POWER ELECTRONICS AND DRIVES

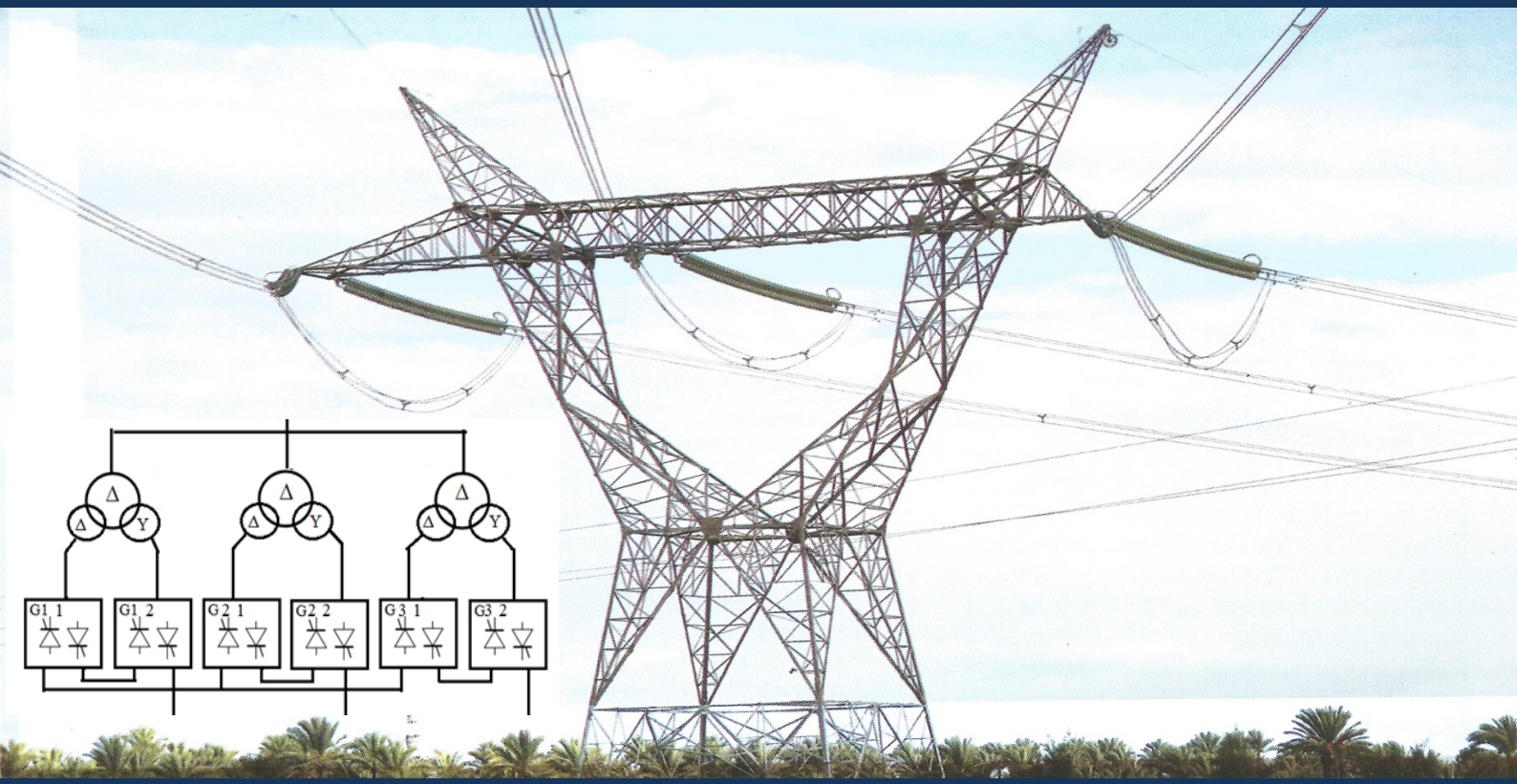

Mohammed T. Lazim

First Edition

Published with the support of Philadelphia University-Jordan

Power Electronics and Drives

Mohammed T. Lazim Al-Zuhairi

Professor of Electrical and Electronics Engineering
Faculty of Engineering and Technology
Electrical Engineering Department
Philadelphia University-Jordan

First Edition

Philadelphia University-Jordan

Published with the support of Philadelphia University – Jordan
Jarash Road P.O.Box. 1 Philadelphia University 19392 Jordan

First Published 2019

Copyright © 2019

All rights reserved.

Printed in the Hashemite kingdom of Jordan
at Al-Fanar Printing Press - Amman

No part of this work may be reproduced, stored in a retrieval system, or transmitted in any form or by any means, electronic, mechanical, photocopying, recording or otherwise, without the prior written permission of the Author.
drmohamadtofik@yahoo.com.
Power Electronics & drives / by Mohammed T. Lazim.
1. Electronics texts for engineers and scientists 2. Electric motors.
3. Electric driving.

Dedicated

To my family:

Ilham – Chief Senior Pharmacist – Wife

Sawsan – Bsc.Chemical Engineer – Daughter

Ahmed – Msc. Electronic and Communications Engineer –Son

Zahra – Msc. Computer and Control Engineer – Daughter

Noor – Bsc. Architect – Daughter

Sura – Bsc. Pharmacist – Daughter

Ali – H.N.D. Electrical Engineering – Son

About the author

Professor Mohammed T. Lazim

Mohammed T. Lazim is employed by Philadelphia University in Jordan as Professor of Electrical and Electronics Engineering. Previously, He was employed by Nahrain University in Iraq as Head of Electronics and Communications Engineering Department and Chief Consultant of Nahrain University Engineering Bureau. Lazim received his B.Sc. and M.Sc. degrees in Electrical Engineering from the University of Baghdad in 1967 and 1975 respectively, and Ph.D. degree in Electrical and Electronics Engineering from the University of Bradford in the United Kingdom in 1981. Previously, He worked as an Associate Professor of Electrical Engineering and Head of the Electrical and Electronics Engineering Department at the Military Engineering College at Baghdad-Iraq. He also worked as a Visiting Associate Professor of Electrical Engineering at the University of Technology-Iraq and as post graduate lecturer at the Electrical Engineering Department at University of Baghdad, and at the Control and Computer Engineering Department at University of Technology-Baghdad, Head of Computer Science Department, and Head of the Operational Research Department at Mansour University College at Baghdad-Iraq. Lazim was also previously employed as a Design, Development and Consultant Engineer with the Ministry of Defence, Ministry of oil, Ministry of Industry and Ministry of Electricity in Iraq.

Professor Lazim is actively involved in teaching, researching, and lecturing in Power Electronics, Electrical Power Systems, Economics of Energy Resources, Electrical Machines, Electrical Drive Systems, Electrical Installation, Reliability Theory and Control Engineering. He has published 7 books listed in the Iraqi and Jordanian National Libraries and more than 70 technical papers and research reports.

Contents

Preface *Page* (xv)
PART I : Power Electronics 1
Chapter One : Power Electronics Fundamentals 1
1.1 Introduction 1
1.2 Power Electronics Applications 3
1.3 Power Semiconductor Devices 4
1.4 Types of Power Semiconductor Devices 5
1.4.1 Power Diode 6
1.4.1.1 Diode Parameters 7
1.4.1.2 Classifications of Power Diode 8
1.4.2 Thyristors (Silicon Controlled Rectifiers "SCRs") 9
1.4.2.1 Static Characteristics of the Thyristor 10
1.4.2.2 Thyristor Parameters 12
1.4.2.3 Thyristor Turning ON Mechanism 12
1.4.2.4 Thyristor Turning OFF Mechanism 14
1.4.2.5 Types of Thyristors 15
1.4.3 The Triac 16
1.4.4 Gate Turn off Thyristors (GTO) 17
1.4.5 Power Transistors 20
1.4.5.1 Bipolar Junction Transistor (BJT) 20
1.4.5.2 Metal Oxide Semiconductor Field Effect Transistors "MOSFETs " 23
1.4.5.3 Insulated Gate Bipolar Transistor "IGBT" 26
1.4.5.4 MOS-Controlled thyristor (MCT Thyristor) 28
1.5 Other Switching Devices 30
1.5.1 Static Induction Transistors (SITs) , and Static Induction Thyristors (SITHs) 30
1.5.2 Gate Commutated Thyristor (GCT Thyristor) 30
1.6 Wide Band Gap Semiconductor Devices 30
1.7 Switching Losses in a Power Switch 33
1.8 Summary of Power Semiconductor Device Capabilities 34
Review Questions and Problems 35

Chapter Two : AC-DC Conversion : Uncontrolled Rectification 38
2.1 Introduction to Basic Rectifier Circuits 38
2.2 Uncontrolled Rectifications 39
2.2.1 Single-Phase Half-Wave Uncontrolled Rectifier with Resistive Load 39
2.2.2 Single-Phase Half-Wave Uncontrolled Rectifier

with *R-L* Load 44
2.2.3 Single-Phase Half-Wave Uncontrolled Rectifier Circuit for Battery Charging 51
2.3 Single-Phase Full-Wave Uncontrolled Rectifiers 53
2.3.1 Case of Resistive Load 53
2.3.2 Single-phase Full-Wave Bi-Phase (Center-tapped) Uncontrolled Rectifier with Resistive Load 55
2.3.3 Single-Phase Full-Wave Uncontrolled Rectifier Loaded with Highly Inductive Load 57
2.4 Harmonic Considerations of the Output Voltage and Current Waveforms of the Single-Phase Full-Wave Rectifier 58
2.4.1 Voltage Waveform Harmonics 58
2.4.2 Input Current Harmonics 61
2.5 Poly-Phase Uncontrolled Rectification 64
2.5.1 Three-Phase Half-Wave Uncontrolled Rectifier 64
2.5.2 Three-Phase Full-Wave Uncontrolled Bridge Rectifier 68
2.5.3 Six-Phase (Hexa-Phase) Uncontrolled Rectifier 72
2.6 General Formula for the Output Voltage of P-Pulse Uncontrolled Rectifier 75
2.6.1 Output Current of P-Pulse Converter 76
2.6.2 Power Factor of a P-Pulse Rectifier 77
2.7 Harmonic Analysis of P-Pulse Uncontrolled Rectifier 78
2.8 Uses of Poly-Phase Uncontrolled Rectifiers 80
2.9 The Freewheeling Diode 83
Problems 83

Chapter Three : AC-DC Conversion : Controlled Rectifications 91
3.1 Introduction 91
3.2 Single-Phase, Half-Wave, Controlled Rectifier Loaded with Passive Loads 91
3.2.1 Case of Resistive Load 91
3.2.2 Single-Phase, Half-Wave, Controlled Rectifier Loaded with Series Resistive-Inductive Load 94

3.2.3 The Freewheeling Diode in Single-phase Controlled Rectification 96
3.3 Single-Phase, Full-Wave, Fully-Controlled Bridge Rectifier (p = 2) 105
3.3.1 Operation of the Converter with Resistive Load 106
3.3.2 Operation of the Converter with *R-L* load 107
3.4 Single-phase Half-Controlled (Semiconverter) Rectifier 113
3.5 Bi-Phase (Mid-Point) Controlled Rectifier 114
3.6 Poly-Phase Controlled Rectifiers 127
3.6.1 Three- Phase Half-Wave Controlled Rectifier ($p = 3$) 127

3.6.2 Three- Phase Full-Wave Fully-Controlled Rectifier ($p = 6$).... 135
3.6.3 Three- Phase Full-wave, Half-Controlled Rectifier 137
3.7 Overlap and Harmonic Considerations in Uncontrolled AC- DC Conversion..... 147
3.7.1 Principle of Overlap During Commutation 147
3.7.2 Harmonic Considerations in Controlled P-Pulse ac-to-dc Converter-General Solution 160
3.7.3 Harmonic Amplitude Spectra of the Output Voltage Waveform for P-Pulse Controlled Rectifiers 162
Problems 171

Chapter Four : DC-DC Conversion: DC Choppers 179
4.1 Introduction..... 179
4.2 Principle of Step-Down Chopper 181
4.3 Analysis of a Step-Down DC Chopper with Resistive-Load 182
4.4 Analysis of a Step-Down DC Chopper with *R-L* load: Exact Analysis 185
4.5 Analysis of a Step-Down DC Chopper with Load Consisting Back *emf* (*E*) 190
4.5.1 Continuous Current Operation Condition with Back *emf*..... 191
4.5.2 Discontinuous Current Operation Condition 192
4.6 Harmonic Analysis of the Load Voltage Waveform of Class-A Chopper..... 195
4.7 Analysis of a Step-Down DC Chopper with *R-L* load: Approximate Analysis 201
4.8 Step-Up DC-to-DC Converter (Boost Converter) 207
4.9 Other Classes of Choppers 214
4.9.1 Class B Chopper Circuit (Two-Quadrant Operation) 214
4.9.2 Class-C Chopper..... 215
4.9.3 Class-D Chopper 215
4.9.4 Class-E Chopper (Full-Bridge DC-DC Converter) 216
4.10 DC-DC Switch-Mode Converters 217
4.10.1 Forward or (Buck) Regulator Using MOSFET 218
4.10.2 Fly Back Regulator (Boost Regulator) 222
4.10.3 Buck-Boost Regulator 226
Problems 230

Chapter Five : AC-AC Conversion : AC Voltage Controller..... 234
5.1 Introduction..... 234
5.2 Single-Phase AC Voltage Controller 234
5.2.1 AC Voltage Controller Working with Resistive Load and Symmetrical Phase-Angel Triggering 235
5.2.2 The RMS Values of the Load Voltage and Current 237
5.3 Harmonics Analysis of the Load Voltage

Waveform of AC Voltage Controller 239
5.4 Calculation of Power Dissipation in Terms of Harmonics 243
5.5 Operation of Single-Phase AC Controller with *R-L* Load 261
5.5.1 Load Voltage Waveform Analysis 265
5.5.2 Harmonic Properties of the Current Waveform 268
5.5.3 The RMS Value of the Load Current 270
5.6 Three-Phase AC-to-AC Voltage Controllers 274
5.6.1 Fully Controlled Three-Phase AC Voltage Controller 274
5.6.2 Analytical Properties of the Output Voltage Waveform 279
5.7 Other Types of Three-Phase AC Voltage controllers 280
Problems 284

Chapter Six : AC-AC Conversion : Integral-Cycle Control 290
6.1 Introduction 290
6.2 Single-Phase Circuit with Voltage Control by Integral-Cycle Triggering (Case of Resistive Load) 290
6.3 Harmonic Amplitude Spectra of Integral-Cycle Waveforms 292
6.3.1 The Supply Frequency Component ($n=T$) 293
6.3.2 Zero Value Harmonics 293
6.3.3 Higher Order Harmonic Frequency Components (n > T) 294
6.4 RMS Load Voltage, Load Power and Power Factor 295
6.5 Integral-Cycle Control of Series Resistive-Inductive Load 299
6.6 Integral-Cycle Control in Three-Phase Circuits 307
6.6.1 Four-Wire, Star-Connected, Resistive Load 307
6.6.2 Four-Wire, Star-Connected, Series *R-L* Load 312
6.7 Other Forms of Integral-Cycle Control 324
6.7.1 Bi-Phase Power Converter 325
6.7.2 Multi-Conduction and Control Periods Integral-Cycle Triggering Technique 330
6.7.3 Bi-Phase Multi-Control and Conduction Period Integral-Cycle Control (BPMICC) Technique 335
Problems 342

Chapter Seven : AC-AC Conversion : Cycloconverter and Matrix Converters 346
7.1 Introduction 346
7.2 Single-Phase to Single-Phase Cycloconverter 347
7.3 Analytical Properties of the Single-Phase to Single-Phase Cycloconverter Output Voltage Waveforms 351
7.3.1 RMS Load Voltage 351
7.3.2 Fundamental Component of the Load Voltage Waveform 351
7.4 Multi-Phase Cycloconverter 354
7.4.1 Three-Phase to Single-Phase Cycloconverter 354
7.4.2 Three-Phase to Three-Phase Cycloconverter 359

7.4.3 Three-Phase to Single-Phase Full-Wave (Six-Pulse) Cycloconverter 361
7.4.4 Three-Phase to Three-Phase Full-Wave (Six-Pulse) Cycloconverter 361
7.5 Envelope Cycloconverter 365
7.5.1 Performance Characteristics of a Single -Phase Envelope Cycloconverter 366
7.5.2 Harmonic Analysis of the Output Voltage Waveform 367
7.5.3 Three-Phase Cycloconverter with T =2 with R-Load 369
7.5.4 Three-Phase Cycloconverter with T =3 with R-Load 371
7.6 Harmonics Reduction in Envelope Cycloconverter 378
7.7 The Matrix Converter 379
Problems 382

Chapter Eight : DC-AC Conversion: Inverters 384
8.1 Introduction 384
8.2 Parallel Inverter 385
8.2.1 Transistor Parallel Inverter 385
8.2.2 Thyristor Parallel Inverter 386
8.2.3 Inverter Performance Parameters 391
8.3 Single-Phase Bridge-Type Inverters 395
8.3.1 Single-Phase Half-Bridge Inverter 396
8.3.2 Single-Phase Full-Bridge Inverter 400
8.4 Three-Phase Inverter 408
8.4.1 120 – Degree Conduction 409
8.4.2 180 – Degree Conduction 412
8.5 Inverter Output Frequency and Voltage Control 417
8.5.1 Single Pulse Width Modulation 419
8.5.2 Multiple Pulse Width Modulation 421
8.5.3 Sinusoidal Pulse Width Modulation (SPWM) 423
8.5.4 Modified Sinusoidal Pulse Width Modulation 426
8.5.5 Other PWM Methods 426
8.6 Voltage Control of Three-Phase Inverter 428
8.7 Harmonic Reductions in the Inverter Output Voltage 428
8.7.1 Harmonic Reduction by PWM 429
8.7.2 Harmonic Reduction by Transformer Connections 429
8.7.3 Harmonic Reduction by Stepped-Wave Inverter 431
8.7.4 Harmonic Reduction Using Filters 431
8.8 Three-Phase Naturally Commutated Inverter 432
8.9 Current Source Inverter 433
8.9.1 Single-Phase Current Source Inverter 434
8.9.2 Three-Phase Current Source Inverter 435
Problems 436

Chapter Nine : DC-AC Conversion : Resonant
Inverters and Multilevel Inverters 441
9.1 Introduction..... 441
9.2 Single-Phase Series Resonant Inverters 442
9.3 Single-Phase Single-Switch Resonant Inverter 448
9.4 Single-phase Discrete Pulse Modulated Resonant Inverter 453
9.5 Multilevel Inverters 456
9.5.1 Cascaded H-Bridge Multilevel Inverters 457
9.5.2 Diode-Clamped Multilevel Inverters 462
9.5.3 Flying-Capacitor Multilevel Inverters 465
Problems 469

PART II : Electrical Drives 472
Chapter Ten : Introduction to Electrical Drives 472
10.1 Introduction 472
10.2 General Electric Drive System 473
10.2.1 Drive System Components 473
10.2.2 Classification of Electric Drives 475
10.2.3 Advantages of the Drive System 475
10.3 Review of Rotational Mechanics..... 476
10.4 Dynamics of Motor-Load System:
Fundamentals of Torque Equations 477
10.4.1 Types of Loads 478
10.4.2 Classifications of Various Types of Loads 480
10.4.3 Basic Equation of Motion for Drive System 482
10.5 Mechanical Transmissions Employed in Electrical Drive Systems .....
493
10.5.1 Reducers 494
10.5.2 Clutches 496
10.6 Ratings of Motors 499
10.6.1 Rating of the Motor for Continuous Load 500
10.6.2 Rating of the Motor for Intermittent Loads 500
10.6.3 Rating of the Motor for Variable Load 502
Problems 504

Chapter Eleven : DC Drives - DC Machines Review..... 509
11.1 Introduction..... 509
11.2 DC Motors 509
11.3 Types of DC Motors 510
11.4 Principles of DC Motors 512
11.4.1 The Equivalent Circuit of a DC Separately-Excited Motor ... 512
11.4.2 Speed and Torque Equations 513
11.5 Mechanical Characteristics of DC Motors In Driving Conditions .515
11.5.1 Mechanical Characteristics of a Separately-

Excited DC Motor 515
11.5.2 Mechanical Characteristics of Shunt DC Motor 516
11.5.3 Mechanical Characteristics of Series DC Motor 518
11.5.4 Mechanical Characteristics of Compound DC Motor 522
11.6 DC Motors Speed Control 523
11.6.1 Motor Speed Control of Shunt and Separately-Excited DC Motors 523
11.6.2 Safe Ranges of Operation for the Two Common Methods 526
11.6.3 Speed Control of Series DC Motors 532
11.7 Four-Quadrant Operation of a Drive System and Motor Braking 535
11.7.1 Four-Quadrant Operation of DC Machine 535
11.7.2 Electrical Braking of DC motors 537
11.7.3 Types of DC Motor Electric Braking 538
Problems 545

Chapter Twelve : DC Chopper Drives 548
12.1 Introduction 548
12.2 One-Quadrant DC Chopper Drives 548
12.2.1 Armature Voltage Waveform Analysis for Continuous Armature Current Operation 550
12.2.2 Armature Voltage Waveform Analysis for Discontinuous Armature Current Operation 551
12.3 Analytical Properties of the Armature Current Waveform 552
12.4 Power Input, Supply Current, Average Armature Current and Torque Calculations 558
Problems 567

Chapter Thirteen : DC Drives Using Controlled Rectifiers 572
13.1 Introduction 572
13.2 Single-Phase Converter Drives 573
13.2.1 Single-Phase Half-Wave Converter Drives 573
13.2.2 Single-Phase Semiconverter with Separately-Excited DC Motor Load 577
13.2.3 Single-Phase Full-Wave Fully-Controlled Rectifier Drives 582
13.2.4 Single-Phase Dual Converter Drives 591
13.3 Three-Phase DC Drives 593
13.3.1 Three-Phase Half-Wave (or P = 3) Converter 594
13.3.2 Three-Phase Semiconverter Drive 596
13.3.3 Three-Phase Full-Converter Drive 599
13.3.4 Three-Phase Dual Converter Drive 601
Problems 605

Chapter Fourteen : Closed-Loop Variable Speed DC Drives 610
14.1 Introduction 610
14.2 Closed-Loop Variable Speed DC Drive 611
14.2.1 The Triggering (Firing) Circuit 611
14.2.2 Control Signal and Components 612
14.3 Speed control 613
14.3.1 Open-Loop Operation 614
14.3.2 Closed-Loop Operation 614
14.4 DC Motor Control Characteristics 616
14.4.1 Open-Loop Transfer Function of DC Motor 617
14.4.2 Closed-Loop Transfer Function 621
14.5 Practical Closed-Loop Control System for DC Motor with Speed and Current Controllers 623
14.5.1 Speed and Current Controllers Transfer Functions 625
14.5.2 Mathematical Modeling of the Power Converter Units 629
14.5.3 Closed-Loop Current Control with PI-Controller 633
14.5.4 Closed-Loop Speed Control with PI-Controller 636
14.5.5 Closed-Loop Speed and Current Control with PI-Controller Simplified Steady-State Analysis 639
Problems 643

Chapter Fifteen : AC Drives 649
15.1 Introduction 649
15.2 Types of AC Motors 650
15.3 Three-Phase Induction Motor : Revision of Equations 651
15.3.1 Basic Principles of Three- Phase Induction Motor with Sinusoidal Supply Voltages 652
15.3.2 Development of Circuit Model (Equivalent Circuit) Standstill Operation 654
15.3.3 The Approximate Equivalent Circuit 657
15.3.4 Power and Torque in Induction Motor 657
15.4 Speed Control of Induction Motor 662
15.4.1 Speed Control from Stator Side 663
15.4.2 Speed Control from Rotor Side 685
15.5 Synchronous Motor Drives 697
15.5.1 Variable Speed Synchronous Motor Drives (VSD) 698
15.5.2 Types of Inverters Used in Synchronous Motor Drives 701
15.5.3 Cycloconverter Drives of Synchronous Motors 702
15.5.4 Types of Cycloconverter Used in Synchronous Motor Drives 705
Problems 707
Appendices 709
References 717
Index 720

Preface

During the last fifty years the field of power electronics and drives has become more diversified and broader in scope. Power electronics has found an important place in modern technology being a core of power and energy control. Almost all the new electrical and electromechanical equipment contain power electronics circuits.

This book *Power Electronics and Drives* is intended as a textbook for courses on Power Electronics and Motor Control for junior and senior undergraduate students in Electrical; Electronics and Communication; Electronics and Telecommunication; Instrumentation and Control; Electronics and Instrumentation; Industrial Electronics, and Mechatronics Engineering. The content of the book and the level of the presentation are designed to suit the preparation and needs of the average engineering student. The text is written for some flexibility in the order of the topics. The textbook is unique and differs from the general treatment of the subject, through the style of presentation of the material, and through the addition of recent theories and applications of power electronics.

The book consists of two parts. Part-I (Chapter 1 to 9) provides good background and a comprehensive description on power electronics subjects. Part-II (Chapter 10 to 15) covers the motor drive systems, which undergraduate students will also find useful. The text can also be utilised as a textbook for graduate students and as a reference book for technicians and engineers of respective specialties.

A large number of solved examples, theoretical exercises and numerical problems, all of degree standard, have been included in the text. The solution to illustrative examples covering almost all topics and sub-topics makes the entire presentation easy to follow. Exercises and numerical problems with answers given at the end of each chapter help the students in evaluating their unders- tanding of the subject.

The author wishes to thank Philadelphia University for its support in publi- shing this book and also Professor Munther N. Baker for his valuable remarks on the book during the writing phases. Similarly he thanks Professor Kassim Al-Obaidi, Dean of the Faculty of Engineering and Technology and Dr. Mohammed M. Al-Salman, Head of Electrical Engineering Department for their encouragement and support. Thanks are also due to author's previous M.Sc. and Ph.D. students: Dr. Mohammed

Khasbak, Dr. Anas L.Mahmoud , Dr. Ali K.Jabir, Mr.Ahmed Mudhafar Al-Taie and Mr. Jan W.Jan, for their great help with Chapters 6 and 7.

Within this book, every care and attention has been taken to eliminate misprints and errors. However, should the reader become aware of any inaccuracy or misprint that has crept in, then the author would be grateful if this could be brought to his attention. Also, any suggestion for improvement of the book will be acknowledged and well appreciated.

Author
Dr. Prof. Mohammed T.Lazim
Amman 2019
drmohamadtofik@yahoo.com

PART I :POWER ELECTRONICS

CHAPTER ONE

POWER ELECTRONICS FUNDAMENTALS

1.1 INTRODUCTION

The first electronics revolution began in 1948 with the invention of the bipolar silicon transistor at Bell Telephone Laboratories by Bardeen, Bratain, and Schockley. This invention leads to the most recent advanced in electronic technologies seen today. Also, modern microelectronics has evolved over the years from these silicon semiconductors. In 1957, the second electronics revolution started with the development of the four-layer high power commercial thyristor by the General Electric Company in USA. The invention of this device and its later applications in energy processing and motor control fields has initiated a new era of power electronics.

From the early 1960s until quite recently, the thyristor and its family was almost universally used as the high power semiconductor switch which leads to introduction of many different types of energy conversion techniques. The energy conversion using power electronics achieves conversion of electric power from one form to another, using a combination of high-power semiconductor devices and passive components, mainly transformers, inductors, and capacitors. The input and output may be alternating current (a.c.) or direct current (d.c.) and may differ in magnitude and/or frequency. The end goals of a power electronic converter are to achieve high efficiency of conversion, minimize size and weight, and achieve desired regulation of the output.

Power electronic converters can be classified into four different types on the basis of input and output, *dc-dc, dc-ac, ac-dc,* and *ac-ac,* named with the first part referring to the input and the second to the output. Development of power semiconductors with very high voltage and current ratings has enabled the use of power electronic converters in many

industrial and utility applications. The range of applications continues to expand in areas such as power supplies, motor speed control, factory automation, transportation, energy storage, industrial drives, and electric power transmission and distribution. Applications in power transmission include high-voltage d.c. (HVDC) converter stations, flexible a.c. transmission system (FACTS), and static-var compensators. Almost all new electrical or electromechanical equipment, from household air conditioners and computer power supplies to industrial motor controls, contain power electronic circuits and/or systems. Also, engineers involved in conversion and control of power and energy, working in applications ranging from several hundred voltages at a fraction of an ampere for display devices to about 1000 kV at high-voltage d.c. transmission should have a working knowledge of power electronics.

In general these applications require an efficient conversion of voltage and frequency including driving an a.c. electric motor with variable speed requiring in principle constant V/Hz in most industrial applications or variable voltage in d.c. motors in transportation applications as used in electric/hybrid vehicles, electric trains/trams, submarines and ships. Also in utility application to connect various sources of energy (mostly renewable such as wind where wind generator is driven with variable speed /frequency to maximize energy capture and PV where power is generated as d.c. and the voltage available changes heavily with the illumination and proximity to maximum power point) to the a.c. grid (directly or via long high voltage d.c. transmission lines). In addition, in communication engineering, mobile applications may impose additional restrictions regarding size/weight which means higher power densities are required and that can only be achieved (for similar functionality) by power electronics.

By definition, Power Electronics relates power semiconductor devices circuitry, its design and role includes the techniques of converting and processing high power electrical energy. The role of power electronics is shown in Fig.1.1.

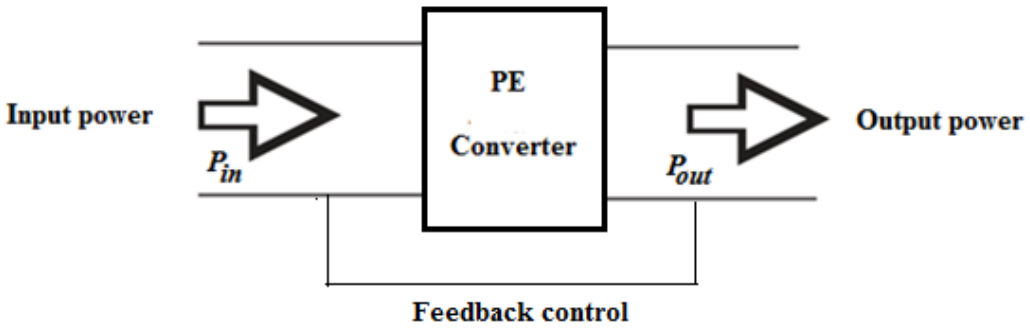

Fig.1.1 The role of power electronics.

Power semiconductor devices are used, such as power diodes, thyristors and power transistors. These power semiconductor devices are so important in modern power control. They are used in switching applications where they compete with “mechanically-operated" or “electrically-operated” switches and they give the following advantages:

1. Faster in operation by a factor of at least a hundred times.
2. Need no routine maintenance.
3. Do not stick, bounce or wear.
4. Give no sparking on break.
5. Have a very long life expectancy when used properly .
6. Are physically small.
7. Are relatively cheap.

The main goal of electronic power conversion systems is to convert electrical energy from one form to another, from the source to the load using power semiconductor devices with, high efficiency, high availability, high reliability, small size, light weight and low cost. Hence, in addition to the simple on-off applications of power semiconductor devices their speed of operation and life expectancy, which are independent of the number of switching actions, make them possible to arrange for smooth control of the mean power from zero to maximum in most applications.

1.2 POWER ELECTRONICS APPLICATIONS

The main fields of applications are in Energy Processing and Drive Technology. Power semiconductor devices are interconnected in a variety of ways to form power control units. These units can be classified in a variety of ways, one of the simplest being to classify them according to their input /output requirements, thus, referring to Fig.1.2.

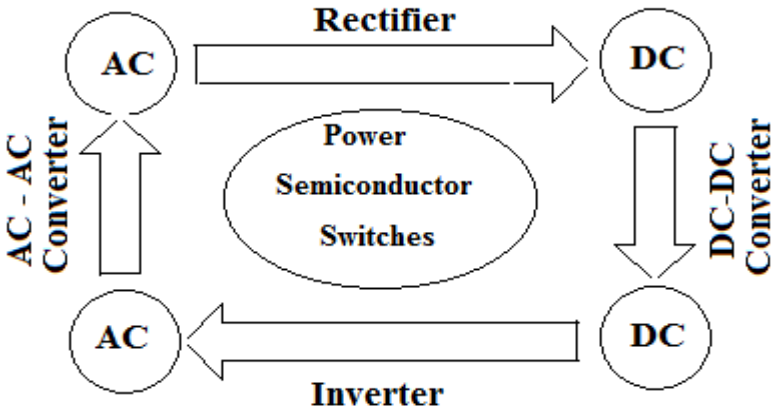

Fig.1.2 Power or energy processing through power electronics converters.

(1) **AC-DC (Rectifiers)** : Circuits for converting a.c. voltage to d.c. voltage or transfer of power from an alternating current (a.c.) supply to direct current (d.c.) form. These circuits can be of two main types:
   (a) AC-DC (Uncontrolled)
   (b) AC-DC (Controlled)

(2) **DC-AC (Inverters)** : Circuits for converting a d.c. voltage to an alternating one or transfer of power from a direct current supply to alternating current form. The output power can be at any desired volage and /or frequency.

(3) **DC-DC Converters** : Circuits change a fixed d.c. voltage into a variable d.c. supply, i.e. transfer of power from a direct current supply directly into a direct current load of different voltage level. These types of converters are usually called d.c. choppers.

(4) **AC-AC Converters** : Circuits change a fixed a.c. voltage into a variable a.c. supply, i.e. transfer of power from an alternating current supply directly into an alternating current load of different voltage level at fixed frequency or variable frequency. These converters are usually of two types:
   (a) AC voltage controllers: Change the a.c. supply voltage magnitude only keeping the frequency unchanged.
   (b) Cycloconverters or matrix converters: Change the a.c. supply directly to a variable a.c. supply both in magnitude and frequency (also called static frequency changers).

1.3 POWER SEMICONDUCTOR DEVICES

Power electronics evolution is a result of the evolution of power semiconductor devices. The Power semiconductor switches are the work-horses of power electronics (PE). There are several power semiconductor devices currently involved in several industrial applications. PE switches work in two states only: Fully on (conducting), and fully off (blocking). Switches are very important and crucial components in power electronic systems. The ideal or good switch must have the following characteristics:

- Very low or negligible power loss during turning ON or OFF.
- Switching times between ON and OFF states should be very low.
- Small power required to turn it ON or OFF.
- Bidirectional and voltage blocking capability.
- Adequate voltage and current ratings.

Practical power semiconductor switches are not perfect. They usually have a very low on-state resistance that result in conduction voltage drop

across the switch itself. In the off-state, these switches possess a very high resistance which results leakage current in both the forward and reverse directions depending on the polarity of the applied voltage. However, the ratings of the power switch in practical case shall include:

- Ratings: blocking voltage and carrying current.
- Speed: any real device requires a definite time to switch.
- Second-order ratings: *di/dt*, *dv/dt*, momentary capabilities.
- Power loss.
- Thermal ratings: need for heat sinks.
- Control ratings: method of operation of the switch.

1.4 TYPES OF POWER SEMICONDUCTOR SWITCHES

The main types of power semiconductor switches are:

1. Power Diodes

2. Thyristor devices
   a. Silicon controlled rectifier (SCR)
   b. Triac (Triode ac switch)
   c. Gate turn-off thyristor (GTO)
   d. MOS controlled thyristor (MCT)
   e. Integrated gated-commutated thyristor (IGCTs)
   f. Static induction thyristor (SITH)

3. Power transistors
   a. Bipolar junction transistor (BJT)
   b. Metal oxide semiconductor field effect transistor (MOSFET and COOLMOS)
   c. Insulated gate bipolar transistor (IGBT)
   d. Static induction transistor (SIT)

4. Power integrated circuit and power modules
   a. Monotholic integration : power integrating circuit
      (i) High voltage integrated circuit (HVIC)
      (ii) Smart power integrated circuit (SPIC)
   b. Packaging integration: power modules
      (i) Ordinery power module: power devices packaged together
      (ii) Intellegent power module (IPM): power devices, drive circuit, protection circuit
      (iii) Integrated power electronics module (IPEM): power devices, drive circuit, protection circuit , control circuit.

These devices are based on the mature and very well established silicon technology. However, Si exhibits some important limitations regarding its voltage blocking capability, operation temperature and switching frequency. In some industrial applications where electronic systems based on traditional Si power devices cannot operate, a new generation of power devices based on Wide Band Gap Semiconductors such as silicon carbide SiC and gallium nitrate GaN are used. These new devices present high-voltage blocking capability, high-temperature operation and high switching frequencies. Therefore, the power switching devices may also be divided into high voltage devices (mostly IGBTs), low voltage devices (mostly discrete MOSFETs), wide band gap devices (GaN and SiC MOSFETs and diodes), and integrated power (also sometimes known as smart power).

1.4.1 Power Diode

Power diode is usually used as a switch; it is the simplest one among other power electronics switches. It is a two terminal device formed of a PN junction as shown in Fig.1.3(a). Terminal A known as the anode and terminal K known as the cathode. It is not controllable and its operating states are determined by the circuit operating point. When diode is forward biased, i.e. terminal A becomes at a higher potential compared to terminal K, it conducts current i_D in the direction as shown, i.e. a forward positive voltage V_F will turn it on. When it reversed biased (a reverse negative current from cathode to anode) will turn it off. With forward biasing a small voltage drop V_D will appear across it typically it ranges from 0.6 to 1.0 V for currents in the normal range, which under ideal conditions is usually ignored. However, when a diode is reverse biased, it does not conduct and the diode then experiences a small current I_s flowing in the reverse direction called the leakage current. Both forward voltage drop and leakage current are ignored in an ideal diode or in power electronics applications.

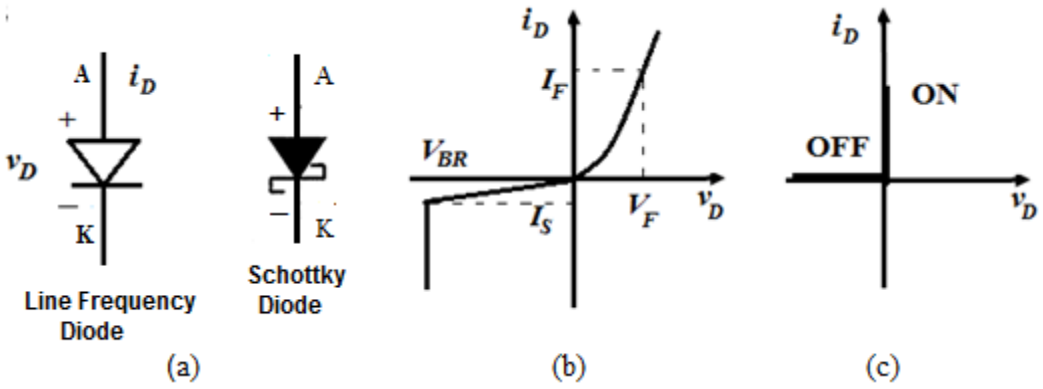

Fig.1.3 Power diode: (a) Symbol, (b) Characteristic, and (c) Ideal characteristic.

Practically, the diode characteristic consists of two regions, as shown in Fig.1.3(b):

(a) A forward bias region (on-state) where both v_D and i_D are positive and the current in this region increases exponentially with the increase in the voltage, and,

(b) A reversed bias region (off-state) where both v_D and i_D, are negative and very small leakage current (μA to mA) flows through the diode until the applied reverse voltage reaches the diode's breakdown voltage limit V_{BR}.

Ideally, the diode is represented by a short circuit when forward biased and as an open circuit when reversed biased with the ideal characteristic shown in Fig.1.3(c). In general, for each diode, there is a small delay in going from off-state to on-state due to the time required for the carriers to build up. During turn-off, the excess carriers in the drift region have to be removed. Thus, for a short time, the diode conducts in the reverse direction with a high voltage across it. This phenomenon, known as reverse recovery, leads to significant power loss and becomes one of the limiting factors in high-frequency circuits.

1.4.1.1 Diode parameters

1. **DC diode parameters**

The most important parameters of a power diode are the following:

- Forward voltage V_F is the voltage drop of a diode across A and K at a defined current level when it is forward biased.
- Breakdown voltage V_{BR} is the voltage drop across the diode at a defined current level when it is beyond reverse-biased level. This is known as avalanche.
- Reverse current I_R is the current at a particular voltage, and which is below the breakdown voltage.

2. **AC diode parameters**

- Forward recovery time t_{FR} is the time required for the diode voltage to drop to a particular value after the forward current starts to flow.
- Reverse recovery time t_{rr} is the time interval between the application of reverse voltage and the reverse current dropped to 0.25 of I_{rm} (reverse maximum current), as shown in Fig. 1.4.

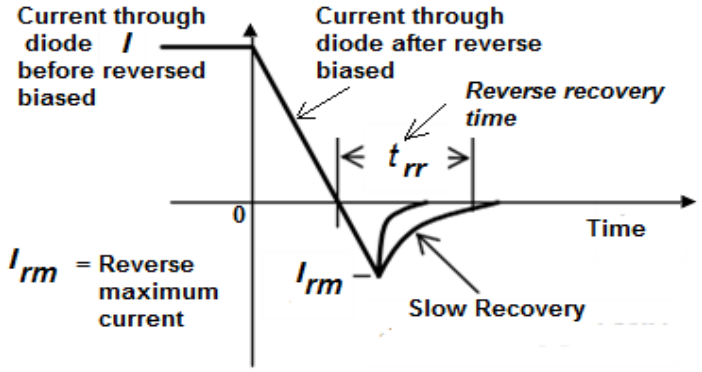

Fig.1.4 Diode reverse recovery process.

1.4.1.2 Classifications of power diode

PN junction type power diodes are classified as:

1. Line frequency diodes: For low frequency rectifications.
   - On-state voltage very low (below 1V).
   - Large reverse recovery time t_{rr} (about 25 μs).
   - Very high current (up to 6 kA) and voltage (8 kV) ratings.
   - Used in line-frequency (50/60 Hz) applications such as rectifiers.
   - Slow recovery, as illustrated in Fig.1.4.

2. Fast and ultra-fast recovery diode: For high frequency rectifications.
   - Very low t_{rr} (< 1 μs).
   - Power levels at several hundred volts and several hundred amperes.
   - Normally used in high frequency circuits.

3. Schottky diode: These are based on metal-semiconductor junctions. These junctions have a lower junction potential leading to a lower forward voltage drop.
   - Silicon-based Schottky power diodes have forward voltage drop ranging from 0.3 to 0.6 V,
   - Can withstand reverse voltages up to 200 V. As opposed to PN junction diodes, Schottkys are majority carrier devices, so they do not have any reverse recovery.
   - They are used in low voltage, high current application such as switched-mode power supplies.

4. SiC Schottky diode: Recently, SiC-based Schottky diodes have been replaced the Si-based diodes due to their thermal capabilities.

1.4.2 Thyristors (Silicon Controlled Rectifiers “SCRs”)

The thyristor, it is also called silicon controlled rectifier (SCR), is a four-layer, three terminal switching semiconductor device, with each layer consisting of an alternately N or P-type material, for example N-P-N-P. The main terminals, labeled anode A and cathode K , are across the full four layers, and the control terminal, called the gate G, is attached to one of the middle layers. The thyristor symbol and its two-transistor analogy is shown in Fig.1.5. In contrast to the linear relation that exists between load and control currents in a transistor, the thyristor is bistable. The anode and cathode terminals are connected in series with the load to which power is to be controlled. The gate electrode which is the control terminal may be connected to an integrated and complex structure as part of the device.

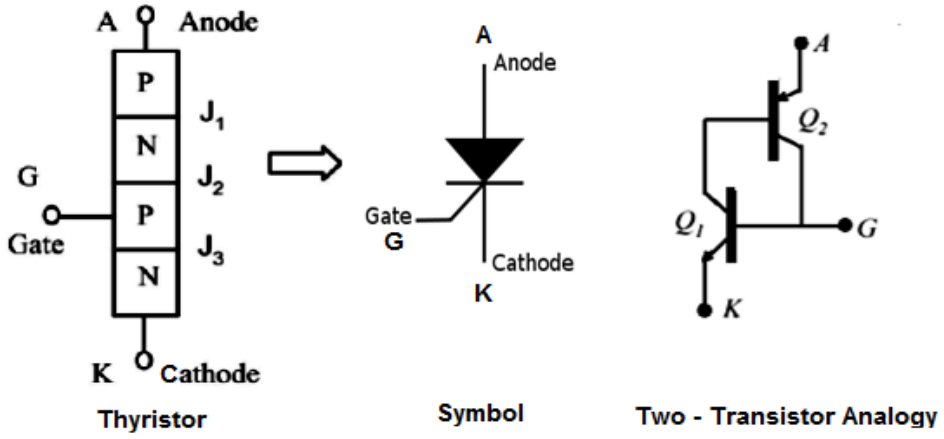

Fig.1.5 The thyristor and its equivalent two-transistor analogue.

Thyristors are mainly used where high currents and voltages are involved, and are often used to control alternating currents, where the change of sign of the current causes the device to automatically switch off. Like a diode, a thyristor conducts only in one direction and used to approximate ideal closed (no voltage drop between anode and cathode) or open (no anode current flow) switch for control of power flow in a circuit. All thyristor types are controllable in switching from a forward blocking state (positive voltage applied to the anode with respect to the cathode) into a forward-conduction state (large forward anode current flowing with a small anode-cathode voltage drop).

Ideally, SCRs are represented by a short circuit when operating within the conduction region and as an open circuit when operating within the blocking region. The ideal characteristic is shown in Fig.1.6(a). After switching from a forward-blocking state into the forward-conduction state, most thyristors have the characteristic that the gate signal can be

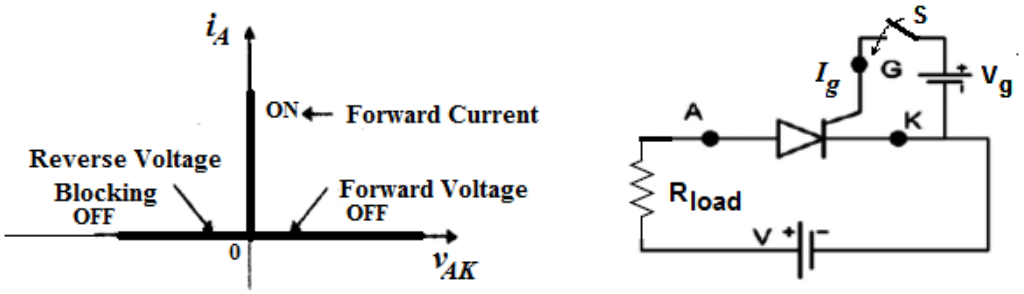

Fig. 1.6 (a) Thyristor ideal characteristic, (b) Thyristor gate circuit.

removed and the thyristor will remain in its forward-conduction mode. This means that once the thyristor is turned-on, the gate loses control. This property, called "latching", is an important distinction between thyristors and other types of power electronic devices. This latching (triggering) process is carried out by injecting current to the gate terminal (i_g) or applying a low voltage, short duration pulse (v_g) to the gate (typically 4 V, 100 µs), Fig.1.6(b), at the required latching instant provided that the device is forward biased (v_{AK} is positive).

1.4.2.1 Static Characteristics of the Thyristor

Practically, the static thyristor characteristic or the Current-Voltage curves for thyristors has three main regions as shown in Fig.1.7.

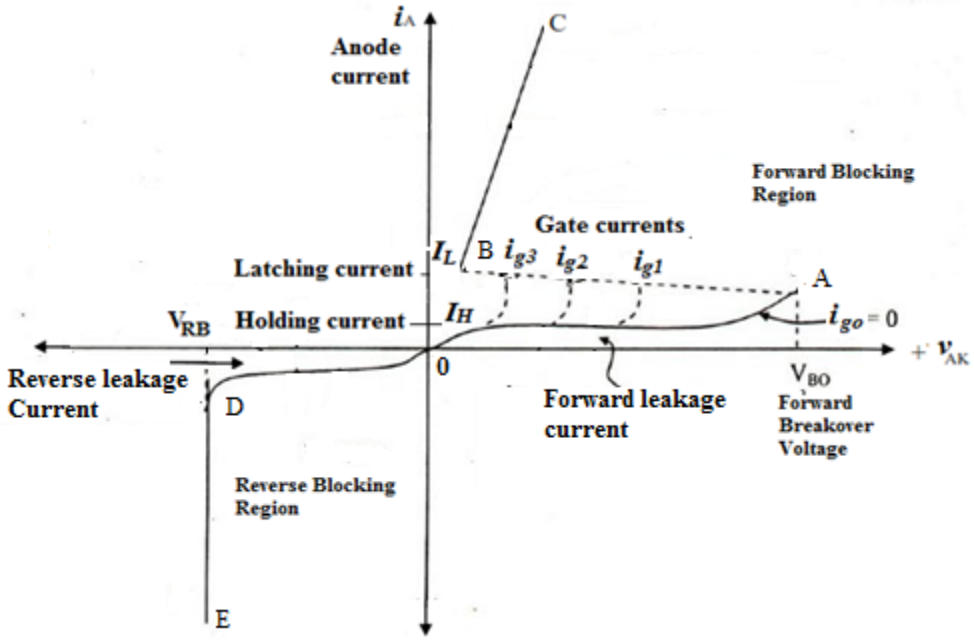

Fig.1.7 Static volt-ampere characteristics of a thyristor.

- The Conduction Region where the thyristor is operating in its on-state,
- The Forward Blocking Region where the thyristor is forward biased but not yet triggered or the voltage did not reach the forward breakover voltage, and
- The Reverse Region that consists of the reverse blocking region and the reverse avalanche region similar to the diode characteristic.

The operation of thyristors is as follows: When a positive voltage is applied to the anode (with respect to a cathode), the thyristor is in its forward-blocking state. The center junction J_2 (see Fig.1.5) is reverse-biased. In this operating mode the gate current is held to zero (open-circuit). As long as the forward applied voltage does not exceed the value necessary to cause excessive carrier multiplication in the depletion region around J_2 (avalanche breakdown), the thyristor remains in an off-state (forward blocking). If the applied voltage exceeds the maximum forward blocking voltage of the thyristor, it will switch to its on-state. However, this mode of turn-on causes non uniformity in the current flow, is generally destructive, and should be avoided.

When a positive gate current is injected into the device, it becomes forward-biased and electrons are injected from the n-emitter into the p-base. Some of these electrons diffuse across the p-base and are collected in the n-base. This collected charge causes a change in the bias condition of J_1. This change will cause holes to be injected from the p-emitter into the n-base. These holes diffuse across the n-base and are collected in the p-base. The addition of these collected holes in the p-base acts the same as gate current. The entire process is regenerative and will cause the increase in charge carriers until J_2 also becomes forward biased and the thyristor is latched in its on-state (forward-conduction). The regenerative action will take place as long as the gate current is applied in sufficient amount and for a sufficient length of time. This mode of turn-on is considered to be the desired one as it is controlled by the gate signal.

This switching behavior can also be explained in terms of the two-transistor analog shown in Fig. 1.5. The two transistors are regeneratively coupled so that if the sum of their forward current gains (α's) exceeds unity, each drives the other into saturation. However ,Thyristor can only be turned on with three conditions:

1. The device must be forward biased, i.e. the anode should be more positive than the cathode.
2. A positive gate current *(i_g)* should be applied at the gate.
3. The current through the thyristor should be more than or equal to the latching current.

Once conducting, the anode current is LATCHED (continuously flowing).

1.4.2.2 Thyristor Parameters

The important points for the thyristor characteristic which can be considered as the thyristor parameters are,

***Latching Current*:** This is the minimum current required to turn on the SCR device and convert it from the Forward Blocking State to the ON State.

***Holding Current*:** This is the minimum forward current flowing through the thyristor in the absence of the gate triggering pulse.

***Forward Breakover Voltage*:** This is the forward voltage required to be applied across the thyristor to turn it on without the gate signal application.

***Max Reverse Voltage*:** This is the maximum reverse voltage to be applied across the thyristor before the reverse avalanche occurs.

Peak Inverse Voltage: It is the maximum voltage which the device can safely withstand in its off-state.

***ON-State Voltage*:** The voltage which appears across the device during its on-state is known as its on-state voltage.

***Rate of rise of voltage dv/dt*:** The rate at which the voltage across the device rises without triggering the device is known as its rate of rise of voltage.

***Current Rating*:** The current carrying capacity of the device is known as its current rating.

It is also worth mentioning that once the SCR is triggered and turned ON the gate signal can be removed without turning it OFF. SCRs are turned OFF when reversing the terminal voltage and current. The thyristor turning ON and OFF mechanisims are illustrated in the following subsuctions.

1.4.2.3 Thyristor Turning ON Mechanism

In reverse-biased mode, the SCR behaves like a diode. It conducts a small leakage current which is almost dependent of the voltage, but increases with temperature. When the peak reverse voltage is exceeded, avalanche breakdown occurs, and large current will flow. In the forward biased mode, with no gate current present (i.e. in the untriggered state, the device exhibits a leakage current. If the forward breakover voltage (V_{Bo}) is exceeded, the SCR "self-triggers" into the conducting state and the voltage collapses to the normal forward volt-drop, typically 1.5-3 V. The presence of any gate current i_g will reduce the forward breakover voltage and will trigger the thyristor at any required instant (α), also called firing angle, see Fig.1.8.

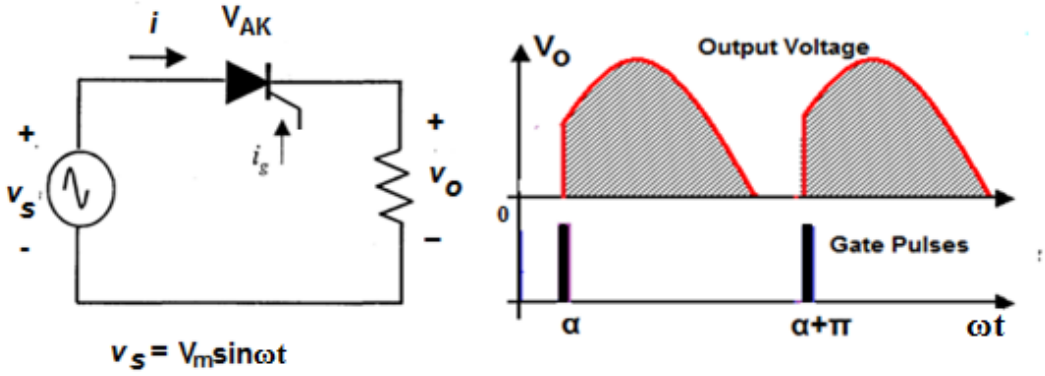

Fig.1.8 Thyristor triggering using gate pulses.

Methods of turning ON the thyristor

The turning on process of the thyristor is known as "Triggering". There are several methods to turn on the thyristor and change its state from Forward-Blocking state to Forward-Conduction state.These methods can be summarized as:

(a) Gate Triggering

This is the most general (practical) method to turn on the thyristor by applying positive voltage between the gate and the cathode to a forward biased thyristor. In this case charge carriers are injected in the inner p-layer, thereby reducing the depletion layer thickness. This will increase the anode current and regenerative action starts. Once the thyristor is turned on, there will be no need to the gate voltage or current, thus, in gate triggering method, instead of applying continuous signal, pulse triggering is preferable.

(b) High Forward Voltage Triggering

In this mode, an additional forward voltage is applied between anode and cathode. When the anode terminal is positive with respect to cathode (V_{AK}), Junction J_1 and J_3 is forward biased and junction J_2 is reverse biased. No current flows due to depletion region in J_2 is reverse biased (except leakage current). As V_{AK} is further increased, at a voltage V_{BO} (Forward Break Over Voltage) the junction J_2 undergoes avalanche breakdown and so a current flows and the device tends to turn ON (even when gate is open).

(c) Thermal (or) Temperature Triggering

The width of depletion layer of SCR decreases with increase in junction temperature. Therefore in SCR when V_{AR} is very near its breakdown voltage, the device is triggered by increasing the junction temperature. By increasing the junction temperature the reverse biased junction collapses thus the device starts to conduct.

(d) Radiation Triggering (or) Light Triggering

For light triggered SCRs a special terminal niche is made inside the inner p-layer instead of gate terminal. When light is allowed to strike this terminal, free charge carriers are generated. When intensity of light becomes more than a normal value, the thyristor starts conducting. This type of thyristors are called as Light Activated SCR " LASCR" .

(e) *dv/dt* Triggering:

When the device is forward biased, J_1 and J_3 are forward biased, J_2 is reverse biased. Junction J_2 behaves as a capacitor, due to the charges existing across the junction. If voltage across the device is V, the charge is represented by Q and capacitance by C then,

$$i_c = dQ/dt$$
$$Q = CV$$
$$i_c = d(CV) / dt$$
$$= C.\, dV/dt + V.\, dC/dt$$
$$as\ dC/dt = 0$$
$$i_c = C.dV/dt$$

Therefore when the rate of change of voltage across the device becomes large, the device may turn on, even if the voltage across the device is small.

1.4.2.4 Thyristor Turning OFF Mechanism (Thyristor Commutation)

The process of turning off a thyristor is defined as "Commutation". Thyristor cannot be turned off by applying negative gate current. It can only be turned off if the current I through it goes negative (reverse). In all commutation techniques, a reverse voltage is applied across the thyristor during the turn off process.
There are two methods by which a thyristor can be turned off.

(a) Natural Commutation
(b) Forced Commutation

For natural commutation , in a.c. circuit, the current always passes through zero for every half cycle. As the current passes through natural zero, a reverse voltage will simultaneously appear across the device. This will turn off the device immediately. This happens when negative portion of the of sine-wave occurs. This process is called as "*natural commutation*" since no external circuit is required for this purpose.

In *forced commutation* , the anode current is "diverted" to another circuitry. To turn off a thyristor, the forward anode current should be brought to zero for sufficient time to allow the removal of charged carriers. In case of d.c. circuits the forward current should be forced to zero by means of some external circuits. One typical thyristor commutation circuit is shown in Fig.1.9. Thyristor T_m is the main thyristor through which the flow of power is controlled. Capacitor C and the four thyristors (T_1,T_2,T_3,T_4) is the commutation circuit. The function of the commutation circuit is to switch off the main thyristor at the end of each on period. During on period of the thyristor, the two auxiliary thyristors T_2 and T_4 are triggered so that the capacitor C is charged such as plate *a* is positive. To switch off, thyristors (T_1,T_3) are triggered on. This results in applying reverse polarity voltage across T_m and hence it will be switched off. Also the capacitor polarity will be reversed; i.e. plate b will now be positive. Thyristor T_m is switched on for the next on period, and now to switch off T_m, thyristors (T_2,T_4) are switched on, and so the cycle is repeated (see Appendix B for more details about forced commutation circuits).

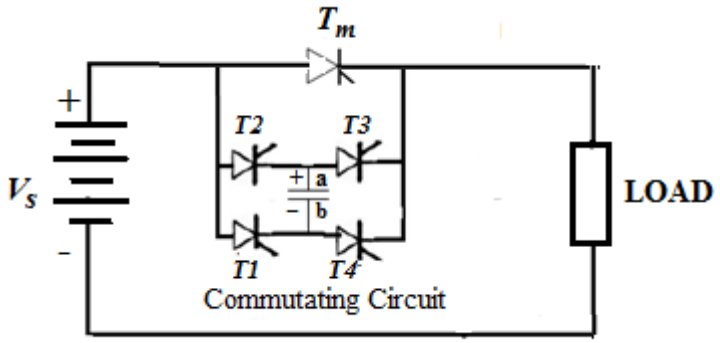

Fig.1.9 Typical forced commutation circuit for a thyristor.

1.4.2.5 Types of Thyristors

1. **Phase Controlled**
   - Rectifying line frequency voltage and current for a.c. and d.c. motor drives.
   - Large voltage (up to 7 kV) and current (up to 5 kA) type-1 capability.
   - Low on-state voltage drop (1.5 to 3 V).

2. **Inverter Grade**
   - Used in inverter and chopper
   - Quite fast, Can be turned-off using "force commutation" method.

3. **Light Activated (Photo Activated)**
   - Similar to phase controlled, but triggered by pulse of light This is mainly used with optocoupler or optoisolator.
   - Normally very high power ratings.

SCR ratings for voltage and current approach those of diodes. Devices for high-voltage d.c. (HVDC) conversion have been built with simultaneous 12 kV and 6 kA type-2 ratings. Fig.1.10 shows phototograph for different types of thyristors used in practice.

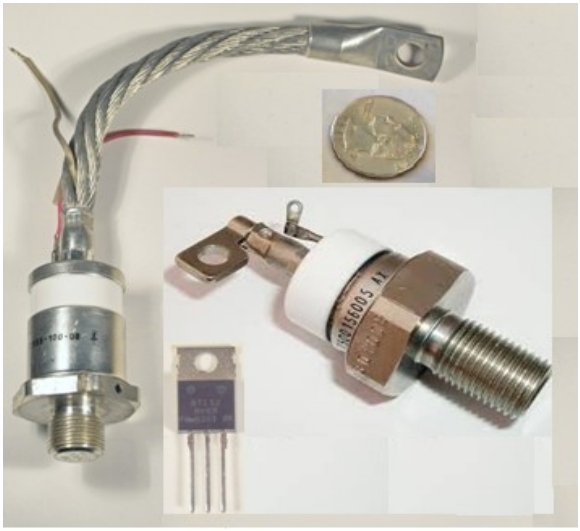

Fig .1.10 Power semiconductor switches (thyristors).

1.4.3 The Triac

The triac, also called '**Bidirectional Thyristor',** is a two thyristors connected back-to-back, used for high or medium power control for both a.c. and d.c. applications, as shown in Fig.1.11. Either of the electrodes MT1 and MT2 can act as anode and either is cathode. The device can be triggered by either positive or negative voltage on the gate with respect to MT1. This device is effectively two thyristors (SCR s) back-to-back in construction with an external n-region which is the gate. Both SCRs are mounted within an encapsulated enclosure and there is one gate terminal. The application of positive anode voltage with positive gate pulse to an inert device causes switch-on in the forward direction. If the anode voltage is reversed, switch-off occurs when the current falls below its holding value, as for an individual SCR. Voltage blocking will then occur in both directions until the device is gated again, in either polarity, to obtain conduction in the desired direction. Hence, the four possible modes of operation of a triac can be summarized as:

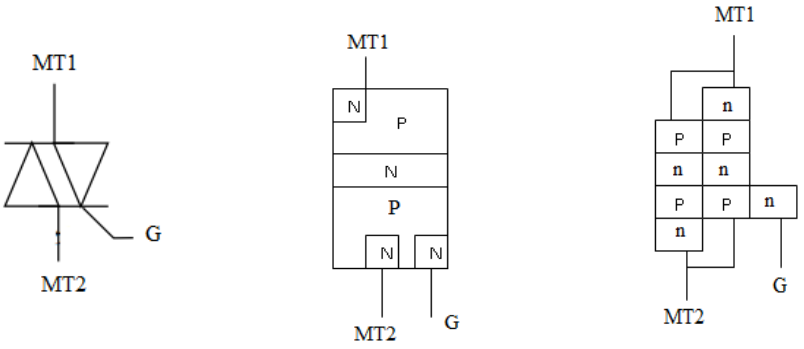

Symbol Triac structure Triac : Two- Thyristor Equivalent Circuit

Fig.1.11 The Triac.

(a) MT2 +, G + : (both relative to MT1) Gate current flows into gate terminal.
(b) MT2 +, G – : Gate current opposite to (a)
(c) MT2 –, G + : Gate current as (a)
(d) MT2 –, G – : Gate current as (b)

Compared with individual SCRs, the triac combination is a low-voltage, lower power, and low-frequency switch with applications usually restricted below 400 Hz. The triac v-i characteristics is shown in Fig.1.12.

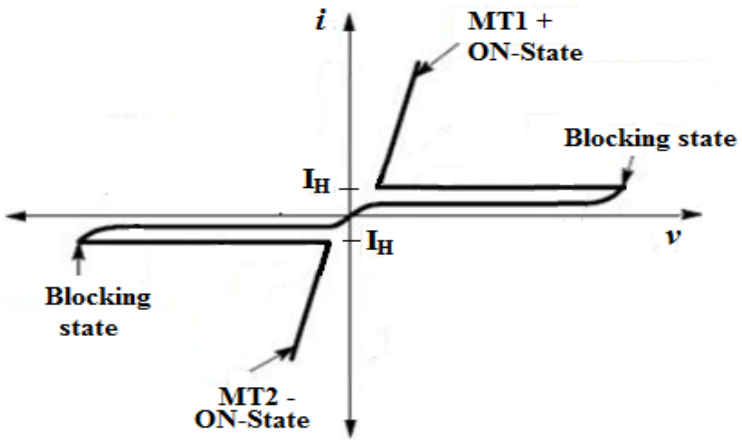

Fig.1.12 Triac characteristic.

1.4.4 Gate Turn off Thyristors (GTO)

A gate turn-off thyristor (known as a GTO) is a three-terminal power semiconductor device that belongs to a thyristor family with a four-layer structure. They also belong to a group of power semiconductor devices that have the ability to fully control on and off states via the control terminal (gate). The design, development, and operation of the GTO are easier to understand if we compare it to the conventional thyristor. Like a

thyristor, applying a positive gate signal to its gate terminal can turn on a GTO. Unlike a standard thyristor, a GTO is designed to turn off by applying a negative gate signal.

There are two types of GTOs: asymmetrical and symmetrical. The asymmetrical GTOs are the most common type on the market. This type is normally used with an anti-parallel diode and hence do not have high reverse-blocking capability. Reverse conducting is accomplished with an anti-parallel diode integrated onto the same silicon wafer. The symmetrical GTOs have equal forward and reverse-blocking capability.

GTO behaves like normal thyristor, but can be turned off using gate signal. The turning off process is difficult, needs very large reverse gate current (normally 1/5 of anode current). It means a 2000 A rating GTO requires 400 A gate current pulse to switch it off but for very short time. Therefore, the gate pulse duration and the power loss due to the gate pulse is small and it can be supplied by low voltage power MOSFETs. The GTO symbol and characteristics are shown in Fig.1.13. The basic structure of a GTO, a four-layer p-n-p-n semiconductor device, is very similar in construction to a thyristor. It has several design features that allow it to be turned on and off by reversing the polarity of the gate signal.

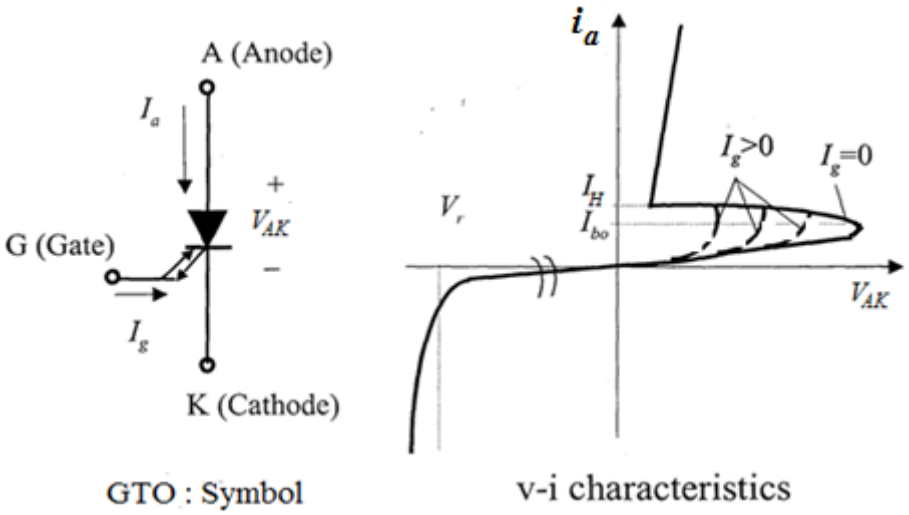

Fig.1.13 Gate turns off (GTO) thyristor.

The turn-on mode is similar to that of a standard thyristor. The injection of the hole current from the gate forward biases the cathode p-base junction, causing electron emission from the cathode. These electrons flow to the anode and induce hole injection by the anode emitter. The injection of holes and electrons into the base regions continues until charge multiplication effects bring the GTO into conduction. This is shown in Fig.1.14(a). The GTO structure is also shown in Fig.1.14(b).

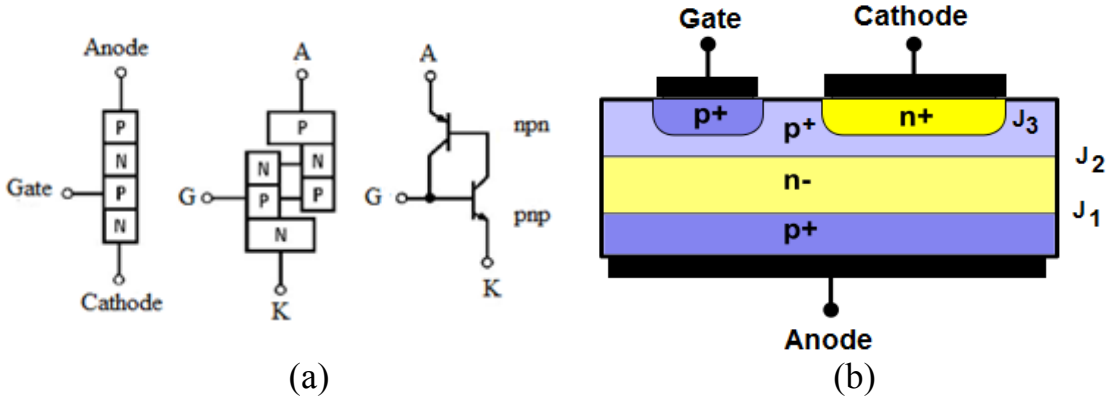

(a) (b)

Fig.1.14 GTO thyristor: (a) Two transistor analogy, (b) GTO structure.

As with a conventional thyristor, only the area of cathode adjacent to the gate electrode is turned on initially and the remaining area is brought into conduction by plasma spreading. However, unlike the thyristor, the GTO consists of many narrow cathode elements, heavily interdigitated with the gate electrode, and therefore the initial turned-on area is very large and the time required for plasma spreading is small.The prime design goal of GTO devices are to achieve fast turn off time and high current turn off capability. The GTO's turn off occurs by removal of excess holes in the cathode base region by reversing the current through the gate terminal. The ratings, merits and demerits of the device are,

- Ratings: Voltage V_{ak} < 6 kV (4500 V), Current I_a < 3 kA.
- Frequency < 5 kHz.
- Gate drive design is very difficult, need very large reverse gate current to turn off.
- GTO normally requires snubbers: A GTO normally requires a *dv*/*dt* snubber circuit to conduct actual turn-off operation under high voltage and high current condition. High power snubbers are expensive.
- A reverse conducting GTO has been fabricated that can block 6 kV in the forward direction, interrupt a peak current of 3 kA, and has a turn-off gain of 5.
- In very high power region (> 6 kV, > 3 kA), a modified GTO structure, called a gate commutated thyristor (GCT), has been designed and manufactured that commutates all of the cathode current away from the cathode region and diverts it out the gate contact. The GCT is similar to a GTO in structure except that it has a low-loss n-buffer region between the n-base and p-emitter; see Fig.1.14. Development in gate-controlled thyristor (GCT) may effectively end the future of GTO.

The Advantages and Disadvantages of GTO are:

Advantages of the GTO include:

1. High current-voltage capability.
2. Low conduction loss.
3. Low cost.

Disadvantages

1. Non-uniform turn-off and *dv*/*dt* snubber required.
2. Non-uniform turn-on *di*/*dt* snubber required.
3. Current control-high gating power.
4. Long switching time-long storage time, minimum on-time and off-time requirements.
5. No current limitation capability.

1.4.5 Power Transistors

There are many different types of Power Transistor include MOSFETs ranging from 500V to 1500V, silicon carbide (SiC) MOSFETs featuring the industry's highest temperature rating of 200 °C, IGBTs with breakdown voltages ranging from 350 V to 1300 V and a wide range of power bipolar transistors. These devices can be turned "ON" and "OFF" by relatively very small control signals, operated in SATURATION and CUT-OFF modes only. No "linear region" operation is allowed due to excessive power loss.

1.4.5.1 Bipolar Junction Transistor (BJT)

Power bipolar junction transistors (BJTs) play a vital role in power circuits. Like most other power devices, power transistors are generally constructed using silicon. The use of silicon allows operation of a BJT at higher currents and junction temperatures, which leads to the use of power transistors in a.c. applications where ranges of up to several hundred kilowatts are essential.

The power transistor is part of a family of three-layer devices. The three layers or terminals of a transistor are the base, the collector, and the emitter. Effectively, the transistor is equivalent to having two *pn*-diode junctions stacked in opposite directions to each other. The two types of a transistor are termed *npn* and *pnp*. The *npn*-type transistor has a higher current-to-voltage rating than the *pnp* and is preferred for most power conversion applications. Fig.1.15 shows the symbol of a BJT *npn*-type transistor and its V-I characteristics.

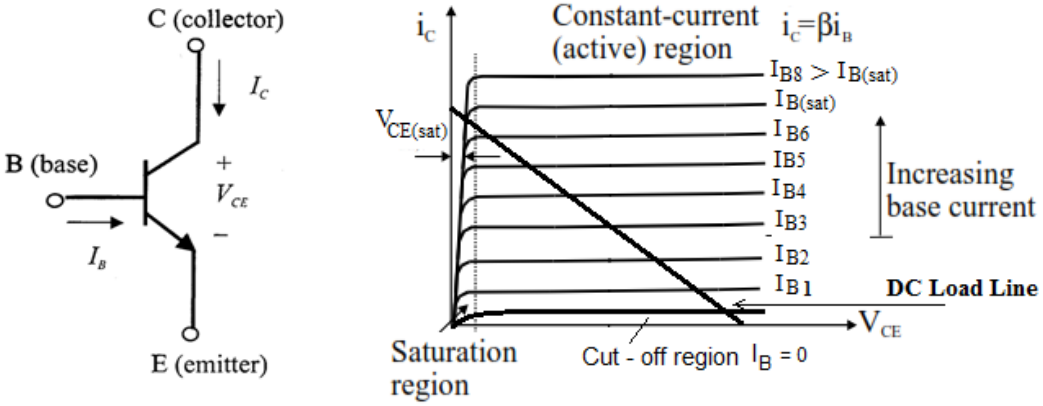

(a) BJT : Symbol (npn) (b) V-I Characteristics

Fig.1.15 BJT power transistor.

With zero base current the transistor behaves like an open switch. With high base current the device saturates and switches into conduction with a low forward voltage drop. Hence, to turn on /off the device, a base drive circuit is connected to the base and emitter terminal. To turn on, current is injected into the base terminal. When turned on, conventional current passes from collector to emitter; current is injected into the base terminal. To turn-off, the base current is removed (made zero value). The current gain β of a BJT ends to be low when operated in the saturated ON condition, $\beta < 10$ is common. It deteriorates as voltage ratings increases.

Safe Operating Area (SOA) of BJT

The safe operating area (SOA) is defined as the voltage and current conditions over which the transistor or any power semiconductor switch can be expected to operate without self-damage. This characteristic is also called the dynamic breakdown characteristics.

The dynamic behavior of a power transistor is bounded by three main parameters:

FBSOA: Forward Bias Safe Operating Area

RBSOA: Reverse Bias Safe Operating Area

BVsus: Breakdown Sustaining

The designer of a given application must carefully check that, under no circumstances, the transistor will operate out of the curves provided in the data sheet: severe damage, or destruction, occurs if the operating point moves outside the specified limits.

The data provided for the FBSOA curve are based on a maximum junction temperature, and is bounded by four points as shown in Fig.1.16:

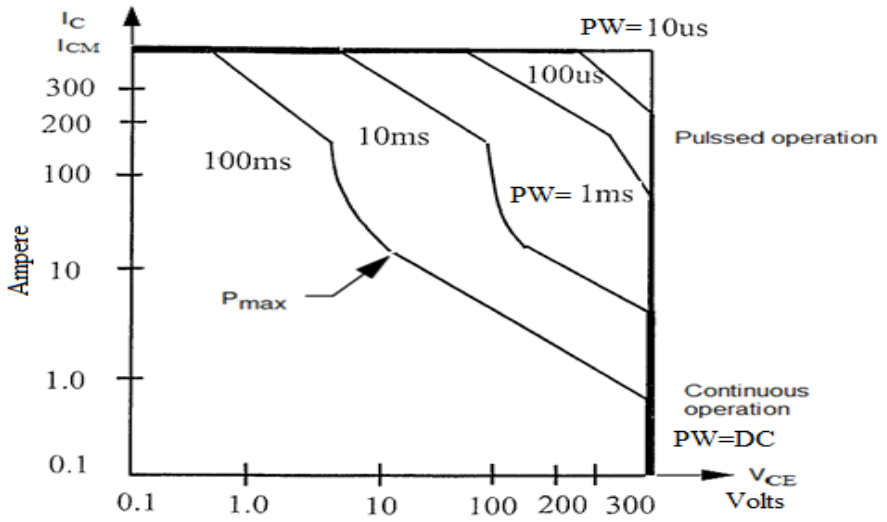

Fig.1.16 Forward biased SOA as the voltage and current.

BV_{CEO} : maximum collector to emitter voltage when base is open circuited
I_{CM} : maximum allowable collector current
P_m : maximum power dissipation
PW: pulse width

RBSOA

The *RBSOA* curves are used to define the maximum current /voltage a transistor can sustain under Base-Emitter reverse bias. These characteristics can be found by special test circuit and depicted in Fig.1.17. The *RBSOA* parameter is essentially an analysis of the breakdown, under dynamic condition, when the device is loaded by an inductor. The *RBSOA* is usually larger than *FBSOA* because of BV_{CBO} at low collector current.

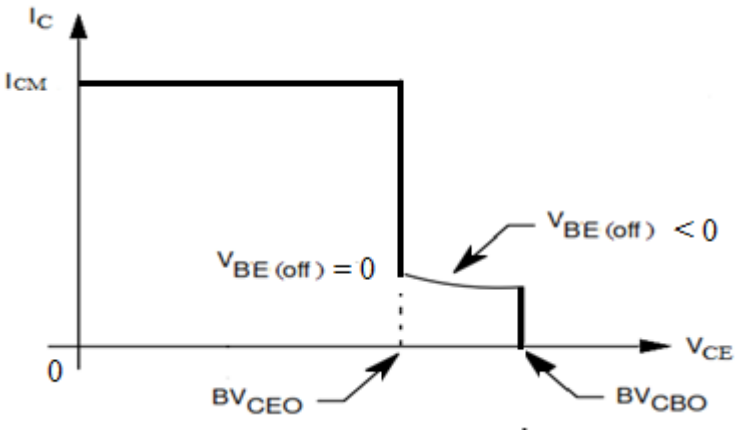

Fig.1.17 The RBSOA of a BJT.

Ratings, Merits and Demerit of BJT

i. Ratings: Voltage V_{CE} < 1600 V, Current I_C < 1000 A.
ii. BJT has small turn-on and turn-off times, hence its switching frequency is higher, up to 5 kHz.
iii. Low on-state voltage V_{CE}: 2-3 V, hence low on-state loss.
iv. Low current gain (β): Need high base current to obtain reasonable I_C.
v. BJT does not require commutation circuits. It is a bipolar device.
vi. The base drive circuit of the BJT is relatively expensive and complex.

1.4.5.2 Metal Oxide Semiconductor Field Effect Transistors "MOSFETs"

Unlike the bipolar junction transistor (BJT) which uses both types of carriers in conduction , the MOSFET device is a unipolar device , because it uses only one type of the majority carriers in conduction (either holes or electrons). The development of metaloxide-semiconductor (MOS) technology for microelectronic circuits opened the way for development of the power metal oxide semiconductor field effect transistor (MOSFET) device in the early 1970s. Since its invention, it has gone through several evolutionary steps. Now days, power MOSFETs are commonly used as switches in power electronics applications.

The invention of the power MOSFET was partly driven by the limitations of bipolar power transistors which, until recently, were the devices of choice in power electronics applications. Although it is not possible to define absolutely the operating boundaries of a power device, we will loosely refer to the power device as any device that is capable of switching at least 1A. The bipolar power transistor is a current-controlled device and a large base drive current as high as one fifth of the collector current is required to keep the device in the on state.

Also, higher reverse base drive currents are required to obtain fast turn-off. Despite the very advanced state of manufacturability and lower costs of bipolar power transistors, these limitations have made the base drive circuit design more complicated and hence more expensive. There are two further limitations to the bipolar power transistor. First, both electrons and holes contribute to conduction in BJTs. Presence of holes with their higher carrier lifetime causes the switching speed to be several orders of magnitude slower than for a power MOSFET of similar size and voltage rating. Secondly, the BJTs suffer from thermal runaway.

The forward voltage drop of a BJT decreases with increasing temperature causing diversion of current to a single device when several devices are paralleled. Power MOSFETs, on the other hand, are majority carrier devices with no minority carrier injection. They are superior to the BJTs in high-frequency applications where switching power losses are impor-

tant and can withstand simultaneous application of high current and voltage without undergoing destructive failure due to second breakdown. Power MOSFETs can also be paralleled easily since the forward voltage drop increases with increasing temperature, ensuring an even distribution of current among all components. However, at high breakdown voltages (>>200V) the on-state voltage drop of the power MOSFET becomes higher than that of a similar size bipolar device with a similar voltage rating, making it more attractive to use the bipolar power transistor at the expense of worse high-frequency performance.

Fig.1.18 shows the present current-voltage limitations of power MOSFETs and BJTs. New materials, structures and processing techniques are expected to push these limits out over time. A relatively new device

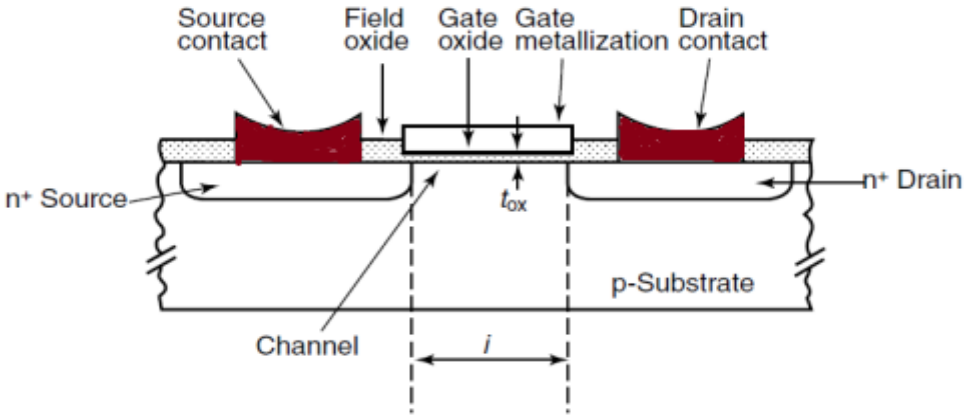

Fig.1.18 Power MOSFET structure.

which combines the high-frequency advantages of the MOSFET with the low on-state voltage drop of high voltage BJTs is the insulated-gate-bipolar transistor (IGBT). The power MOSFETs are also three terminals switches as shown in Fig.1.19 constructed either with electrons as the majority carriers (n-channel type) or with holes as the majority carriers (p-channel type).

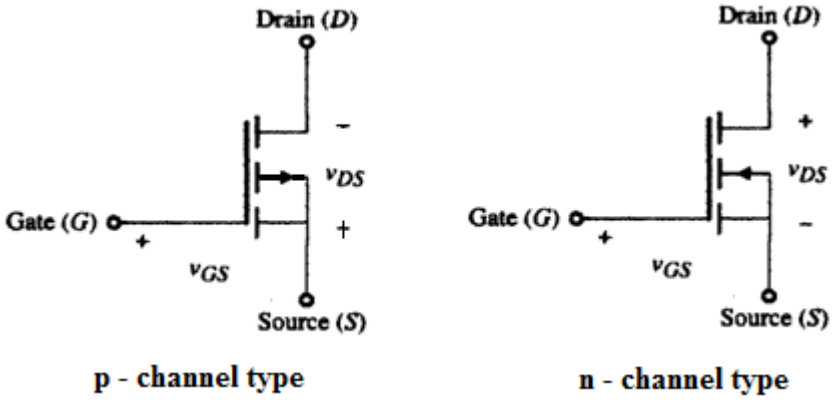

(a) (b)

Fig.1.19 Power MOSFET symbol (a) p-channel , and (b) n-channel.

MOSFET is considered the fastest power switching device (200 kHz) for rating voltages < 500 V, current I_{DS} < 300 A, or 100 kHz, < 1500 V, 300 A.

MOSFET characteristics

- Turning on and off is very simple. Only need to provide V_{GS} = +15V to turn on and 0.0 V to turn off. Gate drive circuit is simple.
- Basically low voltage device. High voltage device are available up to 600 V but with limited current. Can be paralleled quite easily for higher current capability.
- Dominant in high frequency application (>100 kHz). Biggest application is in switched-mode power supplies.
- On-state loss relatively high, V_{DS} > 3 V.

Practically, MOSFET's characteristic consists of three regions, as shown in Fig.1.20 :

- Cut OFF region (OFF state) when $V_{GS} < V_{Th.}$
- Linear region when $V_{DS} < V_{GS} - V_{Th}$, and
- Active region when $V_{DS} > V_{GS} - V_{Th}$.

Ideally, MOSFETs are represented by a short-circuit when operating within the ON state and as an open-circuit when operating within the OFF state.

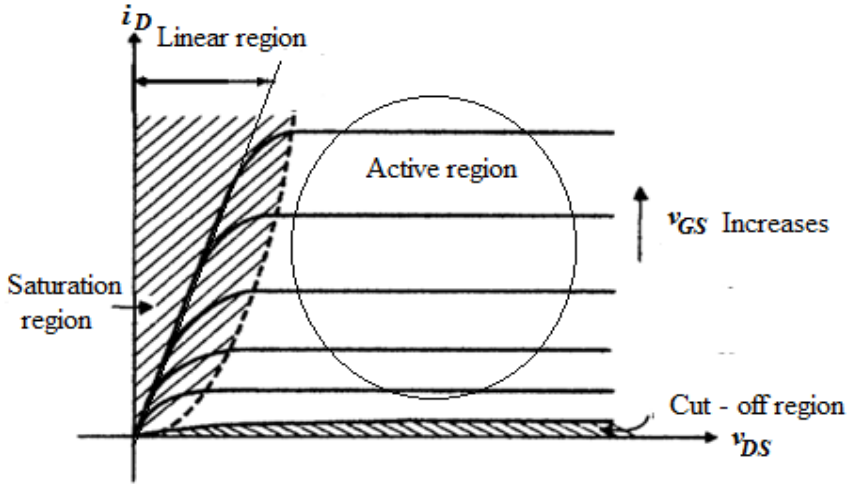

Fig.1.20 Power MOSFET characteristics.

A new power device called COOLMOS is now available which is an improvement of the conventional MOSFET. It is capable of handling 2 to 3 times output power compared with that of a standard MOSFET and its conduction losses are less by a factor of five.

1.4.5.3 Insulated Gate Bipolar Transistor "IGBT"

When the development of power MOSFETs encountered difficulty in increasing their current-handling capability, the idea of a MOS-controlled bipolar device was developed to overcome the problem. This effort led to today's insulated gate bipolar transistor (IGBT). This device, which is also a three terminal switch, combines the high-frequency advantages of the MOSFET with the low on-state voltage drop of high voltage BJTs. Its operation modes and characteristics are almost similar to those for MOSFETs, except for the operating ranges. The IGBT symbol and characteristics are shown in Fig.1.21.

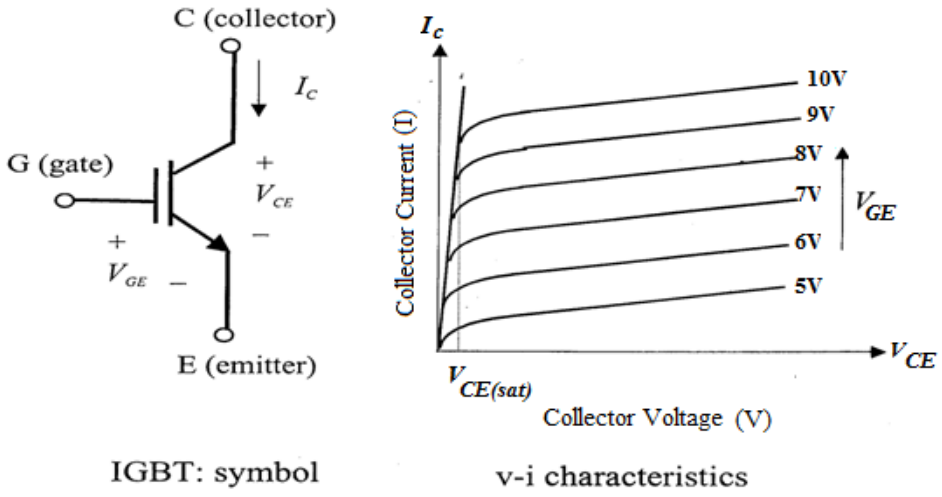

Fig.1.21 The IGBT power transistor.

The IGBT fundamentally changes the BJT current control into voltage control while maintaining the advantages of the BJT. In addition, the use of a wide-base *pnp* transistor in the IGBT structure results in a much improved conductivity modulation effect than a conventional BJT, pushing the voltage rating of the IGBT toward the level of GTOs. The internal *pnp* structure also does not have the second breakdown problem as a conventional *npn* structure because the high voltage is supported by the base region of the *pnp* transistor instead of by the collector region as is the case for a conventional *npn* transistor. IGBTs also have excellent RBSOA and FRSOA. Having undergone several years of development, IGBTs have become the best device for applications in the range of 600 to 3000 V.

The above trend shows that when the power level moves higher, power semiconductor devices limit the maximum system switching frequency, hence the performance of the system, especially at the GTO level. To meet the increasing demand for better performance in high-power systems, many efforts have been made to improve the performance

of high-power semiconductor devices. Among them, one effort is to push the IGBT toward higher power ratings based on the module concept. With its good dynamic performance, high-power systems equipped with IGBTs can operate at a much higher switching frequency and have many benefits compared with a conventional GTO system. The state-of-the-art IGBT rating is currently 3.3 kV/1.2 kA, which is at the low end of that of the GTO.

IGBT Structure and Operation

The name insulated gate bipolar transistor stems from its operation based on an internal interaction between an insulated-gate FET (IGFET) and a bipolar transistor. It has previously been called an IGT (insulated-gate transistor), an IGR (insulated-gate rectifier), a COMFET (conductivity-modulated field effect transistor), a GEMFET (gain-enhanced MOSFET), a BiFET (bipolar FET), and an injector FET. IGBTs have been successfully used since they were first demonstrated in 1982 and are currently the most widely used power semiconductor switches with applications from several kilowatts to a few megawatts. A cross section of the planar junction-based IGBT structure introduced in the 1980s is shown in Fig. 1.22.

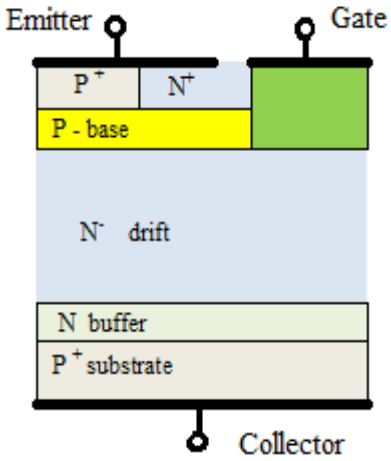

Fig.1.22 IGBT structure.

The IGBT structure is similar to that of a planar power MOSFET except the difference in the substrate doping type. The fabrication of the IGBT therefore is almost the same as a power MOSFET. This makes manufacturing relatively easy immediately after conception, and its ratings have grown at a rapid pace as a result of the ability to scale up both the current and the blocking voltage ratings. IGBT has a combination of BJT and MOSFET characteristics, compromises include:

i. Gate behavior similar to MOSFET - easy to turn on and off.
ii. Low losses like BJT due to low on-state Collector-Emitter voltage V_{CE} (2-3 V).

iii. Ratings: Voltage V_{CE} < 6000 V, Current 2500A currently available.
iv. Good switching capability (up to 100 kHz) for newer devices.
v. Typical application, IGBT is used at 20-50 kHz.
vi. For very high power devices and applications, frequency is limited to several kHz .
vii. Very popular in new products; practically replacing BJT in most new applications.
viii. "Snubberless" operation is possible. Most new IGBTs do not require snubber.

1.4.5.4 MOS-Controlled Thyristor (MCT Thyristor)

An effort to combine the advantages of bipolar junction and field-effect structures has resulted in hybrid devices:

- The IGBT is an improvement over a BJT.
- The MCT is an improvement over a thyristor.

The IGBT power transistor has been discussed in the previous sub-section. In this section, the MOS-controlled thyristor MCT will be discussed and investigated.

MCT can be switched on or off by negative or positive gate voltage, respectively. It has fast turn-on and then off times, with high-speed switching capability, low conduction losses, low switching losses, and high current density. The gating requirements of an MCT are easier than those of the GTO since it needs smaller gate turn-off current due to its high gate input impedance. Compared with the power MOSFET, it has higher current density and lower forward drop. It has great potential in high-power, high-voltage applications. A peak power of 1 MW can be switched off in 2 *ns* by a single MCT. Therefore, the MCT overcomes several of the limitations of the existing power devices and promises to be a better switch for the future. The MCT symbol and equivalent circuit are shown in Fig.1.23. The MCT characteristics are shown in Fig.1.24.

MCT Working Principle

The P-MOS helps turn on the MCT. To it turn on, it needs:

- Forward bias.
- Applying a negative pulse to its gate with respect to the anode.
- The regenerative action within $Q_1$and Q_2 turns the MCT on into full conduction within a very short time and maintains it even after the gate pulse is removed.

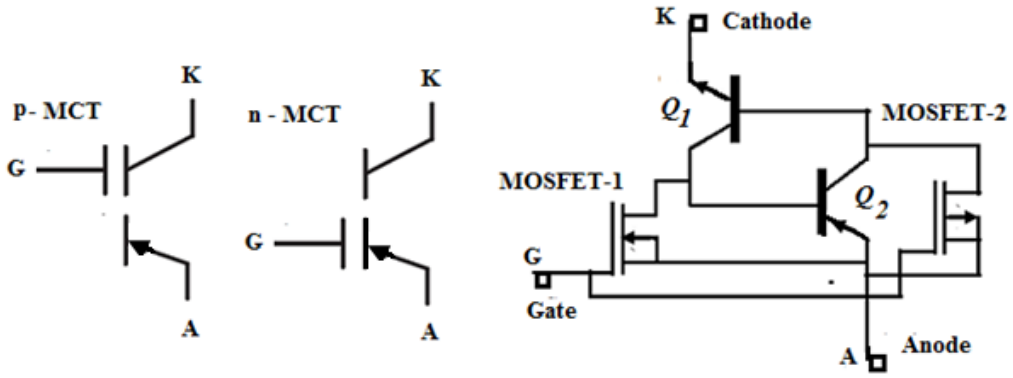

(a) Symbol (b) Equivalent circuit

Fig.1.23 The MCT (a) Symbol and, (b) Equivalent circuit.

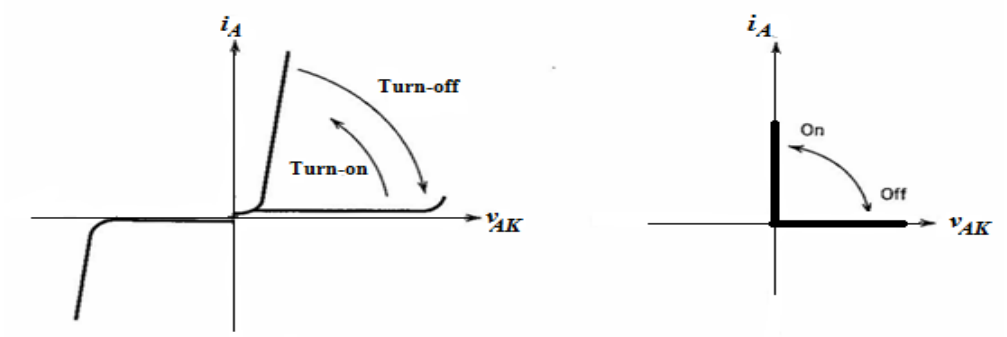

(a) (b)

Fig.1.24 MCT characteristics : (a) MCT *v-i* characteristic,
(b) idealized characteristic.

MCT will remain in the on-state until the device current is reversed or a turn-off pulse is applied to its gate. With a positive pulse the n-MOS helps turn the MCT off by diverting Q_2 current and breaking the latching action of the SCR. The highest current that can be turned off with the application of a gate bias is called the "maximum controllable current". The MCT can be gate controlled if the device current is less than the maximum controllable current.

For small currents rating device, the width of the off pulse doesn't matter. For high currents rating device, the width of the off pulse is critical and probably it should take the entire off time of the switch. The on-state resistance of an MCT is slightly higher than that of an equivalent thyristor.

1.5 OTHER SWITCHING DEVICES

There are several other power switching device available such as: Diac, Static Induction Transistors (SITs), COOLMOS Transistor, Static Induction Thyristors (SITHs) and Gate commutated thyristor (GCT).

1.5.1 Static Induction Transistors (SITs) , and Static Induction Thyristors (SITHs)

The first invention of SIT was in the 1950s where the PIN diode was also invented. This new SIT technology may challenge SCRs, GTOs, MOSFETs, IGBTs, magnetrons and most other power semiconductors. SITs have extremely low forward voltage drop, very fast switching speeds and greater radiation tolerance than most semiconductors. They operate at thousands of volts, hundreds of amperes, frequency up to 10GHz and levels up to one megawatt. It is believed that this new technology will bring revolution in power electronics industry.

The static induction thyristor (SITH) acts like a diode, in the absence of gate signal, conducting current from anode (A) to cathode (K). Negative gate voltage turns the switch off and must be maintained to give reverse voltage blocking. The SITH is similar to the GTO in performance with higher switching speed but lower power rating.

1.5.2 Gate Commutated Thyristor (GCT Thyristor)

The GCT thyristor is designed to obtain a very low parasitic inductance and its package is integrated with a specially designed gate-drive circuit. The specially designed gate drive circuit allows the GCT to be operated without a snubber circuit and switch with higher anode di /dt, than a similar GTO. At blocking voltages of 4.5 kV and higher the GCT seems to provide better performance than a conventional GTO. The speed at which the cathode current is diverted to the gate (*di/dt*) is directly related to the peak snubberless turn-off capability of the GCT. The gate drive circuit can sink current for turn-off at *di/dt* values of 7000 A/ms. This hard gate drive results in a low charge storage time of ≈1 ms. Low storage time and fail-short mode make the GCT attractive for high-voltage series applications.

1.6 WIDE BAND GAP SEMICONDUCTOR DEVICES FOR POWER ELECTRONICS

Nowadays , a real breakthrough in the Power Electronics field may come from the development and use of Wide Band Gap (WBG) semiconductor devices. WBG semiconductors such as silicon carbide (SiC) and gallium nitrite (GaN) and diamond show superior material properties, which allow operation at high-switching speed, high-voltage and high-temperature. These unique performances provide a qualitative

change in their application to energy processing with increased the conversion efficiency.

Table 1.1 summarizes the main material parameters of WBG semi-conductors devices to replace Si in the next generation of power swithes. GaN and especially SiC process technologies are more mature and, therefore, more attractive especially for high power and high temperature electronics (HTE).

Although GaN can offer better high-frequency and high-voltage performances and presents a lower thermal conductivity than SiC, but at present, SiC is considered to have the best trade-off between properties and commercial maturity with considerable potential for both HTE and high power devices. However, the industrial interest for GaN power devices is increasing recently.

Table 1.1. Physical properties of **WBG** for power devices.

Material	**E_g(eV) at 33K**	**μ_n (cm^2/Vs)**	**μ_p (cm^2/Vs)**	**V_{sat} (cm/s)**	**E_c (cm/s)**	**λ (W/cm.^{o}K)**	**ε**
Si	1.2	1450	450	10^7	$3x10^5$	1.3	11.3
4H-SiC	3.3	950	115	$2x10^7$	$3x10^6$	5	10
GaN	3.39	1000	350	$2x10^7$	$5x10^6$	1.3	8.9
Diamond	5.6	2200	1800	$3x10^7$	$5x10^7$	20	5.7

Characteristics of Silicon Carbide Semiconductors

Silicon carbide is naturally occurring in very small quantities because it is only found in meteorites or corundum deposits. It was first identified in its natural state by Dr.Ferdinand Henri Moissan in 1893 as a small component of the Canyon Diablo meteorite in Arizona-USA. Many of silicon carbide's advantages are due to its much larger band gap. SiC has a band gap of 3.3 eV as compared to silicon's band gap of 1.2 eV as given in Table 1.1. By having a band gap three times higher than silicon, SiC material properties are better suited for power semiconductor switches. One such parameter is the critical electric field; this parameter dictates how much electric field a junction can support before avalanche breakdown occurs. SiC's critical electric field is approximately 8 times higher than silicon. This results in much thinner devices for a given operating voltage eading to smaller resistive losses in SiC switches.

Silicon carbide also has a much lower intrinsic carrier concentration (~10-8 cm^3) than silicon (~1012 cm^3) at 300 K. The biggest implication this has on device performance is that is controls the maximum operating temperature. For silicon this results in a maximum temperature of

approximately 450 K (150˚C). For SiC the resulting maximum operating temperature can be as high as 900 K. So, not only are SiC devices generally more efficient than their silicon counterparts but they also operate reliably at lower efficiencies. This simplifies many of design requirements on power electronics systems making these switches easier to implement into industry. There are many emerging markets that can benefit from the advantages presented by silicon carbide based power electronic systems. For example, green energy initiatives such as solar power generation and wind power generation can benefit from the higher efficiency offered by SiC based inverters that are used to tie these systems to the electric grid. Hybrid electric vehicles benefit greatly by the higher operating temperatures and power densities that silicon carbide offers for the dc-dc converters used to distribute energy to and from the motors.

The use of silicon carbide as a raw material for power semiconductor switches is a relatively new technology in terms of semiconductor research. It was not until the early 90's that it became aviable alternative to silicon and significant investment into the technology started to occur.
The silicon carbide is a compound of silicon and carbon with chemical formula SiC. It is a semiconductor, which can be doped n-type by nitrogen or phosphorus and p-type by beryllium, boron, aluminum, or gallium. Metallic conductivity has been achieved by heavy doping with boron, aluminum or nitrogen. SiC is used in semiconductor electronics devices that operate at high temperatures or high voltages, or both.

Compared to Si, the silicon carbide has a bandgap almost three times wider than Si, meaning that the electrons need higher activation energy to jump to the conduction band. As a result, SiC junctions can operate at higher temperature, without any unwanted conduction.

Another advantage is that its electric breakdown field is almost ten times higher than silicon's, so either it can withstand much higher electric field, or we can make the transistor thinner. By making it thinner we achieve much better switching characteristics, as turn-on and turn-off times are smaller, thus having lower switching losses over the transistors.
In power electronics, SiC based power electronic devices have significant advantages over silicon (Si) in capabilities. They operate at much higher frequencies and temperatures and convert electric power at higher efficiency or lower losses. Additionally, SiC-based devices manage the same level of power as Si devices at half the size, which will enable dramatic increases in power density and reliability.

The first devices available were Schottky diodes, and MOSFETs. MOSFET and SiC Schottky diodes can be superior to a traditional all-silicon system. SiC devices allow power circuits to operate at higher switching speeds, which reduce the cost of magnetic components as well as system size and weight. In addition, thermal management consider-ations such as heat sinking and cooling are less stringent, because these

systems are more thermally efficient. SiC MOSFETs in an n-channel configuration rated higher than 1200 V, is available now in the markets and for high-power switching, bipolar transistors and thyristors are currently developed.

SiC features can be summarised as :

i. Extremely low switching losses.
ii. Zero reverse recovery charge-improves system efficiency (High Power Density).
iii. Smaller footprint device reduces system size and weight. High thermal conductivity and high thermal staibility.
iv. 2.5 × more thermally conductive than silicon.
v. Reduced sink requirements results in lower cost and smaller size.
vi. High temperature operation.
vii. Increased power density and improved reliability.
viii. High breakdown electric field strength (about ×10 of Si),
ix. Wide bandgap.

1.7 SWITCHING LOSSES IN A POWER SWITCH

When a power switch is switched on, voltage and current are switched instantaneously in the ideal switch as shown in Fig.1.25 (a). The ideal switch requires zero transition time, hence the voltage across it will fall to zero and the current through it will raise to its maximum value *I* depending on the load.

In real switch, due to the non-idealities of power switches, the switching profile is as shown in Fig.1.25(b). The switching losses occur as a result of both the voltage and current changing simultaneously during the switching period.

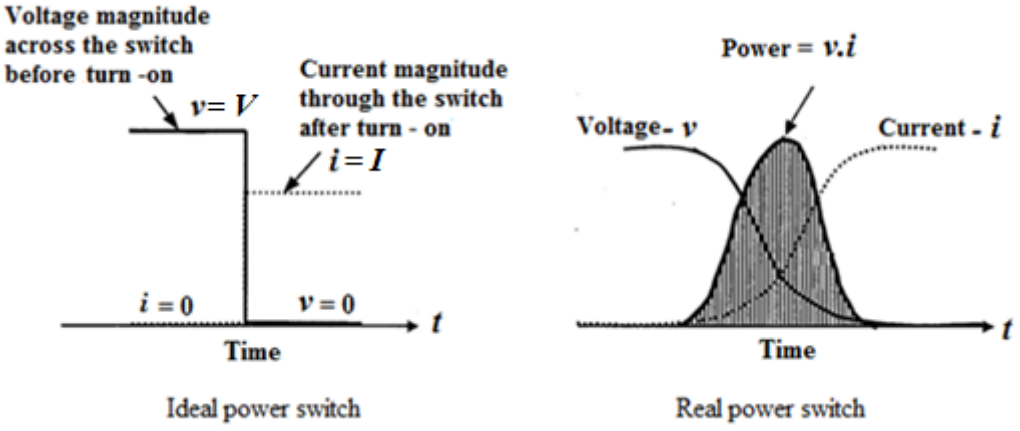

(a) (b)

Fig.1.25 Transition of voltage and current in a power switch during turn-on: (a) Ideal switching profile, (b) Real switching profile.

The product of device voltage and current gives instantaneous power dissipated in the device. The heat energy that developed over the switching period is the integration (summation) of instantaneous power over time as shown by the shaded area under the power curve (Fig.1.25(b). The average power loss is the sum of the turn-on and turn-off energies multiplied by the switching frequency. When frequency increases, switching losses increases. This limits the usable range of power switches unless proper heat removal mechanism is employed.

1.8 SUMMARY OF POWER SEMICONDUCTOR DEVICE CAPABILITIES

Although there are a number of other devices that have been developed or are being developed, the workhorse power semiconductor devices today are SCRs, GTOs, MOSFETs, and IGBTs. Each of these devices dominates a specialized power arena. The MOSFET has excellent dynamic and static performance. It dominates low voltage applications below 600 V. The IGBT is slower than the MOSFET but has better forward voltage drop above 600 V. It dominates applications from 600 to 3000 V. At an even higher voltage level, the GTO becomes the dominant device with better current-carrying capability but much slower dynamic response. Without turn-off capability, the SCR has an even better current conduction capability, so it is suitable for even higher power a.c. applications where gate-controlled turn-off capability is not necessary. For a typical application, the switching frequency is an important index in determining system performance. Generally, the higher the switching frequency, the better the dynamic performance of the system, the smaller the size of the system due to reduced passive components and the lower the cost of the system due to savings on passive components. The practical switching frequency of an application system is a trade-off of many issues including maximum device switching frequency, maximum magnetic switching frequency, switching losses of the power switches, overall system efficiency, etc. In the low power field where the MOSFET plays the major role, the switching frequency is normally subject to system efficiency and /or magnetic considerations instead of device limitations. In the medium power field, where the IGBT plays the major role, the situation changes.

At the lower end, the limitation of the device does not dominate since the lower-rating IGBT is normally fast enough. However, when the power rating is higher, the IGBT switching speed decreases and the switching losses increase significantly. The practical switching frequency is thus subject to the limitation of the device. When the power level moves even higher, the GTO is the only available device. Since it has several tens of microseconds switching time, significant turn-off, and dv/dt snubber loss, the GTO is traditionally the limitation of the switching frequency of

the system. Fig.1.26 gives a summary of power semiconductor device capabilities for clarity.

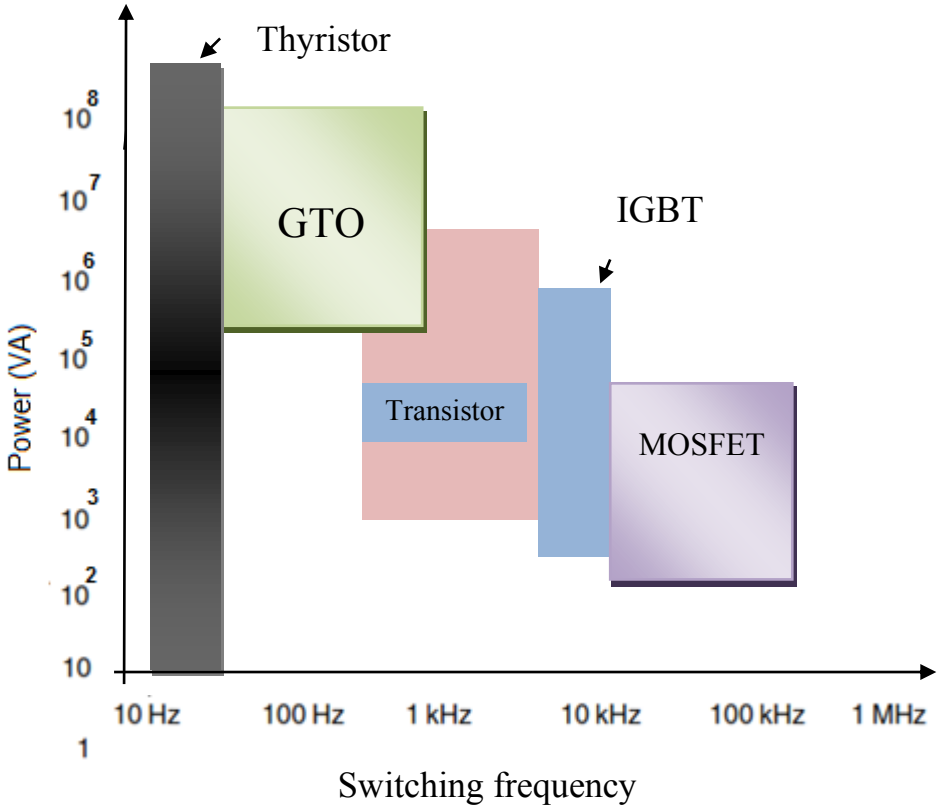

Fig.1.26 Summary of power semiconductor device capabilities.

.

REVIEW QUESTIONS AND PROBLEMS

1.1 Explain the terms latching current and holding current in a thyristor device.

1.2 What are the conditions that must be satisfied to make a thyristor be on?

1.3 Why does a thyristor have a $(di/dt)_{max}$ rating ?

1.4 Explain the principle of turning off a thyristor in a d.c. circuit, why we need force commutation circuit to achieve turn off ? How the forced turn-off of an SCR is different from natural turn-off.

1.5 Give the broad classification of power semiconductor devices.

1.6 What are the types of power diodes?
1.7 Why the current in power diodes varies linearly rather than exponentially with voltage.
1.8 Describe, with the aid of a sectional diagram, the construction of a triac. Draw an equivalent circuit of the device and explain why force commutation cannot be applied to triac ?
1.9 Compare the relative advantages of triacs and thyristors and hence give two examples of application: one in which a triac is particularly suitable and the other where silicon controlled rectifier type of thyristor is preferable. Give the reasons for your selection.
1.10 What is GTO ? How GTO can be turned on and turned off ?
1.11 Give the merits and demerits of GTO, as compared to conventional SCR.
1.12 Sketch typical static characteristics of a gate turn-off device and explain briefly how can this device turned on and off from its gate.
1.13 What are the types of power transistors ?
1.14 What are the advantages of MCT ?
1.15 What is an IGBT ? Sketch the symbol and characteristics of an IGBT Discuss its advantages and disadvantages.
1.16 Compare IGBT with the power MOSFET and give the applications of IGBTs.
1.17 What are the advantages of power bipolar transistors over FETs and thyristors for use in inverter circuits for power applications ? What are the factors limit their usage?

Are the following statements True or False?

1.18 Thyristors are used only for low voltage, low current applications.
1.19 MOSFETs are used for high frequency applications.
1.20 BJT is more efficient than IGBT in high power applications.
1.21 GTO requires very low current applied to its gate to be turn off.
1.22 IGBT is a voltage driven device.
1.23 Thyristors are preferred to be used in the output stage of 10W 1MHz transmitter.
1.24 MOSFETs are preferred to be used for 1000 kW motor control circuit.
1.25 TRIAC is used for lighting dimmer circuits.
1.26 IGBT used in high voltage d.c. rectifier circuits (above 5 kV level).
1.27 BJT is the fastest switching device in power applications.

Choose the correct answer for the following questions:

1.28 The conditions which must be satisfied to turn on the thyristor with its current is more than its latching current are:

(a) The anode is more positive than the cathode and a positive current pulse is applied to the gate.
(b) The anode is more negative than the cathode and a positive current pulse is applied to the gate.
(c) The cathode is more positive than the anode and a negative current pulse is applied to the gate.
(d) The cathode is more negative than the cathode and a negative current pulse is applied to the gate.

1.29 The latching and holding currents are terms applicable to:

(a) Thyristor (b) BJT (c) IGBT (d) MOSFET

1.30 For a certain applications of power supply a power semiconductor switch is required to operate with 3000 V, 2000 A load and switching frequency of 30 kHz. The power switching device suitable for this task is:

(a) Thyristor (b) Diode (c) IGBT (d) MOSFET

1.31 A thyristor (SCR) has a latching current of 100 mA is connected between a d.c. source of 200 V and a purely inductive load of L= 0.2 H. The minimum width of the gate pulse current required to turn on this SCR is:

(a) 50 ms (b) 50 µs (c) 100 µs (d) 40ms (e) 60 µs

1.32 For certain applications of power supply a power semiconductor switch is required to operate with 400 V, 200 A load and switching frequency of 100 kHz. The power switching device suitable for this task is:

(a) GTO (b) IGBT (c) MOSFT (d) BJT (e) Triac

[Ans: 1.18 **F**, 1.19 **T**, 1.20 **F**, 1.21 **F**, 1.22 **T**, 1.23 **F**, 1.24 **F**, 1.25 **T**, 1.26 **F**, 1.27 **F**, 1.28 **(a)**, 1.29 **(a)** , 1.30 **(c)** , 1.31 **(c)** , 1.32 **(c)]**

CHAPTER TWO

AC-DC CONVERSION: UNCONTROLED RECTIFICATIONS

2.1 INTRODUCTION TO BASIC RECTIFIER CIRCUITS

Several types of rectifier circuits are available: Single-phase and three-phase, half-wave and full-wave, controlled and uncontrolled, etc. For a given application, the type used is determined by the requirements of that application. In general the types of rectifiers are:

1. Uncontrolled Rectifiers : Provide a fixed d.c. output voltage for a given a.c. supply where diodes are used only.

2. Controlled Rectifiers : Provide an adjustable d.c. output voltage by controlling the phase at which the devices are turned on, where thyristors and diodes are used. These are of two types:

   (a) Half-controlled : Allows electrical power flow from a.c. to d.c. (i.e. rectification only) .
   (b) Fully-controlled : Allows power flow in both directions (i.e. rectification and inversion).

There are many applications for rectifiers. Some of them are:

» Variable speed d.c. drives,
» Battery chargers,
» DC power supplies for electric railways and,
» Power supply for a specific application like electroplating.

The power rating of a single-phase rectifier tends to be lower than 10 kW, whereas the three-phase bridge rectifiers are used for delivering higher power output, up to 500 kW at 500 V d.c. or even more.

In study of the rectifier circuits; there are certain electrical properties of interest that should be taken into consideration. These are the properties on the supply side and the properties on the load side of the rectifier respectively. The supply-side will be assumed to have zero impedance such that the sinusoidal supply voltages remains undistorted even when the rectifier current pulses drawn from the supply are nonsinusoidal.

Basically the study of rectifier circuit is concentrated on study of waveforms as well as circuit analysis with the assumptions that:

(1) No energy is stored within a rectifier.
(2) The forward vo1tge drop, and reverse and forward leakage currents in diodes and thyristors are neglected.
(3)The pulse is of sufficient amplitude to switch on the appropriate thyristor.

Although the controlled rectification is the most important type that is mainly used in many industrial applications, it is of interesting to demonstrate first the uncontrolled diode rectifiers to clarify the presentation. Hence, the single-phase and poly-phase, half-wave and full -wave uncontrolled rectifiers loaded with different types of load will be discussed in the following sections.

2.2 UNCONTROLLED RECTIFICATIONS

In this type of rectifier, the produced d.c. output power is fixed with the converter used. They usually employ diodes as their power switches. The following subsections deal with the basic operation of some examples of uncontrolled rectifiers single-phase half-wave rectifier loaded with resistive and series resistive inductive loads.

2.2.1 Single-Phase Half-Wave Uncontrolled Rectifier with Resistive Load

Fig.2.1 shows the basic circuit for a single-phase, half-wave uncontrolled rectifier supplying a resistive load. The circuit is supplied by a single-phase transformer whose secondary represents the rectifier's circuit a.c. source (v_s) that is represented by a sinusoidal wave given by,

$$v_s(\omega t) = V_m sin\omega t \qquad (2.1)$$

where v_s is the instantaneous supply voltage, V_m is the peak value of the supply voltage, $\omega = 2\pi f$ is the angular frequency, and t and is the time.

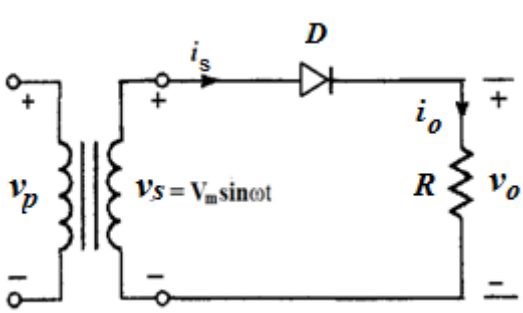

(a)

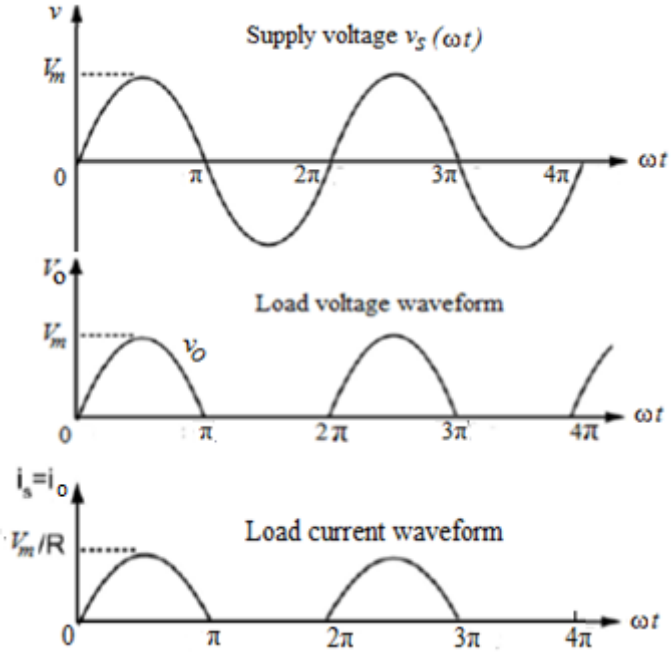

(b)

Fig.2.1 Single-phase half-wave rectifier: (a) Circuit and, (b) Waveforms.

For this configuration, the diode will conducts (becomes forward biased) whenever the supply voltage v_S is positive. This means that, during the positive half cycle, ($0 < \omega t < \pi$), The diode conducts and behaves like a closed switch connecting the supply to the load. Current i_o will flow through the load with value $i_o = v_o / R$ and since the load is resistive, the load current waveform will be replica of the voltage waveform.

The average value of the load voltage V_{dc} can be calculated as follows:

$$V_{dc} = \frac{1}{2\pi}\int_0^{\pi} v_s\,(\omega t)d\omega t \qquad (2.2)$$

$$= \frac{1}{2\pi}\int_0^{\pi} V_m sin\omega t\, d\omega t = \frac{V_m}{2\pi}\,(-cos\pi + cos0^o) = \frac{V_m}{\pi} \qquad (2.3)$$

Since the load is resistive, therefore the load voltage and current are in-phase and they are related by $i_o = v_o / R$. Consequently, the average value of the load current I_{dc} is

$$I_{dc} = \frac{V_{dc}}{R} = \frac{V_m}{\pi R} \qquad (2.4)$$

The output d.c. power is given by:

$$P_{dc} = V_{dc}I_{dc} = \frac{V_{dc}^2}{R} \quad (2.5)$$

The *rms* value of the load voltage V_{orms} can be calculated over one cycle as follows:

$$V_{orms} = \sqrt{\frac{1}{2\pi}\int_0^{\pi} v_s^2\,(\omega t)d\omega t} \quad (2.6)$$

$$= \sqrt{\frac{1}{2\pi}\int_0^{\pi} (V_m sin\omega t)^2\, d\omega t}$$

$$= \sqrt{\frac{(V_m)^2}{2\pi}\int_0^{\pi} \frac{1}{2}(1 - cos2\omega t)d\omega t} = \frac{V_m}{2} \quad (2.7)$$

Since: $(sin\omega t)^2 = \frac{1}{2}(1 - cos2\omega t)$

Therefore, the *rms* value of the load current I_{orms} is :

$$I_{orms} = \frac{V_{orms}}{R} = \frac{V_m}{2R} = \frac{I_m}{2} \quad (2.8)$$

The *rms* value $I_{orms} = I_m/2$ for half-wave operation compared with the corresponding value for pure sinusoidal operation which is $I_{orms} = I_m/\sqrt{2}$.

The output a.c. power is given by:

$$P_{ac} = V_{orms}I_{orms} = \frac{V_{orms}^2}{R} = \frac{(0.5V_m)^2}{R} \quad (2.9)$$

Performance parameters

From the above discussion, the performance of a rectifier can be, therefore, evaluated in terms of the following parameters:

1. The output d.c. power is given by

$$P_{dc} = V_{dc}I_{dc} \quad (2.10)$$

2. The output a.c. power is given by

$$P_{ac} = V_{orms}I_{orms} \quad (2.11)$$

3. The efficiency of the converter is given by

$$\eta = \frac{P_{dc}}{P_{ac}} \tag{2.12}$$

4. Output a.c. component

The output voltage can be considered to have two components: including (i) d.c. value and (ii) the a.c. components or ripple. The *rms* value of the a.c. component of the output voltage is

$$V_{ac} = \sqrt{V_{orms}^2 - V_{dc}^2} \tag{2.13}$$

5. Form Factor, *FF* : It is a measure of the shape of the output voltage.

$$FF = \frac{V_{orms}}{V_{ac}} \tag{2.14}$$

6. Ripple factor, *RF* : It is a measure of the ripple content or the degree of distortion in a rectified voltage waveform which can be calculated as

$$RF = \frac{\text{rms value of the ac components}}{\text{average value}} = \frac{V_{ac}}{V_{dc}}$$

$$= \frac{\sqrt{V_{orms}^2 - V_{dc}^2}}{V_{dc}} \tag{2.15}$$

7. Transformer utilization factor, *TUF* : This is defined as

$$TUF = \frac{P_{dc}}{V_s I_s} \tag{2.16}$$

where

V_s : *rms* voltage of the transformer secondary
I_s : *rms* current of the transformer secondary

8. Displacement Factor, *DF*

$$DF = cos\emptyset \tag{2.17}$$

"Ø" is the phase angle between the fundamental component of the input current and voltage.

9. Harmonic Factor, *HF*

$$HF = \frac{\sqrt{I_s^2 - I_1^2}}{I_1} \tag{2.18}$$

where
I_1 : the fundamental *rms* component of the input current.

10. Power factor *PF* : For rectifier , this is defined as

$$PF = \frac{\text{a. c. output power}}{\text{input volt ampere}} = \frac{P_{ac}}{S_{in}} \tag{2.19}$$

Example 2.1

An ideal single-phase source, 240 V, 50 Hz, supplies power to a load resistor R = 100 Ω via a single ideal diode.

(a) Calculate the average and *rms* values of the load current and the power dissipation.
(b) Calculate the circuit power factor and the ripple factor.
(c) What must be the rating of the diode?

Solution

$$I_{dc} = \frac{V_m}{\pi R} = \frac{240\sqrt{2}}{\pi \times 100} = 1.08\text{A}$$

$$I_{orms} = \frac{V_m}{2R} = \frac{240\sqrt{2}}{2 \times 100} = 1.7\text{A}$$

The average power dissipation in the load resistor R is given by the average a.c. power:

$$P_{ac} = I_{orms}^2 \times R = \left(\frac{V_m}{2R}\right)^2 = \frac{{V_m}^2}{4R^2} = (1.7)^2 \times 100 = 289\text{ W}$$

$$S_{in} = V_s \times I_{orms} = 240 \times 1.7 = 408\text{ W}$$

$$PF = \frac{P_{ac}}{S_{in}} = \frac{289}{408} = 0.708$$

$$RF = \frac{\sqrt{V_{orms}^2 - V_{dc}^2}}{V_{dc}} = \frac{\sqrt{I_{orms}^2 - I_{dc}^2}}{I_{dc}} = \sqrt{(\frac{1.7}{1.08})^2 - 1} = 1.21$$

The value 1.21 for half-wave rectification is large, since the ideal value of the ripple factor should be zero for the output d.c. voltage. The diode must be rated in terms of a peak reverse voltage and a mean forward current.

Diode $PRV = V_m = \sqrt{2} \times 240 = 339.4V \longrightarrow$ Choose 400V diode.

Either the *rms* or the mean (average) current could be use as the basis of current rating: Since I_{orms} = 1.7A choose 2A diode rating.

2.2.2 Single-Phase Half-Wave Uncontrolled Rectifier with *R-L* Load

If the load consists of a series resistor and inductor, the current will flow through the negative cycle as well; Fig.2.2 shows the circuit diagram and Fig.2.3 shows the load voltage and current waveform for this case.

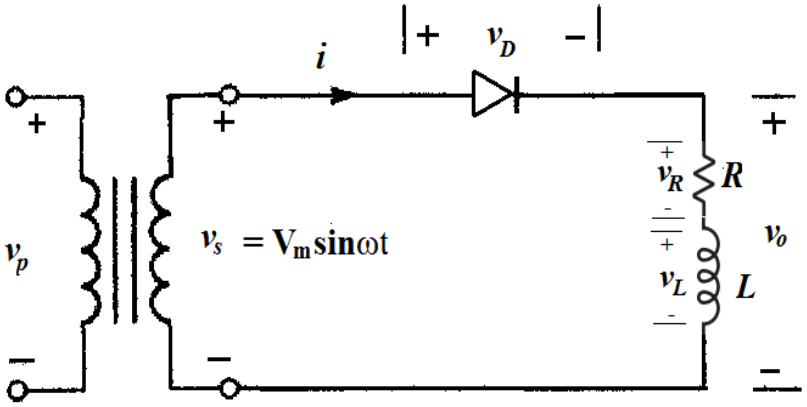

Fig .2.2 Single-phase half-wave rectifier with *R -L* load.

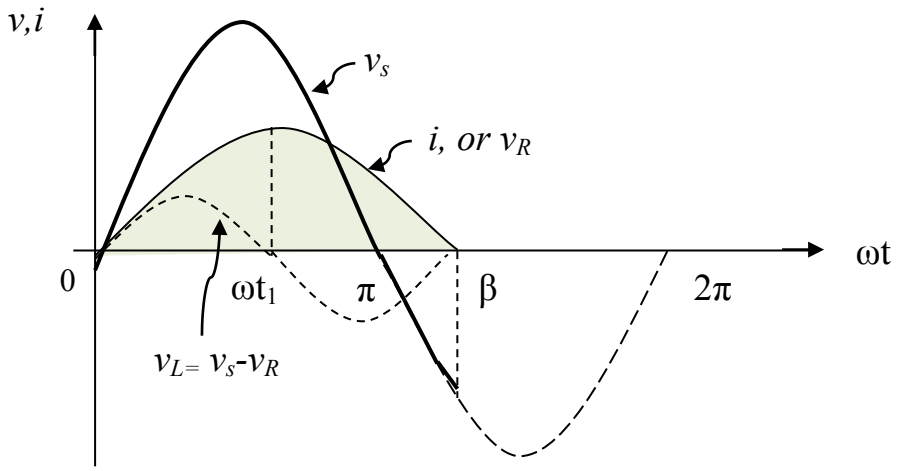

Fig.2.3 Waveforms for the circuit of Fig.2.2.

During conduction period, we have by KVL;

$$v_s = v_o = v_R + v_L$$

$$V_m sin\omega t = i\,R + L\frac{di}{dt} \qquad (2.20)$$

Each supply period (cycle) in Fig.2.3 can be divided into 4-distinct regions:-

- From 0 – ωt_1: The current rises from zero to peak, which lags the voltage peak due to circuit inductance; v_L is positive and the inductor store energy.
- From $\omega t_1 - \pi$: The current decays, and hence v_L is negative. Both source and inductor supply energy to *R*.
- From $\pi - \beta$: The current continues to decay until it reaches zero, v_L remains negative, and hence energy is supplied by the inductor to both source and resistor.
- From β – 2π : At β current reaches zero and the diode cut-out. Current remains zero until the beginning of the next positive half cycle. The average output voltage is

$$V_{dc} = \frac{1}{2\pi}\int_0^{\beta} v_s\,(\omega t)d(\omega t) = \frac{1}{2\pi}\int_0^{\beta} V_m sin\omega t\; d(\omega t)$$

$$V_{dc} = \frac{V_m}{2\pi}\Big[-\cos\omega t\Big\{_0^{\beta}\Big] = \frac{V_m}{2\pi}[-\cos\beta + \cos 0]$$

$$= \frac{V_m}{2\pi}[1 - \cos\beta] \qquad (2.21)$$

The average output current is

$$I_{dc} = \frac{V_m}{2\pi R}[1 - \cos\beta] \qquad (2.22)$$

Equation of the current:
The equation for the current through *R-L* load can be found from the solution of the differential equation (2.20) which can be re-written as:

$$L\frac{di}{dt} + i\,R = V_m sin\omega t \qquad (2.23)$$

This is a first order differential equation. The solution of this equation has two parts:

1- Steady state solution : $i_{ss}(\omega t) = \frac{V_m}{|Z|}\sin(\omega t - \theta)$

2- Transient solution : $i_{tr}(\omega t) = Ae^{-\frac{t}{\tau}}$

where

$$|Z| = \sqrt{R^2 + (\omega L)^2} \quad , \quad \tan\theta = \frac{\omega L}{R}$$

and

$$\tau = \frac{L}{R} = \text{time constant}, \qquad A = \text{constant}$$

The complete solution is : $i(\omega t) = i_{ss}(\omega t) + i_{tr}(\omega t)$

$$i(\omega t) = \frac{V_m}{|Z|}\sin(\omega t - \theta) + Ae^{-\frac{t}{\tau}} \qquad (2.24a)$$

The constant A can be found from initial conditions: when t =0 , $i(\omega t) = 0$:

$$0 = \frac{V_m}{|Z|}\sin(-\theta) + Ae^{-0}$$

$$\therefore A = \frac{V_m}{|Z|}\sin(\theta) \qquad (2.24b)$$

Substitute Eq. (2.24b) into Eq. (2.24a) yields

$$i(\omega t) = \frac{V_m}{|Z|}\sin(\omega t - \theta) + \frac{V_m}{|Z|}\sin(\theta)\, e^{-\frac{t}{\tau}}$$

The final equation of the current is

$$i(\omega t) = \frac{V_m}{\sqrt{R^2 + (\omega L)^2}}[\sin(\omega t - \theta) + sin\theta e^{-cot\theta\,.\omega t}] \qquad (2.25)$$

The current extinction angle β at which the current becomes zero can be determined for a given load impedance angle θ as:
From the final condition of the current, when $\omega t = \beta$, $i = 0$, hence from the above equation (2.25) :

$$0 = \frac{V_m}{\sqrt{R^2 + (\omega L)^2}}[\sin(\beta - \theta) + sin\theta e^{-cot\theta\,.\beta}]$$

$$0 = [\sin(\beta - \theta) + sin\theta e^{-cot\theta\,.\beta}]$$

$$\sin(\beta - \theta) = -\sin\theta e^{-\cot\theta \cdot \beta} \qquad (2.26)$$

This is a transcendental equation which cannot be solved analytically. It can only be solved numerically by iteration technique. The initial guess of β is : $\beta_o = 180^o + \theta + \Delta$, where Δ is few degrees.

Example 2.2

For the half-wave uncontrolled rectifier circuit supplying a series resistive-inductive load shown in Fig.2.2. The supply voltage is $v_s(\omega t) = \sqrt{2} \times 220 \sin\omega t$ and the supply frequency is 50 Hz and the load parameter values are: $R = 5\ \Omega$, and $L = 16$ mH.

(a) Sketch the load voltage and current waveforms for two cycles.
(b) Calculate the current extinction angle β.
(c) Calculate the average value of the d.c. load voltage (V_{dc}) .
(d) Calculate the angle of maximum current (ωt_1) .

Solution

(a) The output voltage and current waveforms are as shown in Fig.2.4.

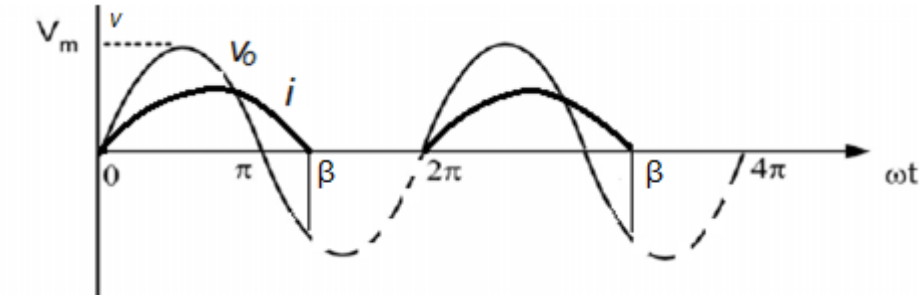

Fig.2.4 Waveforms.

(b) From the final condition of the current, when $= \beta$, $i(\beta) = 0$, hence substitute these values in Eq.(2.25) to find β ,

$$i(\beta) = 0 = \frac{V_m}{\sqrt{R^2 + (\omega L)^2}}[\sin(\beta - \theta) + \sin\theta e^{-\cot\theta \cdot \beta}]$$

$$0 = [\sin(\beta - \theta) + \sin\theta e^{-\cot\theta \cdot \beta}]$$

$$\sin(\beta - \theta) = -\sin\theta e^{-\cot\theta \cdot \beta}$$

The solution of this transcendental equation numerically by iteration technique is as follows:
The initial guess of β is : $\beta_o = 180^o + \theta + \Delta$, where Δ is few degrees.

$\tan\theta = \omega L/R = 2\pi fL/R = (100\pi \times 16 \times 10^{-3})/5 = 1$

hence $\theta = 45^{\circ}$. and therefore : $\beta_o = 180^{\circ} + \theta + \Delta = 180^{\circ} + 45^{\circ} + 0 = 225^{\circ}$ as a starting value for iteration (here choose $\Delta = 0^{\circ}$):

Table 2.1.

Estimated β			
β (degrees)	**β (rad)**	**$\sin(\beta - \theta)$**	**$-\sin\theta\, e^{-\beta}$**
210°	**3.663**	**0.2588**	**- 0.0181**
220°	**3.837**	**0.0870**	**-0.0152**
225°	**3.925**	**0.0000**	**-0.0139**
226°	**3.942**	**-0.013**	**-0.0136**

By intuition : $\beta = 225.8^{\circ}$.

(c)The average DC output voltage is :

$$V_{dc} = \frac{1}{2\pi}\int_0^{\beta} v_s(\omega t)d(\omega t) = \frac{1}{2\pi}\int_0^{\beta} V_m \sin\omega t\, d(\omega t)$$

$$V_{dc} = \frac{V_m}{2\pi}\left[-\cos\omega t\right\{_0^{\beta}] = \frac{V_m}{2\pi}[-\cos\beta + \cos 0^{\circ}]$$

$$= \frac{V_m}{2\pi}[1 - \cos\beta]$$

$$V_{dc} = \frac{\sqrt{2}\times 220}{2\pi}[1 - \cos 225.8] = 84\ \text{V}$$

(d) Angle of maximum current can be found by differentiating Eq.(2.25) and equating to zero , hence

$$\frac{di(\omega t)}{dt} = \frac{V_m}{\sqrt{R^2 + (\omega L)^2}}[\omega\cos(\omega t - 45^{\circ}) - \omega \sin 45^{\circ} e^{-(\cot 45)\,.\omega t}] = 0$$

$$\frac{di(\omega t)}{dt} = [\cos(\omega t - 45^{\circ}) - \sin 45^{\circ} e^{-(\cot 45^{\circ})\,.\omega t}] = 0$$

Maximum current occurs at $\omega t = \omega t_1$ as shown in Fig. 2.5, thus

$$\cos(\omega t_1 - 45^{\circ}) = \sin 45^{\circ} e^{-(\cot 45^{\circ})\,\omega t_1}$$

Solve the above transcendental equation numerically by starting at $\omega t_1 = 110^\circ$, we get the final solution $\omega t_1 = 146^\circ$.

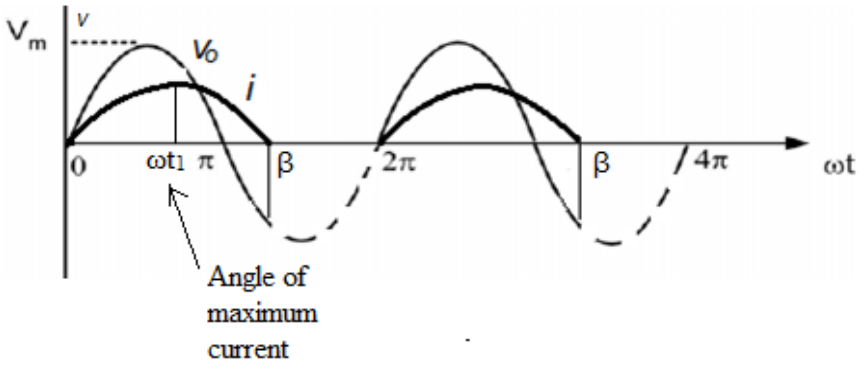

Fig.2.5 Angle of maximum current.

Example 2.3

A circuit is connected as shown in Fig.2.6 to a 240 V, 50 Hz supply. Neglect the diode voltage drop; determine the current waveform, the average load voltage and the average load current of (a) A pure resistor of 10 Ω, (b) An inductance of 0.1 H in series with a 10 Ω resistor. Assume the extinction angle $\beta = 265$ °.

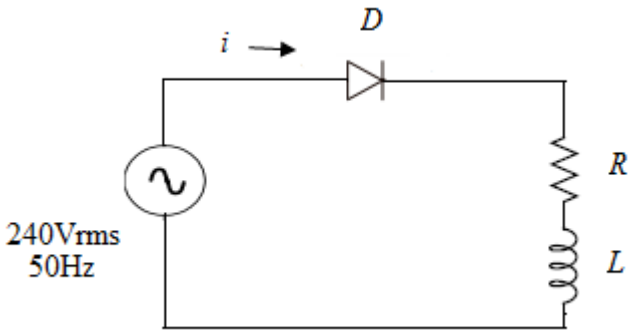

Fig.2.6.

Solution

(a) For resistive load

$$v_s = V_m \sin \omega t = \sqrt{2} \times 240 \sin 2\pi \times 50t = 339.4 \sin 314t$$

For single-phase half-wave uncontrolled rectifier:

$$V_{dc} = \frac{V_m}{\pi} = \frac{339.4}{\pi} = 108 \text{ V}$$

$$I_{dc} = \frac{V_{dc}}{R} = \frac{108}{10} = 10.8\ \text{A}$$

The voltage and current waveforms are shown in Fig.2.7 (a).

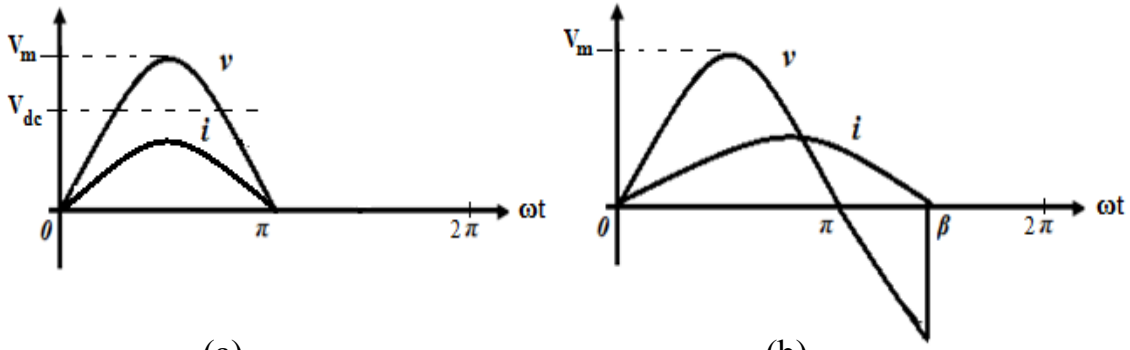

(a) (b)

Fig.2.7 Current and voltage waveforms : (a) Case of *R*-load, (b) Case of *R-L* load.

(b) For *R-L* load :

$$i(\omega t) = \frac{V_m}{|Z|}\sin(\omega t - \theta) + \frac{V_m}{|Z|}\sin\theta\, e^{-\frac{R}{L}t}$$

$$|Z| = \sqrt{R^2 + (\omega L)^2} = \sqrt{10^2 + (2\pi \times 50 \times 0.1)^2} = 32.97\ \Omega$$

$$\theta = \tan^{-1}\frac{\omega L}{R} = \tan^{-1}\frac{31.4}{10} = 72.3^\circ = 1.262\ \text{rad}$$

$$i(\omega t) = \frac{339.4}{32.47}[\sin(\omega t - 72.3^\circ) + \sin 72.3^\circ e^{-\frac{10}{0.1}t}]$$

$$= 10.29\sin(100\pi t - 72.3^\circ) + 9.1\, e^{-100t}$$

$$V_{dc} = \frac{1}{2\pi}\int_0^{4.62=265^\circ} 339.4\ \sin\omega t\ d\omega t = 58.8\ \text{V}$$

$$I_{dc} = \frac{V_{dc}}{R} = \frac{58.8}{10} = 5.88\ \text{A}$$

2.2.3 Single-Phase Half-Wave Uncontrolled Rectifier Circuit for Battery Charging

The single-phase half-wave controlled rectifier circuit containing simple diode and a current limiting resistance *R* can be used to charge a battery of *emf E* from a single-phase supply (Fig.2.8). The battery opposes the unidirectional flow of current so that the net driving voltage is v_s-*E*.

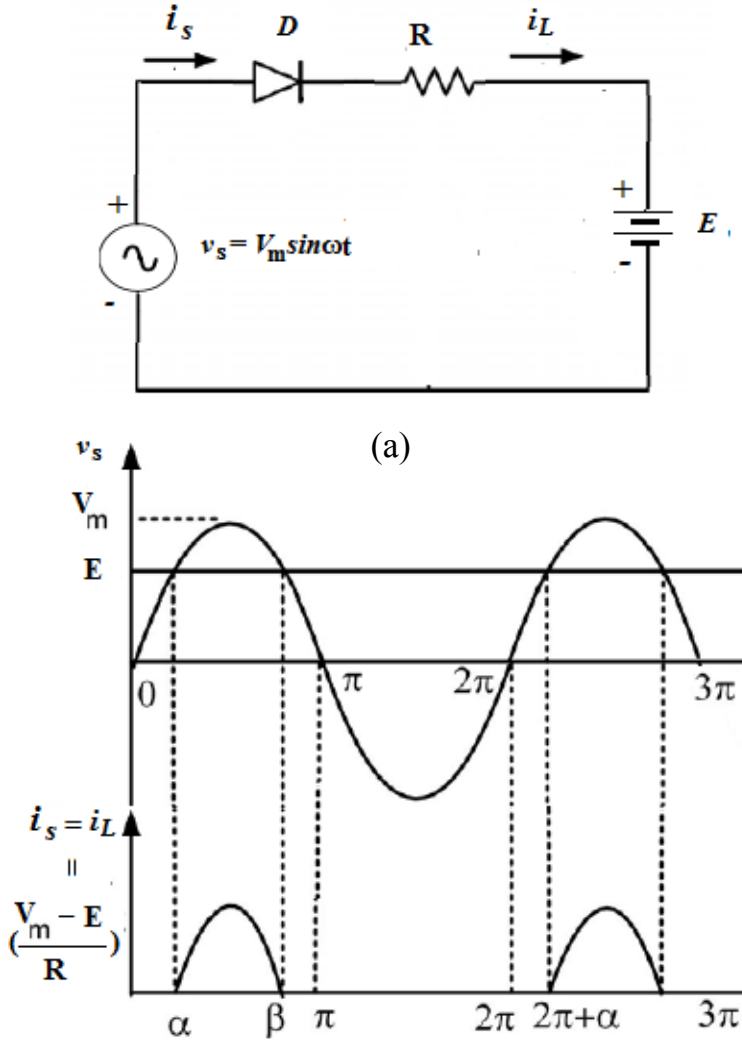

Fig.2.8 Single-phase half-wave controlled rectifier circuit for battery charging: (a) Circuit, (b) Waveforms.

Neglecting any voltage drop on the diode (which is of the order 1–2 V) the current flows in the circuit is therefore,

$$i_L = \frac{v_s - E}{R} = \frac{1}{R}(V_m \sin\omega t - E) \qquad \alpha \leq \omega t \leq \beta \qquad (2.27)$$

where α and β define the current pulse in Fig. 2.8(b). These angles are defined as

$$v_s - E = V_m \sin\alpha - E = 0$$

Therefore

$$\alpha = \sin^{-1}\frac{E}{V_m} \tag{2.28}$$

and $$\beta = \pi - \alpha \tag{2.29}$$

The average value I_{av} of the battery charging current is defined by

$$I_{av} = \frac{1}{2\pi}\int_0^{2\pi} i_L\,(\omega t)d\omega t$$

Substituting Eq. (2.27) into the above defining integral expression gives

$$I_{av} = \frac{1}{2\pi}\int_\alpha^\beta \frac{1}{R}(\,V_m \sin\omega t - E)\,d\omega t$$

$$= \frac{1}{2\pi R}[V_m(\cos\alpha - \cos\beta) + E(\alpha - \beta)]$$

$$\therefore\ I_{av} = \frac{1}{2\pi R}[2V_m\cos\alpha + E(2\alpha - \pi)] \tag{2.30}$$

Example 2.4

The battery charger circuit of Fig. 2.8 is used to charge a 270 V battery of electric vehicle from the main supply voltage of 230 V, 50 Hz through a limiting resistor R =5 Ω. Calculate the average charging current of the battery.

Solution

From equations (2.28) and (2.29)

$$V_m = 230 \times \sqrt{2} = 325.2\ V$$

$$\alpha = \sin^{-1}\frac{E}{V_m} = \frac{270}{325.2} = 0.830$$

$$\alpha = 56° \qquad \text{and} \qquad \beta = \pi - \alpha = 124°$$

Now from Eq.(2.30) :

$$I_{av} = \frac{1}{2\pi R}[2V_m \cos\alpha + E(2\alpha - \pi)]$$

$$= \frac{1}{2\pi \times 5}[2 \times 325.2 \cos 56° + 270(2 \times 0.976 - \pi)] = 1.38 \text{ A}$$

2.3 SINGLE-PHASE FULL-WAVE UNCONTROLLED RECTIFIERS

2.3.1 Case of Resistive Load

Fig.2.9 (a) presents the circuit connection for a single-phase full-wave, bridge rectifier loaded with a resistive load. It is sometimes referred to as the full-wave bridge rectifier. For this configuration, two diodes always conducting during the same interval to provide a closed loop for the current. D_1 and D_2 conduct whenever the supply voltage (v_S) is positive while D_3 and D_4 conduct whenever the supply voltage (v_S) is negative as illustrated by Fig .2.9 (b).

Since the load is a resistive load. Then, the load current will have the same waveform as the load voltage , $i_o = \frac{v_o}{R}$.

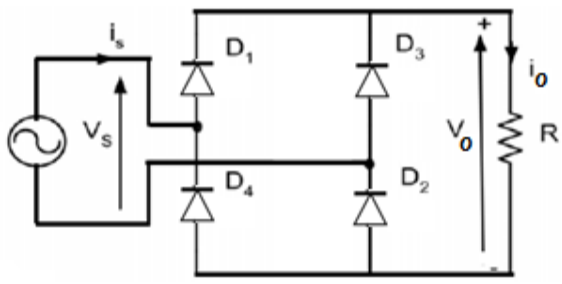

(a) Circuit.

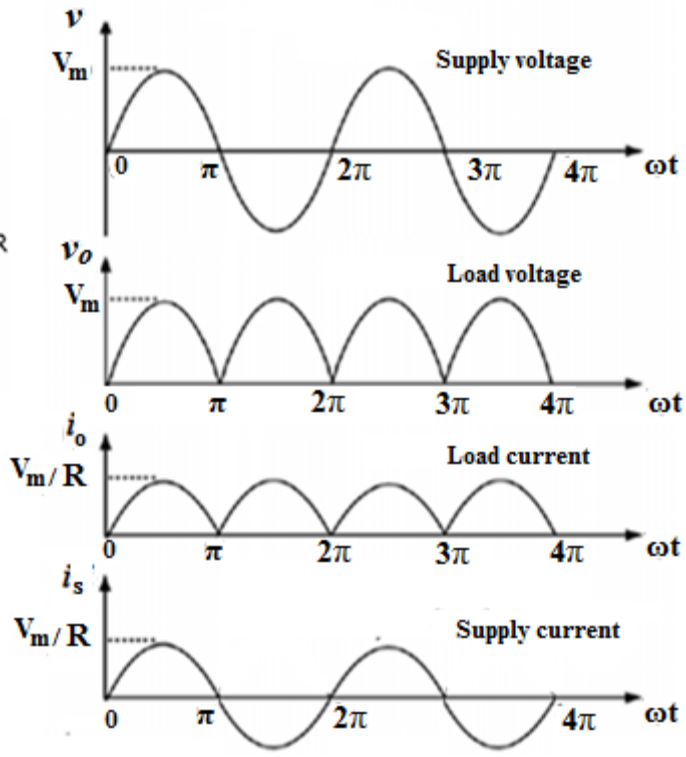

(b) Waveforms

Fig.2.9 Single-phase full-wave rectifier with resistive load.

The average value of the load voltage V_{dc} can be calculated as follows:

$$V_{dc} = \frac{1}{\pi}\int_0^{\pi} V_m sin\omega t\, d\omega t = \frac{V_m}{\pi}\,(-cos\pi + cos0^o) = \frac{2V_m}{\pi} \qquad (2.31)$$

The value of Eq. (2.31) is seen to be twice the corresponding value of the half-wave rectifier given in Eq. (2.3).

The average value of the load current I_{dc} is

$$I_{dc} = \frac{V_{dc}}{R} = \frac{2V_m}{\pi R} \qquad (2.32)$$

$$P_{dc} = V_{dc}I_{dc} = \frac{V_{dc}^2}{R} \qquad (2.33)$$

The *rms* value of the load voltage V_{orms} can be calculated as follows:

$$V_{orms} = \sqrt{\frac{1}{\pi}\int_0^{\pi} v_s^2\,(\omega t)d\omega t} = \sqrt{\frac{1}{\pi}\int_0^{\pi} (V_m sin\omega t)^2\, d\omega t}$$

$$= \sqrt{\frac{(V_m)^2}{\pi}\int_0^{\pi}\frac{1}{2}(1 - cos2\omega t)d\omega t} = \frac{V_m}{\sqrt{2}} \qquad (2.34)$$

The value of V_{orms} is seen to be √2 times the corresponding value of the half-wave rectifier given in Eq. (2.34). It should be noted that V_{orms} has the same *rms* value as a sinusoidal voltage of same maximum value . This means that the *rms* value is not affected by the polarity of the waveform.

The *rms* value of the load current I_{orms} is ,

$$I_{orms} = \frac{V_{orms}}{R} = \frac{V_m}{\sqrt{2}R} \qquad (2.35)$$

The output a.c. power is given by:

$$P_{ac} = V_{orms}I_{orms} = \frac{V_{orms}^2}{R} = \frac{(0.707V_m)^2}{R} \qquad (2.36)$$

The *PRV* for any diode in this configuration is (V_m) ; and The load voltage ripple factor is

$$RF = \frac{\sqrt{V_{orms}^2 - V_{dc}^2}}{V_{dc}} = 0.48$$

which is smaller than the corresponding *RF* value of the half-wave rectifier (see Example 2.1).

The supply current i_s is a pure sinusoidal as shown in Fig.2.9 (b). This is because the application of sinusoidal voltage to the resistive load causes sinusoidal supply current which is in-phase with the voltage. The average and *rms* values of the supply current are,

$$I_{s(av)} = \frac{1}{2\pi}\int_0^{2\pi} V_m sin\omega t \, d\omega t = 0 \qquad (2.37)$$

$$I_{s(rms)} = \sqrt{\frac{1}{2\pi}\int_0^{2\pi} (\frac{V_m}{R} sin\omega t)^2 \, d\omega t} = \frac{V_m}{\sqrt{2}R} \qquad (2.38)$$

If we neglect the voltage drops across the diodes, the input power will be equal to the output power and therefore the power factor of the circuit will be unity.

2.3.2 Single-Phase Full-Wave Bi-Phase (Center-Tapped) Uncontrolled Rectifier with *R*-Load

This rectifier is shown in Fig.2.10. The waveforms and analysis are same as that for the bridge rectifier of Fig.2.9. Hence, it will not be repeated here.

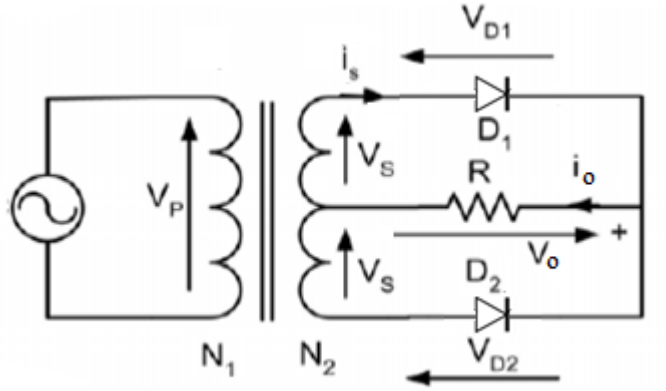

Fig.2.10 Bi-phase (center- tapped) full wave uncontrolled rectifier.

Example 2.5

For the single-phase, full-wave, uncontrolled rectifier shown in Fig.2.9, the supply voltage is 110 V, 50 Hz. The load resistor is 25 Ω, calculate:

(a)The average values of the output voltage and current.

(b)The *rms* values of the output voltage and current.

(c) The d.c. power consumed by the load (P_{dc}) and the average value of the power delivered to the load (P_{ac}).

Sketch the appropriate load voltage and diode voltage waveforms.

Solution

(a) The average value of the load voltage V_{dc}

$$V_{dc} = \frac{1}{\pi}\int_0^{\pi} V_m \sin \omega t \, d\omega t = \frac{2V_m}{\pi} = \frac{2\sqrt{2} \times 110}{\pi} = 99.035 \text{ V}$$

The average value of the load current

$$I_{dc} = \frac{V_{dc}}{R} = \frac{99.035}{25} = 3.961 \text{ A}$$

(b) the *rms* value of the load voltage V_{orms} is calculated from Eq.(2.34) :

$$V_{orms} = \frac{V_m}{\sqrt{2}} = \frac{\sqrt{2} \times 110}{\sqrt{2}} = 110 \text{ V}$$

$$I_{orms} = \frac{V_{orms}}{R} = \frac{110}{25} = 4.4 \text{ A}$$

(c) The d.c. and a.c. power,

$$P_{dc} = \frac{V_{dc}^2}{R} = \frac{(99.035)^2}{25} = 392.31 \text{ W}$$

$$P_{ac} = \frac{V_{orms}^2}{R} = \frac{(110)^2}{25} = 484 \text{ W}$$

The load voltage and diode voltage waveforms are shown in Fig.2.11.

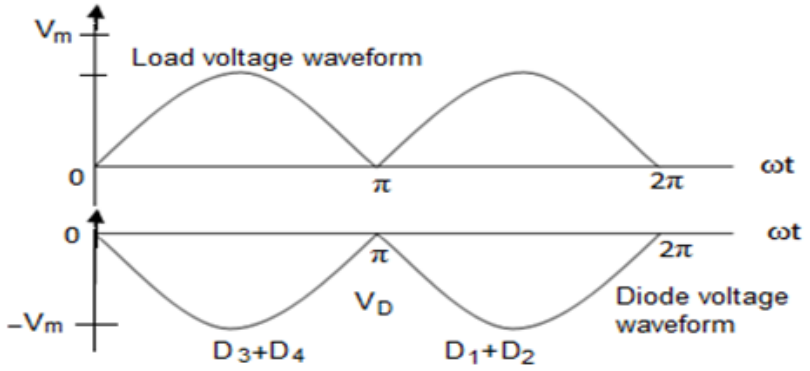

Fig.2.11 Voltage and current waveforms for Example 2.5.

2.3.3 Single-Phase Full-Wave Uncontrolled Rectifier Loaded with Highly Inductive Load

Fig. 2.12 (a) presents the circuit connection for a single-phase, full-wave, rectifier loaded with a highly inductive load. Highly inductive loads are basically *R-L* loads where $L >>> R$. Therefore, the load time constant $\tau = L / R$ is very high and can be considered infinity. Consequently, the load current is assumed constant. For one total period of operation of this circuit, the corresponding waveforms are shown in Fig. 2.12 (b).

During the conduction of D_1 and D_2 simultaneously the supply voltage appears directly across the load so that the load voltage $v_o(\omega t)$ remains the same form as shown in Fig.2.9 (b) (same as the case of resistive load). Hence, the average value of the load voltage V_{dc} can be calculated as follows:

$$V_{dc} = \frac{1}{\pi}\int_0^{\pi} V_m sin\omega t \, d\omega t = \frac{V_m}{\pi}(-cos\pi + cos0^o) = \frac{2V_m}{\pi} \qquad (2.39)$$

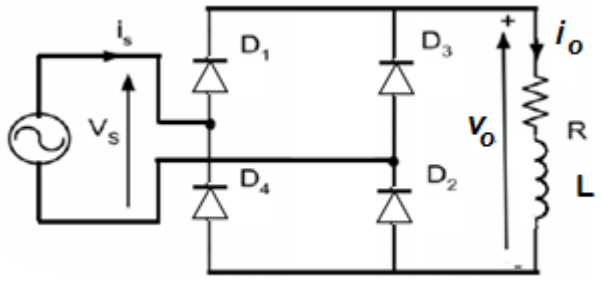

(a) Circuit.

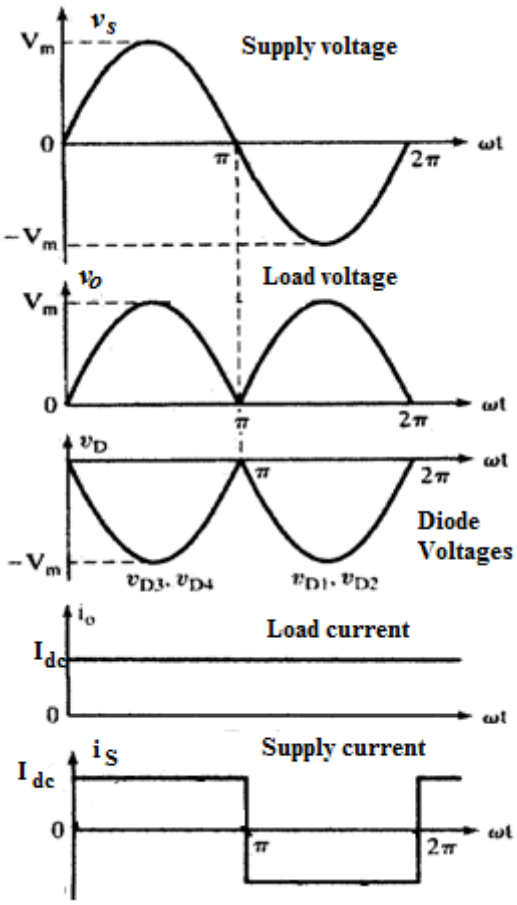

(b) Waveforms.

Fig.2.12 Single-phase full-wave rectifier loaded with highly inductive load.

Since the load is a highly inductive load. Then, the load current is considered constant (ripple free current) and its average value is

$$I_{dc} = \frac{V_{dc}}{R} = \frac{2V_m}{\pi R} \tag{2.40}$$

and the d.c. power is

$$P_{dc} = V_{dc} I_{dc} = \frac{V_{dc}^2}{R} \tag{2.41}$$

The *rms* value of the load voltage V_{orms} can be calculated as follows:

$$V_{orms} = \sqrt{\frac{1}{\pi}\int_0^{\pi} (V_m sin\omega t)^2 \, d\omega t}$$

$$= \sqrt{\frac{(V_m)^2}{\pi}\int_0^{\pi} \frac{1}{2}(1 - cos2\omega t) d\omega t} = \frac{V_m}{\sqrt{2}} \tag{2.42}$$

Therefore the *rms* value of the load current I_{orms} is

$$I_{orms} = \frac{V_{rms}}{R} = \frac{V_m}{\sqrt{2}R} \tag{2.43}$$

Since the load current is constant over the studied period, therefore, the rms value of the load current I_{orms} is

$$I_{orms} = I_{dc} = I_s \tag{2.44}$$

The output a.c. power is given by:

$$P_{ac} = V_{orms} I_{orms} = \frac{V_{orms}^2}{R} = \frac{(0.707V_m)^2}{R} \tag{2.45}$$

2.4 HARMONIC CONSIDERATIONS OF THE OUTPUT VOLTAGE AND CURRENT WAVEFORMS OF THE SINGLE-PHASE FULL - WAVE RECTIFIER

2.4.1 Voltage Waveform Harmonics

The output voltage waveform of the single-phase full-wave rectifier is shown in Fig.2.13. It is re-drawn with the supply voltage is taken as cosine wave instead of sine wave for sake of simplifying analysis.

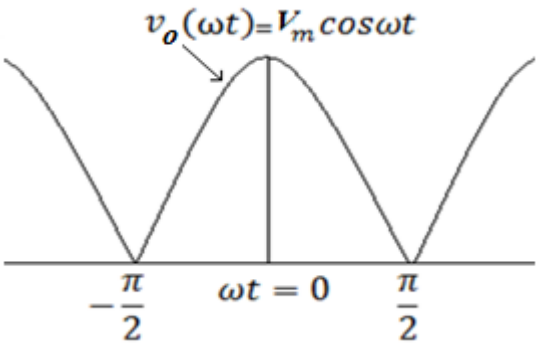

Fig.2.13. Voltage waveform of full-wave rectifier.

The output voltage waveform can be expressed in a Fourier series as,

$$v_o(\omega t) = a_0 + \sum_{n=1,2,3,..}^{\infty} (a_n \cos n\omega t + b_n \sin n\omega t) \qquad (2.46)$$

where $n =$ is the order of harmonic.

The Fourier coefficients are defined as (See Appendix-A)

$$\frac{a_o}{2} = \frac{1}{2\pi}\int_0^{2\pi} v_o(\omega t)d\omega t \qquad (2.47)$$

$$a_n = \frac{1}{\pi}\int_0^{2\pi} v_o(\omega t)\cos n\omega t\, d\omega t \qquad (2.48)$$

$$b_n = \frac{1}{\pi}\int_0^{2\pi} V_o(\omega t)\sin n\omega t\, d\omega t \qquad (2.49)$$

where

a_o is the average value or the d.c. component of the output voltage waveform.
a_n is the cosine-term of the nth order harmonic.
b_n is the sine-term of the nth order harmonic.

In this case, the Fourier coefficients are:

$$a_0 = V_{dc} = \frac{1}{\pi}\int_{-\frac{\pi}{2}}^{\frac{\pi}{2}} V_m \cos\omega t\, d\omega t = \frac{2V_m}{\pi} \qquad (2.50)$$

$$a_n = \frac{1}{\pi}\int_{-\frac{\pi}{2}}^{\frac{\pi}{2}} V_m \cos\omega t \cos n\omega t \; d\omega t$$

$$a_n = \frac{4V_m}{\pi}\sum_{n=2,4,6,..}^{\infty}\frac{1}{(n+1)(n-1)} \tag{2.51}$$

$$b_n = \frac{1}{\pi}\int_{-\frac{\pi}{2}}^{\frac{\pi}{2}} V_m \cos\omega t \sin n\omega t \; d\omega t = 0 \tag{2.52}$$

The amplitude of the nth order harmonic c_n can be found as,

$$C_n = \sqrt{a_n^2 + b_n^2} \tag{2.53}$$

and the phase-angle ψ_n of the nth harmonic component is given as,

$$\psi_n = \tan^{-1}\frac{a_n}{b_n} \tag{2.54}$$

Hence, the output voltage waveform expressed in Fourier series as,

$$v_o(\omega t) = \frac{2V_m}{\pi} - \frac{4V_m}{3\pi}\cos 2\omega t + \frac{4V_m}{15\pi}\cos 4\omega t - \frac{4V_m}{35\pi}\cos 6\omega t + \cdots + \cdots \tag{2.55}$$

The first term on the RHS is the d.c. value. The second term is the dominant output ripple, which in this case is at twice the supply frequency; the third other terms are the higher order ripples. The amplitude of this ripples reduce as the harmonics number increases. All ripple components are unwanted.

For the half-wave rectifier, it is found that the Fourier series for the voltage waveform of Fig.2.1 is

$$v_o(\omega t) = \frac{V_m}{\pi} + \frac{V_m}{2\pi}\sin\omega t - \frac{2V_m}{3\pi}\cos 2\omega t - \frac{2V_m}{15\pi}\cos 4\omega t + \cdots + \cdots \tag{2.56}$$

Harmonic spectra of the output voltage waveform of the full-wave rectifier are shown in Fig.2.14 for the case when the load is purely resistive.

From Fig.2.14, it is seen that the zero frequency component n = 0 or the d.c. component is the dominant one in the spectrum, and that the second harmonic, corresponding to n=2 is the most significant harmonic amplitudes. Only even harmonics are existing and any odd harmonic number are all of zero value in this case. The harmonic spectrum of Fig.2.14 has an envelope identical to a Fourier integral of the mathematical form *sincx*.

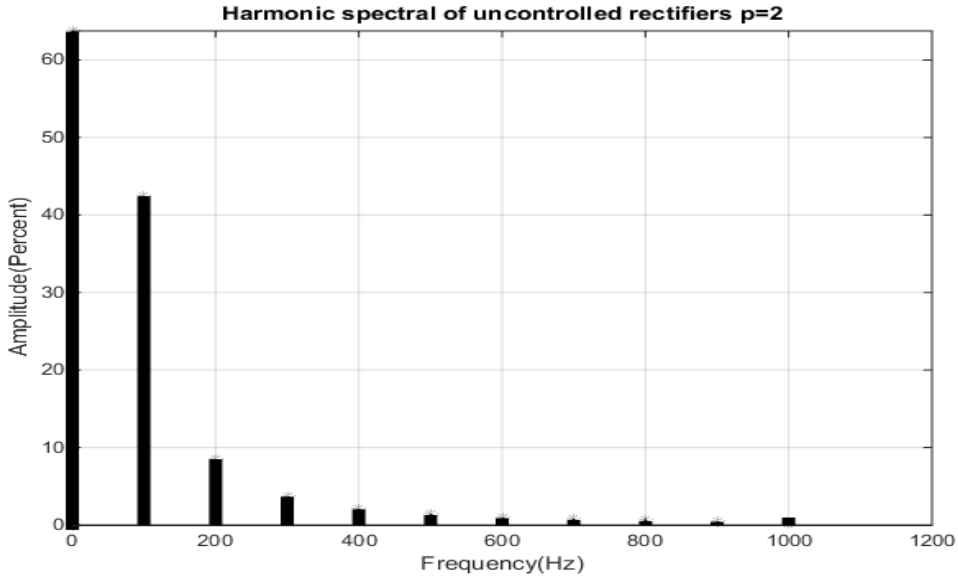

n	0	2	4	6	8	10	12	16	20
Hz	0	100	200	300	400	500	600	800	1000
c(n)	63.63635	42.42423	8.484847	3.636363	2.020202	1.285583	0.890019	0.499109	0.318979

Fig.2.14 Harmonic spectra for the output voltage of the single-phase full-wave rectifier, with normalised V_m (=100%).

2.4.2 Input Current Harmonics

If ripple-free load current in steady-state is assumed, the input current i_s waveform of the single-phase full-wave rectifier may then be depicted as shown in Fig.2.15 for an ideal input transformer.

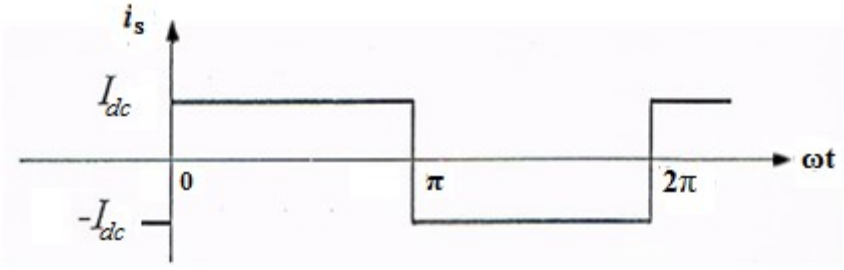

Fig.2.15 Input current waveform for single-phase full-wave rectifier.

Diodes D_1 and D_2 carry each half cycle of the load current and input current i_s is a square wave a.c. waveform as indicated. The actual input current waveform includes the transient behavior of the load in each half cycle and its harmonics are quite difficult to obtain analytically. With the assumption that the supply is ideal and perfectly smooth and ripple free load current, which implies an infinitely large load inductance, it is quit straightforward to obtain an analytical expression for the input current harmonics.

The rectangular wave of Fig.2.15 is defined as,

$$f(\omega t) = i_s(\omega t) = I_{dc} \qquad 0 \le \omega t \le \pi$$

$$= -I_{dc} \qquad \pi \le \omega t \le 2\pi$$

Hence, the Fourier coefficients of the rectangular wave are,

$$a_0 = \frac{1}{2\pi}\int_0^{\pi} i_s(\omega t)\ d\omega t + \frac{1}{2\pi}\int_{\pi}^{2\pi} i_s(\omega t)\ d\omega t$$

$$= \frac{1}{2\pi}\int_0^{\pi} (I_{dc})\ d\omega t + \frac{1}{2\pi}\int_{\pi}^{2\pi} (-I_{dc})\ d\omega t\ = 0 \qquad (2.57)$$

$$a_n = \frac{1}{\pi}\int_0^{\pi} (I_{dc})\, cosn\omega t\ d\omega t + \frac{1}{2\pi}\int_{\pi}^{2\pi} (-I_{dc}) cosn\omega t\ d\omega t\ = 0 \qquad (2.58)$$

$$b_n = \frac{1}{\pi}\int_0^{\pi} (I_{dc})\, sinn\omega t\ d\omega t + \frac{1}{\pi}\int_{\pi}^{2\pi} (-I_{dc}) sinn\omega t\ d\omega t$$

$$= \frac{I_{dc}}{n\pi}\left[-\ cosn\omega t\ \Big|_0^{\pi} +\ cosn\omega t\ \Big|_{\pi}^{2\pi}\ \right]$$

$$= \frac{I_{dc}}{n\pi}\left[(coso - cosn\pi) + (1 -\ cosn\pi\ )\ \right]$$

$$= \frac{I_{dc}}{n\pi}[1 - cosn\pi + 1 - cosn\pi] = \frac{I_{dc}}{n\pi}(1 - cosn\pi)$$

- When n is even (2, 4, 6…) cosnπ = 1, $\Longrightarrow$ $b_n = 0$.
- When n is odd (3, 5, 7…) cosnπ = -1

$$\therefore b_n = \frac{4I_{dc}}{n\pi} \qquad (2.59)$$

The Fourier series is given by:

$$i_s(\omega t) = a_o + \sum_{n=1}^{\infty}(a_n\, cosn\omega t + \, b_n sinn\omega t)$$

Hence the input current can be represented by Fourier series as,

$$i_s(\omega t) = 0 + \sum_{n=1}^{\infty}(0 + \frac{4I_{dc}}{n\pi} sinn\omega t)$$

$$or \qquad i_s(\omega t) = \sum_{n=1}^{\infty} \frac{4I_{dc}}{n\pi} sinn\omega t$$

$$= \frac{4I_{dc}}{\pi}\sin\omega t + \frac{4I_{dc}}{3\pi}\sin 3\omega t + \frac{4I_{dc}}{5\pi}\sin 5\omega t + \cdots \qquad (2.60)$$

In more general form (2.60) may be written as

$$i_s(\omega t) = \frac{4I_{dc}/k}{\pi}\sin\omega t + \frac{4I_{dc}/k}{3\pi}\sin 3\omega t + \frac{4I_{dc}/k}{5\pi}\sin 5\omega t + \cdots \qquad (2.61)$$

where k is the transformer turns ratio between primary and secondary windings. The transformer magnetizing current has been neglected in this analysis .

Note that in the above circuit, the input current waveform i_s has no d.c. value. The first term for n = 1, is called the fundamental and the higher order terms are the harmonics which are unwanted. The harmonic spectrum of the input current wave is as shown in Fig.2.16.

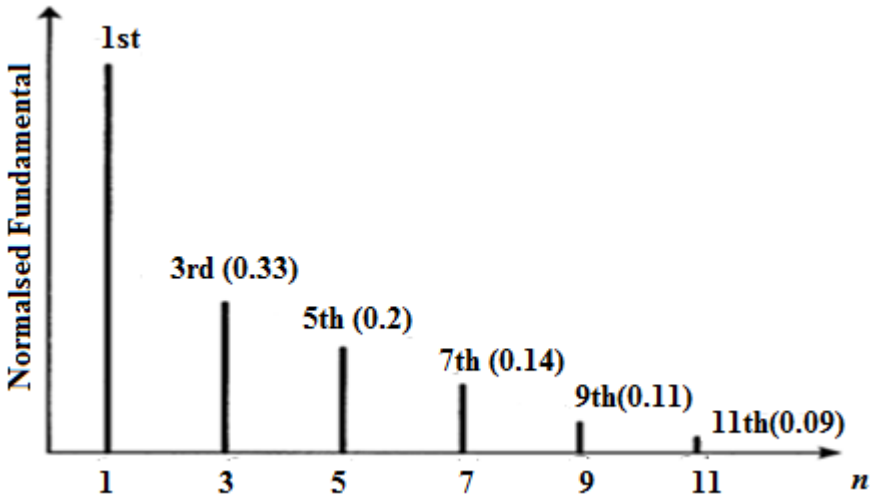

Fig.2.16 Harmonic spectrum of the input current wave.

It is clear from Fig.2.16 that:

- The harmonic amplitudes reduce as the harmonic number increases.
- No even harmonics.
- Nearest harmonic is the third, if the fundamental is 50 Hz, then the third harmonic is 150Hz and the fifth harmonic 250 Hz as shown in Fig.2.16.

2.5 POLY-PHASE UNCONTROLLED RECTIFICATION

For most industrial applications poly-phase rectifier circuits are used. The circuit employed may give either half-wave or full-wave, controlled or uncontrolled rectifier circuits. In these rectifier circuits, the commutation processes involved are purely natural by the cycling of the supply-side voltages. Hence there is no reason in using gate turn-off devices and such rectifiers can employ thyristors as switches. When poly-phase a.c. is rectified, phase-shifted pulses overlap each other to produce d.c. output that is much "smoother", i.e. has less a.c. content than that produced by single-phase rectification. This is considered as an advantage in high-power rectifier circuits, where sheer physical size of filtering components would be prohibitive but low-noise d.c. power must be obtained.

The following assumption are made during the studying and analysing the polly-phase rectifier circuits :

(a) All phases of the supply are identical, balanced, pure sinusoidal and displaced exactly by 360˚/p from each other, where p = number of phases (p = 3 for three-phase system and P = 6 for six-phase system …etc).

(b) The leakage reactances of the supply are neglected for all the phases.

(c) The switching functions are symmetrical and are phase shifted by 360˚/ p with respect to each other.

2.5.1 Three-Phase Half-Wave Uncontrolled Rectifier

Fig.2.17 shows a three-phase half-wave uncontrolled rectifier with resistive load. The rectifier is fed from an ideal three-phase supply through delta-star three-phase transformer.

The principle of operation of this convertor can be explained as follows:

- Diode 1 which has a more positive voltage at its anode conducts for the period from $\pi/6$ to $5\pi/6$. In this period D_2 and D_3 are off. The neutral wire provides a return path to the load current.
- Similarly, diode 2, and 3, whichever has more positive voltage at its cathode conducts.
- The conduction pattern is: D_1 ,D_2, D_3.

The output voltage and current waveforms are shown in Fig.2.18.

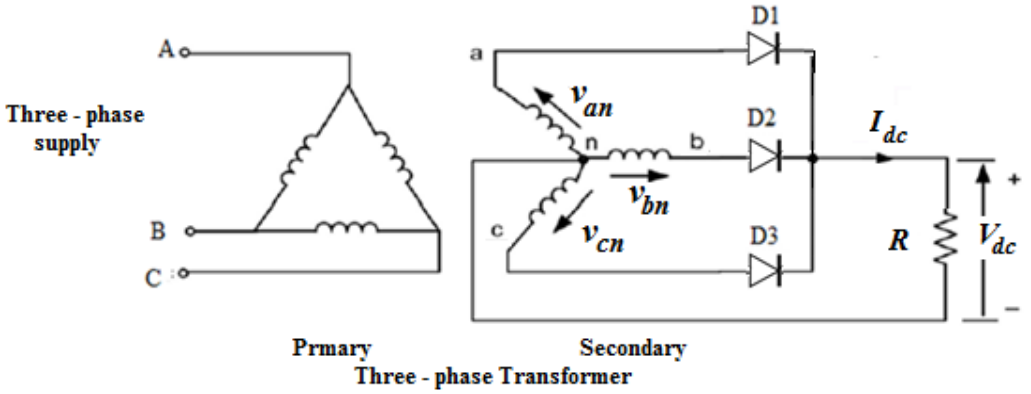

Fig.2.17 Three-phase half-wave uncontrolled rectifier with *R*-Load.

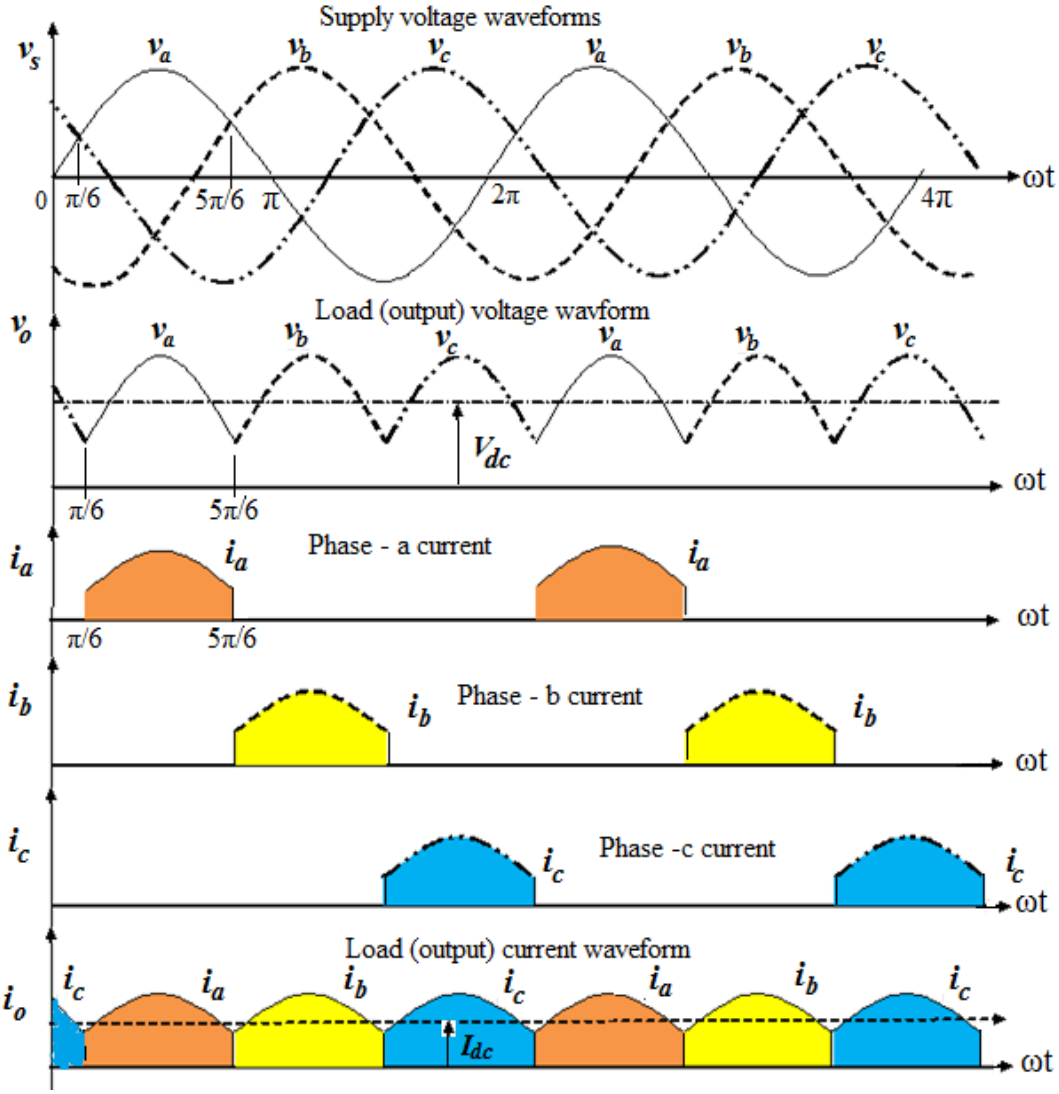

Fig .2.18 Load voltage and current waveforms for the three-phase, half-wave uncontrolled rectifier.

Analytical properties of the output voltage waveform

Let $v_{an} = V_m \sin \omega t$
$v_{bn} = V_m \sin (\omega t - 2\pi / 3)$
$v_{cn} = V_m \sin (\omega t - 4\pi / 3)$

The average value V_{dc} of the output (load) voltage waveform $v_o(\omega t)$ shown in Fig.2.17 can be found as

$$V_{dc} = \frac{1}{\frac{2\pi}{3}} \int_{\pi/6}^{5\pi/6} V_m \sin\omega t \, d\omega t = \frac{3V_m}{2\pi} [-cos\omega t]_{\pi/6}^{5\pi/6}$$
$$= \frac{3V_m}{2\pi}\left[-(\cos\frac{5\pi}{6} - cos\frac{\pi}{6})\right] = \frac{3V_m}{2\pi}\left[-(-\frac{\sqrt{3}}{2} - \frac{\sqrt{3}}{2})\right]$$
$$= \frac{3\sqrt{3}V_m}{2\pi} \qquad (2.62)$$

The load current I_{dc} is:

$$I_{dc} = \frac{3\sqrt{3}V_m}{2\pi R} \qquad (2.63)$$

Note that the secondary windings of the supply transformer carry unidirectional currents, which leads d.c. magnetization of the transformer core. This implies that the transformer cores have d.c. flux, so that for the same a.c. voltage and hence flux swing, it must have larger core size than is necessary. This problem of d.c. magnetization is avoided using bridge rectifier circuit.

Example 2.6

Power is supplied to a load resistor R from a three-phase zero-impedance supply of balanced sinusoidal voltages using half-wave bridge circuit of Fig.2.19 . The three diodes may be considered as ideal switches.

(a) Sketch the phase current waveform i_a (ωt) in phase-a with respect to the phase voltage v_{an} (ωt) = $V_m \sin \omega t$.

(b) Show that the rms value of the phase current current is:

$$I_a = 0.485 \frac{V_m}{R}$$

Hence, calculate I_a of the phase current, compare with the value for sinusoidal operation.

(c) Sketch the load current waveform and specify, by observation, the lowest ripple frequency.

Fig.2.19 Three-phase Half-wave rectifier.

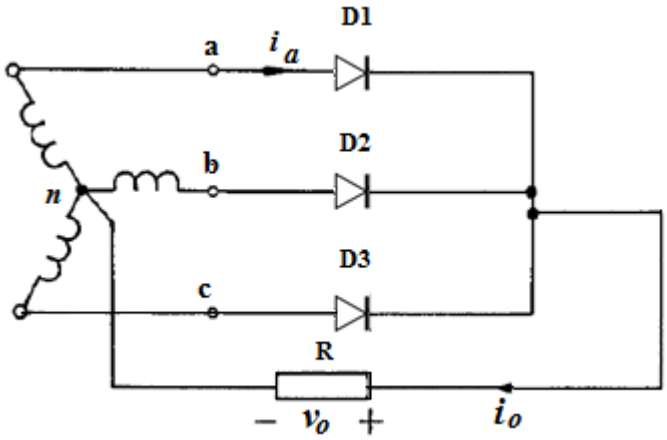

Solution

(a) The waveform of the current in phase - a is depicted in Fig.2.20.

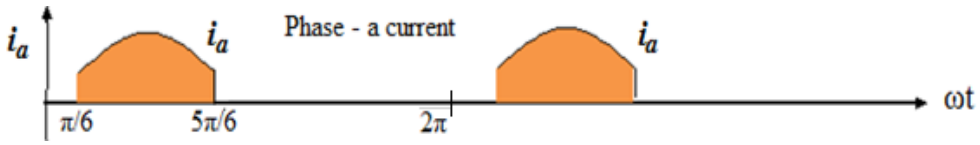

Fig.2.20 Current waveform in phase - a.

(b) Phase current (i_a) :
Let the phase current $i_a(\omega t)$ in phase - a with resistive load be ,

$$i_a(\omega t) = I_m \sin\omega t$$

where : $I_m = V_m / R$, hence the *rms* value of i_a is:

$$I_a = \sqrt{\frac{1}{T}\int_0^T i_a^2(\omega t)dt} = \sqrt{\frac{1}{2\pi}\int_{\frac{\pi}{6}}^{\frac{5\pi}{6}} I_m^2 sin^2(\omega t)d(\omega t)}$$

$$\therefore I_a = \frac{I_m}{\pi\sqrt{2}}\sqrt{\frac{1}{2}\int_{\frac{\pi}{6}}^{\frac{5\pi}{6}}(1-cos\omega t)d(\omega t)} = 0.485I_m$$

For sinusoidal operation

$$I_{arms} = \frac{I_m}{\sqrt{2}} = 0.707I_m$$

(c) The ripple period is given by $\frac{2\pi}{3}$ which represents the lowest ripple frequency = 3 times the supply frequency as depicted in Fig.2.21.

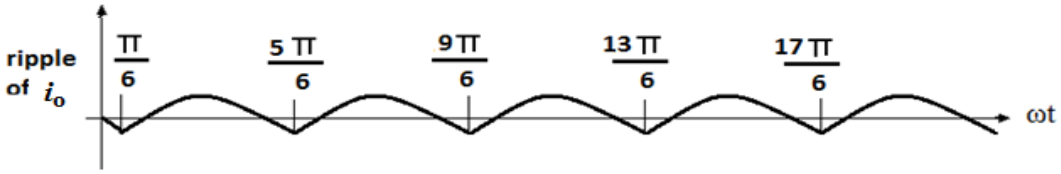

Fig.2.21 The ripple frequency.

2.5.2 Three-Phase Full-Wave Uncontrolled Bridge Rectifier

Fig.2.22 shows a three-phase full-wave uncontrolled bridge rectifier with resistive load. The rectifier is fed from an ideal three-phase supply through delta-star three-phase transformer. The principle of operation of this convertor can be explained as follows:

Each three-phase line connects between pair of diodes, one to route power to positive (+) side of load, and other to route power to negative (-) side of load.

- Diode 1, 3 and 5, whichever has a more positive voltage at its anode conducts.
- Similarly, diode 2, 4 and 6, whichever has more negative voltage at its cathode return the load current.
- The conduction pattern is: **16-36-34-54-52-12.**
- Each diode conducts for 120˚ in each supply cycle as shown in Fig.2.23.

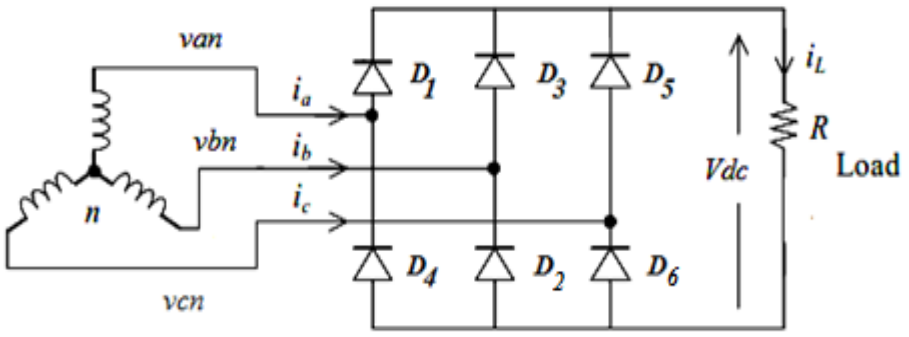

Fig.2.22 The three-phase full-wave, uncontrolled rectifier.

The output voltage is the instantaneous difference between two appropriate phases at each instant as depicted in Fig.2.23, and the resultant d.c. output voltage wave is shown in Fig.2.24.

To find the average voltage V_{dc} on the load, assume that the line to line voltages are represented by the following equations,

$$v_{ab} = v_{an} - v_{bn} = V_m \sin(\omega t) - V_m \sin(\omega t + 2\pi/3),$$

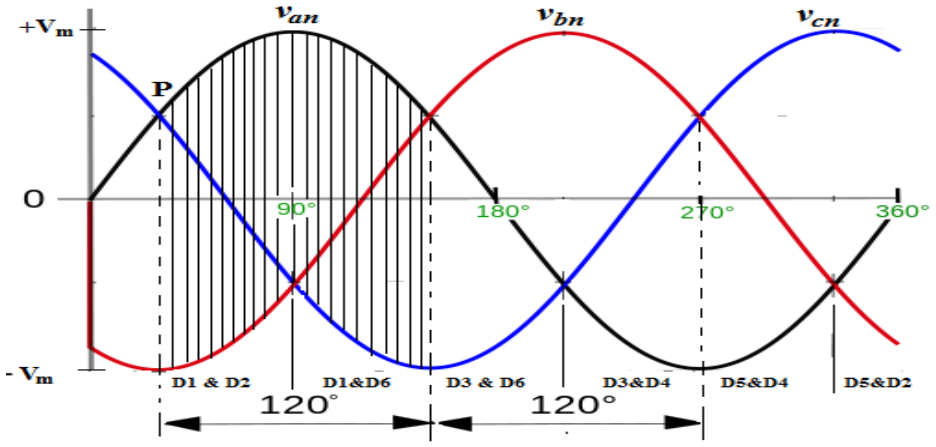

Fig.2.23 Each diode conducts for 120˚.

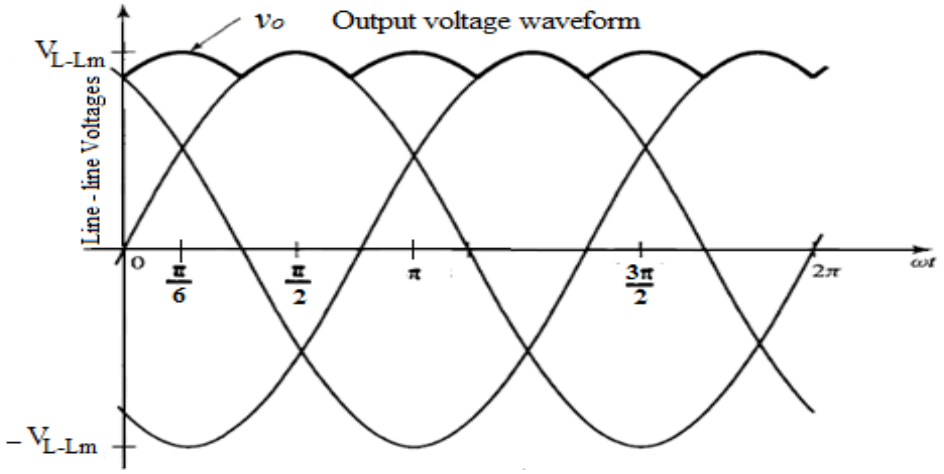

Fig.2.24 The line to line supply voltage and the output voltage waveforms.

hence

$$v_{ab}(\omega t) = \sqrt{3}\, V_m sin\left(\omega t + \frac{\pi}{6}\right) \quad (2.64)$$

Similarly,

$$v_{bc}(\omega t) = \sqrt{3}\ V_m sin\left(\omega t - \frac{\pi}{2}\right) \quad (2.65)$$

$$v_{ca}(\omega t) = \sqrt{3}\ V_m sin\left(\omega t - \frac{7\pi}{6}\right) \quad (2.66)$$

The resultant output voltage waveform appears across the load is the line to line values of the three-phase supply as shown in Fig.2.25.

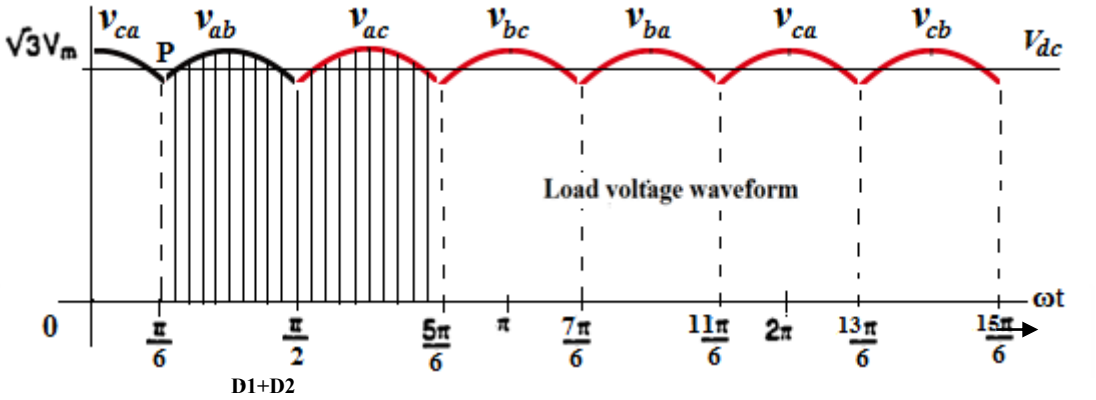

Fig.2.25 The d.c. output voltage waveform.

The average value V_{dc} of the output voltage can be calculated by integrating over 1/6 of a cycle,

$$V_{dc} = \frac{3}{\pi}\int_{\pi/6}^{\pi/2} v_{ab}(\omega t)\, d\omega t$$

$$= \frac{3}{\pi}\int_{\frac{\pi}{6}}^{\frac{\pi}{2}} \sqrt{3}V_m sin\left(\omega t + \frac{\pi}{6}\right) d\omega t$$

$$= \frac{3}{\pi}\int_{\pi/6}^{\pi/2} \sqrt{3}V_m(\sin\omega t \cos\frac{\pi}{6} - \cos\omega t \sin\frac{\pi}{6})d\omega t$$

$$= \frac{3}{\pi}\int_{\pi/6}^{\pi/2} \sqrt{3}V_m\left(\sin\omega t\ \frac{\sqrt{3}}{2} + \cos\omega t \frac{1}{2}\right) d\omega t$$

$$= \frac{3\sqrt{3}V_m}{\pi}\left[\left(-\cos\left(\frac{\pi}{2}\right) + \cos\left(\frac{\pi}{6}\right)\right)\frac{\sqrt{3}}{2} + (\sin\left(\frac{\pi}{2}\right) - \sin\left(\frac{\pi}{6}\right))\frac{1}{2}\right]$$

$$\therefore\ V_{dc} = \frac{3\sqrt{3}V_m}{\pi} \qquad (2.67)$$

The load current I_{dc} is:

$$I_{dc} = \frac{3\sqrt{3}V_m}{\pi R} \qquad (2.68)$$

The average power is:

$$P_{dc} = V_{dc} I_{dc} = \frac{3\sqrt{3}V_m}{\pi} \times \frac{3\sqrt{3}V_m}{\pi R} = \frac{27\ V_m^2}{\pi^2 R} \qquad (2.69)$$

The waveforms of the supply line current through phase-a and the current through diode D_1 are shown in Fig.2.26 for resistive and inductive loads .

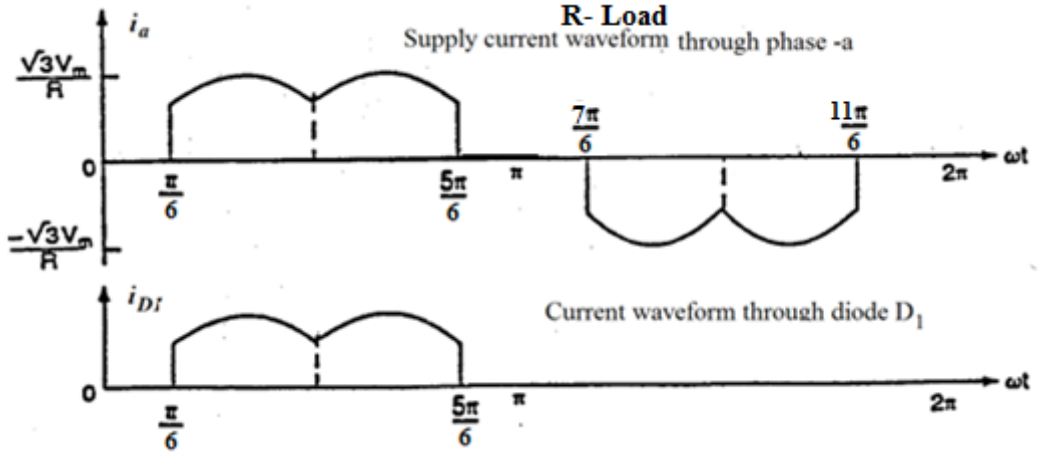

(a)

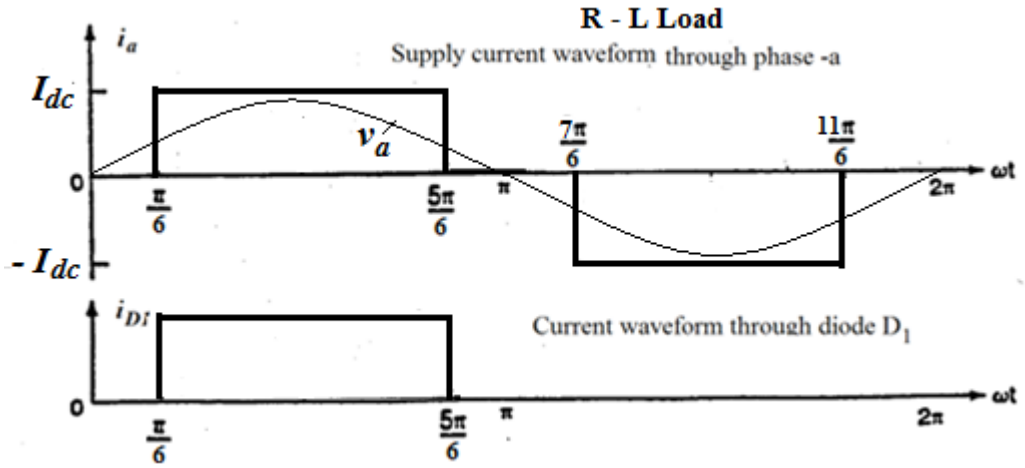

(b)

Fig.2.26 Waveforms of the supply line current through phase-a and the current through diode D_1 in a three-phase full-wave rectifier bridge: (a)With resistive load, and (b)With highly inductive load.

To calculate the power factor, for phase - a for example:

$$I_{arms} = \sqrt{\frac{1}{\pi}\int_{\pi/6}^{5\pi/6} I_{dc}^2 \; d\omega t}$$

$$I_{arms} = \sqrt{\frac{I_{dc}^2}{\pi}\left[\frac{5\pi}{6} - \frac{\pi}{6}\right]} = \sqrt{\frac{2}{3}}\, I_{dc} \tag{2.70}$$

$$P = \frac{1}{\pi}\int_{\pi/6}^{5\pi/6} I_{dc} V_m sin\omega t \; d\omega t = \frac{\sqrt{3}}{\pi} V_m I_{dc} \tag{2.71}$$

$$PF = \frac{P}{V_{rms}\, I_{rms}} = \frac{\left[\frac{\sqrt{3}}{\pi} V_m I_{dc}\right]}{\left[\frac{V_m}{\sqrt{2}}\sqrt{\frac{2}{3}}\, I_{dc}\right]} = \frac{3}{\pi} \approx 0.96 \tag{2.72}$$

Compare to 0.91 for the single-phase full-wave bridge rectifier. Also the three-phase bridge rectifier uses 6 diodes, while single-phase bridge rectifier uses only 4 diodes.
Regarding the ripple voltage for the three-phase bridge rectifier it is at 6*f* and is small in magnitude, while for single-phase bridge rectifier it is at 2*f*. This means that the three-phase bridge rectifier output voltage is easier to filter.

2.5.3 Six-Phase (Hexa-Phase) Uncontrolled Rectifier

To get more smooth output voltage waveform, higher phase numbers than three may be used. Poly-phase systems with more than three phases are easily accommodated into bridge rectifier scheme. Once poly-phase power is available, it may be converted to any desired number of phases with a suitable arrangement of transformers. Common practice for rectifier installations and in HVDC converters is to provide six phases, with 60 degree phase spacing, to reduce harmonic generation in the a.c. supply system and to provide smoother direct current. Six-phase power has the same voltage between adjacent phases as between phase and neutral.

Six-phase half-wave (6-puls) rectifier circuit

A six-phase supply is obtained from a three-phase system using transformer with centre tapped secondary winding as shown in the Fig.2.27. This circuit is, in fact, a six-phase, half-wave rectifier. Obviously, each diode in this circuit conducts for one-sixth of a cycle.

Hence, the conduction angle of each diode will be 60˚ only. The supply and output voltage waveforms are shown in Fig.2.28.

Referring to Fig.2.27, the average output voltage may be given by,

$$V_{dc} = \frac{3}{\pi}\int_{\pi/3}^{2\pi/3} V_m \sin \omega t \, d\omega t = \frac{3V_m}{\pi}[\cos 120^\circ - cos60^\circ]$$

$$\therefore \quad V_{dc} = \frac{3V_m}{\pi} \qquad (2.73)$$

The output voltage has a mean value of 0.955 V_m. Ripple has a very small value and a fundamental frequency six times the supply frequency.

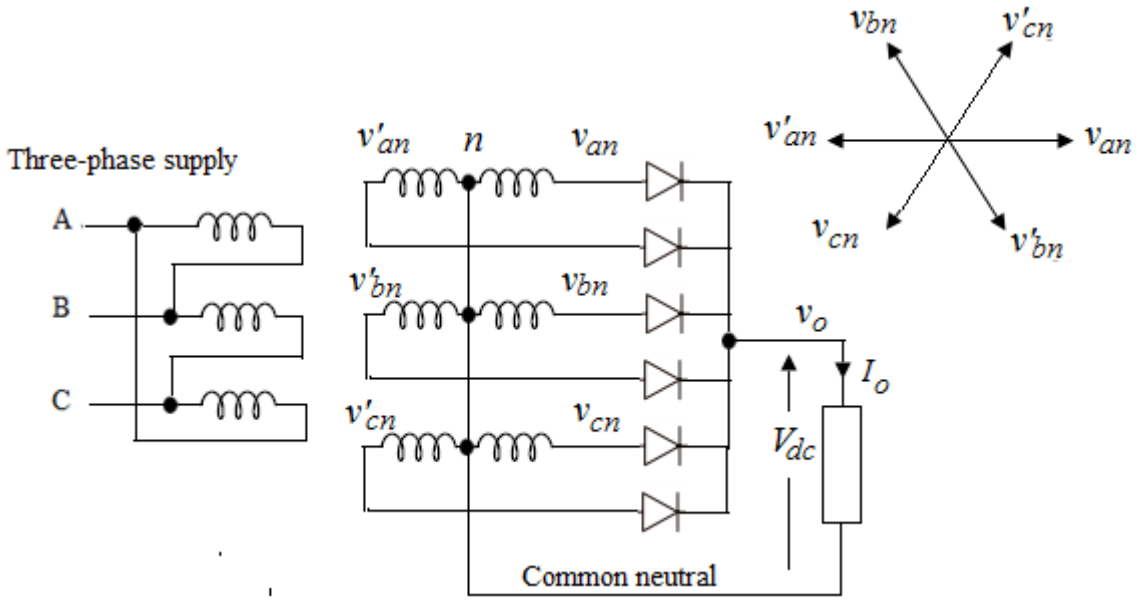

Fig.2.27 Six-phase rectifier.

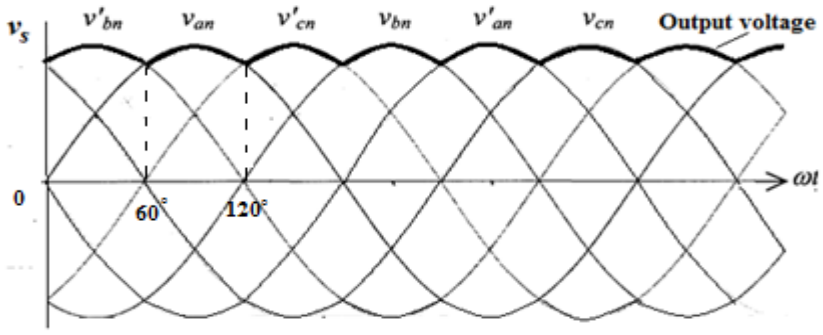

Fig.2.28 Six-phase rectifier: Input and output voltage waveforms .

Six-phase full-wave (12-puls) rectifier circuit

In many applications, it is necessary to reduce ripple in the output d.c. voltage waveform as much as possible. For example the ripple of a three-phase full-wave rectifier is about 4.2%. This can be reduced to about 1% by increasing the ripple frequency to twelve times the input frequency by using six-phase full-wave rectifier circuit. To construct a six-phase full-wave rectifier circuit, two three-phase full-wave bridges are connected in parallel as shown in Fig. 2.29.

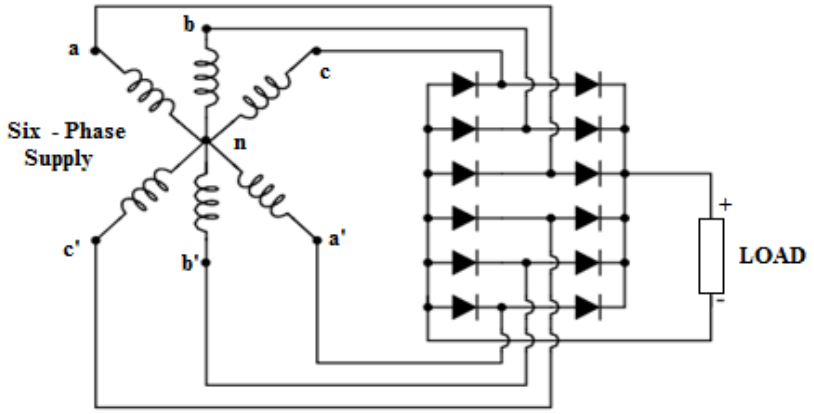

Fig.2.29 Six-phase full-wave rectifier.

The conduction period for each two diodes will be 30˚ in this case. The six voltages to neutral will be:

$$v_a = V_m \sin \omega t \quad , \quad v_{a'} = V_m \sin(\omega t - 180°)$$

$$v_b = V_m \sin(\omega t - 60°) \quad , \quad v_{b'} = V_m \sin(\omega t - 240°)$$

$$v_c = V_m \sin(\omega t - 120°) \quad , \quad v_{c'} = V_m \sin(\omega t - 300°)$$

$$v_{ab} = V_m \sin \omega t - V_m \sin(\omega t - 60°)$$

$$v_{ab} = V_m[\sin \omega t - (\sin \omega t \cos 60° - \cos \omega t \sin 60°)]$$

$$v_{ab} = V_m[\frac{1}{2}\sin \omega t + \frac{\sqrt{3}}{2}\cos \omega t]$$

$$= V_m[\sin \omega t \sin 30° + \cos \omega t \cos 30°]$$

$$\therefore \quad v_{ab} = V_m \cos(\omega t - 30°) \qquad (2.74)$$

2.6 GENERAL FORMULA FOR THE OUTPUT VOLTAGE OF A P-PULSE UNCONTROLLED RECTIFIER

A general expression for the average d.c. output voltage can be derived for any number of phases (p-pulse) when the load is connected between the cathode rail of the converter and the neutral of the transformer secondary.

Let us consider a p-phase rectifier having maximum voltage V_m / phase. The waveform of the output voltage will be as shown in Fig.2.30.

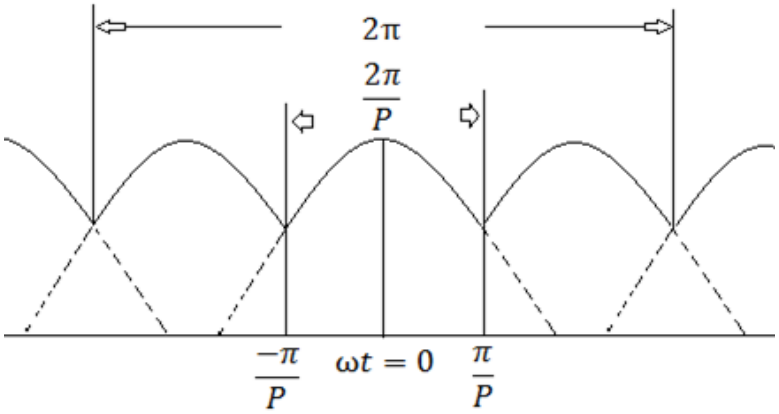

Fig.2.30 P-phase rectifier voltage waveforms .

The average d.c. voltage V_{dc} is,

$$V_{dc} = \frac{1}{\frac{2\pi}{\mathrm{p}}} \int_{(-\frac{\pi}{\mathrm{p}})}^{(+\frac{\pi}{\mathrm{p}})} \mathrm{V_m} \cos \omega t \, d\omega t$$

$$= \left(\frac{\mathrm{p}}{2\pi}\right) \mathrm{V_m} \left[\sin\left(\frac{\pi}{\mathrm{p}}\right) - \sin(-\frac{\pi}{\mathrm{p}})\right] \quad = \frac{\mathrm{P\,V_m}}{2\pi}\left[2 \sin \frac{\pi}{\mathrm{P}}\right]$$

$$\therefore V_{dc} = \frac{p}{\pi} V_m \sin\frac{\pi}{p} \qquad (2.75)$$

For a three-phase, half-wave circuit, p = 3, hence,

$$V_{dc} = \frac{3}{\pi} V_m \sin\frac{\pi}{3} = \frac{3\sqrt{3}V_m}{2\pi}$$

which is the same result as that given in Eq. (2.62).

2.6.1 Output Current of P-Pulse Converter

The current in p-pulse rectifier is supplied by each phase of the transformer secondary windings for a period of 2π/p only of each cycle. Hence the secondary current is a train of pulses as shown in Fig.2.31.

The mean current per phase - *a*

$$I_{d(av)} = \frac{1}{2\pi}\int_0^{2\pi/p} I_{dc}\, d\omega t$$

Fig.2.31.

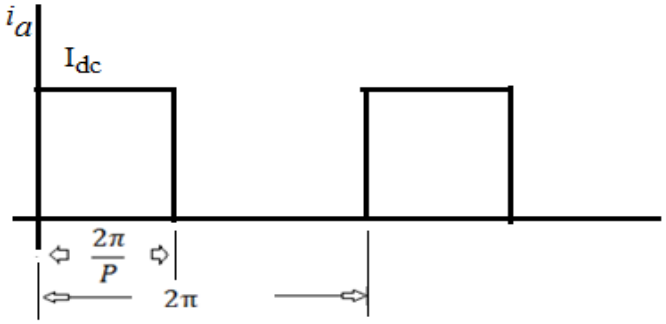

$$I_{d(av)} = \frac{I_{dc}}{p} \qquad (2.76)$$

The *rms* current, I_{rms} , per phase is,

$$I_{arms} = \sqrt{\frac{1}{2\pi}\int_0^{2\pi/p} I_{dc}^2\, d\omega t} \quad = \frac{I_{dc}}{\sqrt{p}} \qquad (2.77)$$

Hence for 6 – pulse converter

$$I_{arms} = \frac{I_{dc}}{\sqrt{6}} \qquad (2.78)$$

For 12 – pulse converter

$$I_{arms} = \frac{I_{dc}}{\sqrt{12}} = \frac{I_{dc}}{\sqrt{2}\sqrt{6}} \qquad (2.79)$$

So for the 12- pulse converter I_{arms} decreases by factor of $\sqrt{2}$, but twice as many devices , each device carries the full current for half the time; and ohmic loss in devices, transformers lines depends on the *rms* value of the current itself.

2.6.2 Power Factor of a P-Pulse Rectifier

The power factor of a rectifier is , as defined before, is the ratio of power output in watt and the volt-amperes drawn from the supply, hence,

$$PF = \frac{\text{Watts output}}{\text{Volt Amperes supplied}} = \frac{\mathrm{V_{dc}I_{dc}}}{\mathrm{p}\frac{\mathrm{V_m}}{\sqrt{2}}\mathrm{I_{arms}}}$$

$$\therefore \quad PF = \frac{\frac{p}{\pi}\, V_m\sqrt{p}\; I_{arms}\sin\frac{\pi}{p}}{p\frac{V_m}{\sqrt{2}}I_{arms}} = \frac{\sqrt{2p}}{\pi}\sin\frac{\pi}{p} \qquad (2.80)$$

Example 2.7

A three-phase (3-pulse) half-wave uncontrolled rectifier supplies a load of 5 kW at 240 V. Detrmine the rating of the secondary winding of the supply transformer and the input power factor.

Solution

For 3-pulse rectifier, the average output d.c. voltage of the rectifier V_{dc} is,

$$V_{dc} = \frac{3}{\pi}\, V_m\, \sin\frac{\pi}{3} = \frac{3\sqrt{3}V_m}{2\pi} = 240 \text{ V}$$

$$240 = \frac{3\sqrt{3}V_m}{2\pi} \quad \rightarrow \quad V_m = \frac{2\pi \times 240}{3\sqrt{3}} = 290 \text{ V}$$

The *rms* value of the supply voltage is

$$V_s = \frac{V_m}{\sqrt{2}} = 205.14 \text{ V}$$

$$\text{Output current} \quad I_{dc} = \frac{5000}{240} = 20.8 \text{ A}$$

The *rms* value of the secondary phase current, I_{arms} ,

$$I_{arms} = \frac{I_{dc}}{\sqrt{p}} = \frac{20.8}{\sqrt{3}} = 12 \text{ A}$$

Transformer rating per phase = $V_s I_{arms} = 205.14 \times 12 = 2461.68$ VA

Total transformer rating in kVA = $2461.68 \times 3 = 7.385$

$$PF = \frac{\sqrt{2p}}{\pi}\sin\frac{\pi}{p} = \frac{\sqrt{2\times 3}}{\pi}\sin\frac{\pi}{3} = 0.675$$

2.7 HARMONIC ANALYSIS OF P-PULSE UNCONTROLLED RECTIFIER

The output voltage waveform $v_o(\omega t)$ of a p-pulse converter shown in Fig.2.30 may be represented in terms of its harmonic components using Fourier series as,

$$v_o(\omega t) = a_0 + \sum_{n=1}^{\infty} a_0 \cos(n\omega t) + \sum_{n=1}^{\infty} b_n \sin(n\omega t)$$

where , a_o , a_n and b_n are the Fourier coefficient that may be written as:

$$a_0 = \frac{1}{\omega t}\int_{-\frac{\omega t}{2}}^{\frac{\omega t}{2}} v(\omega t)d\omega t$$

,

$$a_n = \frac{2}{\omega t}\int_{\frac{-\omega t}{2}}^{\frac{\omega t}{2}} v(\omega t)\cos(\omega t)\, d\omega t$$

$$b_n = \frac{2}{\omega t}\int_{\frac{-\omega t}{2}}^{\frac{\omega t}{2}} v(\omega t)\sin(\omega t)\, d\omega t = 0$$

for function $f(\omega t)$ symmetrical about $\omega t = 0$ (even function harmonic series only).

$$a_0 = V_m \frac{p}{\pi} sin\frac{\pi}{p} \qquad \therefore V_{dc} = a_0 = \frac{p}{\pi}\, V_m\, \sin\frac{\pi}{p} \qquad (2.81)$$

This result is the same as that given in Eq.(2.75).
For evaluating, a_n, regain integration productivity

$\int \cos(\omega t)\cos(n\omega t)\, d\omega t.$

Now $\int udv = vu - \int v.du$ (integration by parts)

$\int \cos(\theta)\cos(n\theta)\,d\omega t.$ cos (θ) =dv, $\cos(n\theta) = u$

$$\int \cos(\theta)\cos(n\theta)\,d\omega t. = \sin(\theta)\cos(n\theta) + n\int sin\,(\theta)\sin(n\theta)\,.d\theta$$

Also $\sin(\theta) = dv$, $\sin(n\theta) = u$

So

$$\int sin\,(\theta)\sin(n\theta)\,.d\theta = -\cos(\theta)\sin(n\theta) - n\int(-\cos(\theta))\cos(n\theta)\,.d\theta$$

$$\therefore \int \cos(\theta)\cos(n\theta)\,d\omega t = \sin(\theta)\cos(n\theta) + n[-\cos(\theta)\sin(n\theta) + \int \mathrm{ncos}(n\theta)\mathrm{cos}(\,\theta).d\theta$$

$$\therefore \int \cos(\theta)\cos(n\theta)\,d\omega t = \frac{1}{n^2-1}[ncos(\theta)\sin(n\theta) - \sin(\theta)\cos(\theta)]$$

$$\therefore a_n = \frac{p}{\pi}\int_{\frac{-\pi}{P}}^{\frac{\pi}{P}} v_m\cos(\omega t)\cos(n\omega t)\,.d\omega t$$

$$= \frac{V_m p}{\pi(n^2-1)}[ncos(\omega t)\sin(\omega t) - \sin(\omega t)\cos(\omega t)]_{\frac{-\pi}{P}}^{\frac{\pi}{P}}$$

$$= \frac{V_m p}{\pi(n^2-1)}\left[ncos\left(\frac{\pi}{P}\right)\sin\left(\frac{\pi}{P}\right) - \sin\left(\frac{\pi}{P}\right)\cos\left(\frac{\pi}{P}\right) - \sin\left(\frac{\pi}{P}\right)\cos(n\left(\frac{\pi}{P}\right)\right.$$
$$\left. -ncos\left(-\frac{\pi}{P}\right)\sin\left(n\left(-\frac{\pi}{P}\right) + sin\left(-\frac{\pi}{P}\right)cos\left(n\left(-\frac{\pi}{P}\right)\right)\right)\right]$$

Now n = cp , i.e. a multiple of p.

$$\therefore \sin\left(\frac{n\pi}{P}\right) = 0, \qquad \cos\left(\frac{n\pi}{p}\right) = \pm 1$$

$$a_n = \frac{V_m p}{\pi(n^2-1)}\left[-\sin\left(\frac{\pi}{P}\right)\cos\left(n\frac{\pi}{P}\right) - \sin\left(\frac{\pi}{P}\right)\cos\left(n\frac{\pi}{P}\right)\right]$$

$$= -\frac{P}{\pi}V_m\sin\left(\frac{\pi}{P}\right)\frac{2\cos\left(\frac{n\pi}{P}\right)}{(n^2-1)} \qquad (2.82)$$

The amplitude c_n of the n[th] order harmonic is:

$$c_n = \sqrt{{a_n}^2 + {b_n}^2} = \sqrt{{a_n}^2 + 0} = a_n \qquad (2.83)$$

The phase angle ψ_n of the n[th] order harmonic is:

$$\psi_n = \tan^{-1}\frac{a_n}{b_n} = \tan^{-1}\frac{a_n}{0} = \infty \qquad \therefore \psi_n = 90°. \tag{2.84}$$

Application of the general equation to single-phase full wave:

For P =2 full wave single-phase converter, applying Eq. (2.75) yields

$$a_0 = V_m\left(\frac{2}{\pi}\right)\sin\left(\frac{\pi}{2}\right) = \frac{2V_m}{\pi}$$

.

$$a_n = -\frac{2P}{\pi}\left(\frac{V_m}{n^2-1}\right)\sin\left(\frac{\pi}{P}\right)\cos\left(n\frac{\pi}{P}\right)$$

$$= \frac{-4}{\pi}\left(\frac{V_m}{n^2-1}\right)\sin\left(\frac{\pi}{2}\right)\cos\left(n\frac{\pi}{2}\right)$$

and $c_n = \dfrac{-4V_m}{(n^2-1)}$

$$\therefore v_0(\omega t) = \frac{2V_m}{\pi} - \frac{4V_m}{3\pi}\cos(2\omega t) + \frac{V_m}{15T}\cos(4\omega t) - \frac{4V_m}{35\pi}\cos(6\omega t) + \cdots \tag{2.85}$$

which is the same as that obtained in Eq.(2.55). The amplitude of the fundamental component is: c_1= 0, since the function contains even harmonics only. Harmonic spectra for the output voltage waveform for 3- pulse (p = 3) , and 6-pulse (p = 6) converters are shown in Fig. 2.32 . It is clear that as the number of pulses is increased, the value of the output d.c. voltage is increased. The second order harmonic is also increased significantly, however, the higher order even harmonics are increased also but their increasing is small compared with the second harmonic.

Now if the number of pulse is increased to 12 , the d.c. value will not increase a lot as expected, and the second harmonic remains the dominant one in the spectrum beside the d.c. component. This shown in Fig.33 which gives the frequency spectra of the output voltage for 12-pulse converter.

2.8 USES OF POLY-PHASE UNCONTROLLED RECTIFIERS

Uncontrolled rectifiers are extensively used in a number of power electronic based converters. In most cases, they used to provide an intermediate unregulated d.c. voltage source, which is further processed to obtain a regulated d.c. or a.c. output. They have, in general, been proved efficient and robust power stages. However, they suffer from few distinct

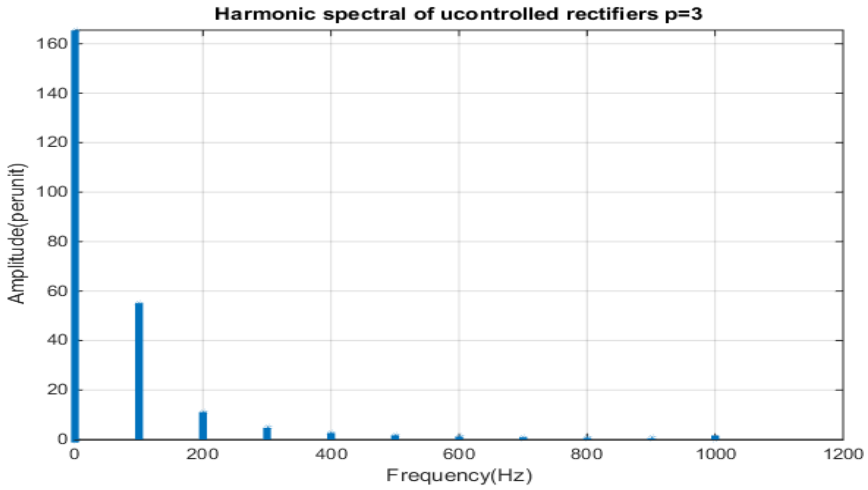

n	0	2	4	6	8	10	12	16	20
Hz	0	100	200	300	400	500	600	800	1000
c(n)	165.372	55.1241	11.0248	4.72492	2.62496	1.67043	1.15645	0.64852	0.41447

(a)

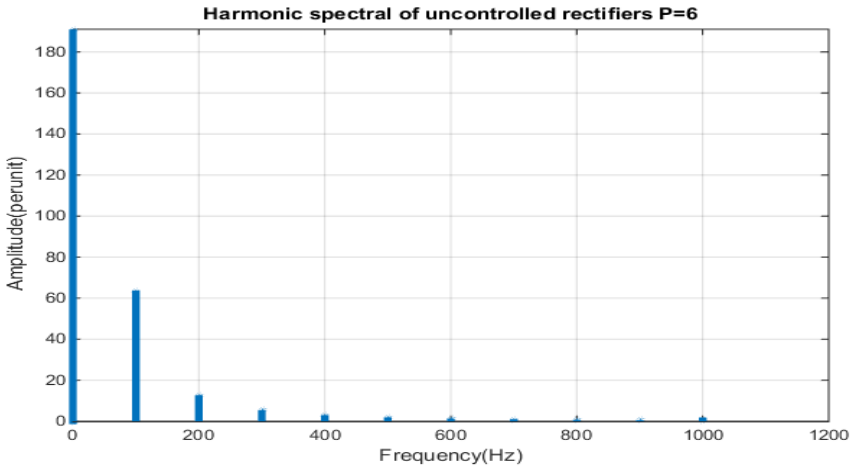

n	0	2	4	6	8	10	12	16	20
Hz	0	100	200	300	400	500	600	800	1000
c(n)	190.979	63.6596	12.7319	5.45654	3.03141	1.92908	1.33552	0.74894	0.47864

(b)

Fig.2.32 Harmonic frequency spectra for the output voltage waveform for: (a) 3-pulse (p =3), and (b) 6-pulse (p = 6) converters.

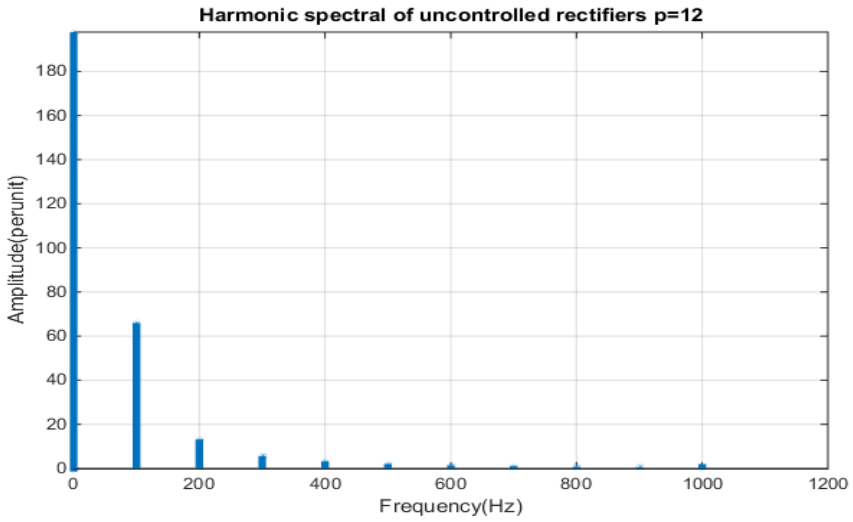

n	0	2	4	6	8	10	12	16	20
Hz	0	100	200	300	400	500	600	800	1000
c(n)	197.721	65.9071	13.1814	5.64918	3.13843	1.99719	1.38267	0.77538	0.49554

Fig.2.33 Harmonic spectra for the output voltage waveform for the 12-pulse converters (p = 12).

disadvantages. The main among them is their inability to control the output d.c. voltage / current magnitude when the input a.c. voltage and load parameters remain fixed. They are also unidirectional in the sense that they allow electrical power to flow from the a.c. side to the d.c. side only. These two disadvantages are the direct consequences of using power diodes in these converters, which can block voltage only in one direction.

It has been shown in the analysis carried on in this chapter that, the output d.c. voltages for half-wave and full-wave three-phase rectifier circuits in terms of the *rms* value of the supply phase voltages are 1.17 V_s and 2.34V_s respectively. Apart from greatly increasing the output voltage, using three-phase rectification reduces the magnitude of the ripple voltage and increases its frequency to either three (for half-wave) or six (for the full-wave) times the supply frequency.

Hence, poly-phase rectifiers are only used where the efficiency of rectific- ation is more important than the cost of the rectifier itself. This is generally the case when the output d.c. power of the rectifier exceeds about 11kW. Many industrial plants, broadcast, and television stations requiring up to 20,000 volts d.c. at peak currents of 10A or more utilize poly-phase rectifiers. Poly-phase circuits have also the advantage over single-phase types of developing fairly steady output d.c. voltages that requires little filtering.

2.9 THE FREEWHEELING DIODE

The operation of both single-phase and poly-phase circuits is normally modified by including a freewheeling diode across the load whenever the load is inductive. This diode blockes the flow of rectifier current but allows the load current to circulate during period of negative supply voltage. Fig.2.34 shows a simple single-phase, half-wave rectifier with inductive load and freewheeling diode. When the freewheeling diode

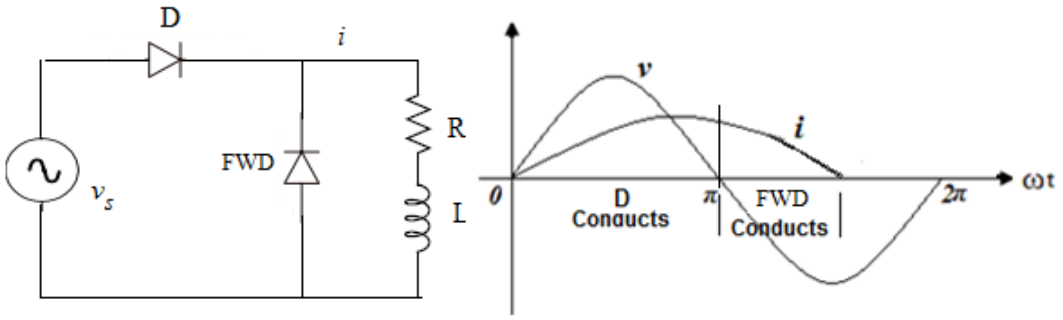

Fig.2.34 The freewheel diode FWD.

FWD is removed from the circuit, the inductive load maintains a continuous current and forces rectifier current flow during periods of negative output voltage. When the freewheeling diode is connected to the circuit, it immediately comes into conduction whenever the supply voltage reverses.This allows the load current which is maintained by the load *emf* to circulate during period of negative supply voltage at the load and the rectifier current becomes zero. The load is effectively short circuited by the freeeheeling diode until suplly voltage becomes positive.

For all the above circuits the d.c. output voltage is directly proportional to the a.c. supply voltage and it cannot be regulated or controlled. By replacing the simple diodes by thyristors (SCRs) such control becomes possible.

PROBLEMS

2.1 A circuit consists of a resistor R ,inductor L and diode D in series , supplied from an ideal source of instantaneous value $v = V_m \sin\omega t$.

(a) Derive an expression for the time variation $i(\omega t)$ of the instantaneous current in terms of V_m , ($Z=\sqrt{R^2 + X^2}$) and $\emptyset = \tan^{-1} \omega L/R$.

(b) Sketch roughly to scale ,consistent time variations of v , i and the inductor induced *emf* v_L if $\emptyset = 60°$.

(c) Show that , with a load time constant $\tau = L/R$, the instant of the cycle when the inductor *emf* is zero is given by the transcendental equation

$$\cos(\omega t - \emptyset) = \cos\emptyset\, e^{-t/\tau}$$

2.2 For the half-wave uncontrolled rectifier circuit supplying a series resistive-inductive load shown in Fig.2.35. The supply voltage is $v = \sqrt{2}\times 220 \sin\omega t$ and the supply frequency is 50 Hz and the load parameter values are: R =10 Ω , and X_L = 20 Ω . The current i for the conduction interval $\omega t = 0$ to $\omega t = \beta$ is given by:

$$i(\omega t) = \frac{V_m}{|z|}[\sin(\omega t - \theta) + sin\theta e^{-cot\theta\,.\omega t}]$$

where $|z| = \sqrt{R^2 + (\omega L)^2}$ and $\tan\theta = \omega L/R$

(a) Sketch the load voltage and current waveforms.
(b) Calculate the current extinction angle β.
(c) Calculate the average d.c. load voltage V_{dc}.

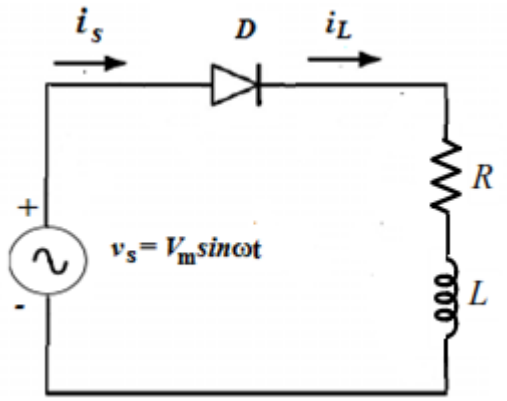

Fig.2.35.

[Ans: β =249.25° , V_{dc} = 64.69 V]

2.3 A single-phase half-wave uncontrolled rectifier supplied from 70 V a.c. supply is used to charge a 50 V battery through a 10 Ω resistance as shown in Fig.2.36. Determine the average value of the current in the circuit.

[Ans: 1.053 A]

Fig.2.36.

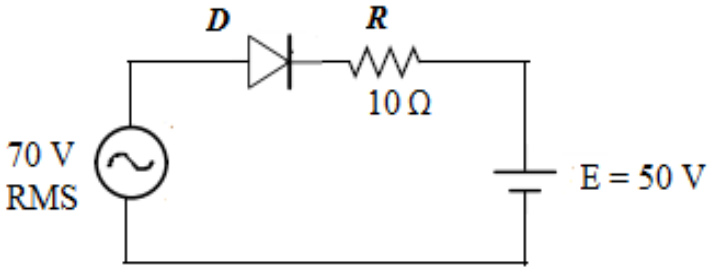

2.4 An ideal single-phase source, 230 V, 50 Hz, supplies power to a load resistor R = 40 Ω via a single ideal diode. Calculate the average and *rms* values of the current and the power dissipation. What must be the rating of the diode?

[Ans: I_{dc} =2.59 A, I_{Lrms} = 2.875 A , P_L = 330.6 W , I_D = 3 A , V_D = 400 V]

2.5 A single-phase, full-wave diode bridge is used to supply power to a resistive load of value R = 75 Ω. If the supply voltage is sinusoidal, v_s = 400 sin ωt, calculate the average and rms values of the load current. Calculate the ripple factor for the load current and compare this with half-wave operation.

[Ans : 7.63A , I_L = 8.5 A , RF = 0.487 compared with 1.21 for half-wave operation]

2.6 Derive expressions for the average and *rms* currents for a single-phase, full-wave uncontrolled diode bridge circuit loaded with pure resistive load. Show that the ripple factor is less than the value for half-wave uncontrolled rectifier circuit with resistive load. What is the ideal value of ripple factor?

2.7 A single-phase supply $v_s = V_m$ sin ωt supplies power to a resistor R through an ideal diode. Show that the load voltage $v_L(\omega t)$ can be represented by the Fourier series

$$v_L(\omega t) = V_m\left(\frac{1}{\pi} + \frac{1}{2}\sin\omega t - \frac{2}{3\pi}\cos 2\omega t + \cdots.\right)$$

2.8 A single-phase supply v_s = √2 × 240 sin ωt, 50 Hz, supplies power to an *R-L* through an ideal diode as shown in Fig.2.37.

(a) Sketch , approximately to scale for at least two cycles , the waveforms for v_s , v_o and i_o given that the current i_o conducts for 222° before it goes zero. Neglect source impedances.

(b) Show that average value of the output voltage is: V_o = 95.4V.

Fig.2.37.

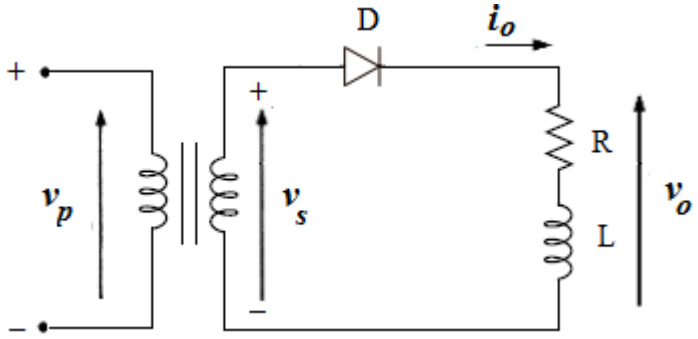

2.9 For a single-phase, half-wave diode rectifier circuit with resistive load and supply voltage $v_s = V_m \sin \omega t$, obtain an expressions for the Fourier coefficients a_1, b_1 and c_1 of the fundamental component of the load current.

2.10 For the circuit shown in Fig.2.38 ,

(a) If the current is assumed to be continuous, prove that the load current i_o is given by

$$i_o = \frac{V_m}{\sqrt{R^2 + (\omega L)^2}}\left[\sin(\omega t - \theta) + \frac{2}{1 - e^{-(R/L)(\frac{\pi}{\omega})}} \sin\theta \; e^{-(R/L)t}\right]$$

where

$$\theta = \tan^{-1}\frac{\omega L}{R}$$

Fig. 2.38.

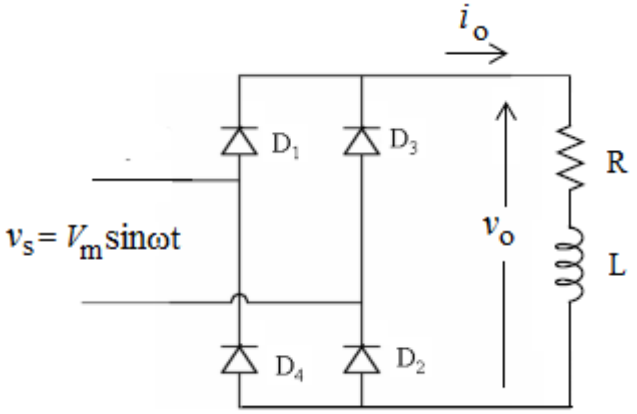

(b) If the current is assumed to be discontinuous starting from zero , prove that the load current i_o is given by

$$i_o = \frac{V_m}{\sqrt{R^2 + X^2}}\left[\sin(\omega t - \theta) + \sin\theta \; e^{-(R/L)t}\right]$$

2.11 A single-phase full-wave uncontrolled bridge rectifier is supplying a highly inductive load (L/R ratio is very large), the load current is assumed to be smooth and ripple-free. If the supply voltage is 220 V, 50 Hz, and the inductor load resistance $R = 22\ \Omega$, Calculate:

(a) The average output voltage V_{dc} and current I_{dc}.

(b) The *rms* value of the output voltage V_{orms} and current I_{orms} .

(c) The *rms* value of the diode current I_{Drms} and the *PRV* of each diode.

[Ans: (a) 198.1 V, 9 A , (b) 220 V, 10 A , (c) 4.5 A, 155.5 V]

2.12 Repeat problem (2.11) with Bi-phase rectifier type and compare your results.

2.13 A single-phase, full-wave, uncontrolled diode bridge rectifier is used to supply to an inductive load with a resistive component of 20 Ω and inductance of 50 mH from a 240 V (*rms*), 50 Hz supply. The electrical diagram is as shown in Fig.2.39. Use the current formula obtained in Problem 2.10,

(a) Calculate the average output current and voltage supplied to the load, ignore the voltage drops across the diodes.

(b) Calculate the new value of the average output current if the load resistor is halved while retaining the same circuit parameters as before. Comment on the results.

Fig.2.39.

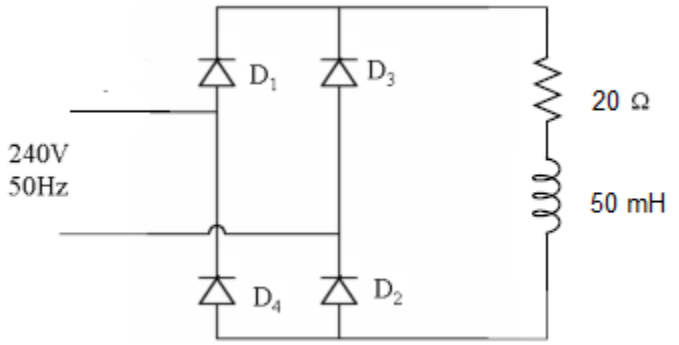

[Ans: (a) 10.8A, (b) 5.4A]

2.14 An electroplating bath is to be supplied from a single-phase full wave rectifier. The load requires 10 A at 100 V. The a.c. supply is from the 230 V mains. Produce the design details of using bi-phase and bridge rectifier circuits and compare the two designs. Assume the load is highly inductive such that the current is continuous and ripple free, and the voltage drop across the diode is neglected.

[Ans: Bi-Phase rectifier: PRV = 314V, Transformer kVA = 1570, I_{Drms} = 7.07A, I_{Ddc} = 5A, Bridge rectifier: PRV = 157V, I_{Drms} = 7.07A, Transformer kVA = 1110]

2.15 Develop expressions for average and *rms* load voltages for a three-phase half-wave uncontrolled rectifier connected to a resistive load.

2.16 Compare the power factor of the 3-phase bridge rectifier supplied from a Y-connected supply with that of a single-phase bridge rectifier. Assume ripple-free load current in each case.

2.17 A three-phase, half-wave uncontrolled rectifier shown in Fig.2.40 contains three ideal diodes and is fed from an ideal three-phase voltage source of 380V (*rms*, line-to-line), 50 Hz. The load is resistive with R =15 Ω. Calculate:

(a) The average output voltage and average load current of the rectifier.
(b) The d.c. and a.c. power dissipations in the load.
(c) The diode ratings.
(d) What is the lowest ripple frequency of the output voltage waveform.

Fig.2.40.

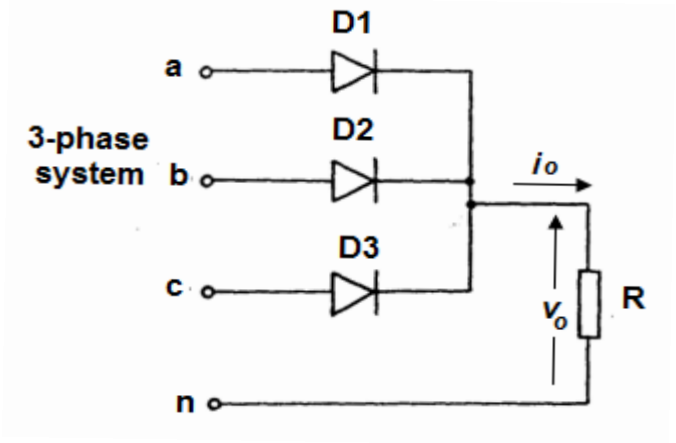

[Ans: (a) 256.5V, 17.1A, (b) P_{dc}= 4388W, P_{ac} = 4525.6W, (c) I_D= 10A, V_D = PRV= √3 V_m= 537.3 (say 600V), (d) Lowest ripple = 3f =150Hz]

2.18 Using notation of Fig.2.30 show that for the case of uncontrolled rectification (α = 0) the harmonic of the d.c. voltage produced by an a.c. to d.c. converter with continuous d.c. current flow are contained in the following expression for d.c. voltage :

$$v(\omega t) = V_m \frac{p}{\pi} \sin\frac{\pi}{p}\left[1 - \sum_{n=1}^{n=\infty} \frac{2\cos n\pi/p}{n^2-1}\cos n\omega t\right]$$

where V_m is the peak value of the transformer secondary voltage per-phase.
p is the pulse number.
N= cp with c is a positive integer.

2.19 Power is supplied to a load resistor *R* from a three-phase, zero-impedance supply of balanced sinusoidal voltages, using full-wave uncontrolled bridge circuit of Fig.2.41. The six diodes may be considered as ideal switches.

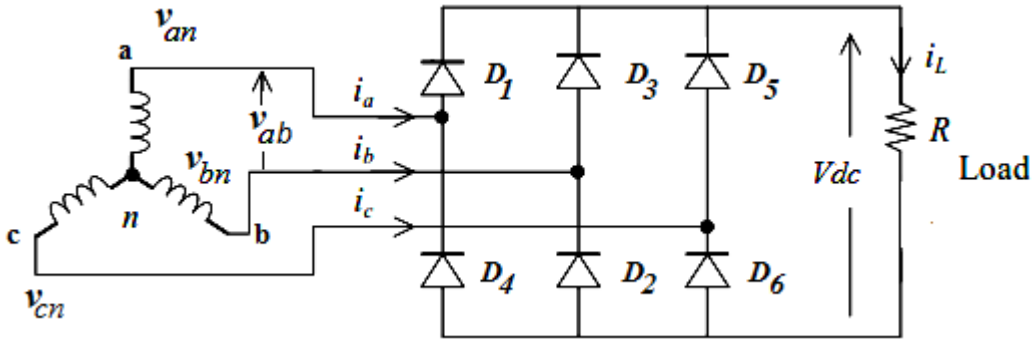

Fig.2.41.

(a) If the supply voltage for phase- a is $v_{an} = V_m \sin \omega t$, and the line- to -line voltage is

$$v_{ab}(\omega t) = \sqrt{3}\, V_m sin\left(\omega t + \frac{\pi}{6}\right) ,$$

show that the average value of the load current is given by :

$$I_{dc} = \frac{3\sqrt{3}V_m}{\pi R}$$

(b) Calculate V_{dc}, I_{dc} and P_{dc} if $V_m = 300$ V, $R = 50\ \Omega$.

[Ans : (b) $V_{dc} = 496.43$ V, $I_{dc} = 9.92$ A , $P_{dc} = 4928.8$ W]

2.20 A three-phase, full-wave uncontrolled bridge rectifier contains six ideal diodes and is fed from an ideal three-phase voltage source of 240 V, 50 Hz. The load is resistive with R =10 Ω. Calculate the average load voltage and the power dissipation. Also calculate the required voltage and current ratings of the diodes.

[Ans: $V_{dc} = 324$ V, $P_{dc} = 10.497$ kW, $I_{Drms} = 18.7$ A, V_D =339.4 V]

Test Questions

Mark the correct answer:

2.21 In a single phase uncontrolled half-wave rectifier, if the *rms* value of the input voltage is $V_s = 220$ V, the average d.c. voltage is

(a) 104V (b) 120V (c) 99V (d) 85V

2.22 In a single-phase full-wave uncontrolled bridge rectifier supplying resistive load, if the input voltage is v_s =311sinωt, then the average output voltage is

(a) 209 (b) 106 V (c) 198 V (d) 99 V

2.23 Each diode of a three-phase half-wave uncontrolled rectifier conducts for:

(a) 60 (b) 120° (c) 180° (d) 90°.

2.24 In a Bi-phase full-wave uncontrolled rectifier, if per-phase *rms* input voltage is 230 V, then the average output voltage is

(a) 257.3 V (b) 116.95 V (c) 207.00 V (d) 101.28 V

2.25 The supply voltage for a single-phase half-wave uncontrolled rectifier is v_s = 220√2 sin314t. The rectifier is loaded with resistive load R = 10 Ω. The d.c. power absorbed by the load is

(a) 980.1 W (b) 875.9 W (c) 1073.0 W (d) 790.9 W

2.26 In a single-phase full-wave uncontrolled rectifier supplying resistive load, the input voltage has an *rms* value of 250 V, if the load is resistive with R = 25 Ω , then the average current I_{dc} is

(a) 4A (b) 9A (c) 15 A (d) 20A

2.27 In a three-phase full-wave uncontrolled bridge rectifier, if per-phase peak input voltage is V_m , the average output voltage is given by

(a) $V_m/2\pi$ (b) $\sqrt{3}V_m/2\pi$ (c) $3\sqrt{3}V_m/4\pi$ (d) $3\sqrt{3}V_m/\pi$

2.28 Each diode of a hexa-phase uncontrolled diode rectifier conducts for:

(a) 60° (b) 120° (c) 180° (d) 90°

2.29 In a three-phase half-wave uncontrolled rectifier, if per-phase peak input voltage is V_m , then the average output voltage is given by

(a) $V_m/2\pi$ (b) $\sqrt{3}V_m/2\pi$ (c) $3\sqrt{3}V_m/\pi$ (d) $3\sqrt{3}V_m/2\pi$

[Ans : 2.21(**c**) , 2.22 (**c**) , 2.23 (**b**), 2.24 (**c**) , 2.25 (**a**) , 2.26(**b**) , 2.27 (**d**), 2.28 (**a**), 2.29 (**d**)]

CHAPTER THREE

AC-DC CONVERSION: CONTROLLED RECTIFICATIONS

3.1 INTRODUCTION

The disadvantages of the uncontrolled rectifiers discussed in the previous chapter are overcome if the diodes are replaced by controllable power semiconductor switch; the resulting converters are called controlled converters. In Controlled Rectifications, the generated d.c. power is controllable and variable. They usually use SCRs as their power switches. For fast switching operation, MOSFETs and IGBTs are used. The following sections deal with the basic operation of some examples of controlled rectifiers starting with the simplest type which is the single-phase half-wave controlled rectifier loaded with resistive load.

3.2 SINGLE-PHASE, HALF-WAVE, CONTROLLED RECTIFIER LOADED WITH PASSIVE LOADS

3.2.1 Case of Resistive Load

Fig.3.1(a) shows the basic circuit for a single-phase, half-wave, controlled rectifier loaded with a resistive load. For this configuration, during the positive half cycle of the supply voltage v_S , the anode of the thyristor is connect to the positive terminal of the supply, the cathode is connect to negative terminal of supply, and the thyristor is forward biased. Hence, the thyristor will conduct only when triggered using gate pulses.

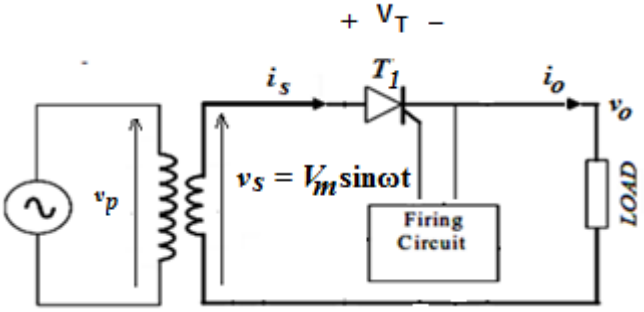

(a) Circuit

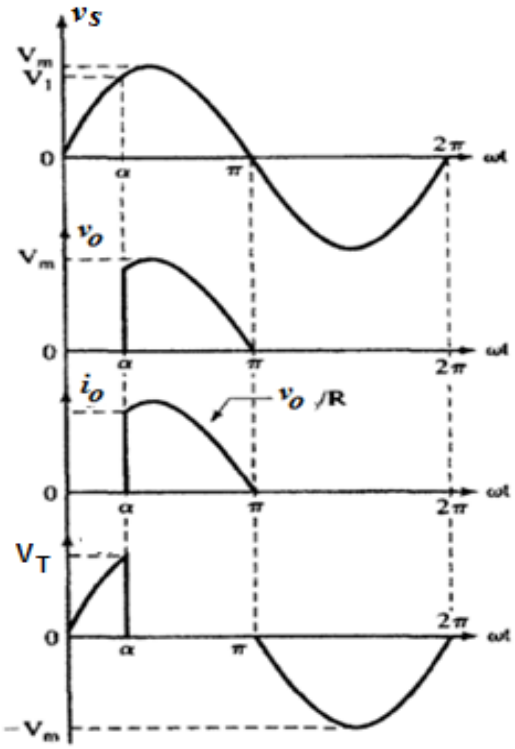

(b) Waveforms.

Fig.3.1 Single-phase half-wave controlled rectifier.

The thyristor is fired at ωt = α, and the input voltage appears across the load. The voltage across the thyristor collapses to almost zero and the full supply voltage appears across the load. From this point onwards, the load voltage follows the supply voltage. The load being purely resistive the load current i_o is proportional to the load voltage.

At ωt = π, T_1 is reverse-biased by the negative half-cycle of the supply and during the period $\pi < \omega t \leq 2\pi$, the thyristor is turned off and blocks the supply voltage and the load voltage remains zero as shown in Fig.3.1(b). Consequently, no load current flows during this interval. Since the output voltage and current are both positive, the converter is said to operate in the first quadrant. This converter is not normally used in the industrial application because of its high ripple current and low ripple frequency. The waveforms for one total period of operation of this circuit are shown in Fig.3.1(b).

The average value of the load voltage V_{dc} can be calculated as follows:

$$V_{dc} = \frac{1}{2\pi}\int_{\alpha}^{\pi} v_s\,(\omega t)d\omega t = \frac{1}{2\pi}\int_{\alpha}^{\pi} V_m sin\omega t\, d\omega t$$

$$\therefore \; V_{dc} = \frac{V_m}{2\pi}(-cos\pi + cos\alpha) = \frac{V_m}{2\pi}(1 + cos\alpha) \qquad (3.1)$$

Therefore, the average output voltage can vary from 0 to V_m/π and the average load current will vary from 0 to $V_m/\pi R$ when varying α from π to 0, respectively.
Since the load is resistive, therefore the load voltage and current are in phase and they are related by $i = v/R$. Consequently, the average value of the load current I_{dc} is

$$I_{dc} = \frac{V_{dc}}{R} = \frac{V_m}{2\pi R}(1 + cos\alpha) \qquad (3.2)$$

The output d.c. power is given by:

$$P_{dc} = V_{dc}I_{dc} = \frac{V_{dc}^2}{R} \qquad (3.3)$$

The *rms* value of the load voltage V_{orms} can be calculated as follows:

$$V_{orms} = \sqrt{\frac{1}{2\pi}\int_{\alpha}^{\pi} v_s^2\,(\omega t)d\omega t} = \sqrt{\frac{1}{2\pi}\int_{\alpha}^{\pi}(V_m sin\omega t)^2\,d\omega t}$$

$$= \sqrt{\frac{(V_m)^2}{2\pi}\int_{\alpha}^{\pi}\frac{1}{2}(1 - cos2\omega t)d\omega t}$$

$$= \frac{V_m}{2}\sqrt{\frac{1}{\pi}(\pi - \alpha + \frac{1}{2}sin2\alpha)} \qquad (3.4)$$

$$\text{since}: \quad (\sin\omega t)^2 = \frac{1}{2}(1 - cos2\omega t)$$

Therefore the *rms* value of the load current I_{orms} is :

$$I_{orms} = \frac{V_{orms}}{R} = \frac{V_m}{2R}\sqrt{\frac{1}{\pi}(\pi - \alpha + \frac{1}{2}sin2\alpha)} \qquad (3.5)$$

The output a.c. power is given by:

$$P_{ac} = V_{orms}I_{orms} = \frac{V_{orms}^2}{R} = \frac{(0.5V_m)^2}{R} \qquad (3.6)$$

The *PRV* of the thyristor for this configuration is V_m.

To find the power factor of the circuit, the current drawn from the source i_s is the same as the load current. Hence,

$$P_{ac} = V_{orms} I_{orms}$$

$$PF = \frac{P_{ac}}{S} \quad , \text{ but } \quad S = V_s\, I_{orms}$$

$$\text{Hence} \quad PF = \frac{V_{orms} I_{orms}}{V_s\, I_{orms}} = \frac{V_{orms}}{V_s}$$

$$= \frac{V_m}{2V_s}\sqrt{\frac{1}{\pi}(\pi - \alpha + \frac{1}{2}sin2\alpha)}$$

$$= \frac{\sqrt{2}V_s}{2V_s}\sqrt{\frac{1}{\pi}(\pi - \alpha + \frac{1}{2}sin2\alpha)}$$

$$\therefore \quad PF = \sqrt{\frac{1}{2\pi}(\pi - \alpha + \frac{1}{2}sin2\alpha)} \qquad (3.7)$$

3.2.2 Single-Phase, Half-Wave, Controlled Rectifier Loaded with Series Resistive – Inductive Load

Fig.3.2 shows a single-phase half-wave controlled rectifier with *R-L* load. This circuit is the same as that of Fig.3.1(a) except that the load consists of a resistor and inductor connected in series. At ωt = α, the voltage across the load will be the instantaneous value of the supply voltage at this firing angle. At this instant, because of the existence of the inductor, the current will increase slowly in the same manner as the diode case discussed in ChapterTwo. The load voltage and current waveforms are as depicted in Fig.3.3.

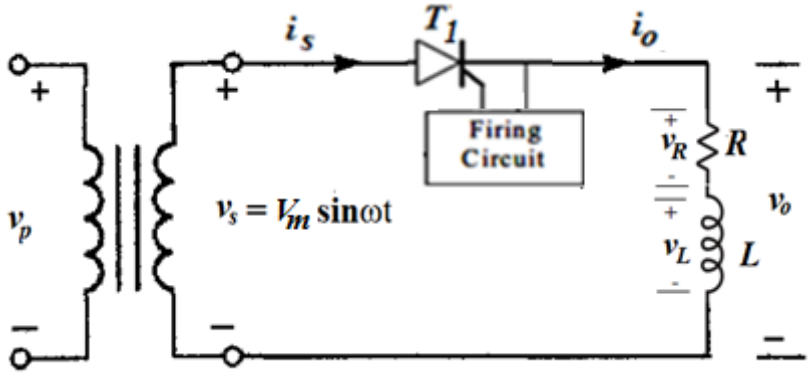

Fig.3.2 Single-phase half-wave controlled rectifier with series *R-L* load.

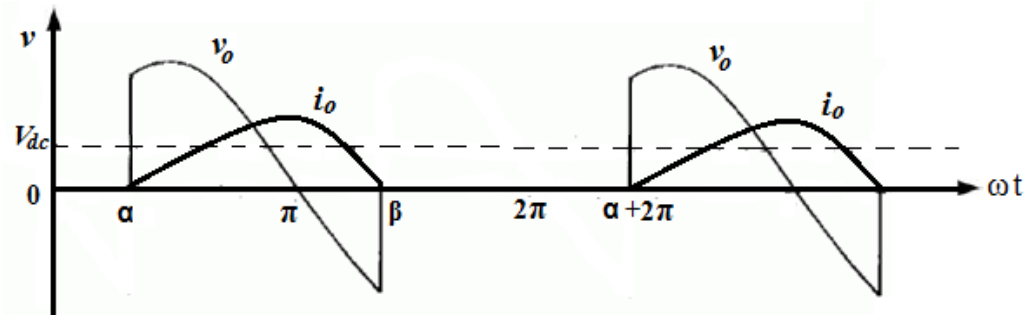

Fig.3.3 Waveforms for the single-phase half-wave controlled rectifier with *R-L* load.

The average value of the load voltage V_{dc} can be calculated as follows:

$$V_{dc} = \frac{1}{2\pi}\int_{\alpha}^{\beta} v_s\,(\omega t)d\omega t \;= \frac{1}{2\pi}\int_{\alpha}^{\beta} V_m sin\omega t\, d\omega t$$

$$= \frac{V_m}{2\pi}\,(-cos\beta + cos\alpha)$$

$$= \frac{V_m}{2\pi}\,(cos\alpha - cos\beta) \qquad (3.8)$$

Consequently, the average value of the load current I_{dc} is

$$I_{dc} = \frac{V_{dc}}{R} = \frac{V_m}{2\pi R}(cos\alpha - cos\beta) \qquad (3.9)$$

The output d.c. power is given by:

$$P_{dc} = V_{dc}I_{dc} = \frac{V_{dc}^2}{R} \qquad (3.10)$$

The *rms* value of the load voltage V_{orms} can be calculated as follows:

$$V_{orms} = \sqrt{\frac{1}{2\pi}\int_{\alpha}^{\beta} v_s^2\,(\omega t)d\omega t}$$

$$= \sqrt{\frac{1}{2\pi}\int_{\alpha}^{\beta} (V_m sin\omega t)^2\, d\omega t} = \sqrt{\frac{(V_m)^2}{2\pi}\int_{\alpha}^{\beta}\frac{1}{2}(1 - cos2\omega t)d\omega t}$$

$$= \frac{V_m}{2}\sqrt{\frac{1}{\pi}[(\beta-\alpha)-\frac{1}{2}(sin2\beta - sin2\alpha)]} \qquad (3.11)$$

Therefore, the *rms* value of the load current I_{orms} is :

$$I_{orms} = \frac{V_{orms}}{R} = \frac{V_m}{2R}\sqrt{\frac{1}{\pi}[(\beta-\alpha)-\frac{1}{2}(sin2\beta - sin2\alpha)]} \qquad (3.12)$$

The output a.c. power is given by:

$$P_{ac} = V_{orms} I_{orms} \qquad (3.13)$$

The *PRV* of the thyristor for this configuration is V_m . To find the power factor of the circuit, the current drawn from the source i_s is the same as the load current. Hence,

$$S = V_s\, I_{orms} \qquad (3.14)$$

But $PF = \frac{P_{ac}}{S}$

Hence $PF = \frac{V_{orms} I_{orms}}{V_s\, I_{orms}} = \frac{V_{orms}}{V_s}$

$$= \frac{V_m}{2V_s}\sqrt{\frac{1}{\pi}[(\beta-\alpha)-\frac{1}{2}(sin2\beta - sin2\alpha)]}$$

Since $V_m/2V_s = \sqrt{2}V_s/2V_s$

$$\therefore \quad PF = \sqrt{\frac{1}{\sqrt{2}\pi}[(\beta-\alpha)-\frac{1}{2}(sin2\beta - sin2\alpha)]} \qquad (3.15)$$

3.2.3 The Freewheeling Diode in Single-Phase Controlled Rectification

The freewheeling diode (FWD) is connected in the circuit across an *R-L* load in such a way as to provide an alternative path for the decaying load current so that the thyristor current is al1owed to become zero and the thyristor is allowed to turn off.

Consider the half-wave rectifier of Fig.3.4(a) where FWD is the freewheeling diode. If switch *S* is opened, i.e. the converter operates

without FWD, then the output voltage and current waveforms are as shown in Fig.3.4(b). If *S* is closed, then the supply voltage is positive, from α to π, FWD is in reverse and passes approximately no current (open circuited), so that source and load current are equal ($i_s = i_o$) as shown in Fig.3.4(d).

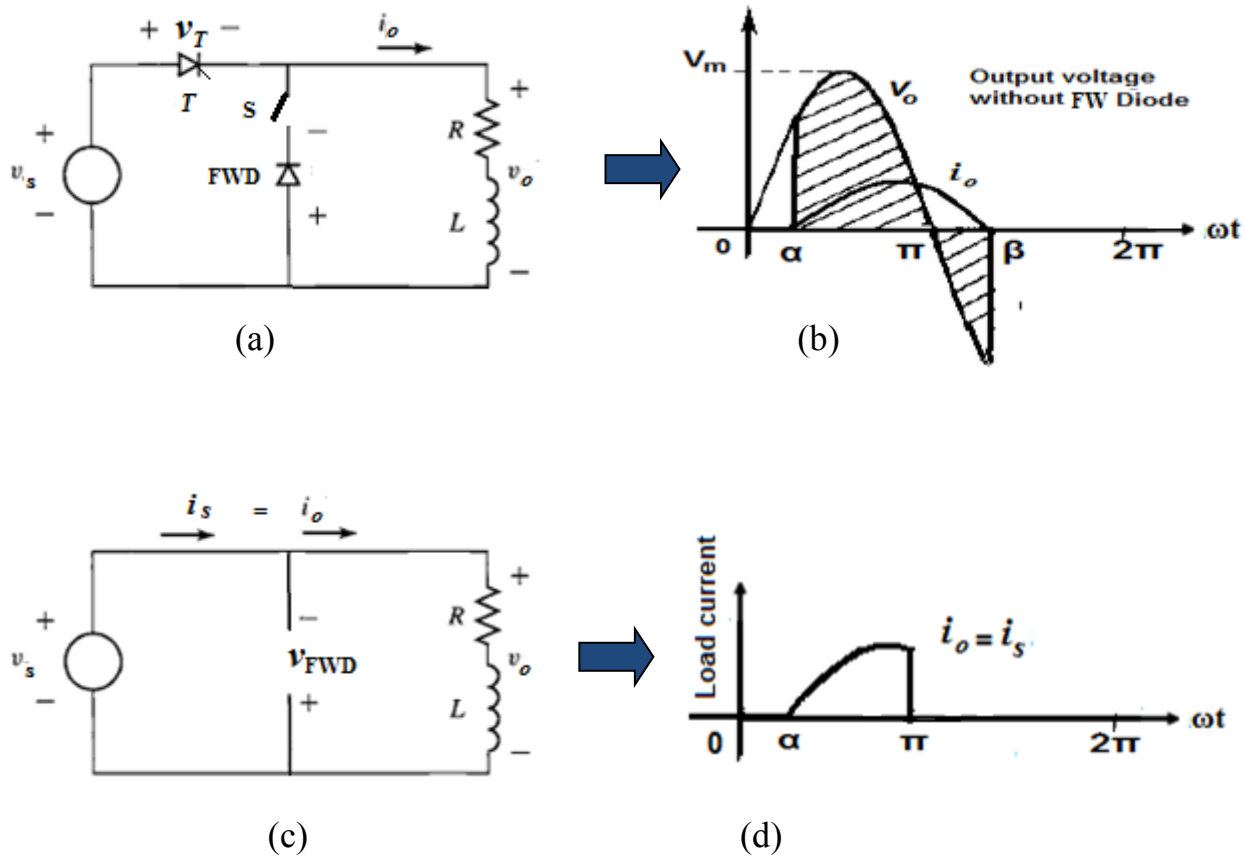

Fig.3.4 Converter operation : (a) Without freewheeling diode, (b)Voltage and current waveforms without freewheeling diode, (c) Operation with freewheeling diode, (d) Supply and load Currents during the positive half-cycle.

During the negative half-cycle of the supply, the load current i_o flows through the low resistance path provided by FWD rather than against the negative supply voltage, so that $i_{FWD} = i_o$, and $i_s = 0$. Hence the thyristor *T* is allowed to switch off. In this part of the half-cycle, the current is driven by the energy stored in *L*; it decays according to the time constant of the circuit (*R*, *L*, and FWD), Fig.3.5; v_o is very small and negative, being equal to the voltage drop across FWD. Therefore, the output voltage waveform will be as depicted in Fig.3.6 which is exactly similar to the case of resistive load.

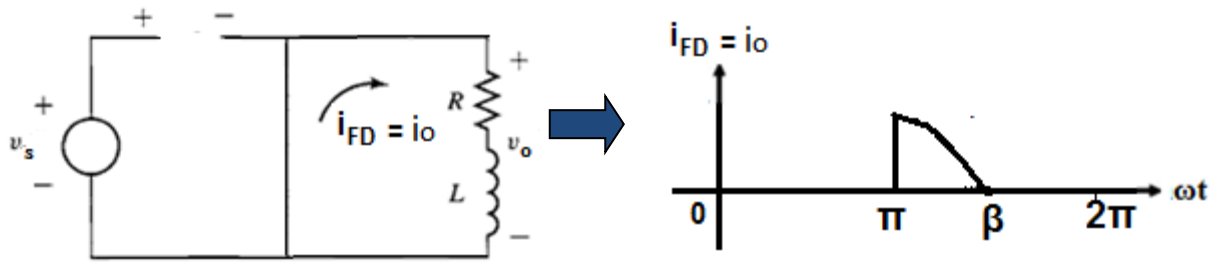

Fig.3.5 Load current during the supply negative half-cycle.

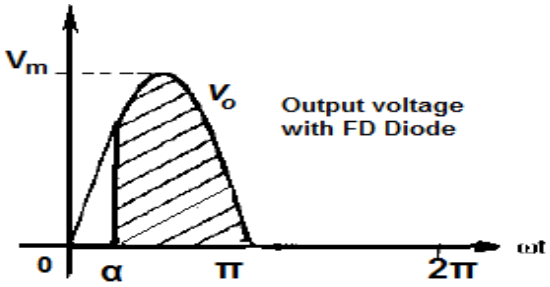

Fig.3.6 Output voltage waveform for *R -L* load with freewheeling diode.

To derive an expression for the average value of the output voltage for single-phase half-wave controlled rectifier with *R-L* load and freewheeling diode, referring to the voltage waveform shown in Fig.3.6 one can write,

$$V_{dc} = \frac{1}{2\pi}\int_{\alpha}^{\pi} v_s\,(\omega t)d\omega t \;= \frac{1}{2\pi}\int_{\alpha}^{\pi} V_m sin\omega t\, d\omega t$$

$$= \frac{V_m}{2\pi}\,(-cos\pi + cos\alpha) \;= \frac{V_m}{2\pi}\,(1 + cos\alpha) \qquad (3.16)$$

which is the same expression as that of resistive load case given in Eq.(3.1).

Example 3.1

The single-phase half-wave controlled rectifier shown in Fig.3.2(a) supplies a resistive load draws an average current of 1.62 A. If the converter is operated from a 240 V, 50 Hz supply and if the average value of the output voltage is 81V, calculate the following:

(a) The firing angle α.
(b) Load resistance .

(c)The *rms* load voltage.
(d) The *rms* load current.
(e) DC power.
(f) The ripple factor .

Solution

(a) For single-phase half-wave controlled rectifier with resistive load; the average value of the output voltage is calculated from Eq.(3.1) as

$$V_{dc} = \frac{V_m}{2\pi}(1 + cos\alpha)$$

$$81 = \frac{240 \times \sqrt{2}}{2\pi}(1 + cos\alpha) \quad \rightarrow \quad \text{Hence } \alpha = 60^{\circ}.$$

(b) $$R = \frac{V_{dc}}{I_{dc}} = \frac{81}{1.62} = 50\ \Omega$$

(c) The *rms* load voltage is calculated using Eq.(3.4) as

$$V_{orms} = \frac{V_m}{2}\sqrt{\frac{1}{\pi}(\pi - \alpha + \frac{1}{2}sin2\alpha)}$$

$$= \frac{240 \times \sqrt{2}}{2}\sqrt{\frac{1}{\pi}(\pi - \frac{\pi}{3} + \frac{1}{2}sin120^{\circ})} = 152.14\ \text{V}$$

(d) The *rms* load current

$$I_{orms} = \frac{V_{orms}}{R} = \frac{152.14}{50} = 3.04\ \text{A}$$

(e) The output d.c. power is given by:

$$P_{dc} = V_{dc}I_{dc} = \frac{V_{dc}^2}{R} = \frac{81^2}{50} = 131.22\ \text{W}$$

(f) $$\text{Ripple factor} = \frac{\sqrt{V_{orms}^2 - V_{dc}^2}}{V_{dc}} = \frac{\sqrt{152.14^2 - 81^2}}{81} = 1.57$$

Example 3.2

The thyristor shown in Fig.3.7 is triggered by *RC* phase-shift bridge circuit connected to its cathode and gate through 1:1 center tapped transformer. For the resistor *R*, the minimum value is R_{min} = 1 kΩ and maximum value R_{max} = 11 kΩ. The value of the capacitor C = 0.4 μF. Assuming that the SCR fires at the instant when the gate / cathode voltage goes positive, determine the range of firing angles available.

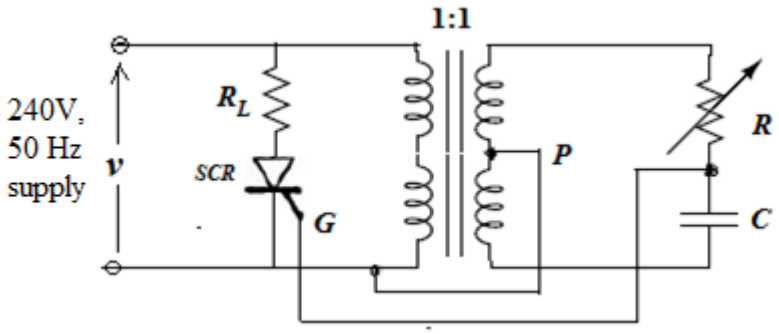

Fig.3.7.

Solution

(a) For $R = R_{min}$ = 1kΩ

Center-tap voltage:

$$V_p = \frac{240\angle 0°}{2} = 120\angle 0° \text{ Volts}$$

The impedance of the *RC* circuit Z_{min} is,

$$|Z_{min}| = \sqrt{R_{min}^2 + (\frac{-1}{\omega c})^2} = \sqrt{1000^2 + (\frac{-1}{100\pi \times 0.4 \times 10^{-6}})^2}$$

$$= \sqrt{10^6 + 7990^2} = 8024.33\Omega\angle 0°$$

$$I_{max} = \frac{240\angle 0°}{|Z_{min}|} = \frac{240\angle 0°}{8024.33\angle -83°} = 0.02992 \text{ A}\angle 83°$$

$$V_R = R_{min}\ I_{max} = 1000 \times 0.02992 = 29.92 \text{ V}\angle 83°$$

Taking voltage V_p as a reference,

$$V_{GP} = 120\angle\, 0° - 29.92\, V\angle 83°$$
$$= 120 - 29.92\, cos83° - j29.92 sin83°$$
$$= 116.35 - j29.69 = 120\angle 14.3°\ \text{V} \quad \therefore\ \alpha_1 = 14.3°$$

(b) For $R = R_{max} = 11\ \text{k}\Omega$

$$|\, Z_{max}| = \sqrt{R_{max}^2 + (\frac{-1}{\omega c})^2} = \sqrt{11000^2 + (\frac{-1}{100\pi \times 0.4\ \times 10^{-6}})^2}$$
$$= \sqrt{11^6 + 7990^2}\ \Omega$$

$$V_R = I_{min}\, .R_{max} = \frac{240\angle 0°}{Z_{max}} = 194\, V\angle 36°$$
$$V_{GP} = 120\angle\, 0° - 194\, V\angle 36°$$
$$= 120 - 194\, cos36° - j194\, sin36°$$
$$= 123\angle\, 108.2° \quad \therefore\ \alpha_2 = 108.2°$$

Hence the range of angles: $14.3° - 108.2°$

Example 3.3

The circuit of Example 3.2 is used as a half-wave controlled rectifier supplying resistive load with R_L = 1 kΩ. For the firing angles obtained in the previous example draw the load current waveforms for both angles and, determine the corresponding power dissipation in the load resistor.

Solution

The load current waveform is shown in Fig.3.8 (a) when α = 14.3˚ = 0.249 rad.

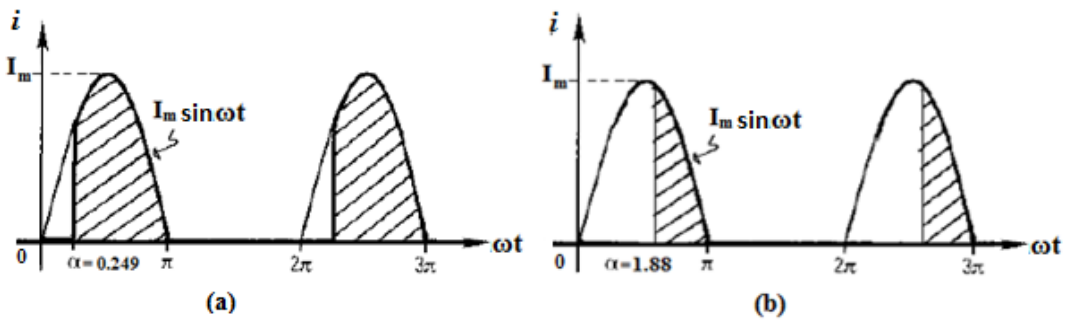

Fig.3.8.

The *rms* value of the load current may be given by,

$$I_{orms}^2 = \frac{V_m^2}{2\pi R_L}\int_{0.249}^{\pi} sin^2\omega t\, d\omega t$$

$$I_{orms}^2 = \frac{V_m^2}{2\pi R_L}\int_{0.249}^{\pi} \frac{1}{2}\,(1 - cos2\omega t)d\omega t$$

$$= \frac{V_m^2}{2\pi R_L} \times \frac{1}{2}\,(1 - sin2\omega t)\Big\{_{0.249}^{\pi} = 0.02863 \text{ A}$$

$$P = I_{orms}^2 . R_L = I_{rms}^2 \times 1000 = 28.63 \text{ W}$$

Similarly for $\alpha_2 = 108.2°$ (Fig.3.8(b)) , $P = 8.64$ W

Example 3.4

A single-phase half-wave controlled rectifier shown in Fig.3.2 supplied from 230V a.c. supply is operating at α = 60º. If the load resistor is 10Ω, determine:

(a) The power absorbed by the load (P_{dc}).
(b) The power drawn from the supply (P_{ac}).
(c) The power factor at the a.c. source.

Solution

(a) The d.c. power absorbed by the load (P_{dc}) :

$$P_{dc} = V_{dc} I_{dc} = \frac{V_{dc}^2}{R}$$

$$V_{dc} = \frac{V_m}{2\pi}\,(1 + cos\alpha) = \frac{\sqrt{2} \times 230}{2\pi}\,(1 + cos60°) = 77.68 \text{ V}$$

$$P_{dc} = \frac{77.68^{\,2}}{10} = 603.4 \text{ W}$$

(b) The power drawn from the supply P_{ac} :

$$P_{ac} = V_{orms} I_{orms} = \frac{V_{orms}^2}{R} = \frac{(0.5V_m)^2}{R} = \frac{1}{4} \times \frac{(\sqrt{2} \times 230)^2}{10}$$
$$= 2644.2 \text{ W}$$

(c) The power factor at the a.c. source.

The power factor can be calculated from Eq.(3.7) as

$$PF = \sqrt{\frac{1}{2\pi}(\pi - \alpha + \frac{1}{2}sin2\alpha)} = \sqrt{\frac{1}{2\pi}(\pi - \frac{\pi}{3} + \frac{1}{2}sin120°)}$$
$$= 0.633 \text{ lagging}$$

Example 3.5

For the single-phase half-wave controlled rectifier shown in Fig.3.9, thyristor T_1 is operating at $\alpha_1 = 80°$. Thyristor T_2 is connected across the load and operating with a delay angle α_2 of 40º. Assume the load is highly inductive such that I_L is continuous. Plot waveforms for the instantaneous values of v_L, i_{T1} , i_{T2} ,i_L , v_{T1} and v_{T2}. Derive an expression for the average load voltage V_{dc} as a function of α_1 and α_2 (with $\alpha_1 < \alpha_2$).

Fig.3.9.

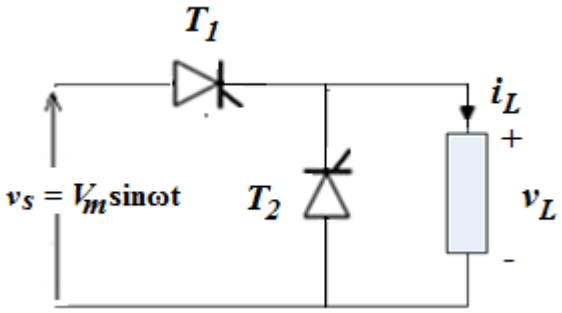

Solution

The voltage and current waveforms are shown in Fig.3.10.

The average d.c. voltage may be obtained as

$$V_{dc} = \frac{1}{2\pi}\int_{\alpha_1}^{\alpha_2} V_m sin\omega t\, d\omega t = \frac{V_m}{2\pi}\int_{\alpha_1}^{\alpha_2} sin\omega t\, d\omega t$$

$$= \frac{V_m}{2\pi}\left\{-cos\omega t\Big|_{\alpha_1}^{\alpha_2}\right\} = \frac{V_m}{2\pi}\{cos\alpha_1 - cos\alpha_2\}$$

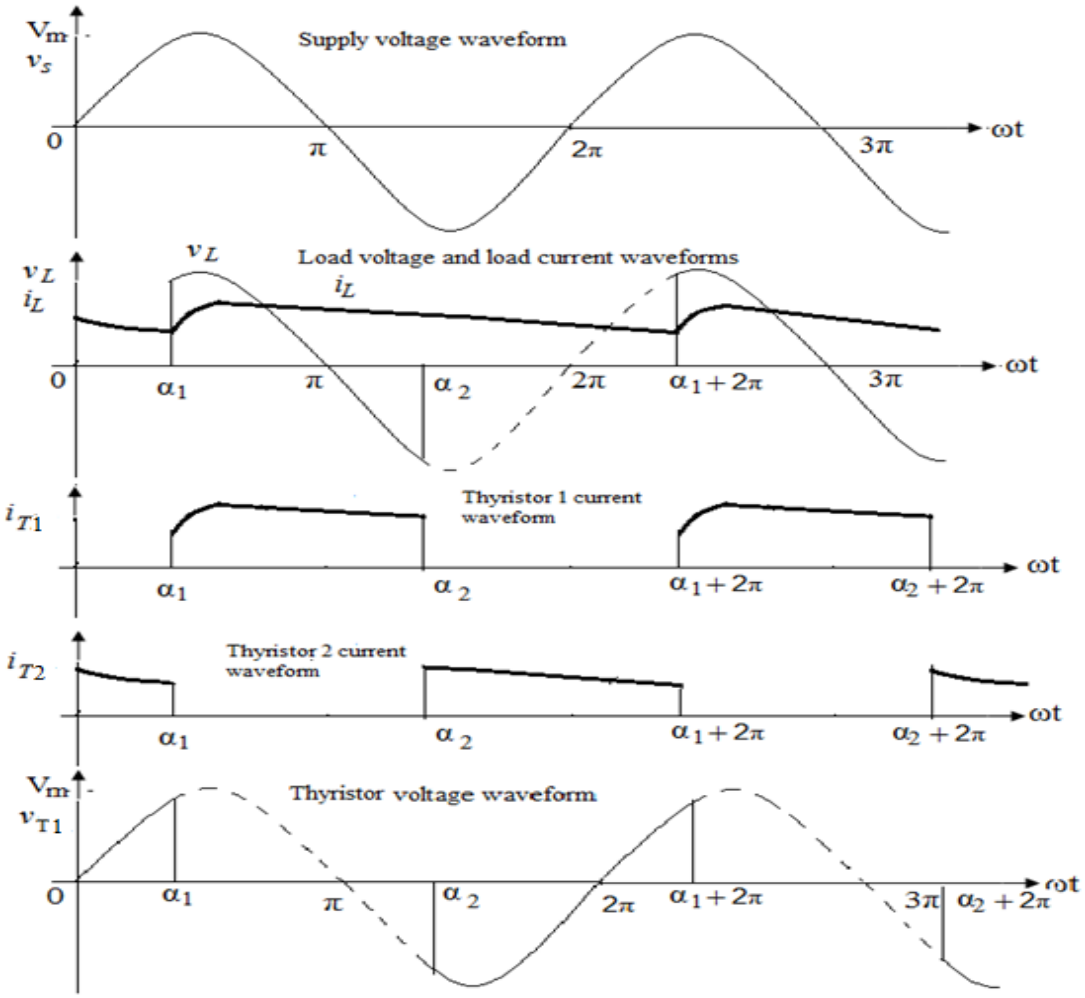

Fig.3.10 The voltage and current waveforms of Example 3.5.

Example 3.6

The single-phase half-controlled rectifier shown in Fig.3.11 operating at a triggering angle of 60º from a.c. source v_s = 300 sinωt. Assuming the load is resistive, express V_{dc} of the load as a function of α, and calculate its value.

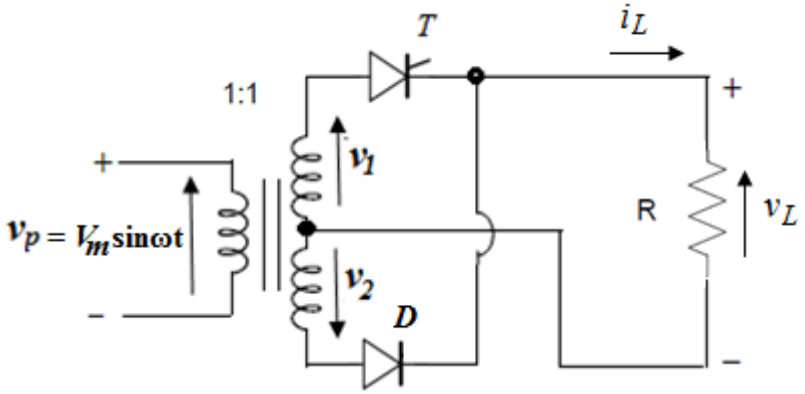

Fig.3.11

Solution

$$V_{dc} = \frac{1}{2\pi}\{\int_{\alpha}^{\pi} V_m sin\omega t\, d\omega t + \int_{\pi}^{2\pi} -V_m sin\omega t\, d\omega t\}$$

$$= \frac{V_m}{2\pi}\left[-cos\omega t\,\right]_{\alpha}^{\pi} - \left\{-cos\omega t\,\right\}_{\pi}^{2\pi}$$

$$= \frac{V_m}{2\pi}\{1 + cos\alpha + 1 + 1\} \quad = \frac{V_m}{2\pi}\{3 + cos\alpha\}$$

For $\alpha = 60°$: $V_{dc} = \frac{V_m}{2\pi}\{3 + cos60^o\} = 167.2$ V

3. 3 SINGLE-PHASE, FULL-WAVE, FULLY-CONTROLLED BRIDGE RECTIFIER (P = 2)

The single-phase, fully-controlled full-wave rectifier bridge is shown in Fig.3.12(a). In this circuit, two thyristors must be triggered simultaneously to permit current to flow. For example, with the instantaneous polarity of the sinusoidal supply voltage indicated in Fig.3.12 (b), T_1 and T_2 must be triggered, while in reverse, T_3 and T_4 must triggered at the same time. The output voltage and current waveforms are shown in Fig.3.12 (b) for the case of resistive load.

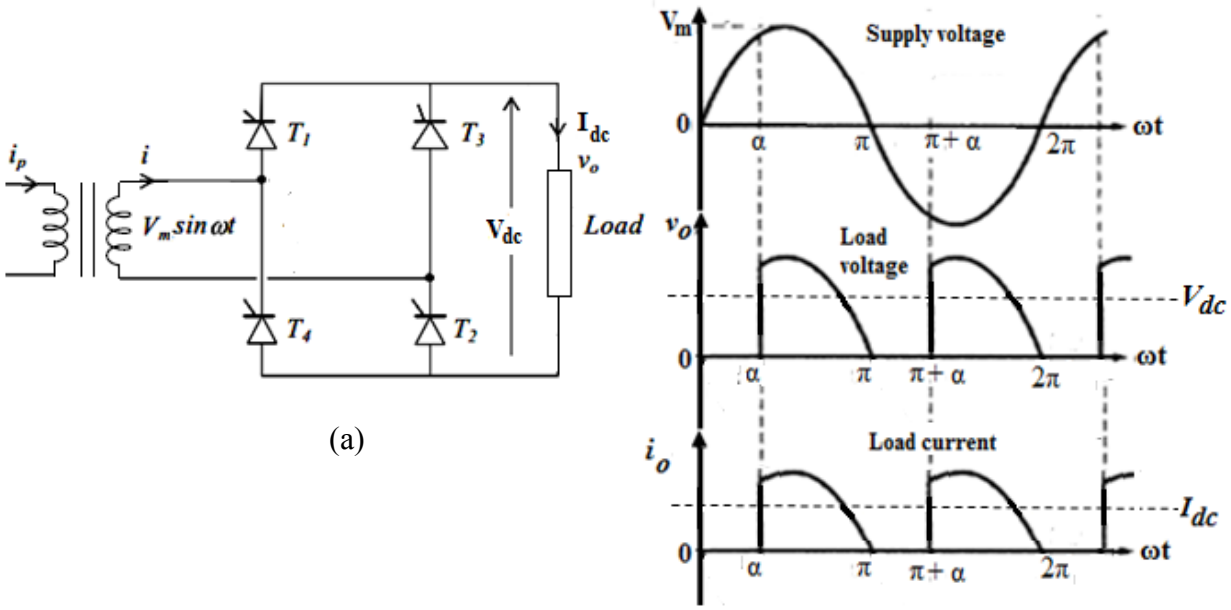

Fig. 3.12 Single-phase fully-controlled full-wave rectifier bridge with *R*-load , (a) Circuit, (b) Waveforms.

The single-phase supply to the rectifier is usually taken from the secondary of a transformer and not directly from the main and is generally expressed as

$$v_s\,(\omega t) = V_m sin\omega t$$

In the following analysis, the rectifier will be considered to operate with three types of passive loads, namely: pure resistive load, *R-L* load with small *L/R* ratio (in which the resistance is dominant, *R-L* load with large *L/R* ratio (in which ωL is larger than *R*) and *R-L* load which is highly inductive ($L>>R$).

3.3.1 Operation of the Converter with Resistive Load

Referring to Fig.3.12(b), the average d.c. output voltage of the converter with resistive load is given by,

$$V_{dc} = \frac{1}{\pi}\int_{\alpha}^{\pi} V_m\, sin\ \omega t\ d\omega t = \frac{V_m}{\pi}(1 + cos\alpha) \qquad (3.17)$$

The *rms* value of the load voltage V_{orms} can be calculated as follows:

$$V_{orms} = \sqrt{\frac{1}{\pi}\int_{\alpha}^{\pi} v_s^2\,(\omega t) d\omega t}$$

$$= \sqrt{\frac{1}{\pi}\int_{\alpha}^{\pi} (V_m sin\omega t)^2\, d\omega t} = \sqrt{\frac{(V_m)^2}{\pi}\int_{\alpha}^{\pi}\frac{1}{2}(1 - cos2\omega t) d\omega t}$$

$$= \frac{V_m}{\sqrt{2}}\sqrt{\frac{1}{\pi}(\pi - \alpha + \frac{1}{2}sin2\alpha)} \qquad (3.18)$$

Therefore , the *rms* value of the load current I_{orms} is

$$I_{orms} = \frac{V_{orms}}{R} = \frac{V_m}{\sqrt{2}R}\sqrt{\frac{1}{\pi}(\pi - \alpha + \frac{1}{2}sin2\alpha)} \qquad (3.19)$$

3.3.2 Operation of the Converter with *R-L* load

(i) Case of *R-L* load with small *L / R* ratio: Discontinuous load current

In this case the current will be discontinuous as shown in Fig.3.13. For $\alpha \leq \omega t \leq \beta$, the circuit equation is given by

$$V_{dc} = \frac{1}{\pi}\int_{\alpha}^{\beta} V_m \sin \omega t \, d\omega t = \frac{V_m}{\pi}(\cos\alpha - \cos\beta) \qquad (3.20)$$

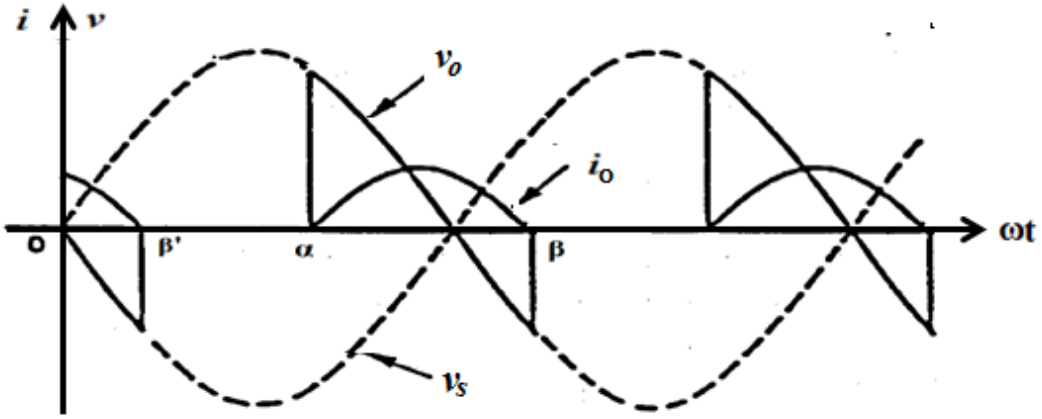

Fig.3.13 Waveforms of the output voltage and current for discontinuous current operation.

(ii) Case of *R-L* load with large L / R ratio: Continuous load current

Under these conditions, a thyristor is still conducting when another is forward-biased and is turned on. The first device is instantaneously reverse-biased by the second device which has been turned on. The first device is commutated and load current is instantaneously transferred on the incoming device. In this case the current is continuous as shown in Fig.3.14.

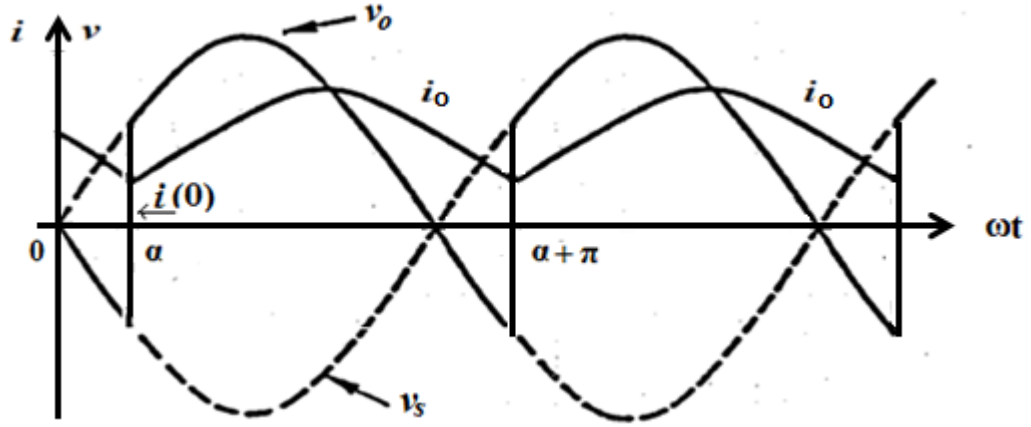

Fig. 3.14 Waveforms of the output voltage and current for continuous current operation.

The average value of the load voltage V_{dc} can be calculated as follows:

$$V_{dc} = \frac{1}{\pi}\int_{\alpha}^{\alpha+\pi} V_m \sin \omega t \, d\omega t \; = \frac{2V_m}{\pi}\cos\alpha \qquad (3.21)$$

Under all delay angle condition, the average current is given by:

$$I_{dc} = \frac{V_{dc}}{R} \qquad (3.22)$$

From the above voltage equation, (3.21), it is clear that, if the firing angle is greater than 90˚, the average voltage can be negative because cosα is negative. Thus if the firing angle is suddenly increased to, say, 160˚, a large negative voltage will be applied to the load and the power is fed back to the supply. This process is known as 'INVERSION'. The current remains positive while the voltage is negative. Hence a negative pulse of energy will be produced which is fed back to the supply. In this case m the converter is said to operate in two quadrants as shown in Fig.3.15(a). The graph shown in Fig. 3.15(b) gives the relation between the firing angle and the output voltage in percentage for the two modes of operation (continuous and discontinuous) for full-wave single-phase rectifier.

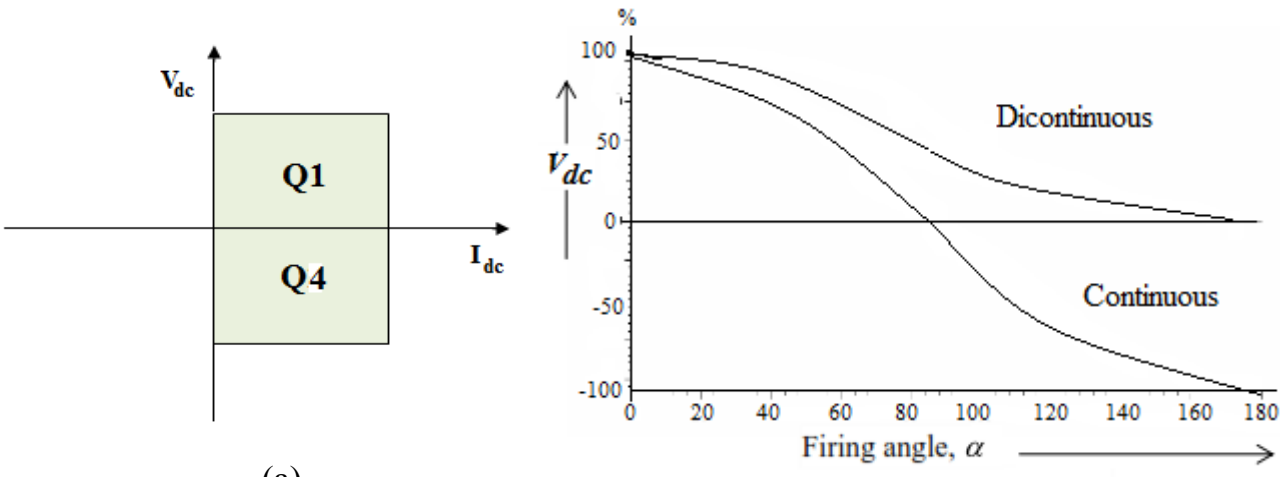

(a)

(b)

Fig. 3.15 Full-wave fully-controlled single-phase rectifier: (a)Two quadrants operation, (b) The relation between the firing angle and the output voltage in p.u. for the two modes of operation, continuous and discontinuous current.

To find roughly whether the converter is operating in continuous or discontinuous current mode , the following simple rule- of- thumb may be used:

If	$\pi + \alpha < \beta$	the current is continuous
If	$\pi + \alpha > \beta$	the current is discontinuous

(iii) Case of highly inductive load (*L* > > *R*)

Fig. 3.16 (a) shows the circuit connection for a single-phase, full-wave, controlled rectifier loaded with a highly inductive load. For one total period of operation of this circuit, the corresponding waveforms are shown in Fig. 3.16 (b).

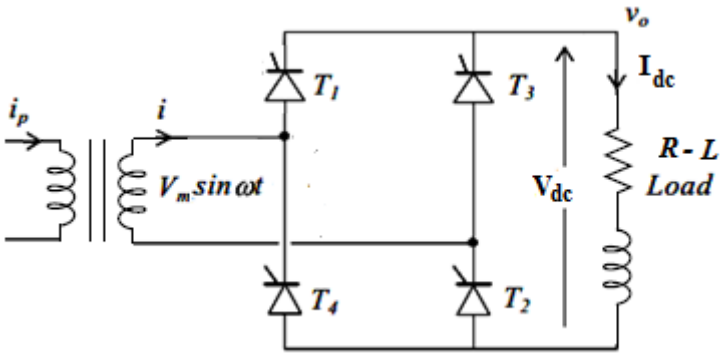

(a) Circuit

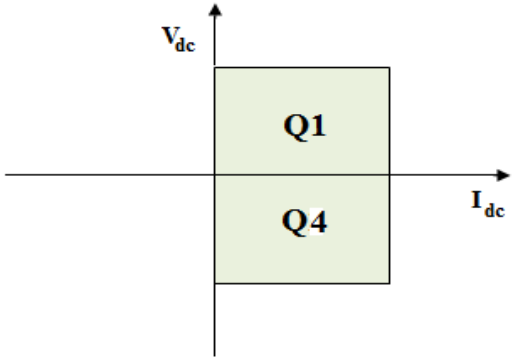

(c) Operating quarters

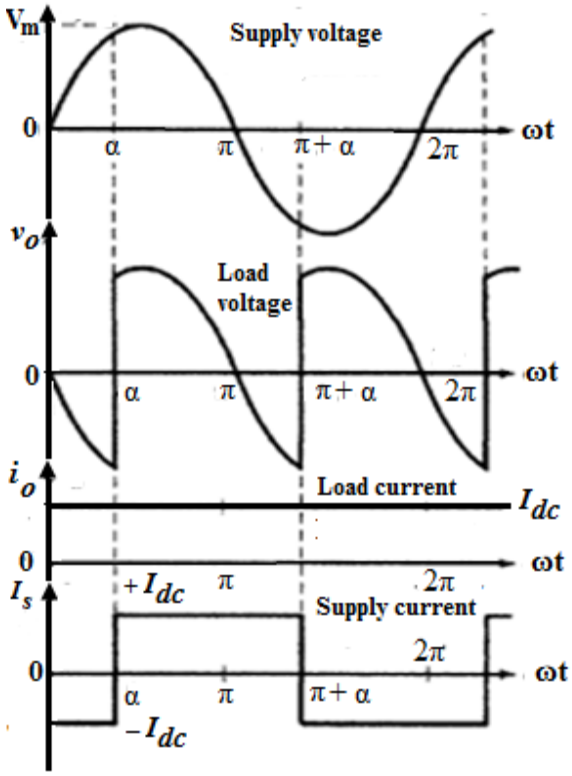

(b) Waveforms.

Fig.3.16 Single phase full-wave rectifier loaded with highly inductive load.

The average value of the load voltage V_{dc} can be calculated as follows,

$$V_{dc} = \frac{1}{\pi}\int_{\alpha}^{\alpha+\pi} V_m \sin \omega t \, d\omega t \quad = \quad \frac{2V_m}{\pi}\cos\alpha \qquad (3.23)$$

Which is the same as Eq.(3.21) for continuous current operation mode. Therefore, the average output voltage can vary from $+2V_m/\pi$ to $-2V_m/\pi$ when varying α from π to 0, respectively. Moreover, since the load voltage for this configuration can be positive or negative while the load current is always positive because the thyristors prevents a reverse current flow. Therefore, this converter operates in the first and the fourth quadrants as shown in Fig.3.16 (c).

The *rms* value of the load voltage V_{orms} can be calculated as follows,

$$V_{orms} = \sqrt{\frac{1}{\pi}\int_{\alpha}^{\pi+\alpha} v_s^2\,(\omega t)d\omega t} = \sqrt{\frac{1}{\pi}\int_{\alpha}^{\pi+\alpha} (V_m sin\omega t)^2\,d\omega t}$$

$$= \sqrt{\frac{V_m^2}{\pi}\int_{\alpha}^{\pi+\alpha} \frac{1}{2}(1-cos2\omega t)d\omega t} = \frac{V_m}{\sqrt{2}} \qquad (3.24)$$

Since the load current is constant over the studied period, therefore the *rms* value of the load current I_{orms} is : $I_{orms} = I_{dc} = I_a$

The *PRV* for any thyristor in this configuration is (V_m).

(iv) Case of resistive-inductive load in series with d.c. source (*R-L-E*)

Fig.3.17(a) shows the circuit diagram for a single-phase, full-wave, controlled rectifier supplying *RLE* load. When the current is continuous, the output voltage and current waveforms are similar to the case of inductive load with large *L/R* ratio, Fig.3.14. This means that *E* has no effect on the waveforms as long as the current remains continuous. Hence the equations for the average and *rms* values of the output voltages are same as that given in Eqs.(3.21) and (3.24).

To find the average load current for continuous case, referring to Fig.3.14, by applying KVL, for the interval $\alpha \le \omega t \le \alpha + \pi$ which is repeated every π :

$$v_s\,(\omega t) = V_m sin\omega t = R\,i + L\frac{di}{dt} + E \qquad (3.25)$$

This is a first order differential equation. The solution of this equation has three parts:

1- Steady-state solution due to source voltage:

$$i_{ss1}(\omega t) = \frac{V_m}{Z}\sin(\omega t - \theta)$$

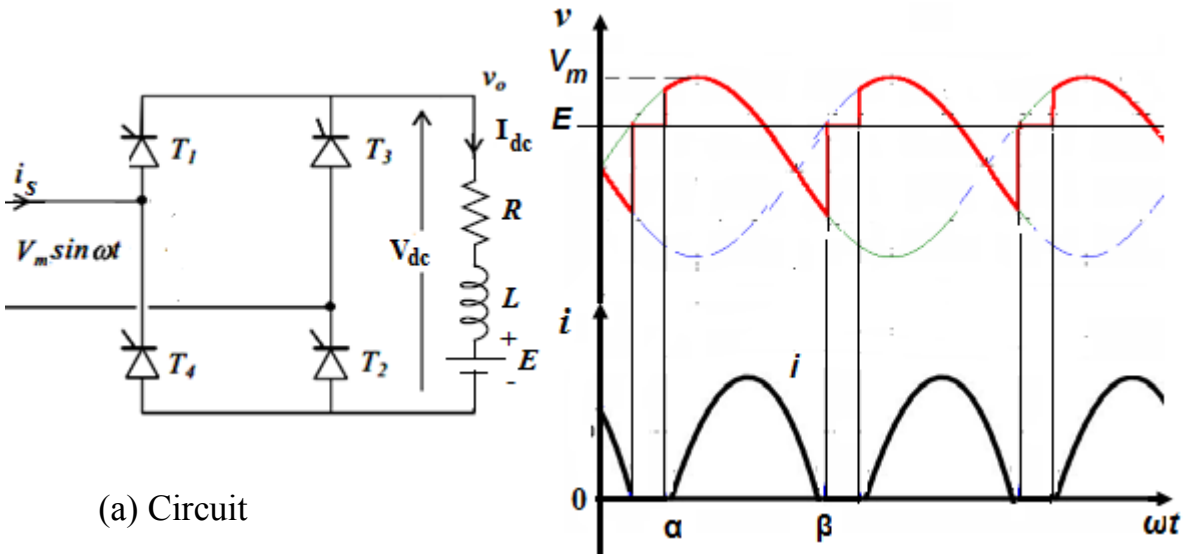

(a) Circuit

(b) Waveforms

Fig.3.17 Single-phase full-wave rectifier operating with *RLE* load.

2- Steady-state solution due to d.c. voltage E : $i_{ss2}(\omega t) = -\frac{E}{R}$

3- Transient solution: $i_{tr}(\omega t) = Ae^{-\frac{t}{\tau}}$

where

$$|Z| = \sqrt{R^2 + (\omega L)^2}$$

$$\theta = \tan^{-1}(\frac{\omega L}{R})$$

$$\tau = \frac{L}{R} = \text{time constant} \quad \text{and} \quad A = \text{Constant}$$

The complete solution is: $i(\omega t) = i_{ss1}(\omega t) + i_{ss2}(\omega t) + i_{tr}(\omega t)$

$$i(\omega t) = \frac{V_m}{|Z|}\sin(\omega t - \theta) - \frac{E}{R} + Ae^{-\frac{t}{\tau}} \qquad (3.26)$$

For continuous current case, the constant A can be found from initial conditions: $i(\omega t = \alpha) = i(0)$,

$$i(\alpha) = i(0) = \frac{V_m}{|Z|}\sin(\alpha - \theta) - \frac{E}{R} + Ae^{-\frac{R}{\omega L}\alpha}$$

$$\therefore A = [i(0) - \frac{V_m}{|Z|}\sin(\alpha - \theta) + \frac{E}{R}]\ e^{-\frac{R}{\omega L}\alpha} \qquad (3.27)$$

Substitute Eq.(3.27) into Eq.(3.26) and simplify yields

$$i(\omega t) = \frac{V_m}{|Z|}\sin(\omega t - \theta) - \frac{E}{R} + [i(0) - \frac{V_m}{|Z|}\sin(\alpha - \theta) + \frac{E}{R}]\ e^{\frac{-R}{\omega L}(\omega t - \alpha)} \quad (3.28)$$

Note that, $i(0)$ is the initial value of the load current at $\omega t = \alpha$, $\alpha + \pi$, $2\pi + \alpha$,….. This is can be obtained by substituting this value into Eq.(3.28) and solving for $i(0)$ we get,

$$i(0) = -\frac{V_m}{|Z|}\sin(\alpha - \theta)\left[\frac{1 + e^{-\frac{\pi R}{\omega L}}}{1 - e^{-\frac{\pi R}{\omega L}}}\right] - \frac{E}{R} \quad (3.29)$$

Once $i(0)$ in Eq.(3.29) is found ,the average value of $i(\omega t)$ can be found as

$$I_{av} = \frac{1}{\pi}\int_{\alpha}^{\alpha+\pi} i(\omega t)\ d\omega t$$

$$I_{av} = \frac{1}{\pi}\int_{\alpha}^{\alpha+\pi} \{\frac{V_m}{|Z|}\sin(\omega t - \theta) - \frac{E}{R} + \left[i(0) + \frac{E}{R} - \frac{V_m}{|Z|}\sin(\alpha - \theta)\right] e^{cot\theta(\alpha - \omega t)}\}\ d\omega t \quad (3.30)$$

For discontinuous current case, one can find the average value of the current I_{av} by referring to Fig.3.17(b) for the interval $\alpha \le \omega t \le \beta$ as

$$I_{av} = \frac{1}{\pi}\int_{\alpha}^{\beta} \{\frac{V_m}{|Z|}\sin(\omega t - \theta) - \frac{E}{R} + \left[i(0) + \frac{E}{R} - \frac{V_m}{|Z|}\sin(\alpha - \theta)\right] e^{cot\theta(\alpha - \omega t)}\}\ d\omega t \quad (3.31)$$

where

$$\alpha = sin^{-1}\frac{E}{V_m} \quad , \quad \beta = \pi - sin^{-1}\frac{E}{V_m} \quad \text{and} \quad i(0) = 0$$

Equation (3.31) above can also be applied to single-phase half-wave controlled rectifier of Fig.3.1 operating with *RLE*-load by modifying it as:

$$I_{av} = \frac{1}{2\pi}\int_{\alpha}^{\beta}\{\frac{V_m}{Z}\sin(\omega t-\theta)-\frac{E}{R} + \left[\frac{E}{R}-\frac{V_m}{Z}\sin(\alpha-\theta)\right]e^{cot\theta(\alpha-\omega t)}\}\,d\omega t \qquad (3.32)$$

3.4 SINGLE-PHASE HALF-CONTROLLED (SEMICONVERTER) RECTIFIER

Fig.3.18(a) shows a single-phase half-controlled (semiconverter) rectifier. This configuration consists of a combination of thyristors and diodes to reduce the cost of the full-wave fully-controlled rectifier. With resistive load, the converter operates in the same manner as fully contr-olled one. The load current and voltage have the same form as presented in Subsection 3.3.1 also apply to this circuit.

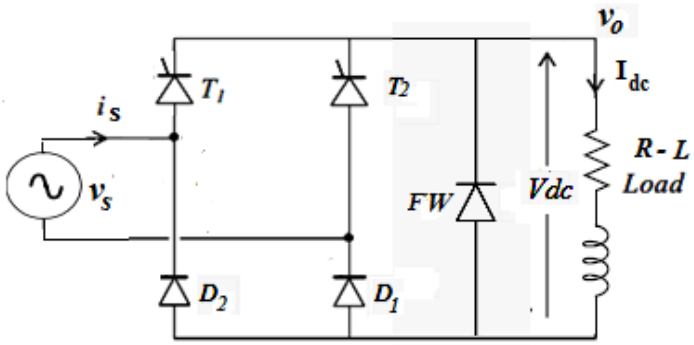

(a) Circuit

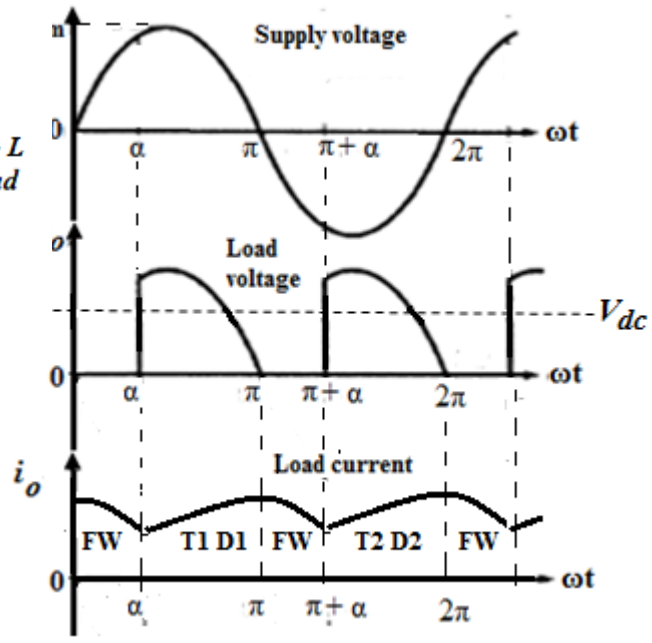

(b) Waveforms

Fig.3.18 Single-phase, half-controlled (Semiconverter): (a) Circuit, (b) Waveforms.

Equations (3.17) to (3.19) for the voltage and current are also applied for the semiconverter with resistive load. However with resistive-inductive load the converter can operates in continuous or discontinuous modes depend on the *L/R* ratio as discussed in Subsection 3.3.2.

In continuous current mode, freewheeling diode must be used to eliminate any negative voltage occurrence at the load terminals as shown in Fig.3.18 (a). This is because the diode FWD is always activated (forward biased) whenever the load voltage tends to be negative. For one total period of operation of this circuit, the corresponding waveforms are

shown in Fig. 3.18 (b). The average value of the load voltage V_{dc} in case of *R-L* load can be calculated as follows,

$$V_{dc} = \frac{1}{\pi}\int_{\alpha}^{\pi} V_m \sin \omega t \, d\omega t \; = \frac{V_m}{\pi}(1 + cos\alpha) \qquad (3.33)$$

which is the same expression for the case of pure resistive load. Therefore, the average output voltage can vary from 0 to V_m/π when varying α from π to 0 respectively. The average value of the load current I_{dc} is calculated as : $I_{dc} = \frac{V_{dc}}{R}$

The *rms* value of the load voltage V_{orms} can be calculated as follows:

$$V_{orms} = \sqrt{\frac{1}{\pi}\int_{\alpha}^{\pi} v_s^2\,(\omega t) d\omega t} = \sqrt{\frac{1}{\pi}\int_{\alpha}^{\pi} (V_m sin\omega t)^2 \, d\omega t}$$

$$= \sqrt{\frac{(V_m)^2}{\pi}\int_{\alpha}^{\pi} \frac{1}{2}(1 - cos2\omega t) d\omega t}$$

$$= \frac{V_m}{\sqrt{2}}\sqrt{\frac{1}{\pi}(\pi - \alpha + \frac{1}{2} sin2\alpha)} \qquad (3.34)$$

3.5 BI-PHASE (MID-POINT) CONTROLLED RECTIFIER

Fig.3.19 shows the circuit diagram of a bi-phase (mid-point) controlled rectifier. This circuit acts exactly as the single-phase full-wave rectifier discussed in the previous section. The only difference is that it uses two thyristors T_1 and T_2 only which is considered as an advantage over the bridge type rectifier. However, the voltage rating of each thyristor must be twice as that of the bridge type, i.e. $PRV = 2V_m$ on the secondary side whereas it is only V_m on the bridge type. The major disadvantage of the bi-phase converter is that it needs large center-tapped transformer which adds cost to the circuit.

.

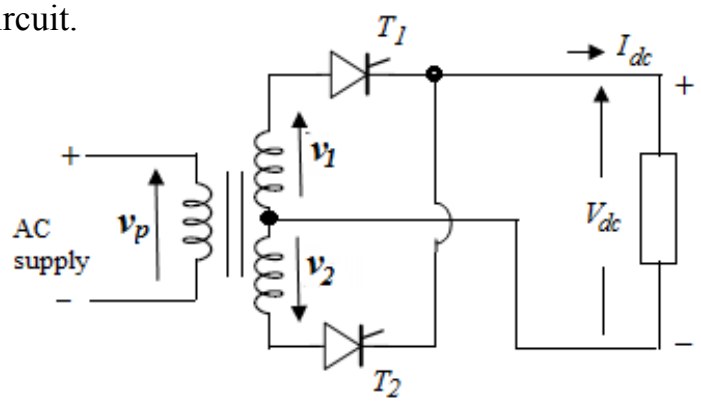

Fig.3.19

The operation of the converter can be illustrated as follows:
During positive half cycle of v_1 , T_1 is forward biased while T_2 is reversed biased since v_2 is now negative. T_1 conducts from its firing angle α till π and positive voltage appears across the load. From π to 2π, v_2 becomes positive T_1 is reversed biased whereas T_2 is forward biased and positive voltage also appears on the load same as the full-wave bridge rectifier output. Therefore, this converter is considered as an alternative to the bridge converter for producing full-wave rectification. Hence all mathematical analysis and waveforms for the output voltage, current, power and power factor are the same for that of the bridge type converter, so it will not be repeated here.

Example 3.7

A fully-controlled single-phase bridge rectifier is supplied from a 50Hz, 230/100V transformer .The rectifier supplying a highly inductive load of 10Ω resistor. For a firing angle of 45º, determine the rectified voltage, the rectified current and the power factor.

Solution

For highly inductive load, referring to Fig. 3.16(b), the average output voltage V_{dc} is calculated as follows,

$$V_{dc} = \frac{1}{\pi}\int_{\alpha}^{\alpha+\pi} V_m sin\omega t \, d\omega t = \frac{V_m}{\pi}\left\{ -cos\omega t]_{\alpha}^{\alpha+\pi} \right\} = \frac{2V_m}{\pi} cos\alpha$$

$$V_m = 100 \times \sqrt{2} = 141.42 \text{ V} \qquad \text{since } V_m = \sqrt{2}\, V_{rms}$$

$$\therefore V_{dc} = \frac{2 \times 141.24}{\pi} cos45^o = 63.64 \text{ V}$$

$$I_{dc} = \frac{V_{dc}}{R} = \frac{63.64}{10} = 6.364 \text{ A}$$

$$PF = \frac{\text{Average Power}}{V_{orms} \times I_{orms}} = \frac{(\frac{2V_m}{\pi} cos\alpha) \times I_{orms}}{V_{orms} \times I_{orms}}$$

$$= \frac{2\sqrt{2}}{\pi} cos\alpha = \frac{2\sqrt{2}}{\pi} cos45° = 0.636$$

Example 3.8

A single-phase, fully-controlled bridge rectifier supplies a constant current to a highly inductive load. Derive an expression for the average d.c. output voltage from the bridge and also the *rms* value of the fundamental component of the alternating line current assuming (a) that there is no freewheel diode, and (b) that a freewheel diode is used.

Solution:

(a) No freewheeling diode:
The load voltage and current waveforms will be as shown in Fig.3.20 (a) and (b) respectively.

$$V_{dc} = \frac{1}{\pi}\int_{\alpha}^{\alpha+\pi} V_m \sin\omega t \, d\omega t$$

$$= \frac{2V_m}{\pi}\cos\alpha$$

Current seen by the input transformer is as depicted in Fig.3.20 (c) ,

$$I_s = I_{dc} \quad 0 < \omega t < \pi$$

$$I_s = -I_{dc} \quad \pi < \omega t < 2\pi$$

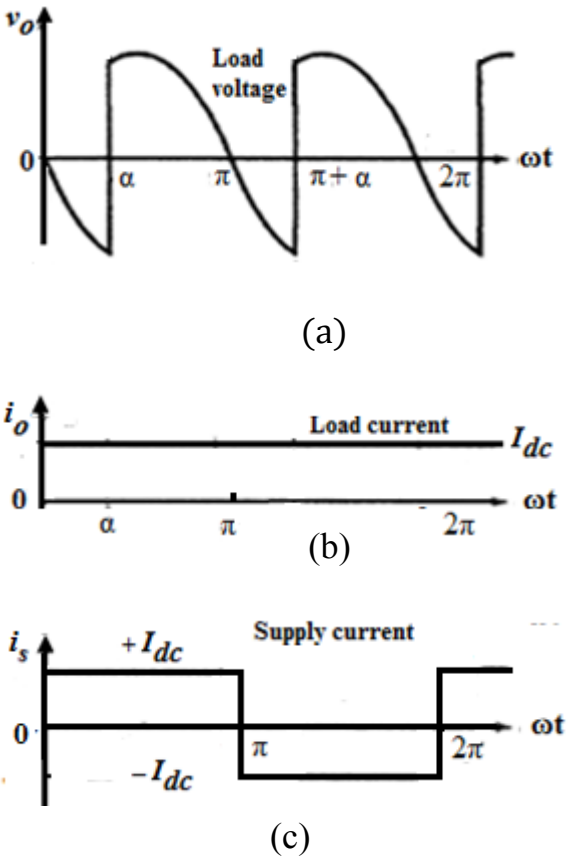

Fig.3.20 Waveforms.

Using Fourier series analysis, the Fourier coefficients are,

$$a_1 = \frac{2}{\pi}\int_0^{\pi} \mathrm{I_{dc}} \cos\omega t \, d\omega t = \frac{2\mathrm{I_{dc}}}{\pi}\left\{\sin\omega t\right\}_0^{\pi} = 0$$

$$b_1 = \frac{2}{\pi}\int_0^{\pi} \mathrm{I_{dc}} \sin\omega t \, d\omega t \frac{2\mathrm{I_{dc}}}{\pi}\left\{-\cos\omega t\right\}_0^{\pi} = \frac{4\mathrm{I_{dc}}}{\pi}$$

The amplitude c_1 of the fundamental component is given by

$$c_1 = \sqrt{a_1^2 + b_1^2} = \frac{4I_{dc}}{\pi}$$

The *rms* value of the fundamental component is

$$V_{o1} = \frac{c_1}{\sqrt{2}} = \frac{1}{\sqrt{2}} \times \frac{4I_{dc}}{\pi} = \frac{2\sqrt{2}}{\pi} I_{dc}$$

(b) With freewheeling diode : In this case the output current will be discontinuous as depicted in Fig.3.21 (b),

$$V_{dc} = \frac{1}{\pi}\int_{\alpha}^{\pi} V_m sin\omega t \, d\omega t$$

$$V_{dc} = \frac{V_m}{\pi}\left\{-cos\omega t\right\}_{\alpha}^{\pi}$$

$$= \frac{V_m}{\pi}(1 + cos\alpha)$$

$$a_1 = \frac{2}{\pi}\int_{\propto}^{\pi} I_{dc}\, cos\omega t \, d\omega t$$

$$= \frac{2\ I_{dc}}{\pi}\left\{sin\omega t\right\}_{\alpha}^{\pi}$$

$$= \frac{2\ I_{dc}}{\pi} sin\alpha$$

$$b_1 = \frac{2}{\pi}\int_{\propto}^{\pi} I_{dc}\ sin\omega t \, d\omega t$$

$$= \frac{2\ I_{dc}}{\pi}\left\{-cos\omega t\right\}_{\alpha}^{\pi} = \frac{2\ I_{dc}}{\pi}(1 + cos\alpha)$$

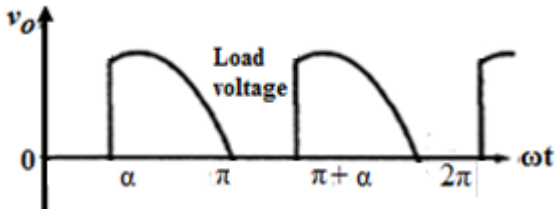

(a)

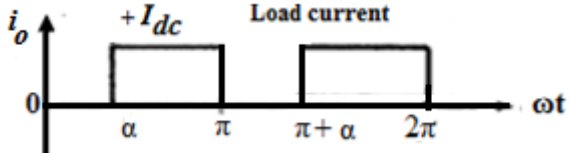

(b)

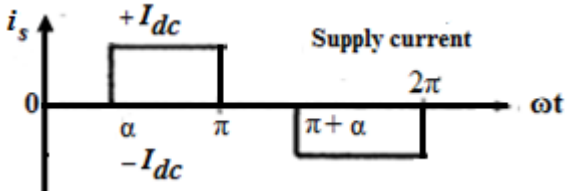

(c)

Fig. 3.21.

Hence, $V_{o1} = \frac{1}{\sqrt{2}}\sqrt{a_1^2 + b_1^2} = \frac{2\sqrt{2}\ I_{dc}}{\pi}\cos\frac{\alpha}{2}$

Example 3.9

For a single-phase, fully-controlled, bridge rectifier derive an expression for the a.c. power dissipated in a resistive load as the triggering angle is varied. If one thyristor remains in the non-conducting state, calculate the firing angle which results in 25% of maximum power dissipation in the load.

Solution

The power dissipated in resistive load is given by,

$$P = I_{orms}^2 \times R$$

$$I_{orms} = \sqrt{\frac{1}{\pi}\int_{\propto}^{\pi} (\frac{V_m}{R} sin\omega t\,^2)\, d\omega t}$$

$$I_{orms}^2 \times R = \frac{{V_m}^2}{2\pi R}\left(\pi - \alpha + \frac{1}{2}\, sin2\alpha\right)$$

$$P_{max} = \frac{dP}{d\alpha} = \frac{{V_m}^2}{2\pi R} \quad \frac{d\left(\pi - \alpha + \frac{1}{2}\, sin2\alpha\right)}{d\alpha} = 0$$

$$\therefore\ P_{max} = \frac{V_m^2}{2R}$$

If one thyristor is open circuit

$$P_o = \frac{1}{2}P = \frac{1}{2}\frac{{V_m}^2}{2\pi R}\left(\pi - \alpha + \frac{1}{2}\, sin2\alpha\right) = 0.25P_{max}$$

$$0.25\frac{{V_m}^2}{2R} = \frac{1}{2}\frac{{V_m}^2}{2\pi R}\left(\pi - \alpha + \frac{1}{2}\, sin2\alpha\right) = \alpha + \frac{1}{2}\, sin2\alpha = \frac{\pi}{2}$$

Since : $\frac{1}{2}\, sin2\alpha$ is very small, $\therefore \alpha = \frac{\pi}{2}$.

Example 3.10

A single-phase fully controlled, full-wave, bridge rectifier has a source of 230 V *rms* at 50 Hz, and is feeding a load R = 25 Ω and L = 10 mH. The

firing angle α = 45˚ and the current extinction angle β =230˚. It is required to:

(a) Sketch the appropriate load voltage and load current waveforms.
(b) Determine whether the current is continuous or discontinuous.
(d) Determine the average load voltage and current.
(e) Determine the *rms* load voltage and current.
(f) Determine the a.c. and d.c powers absorbed by the load.
(g) Determine the efficiency of the converter.

Solution

(a) Since $\pi + \alpha = 180° + 45° = 225° < \beta$, then the current is continuous.

(b) The waveforms for v_o, and i_o are as shown in Fig.3.22,

Fig.3.22.

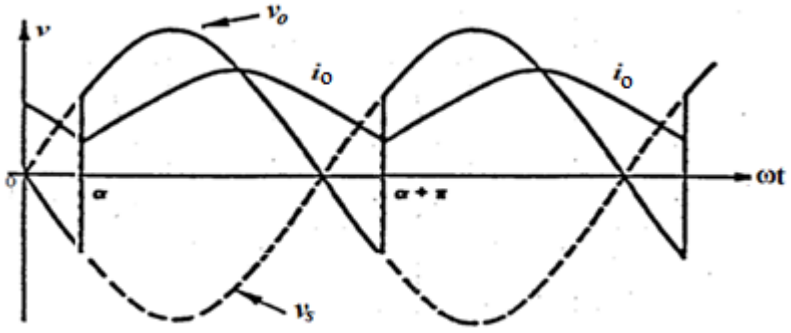

(c) $$V_{dc} = \frac{1}{\pi}\int_{\alpha}^{\alpha+\pi} V_m sin\omega t \, d\omega t = \frac{2\,V_m}{\pi} cos\alpha$$

$$= \frac{2 \times 230 \times \sqrt{2}}{\pi} \cos 45 = 146.45 \text{ V}$$

$$I_{dc} = \frac{V_{dc}}{R} = \frac{146.45}{25} = 5.85 \text{ A}$$

(d) The *rms* values of the output voltage and current: Using Eq.(3.24),

$$V_{orms} = \frac{V_m}{\sqrt{2}} = \frac{230 \times \sqrt{2}}{\sqrt{2}} = 230 \text{ V}$$

$$I_{orms} = \frac{V_{rms}}{Z_L} = \frac{V_{rms}}{\sqrt{R^2 + (\omega L)^2}} = \frac{230}{\sqrt{25^2 + (2\pi \times 50 \times 10 \times 10^{-3})^2}}$$

∴ $I_{orms} = 9.12$ A

(f) The d.c. and a.c. powers are,

$$P_{dc} = V_{dc}\, I_{dc} = 146.45 \times 5.85 = 856.73 \text{ W}$$

$$P_{ac} = V_{rms}\, I_{rms} = 230 \times 9.12 = 2097.6 \text{ W}$$

(g) The efficiency of the converter,

$$\eta = \frac{P_{dc}}{P_{ac}} = \frac{856.73}{2097.6} = 0.408 = 40.8\%$$

Example 3.11

The circuit of Fig.3.23 consists of identical resistors $R_1 = R_2 = 200\ \Omega$, an ideal diode D and an ideal thyristor T supplied from an ideal power supply $v_s = 200 \sin\omega t$.
(a) Sketch, to scale, corresponding waveforms of the supply voltage and the currents in R_1, R_2, D and T if the thyristor firing angle is 90°.
(b) What is the average value of the current in R_1 for a supply cycle?

Fig. 3.23.

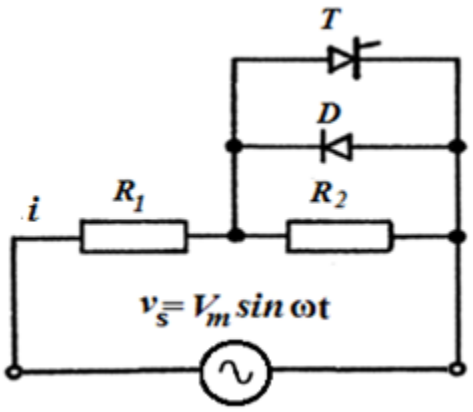

Solution

(a) The waveforms are as shown in Fig.3.24,

(b) $$i_1 = \frac{V_m}{R_1 + R_2} sin\omega t = \frac{200}{400} sin\omega t = 0.5\, sin\omega t$$

$$i_2 = \frac{V_m}{R_1} sin\omega t = \frac{200}{200}\, sin\omega t = sin\omega t$$

$$I_{dc} = \frac{1}{2\pi}\int_0^{\frac{\pi}{2}} 0.5\, sin\omega t\, d\omega t + \frac{1}{2\pi}\int_{\pi/2}^{2\pi} sin\omega t\, d\omega t$$

$$= \frac{1}{2\pi}\left[-\cos\frac{\pi}{2} + 0.5 - 1 + \cos\frac{\pi}{2}\right] = \frac{-1}{4\pi} = -79.6 \text{ mA}$$

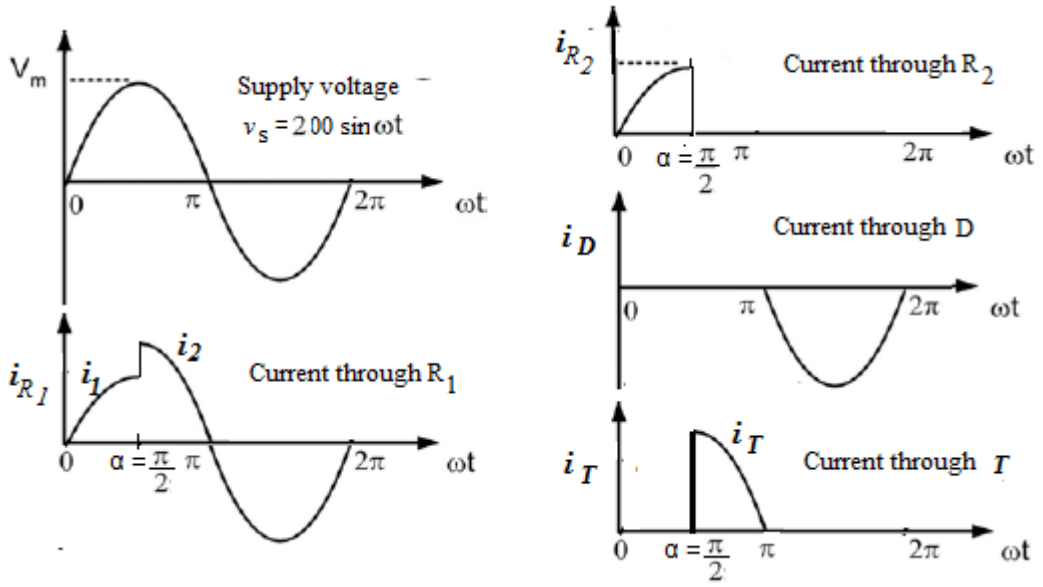

Fig.3.24 Waveforms for example 3.11.

Example 3.12

A single-phase full-wave fully-controlled bridge rectifier is feeding an *R-L* load with R = 15 Ω and L = 20 mH as shown in Fig.3.25. The *rms* value of the a.c. input voltage is 230 V. The firing angle α is maintained constant at 45° so that the load current has an extinction angle of β =235°.

(a) Specify whether the current is continuous or discontinuous.
(b) Determine the average load voltage V_{dc} and current I_{dc}.
(c) Assume that load resistance remains the same; find the voltage V_{dc} and current I_{dc} if a freewheeling diode D_{FW} is used across the load.
(d) If T_3 is open circuited, find the load voltage and d.c. power while freewheeling diode D_{FW} is still connected and α is the same.

Fig.3.25.

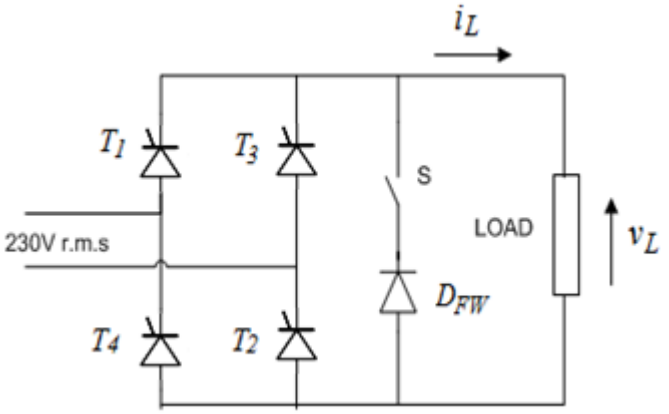

Solution

(a) The current is continuous or discontinuous is found as follows:

Since 180˚ + 45˚ = 225, which is < β (=235°). Hence , the current is continuous.

(b) The average load voltage V_{dc} and current I_{dc} for continuous current operation are

$$V_{dc} = \frac{2V_m}{\pi} cos\alpha$$

$$\therefore V_{dc} = \frac{2 \times 230 \times \sqrt{2}}{\pi} cos45^o = 146.5 \text{ V}$$

$$I_{dc} = \frac{V_{dc}}{R} = \frac{146.5}{15} = 9.76 \text{ A}$$

(c) When the freewheeling diode D_{FW} is used across the load, and the load resistance remains the same; the waveform of the voltage will be as depicted in Fig.3.26.

The voltage V_{dc} and current I_{dc} are

$$V_{dc} = \frac{1}{\pi}\int_{\alpha}^{\pi} V_m sin\omega t \, d\omega t$$

$$= \frac{V_m}{\pi}\left\{-cos\omega t\right]_{\alpha}^{\pi}\right\}$$

$$= \frac{V_m}{\pi}(1 + cos\alpha)$$

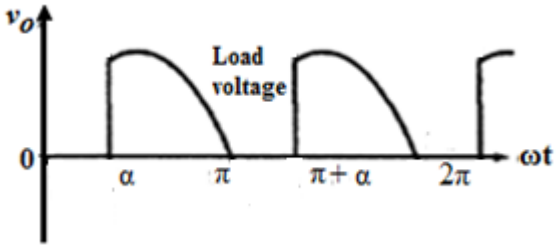

Fig. 3.26.

$$= \frac{325.2}{\pi}(1 + cos45°) = 176.67 \text{ V}$$

$$I_{dc} = \frac{V_{dc}}{R} = \frac{176.67}{15} = 11.77 \text{ A}$$

(d) If T_3 is open circuited, the circuit and the output voltage will be as in Fig.3.27.

$$V_{dc} = \frac{1}{\pi}\int_{\alpha}^{\pi} V_m sin\omega t \, d\omega t = \frac{V_m}{2\pi}\left\{-cos\omega t\right]_{\alpha}^{\pi}\right\} = \frac{V_m}{2\pi}(1 + cos\alpha)$$

$$= \frac{325.2}{2\pi}(1 + cos45°) = 88.33 \text{ V}$$

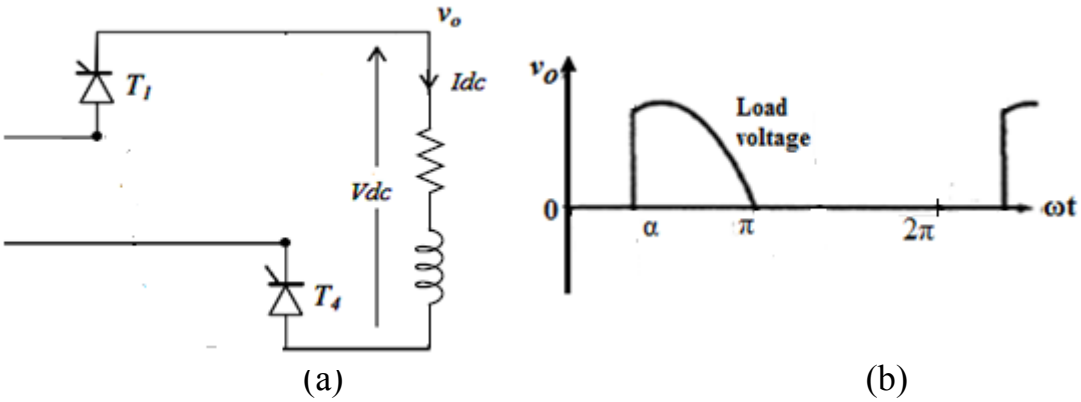

(a) (b)

Fig.3.27.

$$I_{dc} = \frac{V_{dc}}{R} = \frac{88.33}{15} = 5.89 \text{ A}$$

$$P_{dc} = V_{dc} \times I_{dc} = 88.33 \times 5.89 = 520.17 \text{ W}$$

Example 3.13

The firing angle of the circuit shown in Fig.3.16 is kept constant to produce an average output voltage of 54 V d.c. and steady load current of 3.6 A. The load has a fixed resistance and infinite inductance. The primary voltage V_p = 240 V *rms* and the transformer has 2:1 voltage ratio.

(a) Find the triggering angle α and the load resistance *R*.
(b) Assume a FWD diode is connected across the load. Find the load current.
(c) If one thyristor is damaged (open-circuited), find the new load current.
(d) Specify the required ratings of thyristors and transformer.

Solution

(a) For highly inductive load the d.c. voltage is given by Eq.(3.31) as

$$V_{dc} = \frac{2V_m}{\pi} cos\alpha$$

$$V_m = \sqrt{2}V_p \times \frac{1}{a} = \sqrt{2} \times 240 \times \frac{1}{2} = 169.7 \text{ V}$$

where *a* is the transformer voltage ratio.

$$V_{dc} = 54 = \frac{2 \times 169.7}{\pi} cos\alpha \qquad \rightarrow cos\alpha = 0.5002$$

$\cos^{-1} 0.5002 \cong 60°$

The load resistance R is found as

$$R = \frac{V_{dc}}{I_{dc}} = \frac{54}{3.6} = 15\Omega$$

(b) When a freewheel diode is connected across the load, the output voltage waveform will be as depicted in Fig.3.28 and its average value is given by

$$V_{dc} = \frac{1}{\pi}\int_{\alpha}^{\pi} V_m sin\omega t \, d\omega t$$

$$V_{dc} = \frac{V_m}{\pi}\{-cos\omega t\ {}^{\pi}_{\alpha}\}$$

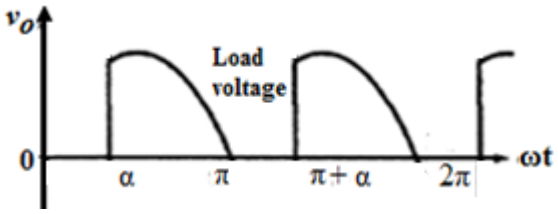

Fig.3.28.

$$= \frac{V_m}{\pi}(1 + cos\alpha) \quad \frac{169.7}{\pi}(1 + cos60°) = 81 \text{ V}$$

$$I'_{dc} = \frac{V_{dc}}{R} = \frac{81}{15} = 5.4 \text{ A}$$

(c) If one thyristor is damaged, the circuit becomes single-phase, half-wave rectifier, and

$$V_{dc} = \frac{1}{2\pi}\int_{\propto}^{\alpha} V_m sin\omega t \, d\omega t$$

$$V_{dc} = \frac{V_m}{2\pi}\{-cos\omega t\ {}^{\pi}_{\alpha}\} = \frac{V_m}{2\pi}(1 + cos\alpha) = \frac{169.7}{2\pi}(1 + 0.5) = 40.5\text{V}$$

$$I''_{dc} = \frac{V_{dc}}{R} = \frac{40.53}{15} = 2.7 \text{ A}$$

(d) Thyristors voltage ratings:

PRV = 2 V_m = 2 × 169.7 = 339.4 V

and PFV = 2 V_m = 2 ×169.7 = 339.4 V

Thyristor average current , since the current is steady (constant) , for highly inductive load ,the current through each thyristor is a rectangular

pulse start from α to α + π for a complete cycle of 2π as shown in Fig.3.29, hence its average value is

$$I_{Tav} = \frac{1}{2\pi}\int_{\alpha}^{\alpha+\pi} I_{dc}\, d\omega t = \frac{I_{dc}}{2\pi}(\alpha + \pi - \alpha) = \frac{I_{dc}}{2} = \frac{3.6}{2} = 1.8\ \text{A}$$

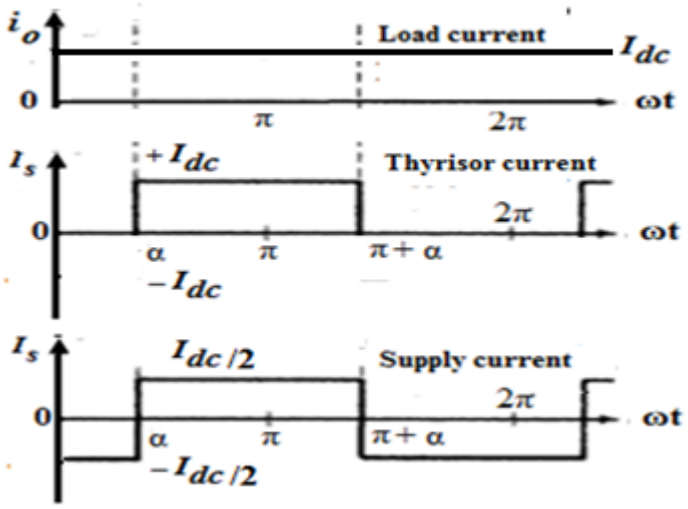

Fig.3.29 Current waveforms.

The *rms* value of the thyristor current is

$$I_{Trms} = \sqrt{\frac{1}{2\pi}\int_{\alpha}^{\alpha+\pi} {I_{dc}}^2\, d\omega t} = \frac{I_{dc}}{\sqrt{2}} = \frac{3.6}{\sqrt{2}} = 2.54\ \text{A}$$

$$(VA)_s = 2 \times \frac{I_{dc}}{\sqrt{2}} \times \frac{V_m}{\sqrt{2}} = I_{dc}V_m = 3.6 \times 169.7 = 610.9$$

$$(VA)_p = \frac{I_{dc}}{2} \times V_{prms} = \frac{3.6}{2} \times 240 = 432$$

The transformer rating is:

$$(VA)_{TR} = \tfrac{1}{2}\big((VA)_s + (VA)_p\big) = \tfrac{1}{2}(610.9 + 432) = 521.45$$

Example 3.14

A full-wave, fully-controlled bridge rectifier is fed from 230 V, 50 Hz, single-phase supply. The rectifier is used to charge a 48 V d.c. battery bank through *R*-*L* circuit of *R* = 0.48 Ω and *L*= 0.79 mH. The firing angle is maintained at 41˚. Find the required average charging current.

Solution

$$V_m = 230 \times \sqrt{2} = 325.2 \text{ V}$$

To find the average charging current using Eq.(3.28) and Eq.(3.29) as follows :
From equation (3.29),

$$i(0) = -\frac{V_m}{Z}\sin(\alpha - \theta)\left[\frac{1 + e^{-\frac{\pi R}{\omega L}}}{1 - e^{\frac{\pi R}{\omega L}}}\right] - \frac{E}{R}$$

$$Z = \sqrt{R^2 + (\omega L)^2} = \sqrt{(0.48)^2 + (2\pi \times 50 \times 0.79 \times 10^{-3})^2}$$
$$= 2.526\ \Omega$$

$$\theta = \tan^{-1}(\frac{\omega L}{R}) = \tan^{-1}(\frac{2\pi \times 50 \times 0.79 \times 10^{-3}}{0.48}) = \tan^{-1}\frac{2.48}{0.48}$$
$$= 79° = 0.715 \text{ rad}$$

$$\frac{\pi R}{\omega L} = \frac{3.14 \times 0.48}{2.48} = 0.607$$

$$i(0) = -\frac{325.2}{2.526}\sin(41° - 79°)\left[\frac{1 + e^{-0.607}}{1 - e^{-0.607}}\right] - \frac{48}{0.48} = 169.13 \text{ A}$$

Substituting this value into Eq.(3.28),

$$i(\omega t) = \frac{325.2}{2.526}\sin(\omega t - 79°) - \frac{48}{0.48} + [169.13$$
$$- \frac{325.2}{2.526}\sin(41° - 79°) + \frac{48}{0.48}]\ e^{\frac{-0.48}{2.48}(\omega t - 0.193)}$$

$$i(\omega t) = 128.74\sin(\omega t - 79°) - 100 + 400e^{-193\omega t}$$

To find the average value of the current using Eq.(3.30),

$$I_{av} = \frac{1}{\pi}\int_{\alpha}^{\alpha+\pi} i(\omega t)\ d\omega t$$

$$= \frac{1}{\pi}\int_{0.715}^{0.715+\pi} \{128.74\sin(\omega t - 79°) - 100 + 400e^{-193\omega t}\}\, d\omega t$$
$$\cong 220 \text{ A}$$

3.6 POLY-PHASE CONTROLLED RECTIFIERS

The poly-phase controlled rectifiers are used to convert a.c. input power supply into d.c. variable output voltage across the load. The features of poly-phase controlled rectifiers are:

- Operate from poly-phase a.c. supply voltage.
- They provide higher d.c. output voltage and higher d.c. output power.
- Higher output voltage ripple frequency.
- Filtering requirements are simplified for smoothing output load voltage and load current.

Poly-phase controlled rectifiers are classified into half-wave and full-wave, three-phase, six-phase, twelve-phase depending on the number of input phases which indicates the number of pulses *p* of the output voltage waveform.

3.6.1 Three-Phase Half-wave Controlled Rectifier (*p = 3*)

The Three-phase half-wave controlled rectifier is shown in Fig.3.30 (a). The waveforms for the supply voltage, output voltage, and load current are shown in Fig.3.30 (b) for case of resistive load.

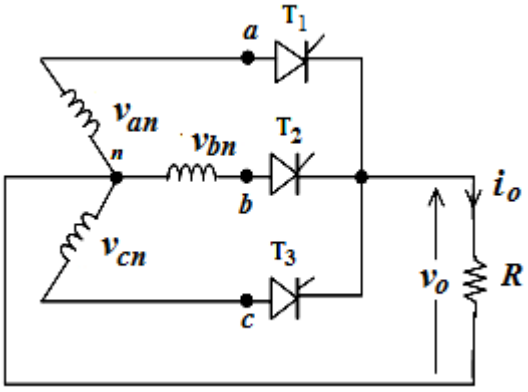

(a) Circuit.

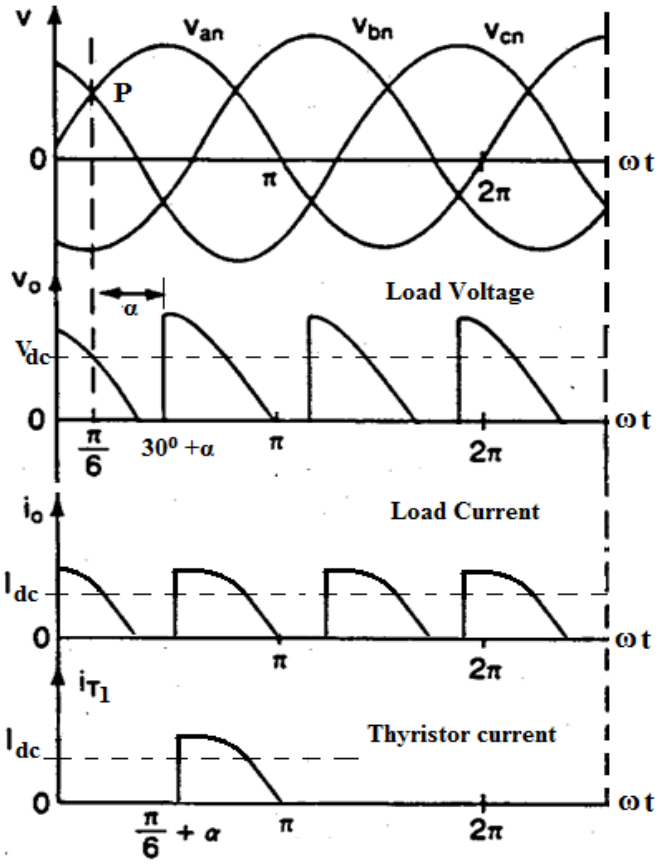

(b) Waveforms.

Note: α is usually measured from point *P* in Fig.3.30 (b).

Fig.3.30 Three-phase half-wave controlled rectifier. Case of resistive load.

As for the half-wave 3-phase uncontrolled diode rectifier, the load is connected between the converter positive terminal (cathodes of all thyristors) and the supply neutral. The thyristor with the highest voltage with respect to the neutral, when triggered, conducts. As the voltage of another thyristor becomes the highest, the load current is transferred to that device when triggered, and the previously conducting device is reverse-biased and naturally commutated. This process can be illustrated with the aid of Fig.3.30 (a) and assuming resistive load as follows:

The three-phase half-wave converter can be considered as it combines three single-phase half-wave controlled rectifiers in one single circuit feeding a common load. The thyristor T_1 in series with one of the supply phase windings 'v_{an}' acts as one half-wave controlled rectifier. The second thyristor T_2 in series with the supply phase winding 'v_{bn}' acts as the second half-wave controlled rectifier. The third Thyristor T_3 in series with the supply phase winding 'v_{cn}' acts as the third half-wave controlled rectifier. The 3-phase input supply is applied through the star-connected supply transformer. The common neutral point of the supply is connected to one end of the load while the other end of the load connected to the common cathode point.

- When the thyristor T_1 is triggered at $\omega t = (30° + \alpha)$ the phase voltage v_{an} appears across the load when T_1 conducts. The load current flows through the supply phase winding $'a - n'$ and through thyristor T_1 as long as T_1 conducts.
- When thyristor T_2 is triggered at $\omega t = (150° + \alpha)$ T_1 becomes reverse biased and turns-off. The load current flows through the thyristor T_2 and through the supply phase winding $'b - n'$. When T_2 conducts the phase voltage v_{bn} appears across the load until the thyristor T_3 is triggered .
- When the thyristor T_3 is triggered at $\omega t = (270° + \alpha)$ T_2 is reversed biased and hence T_2 turns-off. The phase voltage v_{cn} appears across the load when T_3 conducts.
- When T_1 is triggered again at the beginning of the next input cycle the Thyristor T_3 turns off as it is reverse biased naturally as soon as T_1 is triggered . The output voltage which appears across the load, and the load current assuming a constant and ripple free load current for a highly inductive load and the current through the thyristor T_1 .

For a purely resistive load where the load inductance '$L = 0$' and the trigger angle $\alpha > 30°$ the load current appears as discontinuous load current and each thyristor is naturally commutated when the polarity of the corresponding phase supply voltage reverses. The frequency of output ripple frequency for a three-phase half wave converter is $3\,f_s$, where f_s is the input supply frequency.

Analytical properties of the output voltage waveform of the three-phase half-wave controlled rectifier

(A) Case of resistive load

The waveforms for the supply voltage, output voltage, and load current are shown in Fig.3.29 for the case of resistive load. The average value of the output voltage V_{dc} can be found as:

Let $v_{an} = V_m \sin \omega t$

$v_{bn} = V_m \sin(\omega t - 2 \pi / 3)$

$v_{cn} = V_m \sin(\omega t - 4 \pi / 3)$

The average value of the load voltage wave is

$$V_{dc} = \frac{1}{\frac{2\pi}{3}} \int_{30°+\alpha}^{180°} V_m \ sin\omega t \ d\omega t = \frac{3V_m}{2\pi} [-cos\omega t]_{30° + \alpha}^{180°}$$

$$= \frac{3V_m}{2\pi} [-(\cos(180°) + \cos(30° + \alpha)]$$

$$= \frac{3V_m}{2\pi} [1 + \cos(\alpha + 30°)] \qquad (3.35)$$

The load current I_{dc} is:

$$I_{dc} = \frac{3V_m}{2\pi R} [1 + \cos(\alpha + 30°)] \qquad (3.36)$$

In case of resistive load, each thyristor ceases to conduct as soon as its anode voltage goes negative. This causes discontinuous current flow in the rectifier circuit when the angle exceeds $30°$ as shown in Fig.3.30.

(B) Case of series resistive-inductive (*R-L*) load

When the load is highly inductive it tends to maintain constant output current even with large delay angles, and the thyristor current remains rectangular as shown in Fig.3.31. Consequently, the induced *emf* in the load inductor maintains current flow even when the anode polarity has reversed. This means that energy is being returned from the magnetic field of the inductor through the transformer to the supply, and the circuit is temporarily acting as an inverter.The average value of the load voltage wave is

$$V_{dc} = \frac{1}{\frac{2\pi}{3}} \int_{30°+\alpha}^{30°+\alpha+120°} V_m \ sin\omega t \ d\omega t = \frac{3V_m}{2\pi} [-cos\omega t]_{30° + \alpha}^{150° + \alpha}$$

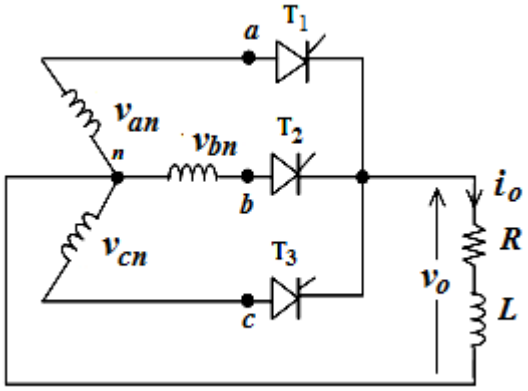

(a) Circuit.

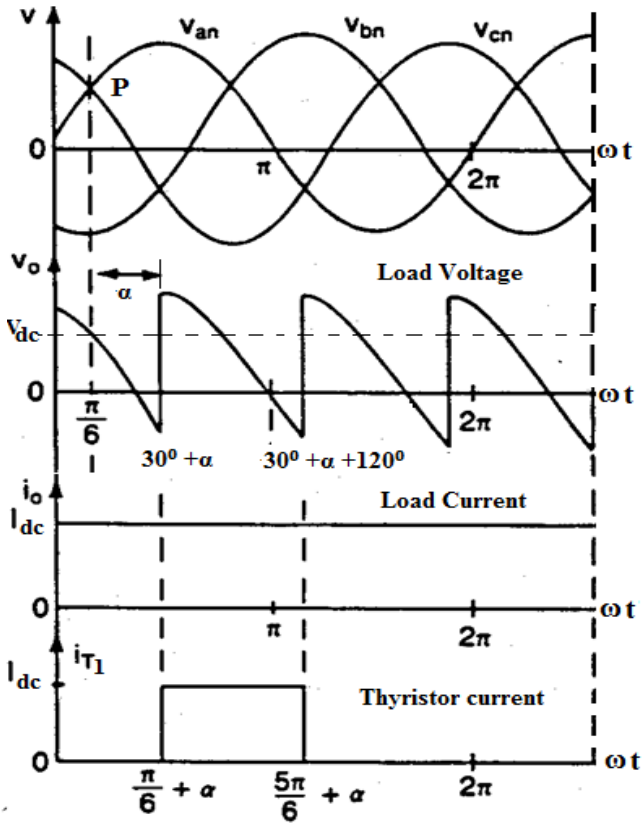

(b) Waveforms

Fig.3.31 Three-phase half-wave controlled rectifier with *R-L* load.

$$V_{dc} = \frac{3V_m}{2\pi}[-(\cos(150° + \alpha) - \cos(30° + \alpha))]$$

$$= \frac{3\sqrt{3}V_m}{2\pi}cos\alpha \qquad (3.37)$$

The load current I_{dc} is:

$$I_{dc} = \frac{3\sqrt{3}V_m}{2\pi R}cos\alpha \qquad (3.38)$$

The operation of the three- phase, half-wave rectifier with different values of α is illustrated in Fig.3.32. It can be seen that this converter can operate either as a rectifier or as an inverter as

For $0^0 < \alpha < 90^0$ ⟹ Rectification process

$90^0 < \alpha < 180^0$ ⟹ Inversion process

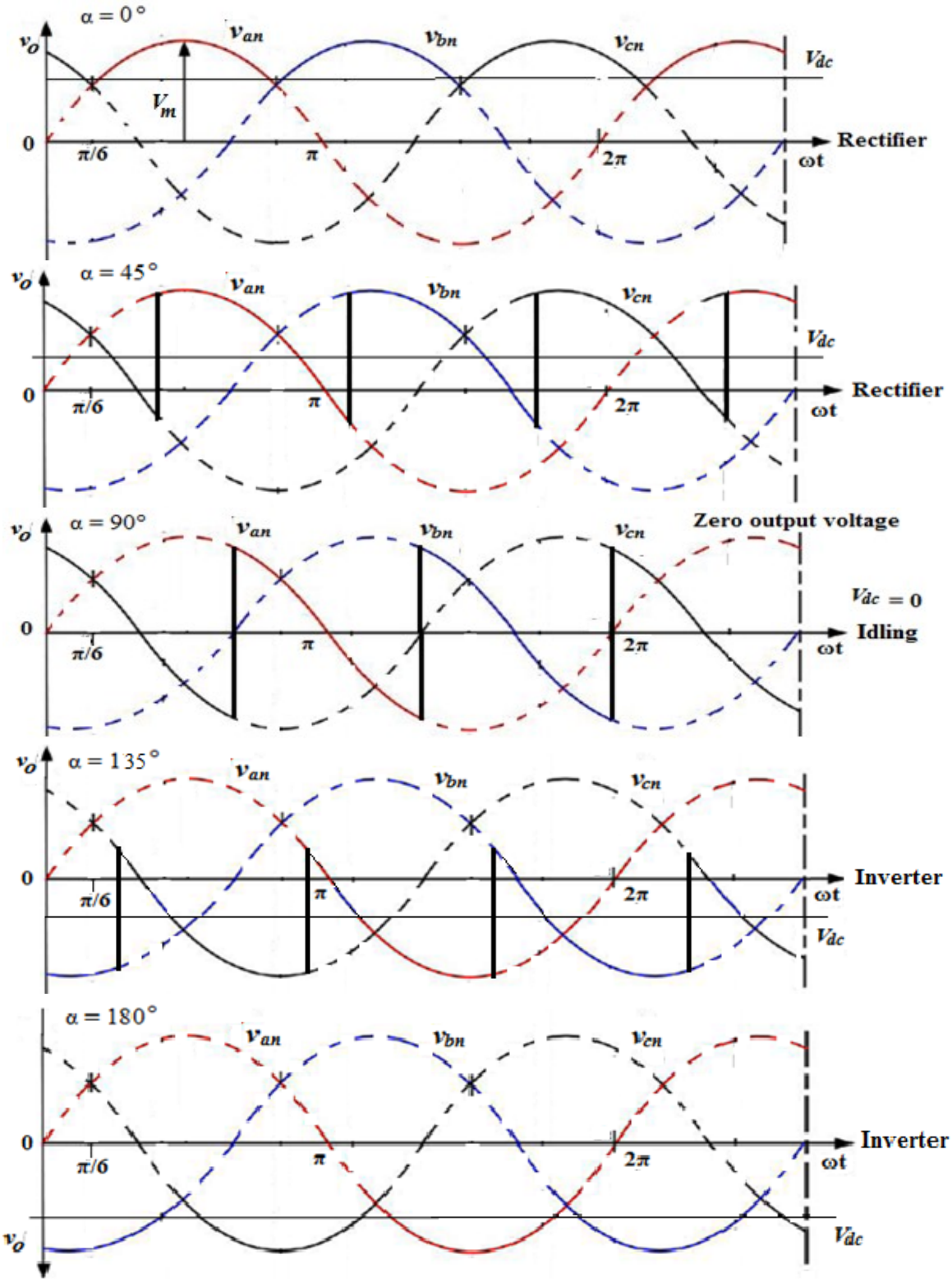

Fig.3.32 Output voltage waveform of the three-phase half-wave rectifier for different values of firing angle α. Case of *R-L* load.

Notes:

1. The mean output voltage is zero for α = π/2. The converter is idle (no output).
2. Negative average output voltage occurs when α > π/2.
3. Power inversion is possible, if a load with an *emf* to assist the current flow.

The three-phase half-wave converter is not normally used in practical converter systems because of the disadvantage that the supply current waveforms contain d.c. components (i.e. the supply current waveforms have an average or d.c. value).

Example 3.15

The load in Fig.3.31 consists of a resistance and a very large inductance. The inductance is so large that the output current I_o can be assumed to be continuous and ripple-free. For α = 60°,

(a) Draw the wave forms of V_o and I_o.
(b) Determine the average value of the output voltage, if phase voltage V_{an} = 120 V.
(c) Find the average output voltage if a free wheel diode is connected across the load.

Solution

(a) The waveforms of V_o and I_o are as shown in Fig.3.31(b),
(b) The average value of the output voltage is given in Eq.(3.37) as,

$$V_{av} = \frac{3\sqrt{3}\,V_m}{2\pi}\cos\alpha$$

For $\alpha = 60°$: $\quad V_m = \sqrt{2}\,V_{an} = \sqrt{2} \times 120\text{ V} = 169.7\text{ V}$

$$\therefore V_{dc} = \frac{3\sqrt{3}}{2\pi} \times 169.7\cos 60^o = 70.2\text{ V}$$

(c) If a freewheel diode is connected across the load, the circuit and output voltage waveform will be as shown in Fig.3.33.

The average voltage of the waveform of Fig.3.33 (b) can be evaluated as

$$V_{dc} = \frac{1}{\frac{2\pi}{3}}\int_{30°+\alpha}^{\pi} V_m\ sin\omega t\ d\omega t = \frac{3V_m}{2\pi}\,[-cos\omega t]_{30°+\alpha}^{\pi}$$

$$V_{dc} = \frac{3V_m}{2\pi}(1 + \cos(30° + \alpha))$$

$$\therefore V_{dc} = \frac{3\sqrt{3}}{2\pi} \times 169.7\,(1 + \cos(30^o + 60^o)) = 81\ \text{V}$$

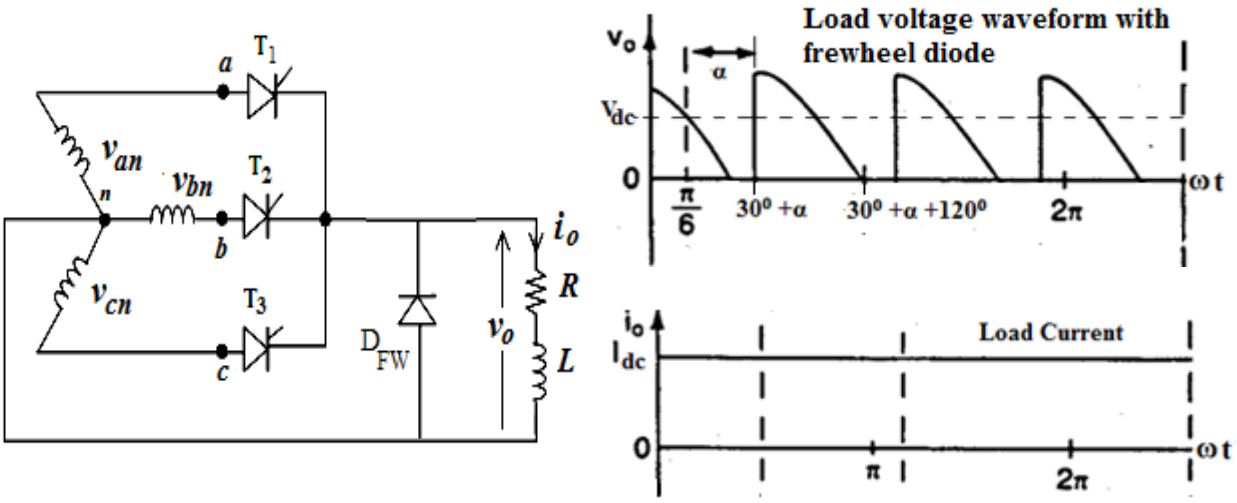

(a) Circuit

(b) Waveform

Fig.3.33.

General solution of *p*-pulse half-wave controlled rectifier

For p-pulse (or p-phase, i.e.: 3-phase, 6-phase, 12-phase …. etc) half-wave rectifier circuit, a general formula can be obtained as follows:
The output voltage v_o waveform of a p-pulse, fully controlled converter with continuous current operating mode would be as shown in Fig.3.35.

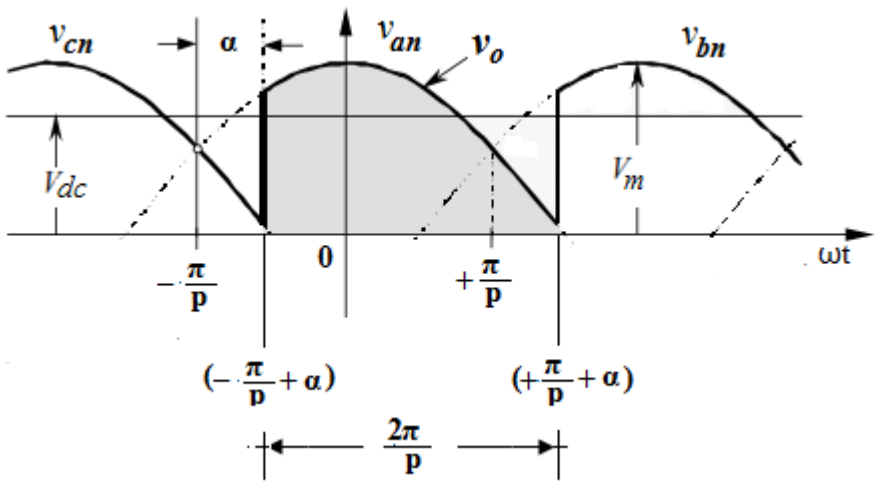

Fig.3.34.

It has been found useful for calculation to express the a.c. voltages on the thyristor side by cosine functions to avoid the mistake in the polarity sign. Hence:

$v_{an} = V_m \cos(\omega t + 120)$
$v_{bn} = V_m \cos \omega t$
$v_{cn} = V_m \cos(\omega t - 120)$

The average d.c. voltage V_{dc} is,

$$V_{dc} = \frac{1}{\frac{2\pi}{p}} \int_{(-\frac{\pi}{p}+\alpha)}^{(+\frac{\pi}{p}+\alpha)} V_m \cos \omega t \, d\omega t$$

$$= \left(\frac{p}{2\pi}\right) V_m \left[\sin\left(\frac{\pi}{p} + \alpha\right) - \sin\left(-\frac{\pi}{p} + \alpha\right)\right]$$

$$= \left(\frac{p}{2\pi}\right) V_m \left[\sin\frac{\pi}{p}\cos\alpha + \sin\alpha\cos\frac{\pi}{p} - \sin\left(-\frac{\pi}{p}\right)\cos\alpha + \cos\left(\frac{-\pi}{p}\right)\sin\alpha\right]$$

$$= \frac{P\, V_m}{2\pi}\left[2 \sin\frac{\pi}{P}\cos\alpha\right]$$

$$\therefore V_{dc} = \frac{p}{\pi} V_m \sin\frac{\pi}{p}\cos\alpha \qquad (3.39)$$

or , for a three-phase, half-wave circuit, $p = 3$, hence,

$$V_{dc} = \frac{3}{\pi} V_m \sin\frac{\pi}{3}\cos\alpha = \frac{3\sqrt{3}V_m}{2\pi}\cos\alpha$$

which is the same as Eq.(3.37) obtained previously.

Notes :
-The diode conduction angle is $120^\circ + \alpha$.

-The variation of the average output voltage V_{dc} with the triggering angle α is shown in Fig.3.35 .

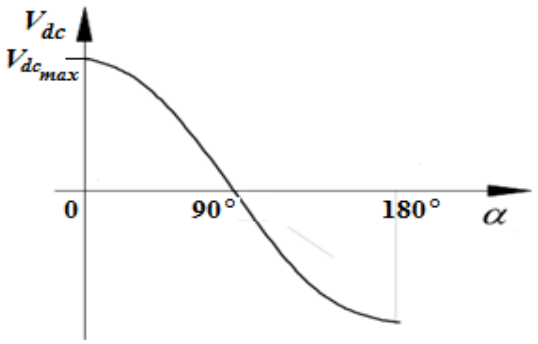

Fig.3.35 variation of the average output voltage V_{dc} with the triggering angle α.

3.6.2 Three-Phase Full-Wave Fully-Controlled Rectifier ($p = 6$)

Three-phase , full-wave converter is a fully-controlled bridge rectifier using six thyristors connected as shown in Fig.3.36(a). All the six thyristors are controlled switches which are turned on at an appropriate time by applying suitable gate trigger signals. The three-phase full-converter is extensively used in industrial power applications up to about 150kW output power level, where two-quadrant operation is required. This circuit is also known as three-phase full wave bridge or as a six-pulse converter. The frequency of output ripple voltage is 6 f_s and the filtering requirement is less than that of three-phase half-wave converters.

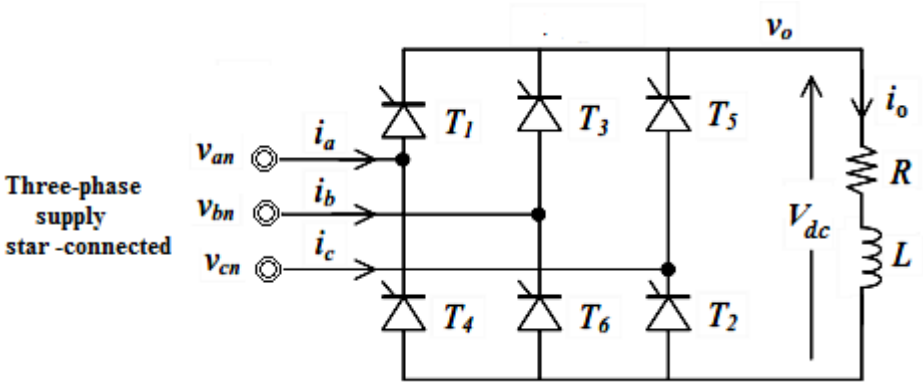

Fig.3.36 Three-phase full-wave fully-controlled rectifier.

In the circuit configuration of the three-phase full-wave controlled rectifier, the thyristor which has the most positive voltage at its anode conducts when triggered, and the thyristor with the most negative voltage at its cathode returns the load current, if triggered. The waveforms are as shown in Fig.3.37.

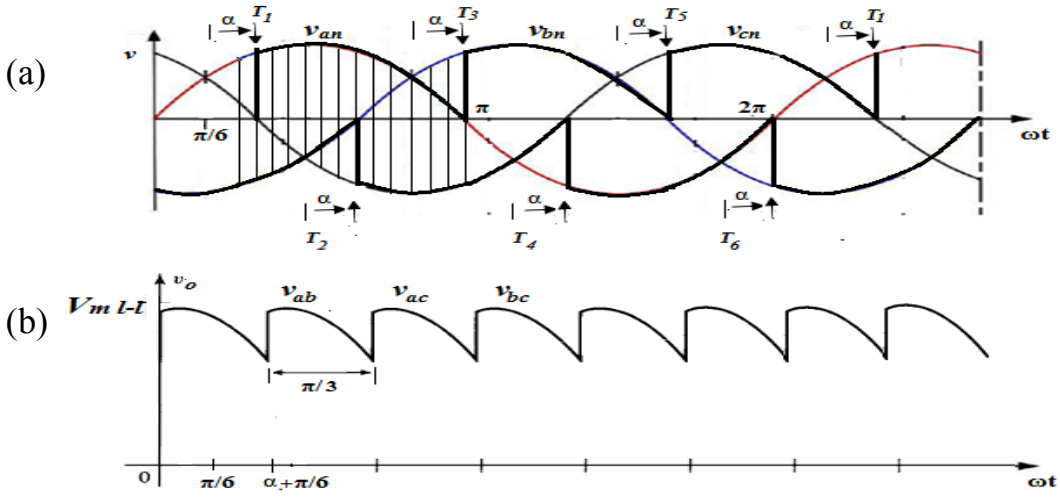

Fig.3.37 Three-phase full-wave fully-controlled rectifier output voltage waveform.

- Commutation of the load current from one thyristor to the next occurs at the firing instant, when the incoming thyristor reverse biases the previously conducting thyristor.
- The output d.c. voltage waveform is determined by the difference of potentials of the positive and negative rails.

Assuming continuous conduction, with highly inductive load, the average d.c. output voltage can be found by referring to Fig.3.37(b) as follows,

$$V_{dc} = \frac{6}{2\pi}\int_{\alpha+\frac{\pi}{6}}^{\alpha+\frac{\pi}{2}} v_s(\omega t)d\omega t$$

where $v_s(\omega t) = v_{ab} = \sqrt{3}V_m \sin(\omega t + 30°)$

hence $$V_{dc} = \frac{3}{\pi}\int_{\alpha+\frac{\pi}{6}}^{\alpha+\frac{\pi}{2}} \sqrt{3}V_m \sin(\omega t + 30°)\, d\omega t$$

$$\therefore \quad V_{dc} = \frac{3\sqrt{3}V_m}{\pi} cos(\alpha) \qquad (3.40)$$

The *rms* value of the output voltage waveform is

$$V_{o(rms)} = [\frac{6}{2\pi}\int_{\alpha+\frac{\pi}{6}}^{\alpha+\frac{\pi}{2}} {v_o}^2(\omega t)d\omega t]^{\frac{1}{2}}$$

$$V_{o(rms)} = [\frac{3}{\pi}\int_{\alpha+\frac{\pi}{6}}^{\alpha+\frac{\pi}{2}} 3{V_m}^2 \sin^2(\omega t + 30°)\, d\omega t]^{\frac{1}{2}}$$

$$V_{o(rms)} = \sqrt{3}V_m[\frac{1}{2} + \frac{3\sqrt{3}}{4\pi}\cos(2\alpha)]^{\frac{1}{2}} \qquad (3.41)$$

Alternatively , V_{dc} can be evaluated from the general p-phase formula, Eq.(3.30), as

$$V_{dc} = \frac{p}{\pi} V_{ml-l} \sin\frac{\pi}{p} \cos\alpha \quad ,$$

Here p = 6 , V_{ml-l} = Maximum line-to-line voltage = √3 V_m , here V_m = maximum line-to-neutral voltage, hencee,

$$V_{dc} = \frac{6\sqrt{3}}{\pi} V_m \sin\frac{\pi}{6} \cos\alpha = \frac{3\sqrt{3}V_m}{\pi} cos(\alpha)$$

which is the same result as in Eq. (3.40).

This converter operates in quadrants Q1 and Q4, developing both positive and negative polarity d.c. output voltage. For firing angles, $0^\circ \leq \alpha \leq 90^\circ$, the converter operates in quadrant-1 (Q1) (giving positive output power, i.e. rectifier operation) and for $90^\circ \leq \alpha \leq 180^\circ$, the operation is in quadrant-4 (giving negative output power, i.e. inverter operation). Operation in quadrant-4 is possible only when the load includes an active d.c. source, able to source power into the a.c. supply circuit. See Fig.3.38.

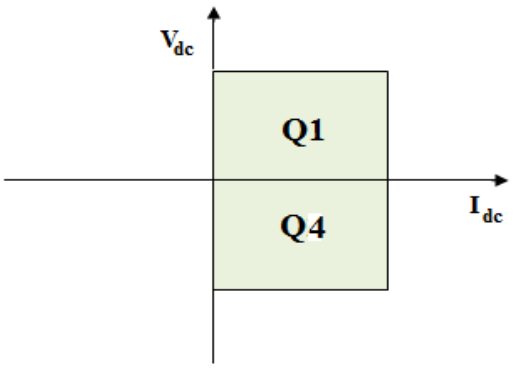

Fig. 3.38 Quadrants of operation of the three-phase fully-controlled converter.

3.6.3 Three-Phase Full-Wave Half-Controlled Rectifier

This converter is shown in Fig.3.39. It consists of three thyristors and three diodes with freewheeling diode across the load. It gives positive voltage and positive current only (not regenerative converter) i.e. it operates in the first quadrant only.

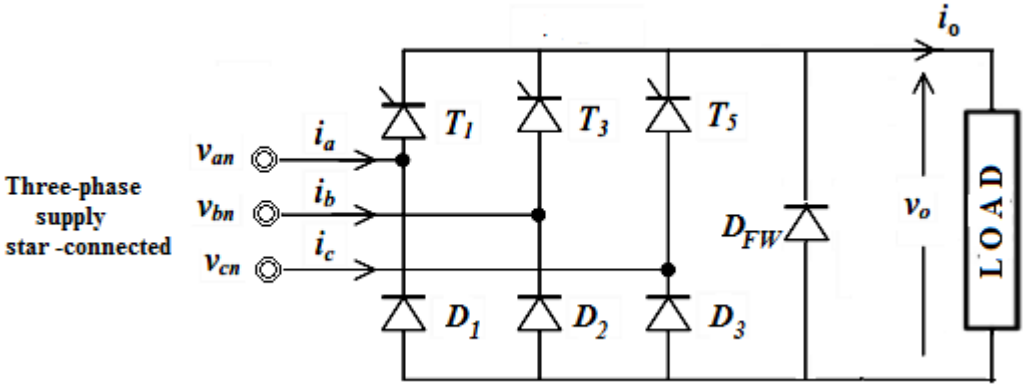

Fig.3.39 Three-phase full-wave, half-controlled rectifier.

In order to understand the principle of operation of this converter, assume that the output (load) current is continuous and ripple free.

- At $\omega t = \pi/6 + \alpha$, T_1 is triggered, hence T_1 and D_3 conduct and voltage $v_o = v_{ac}$ appears across the load.
- At $\omega t = 7\pi/6$ (210˚), $v_o = 0$, and from this instant onward v_{an} becomes the most negative phase and diode D_1 becomes forward biased and start conducting . Now since T_1 is still conducting, the

output current i_o will freewheel through T_1 and D_1 if D_{FW} is not connected making $v_o = 0$.

- When T_2 is triggered, current i_o will flow through T_2 and D_1 and voltage v_{ba} appears across the load.
- The process repeated every $2\pi/3$ whenever a thyristor is triggered.

The output voltage and current waveforms of the three-phase half-controlled rectifier bridge are as shown in Fig.3.40 for $\alpha = 90^\circ$. The instants of triggering the thyristors and duration of conduction of the diodes are also on the same figure.

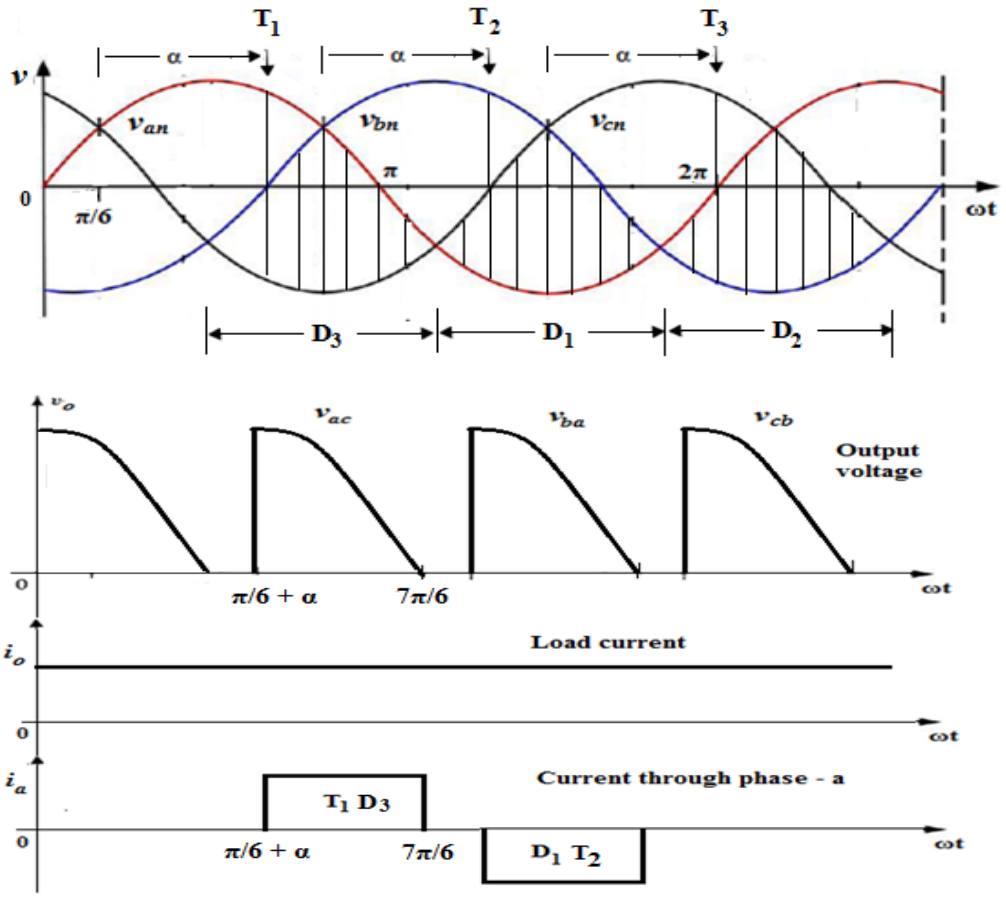

Fig.3.40 Waveforms of three-phase full-wave, half-controlled rectifier.

The output voltage is given by:
For the period $\pi/6 + \alpha$ and $7\pi/6$, the voltage appears across the load is

$$v_o = v_{ac}(\omega t) = \sqrt{3}V_m \sin(\omega t - 30^\circ)$$

$$v_{dc} = \frac{3}{2\pi}\int_{\alpha+\frac{\pi}{6}}^{\frac{7\pi}{6}} v_{ac}(\omega t)d\omega t$$

$$= \frac{3}{2\pi}\int_{\alpha+\frac{\pi}{6}}^{\frac{7\pi}{6}} \sqrt{3}V_m \sin(\omega t - 30°)d\omega t$$

$$\therefore \quad v_{dc} = \frac{3\sqrt{3}V_m}{2\pi}(1 + cos\alpha) \qquad (3.42)$$

Example 3.16

A three-phase full-wave fully-controlled rectifier supply a highly inductive load with R = 10 Ω the supply is a three-phase star-connected with 400 V *rms*, calculate:

(a) The load current when the firing angle α = 45°.
(b) The power drawn from the supply.
(c) If the current value kept at (a) and α changed to 135°, calculate the power returned to the supply.

Solution

(a) For α = 45 °

$$V_m = \frac{\sqrt{2} \times 400}{\sqrt{3}} = 326.6 \text{ V}$$

$$V_{dc} = \frac{3\sqrt{3}\ V_m}{\pi}\cos\alpha \quad = \frac{3\sqrt{3}\ \times 326.6}{\pi}\cos 45° \quad = 381.97 \text{ V}$$

$$I_{dc} = \frac{V_{dc}}{R} = \frac{381.97}{10} = 38.197 \text{ A}$$

(b) The power drawn from the source = the power dissipated at the resistance of the load

$$P_s = P_{load} = V_{dc}\, I_{dc} = 381.97 \times 38.197 = 14590.21 \text{ W}$$

(c) For α = 135° , $I_o = I_{dc}$ = 38.197 A

$$V_{dc} = \frac{3\sqrt{3}\, V_m}{\pi}\cos 135° = \frac{3\sqrt{3}\ \times 326.6}{\pi}\cos 135° = -381.97 \text{ V}$$

Power return to the source:

$$P_s = V_{dc} \, . \, I_{dc} = -381.97 \times 38.197 = -14590.21 \text{ W}$$

Example 3.17

If the converter in Example 3.16 is replaced by a full-wave half-controlled converter, calculate:

(a) V_{dc} when $\alpha = 45°$
(b) V_{dc} when $\alpha = 75°$
(c) V_{dc} when $\alpha = 135°$
(d) Maximum value of V_{dc}
(e) The value of α to obtain $I_{dc} = 15$ A

Solution

(a) For a three-phase semiconverter , the average d.c. voltage is

$$V_{dc} = \frac{3\sqrt{3}\ V_m}{2\pi}(1 + \cos\alpha)$$

For $\alpha = 45°$:

$$V_{dc} = \frac{3\sqrt{3} \times 326.6}{2\pi}(1 + \cos 45°) = 461 \text{ V}$$

(b) For $\alpha = 75°$:

$$V_{dc} = \frac{3\sqrt{3}\ \times 326.6}{2\pi}(1 + \cos 75°) = 340 \text{ V}$$

(c) For $\alpha = 135°$

$$V_{dc} = \frac{3\sqrt{3}\ \times 169.83}{2\pi}(1 + \cos 135°) = 79.53 \text{ V}$$

(d) Maximum voltage output is when $\alpha = 0°$

$$V_{dc} = \frac{3\sqrt{3}\ \times 326.6}{2\pi}(1 + \cos 0°) = 540 \text{ V}$$

(e)

$$I_{dc} = \frac{V_{dc}}{\text{R}} = 15 \text{ A}$$

or $V_{dc} = 15 \times R = 15 \times 10 = 150$ V

$$150 = \frac{3\sqrt{3} \times 326.6}{2\pi}(1 + \cos\alpha)$$

From which $\alpha = 116.4°$

Example 3.18

A d.c. load requires control of V_{dc} from maximum to 1/10 of the maximum value. If a half-controlled three-phase bridge is to be used, determine the range of angles required to trigger the thyristors.

Solution

Maximum V_{dc} is obtained when $\alpha = 0^{\circ}$, hence for the three-phase half-controlled bridge

$$V_{dcmax} = \frac{3\sqrt{3}\ V_m}{2\pi}(1 + \cos 0°) = \frac{3\sqrt{3}\ V_m}{\pi}$$

$$V_{dc} = \frac{V_{dcmax}}{2}(1 + \cos\alpha)$$

$$\frac{V_{dc}}{V_{dcmax}} = \frac{1}{10} = \frac{1}{2}(1 + \cos\alpha)$$

From which

$$\cos\alpha = \frac{1}{5} - 1 = -0.8 \qquad \therefore \alpha = 143°$$

The range of α is : $0^{\circ} \leq \alpha \leq 143^{\circ}$

Example 3.19

The load in Fig.3.41 consists of a resistance and a very large inductance. The inductance is so large that the output i_o can be assumed to be continuous and ripple-free. The load is supplied from an ideal three-phase half-wave controlled rectifier.

(a) Sketch a set of waveforms, for thyristor firing angle $\alpha = 45°$, showing: supply voltages (v_{an}, v_{bn}, v_{cn}), load voltage v_o, and load current i_o.

(b) Derive and expression for the average value V_{dc} of the load voltage.

(c) Determine the average value of the output voltage and current if the phase voltage peak is V_{max} = 450 V and R =100 Ω when α = 0°, α = 60°, and α = 120°.

(d) How is the average load voltage affected if thyristor T_2, failed to open circuit?

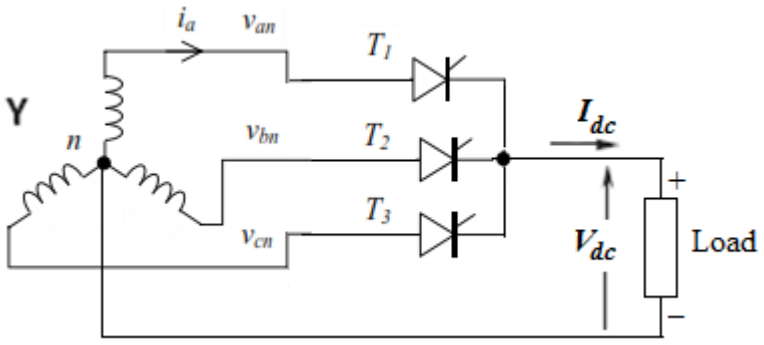

Fig.3.41

Solution

(a) Waveforms as shown in Fig.3.42.

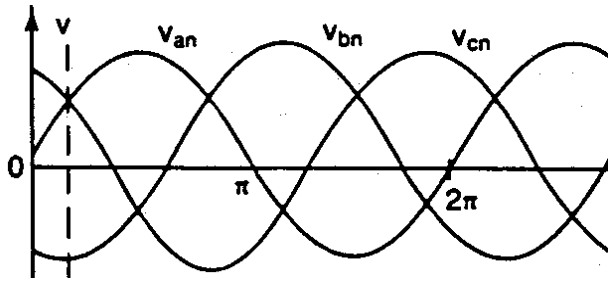

(a) Supply voltage waveforms

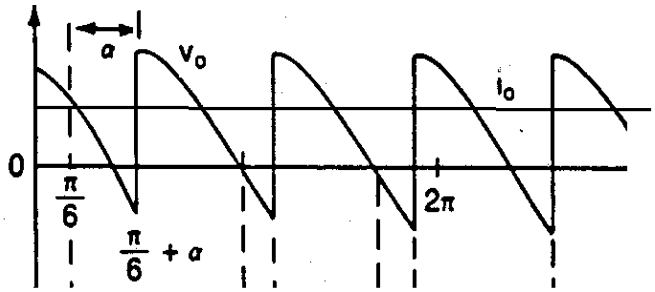

(b) Load voltage and current

Fig.3.42.

(b) Let $v_{an} = V_m \sin\omega t$,

$$V_{dc} = \frac{1}{\frac{2\pi}{3}} \int_{30°+\alpha}^{30°+\alpha+120°} V_{an}(\omega t)\, d\omega t$$

$$= \frac{1}{\frac{2\pi}{3}} \int_{30°+\alpha}^{30°+\alpha+120°} V_m sin\omega t d\omega t$$

$$= \frac{1}{\frac{2\pi}{3}} \int_{30°+\alpha}^{30°+\alpha+120°} V_m sin\omega t d\omega t$$

$$= \frac{3V_m}{2\pi}[-\cos(\alpha + 150) + \cos(\alpha + 30)] = \frac{3\sqrt{3}\,V_m}{2\pi} cos\alpha$$

(c) For α = 0°

$$V_{dc} = \frac{3\sqrt{3} \times 450}{2\pi} cos0° = 372\text{V} \quad \rightarrow \quad I_{dc} = \frac{372}{100} = 3.72\text{ A}$$

For $\alpha = 60°$

$$V_{dc} = \frac{3\sqrt{3} \times 450}{2\pi} \cos 60° = 189\text{ V} \quad \rightarrow \quad I_{dc} = \frac{189}{100} = 1.89\text{ A}$$

For α = 120°

$$V_{dc} = \frac{3\sqrt{3} \times 450}{2\pi} \cos(120°) = -322\text{ V}$$

(d) If T_2 failed to open circuit, phase-b will be eliminated and the voltage and current waveforms will appear as depicted in Fig.3.43 ,

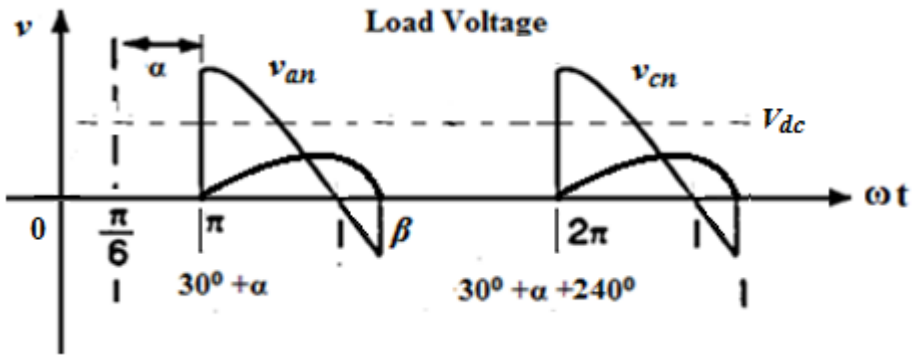

Fig.3.43 Voltage and current waveforms when T_2 fails to open circuit.

The average voltage will be,

$$V_{dc} = \frac{1}{2\pi}\int_{\alpha+30^\circ}^{\beta} V_m \sin\omega t\, d\omega t + \int_{\alpha+30^\circ+240^\circ}^{\beta+240^\circ} V_m \sin\omega t\, d\omega t$$

Example 3.20

Sketch the waveform across an *R-L* load (L→ ∞) for a 3-phase, half-wave converter with delay angle α = 60° (a) without, (b) with freewheeling diode. Drive, in each case, expressions for the average output d.c. voltage and deduce waveforms of transformer secondary current.

Solution

a) Without freewheeling diode, the load voltage is as shown in Fig.3.44.

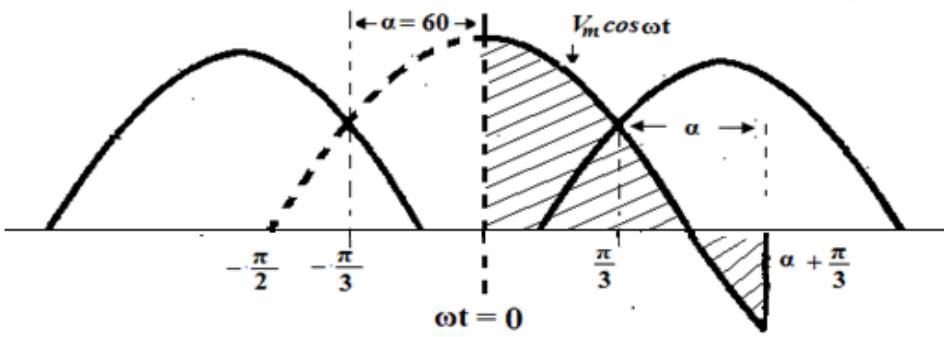

Fig.3.44

$$V_{dc} = \frac{3}{2\pi}\int_{\frac{-\pi}{3}}^{\frac{\pi}{3}} \sqrt{2}\, V_s \cos\omega t\, d\omega t = \frac{3}{2\pi}\left[\sqrt{2}\ V_s \sin\omega t\right]_{-\frac{\pi}{3}+\alpha}^{\frac{\pi}{3}+\alpha}$$

$$= \frac{3\sqrt{2}V_s}{2\pi}\left[\sin\left(\frac{\pi}{3}+\alpha\right) - \sin\left(-\frac{\pi}{3}+\alpha\right)\right]$$

$$= \frac{3\sqrt{2}\,V_s}{2\pi}\left[\sin\frac{\pi}{3}\cos\alpha + \cos\frac{\pi}{3}\sin\alpha\right.$$

$$\left. = \sin\left(-\frac{\pi}{3}\right)\cos\alpha - \cos\left(-\frac{\pi}{3}\right)\sin\alpha\right]$$

$$= \frac{3\sqrt{2}V_s}{2\pi}\ 2\sin\frac{\pi}{3}\cos\alpha \quad = \sqrt{2}\ V_s\left(\frac{3}{\pi}\right)\sin\frac{\pi}{3}\cos\alpha$$

With freewheeling diode, the negative voltage areas are eliminated

$$= \frac{3}{2\pi} \int_{-\frac{\pi}{3}+\alpha}^{\frac{\pi}{2}} \sqrt{2}\ V_s \cos \omega t\ d\omega t = \frac{3}{2\pi} \left[\sqrt{2}\ V_s \sin \omega t\right]_{-\frac{\pi}{3}+\alpha}^{\frac{\pi}{2}}$$

$$= \frac{3}{2\pi}\sqrt{2}\ V_s \left[\sin\frac{\pi}{2} - sin\left(-\frac{\pi}{3}+\alpha\right)\right]$$

$$= \frac{3}{2\pi}\sqrt{2}\ V_s \left[\sin\frac{\pi}{3}cos\alpha = cos\frac{\pi}{3}sin\alpha + sin\frac{\pi}{2}\right]$$

$$= \frac{3}{2\pi}\sqrt{2}\ V_s \left[1 - sin\left(\alpha - \frac{\pi}{3}\right)\right]$$

Example 3.21

Show that for a p-pulse converter with purely resistive load, where the delay angle α is restricted so that the load current is continuous, the *rms* value of d.c. voltage is given by:

$$V_{orms} = \frac{V_m}{\sqrt{2}}\sqrt{1 + \frac{P}{2\pi}cos2\alpha sin\frac{2\pi}{P}}$$

where V_m is the peak value of the transformer secondary voltage secondary voltage per phase.

Solution

From Fig. 3.45, the *rms* value of the output voltage is

$$V_{orms}^2 = \frac{P}{2\pi} \int_{-\frac{\pi}{P}+\alpha}^{\frac{\pi}{P}+\alpha} (V_m)^2 cos^2\omega t\ d\omega t$$

$$= \frac{P}{2\pi} V_m^2 \int_{-\frac{\pi}{P}+\alpha}^{\frac{\pi}{P}+\alpha} \left(\frac{1}{2} + \frac{cos2\omega t}{2}\right) d\omega t$$

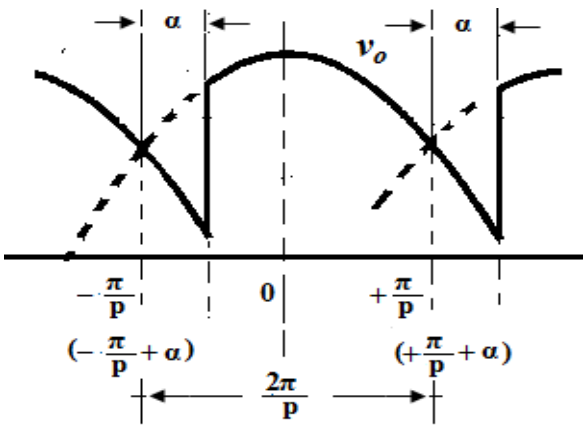

Fig. 3.45.

$$= \frac{P}{2\pi} V_m^2 \left[\frac{1}{2}\omega t + \frac{sin2\omega t}{4}\right] \begin{cases} \frac{\pi}{P} + \alpha \\ -\frac{\pi}{P} + \alpha \end{cases}$$

$$= \frac{P}{2\pi} V_m^2 \left\{ \begin{matrix} \frac{1}{2}\frac{\pi}{P} + \frac{1}{2}\alpha + \frac{1}{4}\left[sin2\alpha cos\frac{2\pi}{P} + cos2\alpha sin\frac{2\pi}{P}\right] - \frac{1}{2}\alpha - \frac{1}{2}\frac{\pi}{P} \\ -\frac{1}{4}\left[sin2\alpha cos\frac{2\pi}{P} - cos2\alpha sin\frac{2\pi}{P}\right] \end{matrix} \right\}$$

$$= \frac{P}{2\pi} V_m^2 \left[\frac{\pi}{P} + \frac{1}{2} cos2\alpha sin\frac{2\pi}{P}\right]$$

$$\therefore \quad V_{orms} = \frac{V_m}{\sqrt{2}} \sqrt{1 + \frac{P}{2\pi} cos2\alpha \, \sin(\frac{2\pi}{P})}$$

Example 3.22

Show that for a *P*-pulse converter with a purely resistive load, where the delay angle α is such that the load current is discontinuous, the *rms* value of the output voltage is given by

$$V_{orms} = V_s \sqrt{\frac{P}{4} - \frac{1}{2}\frac{\alpha}{\pi}P + \frac{1}{2} - \frac{1}{4}\frac{P}{\pi} sin2\left(\alpha - \frac{\pi}{P}\right)}$$

where V_s is the *rms* value of the transformer secondary voltage per phase.

Solution:
The *rms* value of the output voltage waveform for a *p*-pulse converter is

$$V_{orms}^2 = \frac{P}{2\pi} \int_{-\frac{\pi}{P}+\alpha}^{\frac{\pi}{2}} \left(\sqrt{2}\ V_s\right)^2 cos^2\omega t \, d\omega t$$

$$= \frac{P}{\pi} V_s^2 \left[\frac{1}{2}\omega t + \frac{sin2\omega t}{4}\right]_{-\frac{\pi}{P}+\alpha}^{\frac{\pi}{2}}$$

$$= \frac{P}{\pi} V_s^2 \left[\frac{\pi}{4} - \frac{\alpha}{2} + \frac{\pi}{2p} - \frac{1}{4} \left(sin2\alpha cos^2 \frac{2\pi}{P} - cos2\alpha sin \frac{2\pi}{P} \right) \right]$$

$$\therefore V_{orms} = V_s \sqrt{\frac{P}{4} - \frac{1}{2}\frac{\alpha}{\pi} P + \frac{1}{2} - \frac{1}{4}\frac{P}{\pi} sin2\left(\alpha - \frac{\pi}{P}\right)}$$

3.7 OVERLAP AND HARMONIC CONSIDERATIONS IN CONTROLLED AC- DC CONVERTORS

3.7.1 Principle of Overlap During Commutation

Overlap is the phenomenon due to the effect of source inductance on the a.c. side. The current commutation is delayed due to the source inductance which is normally the leakage reactance of a transformer (as X >> R for a transformer, the source resistance is usually neglected).Current commutation with diodes starts when the voltage of the incoming diode exceeds that of the outgoing diode. With thyristors, the comm- utation process starts by triggering the incoming thyristor while its voltage is higher than that of the outgoing one. Due to the inductive reactances of the source (including the reactances of the feeders, up to the rectifying element), certain time is required until the current transfer is completed. Note that, load inductance is not involved in this transfer.

In the following analyses, the source is represented by the equivalent phase reactances or inductances and emfs (v_1 and v_2).The current of the outgoing thyristor T_1 at the instant of triggering T_2 is I. The current of the incoming thyristor i_2 cannot jump immediately to I and T_1 cannot cease conduction. After triggering T_2, both T_1 and T_2 are conducting, and i_2 starts increasing from zero up to I while i_1 start decreasing from I down to zero, such that $i_1+i_2=I$, as depicted in Fig. 3.46. The period of this transition is called the overlap period of current during commutation. The angular period μ is known as the overlap angle or the commutation angle.

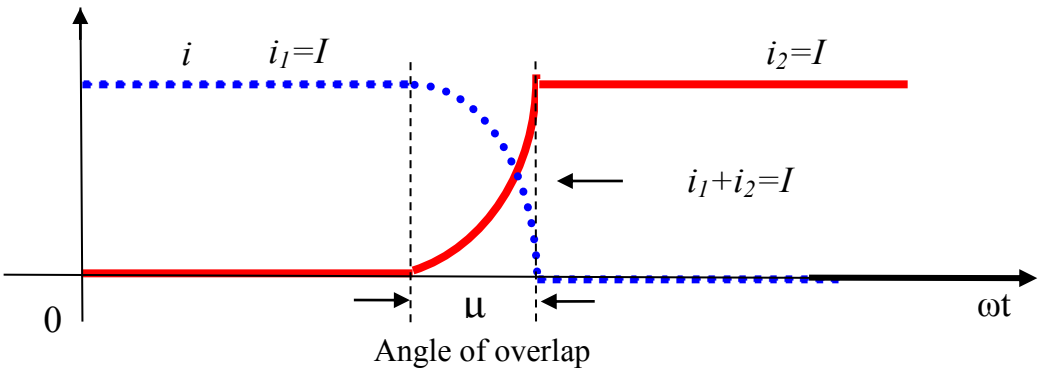

Fig.3.46 Overlap angle during commutation.

Effect of source inductance in single-phase fully-controlled converters

To generalize the problem, the following analyses are based on controlled rectifiers, and for uncontrolled rectifiers the final result and relation are simply obtained by setting α = 0. Hence let us first consider the general case when two thyristors T_1 and T_2 encountering commutation process as depicted in Fig.3.47. If we assume that the load is highly inductive such that the loads current is continuous and ripple free, then

Initial condition: $i_1=I$, $i_2=0$

Final condition: $i_1=0$, $i_2=I$

During overlap period: $i_1+i_2=I$

or $\dfrac{di_1}{dt}+\dfrac{di_2}{dt}=0$

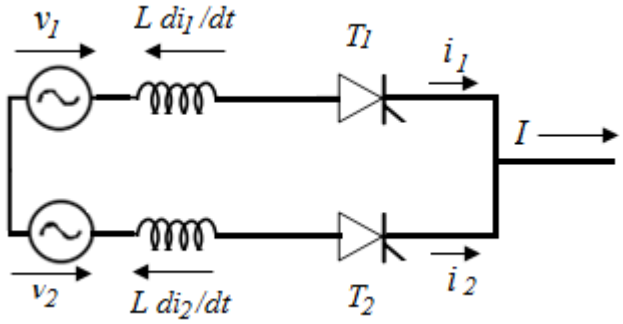

Fig.3.47.

and around the loop shown in Fig.3.47:

$$v_2 - v_1 = L\frac{di_2}{dt} - L\frac{di_1}{dt} = 2L\frac{di_2}{dt} \qquad (3.43)$$

Equation (3.43) above will be used as basic relation for the following analysis for the overlap effect in rectifier circuit.

(A) Bi-phase (2-pulse) Converter

For the bi-phase controlled rectifier circuit shown in Fig.3.48,
Let $v_1 = -V_m sin\omega t$, and $v_2 = V_m sin\omega t$

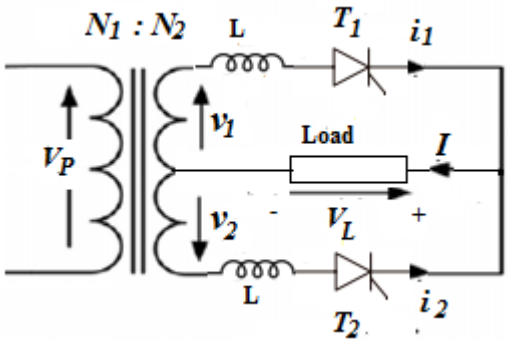

Fig.3.48.

During overlap period, the voltage waveforms will be as depicted in Fig.3.49, where,

$$v_L = \frac{v_1 + v_2}{2} = 0$$

$v_2 - v_1 = 2V_m sin\omega t$; the forcing voltage, hence from Eq.(3.43):

$$L\frac{di_2}{dt} = V_m \sin\omega t$$

Integrating both sides:

$$\int_0^{i_2} di_2 = \frac{1}{L}\int_{t=\frac{\alpha}{\omega}}^{t} V_m \sin\omega t \, d\omega t$$

$$= \frac{V_m}{\omega L}\int_{\omega t=\alpha}^{\omega t} \sin\omega t \, d\omega t$$

$$i_2 = \frac{V_m}{\omega L}(-cos\omega t)\Big|_{\alpha/\omega}^{t}$$

$$= \frac{V_m}{\omega L}(cos\alpha - cos\omega t)$$

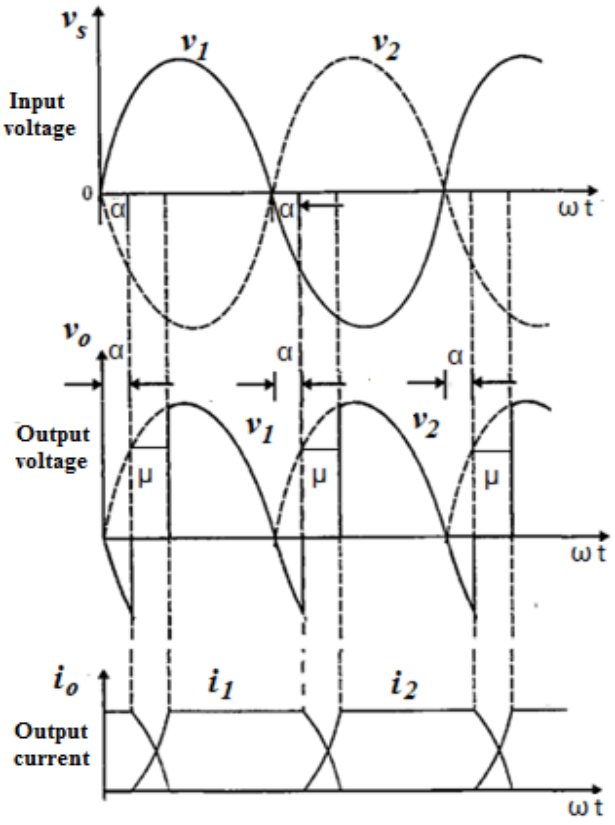

Fig.3.49 Waveforms.

$$i_1 = I - i_2 = I - \frac{V_m}{\omega L}(cos\alpha - cos\omega t)$$

From the final conditions: At $\omega t = \alpha + \mu$, $i_2 = I$, $i_1 = 0$

Therefore,

$$cos\alpha - cos(\alpha + \mu) = \frac{\omega L I}{V_m} \qquad (3.44)$$

The average output voltage V_{dc} is:

$$V_{dc} = \frac{1}{\pi}\left[\int_{\alpha}^{\alpha+\mu}\left(\frac{v_1 + v_2}{2}\right)d\omega t + \int_{\alpha+\mu}^{\pi+\alpha} v_2 \, d\omega t\right]$$

$$= \frac{1}{\pi}\left[\int_{\alpha+\mu}^{\pi+\alpha} V_m \sin\omega t \, d\omega t\right]$$

$$= \frac{V_m}{\pi}\left(cos\alpha + cos(\alpha + \mu)\right)$$

Using Eq.(3.44) V_{dc} can be expresses as

$$V_{dc} = \frac{2V_m}{\pi}\cos\alpha - \frac{\omega LI}{\pi} = \frac{2\,V_m}{\pi}\cos(\alpha+\mu) + \frac{\omega LI}{\pi} \qquad (3.45)$$

This is the output d.c. voltage of the converter considering the effect of the source inductance L which causes overlap. The effect of overlap is, then equivalent to voltage loss of ($\omega LI/\pi$) . This lost voltage can also be determined by calculating the area A which occurs every half cycle or every $\frac{\pi}{\omega}$ second. Thus referring to Fig.3.50, A can be determined as:

$$A = \int_{t=\frac{\alpha}{\omega}}^{(\alpha+\mu)/\omega} \left(v_2 - \frac{v_1+v_2}{2}\right) dt$$

$$= \int_{t=\frac{\alpha}{\omega}}^{(\alpha+\mu)/\omega} \left(\frac{v_2-v_1}{2}\right) dt$$

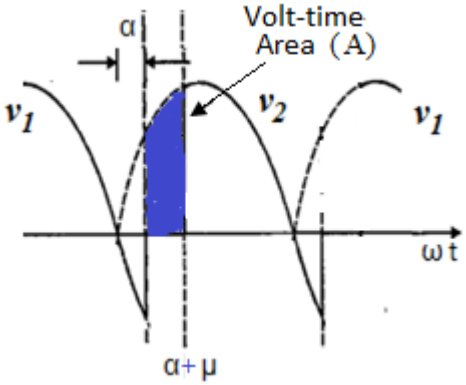

Fig.3.50 Volt-time area.

since $\frac{v_1+v_2}{2} = L\frac{di_2}{dt}$, then

$$A = \int_{t=\frac{\alpha}{\omega}}^{(\alpha+\mu)/\omega} L di_2 = L(I-0) = LI$$

The average lost voltage during commutation is,

$$V_{dc(lost)} = \frac{A}{\pi/\omega} = \frac{LI}{\pi/\omega} = \frac{\omega L\, I}{\pi} \qquad (3.46)$$

The net output d.c. voltage for the bi-phase converter will be:

$$V_{dc} = V_{dc}(\text{without } L) - V_{dc(lost)} = \frac{2V_m}{\pi}\cos\alpha - \frac{\omega LI}{\pi} \qquad (3.47)$$

(B) Single-phase full-wave bridge rectifier

For the single-phase full-wave bridge rectifier, the equivalent circuit during overlap is shown in Fig.3.51. The supply current i_s is common between T_1 and T_3. Hence, by KVL;

$$v_s = V_m \sin\omega t = L\frac{di_s(t)}{dt}$$

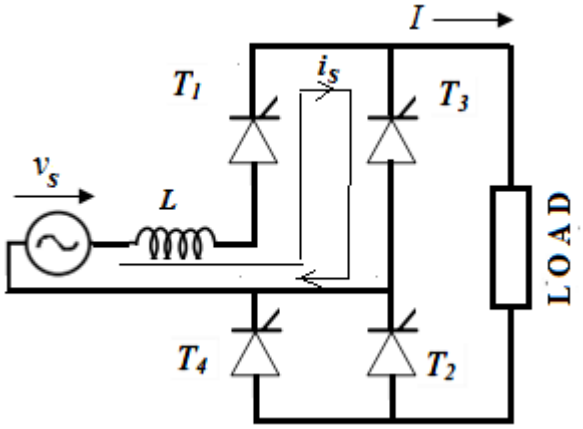

Fig.3.51.

Initial condition: $i_s = I$,

Final condition: $i_s = -I$

$$V_m \sin\omega t\, dt = L\, di_s(t)$$

Integrating both the sides :

$$\int_{\alpha}^{\alpha+\mu} V_m \sin\omega t\, dt = \int_{I}^{-I} L\, di_s(t) = -2LI$$

$$= \frac{V_m}{\omega}\left(-cos\alpha + cos(\alpha+\mu)\right) = -2LI$$

$$cos\alpha - cos(\alpha+\mu) = \frac{2\omega LI}{V_m} = V_{dc(lost)}$$

Therefore, the net output d.c. voltage for the single-phase converter will be:

$$V_{dc} = V_{dc}(\text{without L}) - V_{dc(lost)} = \frac{2V_m}{\pi}\, cos\alpha - \frac{2\omega LI}{\pi} \qquad (3.48)$$

(C) Three-phase half-wave rectifier

For the three-phase half-wave controlled rectifier circuit shown in Fig.3.30, the output voltage waveform considering overlap angle is depicted in Fig.3.52. Now let :

$$v_1 = V_m sin\omega t \ , \quad v_2 = V_m \sin(\omega t + 120°)$$

and $v_3 = V_m \sin(\omega t - 120°)$

Hence,

$$v_1 + v_2 = V_m \sin(\omega t + 60°)$$

$$= V_m \cos(\omega t + 60° - 90°) = V_m \cos(\omega t - 30°)$$

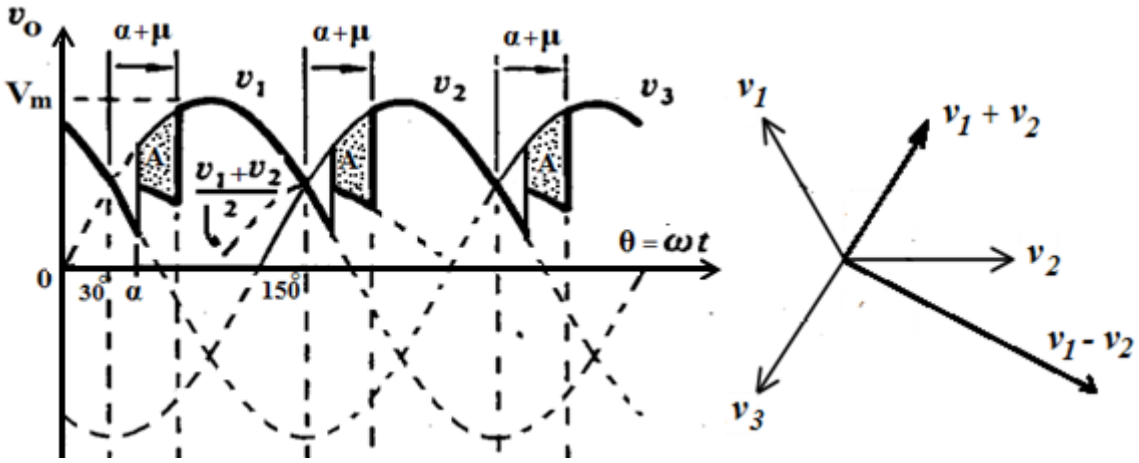

(a) (b)

Fig.3.52 Three-phase half-wave controlled rectifier considering overlap: (a) Output voltage waveform, (b) Voltage phasor diagram.

$$v_1 - v_2 = \sqrt{3}V_m sin\omega t$$

Using Eq.(3.43) gives :

$$L\frac{di_2}{dt} = \frac{\sqrt{3}}{2}V_m sin\omega t \qquad (3.49)$$

Taking integration of both sides of Eq.(3.49) yields

$$\int_0^{i_2} di_2 = \int_{t=\frac{\alpha}{\omega}}^{t} \frac{\sqrt{3}}{2L} V_m sin\omega t\, dt$$

$$i_2 = \frac{\sqrt{3}\,V_m}{2\omega L}(cos\alpha - cos\omega t) \qquad (3.50)$$

Now, at $\omega t = \alpha + \mu$, $i_2 = I = (I_{dc})$ and $i_1 = 0$

$$cos\alpha - cos(\alpha + \mu) = \frac{2\omega LI}{\sqrt{3}\,V_m} \qquad (3.51)$$

$$V_{dc} = \frac{1}{T}\int_0^T V_L\, dt = \frac{1}{\frac{2\pi}{3}}\left[\int_{30°+\alpha}^{30°+\alpha+\mu}\left(\frac{v_1+v_2}{2}\right)d\omega t + \int_{30°+\alpha+\mu}^{150°+\alpha} v_2\, d\omega t\right]$$

Using $\emptyset = \omega t - 30°$ and $d\emptyset = d\omega t$ gives,

$$V_{dc} = \frac{3}{2\pi}\left[\int_{\emptyset=\alpha}^{\alpha+\mu} \frac{V_m}{2} cos\emptyset \, d\emptyset + \int_{\omega t=30°+\alpha+\mu}^{150°+\alpha} v_2 d\omega t\right]$$

$$= \frac{3\sqrt{3}\, V_m}{4\pi}\left(cos\alpha + cos(\alpha+\mu)\right)$$

With the aid of Eq.(3.51):

$$V_{dc} = \frac{3\sqrt{3}\, V_m}{2\pi} cos\alpha - \frac{3\omega LI}{2\pi}$$

$$= \frac{3\sqrt{3}\, Vm}{2\pi} Cos(\alpha+\mu) + \frac{3\omega LI}{2\pi} \qquad (3.52)$$

(D) P-pulse converter

For p-pulse converter the voltage waveforms and the overlap angles are depicted in Fig.3.53. Let the voltage at the anode of the incoming thyristor be $v_2 = V_m \cos\theta$. Since the phase voltages are displaced by $\frac{2\pi}{p}$ radians, then, the voltage at the anod of the outgoing thyristor v_1 is given by:

$$v_1 = V_m \cos(\theta + \frac{2\pi}{p})$$

$$v_2 - v_1 = V_m\,[\cos\theta - \frac{2\pi}{p}] = 2V_m \sin\frac{\pi}{p}\sin\left(\theta + \frac{\pi}{p}\right)$$

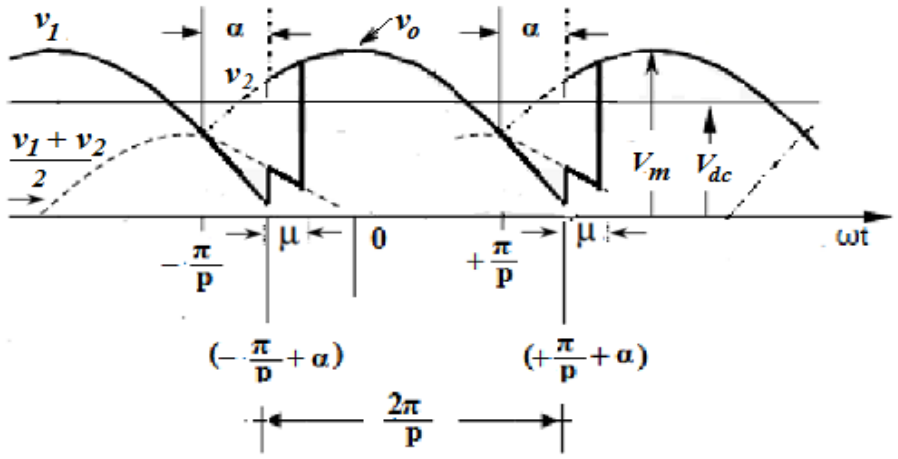

Fig.3.53

Using $\emptyset = \theta + \frac{\pi}{p} = \omega t + \frac{\pi}{p}$; $d\emptyset = \omega dt$
From Eq.(3.43) :

$$\frac{v_2 - v_1}{2} = V_m \sin\frac{\pi}{p}\sin\emptyset = L\frac{di_2}{dt}$$

The overlap starts with $\emptyset = \alpha$ with $i_2 = 0$ and it lasts at $\emptyset = \alpha + \mu$ with $i_2 = I$. Therefore, the average d.c. output voltage

$$L\int_0^{i_2} di_2 = \int_{\alpha}^{\alpha+\mu} V_m \sin\frac{\pi}{p}\sin\emptyset\frac{d\emptyset}{\omega}$$

$$\omega LI = V_m \sin\frac{\pi}{p}[-\cos\emptyset\{^{\alpha+\mu}_{\alpha}]$$

$$cos\alpha - cos(\alpha+\mu) = \frac{\omega L\, I}{V_m \sin\frac{\pi}{p}} \qquad (3.53)$$

And the average d.c. output voltage can be evaluated as,

$$V_{dc} = \frac{p}{2\pi}\left[\int_{\frac{-\pi}{p}+\alpha}^{\frac{-\pi}{p}+\alpha+\mu}\left(\frac{v_2 - v_1}{2}\right)d\emptyset + \int_{-\frac{\pi}{p}+\alpha+\mu}^{\frac{\pi}{p}+\alpha} v_2 d\omega t\right]$$

$$= \frac{p}{2\pi}\left[\int_{\alpha}^{\alpha+\mu} V_m \cos\frac{\pi}{p}cos\emptyset\, d\emptyset + \int_{-\frac{\pi}{p}+\alpha+\mu}^{\frac{\pi}{p}+\alpha} V_m\cos\theta\; d\omega t\right]$$

$$= \frac{p}{2\pi}V_m \sin\frac{\pi}{p}[cos\alpha + cos(\alpha+\mu)]$$

$$\therefore\; V_{dc} = \frac{p}{\pi}V_m \sin\frac{\pi}{p}cos\alpha - \frac{p\omega L\, I}{2\pi} \qquad (3.54)$$

or $$V_{dc} = \frac{p}{\pi}V_m \sin\frac{\pi}{p}\cos(\alpha+\mu) - \frac{p\omega L\, I}{2\pi} \qquad (3.55)$$

Alternatively, one can use the lost voltage due to commutation to derive V_{dc} . $A=LI$ (as derived before) and its average value $V_{dc(lost)}$ for p-pulse converter is thus,

$$V_{dc(lost)} = \frac{A}{(\frac{2\pi}{p\omega})} = \frac{p\omega L\, I}{2\pi}$$

Therefore the net output d.c. voltage for the p-pulse converter will be:

$$V_{dc} = V_{dc}(\text{without L}) - V_{dc(lost)}$$

$$= \frac{p}{\pi} V_m \sin\frac{\pi}{p} \cos\alpha - \frac{p\omega L\, I}{2\pi} \qquad (3.56)$$

Notes:

1. ωL = X is the supply reactance per phase (up to the anode of the thyristor) and $\frac{\omega L}{2\pi} = f\ L$ where f is the frequency of the supply.

2. For a given frequency and input voltage (V_m) the overlap angle μ depends upon:
   - α : the triggering angle.
   - L : the leakage inductance of the supply
   - I : the load current or the d.c. side current

3. Minimum overlap angle occurs when the triggering happens near the maximum voltage differences between the phases (v_2-v_1).

4. With a three-phase bridge, the overlap occurs every 60˚ and the lost voltage is $\frac{A}{(\frac{2\pi}{6\omega})}$ or $\frac{3\omega L\, I}{\pi}$. With a single-phase bridge rectifier, the overlap is equivalent to that taking place every 90˚ or π/2 and the lost voltage is $\frac{A}{(\frac{2\pi}{4})}$ or $\frac{2\omega L}{I}$. Hence, the output of bridge rectifier is given by (let $I = I_{dc}$)

   For bi-phase rectifier

$$V_{dc} = \frac{2\, V_m}{\pi} cos\alpha - \frac{\omega L}{\pi} I_{dc}$$

   For single-phase bridge

$$V_{dc} = \frac{2\, V_m}{\pi} cos\alpha - \frac{2\omega L}{\pi} I_{dc}$$

For three-phase bridge rectifier

$$V_{dc} = \frac{3\sqrt{3}\ V_m}{2\pi} cos\alpha - \frac{3\omega L}{2\pi}\ I_{dc}$$

For a bi-phase rectifier

$$cos\alpha - cos(\alpha + \mu) = \frac{\omega L}{V_m} I_{dc}$$

For a single-phase bridge rectifier

$$cos\alpha - cos(\alpha + \mu) = \frac{2\omega L}{V_m} I_{dc}$$

which is double of a bi-phase rectifier.

For a three-phase half-wave rectifier

$$cos\alpha - cos(\alpha + \mu) = \frac{2\omega L}{\sqrt{3}\, V_m} I_{dc}$$

For a three-phase bridge rectifier

$$cos\alpha - cos(\alpha + \mu) = \frac{2\omega L}{\sqrt{3}\, V_m} I_{dc}$$

This is the same as a three-phase half-wave rectifier but of double occurrence.

For p-pulse converter

$$cos\alpha - cos(\alpha + \mu) = \frac{\omega L}{V_m \sin\frac{\pi}{p}} I_{dc}$$

Example 3.23

A single-phase mid-point (bi-phase) converter supplied from 240/120 V, 50Hz transformer is connected to load of 15 Ω resistance and infinite inductance. If the secondary winding of the transformer has a line inductance of 20 mH. Determine the load voltage and current at a firing angle of 60^o. Find the overlap angle.

Solution

For bi-phase or mid-point rectifier

$$V_{dc} = \frac{2\,V_m}{\pi} cos\alpha - \frac{\omega L I_{dc}}{\pi}$$

or $$R\ I_{dc} = \frac{2\,V_m}{\pi} cos\alpha - \frac{\omega L}{\pi} I_{dc}$$

$$I_{dc}\,[R + \frac{\omega L}{\pi}] = \frac{2\,V_m}{\pi} cos\alpha$$

$$I_{dc} = \frac{\frac{2\,V_m}{\pi} cos\alpha}{[R + \frac{\omega L}{\pi}]} = \frac{\frac{2 \times 120 \times \sqrt{2}}{\pi}}{15 + \frac{100\pi \times 20}{1000\pi}} = 3.17\ \text{A}$$

$$V_{dc} = R\ I_{dc}\ 15 \times 3{,}17 = 47.6\ \text{V}$$

For bi-phase rectifier

$$cos\alpha - cos(\alpha + \mu) = \frac{\omega L}{V_m} I_{dc}$$

$$cos(\alpha + \mu) = -\frac{\omega L}{V_m} I_{dc} + cos\alpha$$

$$= -\frac{2\pi \times 50 \times\ 20 \times 10^{-3}}{169.7} \times 3.17 + \cos 60°$$

$$cos(\alpha + \mu) = -\ 0.1173 + 0.5 = 0.3886$$

$$\alpha + \mu = 67.5\ ° \qquad \therefore\ \mu = 67.5° - \alpha = 67.5° - 60° = 7.5°$$

Example 3.24

A three-phase, half-wave controlled rectifier shown in Fig.3.54 is supplied by 150 V per phase, at 50 Hz. The source inductance and resistance are 1.2 mH and 0.07 Ω per phase respectively. Assuming a thyristor voltage drop of 1.5 V and a continuous load current of 30 A, determine the mean load voltage at firing angles of 0˚, 30˚ and 60˚.

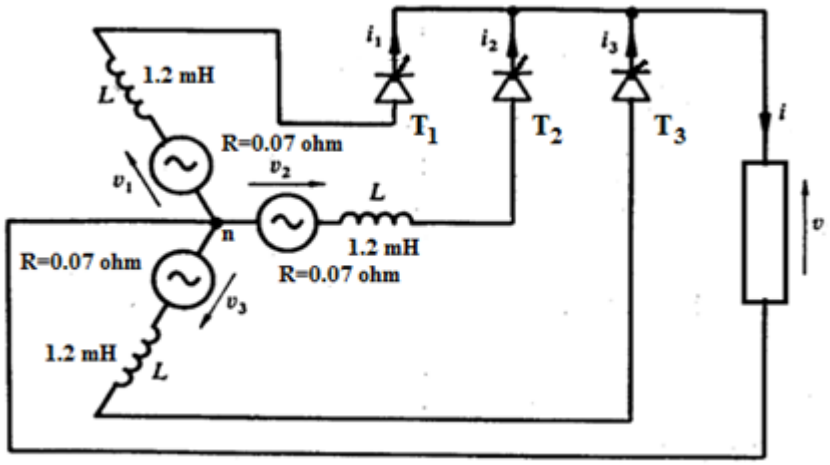

Fig.3.54.

Solution

At all time there is a voltage drop across the thyristor which is 1.5 V, also there is a constant voltage drop across the source resistance which is equal to: $30 \times 0.07 = 2.1$ V.

$$V_{dc} = \frac{3\sqrt{3}}{2\pi} V_m cos\alpha - \frac{3\omega L}{2\pi} I_{dc}$$

$$\frac{3\omega L}{2\pi} I_{dc} = \frac{3 \times 2\pi \times 50 \times 1.2 \times 10^{-3}}{2\pi} = 5.4 \text{ V}$$

$$\frac{3\sqrt{3}\ V_m}{2\pi} = \frac{3\sqrt{3} \times 150 \times \sqrt{2}}{2\pi} = 175.4$$

at

$\alpha = 0^{\circ}$ $\quad V_d = 175.4 \cos 0° - 1.5 - 2.1 - 5.4 = 166$ V

$\alpha = 30°$ $\quad V_d = 175.4 cos30° - 1.5 - 2.1 - 5.4 = 142.9$ V

$\alpha = 60°$ $\quad V_d = 175.4\ cos60° - 1.5 - 2.1 - 5.4 = 78.7$ V

Example 3.25

A three-phase fully-controlled thyristor bridge rectifier is supplied from three-phase source of 400 V, 50 Hz with an inductive reactance of 0.25 Ω per phase and negligible resistance. The output is smoothed by an inductor which has a resistance of 0.15 Ω and the load current is 200 A. Determine the mean bridge output voltage, the mean load voltage and the overlap angle when the delay angle is 45°. Ignore any voltage drop in the thyristors.

Solution

From Eq.(3.55), for p-pulse converter :

$$V_{dc} = \frac{p}{\pi} V_m \sin\frac{\pi}{p} \cos\alpha - \frac{p\omega L I}{2\pi}$$

For three-phase fully-controlled thyristor bridge rectifier p = 6, hence

$$V_{dc} = \frac{6}{\pi} V_m \sin\frac{\pi}{6} \cos\alpha - \frac{6\,\omega L I}{2\pi}$$

$$V_{dc} = \frac{6}{\pi} V_m \frac{\sqrt{3}}{2} \cos\alpha - \frac{3\,\omega L I}{\pi}$$

$$V_m = \sqrt{2}\,\frac{400}{\sqrt{3}} = 326.6\,V \quad \rightarrow \quad \sqrt{3}V_m = \sqrt{2} \times 400$$

$$V_{dc} = \frac{6}{\pi} \times \sqrt{2}\,\frac{400}{\sqrt{3}} \times \frac{\sqrt{3}}{2} \cos 45° - \frac{3 \times 0.25 \times 200}{\pi} = 334.28\ \text{V}$$

$$V'_{dc} = 334.28 - 200 \times 0.15 = 304.28\ \text{V}$$

$$V_{dc} = \frac{PV_m}{2\pi} \sin\frac{\pi}{P}\left(cos\alpha + cos(\alpha + \mu)\right)$$

$$334.28 = \frac{6}{2\pi} \times \sqrt{2} \times 400 \times \frac{1}{2}\left(cos\alpha + cos(\alpha + \mu)\right)$$

$$334.28 = 270.2\left(cos\alpha + cos(\alpha + \mu)\right)$$

$$cos\alpha + cos(\alpha + \mu) = 1.237$$

$$cos(45° + \mu) = 1.237 - 0707 = 0.530$$

$$45° + \mu = \cos^{-1} 0.530 = 57.98°$$

$$\therefore \quad \mu = 57.98° - 45° = 12.98°$$

3.7.2 Harmonic Considerations in Controlled P-Pulse ac-to-dc Converter – General Solution

The d.c. output voltage waveform of a p-pulse controlled converter may be represented by Fourier series as

$$v(\omega t) = a_o + \sum_{n=2}^{\infty} a_n \cos(n\omega t) + \sum_{n=2}^{\infty} b_n \sin(n\omega t)$$

Referring to the waveform of p-pulse converter shown in Fig. 3.34, the Fourier coefficients can be evaluated as follows:

$$a_o = V_{dc} = \frac{1}{\frac{2\pi}{p}} \int_{(-\frac{\pi}{p}+\alpha)}^{(+\frac{\pi}{p}+\alpha)} V_m \cos \omega t \, d\omega t$$

$$a_o = \frac{p}{\pi} V_m \sin\frac{\pi}{p} \cos\alpha = V_{dc} \cos\alpha \qquad (3.57)$$

The Fourier coefficients of the n^{th} order harmonics are (for $n \neq 1$):

$$a_n = \frac{1}{\frac{2\pi}{p}} \int_{(-\frac{\pi}{p}+\alpha)}^{(+\frac{\pi}{p}+\alpha)} V_m \cos \omega t \cos n\omega t \, d\omega t$$

$$b_n = \frac{1}{\frac{2\pi}{p}} \int_{(-\frac{\pi}{p}+\alpha)}^{(+\frac{\pi}{p}+\alpha)} V_m \cos \omega t \sin n\omega t \, d\omega t$$

Evaluating this integration by the same method as that given in chapter two for uncontrolled case we get,

$$a_n = \frac{2V_{dc}}{(n^2-1)} [n \sin n\alpha \sin\alpha + \cos n\alpha \cos\alpha] \qquad (3.58)$$

$$b_n = \frac{2V_{dc}}{(n^2-1)} [n \cos n\alpha \sin\alpha + \sin n\alpha \cos\alpha] \qquad (3.59)$$

where :

V_{dc}= d.c. output value for uncontrolled case
n = cp with c any integer
V_m = the maximum value of converter secondary voltage /phase
α = the triggering (delay) angle

The fundamental component coefficients a_1 , b_1 and c_1 (when n = 1) are:

$$a_1 = \frac{V_m}{\pi}\int_{\frac{-\pi}{p}+\alpha}^{\frac{\pi}{p}+\alpha} \sin(\omega t)\cos(\omega t)\, d\omega t$$

$$= \frac{V_m}{\pi}\int_{\frac{-\pi}{p}+\alpha}^{\frac{\pi}{p}+\alpha} \frac{1}{2}\sin(2\omega t)\, d\omega t$$

$$= \frac{V_m}{4\pi}[-\cos(2\omega t)]_{\frac{-\pi}{p}+\alpha}^{\frac{\pi}{p}+\alpha}$$

$$= \frac{V_m}{4\pi}[-\cos\ (\frac{2\pi}{p}+2\alpha)+\cos\ (-\left(\frac{2\pi}{p}+2\alpha\right))]$$

$$= \frac{V_m}{4\pi}\ [(\cos\left(\frac{2\pi}{p}\right)\cos(\,2\alpha)-\sin\left(\frac{2\pi}{p}\right)\sin(2\alpha)) + \cos\left(-\frac{2\pi}{p}\right)\cos(2\alpha)-\sin\left(-\frac{2\pi}{p}\right)\sin(2\alpha)]$$

After further simplification

$$\therefore a_1 = \frac{V_m}{2\pi}\left[\sin\left(\frac{2\pi}{p}\right)\sin(2\alpha)\right] \qquad (3.60)$$

$$b_1 = \frac{V_m}{\pi}\int_{\frac{-\pi}{p}+\alpha}^{\frac{\pi}{p}+\alpha} \sin(\omega t)\sin(\omega t)\, d\omega t$$

$$= \frac{V_m}{\pi}\int_{\frac{-\pi}{p}+\alpha}^{\frac{\pi}{p}+\alpha} \sin^2(\omega t)\, d\omega t = \frac{V_m}{2\pi}\int_{\frac{-\pi}{p}+\alpha}^{\frac{\pi}{p}+\alpha}[1-\cos(2\omega t)]d\omega t$$

$$= \frac{V_m}{2\pi}[\omega t-\frac{1}{2}\sin(\,2\omega t)]_{\frac{-\pi}{p}+\alpha}^{\frac{\pi}{p}+\alpha}$$

$$= \frac{V_m}{2\pi}[\frac{\pi}{p}+\alpha+\frac{\pi}{p}-\alpha-\frac{\sin\left(\frac{2\pi}{p}+2\alpha\right)}{2}+\frac{\sin\left(-\frac{2\pi}{p}+2\alpha\right)}{2}$$

$$= \frac{V_m}{2\pi}[\frac{2\pi}{p}-\frac{1}{2}(\sin\left(\frac{2\pi}{p}+2\alpha\right)-\sin\left(2\alpha-\frac{2\pi}{p}\right))$$

$$= \frac{V_m}{2\pi}\left[\frac{2\pi}{p} - \frac{1}{2}\left(\sin\left(\frac{2\pi}{p}\right)\cos(2\alpha) + \sin(2\alpha)\cos\left(\frac{2\pi}{p}\right)\right.\right.$$
$$\left.\left. - \sin(2\alpha)\cos\left(\frac{2\pi}{p}\right) + \sin\left(\frac{2\pi}{p}\right)\cos(2\alpha)\right)\right.$$

$$\therefore \quad b_1 = \frac{V_m}{2\pi}\left[\frac{2\pi}{p} - \sin\left(\frac{2\pi}{p}\right)\cos(2\alpha)\right] \qquad (3.61)$$

The amplitude c_1 of the fundamental component is, $c_1 = \sqrt{{a_1}^2 + {b_1}^2}$

3.7.3 Harmonic Amplitude Spectra of the Output Voltage Waveform for P-Pulse Controlled Rectifiers

(i) Single-phase full-wave controlled rectifier (p= 2)

Harmonic amplitude spectra of the output voltage waveform for single-phase full-wave rectifier (p = 2) is shown in Fig.3.55 for triggering angle α = 30˚. It is clear that the zero frequency component (the d.c. value which has an amplitude of 55.1 percent) is not the dominant one in the frequency spectrum. The second order harmonic (f =100Hz) has amplitude of 66.22 percent, whereas the fundamental component (f = 50 Hz) has amplitude of 50.01 percent. For all higher order harmonic frequency components, the harmonic amplitude c_n indicates that the output voltage waveform contains both even and odd harmonics. The values of the harmonic amplitudes c_n in percentage (V_m=100%) are given in Table 3.1 for convenience.

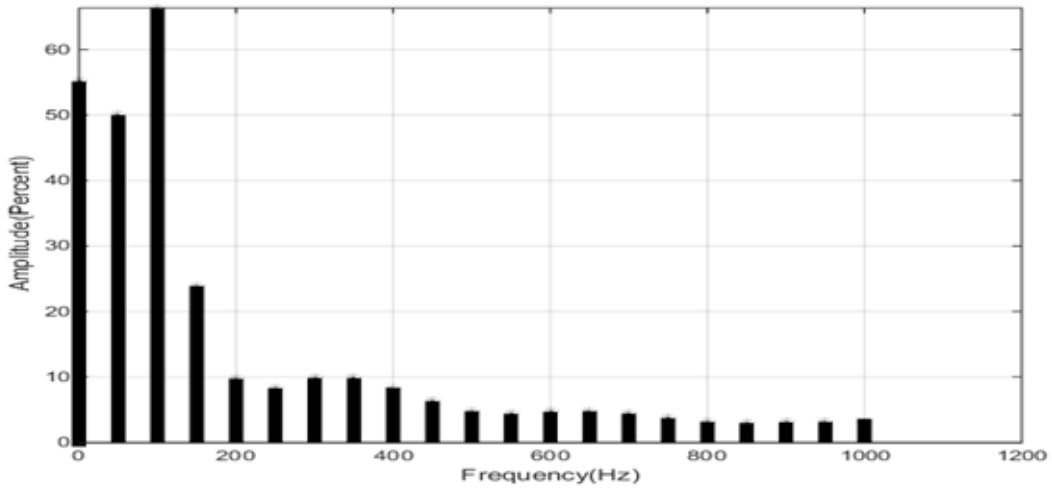

Fig.3.55 Harmonic amplitude spectra for the output voltage waveform of single-phase full-wave rectifier (p = 2) for triggering angle α = 30˚.

Table 3.1 Harmonic amplitudes for the output voltage waveform of single - phase full-wave rectifier (p = 2) for triggering angle α = 30˚.

n	0	1	2	4	6	8	10	12	16	20
Hz	0	50	100	200	300	400	500	600	800	1000
c(n)	55.10399	50.01005	66.22861	9.716907	9.841967	8.344014	4.75539	4.677029	3.138863	2.971708

(ii) Three -phase half-wave controlled rectifier (p= 3)

Harmonic amplitude spectra of the output voltage waveform for three-phase half-wave rectifier (p = 3) is shown in Fig.3.56 for triggering angle α = 30˚.

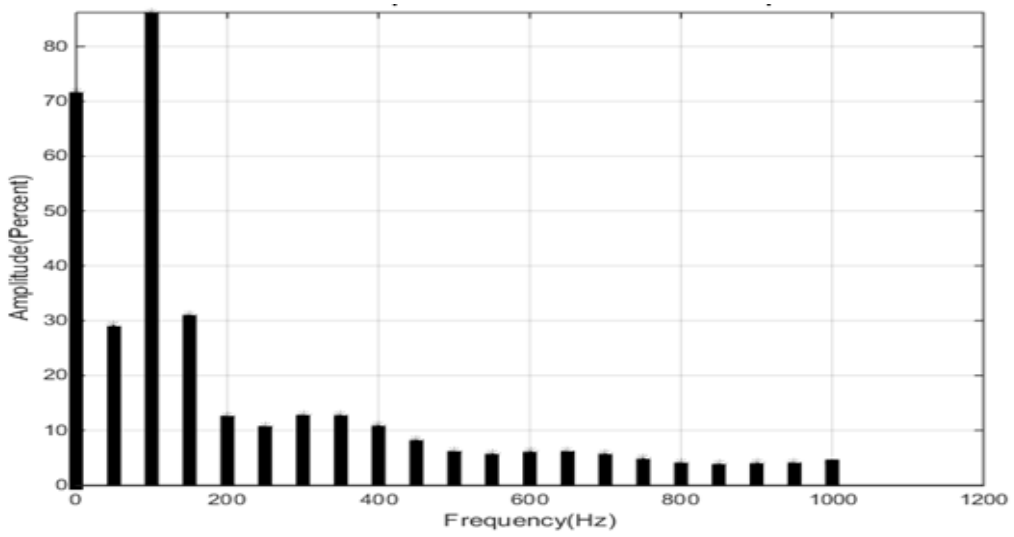

Fig. 3.56 Harmonic amplitude spectra for three-phase half-wave rectifier (p = 3) for triggering angle α = 30˚.

It is clear that the zero frequency component (the d.c. value which has an amplitude of 71.59 percent) is not the dominant one in the frequency spectrum. The second order harmonic (f = 100 Hz) has amplitude of 86.05 percent, whereas the fundamental component (f = 50 Hz) has amplitude of 29.01 percent. For all higher order harmonic frequency components, the harmonic amplitude c_n indicates that the output voltage waveform contains both even and odd harmonics.

The values of the harmonic amplitudes c_n in percentage (V_m=100%) are given in Table 3.2 for convenience.

Table 3.2 Harmonic amplitudes for the output voltage waveform three - phase half - wave rectifier (p = 3) for triggering angle α = 30˚.

n	0	1	2	4	6	8	10	12	16	20
Hz	0	50	100	200	300	400	500	600	800	1000
c(n)	71.59961	29.01816	86.05443	12.62571	12.7882	10.84183	6.178937	6.077118	4.078496	3.861302

(iii) Three-phase full-wave fully-controlled rectifier (p= 6)

Harmonic amplitude spectra of the output voltage waveform for three-phase full-wave rectifier (p = 6) is shown in Fig.3.57 for triggering angle α = 30˚. It is clear that the zero frequency component (the d.c. value which has an amplitude of 82.68 percent) is not the dominant one in the frequency spectrum. The second order harmonic (f =100Hz) has amplitude of 99.37 percent, whereas the fundamental component (f =50Hz) has amplitude of 15.43 percent. For all higher order harmonic frequency components, the harmonic amplitude c_n indicates that the output voltage waveform contains both even and odd harmonics.

The values of the harmonic amplitudes c_n in percentage (V_m=100%) are given in Table 3.3.

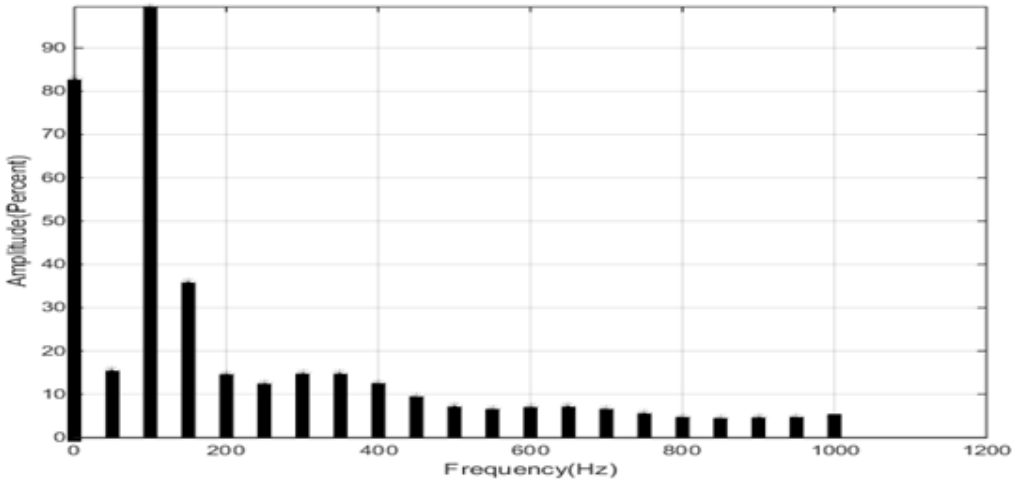

Fig. 3.57 Harmonic amplitude spectra for three-phase full-wave rectifier (p = 6) for triggering angle α = 30˚.

Table 3.3 Harmonic amplitudes for the output voltage waveform three-phase full-wave rectifier (p = 6) for triggering angle α = 30˚.

n	0	1	2	4	6	8	10	12	16	20
Hz	0	50	100	200	300	400	500	600	800	1000
c(n)	82.68617	15.43303	99.37919	14.58068	14.76834	12.52059	7.13569	7.018106	4.710015	4.45919

(iv) Poly-phase 12-pulse rectifier (p=12)

Harmonic amplitude spectra of the output voltage waveform for twelve - phase full-wave rectifier (p = 12) is shown in Fig.3.58 for triggering angle α = 30˚. It is clear that the zero frequency component (the d.c. value which has an amplitude of 82.68 percent) is not the dominant one in the frequency spectrum. The second order harmonic (f=100Hz) has amplitude of 99.37 percent, whereas the fundamental component (f =50 Hz) has

amplitude of 15.43 percent. For all higher order harmonic frequency components, the harmonic amplitude c_n indicates that the output voltage waveform contains both even and odd harmonics. The values of the harmonic amplitudes c_n in percentage (V_m=100%) are given in Table 3.4.

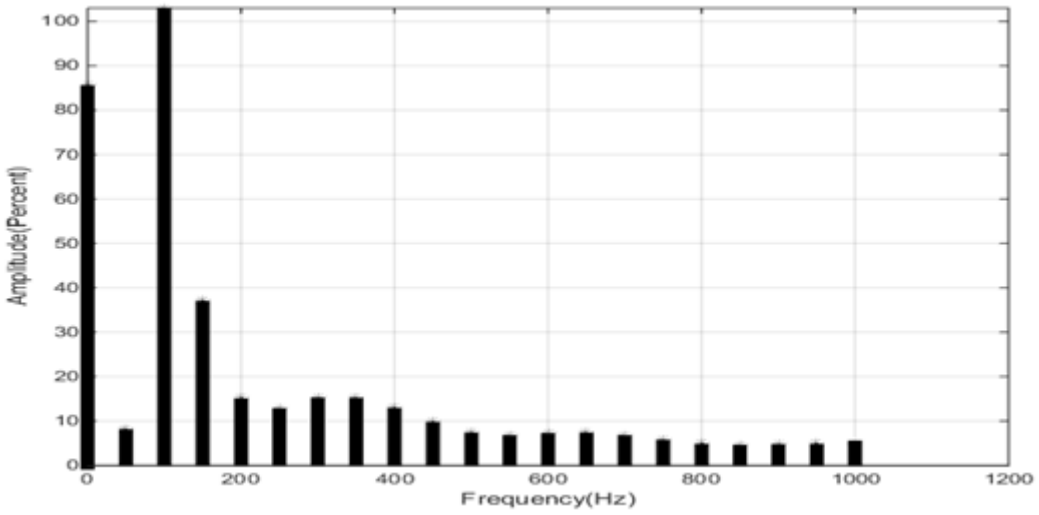

Fig. 3.58 Harmonic amplitude spectra for poly-phase 12- pulse rectifier for triggering angle α = 30˚.

Table 3.4 Harmonic amplitudes for the output voltage waveform poly-phase rectifier (p = 12) for triggering angle α = 30˚.

n	0	1	2	4	6	8	10	12	16	20
Hz	0	50	100	200	300	400	500	600	800	1000
c(n)	85.60544	8.154862	102.8878	15.09546	15.28974	12.96264	7.387619	7.265883	4.876304	4.616623

From the above results, it is evident that as the number of pulse (p) in an a.c. to d.c. converter increases, the d.c. output voltage is increases. The most significant harmonic is the second harmonic of the supply frequency which, for the same delay angle α, increases as the number of pulse p increases. On contrast, the first order harmonic is decreases as the number of pulse p increases. The variation of the d.c. component (V_{dc}) with the delay angle α is given in Table 3.5 for clarity.

Figs.3.59 to 62 show harmonic spectra for rectifiers with different number of pulses (p = 2,3,6, and 12) with $V_m = 100$ and $0 \leq \alpha \leq 180°$,

Table 3.5

Variation of V_{dc} with delay angle α for p =2,3,6, and 12 pulse.

P	2						
α	0	30˚	60˚	90˚	120˚	150˚	180˚
V_{dc}(V)	63.6	55.1	31.8	0	-31.8	-55.1	-63.6
P	3						
α	0	30˚	60˚	90˚	120˚	150˚	180˚
V_{dc}(V)	82.6	71.6	41.3	0	-41.3	-71.6	-82.6
P	6						
α	0	30˚	60˚	90˚	120˚	150˚	180˚
V_{dc}(V)	95.5	82.6	47.7	0	-47.7	-82.6	-95.5
P	12						
α	0	30˚	60˚	90˚	120˚	150˚	180˚
V_{dc}(V)	98.9	85.6	49.4	0	-49.5	-85.7	-98.9

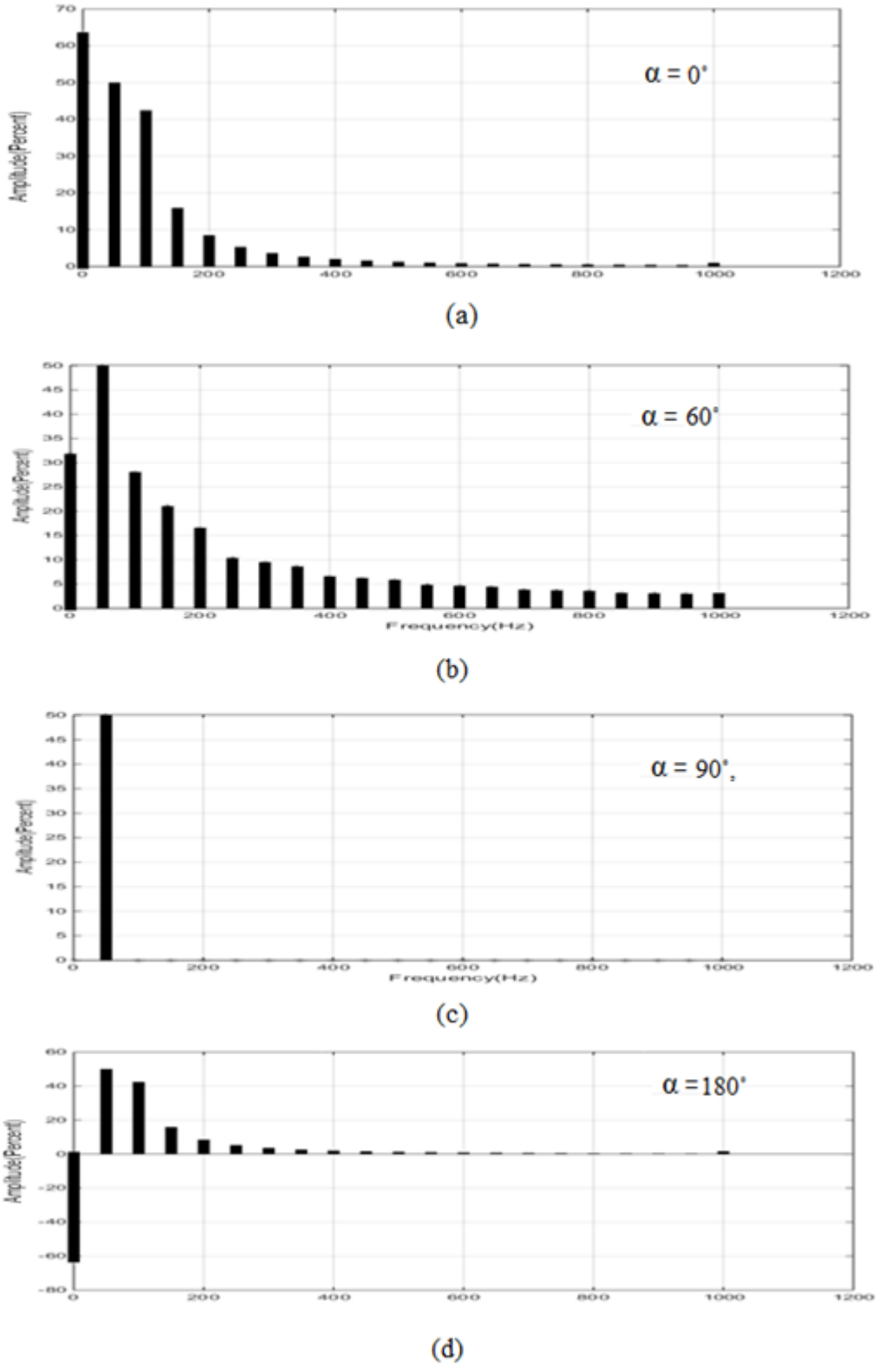

Fig.3.59 Harmonic frequency spectra for p =2 rectifier with different firing angles: (a) α = 0˚, (b) α = 60˚, (c) α = 90˚, and (d) α = 180˚.

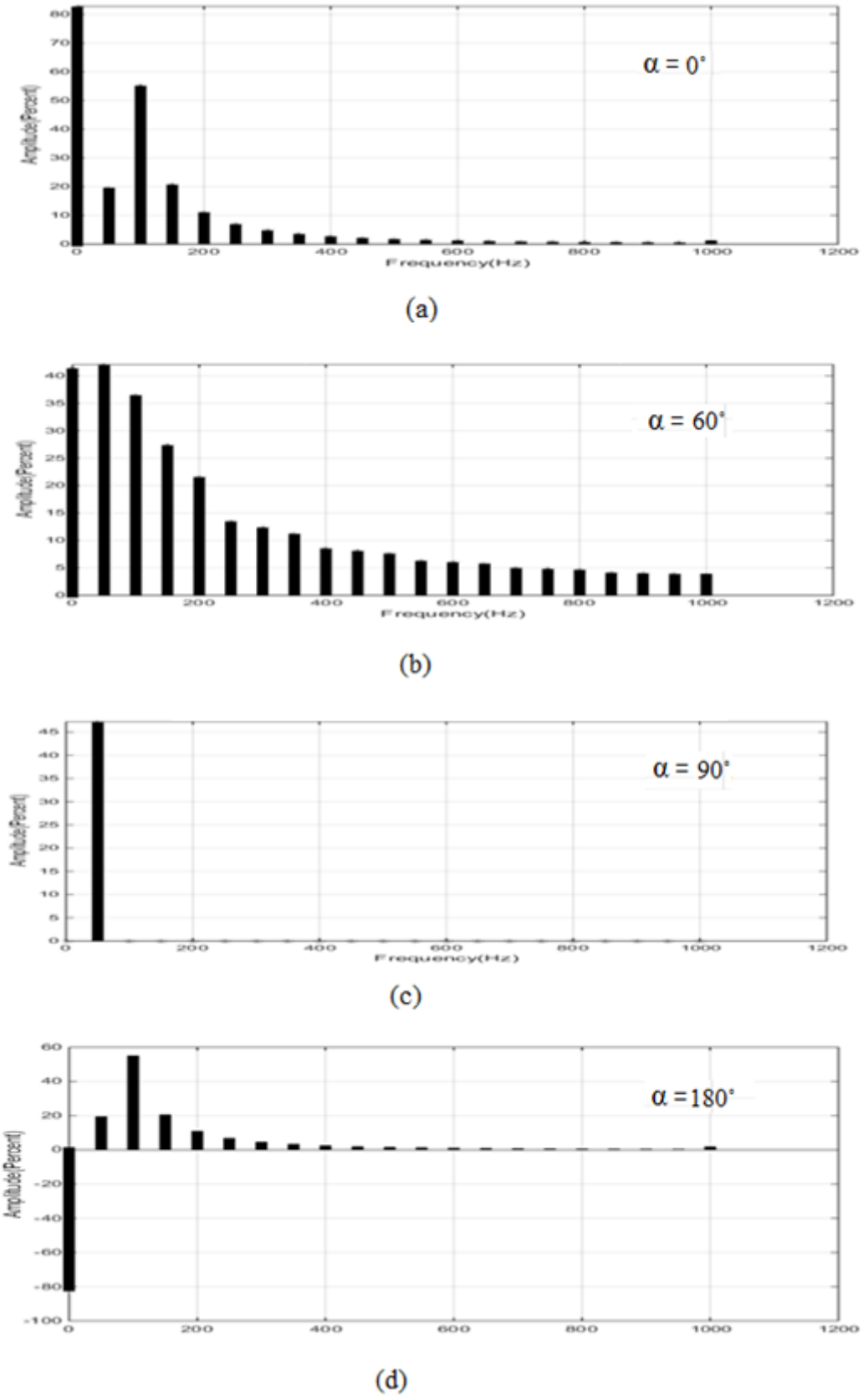

Fig.3.60 Harmonic frequency spectra for p =3 rectifier with different firing angles: (a) α = 0˚, (b) α = 60˚, (c) α = 90˚, and (d) α = 180˚.

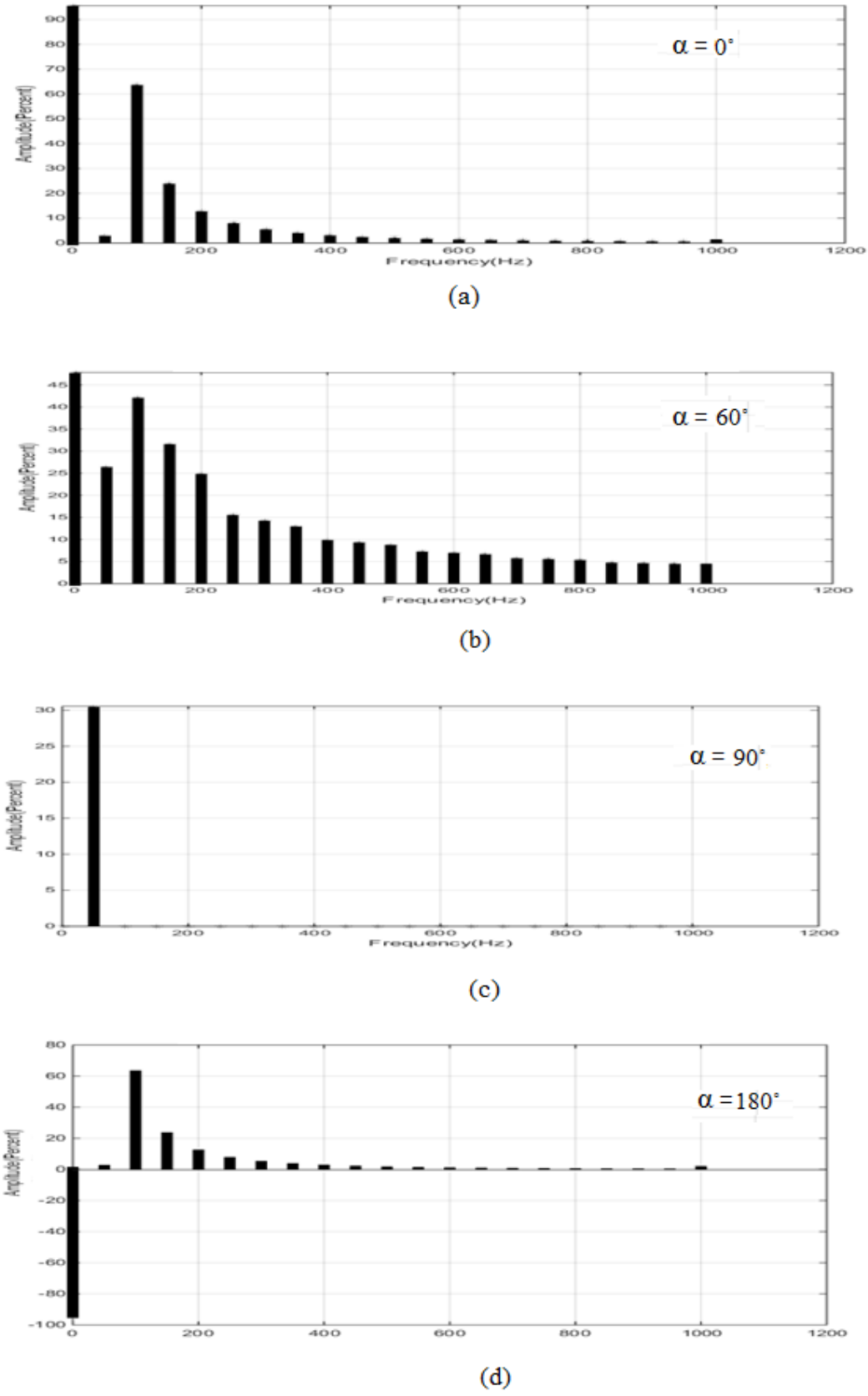

Fig.3.61 Harmonic frequency spectra for p = 6 rectifier with different firing angles: (a) α = 0˚, (b) α = 60˚, (c) α = 90˚, and (d) α = 180˚.

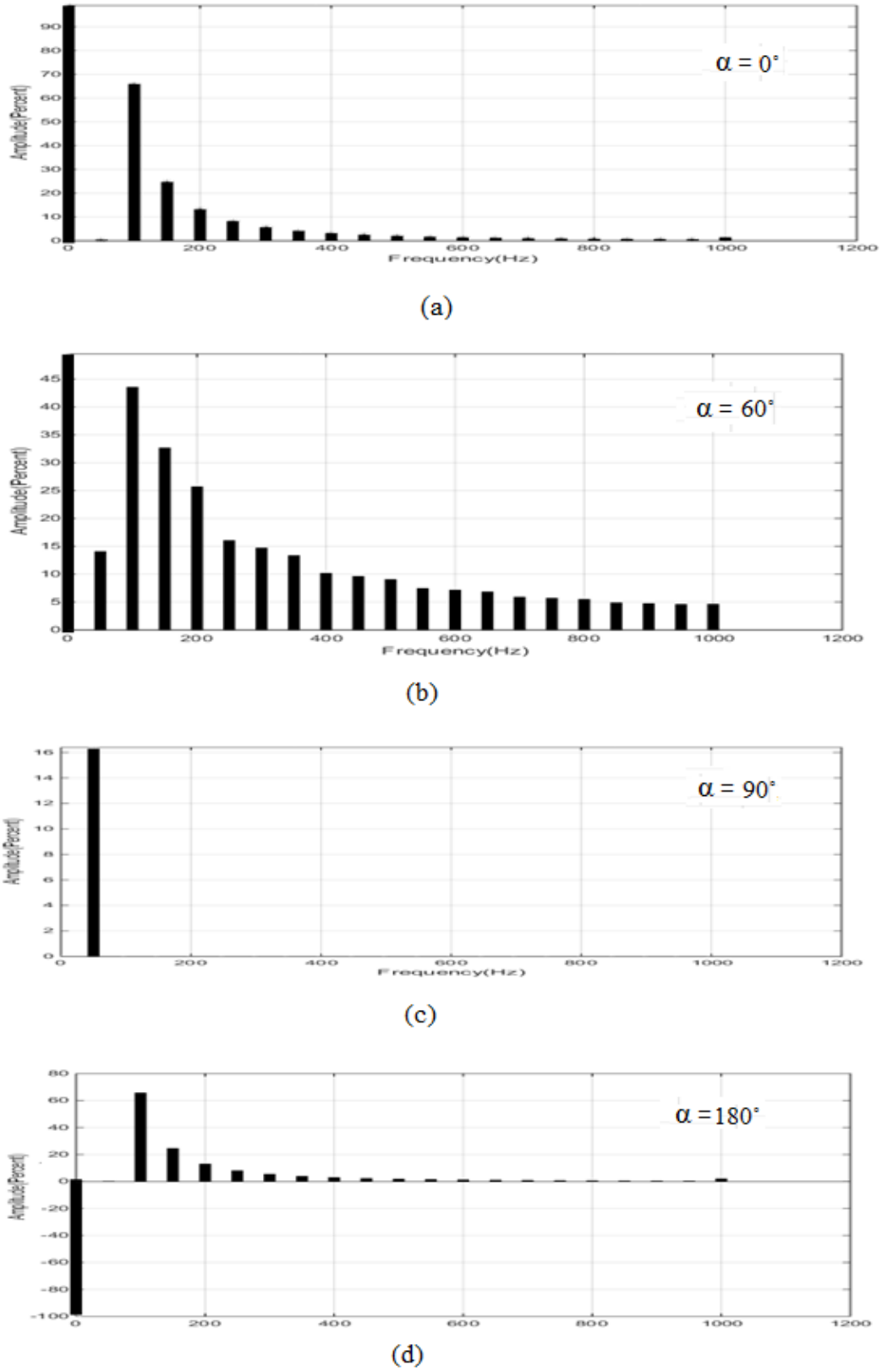

Fig.3.62 Harmonic frequency spectra for p=12 rectifier with different firing angles: (a) α = 0˚, (b) α = 60˚, (c) α = 90˚, and (d) α = 180˚.

PROBLEMS

3.1 A single- phase half - wave controlled rectifier shown in Fig.3.63, operates from an ideal sinusoidal source with v_s = 325 sinωt, at 50Hz. If the load is purely resistive, and at a certain triggering α , the output d.c. voltage is V_{dc} = 95 V, and the average value of the load current is 2.2 A. It is required to calculate the following:

(a) The triggering angle α
(b) Load resistance
(c) The *rms l*oad voltage
(d) The *rms* load current
(e) DC power
(f) What are the current and voltage ratings of the thyristor used?

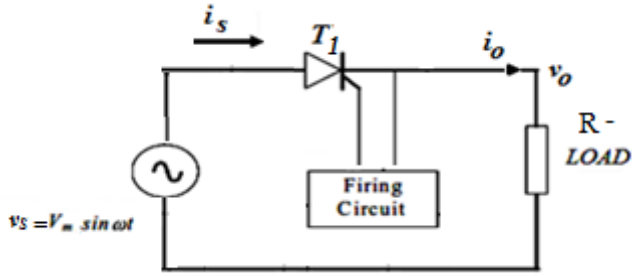

Fig.3.63.

[Ans : (a) 33.31˚, (b) 43.18 Ω, (c) 159.34 V , (d) 3.63 A, (e) 209 W, (f) 4 A, 400 V]

3.2 A single-phase half-wave controlled rectifier supplied from 230 V, 50 Hz a.c. supply is operating at α = 60º. If the load resistor is 15 Ω, determine:

(a) The power absorbed by the load (P_{dc}), the power drawn from the supply (P_{ac}) and the efficiency of the rectifier.
(b) The form factor and the ripple factor.
(c) The volt ampere rating of the transformer and the transformer utilization factor.
(d) The power factor at the a.c. source.

[Ans : (a) P_{dc} =178.6, P_{ac} = 880.74 W , η = 0.202 , (b) *FF*= 2.22, *RF* =1.98 , (c) VA rating of the transformer =1761.78, *TUF* = 0.10, (d) *PF* = 0.1013]

3.3 A bi-phase rectifier supplied from 230/110 V, 50 Hz ideal transformer is connected to load of 10 Ω resistance and infinite inductance.

(a) Determine the average output voltage, and current at a firing angle of 60º.
(b) Prove that the input power factor of the rectifier is given by

$$PF = \frac{2\sqrt{2}}{\pi} \cos\alpha$$

and find its value at α = 60º

[Ans: (a) 49.5 V, 4.95 A, (b) 0.450]

3.4 What are the required delay angles of a bi-phase controlled rectifier to obtain 60% and 25 % of its maximum output voltage? Assuming :

(a) A highly inductive load.

(b) A pure resistive load.

[Ans : (a) 53°, 75.5°, (b) 113.6 °, 104.5 °]

3.5 A single-phase mid-point (bi-phase) rectifier supplied from 240/120 V, 50 Hz ideal transformer is connected to load of 15 Ω resistance and infinite inductance. Determine the average output voltage, current and the power factor at a firing angle of 60°.

[Ans: 54 V, 3.6 A, 0.450]

3.6 A fully-controlled single-phase bridge rectifier is supplied from a 50 Hz 240/100 V transformer. It is supplying a highly inductive load of 5.5 Ω resistance. For a firing angle of 45°, determine the average output voltage, the average output current and the input power factor of the rectifier.

[Ans: 63.7 V, 11.57 A, 0.637]

3.7 If the line side of the transformer in the above example has an inductance of 5 mH, determine the output voltage, current and the angle of overlap.

[Ans: 61.4 V, 11.16 A, 9.35°]

3.8 Fig. 3.64 shows an SCR – Diode converter fed from 230V *rms* a.c. supply. The converter consists of one SCR and three diodes. Assume that load current is continuous and load resistance is 15 Ω.

(a) Prove that the average d.c. output voltage is given by

$$V_{dc} = \frac{V_m}{2\pi}(3 + cos\alpha)$$

(b) Draw waveforms of output voltage, load current and currents through thyristor and diodes for a firing angle of 60°.

(c) Find d.c. output voltage, d.c. current and d.c. output power.

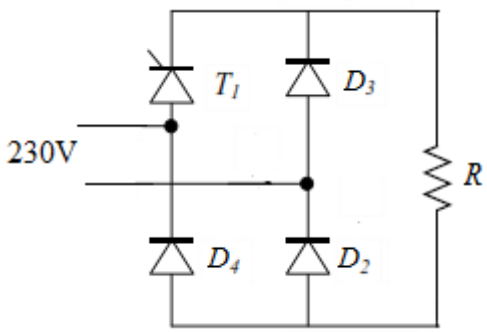

Fig.3.64.

[Ans: 181.3 V , 12 A , 2.2 kW]

3.9 A freewheel diode is connected across a single-phase fully-controlled, full-wave, bridge rectifier as shown in Fig. 3.65. The bridge has a source of 120 V *rms* at 50 Hz, and is feeding an *R-L* with load R =10 Ω and L = 20mH. The firing angle α = 30˚ and the current extinction angle β =216˚. It is required to:

(a) Determine whether the current is continuous or discontinuous.
(b) Determine the average load voltage and current.
(c) Calculate the *rms* load voltage and current.
(d) Determine the a.c. and d.c. powers absorbed by the load.
(e) Determine the efficiency of the converter.

Fig.3.65.

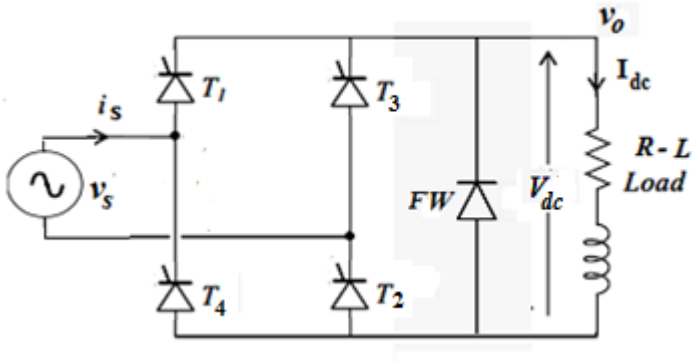

[Ans: (a) Current is continuous (b) 100.8 V, 10.08 A, (c) 118.28 V, 10.03 A, (d) 1184.14 W, 1018 W, (e) 85%]

3.10 A single -phase full-converter bridge circuit is feeding an *RLE* load and is fed from single-phase sinusoidal a.c. supply v_s = 300 sinωt , 50Hz. The load current is constant at 20 A. R = 0.25 Ω, L = 0.2 H. Find (a) firing angle if E = 75 V, (b) firing angle if E = -75 V, (c) input power factor in bath cases, and (d) draw output voltage waveform.

[Ans : 65.25 ˚, 111.49˚, 0.377, 0.33]

3.11 A three-phase, star-connected, sinusoidal voltage supply has a peak voltage V_m per phase. This supplies power to a load resistor through a three-phase, full-wave bridge rectifier. Sketch the circuit arrangement and give the waveform of a phase current in correct time-phase to the corresponding supply phase voltage. Sketch the waveform of the load current for a supply cycle and derive an expression for its average value in terms of V_m and R. Explain what you would expect to be the lowest order of harmonic ripple frequency in the load current. What effect would be caused to the phase current waveform by (i) large load inductance, (ii) large supply inductance and large load inductance?

3.12 Show from first principle that the *rms* value of primary line current for a three-phase converter transformer is given by

$$I_p = \frac{\sqrt{2}}{3}\, I_{dc}$$

where I_{dc} is the value of well-smoothed d.c. current. The transformer has equal primary and secondary turns and star-connected primary winding.

3.13 Show that the line current supplying the primary winding of a 3-pulse converter with delta-connected primary, having equal primary and secondary turns and well-smoothed dc current I_d, i_p given by:

$$i_p = 3\,\frac{I_{dc}}{\pi}\left[\cos\omega t - \frac{sin2\omega t}{2} + \frac{sin4\omega t}{4} + \frac{cos5\omega t}{5} - \frac{cos7\omega t}{7} + \frac{sin\,8\omega t}{8} - \frac{sin10\omega t}{10} - \frac{cos11\omega t}{11} + \frac{cos13\omega t}{13}\right]$$

Take the reference point $\omega t = 0$ on the waveform of i_p so as to correspond with the maximum positive voltage for the reference phase of a line currying current i_p.

3.14 Show that the 'short- circuit 'current flowing in the lagging phase of two involved in commutation of d.c. load current is given by

$$i_{sc} = i_{s2} = \frac{V_m}{\omega L_s}$$

3.15 A single-phase semiconverter bridge rectifier operating at a delay angle α and connected to highly inductive load such that the load current (I_{dc}) is continuous and ripple-free. Sketch the relevant waveforms during the development of your answer :

(a) Prove that the *rms* value of the input current of the rectifier is given by

$$I_{in} = I_{dc}\sqrt{1 - \frac{\alpha}{\pi}}$$

(b) Prove that the power factor of the fundamental component of the input current is

$$PF_1 = \cos\frac{\alpha}{2}$$

(c) Prove that the power factor of the input current is

$$PF_{in} = (\sqrt{2}/\pi) \times (1 + cos\alpha)/\sqrt{1 - \frac{\alpha}{\pi}}$$

(d) Use the results obtained above to prove that the distortion factor of the input current can be expressed as

$$\text{Distortion factor} = \frac{0.9}{\sqrt{1-\frac{\alpha}{\pi}}} \times \cos\frac{\alpha}{2}$$

3.16 A three-phase, full-wave half-controlled rectifier bridge circuit is operating at a delay angle $\alpha = 67^{o}$ when supplying full power. The per-phase inductance of the coupled transformer is 2 mH. The input voltage has an *rms* magnitude of 230 V per phase at 50 Hz. The load current in the d.c. side is 15 A at 200 V. It is required to:

(a) Obtain the drop in the d.c. voltage due to current overlap.
(b) Calculate the *rms* secondary voltage of the transformer.
(c) Calculate the overlap angle.
(d) Obtain the recovery angle while the converter in operating in the inversion mode with 15 A, 200 V d.c. input.
(e) Obtain the firing angle for the conditions in (d).

[Ans : (a) 4.5 V, (b) 450 V, (c) 1.06˚, (d) 67.14˚, (e) 111.8˚]

3.17 In problem 3.16**,** if the converter (and the input transformer) is replaced by a three-phase full-wave fully-controlled one to deliver the same output power (voltage and current) when operating at the same firing angle α of that problem in rectification mode. It is required to:

(a) Obtain the drop in the d.c. voltage due to a.c. source internal reactance.
(b) Calculate the overlap angle.
(c) Calculate the extinction angle when the circuit is to function as inverter with 15 A and 200 V power.
(d) Obtain the firing angle for the case stated in (c).

[Ans: (a) 9 V, (b) 2.06˚, (c) 67.14˚, (e) 110.8˚]

3.18 In a single-phase half-wave ac-dc converter, the average value of the load current is 1.78 A. If the converter is operated from a 240 V, 50 Hz supply and if the average value of the output voltage is 27% of the maximum possible value, calculate the following, assume the load to be resistive.

(a) Load resistance
(b) Firing angle
(c) Average output voltage
(d) The *rms* load voltage
(e) The *rms* load current
(f) DC power

(g) AC power
(h) Rectifier efficiency
(i) Form factor
(j) Ripple factor

[Ans: (a) 51.4 Ω , (b) 45 °, (c) 91 V , (d) 134 V, (e) 2.6 A , (f) 162 W, (g) 349 W, (h) 46.4% , (i) 1.362 , (j) 1.08]

3.19 For the circuit arrangement shown in Fig.3.66 and for a pure resistive load, sketch a set of waveforms for thyristor triggering α = 90° showing the supply current,load current and thyristors voltage .
Derive an expression for the average value of the load current I_{dc} and calculate its values for α = 0° , 60° , and 120° if the the supply voltage is ideal sinusoid with V_m = 400 V, 50 Hz and the load resisror R =10 Ω. How is the average load current affected if diode D_2 fails to open circuit?

Fig.3.66.

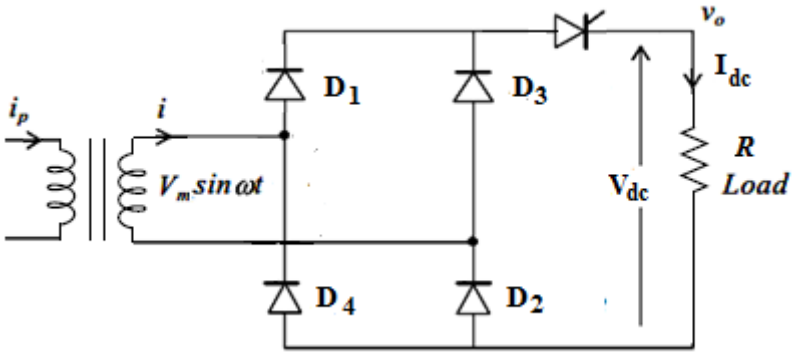

[Ans : 12.7 A, 9.5 A, 3.17 A .When diode D_2 failed to open circuit, the circuit will act as a half-wave rectifier]

3.20 For the three-phase half-wave fully controlled rectifier shown in Fig.3.67, the load consists of a resistance and a very large inductance. The inductance is so large that the output current i_o can be assumed to be continuous and ripple-free. For triggering angle α = 30°.

Fig.3.67.

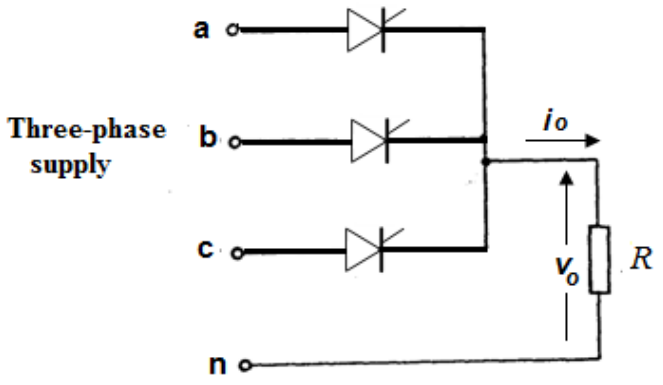

(a) Draw the waveforms of v_o and i_o.
(b) Prove that the d.c. power delivered to the load is given by:

$$P_{dc} = 0.684\frac{V_m^2}{R}cos^2\alpha$$

(c) Determine the mean value of the output voltage, current and d.c. power if phase voltage is V_{an} = 220 V (*rms*), α = 30° and R = 50 ohms.

[Ans: (c) 121.6 V, 6.08 A , 740 W]

3.21 A three-phase half-wave controlled rectifier is connected to a star supply and a resistive load R =10 Ω. If the rectifier is turned-on at a firing angle of 60˚, calculate average and *rms* output voltages and currents. Assume phase supply voltage to be 120 V.

[Ans: 70 V, 106.8 V, 7 A, 10.68 A]

3.22 A large magnet load consists of an inductance of 18.5 H and resistance of 50 Ω is to be supplied from a 400 V, 50 Hz, three-phase source through a fully controlled full-wave, three-phase rectifier bridge as shown in Fig.3.68. It is required to determine:

(a) The power delivered to the magnet at firing angle of 60˚.
(b) The maximum d.c. voltage $V_{dc,max}$ and maximum current $I_{dc,max}$ which can be supplied from this rectifier ,
(c) The delay angle α required to give a magnet current of 4A.

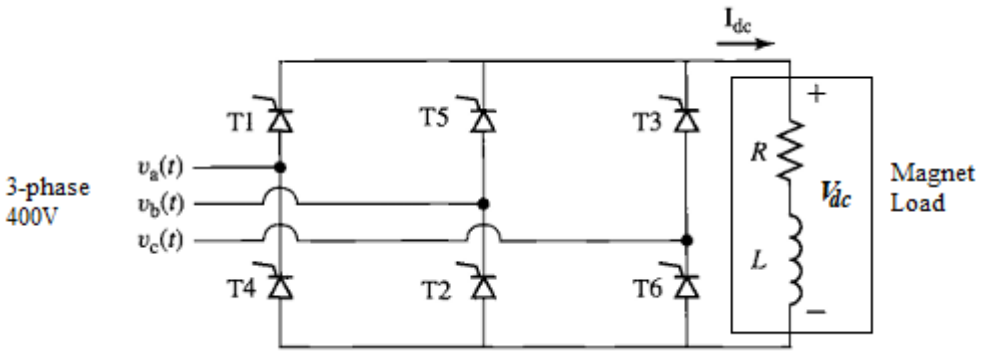

Fig.3.68.

[Ans : P_o = 1.447 kW, $V_{dc,max}$ = 538V , $I_{dc,max}$ = 10.76A , α = 68.18˚]

3.23 For a p-pulse convertor, show that the average voltage V_{dc} considering the overlap period is given by:

$$V_{dc} = \frac{PV_m}{2\pi}\sin\frac{\pi}{P}\left(cos\alpha + cos(\alpha+\mu)\right)$$

$$V_{dc} = \frac{PV_m}{\pi}sin\frac{\pi}{P}cos\alpha - \frac{P\omega LI}{2\pi}$$

$$\text{or } = \frac{PV_m}{\pi}sin\frac{\pi}{P}\cos(\alpha+\mu) + \frac{P\omega LI}{2\pi}$$

3.24 When a controlled rectifier circuit operates with pure inductive load, the average output voltage across the load is zero but unidirectional current flows in the load. If the delay angle exceeds a certain value, dependent of the pulse number, this load current becomes discontinuous. Determine the relationship between pulse number and the minimum value of α at which load current becomes discontinuous and show that, with discontinuous current flow, the average value of the d.c. load current in p.u. of its peak value is given by :

$$\frac{I_{dc}}{I_m} = \frac{p}{2}[(\beta' - \alpha')\cos\alpha' + \sin\alpha' - \sin\beta']$$

Where α' and β' are respectively the delay angle and current extinction angle measured from the instant of zero transit into the positive half cycle for a phase about to conduct.

3.25 (a) Show that for a 6-pulse converter with a purely resistive load, where the triggering angle α is such that load current is discontinuous, the *rms* value of d.c. voltage is given by :

$$V_{orms} = V_m\sqrt{1 - \frac{3\alpha}{2\pi} - \frac{3}{4\pi}sin2\alpha}$$

where V_m is the maximum value of the transformer secondary voltage per-phase.

(b) For 400 V three-phase voltage supplying 6-pulse converter operating such that the load current is discontinuous, find the *rms* value of the output voltage and the *rms* value of the load current when the triggering angle is 75°. Assume the load is resistive with R = 20 Ω.

[Ans : (b) 123.5V , 6.17A]

CHAPTER FOUR

DC-DC CONVERSION: DC CHOPPERS

4.1 INTRODUCTION

A dc-to-dc converter, also known as d.c. chopper, is a static device which is used to obtain a variable d.c. voltage from a constant d.c. voltage source. Also the dc-to-dc converter is defined in more general way as an electrical circuit that transfers energy from a d.c. voltage source to a load. The energy is first transferred via power electronic switches to energy storage devices and then subsequently switched from storage into the load. The switches used are GTO, IGBT, Power BJT, and Power MOSFET for low power application and thyristors or SCRs for high power application. The storage devices are inductors and capacitors. The power source is either a battery (d.c. volt) or a rectified a.c. volt. This process of energy transfer results in an output voltage that is related to the input voltage by the duty ratios of the switches.

The dc-to-dc converter products are used extensively for divers applications in the healthcare (bio-life science, dental, imaging, laboratory, medical), communications, computing, storage, business systems, test and measurement, instrumentation, and industrial equipment industries. They are used in electric motor drives, in switch mode power supplies (SMPS), trolley cars, battery operated vehicles, traction motor control, control of large number of d.c. motors, etc. They are also used as d.c. voltage regulators.

Types of dc-to-dc converters

There are mainly two types of dc-to-dc converters: (1) Step-down choppers, and (2) Step-up choppers. In step-down choppers, the output

voltage will be less than the input voltage, whereas in step-up choppers output voltage will be more than the input voltage. Hence a chopper is considered as d.c. equivalent of an a.c. transformer since it behaves in an identical manner. Also dc-to-dc converters can be categorized into two groups:

1) DC-to-DC converters without isolation

These dc-to-dc converters do not have any isolation transformer between input and output stages. Some of the commonly used dc-to-dc converters without isolation are:

a. Buck converter
b. Boost converter
c. Buck-boost converter

The buck converter is step-down converter (output voltage < input voltage) whereas Boost converter is a step-up converter (output voltage > input voltage). The buck-boost converter is derived from step-up and step-down converters. The buck-boost converter can be operated in step-up or step-down mode depends on the duty cycle of switch (t_{on} / T), where t_{on} is the duration for which switch is on and T is the switching time period).

2) DC-to-DC converters with isolation

A transformer is provided in between to isolate the input and output stages. The electrical isolation is an additional feature and is mainly useful in cases where the input voltage level (V_{in}) and output voltage level (V_{out}) differs significantly i.e. high or low values of V_{out} / V_{in}. The dc-to-dc converters with isolation is again divided into two types based on polarity of transformer core excitation:

- Unidirectional core excitation, core is excited with forward currents of only one direction. In these dc-to-dc converters the isolation transformer core is operated in only the positive part of B-H curve.
- Bidirectional core excitation, core is excited with currents in either direction. In these dc-to-dc converters the isolation transformer core is operated alternatively in positive and negative portions of B-H curve.

Some of the commonly used dc-to-dc converters with isolation are:

a. Cuk converter (can be used in non-isolated mode also)
b. Fly-back converter
c. Forward converter
d. Full-bridge converter
e. Half-bridge converter
f. Push-pull converter

4.2 PRINCIPLE OF STEP-DOWN CHOPPER

The basic chopper circuit, often referred to as a class-A chopper, with resistive load is shown in Fig.4.1. It consist of a semiconductor switch S (often a thyristor) and its commutation circuit. The thyristor in the circuit acts as a switch. By the action of the switch, i.e. when thyristor is ON, supply voltage appears across the load and when thyristor is OFF, the voltage across the load will be zero. The output voltage waveform is as shown in Fig.4.2 which has an average value $V_{ave} = V_o$.

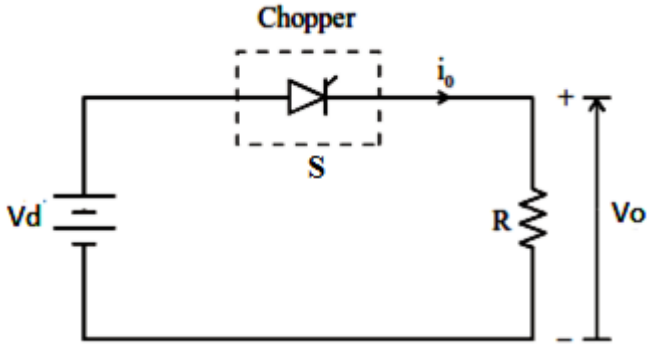

Fig.4.1 Step-down simple chopper circuit.

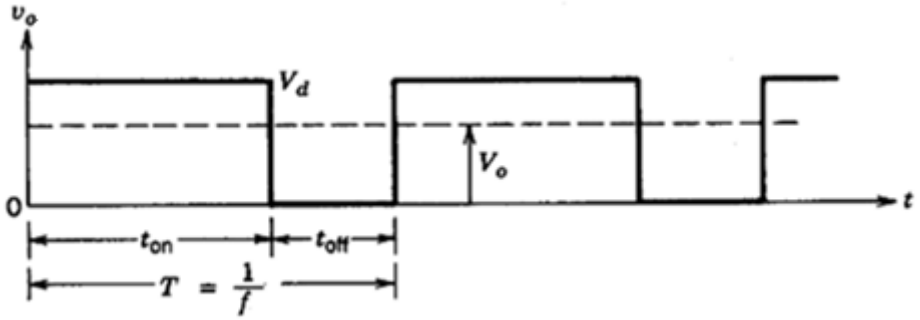

Fig.4.2 Chopper output voltage waveform, case of *R*-load.

The applied voltage is therefore "chopped" by the action of the switch. Since the average load voltage V_o is less than the input voltage, this circuit is called "step-down chopper". For all loads the current is unidirectional and the polarity of the load voltage is non-reversible. Operation takes place only in the positive voltage, positive current quadrant of the load voltage/load current plane so the circuit is referred to as a one-quadrant chopper.

Methods of Control

The output d.c. voltage can be varied by the following methods.

(a) Pulse width modulation control or constant frequency operation.

(b) Variable frequency control.

Pulse Width Modulation

- t_{on} is varied keeping chopping frequency 'f' and chopping period 'T' constant.
- Output voltage is varied by varying the ON time $t_{on.}$

Typical thyristor chopper circuit:

Fig.4.3 shows one typical thyristor chopper circuit. Thyristor (T_m) is the main thyristor through which the flow of power is controlled. The capacitor C and the four Thyristors (T_1,T_2 ,T_3 ,T_4) is the commutation circuit (this circuit had been already discussed in Chapter One).

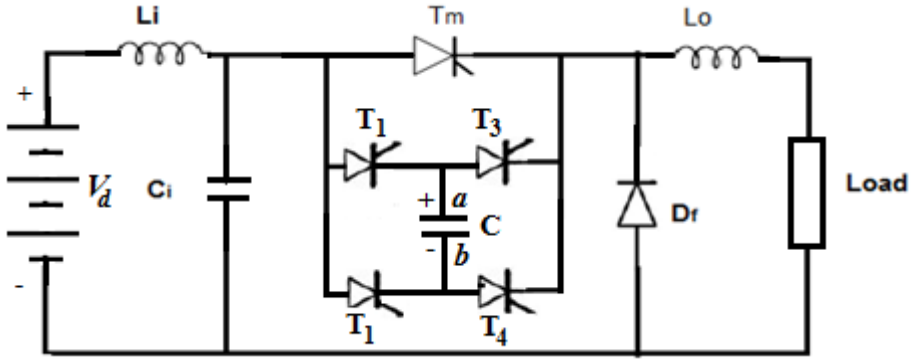

Fig.4.3 Typical thyristor d.c. chopper with forced commutation circuit.

The function of the commutation circuit is to switch off the main thyristor at the end of each ON period. If the capacitor is charged such as plate ***a*** is positive. To switch OFF (T_m) , Thyristors (T_1,T_3) are triggered ON. This results in applying reverse polarity voltage across (T_m) and hence it will be switched OFF. Also the capacitor polarity will be reversed; i.e. plate *b* will now be positive. Thyristor (T_m) is switched ON for the next ON period, and now to switch OFF (T_m) , Thyristors (T_2,T_4) are switched ON , and so the cycle is repeated . However , the thyristor commutation circuits are discussed in details in Appenix-B.

The L_i-C_i circuit in the input terminal is a filter circuit that reduces the harmonics injected into the power source. The inductance (L_o) in the output terminal is filter that smooth the current passing through the load. The diode (D_f) is a freewheeling diode, its function is to circulate the d.c. current through it when the main Thyristor (T_m) is OFF.

4.3 ANALYSIS OF A STEP- DOWN DC CHOPPER WITH RESISTIVE - LOAD

Referring to Fig.4.2, the average output voltage V_o can be found as:

Let T = control period = $t_{on} + t_{off}$ (4.1)

and,

$$f = \text{chopping frequency} = \left(\frac{1}{control\ \ period\ (T)}\right) = 1/T \qquad (4.2)$$

Typical chopping of the frequencies are usually in the range $10\,\text{Hz} < (f = \omega/2\pi) < 1000\text{Hz}$ for thyristor chopper and up to 10kHz for transistor choppers. In low power applications MOSFET switches can be used at frequencies in excess of 200 kHz.
The average value of the load voltage waveform shown in Fig. 4.2 may be expressed by the basic relationship,

$$V_o = V_{av} = \frac{1}{T}\int_0^{t_{on}} V_d\ dt \qquad (4.3)$$

Evaluating this integration gives,

$$V_o = \frac{t_{on}}{T} V_d = \gamma V_d \qquad (4.4)$$

$$\text{where},\ \gamma = \frac{t_{on}}{T} = \text{Duty cycle} \qquad (4.5)$$

- Maximum value of $\gamma = 1$ when $t_{on} = T$ $(t_{off} = 0)$
- Minimum value of $\gamma = 0$ when $t_{on} = 0$ $(t_{off} = 0)$

The output voltage is stepped-down by the factor γ, $(0 \le V_o \le V_d)$.

Therefore, this form of chopper is a step-down chopper. Since the load is resistive the average load current is given by the basic equation

$$I_o = \frac{V_o}{R} \qquad (4.6)$$

$$I_o = \frac{1}{R}(\gamma V_d) \qquad (4.7)$$

The average power transferred to the load may be expressed by the basic relationship.

$$P_o = \frac{1}{T}\int_0^{\mathrm{T}} v_o i_o dt = V_o \times I_o \qquad (4.8)$$

The *rms* value of the load voltage waveform is given by,

$$V_{orms} = \sqrt{\frac{1}{T}\int_0^{t_{on}} v_o^2(t)d\omega t} = \sqrt{\frac{V_d^2}{T}[t]_0^{t_{on}}} = \sqrt{\gamma}\, V_d \qquad (4.9)$$

The *rms* value of the load current,

$$I_{orms} = \frac{V_{orms}}{R} \qquad (4.10)$$

In the equivalent circuit of the Fig.4.1 the load power can be written, in a form more convenient for calculation as

$$P_o = I_{orms}^2 \times R \qquad (4.11)$$

Since the input voltage V_d is constant, average power is only transferred from the supply to the chopper by the combination of V_d with the average value of the input current $I_{S(av)}$,

$$P_{in} = V_d \times I_{s(av)} \qquad (4.12)$$

The ripple factor, *RF* : It is a measure of the ripple content. Also, the ripple factor, defining the ratio of the a.c. components to the average value, is given by

$$\text{ripple factor} = \frac{\sqrt{V_{orms}^2 - V_o^2}}{V_o} \qquad (4.13)$$

$$RF = \frac{V_d\sqrt{\gamma - \gamma^2}}{V_d\,\gamma} == \sqrt{\frac{1-\gamma}{\gamma}} \qquad (4.14)$$

For full conduction $\gamma = 1$ and *RF= 0.*

Note1: In this type of chopper both the voltage and current are always positive, hence this chopper is called a single-quadrant Buck converter or class-A chopper.

Note2: The chopper switch can also be implemented by using a power BJT, power MOSFET, GTO, and IGBT transistor. The practical devices have a finite voltage drop ranging from

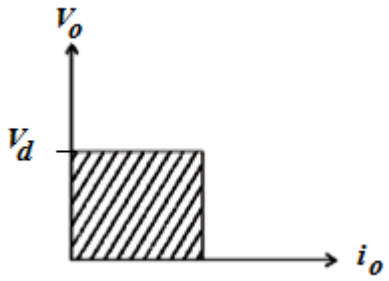

Fig.4.4 Single-quadrant operation.

0.5V to 2V, and for the sake of simplicity, the voltage drop of these power semiconductor devices are generally neglected.

Example 4.1

A class-A d.c. chopper circuit (Buck converter) is supplied with power form an ideal battery of 100 V. The load voltage waveform consists of rectangular pulses of duration 1 ms in an overall cycle time of 2.5 ms. For resistive load of R =10 Ω , it is required to calculate:

(a) The duty cycle γ.
(b) The average value of the output voltage V_o.
(c) The *rms* value of the output voltage V_{orms}.
(d) The ripple factor *RF*.
(e) The output d.c. power.

Solution

(a) t_{on} = 1ms , T = 2.5 ms

$$\gamma = \frac{t_{on}}{T} = \frac{1\ ms}{2.5\ ms} = 0.4$$

(b) $V_{av} = V_o = \gamma\ V_d = 0.4 \times 100 = 40$ V.

(c) $V_{orms} = \sqrt{\gamma}\ V_i = \sqrt{0.4} \times 100 = 63.2$ V.

(d) $$RF = \sqrt{\frac{1-\gamma}{\gamma}} = \sqrt{\frac{1-0.4}{0.4}} = 1.225$$

(e) The load (output) current and the average power are

$$I_o = \frac{V_o}{R} = \frac{40}{10} = 4 \text{ A}$$

$$P_{av} = I_o\ V_o = 4 \times 40 = 160 \text{ W}$$

4.4 ANALYSIS OF A STEP-DOWN DC CHOPPER WITH *R-L* LOAD: EXACT ANALYSIS

Referring to Fig.4.5 which shows typical class-A chopper operating with series resistive-inductive load, the current "i_o"will alter between certain maximum and minimum values. These values depend on the parameters of the circuit and the value of the duty cycle (operation conditions). The waveforms of the output voltage and current are shown in Fig. 4.6. However, class-A chopper can operates in two modes with *R-L* loads:

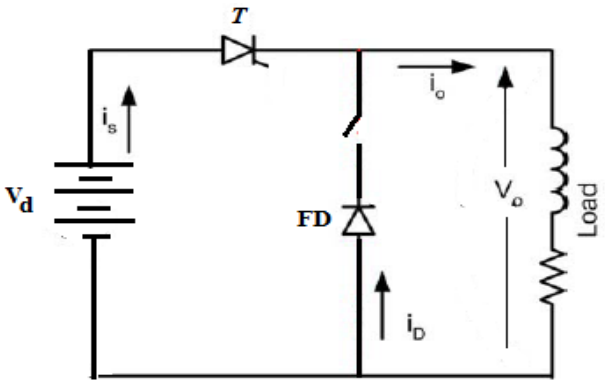

Fig.4.5 Class-A chopper operating with series resistive-inductive load.

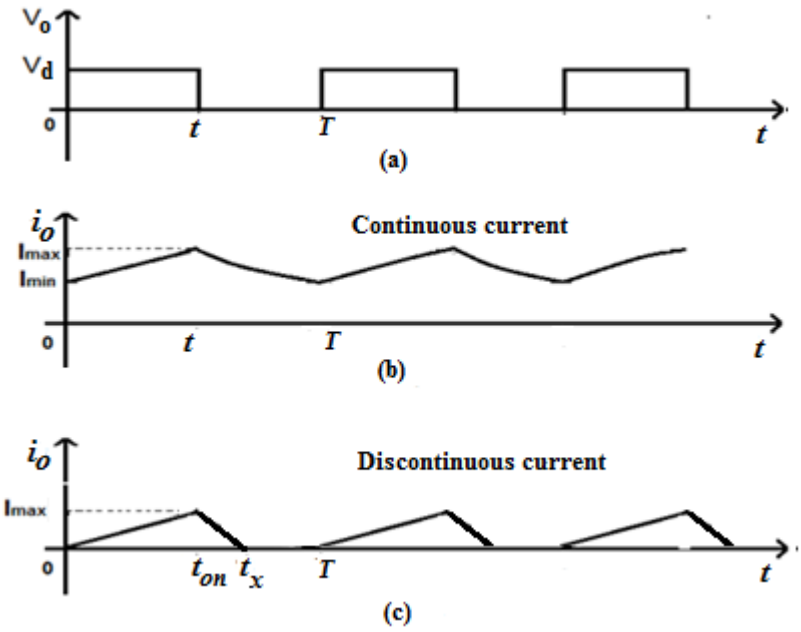

Fig.4.6 Load current and voltage waveforms with inductive load: (a) Load voltage waveform, (b) Continuous load current, (c) Discontinuous load current (t_x is the instant when the current falls to zero).

- For high values of γ, the load current fluctuates in magnitude but it is more or less "continuous", as shown in Fig.4.6(b).
- For low values of γ , the load current may fall to zero during the OFF periods "discontinuous", as shown in Fig.4.6(c). However the load voltage waveform is the same for both cases as shown in Fig.4.6(a).

Analytical properties of the load current waveform

With an *R-L* load, during the ON-state, when switch S closed, the equivalent circuit is represented by Fig.4.7. The current flows through the circuit is governed by the following equation:

$$V_d = Ri_o + L\frac{di_o}{dt} \qquad \text{for} \qquad 0 \le t \le t_{on} \qquad (4.15)$$

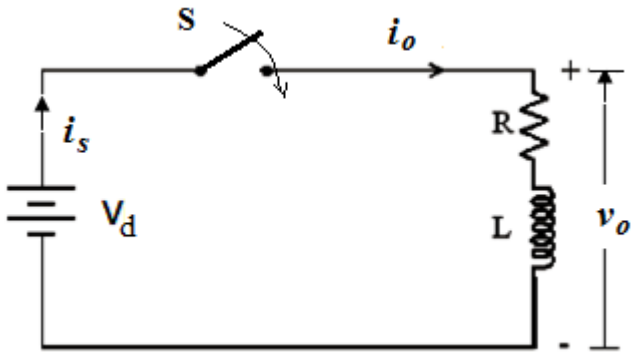

Fig.4.7 ON-state equivalent circuit.

To solve this equation, we re-arrange it as,

$$(V_d - Ri_o)dt = L\, di_o \qquad (4.16)$$

Integrating both sides and simplify,

$$\int \frac{di_o}{i_o - \frac{V_d}{R}} = \int \frac{-R}{L} dt$$

$$\ln\left(i_o - \frac{V_d}{R}\right) = \frac{-R}{L}t + K$$

$$i_o - \frac{V_d}{R} = e^{\frac{-R}{L}t+K} = e^K e^{\frac{-R}{L}t} = K'e^{\frac{-R}{L}t}$$

where *K* and *K'* are constants.

- Special case : at *t = 0* , $i_o = 0$

$$0 - \frac{V_d}{R} = K'e^0 \qquad \therefore\ K' = -\frac{V_d}{R}$$

Hence, the equation for the current is,

$$i_o(t) = \frac{V_d}{R} - \frac{V_d}{R}e^{\frac{-R}{L}t} = \frac{V_d}{R}\left(1 - e^{-t/\tau}\right)$$

Where τ = time constant = L / R,

- The general case when : at $t = 0$, $i_o = I_o$

$$I_o - \frac{V_d}{R} = K'e^0 \qquad \therefore\ K' = I_o - \frac{V_d}{R}$$

$$i_o(t) = \frac{V_d}{R} + (I_o - \frac{V_d}{R})\, e^{-t/\tau}$$

$$i_o(t) = \frac{V_d}{R}\left(1 - e^{-t/\tau}\right) + I_o e^{-t/\tau} \qquad (4.17)$$

This general equation of the current can be re-written in terms of ωt as,

$$i_o(\omega t) = \frac{V_d}{R}\left(1 - e^{-\omega t/\omega\tau}\right) + I_o e^{-\omega t/\omega\tau} \qquad (4.18)$$

where $\omega\tau = \omega L/R$

Equation (4.18) can be considered as a general solution for the instantaneous current flowing through an *R-L* load fed by d.c. chopper circuit, and when applied to the chopper circuit shown in Fig.4.5 yields,

At the end of the ON period $t=t_{on} = \gamma T$, $i_o = I_2$ (or I_{max}) and therefore ,

$$I_2 = \frac{V_d}{R}\left(1 - e^{-\gamma T/\tau}\right) + I_1 \qquad (4.19)$$

On opening S , Fig.4.8 , the current " i_o " is commutated to the freewheeling diode and falls exponentially from I_2 to I_1 (or I_{min}) according to

$$0 = Ri_o + L\,\frac{di_o}{dt} \qquad t_{on} \le t \le T \qquad (4.20)$$

Thus $\quad i_o = I_2 e^{-(t-t_{on})/\tau} \qquad t_{on} \le t \le T \qquad (4.21)$

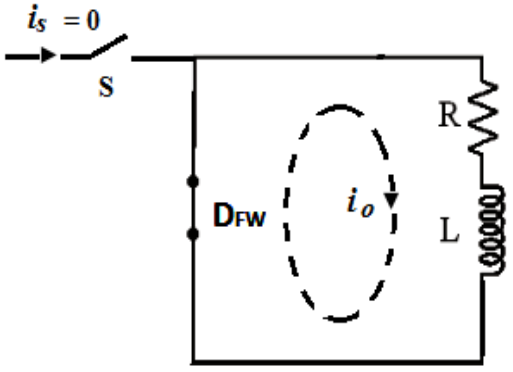

Fig.4.8 OFF-state equivalent circuit.

At the end of the OFF period, $t = T$, $I = I_1$ and therefore,

$$I_1 = I_2 e^{-(1-\gamma)T/\tau} \qquad (4.22)$$

or

$$I_2 = \mathrm{I}_1 \mathrm{e}^{(1-\gamma)\mathrm{T}/\tau} \tag{4.23}$$

The variation of the current is shown in Fig.4.9.

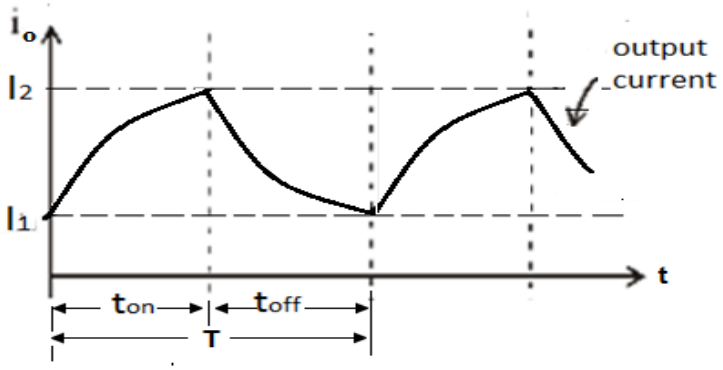

Fig.4.9 Current waveform for *R-L* load.

The average value of load current is defined by,

$$I_{oav} = \frac{1}{T}\int_{t=0}^{T} i_o(t)\, dt \tag{4.24}$$

The average value of the current drawn from the source is

$$I_{sav} = \frac{1}{T}\int_{t=0}^{T} i_s(t)\, dt \tag{4.25}$$

where $i_s = i_o$ $\qquad 0 \le t \le t_{on}$

$i_s = 0$ $\qquad t_{on} \le t \le T$

The peak-to-peak ripple of the load current I_r is given by $I_r = \Delta I = I_2 - I_1$. From above equations, with simple algebraic manipulation one can show that:

$$\frac{I_r}{I_m} = \frac{1 - e^{-\gamma \mathrm{T}/\tau} - \mathrm{e}^{-(1-\gamma)\mathrm{T}/\tau} + e^{-\mathrm{T}/\tau}}{1 - e^{-\mathrm{T}/\tau}} \tag{4.26}$$

where $I_m = V_d / R$: Maximum ON-state load current (i.e. , when $\gamma = 1$). Thus, for given circuit parameters (namely *R* and *L*) and the cycle time, $\frac{I_r}{I_m}$ is function of γ. The variation of $\frac{I_r}{I_m}$ with γ is shown in Fig.4.10 for different values of (T/τ). From this figure one can simply draw the following conclusions:

1. The maximum ripple occurs at $\gamma = 0.5$.
2. The ripple is very small when ($T < 0.1\tau$) , (or when $f > 10/\tau$).

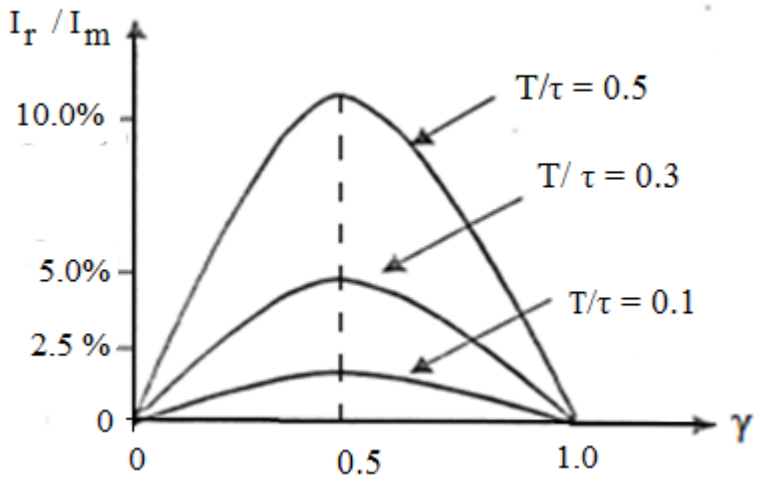

Fig.4.10. The variation of $\frac{I_r}{I_m}$ with γ.

4.5 ANALYSIS OF A STEP-DOWN DC CHOPPER WITH LOAD CONSISTING BACK EMF (*E*)

When the load has a back *emf E* (such as battery or motor), Fig.4.11, the governing equations during the ON and OFF periods are respectively:

$$V_o = V_d = Ri_o + L\frac{di_o}{dt} + E \qquad 0 \le t \le t_{on} \qquad (4.27)$$

$$0 = Ri_o + L\frac{di_o}{dt} + E \qquad t_{on} \le t \le T \qquad (4.28)$$

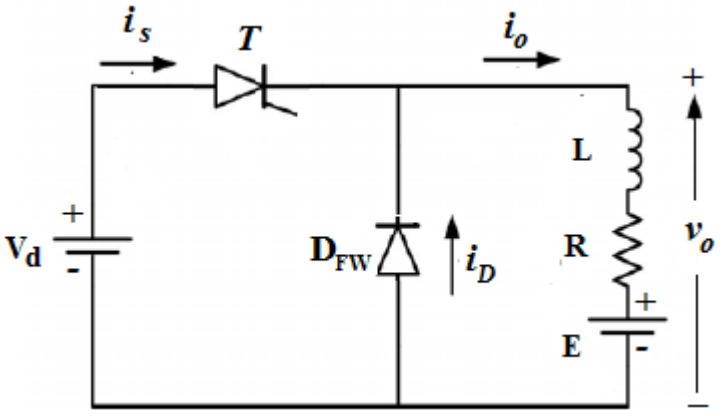

Fig.4.11 Operation with load consisting back *emf*.

In this case the current will be either continuous or discontinuous depending on the values of E and the duty cycle γ. However, the output voltage waveform is assumed to be the same for both continuous and discontinuous current operation which is also the same for resistive load.
It should be noted that the voltage forcing the current build up during the ON period is $(V_d - E)$, and during the OFF period, the decay of the current is aided by E. Thus a slower ON-state increase and faster OFF-state decrease in the current is expected.

4.5.1 Continuous Current Operation Condition with Back - *emf*

For analysis of class-A chopper circuit operation with back *emf* E, it is convenient to start by considering the case of continuous current conditions, when the back *emf* E is small, and the waveform of the current alter between I_{max} and I_{min} as in Fig.4.6(b) as follows:

When switch S is ON (and D_{FW} OFF) at t = 0, then at t = 0^+ (just after switching), $v_o = V_d$, $i_o = I_{min}$. From Eq.(4.17) and these initial conditions,

$$i_o(t) = \frac{V_d - E}{R}\left(1 - e^{-t/\tau}\right) + \mathrm{I_{min}}\mathrm{e}^{-\mathrm{t}/\tau} \qquad 0 \le t \le t_{on} \qquad (4.29)$$

At $t = t_{on}$, when S is opened, $i_o = I_{max}$, and:

$$i_o(t) = I_{max} = \frac{V_d - E}{R}\left(1 - e^{-t_{on}/\tau}\right) + I_{min}\mathrm{e}^{-t_{on}/\tau} \qquad (4.30)$$

Equation (4.30) is not time dependent and remains true after S switches off.
When switch S is off (and D on),
With $t = t_{on}^{+}$, in Fig.4.9, $v_o = 0$ and $i_o(t) = I_{max}$ and in the interval $t_{on} \le t \le T$, the load current is given by

$$i_o(t) = \frac{-E}{R}\left(1 - e^{-(t-t_{on})/\tau}\right) + \mathrm{I_{min}}e^{-(t-t_{on})/\tau} \qquad (4.31)$$

But at $t = T$, $i_o(t) = I_{min}$, equation Eq.(4.31) may then be rewritten as

$$i_o(t) = I_{min} = \frac{-E}{R}\left(1 - \varepsilon^{-(T-t_{on})/\tau}\right) + \mathrm{I_{max}}\varepsilon^{-(T-t_{on})/\tau} \qquad (4.32)$$

The simultaneous solution of Eq.(4.32) and Eq.(4.30) yields

$$I_{max} = \frac{V_d}{R}\left(\frac{1 - e^{-t_{on}/\tau}}{1 - e^{-T/\tau}}\right) - \frac{E}{R} \qquad (4.33)$$

$$I_{min} = \frac{V_d}{R}\left(\frac{e^{t_{on}/\tau} - 1}{e^{T/\tau} - 1}\right) - \frac{E}{R} \tag{4.34}$$

For full conduction of switch S in Fig.4.11, $\gamma = 1$, so that $I_{max} = I_{min} = (V_d - E)/R$. The use of Eq.(4.33) and Eq.(4.34) permits solution of Eq.(4.29) and Eq.(4.30) to determine a value for $i_o(t)$ at any instant of the cycle during continuous conduction.

4.5.2 Discontinuous Current Operation Condition

Under certain circuit conditions, depending on the duty cycle and the value of the back *emf E*, the load current $i_o(t)$ may fall to zero resulting in the discontinuous pulse pattern of Fig.4.12; this waveform consists of two parts that may be classified according to the conduction of switch S, as in subsection (4.1.1) above. The maximum current is now, in general, different from the value I_{max} obtained with continuous operation and it occurs for a different value of t_{on}. The minimum current for discontinuous operation is, by definition, zero.

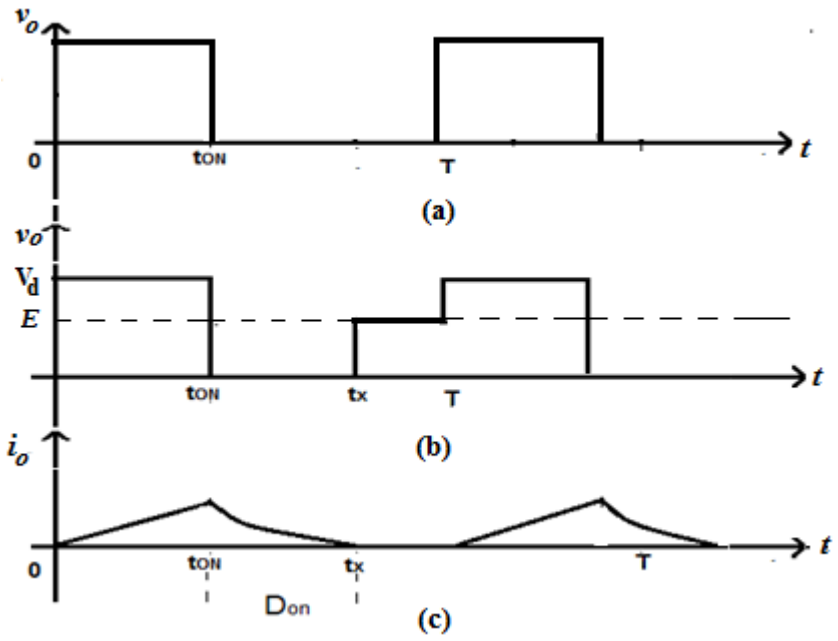

Fig.4.12 Load voltage and current waveforms for discontinuous current operation.

- With switch S on (and diode D off),

In the interval $0 \leq t \leq t_{on}$ of Fig.4.12 (c) the current equation Eq.(4.30) applies with the limits that $v_o = V_d$, and $i_o(t) = 0$ at $t = 0+$. This gives

$$i_o(t) = \frac{V_d - E}{R}\left(1 - e^{-t/\tau}\right) \tag{4.35}$$

Maximum $i_o(t)$ occurs at $t = t_{on}$ so that

$$I_{max_d} = \frac{V_d - E}{R}\left(1 - e^{-t_{on}/\tau}\right) \tag{4.36}$$

Where I_{max_d} is defined as the maximum current value for discount-inuous current operation.

- With switch S off (and D_{FW} on)

When S switches off in Fig.4.11 the load voltage $v_o(t)$ falls to zero due to the conduction through diode D_{FW}. The circuit differential equation (4.28) is then modified to:

$$\frac{di_o}{dt} + \frac{R}{L} i_L = \frac{-E}{L} \tag{4.37}$$

This has the solution of Eq.(4.38) except that the maximum current is now given by Eq.(4.36) to result in

$$i_o(t) = \frac{-E}{R}\left(1 - e^{-(t-t_{on})/\tau}\right) + \frac{V_d - E}{R}\left(1 - e^{-t_{on}/\tau}\right) e^{-(t-t_{on})/\tau} \tag{4.38}$$

The current extinction angle *x*

To find the current extinction angle *x,* let the repetition periodicity $\mathrm{t_{on}} + \mathrm{t_{off}}$, Fig.4.2, be designated as 2π radians, hence

$$\mathrm{t_{on}} + \mathrm{t_{off}} = 2\pi \tag{4.39}$$

Since the independent variable is chosen as ωt at the periodic time of the over all (ON + OFF) cycle is

$$\text{Periodic time} = \frac{2\pi}{\omega} \tag{4.40}$$

The frequency of the chopper operation is the inverse of the periodic time,

$$\text{Chopping frequency} = f_c = \frac{\omega}{2\pi} \tag{4.41}$$

The ON period of the chopper t_{on} is,

$$\mathrm{t_{on}} = \gamma(\mathrm{t_{on}} + \mathrm{t_{off}}) = 2\pi\gamma \tag{4.42}$$

The ON time of the switch in seconds is therefore

$$\text{Switch ON – time} = 2\pi\gamma/\omega \tag{4.43}$$

The terms t_{on}, t_{off} now serve the double purpose of identifying the conduction state of switch S in Fig.4.11 and also defining its period of conduction or extinction in radians.

Let current extinction occur at $t = t_x$ ($\omega t = x$) in Fig.4.12 (b), where *x* is

the current extinction angle which occurs at time t_x. Putting $i_o(x) = 0$ and $\omega t_x = x$ into Eq.(4.38) gives expression for x,

$$x = \omega\tau \ln\left[e^{\,t_{on}/\omega\tau}\left\{1 + \frac{V_d - E}{E}\left(1 - e^{-\,t_{on}/\omega\tau}\right)\right\}\right] \qquad (4.44)$$

Or in terms of the duty cycle γ,

$$x = \omega\tau \ln\left[e^{(\,2\pi\gamma)/\omega\tau}\left\{1 + \frac{V_d - E}{E}\left(1 - e^{-2\pi\gamma/\omega\tau}\right)\right\}\right] \qquad (4.45)$$

In terms of time in seconds, we can re-write Eq.(4.44) above as,

$$t_x = \tau \ln\left[e^{(t_{on})/\tau}\left\{1 + \frac{V_d - E}{E}\left(1 - e^{-t_{on}/\tau}\right)\right\}\right] \text{ seconds} \qquad (4.46)$$

where $t_x = \frac{x}{\omega}$ and $\frac{2\pi\gamma}{\omega} = t_{on}$

If t_{on} is decreased to the value t_{on}^x at which $I_{min} = 0$ that represent the boundary between continuous and discontinuous operation. i.e. the converter is operating at the point of changeover from continuous current operation to discontinuous current operation. Then, from Eq. (4.5),

$$\gamma' = \frac{t_{on}^x}{T} = \frac{t_{on}^x}{t_{on}^x + t_{off}} \qquad (4.47)$$

For this boundary condition, from Eq. (4.34)

$$\frac{E}{V_d} = \frac{\mathrm{e}^{t_{on}^x/\mathrm{T})(\mathrm{T}/\tau)} - 1}{\mathrm{e}^{\mathrm{T}/\tau} - 1} \qquad (4.48)$$

or $$m = \frac{\mathrm{e}^{\gamma'\sigma} - 1}{\mathrm{e}^{\sigma} - 1}$$

where $$m = \frac{E}{V_d}$$

and $$\sigma = \mathrm{T}/\tau$$

The relationship between $m = \left(\frac{E}{V_d}\right)$ and γ' is shown in Fig.4.13 with the factor $\sigma = (T/\tau)$ as parameter. If a circuit operate with a specified value of γ, then the criteria for continuous or discontinuous operation are,

$$\left.\begin{array}{l}\gamma > \gamma' \text{ , continuous current} \\ \gamma < \gamma' \text{ , discontinuous current}\end{array}\right\} \qquad (4.49)$$

where γ' is defined by Eq.(4.47).

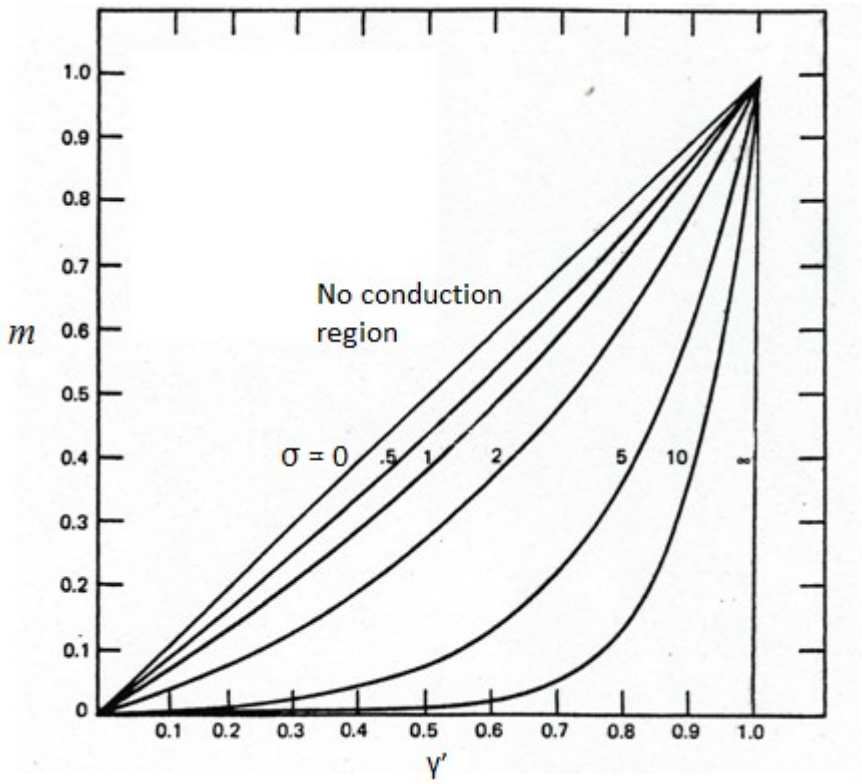

Fig.4.13 Relation between m and γ' for different values of σ.

If the circuit is passive, $E = 0$ and Eq.(4.38) can only be satisfied by $\gamma' = 0$ in other words, there is no finite value of t_{on} that will result in discontinuous operation. Although the current may become small it is finite and operation is, therefore, continuous.

4.6 HARMONIC ANALYSIS OF THE LOAD VOLTAGE WAVEFORM OF CLASS-A DC CHOPPER

As it had been considered that the repetition periodicity $t_{on} + t_{off}$, Fig.4.2, be designated as 2π radians to facilitate harmonics analysis, so that, $t_{on} + t_{off} = 2\pi$. Hence, $t_{on} = \gamma(t_{on} + t_{off}) = 2\pi\gamma$.
In many cases it had been found that the output voltage waveform $v_o(\omega t)$ is a very close approximation to one of the ideal waveforms shown in Fig.4.2 for both continuous and discontinuous current operation. When this is so, the waveform may be represented as,

$$v_o(\omega t) = V_d \Big|_{0}^{2\pi\gamma} + 0 \Big|_{2\pi\gamma}^{2\pi} \tag{4.50}$$

Since this waveform is periodic function, the time variation of v_o may be represented by Fourier series as,

$$v_o(\omega t) = \frac{a_o}{2} + \sum_{n=1}^{\infty} a_n \cos n\omega t \; + \sum_{n=1}^{\infty} b_n \sin n\omega t$$

$$= V_o + \sum_{n=1}^{\infty} C_n \sin(n\omega t + \varphi_n)$$

where, the Fourier coefficients are:

$$\frac{a_o}{2} = \frac{1}{2\pi} \int_0^{2\pi} v_o^2(\omega t) d\omega t$$

$$= \frac{1}{2\pi} \int_0^{2\pi\gamma} V_d d\omega t = \frac{V_d}{2\pi} [\omega t]_0^{2\pi\gamma}$$

$$\therefore \frac{a_o}{2} = V_o = \gamma V_d \tag{4.51}$$

This value is the average value of the output voltage waveform which represents the zero frequency components in the series or the d.c. value of v_o . The Fourier coefficients for the nth harmonic (higher order harmonics) of the load voltage waveform are given by,

$$a_n = \frac{1}{\pi} \int_0^{2\pi} v_o(\omega t) \cos n\omega t \; d\omega t$$

$$a_n = \frac{V_d}{\pi} \int_0^{2\pi\gamma} \cos n\omega t \; d\omega t = = \frac{V_d}{n\pi} \sin 2\pi n\gamma \tag{4.52}$$

$$b_n = \frac{1}{\pi} \int_0^{2\pi} V_o(\omega t) \sin n\omega t \; d\omega t$$

$$b_n = \frac{V_d}{\pi} \int_0^{2\pi\gamma} \sin n\omega t \; d\omega t \; = = \frac{V_d}{n\pi} (1 - \cos 2\pi n\gamma) \tag{4.53}$$

The peak amplitude $\hat{V}_{o_n}$ and phase-angle φ_n of nth load voltage harmonic are therefore given by,

$$\hat{V}_{o_n} = c_n = \sqrt{a_n^2 + b_n^2}$$

$$= \frac{V_d}{n\pi}\sqrt{[sin^2 2\pi n\gamma + (1 - \cos 2\pi n\gamma)^2]} \qquad (4.54(a))$$

$$= \frac{2V_d}{n\pi}\sin n\pi\gamma \qquad (4.54(b))$$

$$\varphi_n = \tan^{-1}\left(\frac{a_1}{b_1}\right) = \tan^{-1}\left(\frac{\sin 2\pi n\gamma}{1 - \cos 2\pi n\gamma}\right) \qquad (4.55(a))$$

$$= \frac{\pi}{2} - n\pi\gamma \qquad (4.55(b))$$

The fundamental component of the output voltage waveform is found for *n =1*, thus:

$$c_1 = \frac{V_d}{\pi}\sqrt{[sin^2 2\pi n\gamma + (1 - \cos 2\pi n\gamma)^2]}$$

$$= \frac{V_d}{\pi}\sqrt{[sin^2 2\pi\gamma + 1 - 2\cos 2\pi\gamma + \cos^2 2\pi\gamma]}$$

But $\frac{2\pi\gamma}{\omega} = t_{on}$, hence:

$$c_1 = \frac{\sqrt{2}V_d}{\pi}\sqrt{[1 - \cos 2\pi\gamma]}$$

$$= \frac{\sqrt{2}V_d}{\pi}\sqrt{[1 - \cos\omega t_{on}]} \qquad (4.56)$$

Example 4.2

In a class-A chopper circuit an ideal battery of terminal voltage 100 V supplies a series load of resistance 0.25 Ω, and a series inductor of 1 mH. The load consists of a series battery of 10 V. The control time *T* of the chopper is 2.5 ms and the ON time is 1 ms.

(a) Specify whether the current will be continuous or discontinuous?
(b) Calculate the average output voltage V_o, and average output current I_o.
(c) Calculate the maximum and minimum values of the output current.
(d) Sketch to scale compatible waveforms for v_o, i_o, i_D, and i_s.

(e) Calculate the fundamental component of output harmonic voltage and the first order harmonic current.

Solution

(a) To find whether the current will be continuous or discontinuous, we have to calculate the parameters $\gamma, \mathrm{m}, \sigma, \text{and } \gamma'$ first,

$$\gamma = \frac{\mathrm{t_{on}}}{\mathrm{T}} = \frac{1}{2.5} = 0.4$$

$$m = \frac{E}{V_d} = \frac{10}{100} = 0.1$$

$$\sigma = \mathrm{T}/\tau = 2.5 \times 10^{-3} \times \frac{R}{L} = 2.5 \times 10^{-3} \frac{0.25}{1 \times 10^{-3}} = 0.625$$

But

$$m = \frac{\mathrm{e}^{\gamma' \sigma} - 1}{\varepsilon^{\sigma} - 1} = 0.1 = \frac{\mathrm{e}^{0.625\,\gamma'} - 1}{e^{0.625} - 1}$$

$$\mathrm{e}^{0.625\,\gamma'} = 1.0868$$

$$0.625\,\gamma' = \ln 1.0868 \qquad \rightarrow \qquad \gamma' = 0.1332$$

$$\gamma' = 0.1332$$

Since $\gamma' < \gamma$ $\therefore$ the current is continuous.

(b) From Eq.(4.4), the average output voltage V_o is,

$$V_o = 0.4 \times 100 = 40\,V$$

$$I_o = \frac{V_o - E}{R} = \frac{40 - 10}{0.25} = 120\ \mathrm{A}$$

(c) Expressions for I_{max} and I_{min} are given in equations (4.33) and (4.34),

$$t_{on}/\tau = \frac{0.25 \times 10^{-3}}{1 \times 10^{-3}} = 0.25$$

$$I_{max} = \frac{100}{0.25}\left(\frac{1 - e^{-0.25}}{1 - e^{-0.625}}\right) - \frac{10}{0.25} = 150.4\ \mathrm{A}$$

$$I_{min} = \frac{100}{0.25}\left(\frac{e^{0.25}-1}{e^{0.625}-1}\right) - \frac{10}{0.25} = \quad 90.8 \text{ A}$$

(d) Waveforms for v_o, i_o, i_D, and i_s are shown in Fig.4.14.
(e) The fundamental component of output harmonic voltage is calculated from Eq.(4.56),

$$V_{o1} = \frac{c_1}{\sqrt{2}} = \frac{V_d}{\pi}\sqrt{[1-\cos\omega t_{on}]}$$

$$\omega = \frac{2\pi}{T} = \frac{2\pi}{2.5\times10^{-3}} = 2513 \text{ rad/s}$$

$$= \frac{100}{\pi}\sqrt{[1-\cos(2513\times10^{-3})]} = 42.18 \text{ V}$$

$$I_{o1} = \frac{V_{o1}}{Z_{o1}} = \frac{V_{o1}}{\sqrt{R^2 + (\omega L)^2}} = \frac{42.18}{\sqrt{0.25^2 + (2.513)^2}} = 16.7 \text{ A}$$

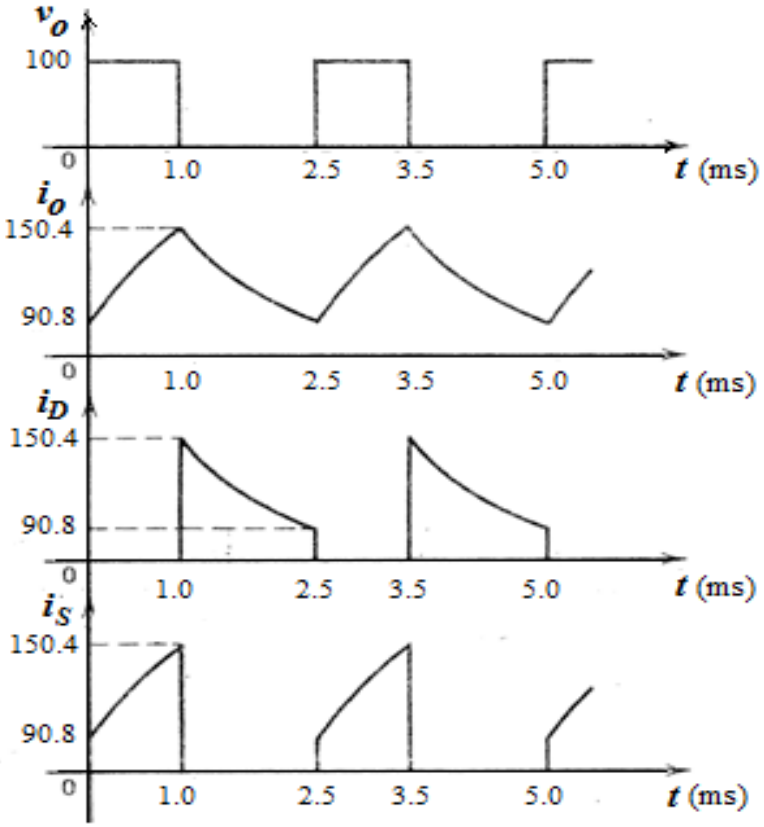

Fig.4.14 Class-A chopper waveforms.

Example 4.3

Repeat Example 4.2 when V_d = 100 V, L= 0.2 mH. R = 0.25 Ω, E = 40 V, T = 2.5 ms , t_{on} = 1.25 ms.

Solution

(a) To find whether the current is continuous or discontinuous,

$$m = \frac{E}{V_d} = \frac{40}{100} = 0.4$$

$$\sigma = \mathrm{T}/\tau = 2.5 \times 10^{-3} \times \frac{R}{L} = 2.5 \times 10^{-3} \frac{0.25}{0.2 \times 10^{-3}} = 3.125$$

$$m = \frac{\mathrm{e}^{\gamma' \sigma} - 1}{\varepsilon^{\sigma} - 1} = 0.4 = \frac{\mathrm{e}^{3.125\,\gamma'} - 1}{e^{3.125} - 1} \qquad \rightarrow \gamma' = 0.692$$

$$\gamma = \frac{\mathrm{t_{on}}}{\mathrm{T}} = \frac{1.25}{2.5} = 0.5$$

Since $\gamma' > \gamma$ $\therefore$ the current is discontinuous.

$$\tau = \frac{0.2 \times 10^{-3}}{0.25} = 0.8 \text{ x } 10^{-3} \text{ s}$$

$$\frac{\mathrm{t_{on}}}{\tau} = \frac{1.25 \times 10^{-3}}{0.8 \times 10^{-3}} = 1.56$$

From Eq.(4.46)

$$t_x = \tau \ln\left[e^{(t_{on})/\tau}\left\{1 + \frac{V_d - E}{E}\left(1 - e^{t_{on}/\tau}\right)\right\}\right]$$

$$t_x = 0.8 \times 10^{-3} \ln(\mathrm{e}^{1.56}\left\{1 + \frac{100 - 40}{40}(1 - e^{-1.56})\right\}) = 1.87 \text{ ms}$$

$$V_o = \gamma V_d + \frac{T - t_x}{T} E = 0.5 \times 100 + \frac{(2.5 - 187) \times 10^{-3}}{2.5 \times 10^{-3}} \times 40$$
$$= 60 \text{ V}$$

(b) Since the current is discontinuous, I_{min} = 0. From Eq.(4.36)

$$I_{max_d} = \frac{V_d - E}{R}\left(1 - e^{-t_{on}/\tau}\right) = \frac{100 - 40}{0.25}(1 - e^{-1.56}) = 189.5 \text{ A}$$

(c) Waveforms for v_o, i_o, i_D, and i_s are shown in Fig.4.15.

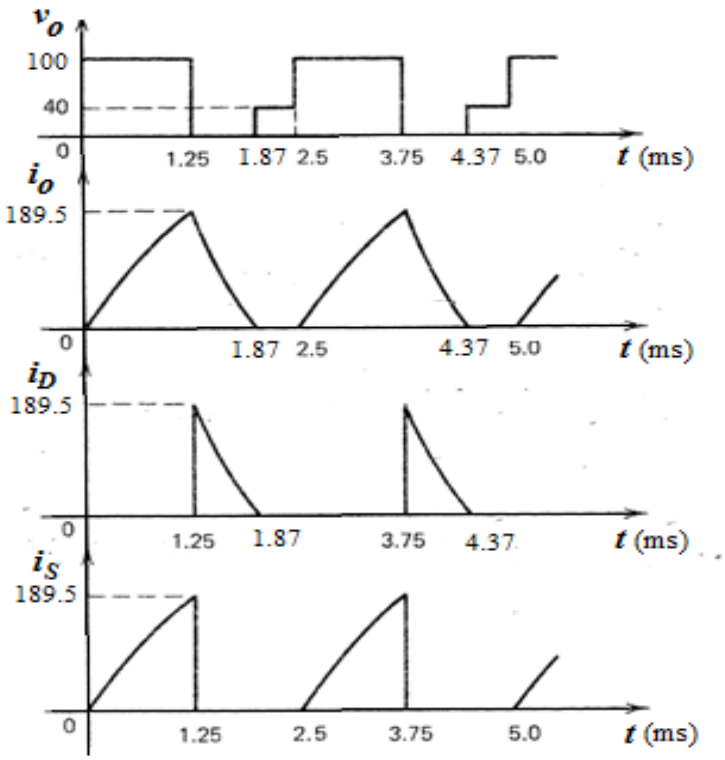

Fig.4.15 Waveforms.

4.7 ANALYSIS OF A STEP-DOWN DC CHOPPER WITH *R-L* LOAD: APPROXIMATE ANALYSIS

Consider a class-A chopper circuit with *R-L* load as shown in Fig.4.16(a). This is a step down chopper with one quadrant operation.
If we use the simplified linear analysis by considering that $T \ll \tau$, where ($T = t_{on} + t_{off}$). In this case the current is continuous as shown in Fig.4.16(b).

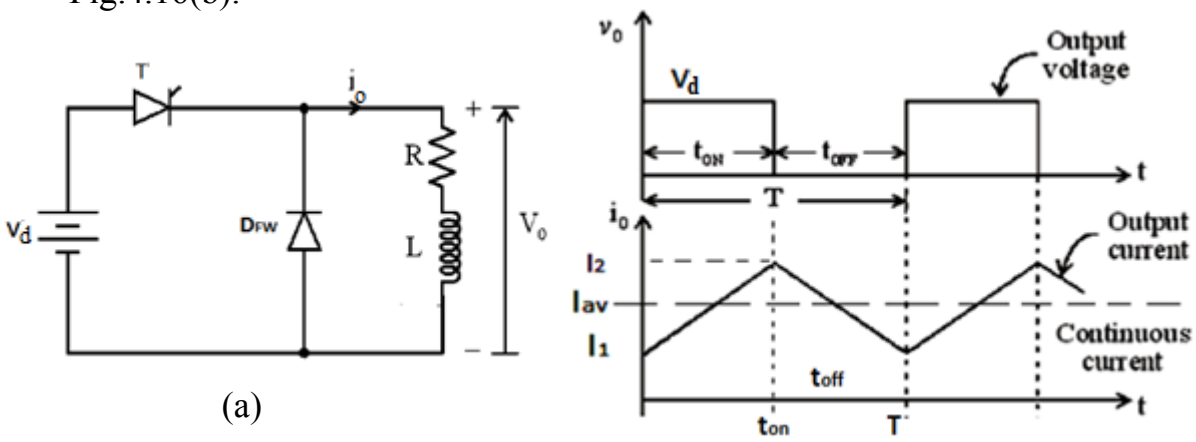

Fig.4.16 Class-A chopper circuit with *R-L* load : (a) Circuit, and (b) Voltage and current waveforms.

Referring to Fig.4.16:

- The current variation is almost linear and the current waveform becomes triangular.
- During the ON period , the equation govern the circuit is,

$$V_d = Ri + L\frac{di}{dt} \qquad (4.57a)$$

Since $\frac{di}{dt}$ = constant, hence during ON period:

$$\frac{di}{dt} = \frac{I_2 - I_1}{t_{on}} = \frac{\Delta I}{t_{on}} \qquad (4.57b)$$

Where ΔI is the peak-to-peak of the load current .Thus the equation of the current is given by:

$$i_1 = I_1 + \frac{\Delta \mathrm{I}}{\gamma T}t \qquad 0 \le t \le t_{on} \qquad (4.58)$$

where $\gamma = \frac{t_{on}}{T}$

During the off period:

$$\frac{di}{dt} = \frac{I_1 - I_2}{t_{off}} = -\frac{\Delta I}{t_{off}} = -\frac{\Delta \mathrm{I}}{T - t_{on}} = -\frac{\Delta \mathrm{I}}{T - \gamma T} = -\frac{\Delta \mathrm{I}}{(1-\gamma)T} \qquad (4.59)$$

Hence, during the off the equation of the current is

$$i_2 = I_2 - \frac{\Delta \mathrm{I}}{(1-\gamma)T}(t - t_{on}) \qquad t_{on} \le t \le T \qquad (4.60)$$

The average value of the output current is

$$I_{av} = \frac{1}{T}\left[\frac{1}{2}\, t_{on}(I_2 - I_1) + \frac{1}{2}\, t_{off}(I_2 - I_1) + I_1 T\right] \qquad (4.61)$$

$$I_{av} = \frac{1}{2}(I_2 + I_1) \qquad (4.62)$$

Example 4.4

A 140V battery supplies *R-L* load through a class-A d.c. chopper. The load has a freewheeling diode across it is composed of 0.4 H in series with 10 Ω resistor. Load current, due to improper selection of frequency of chopping, varies widely between 8 A and 9.2 A.

(a) Find the average load voltage, current and the duty cycle of the chopper.
(b) What is the operating frequency *f* ?
(c) Find the ripple current to maximum current ratio.

Solution

(a) The average load current is:

$$I_{av} = \frac{1}{2}(I_2 + I_1) = \frac{9.2 + 8}{2} = 8.6A$$

$$I_{av} = \frac{V_{av}}{R} = \frac{\gamma V_d}{R} \qquad \text{or} \qquad \gamma = \frac{I_{av}\ R}{V_d} = \frac{8.6\ \times\ 10}{140} = 0.614$$

The average load voltage is

$V_{av} = V_o = \gamma\ V_d$

$V_{av} = 0.614 \times 140 = 86$ V.

(b) To find the operating (chopping) frequency:

During the ON period,

$$V_d = Ri + L\frac{di}{dt}$$

Assuming $\frac{di}{dt} \cong constant$

$$\frac{di}{dt} \cong \frac{\Delta I}{t_{on}} = \frac{9.2 - 8}{\gamma T} = \frac{1.2}{\gamma T}$$

From Eq. (4.5a)

$$L\frac{di}{dt} \cong V_d - I_{av}\ R = 140 - 10 \times 8.6 = 54\ \text{V}$$

or $$\frac{di}{dt} = \frac{54}{L} = \frac{54}{0.4} = 135\ \text{A.s}$$

but $$\frac{di}{dt} = \frac{1.2}{\gamma T} = 135 = \frac{1.2}{0.614\ T}$$

$$\therefore T = \frac{1.2}{0.614 \times 135} = 14.47\ \text{ms}$$

hence $$f = \frac{1}{T} = \frac{1}{14.47 \times 10^{-3}} = 69\ \text{Hz}$$

The maximum current I_m occurs at $\gamma = 1$,

$$\therefore\ I_m = \frac{\gamma V_d}{R} = \frac{1 \times 140}{10} = 14\ \text{A}$$

Ripple current I_r = ΔI = 9.2 - 8 =1.2 A

$$\therefore \frac{I_r}{I_m} = \frac{1.2}{14} = 0.085 \quad \text{or} \quad 8.5\% .$$

Input Current I_s

For the class-A chopper shown in Fig.4.16(a), the ON-state and OFF-state equivalent circuits are as depicted in Fig.4.17. When the thyristor is closed (during the ON period), the load current "*i*" rises from I_1 to I_2 and falls from I_2 to I_1 during the off period as shown in Fig.4.18(a).The input current i_s flows during the ON period only is as shown in Fig .4.18 (b).

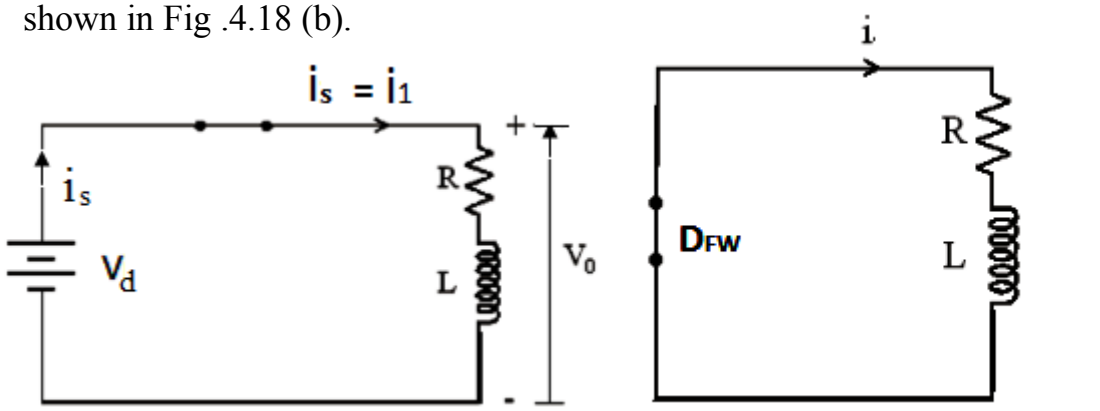

(a) ON-State equivalent circuit. (b) OFF-State equivalent circuit.

Fig.4.17 ON and OFF-states equivalent circuits.

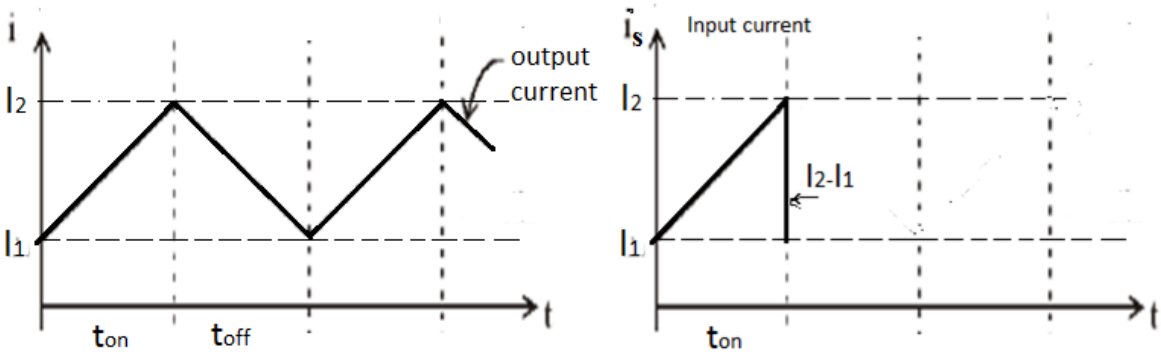

(a) (b)

Fig.4.18 Class-A d.c. chopper : (a) Load Current, (b) Input current.

The equation of the input current is

$$i_s = i_1 = I_1 + \frac{\Delta I}{\gamma T} t \qquad 0 \le t \le t_{on}$$

$$i_s = 0 \qquad t_{on} \le t \le T$$

The average value of the current drawn from the supply is simply found by,

$$I_{s(av)} = \frac{1}{T}\left[\frac{1}{2}\, t_{on}(I_2 - I_1)\right] + \frac{t_{on} I_1}{T}$$

$$I_{s(av)} = \frac{1}{T}\left[\frac{1}{2}\, t_{on}(I_2 + I_1)\right] = \frac{t_{on}}{2T}\,(I_2 + I_1) = \gamma I_{av} \qquad (4.63)$$

Approximate equations for the minimum and maximum load currents

To find approximate formulae for the minimum current I_1 and maximum current I_2 in a chopper circuit let us consider the equivalent circuit of the chopper during the OFF-state period t_{off} as depicted in Fig.4.17 (b).

During the OFF period, the only voltage source is the inductor voltage which its average value is given by

$$V_{L(av)} = L\frac{di}{dt} \cong -L\frac{I_1 - I_2}{t_{off}} \qquad (4.64)$$

or $$V_{L(av)}\frac{t_{off}}{L} = I_2 - I_1 \qquad (4.65)$$

But

$$I_{av} = \frac{1}{2}(I_2 + I_1)$$

$$I_1 = 2\ I_{av} - I_2 \qquad (4.66)$$

Substituting Eq.(4.66) into Eq.(4.65) yields

$$\frac{t_{off}}{L}\, V_{L(av)} = I_2 - (2\ I_{av} - I_2) = 2I_2 - 2\ I_{av}$$

For further simplification of the above equation yields

$$I_2 = I_{max} = \frac{V_o}{R} + \frac{t_{off}}{2L} V_o \qquad (4.67)$$

$$I_1 = I_{min} = \frac{V_o}{R} - \frac{t_{off}}{2L} V_o \qquad (4.68)$$

where $V_o = V_{L(av)} = V_{(av)}$ and $I_{av} = \frac{V_o}{R}$

Example 4. 5

A d.c. Buck converter operates at frequency of 2000 Hz from 200 V d.c. source supplying a 5 Ω resistive load. The inductive component of the load is 5 mH. For output average voltage of 100 V, find:

(a) The duty cycle.
(b) t_{on} .
(c) The *rms* value of the output current.
(d) The average value of the output current.
(e) I_{max} and I_{min} .
(f) The input power.
(g) The peak-to-peak ripple current.

Solution

(a) $V_{av} = V_o = \gamma V_d$

$$\gamma = \frac{V_{av}}{V_d} = \frac{200}{100} = 0.5$$

(b) T= 1/ f = 1 / 2000 = 0.5 ms

$$\gamma = \frac{t_{on}}{T} \quad \rightarrow \quad t_{on} = \gamma T = 0.5 \times 0.5 = 0.25 \text{ ms}$$

(c) $V_{orms} = \sqrt{\gamma}\, V_d = \sqrt{0.5} \times 200 = 140.14$ V

$$I_{orms} = V_{orms}/R = 140.14 / 5 = 28 \text{ A}$$

(d)

$$I_{av} = \frac{V_{av}}{R} = \frac{100}{5} = 20 \text{ A}$$

(e)

$$I_{max} = \frac{V_{av}}{R} + \frac{t_{off}}{2L} V_{av} = \frac{100}{5} + \frac{(0.5 - 0.25) \times 10^{-3}}{2 \times 5 \times 10^{-3}} \times 100$$

$$= 20 + 2.5 = 22.5 \text{ A}$$

$$I_{min} = \frac{V_{av}}{R} - \frac{t_{off}}{2L} V_{av} = \frac{100}{5} - \frac{(0.5 - 0.25) \times 10^{-3}}{2 \times 5 \times 10^{-3}} \times 100$$

$$= 20 - 2.5 = \ 17.5 \text{ A}$$

(f)

$$I_{s(av)} = \frac{\gamma}{2} (I_{min} + I_{max}) = \gamma I_{av} = 0.5 \times 20 = 10 \text{ A}$$

$$P_{in} = I_{s(av)} V_d = 10 \times 200 = 2000 \text{ W}$$

(g)

$$I_{p-p} = \Delta I = I_{max} - I_{min} = 22.5 - 17.5 = 5 \text{ A}$$

4.8 STEP-UP DC CHOPPER (BOOST CONVERTER)

The boost converter, also called fly-back converter**,** is a dc-to-dc converter that steps up the dc voltage from low value to a desired high value. In contrast to the step-down chopper, the minimum average output voltage of the step-up chopper equals the input voltage V_d . Again changing the duty cycle can change the average output voltage V_o . The boost converter basic circuit is shown in Fig. 4.19.

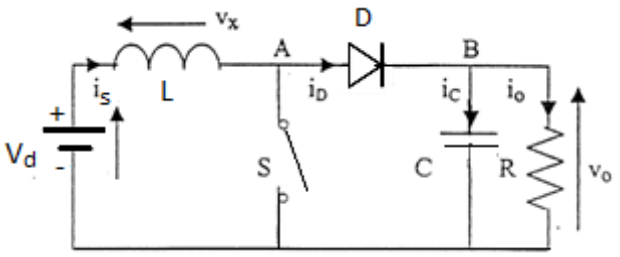

Fig.4.19 Boost converter.

The principle of operation of this chopper is the storage of energy at low supply voltage (in an inductor) and its release at higher voltage. i.e. the energy transfer, from the source to the load, takes place only during the off period of the switch. This is why it is called fly-back converter. A thyristor or a transistor is usually used to act as a switch for transferring the energy in the storage component (the inductor) to the output circuit.
Since the energy is supplied in pulses, a large capacitor at the output is required to smooth the output voltage. The essential parts of the circuit are shown, where "S" represents the main switching element.

Let us assume that the circuit has been operating for a long time and the inductor current varies between minimum value I_1 and maximum value I_2 as a function of time. We begin our analysis when the inductor current is at its minimum and the switch S is closed at t = 0, see

Fig.4.20(a), the inductor current builds up during the period $0 \leq t \leq t_{on}$ according to the differential equation,

$$V_d - L\frac{di_s}{dt} = 0 \qquad (4.69)$$

With high chopping frequency and assuming linear and small current variation, its solution is,

$$V_d = L\frac{I_2 - I_1}{t_{on}} = L\frac{\Delta I}{t_{on}} \qquad (4.70)$$

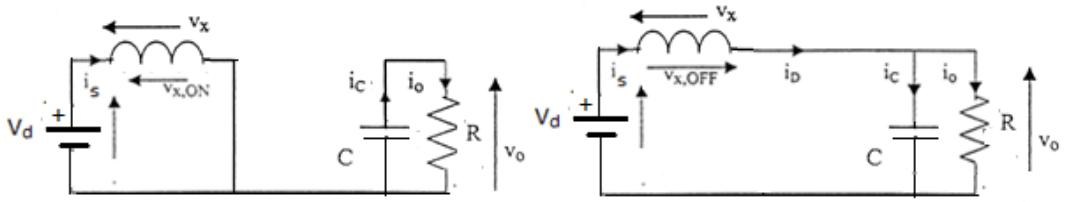

(a) (b)

Fig.4.20 Boost converter equivalent circuits : (a) ON-state equivalent circuit, (b) OFF-state equivalent circuit.

During the ON time the inductor current increases from its minimum value toward its maximum value. In other words, the stored energy in the inductor increases during the time the switch is in the closed position.

At the beginning of the OFF time, S will be open (chopper becomes OFF) and the inductor current i_s will start reducing from I_2 to I_1 , Fig.4.20 (b). Due to the reversal of current change (it is reducing now, not increasing) the inductor voltage reverses polarity. Therefore, the voltage at point "A" in Fig.4.19 will be higher than that at point "B' thus, with the beginning of the OFF period the diode D becomes forward biased and the current is directed toward the load via diode D. The inductor current, therefore, charges the capacitor and supplies the load current. The diode D blocks not only the current flow toward the source when the switch is in the closed position but also stops the output voltage from appearing across the closed switch. The inductor also helps control the percent current ripple and determines whether or not the circuit is operating in the continuous conduction mode. The capacitor C provides the filtering action by providing a path for the harmonic currents away from the load. In addition, its value is large enough so that the output voltage ripple is very small. Referring to Fig.4.20 (b) , during the OFF period :

$$V_x = L\,\frac{I_1 - I_2}{t_{off}} = -L\frac{\Delta I}{t_{off}} \tag{4.71}$$

$$V_{x,OFF} = L\frac{I_2 - I_1}{t_{off}} = L\frac{\Delta I}{t_{off}} \tag{4.72}$$

$$V_o = V_d + V_{x,OFF} = V_d + L\frac{\Delta I}{t_{off}} \tag{4.73}$$

Using

$$L\Delta I = t_{on}V_d$$

$$V_o = V_d + V_d\frac{t_{on}}{t_{off}} = \frac{T}{t_{off}}V_d$$

$$V_o = \frac{V_d}{1-\gamma} \tag{4.74}$$

where $= \frac{t_{on}}{T}$: the ON time ratio.

Therefore, V_o can be controlled by controlling the ON and OFF time of the chopper.

Equation (4.73) states that the output voltage of the boost converter is indirectly proportional to (1-γ) and directly proportional to the source voltage V_d. Since the duty cycle is usually less than unity, the output voltage is greater than the applied voltage. This is the reason why a boost converter is commonly called the *step-up converter*. When the switch, the inductor, and the capacitor are treated as ideal elements, or low-loss chopper circuit, the average power dissipated by these components is zero. Consequently, the average power supplied by the source must be approximately equal to the average power delivered to the load. That is,

$$P_{in} \cong P_{out} \tag{4.75}$$

or

$$I_S V_d \cong I_o\, V_o \tag{4.76}$$

and from Eq. (4.73)

$$I_o = \frac{V_d}{V_o} I_S = (1-\gamma) I_S \tag{4.77}$$

or the average input (source) current can be expressed in terms of the average output (load) current as :

$$I_S = \frac{I_o}{(1-\gamma)} \tag{4.78}$$

Since the source current is exactly the same as the inductor current, the average inductor current is,

$$I_{L,avg} = I_S = \frac{I_o}{(1-\gamma)} \tag{4.79}$$

It is to be noted that the average current in the inductor for the boost converter is not the same as the average load current, which was true for the buck converter. The expressions for the maximum and minimum currents through the inductor may now be written as

$$I_{L,max} = I_2 = I_{L,avg} + \frac{\Delta I_L}{2} = \frac{V_o}{R(1-\gamma)} + \frac{V_o}{2fL}(1-\gamma)\gamma \tag{4.80}$$

$$I_{L,min} = I_1 = I_{L,avg} - \frac{\Delta I_L}{2} = \frac{V_o}{R(1-\gamma)} - \frac{V_o}{2fL}(1-\gamma)\gamma \tag{4.81}$$

The inductor current variation between its maximum and minimum values is as shown in Fig.4.21, keeping in mind that it also represents the source current.

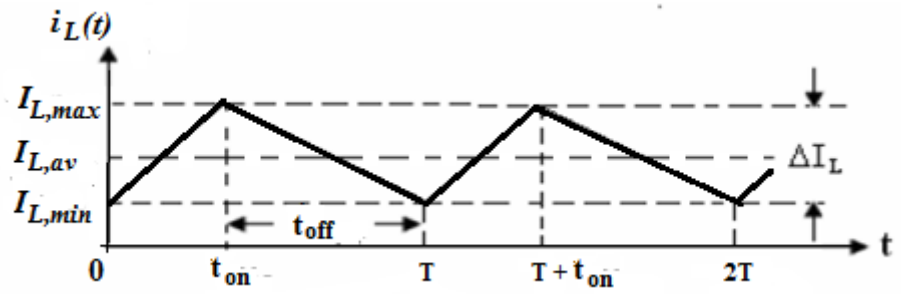

Fig.4.21 Inductor and source currents waveforms.

The peak-to-peak current ripple can be expressed in terms of the output voltage, by subtracting Eq.(4.80) from Eq.(4.79) above, as

$$\Delta I_L = \frac{V_o}{fL}(1-\gamma)\gamma \tag{4.82}$$

The current through the diode is shown in Fig.4.22. Its average value is,

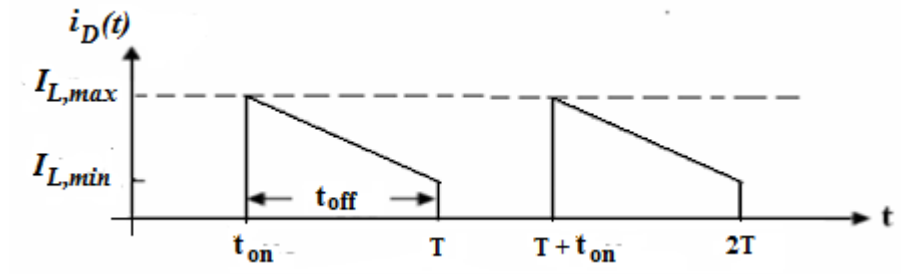

Fig.4.22 The diode current waveform.

$$I_{D,av} = \frac{I_{L,max}+I_{L,min}}{2} \times \frac{t_{off}}{T} = \frac{V_o}{R} \tag{4.83}$$

Since the average current in the diode is equal to the average current through the load resistor R, the average current in the capacitor, as expected, is zero. When the switch S is in its closed position, the capacitor supplies the load current. Hence, from $0 \leq t \leq t_{on}$, the capacitor current is

$$i_C(t) = -I_o = -\frac{V_o}{R} \tag{4.84}$$

When the switch S is opened, the inductor current supplies both the capacitor current and the load current. Thus, during the time interval $t_{on} \leq t' \leq T$, the capacitor current is

$$i_C(t) = i_L(t) - I_o \tag{4.85}$$

The maximum and minimum values of the capacitor current when the switch S is in its open position as

$$I_{C,max} = I_{L,max} - I_o = \frac{V_o\gamma}{R(1-\gamma)} + \frac{V_o}{2fL}(1-\gamma)\gamma \tag{4.86}$$

$$I_{C,min} = I_{L,min} - I_o = \frac{V_o\gamma}{R(1-\gamma)} - \frac{V_o}{2fL}(1-\gamma)\gamma \tag{4.87}$$

It is also must be noted that

$$\Delta I_L = I_{C,max} - I_{C,min} \tag{4.88}$$

The capacitor current waveform is shown in Fig. 4.23.

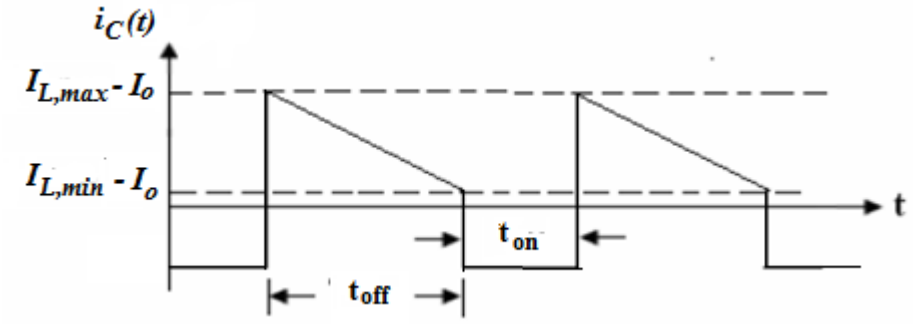

Fig.4.23 Current through capacitor C.

The input resistance at the chopper terminal (the equivalent resistance appearing across the source) is

$$R_{in} = \frac{V_d}{I_S} = \frac{(1-\gamma)V_o}{I_o/(1-\gamma)} = (1-\gamma)^2 \frac{V_o}{I_o}$$

$$R_{in} = (1-\gamma)^2 R \qquad (4.89)$$

The voltage regulation of practical chopper is very poor. A feedback regulator is therefore very essential for operation with variable load to stabilize the output voltage. This is depicted in Fig.4.24 .

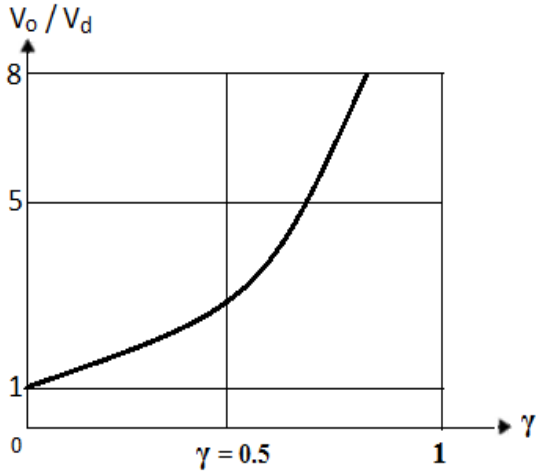

Fig.4.24 Chopper voltge regulation.

Example 4.6

A boost converter is used to convert 12 V input to supply 50 W at an output voltage of 48 V ± 0.5 %. The input current variation shall be no more than ± 1%. If the switching frequency is 10 kHz, specify the smallest inductance and capacitance to meet the given specifications.

Solution

$$V_o = 48\ V$$
$$\gamma = 1 - \frac{V_d}{V_o} = 1 - \frac{12}{48} = 0.75$$
$$T = \frac{1}{f} = \frac{1}{10\ \text{kHz}} = 100\ \mu\text{s}$$

$$t_{on} = \gamma T = 0.75 \times 100 = 75\ \mu\text{s}$$

$$t_{off} = (1-\gamma)T = (1-0.75)100\ \mu\text{s} = 25\ \mu\text{s}$$

$$P_{out} = I_o\ V_o$$

$$I_o = \frac{50}{48} = 1.04 \text{ A} \quad ,$$

Assuming the converter is operating with low – loss, i.e. $P_{in} \cong P_{out}$, hence

$$I_s = \frac{50}{12} = 4.16 \text{ A}$$

During the ON period of the chopper,

$$V_d = L\frac{di_s}{dt} = L\frac{\Delta I_s}{t_{on}}$$

The maximum allowable variation in the input current is $\pm 1\%$, the peak-to-peak variation at the input current is therefore 2% . Hence,

$$\Delta I_s = \frac{2}{100} I_s = \frac{2}{100} \times 4.16 = 0.08 \text{ A}$$

since from the relation: $V_d = L\frac{\Delta I_s}{t_{on}}$ $L > \frac{V_d t_{on}}{\Delta I_s}$

$\therefore \quad L > 11.25 \text{ mH}$

The capacitor has to supply 1.04 A for the entire ON-period (t_{on}) such that V_o will not changed more than ± 0.5 % of the rated value . Thus, the peak-to-peak variation of the output voltage is

$$\Delta V_O = \frac{1}{100} \times 48 \ = \ 0.48 \text{ V}$$

The variation in the input voltage is approximately determined from,

$$I_o = I_c = C\frac{dV_o}{dt} = C\frac{\Delta V_o}{t_{on}} \ , \quad \Delta V_o = \frac{I_o t_{on}}{C}$$

$$C > \frac{I_o t_{on}}{\Delta V_o} \ , \qquad \text{or} \qquad C > \frac{1.04 \times 75 \times 10^{-6}}{0.48}$$

$\therefore \quad C > 162.5 \ \mu\text{F}$

The required capacitor is 160 μF

4.9 OTHER CLASSES OF CHOPPERS

In the previous sections, we discuss the basic principle of class-A chopper (one-quadrant) operation in its two types, the step down chopper, also called Buck converter and the step up chopper which is called Boost converter. However, there are other types of choppers that are classified depending upon the directions of current flow and voltage. These choppers are:

1- Class-B chopper
2- Class-C chopper
3- Class-D chopper
4- Class-E chopper

4.9.1 Class-B Chopper Circuit (Two-Quadrant Operation)

If the supply voltage V_d is not reversible, reversal of load current can be realized in the circuit of Fig.4.25(a). In this circuit, converter is capable of regeneration. When the thyristor T_1 switched on the supply voltage is

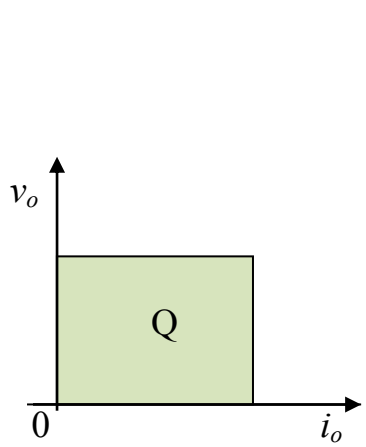

+ Current i_o : T_1 and D_1

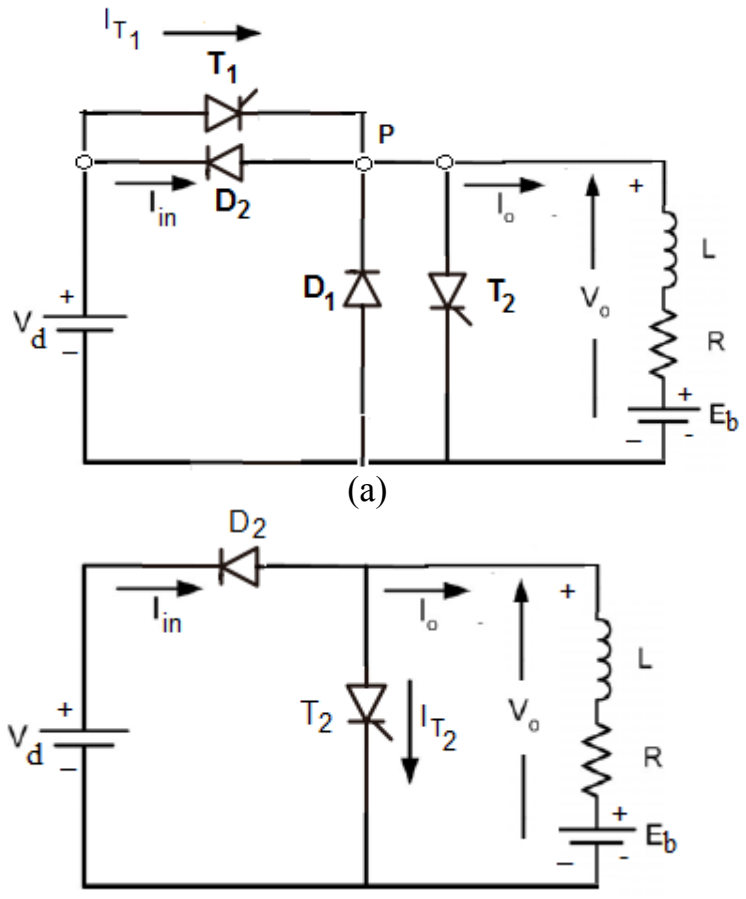

(a)

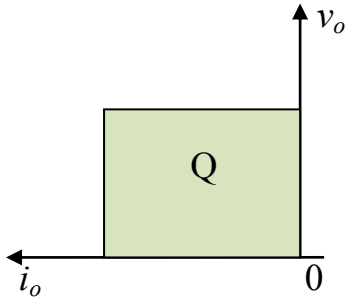

- Current i_o : T_2 and D_2

(b)

Fig.4.25 Class-B, chopper : (a) Positive current mode,(b) Negative current mode.

clamped across the passive *R-L* load and active load E_b (which is may be a motor). Hence, positive or 'motoring' current flows causing diode D_1 to be reverse biased. When T_1 is switched off the potential of point p drops from V_S to zero. The load current cannot change instantaneously and a return path is provided via diode D_1. When this current has been driven down to zero by the back *emf*, thyristor T_2 switches on to provide a path for negative armature current. Thyristor T_2 is then switched off and the instantaneous negative armature current i_o transferred through diode D_2 to the supply, and constitutes a regenerative current pulse. The opposition of supply voltage V_d reduces the negative current to zero and thyristor T_1 is switched on to restart the cycle of events.

The circuit of Fig.4.25 therefore operates in the two positive voltage quadrant of the load voltage / load current plane. Hence diode D_2 allows the current flow only from load to source and the back *emf* E_b is responsible for negative current flow.

4.9.2 Class-C Chopper

In some texts the circuit of class-B chopper shown in Fig.4.25(b) (only operation in Q2) is called class-B chopper, while the circuit shown in Fig.4.25(a) is called class-C chopper when class-B chopper operates in two-quadrant Q1 and Q2, i.e. as rectifier and as inverter. Fig.4.26 shows the quadrant of operation of this type of chopper.

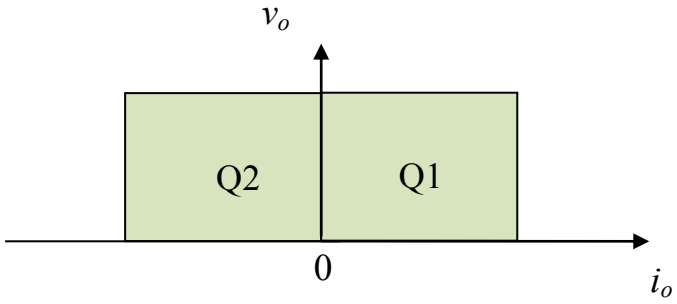

Fig.4.26 Two-quadrant operation of class-C chopper.

4.9.3 Class-D Chopper

The schematic circuit diagram of the chopper is shown in Fig.4.27(a). This type of chopper also operates in two quadrants as shown in Fig.4.27(b). The output i_o is always positive ,whereas the load voltage v_o may be either positive or negative. Rectifying process occurs when v_o and i_o are both being positive, however, when the voltage is reversed inverting process takes place and the energy fed from load to the source. The operation of class-D chopper can be summarized as follows:

- When T_1 and T_2 conduct simultaneously, the chopper operates in the 1st quadrant. In this case v_o and i_o both are positive. The converter is rectifying and the inductor *L* stored energy.

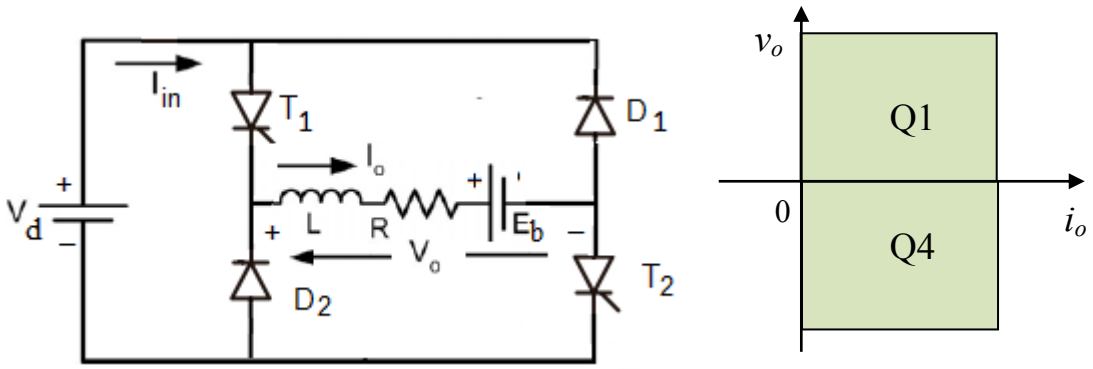

(a) (b)

Fig.4.27 Class-D chopper: (a) Circuit, (b) Quadrants of operation.

- When T_1 and T_2 are switched off , the load inductor produces sufficient voltage across it to maintain the current i_o in the same direction. The inductor voltage forward biases D_1 and D_2 causing these diodes to conduct and supply energy from load to the source.

4.9.4 Class-E Chopper (Full-Bridge DC-DC Converter)

Fig.4.28(a) shows the circuit diagram of a full bridge dc-to-dc converter which is also called a class-E chopper. This chopper operates in the four quadrants of $v_o - i_o$ diagram, i.e. the output voltage as well as the output current both can take positive or negative values as shown in Fig.4.28(b).

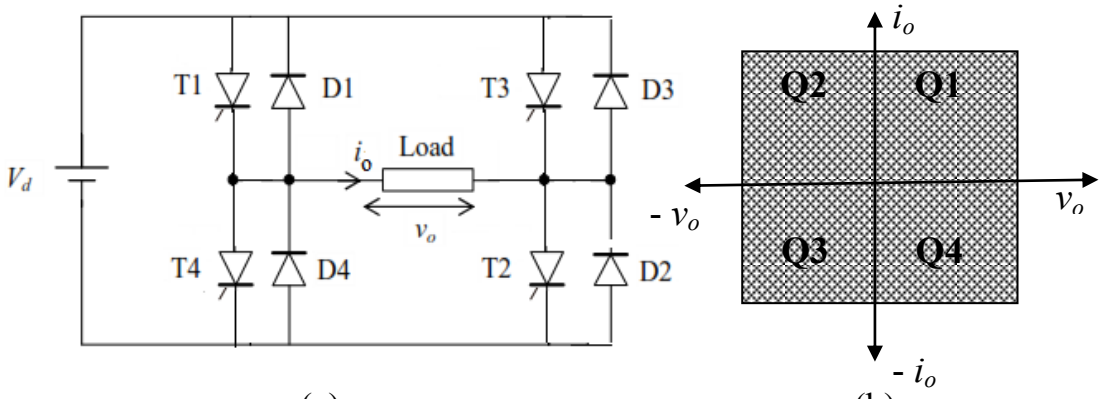

(a) (b)

Fig.4.28 Full bridge dc-to-dc converter (Class-E Chopper): (a) Circuit, (b) Four quadrants operation.

- When T_1 and T_2 conduct simultaneously, the chopper operates in the 1st quadrant. In this case v_o and i_o both are positive.
- When T_3 and T_4 conduct simultaneously, the chopper operates in the 3st quadrant. In this case v_o and i_o both are negative.

- If T_4 is turned off, the inductor of the *R-L* load will force the current to flow through D_1 and D_2 and load power is fed to the source. In this case i_o is negative and v_o is positive, inverting operation, and the chopper is operate in the 2nd quadrant.
- Similarly, if T_2 is turned off, the inductor of the *R-L* load will force the current to flow through D_3 and D_4 and load power is fed to the source. In this case i_o is positive and v_o is negative, inverting operation, and the chopper is operate in the 4nd quadrant.

Class-E chopper is, therefore, can operate in the four quadrants which is suitable for use in reversible d.c. drives to operate a d.c. motor in forward, reversing, breaking and regenerating modes. Hence the d.c. drives using class-E choppers are considered to be highly efficient and their dynamic response is also fast.

4.10 DC-DC SWITCH-MODE CONVERTERS

These types of converters are widely used in industry as regulated switch-mode power supplies. They are basically chopper circuits that may use BJT transistor, MOSFET, IGBT, thyristor or GTO for switching operation.

Power supplies in industrial applications have to meet the following specifications:

1. Isolation between the source and load.
2. High power density for reduction of size and weight.
3. Controlled direction of power flow.
4. High conversion efficiency.
5. Input and output waveforms with a low " *THD* " for small filters.
6. Controlled *PF* of the source in an a.c. voltage.

Power supplies can be categorized into two types:

1. DC power supplies.
2. AC power supplies.

In d.c. power supplies, usually two-stage converter (ac-dc) is used, however this type is known as a rectifier either controlled or uncontrolled, but the voltage output is always stepped down and often unregulated .

There is, however, another type of ac-dc converter which uses three-stage (ac-dc, dc-ac, and ac-dc) which can be accomplished by PWM or switching regulator or resonant oscillation switched mode power supplies SMPS. Typical block diagram of a three-stage switch-mode power supply is depicted in Fig.4.29.

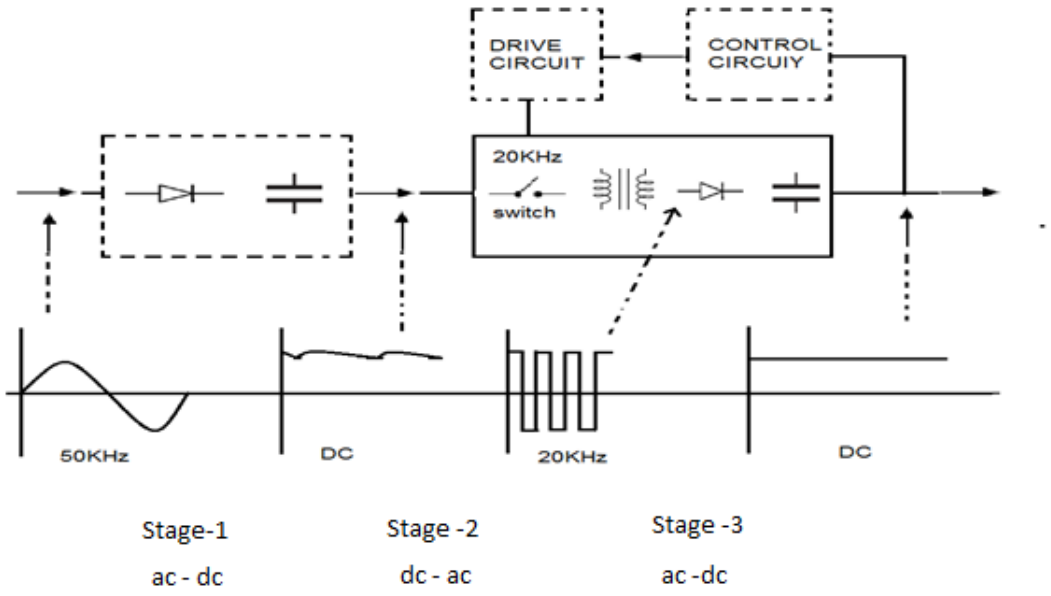

Fig.4.29 Block diagram of three-stage switch-mode power supply.

The output d.c. voltage of stage-1 in Fig.4.29 which is obtained by rectifying the main supply line voltage will be greatly affected by the fluctuation of the line voltage magnitude. However, using switch-mode dc-to-dc converters in stage-2 and stage-3 will convert the unregulated d.c. input to these sages into a d.c. output voltage at a desired level.

Depending on requirement of application switched-mode dc-to-dc converter can be one of three basic converter types:

(a) Forward (Buck).
(b) Fly back.
(c) Balanced (Buck Boost).

4.10.1 Forward or (Buck) Regulator Using MOSFET

This converter is basically like a step-down d.c. chopper with low pass *LC* filter connected across the load as shown in Fig.4.30. The load is assumed to be pure resistance and the transistor is ideal. The converter operates in two modes:

Mode 1: When the transistor *Q* is ON at $t = 0$, here the input current is flowing through *LC* and load.
Mode 2: When the transistor *Q* is OFF at $t = t_1$, *FW* diode conducts and current flow through *LC* and load.
Waveforms of the output voltage and current for the two modes of operation of the converter ar depicted in Fig.4.31.

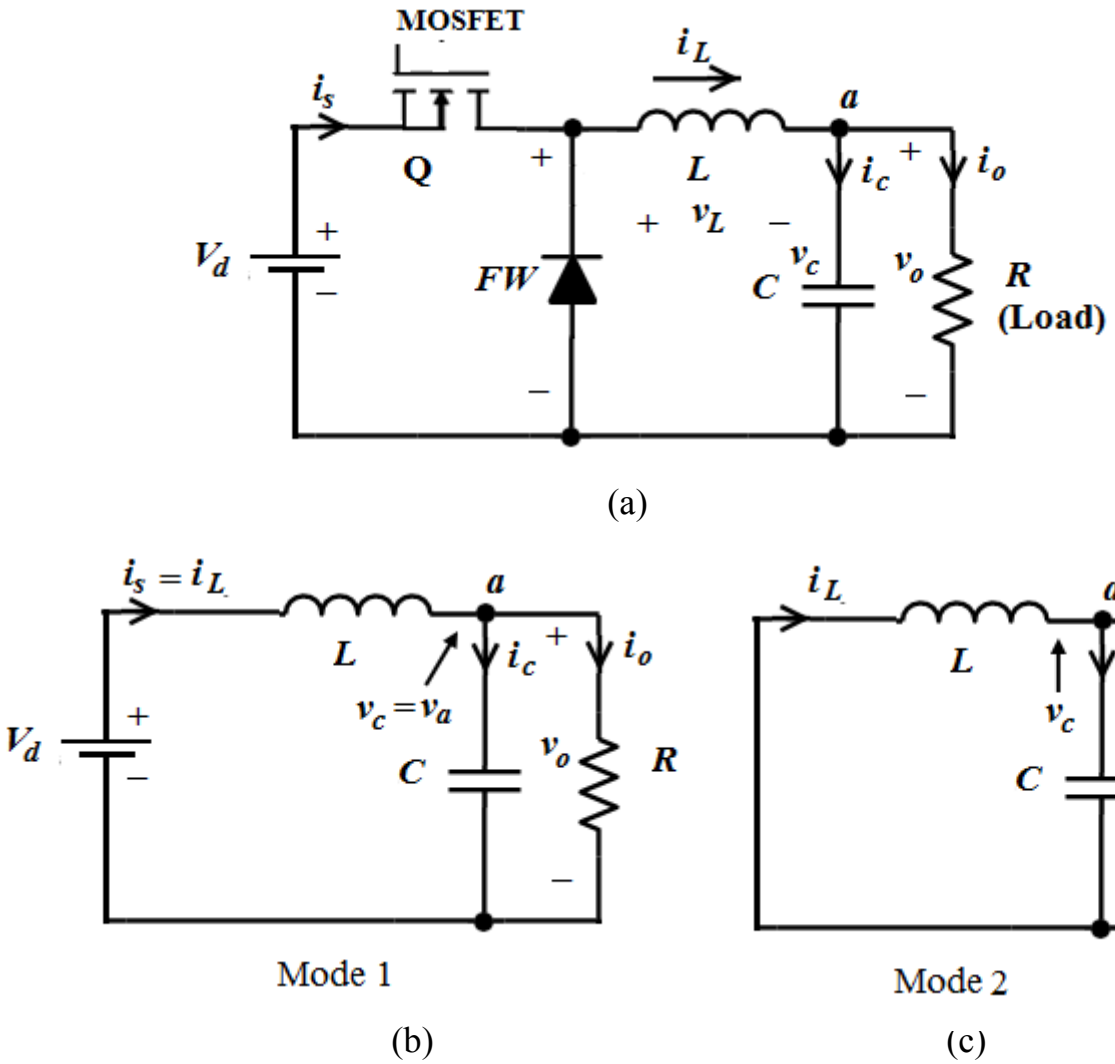

Fig. 4.30 Forward converter operation in two modes : (a) Regulator circuit, (b) Mode-1 equivalent circuit, (c) Mode-2 equivalent circuit.

Analytical properties of the forward Buck regulator

The voltage across inductor is $v_L = L \frac{di}{dt}$

Assuming that inductor current rises linearly from a minimum current I_1 to a maximum current I_2 in time t_1 , then

$$V_s - V_a = L \frac{I_1 - I_2}{t_1} = L \frac{\Delta I}{t_1}$$

and falls linearly from I_2 to I_1 in time t_2

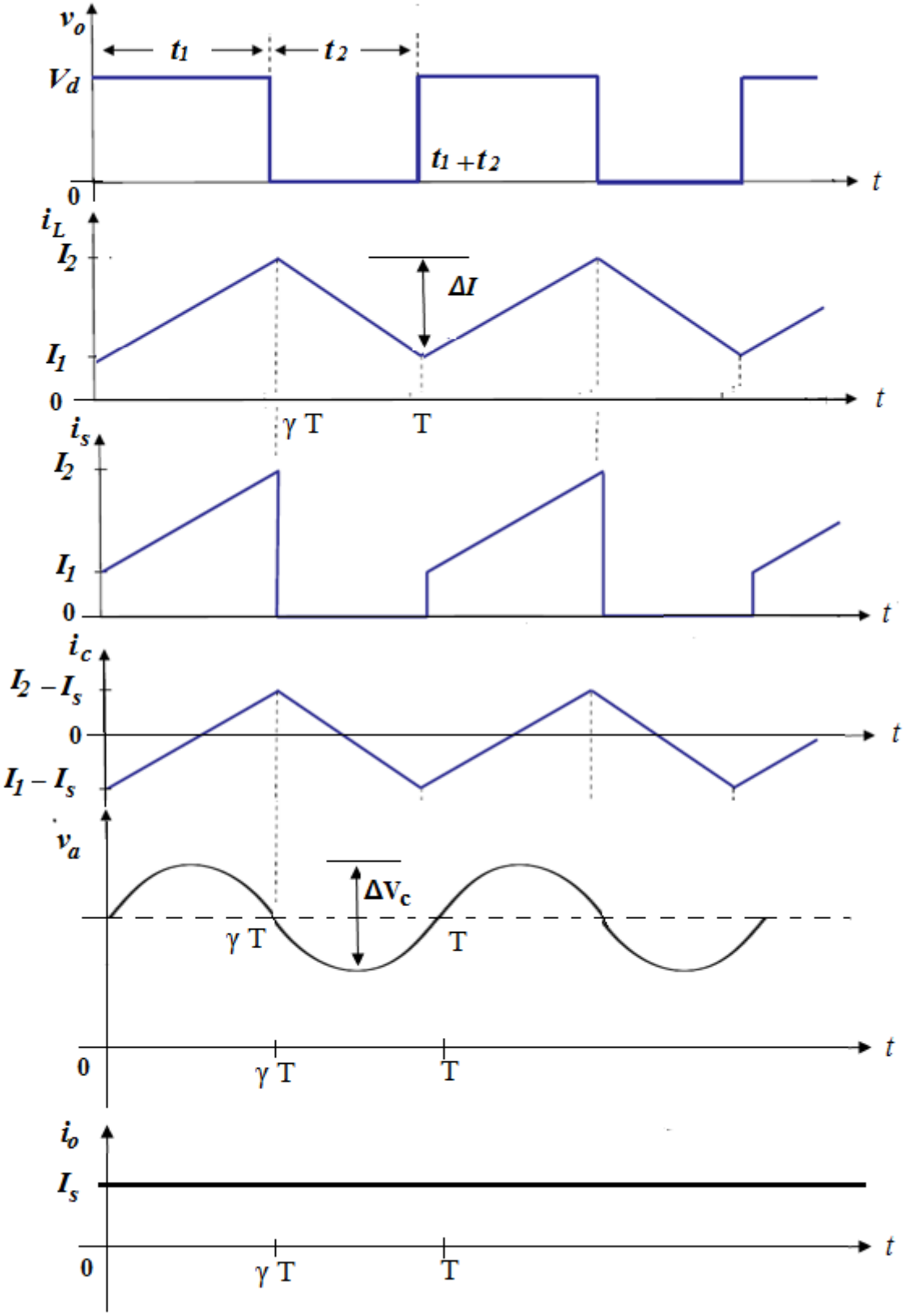

Fig. 4.31 Forward regulator waveforms.

$$-V_{\mathrm{a}} = L\,\frac{I_2 - I_1}{t_1}$$

$$\therefore\ V_{\mathrm{a}} = L\,\frac{\Delta I}{t_2}$$

$$\Delta I = \frac{(V_d - V_a)}{L}t_1 = \frac{V_a}{L}t_2$$

$$t_1 = \gamma T \qquad \text{and} \quad t_2 = (1-\gamma)T \qquad\qquad \therefore\ V_a = \gamma V_d$$

Assuming a lossless transistor switch:

$$V_d I_{\mathrm{s}} = \mathrm{V_a I_a} = \gamma \mathrm{V_d I_a}$$

Hence the average input current is $I_s = \gamma I_a$
The switching period T,

$$T = \frac{1}{f} = t_1 + t_2 = L\,\frac{\Delta I}{V_d - V_a} + L\,\frac{\Delta I}{V_a} = L\,\frac{\Delta I\, V_d}{V_a(V_d\_V_a)}$$

Which gives a peak – peak ripple current as

$$\Delta I = \frac{V_a(V_d - V_a)}{f\ L\ V_d} \ \text{ or } \ = \frac{V_d\ \gamma\ (1-\gamma)}{f\ L} \qquad (4.90)$$

Using KCL:

$$i_L = i_c + i_a$$

If we assume load ripple is very small that can be neglected , thus
$\Delta i_L = \Delta i_c$
The average capacitor current which flow for $\frac{t_1}{2} + \frac{t_2}{2} = \frac{T}{2}$ is

$$I_c = \frac{\Delta I}{4}$$

$$v_c = \frac{1}{c}\int i_c\, dt + \ v_c\,(t=0)$$

Peak-peak ripple voltage of *C* is thus:

$$\Delta V_c = v_c - v_c(t=0) = \frac{1}{c}\int_0^{T/2} \frac{\Delta I}{4} dt = \frac{\Delta I}{8fC}$$

$$\Delta V_c = \frac{V_a(V_d - V_a)}{8fLCV_d} \qquad (4.91)$$

Advantages:

1- Use one transistor.
2- High efficiency.
3- I/p current is continuous.
4- Step-up convertor without transformer.

Disadvantages:

1- High peak of current flows through the transistor.
2- Output voltages very sensitive to change.
3- Difficult to protect the transistor in case of short-circuit.
4- Average output current is less than average of inductor current.

Example 4.7

A forward buck regulator has V_d =15 V. The average output voltage required is V_a = 6 V with peak-to-peak ripple input of 10 mV, the switching frequency is 20 kHz and the peak-to-peak ripple of current of the inductor L is 0.6 A. Calculate the duty cycle and the values of L and C required.

Solution

$$V_a = \gamma V_d \qquad \rightarrow \quad \gamma = \frac{V_a}{V_d} = \frac{6}{15} = 0.4$$

$$L = \frac{V_a(V_d - V_a)}{\Delta I\, V_d}\, T = \frac{V_a(V_d - V_a)}{\Delta I\, V_d\, f} = \frac{6 \times (15-6)}{0.6 \times 15 \times 20 \times 10^3} = 300\ \mu H$$

$$C = \frac{\Delta I}{8\, \Delta V_c\, f} = \frac{0.6}{8 \times 10 \times 10^{-3} \times 20 \times 10^3} = 375\ \mu F$$

4.10.2 Fly Back Regulator (Boost Regulator)

The principle of operation of the fly back converter is that the energy is stored in an inductor and then transfers it to the load storage capacitor such that the output voltage is in excess of the input voltage. There are two types of fly back convertors:

(1) Step-up voltage called boost regulator.
(2) Step-up/step-down voltage fly back regulator called Buck-boost.

Boost regulator (step-up chopper)

The boost regulator provides output voltage which is higher than the input voltage. Hence it works like step-up d.c. voltage transformer. Fig.4.32 shows a typical circuit diagram of the boost regulator using MOSFET as a switching device. Waveforms of the output voltage and current for the operation of the converter are depicted in Fig.4.33.

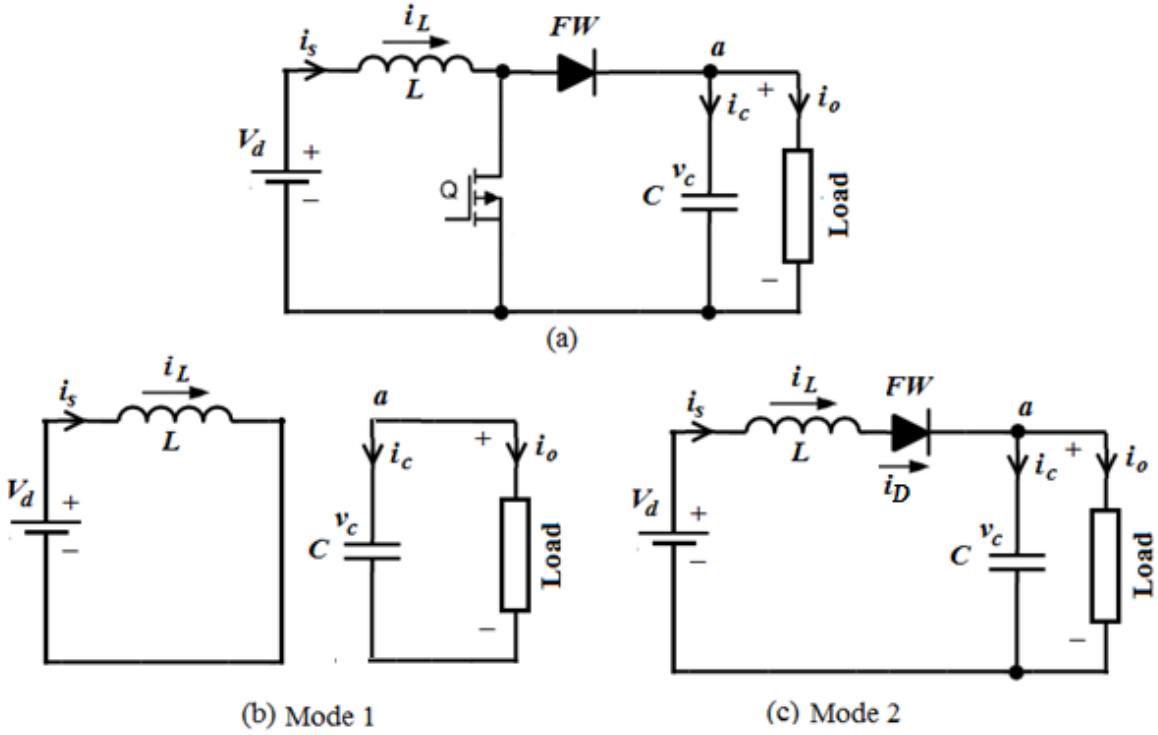

Fig. 4.32 Boost converter operation in two modes : (a) Converter circuit, (b) Mode-1 equivalent circuit, (c) Mode-2 equivalent circuit.

The operation of the regulator can be illustrated as follows:

Mode 1: At t = 0 transistor Q is ON, input current flows through the inductor L and transistor Q. The diode FW is reversed biased, thus isolating the output stage. The inductor L stores energy from the supply.
Mode 2: At t = t_1 transistor Q is OFF, current flows through L,C, load and the freewheeling diode FW. Both the input V_d and inductor L supply energy to the load.

Assuming the inductor current floes continuously and rises linearly from I_1 to I_2 in time t_1 , then

$$V_d = L\,\frac{\Delta I}{t_1} \qquad (4.92)$$

Inductor current falls linearly from I_2 to I_1 in t_2 .

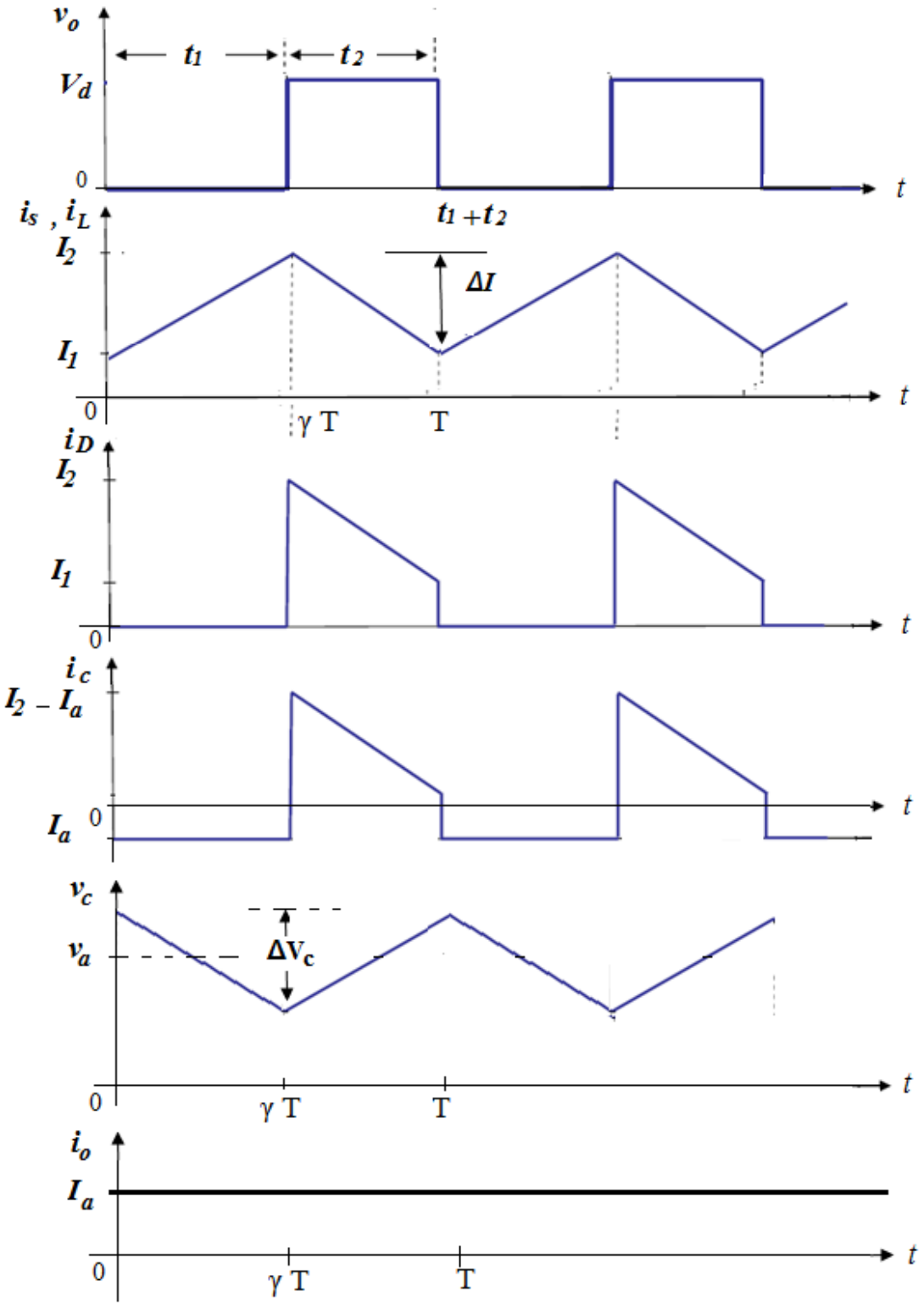

Fig. 4.33 Boost regulator waveforms.

$$V_a - V_d = L\,\frac{\Delta I}{t_2} \quad \text{or} \quad t_2 = \frac{\Delta I\, L}{(V_a - V_d)}.$$

$$\Delta I = \frac{V_d\, t_1}{L} = \frac{(V_a - V_d\,)t_2}{L}$$

$$t_1 = \gamma T \tag{4.93}$$

and $t_2 = (1-\gamma)T$ (4.94)

$$V_d\,\gamma T = (V_a - V_d)(1-\gamma)T$$

Dividing both sides by T and rearranging terms yields,

$$\frac{\mathrm{V_a}}{\mathrm{V_d}} = \frac{1}{(1-\gamma)} \quad \rightarrow \quad \frac{\mathrm{V_o}}{\mathrm{V_d}} = \frac{1}{(1-\gamma)} \tag{4.95}$$

so that $V_o > V_d$ for this converter. Theoretically, at least, $Vo \rightarrow \infty$ when $\gamma = 1$.
Assuming a lossless transistor switch:

$$V_d I_\mathrm{s} = V_a I_a = \frac{\gamma \mathrm{V_d I_a}}{(1-\gamma)}$$

Two useful equations can be obtained from the above equation

$$\frac{V_a}{V_d} = \frac{\gamma}{(1-\gamma)} \quad \rightarrow \quad \frac{\mathrm{V_o}}{\mathrm{V_d}} = \frac{\gamma}{(1-\gamma)} \tag{4.96}$$

Hence the average input current is

$$I_s = \frac{1}{1-\gamma} I_a \quad \rightarrow \frac{\mathrm{I_a}}{I_s} = 1-\gamma \;\rightarrow \frac{\mathrm{I_o}}{I_s} = 1-\gamma \tag{4.97}$$

$$T = \frac{1}{f} = t_1 + t_2 = L\,\frac{\Delta I}{V_d} + L\,\frac{\Delta I}{V_a - V_d} = L\,\frac{\Delta I\, V_d}{V_d(V_a\_V_d)}$$

which gives a peak-to-peak inductor ripple current as

$$\Delta I = \frac{V_d(V_a - V_d)}{f\, L\, V_a} \quad \text{or} \quad \Delta I = \frac{V_d \gamma}{f\, L} \tag{4.98}$$

The peak-to-peak capacitor ripple voltage can be obtained by considering that the capacitor supplies current to the load during the period when

transistor Q is ON for $t = t_1$. Under this condition, the average capacitor current is I_a, and hence ΔV_c is

$$\Delta V_c = v_c - v_c(t=0) = \frac{1}{c}\int_0^{t_1} I_c\, dt = \frac{I_a}{C} t_1 \qquad (4.99)$$

Using Eq.(4.99) and Eq.(4.96) one can get

$$\Delta V_c = \frac{I_a(V_a - V_s)}{fCV_a} \qquad (4.100)$$

Advantages :

1- Uses one transistor .
2- High efficiency.
3- Input current is always continuous.
4- Step-up converter without using external transformer.

Disavantages

1- High peak of current flows through the transistor.
2- The output voltage is very sensitive to the change in duty cycle γ.
3- Difficult to protect the transistor in case of short circuit.
4- Average output voltage is less than average inductor current by a factor of (1-γ) and a much higher *rms* current flow through filter capacitor resulting in the use of a large capacitor and inductor (filters) than those of Buck regulator.

4.10.3 Buck-Boost Regulator

In this type of regulators , the output voltage may be less than or greater than the input voltage V_d. The output voltage is always opposite to the input voltage, hence the Buck-boost regulator is also called as inverting regulator. The ciccuit diagram of the regulator is typically shown in Fig.4.34. The *L*-*C* and *FW* diode are the filtering components whearas *Q* is the transistor switch. Waveforms of the output voltage and current for the operation of the converter are depicted in Fig.4.35.

Two modes are exist in operation of Buck-boost regulator:

Mode-1:

Here when the transistor *Q* is ON and diode *FW* is reversed biased, the input current rises through inductor *L* and transistor *Q* , hence inductor *L* stores energy from $t = 0$ to $t_1 (= \gamma T)$. The capacitor discharges and supply current to the load.The output voltage takes the form of the capacitor voltage exactly.

Mode-2:

At $t = t_1$, transistor Q is turned off .The equivalent circuit will be as shown in Fig.4.34 (c) and current through L will through L , C , FW diode and load.

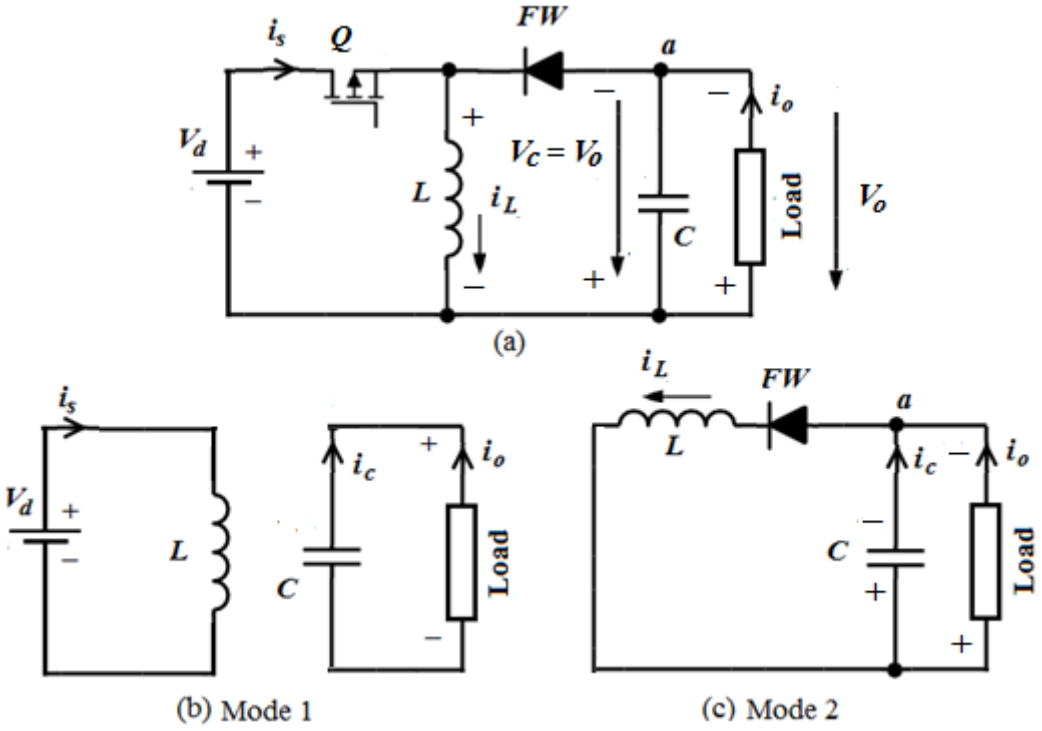

Fig. 4.34 Buck-Boost regulator operation in two modes: (a) Converter circuit, (b) Mode 1 equivalent circuit, (c) Mode 2 equivalent circuit.

The inductor generates voltage $v_L = V_d = L\ di/dt$ in the direction shown which forward biased FW diode. Thus inductor L supplies energy to the load from $t = t_1$ to $t = T$. Assuming that the load current is continuous and ripple-free, and that the inductor current rises linearly from I_1 to I_2 in time t_1, thus

$$V_d = L\,\frac{I_2 - I_1}{t_1 - 0} = L\frac{\Delta I}{t_1}$$

$$\therefore\ t_1 = \frac{L\,\Delta I}{V_d}$$

where ΔI is the peak-peak ripple current of L.

Inductor current falls linearly from I_2 to I_1 in time t_2, thus

$$V_a = L\frac{\Delta I}{t_2}$$

$$\Delta I = \frac{V_d t_1}{L} = \frac{-V_a t_2}{L}$$

$$V_o = \frac{-V_d\,\gamma}{1-\gamma} \qquad (4.101)$$

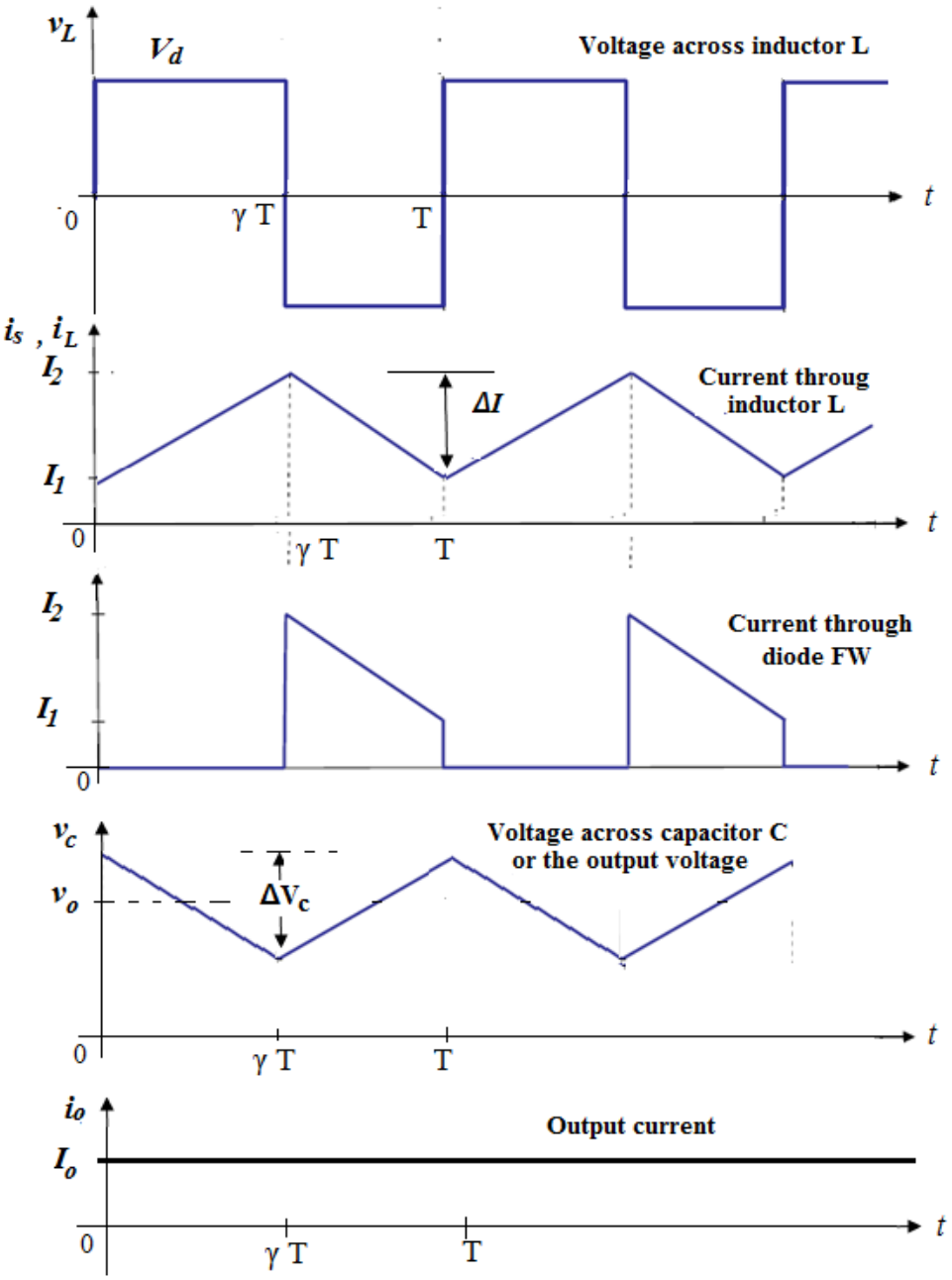

Fig. 4.35 Buck-Boost regulator waveforms.

Assuming a lossless transistor switch:

$$V_d I_s = V_o I_o$$

Hence, the average input current related to the average current by

$$I_s = \frac{I_o \gamma}{1-\gamma}\,. \tag{4.102}$$

To find the peak-to-peak inductor ripple current ,the control period *T* can be be obtained from

$$T = \frac{1}{f} = t_1 + t_2 = L\frac{\Delta I}{V_d} - L\frac{\Delta I}{V_o} = L\frac{\Delta I(V_o - V_d)}{V_d V_o} \tag{4.103}$$

From this equation , the peak-to-peak ripple current can be obtained

$$\Delta I = \frac{V_d V_o}{f.L(V_o - V_d)} \tag{4.104}$$

or $$\Delta I = \frac{V_d \gamma}{f.L} \tag{4.105}$$

The average inductor current , assuming continuous current, is therefore given by

$$I_L = \; I_s + I_o = \frac{I_o \gamma}{1-\gamma} + I_o = \frac{I_o}{1-\gamma} \tag{4.106}$$

To find the peak-to-peak capacitor ripple voltage consider the circuit when transistor *Q* is ON. At this condition, the capacitor *C* supply current to the load for the period from $t = 0$ to $t = t_1$ in average discharging current $I_c = -I_o$. Therefore, the peak-to-peak ripple voltage of the capacitor is

$$\Delta V_c = \frac{1}{c}\int_0^{t_1} I_c \; dt = \frac{1}{c}\int_0^{t_1} I_o \; dt = \frac{I_o t_1}{c}\,.$$

$$t_1 = \frac{V_o}{(V_o - V_d)f} \qquad\qquad \therefore \; \Delta V_c = \frac{I_o V_o}{(V_o - V_d)fc}$$

or $$\Delta V_c = \frac{I_o \gamma}{fc} \tag{4.107}$$

Advantages:

1- Provide reversal output voltage without using transformer.

2- High efficiency.

3- Under fault, *di/dt* of fault current would be V_d /*L* and limited by *L*.

4- Output short circuit protection would be easy implemented.

Disadvantages:

1- Output current is discontinuous.

2- High peak current flows through transistor *Q*.

PROBLEMS

4.1 A class-A transistor chopper circuit shown in Fig.4.36 supplied with power from an ideal battery of terminal voltage 150 V. The load voltage waveforms consists of rectangular pulses of duration 1 ms in an overall cycle of 3 ms.

(a) Sketch the waveforms of v_L and i_L.

(b) Calculate the duty cycle γ.

(c) Calculate the average and *rms* values of the load voltage.

(d) Find the average value of the load current if $R = 10\ \Omega$.

(e) Calculate the input power and the ripple factor *RF*.

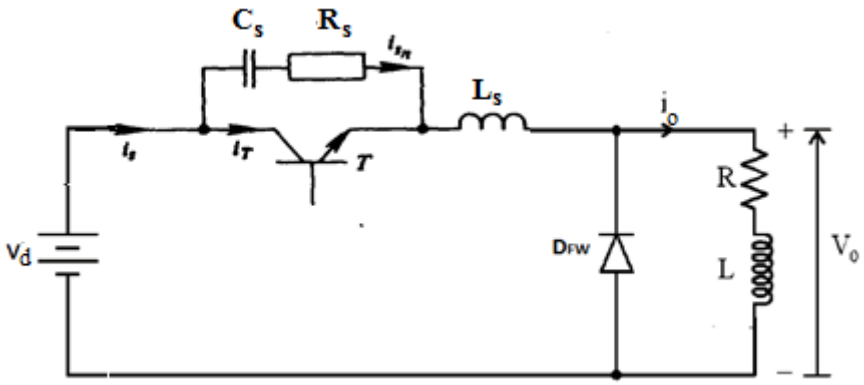

Fig.4.36

[Ans : (b) 0.333, (c) 50 V, 86.6V, (d) 2.5 A , (e) 0.833 A, 125 W, 1.414]

4.2 A class-A thyristor d.c. chopper shown in Fig.4.37 is operating at a frequency of 2 kHz from 96 V d.c. source to supply a resistive load of 8 Ω. The load time constant is 6 ms. If the mean load voltage is 57.6 V, find duty cycle (mark to space ratio), the mean load current, and the magnitude of the current ripple. Derive any formula used.

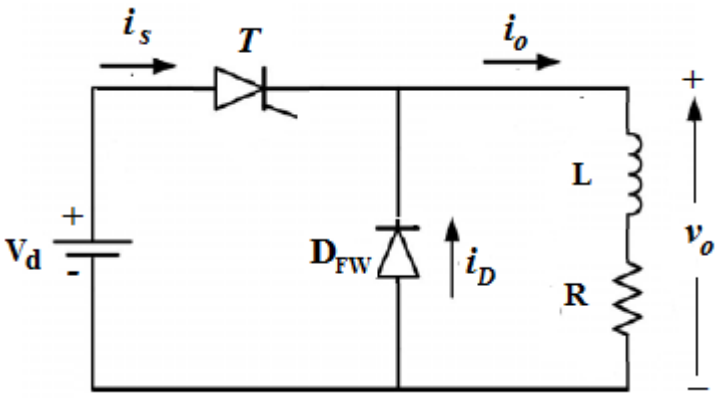

Fig.4.37

[Ans: γ = 0.6 , I_{av} = 7.2 A, ΔI = 0.24 A]

4.3 A d.c. Buck converter (class-A chopper) shown in Fig.4.37 supplies power to a load having 6 Ω resistance and 20 mH inductance. The source voltage is 100 V d.c. and the output load voltage is 60 V. If the ON time is 1.5 ms, find:

(a) Chopper switching frequency.
(b) I_{max} and I_{min} (I_2 and I_1).
(c) The average diode current.
(d) The average input current.
(e) Peak-to-peak ripple current.

[Ans: (a) f_c = 40 Hz , (b) I_{max} = 1.5 A, I_{min} = 8.5 A, (c) $I_{avD} = I_{av}$ = 10 A , (d) ΔI= 3 A]

4.4 In a class-A chopper circuit an ideal battery of terminal voltage 100V supplies a series load of resistance 0.5 Ω and inductance of 1.0 mH. The thyristor is switched on for 1 ms in an overall period of 3 ms. Calculate the average values of the load voltage and current and the power taken from the battery. Assuming continuous current conduction. Also calculates the *rms* value of the load current taking the first two harmonics of the Fourier series.

[Ans: V_{av} = 33.3 V, I_{av} = 66.7 A , P_{in}= 2223 W, I_{Lrms} = 69.1 A]

4.5 In a class-A chopper circuit an ideal battery of terminal voltage 220 V supplies a load of resistance10 Ω. The chopping frequency is f =1 kHz and the duty cycle is set to be 0.5. Determine:

(a) The average output voltage.
(b) The *rms* output voltage.
(c) The chopper efficiency.
(d) The ripple factor.
(e) The fundamental component of output harmonic voltage.

[Ans: (a) V_{av} = 110 V, (b) $V_{Lr.m.s}$ = 155.56 V, (c) $\acute{\eta}$ = 100%, (d) RF = 1.0, (e) $V_{L1\ r.m.s}$ = 99 V]

4.6 In the transistor chopper circuit shown in Fig.4.36 (problem 4.1) V_d = 300 V, L = 3 mH, R = 1.0 Ω and it operating with T = 3 ms, and t_{on} = 1.5 ms. Using the approximate solution to:

(a) Determine the minimum, maximum and average values of load current.
(b) Express the load current variation in during the of ON and OFF periods.

[Ans: (a) I_{min} = 112.5 A, I_{max}=187.5 A, I_{av} = 150 A,
(b) i_1 = 112.5+50000t , i_2 =212 – 50000t]

4.7 Repeat problem 4.6 , determine the minimum, maximum and average values of load current using exact solution and compare your results.

[Ans: I_{min} = 113.15A, I_{max} = 186.7A, I_{av} = 149.925A]

4.8 Repeat problem 4.7 assuming that E_b = 40 V.

[Ans: I_{min} =78.18 A, I_{max}= 146.7 A, I_{av} 112.44 A]

4.9 In the thyristor chopper circuit shown in Fig.4.37, V_d = 220V, L = 30 mH, R = 0.5 Ω and it operating with T = 3 ms, t_{on} = 1.5 ms and E_b =30V. State clearly any approximation you may make to simplify the solution. Find the minimum, maximum, average load current and average value of the current drawn from the 220V source. Draw the equivalent circuit appearing across the source terminals.

[Ans:157.25 A, 162.75 A, 160 A, 80 A. Equivalent circuit parameters are: 60 V source in series with 2 Ω resistance.]

4.10 A dc-dc converter is connected to a 100 V d.c. source to supply an inductive load having 40 mH in series with 5 Ω resistance. FWD is placed across the load. Load current varies between two limits of 10 A and 12 A.

(a) Find the time ratio (duty cycle) and the frequency of the chopper.

(b) Find the equivalent Thevenin resistance across the source and determine the average source current.

[Ans: (a) 0.55, 309 pps; (b) 16.53 Ω, 6.05 A]

4.11 Sketch the power circuit diagram for a class-A thyristor chopper. Show waveforms of the load voltages for the two duty cycle conditions (a) γ = 0.25, and (b) γ = 0.8. For both conditions calculate the average value, *rms* value and ripple factor of the load voltage waveform for V_d = 100 V.

[Ans : (a) 25 V, 50 V, 1.224, (b) 80 V, 89.44 V, 0.5]

4.12 A class-A d.c. chopper circuit is supplied with power from an ideal battery of 120 V. The load voltage wave form consists of rectangular pulses of duration 1ms in an overall cycle time of 2.5 ms. Calculate the *rms* values of the fundamental component and the third harmonic component of the load voltage waveform .

{Ans: 51.36 V, 12.73 V]

4.13 The output d.c. voltage V_o of a step-down (Buck) converter is maintained at 5 V by controlling the duty cycle γ. The input d.c. voltage V_d to the converter varies in the range of 10 - 40 V. The chopping frequency f_c of the converter is 20 kHz. The minimum load current, I_o , of the converter is 1A. Assuming ideal devices and componenents, calculate the minimum inductance required for operation of the converter in continuous conduction mode.

[Ans : L = 108.9 μH]

4.14 The output d.c. voltage V_o of a boost (step-up) converter is maintained at 24V by controlling the duty cycle γ. The input d.c. voltage V_d to the converter varies in the range of 8 - 16 V. The switching frequency f_c of the converter is 20 kHz. The minimum load of the converter is 5 W. Assuming ideal devices and components, calculate the minimum inductance L required for operation of the converter in continuous conduction mode.

[Ans: L = 427 μH]

CHAPTER FIVE

AC-AC CONVERSION: AC VOLTAGE CONTROLLER

5.1 INTRODUCTION

There are numerous systems in use today that convert the fixed voltage and fixed frequency a.c. supply into variable voltage or /and variable frequency supply using power semiconductor devices. The simplest forms of ac-to-ac converters are the a.c. voltage controllers that convert fixed voltage fixed frequency into variable voltage fixed frequency. These voltage controllers are also called a.c. choppers or a.c. voltage regulators. Some of the applications are motor drive systems; electric furnaces heat control, light dimmers, HVAC systems, welding and other industrial applications. This chapter discusses the single-phase and three-phase a.c. voltage controller (a.c. choppers) and their performance with resistive and resistive-inductive loads.

5.2 SINGLE-PHASE AC VOLTAGE CONTROLLER

A single-phase a.c. voltage controller is shown in Fig.5.1. In this controller two thyristors (SCRs) are connected in inverse-parallel (back-to -back) to perform the function of an electronic switch suitable for use with a.c supply. If suitable gating pulses are applied to the thyristors while their respective anode voltage is positive, current conduction is initiated. The conduction angle depends on the triggering-angle, which is measured form anode voltage zero.

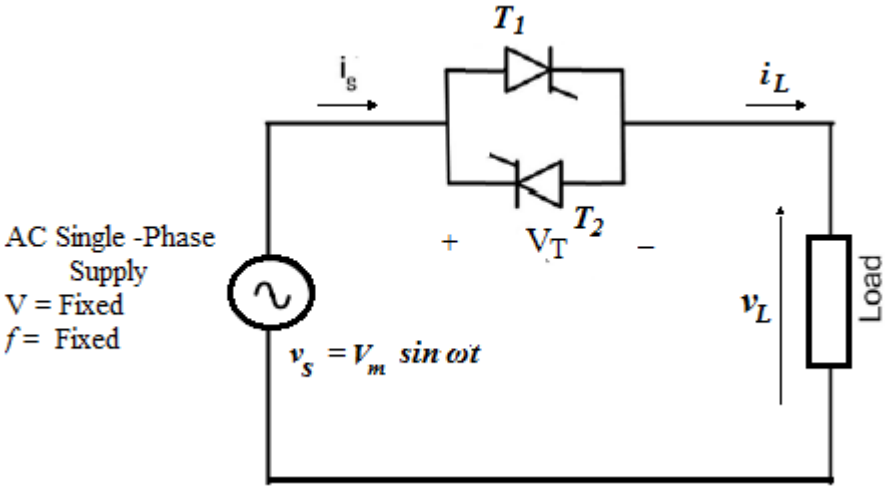

Fig.5.1 Basic circuit arrangement of single-phase inverse-parallel connected thyristor pair.

Two different modes of switching operation are mainly used:

(a) If each switch triggered at some non-zero point on its respective anode voltage cycle, the voltage waveform is described as phase-angle control.
(b) If triggering is used to permit complete cycles of load current followed by complete cycles of extinction, the load voltage and current waveform is variously described as burst firing, zero voltage switching, cycle selection, on-off control or integral-cycle switching.

Also in phase-angle control mode of operation, two different modes may be obtained:

(c) If $\alpha_1 = \alpha_2 = \alpha$, i.e. the two thyristors are triggered at same angle value, then the triggering mode is called *symmetrical* angle triggering.
(d) If triggering is used with two different values of angles $\alpha_1 \neq \alpha_2$, then the triggering mode is called *asymmetrical* angle triggering.

5.2.1 AC Voltage Controller Working with Resistive Load and Symmetrical Phase-Angel Triggering

With resistive load single gating pulse of magnitude 1-3 V is usually sufficient to switch on an SCR. Waveforms for sinusoidal supply voltage with an arbitrary triggering angle $\alpha = 60°$ is given in Fig.5.2. The gate current pulse i_g in both the thyristors shoud be positve, since the thyristor does not work with negative gate current at all.

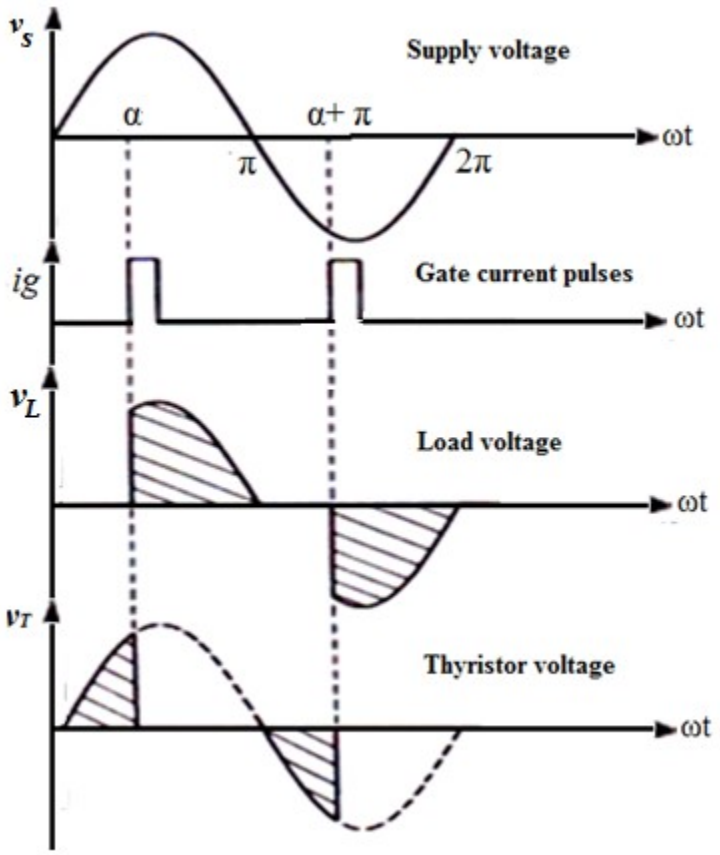

Fig.5.2 Theoretical voltage waveforms for the circuit of Fig.5.1, for *R*-load and α = 60°.

Analytical properties of the output voltage waveform

The voltage waveforms are defined in terms of the maximum value of the supply phase voltage V_m by

- The supply voltage v_s

$$v_s(\omega t) = V_m sin\omega t \tag{5.1}$$

- The load voltage v_L

$$\left.\begin{array}{l} v_L = V_m sin\omega t \begin{cases} \pi\ ,\ 2\pi, \ldots \\ \alpha,\ \pi + \alpha, \ldots \end{cases} \\ v_L = 0 \qquad \text{elsewhere} \end{array}\right\} \tag{5.2}$$

- The thyristor voltage v_T

$$v_T = V_m sin\omega t \begin{cases} \alpha\ , \pi + \alpha, \ldots \\ 0\ , \quad \pi, \ldots \end{cases} \tag{5.3}$$

5.2.2 The *rms* Values of the Load Voltage and Current

Any function $v_L(\omega t)$ that is periodic in 2π radians has a root mean square (*rms*) or effective value defined by:

$$V_L = \sqrt{\frac{1}{2\pi}\int_0^{2\pi} v_L^2(\omega t)d\omega t} \tag{5.4}$$

The function $v_L(\omega t)$ is defined by Eq.(5.2) for the circuit of Fig.5.1. Substituting Eq.(5.2) into Eq.(5.4) gives:

$$V_L = \sqrt{\frac{1}{2\pi}\int_\alpha^\pi (V_m sin\omega t)^2\, d\omega t + \frac{1}{2\pi}\int_{\alpha+\pi}^{2\pi} (V_m sin\omega t)^2\, d\omega t}$$

But $$\frac{1}{2\pi}\int_\alpha^\pi (V_m sin\omega t)^2\, d\omega t = \frac{1}{2\pi}\int_{\alpha+\pi}^{2\pi} (V_m sin\omega t)^2\, d\omega t$$

Hence , it can be written as

$$V_L = \sqrt{\frac{1}{\pi}\int_\alpha^\pi (V_m sin\omega t)^2\, d\omega t} = \sqrt{\frac{V_m^2}{\pi}\int_\alpha^\pi \frac{1}{2}(1 - cos2\omega t)\, d\omega t}$$

$$V_L = \frac{V_m}{\sqrt{2}}\sqrt{\frac{1}{\pi}\{(\pi - \alpha) + \frac{sin2\alpha}{2}\}} \tag{5.5}$$

The *rms* vale of the sinusoidal supply voltage is given by the standard relationship :

$$V_s = \frac{V_m}{\sqrt{2}}$$

The *rms* load voltage V_L given in Eq.(5.5) can, therefore , be re-written as

$$V_L = V_s\sqrt{\frac{1}{\pi}\{(\pi - \alpha) + \frac{sin2\alpha}{2}\}} \tag{5.6}$$

With resistive load the instantaneous current is given by:

$$i_L = \frac{v_L}{R} = \frac{V_m}{R} sin\omega t \begin{cases} \pi\ ,\ 2\pi, \ldots \\ \alpha\ , \pi + \alpha, \ldots \end{cases} \tag{5.7}$$

The *rms* load current I_L can therefore by written directly from:

$$I_L = \frac{V_m}{\sqrt{2}R}\sqrt{\frac{1}{\pi}\{(\pi-\alpha)+\frac{sin2\alpha}{2}\}} \tag{5.8}$$

In terms of the *rms* supply voltage V_s the *rms* current is given by:

$$I_L = \frac{V_s}{R}\sqrt{\frac{1}{\pi}\{(\pi-\alpha)+\frac{sin2\alpha}{2}\}} \tag{5.9}$$

Power and power factor

The average power delivered to the load:

For resistive load, the average load power P_L is

$$P_L = I^2R \qquad or \qquad P_L = \frac{V^2}{R} \tag{5.10}$$

$$P_L = \frac{V_s^2}{R}\left[\frac{1}{\pi}\{(\pi-\alpha)+\frac{sin2\alpha}{2}\}\right] \tag{5.11}$$

The apparent power taken from the supply

$$P_s = V_s \,.\, I_L$$

$$P_s = \frac{V_s^2}{R}\sqrt{\frac{1}{\pi}\{(\pi-\alpha)+\frac{sin2\alpha}{2}\}} \tag{5.12}$$

Input power factor

$$PF = \frac{\text{Average power}}{\text{Apparent power}}$$

$$PF = \frac{V_L \,.\, I_L}{V_s \,.\, I_L} = \frac{V_L}{V_s} = \sqrt{\frac{1}{\pi}\{(\pi-\alpha)+\frac{sin2\alpha}{2}\}} \tag{5.13}$$

5.3 HARMONICS ANALYSIS OF THE LOAD VOLTAGE WAVEFORM OF AC VOLTAGE CONTROLLER

The load voltage v_L waveform shown in Fig.5.3 is a nonsinusoidal waveform that contains harmonic components.

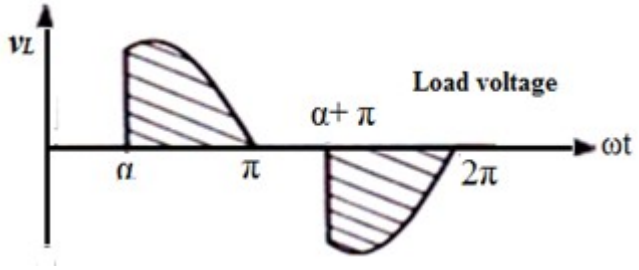

Fig.5.3 Load voltage waveform of a single-phase a.c. voltage controller with resistive load.

In terms of harmonics, this waveform can be expressed in Fourier series (see Appendix-A) as

$$v_L(\omega t) = \frac{a_o}{2} + \sum_{n=1}^{\infty} a_n \cos n\omega t \; + \sum_{n=1}^{\infty} b_n \sin n\omega t \tag{5.14}$$

$$= \frac{a_o}{2} + \sum_{n=1}^{\infty} c_n \sin(n\omega t + \psi_n) \tag{5.15}$$

where, the Fourier coefficients are,

$$\frac{a_o}{2} = \frac{1}{2\pi} \int_0^{2\pi} V_L(\omega t) d\omega t \tag{5.16}$$

$$a_n = \frac{1}{\pi} \int_0^{2\pi} v_L(\omega t) \cos n\omega t \, d\omega t \tag{5.17}$$

$$b_n = \frac{1}{\pi} \int_0^{2\pi} V_L(\omega t) \sin n\omega t \, d\omega t \tag{5.18}$$

n = the nth order harmonics (n =1,2,3,…….)

c_n = the amplitude of the nth order harmonics

$$c_n = \sqrt{a_n^2 + b_n^2} \tag{5.19}$$

ψ_n = phase angle of the n[th] harmonic component given as,

$$\psi_n = \tan^{-1}\frac{a_n}{b_n} \tag{5.20}$$

For the fundamental component (n =1):

$$a_1 = \frac{1}{\pi}\int_0^{2\pi} v_L(\omega t)\cos\omega t\, d\omega t \tag{5.21}$$

$$b_1 = \frac{1}{\pi}\int_0^{2\pi} V_L(\omega t)\sin\omega t\, d\omega t \tag{5.22}$$

The amplitude of the fundamental component is

$$c_1 = \sqrt{a_1^2 + b_1^2} \tag{5.23}$$

The phase angle of the fundamental component is given as,

$$\psi_1 = \tan^{-1}\frac{a_1}{b_1} \tag{5.24}$$

For the fundamental component of the load voltage, referring to Fig.5.5,

$$a_1 = \frac{1}{\pi}\int_0^{2\pi} V_m sin\omega t\cos\omega t\, d\omega t$$

$$= \frac{1}{\pi}\int_\alpha^{\pi} V_m sin\omega t\cos\omega t\, d\omega t + \frac{1}{\pi}\int_{\alpha+\pi}^{2\pi} V_m sin\omega t\cos\omega t\, d\omega t$$

$$= \frac{2}{\pi}\int_\alpha^{\pi}\frac{1}{2}V_m\sin 2\,\omega t\, d\omega t \quad , \text{ (since : } sin2\omega t = 2sin\omega t cos\omega t)$$

$$= \frac{1}{\pi}\int_\alpha^{\pi} V_m\sin 2\,\omega t\, d\omega t = \frac{V_m}{2\pi}\,[-(\cos 2\pi - cos2\alpha)]$$

$$\therefore\ a_1 = \frac{V_m}{2\pi}(\cos 2\alpha - 1) \tag{5.25}$$

Similarly,

$$b_1 = \frac{1}{\pi}\int_0^{2\pi} V_m sin\omega t \ \sin\omega t \ d\omega t$$

$$= \frac{1}{\pi}\int_\alpha^{\pi} V_m sin\omega t \sin\omega t \ d\omega t + \frac{1}{\pi}\int_{\alpha+\pi}^{2\pi} V_m sin\omega t \ \sin\omega t \ d\omega t$$

$$= \frac{2}{\pi}\int_\alpha^{\pi} \frac{1}{2} V_m (1 - \cos 2\omega t)\, d\omega t$$

since $(sin\omega t)^2 = \frac{1}{2}(1 - cos2\omega t)$

$$\therefore \quad b_1 = \frac{V_m}{2\pi}(2\pi - 2\alpha + \sin 2\alpha) \tag{5.26}$$

$$c_1 = \sqrt{[\frac{V_m}{2\pi}(\cos 2\alpha - 1)]^2 + [\frac{V_m}{2\pi}(2\pi - 2\alpha + \sin 2\alpha)]^2} \tag{5.27}$$

$$\psi_1 = \tan^{-1}\frac{(\cos 2\alpha - 1)}{(2\pi - 2\alpha + \sin 2\alpha)} \tag{5.28}$$

For the n[th] Fourier harmonic component, using Eq.(5.17) and Eq.(5.18), we get,

$$a_n = \frac{V_m}{2\pi}\left[\begin{array}{l} \frac{1}{n+1}\{1 + (-1)^{n+1}\}\{\cos(n+1)\,\alpha - 1\} \\ -\frac{1}{n-1}\{1 + (-1)^{n-1}\}\{\cos(n-1)\,\alpha - 1\} \end{array}\right] \tag{5.29}$$

$$b_n = \frac{V_m}{2\pi}\left[\begin{array}{l} \frac{1}{n+1}\{1 + (-1)^{n+1}\}\{\sin(n+1)\,\alpha - 1\} \\ -\frac{1}{n-1}\{1 + (-1)^{n-1}\}\{\sin(n-1)\,\alpha - 1\} \end{array}\right] \tag{5.30}$$

- For even order harmonic terms (n = 2,4,6,…….) the values of (-1)$^{n+1}$ and (-1) $^{n-1}$ are (-1), hence $a_n = 0$ and $b_n = 0$ (no even harmonics).
- For odd harmonic terms (n =3,5,7,…….) the values of (-1)$^{n+1}$ and (-1) $^{n-1}$ are unity. Hence $a_n \neq 0$ and $b_n \neq 0$.

Hence, this will modify the above equations to:

$$a_n = \frac{V_m}{2\pi}\left[\begin{matrix}\frac{2}{n+1}\{\cos(n+1)\,\alpha - 1\} \\ -\frac{2}{n-1}\{\cos(n-1)\,\alpha - 1\}\end{matrix}\right] \tag{5.31}$$

$$b_n = \frac{V_m}{2\pi}\left[\begin{matrix}\frac{2}{n+1}\{\sin(n+1)\,\alpha - 1\} \\ -\frac{2}{n-1}\{\sin(n-1)\,\alpha - 1\}\end{matrix}\right] \tag{5.32}$$

Therefore, only odd harmonics: 3^{rd} ,5^{th} ,7^{th} , 9^{th} ,11^{th} …etc are exist in the load voltage waveform of Fig.5.3. The fundamental component $v_1 = c_1 \sin\omega t$ has same frequency as that of the load voltage waveform (i.e.50Hz in our case) whereas the third order harmonics $v_3 = c_3 \sin 3\omega t$ (i.e. has frequency 3x50 =150 Hz) . The variation of these harmonics with the triggering angle α is shown in Fig.5.4. Also, Fig. 5.5 shows the time variation of the fundamental, third and fifth order harmonic components of the load voltage waveform for clarity.

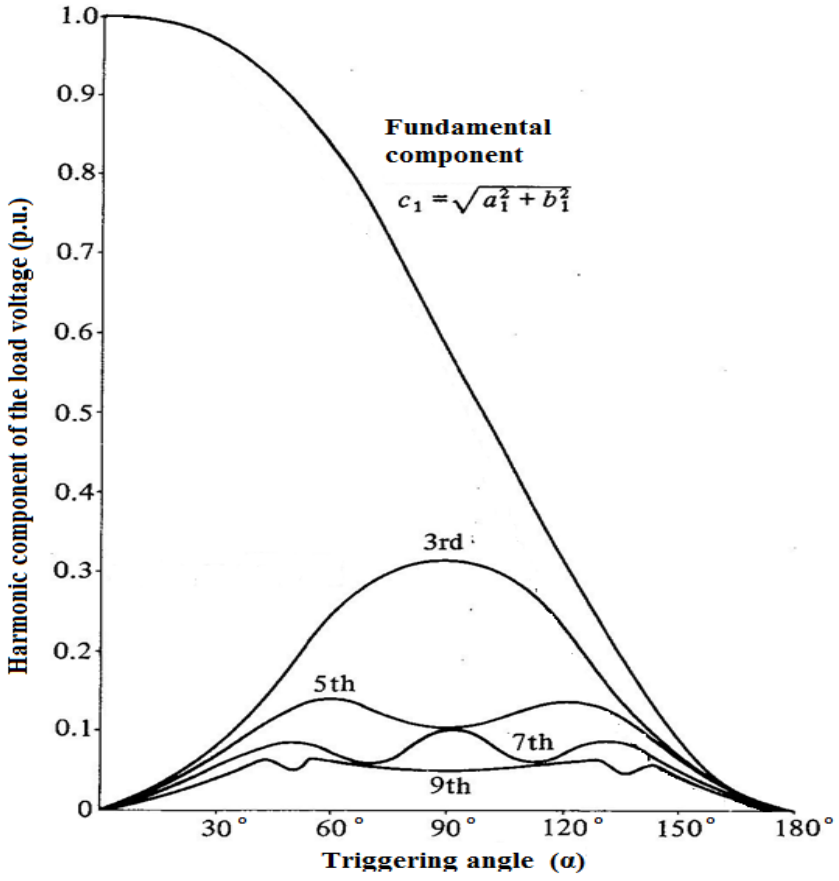

Fig.5.4 Variation of harmonic amplitudes with the triggering angle α in terms of the fundamental component.

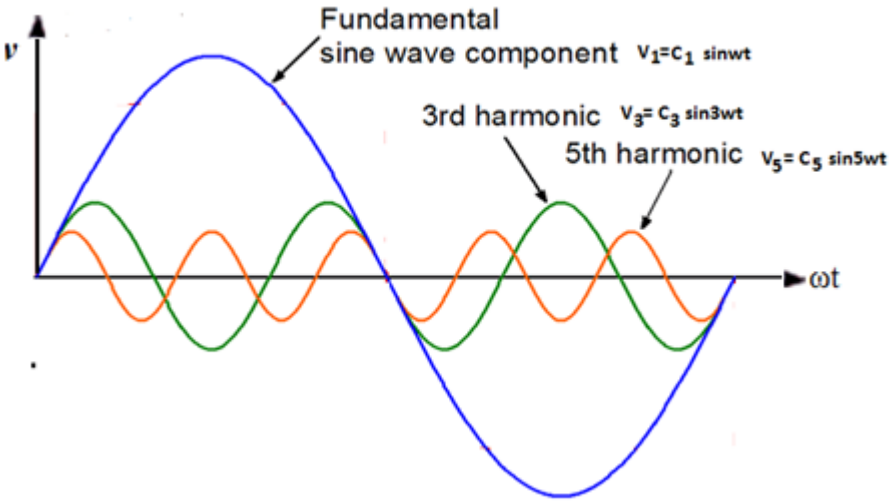

Fig.5.5 Harmonic components time variation up to fifth order of the load voltage waveform.

5.4 CALCULATION OF POWER DISSIPATION IN TERMS OF HARMONICS

In general the average value of the power is calculated as given in Eq.(5.13). However, the power calculation in terms of harmonic components is

$$P_L = R\,(I_1^2 + I_3^2 + \ \ldots\ldots\ldots) = \frac{1}{R}(V_{L1}^2 + V_{L3}^2 + (V_{L5}^2 + \ \ldots\ldots\ldots) \quad (5.33)$$

$$P_L = V_s\, I_1 \cos\psi_1 \quad (5.34)$$

Where I_1 is the *rms* value of the fundamental current,

$$I_1 = \frac{V_1}{\sqrt{2}} \times \frac{1}{R} \quad (5.35)$$

$$\cos\psi_1 = \frac{b_1}{c_1} \quad (5.36)$$

Power factor in systems with sinusoidal voltage (at supply) but non-sinusoidal current

In general, the power factor is defined as

$$PF = \frac{\text{Average power}}{\text{Apparent power}} = \frac{P_L}{V_s\, I_s}$$

where

$V_s = rms$ value of the supply voltage
$I_s = rms$ value of the supply current

$i(\omega t)$ is periodic in 2π but is non-sinusoidal.

Average power is obtained by combining in-phase voltage and current components of the same frequency.

$$P_L = V_s\, I_1 cos\psi$$

$$PF = \frac{V_s\, I_1 cos\psi}{V_s\, I_s} = \frac{I_1}{I_s} cos\psi$$

PF = Distortion factor × Displacement factor

where

$$\text{Distortion factor} = \frac{I_1}{I_s} \qquad (5.37)$$

$$\text{Displacement factor} = \cos\psi_1 \qquad (5.38)$$

- Distortion Factor = 1 for sinusoidal operation.
- Displacement factor is a measure of displacement between $v(\omega t)$ and $i(\omega t)$.
- Displacement Factor = 1 for sinusoidal resistive operation.

Example 5.1

In a single-phase resistive circuit in which the load voltage is controlled by symmetrical phase angle triggering of a pair of inverse-parallel connected thyristors as shown in Fig.5.1. The output voltage waveform is as shown in Fig.5.2. If the supply voltage is $v_s = 200 \sin\omega t$, $\alpha = 60^\circ$ and $R = 50\ \Omega$, calculate :

(a) The *rms* value of the fundamental component of the load current,
(b) The value of the displacement angle ψ_1 between the supply voltage and the fundamental component of the load current,
(c) The *rms* value of the load voltage and the power factor of the circuit.
(d) The displacement factor and the distortion factor.

Solution

(a) The peak value of the fundamental component of the load voltage is found as,

$$c_1 = \frac{V_m}{2\pi}\sqrt{(cos2\alpha - 1)^2 + [2(\pi - \alpha) + sin2\alpha]^2}$$

V_m = 200 V, α = 60˚ = π/3

$$c_1 = \frac{200}{2\pi}\sqrt{(cos2 \times 60° - 1)^2 + [2\left(\pi - \frac{\pi}{3}\right) + sin2 \times 60°]^2}$$

$$c_1 = 167.8 \text{ V}$$

The *rms* value of the fundamental component of load voltage V_{L1} is calculated as,

$$V_{L1} = \frac{c_1}{\sqrt{2}} = \frac{167.8}{\sqrt{2}} = 118.7 \text{ V}$$

The fundamental component of the load current is,

$$I_{L1} = \frac{V_{L1}}{R} = \frac{118.7}{50} = 2.37 \text{ A}$$

(b) The displacement angle ψ_1

$$\psi_1 = tan^{-1}\frac{a_1}{b_1} = tan^{-1}\frac{cos2\alpha - 1}{2(\pi - \alpha) + sin2\alpha}$$

$$\psi_1 = tan^{-1}\frac{cos2 \times 60 - 1}{2\left(\pi - \frac{\pi}{3}\right) + sin2 \times 60} = -16.5^o$$

(c) The *rms* value of the load voltage is given by ,

$$V_L = V_m\sqrt{\frac{1}{2\pi}\{(\pi - \alpha) + \frac{sin2\alpha}{2}\}}$$

$$V_L = 200\sqrt{\frac{1}{2\pi}\{\left(\pi - \frac{\pi}{3}\right) + \frac{sin120^o}{2}\}} = 126.85 \text{ V}$$

$$PF = \frac{V_L \cdot I_L}{V_s \cdot I_L} = \frac{V_L}{V_s} = \sqrt{\frac{1}{\pi}\{(\pi - \alpha) + \frac{1}{2}sin2\alpha\}}$$

$$PF = \frac{V_L \cdot I_L}{V_s \cdot I_L} = \frac{V_L}{V_s} = \frac{126.85}{200/\sqrt{2}} = 0.897$$

or $$PF = \sqrt{\frac{1}{\pi}\{\left(\pi - \frac{\pi}{3}\right) + \frac{1}{2}sin120^o\}} = 0.897$$

(d) The displacement factor :

$$cos\psi_1 = \cos(-16.5) = \cos 16.5° = 0.9588$$

The distortion factor :

$$DF = \frac{I_{L1}}{I_L} = \frac{2.37}{(\frac{126.85}{50})} = 0.934$$

PF can also be calculated from :

PF = displacement factor × distortion factor

PF = 0.9588 × 0.934 = 0.897

Eample 5.2

The a.c. controller in Example 5.1, is used to control the power supplied to a 25 Ω resistor from a single-phase, 230 V, 50 Hz supply. When the triggering angle is 30˚ the measured *rms* load current and voltage are 9 A and 216 V respectively. Determine the ideal theoretical values for the *rms* current and voltage and suggest reasons for any difference.

Solution

The theoretical value of the *rms* load voltage is obtained using Eq.(5.6),

For α = 30° or $\frac{\pi}{6}$ rad

$$V_L = V_s\sqrt{\frac{1}{\pi}\left(\pi - \alpha + \frac{1}{2}\sin 2\alpha\right)}$$

$$V_L = 230\sqrt{\frac{1}{\pi}\left[\left(\pi - \frac{\pi}{6}\right) + \frac{1}{2}\sin 120°\right]}$$

$$= 230 \times \sqrt{0.985} = 226.6 \text{ V}$$

$$I_L = \frac{V_L}{20} = \frac{226.6}{25} = 9.06 \text{ A}$$

The measured values are : $V_{Lrms} = 216$ V
$I_{Lrms} = 9.06$ A

The mulimeter or the moving coil instrument measure only the 50 Hz component which is in V_{Lrms} while the theoretical value of *rms* of the waveform include all the *rms* values of the harmonic components associated with the waveform, therefore it is 226.6 V.

Example 5.3

An a.c. voltage controller shown in Fig.5.1 is used to provide power to a single-phase *R*-load fron an ideal supply $v_s = V_m \sin\omega t$ by symmetrical phase-angle triggering of a pair of inverse-parallel connected SCRs in the supply lines. Sketch, approximately to scale, the load voltage waveform for firing-angle for $\alpha = 90°$ and also sketch the corresponding fundamental component of the load current. Derive, from first principle, an expression for the *rms* load current I_L at any arbitrary angle α, in terms of V_m , R and α. Use I_L , calculate the per-unit average power dissipated in the load at $\alpha = 90°$.

Solution

The waveforms of the load voltage and current are shown in Fig. 5.6.

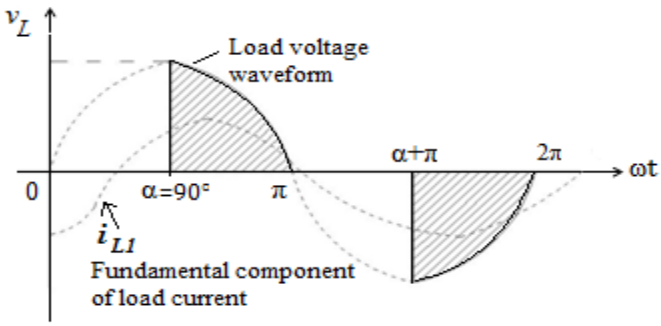

Fig.5.6 Waveforms.

From Eq.(5.5) the *rms* value of the load voltage is

$$V_L = V_m \sqrt{\frac{1}{2\pi}\left[(\pi - \alpha) + \left(\frac{sin2\alpha}{2}\right)\right]}$$

The load current is given by

$$i_L(\omega t) = \frac{V_m}{R} \sin \omega t$$

Therefore, the *rms* value of the load current is

$$I_L = \frac{V_L}{R} = \frac{V_m}{\sqrt{2}R} \sqrt{\frac{1}{\pi}\left[(\pi - \alpha) + \frac{sin2\alpha}{2}\right]}$$

$$P = I^2{}_L R = \frac{V_L^2}{R}\left[\frac{1}{\pi}\left[(\pi - \alpha) + \frac{sin2\alpha}{2}\right]\right]$$

Let $\frac{V_L^2}{R} = 1.0$ p. u.

For $\alpha = 80° = 1.3$ rad

$$P = 1.0\left[\frac{1}{\pi}\left[\left(\pi - \frac{\pi}{2}\right) + \frac{sin180°}{2}\right]\right] = 0.707 \text{ p. u.}$$

Example 5.4

A single-phase resistive heating load is to be controlled from a single-phase, 50 Hz, a.c. supply by means of an inverse parallel pair of thyristors. What will be the firing angle of the thyristors when a load has 67% of its maximum value?

Solution

From Eqs.(5.6) and (5.9), the *rms* values of the load voltage and load current are

$$V_L = \frac{V_m}{\sqrt{2}} \sqrt{\frac{1}{\pi}\left(\pi - \alpha + \frac{1}{2} sin2\alpha\right)}$$

$$I_L = \frac{V_L}{R} = \frac{V_m}{\sqrt{2}R} \sqrt{\frac{1}{\pi}\left(\pi - \alpha + \frac{1}{2} sin2\alpha\right)}$$

$$\therefore \quad P = I_L{}^2 R = \frac{V_m{}^2}{2\pi R}\left[\pi - \alpha + \frac{1}{2}sin2\alpha\right]$$

$$P_{max} = P\Big|_{\alpha=0} = \frac{V_m{}^2}{2R}$$

When $P_{load} = 0.67 \quad \rightarrow \quad P_{max} = 0.67\left(\frac{V_m{}^2}{2R}\right)$

$$0.67\frac{V_m{}^2}{2R} = \frac{V_m{}^2}{2\pi R}\left[\pi - \alpha + \frac{1}{2}\sin 2\alpha\right]$$

$$0.67 = \frac{1}{\pi}\left(\pi - \alpha + \frac{1}{2}sin2\alpha\right)$$

$$0.67\pi - \pi = -\alpha + \frac{1}{2}sin2\alpha$$

$$\therefore \quad \alpha - \frac{1}{2}sin2\alpha = 0.33\pi = 1.036$$

Solve numerically for α :

α (degree)	α (rad..)	$RHS = \alpha - \frac{1}{2}sin2\alpha$	LHS
60°	1.046	0.618	0.613
70°	1.22	0.899	0.898
80°	1.40	1.229	1.228
75°	1.308	1.058	1.058

$\therefore \alpha \simeq 75° \longrightarrow$ LHS=RHS

Example 5.5

A single-phase full-wave a.c. voltage controller consists of two thyristors connected in inverse-parallel as shown in Fig.5.7. The supply voltage is V_s =230 V(*rms*) at 50 Hz. The controller is used as a light dimmer to control the light intensity of a group of lamps with total resistance of 10 Ω. The triggering mode of the thyristors is symmetrical with α = 60°.

(a) Sketch compatible waveforms for the supply, load and thyristor voltages.

(b) Calculate the *rms* value of the load voltage.

(c) Determine the input power factor of the circuit.
(d) If one thyristor is replaced by a diode, what will be the *rms* value of the load voltage?

Fig.5.7 The circuit.

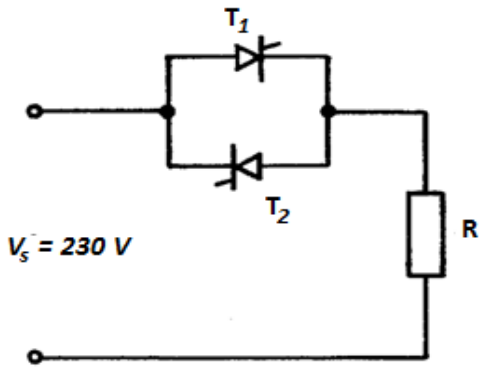

Solution

(a) The waveforms for the supply, load and thyristor voltages are shown in Fig.5.2,

(b) The *rms* value of the load voltage is given by Eq. (5.6) as,

$$V_L = V_s\sqrt{\frac{1}{\pi}\{(\pi-\alpha)+\frac{1}{2}sin2\alpha\}}$$

$$= 230\sqrt{\frac{1}{\pi}\{\left(\pi-\frac{\pi}{3}\right)+\frac{1}{2}sin2\times 60°\}}$$

Hence $V_L = 206.3$ V

(c) The input power factor of the circuit,

$$PF = \frac{V_L \cdot I_L}{V_S \cdot I_L} = \frac{V_L}{V_S} = \frac{206.3}{230} = 0.896$$

(d) If one thyristor is replaced by a diode, the circuit will be as shown in Fig.5.8(a), and the load voltage waveform will is as depicted in Fig.5.8(b). Hence, the *rms* value of the output voltage will be given by

$$V_L = \sqrt{\frac{1}{2\pi}\int_{\alpha}^{2\pi}(V_m sin\omega t)^2\, d\omega t}$$

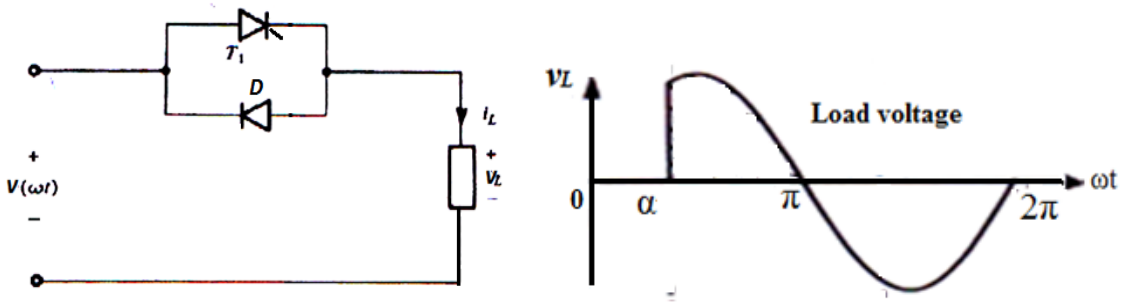

(a) (b)

Fig.5.8.

and the *rms* value of the output voltage is, therefore

$$V_L = \sqrt{\frac{V_m^2}{2\pi}\int_{\alpha}^{2\pi}\frac{1}{2}(1-cos2\omega t)\,d\omega t} = \frac{V_m}{2}\sqrt{\frac{1}{\pi}\left\{(2\pi-\alpha)+\frac{sin2\alpha}{2}\right\}}$$

$$= \frac{\sqrt{2}\times 230}{2}\sqrt{\frac{1}{\pi}\left[2\pi-\frac{\pi}{3}+\frac{sin2\times 60°}{2}\right]} = = 218.46\ \text{V}$$

Thus, the *rms* value of the output voltage is increased.

Example 5. 6

The circuit arrangement shown in Fig.5.9 is used to vary the current in resistor R_B. The triac is triggered so as to produce a periodic load voltage with identical positive and negative alternations.

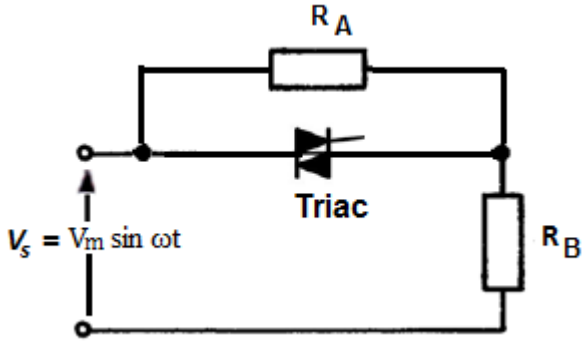

Fig.5.9 The circuit.

(a) Sketch the waveform of current in resistor R_B if the triac firing angle is α = 90°. Assume that $v = V_m \sin \omega t$.

(b) Show that the Fourier coefficients for the fundamental component of the current are given by:

$$a_1 = \frac{V_m}{2\pi} \ (\cos 2\alpha - 1) \ \frac{R_A}{R_B(R_A + R_{B)}}$$

$$b_1 = \frac{V_m}{2\pi} \ \{\sin 2\alpha + 2(\pi - \alpha)\} \frac{R_A}{R_B(R_A + R_B)} \ + \frac{V_m}{(R_A + R_B)}$$

(c) Calculate the value of the fundamental current I_{B1} in resistor R_B when $R_A = R_B = 10\ \Omega$, $V_m = 100$ V and α = π/2. also calculate the phase-angle of the fundamental current I_B with respect to the supply voltage. Does this value of phase-angle suggest a power factor other than unity? If so, what happens to the fundamental reactive power?

Solution

(a) Current through resistance R_B , i_B is shown in Fig.5.10 .

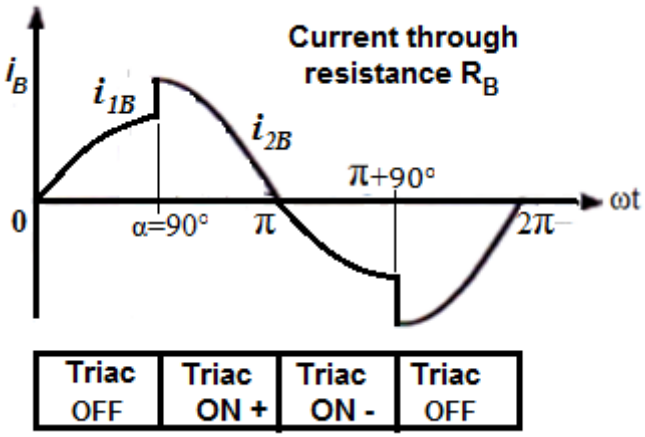

Fig.5.10 Waveforms.

(b) When triac is OFF for the intervals $(0 \le \omega t \le 90^\circ)$ and $(\pi < \omega t \le \pi + 90^\circ)$, the current i_{1B} through resistance R_B is :

$$i_{1B} = \frac{V_m sin\omega t}{R_A + R_B}$$

When triac is ON for the positive and negative half-cycles of the supply for the interval $(90^\circ < \omega t \le \pi)$ and $(90^\circ + \pi < \omega t \le 2\pi)$ respectively, the current through resistance R_B , i_{2B} is :

$$i_{2B} = \frac{V_m sin\omega t}{R_B}$$

The Fourier coefficients of the fundamental component of the current i_B are ,

$$a_1 = \frac{2}{\pi}\left[\int_0^{\alpha} \frac{V_m sin\omega t}{R_A + R_B} \cos\omega t \, d\omega t + \int_{\alpha}^{\pi} \frac{V_m \sin\omega t}{R_B} \cos\omega t \, d\omega t\right]$$

$$= \frac{2V_m}{\pi}\left[\frac{1}{R_A + R_B}\int_0^{\alpha} \frac{1}{2}\sin 2\omega t \, d\omega t + \int_{\alpha}^{\pi} \frac{1}{2R_B}\sin 2\omega t \, d\omega t\right]$$

$$= \frac{2V_m}{\pi}\left[\frac{1}{R_A + R_B}\left[-\frac{1}{2}\cos 2\omega t\right] + \frac{1}{R_B}\left[-\frac{1}{2}\cos 2\omega T\right] \right]$$

$$= \frac{2V_m}{\pi}\left[\frac{1}{R_A + R_B}\left(\frac{1}{2} - \frac{1}{2}\cos 2\alpha\right) + \frac{1}{R_B}\left(-\frac{1}{2} + \frac{1}{2}\cos\alpha\right)\right]$$

$$= \frac{2V_m}{\pi}(\cos 2\alpha - 1)\left[\frac{-1}{R_A + R_B} + \frac{1}{R_B}\right]$$

$$= \frac{2V_m}{\pi}(\cos 2\alpha - 1)\left[\frac{R_A + R_B - R_B}{R_B(R_A + R_B}\right]$$

$$= \frac{V_m}{\pi}(\cos 2\alpha - 1)\left[\frac{R_A}{R_B(R_A + R_B)}\right]$$

$$b_1 = \frac{2}{\pi}\left[\int_0^{\alpha} \frac{V_m sin\omega t}{R_A + R_B} \sin\omega t \, d\omega t + \int_{\alpha}^{\pi} \frac{V_m sin\omega t}{R_B} \sin\omega t \, d\omega t\right]$$

$$= \frac{2V_m}{\pi}\left[\frac{1}{R_A + R_B}\int_o^{\alpha} sin^2\omega t \, d\omega t + \frac{1}{R_B}\int_{\alpha}^{\pi} \sin^2\omega t \, d\omega t\right]$$

$$= \frac{2V_m}{\pi}\left[\frac{1}{2(R_A + R_B)}\int_o^{\alpha} (1 - \cos 2\omega t) \, d\omega t \right]$$

$$+ \frac{1}{2R_B}\int_{\alpha}^{\pi} (1 - \cos 2\,\omega t) \, d\omega t$$

$$= \frac{V_m}{\pi}\left[\frac{1}{R_A + R_B}\left[\omega t - \frac{1}{2}\sin 2\omega t\right] + \frac{1}{R_B}\left[\left(\pi - \alpha + \frac{1}{2}\sin 2\alpha\right)\right]\right]$$

$$= \frac{V_m}{\pi}\left[\frac{1}{R_A + R_B}\left[\alpha - \frac{1}{2}\sin 2\alpha\right] + \frac{1}{R_B}\left[\left(\pi - \alpha + \frac{1}{2}\sin 2\alpha\right)\right]\right]$$

$$= \frac{V_m}{\pi}\left[\frac{1}{R_A + R_B}\left[\alpha - \frac{1}{2}\sin 2\alpha\right] + \frac{1}{R_B}\left[\left(\pi - \alpha + \frac{1}{2}\sin 2\alpha\right)\right]\right]$$

$$= \frac{V_m}{\pi(R_A + R_B)}\left(\alpha - \frac{1}{2}\sin 2\alpha\right) + \frac{V_m}{R_B}\left(\pi - \alpha + \frac{1}{2}\sin 2\alpha\right)$$

$$= \frac{V_m}{2\pi}\left[(\sin 2\alpha) + 2(\pi - \alpha))\frac{R_A}{R_A + R_B}\right] + \frac{V_m}{R_A + R_B}$$

Since $R_A = R_B = 10\ \Omega$, $V_m = 100$ V and $\alpha = 90°$,

$$a_1 = \frac{100}{2\pi}(\cos 180° - 1)x\ \frac{100}{10} = -1.59\ \text{A}$$

$$b_1 = \frac{100}{\pi(10 + 10)}\left(\frac{\pi}{2} - \frac{1}{2}\sin 180°\right) + \frac{100}{10}(\pi - \frac{\pi}{2} + \frac{1}{2}\sin 180°)$$

$$\frac{100}{20\pi} \times \frac{\pi}{2} + \frac{100}{20\pi}\pi = \frac{100}{40} + \frac{100}{20} = 2.5 + 5 = 7.5\ \text{A}$$

$$I_B = \frac{\sqrt{a_1{}^2 + b_1{}^2}}{\sqrt{2}} = \frac{\sqrt{(-1.59)^2 + (7.5)^2}}{\sqrt{2}} = 5.42\ \text{A}$$

$$\psi = \tan^{-1}\frac{a_1}{b_1} = \tan^{-1}\frac{-1.59}{7.5} = -11.96°$$

Although the load is resistive, a lagging *PF* is introduced due to the chopping action.The reactive power here is fiction, since there is no energy storage element.

Example 5.7

A full-wave rectifier bridge supplying a 10 Ω resistive load via an a.c. voltage controller from an ideal single-phase supply $v_s = V_m \sin\omega t$ in an arrangement as shown Fig.5.11. The SCRs of the inverse-parallel pair are gated to provide symmetrical phase-angle triggering.

(a) Sketch waveforms, for two cycles, of the supply voltage, load current and supply current.

(b) Derive an expression for the load power dissipation in terms of V_m, R and α. Calculate the power at α = 30° if V_m = 325 V.

(c) If diode D_1 is failed to open circuit, what will be the value of the load current?

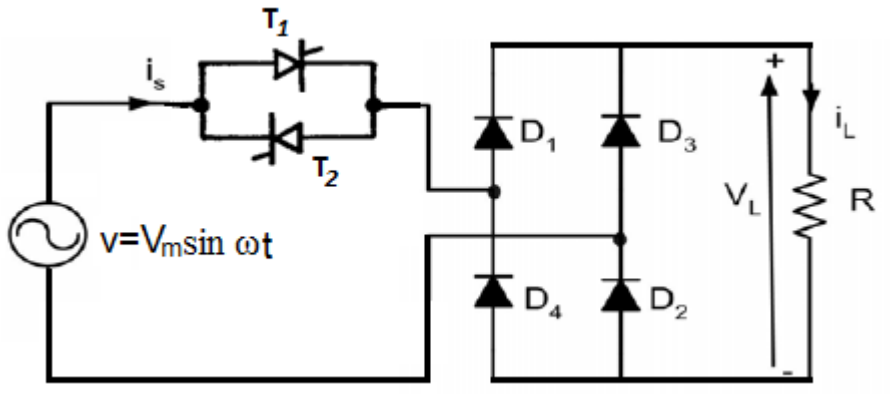

Fig.5.11.

Solution

(a) The waveforms, for two cycles of the supply voltage, supply current and load current are shown in Fig.5.12.

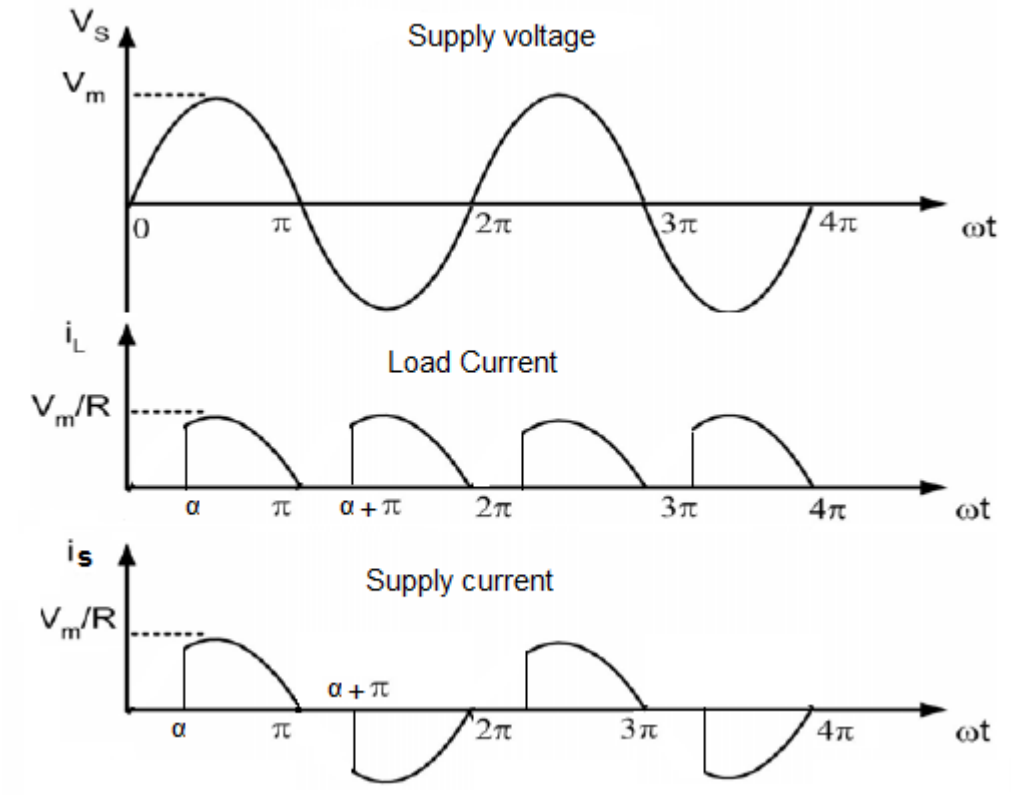

Fig.5.12. Waveforms.

(b) $V_L = \sqrt{\frac{1}{2\pi}\int_o^{2\pi}(V_m sin\omega t)^2 d\omega t} = \sqrt{\frac{1}{\pi}\int_\alpha^{\pi} {V_m}^2 sin^2\omega t d\omega t}$

$$= \sqrt{\frac{{V_m}^2}{2\pi}\left[\int_\alpha^{\pi}(1-\cos 2\omega t)d\omega t\right]} = \sqrt{\frac{{V_m}^2}{2\pi}\left[1-\frac{\alpha}{\pi}+\frac{1}{2\pi}\sin 2\alpha\right]}$$

Power $P = \frac{V_L^2}{R} = \frac{{V_m}^2}{2\pi R}\left[1-\frac{\alpha}{\pi}+\frac{1}{2\pi}\sin 2\alpha\right]$

$$= \frac{{V_m}^2}{2R}\left[1-\frac{\alpha}{\pi}+\frac{1}{2\pi}\sin 2\alpha\right]$$

For $\alpha = 30° \Rightarrow \frac{\pi}{3}$ and $V_m = 325\ V$

$$P = \frac{(325)^2}{2\times 10}\left[1-\frac{\pi/6}{\pi}+\frac{1}{2\pi}\sin 60°\right] = 5371\ \text{W}$$

(c) If D_1 is failed to open circuit, the load current will be halved as shown in Fig.5.13, hence the power will be halved.

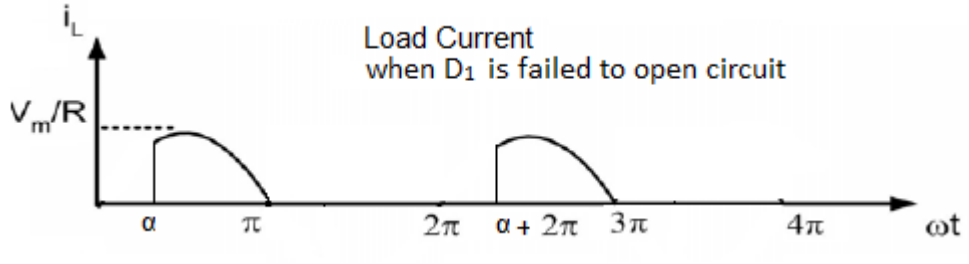

Fig.5.13 The load current waveform when D_1 failed to open circuit.

Example 5.8

A single-phase a.c. controller shown in Fig.5.1 is used to control power flow to a resistive load R from an ideal sinusoidal supply $v_s = V_m \sin \omega t$. The SCRs are gated to produce symmetrical angle triggering of the output voltage and current waveforms.

(a) Derive an expression for the load power dissipation P in terms of V_m, R and α. Calculate the power dissipation if the *rms* supply voltage is 230 V, R = 10 Ω, and α = 90˚?

(b) The fundamental component of the current at α = 90° can be described by the expression

$$i_{L1}(\omega t) = 0.65\ \frac{V_m}{R}\sin(\omega t - 39.71°)$$

Calculate the displacement factor, distortion factor and hence power factor of the circuit at α = 90°.

Solution

(a) For single-phase a.c. controller , the *rms* value of the output voltage is given by Eq.(5.6) as ,

$$V_L = V_s\sqrt{\frac{1}{\pi}\left[(\pi - \alpha) + \frac{\sin 2\alpha}{2}\right]}$$

and the *rms* value of the load current is

$$I_L = \frac{V_L}{R} = \frac{V_s}{R} = \frac{V_s}{R}\sqrt{\frac{1}{\pi}\left[(\pi - \alpha) + \frac{\sin 2\alpha}{2}\right]}$$

The power consumed by the load is

$$P = V_L\, I_L$$

$$= \frac{{V_s}^2}{R}\left[\frac{1}{\pi}\left((\pi - \alpha) + \left(\frac{\sin 2\alpha}{2}\right)\right)\right]$$

For V_s = 240 V , R=25 Ω , α = $\frac{\pi}{2}$

$$\therefore P = \frac{(230)^2}{10}\left[\frac{1}{\pi}\left\{\pi - \frac{\pi}{2} + \frac{\sin 180°}{2}\right\}\right] = 2645\ \text{W}$$

(b) The displacement factor (cosψ$_1$)is

$$i_{L1}(\omega t) = 0.65\frac{V_m}{R}\sin(\omega t - 32.5°)$$

$$\mathrm{I}_{Lmax} = 0.65 \times \frac{V_m}{R} = 0.65 \times \frac{230 \times \sqrt{2}}{10} = 21.13\ \text{A}$$

The *rms* value of the fundamental component of the current is

$$I_{L1} = \frac{I_{Lmax}}{\sqrt{2}} = \frac{21.13}{\sqrt{2}} = 14.95\ \text{A}$$

Thus $P = V_s I_{L1} \cos\psi_1$

$2645 = 230\ 14.95\ \cos\psi_1$

$\therefore\ \cos\psi_1 = 0.7692$

or $\cos\psi_1 = \cos(-39.71°) = 0.7692$

Distrotion Factor, $DF = \frac{I_{L1}}{I_L}$

$$I_L = \frac{V_L}{R} = \sqrt{\frac{P}{R}} = \sqrt{2645/10} = 16.26\ \text{A}$$

$$\therefore DF = \text{distortion factor} = \frac{14.95}{16.26} = 0.9194$$

$PF = DF\ \times$ Displacement factor $= 0.9194\ \times\ 0.7692 =\ 0.707$

Example 5.9

The single-phase a.c. controller shown in Fig .5.1 has a resistive load of R = 15 Ω and the input voltage is V_s = 230 V (*rms*), 50 Hz. The firing angles of thyristors T_1 and T_2 are equal : $\alpha_1 = \alpha_2 = \frac{\pi}{2}$, Determine :

(a) The *rms* value of the output voltage.
(b) The input power factor.
(c) The average and *rms* and values of the thyristor currents.

Solution

(a) Using Eq.(5.6) ,

$$\mathrm{V}_m = \sqrt{2}\,\mathrm{V}_s$$

$$V_L = \frac{\mathrm{V}_m}{\sqrt{2}}\left[\frac{1}{\pi}\left(\pi - \alpha + \frac{1}{2}sin2\alpha\right)\right]^{\frac{1}{2}}$$

For $\alpha = \frac{\pi}{2}$

$$V_L = 230\ (\frac{1}{\pi}\ (\pi - \frac{\pi}{2} + \frac{\sin\pi}{2}))^{\frac{1}{2}} = \frac{230}{\sqrt{2}}\ =\ 162.6\ \text{V}$$

(b) The *rms* value of the load current is

$$I_L = \frac{V_L}{R} = \frac{162.6}{15} = 10.85 \text{ A}$$

Load Power is

$$P = I_L{}^2 R = (10.85)^2 \times 15 = 1763.86 \text{ W}$$

Because the input current is the same as the load current, the input VA rating is:

$$\text{VA} = V_s \ I_s = 230 \times 10.85 = 2495.5$$

The input *PF* is

$$PF = \frac{V_L \cdot I_L}{V_s \cdot I_L} = \frac{V_L}{V_s} = \frac{162.6}{230} = 0.707$$

(c) The average thyristor current

$$I_{T(avg)} = \frac{1}{2\pi R} \int_{\alpha}^{\pi} \text{V}_m \sin \omega t \, d\omega t$$

$$= \frac{\text{V}_s\sqrt{2}}{2\pi R} (cos\ \alpha + 1) = \frac{\sqrt{2} \times 230}{2\pi \times 15} = 3.45 \text{ A}$$

The *rms* value of the thyristor current

$$I_{T(rms)} = \sqrt{\frac{1}{2\pi}\int_{0}^{\pi} (\frac{\sqrt{2}}{R} \text{V}_s \ sin\ \omega t)^2 \, d\omega t}$$

$$= \frac{V_s}{\sqrt{2}R} \left[\frac{1}{\pi}(\pi - \alpha + \frac{\sin 2\alpha}{2})\right]^{\frac{1}{2}} = \frac{230}{2 \times 115} = 7.66 \text{ A}$$

Example 5.10

A pair of thyristors connected in inverse-parallel, Fig.5.1, is used to supply adjustable current to a resistive load R = 12 Ω. If the supply voltage is $v = \sqrt{2} \times 230$ sinωt and the thyristors are each triggered at an angle α after their respective anode voltage zeros, it is required to:

(a) Calculate the power delivered to the load for α = 30°.
(b) Determine the delay angle required to deliver 750 W to a 20 Ω load.

(c) Calculate the *rms* of the source current and the *rms* and average value of the current in the thyristor for the angle obtained in (b) above.

Note that $V_{L\,normalized} = \dfrac{V_L}{V_m/\sqrt{2}}$

and the relation between the normalized *rms* load voltage and the delay angle a for a single-phase a.c. voltage controller with a resistive load is given in Fig.5.14.

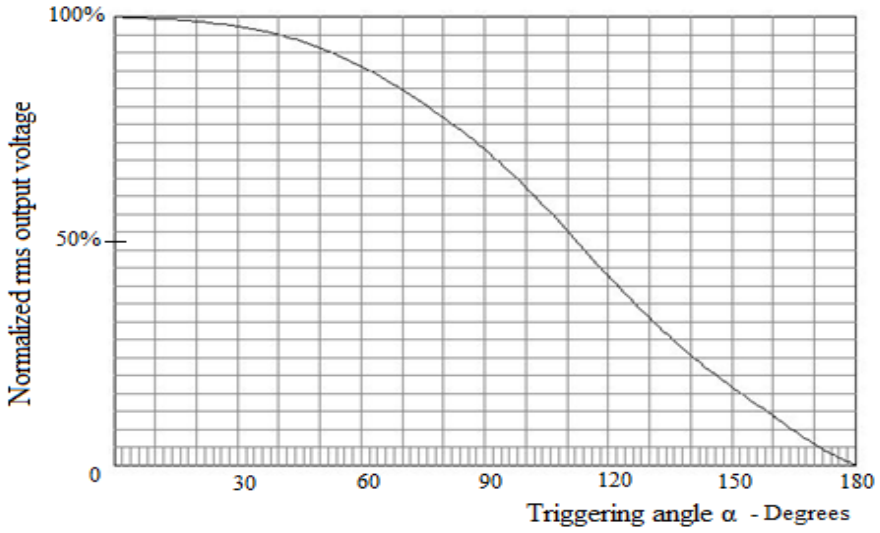

Fig.5.14 Relation between output voltage and the triggering angle.

Solution

(a) For a single-phase a.c. voltage controller, the *rms* value of the output voltage is given by Eq.(5.5) as

$$V^2{}_L = \frac{V_m{}^2}{2\pi}\left[\pi - \alpha + \frac{sin2\alpha}{2}\right]$$

For $\alpha = 30° = \dfrac{\pi}{6}$ rad.

$$V^2{}_L = \frac{V_m{}^2}{2\pi}\left[\frac{5\pi}{6} + 0.44330\right] = 0.487\ V_m{}^2$$

$$\therefore\ V_L = 0.698\ V_m$$

or $V_L = 0.698 \times 230 \times \sqrt{2} = 227\ \text{V}$

$$I_L = \frac{V_L}{R} = \frac{227}{12} = 18.9\ \text{A}$$

$$P = \frac{V^2{}_L}{R} = \frac{(227)^2}{12} = 4294 \text{ W}$$

(b) The required voltage to deliver 750 W to a 20 Ω load is

$$P = \frac{V_L{}^2}{R} \Rightarrow \quad V_L = \sqrt{PR} = \sqrt{750 \times 20} = 122.5 \text{ V}$$

From the graph, the delay angle required to obtain a normalized output of $\frac{122.5}{230} = 0.532$ is approximately : α = 110°.

(a) Source current i_s:

$$I_s = I_L = \frac{V_L}{R} = \frac{122.5}{20} = 6.125 \text{ A}$$

The thyristor currents are determined as follows:

The *rms* value is given by,

$$I_{SCR,rms} = \frac{I_L}{2} = \frac{6.125}{2} = 3.062 \text{ A}$$

The average value is given by,

$$I_{SCR,(av)} = \frac{1}{2\pi}\int_{\alpha}^{\pi} \frac{V_m}{R} sin\omega t d\omega t = \frac{V_m}{2\pi R}(1 + \cos\alpha)$$

$$= \frac{\sqrt{2} \times 230}{2\pi \times 20}(1 + \cos 110°) = 1.71 \text{ A}$$

5.5 OPERATION OF SINGLE-PHASE AC CONTROLLER WITH *R-L* LOAD

The single-phase a.c. voltage controller with resistive-inductive load is shown in Fig.5.15. Due to the inductance in the circuit, the current in thyristor T_1 would not fall to zero at ωt = π, when the source voltage v_s start to be negative. Thyristor T_1 continues to conduct until its current i_L falls to zero at ωt = β .

The instantaneous supply voltage, v_s, is now the sum of three components, consisting of the SCR voltage drop, v_T, the resistance drop, $v_R = iR$, and the voltage v_L across the inductor.

By KVL,

$$v_s = v_R + v_L + v_T = v_s \qquad (5.39)$$

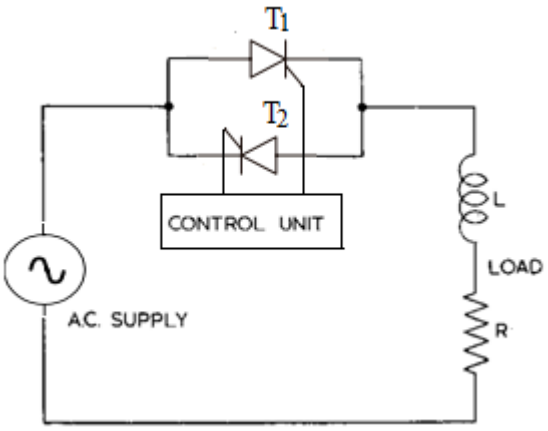

(a) Circuit.

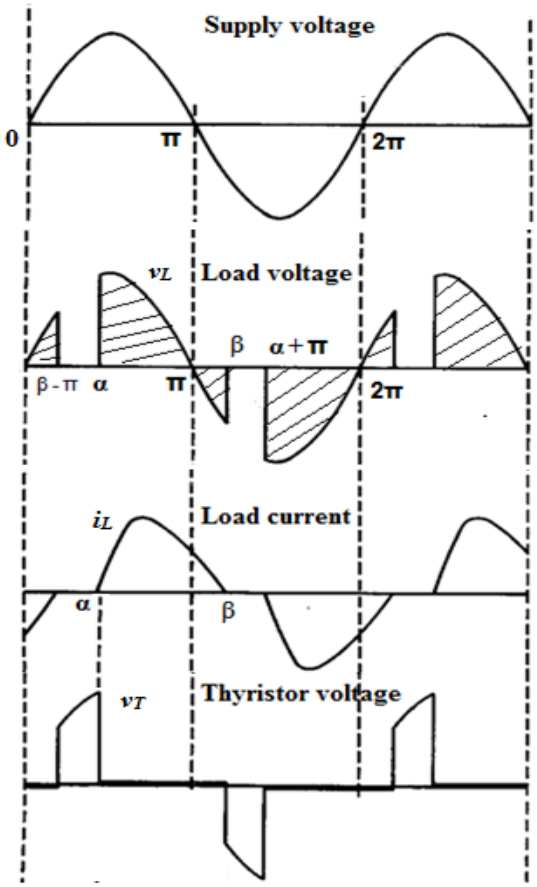

(b)Waveforms.

Fig.5.15 Single-phase controller with series *R-L* load.

Neglecting the voltage drop across the thyristor, the equation for the current through R-L load can be found from the solution of the differential equation:

$$L\frac{di}{dt} + iR = V_m \sin \omega t \qquad (5.40)$$

The solution of this differential equation is:

The start of conduction is delayed until ωt = α subsequent to triggering, let the instantaneous current $i(\omega t)$ consists of hypothetical steady-state components $i_{ss}(\omega t)$ and transient component i_{tr} (ωt), these analytical components of the current waveform are demonstrated in Fig 5.16. At the instant of SCR triggering the load current is zero. If the applied voltage $v(\omega t)$ is given by Eq.(5.1) then the steady-state component of current $i_{ss}(\omega t)$ in Fig.5.16 is given by:

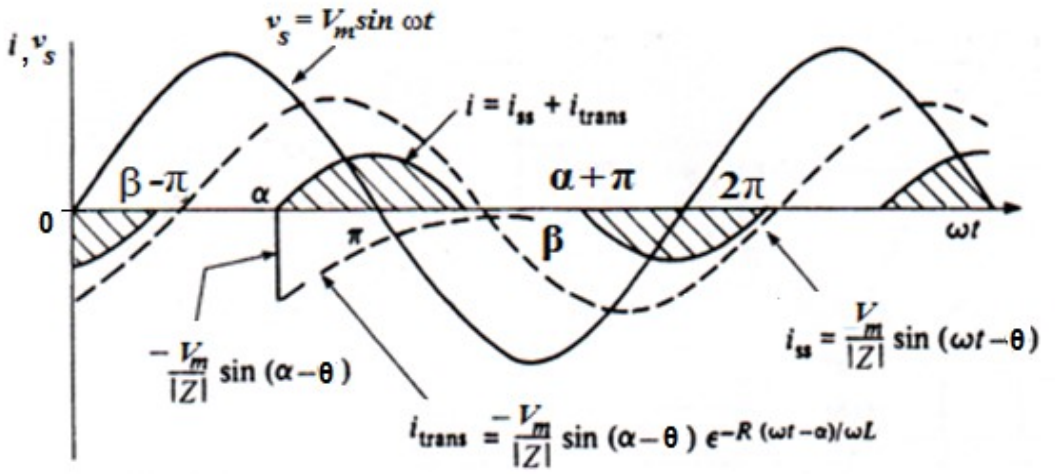

Fig.5.16 Analytical components of current waveform for single-phase a.c. voltage controller with series *R-L* load, θ = 60°, α = 120°.

$$i_{ss}(\omega t) = \frac{V_m}{Z}\sin(\omega t - \theta)$$

and the transient solution is

$$i_{tr}(\omega t) = Ae^{-\frac{t}{\tau}}$$

where

$$Z = \sqrt{R^2 + (\omega L)^2}$$

$$\tan\theta = \frac{\omega L}{R}$$

$$\tau = \frac{L}{R} = \text{time constant}$$

A = constant

The complete solution is : $i(\omega t) = i_{ss}(\omega t) + i_{tr}(\omega t)$

In the interval α< ωt < β, the total current is therefore described by the equation

$$i(\omega t) = \frac{V_m}{Z}\sin(\omega t - \theta) + Ae^{-\frac{t}{\tau}} \qquad (5.41)$$

The constant A can be found from initial conditions:
when ωt = α , $i(\omega t) = 0$

$$0 = \frac{V_m}{Z}\sin(\alpha - \theta) + Ae^{-\frac{\alpha}{\omega\tau}}$$

$$A = -\frac{V_m}{Z}\sin(\alpha - \theta)\, e^{\frac{\alpha}{\omega\tau}} \qquad (5.42)$$

Substitute Eq.(5.42) into Eq.(5.41) yields

$$i(\omega t) = \frac{V_m}{Z}\sin(\omega t - \theta) - \frac{V_m}{Z}\sin(\alpha - \theta)e^{\frac{\alpha}{\omega\tau}}\, e^{-\frac{\omega t}{\omega\tau}}$$

The complete solution for the current at first cycle

$$i(\omega t) = \frac{V_m}{\sqrt{R^2 + (\omega L)^2}}[\sin(\omega t - \theta) - \sin(\alpha - \theta)e^{\frac{-(\omega t - \alpha)}{\omega\tau}}] \quad (5.43)$$

In Fig. 5.16 for the part of the current cycle such that $\beta \leq \omega t \leq \pi + \theta$, the resultant current is mathematically negative. However, the conducting switch will not permit the flow of reverse current so that conduction ceases at point β, which is called the extinction angle or cut-off angle. The extinction angle β can be obtained from Eq.(5.43) by noting that when $\omega t = \beta$, $i(\beta) = 0$. This results in the the following transcendental equation (5.44):

$$0 = \frac{V_m}{\sqrt{R^2 + (\omega L)^2}}[\sin(\beta - \theta) - \sin(\alpha - \theta)\, e^{\frac{-(\beta - \alpha)R}{\omega L}}]$$

$$0 = [\sin(\beta - \theta) - \sin(\alpha - \theta)\, e^{-(\beta - \alpha).\cot\theta}] \qquad (5.44)$$

since $\frac{R}{\omega L} = \cot\theta$

If α and θ are known, β can be calculated. However, this is a transcendental equation (i.e. cannot be solved explicitly and no way of obtaining the angle $\beta = f(\alpha, \theta)$). Method of solution is by iteration as discussed in Chapter Two. However, an approximate value of the extinction angle β can be found from the simple relationship:

$$\beta = 180° + \theta - \Delta$$

where

$\Delta = 5° \sim 10°$ for large R and small ωL

$\Delta = 10° \sim 15°$ for $R = \omega L$

$\Delta = 15° \sim 20°$ for small R and large ωL

For example, If $\theta = 60^0$, $\alpha = 120^0 = 2\pi / 3$, $\cot\theta = 0.578$

Using Eq.(5.41) and solve by iterative method:

$$\sin(\beta - 60°) = \sin(120° - 60°)e^{-0.578(\beta-(2\pi/3))} \rightarrow \beta = 222°$$

Using the approximate solution:

$$\theta = 60°, \qquad \Delta = 15° - 20°$$

$$\beta = 180° + 60° - 15° = 225°$$

$$\text{or } \beta = 180° + 60° - 20° = 220° \rightarrow \beta = \frac{225 + 220}{2} = 222.5^0$$

5.5.1 Load Voltage Waveform Analysis

The load voltage waveform for *R-L* load with a.c. voltage controller is shown in Fig.5.17.

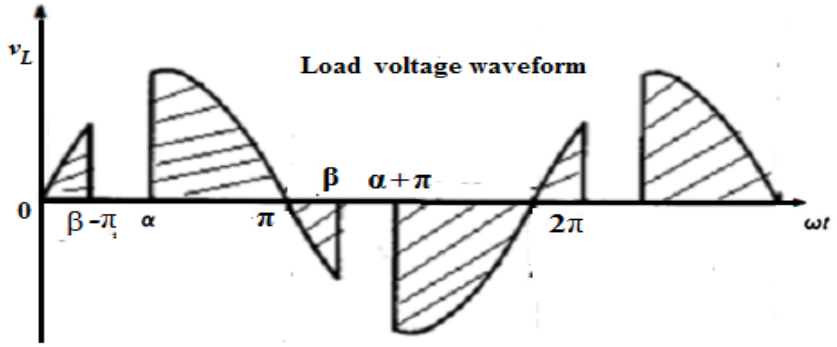

Fig.5.17 The load voltage waveform for *R-L* load.

This waveform can be represented as :

$$v_L = V_m sin\omega t \begin{cases} \beta - \pi, & \beta \quad , 2\pi, \ldots \\ 0, & \alpha, \quad \pi + \alpha, \ldots \end{cases}$$

$$v_L = 0 \qquad \text{elsewhere} \qquad (5.45)$$

The *rms* value of the load voltage can be evaluated as

$$V_L = \sqrt{2 \times \frac{1}{2\pi}\int_{\alpha}^{\beta} (V_m sin\omega t)^2 \, d\omega t}$$

$$= \sqrt{\frac{V_m^2}{\pi}\int_{\alpha}^{\beta} \frac{1}{2}(1 - cos2\omega t)\, d\omega t}$$

$$= V_m \left[\frac{1}{2\pi}(\beta - \alpha + \frac{\sin 2\alpha}{2} - \frac{\sin 2\beta}{2})\right]^{1/2} \quad (5.46)$$

Fourier analysis of the above waveform,

$$a_o = \frac{1}{\pi}\int_0^{2\pi} v_L(\omega t) d\omega t = 0 \quad (5.47)$$

The fundamental component is given by

$$a_1 = \frac{1}{\pi}\int_0^{2\pi} v_L(\omega t)\, cos\omega t \, d\omega t$$

$$a_1 = \frac{1}{\pi}\int_0^{\beta-\pi} V_m sin\omega t \;\; cos\omega t \, d\omega t + \frac{1}{\pi}\int_{\alpha}^{\beta} V_m sin\omega t \;\; cos\omega t \, d\omega t + \frac{1}{\pi}\int_{\alpha+\pi}^{2\pi} V_m sin\omega t \;\; cos\omega t \, d\omega t$$

Use the trigonometric relation: $\sin 2x = 2 \sin x \cos x$

$$a_1 = \frac{V_m}{2\pi}\left[\int_0^{\beta-\pi} sin2\omega t \;\; d\omega t + \int_{\alpha}^{\beta} sin2\omega t \;\; d\omega t + \int_{\alpha+\pi}^{2\pi} sin2\omega t \;\; d\omega t\right]$$

$$a_1 = \frac{V_m}{4\pi}\left[-cos2\omega t\left\{\begin{matrix}\beta-\pi \\ 0\end{matrix} - cos2\omega t\left\{\begin{matrix}\beta \\ \alpha\end{matrix} - cos2\omega t\right\{\begin{matrix}2\pi \\ \pi+\alpha\end{matrix}\right]$$

$$a_1 = \frac{V_m}{2\pi}[cos2\alpha - \cos 2\beta] \quad (5.48)$$

Similarly

$$b_1 = \frac{1}{\pi}\int_0^{2\pi} v_L(\omega t)\, sin\omega t \, d\omega t$$

$$b_1 = \frac{1}{\pi}\int_0^{2\pi} V_m sin\omega t \ cos\omega t \, d\omega t$$

$$b_1 = \frac{1}{\pi}\int_0^{\beta-\pi} V_m sin\omega t \ sin\omega t \, d\omega t + \frac{1}{\pi}\int_\alpha^{\beta} V_m sin\omega t \ sin\omega t \, d\omega t + \frac{1}{\pi}\int_{\alpha+\pi}^{2\pi} V_m sin\omega t \ sin\omega t \, d\omega t$$

$$b_1 = \frac{V_m}{2\pi}[2(\beta-\alpha) - \sin 2\beta + sin2\alpha] \quad (5.49)$$

In the usual way, the peak value of the fundamental load voltage is given by

$$c_1 = \sqrt{a_1^2 + b_1^2}$$

$$c_1 = \frac{V_m}{2\pi}\sqrt{[cos2\alpha - \cos 2\beta]^2 + [2(\beta-\alpha) - \sin 2\beta + sin2\alpha]^2} \quad (5.50)$$

The fundamental component of the load voltage will be phase displaced from the supply voltage by an angle ψ_{v1} , which is different from the current displacement angle, hence

$$\psi_{v1} = \tan^{-1}\frac{cos2\alpha - \cos 2\beta}{2(\beta-\alpha) - \sin 2\beta + sin2\alpha} \quad (5.51)$$

Fourier coefficients for the nth higher harmonic of the load voltage waveform are found to be

$$a_n = \frac{1}{\pi}\int_0^{2\pi} v_L(\omega t)\cos n\omega t \, d\omega t$$

$$a_n = \frac{V_m}{2\pi}\left[\frac{2}{n+1}\{\cos(n-1)\alpha - \cos(n-1)\beta\} - \frac{2}{n-1}\{\cos(n-1)\alpha - \cos(n-1)\beta\}\right] \quad (5.52)$$

$$b_n = \frac{1}{\pi}\int_0^{2\pi} V_L(\omega t)\sin n\omega t \, d\omega t$$

$$b_n = \frac{V_m}{2\pi}\left[\begin{array}{l} \frac{2}{n+1}\{\sin(\mathrm{n}+1)\,\alpha - \sin(\mathrm{n}+1)\,\beta\} \\ -\frac{2}{n-1}\{\sin(n-1)\,\alpha - \sin(\mathrm{n}-1)\,\beta\} \end{array}\right] \quad (5.53)$$

5.5.2 Harmonic Properties of the Current Waveform

The Fourier harmonic components of the current function *i*(ωt), equation (5.43), are found to be:

$$\frac{a_o}{2} = \frac{1}{2\pi}\int_0^{2\pi} i_L(\omega t)d\omega t = 0 \quad (5.54)$$

The fundamental component of the current is found as

$$a_1 = \frac{1}{\pi}\int_0^{2\pi} i(\omega t)\, cos\omega t\, d\omega t$$

$$a_1 = \frac{V_m}{2\pi|Z|}[\cos(2\alpha-\theta) - \cos(2\beta-\theta) - \sin\theta(2\beta-2\alpha)$$

$$+ 4sin\theta\sin(2\alpha-\theta) - \{\cos(\theta+\beta)e^{cot\theta(\beta-\alpha)} - \cos(\theta+\alpha)\}] \quad (5.55)$$

$$b_1 = \frac{1}{\pi}\int_0^{2\pi} i(\omega t)\, sin\omega t\, d\omega t$$

$$b_1 = \frac{V_m}{2\pi|Z|}[\sin(2\alpha-\theta) - \sin(2\beta-\theta) + \cos\theta(2\beta-2\alpha)$$

$$+4sin\theta\sin(\alpha-\theta)\{\sin(\theta+\beta)e^{cot\theta(\beta-\alpha)} - \sin(\theta+\alpha\}] \quad (5.56)$$

Variation of the fundamental component of the current with triggering angle is shown in Fig.5.18 for different values of phase-angle θ. With purely resistive load, the exponential terms of the current equation (5.43) have zero value and the current wave consists of a sinusoid with symmetrical pieces chopped out. With a highly inductive load the current waveform is symmetrical about ωt=0 and fundamental Fourier coefficient b_1 is therefore zero. By putting, θ = 90° and β = 2π – α into Eq. (5.55) and Eq.(5.56), it is found that :

$$a_1 = \frac{-V_m}{\pi\omega L}[(\pi-\alpha) + sin2\alpha] \quad (5.57)$$

and

$$b_1 = 0 \quad (5.58)$$

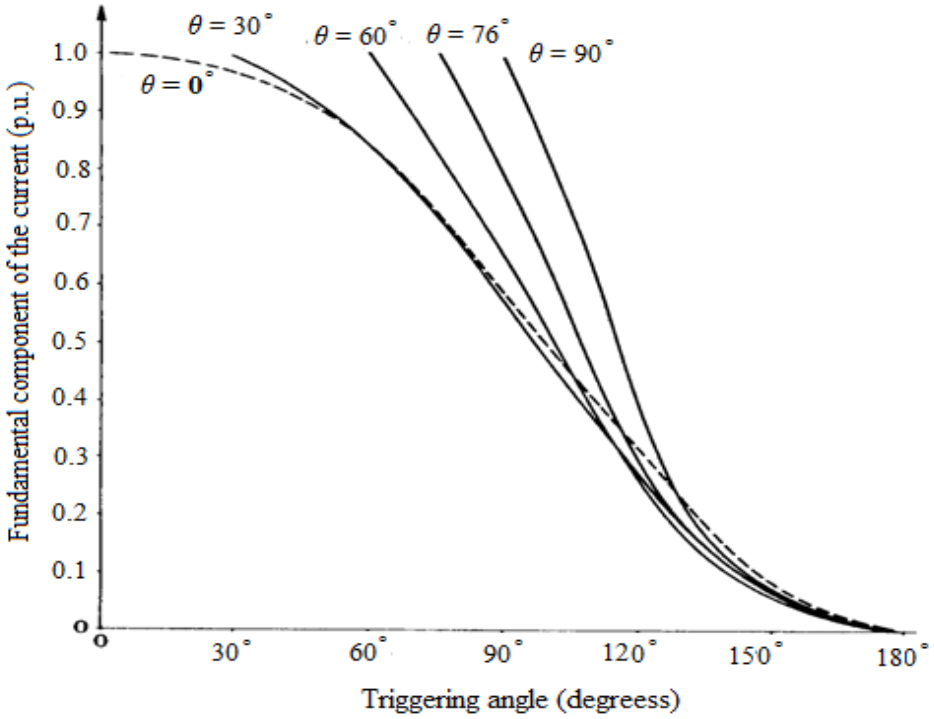

Fig.5.18 Fundamental component of the current versus firing-angle for a single-phase a.c. voltage controller with series *R-L* load.

For the n[th] harmonic Fourier coefficients a_n , b_n are given, for general load phase-angle θ, by

$$a_n = \frac{1}{\pi}\int_0^{2\pi} i(\omega t)\, cosn\omega t\, d\omega t$$

$$b_n = \frac{1}{\pi}\int_0^{2\pi} i(\omega t)\, sinn\omega t\, d\omega t$$

Solutions of the above two Fourier equations yield

$$\begin{aligned} a_n = \frac{V_m}{2\pi|Z|}\Bigg\{ & \frac{2}{n+1}[\cos\{(n+1)\alpha-\theta)\} - \cos\{(n+1)\beta-\theta\}] \\ & -\frac{2}{n-1}[cos\{(n-1)\alpha-\theta)\} - \cos\{(n-1)\beta-\theta\}] \\ & +[(\cos n\beta\cot\theta - n\, sinn\beta)\, e^{-cot\theta(\beta-\alpha)} \\ & -(\cos n\alpha\cot\theta - n\sin n\alpha)]\frac{4\sin(\alpha-\theta)}{n^2+cot\theta^2}\Bigg\} \end{aligned} \qquad (5.59)$$

$$b_n = \frac{V_m}{2\pi|Z|}\left\{\frac{2}{n+1}[\sin\{(n+1)\alpha-\theta)\}-\sin\{(n+1)\beta-\theta\}]\right.$$
$$-\frac{2}{n-1}[sin\{(n-1)\alpha-\theta)\}-\sin\{(n-1)\beta-\theta\}]$$
$$+[(\sin n\beta\cot\theta - n\,cosn\beta\,)\,e^{-cot\theta(\beta-\alpha)}$$
$$\left.-\,(\sin n\alpha\cot\theta - n\cos n\alpha)]\frac{4\sin(\alpha-\theta)}{n^2+cot\theta^2}\right\} \qquad (5.60)$$

5.5.3 The *rms* Value of Load Current

The dissipation in a series circuit is proportional to the square of the total *rms* current. If the magnitudes of the steady-state *rms* current harmonics are now denoted by I_n, the resultant *rms* current is given by

$$I_{Lrms} = \sqrt{I_1^2 + I_3^2 + I_5^2 + I_7^2 + \cdots} \qquad (5.61)$$

For *R-L* loads the *rms* current can also be obtained from its defining integral

$$I_{Lrms} = \sqrt{\frac{1}{2\pi}\int_0^{2\pi} i(\omega t)^2\, d\omega t} \qquad (5.62)$$

Example 5.11

A resistive-inductive load is supplied from a 240 V, 50 Hz supply via inverse-parallel connected thyristors. If the load impedance is 20 Ω and θ = 40˚ and the triggering angle is 60˚, sketch the waveform for the current flowing through each thyristor and determine their conduction angle. Using the approximate method of findig β.

Solution

Since θ = 50° > 45° , hence Δ ≈ 10° - 15°
The current waveform is shown in Fig.5.19.

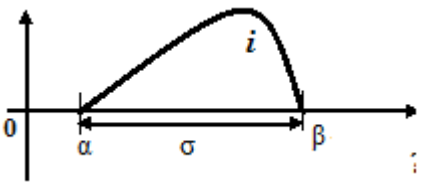

Fig.5.19.

Using approximate method:

β = 180° + θ - Δ
β_1 = 180° + 50° – 10° = 220°
β_2 = 180° + 50° – 15° = 210°

$$\therefore \quad \beta = \frac{\beta 1 + \beta 2}{2} = \frac{220° + 215°}{2} = 217.5°$$

Conduction angle $\sigma = \beta - \alpha = 217.5° - 60° = 157.5°$

Example 5.12

A series *R-L* load of phase angle 45° is controlled by a pair of symmetrically triggered thyristors connected in inverse-parallel. Find an expression showing, approximately, the relationship between the fundamental load voltage and the thyristor firing angle.

Solution

The variation of the fundamental component with the firing angle for *R-L* load is given by:

$$V_{1rms} = \frac{c_1}{\sqrt{2}} = \sqrt{\frac{a_1^2 + b_1^2}{2}}$$

From Eq. (5.47) ,

$$c_1 = \frac{V_m}{2\pi}\sqrt{[cos2\alpha - \cos 2\beta]^2 + [2(\beta - \alpha) - \sin 2\beta + sin2\alpha]^2}$$

$$\therefore \quad V_{1rms} = \frac{V_m}{2\sqrt{2}\pi} \times \sqrt{[cos2\alpha - \cos 2\beta]^2 + [2(\beta - \alpha) - \sin 2\beta + sin2\alpha]^2}$$

To find β , using the approximate method :

$$\beta = 180 + \theta - \Delta$$

For $\theta = 45°$ $\quad \Delta \approx 10°$

$$\beta = 180^o + 45^o - 10^o = 215° = 3.75 \text{ rads}.$$

Let $V_m = 1.0$ p.u. , $\theta = 45° = 0.785$ rad

$$\therefore V_{1rms} = 0.1126 \times \sqrt{[cos2\alpha - 0.342]^2 + [2(3.75 - \alpha) - 0.939 + sin2\alpha]^2}$$

$$= 4.05 \text{ p.u.}$$

Example 5.13

Two thyristors are connected in anti-parallel for the voltage control of a single-phase, series *R-L* load of phase angle θ to sinusoidal currents of supply frequency. If the thyristors are each triggered at angle after their respective anode voltage waveforms ($\alpha > \theta$).

(a) Calculate the extinction angle for $\theta = 60^{\circ}$ and $\alpha = 120^{\circ}$.
(b) Sketch the load voltage waveform and calculate its Fourier coefficients a_1, b_1, c_1, and ψ_1 for the fundamental (supply frequency) component.

Solution

(a) Finding β : Using the approximate method,

$$\beta = 180 + \theta - \Delta \qquad \rightarrow \qquad \Delta = 15^{\circ} - 20^{\circ}$$

$$\beta_1 = 180^{\circ} + 60^{\circ} - 15^{\circ} = 225^{\circ}$$

$$\beta_2 = 180^{\circ} + 60^{\circ} - 20^{\circ} = 220^{\circ}$$

$$\therefore \quad \beta = \frac{\beta_1 + \beta_2}{2} = \frac{225^{\circ} + 220^{\circ}}{2} = 222.5^{\circ}$$

(b) The load voltage waveform is as shown in Fig.5.17.The Fourier coefficients are

$$a_1 = \frac{V_m}{2\pi}(\cos 2\alpha - \cos 2\beta) = \frac{V_m}{2\pi}(-0.5 - 0.08) = -0.0923V_m$$

$$b_1 = \frac{V_m}{2\pi}[2(\beta - \alpha) - \sin 2\beta + sin2\alpha]$$

$$= \frac{V_m}{2\pi}\left[2\left(\frac{222.5^{\circ} - 220^{\circ}}{180}\right)\pi - \sin 445^{\circ} + \sin 240^{\circ}\right] = 0.27V_m$$

$$c_1 = \sqrt{a_1^2 + b_1^2} = \sqrt{(-0.0923)^2\, {V_m}^2 + (0.27)^2\, {V_m}^2} \cong 0.28V_m$$

$$\psi_1 = tan^{-1}\frac{a_1}{b_1} = tan^{-1}\frac{-0.0923}{0.27} = -18.82^{\circ}$$

Example 5.14

A pair of thyristors connected in inverse-parallel is controlled so as to gate at identical points of their respective anode voltages. This device controls the flow of current through a series *R-L* load having a phase-angle of 30◦. The supply voltage is given by $v = V_m \sin\omega t$.

(a) Sketch one cycle of the load voltage waveform $v(\omega t)$ for a firing angle $\alpha = 90^\circ$. Indicate on your diagram the extinction angle β at the end of the completed conduction interval. Estimate, roughly, the conduction angle $\beta - \alpha$.

(b) Calculate, from first principles, an expression for the half-wave average value of the load voltage.

(c) The coefficient a_1 is given by

$$a_1 = \frac{V_m}{2\pi}(\cos 2\alpha - \cos 2\beta)$$

Derive an expression for the corresponding coefficient b_1 in terms of the firing angle α and current extinction angle β.

Solution

(a) $\theta = 30^\circ$, $\Delta = 5^\circ$

$\beta = 180 + 30 - \Delta = 210^\circ - 5^\circ = 205^\circ$

σ = conduction angle = $\beta - \alpha = 205^\circ - 30^\circ = 175^\circ$

(b) For half -wave, the average value is

$$V_{av(h.w)} = \frac{1}{2\pi}\int_0^{\beta-\pi} V_m \sin\omega t\, d\omega t + \frac{1}{2\pi}\int_\alpha^{\pi} V_m \sin\omega t\, d\omega t$$

$$= \frac{V_m}{2\pi}[(-\cos\omega t)\Big|_0^{\beta-\pi} + (-\cos\omega t)\Big|_\alpha^{\pi}]$$

$$= \frac{V_m}{2\pi}[-\cos(\beta - \pi + 1 + 1 + \cos\alpha]$$

$$= \frac{V_m}{2\pi}[2 + \cos\alpha - \cos(\pi - \beta)]$$

$$= \frac{V_m}{2\pi}[2 + \cos 30^\circ - \cos 205^\circ] = 1.95\, V_m$$

(c) $a_1 = \frac{V_m}{2\pi}[\cos 2\alpha - \cos 2\beta]$

$$b_1 = \frac{1}{\pi}\int_0^{2\pi} v_L(\omega t)\sin\omega t\, d\omega t$$

$$= \frac{1}{\pi}\int_0^{\beta-\pi} V_m \sin^2\omega t\, d\omega t + \frac{1}{\pi}\int_\alpha^{\beta} V_m \sin^2\omega t\, d\omega t + \int_{\alpha+\pi}^{2\pi} V_m \sin^2\omega t\, d\omega t$$

$$\therefore \quad b_1 = \frac{V_m}{2\pi}[2(\beta-\alpha) - \sin\beta - \sin 2\alpha]$$

5.6 THREE-PHASE AC-TO-AC VOLTAGE CONTROLLERS

5.6.1 Fully-Controlled Three-Phase AC Voltage Controller

In three-phase system, where large power is to be controlled, several possible circuit configurations for three-phase ac-to-ac voltage controllers are available. These various circuits are shown in Fig.5.20.

The circuits in Fig.5.20(a) and (b) are three-phase full-wave fully-controlled a.c. controller which are three-wire circuits and are difficult to analyse. In both these circuits, for current to flow, it is necessary to trigger at least two thyristors at a time one in each phase to get the controller started by establishing a current path between the supply lines. This necessitates two firing pulses spaced at 60° apart per cycle for firing each thyristor. The operation modes are defined by the number of thyristors conducting in these modes. The firing control range is 0˚ to l50°. The triplen harmonics are absent in both these configurations.

Let us consider first the three-wire circuit with a star-connected balanced resistive load as shown in Fig. 5.21. The analysis of operation of this three-phase a.c. controller can be understood by observing that the three-phase star-connected supply is applied to the star-connected resistive-load through two inverse-parallel thyristors in each phase. The six thyristors are turned on in the sequence T_1-T_2-T_3-T_4-T_5-T_6 at 60° intervals (one-sixth of the time period ($T=2\pi/\omega$) of a complete cycle) and the gate signals are remain throughout the entire conduction angle.

For current to flow it is necessary to trigger at least two thyristors at a time. Hence at any interval, current flows in either three phases or two phases whereas the third phase is open, or no thyristor may be on and the instantaneous output voltages to the load are either line-to-neutral

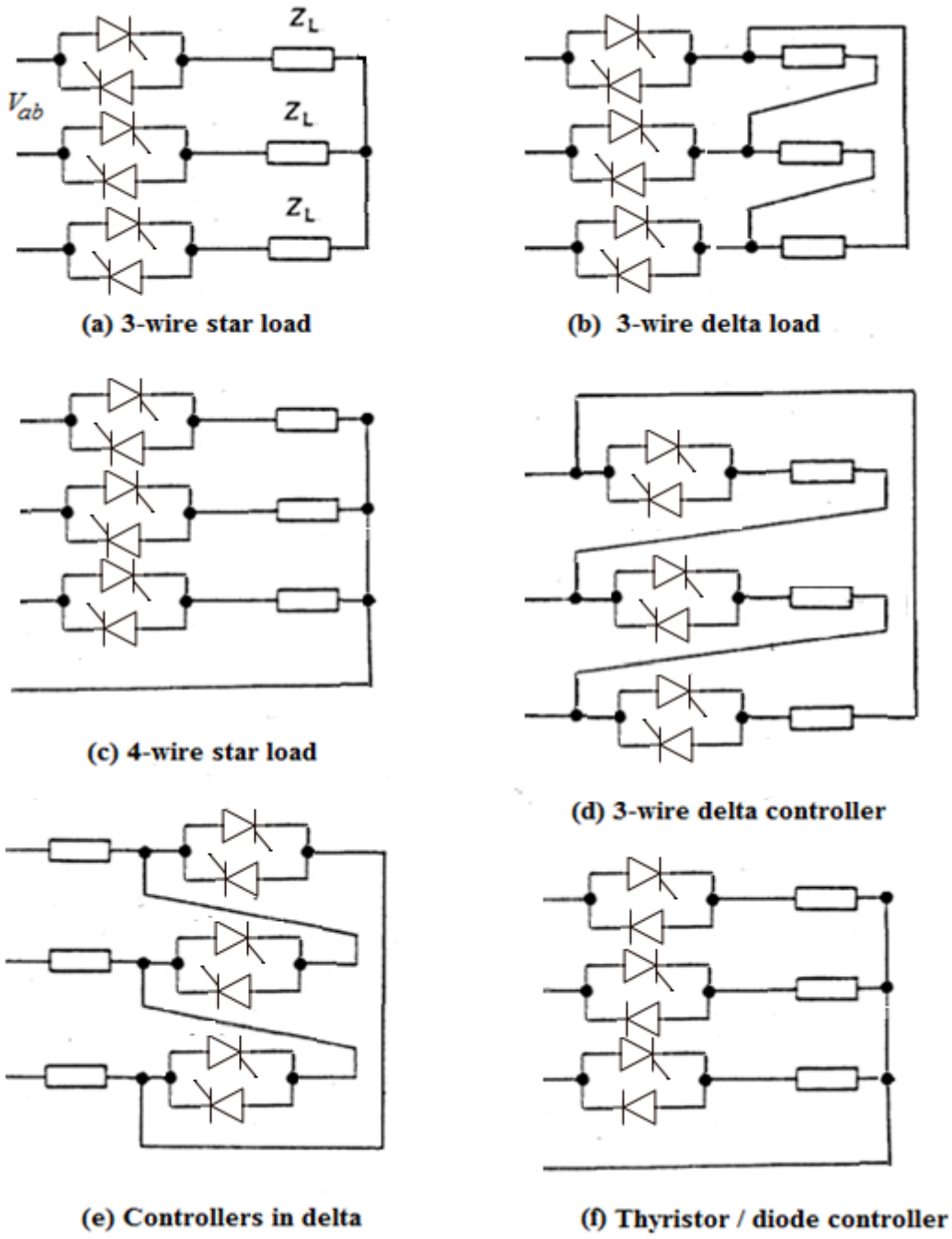

Fig.5.20 Typical three-phase a.c. voltage controller circuit configurations.

voltages (three thyristors on), or one-half of the line-to-line voltage (two thyristors on) or zero (no thyristor on).The thyristors are triggered after a delay angle α from the natural commutation point. The natural commutation point is the starting of a cycle with ωt = 60˚ of output voltage waveform, if six thyristors are replaced by diodes.

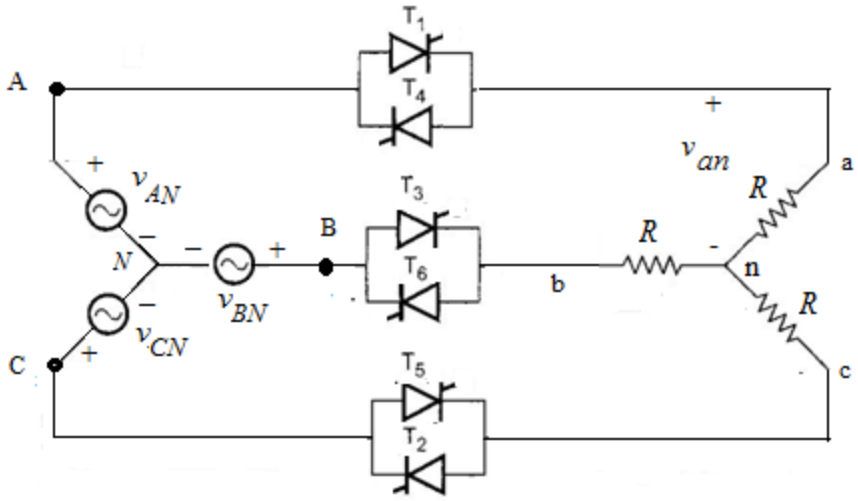

Fig.5.21 Three-phase a.c. voltage controller with star-connected *R*-load.

In the voltage controller of Fig.5.21, depending on the firing angle α, there may be three operating modes as follows:

1. Operating Mode-I: $0 \leq \alpha \leq 60°$

This mode is also known as mode 2/3. There are periods when three thyristors are conducting, one in each phase for, either direction or periods when just two thyristors conduct. To understand the operation of the three-phase controller in mode-I , consider the output phase voltage waveform v_{an} with $\alpha = 30°$ shown in Fig. 5.22. Assume that at $\omega t = 0$, the

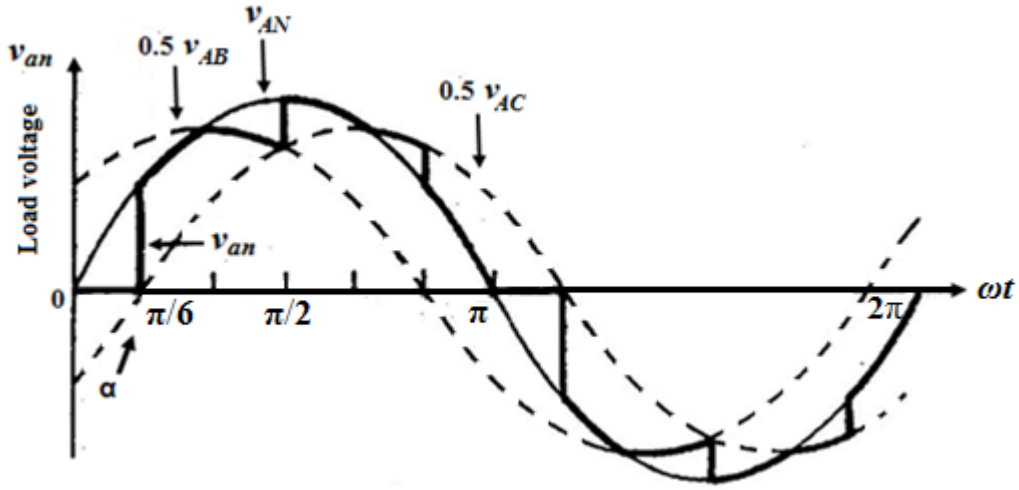

Fig.5.22 Operating Mode-I: $0 \leq \alpha \leq 60°$, $\alpha = 30°$ with *R*-load.

two thyristors T_5 and T_6 are conducting, and the current through the *R*-load in phase-a is zero making $v_{an} = 0$. At ωt = 30°, T_1 is triggered by a gate pulse and starts conducting; T_5 and T_6 remain on and the output voltage is equal to the phase voltage v_{an} . The current in T_6 reaches zero at 60°, turning T_6 off. With T_1 and T_6 staying on, $v_{an} = 0.5\ v_{AB}$. At α = 90°, T_2 is turned on, the three thyristors T_1, T_2, and *T6* are then conducting and the output voltage = v_{AN} . At 120°, T_6 turns off, leaving T_1 and T_2 on, so $v_{an} = 0.5\ v_{AC}$. Thus with the progress of firing in sequence until or α = 60°, the number of the thyristors conducting at a particular instant alternates between two and three.

The instantaneous output phase voltage is therefore, depends on the number of conducting devices which, in turns, constructs its wave shape and it can be determined from Fig.5.22 as follows:

$v_{an} = 0$	For $0 \le \omega t < \pi/6$
$v_{an} = v_{AN}$	For $\pi/6 \le \omega t < \pi/3$
$v_{an} = 0.5\ v_{AB}$	For $\pi/3 \le \omega t < \pi/2$
$v_{an} = v_{AN}$	For $\pi/2 \le \omega t < 2\pi/3$
$v_{an} = 0.5\ v_{AC}$	For $2\pi/3 \le \omega t < 5\pi/6$
$v_{an} = v_{AN}$	For $5\pi/6 \le \omega t < \pi$
$v_{an} = 0$	For $\pi \le \omega t < 7\pi/6$
$v_{an} = v_{AN}$	For $7\pi/6 \le \omega t < 4\pi/3$
$v_{an} = 0.5\ v_{AB}$	For $4\pi/3 \le \omega t < 3\pi/2$
$v_{an} = v_{AN}$	For $3\pi/2 \le \omega t < 5\pi/3$
$v_{an} = 0.5\ v_{AC}$	For $5\pi/3 \le \omega t < 11\pi/6$
$v_{an} = v_{AN}$	For $11\pi/6 \le \omega t < 2\pi$

The gating sequence can be generated by obtaining a pulse signal at the positive zero crossing of the supply phase voltage v_{an} . These pulses are, then , delayed by angles α , α + π/3 and α + 2π/3 for gating T_1 , T_3 and T_5. Similarly we have to generate pulses with delay angles π+ α, 4π/3+α and 5π/3+α for gating T_2, T_4, and T_6 .

2. Operating Mode-II: 60° ≤ α ≤ 90°

This mode is also known as Mode 2/2 in which two thyristors, one in each phase, always conduct. For example when α = 75° the output voltage waveform is as shown in Fig.5.23.

Just prior to or α = 75°, thyristor T_5 and T_6 were conducting and $v_{an} = 0$. At α =75°, T_1 is turned on, T_6 continues to conduct while T_5 turns off as v_{CN} is negative; $v_{an} = 0.5\ v_{AB}$. When T_2 is turned on at α = l35°, T_6 is turned off and on and $v_{an} = 0.5\ v_{AC}$. The next thyristor to turn on is T_3, which turns off T_1 and $v_{an} = 0$. One thyristor is always turned off when

another is turned on in this range of the triggering angle α and the output is either one-half line-to-line voltage or zero.The gating sequence can be generated by obtaining a pulse signal at the positive zero crossing of the

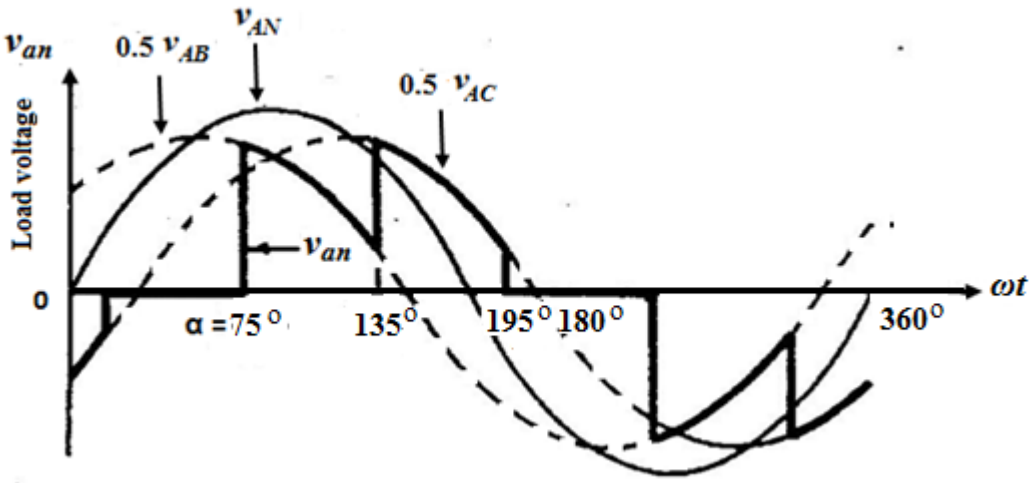

Fig.5.23 Operating Mode-II: $60° \leq \alpha \leq 90°$, $\alpha = 75°$ with *R*-load.

supply phase voltage v_{an} . These pulses are, then, delayed by angles α , $\alpha + 2\pi/3$, and $\alpha + 4\pi/3$ for gating T_1 , T_3 and T_5. Similarly we have to generate pulses with delay angles $\pi+ \alpha$, $5\pi/3+\alpha$, and $7\pi/3+\alpha$ for gating T_2, T_4, and T_6.

3. Operating Mode-III: $90° \leq \alpha \leq 150°$

This mode is also known as Mode 0/2 in which two thyristors conduct in two phases whereas the third phase is open. The output phase voltage, for example, is shown in Fig.5.24 for α =120°.

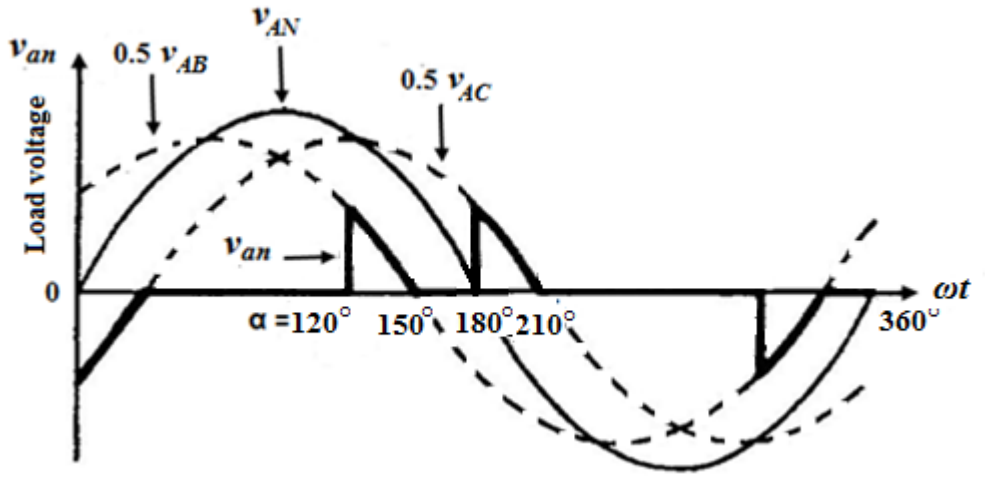

Fig.5.24 Operating Mode-III: $90° \leq \alpha \leq 120°$, $\alpha = 120°$ with *R*-load.

For the interval α = 0 to α = 120°, no thyristors were conduct and v_{an} = 0. At α = l20°, thyristor T_1, is triggered while T_6 has been already triggered. Since v_{AB} is positive, T_l and T_6 are forward-biased and they begin to conduct and v_{an} = 0.5 v_{AB}. Both T_l and T_5 turn off when v_{AB} becomes negative. When a gate signal is given to T_2, it turns on and T_1 turns on again. For α > 150°, there is no period when two thyristors are conducting and the output voltage is zero at α = l50°. Thus, the range of the firing angle control is 0° ≤ α ≤ 150°.

5.6.2 Analytical Properties of the Output Voltage Waveform

The procedure for obtaining an expression of the *rms* value of the output voltage per phase for balanced star-connected *R*-load, which depends on the range of the triggering angle α , as discussed before . If we define the instantaneous input phase voltages, taking v_{an} as reference, as

$$\left.\begin{aligned} v_{AN} &= V_m \sin \omega t \\ v_{BN} &= V_m \sin (\omega t - 2\pi / 3) \\ v_{CN} &= V_m \sin (\omega t - 4\pi / 3) \end{aligned}\right] \qquad (5.63)$$

then the instantaneous input line-to-line voltages are

$$\left.\begin{aligned} v_{AB} &= \sqrt{3}\, v_{AN} = \sqrt{3}\, V_m \sin (\omega t + \pi/6) \\ v_{BC} &= \sqrt{3} v_{BN} = \sqrt{3}\, V_m \sin (\omega t - \pi/2) \\ v_{CA} &= \sqrt{3}\, v_{CN} = \sqrt{3}\, V_m \sin (\omega t - 7\pi/6) \end{aligned}\right] \qquad (5.64)$$

The *rms* values of the output voltage waveform per phase for *R*-load for the three ranges of the triggering angle are found using Eq.(5.4) as follows:

For 0 ≤ α ≤ 60°,

$$V_L = \sqrt{3}V_m \left[\frac{2}{2\pi}\left[\int_{\alpha}^{\pi/3} \frac{(sin\omega t)^2}{3} d\omega t + \int_{\pi/2}^{\alpha+\pi/2} \frac{(sin\omega t)^2}{4} d\omega t + \int_{\alpha+\pi/3}^{2\pi/3} \frac{(sin\omega t)^2}{3} d\omega t + \int_{\pi/2}^{\alpha+\pi/2} \frac{(sin\omega t)^2}{4} + \int_{\alpha+2\pi/3}^{\pi} \frac{(sin\omega t)^2}{3} d\omega t\right]\right]^{1/2} \qquad (5.65)$$

This leads to

$$V_L = \sqrt{3}V_m\sqrt{\frac{1}{\pi}\left(\frac{\pi}{6}-\frac{\alpha}{4}+\frac{sin2\alpha}{8}\right)} \tag{5.66}$$

For $60 \le \alpha \le 90°$,

$$V_L = \sqrt{3}V_m\left[\frac{2}{2\pi}\left[\int_{\alpha+\frac{\pi}{2}-\frac{\pi}{3}}^{\alpha+\frac{5\pi}{6}-\frac{\pi}{3}}\frac{(sin\omega t)^2}{4}d\omega t+\int_{\alpha+\frac{\pi}{2}-\frac{\pi}{3}}^{\alpha+\frac{5\pi}{6}-\frac{\pi}{3}}\frac{(sin\omega t)^2}{4}d\omega t\right]\right]^{1/2}$$

$$V_L = \sqrt{3}V_m\sqrt{\frac{1}{\pi}\left(\frac{\pi}{12}-\frac{3sin2\alpha}{16}+\frac{\sqrt{3}cos2\alpha}{16}\right)} \tag{5.67}$$

For $90 \le \alpha \le 150°$,

$$V_L = \sqrt{3}V_m\left[\frac{2}{2\pi}\left[\int_{\alpha+\frac{\pi}{2}-\frac{\pi}{3}}^{\pi}\frac{(sin\omega t)^2}{4}d\omega t+\int_{\alpha+\frac{\pi}{2}-\frac{\pi}{3}}^{\pi}\frac{(sin\omega t)^2}{4}d\omega t\right]\right]^{1/2}$$

$$V_L = \sqrt{3}V_m\sqrt{\frac{1}{\pi}\left(\frac{5\pi}{24}-\frac{\alpha}{4}-\frac{sin2\alpha}{16}+\frac{\sqrt{3}cos2\alpha}{16}\right)} \tag{5.68}$$

where V_L = *rms* load voltage per-phase.

V_m = Peak value of the supply voltage per-phase.

5.7 OTHER TYPES OF THREE-PHASE AC CONTROLLERS

Other three-phase configurations are shown in Fig.5.20 (c) and (d) that can be considered as three single-phase a.c. controllers working independently of each other and they are easy to analyse. In Fig.5.20 (c), the thyristors are to be rated to carry line currents and withstand phase voltages, whereas in Fig. 5.20 (d) they should be capable of carrying phase currents and withstand the line voltages. Also, in Fig. 5.20 (d) the line currents are free from triplen harmonics while these are present in the closed delta. The power factor in Fig.5.20 (d) is slightly higher. The Firing angle control range for both these circuits is 0° to 180° for *R*-load.

Another configuration is shown in Fig.5.20 (e) when the controllers are delta connected and the load is connected between the supply and the converter. Here, current can flow between two lines even if one thyristor is conducting, so each thyristor requires one fixing pulse per cycle. The voltage and current ratings of the thyristors are nearly the same as those of the circuit in Fig.5.20 (d).

It is also possible to reduce the number of thyristors to three and replace the other three thyristors by diodes in three-phase controller as shown in Fig.5.20 (f). This controller is called thyrode controller or half-controlled a.c. controller.

Three- Phase Delta-Connected AC Voltage Controller with Balanced Resistive Load

The circuit of a three-phase, delta-connected a.c. voltage controller (termed as three-phase ac-to-ac voltage regulator) with balanced resistive load is shown in Fig.5.25.

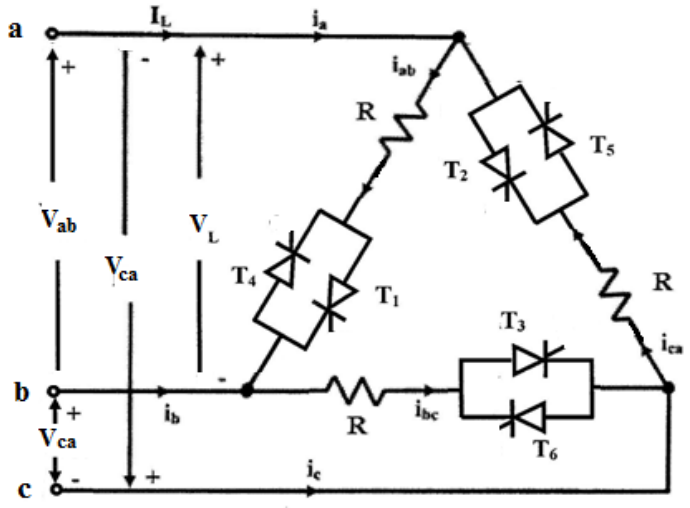

Fig.5.25 Three-phase delta-connected a.c. voltage controller with *R*-load.

It may be noted that the resistance connected in all three phases are equal. Two thyristors connected back-to-back are used per-phase, thus needing a total of six thyristors. As stated earlier, the numbering scheme may be noted. It may be observed that one phase of the balanced circuit is similar to that used for single-phase a.c. voltage controller described in Section 5.1. Since the phase current in a balanced three-phase system is only (l/√3) of the line current, the current rating of the thyristors would be lower than that if the thyristors are placed in the line.

Assuming the line voltage V_{ab} as the reference, the instantaneous input line voltages are,

$$\left.\begin{aligned} v_{ab}(\omega t) &= V_m \sin\omega t \\ v_{bc}(\omega t) &= V_m \sin(\omega t - 120°) \\ v_{ca}(\omega t) &= V_m \sin(\omega t - 240°) \end{aligned}\right\} \qquad (5.69)$$

It may be noted that V_m is the peak value of the line voltage in this case. The waveforms of the input line voltages, phase and line currents, and the thyristor gating signals, for α = l20˚ are shown in Fig.5.26.

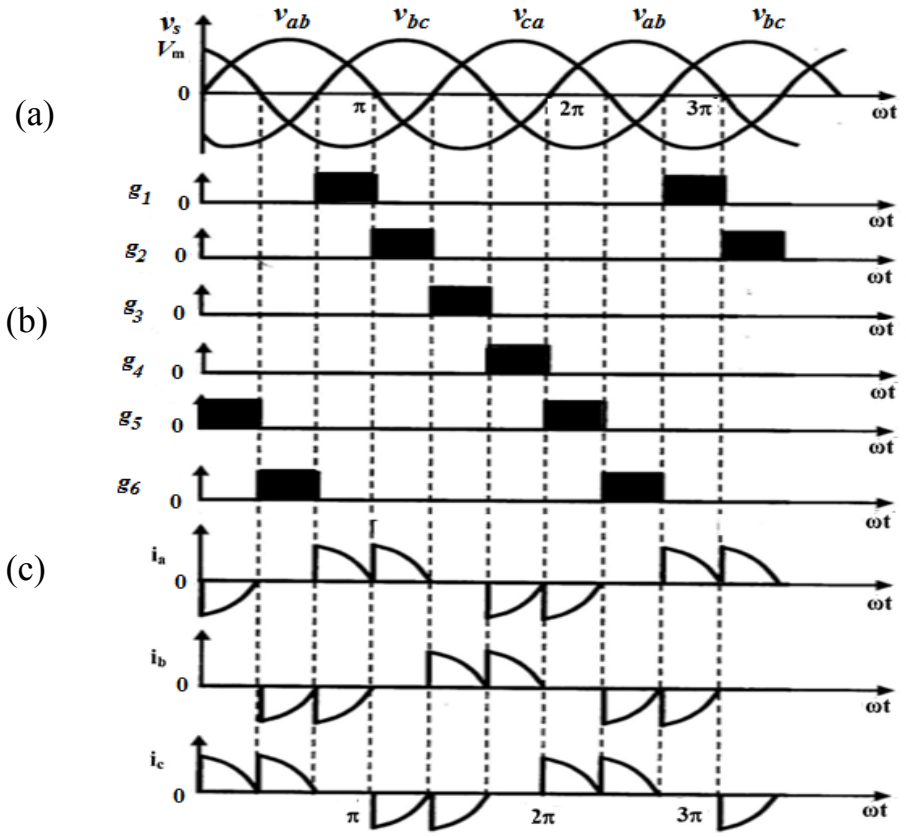

Fig.5.26 Waveforms for delta-connected three-phase a.c. voltage controller with α =120˚: (a) Input line voltages, (b) Thyristors gate pulses, and (c) Load line currents.

Example 5.15

The three-phase a.c. voltage controller shown in Fig.5.21 is used to supply a star-connected resistive load of R =15 Ω. The line-to-line voltage is 400 V *rms* and f = 50 Hz. For the delay α = π/6 determine:

(a)The output power.

(b)The input power factor *PF*.

(c) Find an expression for the instantaneous phase load voltage .

Solution

(a) For $0^\circ \leq \alpha < , 60^\circ$

$$V_L = \sqrt{3}V_m\sqrt{\frac{1}{\pi}\left(\frac{\pi}{6}-\frac{\alpha}{4}+\frac{sin2\alpha}{8}\right)}$$

$$V_m = \frac{400\times\sqrt{2}}{\sqrt{3}} = 326.5\text{ V}$$

$$V_L = \sqrt{3}\times 326.5\times\sqrt{\frac{1}{\pi}\left(\frac{\pi}{6}-\frac{\pi}{6\times 4}+\frac{sin60^\circ}{8}\right)} = 226.2\text{ V}$$

$$I_L = \frac{V_L}{R} = \frac{226.2}{15} = 15.08\text{ A}$$

$$P_L = 3I_L^2R = 3\times(15.08)^2\times 15 = 10.233\text{ kW}$$

(b) Since the load is star-connection the phase current = line current. Thus the input volt-ampere power is

$$S = 3V_s\ I_L = 3\times 230\times 15.08 = 10.405\text{ kVA}$$

$$PF = \frac{P_L}{S} = \frac{10.233}{10.405} = 0.983 \quad \text{lagging}$$

$$V_L = \sqrt{3}\times 326.5\times\sqrt{\frac{1}{\pi}\left(\frac{\pi}{6}-\frac{\pi}{6\times 4}+\frac{sin60^\circ}{8}\right)} = 226.2\text{ V}$$

$$I_L = \frac{V_L}{R} = \frac{226.2}{15} = 15.08\text{ A}$$

$$P_L = 3I_L^2R = 3\times(15.08)^2\times 15 = 10.233\text{ kW}$$

(c) If we take phase – a for the input voltage as reference ,
$v_{AN} = 230\sqrt{2}\ \sin\omega t = 326.5\ \sin\omega t$, the input line voltages are ,

$v_{AB} = 400\ \sqrt{2}\ \sin(\omega t + \pi/6) = 565.6\ \sin(\omega t + \pi/6)$
$v_{BC} = 565.6\ \sin(\omega t - \pi/2)$
$v_{CA} = 565.6\ \sin(\omega t - 7\pi/6)$

For α = π/6 ,the instantaneous load phase voltage is therefore,

$v_{an} = 0$ For $0 \leq \omega t < \pi/6$

$v_{an} = v_{AN} = 326.5 \sin \omega t$ For $\pi/6 \leq \omega t < \pi/3$

$v_{an} = 0.5\, v_{AB} = 282.8 \sin(\omega t + \pi/6)$ For $\pi/3 \leq \omega t < \pi/2$

$v_{an} = v_{AN} = 326.5 \sin \omega t$ For $\pi/2 \leq \omega t < 2\pi/3$

$v_{an} = 0.5\, v_{AC} = 282.8 \sin(\omega t + 7\pi/6)$ For $2\pi/3 \leq \omega t < 5\pi/6$

$v_{an} = v_{AN} = 326.5 \sin \omega t$ For $5\pi/6 \leq \omega t < \pi$

$v_{an} = 0$ For $\pi \leq \omega t < 7\pi/6$

$v_{an} = v_{AN} = 326.5 \sin \omega t$ For $7\pi/6 \leq \omega t < 4\pi/3$

$v_{an} = 0.5\, v_{AB} = 282.8 \sin(\omega t + \pi/6)$ For $4\pi/3 \leq \omega t < 3\pi/2$

$v_{an} = v_{AN} = 326.5 \sin \omega t$ For $3\pi/2 \leq \omega t < 5\pi/3$

$v_{an} = 0.5\, v_{AC} = 282.8 \sin(\omega t + 7\pi/6)$ For $5\pi/3 \leq \omega t < 11\pi/6$

$v_{an} = v_{AN} = 326.5 \sin \omega t$ For $11\pi/6 \leq \omega t < 2\pi$

PROBLEMS

5.1 A single-phase full-wave a.c. voltage controller shown in Fig.5.1 has a resistive load of R = 10 Ω and the input voltage is V_s = 120 V (*rms*), 50Hz. The firing angles of thyristors T_1 and T_2 are equal : $\alpha_1 = \alpha_2 = \frac{\pi}{2}$. Determine:

(a) The *rms* value of the output voltage V_L.
(b) The input power factor.
(c) The average and *rms* values of the thyristor currents.

[Ans: (a) 141.44 V, (b) 0.707 lagging , (c) I_{Tav} = 4.5 A, I_{Trms} = 10 A]

5.2 A pair of thyristors connected in inverse-parallel, as shown in Fig.5.27, is used to supply adjustable current to a resistive load of R = 8 Ω. If the supply has an input voltage of 120 V (*rms*) and the thyristors are each triggered at an angle α after their respective anode voltage zeros. For $\alpha = 60°$:

(a) Calculate the *rms* value V_L of the load voltage and the *rms* value I_L of the load current.
(b) Estimate the power absorbed by the load and the input power factor.
(c) Calculate the average and *rms* values of the thyristor current.
(d) Calculate the *rms* value of the fundamental component of the load voltage V_{L1} and its phase angle ψ_1.

Fig.5.27

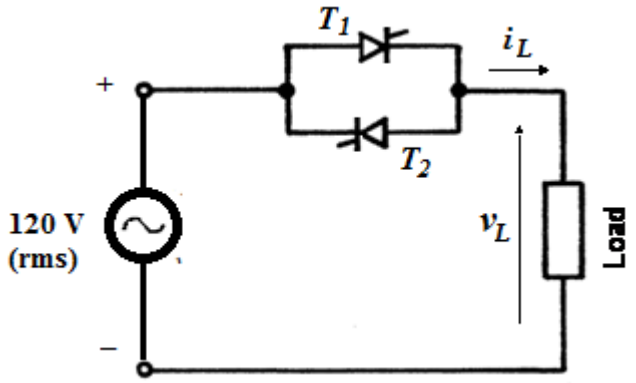

[Ans : (a) 107.6 V, 13.45 A, (b) 1447.62 W, 0.897 Lagging, (c) 5.06 A, 10.9 A, (d) 100.6 V, -16.57˚]

5.3 A single-phase full-wave a.c. voltage controller consists of two thyristors connected in inverse-parallel as shown in Fig.5.1. The supply voltage is V_s = 230 V (*rms*) at 50 Hz. The controller is used to regulate power to 1.5kW electric oven. Find the triggering angle α such that the power delivered to the oven is 0.5 kW.

[Ans: $\alpha = 74.5^o$]

5.4 A single-phase a.c. voltage controller consists of two thyristors connected in inverse-parallel as shown in Fig.5.1. The supply voltage is V_s = 230 V (*rms*) at 50 Hz. The controller is used as a static step-down voltage transformer to control power transfer to a 20 Ω resistor. The triggering mode of the two thyristors is symmetrical with $\alpha = 60°$.

(a) Sketch compatible waveforms for the supply, load and thyristor voltages.
(b) Calculate the *rms* value of the load voltage.
(c) Determine the input power factor of the circuit.
(d) Calculate the average value of the thyristor current.

(e) Explain why we have a power factor not unity while the load is purr resistance ?

[Ans: (b) 207 V, (c) 0.896 , (d) 10.31A]

5.5 A pair of thyristors connected in inverse-parallel, as shown in Fig.5.1, is used to supply adjustable current to a resistive load of R = 20 Ω. If the supply voltage is v_s = 240 sinωt and the thyristors are each triggered at an angle α after their respective anode voltage zeros. For α = 60°:

(a) Calculate the *rms* value V_L of the load voltage and the *rms* value I_L of the load current, hence estimate the power absorbed by the load.
(b) Calculate the *rms* value of the fundamental component of the load voltage V_{L1} and its phase angle ψ_1.
(c) Calculate the displacement factor, the distortion factor and the power factor.
(d) If thyristor T_2 *i*s fail to operate , what effect would this have on the value of the output voltage of the converter at α = 60°.

[Ans: (a) 152.27 V, 7.6 A, 1157 W, (b) 201.13 V, 142.2 V, -16.54°, (c) 0.958, 0.9358, 0.897, (d) If T_2 fails to operate, the circuit will behave as a half-wave controlled rectifier :

$$V_{dc} = \frac{V_m}{2\pi}\,(1 + cos\alpha) = \frac{240}{2\pi}\,(1 + \cos 60)° = 57.32\,V\ ]$$

5.6 A single-phase full-wave a.c. voltage controller consists of two thyristors connected in inverse-parallel as shown in Fig.5.28. The supply voltage is V_s = 220 V (*rms*) at 50 Hz. The controller is used to control heater element of 2500 W in an electric oven. The triggering mode of the thyristors is symmetrical with α =30°.

(a) Sketch compatible waveforms for the supply, load and thyristor voltages.
(b) Calculate the *rms* value of the load voltage and current.
(c) Determine the input power factor of the circuit.
(d) Calculate the average value of the thyristor current.

[Ans : (b) 216.8 V , 11.53 A, (c) 0.983]

Fig.5.28

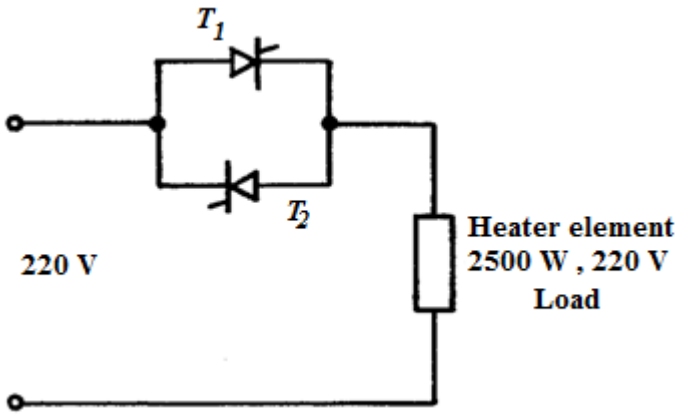

5.7 A pair of thyristors connected in inverse-parallel is used to supply adjustable current to a resistive load of R =10 Ω. If the supply voltage is vs = 220 √2 sinωt and the thyristors are each triggered at an angle α after their respective anode voltage zeros,

(a) Sketch the circuit arrangement of the converter.

(b) Prove that the *rms* value V_L of the load voltage is given by

$$V_L = V_m \sqrt{\frac{1}{2\pi}\left[(\pi - \alpha) + \left(\frac{sin2\alpha}{2}\right)\right]}$$

(c) Calculate the value of V_L for α = 30° and sketch its waveform.

(d) Calculate the *rms* value I_L of the load current and the power delivered to the load.

[Ans: (c) 216.8 V, (d) 21.68 A , 4.7 kW]

5.8 A pair of thyristors connected in inverse-parallel is used to supply adjustable current to a resistive load of R =6 Ω in series with an inductance of L = 33 mH. If the supply voltage is V_s is 240 V, 50 Hz and the thyristors are each triggered at an angle α = 60˚ after their respective anode voltage zeros, find (a) the conduction angle of each thyristor, (b) the *rms* output voltage .

[Ans: (a)162.3 ˚, (b) 225.29 V]

5.9 A single-phase a.c. controller shown in Fig.5.1 is used to supply adjustable current to a resistive load of R =10 Ω. If the supply voltage is v_s = 230 √2 sinωt and the thyristors are each triggered at an angle α after their respective anode voltage zeros,

(a) Prove that the *rms* value I_o of the adjustable load current is given by

$$I_o = \frac{V_m}{\sqrt{2}R}\sqrt{1 - \frac{\alpha}{\pi} + \frac{sin2\alpha}{\pi}}$$

(b) Calculate the value of I_o for α = 45 ° and sketch its waveform.
(c) Calculate the power delivered to the load and the power factor of the circuit.

[Ans: (b) 22 A , (c) 4796.1 W , 0.952]

5.10 A pair of thyristors connected in inverse-paralle, Fig.5.1 , is used to supply adjustable current to a resistive load of 20 Ω. If the supply voltage is $v_s = V_m$ sin ωt and the thyristors are each triggered at an angle α after their respective anode voltage zeros,

(a) Sketch the load current waveform for α = 60°.
(b) Obtain an expression for the *rms* value I_L of the load current in terms of V_m, R and α .
(c) Calculate the value of I_L for α = 60° if V_m = 350 V.
(d) Calculate the power dissipated at the load for α = 60° and the power factor of the circuit.
(e) Calculate the fundamental (first harmonic) component of the load voltage when α = 90°.

[Ans: (c) 11.1 A, (d) 2464.2 W, (e) 146.6 V]

5.11 A pair of thyristors connected in inverse-parallel as shown in Fig.5.1 is used to control the power flow to heating load from an ideal sinusoidal single-phase supply $v_s(\omega t)$ = 325 sinωt. These thyristors are gated to produce symmetrical angle triggering of the current waveform.

(a) If the heating load is pure resistance of R = 20 Ω, calculate the *rms* value of the output voltage and the power dissipation in the load at α = 90˚.
(b) The fundamental component of the load current at α = 90° can be described by the expression

$$i_1(\omega t) = 0.83\,\frac{V_s}{R}\sin(\omega t - 30°)$$

where V_s = *rms* value of the supply voltage .

Calculate the displacement factor, distortion factor and hence the power factor of the circuit.

(c) If the load in (a) is replaced by a series resistor-inductor, estimate (do not calculate) the extinction angle of the current β for $\theta = 50^o$ and $\alpha = 110^o$.

[Ans: (a) 162.5 V, 1320 W, (b) 0.843, 0.830, 0.700, (c) 212.5^o]

5.12 The three-phase bidirectional a.c controller shown in Fig.5.21 suppli a star-connected resistive load of $R = 20\ \Omega$ and the line-to-line input voltage is 415 V *rms*, 50 Hz. For firing angle $\alpha = 45^\circ$, determine (a) The *rms* value of the output voltage per phase, (b) The line current, (c) The output power P_o, and (d) The input power factor of the controller.

[Ans : (a) $V_L = 222.6$ V, (b) $I_L = 11.13$ A, (c) $P_o = 7438$ W, (d) $PF = 0.929$ lagging.]

5.13 The three-phase bidirectional controller shown in Fig.5.21 supplies a star-connected resistive load of $R = 10\ \Omega$ and the line-to-line input voltage is 400 V (*rms*), 50 Hz. Determine the *rms* value of the output voltage and the power delivered to the load for the following triggering angles:
(a) $\alpha = 30^\circ$, (b) $\alpha = 75^\circ$ and (c) $\alpha = 120^\circ$.

[Ans: (a) $V_L = 225$ V, $P_L = 15190$ W, (b) $V_L = 162.66$ V, $P_L = 7937$ W, and (c) $V_L = 47.83$ V, $P_L = 6863.12$ W.]

5.14 The voltage of a three-phase heating load is to be controlled by using three-phase a.c. voltage controller as shown in Fig.5.21. The three-phase supply is star-connected with 400 V, 50 Hz line-to-line voltage. The load is 40 kW, (a) Find the current and voltage ratings of the thyristors assuming safety factor of 1.25 for both the current and voltage, (b) If the two inverse-parallel connected thyristors in each phase are replaced by triacs, what will be their current and voltage ratings?

[Ans: (a) For each thyristor: 36 A, 500 V, (b) For each triac: 72.15 A, 500 V]

CHAPTER SIX

AC-AC CONVERSION: INTEGRAL-CYCLE CONTROL

6.1 INTRODUCTION

When a full supply voltage of complete cycles is applied across the load by two thyristors connected back-to-back or triac in the circuit shown in Fig.5.1, Chapter Five, followed by complete cycles of extinction, the load voltage waveforms are described as "integral-cycle" or "burst firing" control. The advantage of this form of control is that when the ON-OFF switching takes place at zero voltage, the higher order harmonics due to switching are greatly reduced. Moreover, large current transient resulting from switching at any arbitrary angle during the voltage cycle as in the case of phase-angle control, are eliminated.

6.2 SINGLE-PHASE CIRCUIT WITH VOLTAGE CONTROL BY INTEGRAL-CYCLE TRIGGERING (CASE OF RESISTIVE LOAD)

Fig. 6.1 shows a typical cycle consists of N conducting cycles in a total period of T supply cycles. The load voltage with resistive load may be defined in terms of the supply period by the following equation:

$$v_L = V_m \sin \omega t \Big|_{2\pi kT}^{2\pi(N+kT)} \qquad k = 0,1,2,\ldots. \qquad (6.1)$$

Fourier analysis of Eq.(6.1) for the period 2π is found to be indeterminate. However, the waveform of Fig.6.1(b) is periodic in the control period of T supply cycles; hence it is mathematically convenient to express v_L in terms of the control period T rather than of the supply period 2π as suggsted in reference [36], hence, Eq.(6.1) may be written as:

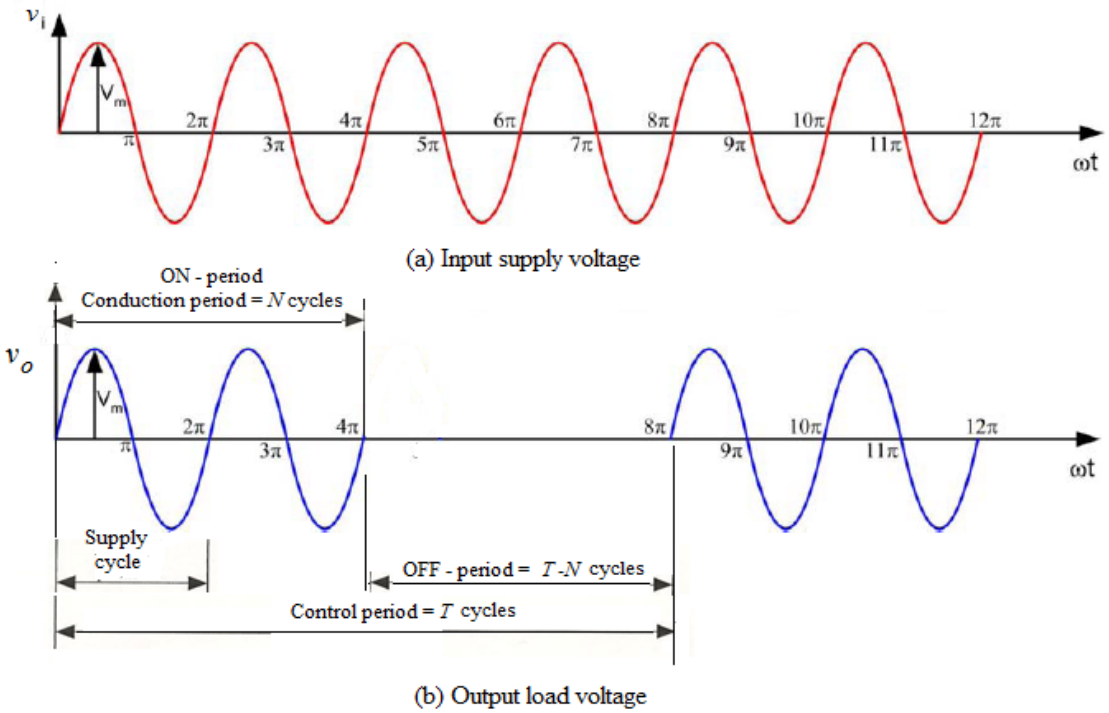

Fig.6.1 Typical load voltage waveform for integral-cycle control of resistive load for $N = 2$, $T = 4$.

$$v_L(T\omega t) = V_m \sin T\omega t \Big|_0^{2\pi(N/T)} + 0 \Big|_{2\pi(N/T)}^{2\pi} \tag{6.2}$$

where V_m is the peak value of the supply voltage. Fourier coefficients for the function of Eq.(6.2) are found to be :

For n ≠ T

$$a_0 = \frac{1}{\pi}\int_0^{2\pi(N/T)} v_L(T\omega t)d\omega t = 0 \tag{6.3}$$

$$a_n = \frac{1}{\pi}\int_0^{2\pi(N/T)} v_L(T\omega t)\cos n\omega t\, d\omega t \tag{6.4}$$

$$= \frac{V_m T}{\pi(T^2 - n^2)}\left[1 - \cos\frac{2\pi nN}{T}\right] \tag{6.5}$$

$$b_n = \frac{1}{\pi}\int_0^{2\pi(N/T)} v_L(T\omega t)\sin n\omega t\, d\omega t \tag{6.6}$$

$$= \frac{V_m T}{\pi(T^2 - n^2)}\left[-\sin\frac{2\pi nN}{T}\right] \tag{6.7}$$

The magnitude c_n of the n^{th} harmonic, for n≠T, is found to be:

$$c_n = \sqrt{a_n^2 + b_n^2} \tag{6.8}$$

$$= \frac{V_m T}{\pi(T^2 - n^2)} [2(1 - \cos\frac{2\pi nN}{T})]^{\frac{1}{2}} \tag{6.9}$$

or $$c_n = \frac{V_m T}{\pi(T^2 - n^2)} 2 \sin\left(\frac{\pi nN}{T}\right) \tag{6.10}$$

The phase angle Ψ_n between the supply voltage and the n^{th}current harmonic is given by

$$\Psi_n = \tan^{-1}\frac{a_n}{b_n} \tag{6.11}$$

Substituting Eqs.(6.5) and (6.7) into Eq.(6.11) above yields

$$\Psi_n = \tan^{-1}[\frac{1 - \cos(2\pi nN/T)}{-\sin(2\pi nN/T)}] \tag{6.12}$$

$$= \tan^{-1}[\frac{\sin(\pi nN/T)}{-\cos(\pi nN/T)}] \tag{6.13}$$

6.3 HARMONIC AMPLITUDE SPECTRA OF INTEGRAL-CYCLE WAVEFORMS

Integral-cycle control is found to generate waveforms that produce both subharmonic components of the supply frequency and higher order harmonics. Hence, this type of voltage control is differing from the phase-angle control discussed in Chapter Five which produces only higher order harmonics. For example, with integral cycle control, the case n = 1 in Eqs.(6.4) to (6.10) represents the $(1 / T)^{th}$ subharmonic of supply frequency which is generally represents the lowest subharmonic that can occur. In Fig.6.1, for example, the lowest subharmonic voltage is one-fourth of supply frequency since T = 4. The *1 / T* subharmonic is not necessarily the harmonic of smallest magnitude, since with certain values of N and T it is possible for a subharmonic to exceed the value of the supply frequency component as it will be seen from the examples of the following subsections.

6.3.1 The Supply Frequency Component (*n* =*T*)

Unlike the phase-angle control, in integral-cycle, the value $n = T$, representing the supply frequency, which forms a special case for which Eqs.(6.4) to (6.10) are indeterminate. If one proceeds from the basic integrals, the following results are obtained:

$$a_{n=T} = \frac{1}{\pi}\int_0^{2\pi(N/T)} v_L(\omega t)\cos T\omega t\, d\omega t \tag{6.14}$$

$$= \frac{V_m}{4\pi T}[-\cos 2T\omega t]_0^{2\pi N/T} = 0 \tag{6.15}$$

$$b_{n=T} = \frac{1}{\pi}\int_0^{2\pi(N/T)} v_L(\omega t)\sin T\omega t\, d\omega t \tag{6.16}$$

$$b_{n=T} = \frac{V_m}{2\pi}\left[\frac{2\pi N}{T}\right] = V_m\frac{N}{T} \tag{6.17}$$

The magnitude $c_n = T$ of the supply frequency component is therefore given in terms of the *rms* value of the supply voltage, V_s, thus

$$c_{n=T} = \sqrt{2}V_s\frac{N}{T} \qquad \text{since} \qquad V_m = \sqrt{2}V_s \tag{6.18}$$

Since $a_{n=T} = 0$, the supply frequency component of current is always in time phase with the supply voltage. However, this result does not mean that an integral-cycle circuit operates at unity power factor because, for part of the control period, the supply current is not in time phase with the supply voltage. But actually, for part of the control period during which there is no conduction, *T-N* cycles, the supply current is zero. For the waveform of Fig.6.1(b) the magnitude of the supply frequency component of current is, from Eq.(6.10), of value $2/4 = 0.5$ per unit of the corresponding sinusoidal value at the same supply voltage. It is to be noted that the magnitude of the supply frequency component of current is proportional to the number of conducting cycles *N*.

6.3.2 Zero-Value Harmonics

By examining Eq.(6.6), it is seen that, provided $n \neq T$, the term $sin(n\pi N/T)$ is zero if $n\pi / T$ has any integral value. Since $N / T \leq 1$ this means that c_n is zero for certain values of $n > 1$. Hence, $sin(n\pi N/T)$ is zero if :

$$n = \frac{Tk}{N}, \qquad \text{where k} = 1, 2, 3, \ldots\ldots \tag{6.19}$$

when $N = 2$, $T = 4$, as in Fig.6.1(b), the amplitude c_n of harmonics is zero when n =2,6,8 etc, corresponding to k = 1,3,4, respectively. The harmonic spectrum for $N = 2$, $T = 4$ is given in Fig.6.2, it is seen that the supply frequency component n = T is dominant and that the subharmonic n =3, corresponding to 3 / 4 of supply frequency, is the greatest non-supply frequency harmonic.

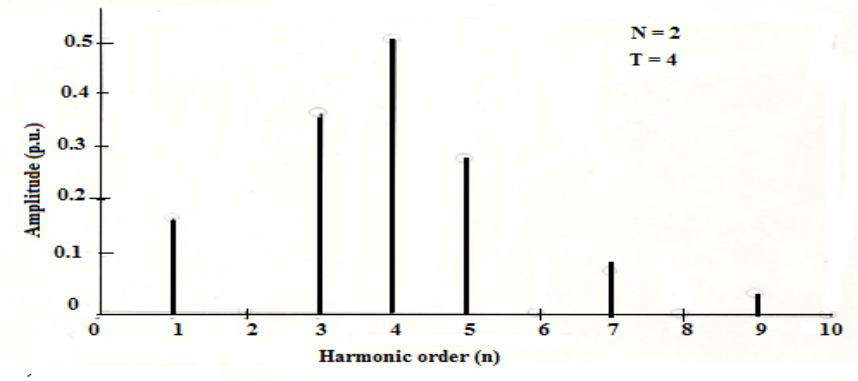

Fig.6.2 Harmonic amplitudes of load voltage for integral-cycle control for $N = 2$, $T = 4$.

6.3.3 Higher Order Harmonic Frequency Components (n > *T*)

Eq.(6.10) gives the harmonic amplitude of all higher order harmonic frequency components. The harmonic phase-angle of any indinidual harmonic is given by Eq.(6.13). However, it is found that, with certain N/T ratios give rise to subharmonic amplitudes, which exceed that of the supply frequency component. An example of this occurs in the harmonic spectrum produced with N =1, T = 4 (Fig.6.3) where, for a 50 Hz supply, the n = 3 harmonic component exceeds the T^{th} (supply frequency) component. The large subharmonic current components that produced in this technique may be used in a.c. motor drives.

Fig.6.3 Harmonic amplitude spectrum for integral-cycle waveform N=1, T=4 .

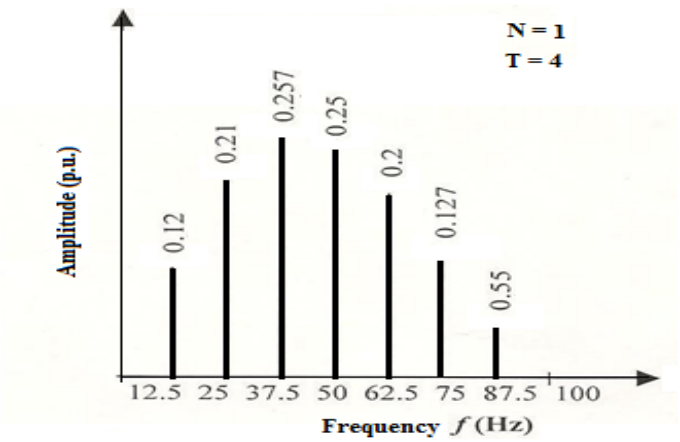

6.4 RMS LOAD VOLTAGE, LOAD POWER AND POWER FACTOR

The *rms* voltage V_L of the function $v_L(\omega t)$ in Fig.6.1(b) is given by:

$$V_L = V_s \sqrt{\frac{N}{T}} \tag{6.20}$$

with sinusoidal operation $N=T$ and therefore, $V_L=V_s$, voltage V_L is not a continuous function but can only exist at the discrete steps defined by the values of N and T. This is true in general for all voltage, current and power relationships in integral-cycle systems. In a resistive circuit the load voltage and current have identical waveforms. The average power in the load is, irrespective of waveform, given by

$$P = \frac{V_L^2}{R} \tag{6.21}$$

where R is the load resistance in (Ω).

In a circuit with resistive load of resistance R, the average power is defined by

$$P = V_s^2 \frac{N}{R\,T} = \frac{V_m^2}{2R} \times \frac{N}{T} \tag{6.22}$$

The distortion factor of the load voltage is defined by ratio of the *rms* value of the supply frequency component to the total *rms* value. For an integral-cycle waveform

$$\text{Distortion factor} = \frac{V_{L(n=T)}}{V_L} = \sqrt{\frac{N}{T}} \tag{6.23}$$

Since the displacement angle ψ_T is zero, the supply frequency component of the current is always in time-phase with the supply voltage. This does not mean that an integral-cycle circuit operates at unity power factor because, for part of the control period, the supply current is not in time-phase with the supply voltage. Indeed for part of the control cycle, there is no supply current at all, hence

$$\text{Displacement factor} = \cos\psi_T = cos\tan^{-1}\frac{a_{n=T}}{b_{n=T}} = 1 \tag{6.24}$$

The power factor is therefore:

$$PF = \text{Distortion factor} \times \text{Displacement factor} = \sqrt{N/T} \tag{6.25}$$

Example 6.1

Two thyristors are connected in inverse-parallel for control of the power flow from a single-phase a.c. supply $v_s = 300 \sin\omega t$ to a resistive load with $R = 10\ \Omega$. The thyristors are operated with integral-cycle triggering mode consisting of two cycles of conduction followed by two cycles of extinction. Calculate:

(a) The *rms* value of the output voltage.
(b) The *rms* value of the current drawn from the source.
(c) The power delivered to the load.

Solution

(a) In this case $N = 2$, $T = 4$. From Eq.(6.21), the *rms* value of the load voltage is

$$V_L = V_s \sqrt{\frac{N}{T}} = \frac{300}{\sqrt{2}} \sqrt{\frac{2}{4}} = 150\ \text{V}$$

(b) The current drawn from the source = current drawn by the load

$$I_s = I_L = \frac{V_L}{R} = \frac{150}{10} = 15\ \text{A}$$

(c) The power delivered to the load. From Eq.(6.23)

$$P = \frac{V_m^2}{2R} \times \frac{N}{T} = \frac{300^2}{2 \times 10} \times \frac{2}{4} = 2250\ \text{W}$$

Example 6.2

In a single-phase resistive circuit in which the load voltage is controlled by integral-cycle triggering mode of a pair of inverse-parallel connected thyristors as shown in Fig.5.1 (Chapter Five). The output voltage waveform consisting of 9 cycle of conduction followed by 18 cycles of extinction. If the *rms* input supply voltage is 230V, 50Hz, and $R = 20\Omega$, calculate :

(a) The *rms* value of the load current.
(b) The input power factor.
(c) Average and *rms* values of the current through the thyristors.
(d) What must be the thyristor ratings?

Solution : The given data is

$$V_s = 230\text{V},\ R = 20\ \Omega\ ,\ N = 9\ \text{ and } T = 9+18=27$$

(a) The *rms* value of the load current, $I_L = \frac{V_L}{R}$

$$\text{Hence}\quad V_L = V_s\sqrt{\frac{N}{T}} = 230\sqrt{\frac{9}{27}} = 132.8\ \text{V}$$

$$I_L = \frac{132.8}{20} = 6.64\ \text{A}$$

(b) Actual load power = $I_L^2 R = \ 6.64^2 \times 20 = 881.8\ \text{W}$

The supply current is the same as the load current, i.e.

$I_s = I_L = 6.64\ \text{A}$,

hence, the input power in VA = $I_s V_s = 6.64\ \times\ 230 = 1527.2$

Therefore the supply power factor is

$$PF = \frac{\text{Actual load power}}{\text{Input power in VA}} = \frac{881.8}{1527.2} = 0.57734$$

The power factor can also be calculate directly from Eq.(6.25) as

$$PF = \sqrt{\frac{N}{T}} = \sqrt{\frac{9}{27}} = \ \sqrt{0.3333} = 0.57734$$

(c) To find the average and *rms* values of the thyristor currents:
Since the load is resistive we can express the current through the load by

$$i(\omega t) = I_m sin\omega t$$

$$\text{where}\qquad I_m = \frac{V_m}{R} = \frac{\sqrt{2}}{R}V_s$$

Each thyristor carries half cycle during one supply period, Fig.6.4, hence the average value of the current during one supply period is

$$I_{T(av)} = \frac{1}{2\pi}\int_0^{\pi} I_m sin\omega t\ d\omega t = \frac{I_m}{2\pi}[-cos\ \pi + cos0] = \frac{I_m}{\pi}$$

Since on thyristor conducts *N* cycles in a total period of *T* cycles, hence the duty cycle of the thyristor will be *N/T* and the average current of the thyristor T_1 is :

$$I_{T1(av)} = \frac{N}{T} \times I_{T(av)} = \frac{N}{T} \times \frac{I_m}{\pi} = \frac{N}{T} \times \frac{\sqrt{2}\,V_s}{\pi \times R} = \frac{9}{27} \times \frac{\sqrt{2}}{\pi \times 20} \times 230$$
$$= 1.726 \text{ A}$$

Since both the thyristors share the load current equally, their average current will be the same, hence

$$I_{T1(av)} = I_{T2(av)} = 1.726 \text{ A}$$

Rms value of the thyristor current can be calculate as

$$I_{T(rms)} = \sqrt{\frac{1}{2\pi}\int_0^{\pi} I_m^2 sin^2\omega t \, d\omega t} = \sqrt{\frac{I_m^2}{4\pi}\int_0^{\pi} (1 - \cos 2\omega t) \, d\omega t}$$

$$I_{T1\,(rms)} = \frac{I_m}{2}\sqrt{\frac{1}{\pi}[\pi - 0 - \frac{1}{2}\sin 2\pi + \frac{1}{2}\sin 0°]} = \frac{I_m}{2} = \frac{\sqrt{2}}{2} \times \frac{V_s}{R}$$
$$= \frac{1}{\sqrt{2}} \times \frac{230}{20} = 8.13 \text{ A}$$

Since both the thyristors share the load current equally, their *rms* current will be the same, hence

$$I_{T1\,(rms)} = I_{T2\,(rms)} = 8.13 \text{ A}$$

(d) Thyristor rating must be: Current I = 10 A, Voltage V = 250 V, PRV = 2×250 = 500V

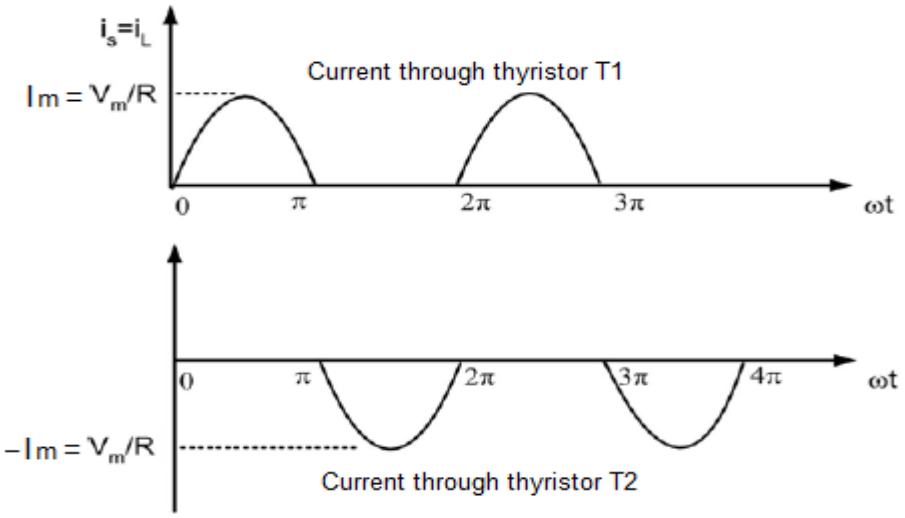

Fig.6.4 Currents through thyristors T_1 and T_2.

6.5 INTEGRAL-CYCLE CONTROL OF SERIES RESISTIVE – INDUCTIVE LOAD

Fig.6.5 shows a single-phase thyristor controller used to feed a series resistance-inductance load. When the thyristors are triggered by long pulses at a triggering angle equal to zero in integral-cycle triggering mode, sinusoidal operation results. A typical steady-state cycle is shown in Fig.6.6 for control period T=3 cycles and conduction period N =2 cycles.

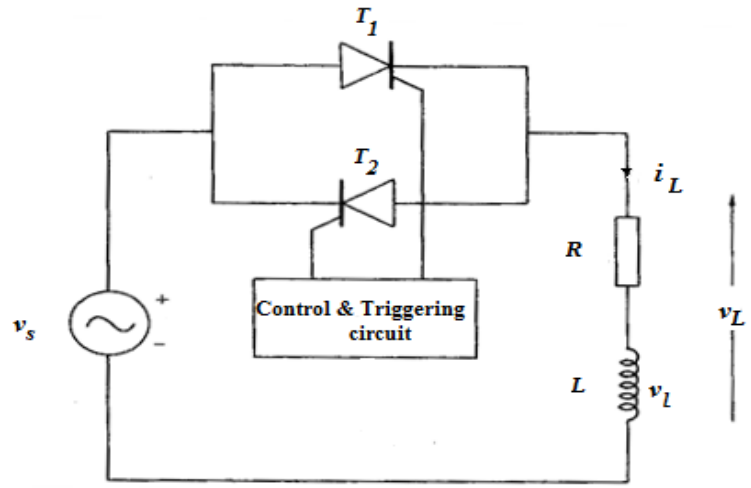

Fig.6.5 Single-phase thyristor controller for series *R-L* load.

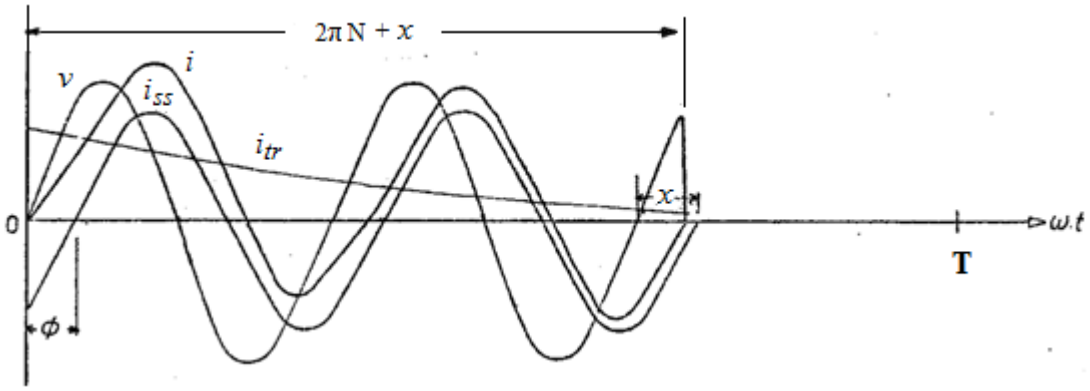

Fig.6.6 Load voltage and current waveforms for series resistance-inductance load with T= 3 and N =2 cycles.

Analysis of the voltage and current waveforms with *R- L* load

For zero voltage triggering the load voltage cycle consists of N conducting cycles in a total period of T supply cycles. Waveforms of the voltage and current at the *R-L* load terminals are shown in Fig. 6.6. It is evident that neither the load voltage nor the load current is zero at the end

of the interval $2\pi N$ as would be the case for resistive load. Extinction of voltage and current occurs by natural commutation at an angle of ($2\pi N+ x$) which is immediately prior to a natural current zero.

Analysis of load voltage waveform (Exact solution)

If the source impedance is neglected, the supply voltage is simply given by

$$v_s = V_m \sin \omega t \tag{6.26}$$

For a control period of T supply cycles, the load voltage is represented by

$$\begin{aligned} v_L(\omega t) &= V_m \sin \omega T t \Big|_{0}^{2\pi N + x} \\ v_L(\omega t) &= 0 \Big|_{2\pi N + x}^{T} \end{aligned} \tag{6.27}$$

Fourier analysis of Eq.(6.27) results in the expression shown below:
For n ≠ T

$$a_0 = \frac{V_m}{\pi T}[\,1 - \cos x] \tag{6.28}$$

$$\begin{aligned} a_n = \frac{V_m}{\pi(T^2 - n^2)} \Big(T \Big\{ 1 - \cos x \cos \frac{n}{T}(2\pi N + x) \Big\} \\ - n \sin x \sin \frac{n}{T}(2\pi N + x) \Big) \end{aligned} \tag{6.29}$$

$$\begin{aligned} b_n = \frac{V_m}{\pi(T^2 - n^2)} \Big(T \Big\{ - \cos x \sin \frac{n}{T}(2\pi N + x) \Big\} \\ + n \sin x \cos \frac{n}{T}(2\pi N + x) \Big) \end{aligned} \tag{6.30}$$

$$\begin{aligned} c_n = \frac{V_m}{\pi(T^2 - n^2)} \Big[T^2 \{ \cos \frac{n}{T}(2\pi N + x) - \cos x \}^2 \\ + T^2 \{ \sin \frac{n}{T}(2\pi N + x) - n \sin x \}^2 \Big]^{1/2} \end{aligned} \tag{6.31}$$

The phase angle Ψ_n between the supply voltage and the n^{th} current harmonic is given by

$$\psi_{n=T} = \tan^{-1} \frac{a_n}{b_n} \tag{6.32}$$

The supply frequency harmonic component, when n =*T,* will be :

$$a_{n=T} = \frac{1}{\pi}\int_{0}^{\frac{2\pi N+x}{T}} V_m \sin T\omega t \ \cos T\omega t \ d(\omega t) \tag{6.33}$$

$$a_{n=T} = \frac{V_m}{4\pi T}[1-\cos(2x)] \tag{6.34}$$

$$b_{n=T} = \frac{1}{\pi}\int_{0}^{\frac{2\pi N+x}{T}} V_m \sin T\omega t \ \sin T\omega t \ d(\omega t) \tag{6.35}$$

$$b_{n=T} = \frac{V_m}{4\pi T}[2\{2\pi N + x\} - \sin(2x)] \tag{6.36}$$

$$c_{n=T} = [\{a_{n=T}\}^2 + \{b_{n=T}\}^2]^{1/2} \tag{6.37}$$

$$\psi_{n=T} = \tan^{-1}\frac{a_{n=T}}{b_{n=T}} \tag{6.38}$$

Approximate analysis

In most practical cases, it is found that the extinction angle of the load current (*x*) is nearly equal to the load angle ∅**.** To simplify the analysis it is convenient to assume that $x \approx \emptyset$. The approximate solution of the previous equations are then

$$a_0 = \frac{V_m}{\pi T}[1-\cos\emptyset] \tag{6.39}$$

$$a_n = \frac{V_m}{\pi(T^2-n^2)}\left(T\left\{1-\cos x\cos\frac{n}{T}(2\pi N+\emptyset)\right\} - n\sin x \sin\frac{n}{T}(2\pi N+\emptyset)\right) \tag{6.40}$$

$$b_n = \frac{V_m}{\pi(T^2-n^2)}\left(T\left\{-\cos x \sin\frac{n}{T}(2\pi N+\emptyset)\right\} + n\sin x\cos\frac{n}{T}(2\pi N+\emptyset)\right) \tag{6.41}$$

$$c_n = \frac{V_m}{\pi(T^2 - n^2)}\Big[T^2\{cos\frac{n}{T}(2\pi N + \emptyset) - \cos\emptyset\}^2 + T^2\{sin\frac{n}{T}(2\pi N + \emptyset) - nsin\,\emptyset\}^2\Big]^{1/2} \quad (6.42)$$

$$a_{n=T} = \frac{V_m}{4\pi T}[1 - \cos(2\emptyset)] \quad (6.43)$$

$$b_{n=T} = \frac{V_m}{4\pi T}[2\{2\pi N + \emptyset\} - \sin(2\emptyset)] \quad (6.44)$$

$$c_{n=T} = \frac{V_m}{4\pi T}\sqrt{[1 - \cos(2\emptyset)]^2 + [2\{2\pi N + \emptyset\} - \sin(2\emptyset)]^2} \quad (6.45)$$

If the angle $\emptyset$ is very small as the case of resistive load Eqs.(6.40) – (6.46) reduced to

$$c_n = \frac{V_m T}{\pi(T^2 - n^2)} 2\sin\left(\frac{\pi n N}{T}\right) \quad (6.46)$$

$$c_{n=T} = V_m \frac{N}{T} \quad (6.47)$$

Current waveform analysis:

The load current waveforms shown in Fig.6.6 resulting from the on-off switching action of the thyristors consists of a steady-state sinusoidal component i_{ss} plus a decaying exponential component i_{tr} with the time constant $\tau = L/R$. During the on period, the current through *R-L* load will be:

$$iR + L\frac{di}{dt} = V_m \sin\omega t \qquad 0 \le \omega t \le 2\pi N + x \quad (6.48)$$

The solution of this equation gives the steady state and transient solutions as follows:

$$i(\omega t) = i_{ss} + i_{tr}$$

or $$i(\omega t) = I_m \sin(\omega t - \emptyset) + I_m \sin\emptyset \; e^{-\cot\emptyset.\omega t}\Big|_0^{2\pi N + x} \quad (6.49)$$

In terms of the control period *T*:

$$i(T\omega t) = I_m \sin(T\omega t - \emptyset) + I_m \sin\emptyset \;\; e^{-\cot\emptyset(T\omega t)} \Big|_0^{\frac{2\pi N+x}{T}} \qquad (6.50)$$

where

$$I_m = \frac{V_m}{|Z|} \qquad (6.51)$$

$$|Z| = \sqrt{R^2 + \omega^2 L^2} \qquad (6.52)$$

$$tan\emptyset = \frac{\omega L}{R} \qquad (6.53)$$

(a) Equation (6.50) must satisfy the initial and final conditions

$$i = 0 \qquad at \qquad \omega t = 0$$
$$i = 0 \qquad at \qquad \omega t = 2\pi N + x$$

If we substitute these values in Eq.(6.49) it will result in the following useful equation

$$\sin(x - \emptyset) = -\sin\emptyset \, e^{-cot\emptyset \,.(2\pi N+x)}$$

(b) Fourier analysis is found to give the following expressions:

The Exact Solution for n ≠ T

$$a_o = \frac{\omega}{\pi}\int_0^{\frac{2\pi N+x}{\omega T}} I_m \sin(Tt\omega - \emptyset)dt + \frac{\omega}{\pi}\int_0^{\frac{2\pi N+x}{\omega T}} I_m \sin\emptyset \;\; e^{-\cot\emptyset(T\omega t)} \; dt \qquad (6.54)$$

$$a_n = \frac{\omega}{\pi}\int_0^{\frac{2\pi N+x}{\omega T}} I_m \sin(Tt\omega - \emptyset)\cos n\omega t \; dt + \frac{\omega}{\pi}\int_0^{\frac{2\pi N+x}{\omega T}} I_m \sin\emptyset \;\; e^{-\cot\emptyset(T\omega t)} \cos n\omega t \; dt \qquad (6.55)$$

$$b_n = \frac{\omega}{\pi}\int_0^{\frac{2\pi N+x}{\omega T}} I_m \sin(T\omega t - \emptyset)\sin \mathrm{n}\omega \mathrm{t} \; dt + \frac{\omega}{\pi}\int_0^{\frac{2\pi N+x}{\omega T}} I_m \sin\emptyset \;\; e^{-\cot\emptyset(T\omega t)} \sin \mathrm{nt}\,\omega \; \mathrm{dt} \qquad (6.56)$$

The solution of the above equations yields:

$$a_0 = \frac{V_m}{\pi T}[\cos\emptyset - \cos(x-\emptyset) + tan\emptyset\{\sin\emptyset + \sin(x-\emptyset)\}] \quad (6.57)$$

$$a_n = \frac{I_m}{\pi(T^2-n^2)}\left[T\left\{\cos - \cos(x-\emptyset)\cos\frac{n}{T}(2\pi N + x) + \frac{I_m \sin\emptyset\tan\emptyset}{\pi(T^2 + tan^2\emptyset n^2)}\right\}\right] \quad (6.58)$$

$$b_n = \frac{I_m}{\pi(T^2-n^2)}\left[-T\sin\frac{n}{T}(2\pi N + x) + n\sin\emptyset\right] + \frac{I_m\, n\tan\emptyset}{\pi(T^2 cot^2\emptyset + n^2)} \quad (6.59)$$

The amplitude c_n of the n^{th} harmonic$(n \neq T)$:-

$$c_n = \frac{I_m T}{\pi(T^2-n^2)}\left[\frac{T^2\left(\cos\frac{n}{T}(2\pi N+\emptyset) - \cos\emptyset\right)^2 + \left(T\sin\frac{n}{T}(2\pi N+\emptyset) - n\sin\emptyset\right)^2}{T^2cos^2\emptyset + n^2 sin^2\emptyset}\right]^{\frac{1}{2}} \quad (6.60)$$

The phase angle ψ_n of the nth harmonic is:

$$\Psi_n = \tan^{-1}\frac{a_n}{b_n} = \pi - \frac{n}{T}(2\pi N + \emptyset) \quad (6.61)$$

The Fourier coefficient of the supply frequency component (n=*T*) are

$$a_T = \frac{\omega}{\pi}\int_0^{\frac{2\pi N+x}{\omega T}} I_m \sin(T\omega t - \emptyset)\cos T\omega t + \frac{\omega}{\pi}\int_0^{\frac{2\pi N+x}{\omega T}} I_m \sin\emptyset\ \ e^{-\cot\emptyset(T\omega t)}\cos T\omega t\, dt \quad (6.62)$$

$$b_T = \frac{\omega}{\pi}\int_0^{\frac{2\pi N+x}{\omega T}} I_m \sin(T\omega t - \emptyset)\sin T\omega t\ dt + \frac{\omega}{\pi}\int_0^{\frac{2\pi N+x}{\omega T}} I_m \sin\emptyset\ \ e^{-\cot\emptyset(T\omega t)} sin\, T\omega t\ \mathrm{dt} \quad (6.63)$$

Solution of these two equations gives

$$a_T = \frac{I_m}{2\pi T}[\sin x \sin(x-\emptyset) - (2\pi N + x)\sin\emptyset + 2\sin\emptyset\{\sin(x-\emptyset)\cos(x+\emptyset) + \sin\emptyset\cos\emptyset\}] \quad (6.64)$$

$$b_T = \frac{I_m}{2\pi T}[(2\pi N + x)\cos\emptyset - \sin x\cos(x-\emptyset) + 2\sin\emptyset\{\sin(x-\emptyset)\ \sin(x+\emptyset) + sin^2\emptyset\}] \quad (6.65)$$

The amplitude of the supply frequency component $c_T(n=T)$ is

$$c_T = \sqrt{a_T^2 + b_T^2}$$

or

$$c_T = \frac{I_m}{2\pi T}[sin^2 x + (2\pi N + x)^2 - (2\pi N + x)\sin 2x]^{\frac{1}{2}} \quad (6.66)$$

and the phase angle is

$$\Psi_T = \tan^{-1}\frac{a_T}{b_T} \quad (6.67)$$

The Approximate Solution

Approximate solution can be achieved when we assume that $x = \emptyset$. In this case the Fourier coefficients of the n^{th} harmonic are:

$$a_0 = \frac{V_m}{\pi T}[\cos\emptyset - 1) + \ tan\emptyset\sin\emptyset\ ] \quad (6.68)$$

$$a_n = \frac{I_m}{\pi(T^2 - n^2)}\left[T\left\{\cos\emptyset - \cos\frac{n}{T}(2\pi N + \emptyset) + \frac{I_m\sin\emptyset\tan\emptyset}{\pi(T^2 + tan^2\emptyset n^2)}\right\}\right] \quad (6.69)$$

$$b_n = \frac{I_m}{\pi(T^2 - n^2)}\left[-T\sin\frac{n}{T}(2\pi N + \emptyset) + n\sin\emptyset\right] + \frac{I_m\, n\tan\emptyset}{\pi(T^2 cot^2\emptyset + n^2)} \quad (6.70)$$

$$a_T = \frac{I_m}{2\pi T}[-(2\pi N + \emptyset)\sin\emptyset + 2\sin^2\emptyset\cos\emptyset\ ] \quad (6.71)$$

$$b_T = \frac{I_m}{2\pi T}[(2\pi N + x)\cos\emptyset - \sin\emptyset\{1 + 2sin^2\emptyset] \quad (6.72)$$

$$c_T = \frac{I_m}{2\pi T}[sin^2\emptyset + (2\pi N + \emptyset)^2 - (2\pi N + \emptyset)\sin 2\emptyset]^{\frac{1}{2}} \quad (6.73)$$

$$\Psi_T = \tan^{-1}\frac{-(2\pi N + \emptyset)\sin\emptyset + 2\sin^2\emptyset\cos\emptyset}{(2\pi N + x)\cos\emptyset - \sin\emptyset(1 + 2sin^2\emptyset)} \quad (6.74)$$

Harmonic content of the load current waveform

Harmonic frequency spectra of the line (load) current in a single-phase circuit with *R-L* load is shown in Fig. 6.6 for *N*=2, *T*=4, representing 50% power transfer. Also Fig.6.7 shows the current waveform frequency spectra of pure resistive load for the same power transfer case for comparison.

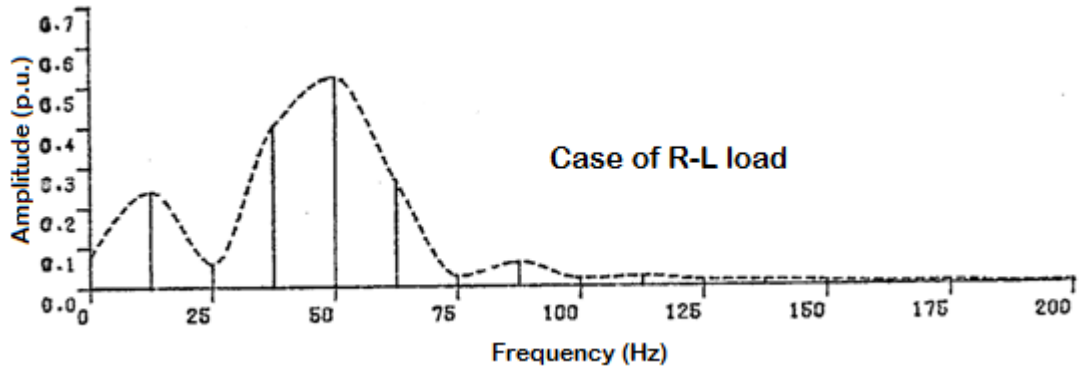

(a)

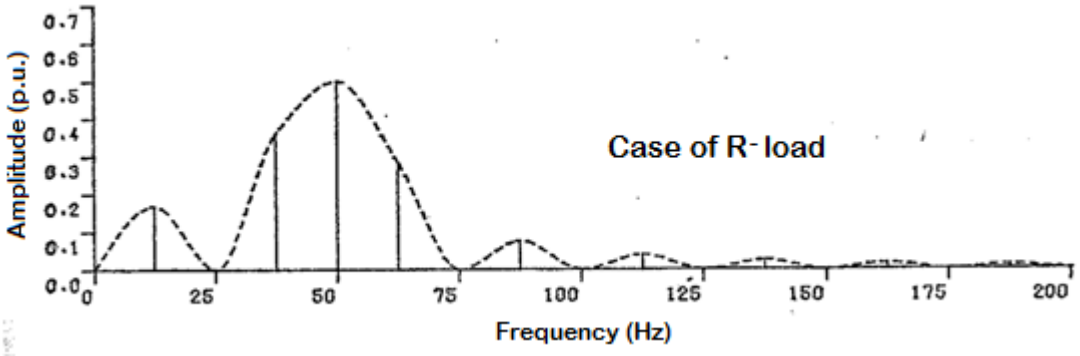

(b)

Fig.6.7 Harmonic amplitude spectra of the load current : (a) With *R-L* load for $N = 2$, $T = 4$, (b) With *R*-load for $N = 2$, $T = 4$.

It is evident from Fig.6.6(a) that the current waveform for *R-L* load has same harmonics as that of the case of resistive load shown in Fig.6.7(b). However, the amplitudes of the harmonics are different in magnitude and phases. Also the load current in case of *R-L* load has a significant d.c.

component which does not exist in case of *R*-load. Table 6.1 gives a comparison between the two cases for clarity.

Table 6.1 comparison between *R-load* and *R-L load* results for *N=2, T=4.*

Harmonic order	**Frequency (Hz)**	**Amplitude(p.u.) Case of *R*-load**	**Amplitude(p.u.) Case of *R-L* load**
DC component	0	0	0.09
1/T	12.5	0.17	0.25
2/T	25	0	0.6
3/T	37.5	0.37	0.43
4/T	50	0.5	0.53
5/T	62.5	0.3	0.28
6/T	75	0	0.14
7/T	87.5	0.9	0.45
8/T	100	0	0.10

6.6 INTEGRAL-CYCLE CONTROL IN THREE-PHASE CIRCUITS

In this section, the analytical properties of an integral-cycle control waveforms of voltage and current in each part of various three-phase loads will be considered. Due to its characteristic feature of permitting complete cycles of load current followed by complete cycles of extinction, integral-cycle control is not feasible for all the connections by which a three-phase load may be supplied with three-phase power. Only those configurations in which each phase operates independently of the other two phases results in symmetrical operation are obviously suitable.

6.6.1 Four-Wire, Star-Connected, Resisitive Load

Consider the four-wire circuit shown in Fig.6.8. This circuit consists of three single-phase circuits with their operations separated in time phase by 120˚. The return current path is provided by the neutral connection. Each series single-phase *R*-load is connected in series with a pair of thyristors in the supply lines. Integral-cycle triggering is used which is symmetrical in the three phases with the onset at voltage zero. The load voltage cycle in each phase consists of *N* conducting cycles in a total period of *T* supply cycles. Waveforms of the voltage and current at the load terminals with $N = 2$, $T = 4$ are shown in Fig.6.9. If the source impedance is negligible, and the supply voltage of phase-a is taken as a reference, then

$$\left.\begin{aligned} v_{an} &= V_m \sin \omega t \\ v_{bn} &= V_m \sin(\omega t - 2\pi / 3) \\ v_{cn} &= V_m \sin(\omega t - 4\pi / 3) \end{aligned}\right\} \qquad (6.75)$$

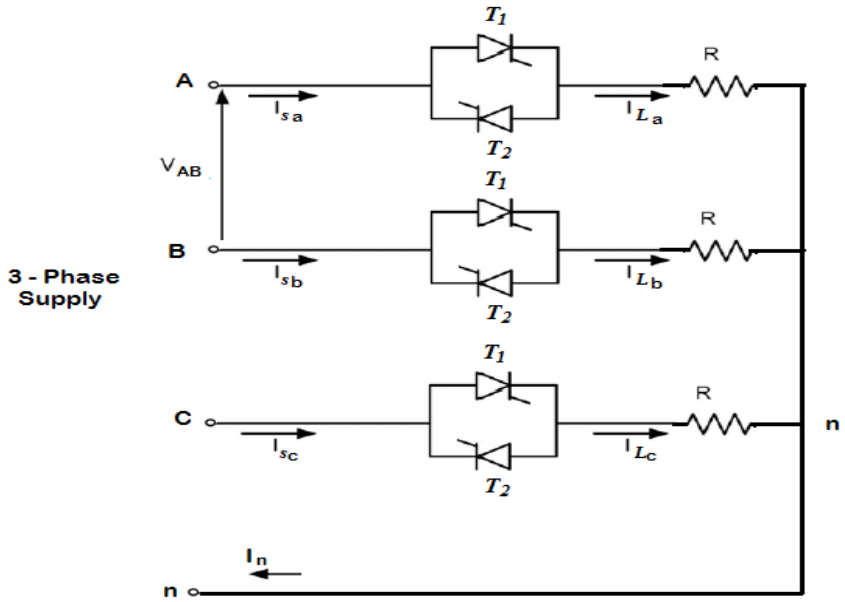

Fig.6.8 Four-wire system with voltage control by integral-cycle triggering mode of thyristors, case of *R*-load.

For a control period of T supply cycles, the load voltage for the three phases are represented by the following equations:

$$v_{\bar{a}\bar{n}} = V_m \sin \omega T t \qquad 0 < \omega t < \frac{2\pi N}{T} \tag{6.76}$$

$$v_{\bar{b}\bar{n}} = V_m \sin(\omega T t - \frac{2\pi}{3T}) \qquad \frac{2\pi}{3T} < \omega t < \frac{2\pi N}{T} + \frac{2\pi}{3T} \tag{6.77}$$

$$v_{\bar{c}\bar{n}} = V_m \sin\left(\omega T t - \frac{4\pi}{3T}\right) \qquad \frac{4\pi}{3T} < \omega t < \frac{2\pi N}{T} + \frac{4\pi}{3T} \tag{6.78}$$

and the current in each phase will be

$$i_{\bar{a}} = I_m \sin \omega T t \qquad 0 < \omega t < \frac{2\pi N}{T} \tag{6.79}$$

$$i_{\bar{b}} = I_m \sin(\omega T t - \frac{2\pi}{3T}) \qquad \frac{2\pi}{3T} < \omega t < \frac{2\pi N}{T} + \frac{2\pi}{3T} \tag{6.80}$$

$$i_{\bar{c}} = I_m \sin(\omega T t - \frac{4\pi}{3T}) \qquad \frac{4\pi}{3T} < \omega t < \frac{2\pi N}{T} + \frac{4\pi}{3T} \tag{6.81}$$

Irrespective of the phase shift between the three phases, Fourier coefficients of the voltage waveform are the same as those given in Eqs.(6.2) to (6.7) for equal control period T. Therefore, harmonic spectra of the three phases are similar to each other as calculated and displayed in Fig.6.10. The current harmonic coefficients for each phase will have the same harmonic coefficients of the voltage since the load is resistive. However the neutral current, for the same control period T for the three phases as shown in Fig.6.9, flows only when one or two phases conduct

simultaneously. When the three phases conduct the neutral current will be zero for balanced load.

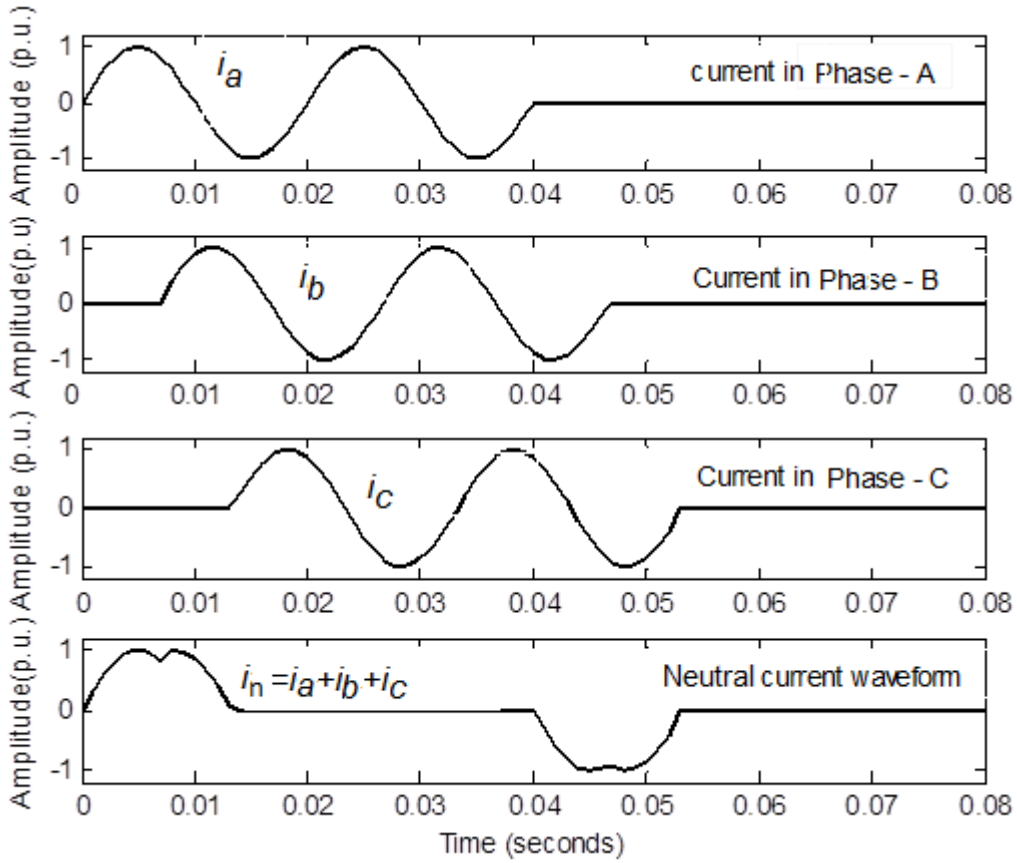

Fig.6.9 Current waveforms in the three phases and neutral for *R*-load with voltage control by integral-cycle triggering mode of thyristors for $N = 2,\ T = 4$.

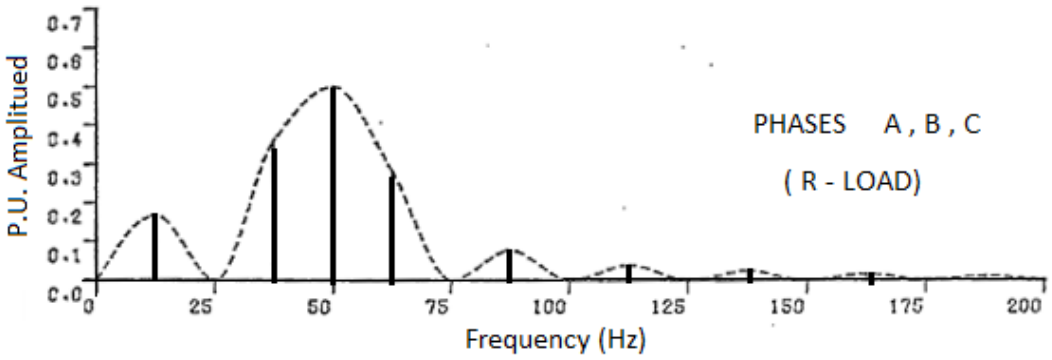

Fig.6.10 Frequency spectra of the load voltage waves in the three phases for *N=2, T=4,*with *R*-load.

Neutral current harmonic analysis

Now using the relations given in Eqs.(6.2) to (6,7) to evaluate Fourier coefficients for the current in each phase one can obtain,

For n ≠ T

$$a_{nA} = \frac{I_m T}{\pi(T^2 - n^2)}\left[1 - \cos\frac{2\pi nN}{T}\right] \quad (6.82)$$

$$a_{nB} = \frac{I_m T}{\pi(T^2 - n^2)}\left[\cos\frac{2\pi n}{3T} - \cos\frac{2\pi n}{3T}\ (3N+1)\right] \quad (6.83)$$

$$a_{nC} = \frac{I_m T}{\pi(T^2 - n^2)}\left[\cos\frac{2\pi n}{3T} - \cos\frac{2\pi n}{3T}\ (3N+2)\right] \quad (6.84)$$

Similarly :

$$b_{nA} = \frac{I_m T}{\pi(T^2 - n^2)}\left[-\sin\frac{2\pi nN}{T}\right] \quad (6.85)$$

$$b_{nB} = \frac{I_m T}{\pi(T^2 - n^2)}\left[\sin\frac{2\pi n}{3T} - \sin\frac{2\pi n}{3T}\ (3N+1)\right] \quad (6.86)$$

$$b_{nC} = \frac{I_m T}{\pi(T^2 - n^2)}\left[\sin\frac{2\pi n}{3T} - \sin\frac{2\pi n}{3T}\ (3N+2)\right] \quad (6.87)$$

For the neutral current since it is the summation of the phase currents, thus,

$$a_{on} = a_{nA} + a_{nB} + a_{nC}$$

$$a_{on} = \frac{I_m T}{\pi(T^2 - n^2)}\left[1 - \cos\frac{2\pi nN}{T} + \cos\frac{2\pi n}{3T} - \cos\frac{2\pi n}{3T}\ (3N+1) + \cos\frac{2\pi n}{3T} - \cos\frac{2\pi n}{3T}\ (3N+2)\right] \quad (6.88)$$

Similarly $b_{on} = b_{nA} + b_{nB} + b_{nC}$

$$b_{on} = \frac{I_m T}{\pi(T^2 - n^2)}\left[-\sin\frac{2\pi nN}{T} + \sin\frac{2\pi n}{3T} - \sin\frac{2\pi n}{3T}\ (3N+1) + \sin\frac{2\pi n}{3T} - \sin\frac{2\pi n}{3T}\ (3N+2)\right] \quad (6.89)$$

Further mathematical simplification of the above two equations yields

$$a_{on} = \frac{I_m T}{\pi(T^2 - n^2)}\left[\cos\frac{2\pi n}{3T} - \cos(\frac{2\pi n}{3T} + \frac{2\pi nN}{T})\right] \times \frac{\sin\frac{\pi n}{T}}{\sin\frac{\pi n}{3T}} \quad (6.90)$$

$$b_{on} = \frac{I_m T}{\pi(T^2 - n^2)}\left[\sin\frac{2\pi n}{3T} - \sin(\frac{2\pi n}{3T} + \frac{2\pi nN}{T})\right] \times \frac{\sin\frac{\pi n}{T}}{\sin\frac{\pi n}{3T}} \quad (6.91)$$

The amplitude c_{on} of the n^{th} order harmonic is,

$$c_{on} = \frac{2\ I_m T}{\pi(T^2 - n^2)}\ \sin\frac{2\pi n}{T} \times \frac{\sin\frac{\pi n}{T}}{\sin\frac{\pi n}{3T}} \quad (6.92)$$

and the phase-angle is:

$$\Psi_{on} = \tan^{-1}\frac{a_{on}}{b_{on}} = \frac{\cos\frac{2\pi n}{3T} - \cos(\frac{2\pi n}{3T} + \frac{2\pi nN}{T})}{\sin\frac{2\pi n}{3T} - \sin(\frac{2\pi n}{3T} + \frac{2\pi nN}{T})} \quad (6.93)$$

Frequency spectrum of the neutral current wave of Fig.6.9 for *N=2, T=4* is shown in Fig.6.11. It should be noted that only odd harmonics exist since, for even harmonics, C_{on} = 0.

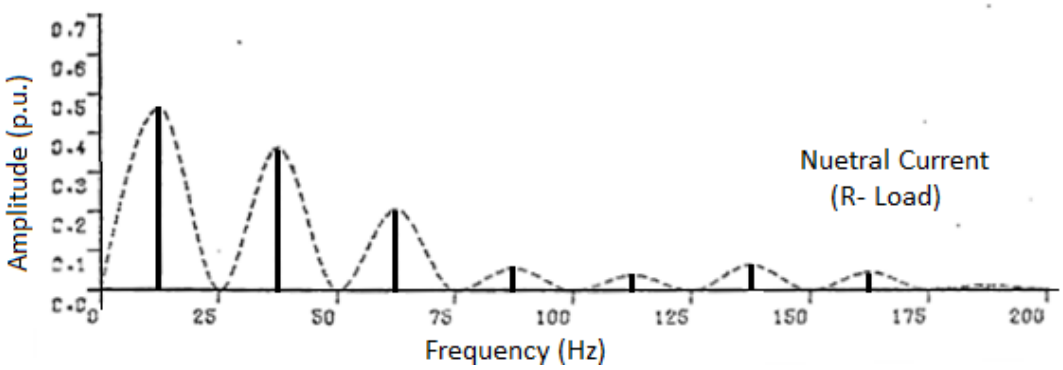

Fig.6.11 Frequency spectrum of the neutral current waveform for *N=2,T=4.*

The supply frequency component when *n = T* of the neutral current

For n=*T*, Fourier coefficients $a_{o(n=T)}$, $b_{o(n=T)}$ and $c_{o(n=T)}$ of Eq.(6.50) can be evaluated for the current in each phase using the relations given in Eqs. (6.28) to (6.30), thus

$$a_{o(n=T)} = 0 \quad (6.94)$$

$$b_{o(n=T)} = 0 \quad (6.95)$$

$$c_{o(n=T)} = 0 \quad (6.96)$$

Hence the supply frequency component is totally suppressed in the neutral current. Oscillogram of phase – a load voltage waveform v_a and neutral current wave i_n with resistive load is shown in Fig.6.12 for clarity.

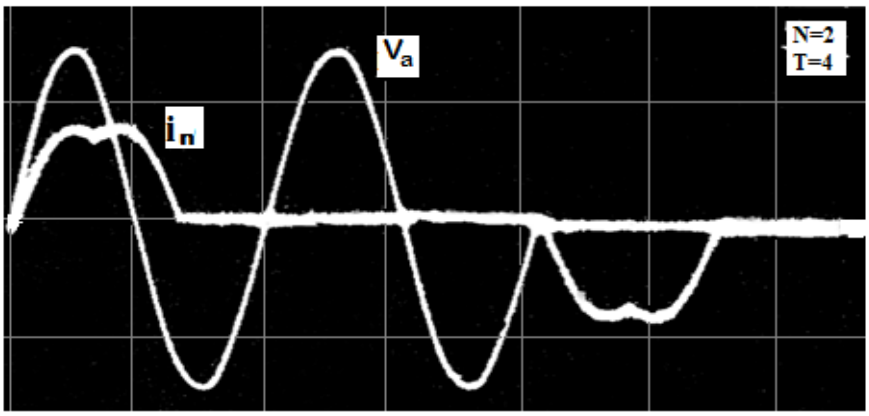

Fig.6.12 Oscillogram of the phase-a load voltage waveform v_a and neutral current wave i_n with resistive load for $N = 2$, $T = 4$.

6.6.2 Four-Wire, Star-Connected, Series *R-L* Load

Figure 6.13 shows a three-phase, four-wire circuit with *R-L* load and voltage controlled by integral-cycle triggering mode of thyristors. Waveforms of the voltage and currents at the load terminals with $N = 2$, $T = 3$ are shown in Fig. 6.14.

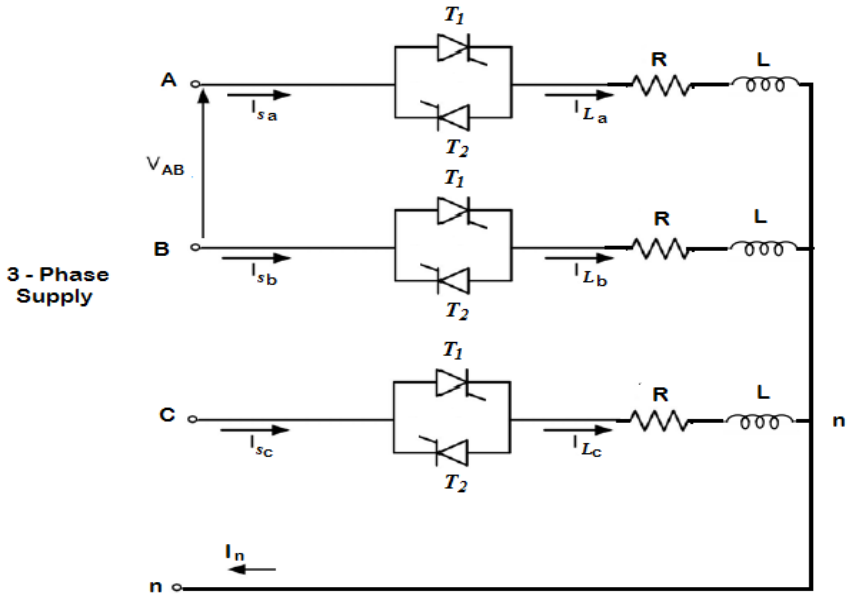

Fig.6.13 Four-wire system with voltage control by integral-cycle triggering mode of thyristors, case of *R-L* load.

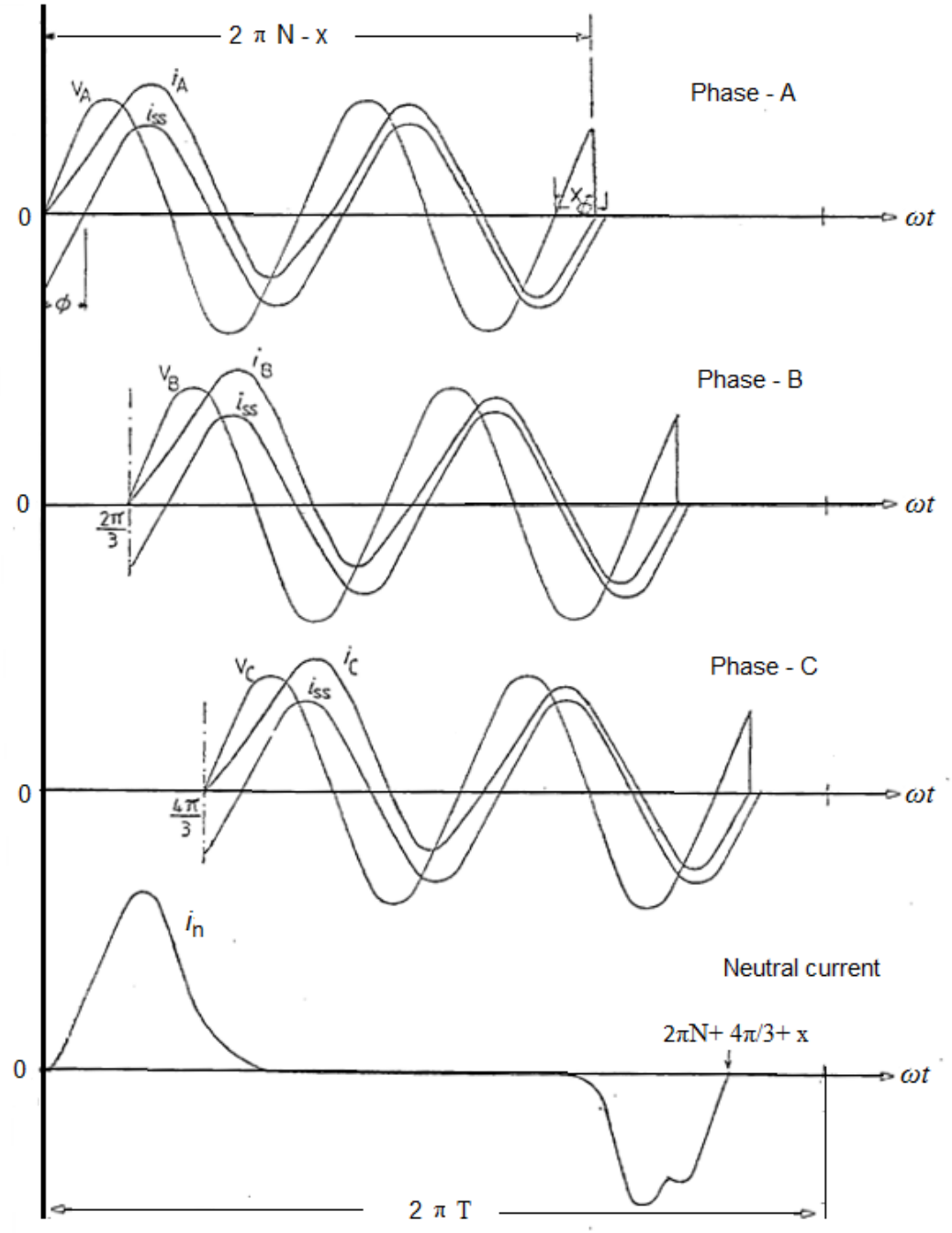

Fig.6.14 Waveforms for the three-phase, four-wire system with voltage control by integral-cycle triggering mode of thyristors for $N = 2$, T=3.

Voltage waveform analysis

Let the notation 1, 2, 3 denote the three phases A, B, and C respectively. Thus the notation for the supply voltage (v_j) for any j^{th} phase will have the general form as follows **:**

$$V_j = V_m \sin(\omega t - \gamma_j) \tag{6.97}$$

where for the three-phase:

$$j = 1, 2, 3$$
$$\gamma_1 = 0, \quad \gamma_2 = 2\pi/3, \quad \gamma_3 = 4\pi/3$$
$$\phi = \tan^{-1}\frac{\omega L}{R}$$

Similarly the general equation of the V_{Lj} will be

$$V_{Lj} = V_m \sin(T\omega t - \gamma_j) \qquad \frac{\gamma_j}{T} < \omega t < \frac{2\pi N + x + \gamma_j}{T} \tag{6.98}$$

Fourier analysis of Eq.(6.98) results in the expressions shown below for the exact solution:

For $n \neq T$

$$a_{0j} = \frac{V_m}{\pi T}[\,1 - \cos x] \tag{6.99}$$

$$a_{nj} = \frac{V_m T}{\pi(T^2 - n^2)}\left(T\left\{\cos\frac{n\gamma_j}{T} - \cos x \cos\frac{n}{T}(2\pi N + x + \gamma_j)\right\} - n\sin x \sin\frac{n}{T}(2\pi N + x + \gamma_j)\right) \tag{6.100}$$

$$b_n = \frac{V_m T}{\pi(T^2 - n^2)}\left(T\left\{\sin\frac{n\gamma_j}{T} - \cos x \sin\frac{n}{T}(2\pi N + x + \gamma_j)\right\} + n\sin x \cos\frac{n}{T}(2\pi N + x + \gamma_j)\right) \tag{6.101}$$

and the amplitude c_n of the n^{th} harmonic is

$$c_n = \frac{V_m T}{\pi(T^2 - n^2)}\left[T^2\{\cos\frac{n}{T}(2\pi N + x) - \cos x\}^2 + T^2\{\sin\frac{n}{T}(2\pi N + x) - n\sin x\}^2\right]^{1/2} \tag{6.102}$$

The phase angle ψ_{nj} between the supply voltage and the n^{th}current harmonic for the j^{th} phase is given by

$$\psi_{nj} = \tan^{-1}\frac{a_{nj}}{b_{nj}} \tag{6.103}$$

The supply frequency harmonic component, when n =*T,* will be:

$$a_{Tj} = \frac{V_m}{4\pi T}\left[\cos\gamma_j - \cos(2x+\gamma_j) - 2(2\pi N + x)\sin\gamma_j\right] \quad (6.104)$$

$$b_{Tj} = \frac{V_m}{4\pi T}\left[\sin\gamma_j + 2\{2\pi N + x\}\cos\gamma_j - \sin(2x+\gamma_j)\right] \quad (6.105)$$

Hence,

$$c_{Tj} = \frac{I_m}{2\pi T}[2(1-\cos 2x) + 4(2\pi N + x)(2\pi N + x) - \sin 2x]^{\frac{1}{2}}$$

and (6.106)

$$\psi_{Tj} = \tan^{-1}\frac{a_{Tj}}{b_{Tj}} \quad (6.107)$$

Approximate analysis

In most practical cases, it is found that the extinction angle if the load current (x) is nearly equal to the load angle $\emptyset$**.** To simplify the analysis it is convenient to assume that $x \approx \emptyset$. Approximate solutions of the previous equations are then

$$a_0 = \frac{V_m}{\pi T}[\,1 - \cos\emptyset] \quad (6.108)$$

$$a_{nj} = \frac{V_m T}{\pi(T^2 - n^2)}\left(T\left\{\cos\frac{n\gamma_j}{T} - \cos\emptyset\cos\frac{n}{T}\left(2\pi N + \emptyset + \gamma_j\right)\right\} - n\sin\emptyset\sin\frac{n}{T}\left(2\pi N + \emptyset + \gamma_j\right)\right) \quad (6.109)$$

$$b_{nj} = \frac{V_m T}{\pi(T^2 - n^2)}\left(T\left\{\sin\frac{n\gamma_j}{T} - \cos\emptyset\sin\frac{n}{T}\left(2\pi N + \emptyset + \gamma_j\right)\right\} + n\sin\emptyset\cos\frac{n}{T}\left(2\pi N + \emptyset + \gamma_j\right)\right) \quad (6.110)$$

$$c_{nj} = \frac{V_m T}{\pi(T^2 - n^2)}\left[T^2\{\cos\frac{n}{T}(2\pi N + \emptyset) - \cos\emptyset\}^2 + T^2\{\sin\frac{n}{T}(2\pi N + \emptyset) - n\sin\emptyset\}^2\right]^{1/2} \quad (6.111)$$

$$\psi_{nj} = \tan^{-1}\frac{\left(T\left\{\cos\frac{n\gamma_j}{T} - \cos\emptyset\cos\frac{n}{T}\left(2\pi N + \emptyset + \gamma_j\right)\right\} - n\sin\emptyset\sin\frac{n}{T}\left(2\pi N + \emptyset + \gamma_j\right)\right)}{\left(T\left\{\sin\frac{n\gamma_j}{T} - \cos\emptyset\sin\frac{n}{T}\left(2\pi N + \emptyset + \gamma_j\right)\right\} + n\sin\emptyset\cos\frac{n}{T}\left(2\pi N + \emptyset + \gamma_j\right)\right)} \quad (6.112)$$

Fourier coefficient of the supply frequency component ($n = T$):

$$a_{Tj} = \frac{V_m}{4\pi T}\left[\cos\gamma_j - \cos(2\emptyset + \gamma_j) - 2(2\pi N + \emptyset)\sin\gamma_j\right] \quad (6.113)$$

$$b_{Tj} = \frac{V_m}{4\pi T}\left[\sin\gamma_j + 2\{2\pi N + \emptyset\}\cos\gamma_j - \sin(2\emptyset + \gamma_j)\right] \quad (6.114)$$

$$c_{Tj} = \frac{I_m}{2\pi T}[2(1 - \cos 2\emptyset) + 4(2\pi N + \emptyset)(2\pi N + \emptyset) - \sin 2\emptyset]^{\frac{1}{2}} \quad (6.115)$$

$$\psi_{Tj} = \tan^{-1}\frac{\cos\gamma_j - \cos(2\emptyset + \gamma_j) - 2(2\pi N + \emptyset)\sin\gamma_j}{\sin\gamma_j + 2\{2\pi N + \emptyset\}\cos\gamma_j - \sin(2\emptyset + \gamma_j)} \quad (6.116)$$

If the angle $\emptyset$ is very small as the case of resistive load, equations (6.108) to (6.111) are reduced to

$$c_{nj} = \frac{V_m T}{\pi(T^2 - n^2)} 2\sin\left(\frac{\pi n N}{T}\right) \quad (6.117)$$

$$c_{Tj} = V_m \frac{N}{T} \quad (6.118)$$

Harmonics phase-angle relationships

Plot of the magnitude and phase-angle of nth frequency component of load current is shown in Fig.6.15. It is seen that, the phase displacement angles of the subharmonics and the higher order harmonics are unbalanced. Evaluating the phase-angle relationships of an individual harmonic or subharmonic, it can be prove that the nth frequency component of load current in phase A (ψ_{n1}) leads that of phase B (ψ_{n2}) by $120^o\frac{n}{T}$ and (ψ_{n2}) leads (ψ_{n3}) by $120^o\frac{n}{T}$ also.

However, if the phase displacement of the j^{th} phase (γ_j) is shifted according to the following relationship:

$$\gamma_j = \gamma_j' + 2\pi m_j \quad (6.119)$$

where, γ_j represent the new shifting angle and

$$m_j = 1,2,...,T-1.\ m_1 = 0,\ \gamma_1' = 0,\ \gamma_2' = 2\pi/3,\ \text{and}\ \gamma_3' = 4\pi/3$$

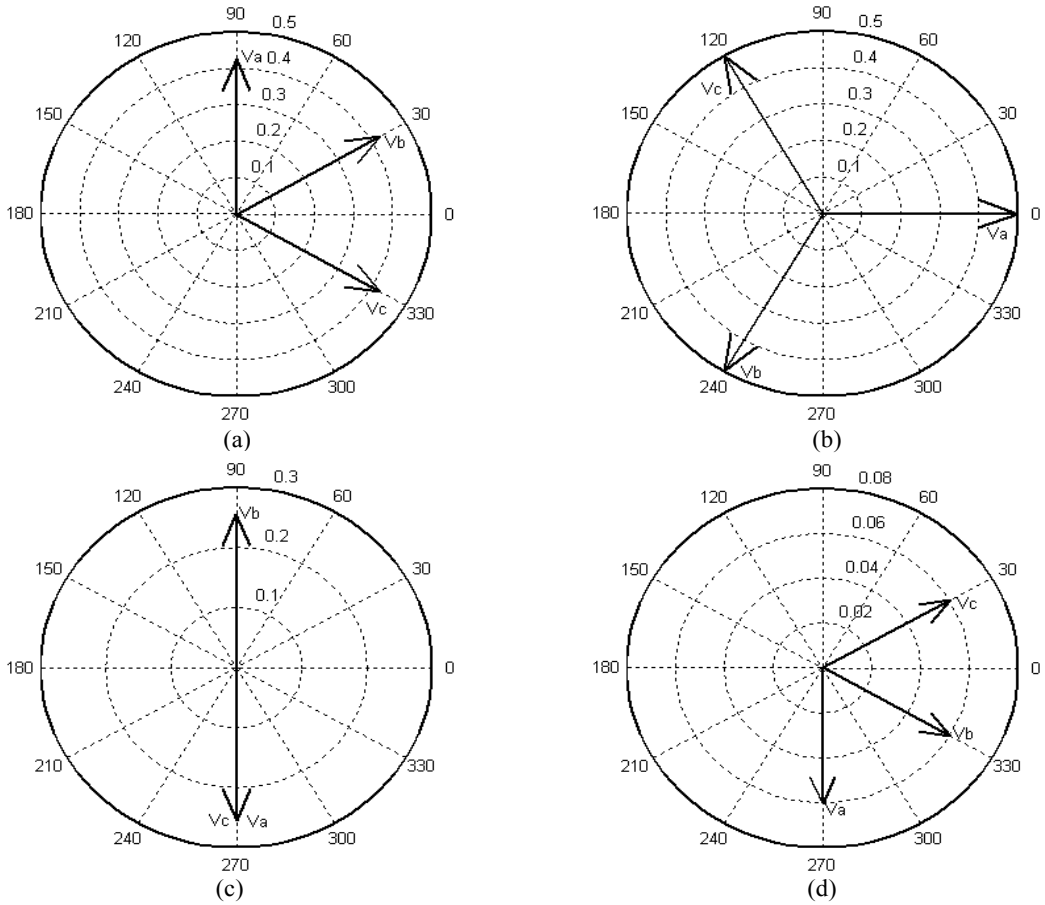

Fig. 6.15 Phase displacement angles for $N = 1$ and $T = 2$, R-load: (a) Phase displacement angles for the 1st harmonic (25 Hz), (b) Phase displacement angles for the supply frequency component, (c) Phase displacement angles for the 3rd harmonic (75 Hz), (d) Phase displacement angles for the 5th harmonic (125 Hz).

This new value of γ_j do not affect the amplitude and phase-angle relationships of the supply frequency component at the load voltages. It can be seen from Eq.(6.111), that the amplitude of the n^{th} harmonic is independent of γ_j, which means that, the variation of γ_j does not affect the harmonic amplitude spectrum of the j^{th} phase. Only the phase-displacement angle ψ_n of the n^{th} harmonic is changed as could be seen from Eq.(6.111). The phase-displacement angle ψ_{nj} of the n^{th} harmonic varies with the variation of m_j.

Now after shifting the load voltage waveform of phase B or C or both by multiple of 2π, the n^{th} frequency component of load current in phase A (ψ_{n1}) will lead that of phase B (ψ_{n2}) by

$$(120^{O} + 360^{O} \times m_2)\frac{n}{T} \qquad (6.120)$$

and (ψ_{n1}) leads (ψ_{n3}) by:

$$(240^{O} + 360^{O} \times m_3)\frac{n}{T} \qquad (6.121)$$

The harmonic amplitude spectrum and the phase-angle relationships for the load voltage waveforms of with N=1, T=2 are shown in Figs.6.16 and 6.17 respectively. It is seen that, the phase-displacement angles of the subharmonics and the higher order harmonics are unbalanced. Now, if the phase-displacement angle of phase B, i.e., ψ_{n2} is shifted by 180° then the phase-displacement angles of the 1st harmonic (25Hz) and the 5th harmonic (125Hz), as for example, become balanced.

The new values of ψ_{n2} for the 1st, 3rd and 5th harmonics which are $\psi_{12} = 210^{o}$, $\psi_{32} = 270°$ and $\psi_{52} = 150^{o}$ respectively give the value $m_2 = 1$ and the new value of γ_2 is equal to 480^{o}. The harmonic amplitude spectrum and the phase-displacement angles of the supply frequency component remains unchanged with the new value of γ_2, while the phase-displacement angles of the 1st, 3rd and 5th harmonics changed as shown in Fig.6.18(a), (c) and (d) respectively. It is found that this shifting technique makes the phase-displacement angles of the nth harmonic order balanced (120° between the phases) except when n is 3 or a multiple of 3 where in this case the phase-displacement angles become in-phase for all values of N and T except when T is a multiple of 3. Also it is noticed that the phase shifting of the phase-displacement angles used in this technique is independ on the value of N. This means that, the values of γ_2 and γ_3 that makes nth order harmonic balanced for certain values of N and T can make it balanced as well for the same value of T with $N = N$-1, N-2,.. ,1.

Table 6.2 shows the values of m_2 and m_3 which make the phase-displacement angle of the nth harmonic either balanced or in phase for typical values of T and N. This technique cannot correct the phase displacement-angles of a particular subharmonic or higher order harmonic if T is a multiple of three.

Table 6.2: The phase-displacement angles for typical values of T and N.

m_3	m_2	N	T
0	1	1	2
2	1	3-1	4
1	3	4-1	5
4	2	6-1	7
2	5	7-1	8
6	3	9-1	10

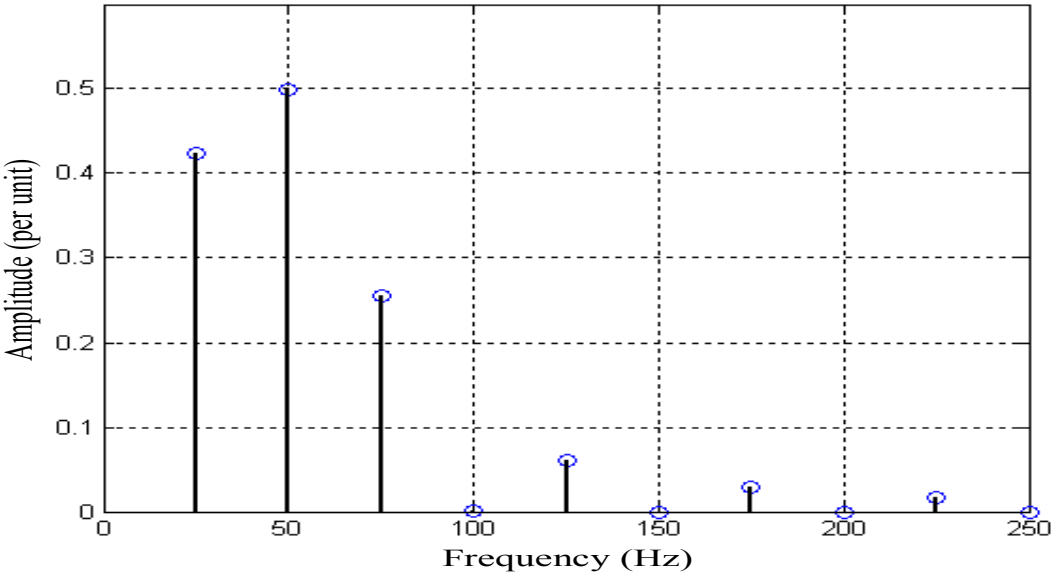

Fig.6.16 Harmonic amplitude spectrum for $T = 2$ and $N = 1$, R-load.

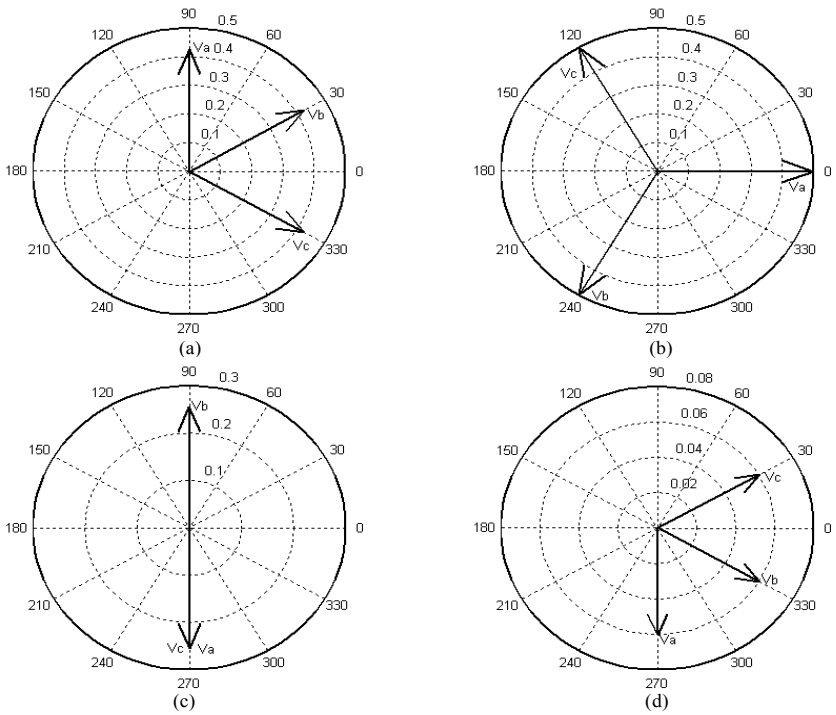

Fig.6.17 Phase displacement angles for $T = 2$ and $N = 1$, R-load (before correction): (a) Phase displacement angles for the 1st harmonic (25Hz), (b) Phase displacement angles for the supply frequency component, (c) Phase displacement angles for the 3rd harmonic (75Hz), (d) Phase displacement angles for the 5th harmonic (125Hz).

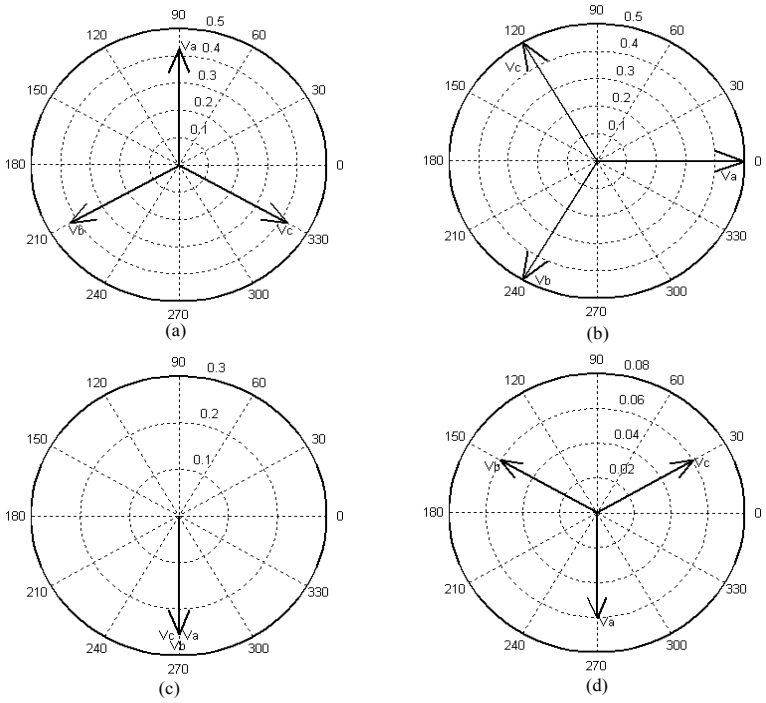

Fig.6.18 Phase displacement angles for $T = 2$ and $N = 1$, R-load (after correction): (a) 1st harmonic (25Hz), (b) Supply frequency component (50Hz), (c) 3rd harmonic (75Hz), (d) 5th harmonic (125Hz)..

2. Analysis of load current waveform

A general solution for the current in any phase can be obtained by expressing the current through the *jth* phase in terms of the control period T as follows:

$$i_j(\omega Tt - \gamma_j) = I_m \sin\left(\omega Tt - \emptyset + \gamma_j\right) + I_m \ \sin(\emptyset + \gamma_j)\ e^{-\cot\emptyset.\omega Tt} \tag{6.122}$$

where

I_m , Z, and $tan\emptyset$ are given in Eqs.(6.51) to (6.53).

(a) Equation (6.122) must satisfy the initial and final conditions

$$i_j = 0 \qquad at \qquad \omega t = \gamma_j \tag{6.123}$$

$$i_j = 0 \qquad at \qquad \omega t = 2\pi N + \emptyset + \gamma_j \tag{6.124}$$

(b) Expressions (6.122) to (6.124) are directly applicable to determine Fourier component of the *jth* phase. Hence for n≠*T*, assuming approximate solution:

$$a_{0j} = \frac{I_m}{\pi T}[\cos\emptyset - 1 + \tan\emptyset \sin\emptyset] \tag{6.125}$$

$$\begin{aligned} a_{nj} = \frac{I_m T}{\pi(T^2 - n^2)}\Big(T\Big\{\cos\emptyset\cos\frac{n\gamma_j}{T} - cos\frac{n}{T}(2\pi N + \emptyset + \gamma_j)\Big\} \\ - n\sin\emptyset\, sin\frac{n}{T}\gamma_j + \frac{I_m \sin\emptyset\tan\emptyset}{\pi(T^2 + tan^2\emptyset n^2)}\{Tcos\frac{n}{T}\gamma_j \\ - n\tan\emptyset\, sin\frac{n}{T}\gamma_j\Big) \end{aligned} \tag{6.126}$$

$$\begin{aligned} b_{nj} = \frac{I_m T}{\pi(T^2 - n^2)}\Big(T\Big\{\cos\emptyset\sin\frac{n\gamma_j}{T} - sin\frac{n}{T}(2\pi N + \emptyset + \gamma_j)\Big\} \\ - n\sin\emptyset\, cos\frac{n}{T}\gamma_j + \frac{I_m \sin\emptyset\tan\emptyset}{\pi(T^2 + tan^2\emptyset n^2)}\{Tsin\frac{n}{T}\gamma_j \\ - n\tan\emptyset\, cos\frac{n}{T}\gamma_j\Big) \end{aligned} \tag{6.127}$$

The amplitude c_{nj} of the nth harmonic of the *jth* phase is

$$c_{nj} = \frac{I_m T}{\pi(T^2 - n^2)}$$

$$\times\left[\frac{T^2\{cos\frac{n}{T}(2\pi N + \emptyset) - \cos\emptyset\}^2 + T^2\{sin\frac{n}{T}(2\pi N + \emptyset) - nsin\emptyset\}^2}{T^2\, cos^2\emptyset + n^2 sin^2\emptyset}\right]^{\frac{1}{2}}$$

(6.128)

The phase-angle ψ_{nj} of the n[th] harmonic of the *jth* phase is

$$\psi_{nj} = \tan^{-1}\frac{a_{nj}}{b_{nj}} = \pi - \frac{n}{T}(2\pi N + \emptyset + \gamma_j) \tag{6.129}$$

The supply frequency component (for n =*T*)

$$\begin{aligned} a_{Tj} = \frac{I_m}{2\pi T}\big[\sin\emptyset\sin\gamma_j + 2sin^2\emptyset\cos(2\emptyset + \gamma_j) \\ - (2\pi N + \emptyset)\sin(\emptyset + \gamma_j)\big] \end{aligned} \tag{6.130}$$

$$b_{Tj} = \frac{I_m}{2\pi T}\big[-\sin\emptyset\cos\gamma_j + 2sin^2\emptyset\,\mathrm{s}\,in(2\emptyset+\gamma_j) + (2\pi N+\emptyset)\cos(\emptyset+\gamma_j)\big] \quad (6.131)$$

$$c_{Tj} = \frac{I_m}{2\pi T}[sin^2\emptyset + (2\pi N+\emptyset)^2 - (2\pi N+\emptyset)\sin 2\,\emptyset]^{\frac{1}{2}} \quad (6.132)$$

$$\psi_{Tj} = \tan^{-1}\frac{\sin\emptyset\sin\gamma_j + 2sin^2\emptyset\cos(2\emptyset+\gamma_j) - 2(2\pi N+\emptyset)\sin(\emptyset+\gamma_j)}{-\sin\emptyset\cos\gamma_j + 2sin^2\emptyset\,\mathrm{s}\,in(2\emptyset+\gamma_j) - 2(2\pi N+\emptyset)\cos(\emptyset+\gamma_j)} \quad (6.133)$$

Neutral current waveform analysis

The waveform of the current flowing through the neutral wire may be obtained by addition of the three instantaneous line current waveforms. For T=3, N=2, the neutral current waveform is shown in Fig.6.14(d). Let i_o be the instantaneous value of the neutral current, where

$$i_o = i_1 + i_2 + i_3 \quad (6.134)$$

Combining Eq.(6.124) and Eq.(6.134) for j = 1, 2, 3, gives

$$\begin{aligned} i_o(t) &= I_m\sin(\omega Tt-\emptyset) + I_m\ \sin\emptyset\ e^{-\cot\emptyset.\omega Tt}\ \Big|_{0}^{2\pi/3\omega T} \\ &+I_m\sin\left(\omega Tt-\emptyset+\frac{\pi}{3}\right) + I_m\ \sin\emptyset\ e^{-\cot\emptyset.\omega Tt} \\ &\times[1+\ e^{-\left(\frac{2\pi}{3}\right)\cot\emptyset}]\Big|_{2\pi/3\omega T}^{4\pi/3\omega T} + I_m\ \sin\emptyset\ e^{-\cot\emptyset.\omega Tt} \\ &\times\ [1+\ e^{\left(\frac{2\pi}{3}\right)\cot\emptyset} + e^{\left(\frac{4\pi}{3}\right)\cot\emptyset}]\ \Big|_{4\pi/3\omega T}^{2\pi N+\emptyset/\omega T} \\ &-I_m\sin(\omega Tt-\emptyset) + I_m\ \sin\emptyset\ e^{-\cot\emptyset.\omega Tt}[\ e^{-\left(\frac{2\pi}{3}\right)\cot\emptyset} \\ &+ e^{\left(\frac{4\pi}{3}\right)\cot\emptyset}]\ \Big|_{\frac{2\pi N+\emptyset}{\omega T}}^{\frac{2\pi N+\emptyset+\frac{2\pi}{3}}{\omega T}} \\ &+I_m\sin\left(\omega Tt-\emptyset-\frac{4\pi}{3}\right) + \ I_m\ \sin\emptyset\ e^{-\cot\emptyset.\omega Tt-\frac{4\pi}{3}}\ \Big|_{\frac{2\pi N+\emptyset+\frac{2\pi}{3}}{\omega T}}^{\frac{2\pi N+\emptyset+\frac{4\pi}{3}}{\omega T}} \\ &+0\Big|_{\frac{2\pi N+\emptyset+\frac{4\pi}{3}}{\omega T}}^{\frac{2\pi}{\omega T}} \end{aligned} \quad (6.135)$$

Fourier analysis of Eq. (6.135) yields,

The d.c. component of the neutral current is

$$a_{0o} = \frac{3I_m}{\pi T}[\cos\emptyset - 1 + \tan\emptyset \sin\emptyset] \tag{6.136}$$

$$c_{no} = \frac{I_m T}{\pi(T^2 - n^2)} \times \frac{\sin\frac{\pi n}{T}}{\sin\frac{\pi n}{3T}} \times \sqrt{\frac{T^2\{cos\frac{n}{T}(2\pi N + \emptyset) - \cos\emptyset\}^2 + T^2\{sin\frac{n}{T}(2\pi N + \emptyset) - nsin\emptyset\}^2}{T^2 cos^2\emptyset + n^2 sin^2\emptyset}} \tag{6.137}$$

Equation (6.137) gives the magnitude c_n of the nth harmonic, for n ≠ T, of the neutral current by simply multiplying the magnitude c_{nj} of the phase current, Eq.(6.128), by the factor $(\sin\frac{\pi n}{T} / \sin\frac{\pi n}{3T})$.The expression (6.137) can be considered as a general solution for R and R-L loads since, for R-load, if we substitute $\emptyset = 0$ into the above expressions , giving a_{oo} = 0, and

$$c_{on} = \frac{2\, I_m T}{\pi(T^2 - n^2)} \sin\frac{2\pi n}{T} \times \frac{\sin\frac{\pi n}{T}}{\sin\frac{\pi n}{3T}} \tag{6.138}$$

Supply frequency harmonic component, corresponding to n = T , does not then exist in the neutral current. This is because the supply frequency components of the three line currents are balanced, with resistive loads.
The phase angle, ψ_{on}, between the n[th] neutral current harmonic and the reference voltage v_a is given, with resistive load, by

$$\psi_{on} = \pi - \frac{2\pi n}{3T}(3N + 1) \tag{6.139}$$

Harmonic content of the load voltage and current waveforms of *R-L* load

With integral-cycle triggering mode of thyristors, it is evident from Fig.6.14, in three-phase 4-wire system, that the three load voltage waveforms are identical and so are the three load current waveforms. The supply frequency components are found to be balanced, since they are 120˚ apart in time-phase. In general the resultant phase voltages are unbalanced in that they do not sum to zero at every instant of the overall cycle. This is due to the fact that the phase-displacement angles $\psi_{nA}, \psi_{nB},$ and ψ_{nC} of a particular harmonic or subharmonic component are given by different functions of N. As a result current flows discontin-

uously in the neutral wire. It is also worth to mention that the neutral current contains a considerable d.c. component, as it is obvious from Eq.(6.136), which is three times of the phase component, Eq.(6.108). .

For *R-L* load, the harmonic frequency spectra of the line currents and neutral current of the 4-wire star-connection are given in Fig. 6.19.

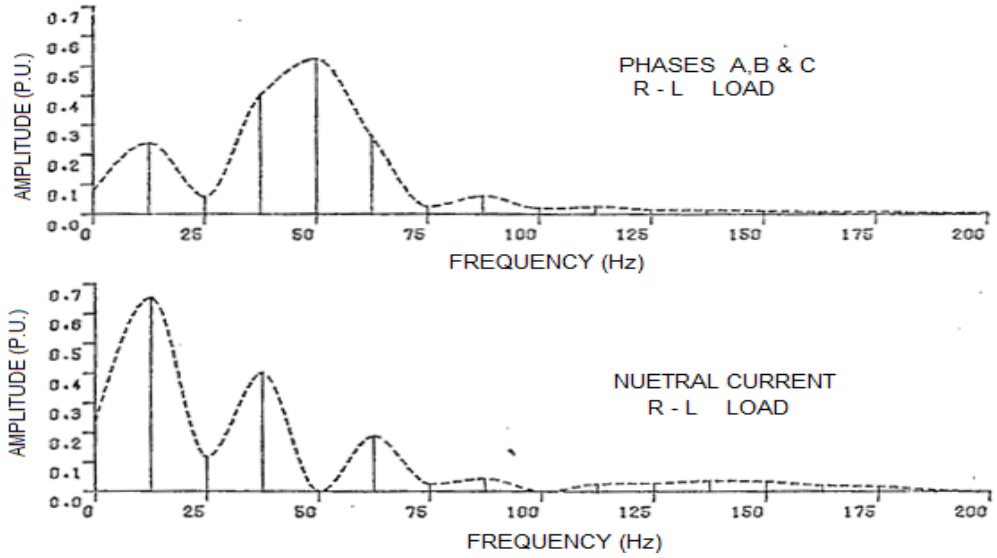

Fig.6.19 Frequency spectra of the line and neutral current waves for *N=2,T=4.*

The per unit values of these current were calculated for given values of *N* and *T*. Frequency spectra for *N*=2 , *T*=4 , $\emptyset = \pi/3$, Fig. 6.19, show that the neutral current contains both subharmonics and higher harmonic components, of the same order as the phase current waveforms, except that there is no supply frequency component or its multiples. If the control period *T* is increases, with ratio *N/T* constant, the neutral current is found to diminish and its value goes to zero for $T >> 1$.

6.7 OTHER FORMS OF INTEGRAL-CYCLE CONTROL

Integral-cycle control often results in considerable power loss but it is preferably used type of control in many industrial applications such as temperature control and d.c. motor drives. As a frequency changer, this type of control proves to be inefficient because the supply frequency component often exists as an effective component in the output voltage. Complete removal of the supply frequency component from the output waveform is considerably difficult due to the necessary use of physically large adding, subtracting, and phase-shifting components because the signals are at high level of power. Moreover, suppression of the supply frequency component using these techniques results in high losses and implementing expensive equipment. On the other hand, ICC has many

advantages over phase-angle control as it generates less number of harmonics, reduces the electromagnetic interference and possesses all the advantages of zero voltage switching techniques.

It was also shown elsewhere, that ICC in its conventional form is not feasible for a.c. drives application. The reason for that is the three-phase waveforms produced are rich of subharmonics of the supply frequency which are unbalanced neither in phases nor in amplitudes.The effects of these subharmonics on the motor causes vibration, noise, and temperature rise in the motor windings. To improve ICC performance, two anti-phase ICC waves are triggered alternatively to produce phase modulated like or bi-phase integral cycle controlled (BPICC) voltage or current waveforms. The technique uses bi-phase integral cycle controlled waveforms is called, elsewhere, angle or phase modulation of discrete form. The bi-phase integral cycle control gives high efficiency of conversion as well as eliminates completely the supply frequency component and most of the power associated with the supply frequency component is transferred to the desired frequency component, and the output voltage waveform contains little harmonics.

6.7.1 Bi-Phase Power Converter

The bi-phase power converter is depicted in Fig.6.20. The converter consists of three single-phase center-tapped transformers supplying three-

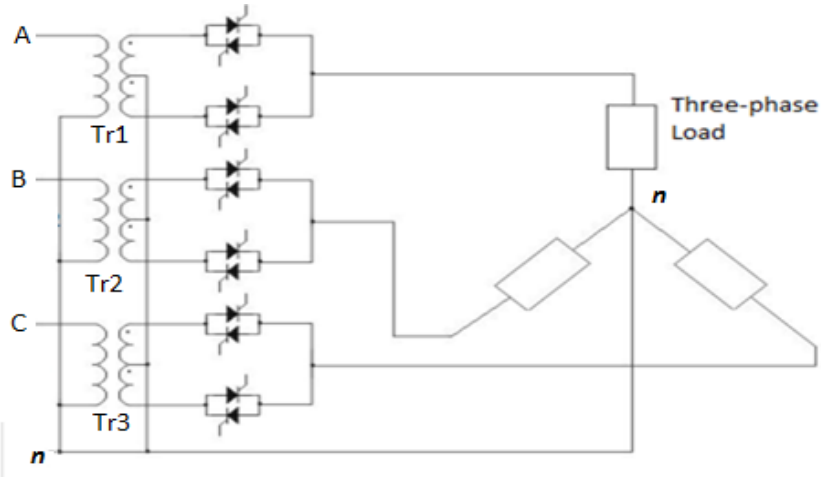

Fig.6.20 Three-phase, 4-wire, star-connected load supplied by a three single-phase centre-tapped power transformers to realize bi-phase ICC waveforms.

phase load via groups of inverse parallel connected thyristors. If the in-phase and anti-phase supply voltage waveforms are switched ON at zero voltage instant alternatively in a control period of T supply cycles, then for the case of R- load, the output voltage waveform per phase will be as shown in Fig.6.21.

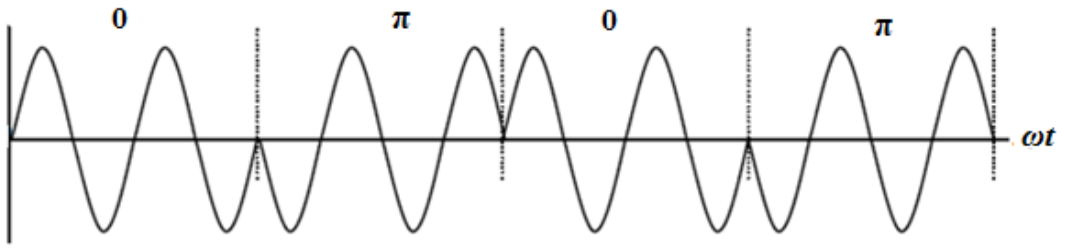

Fig.6.21 Output voltage waveform per phase for the circuit of Fig.6.20 for the case of resistive load.

For the case of *R-L* load, the current will not fall to zero after the end of the zero-phase ICC wave and the load voltage v_{Lj} of the j^{th} phase will be as shown in Fig. 6.22, and it may be defined by the following equation:

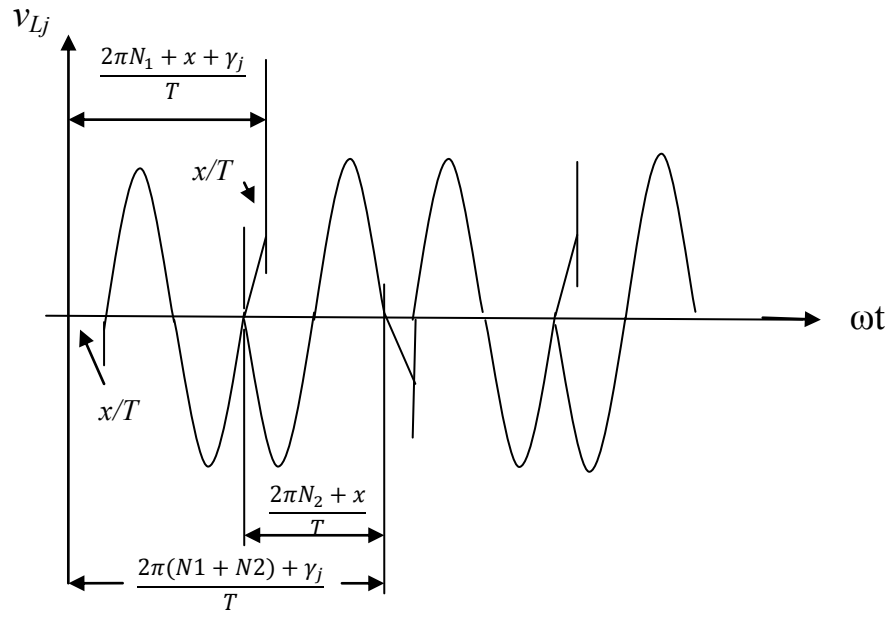

Fig.6.22 Load voltage v_{Lj} of the *jth* phase for a bi-phase ICC wave with *R-L* load.

$$V_{Lj} = V_m sin(\omega Tt - \gamma_j) \begin{cases} \frac{2\pi N_1 + \gamma_j}{T} \\ \frac{\gamma_j}{T} \end{cases}$$

$$- V_m sin(\omega Tt - \gamma_j) \begin{cases} \frac{2\pi(N_1 + N_2) + \gamma_j}{T} \\ \frac{2\pi N_1 + \gamma_j}{T} \end{cases} \qquad (6.140)$$

where $N_1 = N_2 = 1, 2, \ldots, T/2$ and T= the control period.
x = current extinction angle and γ_j = angle of phase j , (j =1,2,3) .
Fourier expansions of Eq.(6.140) gives the following results:

For $n \neq T$ and $x = \emptyset$ (impedance angle), the amplitude c_n and the phase angle ψ_n of the n^{th} harmonic component for the j^{th} phase may be found as:

$$a_{oj} = 0 \tag{6.141}$$

$$\begin{aligned} a_{nj} = \frac{V_m}{\pi(T^2 - n^2)} \Big| \Big(T\{ & cos\frac{n\gamma_j}{T} - cos\frac{n}{T}(2\pi N_1 + \gamma_j) \\ & - \cos\emptyset \, cos\frac{n}{T}(2\pi N_1 + \emptyset + \gamma_j) \\ & + \cos\emptyset \, cos\frac{n}{T}(2\pi(N_2 + N_1) + \emptyset + \gamma_j)\} \\ & + n\{\sin\emptyset \, sin\frac{n}{T}(2\pi(N_1 + N_2) + \emptyset + \gamma_j) \\ & - \sin\varphi \, sin\frac{n}{T}(2\pi(N_1 + \emptyset + \gamma_j)\}\Big)\Big| \end{aligned} \tag{6.142}$$

$$\begin{aligned} b_{nj} = \frac{V_m}{\pi(T^2 - n^2)} \Big| \Big(T\{ & sin\frac{n\gamma_j}{T} - sin\frac{n}{T}(2\pi N_1 + \gamma_j) \\ & - \cos\emptyset \, sin\frac{n}{T}(2\pi N_1 + \emptyset + \gamma_j) \\ & + \cos\varphi \, sin\frac{n}{T}(2\pi(N_1 + N_2) + \emptyset + \gamma_j)\} \\ & + n\{\sin\emptyset \, cos\frac{n}{T}(2\pi N_1 + \emptyset + \gamma_j) \\ & - \sin\emptyset \, cos\frac{n}{T}(2\pi(N_1 + N_2) + \emptyset + \gamma_j)\}\Big)\Big| \end{aligned} \tag{6.143}$$

The amplitude c_{nj} of the nth harmonic component for $n \neq T$ is

$$c_{nj} = \sqrt{a_{nj}^2 + b_{nj}^2} \tag{6.144}$$

and the phase angle ψ_{nj} between the supply voltage and the nth current harmonic is given by

$$\psi_{Tnj} = tan^{-1}\frac{a_{nj}}{b_{nj}} \tag{6.145}$$

For $n = T$, which is the supply frequency component:

$$a_{Tj} = 0 \quad \text{and} \quad b_{Tj} = 0 \tag{6.146}$$

$$c_{Tj} = 0 \quad \text{and} \quad \psi_{Tj} = 0 \tag{6.147}$$

It is obvious from the above two equations that the amplitude of the supply frequency component c_{Tj} equal to zero.This means that the supply frequency component is entirely suppressed by this type of converters. The harmonic amplitude spectrum and phase-displacement angles of the load voltage waveform of a BPICC wave is shown in Fig.6.23(a) for the case where $N_1 = N_2 = 2$ and $T = 4$, for R-load.

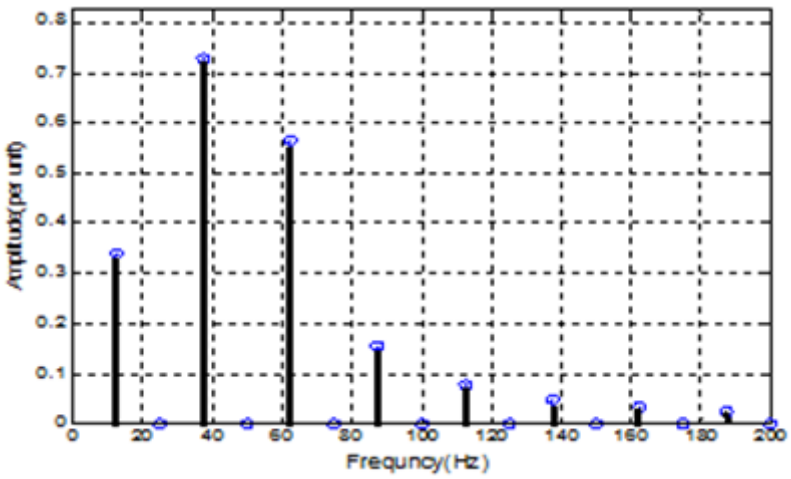

(a)

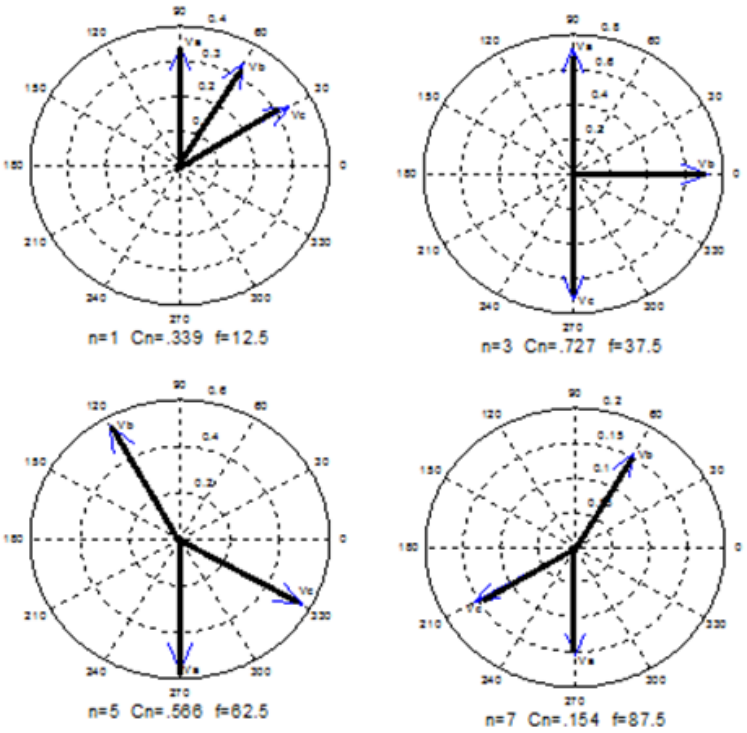

(b)

Fig.6.23 Bi-phase ICC converter : (a) Harmonic amplitude spectrm of phase *A, B,* and *C,* (b) Phase angle relationships for $N_1 = N_2 = 2$ and $T = 4$, R-load.

It is seen from Fig.6.23(a) that the harmonic amplitude spectrum contains odd harmonics only and the amplitudes of the even harmonics as well as the supply frequency component are all equal to zero. Also the harmonic spectrums for the three phases are found to be similar.

As it can be seen from Fig. 6.23(b), the phase displacement angles for any individual harmonic are found to be unbalanced for the three-phase system.The unbalanced phase harmonics generated by this type of converter are found to create severe problem when it is used as an a.c. drive. However, this problem can be solved by using the phase-shifting technique mentioned in the previous section. This technique, although it is simple, it has solved the similar problems associated with integral-cycle triggering for the three-phase systems. The phase-shifting technique involves shifting the load voltagev_{Lj} of phase *B* or phase *C* or both by multiples of 2π with respect to phase *A* which is taken as a reference phase.

By applying the phase shift technique to any BPICC wave , most of the important harmonic components become balanced in amplitude and phase displacement. Nevertheless, few of them becomes in-phase. In any case, the amplitude of an individual harmonic does not affected by the phase-shifting procedure. This fact is illustrated in Fig.6.24 for the case when $N = 2$ and $T = 4$ after phase angle correction for phase B and C. Oscillograms for the voltage and current waveforms for highly inductive load with BPICC are shown in Fig.6.25 for clarity.

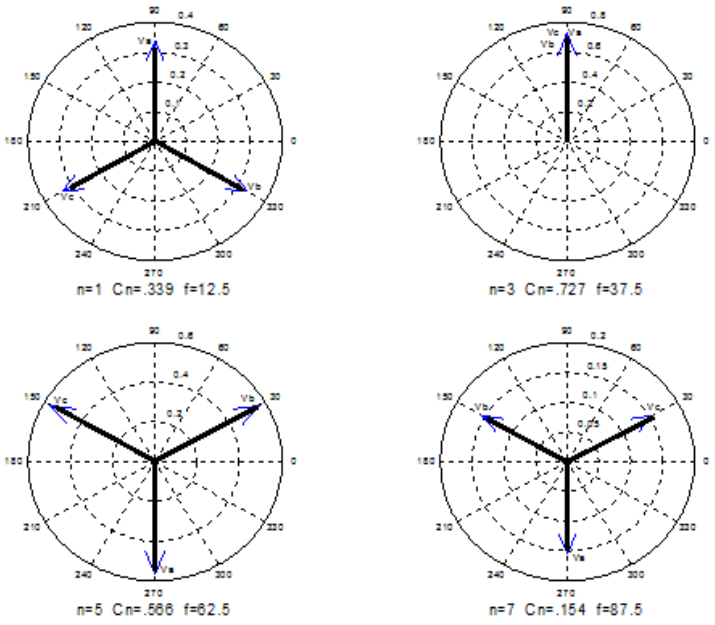

Fig.6.24 Phase angle relationships for $N_1 = N_2$ and $T = 4$, *R*-load after phase-angle correction.

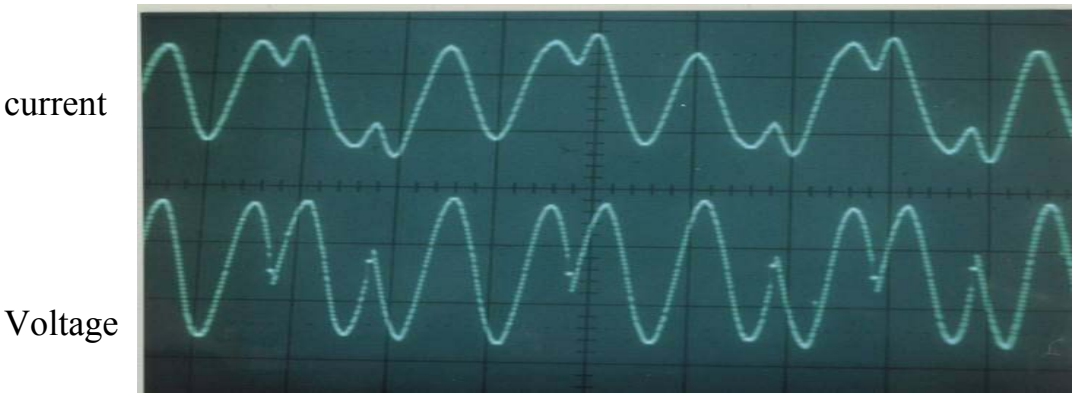

Fig.6.25 Oscillograms of the voltage and current waveforms for highly inductive load.

6.7.2 Multi-Conduction and Control Periods Integral-Cycle Triggering Technique

A typical integral-cycle controlled (ICC) with multi-control period T_1, T_2, T_3,...,T_n and different conduction cycles N_1, N_2, N_3,.... N_n in a total control period of T supply cycles is shown in Fig.6.26. This waveform is periodic in the control period of T supply cycles; hence load voltage with resistive load may be defined in terms of the control periods rather than of supply cycles, as mentioned early in this chapter. Hence for a 3-phase, 4-wire system, let the notation 1, 2, 3 denote the three phases A, B and C respectively. Thus the load voltage v_{Lj} for the *jth* phase (j=1,2,and 3) will have the general form given in Eq.(6.148) :

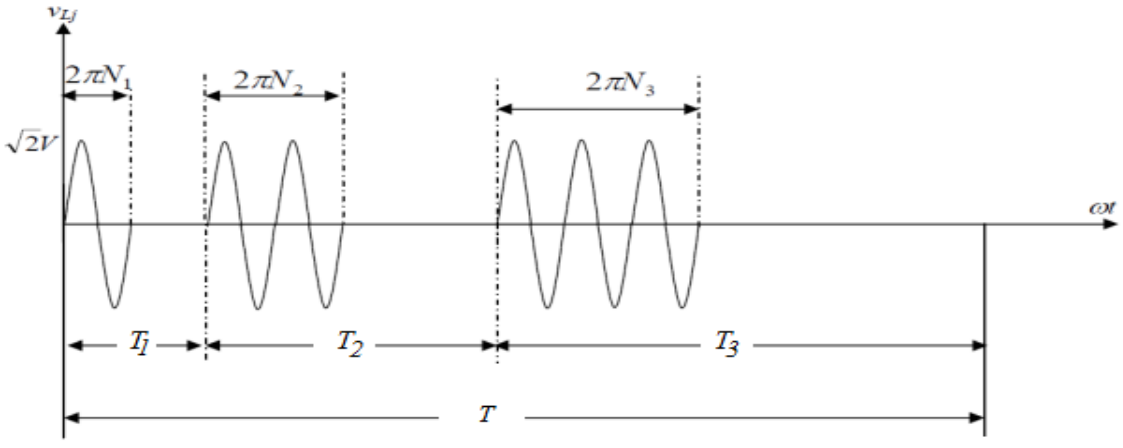

Fig.6.26 Realization of multi-conduction and multi-control period integral-cycle waveform (MICC) using consecutive ICC waves with different control periods.

$$V_{Lj} = V_m sin(\omega Tt - \gamma_j)\begin{cases}\dfrac{2\pi N_1 + \gamma_j}{T} \\ \dfrac{\gamma_j}{T}\end{cases}$$
$$+ V_m sin(\omega Tt - \gamma_j)\begin{cases}\dfrac{2\pi(N_2 + T_1) + \gamma_j}{T} \\ \dfrac{2\pi T_1 + \gamma_j}{T}\end{cases}$$
$$+ V_m sin(\omega Tt - \gamma_j)\begin{cases}\dfrac{2\pi(N_2 + T_1 + T_2) + \gamma_j}{T} \\ \dfrac{2\pi(T_1 + T_2) + \gamma_j}{T}\end{cases} \qquad (6.148)$$

where
$\gamma_1 = 0$, $\gamma_2 = 120^0$ and $\gamma_3 = 240^0$ are the phase angles of the three-phase voltages.
N_i is the number of conduction (ON) cycles.
$T_1 = N_1 + D_1$, $T_2 = N_2 + D_2$ and $T_3 = N_3 + D_3$

Fourier analysis of Eq. (6.148) gives the following results:

The zero frequency (d.c.) component coefficient a_o is

$$a_o = a_{o1} + a_{o2} + a_{o3} = 0$$

The nth harmonic coefficients are

$$a_{nj} = a_{n1j} + a_{n2j} + a_{n3j} \qquad (6.149)$$

$$a_{nj} = \frac{V_m}{\pi(T^2 - n^2)}\left|T\left(cos\frac{n\gamma_j}{T} - cos\frac{n}{T}(2\pi N_1 + \gamma_j)\right.\right.$$
$$+ cos\frac{n}{T}(2\pi T_1 + \gamma_j) - cos\frac{n}{T}(2\pi(N_2 + T_1) + \gamma_j)$$
$$+ cos\frac{n}{T}(2\pi(T_1 + T_2) + \gamma_j)$$
$$\left.\left. - cos\frac{n}{T}(2\pi(N_3 + T_1 + T_2) + \gamma_j)\right)\right| \qquad (6.150)$$

$$b_{nj} = b_{n1j} + b_{n2j} + b_{n3j}$$

$$b_{nj} = \frac{V_m}{\pi(T^2 - n^2)}\left|T\left(sin\frac{n\gamma_j}{T} - sin\frac{n}{T}(2\pi N_1 + \gamma_j) + sin\frac{n}{T}(2\pi T_1 + \gamma_j) - sin\frac{n}{T}(2\pi(N_2 + T_1) + \gamma_j) + sin\frac{n}{T}(2\pi(T_1 + T_2) + \gamma_j) - sin\frac{n}{T}(2\pi(N_3 + T_1 + T_2) + \gamma_j)\right)\right| \quad (6.151)$$

The amplitude C_{nj} of the nth harmonic component for $n \neq T$ is

$$c_{nj} = \sqrt{a_{nj}^2 + b_{nj}^2} \quad (6.152)$$

and the phase angle ψ_{nj} between the supply voltage and the nth current harmonic is given by

$$\psi_{Tnj} = tan^{-1}\frac{a_{nj}}{b_{nj}} \quad (6.153)$$

The supply- frequency harmonic component (n=T) is found to be

$$a_{Tj} = a_{T1j} + a_{T2j} + a_{T3j}$$

$$a_{Tj} = \frac{V_m}{4\pi T}\{-4\pi N_1 sin\gamma_j - 4\pi N_2 sin\gamma_j - 4\pi N_3 sin\gamma_j\} \quad (6.154)$$

$$b_{Tj} = b_{T1j} + b_{T2j} + b_{T3j}$$

$$b_{nj} = \frac{V_m}{4\pi T}\{4\pi N_1 cos\gamma_j + 4\pi N_2 cos\gamma_j + 4\pi N_3 cos\gamma_j\} \quad (6.155)$$

$$c_{Tj} = \sqrt{a_{Tj}^2 + b_{Tj}^2} \quad (6.156)$$

and the phase angle is

$$\psi_{Tj} = tan^{-1}\frac{a_{Tj}}{b_{Tj}} \quad (6.157)$$

If $N = N_1 = N_2 = N_3$ then the above two equation becomes

$$a_{Tj} = \frac{3\,V_m N}{T}\,sin\gamma_j \quad (6.158)$$

$$b_{Tj} = \frac{3\,V_m N}{T}\,cos\gamma_j \tag{6.159}$$

The supply frequency harmonic component C_{Tj} when n=T and $N = N_1 = N_2 = N_3$ is

$$c_{Tj} = \frac{3\,V_m N}{T} \tag{6.160}$$

and the phase angle ψ_{Tj} is

$$\psi_{Tj} = tan^{-1}\frac{a_{Tj}}{b_{Tj}} = tan^{-1}\frac{sin\gamma_j}{cos\gamma_j} \tag{6.161}$$

Fig.6.27 shows harmonic amplitude spectra of two types of discrete frequency MICC waveforms for different value of conduction cycle (N_1, N_2, N_3) and control periods (T_1, T_2, T_3).

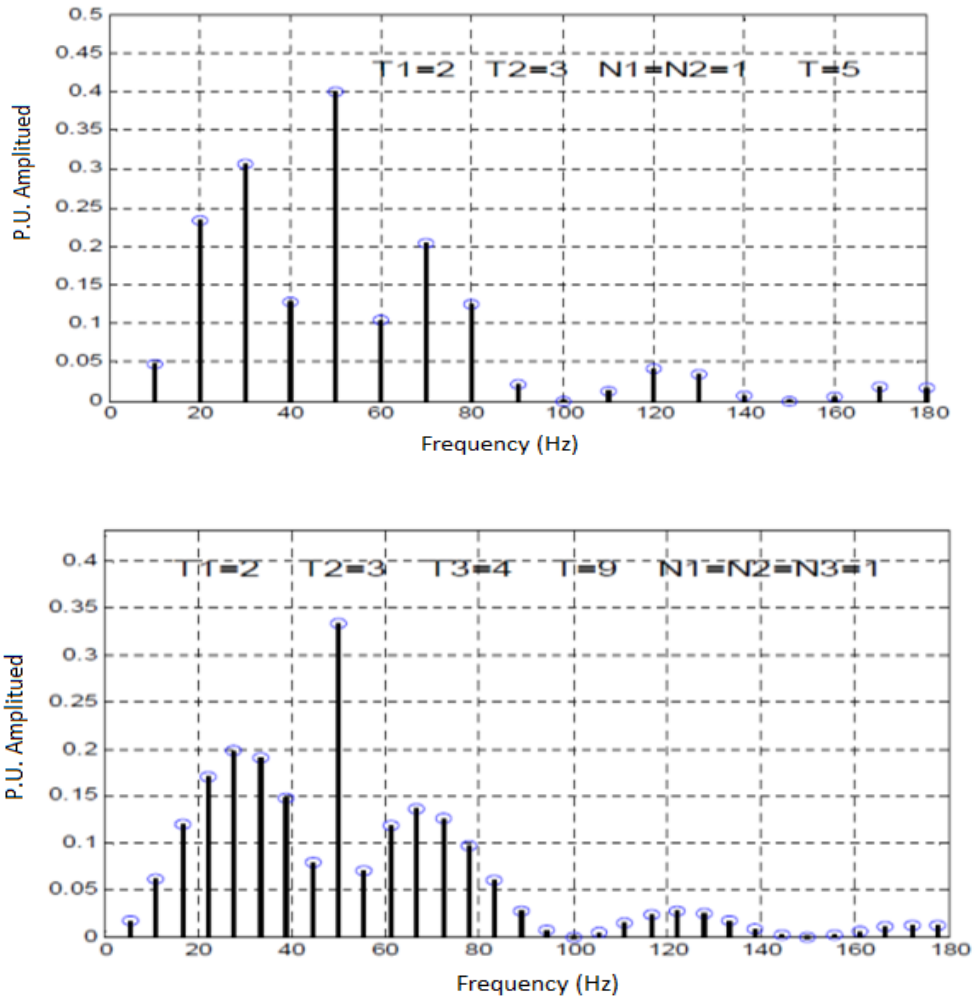

Fig.6.27 Harmonic amplitude spectra of phases (A, B, and C) for two types of MICC waveform.

From Fig.6.27, it is to be noted that this type of control proves to be inefficient as a frequency changing technique because the supply frequency component exists as an effective component in the output voltage. It is also obvious, from Eq.(6.160) that the supply frequency component cannot be suppressed and its peak value depends on the number of conduction cycles N and on the control period T. In general, the harmonic spectrum of the MICC wave shown in Fig.6.27 depends largely on the values of N_1, N_2, N_3 as well as the values T_1, T_2, and T_3 which may be called the MICC parameters. However, the harmonics generation with this type of ICC wave can be selected or controlled by a judicious selection of the values of these parameters. A certain desired frequency component can be enhanced and other undesirable frequency components can be eliminated by this technique.

Fig 6.28, shows the amplitude and phase angle relationship of selected harmonic component for the case N_1=N_2=1, T_1 =2 and T_2=3, R-load, three-phase system. Also from Fig.6.28, it is obvious that the amplitudes of the harmonic components for a certain frequency are balance for the three phases, whereas the phase-angle relationships for these components are found to be unbalanced.

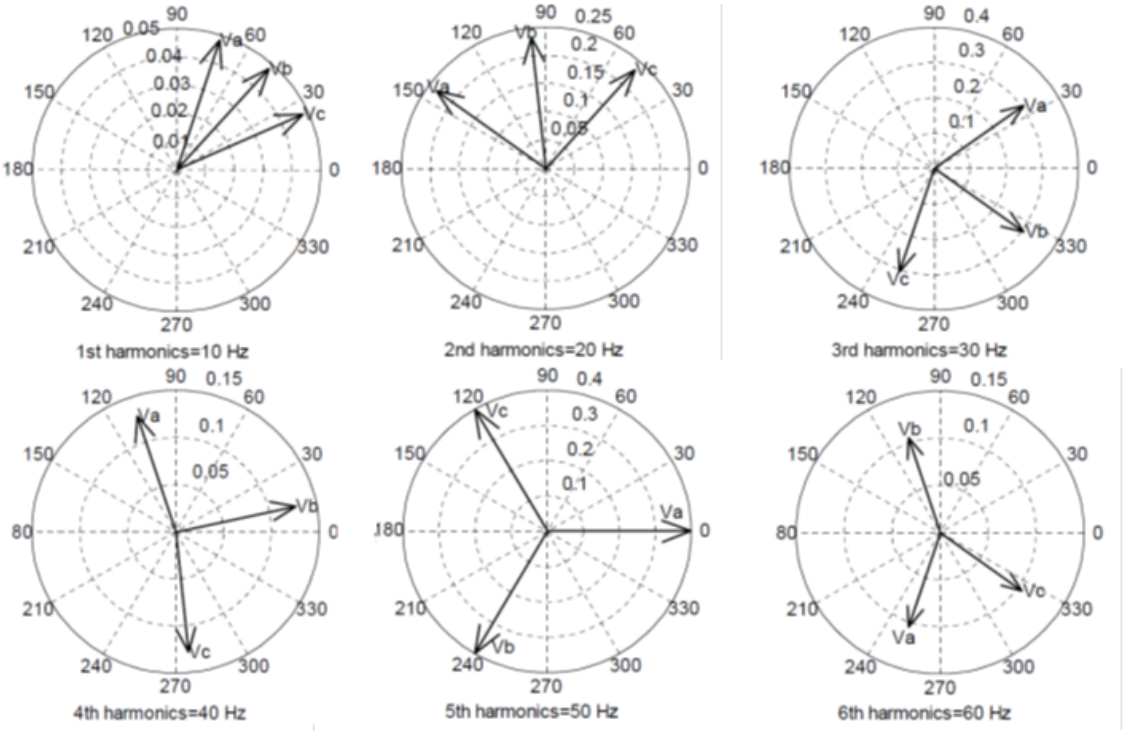

Fig.6.28 Amplitude and phase angle relationship of some selected harmonic components for the case $N_1 = N_2 = 1$, $T_1 = 2$, $T_2 = 3$ and $T = 5$, three-phase system, R-load .

6.7.3 Bi-Phase Multi-Control and and Multi-Conduction Period Integral-Cycle Control (BPMICC) Technique

In the previous converter which is based on ICC , the supply frequency component can be entirely eliminated by using two ICC waves with 0^0 and 180^0 phase shifted as shown in Fig.6.29 which leads to the Bi-phase Multi-period Integral-cycle control (BPMICC).This can be achieved by using the same three-phase converter configuration shown in Fig.6.20.

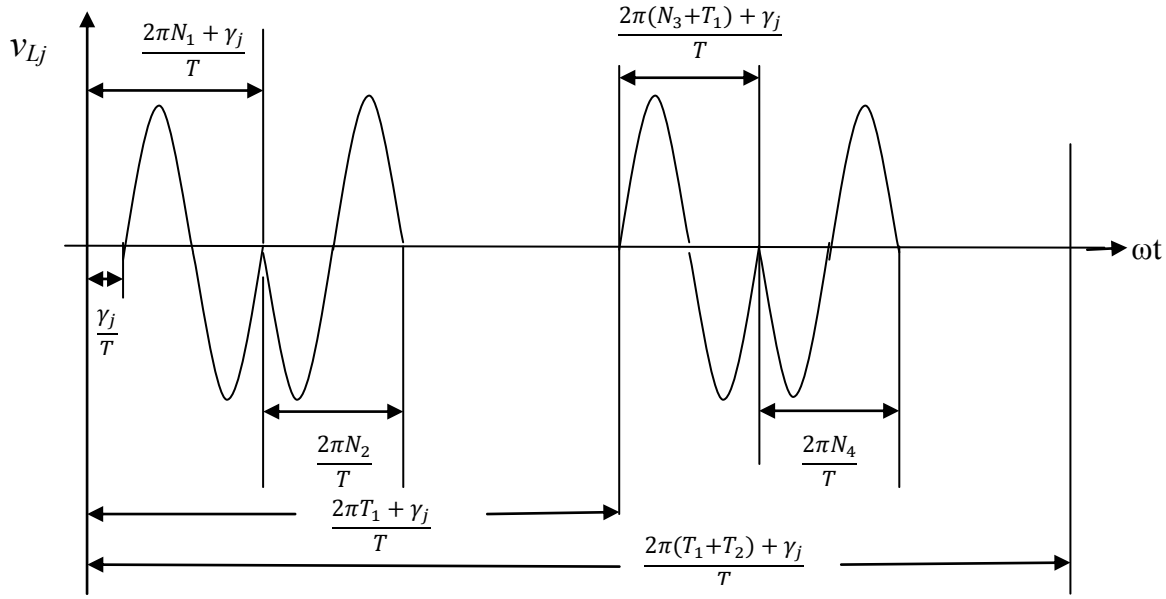

Fig.6.29 Load voltage v_{Lj} of the *jth* phase for a bi-phase ICC wave.

The load voltage v_{Lj} of the j_{th} phase of the waveform of Fig.6.29 may be defined during the control period T by

$$V_{Lj} = V_m sin(\omega Tt - \gamma_j)\begin{cases}\frac{2\pi N_1 + \gamma_j}{T} \\ \frac{\gamma_j}{T}\end{cases}$$

$$- V_m sin(\omega Tt - \gamma_j)\begin{cases}\frac{2\pi(N_1 + N_2) + \gamma_j}{T} \\ \frac{2\pi N_1 + \gamma_j}{T}\end{cases}$$

$$+V_m sin(\omega Tt - \gamma_j)\begin{cases}\dfrac{2\pi(N_3 + T_1)+\gamma_j}{T}\\ \dfrac{2\pi T_1+\gamma_j}{T}\end{cases}$$

$$-V_m sin(\omega Tt - \gamma_j)\begin{cases}\dfrac{2\pi(N_3 + N_4 + T_1)+\gamma_j}{T}\\ \dfrac{2\pi(N_3 + T_1)+\gamma_j}{T}\end{cases} \qquad (6.162)$$

$V_{Lj} = 0$ elsewhere

where $T_1 = N_1 + N_2 + D_1$ and $T_2 = N_3 + N_4 + D_2$

Fourier analysis of Eq.(6.161), gives the following results:

For $n \neq T$

$$a_{nj} = \frac{V_m\, T}{\pi(\,T^2 - n^2)}\Big(cos\frac{n\gamma_j}{T} - 2\,cos\frac{n}{T}(2\pi N_1 + \gamma_j) + cos\frac{n}{T}(2\pi N_1 + \gamma_j) + \,cos\frac{n}{T}(2\pi(N_1 + N_2) + \gamma_j) + cos\frac{n}{T}(2\pi T_1 \,+ \gamma_j) - cos\frac{n}{T}(2\pi(N_3 + T_1) + \gamma_j) + cos\frac{n}{T}(2\pi(N_3 + N_4 + T_1) + \gamma_j)\ \Big) \qquad (6.163)$$

$$b_{nj} = \frac{V_m\, T}{\pi(\,T^2 - n^2)}\Big(sin\frac{n\gamma_j}{T} + \,cos\frac{n}{T}(2\pi(N_1 + N_2) + \gamma_j) + cos\frac{n}{T}(2\pi T_1 \,+ \gamma_j) - cos\frac{n}{T}(2\pi(N_3 + T_1) + \gamma_j) + cos\frac{n}{T}(2\pi(N_3 + N_4 + T_1) + \gamma_j)\ \Big) \qquad (6.164)$$

The amplitude c_{nj} of the nth harmonic component for $n \neq T$ is

$$c_{nj} = \sqrt{a_{nj}^2 + b_{nj}^2} \qquad (6.165)$$

and the phase angle ψ_{nj} between the supply voltage and the nth current harmonic is given by

$$\psi_{nj} = tan^{-1}\frac{a_{nj}}{b_{nj}} \qquad (6.166)$$

The supply-frequency harmonic component (n=*T*) is found to be

$$a_{Tj} = \frac{\sqrt{2}V}{4\pi T}\{-4\pi N_1 sin\gamma_j + 4\pi N_2 sin\gamma_j - 4\pi N_3 sin\gamma_j + 4\pi N_4 sin\gamma_j\} \quad (6.167)$$

$$b_{Tj} = \frac{\sqrt{2}V}{4\pi T}\{-4\pi N_1 cos\gamma_j - 4\pi N_2 cos\gamma_j - 4\pi N_3 cos\gamma_j + 4\pi N_3 cos\gamma_j\} \quad (6.168)$$

The amplitude c_{Tj} of the supply frequency component for $n = T$ and the phase angle ψ_{nj} are

$$c_{Tj} = \sqrt{a_{Tj}^2 + b_{Tj}^2} \quad (6.169)$$

$$\psi_{Tj} = tan^{-1}\frac{a_{Tj}}{b_{Tj}} \quad (6.170)$$

The analysis of the bi-phase ICC wave of Fig.6.29 shows that the amplitude of the supply frequency component (i.e. c_{Tj}) equal to zero only for the cases when $N_1 = N_2$ and $N_3 = N_4$ or $N_1=N_4$ and $N_2=N_3$. Plot of the harmonic amplitude spectrum (per-phase) of the ICC wave for different values of N_1, N_2 ,N_3,N_4 ,T_1 and T_2 for R- load is shown in Fig.6.30.

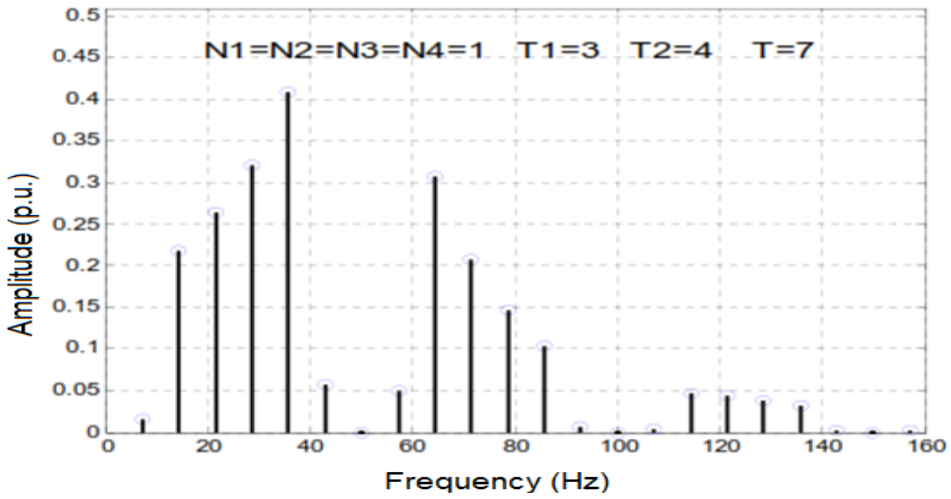

Fig.6.30 Harmonic amplitude spectrum per-phase for a bi-phase ICC wave with $N_1=N_2=N_3=N_4$ =1, and T_1 =3, T_2 = 4 and T=7.

Fig.6.31 shows the amplitude and phase-angle relationship of some selected significant harmonic component for the three phases for the case $N_1 = N_2 = N_3 = N_4 = 1$,$T_1 = 3$ and $T = 7$. It is to be noted that the supply

frequency harmonic component is totally eliminated and the harmonic spectra for the three phases are the same.

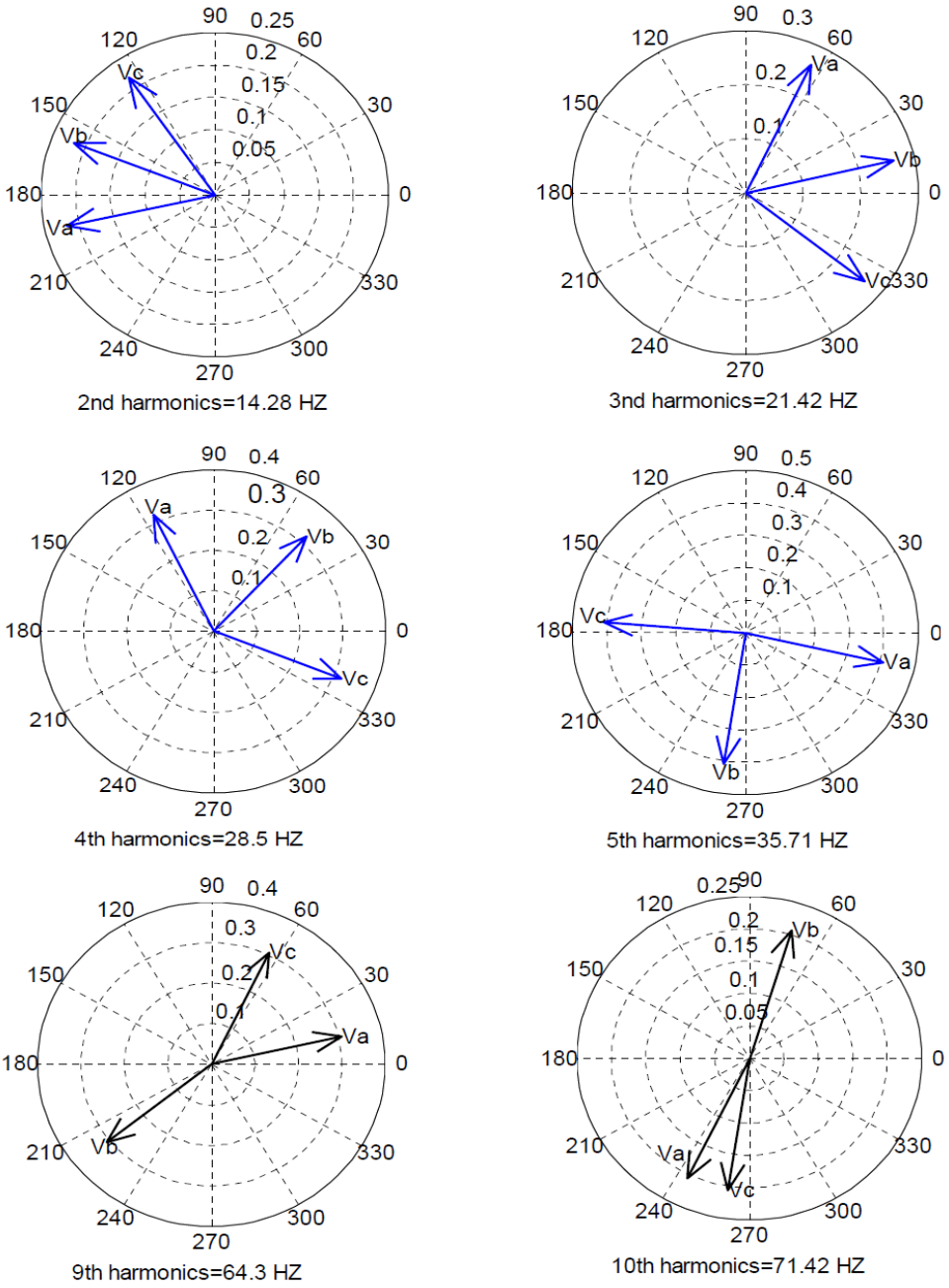

Fig.6.31 Amplitude and phase- angle relation of some selected significant harmonic component in a bi-phase ICC wave for the case $N_1 = N_2 = N_3 = N_4 = 1$, $T_1 = 3$, and T=7, R-load, 3-phase system.

Also from Fig.6.31, it is obvious that the amplitudes of the harmonic components for a certain frequency are balance for the three phases, while the phase-angle relationships for these components are found to be unbalanced. This problem can be solved using the multiple of 2π phase

shifting technique discussed in the previous section. Fig.6.32 shows the phase displacement angle after correction. Matlab program for calculating the frequency spectra and phase relationships is given in Appendix C.

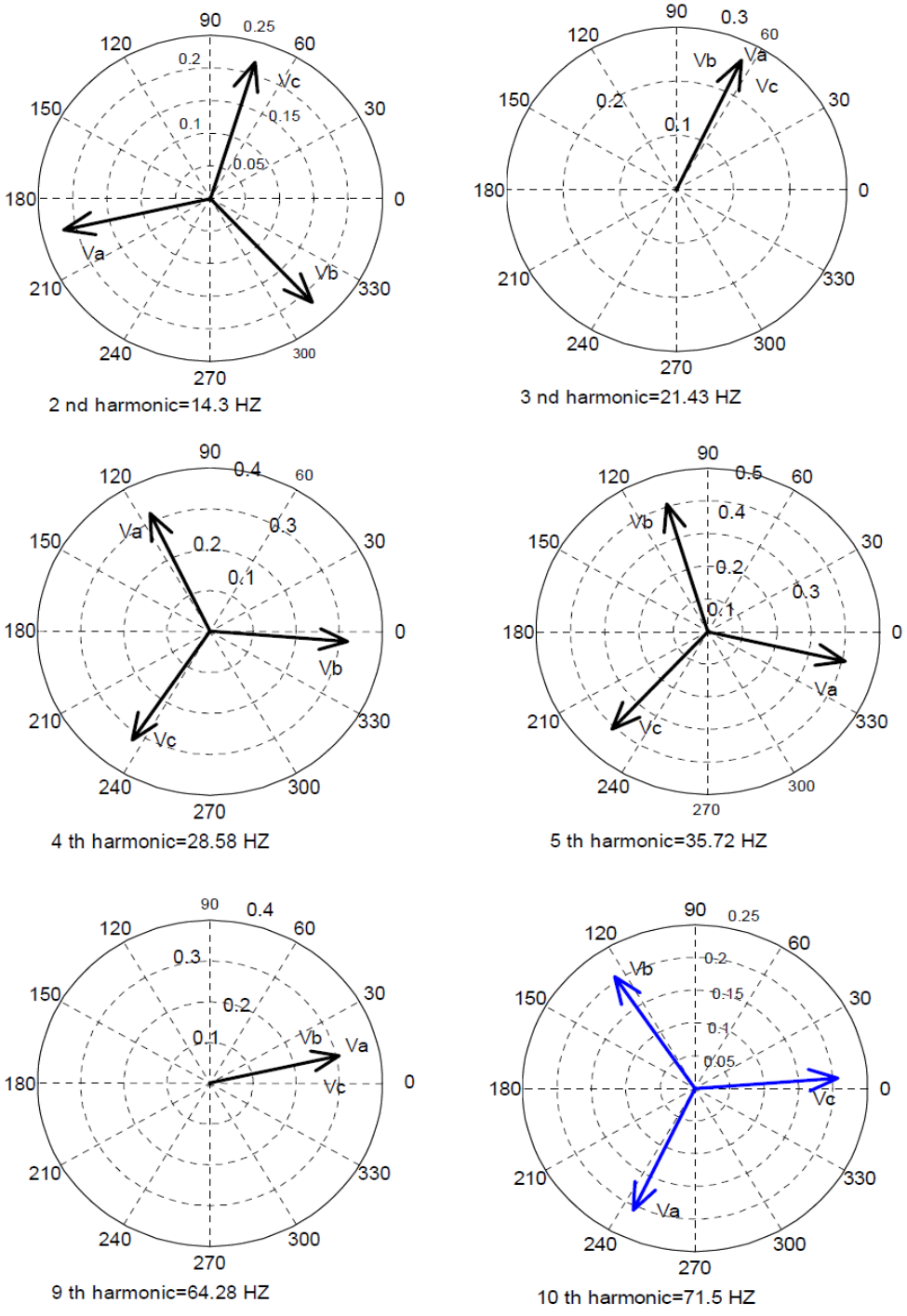
2 nd harmonic=14.3 HZ
3 nd harmonic=21.43 HZ
4 th harmonic=28.58 HZ
5 th harmonic=35.72 HZ
9 th harmonic=64.28 HZ
10 th harmonic=71.5 HZ

Fig.6.32 Amplitude and phase-angle relationship of some selected significant harmonic component in a bi-phase ICC wave for the case N_1 = N_2 = N_3= N_4 = 1, T_1 =3, and T=7, R-load after phase-angle correction.

Fig.6.33 shows oscillograms of the load voltage waveforms v_{LA}, v_{LB} for bi-phase ICC wave for the case when T_1=3, T_2=4,N_1=N_2=N_3=N_4=1.

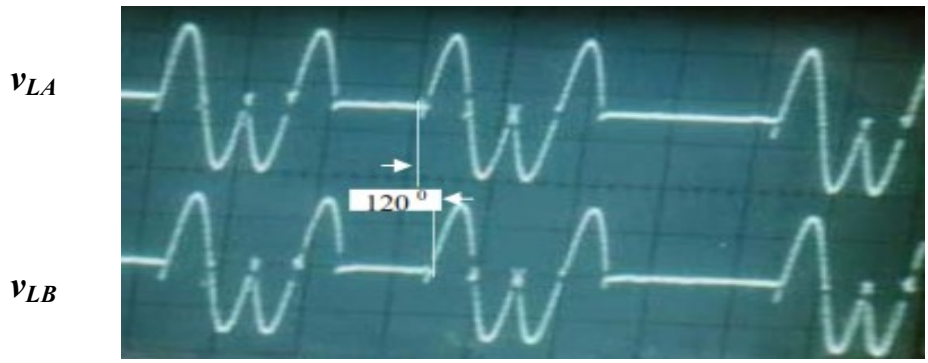

Fig.6.33 Load voltage waveforms (R-load) BPMICC wave for the case when T_1=3, T_2=4,N_1=N_2=N_3=N_4=1 .

Table 6.3 gives comparison between phase-angle triggering and integral-cycle triggering.

Table 6.3

Phase-angle triggering	Integral-cycle triggering
1) DC value = 0, no d.c. component with both resistive and resistive-inductive loads.	1) No d.c. component with resistive load for both the load voltage and current waveforms in single-phase and three-phase systems. However, d.c. component appears significantly in the line and neutral currents with *R-L* load.
2) Odd, higher harmonics.	2) Odd + even harmonics.
3) Higher harmonic voltage < Fundamental voltage.	3) Harmonics (even are troublesome in electricity supply system)
4) No generation of subharmonics.	4) Subharmonics are generated in this type of control. Subharmonic of the fundamental down to the $(1/T)^{th}$ subharmonic. e.g: N=6 , T=8 : Lowest subharmonic is 1/8 supply frequency.

Integral-cycle triggering results in conduction patterns that contain subharmonics of the supply frequency and so constitute a form of step-down frequency changing that can be considered as a form of frequency changer. Also integral-cycle triggering results in a considerable reduction in the amplitudes of the higher order harmonics as compared with other triggering techniques and it is possible that Radio Frequency Interference (RFI) is negligible. The phase-control switching can produce higher order harmonics and heavy inrush current while switching on in a cold start, while integral-cycle control circuits have the advantage of low inrush current due to zero voltage switching ease in construction and low hardware cost. Therefore, integral-cycle control loads have been widely used in resistive loads, such as heaters, oven, furnaces and spot welders. Also it is used in speed control of single-phase induction motor and d.c. series motor.

As a frequency changing scheme, integral-cycle triggering was found not feasible for applications in the three-phase systems exploiting this technique for a.c. motor speed control. This is because the amplitudes and phase-displacement angles of the higher order harmonic and subharmonic components of the integral-cycle controlled waveform are determined by the conduction period N and the control period T and the order of the individual harmonic. However using the modified integral cycle techniques such as bi-phase ICC or multi-bi-phase ICC together with phase-angle correction techniques may rectify the situation.

The choice between integral-cycle triggers and phase-angle triggering, in the circuit of Fig. 6.1 depends partly on whether the long off' time with integral-cycle control in case of unmodified type is acceptable in the particular application.

PROBLEMS

6.1 Power to a resistive load is to be controlled using integral-cycle triggering mode of thyristors. A single-phase voltage source of 230V,50Hz is used to provide current to a 50Ω resistor via a pair of inverse parallel-connected thyristors which is gated to produce integral cycle voltage control with number of conducting cycles N = 6 and the total period T (ON+OFF) is 8 supply cycles. Calculate the power transfer to the resistor, the current and the power factor of the circuit.

[Ans : P_L= 793.5 W, I_L= 3.98 A, PF= 0.866]

6.2 A sinusoidal voltage supply v_s =300 sinωt is connected to a pair of inverse-parallel connected thyristors to control power flow to a 20 Ω resistive heating load. The thyristor are gated to produce burst-firing of the load current. If the number of conducting cycles N = 3 and the total period T = 6 supply cycles. Determine the average percentage power transfer to the load as compared with the operation of the circuit with sinusoidal voltage .What firing angle would be required with phase-angle controlled by thyristors to produce the same *rms* load current?

[Ans : % Power = 50 , α = 90˚]

6.3 A 230V, 50 Hz sinusoidal voltage supply is used to provide power to a resistive load via a pair of inverse-parallel connected thyristors. The two thyristors are triggered to give integral-cycle controlled current waveform in the number of conducting cycles N = 2 and the total control period T =5 supply cycles. Calculate the supply frequency harmonic voltage and the amplitudes of its immediate harmonic neighbors up to the sixth order harmonic.

[Ans : $c_{n=T}$ =130V, $c_{n=1}$ = 43.15V, $c_{n=2}$ = 49.30V, $c_{n=3}$ = 64.70V, $c_{n=4}$ =115V, $c_{n=5}$ = - 49V, $c_{n=6}$ = - 43V]

6.4 One feature of the harmonic properties of integral-cycle controlled thyristor circuits is the presence of subharmonics of the supply frequency. With a control period T (ON time + OFF time), the lowest subharmonic is 1\T of the supply frequency. What are the disadvantages of electrical supplies containing subharmonics of the fundamental?

6.5 For a single-phase integral-cycle controlled thyristor circuit with resistive load, show that the *rms* value of the harmonic load voltage V_H (excluding the supply frequency component when n=T) is given by

$$V_H = \sqrt{N(\frac{1}{T} - \frac{N}{T^2})}$$

Hence prove that, the ratio between the *rms* value of V_H and the *rms* load voltage V_L is given by

$$\frac{V_H}{V_L} = \sqrt{\frac{T-N}{T}}$$

6.6 In an integral-cycle controlled thyristor circuit with resistive load switching at voltage zero, the current, when it flows, is always in time phase with the supply voltage. Does this mean that the circuit operates at unity power factor?

6.7 The two main technical disadvantages semiconductor controlled rectifiers are the generation of radio interference and the distortion of supply voltage.

(a) Explain briefly the types of radio frequency interference caused by semiconductor action. What frequency bands are included in a typical noise spectrum? Describe a simple and cheap way to demonstrate the principle features of radiated interference such as frequency spectrum, amplitude-distance, effect of screening etc. and give typical results of such a demonstration.

(b) Explain how thyristor switching causes distortion of the supply voltage. If the thyristors are to be switched so as to develop 50% power in a resistive load, discuss the modes of thyristor triggering that you would recommend to give (i) minimum supply voltage distortion, (ii) minimum radio interference.

6.8 The voltage of a three-phase 4-wire resistive load is to be controlled by using three-phase a.c. controller with integral-cycle triggering mode of thyristors as shown in Fig.6.34. The Three-phase supply is star-connected with 400V, 50 Hz line to line voltage. (a) For control parameters $N = 2$ and $T = 4$, find the load phase current, and the total power transferred to the load, (b) what is the power factor of the circuit?

[Ans : I_L =16.26 A per-phase, P_L =7.933 kW for three phases, (b) PF = 0.707]

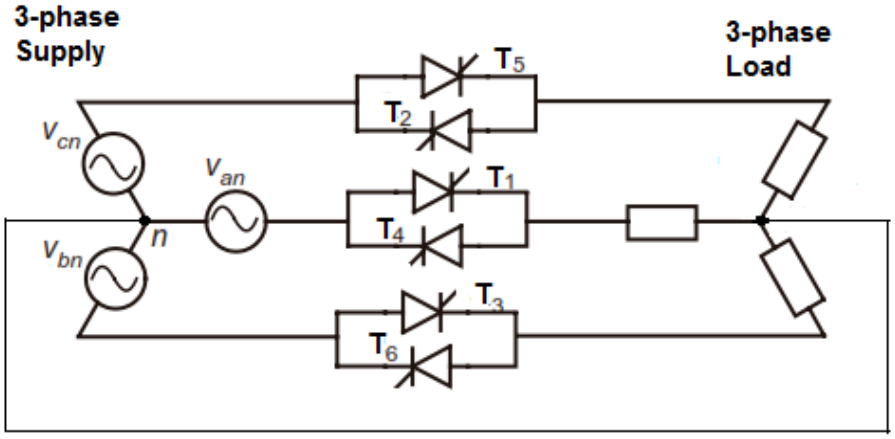

Fig.6.34.

6.9 For the problem 6.8, use equations (6.92) and (6.94) to determine the supply frequency harmonic voltage and the amplitudes of its immediate harmonic neighbors for the neutral current.

Note : Use $I_m = V_m / R$, where V_m is the peak of the phase voltage.

[Ans: $c_{n=T} = 0V$, $c_{n=1}=15V$, $c_{n=2}= 0V$, $c_{n=3} = -11.8V$, $c_{n=5} = 6.73V$]

6.10 An ideal single-phase supply $vs = V_m \sin \omega t$ provides power to a resistive load $R = 100\Omega$ using the circuit of Fig.6.35. The SCRs of the inverse-parallel pair are gated to provide integral cycle control mode of triggering such that the output is d.c. voltage.

(a) Prove that the value of the output d.c. voltage component produced by the circuit is given by

$$V_{dc} = \frac{2V_m}{\pi}\left(\frac{N}{T}\right)$$

(b) Derive an expression for the power transferred to the load in terms of V_m, N and T (the control period).

(c) Calculate the power when $V_m = 300$ V , and $N = 20$, $T = 30$ cycles respectively.

Fig. 6.35.

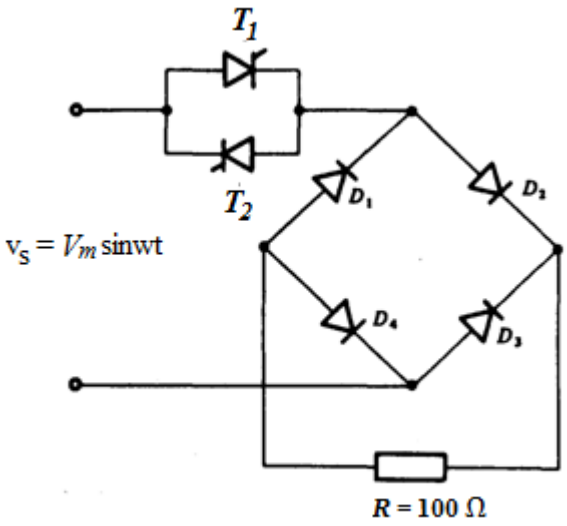

[Ans : (b) $P_{dc} = \left(\frac{2NV_m}{\pi T}\right)^2 \times \frac{1}{R}$, (c) 162.27 W]

6.11 The line currents of a three-phase 3-wire delta-connected resistive load is to be controlled by using three-phase a.c. controller with integral-cycle triggering mode of thyristors as shown in Fig.6.36. Prove that the amplitude c_n^j of the nth harmonic for n ≠ T for the three phases (j =A, B, and C) are given by

$$c_n^A = c_n^B = \frac{\sqrt{3}\, I_m}{\pi(T^2 - n^2)} \sqrt{(3T^2 - n^2)}\, \sin\frac{\pi n N}{T} \qquad \text{For Phases A\&B}$$

$$c_n^C = \frac{n\sqrt{3}\, I_m}{\pi(T^2 - n^2)} \qquad \text{For phase C}$$

and for n=T :

$$c_T^A = c_T^B = c_T^C = 3\, I_m \left(\frac{N}{T}\right)$$

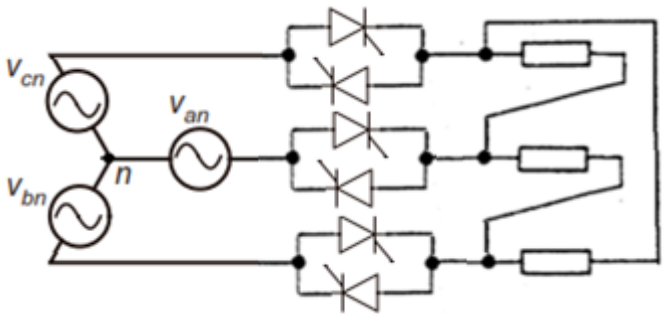

Fig.6.36.

CHAPTER SEVEN

AC-AC CONVERSION: CYCLOCONVERTERS AND MATRIX CONVERTERS

7.1 INTRODUCTION

The ac-to-ac power converters available in industry today do not actually convert power directly from a.c. power of one frequency to a.c. power of another frequency. Instead, these converters first convert electrical power to d.c. using a rectifier, and then convert power back into a.c. using an inverter.These are called two-stage converters. However, a cycloconverter is a frequency changer that converts an a.c. supply of fixed input frequency directly to an a.c. output of another frequency. Cycloconverters not only eliminate the problem of having multiple systems to perform a single function, they also limit the flow of power to a single switch at any one period in time. Therefore, there is no bus link, d.c. or otherwise, included in a cycloconverter topology between power input and power output.

Cycloconverters are used in many industrial applications as one-stage frequency changer for a.c. motor drives and other high power, low speed devices such as gearless cement mills, steel rolling mills, ore grinding mills, pumps and compressors, and mine winders. Cycloconverters can be classified into two categories depending upon the method how the firing angle 'α' is controlled. These are:

1. Phase-controlled cycloconverters, in which the firing angle is controlled by adjustable gate pulses as in controlled rectifier circuits.

2. Envelope cycloconverters, in which the switches remain fully-on like diodes and conduct for consecutive half cycles.

Depending upon the converter use for conversion, the cycloconverters may also be classifies as,

(i) 2-pulse cycloconverters.
(ii) 3-pulse cycloconverters.
(iii) 6-pulse cycloconverters.

Another classification is based on the input and output phases of the cycloconverters as,

(i) Single-phase to single-phase cycloconverters.
(ii) Three-phase to single-phase cycloconverters.
(iii) Three-phase to three-phase cycloconverters

7.2 SINGLE-PHASE TO SINGLE-PHASE CYCLOCONVERTER

The basic circuit of the single-phase two-pulse cycloconverter is shown in Fig.7.1. The converter consist of four thyristor and a center-tap transformer. By the controlled opening and closing of the thyristors, it is possible to fabricate output voltage waveforms having a fundamental component of the desired output frequency.

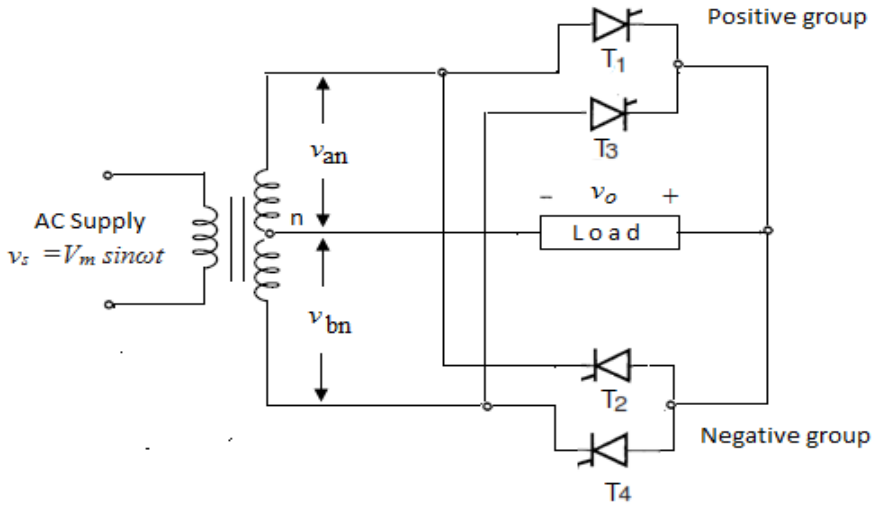

Fig.7.1 Single-phase to single-phase two-pulse cycloconverter basic circuit.

For example, if it is required to generate an output voltage wave of 25 Hz from an input voltage of 50Hz, then in the positive half-cycle of the input voltage v_{an}, thyristor T_1 conducts from 0 to π, and in the positive half-cycle of the input voltage v_{bn} T_3 conducts from π to 2π, hence output voltage is positive. Similarly, during the negative half-cycle of v_{bn}, T_2 conducts from 2π to 3π and during the negative half-cycle of v_{an} T_4 conducts from 3π to 4π, hence the load voltage becomes negative and the sequence is repeated. The waveforms of this converter are shown in

Fig.7.2. The input supply voltage is shown in Fig.7.2 (a) and the 25 Hz output voltage waveform is shown in Fig.7.2(c).

If another output frequency is required, say 16.5 Hz, the waveform will consist of three positive half cycles and thee negative half cycles as shown in Fig.7.2(d). Also, for 12.5 Hz output waveform it is required to trigger four positive half cycles and four negative half cycles. Therefore, if m = number of half supply cycle of frequency f_i, the output frequency f_o will be

$$f_o = \frac{f_i}{m} \qquad \text{where m is integer} = 1,2,3,\ldots\ldots \qquad (7.1)$$

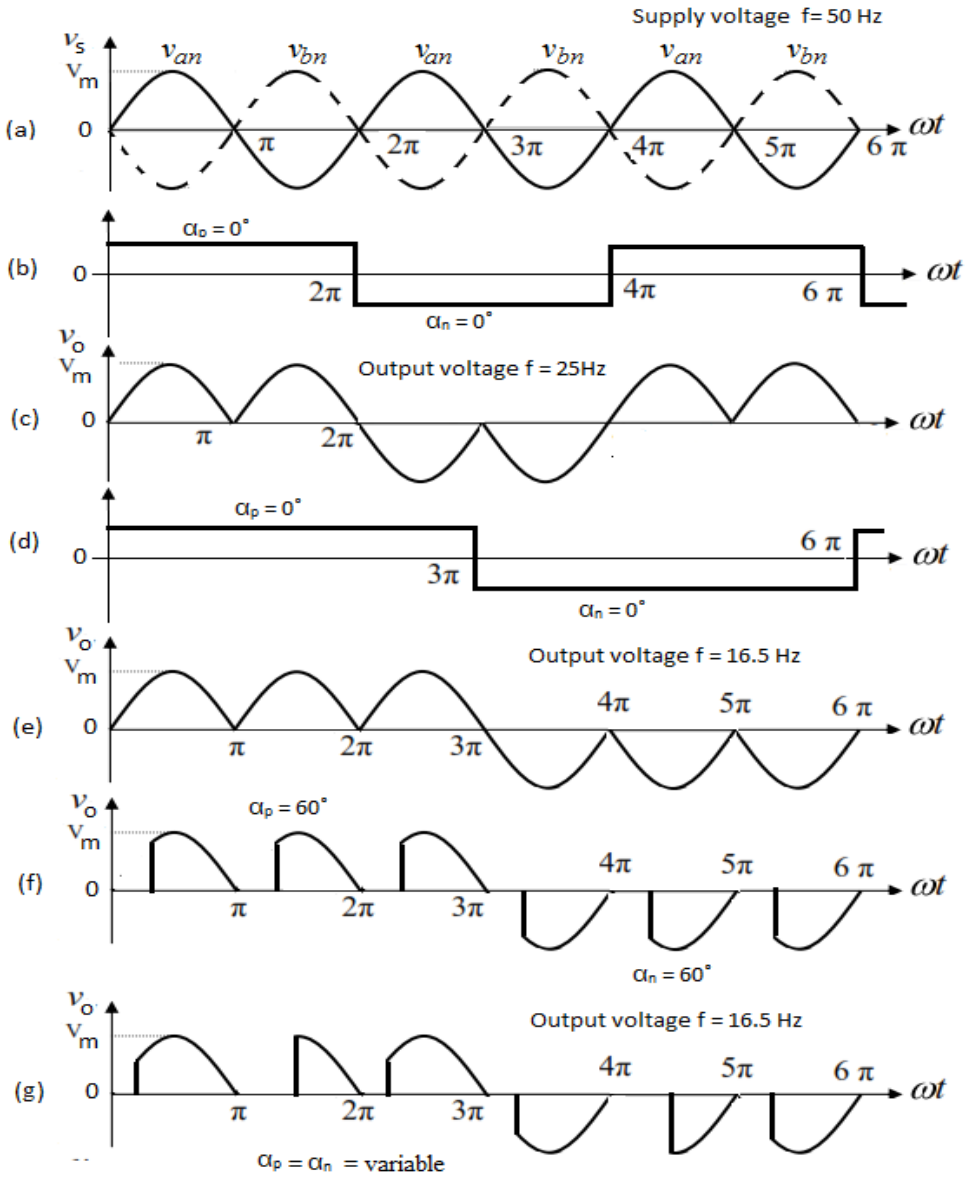

Fig.7.2 Single-phase to single-phase cycloconverter input and output waveforms.

From the output waveforms obtained in Fig.7.2 (c) and (d) , it is to be noted that the converter operates in the mode of half-cycle selection techniques with the triggering α = 0˚ as discussed in Chapter Six. However, if it is required to control the value of the desired fundamental component of the output voltage waveform, the triggering angle α could be set to any value, e.g. α = 60˚ as shown in Fig.7.2(e), or make it variable throughout the whole output cycle using modulation techniques.The cycloconverter generating waveforms of Fig.7.2(c) and (d) is called envelope cycloconverter, whereas cycloconverter generating waveforms of Fig.7.2 (f) and (g) is called phase-angle controlled cycloconverter.

One distinct feature of the cycloconverters is that all of them are naturally commutated devices like controlled rectifiers. It is because of the necessity of producing natural commutation of the current between successive switching that the realizable output frequency is lower than the input frequency. Theoretically, the fundamental component of the highly distorted output voltage waveform is likely to be between 1/3 and 2/3 of the input frequency. Therefore, the cycloconverters are mostly step-down type.

It is possible to implement a cycloconverter in several different forms. The single-phase to single-phase version (Fig.7.1) can also be constructed using two rectifier bridges connected back-to-back or inverse-parallel as shown in Fig.7.3. By the controlled opening and closing of the switches of the two converters it is possible to fabricate output voltage waveforms having a fundamental component of the desired output frequency.

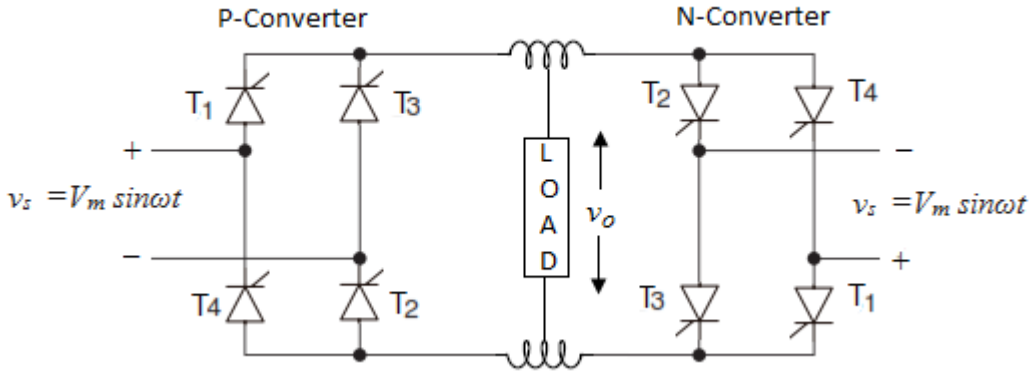

Fig.7.3 Single-phase to single-phase bridge type cycloconverter.

The phase-angle controlled cycloconverter of Fig.7.3 has exactly the same circuit topology as a dual converter. For a dual converter the firing angles of the converter switches are constant in time, as in bridge rectifier circuits, to result in rectifier operation with d.c. output. On the other hand, cycloconverter operation utilizes circuits in which the switch firing angles are functions of time and the output is a.c.voltage.

In the bridge type cycloconverter, each bridge is connected to the same a.c. source but no thyristor firing overlap can be permitted between them as this would short-circuit the supply. In an ideal dual converter the firing angles of the two converters are controlled so that their d.c. output voltages are exactly equal. If the positive bridge is gated at an angle α_p to produce a rectified output voltage V_{dc}, then the negative bridge is simultaneously gated at α_n to also produce the same output voltage V_{dc}, of consistent polarity. Thus the two bridges are delivering identical output d.c. voltages at any instant and the two firing angles must satisfy the relation,

$$\alpha_p - \alpha_n = \pi \qquad (7.2)$$

The phase-angle controlled cycloconverter of Fig.7.3 can operates in two modes, *circulating current free mode* and *circulating current mode*:

1. Circulating current free mode

Since the two bridges are acting alternately only one bridge carries load current at any given time. There is then no current circulating between the two bridges, and the mode of operation is usually called *circulating current free* operation or *noncirculating current* operation. The average value of the rectified load voltage was developed in Section 3.3 in Chapter Three as

$$V_{dc} = \frac{2V_m}{\pi} cos\alpha$$

which can be re-written as

$$V_{dc} = V_{do}\, cos\alpha \qquad (7.3)$$

where $V_{do} = \frac{2V_m}{\pi}$

Hence, when p-converter operating alone, the output voltage is positive half-cycles with average output voltage $V_{d1} = V_{do}\, cos\alpha$. Also when n-converter operating alone, the output voltage is negative half-cycles with average output voltage $V_{d2} = -V_{do}\, cos\alpha = -V_{d1}$. In order to maintain the circulating current free condition, the gating pulses to the thyristors must be controlled so that only the bridge carrying current is kept in conduction. The temporarily idle converter must be blocked by removing its gating pulses altogether.

2. Circulating Current Mode

The circulating current mode is the standard mode of operation in which both the p-converter and n-converter are operating simultaneously.

The p-converter operates as rectifier and the n-converter operates in inversion mode. Thus the two bridges are delivering identical output d.c. voltages at any instant and the two firing angles must satisfy the relation as presented in Eq.(7.3).

An inter-group reactor is included, and allows current to circulate through the positive and negative converters. To keep current flow in both of the converters entirely continuous it is necessary to allow large amounts of circulating current. At times it can reach 57% of the output load current. The purpose of allowing for circulating current is to reduce the number of harmonics in the output voltage. This mode of operation also simplifies the optimal control strategy for the cycloconverter.

7.3 ANALYTICAL PROPERTIES OF THE SINGLE-PHASE TO SINGLE-PHASE CYCLOCONVERTER OUTPUT VOLTAGE WAVEFORMS

7.3.1 RMS Load Voltage

The *rms* value $V_{o(rms)}$ of the output voltage waveform $v_o(\omega t)$ in Fig.7.2 is equal to the *rms* value of any of the half sinusoid sections. This is can be calculated as

$$V_{o(rms)} = \sqrt{\frac{1}{\pi}\int_{\alpha_p}^{\pi} {V_m}^2 \ sin^2\omega t \ d\omega t} = \sqrt{\frac{{V_m}^2}{\pi}\int_{\alpha_p}^{\pi} \frac{1}{2}(1 - cos2\omega t) \ d\omega t}$$

$$= \frac{V_m}{\sqrt{2}}\sqrt{\frac{1}{\pi}[(\pi - \alpha_p) + \frac{1}{2}sin2\alpha_p]} \qquad (7.4)$$

It is to be noted from Eq. (7.4) that the *rms* value of the output voltage of a single-phase to single-phase cycloconverter is independent on the output frequency f_o.

7.3.2 Fundamental Component of the Load Voltage Waveform

The Fourier coefficients a_1 and b_1 of the fundamental component of the output voltage waveform shown in Fig.7.2 (f) can be calculated as:
If there are m half cycles of input in each half period of the output, then

$$a_1 = \frac{2V_m}{m\pi}\left[\int_{\alpha_p}^{\pi} \sin\omega_o t \cos(\frac{\omega_o t}{m})d\omega_o t + \int_{\alpha_p}^{\pi} \sin\omega_o t \cos(\frac{\omega_o t + \pi}{m})d\omega_o t + \int_{\alpha_p}^{\pi} \sin\omega_o t \ \cos(\frac{\omega_o t + (m-1)\pi}{m})d\omega_o t\right]$$

$$= \frac{V_m}{m\pi}\sum_{n=1}^{m}\left\{\frac{m}{m+1}\left[\cos\frac{n\pi}{m}+\cos\left(\alpha_p+\frac{\alpha_p+(n-1)\pi}{m}\right)\right]+\frac{m}{m-1}\left[\cos\frac{n\pi}{m}+\sin\left(\alpha_p-\frac{\alpha_p+(n-1)\pi}{m}\right)\right]\right\} \quad (7.5)$$

Similarly

$$b_1 = \frac{2V_m}{m\pi}\left[\int_{\alpha_p}^{\pi}\sin\omega_o t\sin(\frac{\omega_o t}{m})d\omega_o t+\int_{\alpha_p}^{\pi}\sin\omega_o t\sin(\frac{\omega_o t+\pi}{m})d\omega_o t+\int_{\alpha_p}^{\pi}\sin\omega_o t\sin(\frac{\omega_o t+(m-1)\pi}{m})d\omega_o t\right]$$

$$= \frac{V_m}{m\pi}\sum_{n=1}^{m}\left\{\frac{m}{m-1}\left[\sin\frac{n\pi}{m}-\sin\left(\alpha_p-\frac{\alpha_p-(n-1)\pi}{m}\right)\right]+\frac{m}{m+1}\left[\sin\frac{n\pi}{m}+\sin\left(\alpha_p-\frac{\alpha_p-(n-1)\pi}{m}\right)\right]\right\} \quad (7.6)$$

The amplitude c_1 of the fundamental component is calculated as

$$c_1 = \sqrt{a_1^2+b_1^2} \quad (7.7)$$

Higher harmonic components can be calculated by dividing the parameter *m* inside the square brackets of Eqs.(7.5) and (7.6) by the appropriate order of harmonic.

Example 7.1

The input voltage to the single-phase cycloconverter of Fig.7.1 is 240V, 50 Hz.The load resistance and inductance are 10 Ω and 50 mH respectively. The frequency of the output voltage is 25 Hz. If the converter is to operate with $\alpha_p = 75^\circ$,

(a) Sketch approximately to scale, the input supply voltages and the output voltage waveforms.
(b) Determine the *rms* value of the output voltage.
(c) Determine the *rms* value of the load current.
(d) Determine the input power factor.

Solution

(a) The input and output voltage waveforms are shown in Fig.7.4.

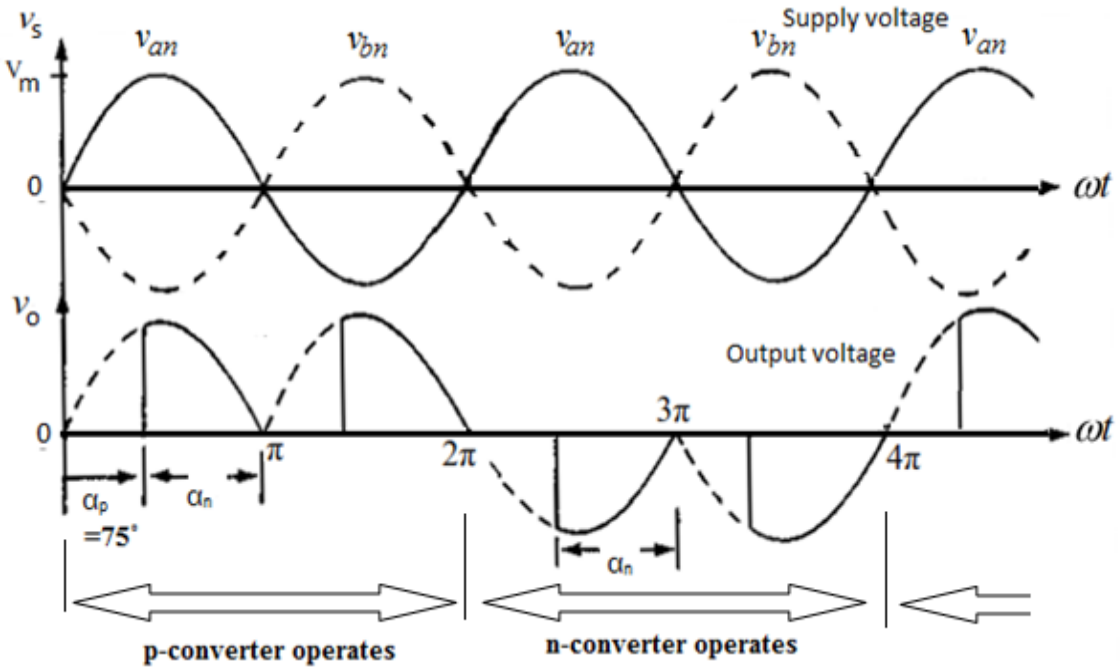

Fig.7.4 Input and output voltage waveforms.

(b) From Eq.(7.4), the *rms* value of the output voltage is

$$V_{o(rms)} = V_m \sqrt{\frac{1}{2\pi}[(\pi - \alpha_p) + \frac{1}{2}sin2\alpha_p]}$$

$$= \sqrt{2} \times 240 \sqrt{\frac{1}{2\pi}[\left(\pi - \frac{75° \times \pi}{180°}\right) + \frac{1}{2}\sin(2 \times 75°)]}$$

$$= 240 \sqrt{\frac{1}{\pi}[(\pi - 0.4167\pi) + 0.25]} \quad = 195.4 \text{ V}$$

The load impedance at 25 Hz is

$$|Z| = \sqrt{R^2 + (\omega L)^2} = \sqrt{10^2 + (2\pi \times 25 \times 0.050)^2} = 12.7\ \Omega$$

$$\theta = \tan^{-1}\frac{7.85}{10} = 38.13°$$

The *rms* value of the load current is

$$I_o = \frac{V_{o(rms)}}{Z} = \frac{195.4}{12.7} = 15.38\ \text{A}$$

(c) The input power factor:

RMS input current $I_s = I_o = 15.38$ A

Input VA = $I_s V_s = 15.38 \times 240 = 3692.6$

Output power $P_o = I_o\, V_{o(rms)}\, cos\theta = 15.38 \times 195.4\, cos38.13°$
$= 2363.9$ W

$$PF = \frac{P_o}{VA} = \frac{2363.9}{3692.6} = 0.64$$

7.4 MULTI-PHASE CYCLOCONVERTER

The single-phase cycloconverter circuits shown in Figs.7.1 and 7.3 are not practical circuits and are seldom used because of their nonsinusoidal output voltage. As many industrial applications require sinusoidal a.c. voltage and in order to construct a 'clean' sinusoidal output, multi-phase cycloconverters are much more effective in producing clean waveforms due to the variety of input to choose from. A nearly sinusoidal output voltage can be synthesized from three-phase input voltages by using three-phase controlled rectifiers as will be discussed in the following subsections.

7.4.1 Three-Phase to Single-Phase Cycloconverter

The three-phase to single-phase cycloconverter is shown in Fig.7.5 which is also called three-pulse cycloconverter since it uses three-phase half-wave converters.

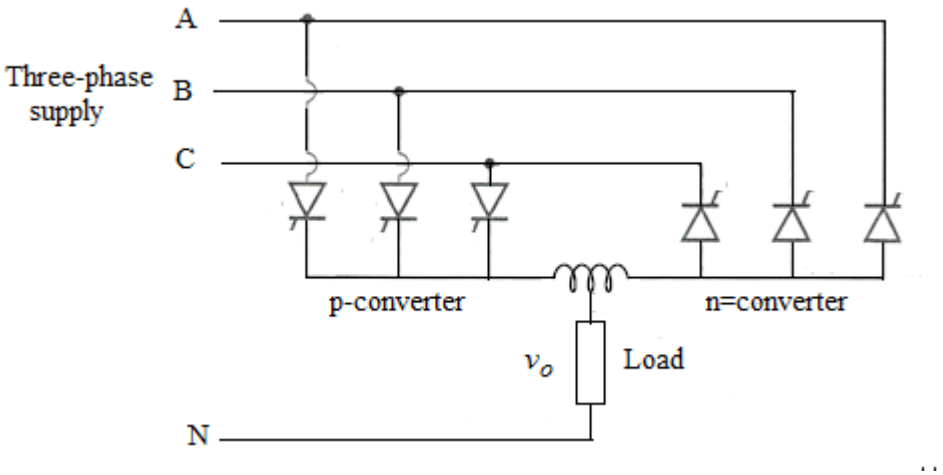

Fig.7.5 Three-phase to single-phase cycloconverter circuit.

The output voltage is positive when the thyristors of the p-converter are conducting, and the output voltage is negative when the thyristor of the n-converter are conducting. The positive (p) and negative (n) converters must operate alternatively without electrically overlap to prevent any circulating current when the two converters operate in the circulating current free mode. The average output voltage of the controlled rectifier of Fig.7.5 is given in Eq.(3.20) which can be rewritten as,

$$V_{dc} = v_o = \frac{3\sqrt{3}V_m}{2\pi} cos\alpha \qquad (7.8)$$

With constant value of the triggering angle α output voltage waveform of the three-phase to single-phase cycloconverter will be as depicted in Fig.7.6.

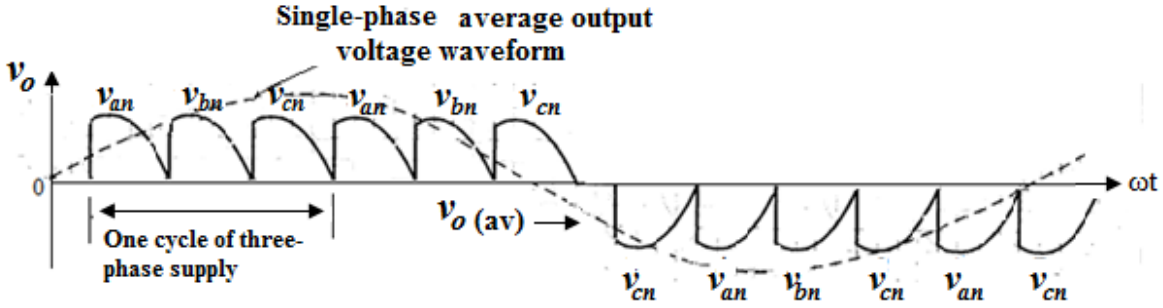

Fig.7.6 Output voltage waveform of the three-phase to single-phase cycloconverter with constant value of the triggering angle α.

For phase-controlled cycloconverters with 50Hz supply the practical maximum output frequency is likely to be about 15Hz for single-way three-phase (three-pulse) rectifier and 30Hz for three-phase (six-pulse) bridge rectifiers. In the dual three-phase converter a.c. operation, the firing angles of the converter switches can be time varied, cycle by cycle. If the time varying firing angle is described as $\alpha(t)$, then the output voltage (no longer d.c.) has a peak amplitude *Vo* given by

$$V_o = \frac{3\sqrt{3}V_m}{2\pi}\cos(\alpha(t)) \qquad (7.9)$$

In Eq.(7.9), when the firing angle $\alpha(t)$ is varied with time in a periodic manner, this means that a process of discrete phase modulation is resulting. The supply frequency acts as a carrier signal, whereas the output frequency ω_o acts as the modulating frequency. This allows the output (modulated) voltage of the converter to be controlled in both amplitude and frequency independently.
A form of modulating function commonly used is

$$\alpha(t) = \pm\ \cos^{-1}(M cos\omega_o\, t) \qquad (7.10)$$

where *M* is the modulation index which is the ratio of maximum modulating voltage to the maximum carrier voltage, and $\omega_o = 2\pi f_o$ (f_o is the desired output frequency). For example, to convert a three-phase supply into a single-phase 15Hz output, it is necessary to use the modulating function (i.e., firing angle)

$$\alpha(t) = \pm\ \cos^{-1}(M cos\omega_o\, t) = \pm\ \cos^{-1}(M cos 2\pi f_o\, t)$$
$$= \pm\ \cos^{-1}(M cos 15\pi\, t)$$

The output voltage waveform of the three-phase to single-phase cycloconverter with variable angle α is shown in Fig.7.7.

In Fig.7.7, it is clear that the cycloconverter output voltage waveform is made up of sections of sine waves which is called concurrent consecutive wave. This wave is highly distorted. The amount of distortion increases as the ratio output frequency/input frequency (i.e., modulating frequency / carrier frequency) increases. In addition to severe output voltage distortion the input current to a cycloconverter is usually significantly distorted. Also, the fundamental component of the input current lags the supply voltage, resulting in poor input power factor, irrespective of whether the load current is lagging, leading, or of unity power factor. Very often both input and output filters may be needed.

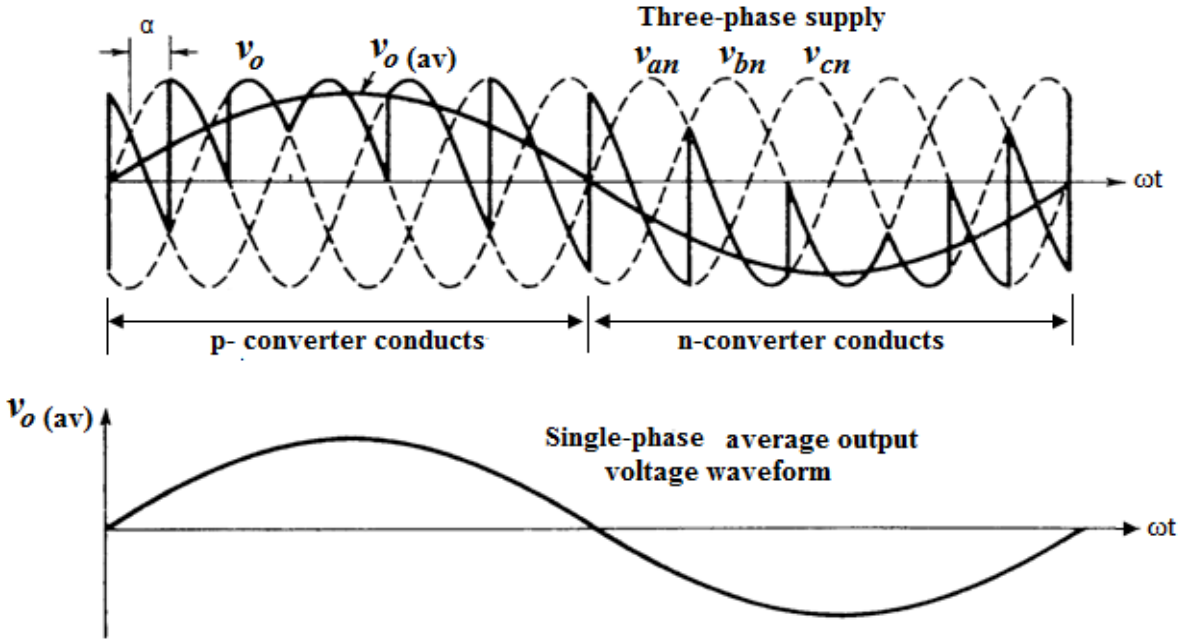

Fig.7.7 Output voltage waveform of the three-phase to single-phase cycloconverter with variable value of the triggering angle α.

The output voltage waveform shown in Fig.7.7 can also be obtained from a three-phase half-wave rectifier shown in Fig.7.8. The average of this controlled rectifier circuit varies as the cosine of the firing angle α (Equation 7.8). By successive variation of α, a nearly sinusoidal output voltage can be obtained . Fabrication of such output voltage is illustrated in Fig.7.9 as follows:

- At point 'A', α = 0° and $V_{dc} = V_{do}$ (from Eq.(7.8)) where $V_{do} = 3\sqrt{3}\, V_m / 2\pi$.
- At point 'B', α > 0 , hence $V_{dc} < V_{do}$ and so on for point 'C'.The converter operates in rectifying mode.
- At point 'D', α = 90°, $V_{dc} = 0$ since cos 90°= 0 and the converter is idling.
- At points 'E','F','G','H'and 'I', α > 90 V_{dc} = negative and the converter operate in inversion mode.

The average value of the output voltage will be maximum at point 'A' (α = 0) and zero at point 'D'(α = 90°). The firing angle is changed from 0° to 90° and then from 90° to 180° and back again to 90° in appropriate steps.

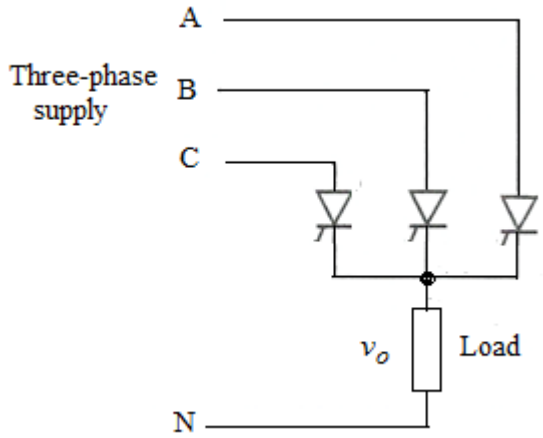

Fig.7.8 Three-phase half-wave rectifier.

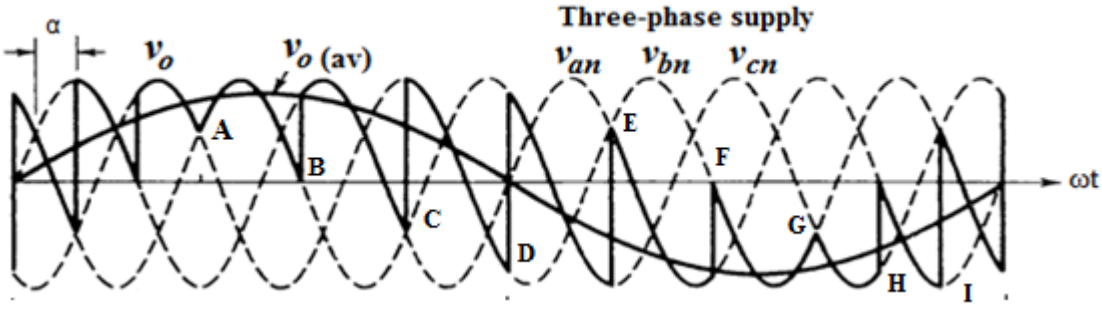

Fig.7.9 Fabrication of output voltage from rectifier-inverter operation of a three-phase half-wave rectifier of Fig.7.8.

Example 7.2

A three-phase to single-phase, three-pulse cycloconverter delivers power to a load rated at 100 V, 30 A, with power factor 0.8 lagging. Estimate the necessary input voltage and power factor.

Solution

From Eq.(7.9) the peak value of the required input voltage is given by

$$\sqrt{2} \times 100 = \frac{3\sqrt{3}V_m}{2\pi} cos\alpha(t)$$

Solve for the worst case when $cos\alpha(t) = 1$

$$V_m = \frac{2\pi\sqrt{2} \times 100}{3\sqrt{3}} = 171 \text{ V}$$

Hence the supply *rms* voltage per phase is

$$V_s = \frac{171}{\sqrt{2}} = 120.93 \text{ V}$$

The *rms* value of the specified single-phase load current is 30A. If this is shared equally between the three input phases, each input line (assuming sinusoidal operation) has an *rms* current per phase,

$$I_{input} = \frac{I_{load}}{\sqrt{3}} = \frac{30}{\sqrt{3}} = 17.32 \text{ A}$$

The load power is

$$P_{load} = V \cdot I \cdot PF = 100 \times 30 \times 0.8 = 2400 \text{ W}$$

The input power per-phase is therefore,

$$P_{input} = \frac{P_{load}}{3} = \frac{2400}{3} = 800 \text{ W}$$

The input power factor is

$$PF = \frac{P_{input}}{V_s \, I_{input}} = \frac{800}{120.93 \times 17.32} = \frac{800}{2094.5} = 0.382 \text{ lagging}$$

Note that this value of input power factor is the maximum possible value, with $\alpha = 0$. If α is increased, the power factor will decrease.

7.4.2 Three-Phase to Three-Phase Cycloconverter

It is possible to implement a cycloconverter in several different forms. The three-phase to three-phase version of the cycloconverter with p = 3 supplying three-phase load is shown in Fig.7.10. In this figure, P_A is thepositive converter of phase-A and N_A is the negative converter for phase-A. Similarly P_B and P_C are the positive converters of phase-B and phase-C respectively, whereas N_B and N_C are the negative converters of phase-B and phase-C respectively. The load voltage v_a is generated by P_A and N_A converters that are connected through an intergroup reactor. The firing schedules of thyristors in $P_B - N_B$ converters and $P_C - N_C$ converters are same as converters $P_A - N_A$ but lag by 120˚ and 240˚ respectively. The output voltage waveforms of the three phases are shown in Fig.7.11 for clarity.

The average value of output voltage can be varied by varying the firing angles of the thyristors on conduction, whereas the frequency of the output voltage can be varied by changing the sequence of firing of the thyristors. Since each converter consists of three thyristors, thus in total

six thyristors per phase. This means, in all 18 thyristors are required for the whole circuit. This is why the cycloconverter considered as a complex device for a.c. to a.c. conversion, since it needs large number of thyristors with more complex triggering circuits.

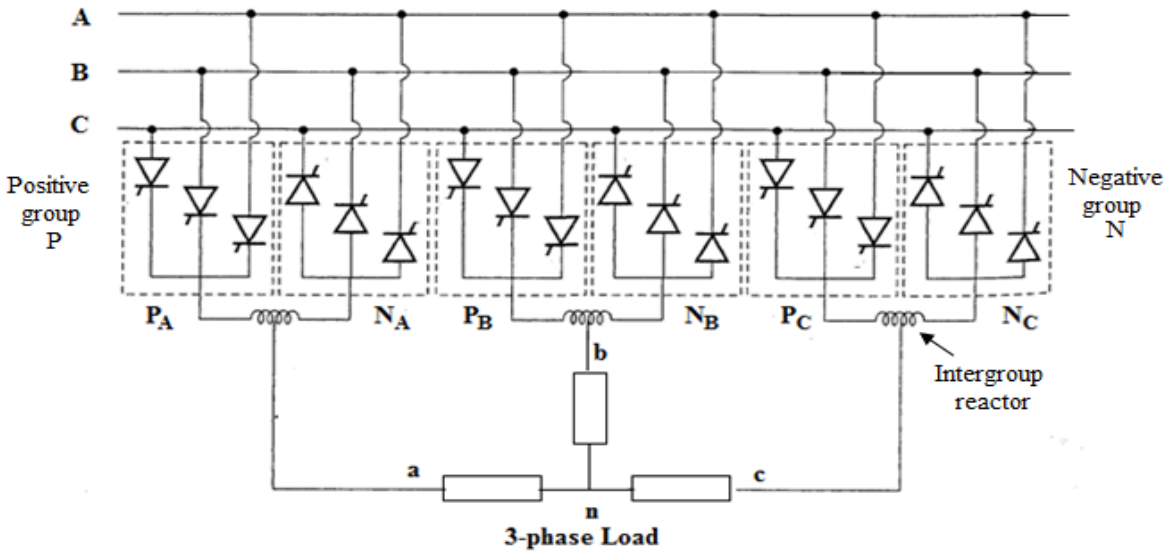

Fig.7.10 Three-phase to three-phase cycloconverter circuit.

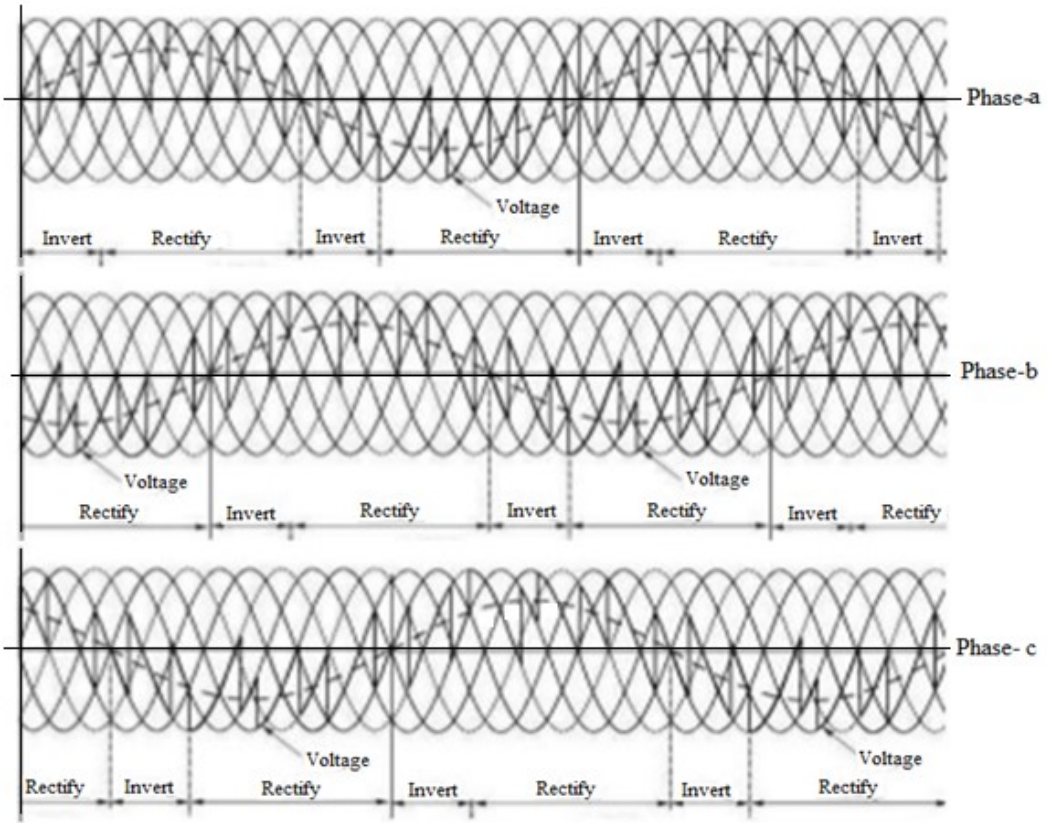

Fig.7.11 Load voltage waveforms for three-phase to three-phase with p =3 cycloconverter.

Circulating current mode

The three-phase to three-phase cycloconverter can also be made to operate in circulating current mode to reduce the control problems arising with discontinuous load current. In this case an intergroup reactor may be connected between the p-converter and n- converter as shown in Fig.7.10 so that circulating current is allowed to circulate between them. In such scheme both the p-converter and n-converter are allowed to conduct simultaneously provided that the average output voltages of the two bridges are identical and must satisfy Eq.(7.2).

The intergroup reactor used in this scheme add cost to the circuit which is considered as disadvantage although it reduce the ripples and improve the quality of the output voltage waveform of the cycloconverter waveforms of this cycloconverter are depicted in Fig.7.12 for circulating current mode.

7.4.3 Three-Phase to Single-Phase Full-Wave (Six-Pulse) Cycloconverter

Fig.7.13 shows the schematic diagram of a three-phase to single-phase bridge type (p = 6) cycloconverter. Two three-phase, full-wave controlled bridge rectifier circuits of the form of P and N converters are connected back-to-back nature representing circulating current free operation. The positive group thyristors conduct for half the period of the output wave whereas the negative group thyristors conduct for the remaining half of the period.

A total of 12 thyristors are implemented in the circuit of this type of cycloconverter. However, the quality of the output voltage waveform is better than that of half-wave three-phase to single-phase converter circuit shown in Fig.7.8. For the three-phase, full-wave converter p = 6, and the peak load voltage may be inferred from Eq.(7.9) to be

$$V_o = \frac{3\sqrt{3}V_m}{\pi}\cos(\alpha(t)) \qquad (7.11)$$

This is seen to be twice the value of the half-wave, three-pulse converter given in Eq.(7.9).

7.4.4 Three-Phase to Three-Phase Full-Wave (Six-Pulse) Cycloconverter

Fig.7.14 shows the schematic diagram of a three-phase to three-phase bridge type (p = 6) cycloconverter in circulating current mode. This converter is constructed using three three-phase to single-phase converters of Fig.7.13. A total of 36 thyristors are implemented in the circuit of this type of cycloconverter 12 for each phase. Fig.7.15 shows the same converter operating in free-circulating current mode.

The output voltages v_o with six-pulse circulating current operation is given by Eq.(7.12) in reference [37] as

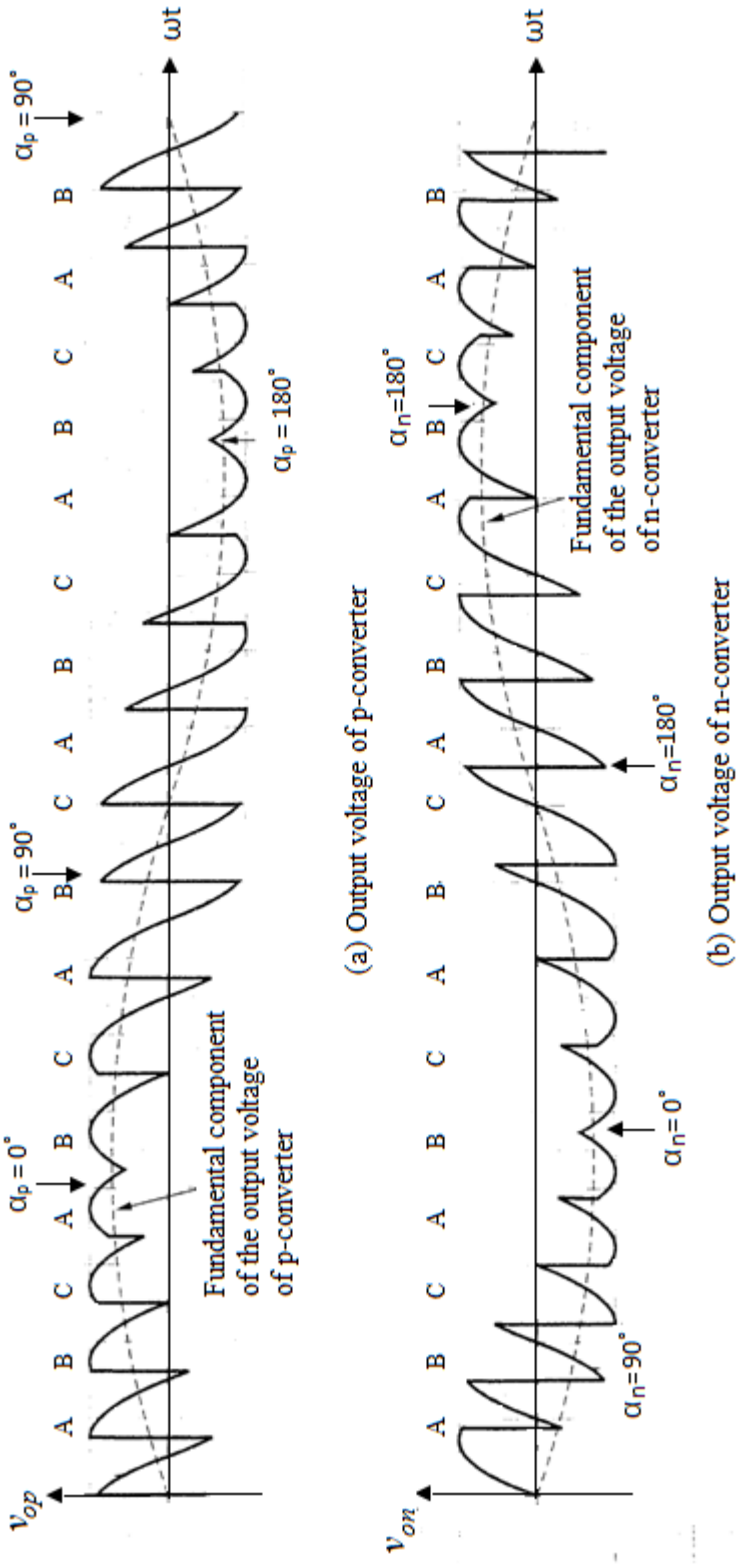

Fig.7.12 Voltage waveforms for the three-phase to three-phase cycloconverter.

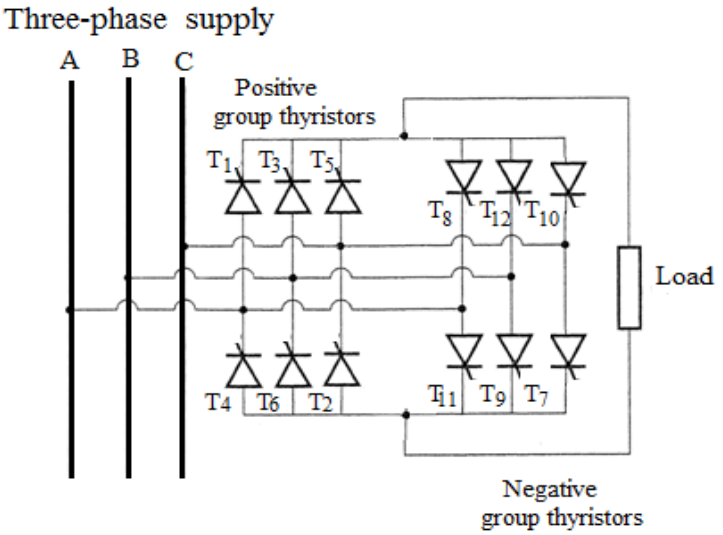

Fig.7.13 Three-phase to single-phase full-wave (six-pulse) cycloconverter.

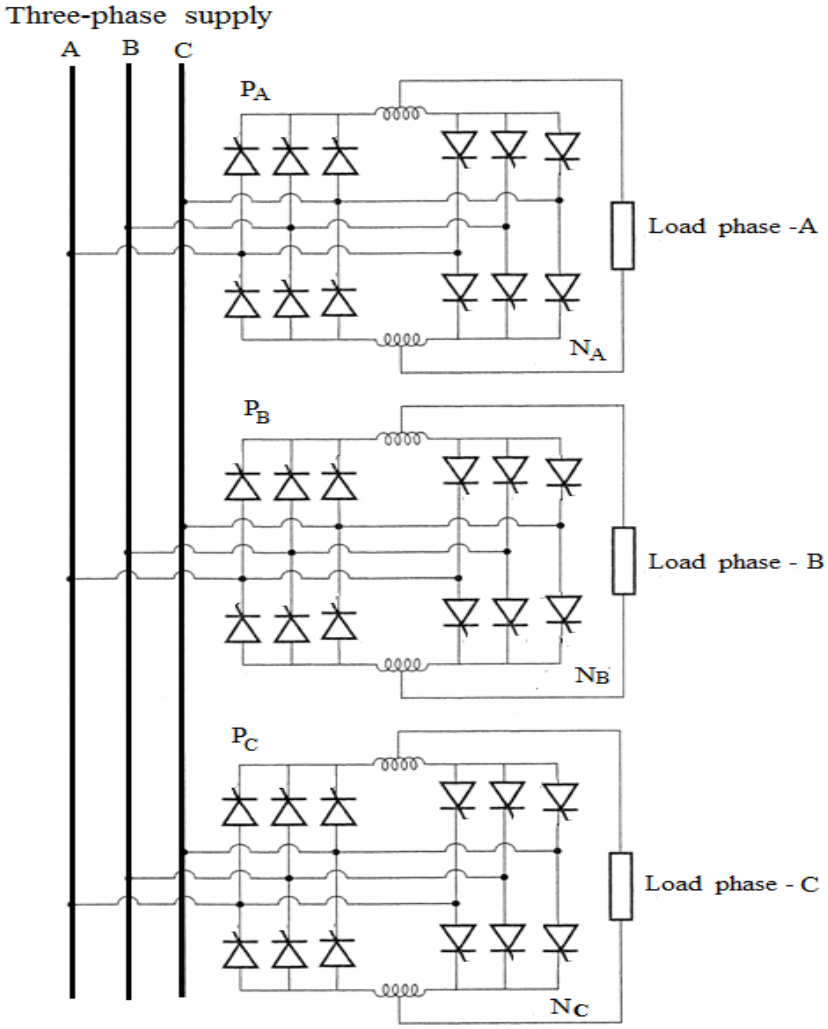

Fig.7.14 Three-phase to three-phase full-wave (six-pulse) cycloconverter operating in circulating current mode.

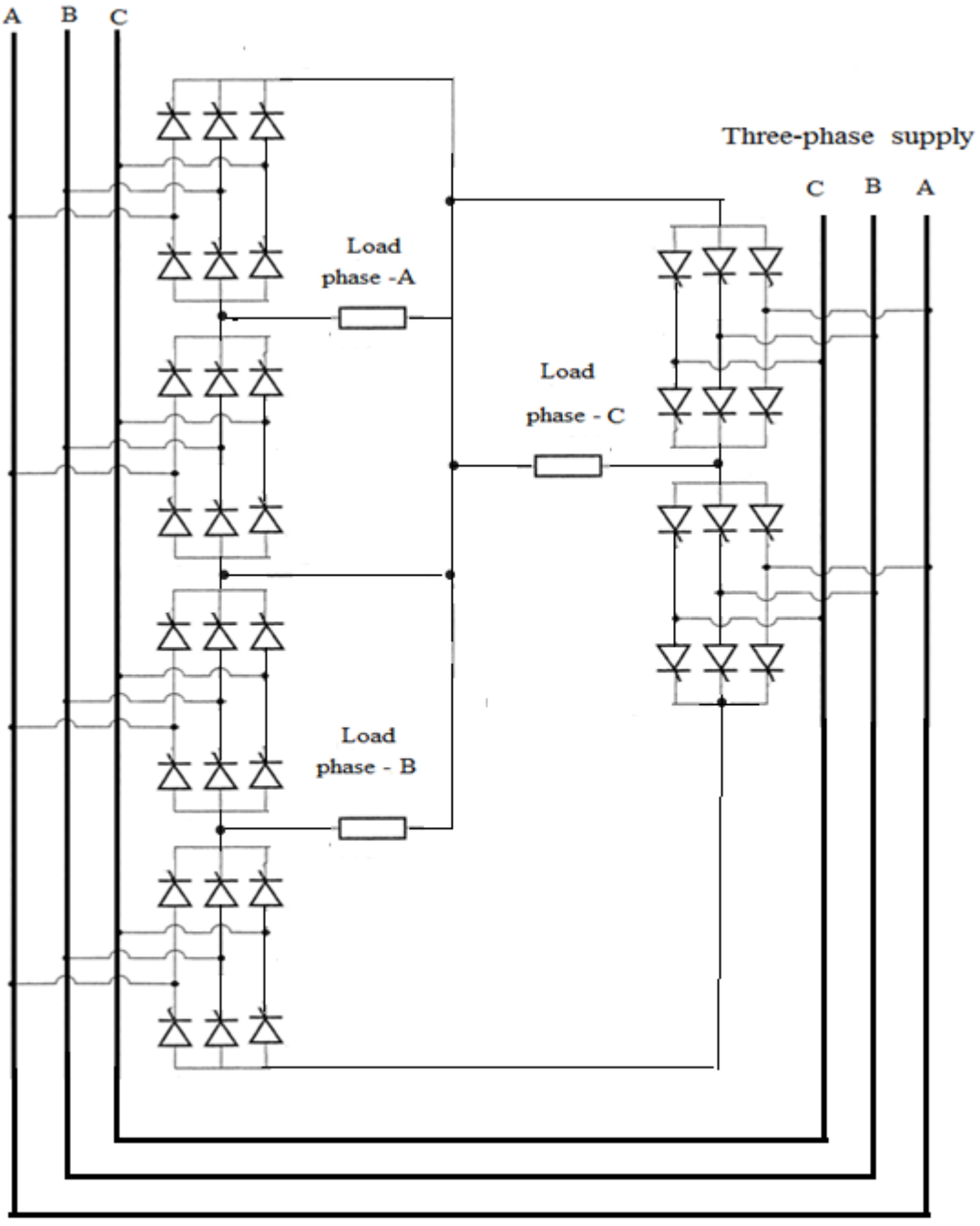

Fig.7.15 Three-phase to three-phase full-wave (six-pulse) cycloconverter operating in non-circulating current mode.

$$v_o = k\,\frac{3\sqrt{3}V_m}{2\pi}\left[M\sin\omega_o\,t + \frac{1}{2}\sum_{p=1}^{\infty}\sum_{n=0}^{2n+1=6p+1}[A]\,[B]\right] \qquad (7.12)$$

where

$$[A] = \left[\frac{a_{(6p-1)(2n+1)}}{6p-1} + \frac{a_{(6p+1)(2n+1)}}{6p+1}\right]$$

$$[B] = \sin[6p\omega_{in}\,t + (2n+1)\omega_o t] - \sin[6p\omega_{in}\,t - (2n+1)\omega_o t]$$

k= 1 for the six-pulse midpoint circuit
k=2 for the six-pulse bridge circuit

From equation (7.12), it is seen that the output voltage contains large number of undesirable harmonic components.

7.5 ENVELOPE CYCLOCONVERTERS

The envelope cycloconverter is an alternative to the phase-controlled cycloconverter discussed in previous sections. The basic idea in operation of this earliest type of frequency changer is that the switches of Fig.7.1 in the envelope cycloconverter can operate continuously, like diodes. The firing angle ' α ' of the component converter is not varied. It is kept constant normally at ' α ' = 0˚ for the positive converter and 'α' =180˚ for negative converter during the positive half cycle of the voltage whereas, during the negative half cycle, α_P = 180˚ and α_n = 0˚. In effect the rectifier valves, usually thyristors, act as on-off switches for the whole of a half cycle. This type of converter is generally called synchronous cycloconverter in which the commutation process of the conducting switches is entirely natural.

The output voltage waveform follows the profile of the a.c. supply voltage v_s , as depicted in Fig.7.16 for simple single-phase version of the converter. These voltage waveforms shows frequency output of ½ f_i, ⅓ f_i and ¼ f_i as shown in Fig.7.16 (b), (c) and (d) respectively. The major advantage of envelope converter is that it has a simple control circuitry. As such, the envelope cycloconverter is preferred if the desired output frequency is constant. However, in case the output voltage control is required, the input voltage has to be varied. The circulating currents may be avoided by turning off the conducting converter completetly.

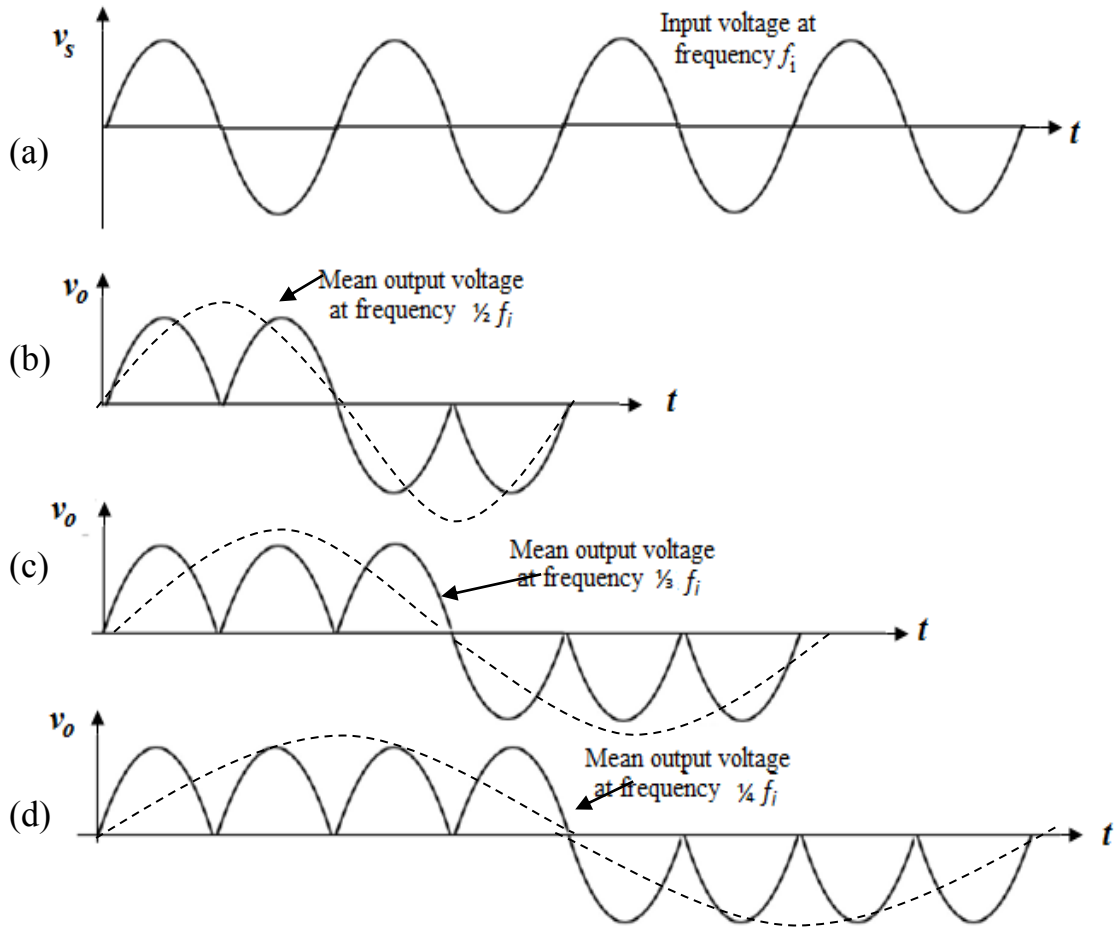

Fig.7.16 Output voltage waveforms from envelope cycloconverter.

7.5.1 Performance Characteristics of a Single-Phase Envelope Cycloconverter

***Rms* Load Voltage**

The *rms* value $V_{o(rms)}$ of the output voltage waveform $v_o(\omega t)$ in Fig. 7.16 (b) is equal to the *rms* value of any of the half sinusoid sections. This is can be calculated as

$$V_{o(rms)} = \sqrt{\frac{4}{4\pi}\int_0^{\pi} {V_m}^2 \, sin^2\omega t \, d\omega t} = \sqrt{\frac{{V_m}^2}{\pi}\int_0^{\pi}\frac{1}{2}(1 - cos2\omega t)\, d\omega t}$$

$$= V_m\sqrt{\frac{1}{2\pi}[(\pi - 0) + \frac{1}{2}(sin2\pi - sin0)]} \quad = \frac{V_m}{\sqrt{2}} \qquad (7.13)$$

It is to be noted from Eq.(7.13) that the *rms* value of the output voltage of a single-phase to single-phase envelope cycloconverter is independent on

the output frequency f_o and has a value same as that of sinusoidal operation.

To generalize the *rms* value of the synchronous envelope cyclo-converter, if m = number of half supply cycle of frequency f_i , the output frequency f_o will be

$$f_o = \frac{2f_i}{m} \qquad \text{where m is integer} = 1,2,3,\ldots\ldots \tag{7.14}$$

and the *rms* value $V_{o(rms)}$ of the output voltage waveform $v_o(\omega t)$ is

$$V_{o(rms)} = \sqrt{\frac{m}{m\pi}\int_0^{\pi} {V_m}^2 \, sin^2\omega t \, d\omega t} \quad = \frac{V_m}{\sqrt{2}}$$

From Eq.(7.14) , it is worth to note that the *rms* value of the output voltage waveform is the same for that of pure sinusoidal operation. However, this does not mean that the waveforms of Fig.7.16 (b), (c) and (d) are pure sinusoids and as a result the output voltage of this converter contains harmonics. These harmonics will be analysed in the following subsection.

7.5.2 Harmonic Analysis of the Output Voltage Waveform

(A) Case when *T*=2 (Double half cycle)

Let $T = 2$ is the number of conducting half cycles of the input supply voltage of frequency f_i in a half period of the output voltage waveform of frequency f_o , hence the load voltage waveform v_o , for case of *R*-load shown in Fig.7.16(b), may be defined for a single-phase system as:

$$\left.\begin{aligned} v_o &= \sqrt{2}\,V_s \sin\omega t && 0 < \omega t < \pi \\ v_o &= -\sqrt{2}\,V_s \sin\omega t && \pi < \omega t < 2\pi \\ v_o &= -\sqrt{2}\,V_s \sin\omega t && 2\pi < \omega t < 3\pi \\ v_o &= \sqrt{2}\,V_s \sin\omega t && 3\pi < \omega t < 4\pi \end{aligned}\right\} \tag{7.15}$$

where V_s = *rms* value of the input supply voltage.

Fourier expansion of Eq.(7.15) gives the following results:

For $n \neq T$

$$a_o = 0 \tag{7.16}$$

$$a_n = \frac{\sqrt{2}V_s\,T}{\pi(T^2 - n^2)}\left[1 + 2\cos\frac{n\pi}{T} - 2\cos\frac{3n\pi}{T} - \cos\frac{4n\pi}{T}\right] \tag{7.17}$$

$$b_n = \frac{\sqrt{2}\,V_s\,T}{\pi(T^2 - n^2)}\left[2\sin\frac{n\pi}{T} - 2\sin\frac{3n\pi}{T} - \sin\frac{4n\pi}{T}\right] \qquad (7.18)$$

The amplitude c_n of the nth order harmonic component is calculated as

$$c_n = \sqrt{a_n^2 + b_n^2} \qquad (7.19)$$

and the phase angle ψ_n of the nth harmonic is

$$\psi_n = \tan^{-1}\frac{a_n}{b_n} \qquad (7.20)$$

For $n = T$, the Fourier coefficients are:

$$a_T = b_T = 0 \qquad (7.21)$$

$$c_T \text{ and } \psi_n = 0 \qquad (7.22)$$

This means that the input frequency component is entirely suppressed and the fundamental component of the output voltage waveform is now define as n = 1 in Eq.(7. 15) with a value given by

$$a_1 = \frac{\sqrt{2}\,V_s T}{\pi(T^2 - 1)}\left[1 + 2\cos\frac{\pi}{T} - 2\cos\frac{3\pi}{T} - \cos\frac{4\pi}{T}\right] \qquad (7.23)$$

$$b_1 = \frac{\sqrt{2}\,V_s\,T}{\pi(T^2 - 1)}\left[2\sin\frac{\pi}{T} - 2\sin\frac{3\pi}{T} - \sin\frac{4\pi}{T}\right] \qquad (7.24)$$

For T =2 ,

$$a_1 = \frac{2\sqrt{2}\,V_s}{3\pi}\left[1 + 2\cos\frac{\pi}{2} - 2\cos\frac{3\pi}{2} - \cos 2\pi\right]$$

$$a_1 = \frac{2\sqrt{2}\,V_s}{3\pi}(1 + 0 - 0 - 1) = 0$$

$$b_1 = \frac{2\sqrt{2}\,V_s}{3\pi}\left[2\sin\frac{\pi}{2} - 2\sin\frac{3\pi}{2} - \sin 2\pi\right]$$

$$b_1 = \frac{2\sqrt{2}\,V_s}{3\pi}[2 + 2 - 0] = \frac{8\sqrt{2}\,V_s}{3\pi} \quad \rightarrow \quad \therefore\ c_1 = b_1 = \frac{8\sqrt{2}V_s}{3\pi}$$

The harmonic amplitude spectrum of the load voltage waveform for T=2 and with R-load is shown in Fig. 7.17. It is clear that the output frequency of the waveform obtained from the envelope cycloconverter with T=2 is half the input frequency (25 Hz for 50 Hz input). Higher order odd harmonics 3rd,5th ,7th and 11th are only present in the spectrum. All even

harmonics (n=2,4,6...) are not present and the supply frequency component is entirely suppressed.

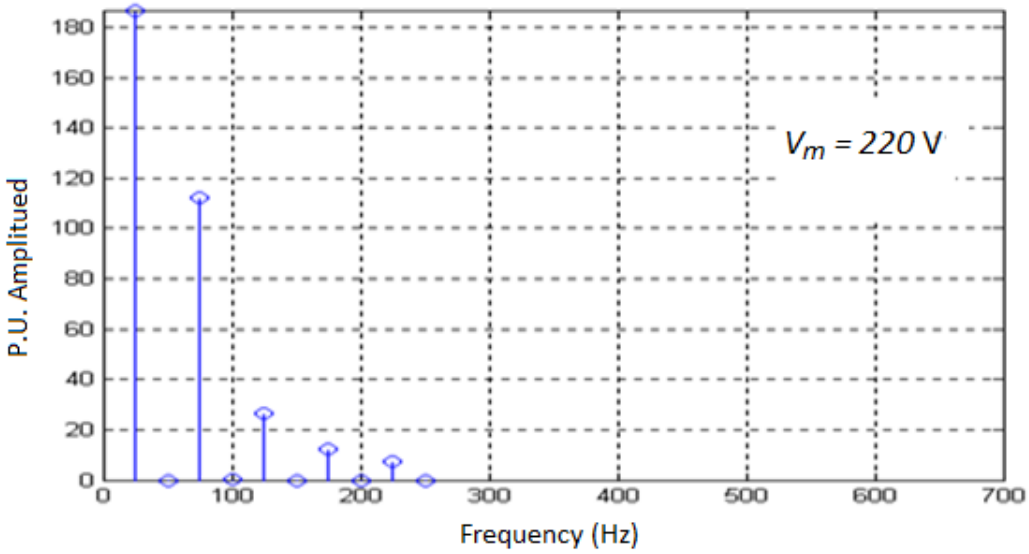

Fig.7.17 Harmonic amplitude spectrum of load voltage waveform for T=2 with R-load.

7.5.3 Three-Phase Cycloconverter with T =2 with R-Load

For medium and high power applications, three-phase cycloconverter is used. A three-phase version of a single-phase synchronous cyclo-converter is shown in Fig.7.18 which consists of three single-phase cycloconverters X,Y, and Z feeding a three-phase star-connected resistive load in 4-wire configuration. The neutral wire is necessary to provide a return path to the load current for the three phases. Other type of connections such as 3-wire system or delta-connected load may not be feasible.

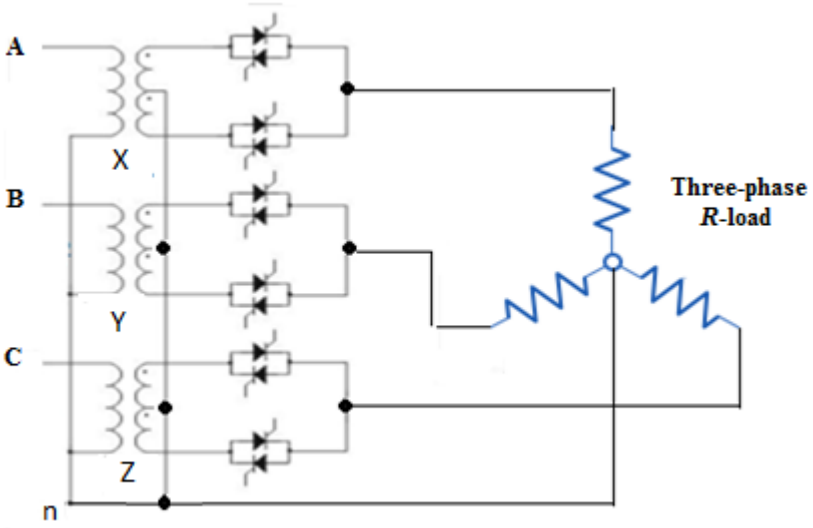

Fig.7.18. Three-phase synchronous cycloconverter.

For T=2 , one can define the output voltage of Fig.7.16(b) in three-phase system as

$$\left.\begin{array}{ll} v_{Lj} = \sqrt{2}\, V_s \sin(\omega t - \gamma_j) & 0 + \gamma_j < \omega t < \pi + \gamma_j \\ v_{Lj} = -\sqrt{2}\, V_s \sin(\omega t - \gamma_j) & \pi + \gamma_j < \omega t < 2\pi + \gamma_j \\ v_{Lj} = -\sqrt{2}\, V_s\ (\sin \omega t - \gamma_j) & 2\pi + \gamma_j < \omega t < 3\pi + \gamma_j \\ v_{Lj} = \sqrt{2}\, V_s \sin(\omega t\ - \gamma_j) & 3\pi + \gamma_j < \omega t < 4\pi + \gamma_j \end{array}\right\} \quad (7.25)$$

where $j = 1,2,3$ and $\gamma_1 = 0, \quad \gamma_2 = 2\pi/3, \quad \gamma_3 = 4\pi/3$

Fourier expansion of Eq.(7.25) $n \neq T$ gives the following results:

$$a_{oj} = 0 \quad (7.26)$$

$$a_{nj} = \frac{\sqrt{2}\, V_s\, T}{\pi(T^2 - n^2)} \left[\cos\frac{n\gamma_j}{T} + 2\cos\frac{n(\pi + \gamma_j)}{T} - 2\cos\frac{n(3\pi + \gamma_j)}{T} - \cos\frac{n(4\pi + \gamma_j)}{T}\right] \quad (7.27)$$

$$b_{nj} = \frac{\sqrt{2}\, V_s\, T}{\pi(T^2 - n^2)} \left[\sin\frac{n\gamma_j}{T} + 2\sin\frac{n(\pi + \gamma_j)}{T} - 2\sin\frac{n(3\pi + \gamma_j)}{T} - \sin\frac{n(4\pi + \gamma_j)}{T}\right] \quad (7.28)$$

For $n = T$, the Fourier coefficients are:

$$a_T = b_T = 0 \quad (7.29)$$

$$c_T \text{ and } \psi_n = 0 \quad (7.30)$$

The harmonic amplitude spectrum for the three phases A, B, and C is found to be same as the harmonic spectrum for single phase presented in Fig.7.17. However, the phase-angle relationships of the three-phase voltage waveforms for *R*-load, for the case when T = 2, are shown in Fig. 7.19. It is clear that the fundamental component as well as the higher order harmonics are balanced in magnitudes but they are unbalanced in phase angles. With passive loads such as *R* and *R-L* loads there will be no problem in operation of the cycloconverter. However, with active load such as motors, the operation of the cycloconverter will encounter problems such as excessive heat, vibration and noise.

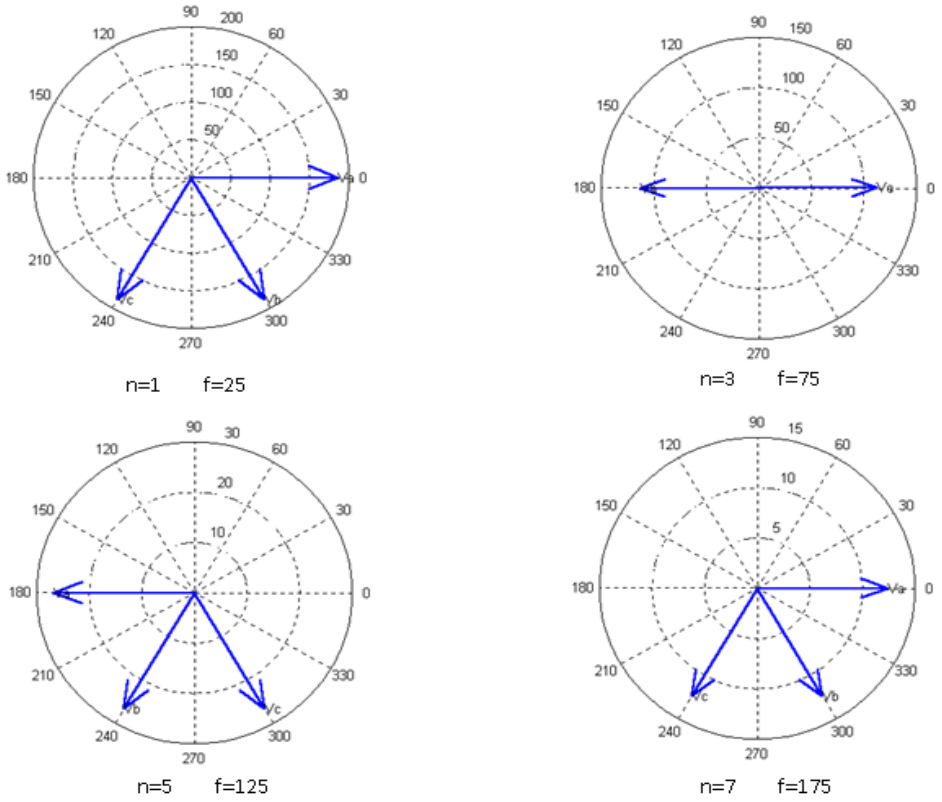

Fig.7.19 Phase angle relationships for T = 2, R-load of the three phases A,B and C.

7.5.4 Three-Phase Cycloconverter with T =3 with R-Load

In the following analysis three-phase version is considered for the case when T=3. Since the output waveforms for the three phase are same only they differ in phase lag of the three-phase system namely 0˚,120 ˚and 240˚.The waveform of the output voltage when T=3 is shown in Fig.7.16 (c) represent the case when T=3 with R-Load above and can be defined in general mathematical form as

$$\left.\begin{aligned}
v_{Lj} &= \sqrt{2}\,V_s \sin(\omega t - \gamma_j) && 0 + \gamma_j < \omega t < \pi + \gamma_j \\
v_{Lj} &= -\sqrt{2}\,V_s \sin(\omega t - \gamma_j) && \pi + \gamma_j < \omega t < 2\pi + \gamma_j \\
v_{Lj} &= \sqrt{2}\,V_s (\sin \omega t - \gamma_j) && 2\pi + \gamma_j < \omega t < 3\pi + \gamma_j \\
v_{Lj} &= \sqrt{2}V_s \sin(\omega t - \gamma_j) && 3\pi + \gamma_j < \omega t < 4\pi + \gamma_j \\
v_{Lj} &= -\sqrt{2V_s} \sin(\omega t - \gamma_j) && 4\pi + \gamma_j < \omega t < 5\pi + \gamma_j \\
v_{Lj} &= \sqrt{2V_s} \sin(\omega t - \gamma_j) && 5\pi + \gamma_j < \omega t < 6\pi + \gamma_j
\end{aligned}\right\} \quad (7.31)$$

Fourier series analysis of Eq.(7.31) for the single-phase version of the converter gives

For $n \neq T$

$$a_o = 0 \tag{7.32}$$

$$a_n = \frac{\sqrt{2}\, V_s T}{\pi(T^2 - n^2)} \tag{7.33}$$

$$b_n = \frac{\sqrt{2}\, V_s\, T}{\pi(T^2 - n^2)} \left[2\sin\frac{n\pi}{T} + 2\sin\frac{2n\pi}{T} - 2\sin\frac{4n\pi}{T} - 2\sin\frac{5n\pi}{T} - \sin\frac{6n\pi}{T}\right] \tag{7.34}$$

For $n = T$, the Fourier coefficients are:

$$a_T = 0 \tag{7.35}$$

$$b_T = \frac{\sqrt{2}\, V_s}{T} \tag{7.36}$$

$$c_T = b_T = \frac{\sqrt{2}\, V_s}{T} \tag{7.37}$$

For $n = T$, the Fourier coefficients are:

Harmonic frequency spectrum of the output voltage waveform for one phase with T=3 is shown in Fig.7.20.The fundamental frequency is ⅓ T (= ⅓ f_i = ⅓ × 50) = 16.66 Hz. The 3rd harmonic is zero, whereas the second significant harmonic is the 5th one followed by the 7th . The other higher order harmonics are negligibly small.

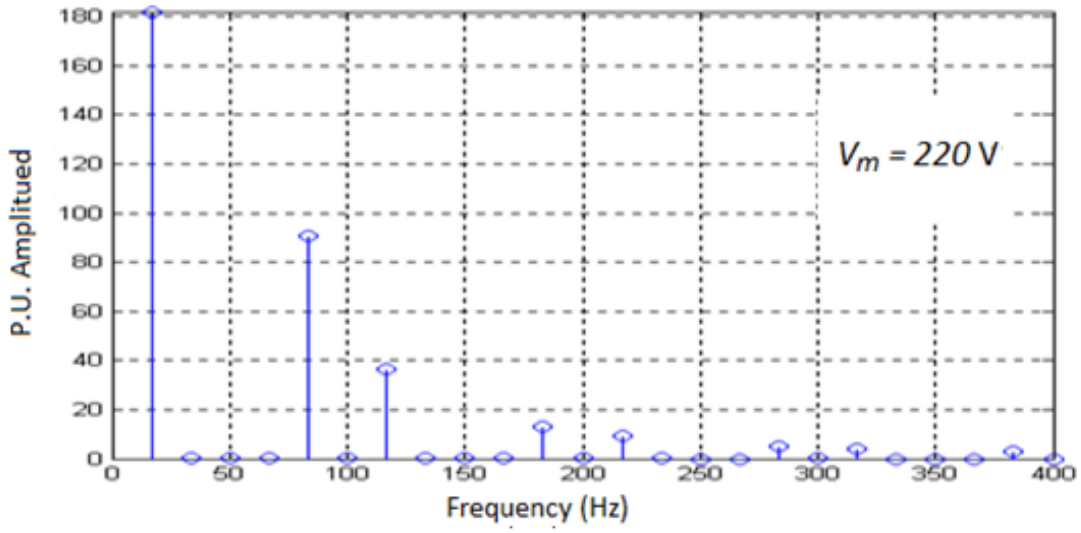

Fig.7.20 Harmonic frequency spectrum of the output voltage waveform for one phase with T=3.

The Fourier analysis for the three-phase version gives:

For $n \neq T$

$$a_{oj} = 0 \tag{7.38}$$

$$a_{nj} = \frac{\sqrt{2}\,V_s T}{\pi(T^2 - n^2)}\left[\cos\frac{n\gamma_j}{T} + 2\cos\frac{n(\pi+\gamma_j)}{T} + 2\cos\frac{n(3\pi+\gamma_j)}{T} - \cos\frac{n(4\pi+\gamma_j)}{T} - 2\cos\frac{n(5\pi+\gamma_j)}{T} - \cos\frac{n(6\pi+\gamma_j)}{T}\right] \tag{7.39}$$

$$b_{nj} = \frac{\sqrt{2}\,V_s\,T}{\pi(T^2 - n^2)}\left[\sin\frac{n\gamma_j}{T} + 2\sin\frac{n(\pi+\gamma_j)}{T} + 2\sin\frac{n(2\pi+\gamma_j)}{T} - 2\sin\frac{n(4\pi+\gamma_j)}{T} - 2\sin\frac{n(5\pi+\gamma_j)}{T} - \sin\frac{n(6\pi+\gamma_j)}{T}\right] \tag{7.40}$$

For $n = T$, the Fourier coefficients are:

$$a_{Tj} = \frac{\sqrt{2}\,V_s}{T}\ \sin\ (-\gamma_j) \tag{7.41}$$

$$b_{Tj} = \frac{\sqrt{2}\,V_s}{T}\cos\ (-\gamma_j) \tag{7.42}$$

$$c_{Tj} = \frac{\sqrt{2}\,V_s}{T} \tag{7.43}$$

$$\psi_{Tj} = \tan^{-1}\frac{a_{Tj}}{b_{Tj}} \tag{7.44}$$

The phase-angle relationships of the load voltages for *R*-load, are shown in Fig. 7.21, for the case of $T = 3$. As in the case when $T = 2$, the harmonic amplitude spectrum for the three phases A, B, and C for $T = 3$ is found to be same as the harmonic spectrum for single phase presented in Fig.7.20. However, the phase-angle relationships of the three-phase voltage waveforms for *R*-load shown in Fig.7.20 for the fundamental component as well as the higher order harmonics are balanced in magnitudes but they are unbalanced in phase angles. Analysis of the output voltage waveform for any number of T = 4,5,6,7,....etc, reveals that the three-phase synchronous envelope cycloconverters generate output voltage waveforms that are balanced in magnitude but they are unbalanced in phase relationship.

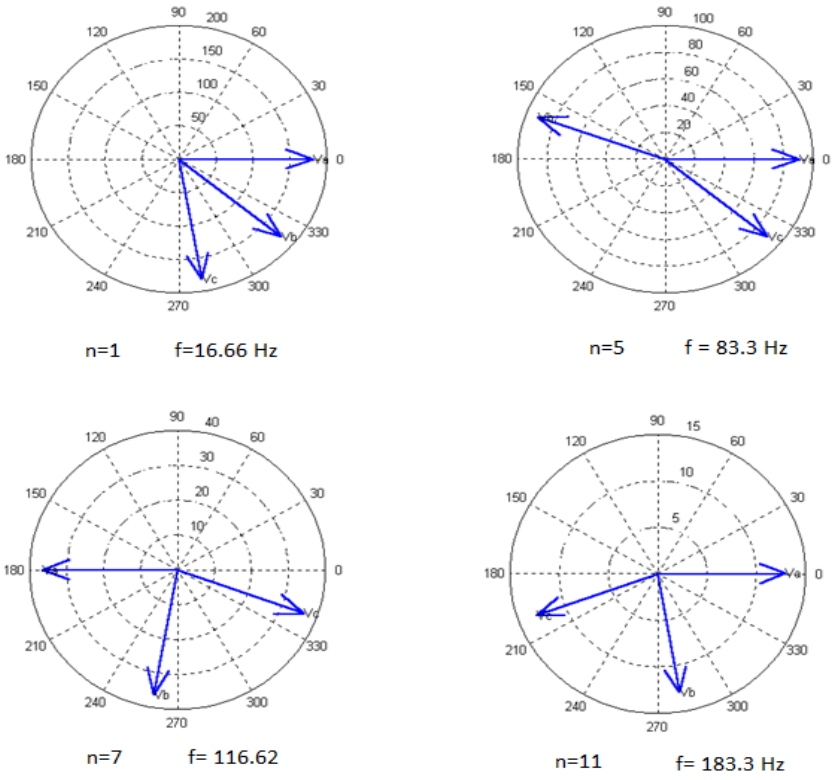

Fig.7.21 Phase angle relationships for $T = 3$, R-load of the three phases A,B and C.

The Generalized Solution

The generalisation of the solution of Fourier expansion of the output voltage waveform generated by synchronous envelop cycloconverter for any value of T is derived in this section for single-phase and multi-phase systems. This generalized solution can be applied easily for any given waveforms as described hereinafter.

1- Generalized equation for single-phase system

Mathematical analysis of voltage waveforms for single-phase systems yields the following general Fourier analysis:

$$a_o = 0 \qquad (7.45)$$

$$a_n = \frac{\sqrt{2}V_s\,T}{\pi(T^2-n^2)}\left[1+2\sum_{k=1}^{k=T-1}\cos\frac{kn\pi}{T}-2\sum_{k=T+1}^{k=2T-1}\cos\frac{kn\pi}{T}-\cos\frac{2Tn\pi}{T}\right] \quad (7.46)$$

$$b_n = \frac{\sqrt{2}\,V_sT}{\pi(T^2-n^2)}\left[2\sum_{k=1}^{k=T-1}\sin\frac{kn\pi}{T}-2\sum_{k=T+1}^{k=2T-1}\sin\frac{kn\pi}{T}-\sin\frac{2Tn\pi}{T}\right] \quad (7.47)$$

where k = integer 1,2,3,.....
The n[th] harmonic amplitude is given by:

$$c_n = \sqrt{a_n^2+b_n^2} \quad (7.48)$$

and the phase angle ψ_n of the nth harmonic is

$$\psi_n = \tan^{-1}\frac{a_n}{b_n} \quad (7.49)$$

2- Generalized equation for multi-phase system.

Mathematical analysis of voltage waveforms for multi-phase systems yields the following general Fourier analysis:

$$a_{oj} = 0 \quad (7.50)$$

$$a_n = \frac{\sqrt{2}\,V_sT}{\pi(T^2-n^2)}\left[\cos n\,\gamma_j+2\sum_{k=1}^{k=T-1}\cos\frac{n(k\pi+\gamma_j)}{T}-2\sum_{k=T+1}^{k=2T-1}\cos\frac{n(k\pi+\gamma_j)}{T}-\cos\frac{n(2T\pi+\gamma_j)}{T}\right] \quad (7.51)$$

$$b_n = \frac{\sqrt{2}\,V_sT}{\pi(T^2-n^2)}\left[\sin n\gamma_j+2\sum_{k=1}^{k=T-1}\sin\frac{n(k\pi+\gamma_j)}{T}-2\sum_{k=T+1}^{k=2T-1}\sin\frac{n(k\pi+\gamma_j)}{T}-\sin\frac{n(2T\pi+\gamma_j)}{T}\right] \quad (7.52)$$

The n[th] harmonic amplitude is given by:

$$c_{nj} = \sqrt{a_{nj}^2 + b_{nj}^2} \tag{7.53}$$

and the phase angle ψ_n is:

$$\psi_{nj} = \tan^{-1}\frac{a_n}{b_n} \tag{7.54}$$

Application of the generalized equations from Eqs.(7.50) to (7.54) to both single-phase and multi-phase system give the same results obtained from the individual analysis of each waveform. From the previous results, it is found that when T is even integer number (T = 2,4,6,8….) the Fourier coefficient of the supply frequency components a_{Tj} and b_{Tj} are always equal to zero, while for odd values of T =3,5,7,9,….., the supply frequency components a_{Tj} and b_{Tj} have significant values. Fig.7.22 shows the frequency spectrum for T = 4. The phase relationship of the three phases is also shown in Fig.7.23 which shows unbalanced phase-angle between the three individual phases A,B, and C.

The problem of unbalanced phase-angle relationships, can be solved using a multiple of 2π phase shifting technique , which is based on shifting the load voltage v_{Lj} of phase B or phase C or both of them, by multiple of 2π, with phase A taken as a reference, i.e when γ_A= 0, the other phase angles will be:

$\gamma_B = (2\,\pi/3) + 2\pi$ $\qquad$ $\gamma_C = (4\,\pi/3) + 4\pi$

It is found that this technique makes the phase displacement angles of the n[th] harmonics balanced except when n is multiple of 3, in this case the phase displacement angles will be in-phase for all cases. The result of implementing this technique is shown in Fig.7.24 as an example for T=4.

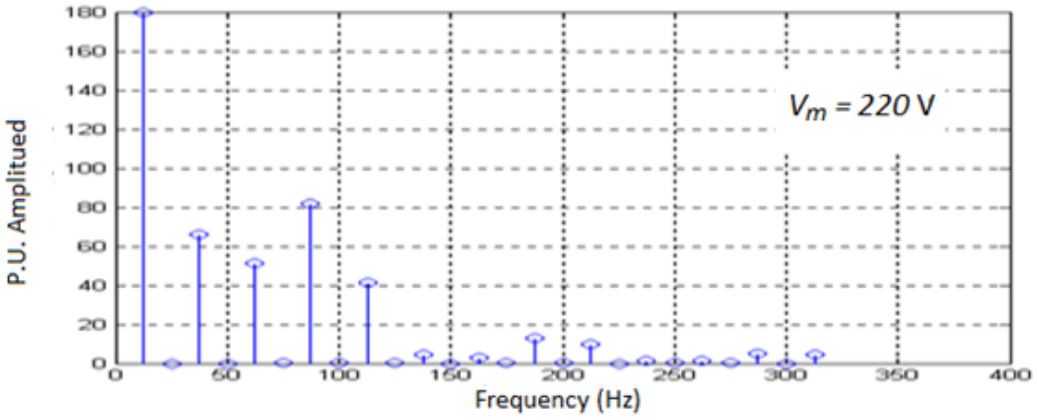

Fig.7.22 Harmonic frequency spectrum of the output voltage waveform for one phase with T=4.

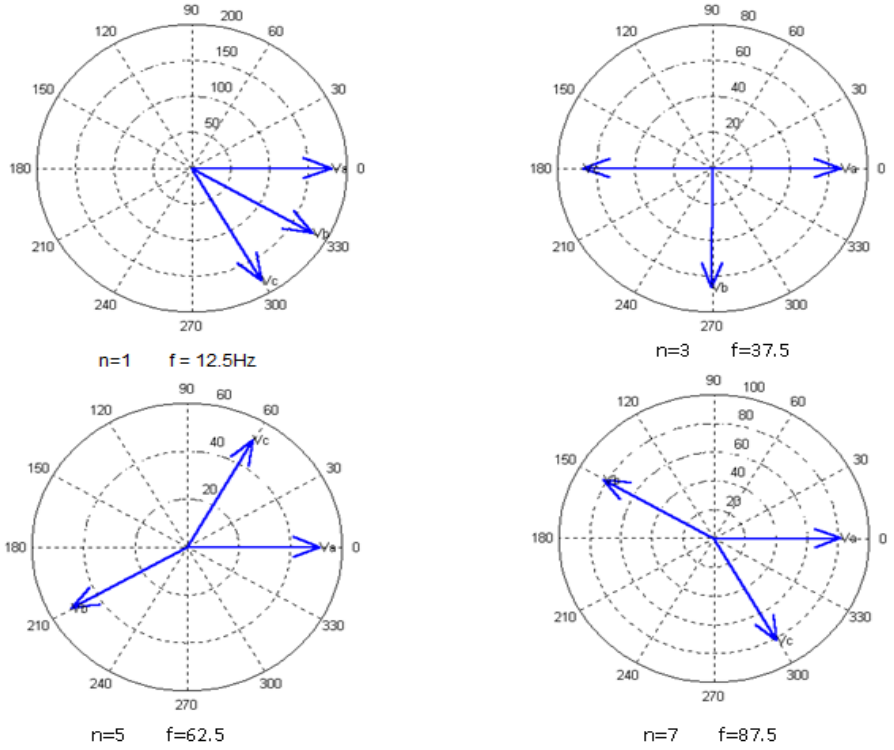

Fig.7.23 Harmonic amplitude spectrum (of phase A, B, and C) and phase angle relationships for $T = 4$, R-load before phase-angle corrections.

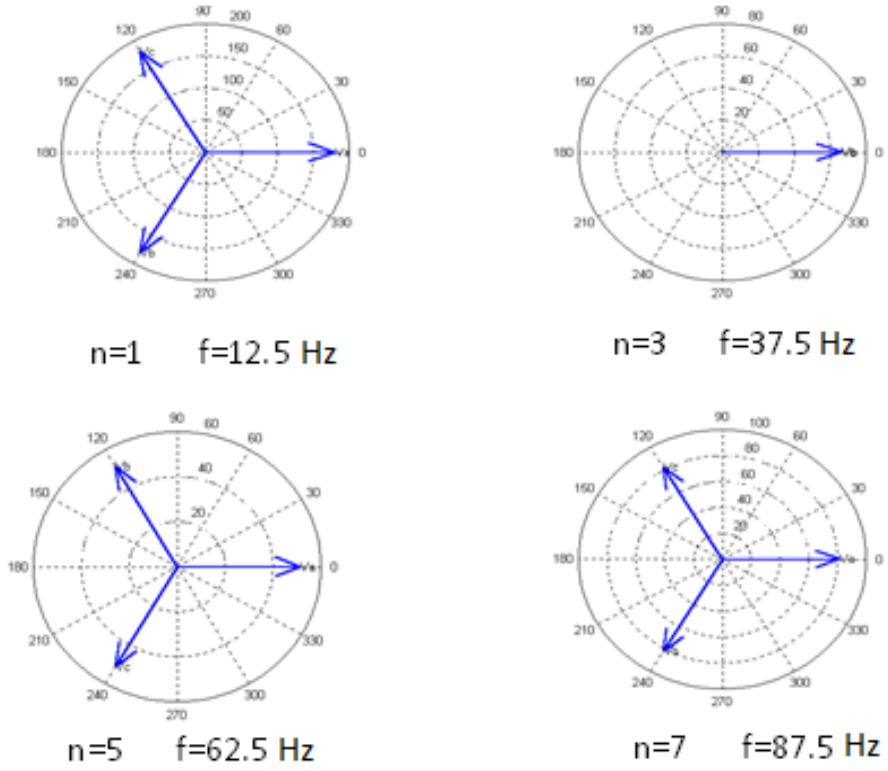

Fig.7.24 Phase-angle relationships of phase A, B, and C for $T = 4$, R-load after phase-angle correction.

7.6 HARRMONICS REDUCTION IN ENVELOPE CYCLOCONVERTER

As it is seen from the previous analysis that the output voltage waveform of the envelope cycloconverter contains harmonics. To reduce these harmonics it is necessary to generate wave shape which is nearly sinusoidal or stepped wave . For single phase source, to generate stepped wave, it is necessary to use some form of input transformer connection. Conduction in successive phases of the transformer secondary windings is made in logic sequence , with respect to the supply voltages, so as to provide an output voltage envelope that is approximately a stepped waveform of the desired output frequency.

In the circuit of Fig. 7.25 (a) , where Triacs are adopted , the voltage applied across the load can be the full supply voltage of either polarity or some fraction V_{m1} , depending on the transformer secondary tap setting. The switches are shown as triacs but can equally well be pairs of inverse-parallel connected silicon controlled rectifiers or any other bidirectional switch. With an ideal supply and ideal switches waveform of the shape shown in Fig. 7.25(b) can be obtained.

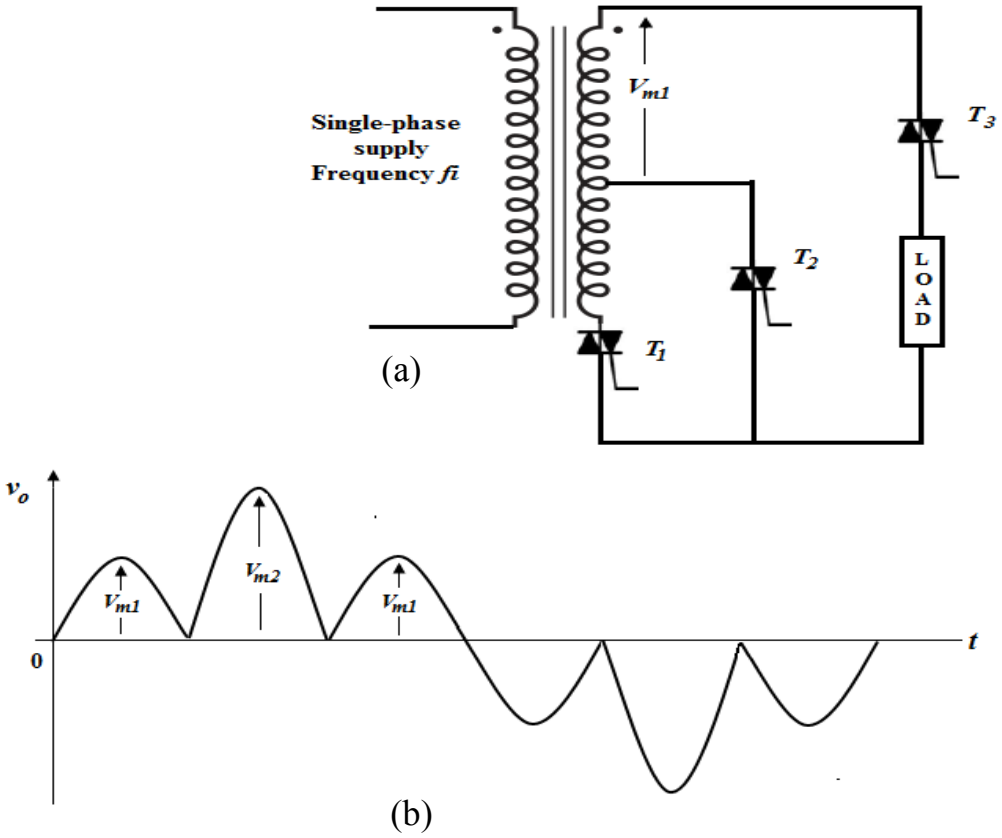

Fig.7.25 Single-phase envelope cycloconverter: (a) Circuit diagram for two-pulse operation and (b) Load voltage waveforms with output frequency $f_o = (1/3)\, f_{in}$.

Basically, a single-phase envelope cycloconverter can be considered to be composed of two converters connected back to back as shown in Fig.7.26. The types of voltage waveforms that can be obtained using envelope converters shown in figure can be improved by increasing the number of pulses using three-phase or multi-phase systems. The waveform is obtained by properly selecting the input voltages to the converter. As with rectifier circuit operation an increase of pulse number reduces the voltage ripple and the higher harmonic content.

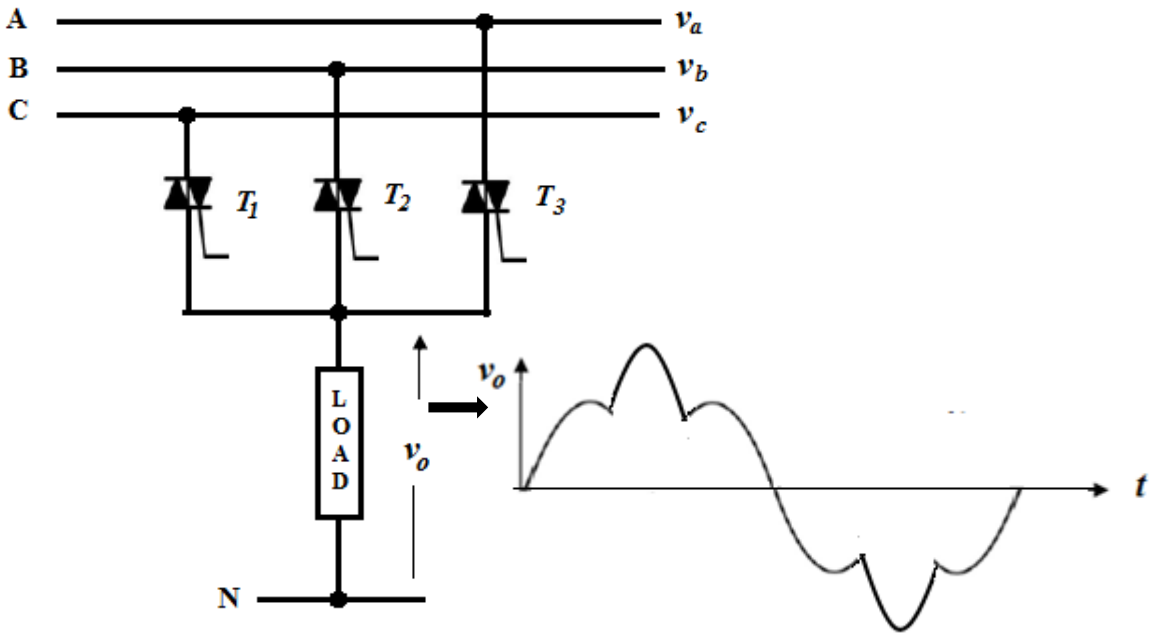

(a) (b)

Fig.7.26 Three-phase to single-phase envelope cycloconverter: (a) Circuit diagram for two-pulse operation and (b) Load voltage waveforms with output frequency $f_o=(1/2)\, f_{in}$.

7.7 THE MATRIX CONVERTER

A matrix converter is defined as an ac to ac converter with a single stage of conversion. It utilizes bidirectional controlled switch to achieve automatic conversion of power. In its topology, the matrix converter can be considered as a three-phase to three-phase forced commutated cycloconverter which, in its simplest form, consists of nine bi-directional switches that allow any output phase to be connected to any input phase as it is shown in Fig.7.27. The input terminal of the converter are connected to a voltage source, usually the grid, while the output terminal are connected to a current source like an induction motor . Only one of the three switches connected to the same output phase can conducts at any instant of time.

The matrix converter has several advantages over other type of ac to ac converters in that

- The output voltage waveforms generated by this converter has minimal higher order harmonic and no subharmonics.
- The bidirectional switches make it possible to have a controllable power factor input since this converter has inherent bidirectional energy flow capability (improved power factor and regeneration capability).
- The lack of d.c. links ensures it has a compact design.
- Generation of output voltage with the desired amplitude and frequency.
- Sinusoidal input current and sinusoidal output voltage .

The main disadvantage of the matrix converter is that it requires more semiconductor devices than a conventional ac to ac indirect power frequency changer.

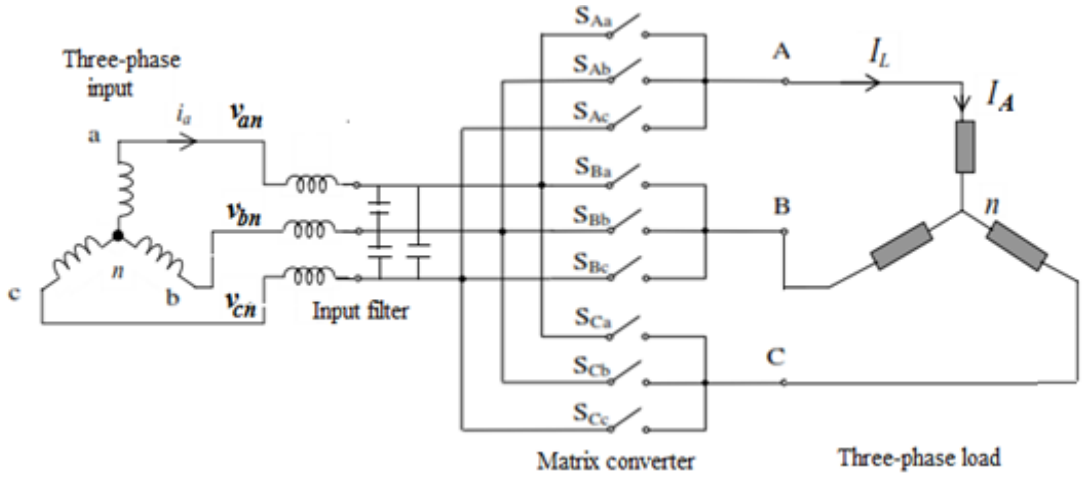

Fig.7.27 Schematic circuit of a three-phase to three-phase matrix converter.

In the matrix converter, if it is assumed that all the switches are ideal and no energy storage components are present between the input and output side of the converter, then, the instantaneous input power must always be equal to the instantaneous output power. Due to this power invariance feature, the phase angles between the voltages and currents at the input can be controlled to give unity displacement factor for any loads. Therefore, for the converter, it is necessary to use ideal bidirectional switches, capable of conducting current and blocking voltage for both polarities depending on the actual control signal.

The required output voltage waveforms are generated directly from the input voltage waveforms and each output voltage waveform is synthesized by sequential sampling of the input voltage waveforms. The sampling rate has to be set much higher than input and output frequencies,

the number of input and output phases do not have to be equal so that rectification, inversion, and frequency conversion are all realizable. The output voltage waveforms are therefore composed of segments of the input voltage waves. The lengths of each segment are determined mathematically to ensure that the average value of the actual output waveform within each sampling period tracks the required output waveform.

Methods of matrix converter control

There are three methods of matrix converter control,

- Venturini-analysis of function transfer
- Pulse width modulation
- Space vector modulation

The Venturini principle can be explained initially using a three-phase output. Consider a three-phase output using a three-phase input voltage as depicted in Fig.7.27, switching elements S_{Aa} –S_{Cc} are nine bidirectional switches connecting the input phases (a, b, and c) to any output phase (A,B, and C) at any instant . Only one of the three switches is turned on at any given time, and this ensures that the input of a matrix converter, which is a voltage source, is not short-circuited while a continuous current is supplied to the load.

During phase connection process, the three voltages v_{AN} ,v_{BN} and v_{CN} are related to the three input voltages by the following mathematical formula :

$$\begin{pmatrix} V_{AN} \\ V_{BN} \\ V_{CN} \end{pmatrix} = \begin{pmatrix} S_{Aa} & S_{Ba} & S_{Ca} \\ S_{Ab} & S_{Bb} & S_{Cb} \\ S_{Ac} & S_{Bc} & S_{Cc} \end{pmatrix} \begin{pmatrix} V_{an} \\ V_{bn} \\ V_{cn} \end{pmatrix} \qquad (7.55)$$

or $$\mathbf{V} = \mathbf{S}\,\mathbf{v}$$

where

$$\mathbf{V} = \begin{pmatrix} V_{AN} \\ V_{BN} \\ V_{CN} \end{pmatrix}, \qquad \mathbf{S} = \begin{pmatrix} S_{Aa} & S_{Ba} & S_{Ca} \\ S_{Ab} & S_{Bb} & S_{Cb} \\ S_{Ac} & S_{Bc} & S_{Cc} \end{pmatrix} \quad \text{and} \quad \mathbf{v} = \begin{pmatrix} V_{an} \\ V_{bn} \\ V_{cn} \end{pmatrix}$$

S = connection matrix consists of the switching variables S_{Aa} through S_{Cc}.

For star-connected load as shown in Fig.7.27, the output phase current are related to the input phase current by

$$\begin{pmatrix} i_A \\ i_B \\ i_C \end{pmatrix} = \begin{pmatrix} S_{Aa} & S_{Ba} & S_{Ca} \\ S_{Ab} & S_{Bb} & S_{Cb} \\ S_{Ac} & S_{Bc} & S_{Cc} \end{pmatrix} \begin{pmatrix} i_a \\ i_b \\ i_c \end{pmatrix} \quad (7.56)$$

Theoretically, with nine bi-directional switches the matrix converter can have $(2)^9 = 512$ different switching states combinations. But not all of them can be usefully employed. Because the converter is supplied by a voltage source and usually feeds an inductive load, the input phases must not be short-circuited and the output currents should not be interrupted. These rules imply that one and only one bi-directional switch per output phase must be switched on at any instant. By this constraint, in a three - phase to three-phase matrix converter only 27 switching combinations are the permitted in practice.

Although the matrix converter has the features that have been briefly described above it might be surprising to establish that this converter topology, today, has not found a wide utilization yet. The reasons for that are due to the number of practical implementation problems that have slowed down the development of this type of ac-to-ac converter.

PROBLEMS

7.1 For the output voltage waveform $v_o(\omega t)$ of Fig.7.4 with peak voltage 200V, calculate the values of the *rms* voltage V_o for the triggering angle α: (a) 30˚, (b) 45˚, (c) 90˚, (d) 125˚, and (e) 150˚.

[Ans: (a) 139.37 V, (b) 131.36 V, (c) 114.84 V, (d) 104.38 V, (e) 70 V]

7.2 Show that the fundamental component of waveform $v_o(\omega t)$ of Fig.7.4 is zero. What is the frequency of the lowest order harmonic?

7.3 In the single-phase cycloconverter shown in Fig.7.3, the input supply voltage is 240V, 50Hz. The load is a pure resistance and the output frequency is 12.5Hz. It is required to:

(a) Sketch the waveforms for the input voltage verses ,output voltage v_o for $\alpha = 0^o$ and $\alpha = 90^o$.

(b) Calculate the *rms* value of the output voltage at $\alpha = 0^o$ and $\alpha = 90^o$.

[Ans: (b) 240 V, 169.73 V]

7.4 A three-phase, four-wire, half-wave rectifier dual converter operated from a 400V, 50-Hz three-phase supply. Calculate the average value of the load voltage for firing angles (a) 30˚, (b) 45˚, (c) 90˚, (d) 125˚, and (e) 150˚.

[Ans: (a) 405.26 V, (b) 330 V, (c) 0 V, (d) - 268.37 V, (e) - 405.26 V]

7.5 The input voltage to the single-phase to single-phase cycloconverter is 240V(*rms*), 50Hz. The load resistance is 10Ω and the load inductance is L = 50 mH. The frequency of the output voltage is 25Hz. If the converter is operating with a delay angle $\alpha_p = 2\pi/3$,

(a) Sketch the circuit configuration of the converter.
(b) Sketch the output voltage waveform.
(c) Determine the *rms* value of the output voltage.
(d) Determine the impedance of the load at the outut frequency.
(e) Calculate the *rms* value of the load current.
(f) Determine the input power factor of the converter.

[Ans : (c) 106 V, (d) 12.7 Ω , (e) 8.34 A, (f) 0.371 (lagging)]

7.6 A single-phase cycloconverter operating in circulating current free dual converter with input 220 V, 50 Hz is used to produce an output voltage waveform of the general form (Fig.7.5). The output frequency is one-third of the input frequency, and α = 45˚. Calculate the amplitude of the fundamental voltage.

[Ans: 135.85 V]

7.7 A three-phase to single-phase three-pulse cycloconverter delivers an output of 240 V, 70 A to a load of 0.9 power factor lagging. Assume that the switches of the converter are ideal and that the output current is nearly sinusoidal. Calculate the input voltage and input power factor.

[Ans: V_s =290 V , PF = 0.4315]

7.8 A three-phase to three-phase, three-pulse cycloconverter operating in circulating current-free such that the input / output frequency ratio is $f_i / f_o = 9$. What are typical frequencies of the low-order higher harmonics?

[Ans : $(2/9) f_o$, $(1/3) f_o$, $(4/9) f_o$, $(5/9) f_o$, $(2/3) f_o$, $(7/9) f_o$,……]

CHAPTER EIGHT

DC-AC CONVERSION: INVERTERS

8.1 INTRODUCTION

Inverter is an electrical device which converts d.c. voltages (or currents) to a.c. voltages (or currents). This device has several important applications in industry such as induction and synchronous motor drives, uninterruptible power supplies (UPSs'), standby power supplies, induction heating, traveling, camping, and HVDC systems. Ideally, the input signal to the inverter is d.c. signal from a battery or an output of a controlled rectifier and the output signal is a.c. which can be square wave, quasi-square wave or nearly sinusoidal wave.

Inverters can be classified as voltage source inverters or current source inverters. Inverter converting voltage is called VOLTAGE SOURCE INVERTER (VSI), whereas inverter converting current is called CURRENT SOURCE INVERTER (CSI). The output of the inverter could be at any desired frequency, voltage or current.

Power transistor such as BJT, MOSFET and IGBT, are widely used in low and medium power inverters. Thyristors (SCRs) or GTOs inverters are used for high power inverter. So there are many types of inverters available in industry today, and each of them is designed to suit particular application or to meet designed performance requirements.However, For VSI inverter, the following types are commonly used in industry:

1- Parallel inverter.
2- Single-phase bridge-type inverter.
   (a) Single-phase half-Bridge inverter.
   (b) Single-phase full-Bridge inverter.
3- Single-phase series inverter.
4- Three-phase inverters.

8.2 PARALLEL INVERTER

The simplest type of voltage source inverter used in low power applications and UPS system for computers is the parallel inverter. Depending on the switching device used , there are two types of parallel inverter namely, transistor parallel inverter and thyristor parallel inverter which is also called parallel capacitor inverter.

8.2.1 Transistor Parallel Inverter

Figure 8.1 shows the diagram of the basic single-phase transistor parallel inverter circuit which consists of two transistors Tr_1 and Tr_2 that are alternatively turned ON and OFF. The transistors employed in the circuit Tr_1 and Tr_2 carry the current in the positive and negative half cycles.

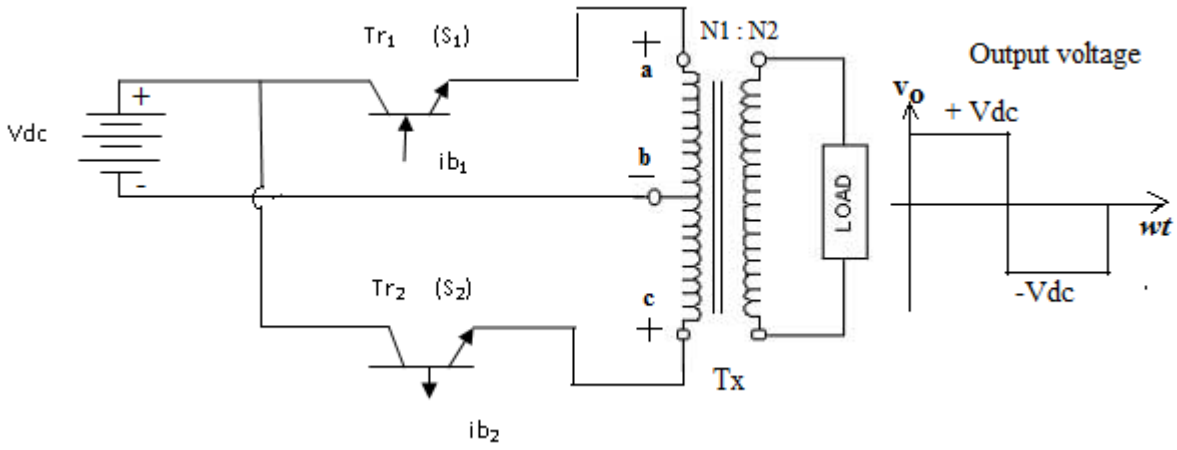

Fig.8.1 Transistor parallel inverter circuit.

Principle of operation

Assuming T_{r1} conducts and Tr_2 OFF, Tr_1 current flows through the primary winding (a-b) of the output transformer Tx and produces an induced voltage on the secondary winding. Hence, supplies a load with positive voltage $+V_{dc}$. When T_{r1} switched off ($i_{b1} \rightarrow 0$) and T_{r2} is switched on by applying current i_{b2} in its base, current flows through the primary winding (c-b) of the output transformer T_x and produce $-V_{dc}$ at the secondary of T_x. Hence a square wave of amplitude V_{dc} is generated. This square or rectangular wave can be approximated to sine wave by using additional filter. Waveforms of this inverter are shown in Fig.8.2 for pure resistive load.

The advantage of the parallel inverter is that, one can use low voltage d.c. source and obtain any output voltage by using appropriate output transformer with proper turns ratio.

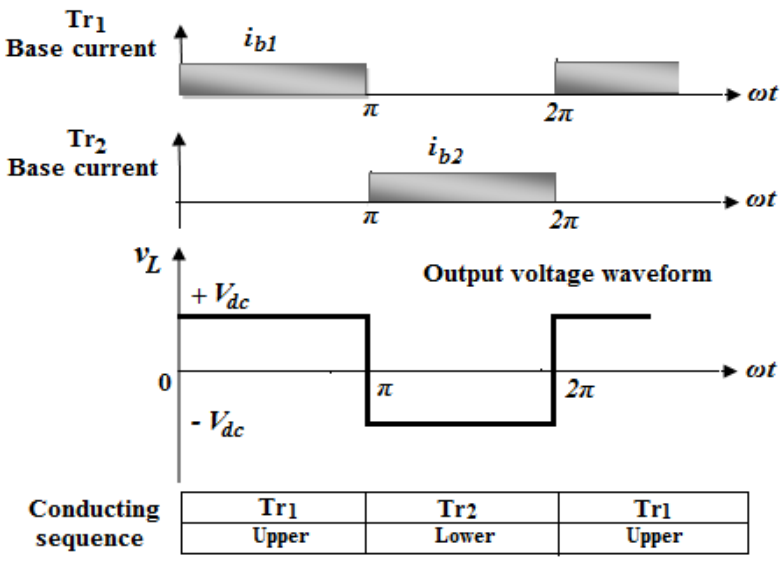

Fig.8.2 Transistor base current and utput voltage waveforms for the parallel transistor inverter.

8.2.2 Thyristor Parallel Inverter

The basic single-phase parallel inverter circuit consists of two SCRs: SCR $_1$ and SCR $_2$, an inductor L, an output transformer, and commutating capacitor C as depicted in Fig.8.3. The output voltage and current are v_o and i_o respectively. The function of L is to make the source current constant and smooth. During the working of this inverter, capacitor C comes in parallel with the load via the transformer and helps to commutate the two thyristors, so it is called a ***parallel capacitor inverter***. The operation of this inverter can be explained in the following modes.

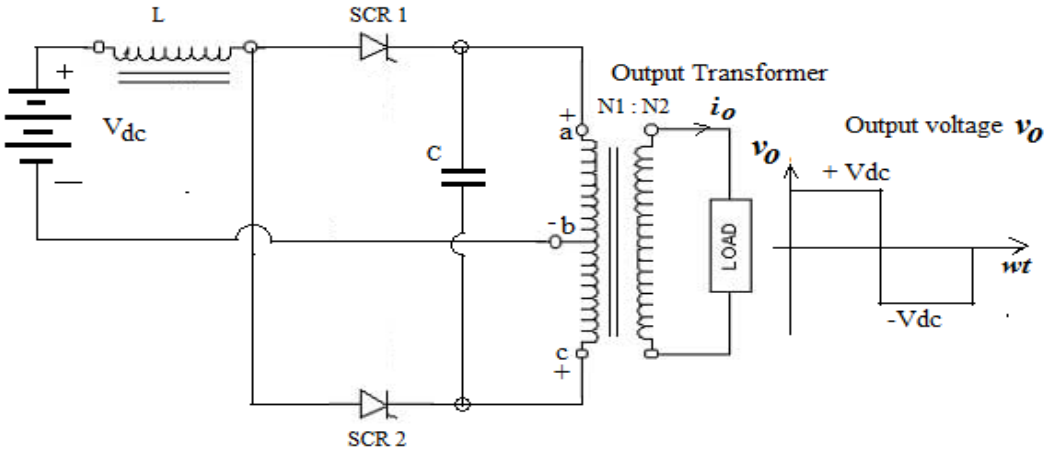

Fig.8.3 Thyristor parallel capacitor inverter circuit.

Mode I

In this mode, SCR_1 is conducting while SCR_2 is OFF. In this case current flows in the upper half of the primary winding (section a-b) of the output transformer. As a result an induced voltage on the secondary is produced and supplied to the load. At this time the voltage between a and c terminals, V_{ac} , is equal two times the d.c. supply voltage. In other words total voltage across primary winding is $2V_{dc}$. Now the capacitor C charges to a voltage of $2V_{dc}$ with upper plate as positive.

Mode II

When SCR_2 is turned ON, by applying a trigger pulse to its gate, at this time (t = 0), capacitor voltage $2V_{dc}$ appears as a reverse bias across SCR_1, it is therefore turned OFF. A current i_o begins to flow through SCR_2 and lower half of primary winding. Now the capacitor has charged (upper plate as negative) from $+2V_{dc}$ to $-2V_{dc}$ at time $t = t_1$. Load voltage also changes from V_{dc} at t = 0 to $-V_{dc}$ at $t = t_1$.

Mode III

When capacitor has charged to $-V_{dc}$, SCR_1 may be tuned ON at any time. When SCR_1 is triggered, capacitor voltage $2V_{dc}$ applies a reverse bias across SCR_2, it is therefore turned OFF. After SCR_2 is OFF, capacitor starts discharging, and charged to the opposite direction, the upper plate as positive. These procedures (Modes) proceed and repeat.

The inductor *L* in Fig.8.3 is used also to limit the commutating current during commutation process. In the absence of *L*, The capacitor will charged and discharged very rapidly during each of SCR s' conduction. The result is that the SCR may have no time to turn off. The waveforms of the SCR and capacitor voltages and currents are shown in Fig.8.4 (a) and (b) respectively.

The *rms* Value of the Output Voltage

The output voltage waveform of the inverter is a square wave as shown in Fig.8.2, the *rms* value of the square wave can be evaluated as follows:

Any function $v_o(\omega t)$ that is periodic in 2π radians has a root mean square *rms* or effective value defined by:

$$V_{o(rms)} = \sqrt{\frac{1}{2\pi}\int_0^{2\pi} v_o^2\,(\omega t)d\omega t} \qquad (8.1)$$

The square wave is defined as,

$$\left.\begin{aligned} f(\omega t) = v_o(\omega t) &= V_{dc} \qquad 0 \le \omega t \le \pi \\ &= -V_{dc} \qquad \pi \le \omega t \le 2\pi \end{aligned}\right\} \qquad (8.2)$$

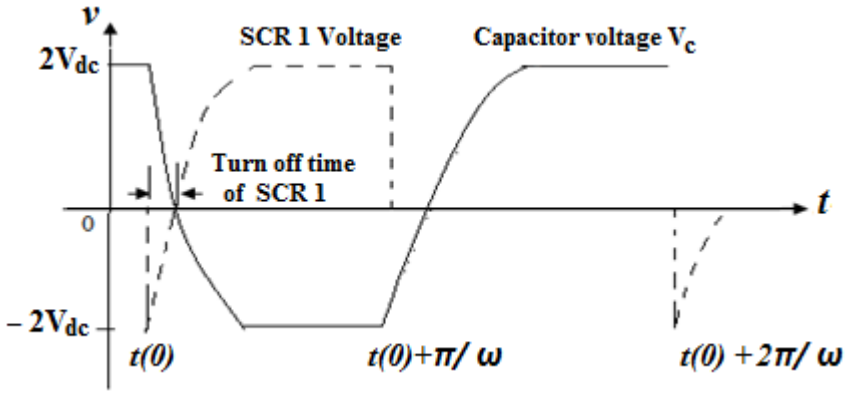

(a)

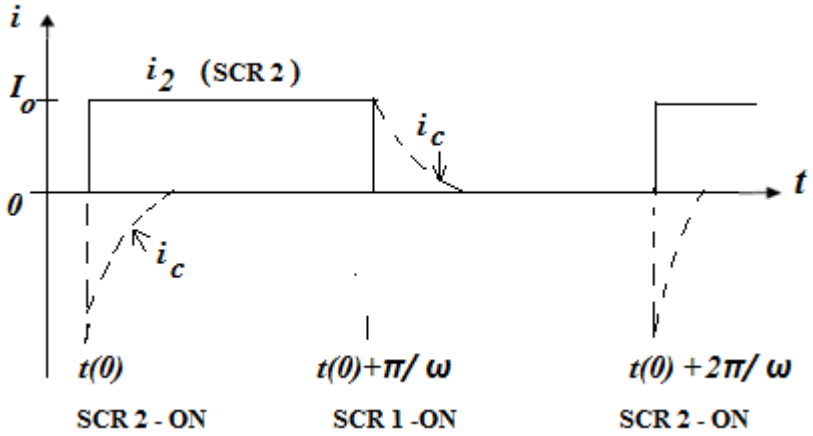

(b)

Fig.8.4 Waveforms of the SCR and capacitor (a) voltage, and (b) current for the parallel inverter.

In the present case,

$$V_{o(rms)} = \sqrt{\frac{1}{\pi}\int_0^{\pi} (V_{dc})^2\, d\omega t} = \sqrt{\frac{V_{dc}^2}{\pi}\int_0^{\pi} d\omega t} = V_{dc} \qquad (8.3)$$

Therefore, the *rms* value of the output voltahe waveform is equal to the d.c. input voltage source. The main disadvantages of the parallel capacitor inverter are the heavy transformer required to carry the load current and the large energy trapped in the commutating capacitor which need to be removed by additional feedback large ratings diodes.

Harmonic Analysis of the Output Voltage Waveform

The output voltage waveform of the inverter is a square wave (Fig.8.2) which is non-sinusoidal. Since this wave is periodic, its harmonic content can be found using Fourier series as follows:

The Fourier coefficients are,

$$\left.\begin{aligned} \frac{a_o}{2} &= \frac{1}{2\pi}\int_0^{2\pi} f(\omega t)d\omega t \\ a_n &= \frac{1}{\pi}\int_0^{2\pi} f(\omega t)cosn\omega t\, d\omega t \\ b_n &= \frac{1}{\pi}\int_0^{2\pi} f(\omega t)sinn\omega t\, d\omega t \end{aligned}\right\} \quad (8.4)$$

Referring to the square wave defined in Eq.(8.2),

The d.c. component is:

$$\frac{a_o}{2} = \frac{1}{2\pi}\left[\int_0^{\pi} V_{dc}\, d\omega t + \int_{\pi}^{2\pi} (-V_{dc})d\omega t\right] = 0 \quad (8.5)$$

The coefficiants a_n and b_n of the nth order harmonic are,

$$a_n = \frac{V_{dc}}{\pi}\left[\int_0^{\pi} cosn\omega t\, d\omega t - \int_{\pi}^{2\pi} cosn\omega t\, d\omega t\right] = 0 \quad (8.6)$$

$$b_n = \frac{V_{dc}}{\pi}\left[\int_0^{\pi} sinn\omega t\, d\omega t - \int_{\pi}^{2\pi} sinn\omega t\, d\omega t\right]$$

$$= \frac{V_{dc}}{n\pi}\left[-cosn\omega t\,\Big|_0^{\pi} + cosn\omega t\,\Big|_{\pi}^{2\pi}\right]$$

$$= \frac{V_{dc}}{n\pi}\left[(coso - cosn\pi) + (1 - cosn\pi)\right]$$

$$\therefore b_n = \frac{2V_{dc}}{n\pi}(1 - cosn\pi)$$

- When n is even (2, 4, 6…) , $cosn\pi = 1$ $\quad\therefore b_n = 0$.
- When n is odd (3, 5, 7…) , $cosn\pi = -1$

$$\therefore \quad b_n = \frac{4\,V_{dc}}{n\pi} \quad (8.7)$$

The Fourier series is given by:

$$f(\omega t) = \frac{a_o}{2} + \sum_{n=1}^{\infty} (a_n \, cosn\omega t + \, b_n sinn\omega t)$$

Hence the output (load voltage) can be represented by Fourier series as,

$$v_o(\omega t) = \sum_{n=1}^{\infty} \frac{4V_{dc}}{n\pi} sinn\omega t \qquad \text{(since: } \frac{a_o}{2} \text{ and } a_n \text{ are zero)} \quad (8.8)$$

From the above equation (8.8), the instantaneous value of the fundamental component (first harmonic, n=1) is

$$v_{o1}(\omega t) = \frac{4}{\pi} V_{dc} sin\omega t \quad (8.9)$$

The fundamental component peak value is,

$$V_{o1p} = c_1 = \frac{4}{\pi} V_{dc} \quad (8.10a)$$

The *rms* value of the fundamental component is,

$$V_{o1(rms)} = \frac{c_1}{\sqrt{2}} = \frac{\frac{4}{\pi} V_{dc}}{\sqrt{2}} = \frac{4V_{dc}}{\sqrt{2}\pi} \quad (8.10b)$$

Similarly, the instantaneous value of the third harmonic component (n=3) is,

$$v_{o3p}(\omega t) = \frac{4}{3\pi} V_{dc} sin3\omega t \quad (8.11)$$

The peak amplitude of third harmonic , n=3 is

$$V_{o3p} = \frac{4}{3\pi} V_{dc} \quad (8.12a)$$

and the *rms* value of the third harmonic is,

$$V_{o3(rms)} = \frac{c_3}{\sqrt{2}} = \frac{\frac{4}{\pi} V_{dc}}{3\sqrt{2}} = \frac{4V_{dc}}{3\sqrt{2}\pi} \quad (8.12b)$$

and so on, the *rms* values for the 5^{th}, 7^{th}, …. odd harmonics can be evaluate. The harmonic spectrum of the square wave is as shown in Fig.8.5(a). It is clear from this figure that:

- Harmonic amplitudes decrease as n increases.
- No even harmonics.

- Nearest harmonic is the third, if the fundamental is 50 Hz, then the third harmonic is 150Hz and the fifth harmonic 250 Hz as shown in Fig.8.5 (b).

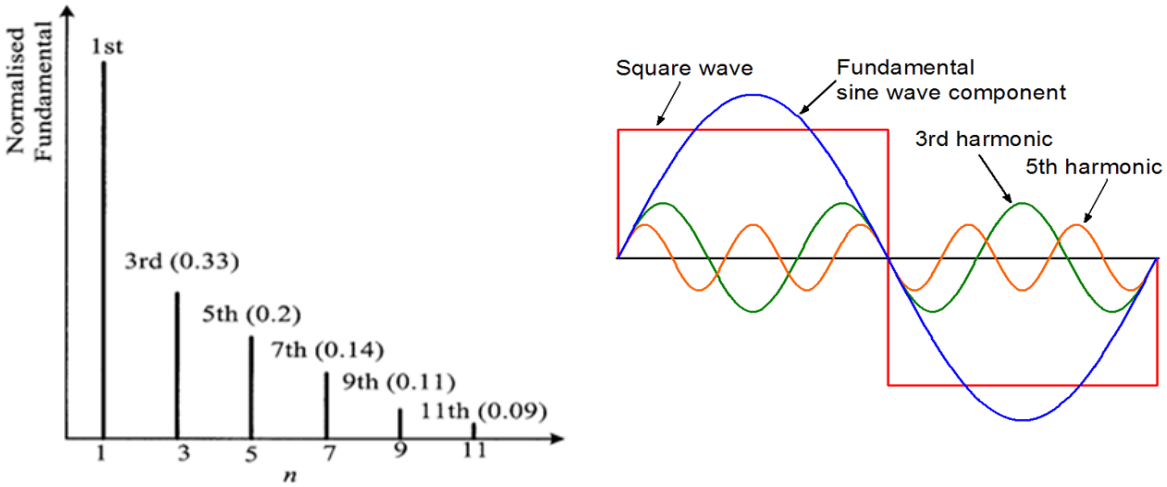

(a) (b)

Fig.8.5 (a) Harmonic spectrum of the square wave, (b) The square wave and its odd harmonics up to the fifth order.

8.2.3 Inverter Performance Parameters

It is obvious from the previous analysis that the output voltage waveform of the inverter is a square wave (or quasi-square wave) which is rich of harmonics. The harmonic components are harmful for the load and the system, because they increase the I^2R losses, generate heat and produce mechanical vibrations when applied to a.c. motors. However, the performance parameters used to assess the amount of distortion produced by the harmonic components in the output voltage waveform of the inverter. These parameters are as follow:

1. The distortion actor *DF*

The distortion factor is defined as

$$DF = \frac{1}{V_1}\left[\sum_{n=2}^{\infty}\left(\frac{V_n}{n^2}\right)^2\right]^{1/2} \tag{8.13}$$

where V_n is the *rms* value of the nth harmonic component.

V_1 is the *rms* value of the fundamental component.

Which is a factor for measuring the harmonic distortion remains in a particular waveform after filtering. The distortion factor of the n^{th} order harmonic component may be calculated as

$$DF_n = \frac{1}{V_1} \times \frac{V_n}{n^2} \tag{8.14}$$

2. The harmonic factor HF_n

The harmonic factor of n^{th} order harmonic is defined as the ratio of the rms value of the n^{th} harmonic component to the *rms* value of the fundamental component.

$$HF_n = \frac{V_n}{V_1} \tag{8.15}$$

This factor represents the contribution of each harmonic component to the harmonic distortion and to evaluate the dominant harmonic component in the output waveform.

3. The total harmonic distortion factor *THD*

This factor gives the ratio of the *rms* values of all harmonic components to the *rms* value of the fundamental component, which is calculated as,

$$THD = \sqrt{\frac{\sum_{n=2,3,..}^{\infty} V_n^2}{V_1^2}} \tag{8.16}$$

The total harmonic distortion factor is very important factor that indicates the amount of distortion in the waveform caused by the harmonic components. It is also represents the measure of closeness of the waveform to pure sine wave. The *THD* can also be written in more general form as:

$$THD = \sqrt{\frac{V^2 - V_1^2}{V_1^2}} \tag{8.17}$$

where V is the *rms* value of the output waveform.

V_1 is the *rms* value of the fundamental component.

4. The lowest order harmonic factor *LOH*

Finally there is another factor which is the lowest order harmonic (*LOH*) that indicates the harmonic of frequency nearest to the fundamental and has amplitude within 3% of the fundamental.

Example 8.1

A single-phase MOSFET parallel inverter has a supply d.c. voltage of 100V supplying a resistive load with R =10 Ω via a center-tap transformer with 1:1 ratio. The output frequency is 50 Hz.

(a) Draw the circuit diagram and the output voltage waveform of the inverter.

(b) Determine the *rms* value of the output voltage waveform.

(c) Determine the amplitude of the Fourier series terms for the square output voltage waveform up to 9th order harmonics.
(d) Calculate the *rms* value of the output voltage in terms of harmonic components that obtained in (b).
(e) Determine the power absorbed by the load consider up to 9th order harmonic.
(f) Draw the frequency spectra of the output voltage waveform.
(g) Calculate the total harmonic distortion factor *THD*.

Solution

(a) The circuit and the output voltage waveform as shown in Fig.8.6.

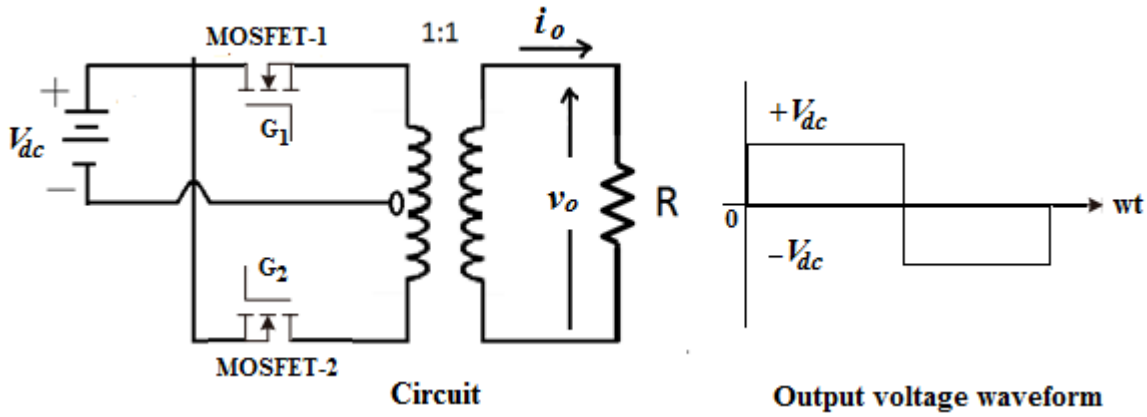

Fig. 8.6.

(b) The *rms* value of the output voltage is found as follows:
Referring to Fig. 8.6,

$$V_{o(rms)} = \sqrt{\frac{1}{T/2}\int_0^{T/2} V_{dc}\, dt} = V_{dc} = 100 \text{ V}$$

(c) From Eq.(8.5), the Fourier series of the output voltage is

$$v_o(\omega t) = \sum_{n=1,3,5,..}^{\infty} \frac{4V_{dc}}{n\pi} sinn\omega t = \sum_{n=1,3,5,..}^{\infty} c_n\, sinn\omega t$$

The amplitude c_n of the n th order harmonic is:

$$c_n = \frac{4V_{dc}}{n\pi} = \frac{4 \times 100}{n\pi} = \frac{127.3}{n}$$

$$v_o(\omega t) = c_1 \sin \omega t + c_3 \sin 3\omega t + c_5 \sin 5\omega t + c_7 \sin 7\omega t + c_9 \sin 9\omega t$$

$$= \frac{127.3}{1}\sin \omega t + \frac{127.3}{3}\sin 3\omega t + \frac{127.3}{5}\sin 5\omega t + \frac{127.3}{7}\sin 7\omega t + \frac{127.3}{9}\sin 9\omega t$$

Hence the output voltage Fourier representation is,

$$v_o(\omega t) = 127.3\sin \omega t + 42.4 \sin 3\omega t + 25.5 \sin 5\omega t + 18.2 \sin 7\omega t + 14.1 \sin 9\omega t$$

(d) In terms of the harmonics , the *rms* value of the output voltage is

$$V_{o(rms)}^{h} = \sqrt{\left(\frac{c_1}{\sqrt{2}}\right)^2 + \left(\frac{c_3}{\sqrt{2}}\right)^2 + \left(\frac{c_5}{\sqrt{2}}\right)^2 + \left(\frac{c_7}{\sqrt{2}}\right)^2 + \left(\frac{c_9}{\sqrt{2}}\right)^2} = 97.94\ V$$

This value is less than $V_{o(rms)}$ since we calculate up to 9th order harmonics only.

(e) To calculate the power we most calculate the *rms* value of the current for each harmonic the amplitude of the nth harmonic current

$$I_n = \frac{c_n}{Z_n}$$

where $Z_n = \sqrt{R^2 + (n\omega L)^2} = R$

$$P_n = I_{n(rms)}^2 R = \left(\frac{I_n}{\sqrt{2}}\right)^2 R$$

n	f_n (Hz)	c_n (V)	Z_n (Ω)	I_n (A)	P_n (W)
1	50	127.3	10	12.73	810
3	150	42.4	10	4.24	89.8
5	250	25.5	10	2.55	32.5
7	350	18.2	10	1.82	16.5
9	450	14.1	10	1.41	9.99

The total power is $\sum P_n = P_1 + P_3 + P_5 + P_7 + P_9 = 958.8$ W

(*f*) The frequency spectrum is given in Fig.8.7 below:

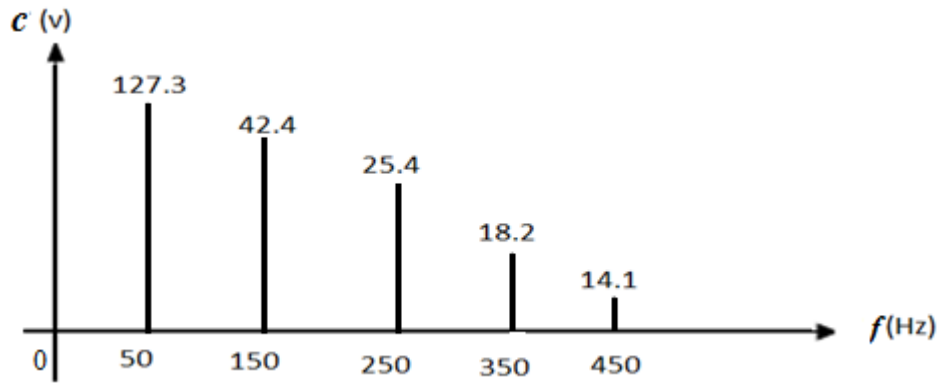

Fig. 8.7 The frequency spectrum of the output voltage waveform.

(*g*) The total harmonic distortion factor

$$THD = \sqrt{\frac{V_{o(rms)}^2 - V_{o1(rms)}^2}{V_{o1(rms)}^2}}$$

$V_{o(rms)} = 100\text{V}$

$V_{o1(rms)} = c_1/\sqrt{2} = 127.3/\sqrt{2} = 90\text{ V}$

$$THD = \sqrt{\frac{100^2 - 90^2}{90^2}} = 0.4843 \rightarrow 48.43\%$$

This is very high *THD* , the practical value of *THD* is about (3-10)% hence we need to use low-pass filter at the output to filter out most of the undesirable harmonic component and to produce nearly sinusoidal output waveform.

8.3 SINGLE-PHASE BRIDGE-TYPE INVERTERS

As it has been stated earlier, the parallel inverter discussed previously has disadvantages in that it uses heavy transformer to carry the load current. Also in the parallel capacitor inverter large amount of energy is trapped in the commutating capacitor which is need to be removed with additional circuit components. These disadvantages may be overcome by using bridge-type inverter which eliminates the need of the magnetic components such as the center-tap transformer or large capacitor. Only semiconductor component are used in this type of inverter.

8.3.1 Single-Phase Half-Bridge Inverter

This type of inverter is very simple in construction. It does not need output transformer like parallel inverter. It sometimes called center-tapped source inverter. The basic configuration of this inverter is shown in Fig 8.8.

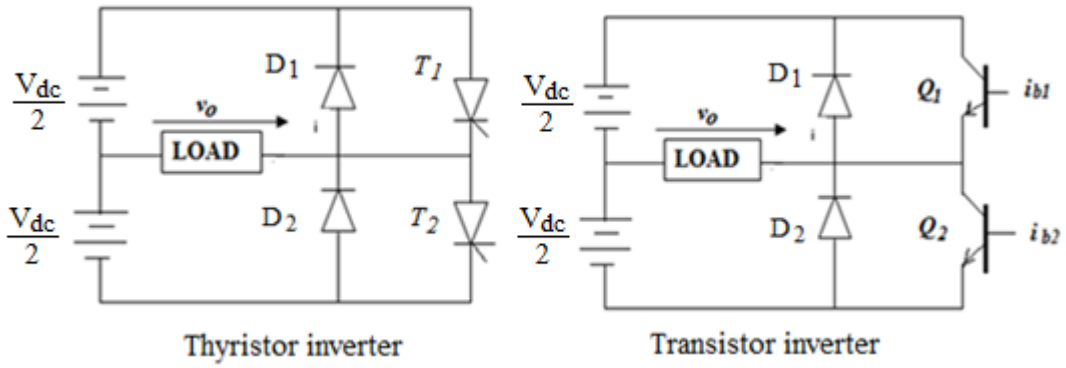

Fig.8.8 Single-phase inverter half-bridge circuit.

The top and bottom switch has to be "complementary" i.e., if the top switch is closed (ON), the bottom must be OFF, and vice-versa. The output voltage waveform is a square wave as that indicated in Fig.8.2. In practice, a dead time between ON and OFF (t_d) for Q_1 & Q_2 is required to avoid short circuit or "shoot-through" faults. This leads to produce quasi-square wave output voltage (Fig.8.9).

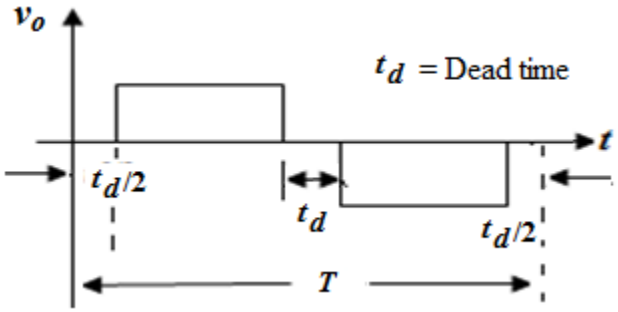

Fig.8.9 Quasi-square output voltage waveform.

Performance of half-bridge inverter with series resistive-inductive loads

If the load is resistive, the output current waveform will be a copy of the voltage waveform as shown in Fig.8.10(a). The output voltage is a square (or quasi-square) wave. However with a series *R-L* load Fig.8.10 (b), the load current *i* is delayed although the output voltage wave is still a square.

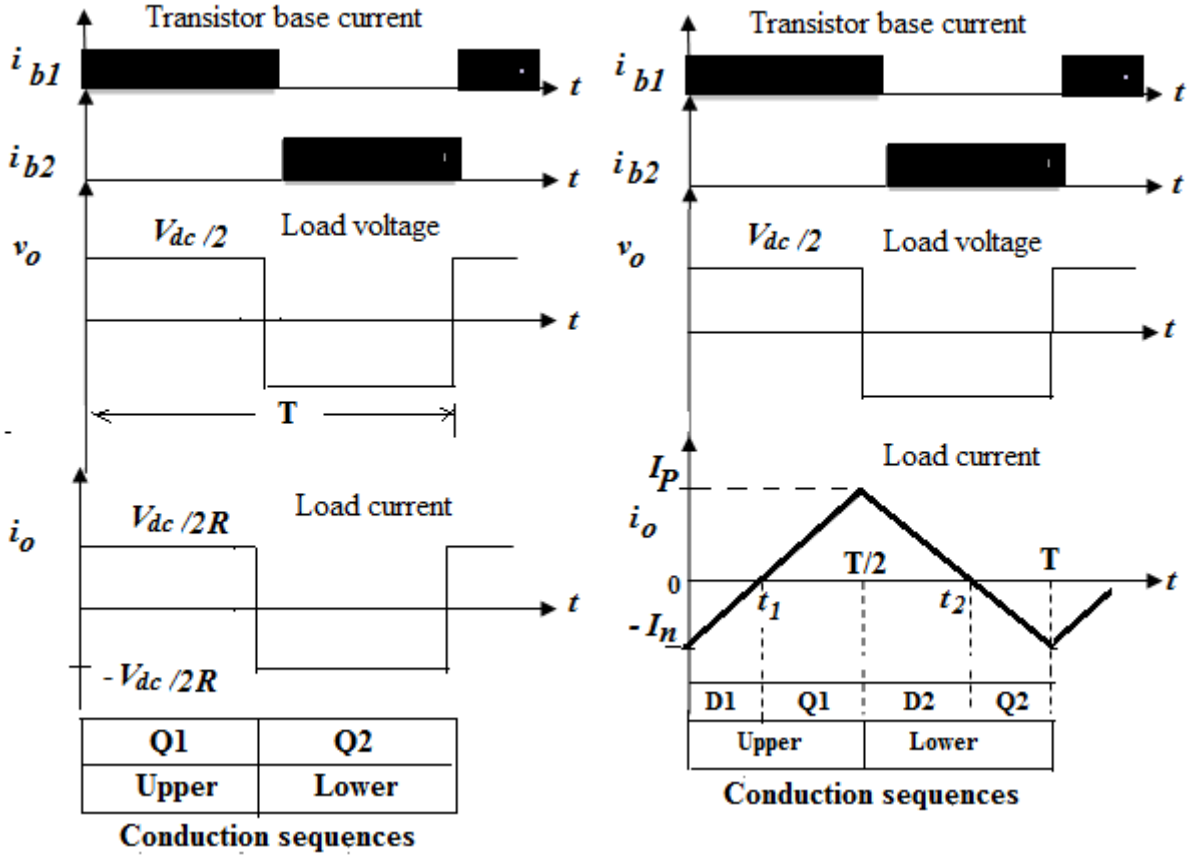

Fig.8.10 Output voltage and current for single-phase half-bridge inverter: (a) Operation with resistive load, (b) Operation with *R-L* load.

In Fig. 8.10(b), Q_1 is applied the driving current i_{b1} from 0 to *T/2*. Since the current is still negative, this cause diode D_1 to conduct from 0 to t_1. The output current i_o increases from $-I_n$ toward zero causing Q_1 to be reversed biased and it does not conduct till D_1 stop conducting at t_1. When Q_1 conducts from t_1 to *T/2*, the output current increases from zero to I_p. Hence, the current i_o will grow exponentially during the positive half-cycle from $-I_n$ to I_p according to the following equation:

$$+\frac{V_{dc}}{2} = Ri + L\frac{di}{dt} \tag{8.18}$$

- Through D_1 [load returning power to the upper half of the source].
- Through Q_1 [load absorbing power from the upper half of the source] until $t = T/2$, whereby $i = I_p$.

At $t = T/2$, Q_1 is turned off and base current drive is applied to Q_2. Negative half cycle starts by conduction of Q_2, but at this instant the current is still positive which cause Q_2 to be reversed bias and D_2 to be forward bias. Current starts to change direction from I_p to zero through D_2 while Q_2 remains off until the it becomes zero at t_2. At this instant Q_2

start to conduct from t_2 to T until i_o = -I_n. The change of current from I_p through D_2 and then to – I_n through Q_2 is governed by the following equation:

$$-\frac{V_{dc}}{2} = Ri + L\frac{di}{dt} \tag{8.19}$$

The *rms* value of the load voltage is

$$V_{o(rms)} = \sqrt{\frac{1}{T}\int_0^T V_o^2 dt} = \left[\frac{1}{T}\left(\frac{V_{dc}}{2}\right)^2 T\right]^{\frac{1}{2}} = \frac{V_{dc}}{2} \tag{8.20}$$

The load voltage $v_o\,(\omega t)$ can be expressed in terms of harmonics by Fourier series as:

$$v_o(\omega t) = \sum_{n=1,3,5}^{\infty} \frac{4}{n\pi}\left(\frac{V_{dc}}{2}\right)\sin n\,\omega t \tag{8.21}$$

Here $v_o(\omega t) = 0$ for n =2,4,6…

where: $\omega = 2\pi f_0$ is the frequency of the output voltage in (rad /sec).

The fundamental component of the load voltage has a peak value of,

$$V_{o1p} = c_1 = \frac{4}{\pi}\,\frac{V_{dc}}{2}$$

and it has *rms* value of

$$V_{o1(rms)} = \frac{c_1}{\sqrt{2}} = \frac{\sqrt{2}}{\pi}V_{dc} = 0.45\,V_{dc} \tag{8.22}$$

For an *R-L* load, the instantaneous load current $i_o(\omega t)$ can be found by dividing the instantaneous output voltage $v_o(\omega t)$ given in Eq.(8.21) by the load harmonic impedance $Z_n = R + jn\omega L$, or

$|Z_n| = \sqrt{R^2 + (n\omega L)^2}$, thus

$$i_o(\omega t) = \frac{v_o(n\omega t)}{|Z_n|}$$

$$i_o(\omega t) = \sum_{n=1,3,5\ldots}^{\infty} \frac{2V_{dc}}{n\pi\sqrt{R^2 + (n\omega L)^2}}\sin(n\omega t - \psi_n) \tag{8.23}$$

where ,

$$\psi_n = tan^{-1}\frac{n\omega L}{R}$$

or $$i_o(\omega t) = \sum_{n=1,3,5\ldots}^{\infty} c_n \sin(n\omega t - \psi_n)$$

If I_{o1} is the *rms* fundamental load current, $c_1 / \sqrt{2}$, then the fundamental output power (for n = 1) is

$$P_1 = V_{o1} I_{o1} cos\psi_1 = I_{o1}^2 R = \left[\frac{2V_{dc}}{\sqrt{2}\pi\sqrt{R^2 + (\omega L)^2}}\right]^2 \times R \qquad (8.24)$$

Note: In most applications (e.g. electric motor drives) the output power due to the fundamental current is generally the useful power, and the power due to harmonic currents is dissipated as heat and increases the load temperature.

Example 8.2

The single-phase half-bridge transistor inverter shown in Fig.8.8 has a resistive load of $R = 3\Omega$ and the d.c. input voltage $V_{dc} = 60$ V. Determine:

(a) The *rms* value of the output voltage.
(b) The *rms* value of the load voltage at the fundamental frequency $V_{o1(rms)}$.
(c) The output power.
(d) The average and peak current of each transistor.
(e) The peak reverse blocking voltage V_{BR} of each transistor.
(f) The total harmonic distortion factor.

Solution

(a) The *rms* value of the output voltage is

$$V_{o(rms)} = \sqrt{\frac{1}{T}\int_0^T V_o^2 dt} = \left[\frac{1}{T}\left(\frac{V_{dc}}{2}\right)^2 T\right]^{\frac{1}{2}} = \frac{V_{dc}}{2} = \frac{60}{2} = 30 \text{ V}$$

(b) The *rms* value of the load voltage at the fundamental frequency is

$$V_{o1(rms)} = \frac{c_1}{\sqrt{2}} = \frac{\sqrt{2}}{\pi} V_{dc} = 0.45\, V_{dc} = 0.45 \times 60 = 27 \text{ V}$$

(c) The output power is

$$P_o = \frac{V_{o1(rms)}{}^2}{R} = \frac{30^2}{3} = 300 \text{ W}$$

(d) The average and peak current of each transistor are

$$I_P = \frac{V_{o(rms)}}{R} = \frac{30}{3} = 10 \text{ A}$$

Because each transistor conducts for a 50% duty cycle, the average current of each transistor is

$$I_{av} = 10 \times 0.5 = 5 \text{ A}$$

(e) The peak reverse blocking voltage V_{BR} of each transistor is

$$V_{BR} = 2 \times 30 = 60 \text{ V}$$

(f) The total harmonic distortion factor is

$$THD = \sqrt{\frac{V_{o(rms)}^2 - V_{o1(rms)}^2}{V_{o1(rms)}^2}} = \sqrt{\frac{30^2 - 27^2}{27^2}} = 0.4843$$

8.3.2 Single-Phase Full-Bridge Inverter

The single-phase half-bridge Inverter discussed in the previous sub-section although it has the advantage that it uses only two semiconductor switches, but it has the distinct disadvantage in that it needs a center-tap d.c. supply. However, this problem can be solved using full-bridge inverter shown in Fig. 8.11.

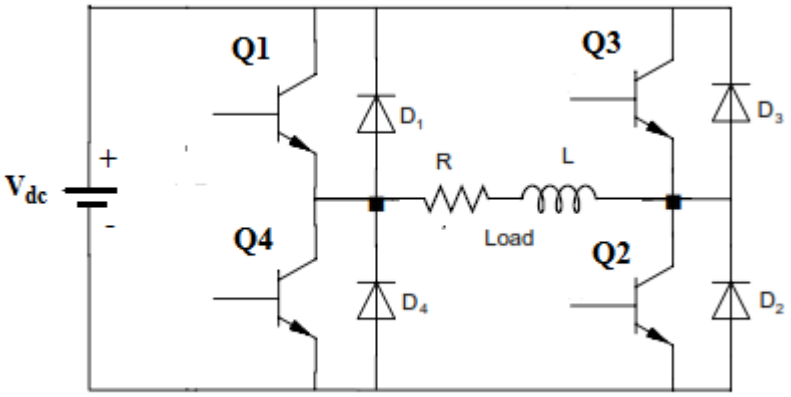

Fig.8.11 Single-phase full-bridge inverter circuit.

The single-phase full-bridge inverter uses four BJT transistors in its operation. Practically, this inverter is constructed from two half-bridge inverter using single d.c. source V_{dc} and the load is connected between the centers of the two legs. The four diodes shown in Fig.8.11 are used for feedback when the load is inductive.

Operation with resistive load

When the load is resistive, the operation of the inverter can be described as follows: Output voltage is a square wave and the current is replica of the voltage shape. In this circuit, Q_1 and Q_2 are triggered simultaneously and so are Q_3 and Q_4. Each device is made to conduct for half-time of the output cycle, the load voltage waveform with the

transistor base currents are shown in Fig 8.12. The output voltage is a square-wave and the current is replica of the voltage shape.

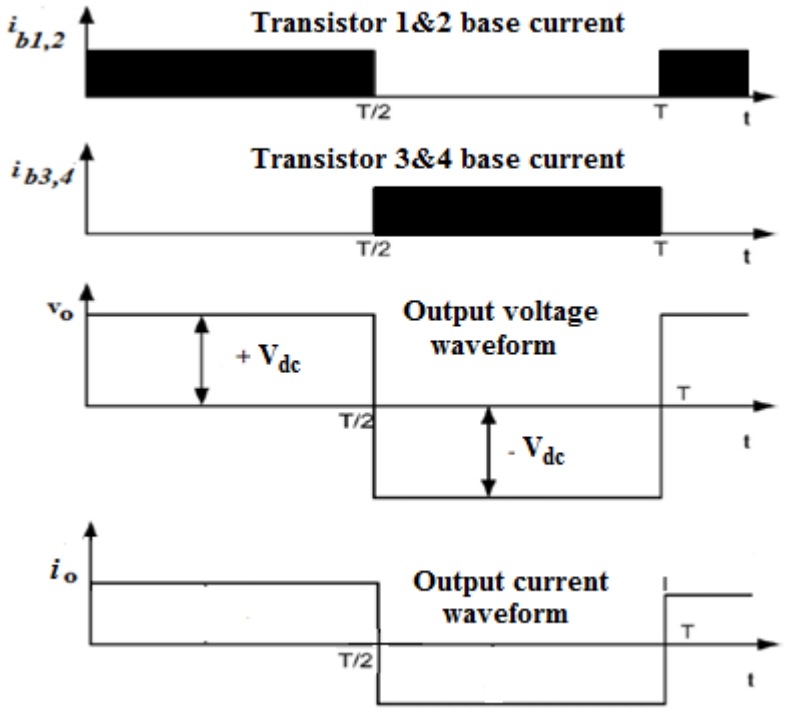

Fig.8.12 Operation of the full-bridge inverter with resistive load.

Operation with resistive-inductive load

With resistive-inductive load, the current i_0 lags the square-wave output voltage v_0 as shown in Fig.8.13. The operation of the inverter in this case can be explained as follows :

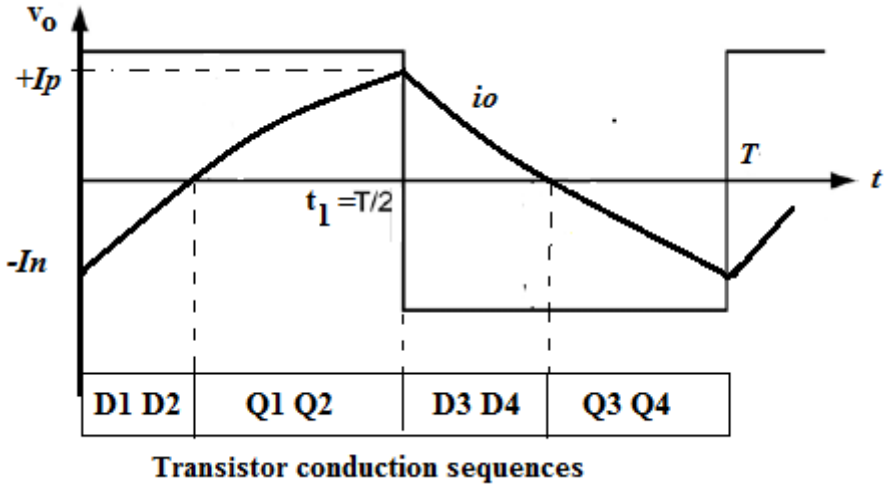

Fig.8.13 Current through a single-phase full-bridge inverter.

- Triggering Q_1 & Q_2 connects the load to V_d . For steady load condition, i_0 grows exponentially through D1& D2 and then through Q_1&Q_2 from $-I_n$ to I_p according to $(V_{dc} = Ri + L\frac{di}{dt})$.
- Triggering Q_1&Q_2 connects the load to V_d. For steady load condition, i_0 grows exponentially through D_1&D_2 and then through Q_1&Q_2 from $-I_n$ to I_p according to $(V_{dc} = Ri + L\frac{di}{dt})$.
- When diodes D_1&D_2 are conducting, the energy fed back to the source, thus they are known as feedback diodes.
- Negative half-cycle starts by triggering Q_3&Q_4 at $t_1 = \frac{T}{2}$, and Q_1&Q_2 goes off when $i_{b1} = i_{b2} = 0$ (base current blocking).
- Load voltage reverses to $-V_{dc}$ and i_o will flow through D_3&D_4 and then through Q_3&Q_4 according to the equation ($-V_d = Ri + L\frac{di}{dt}$). At the end of negative-half cycle $i_o = -I_n$.

Note that:

$$t_1 = \frac{T}{2} = \frac{1}{2f} = \frac{1}{2}\left(\frac{2\pi}{\omega}\right) = \frac{\pi}{\omega}$$

Load *rms* voltage is

$$V_{o(rms)} = \left[\frac{1}{t_1}\int_0^{t_1} V_d^2 dt\right]^{\frac{1}{2}} = V_{dc} \qquad (8.25)$$

Load voltage $v_o(\omega t)$ may be expressed as:

$$v_o(\omega t) = \sum_{n=1,3,5,..}^{\infty} \frac{4V_{dc}}{n\pi} sinn\omega t \qquad (8.26)$$

The peak value of the fundamental component (n=1) of the load voltage is,

$$V_{o1p} = \frac{4}{\pi}V_{dc} \qquad (8.27)$$

The *rms* value of the fundamental component is

$$V_{o1(rms)} = \frac{4V_{dc}}{\sqrt{2}\pi} = 0.9\,V_{dc} \qquad (8.28)$$

Load *rms* current and power can be determine from

$$I_{orms} = \left[\frac{2}{T}\int_0^{T/2} i_o^2 dt\right]^{\frac{1}{2}} \tag{8.29}$$

$$P = \frac{2}{T}\int_0^{T/2} v_o . i_o \, dt \tag{8.30}$$

where the instantaneous value of the load current i_o for an *R-L* load is

$$i_o(\omega t) = \sum_{n=1,3,5}^{\infty} \frac{4V_{dc}}{n\pi\sqrt{R^2 + (n\omega L)^2}} \sin(n\omega t - \psi_n) \tag{8.31}$$

The angle ψ_n by which the load current lags the load voltage is

$$\psi_n = tan^{-1}\frac{n\omega L}{R}$$

The total harmonic distortion factor is,

$$THD = \sqrt{\frac{V_{o(rms)}^2 - V_{o1(rms)}^2}{V_{o1(rms)}^2}}$$

Example 8.3

For the single-phase MOSFET bridge inverter circuit shown in Fig. 8.14, the source V_{dc} =125 V, load resistance R =10 Ω and output voltage frequency f_o = 50 Hz.

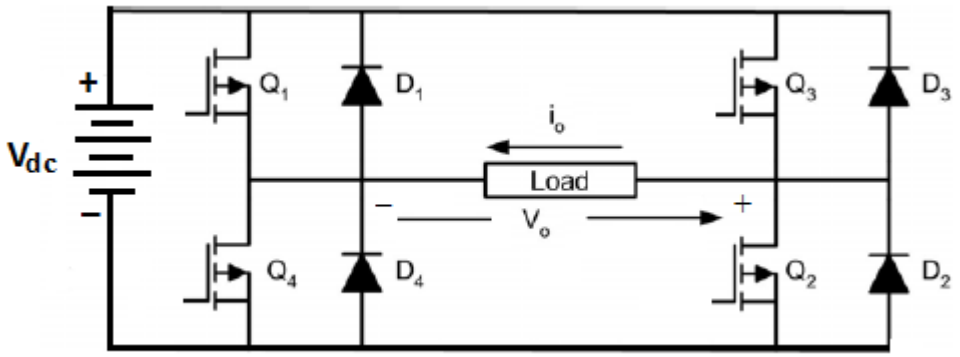

Fig.8.14 Single-phase full-bridge inverter.

(a) Draw the output voltage and load current waveforms.
(b) Derive the *rms* value of the output voltage waveform and hence calculate the output power P_o in terms of the output voltage.
(c) Analyse the amplitude of the Fourier series terms of the output voltage waveform by considering up to the 7th order harmonic. Determine the value of the *rms* output voltage in terms of harmonics *rms* values.
(d) Calculate the average and peak currents of each transistor.
(e) Estimate the total harmonic distortion factor *THD* of the circuit.

Solution

(a) The waveforms of the output voltage and current are depicted in Fig.8.15 as:

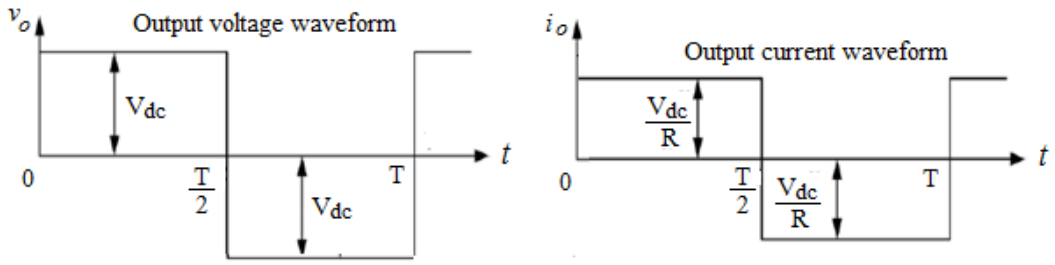

Fig.8.15 Output voltage and current waveforms.

(b) The *rms* value of the output voltage is found from Eq.(8.25) as follows:

$$V_{o(rms)} = \left[\frac{1}{t_1}\int_0^{t_1} V_{dc}^2 dt\right]^{\frac{1}{2}} = V_{dc} = 125\ \text{V}$$

$$P_o = \frac{V_{o(rms)}^2}{R} = \frac{125^2}{10} = 1562.5\ \text{W}$$

(c) The Fourier series of the output voltage is found from Eq.(7.26) as

$$v_o(\omega t) = \sum_{n=1,3,5,..}^{\infty} c_n sinn\omega t$$

The amplitude c_n of the n^{th} harmonic is:

$$c_n = \frac{4V_{dc}}{n\pi} = \frac{4 \times 125}{n\pi} = \frac{159.12}{n}$$

$$v_o(\omega t) = c_1 \sin \omega t + c_3 \sin 3\omega t + c_5 \sin 5\omega t + c_7 \sin 7\omega t$$

$$= \frac{159.12}{1} \sin \omega t + \frac{159.12}{3} \sin 3\omega t + \frac{159.12}{5} \sin 5\omega t + \frac{159.12}{7} \sin 7\omega t$$

Hence the output voltage Fourier representation is,

$$v_o(\omega t) = 159.12 \sin \omega t + 53.04 \sin 3\omega t + 31.82 \sin 5\omega t + 22.73 \sin 7\omega t$$

In terms of the harmonics:

$$V_{o(rms)}^{h} = \sqrt{\left(\frac{c_1}{\sqrt{2}}\right)^2 + \left(\frac{c_3}{\sqrt{2}}\right)^2 + \left(\frac{c_5}{\sqrt{2}}\right)^2 + \left(\frac{c_7}{\sqrt{2}}\right)^2 + \left(\frac{c_9}{\sqrt{2}}\right)^2} = 121.7 \text{ V}$$

This value is less than $V_{o(rms)}$ since we calculate up to 7th order harmonics only.

(d) Since the duty cycle of each transistor is 0.5, the current waveform is as shown in Fig.8.16.

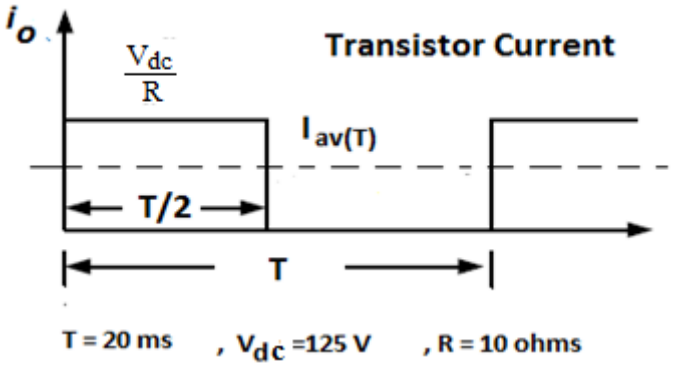

Fig.8.16 Transistor current waveform.

$$I_{av(T)} = \frac{1}{T} \int_0^{1/T} \frac{V_{dc}}{R}\, dt = \frac{V_{dc}}{R} \left[\frac{1}{T} \times \frac{T}{2}\right] = \frac{V_{dc}}{2R} = \frac{125}{20} = 6.25 \text{ A}$$

Peak current

$$\frac{V_{dc}}{R} = \frac{125}{10} = 12.5 \text{ A}$$

(e) The total harmonic distortion factor:

$V_{o1(rms)} = c_1/\sqrt{2} = 159.12/\sqrt{2} = 112.6$ V

$$THD = \sqrt{\frac{V_{o(rms)}^2 - V_{o1(rms)}^2}{V_{o1(rms)}^2}} = \sqrt{\frac{125^2 - 112.6^2}{112.6^2}} = 0.4843$$

Example8.4

For the single-phase full-bridge, transistor inverter shown in Fig.8.14 of the previous example, V_{dc} =100 V, load is a series resistance-inductance with R=10 Ω, and L = 25 mH and the output frequency is 50 Hz. It is required to analyse the circuit by determining: (a)The amplitudes of the Fourier series terms for the output voltage wave up to the 9th order harmonics, (b)The amplitudes of the Fourier series terms for the load current wave up to the 9th order harmonics, (c) The power absorbed by the load in terms of harmonics, (d) Compute the total harmonic distortion factor (THD).

Solution

(a) From Eq.(8.5) ,the Fourier series of the output voltage is

$$v_o(\omega t) = \sum_{n=1,3,5,..}^{\infty} \frac{4V_{dc}}{n\pi} sinn\omega t$$

The amplitude of the n th order harmonic c_n is:

$$c_n = 4V_{dc} / 2\pi = (4x100) / n\pi = 127.3 / n$$

$$v_o(\omega t) = c_1 \sin\omega t + c_2 \sin 3\omega t + c_5 \sin 5\omega t + c_7 \sin 7\omega t + c_9 \sin 9\omega t$$
$$= (127.3/1) \sin\omega t + (127.3/3) \sin 3\omega t + (127.3/5) \sin 5\omega t + (127.3/7) \sin 7\omega t + (127.3/9) \sin 9\omega t$$

Hence the output voltage Fourier representation is,

$$v_o(\omega t) = 127.3 \sin \omega t + 42.4 \sin 3\omega t + 25.5 \sin 5\omega t + 18.2 \sin 7\omega t + 14.1 \sin 9\omega t.$$

(b) From Eq.(8.31) , the Fourier series for the current is ,

$$i_o(\omega t) = \sum_{n=1,3,5}^{\infty} \frac{4V_{dc}}{n\pi\sqrt{R^2 + (n\omega L)^2}} \sin(n\omega t - \psi_n)$$

$$= \sum_{n=1,3,5}^{\infty} \frac{c_n}{Z_n} \sin(n\omega t - \psi_n) = \sum_{n=1,3,5}^{\infty} I_n \sin(n\omega t - \psi_n)$$

where

$$|Z_n| = \sqrt{R^2 + (n\omega L)^2} \quad , \quad I_n = \frac{c_n}{Z_n} \quad \text{, and} \quad \psi_n = tan^{-1}\frac{n\omega L}{R}$$

Calculating I_n from the above equation yields,

$$i_o(\omega t) = 9.29 \sin(\omega t - 43.25^\circ) + 1.42 \sin(3\omega t - 70.52^\circ) + 0.53 \sin(5\omega t - 78.02^\circ) + 0.25 \sin(7\omega t - 81.37^\circ) + 0.17 (\sin 9\omega t - 83.27^\circ).$$

(c) To calculate the power, the *rms* value of the current for each harmonic must be calculated, hence the power P_n of the nth harmonic is

$$P_n = I_{n(rms)}^2 R = \left(\frac{I_n}{\sqrt{2}}\right)^2 R$$

n	f_n (Hz)	c_n (V)	Z_n (Ω)	I_n (A)	P_n (W)
1	60	127.3	13.73	9.29	431
3	180	42.4	30.0	1.42	10
5	300	25.5	48.2	0.53	1.4
7	420	18.2	66.7	0.25	0.34
9	540	14.1	85.4	0.17	0.14

The total power is $\sum P_n = P_1 + P_3 + P_5 + P_7 + P_9 = 443$ W

(d) The total harmonic distortion factor

$$V_{o(rms)} = \sqrt{\frac{1}{T/2}\int_0^{T/2} V_{dc}\, dt} = V_{dc} = 100 \text{ V}$$

$V_{o1(rms)} = c_1/\sqrt{2} = 127.3/\sqrt{2} = 90$ V

$$\therefore \quad THD = \sqrt{\frac{V_{o(rms)}^2 - V_{o1(rms)}^2}{V_{o1(rms)}^2}} = \sqrt{\frac{100^2 - 90^2}{90^2}} = 0.4843$$

or $THD = 48.43\ \%$

8.4 THREE-PHASE INVERTER

In high-power applications, three-phase inverters are normally used. Moreover when three-phase voltage source required from a d.c. source three-phase inverter is needed. However, a three-phase inverter can be constructed using three single-phase parallel inverters which are connected in parallel as shown in Fig.8.17. The gate signals of single-phase inverters should be advanced or delayed by 120^0 with respect to each other in order to obtain three-phase balanced (fundamental) voltages. The transformer secondary windings may be connected in wye or delta whereas the primary windings must be isolated from each other.

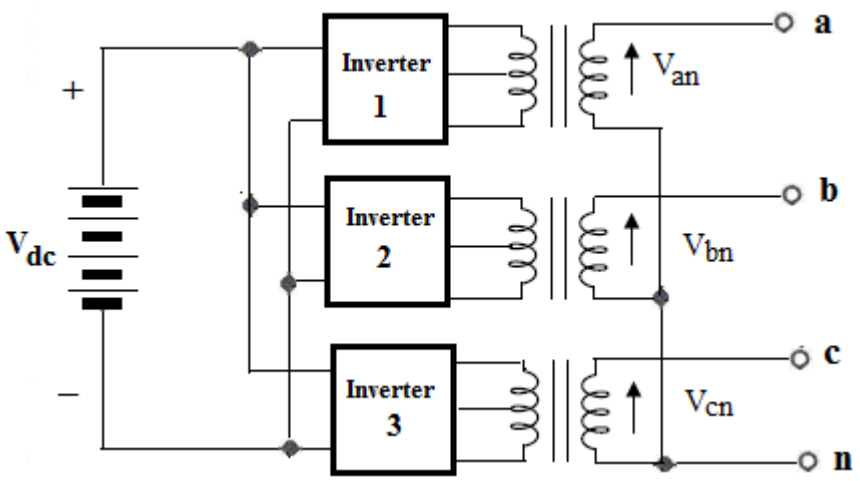

Fig.8.17 Schematic diagram of a three-phase inverter constructed from three single-phase parallel inverters.

Three single-phase half-bridge inverters can be connected as shown in Fig.8.18 to form a configuration of three-phase bridge inverter. In this circuit, there are six BJTs, Q_1, Q_2, Q_3, Q_4, Q_5, and Q_6. Also, there are six diodes connected across each transistor as shown in the figure. Observe that the upper transistors are numbered as Q_1, Q_3, and Q_5. Similarly, the lower transistors are numbered as Q_2, Q_4, and Q_6. Here, Q_1 and Q_4 are connected to phase-a. When Q_1 conducts, phase-a is connected to $+V_{dc}$ and when Q_4 conducts, phase-a is connected to $-V_{dc}$. Similarly, Q_3 and Q_6

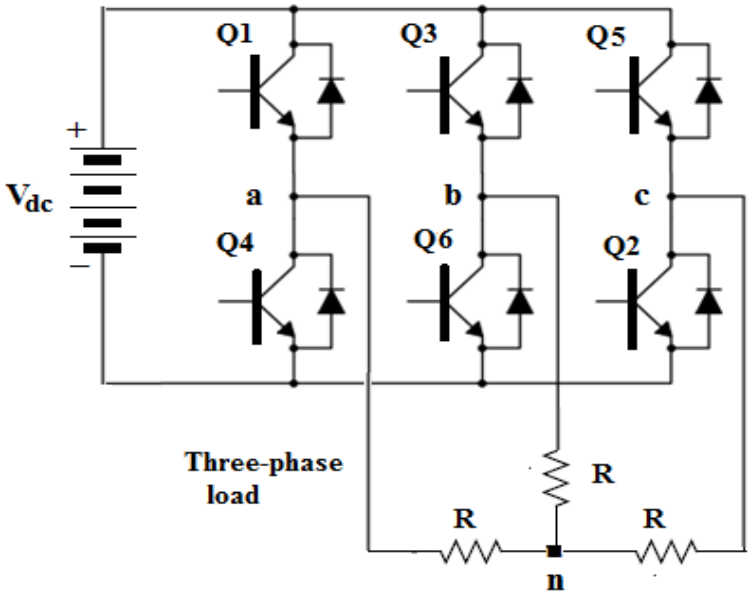

Fig.8.18 Three-phase bridge inverter circuit diagram with star-connected *R*-load.

are connected to phase-b and Q_5 and Q_2 are connected to phase-c.

In practice, for the three-phase bridge inverter there are two types of conduction depending on the control signal used to drive the six transistors with 120˚ or 180˚ conduction. Referring to Fig.8.18 : in 120˚, each BJT transistor conducts for 120˚ and in 180˚, each BJT transistor conducts for 180˚ as it will be described in the following subsection.

8.4.1 120 – Degree Conduction

In this type of control, only two transistors conduct at the same time such that each transistor conducts for 120˚ and remains OFF for 240˚. This means that only two transistors remain "ON" at any instant of time. The per-phase and line-to-line voltage waveforms for this type of operation are shown in Fig.8.19.

The conduction sequence of the transistors is : 1,6-1,2-2,3-3,4-4,5-1,6-1,2-2,3. For star-connected load, three modes for three-phase bridge inverter operation exist. In each case, the effective resistance across the source is 2*R* as shown in Fig.8.20.

- During mode-1 for $0 \leq \omega t \leq \pi/3$ transistor 1and 6 conduct:

$$v_{an} = +\frac{V_{dc}}{2} \quad , \quad v_{bn} = -\frac{V_{dc}}{2} \quad , \quad v_{cn} = 0 \quad , \quad v_{ab} = V_{dc}$$

- During mode-2 for $\pi/3 \leq \omega t \leq 2\pi/3$ transistor 1and 2 conduct:

$$v_{an} = +\frac{V_{dc}}{2} \quad , \quad v_{bn} = 0 \quad , \quad v_{cn} = -\frac{V_{dc}}{2}$$

- During mode-3 for $2\pi/3 \leq \omega t \leq \pi$ transistor 3 and 2 conduct:

$$v_{an} = 0 \quad , \quad v_{bn} = +\frac{V_{dc}}{2} \quad , \quad v_{cn} = -\frac{V_{dc}}{2}$$

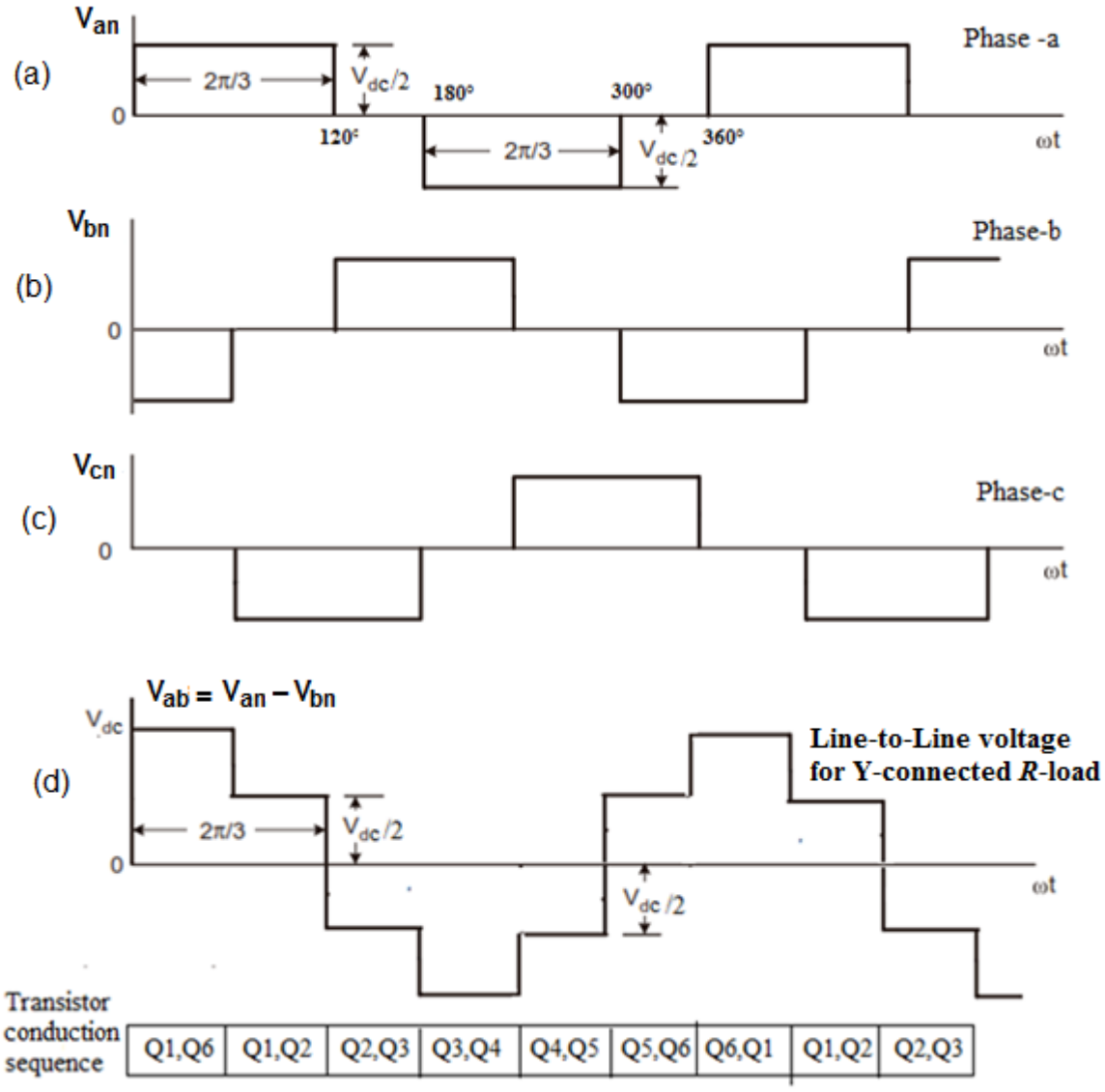

Fig.8.19 Voltage waveforms when two transistor in 120˚conduction.

It should be noted from Fig.8.20 that the phase voltage is a quasi-square waveform. It has peak value of $\pm\frac{V_{dc}}{2}$. They are shifted by 120˚ with respect to each other. The output line to line voltage is a six-step waveform, it has peak value of $\pm V_{dc}$.

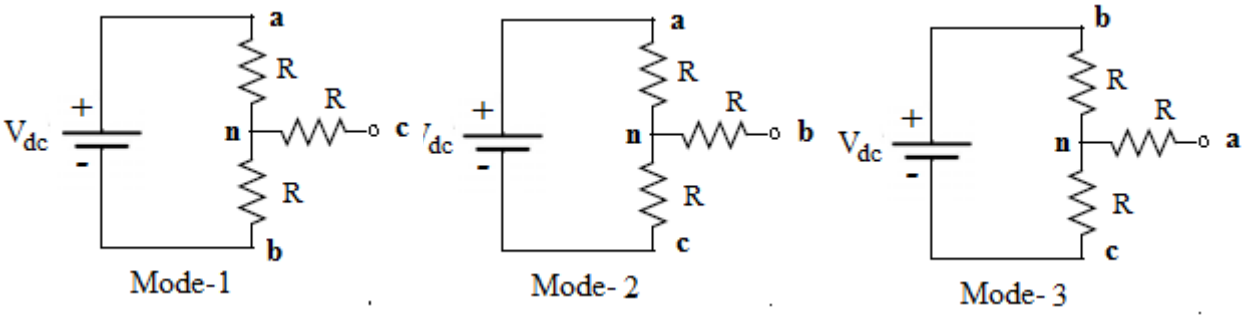

Fig.8.20 Equivalent circuits for the three modes of operation for 120˚ conduction for the three-phase bridge inverter.

Mathematical analysis of 120˚ Mode inverter

The *rms* value of the output voltage waveform of 120˚ mode inverter shown in Fig.8.19 for phase-a can be obtain as,

$$V_{a(rms)} = \frac{1}{2\pi}\int_0^{2\pi} v_a^2 \; d\omega t$$

$$= \frac{1}{2\pi}\sqrt{\int_0^{2\pi/3} (\frac{V_{dc}}{2})^2 \; d\omega t} + \frac{1}{2\pi}\sqrt{\int_{\pi}^{5\pi/3} (-\frac{V_{dc}}{2})^2 \; d\omega t}$$

$$\therefore \quad V_{a(rms)} = \frac{V_{dc}}{2}\sqrt{\frac{2}{3}} = \frac{V_{dc}}{\sqrt{6}} \qquad (8.32)$$

The line-to-line voltages for star-connected load can be found as:

$$V_{L-L} = \sqrt{3}\, V_{phase} = \sqrt{3} \times \frac{V_{dc}}{\sqrt{6}} = \frac{V_{dc}}{\sqrt{2}} \qquad (8.33)$$

The line-to-neutral voltages shown in Fig.8.19 (a) to (c) can be expressed in Fourier series as:

$$V_{an}\,(\omega t) = \sum_{n=1,3,5}^{\infty} \frac{2V_{dc}}{n\pi} \sin\frac{n\pi}{2} \sin\frac{n\pi}{3} \sin n\left(\omega t + \frac{\pi}{6}\right) \qquad (8.34a)$$

$$V_{bn}\,(\omega t) = \sum_{n=1,3,5}^{\infty} \frac{2V_{dc}}{n\pi} \sin\frac{n\pi}{2} sin\frac{n\pi}{3} \sin n\left(\omega t - \frac{\pi}{2}\right) \qquad (8.34b)$$

$$V_{cn}\,(\omega t) = \sum_{n=1,3,5}^{\infty} \frac{2V_{dc}}{n\pi} \sin\frac{n\pi}{2} sin\frac{n\pi}{3} \sin n\left(\omega t - \frac{7\pi}{6}\right) \qquad (8.34c)$$

The peak amplitude of the fundamental component (n=1): for phase a, b or c is:

$$V_{L1P} = \frac{2}{\pi} V_{dc} \sin\frac{\pi}{3} = \sqrt{3}\,\frac{V_{dc}}{\pi} \tag{8.35}$$

The *rms* value of the fundamental component is

$$V_{L1(rms)} = \frac{V_{1P}}{\sqrt{2}} = \sqrt{\frac{3}{2}} \times \frac{V_{dc}}{\pi} \tag{8.36}$$

The line-to-line voltage waveform shown in Fig.8.19(d) is $v_{ab} = \sqrt{3}v_{an}$ with phase lead of 30˚ can be expressed in Fourier series as:

$$V_{ab}\,(\omega t) = \sum_{n=1,3,5}^{\infty} \frac{2\sqrt{3}V_{dc}}{n\pi} \sin\frac{n\pi}{2} \sin\frac{n\pi}{3} \sin[n\,(\omega t + \frac{\pi}{6}) \pm \frac{\pi}{6}] \quad (8.37a)$$

Similarly for the other line voltages v_{bc} and v_{ca} , the Fourier representation are

$$V_{bc}\,(\omega t) = \sum_{n=1,3,5}^{\infty} \frac{2\sqrt{3}V_{dc}}{n\pi} \sin\frac{n\pi}{2} sin\frac{n\pi}{3} \sin[n\,\left(\omega t - \frac{\pi}{2}\right) \pm \frac{\pi}{6}] \; (8.37b)$$

$$V_{ca}\,(\omega t) = \sum_{n=1,3,5}^{\infty} \frac{2\sqrt{3}V_{dc}}{n\pi} \sin\frac{n\pi}{2} sin\frac{n\pi}{3} \sin[n\,\left(\omega t - \frac{7\pi}{6}\right) \pm \frac{\pi}{6}] \; (8.37c)$$

where $+\frac{\pi}{6}$ for positive sequence harmonic components (n=1,7,13,19,……) and $-\frac{\pi}{6}$ for negative sequence harmonic components (n=5,11,17,23,……).

8.4.2 180 –Degree Conduction

In this mode of operation of the three-phase inverter, three transistors remain on at any instant of time. The base current drive of Q_1, in Fig.8.18, is applied for 180˚ (half-cycle) and is off for the remaining 180˚ (next half-cycle). Base current drive of Q_2 is applied with 60˚ delay with respect to Q_1. Hence for half a cycle, the following modes are presented for star-connected load:

- During mode-1 for $0 \leq \omega t \leq \pi/3$, transistor 1,5 and 6 conduct, the equivalent circuit is shown in Fig.8.21 (a).

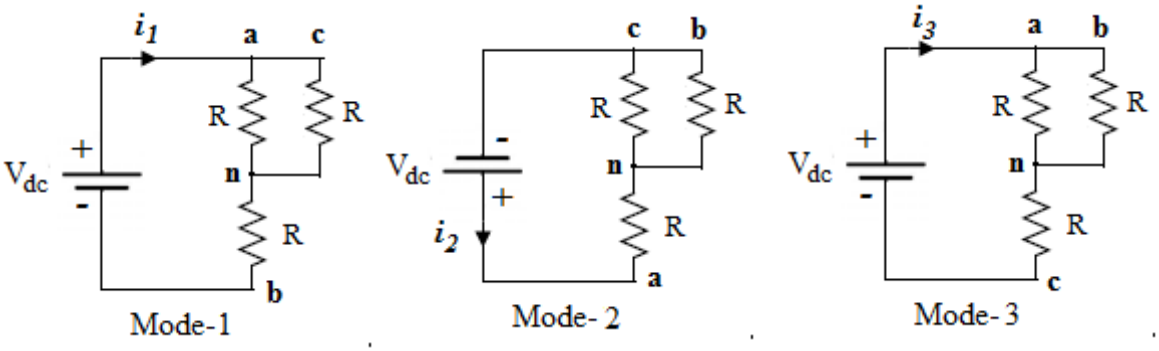

(a) (b) (c)

Fig. 8.21 Equivalent circuits for the three modes of operation for 180˚ conduction.

$$R_{eq} = R + \frac{R}{2} = \frac{3R}{2}$$

$$v_{an} = v_{cn} = +\frac{V_{dc}}{3}$$

$$i_1 = \frac{V_{dc}}{R_{eq}} = \frac{2V_{dc}}{3R}$$

$$v_{bn} = -i_1 R = -\frac{2V_{dc}}{3}$$

- During mode-2 for $\pi/3 \leq \omega t \leq 2\pi/3$, transistor 1,2 and 6 conduct: Equivalent circuit is shown in Fig.8.21 (b).

$$R_{eq} = R + \frac{R}{2} = \frac{3R}{2}$$

$$i_2 = \frac{V_{dc}}{R_{eq}} = \frac{2V_{dc}}{3R}$$

$$v_{an} = i_2 R = \frac{2V_{dc}}{3}$$

$$v_{bn} = v_{cn} = \frac{-i_1 R}{2} = -\frac{V_{dc}}{3}$$

- During mode-3 for $2\pi/3 \leq \omega t \leq \pi$, transistor 1, 3 and 2 conduct: Equivalent circuit is shown in Fig.8.21 (c).

$$R_{eq} = R + \frac{R}{2} = \frac{3R}{2} \quad \Rightarrow \quad i_3 = \frac{V_{dc}}{R_{eq}} = \frac{2V_{dc}}{3R}$$

$$v_{an} = v_{bn} = i_3 \times \frac{R}{2} = \frac{V_{dc}}{3} \quad \text{and} \quad v_{cn} = -i_3 R = -\frac{2V_{dc}}{3}$$

Waveforms for the transistors base currents and load phase voltage and current for *R*-load are shown in Fig.8.22 for 180-degree conduction. The line-to-neural voltage and line current waveform, in case of resistive load, will be replica of the phase voltage waveform as shown in Fig.8.22(e). However, if the load is inductive, the phase current through each load branch would be delayed to its phase voltage as shown in Fig.8.22(f).

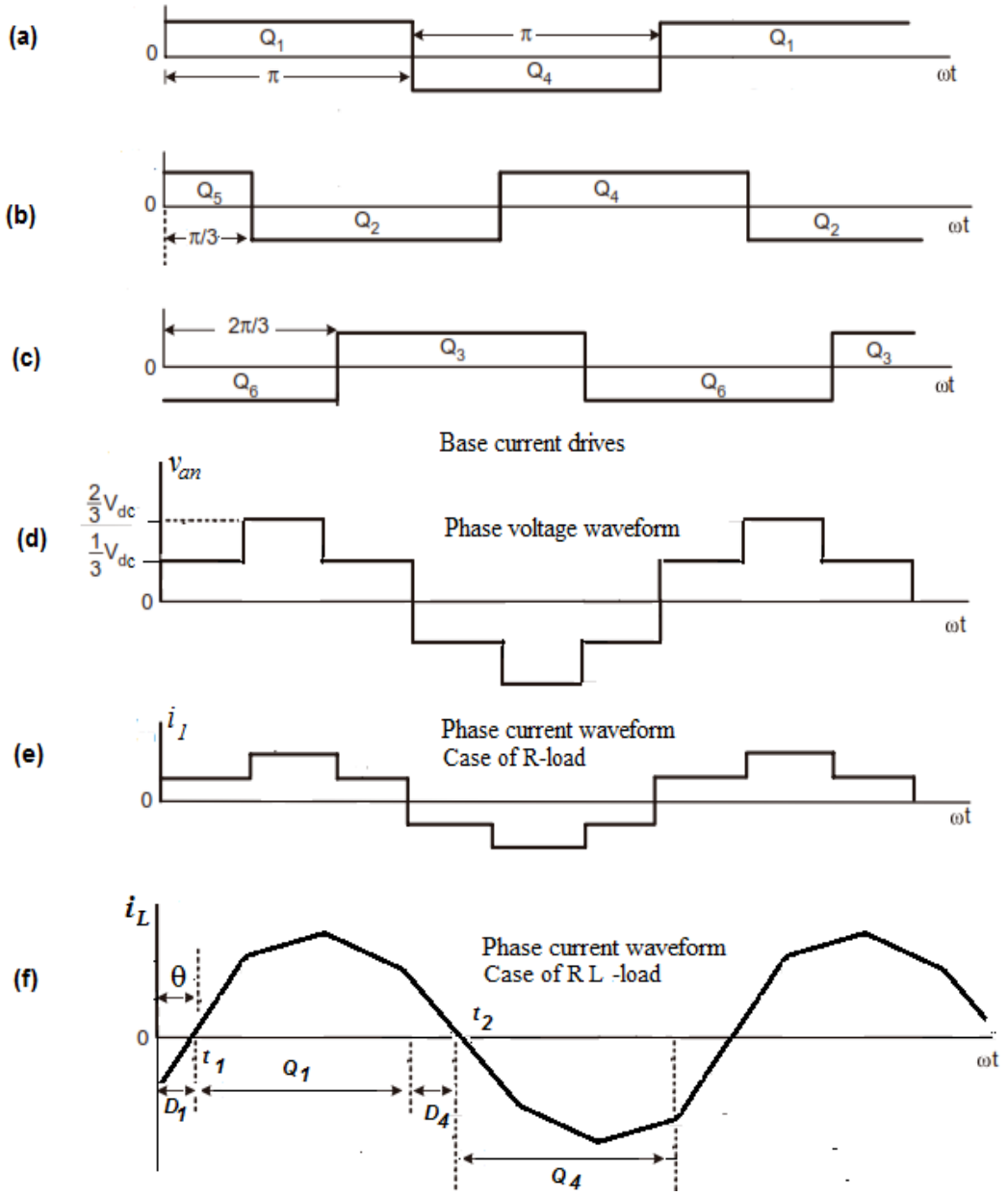

Fig.8.22 Line-to-neural voltage and line current waveforms for 180˚ conduction, case of *R*-load and phase current, (f) in case of *R*-*L* load.

Fourier representation of the phase and line voltages

The line-to-neutral voltage waveform shown in Fig.8.22(d) can be expressed in Fourier series, which is given in many reference and text books for the three phases a, b and c as,

$$v_{an}(\omega t) = \sum_{n=1,3,5}^{\infty} \frac{4V_{dc}}{\sqrt{3}n\pi} \sin\frac{n\pi}{2} \sin\frac{n\pi}{3} \sin[n\left(\omega t + \frac{\pi}{6}\right) \mp \frac{\pi}{6}] \quad (8.38a)$$

$$v_{bn}(\omega t) = \sum_{n=1,3,5}^{\infty} \frac{4V_{dc}}{\sqrt{3}n\pi} \sin\frac{n\pi}{2} sin\frac{n\pi}{3} \sin[n\left(\omega t - \frac{\pi}{2}\right) \mp \frac{\pi}{6}] \quad (8.38b)$$

$$v_{cn}(\omega t) = \sum_{n=1,3,5}^{\infty} \frac{4V_{dc}}{\sqrt{3}n\pi} \sin\frac{n\pi}{2} sin\frac{n\pi}{3} \sin[n\left(\omega t - \frac{7\pi}{6}\right) \mp \frac{\pi}{6}] \quad (8.38c)$$

where : $-\frac{\pi}{6}$ for positive sequence harmonic components (n=1,7,13,19,…) and $+\frac{\pi}{6}$ for negative sequence harmonic components (n=5,11,17,23,…) with respect to the line to line voltage v_{ab} .

For Y-connected load, the line to line voltage is $v_{ab} = \sqrt{3}\ v_{an}$ without $\mp\frac{\pi}{6}$ delay angle, hence the three line-to-line voltages are given by

$$v_{ab}(\omega t) = \sum_{n=1,3,5}^{\infty} \frac{4V_{dc}}{n\pi} \sin\frac{n\pi}{2} \sin\frac{n\pi}{3} \sin n\left(\omega t + \frac{\pi}{6}\right) \quad (8.39a)$$

$$v_{bc}(\omega t) = \sum_{n=1,3,5}^{\infty} \frac{4V_{dc}}{n\pi} \sin\frac{n\pi}{2} sin\frac{n\pi}{3} \sin n\left(\omega t - \frac{\pi}{2}\right) \quad (8.39b)$$

$$v_{ca}(\omega t) = \sum_{n=1,3,5}^{\infty} \frac{4V_{dc}}{n\pi} \sin\frac{n\pi}{2} sin\frac{n\pi}{3} \sin n\left(\omega t - \frac{7\pi}{6}\right) \quad (8.39c)$$

The line current i_L in phase-a for an *R-L* load is obtained by dividing the phase voltage v_{an} in by the load impedance, $Z=R+jn\omega L$

$$i_a(\omega t) = \sum_{n=1,3,5}^{\infty} I_n \sin[n\left(\omega t + \frac{\pi}{6}\right) \mp \frac{\pi}{6} - \theta_n] \quad (8.40)$$

where

$$I_n = \frac{4V_{dc}}{\sqrt{3}n\pi\sqrt{R^2 + (n\omega L)^2}} \sin\frac{n\pi}{2} \sin\frac{n\pi}{3}$$

and $\theta_n = \tan^{-1} n\omega L/R$, the impedance angle for the n[th] order harmonic.

The line-to-line *rms* voltage is

$$V_{L(rms)} = \sqrt{\frac{2}{2\pi}\int_0^{2\pi/3} V_{dc}^2 \, d\omega t} = \sqrt{\frac{2}{3}}\, V_{dc} \qquad (8.41)$$

From (8.38a), the *rms* value of the nth harmonic component of the phase voltage is

$$V_{Ln} = \frac{4V_{dc}}{\sqrt{6}n\pi}\sin\frac{n\pi}{2}\sin\frac{n\pi}{3} \qquad (8.42)$$

From which, the *rms* value of the fundamental component (n =1) of the output phase voltage is

$$V_{L1} = \frac{4V_{dc}}{\sqrt{6}\pi}\sin\frac{\pi}{3} = \frac{2\sqrt{2}}{\pi}\, V_{dc} \qquad (8.43)$$

Example 8.5

The three-phase inverter in Fig.8.18 used to feed a Y-connected resistive load with R =15 Ω per-phase. The d.c. input to the inverter V_{dc} = 300 V and the output frequency is 50 Hz. If the inverter is operating with 120˚ conduction mode, calculate : (a) The peak and *rms* value of the load current I_L, (b) The output power, and the average and *rms* values of the current of each transistor.

Solution

(a) For 120[o] conduction mode, at any time the load resistances of two phases are connected in series, hence, peak value of load current is

$$I_p = \frac{V_{dc}}{2R} = \frac{300}{2 \times 15} = 10 \text{ A}$$

From Eq.(8.32), the *rms* value of the phase voltage is

$$V_{a(rms)} = \frac{V_{dc}}{\sqrt{6}} = \frac{300}{\sqrt{6}} = 122.44\text{V}$$

Hence the *rms* value of the load current is

$$I_{a(rms)} = \frac{V_{a(rms)}}{R} = \frac{122.44}{15} = 8.16 \text{ A}$$

(b) The load power is

$$P_o = 3\, {I_{a(rms)}}^2 R = 3 \times 8.16^2 \times 15 = 3000 \text{ W}$$

(c) For 120° conduction mode, each transistor carries current for (1/3)rd of a cycle, hence the average transistor current is

$$I_{T(av)} = \frac{I_p}{3} = \frac{10}{3} = 3.33 \text{ A}$$

The *rms* value of the thyristor current is

$$I_{T(rms)} = \sqrt{(\frac{I_p}{3})^2} = \sqrt{(\frac{10}{3})^2} = 3.33 \text{ A}$$

8.5 INVERTER OUTPUT FREQUENCY AND VOLTAGE CONTROL

In many applications of the inverter require means of controlling the output voltage as well as its output frequency. In drive systems, the ratio of voltage to frequency (*V/f*) need to be maintained constant in order not to drive the machine into the saturation region of its magnetic circuit. Similarly, in UPS the output voltage of the inverter should be regulated. The output frequency can be easily controlled by controlling the triggering instants of the power switch electronically. However, the control of the voltage in most of these applications is usually required in order to provide stepless adjustment of the inverter output voltage. The methods of voltage control can be grouped into three broad categories:

1. Control of voltage supplies to the inverter.
2. Control of voltage delivered by the inverter.
3. Control of voltage within the inverter.

Control of voltage supplies to the inverter can be achieved by several methods including the use of d.c. choppers and phase-controlled rectifiers. The principal disadvantage of these methods is that the power delivered by the inverter is handed twice, once by the d.c. or a.c. voltage control and

once by the inverter. In the second category, the output may be controlled by means of auto transformer.

In the third category, control of the inverter output voltage may be achieved by incorporating time-ratio controls within the inverter circuit. A more common method of controlling the voltage within an inverter involves the use of pulse width modulation (PWM) techniques. With this technique the inverter output voltage is controlled by varying the duration of the output voltage pulses. Moreover, the output frequency can also be controlled by this technique.

Principle of pulse width modulation (PWM) technique

PWM is simply the variation (modulation) of the duty of a square pulse to produce a controlled average voltage. In its simple form, PWM is obtained by comparing a reference signal, A_r (also called the modulating wave) with a triangular carrier wave, A_c as shown in Fig.8.23.

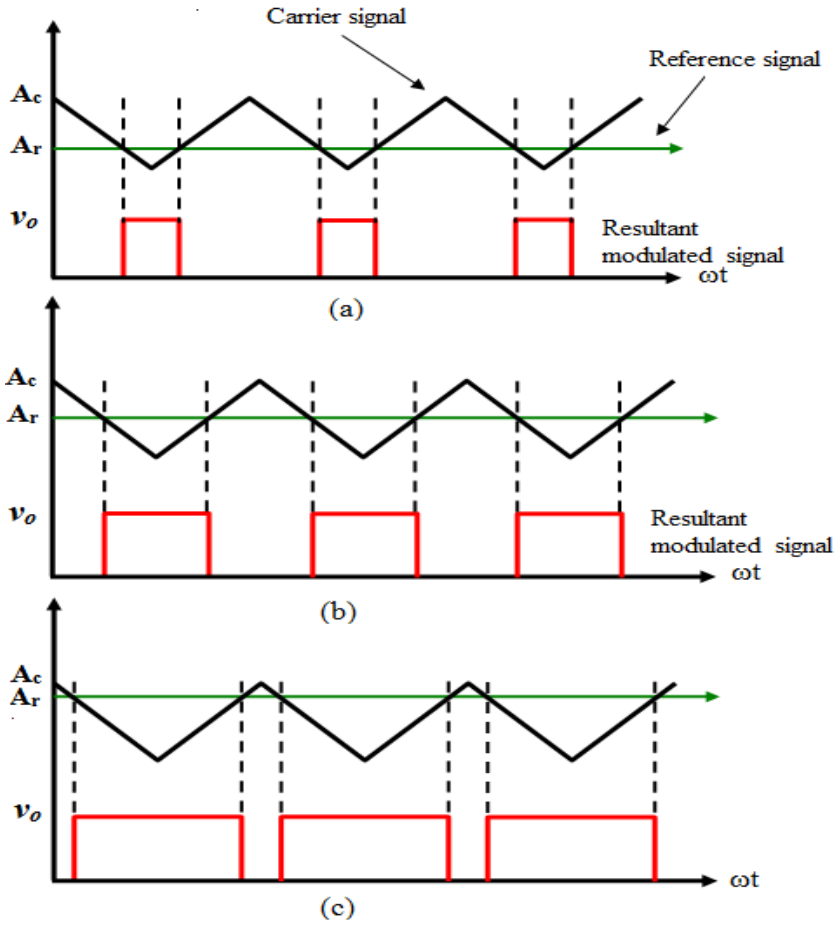

Fig.8.23 PWM technique: (a) low value of modulation index M, (b) moderate value of M, (c) high value of M.

By varying A_r from 0 to A_c, the pulse width δ can be varied from 0^o to 180^o. Thus, the voltage and hence, the amount of power sent to the load is controlled. The modulation index is defined as,

$$\text{Modulation index} = M = \frac{A_r}{A_c} \tag{8.44}$$

In power electronics, the modulating signal is produced by controlling the turn-on and turn-off of the power semiconductor devices such as thyristors, BJTs, MOSFETs, GTOs, etc. The duty of the positive and negative pulses (*rms* value) depends upon switching period which is controlled using PWM in the gate signals in the electronic switches. By the vision of Power Electronic applications, the quality of the PWM technique is measured by its powerful to eliminate the output harmonics or at least to eliminate the low order harmonics (*LOH*) which are difficult to filtered out.

There are many types of PWM, however, the commonly used techniques for controlling output voltage of a single-phase inverter are:

1- Single-pulse width modulation
2- Multiple-pulse-width modulation
3- Sinusoidal pulse-width modulation
4- Modified sinusoidal pulse-width modulation
5- Phase displacement control

Sinusoidal pulse-width modulation (SPWM) is the most commonly used among all these techniques. However, this type of modulation has some drawbacks that will be discussed later on in this chapter. Advanced modulation methods are also used recently such as staircase modulation, harmonic injection modulation, trapezoidal modulation and delta modulation. These methods will not be discussed in this book due to their complex theory. However in all above techniques the aim is to generate a sinusoidal output voltage, but they differ from each other in the harmonic content in their respective output voltage.

8.5.1 Single Pulse Width Modulation

The simplest form of pulse width modulation technique is the single pulse width modulation. This type of modulation gives quasi – square wave output as shown in Fig.8.24(c). According to this figure one can observe that, there is a single pulse of output voltage during each half-cycle and the width of the pulse is varied to control the output voltage. A carrier signal of frequency f_c with amplitude A_c is modulated by another signal or reference signal of amplitude A_r as shown in Fig.8.24 (a).

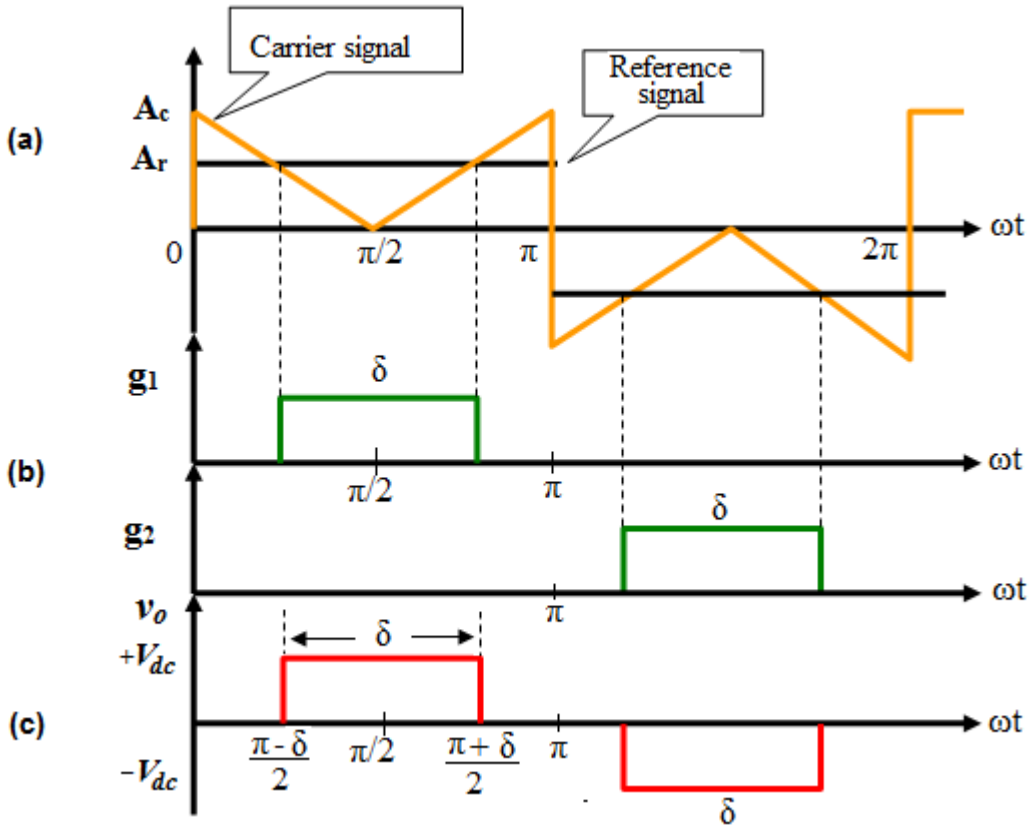

Fig.8.24 Single-pulse width modulation (SPM): (a) Reference signal, (b) Gate signals , (c) Output voltage waveform.

The main objective of using modulation process in power electronics engineering is to generate the gate signal to the power switches and thereby determine the output frequency of the inverter. As mentioned before, the output voltage can be varied by varying the pulse width δ by varying the amplitude A_r from 0 to A_c. i.e by varying the modulation index M from 0 to 1.

Referring to Fig.8.24, the *rms* of the output voltage is given by

$$V_{o(rms)} = \sqrt{\frac{2}{2\pi}\int_{\pi-\delta/2}^{\pi+\delta/2} V_{dc}^2 \, d\omega t} = V_{dc}\sqrt{\frac{\delta}{\pi}} \qquad (8.45)$$

The output voltage waveform has the Fourier series

$$v_o(\omega t) = \sum_{n=1,3,5,..}^{\infty} \frac{4V_{dc}}{n\pi} \sin\frac{n\delta}{2} \sin n\omega t \qquad (8.46)$$

The peak value of the fundamental component is

$$V_1 = \frac{4V_{dc}}{\pi}\sin\frac{\delta}{2} \tag{8.47}$$

Pulse width δ has a maximum value of π radians at which the fundamental term in Eq.(8.47) is a maximum. The n^{th} order harmonic in Eq.(8.46) is seen to have peak value,

$$V_1 = \frac{4V_{dc}}{n\pi}\sin\frac{n\delta}{2} \tag{8.48}$$

The distortion factor of the single-pulse waveform is therefore

$$\text{Distortion factor} = \frac{\frac{V_1}{\sqrt{2}}}{V_{orms}} = \frac{2\sqrt{2}}{\sqrt{\pi\delta}}\sin\frac{\delta}{2} \tag{8.49}$$

which has a maximum value of 0.9 when δ = π.

8.5.2 Multiple-PulseWidth Modulation

An alternative waveform consisting *m* symmetrical spaced pulses per half-cycle can be obtained by control the output voltage of the inverter such that it can be switched on and off rapidly several times during each half-cycle to produce a train of constant magnitude pulses. Fig.8.25 shows the idea of multiple pulse-width modulation.

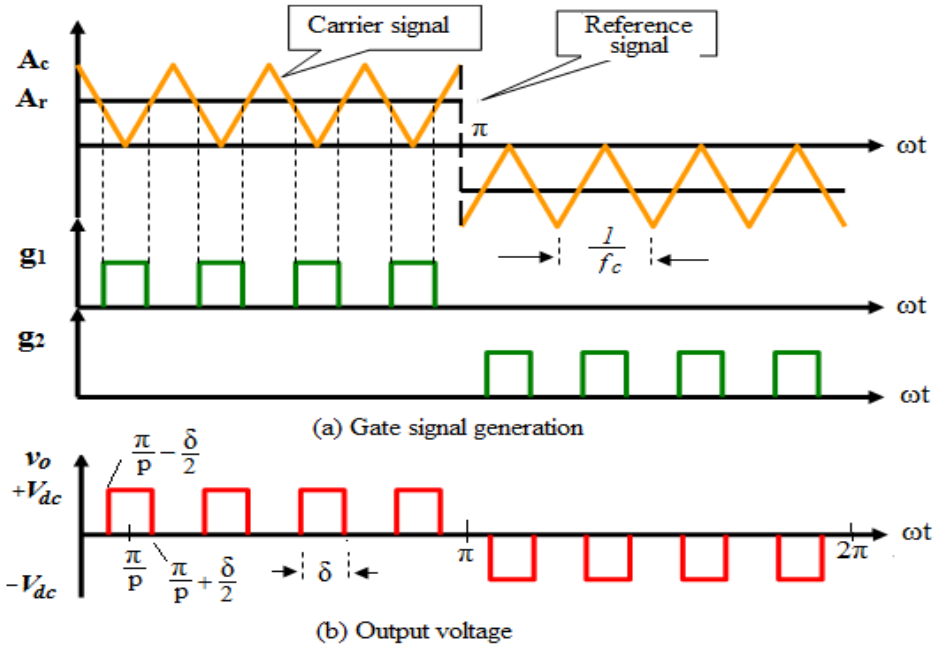

Fig.8.25 Multiple pulse width modulation.

The output voltage waveform consists of p pulses for each half-cycle of the required output voltage. Minimum pulse width is zero and maximum pulse width will be π/p.

Let f_o be the output frequency of the inverter, and $T = 1/f_o = 2\pi$. In this period there are 2p pulses of equal width. The first pulse is located at π/p, then its width is $\frac{\pi}{p} - \frac{\delta}{2}$ to $\frac{\pi}{p} + \frac{\delta}{2}$ as depicted in Fig.8.25. In this case the *rms* value of the output voltage will be:

$$V_{o(rms)} = \sqrt{\frac{2p}{2\pi}\int_{(\pi/p)-(\delta/2)}^{(\pi/p)+(\delta/2)} V_{dc}^2 \, d\omega t}$$

$$V_{o(rms)} = V_{dc}\sqrt{p[\frac{\pi}{p} + \frac{\delta}{2} - \frac{\pi}{p} + \frac{\delta}{2}]} = V_{dc}\sqrt{\frac{p\,\delta}{\pi}} \qquad (8.50)$$

The frequency of the pulses is $f_p = 2\ p\ f_o$ which must be the same frequency of the carrier signal f_c that is always greater than the output frequency f_o. Thus, the number of equal symmetrical pulses p per half-cycle can be calculated as

$$p = \frac{f_c}{2f_o} = \frac{m_f}{2} = \text{integer} \qquad (8.51)$$

where $m_f = f_c / f_o$ is a factor defined as the *frequency modulation ratio.*

The Fourier series of the output voltage is found to be

$$v_o(\omega t) = \sum_{n=1,3,5,..}^{\infty} B_n sinn\omega t \qquad (8.52)$$

where

$$B_n = \sum_{n=1,3,5,..}^{p} \frac{4V_{dc}}{n\pi}\sin\frac{n\delta}{4}[sin\, n\left(\alpha_m + \frac{3\delta}{4}\right) - sin\, n\left(\pi + \alpha_m + \frac{\delta}{4}\right) \qquad (8.53)$$

here the angle α_m (m = 1,2,3,4,……) is the switching angle of each individual pulse in the positive half-cycle of the output voltage wave as depicted in Fig.8.26.

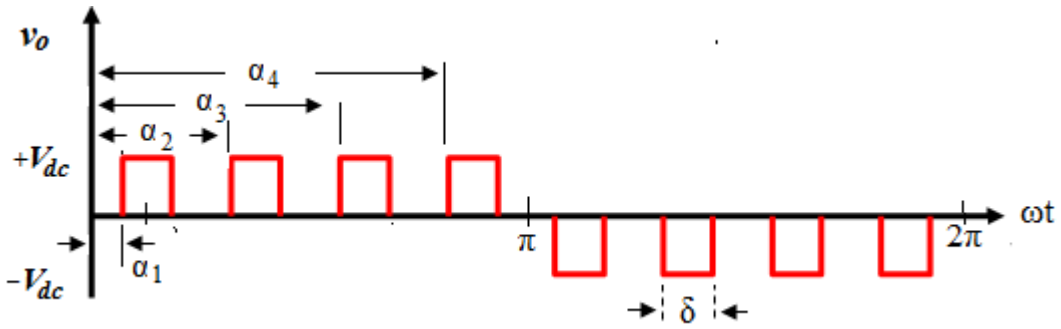

Fig.8.26 The output voltage wave and the meaning of the angle α_m.

The normalized amplitude of harmonics and the percentage distortion factor variation with the modulation index M are shown in Fig.8.27 for p = 5 of the multiple pulse modulation.

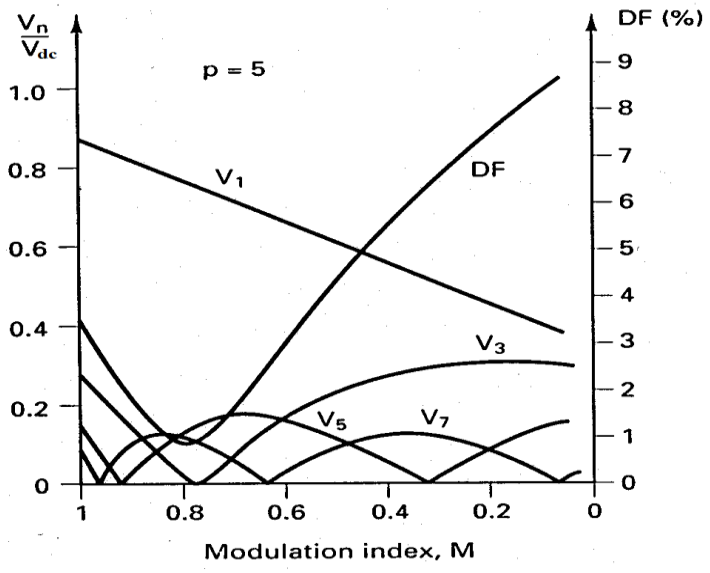

Fig.8.27 Normalized harmonic amplitude and distortion factor variations with the modulation index for p = 5.

8.5.3 Sinusoidal Pulse-Width Modulation (SPWM)

Using sinusoidal reference signal will produce varied width pulses that proportional to the amplitude of the sine wave as shown in Fig.8.28. In this technique, the lower order harmonics of the modulated voltage wave are greatly reduce. The *rms* value of the output voltage of the inverter

depends on the widths of the pulses (δ_m). These widths depend on the mdulation index *M* which controls the output voltage of the inverter.

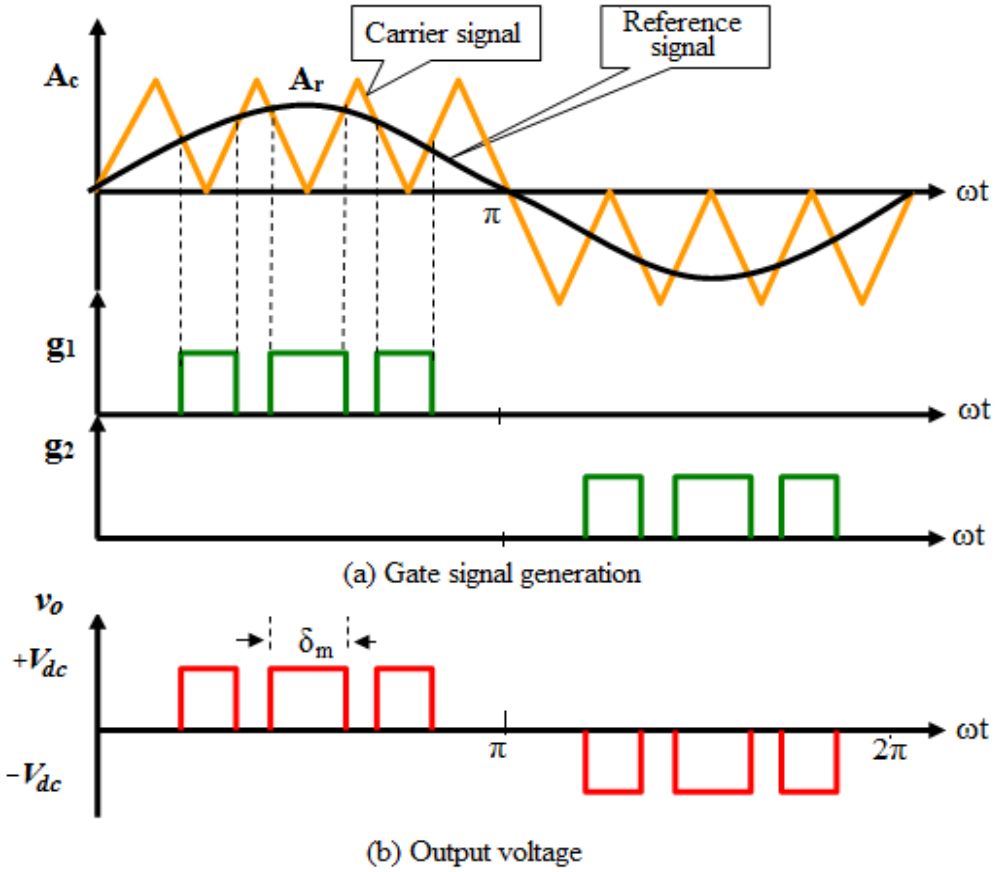

Fig.8.28 Sinusoidal pulse width modulation.

The magnitude of the fundamental component of the output voltage is clearly proportional to the modulation index *Ar /Ac* . But the highest practical value of *M* is unity. If *Ar > Ac* the output voltage waveform $v_o(\omega t)$ approaches a rectangular form and undesirable low frequency harmonics such as the third , fifth and seventh harmonics are introduced and intensified.

The *rms* output voltage is

$$V_o = V_{dc}\sqrt{\sum_{m=1}^{p}\frac{\delta_m}{\pi}} \qquad (8.54)$$

and the coefficient (B_n) of the Fourier series of the output voltage will be

$$B_n = \sum_{n=1.}^{p} \frac{4V_{dc}}{n\pi} \sin\frac{n\delta}{4} [sin\, n\left(\alpha_m + \frac{3\delta_m}{4}\right) - sin\, n\left(\pi + \alpha_m + \frac{\delta_m}{4}\right)] \quad (8.55)$$

Another type of sinusoidal modulation can obtained by using two anti-phase sinusoidal reference (modulating) signal as shown in Fig.8.29. This technique is called double-sided triangular carrier wave modulation. The reference signal v_{ra} produces the resultant modulated wave v_a , Fig.8.29 (b), whereas the reference signal v_{rb} produces the resultant modulated wave v_b , Fig.8.29(c). The corresponding line voltage $v_{ab} = v_a - v_b$ has a fundamental component as shown in Fig.8.29(d).

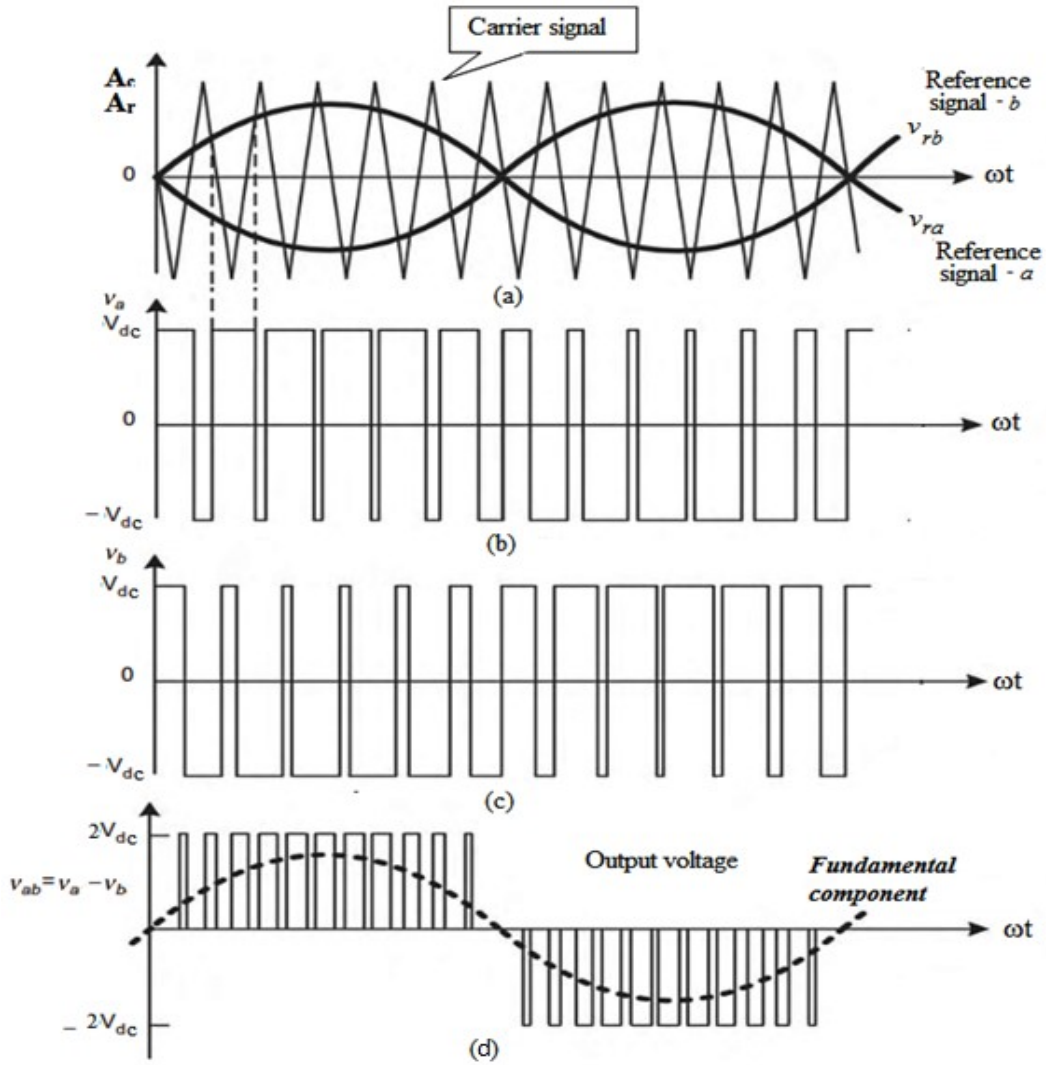

Fig.8.29 PWM voltage waveforms obtained by sinusoidal modulation of double-sided triangular carrier wave.

8.5.4 Modified Sinusoidal PulseWidth Modulation

Here the carrier signal is not symmetry triangle wave. The carrier wave is generated so the widths of the pulses that are near to the peak of the sine wave not change much when modulation index changed. Such scheme is shown in Fig.8.30 and known as MSPWM. Note that the triangular wave is present for the period of first 60˚ of the half cycle of sine wave. The MSPWM increase the fundamental component and improve the harmonic characteristic. This technique reduces the number of switching of power devices and also reduces switching losses.

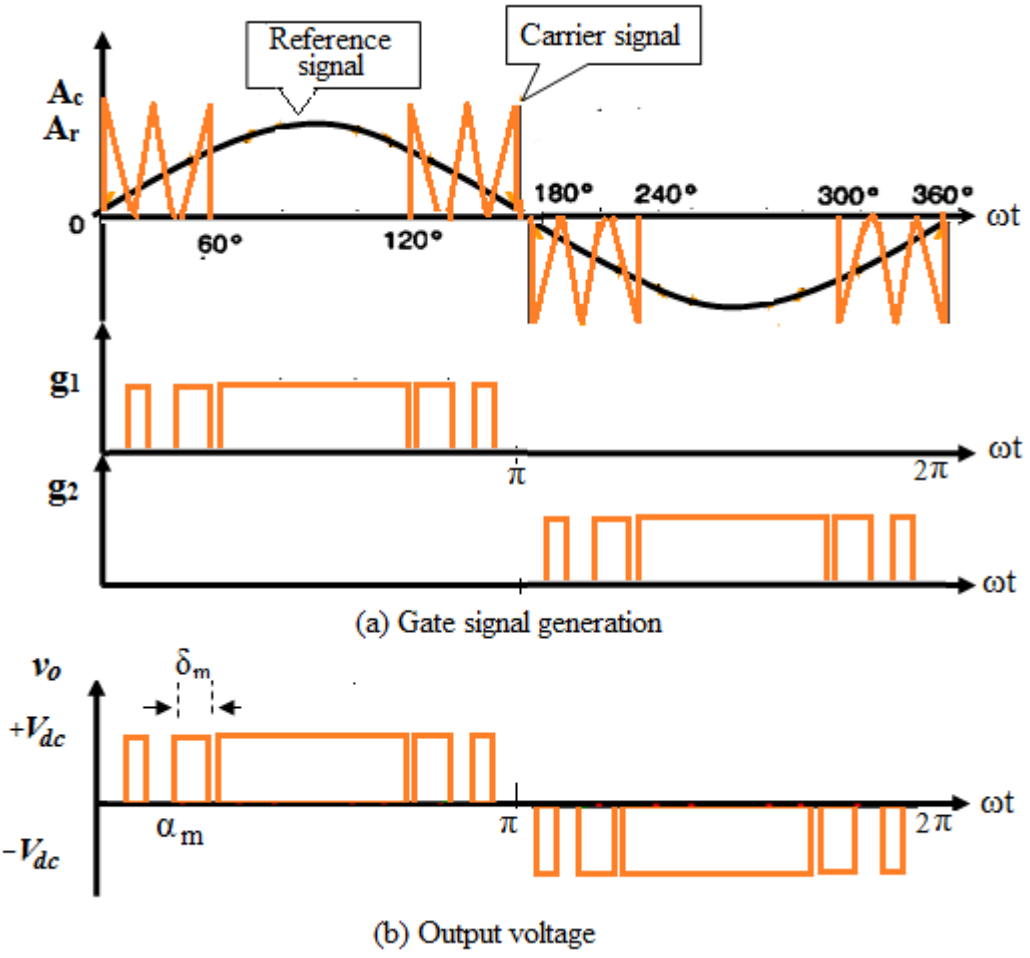

Fig.8.30 Modifide PWM voltage waveforms.

8.5.5 Other PWM Methods

Besides SPWM, other PWM methods are proposed for generating three-phase voltages to deliver more power, including third-harmonic PWM, sixty-degree PWM and space vector PWM. All these methods are aimed at making better use of the d.c. bus voltage and thus increasing

modulation index. These methods are shortly mentioned here without detailed analysis.

1. Third-harmonic PWM

In this method, the reference signal is not a pure sinusoidal wave, but the sum of the fundamental and the third harmonic. It is shown with curve $f(\omega t)$ in Fig.8.31. Same as the SPWM method, this signal will be compared with the triangle signal to generate PWM signals.

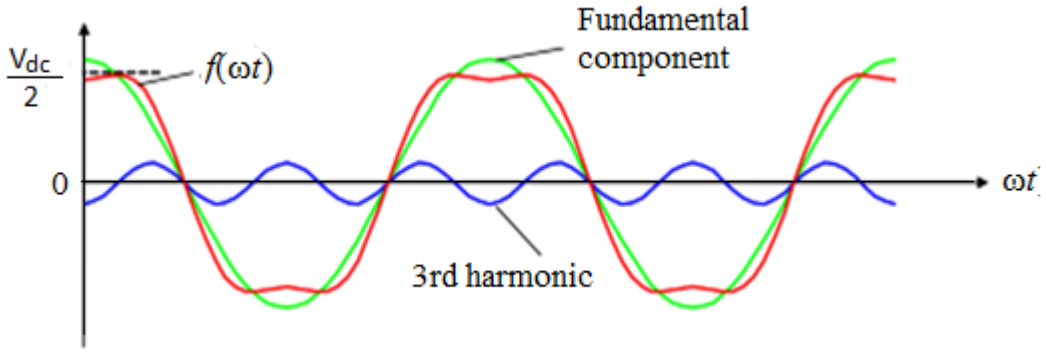

Fig.8.31 Reference signal of third harmonic.

Same as the SPWM method, this signal will be compared with the triangle signal to generate PWM signals. This concept is derived from the nature of three-phase motors that the third harmonic will be filtered out in the windings. Thus only the fundamental part will remain and the modulation index of this method reaches 1.

2. Sixty-degree PWM

The sixty-degree PWM is an extension of third-harmonic PWM. It is based on the nature of the motor that not only third harmonic, but also all none-even triple harmonics are filtered out by the windings. Adding all these harmonics with the fundamental together, a function with flat segments are obtained as shown in Fig.8.32. The period of the flat part covers 60° signal phase. The modulation index of this method can reach 1, too.

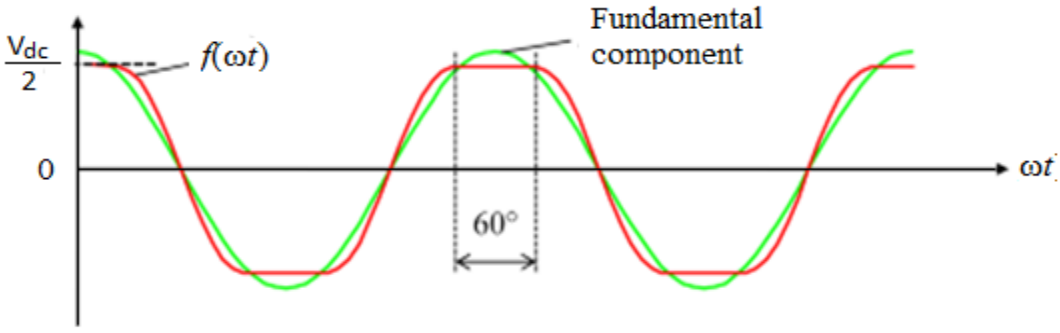

Fig.8.32 Concept of sixty-degree PWM.

Drawbacks of PWM

Pulse width modulation is a simple, flexible process. It is very common in inverter that need to provide adjustable performance and in small battery powered audio amplifiers. However it has a few limitation that preclude certain specialized applications.

- The highest output amplitude is equal to the input.
- Numerous switching operations occur each period. In real switches, a small energy loss is incurred every time a switch turns on or off. In a PMW converter with frequency ratio f_{switch} / f_{out}, the energy lost in switching increases by the same ratio, relative to the loss in a VSI inverter.
- Distortion : Although a low-pass filter should be adequate for recovery modulation function, the inverter output has large harmonics extending to very high frequencies. Even small residual components at megahertz frequencies can interfere with communication equipment, sensors, analog signal processing, and sometime digital logic.

8.6 VOLTAGE CONTROL OF THREE-PHASE INVERTER

For the three-phase inverters, output voltage control can be achieved by the same techniques discussed in the previous section. However, the following methods are mostly used for voltage control in three-phase inverters.

- Sinusoidal pulse width modulation.
- 60˚ pulse width modulation.
- Third harmonic pulse width modulation.
- Space vector modulation.

In sinusoidal pulse width modulation, three reference sinusoidal signals are used one for each phase. These three reference waves have phase shift of 120˚ between each other so that they produce three – phase output voltage waves.

8.7 HARMONIC REDUCTIONS IN THE INVERTER OUTPUT VOLTAGE

The output voltage waveform of the inverter is rich of harmonics; the main objective is to obtain a sinusoidal ac output voltage waveform where the fundamental component can be adjusted within a range and the intrinsic harmonics selectively eliminated and to element the unwanted harmonics.

There are several industrial applications, which may allow a harmonic content of 5 % of its fundamental component if, input voltage when inverter is used. Actually, the inverter output voltage may have harmonic content much higher than 5 % of its fundamental component. In order to bring this content to reasonable limit, there are several methods which can be used:

1- Harmonic reduction by PWM.
2- Harmonic reduction by transformer connections.
3- Harmonic reduction by stepped-wave inverter.
4- Harmonic reduction using phase displacement control.

8.7.1 Harmonic Reduction by PWM

With single pulse width modulation discussed in subsection 8.5.1, the amplitude c_n of the nth order harmonic as given from the Fourier series of the output voltage in Eq.(8.46) ,

$$c_n = \frac{4V_{dc}}{n\pi}\sin\frac{n\delta}{2}$$

where δ is the pulse width
If it is required to eliminate the third order harmonic (n=3) from the output voltage waveform , let

$$\sin\frac{3\delta}{2} = 0 \;\rightarrow\; \frac{3\delta}{2} = 180° \qquad \therefore \quad \delta = 120°$$

To eliminate the fifth order harmonic:

$$\sin\frac{5\delta}{2} = 0 \;\rightarrow\; \frac{5\delta}{2} = 180° \qquad \therefore \quad \delta = 72°$$

It is obvious that m with this method only single specific order harmonic can be eliminated. However, since the third harmonic is the next most predominant one in the output voltage waveform of the inverter, δ must always be 120˚.

8.7.2 Harmonic Reduction by Transformer Connections

The output of two or more inverters may be connected together using separate transformers to produce one output voltage waveform that has other harmonic characteristics. In order to understand the method let us assume that we want to eliminate the third harmonic as well as the triplen order harmonics (9, 15, 18,…), two inverter outputs v_{o1} andv_{o2} are connected through two transformers as shown in Fig.8.33(a).

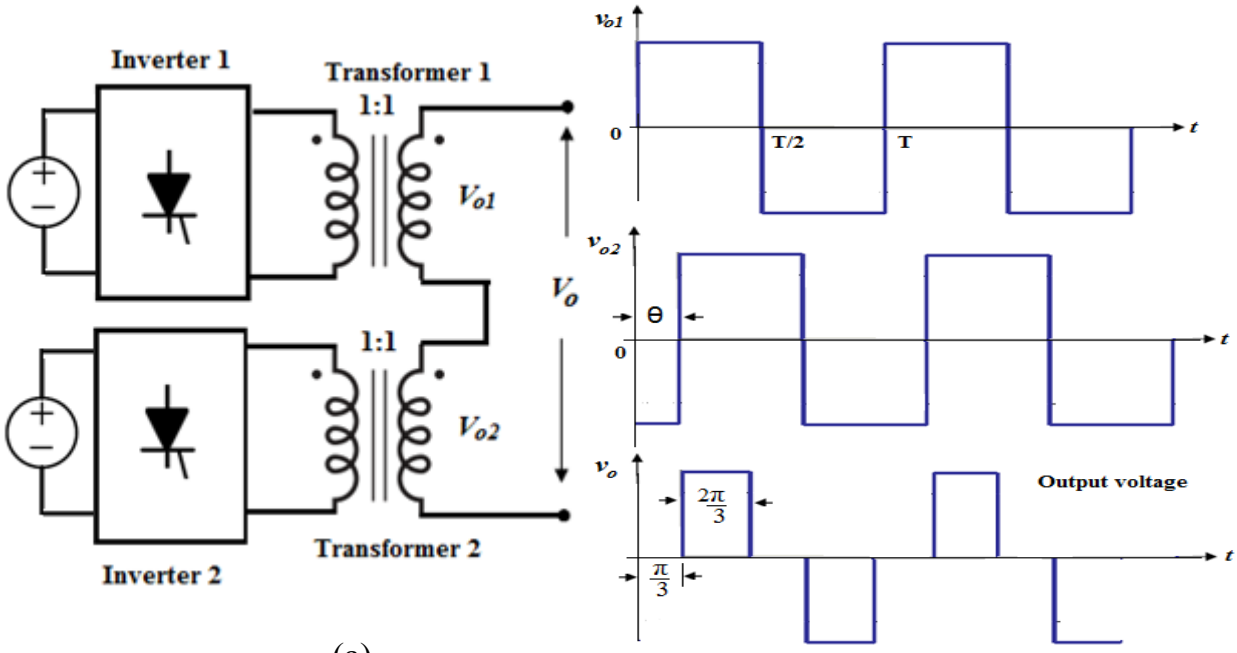

(a) (b)

Fig.8.33 Harmonic elimination using transformer connection: (a) circuit, (b) waveforms.

Let the two voltages are expressed in Fourier series as

For inverter 1

$$v_{o1}(\omega t) = V_{m1}\sin\omega t + V_{m3}\sin 3\omega t + V_{m5}\sin 5\omega t + V_{m7}\sin 7\omega t + V_{m9}\sin 9\omega t + V_{m11}\sin 11\omega t + \cdots \quad (8.56)$$

For inverter 2 , the output voltage v_{o2} is made to lag v_{o1} by π/3, thus

$$v_{o2}(\omega t) = V_{m1}\sin\left(\omega t - \frac{\pi}{3}\right) + V_{m3}\sin(3\omega t - \frac{\pi}{3}) + V_{m5}\sin(5\omega t - \frac{\pi}{3} + V_{m7}(\sin 7\omega t - \frac{\pi}{3}) + V_{m9}(\sin 9\omega t - \frac{\pi}{3}) + V_{m11}(\sin 11\omega t - \frac{\pi}{3}) + \cdots \quad (8.57)$$

The resultant output voltage is $v_o(\omega t) = v_{o1}(\omega t) + v_{o2}(\omega t)$, hence

$$v_o(\omega t) = \sqrt{3}\left[V_{m1}\sin\left(\omega t - \frac{\pi}{6}\right) + V_{m5}\sin\left(5\omega t - \frac{\pi}{6}\right) + V_{m7}(\sin 7\omega t - \frac{\pi}{6}) + V_{m11}(\sin 11\omega t - \frac{\pi}{6}) + \cdots\right] \quad (8.58)$$

It is obvious from Eq.(8.58) that the third order harmonic as well as all the triplen harmonics (n=9,15,18,…) are entirely eliminated from the output

voltage wave. Waveforms of the system are shown in Fig.8.33(b) for clarity.

Alternatively the triplen harmonics can also be suppressed using delta-star transformer at the output of a three-phase inverter, since these harmonic componenets are all in phase and they will cause circulating currents that cancel each other through the delta-connection. Therefore, the output voltage from the star side will not contain any triplen order harmonic voltage.

8.7.3 Harmonic Reduction by Stepped-Wave Inverter

This method of harmonic reduction is similar to the previous one as it also requires two inverters with separate transformers that their secondary windings have different turn ratios and are connected in series as shown in Fig.8.33(a). Transformer 1 has 1:1 turns ratio whereas transformer 1 may has 1:3 turns ratio such that the output resultant waveform is a stepped wave of different amplitudes.

Alternatively, one can use parallel inverter with multi taps on its primary winding as shown in Fig.8.34 (a).When the thyristors on the left side of the battery conduct, the output voltage is positive. When the thyristors on the right side conduct the output voltage is negative. The conduction sequence of the thyristors is 1-2-3-2-1-1'-2'-3'-2'-1'to get 12 steps output voltage waveform.

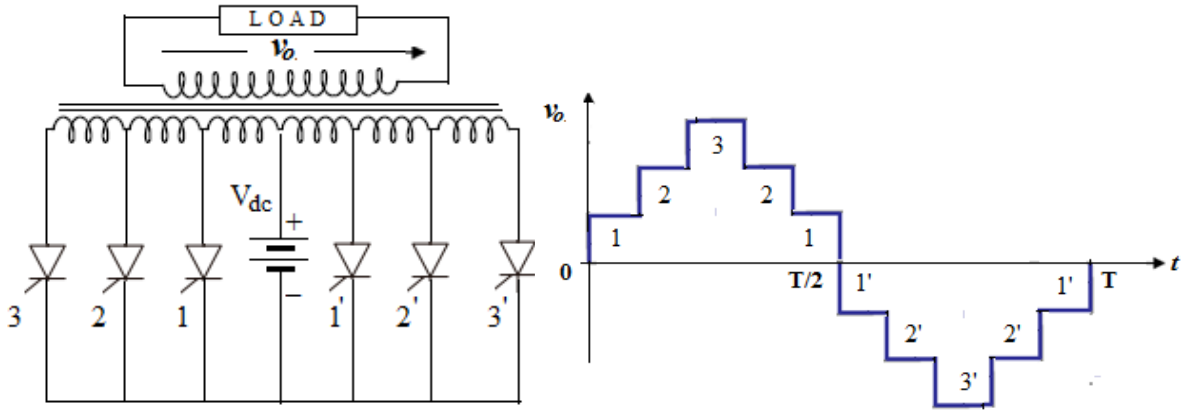

(a) (b)

Fig.8.34 Stepped wave inverter (a) Circuit, (b) output voltage waveform.

8.7.4 Harmonic Reduction Using Filters

Filters of various types such as *LC*, *LCL* or *OTT* are also used to reduce the harmonic contents of the output voltage waveform of an inverter. The reactance ($X_L = 2\pi f L$) of an inductor increases with frequency, therefore the effect of series inductance is to attenuate high

frequencies. On the other hand the reactance of a capacitor ($X_C = 1/2\pi f C$) is inversely proportional to frequency, hence a parallel capacitor provides by-pass to high frequencies. These features are used in combination to eliminate higher order harmonics to some extent. The types of filters in common used for inverter circuits are depicted in Fig. 8.35.

Although *LC* filter shown in Fig.35(a) is simple and gives nearly sinusoidal output voltage waveform , *OTT* filter shown in Fig.8.35(b) gives better performance characteristics due to the generation of high quality and very low harmonic content output voltage waveform. The drastic reduction in the higher order harmonics leads to transfer of their energies to the fundamental component of the desired frequency. However *LC* filter does not has resonance problems as it exist in other types of filters.Hoever , for an inductive load that requires a smooth current (e.g. an electrical machine), the machine inductance provides the filtering because it acts as a low pass filter.

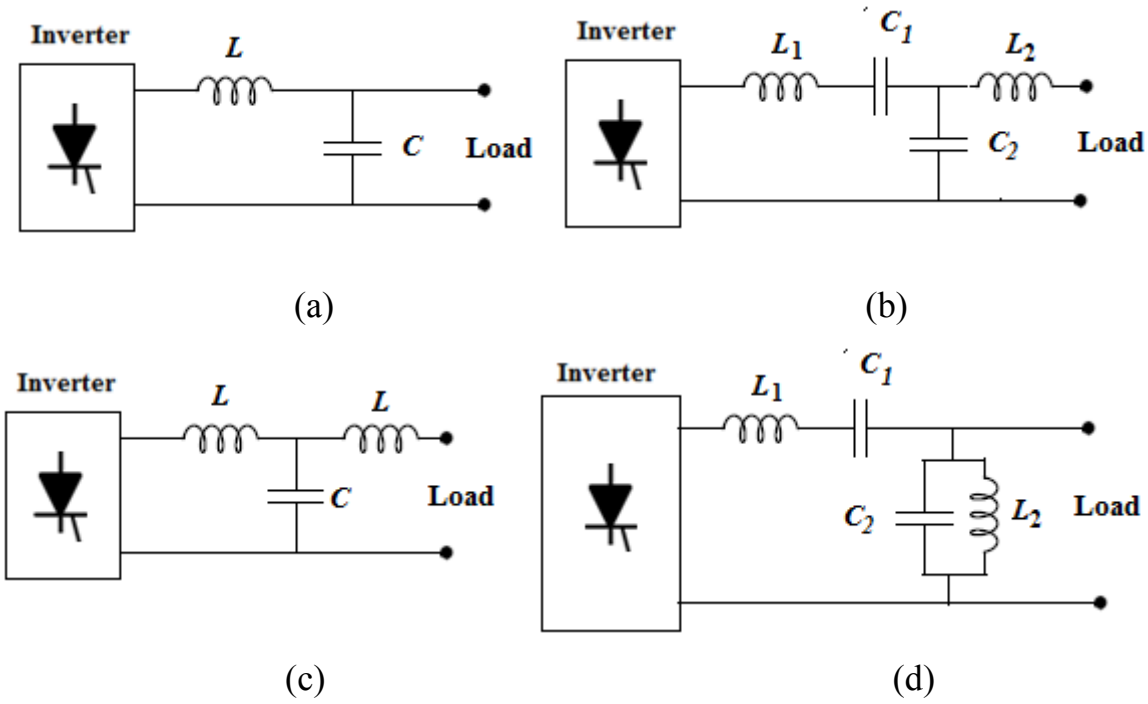

Fig.8.35 Four types of filters commonly used with inverter circuits: (a) Simple *LC* filter, (b) OTT filter, (c) LCL filter, (d) Resonant filter.

8.8 THREE-PHASE NATURALLY COMMUTATED INVERTER

The three-phase full-wave, fully-controlled bridge rectifier, discussed in Chapter Three, can be used as an inverter if the load is replaced by a d.c. supply with reverse polarity voltage as shown in Fig.8.36. The current direction, on the d.c. side is unchanged. If this rectifier bridge is used as inverter, the voltage and frequency as well as the shape of the wave on the a.c. side are set by the bus and cannot be changed.

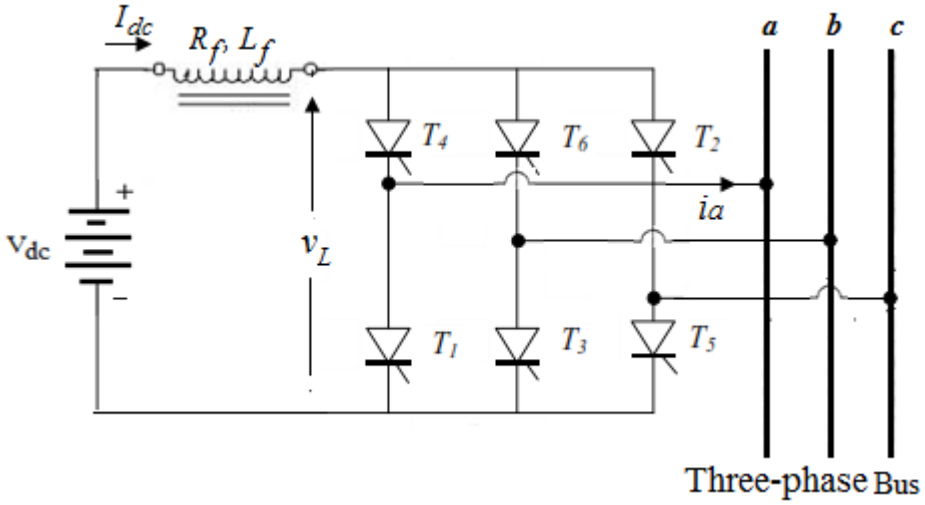

Fig.8.36 Three-phase naturally commutated bridge inverter.

The instantaneous values v_L on the d.c. side of the bridge and the output waveforms are identical to those of rectifier operation with passive load shown in Fig.3.37. For $\alpha < 60^o$, v_L always positive and at $\alpha = 90^o$, $v_L = 0$, whereas for $\alpha > 90^o$, the average value of v_L is negative.
As it was given in Chapter Three , the average value of the bridge voltage is , from Eq.(3.40),

$$V_{Lav} = \frac{3\sqrt{3}V_m}{\pi} cos\alpha \ = 2.34\, V_{sL}\, cos\alpha \qquad (8.59)$$

where V_m is the peak phase voltage and V_{sL} is the *rms* phase voltage.
The average value of the current on the d.c. side is, from Fig.3.36,

$$I_{dc} = \frac{V_{dc} + V_{Lav}}{R_f} = \frac{1}{R_f}[\, V_{dc} + 2.34\, V_{sL}\, cos\alpha] \qquad (8.60)$$

The power on the d.c. side is

$$P = I_{dc} V_{Lav} \qquad (8.61)$$

8.9 CURRENT SOURCE INVERTER

The current source inverter (CSI) is a device that converts the input direct current into an alternating current. It is also called current fed inverter in which the output current is maintained constant irrespective of load on the inverter. This means that, the magnitude and nature of the load current depends on the nature of load impedance. The output voltage of the inverter is independent of the load. The major advantage of current

source inverter is its reliability. In the case of current source inverter a commutation failure in the same leg does not occur due to the presence of a large inductance L_d connected in series with the voltage source.

Compared with a VSI system, the output current of a CSI system is not influenced by the supply voltage, so its output current has low THD and high *PF*. Hence, in the 1980s the current source inverters were the main commonly used electric machine feeding devices. The current source inverter was constructed of a thyristor bridge with large inductance and large commutation capacitors. Serious problems in such drive systems were unavoidable overvoltage cases during the thyristor commutation, as the current source inverter current is supplied in a cycle from a dc-link circuit to the machine phase winding. The thyristor CSI has been replaced recently by the transistor reverse blocking IGBT devices (RBIGBT), where the diode is series-connected and placed in one casing with transistor. The power transistors like RBIGBT or Silicon Carbide (SiC) used in the modern CSIs guarantee superior static and dynamic drive characteristics. The use of current sources for the electric machine control ensures better drive properties than in case of voltage sources, where it may be necessary to use an additional passive filter at the inverter output. Therefore, due to its advantages, the current source inverters are used in many industrial applications such as induction heating, static var compensators (SVC) , variable speed a.c. motors etc.

The freewheeling diodes that are used for voltage source inverters become useless if an inverter is supplied from a d.c. current source, this is because the current in any half-leg of the inverter cannot change its polarity, hence it can only flow through the power semiconductor switches. Therefore, absence of the freewheeling diodes reduces the size and weight of the inverter circuit.

In practice CSI is mainly used for a.c. motor control, hence it invariably of three-phase type. However, we shall describe both the single-phase and three-phase types hereafter.

8.9.1 Single-Phase Current Source Inverter

Fig.8.37 shows the circuit of a single-phase current source inverter. A constant current source is assumed here, which may be realized by using a large inductance L_d of suitable value in series with the current limited d.c. voltage source V_{dc}. The thyristors of the inverter circuits are, T_1 , T_3, T_2 and T_4 , are alternatively turned ON to obtain a nearly square wave current waveform. Two commutating capacitors – C_1 in the upper half, and C_2 in the lower half, are used. Four diodes, D_1, D_2, D_3 and D_4 are connected in series with each thyristor to isolate the commutating capacitors from the load and prevent them from discharging through the load.

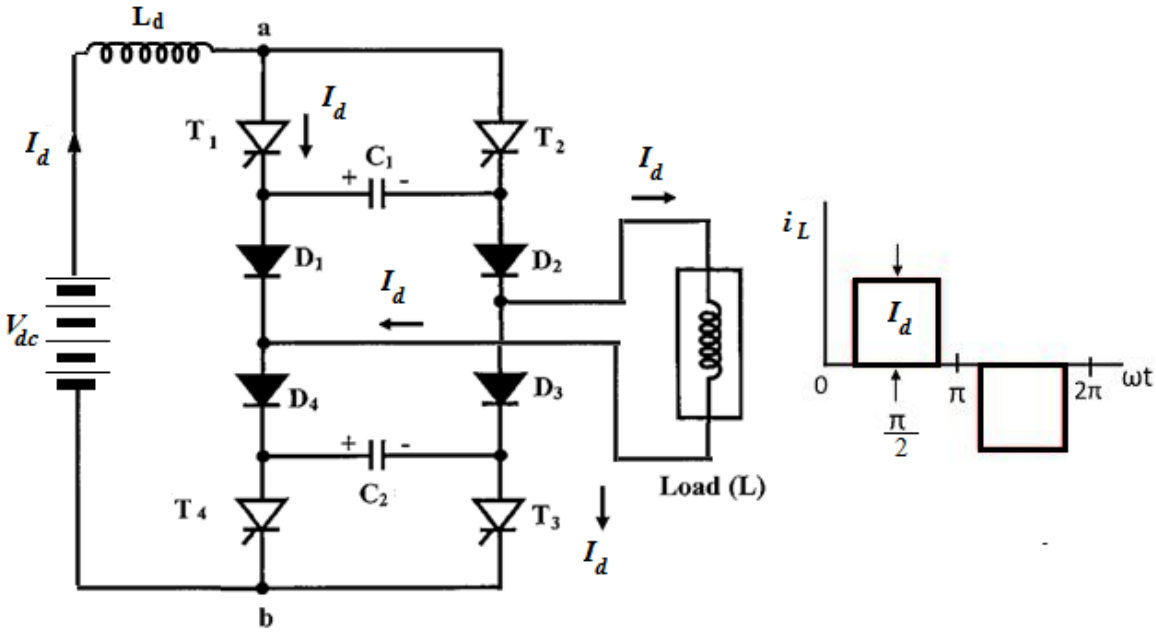

(a) (b)

Fig. 8.37 Single-phase current source inverter: (a) Circuit, (b) Output current waveform.

The output frequency of the inverter is controlled by varying the half time period, (*T/2*), at which the thyristors in pair are triggered by pulses being fed to the respective gates by the control circuit, to turn them ON.
The operation of the circuit can be described as :
In the circuit of Fig.8.37(a), two thyristors must trigger simultaneously to permit current to flow. For example, T_1 and T_3 must be triggered, while in reverse, T_2 and T_4 must trigger at the same time. The output current waveform is shown in Fig.8.37(b) for the case of inductive load.

When T_1 andT_3 conduct, capacitors C_1 and C_2 would be charged with the polarity as shown. When T_2 andT_4 are turned on, thyristors T_1 and T_3 are reversed biased by the capacitors C_1 and C_2 respectively to commutate them. At this instant, the load current flows through $T_2 - C_1 - D_1 -$ load $- D_3 - C_2 - T_4$ charging capacitors C_1 and C_2 with opposite polarity and are ready now to commutate T_2 and T_4 , while the current in the load changes its direction and the cycle is repeated.

8.9.2 Three-Phase Current Source Inverter

The circuit of a three-phase current source inverter is shown in Fig.8.38. As in the circuit of a single-phase CSI, the input is also a constant current source. In this circuit, six thyristors, two in each of three arms, are used, as in a three-phase VSI. Also, six diodes D_1, D_2, D_3, D_4, D_5 and D_6, each one in series with the respective thyristor, are needed here, as used for single-phase CSI.

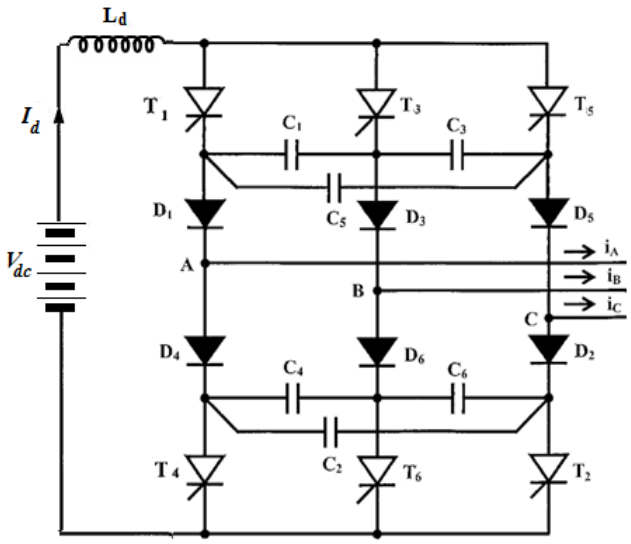

Fig. 8.38 Three-phase current source inverter.

Six capacitors, three each in two (top and bottom) halves, are used for commutation. It may be noted that six capacitors are equal, i.e. C1= C2 = C3.....= C6. The six diodes are needed in CSI, so as to prevent the capacitors from discharging through the load. The numbering scheme for the thyristors and diodes are same, as used in a three-phase VSI, with the thyristors being triggered in sequence as per number assigned in 120˚ conduction mode or 180˚ conduction mode discussed in three-phase voltage source inverter in subsections 8.4.1 and 8.4.2 respectively.

PROBLEMS

8. 1 (a) Draw the circuit diagram of a single-phase half-bridge inverter.
(b) Sketch the output voltage waveform and show conducting devices.
(c) Give an expression for the *rms* values of the inverter output (load) voltage.
(d) Sketch one transistor current and give its average value for a purely resistive load.
(e) What is the peak inverse voltage of the transistors?

8.2 A single-phase half-bridge inverter has a resistive load of 2.5 Ω and input voltage of 50 V. Calculate the following:

(a) The *rms* voltage of the fundamental frequency component,
(b) The output power,
(c) The average current and peak current,
(d) Harmonic *rms* voltage, and
(e) The total harmonic distortion factor.

[Ans : (a) 45 V, (b) 1000 W, (c) 10 A , 20 A , (d) 21.8 V , (e) 48 %]

8.3 For a single-phase transistor bridge inverter, the d.c. supply voltage V_{dc} = 300 V, the load consists of resistance R = 20 Ω in series with L = 40 mH and the output voltage frequency f_o = 50 Hz.

(a) Draw the output voltage and load current waveforms for highly inductive load.
(b) Determine the amplitude of the Fourier series terms of the output voltagewaveform up to the 9th order harmonics.
(c) What is the maximum value of the load current (i_{omax})?
(d) Calculate the power absorbed by the load (consider up to 9th order harmonics).

[Ans : (b) c_1=382 V, c_3 = 127.3 V, c_5 = 76.3 V, c_7 = 54.5 V, c_9 = 42.4 V , (c) I_{omax} = 37.5 A , (d) 4316 W]

8.4 For the single-phase bridge inverter circuit shown in Fig.8.39, V_{dc} =125V, load resistance R =10 Ω and output voltage frequency f_o = 50 Hz.

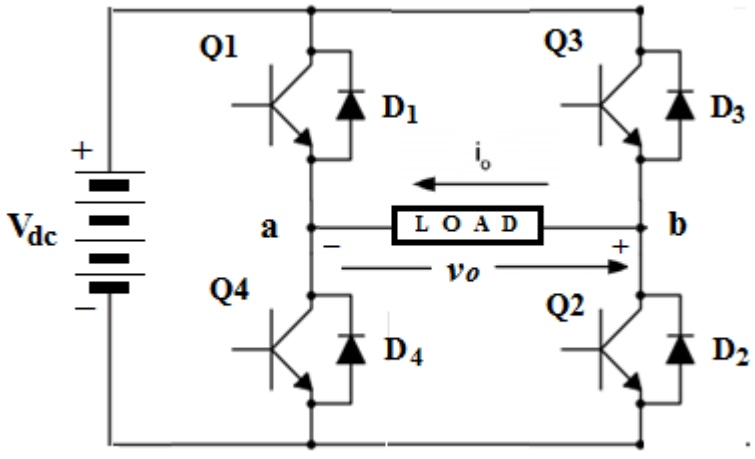

Fig.8.39.

(a) Write the Fourier series terms of the output voltage waveform up to the 7th order harmonic.
(b) Draw the output voltage and load current waveforms.
(c) Determine the value of the *rms* output voltage in terms of

harmonics rms values and the output power P_o (consider up to 7^{th} order harmonics).

(d) Calculate the average and peak currents of each transistor.

(e) Estimate the total harmonic distortion factor *THD* of the circuit.

[Ans : (a) $v_o(\omega t) = 159.12 \sin\omega t + 53.04 \sin 3\omega t + 31.82 \sin 5\omega t + 22.73 \sin 7\omega t$, (c) 121.78 V, 1483 W (d) 6.25 A, 12.5 A , (e) 48.36 %]

8.5 In a single-phase full-bridge PWM inverter, the control logic for power electronics devices is so adjusted that the output voltage waveform produced is a quasi-square as shown in Fig.8.40. The inverter has a resistive load of 5 Ω and input voltage of 100V. Find an expression for the Fourier coefficient of the output voltage for the first sixth harmonics and their corresponding harmonic currents.

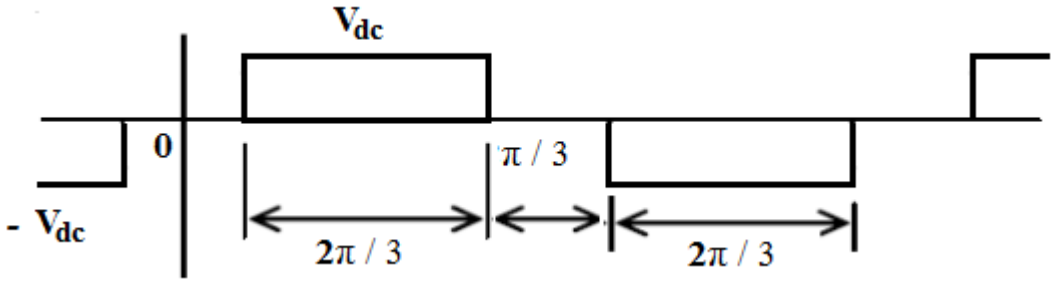

Fig.8.40.

[Ans: The Fourier series is

$$V_{dc} = 0\,, \qquad V_n \frac{4V_d}{n\pi\sqrt{2}} \sin\left(\frac{n\pi}{3}\right) \qquad n = 1,3,5, \ldots\ldots$$

{ Peak harmonics voltage and currents are : $V_1 = 77.97$ V, $V_3 = 0$, $V_3 = -15.95$ V, $I_{dc} = 0$A , $I_1 = 15.58$ A , $I_3 = 0$A , $I_5 = 3.19$ A}

8.6 A three-phase transistor voltage-source inverter supplies a three-phase load, as shown in Fig.8.41. The load consists of star connected resistance of 10 Ω in each phase. The inverter supply voltage is 200V d.c. and each inverter switch conducts for 120˚.

(a) Sketch the switching signals for the six transistors.

(b) Sketch the line-to-neutral voltage for one complete cycle of the output voltage.

(c) Sketch the line-to-line voltage for one complete cycle of the output voltage.

(d) Calculate the *rms* values of the first five harmonics in the line-to-line output voltage, including the fundamental.

(e) Calculate the *rms* values of the first five harmonics in the line-to-neutral output voltage, including the fundamental.

[Ans: (d) $V_{L\text{-}L}$ = 244.95 V, (e) V_{ph} = 141.42 V]

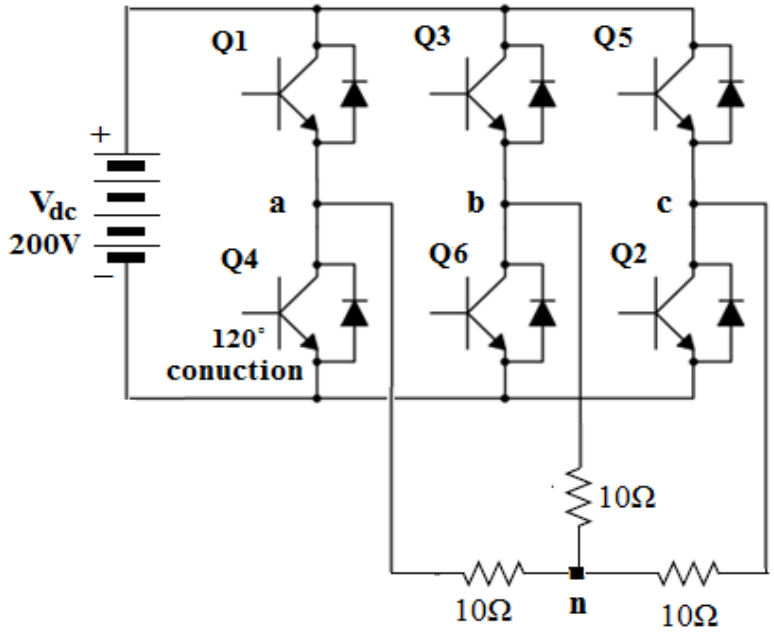

Fig.8.41.

8.7 A single-phase full-bridge voltage source inverter, fed from 200 V d.c. source. The output voltage is controlled by sinusoidal pulse width modulation technique. The carrier and modulating signals are so adjusted that the modulation index produces three pulses per half a cycle of widths, 20˚, 60˚, and 20˚. Assuming the load is purely resistive, find the *rms* value of the output voltage.

[Ans: 149 V]

8.8 For the inverter of problem 8.7, the strategy of output voltage control is changed such that the technique used is multiple pulse width modulation. The width of each pulse is 20˚ and each half cycle has 6 pulses,

(a) Determine the *rms* value of the output voltage,

(b) Find the pulse width to maintain the output *rms* value in (a) constant if the input voltage increases by 20%,

(c) What is the maximum input voltage if the maximum possible pulse width is δ_{max} = 25˚ ?

[Ans: (a) 163.3 V, (b) δ =13.8˚, (c) 179.45 V]

8.9 Repeat problem 8.7 above if single-pulse width modulation technique with $\delta = 120^\circ$ is used to control the output voltage.

[Ans: 163.3V]

8.10 Calculate the *rms* value of the output voltage waveform shown in Fig.8.19. The d.c. input voltage is 200V and the fundamental frequency component of the output voltage waveform is 100Hz.

[Ans: 94V]

8.11 (a) Explain with the aid of neat sketches of waveforms the voltage control using phase-displacement thchnique.

(b) The d.c. supply voltage of a single pulse width modulated inverter is 120V. Calculate the displacement angle to produce rms output voltages of 50V and 100V.

[Ans : 31.25^o , 125^o]

8.12 A three-phase natural commutated inverter is used to transfer power from a 300 V battery to a three-phase 230 V, 50 Hz a.c. bus. A large filter inductor with resistance 10Ω is included in the d.c. side. Estimate the power transferred for (a) $\alpha = 120^o$, (b) $\alpha = 150^o$.

[Hint : Use equations (8.59) – (8.61)]

[Ans: (a) 2248 W, (b) 834 W]

CHAPTER NINE

DC-AC CONVERSION: RESONANT INVERTERS AND MULTILEVEL INVERTERS

9.1 INTRODUCTION

All the inverters discussed in Chapter Eight are characterized by the so-called hard switching. This means that the transition of the switch from the off state to on state or vice versa occurs in the presence of nonzero voltages and currents. As a result, each switching action will associated with certain amount of power loss. This power loss is dependent on the current and voltage levels, and the energy loss due to this power will depend on the switching time.

On the other hand, if the voltage across the switching device subjected to transition from one conduction state to another is zero, or nearly zero current flowing through the device, there will be no losses or electrom-agnetic interference (EMI). This type of switching referred to as soft switching, which allows the device to operate even at high frequencies and leads to minimize the size of filters, transformers and the heat sinks needed.

In general, there are two types of soft switching, the zero-voltage switching (ZVS) and zero-current switching (ZCS), are used in what is called resonant inverters that are mainly used in low capacity power supplies. These types of converters utilize the phenomenon of electric circuit resonance to produce and generate nearly sinusoidal pulses. To explain the basic idea of the resonant inverter, the simple single-phase series resonant converter will first be considered in the following section.

9.2 SINGLE-PHASE SERIES RESONANT INVERTERS

In the series inverter with thyristor switches (unidirectional switches), the commutating circuit consists of an inductor in series with a capacitor as shown in Fig.9.1(a). When T_1 is triggered , current stars flows through the resistance R and the capacitor C start to charge, and the circuit is operates in mode-I as shown in Fig. 9.1(b). Current falls to zero at $t=t_{1m}$ and T_1 is self-commutated. When thyristor T_2 is triggered, the capacitor start discharging through C, L_2, T_2 and R causes a reverse current through the load and T_2 is also self-commutated. The circuit operates in mode-II and the resultant output current waveform will be as depicted in Fig.9.2. The series resonant circuit R LC must be under-damped; hence R, L and C must satisfy the following equation:

$$R^2 < 4L/C \qquad (9.1)$$

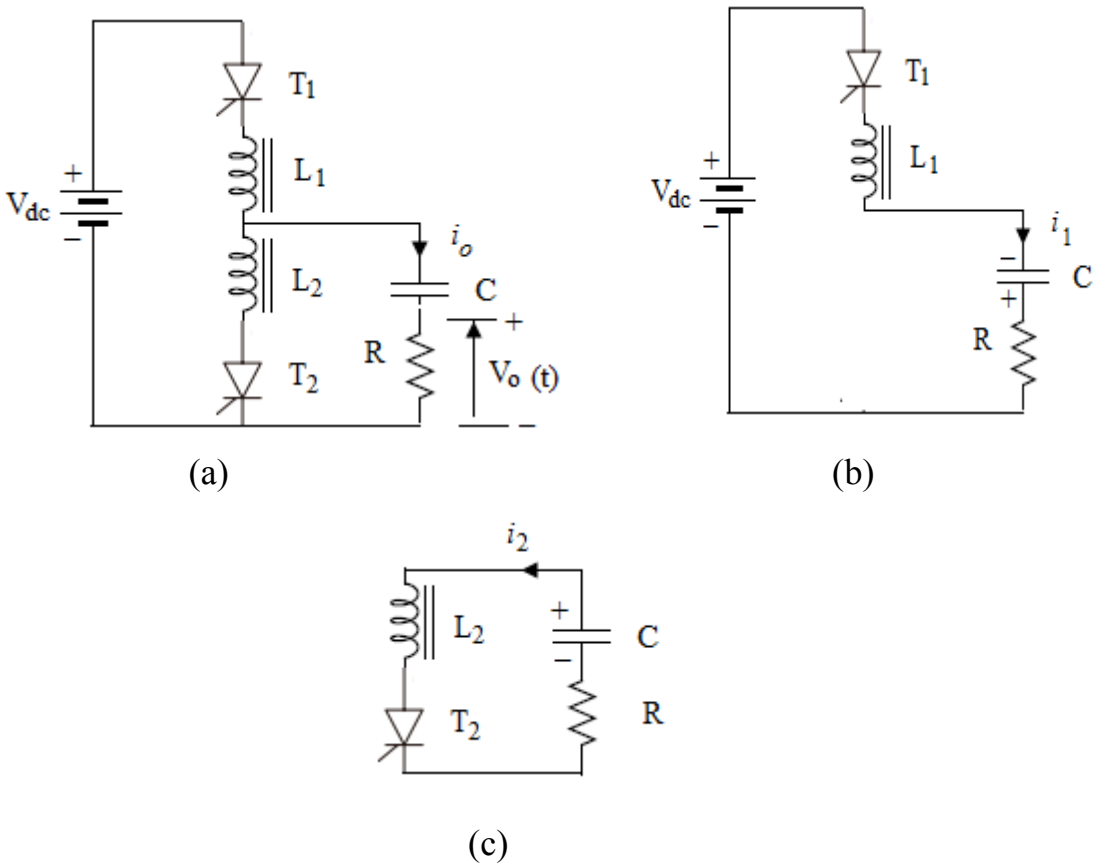

Fig.9.1 Series inverter: (a) Circuit (b) Mode-I operation, (c) Mode-II operation.

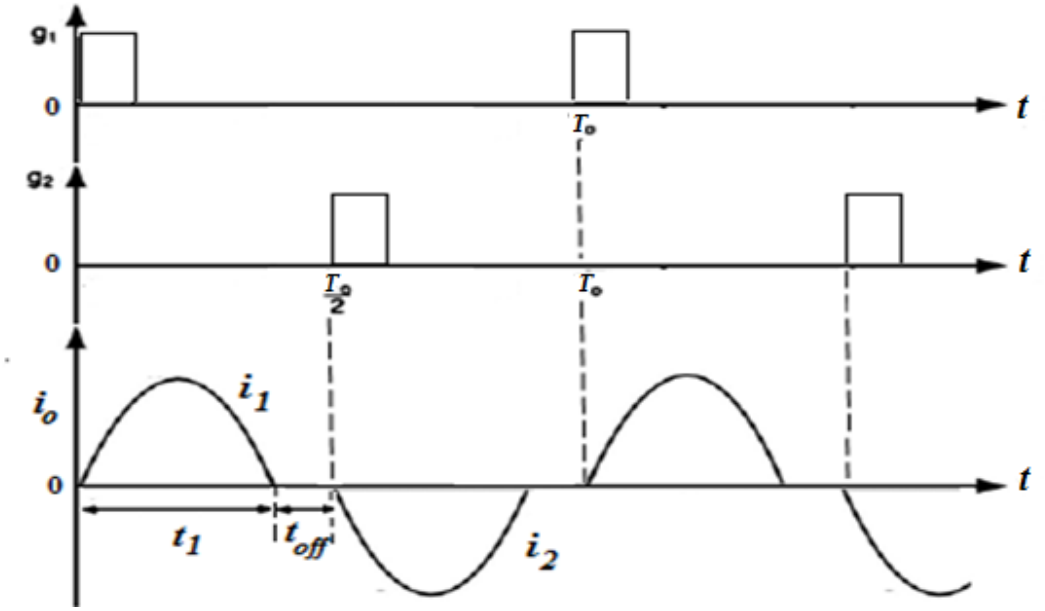

Fig.9.2 The resultant output current waveform of the series inverter.

For mode-I ,the instantaneous load current is described by

$$V_{dc} = Ri_1 + L\frac{di_1}{dt} + \frac{1}{C}\int i_1 dt + v_c(t=0) \qquad (9.2)$$

Solution of Eq.(9.2) for initial conditions : at $t = 0$, $i_1 = 0$, and $v_c = 0$ since the circuit is underdamped yields

$$i_1 = K_1 e^{\frac{-0.5\,R}{L}t} \sin 2\pi f_r\, t \qquad (9.3)$$

where f_r is the resonant frequency given by

$$f_r = \frac{1}{2\pi}\sqrt{\frac{1}{LC} - \frac{R^2}{4L^2}} \qquad (9.4)$$

The full-cycle of *RLC* oscillation T_o is

$$T_o = 2(t_1 + t_{off}) = \frac{2\pi}{\sqrt{\frac{1}{LC} - \frac{R^2}{4L^2}}} \qquad (9.5)$$

The constant K_1 can be found from initial conditions that at $t = 0$, the rate of rise of i_1 is

$$\frac{di_1}{dt} = \frac{V_{dc} + V_c}{2\pi f_r L} = K_1 \qquad (9.6)$$

and $$i_1 = \frac{V_{dc} + V_c}{2\pi f_r L} e^{\frac{-0.5\,R}{L}t} \sin 2\pi f_r\, t \qquad (9.7)$$

For mode-II , the current i_2 can be evaluated as

$$Ri_2 + L\frac{di_2}{dt} + \frac{1}{C}\int i_2 dt \; + \; v_c(t=0) = 0 \qquad (9.8)$$

Solution of Eq.(9.8) yields

$$i_2 = \frac{V_c}{2\pi f_r L} e^{\frac{-0.5\,R}{L}t} \sin 2\pi f_r\, t \qquad (9.9)$$

From Eq. (9.7), the instant of time t_{max} at which the current i_1 is maximum can be found as follows:

At t = t_{max} , $\frac{di_1}{dt} = 0$ and solution of Eq.(9.7) yields

$$t_{max} = \frac{1}{2\pi f_r} \tan^{-1} \frac{4\pi f_r L}{R} \qquad (9.10)$$

Capacitor voltage calculation during Mode-I and Mode-II:

For mode-I, the capacitor voltage can be found from

$$v_c = \frac{1}{C}\int i_1(t)dt \; - \; V_c \qquad 0 \le t \le t_1 \qquad (9.11)$$

where $t_1 = \frac{\pi}{2\pi f_r}$ and $i_1(t = t_1) = 0$

Solution of this equation gives

$$v_c\,(t = t_1) = (\,V_{dc} + V_c) e^{\frac{-\,R}{4Lf_r}t} \; + \; V_{dc} \qquad (9.12)$$

and for mode-III, when the capacitor charges up , the capacitor voltage can be found from

$$v_c = \frac{1}{C}\int i_1(t)dt \; - \; V_c \qquad 0 \le t \le t_2 \qquad (9.13)$$

where $t_2 = \frac{\pi}{2\pi f_r}$ and $i_2(t = t_2) = 0$

$$v_c\,(t = t_2) = (\,V_{dc} + V_c)e^{\frac{-\,R}{4Lf_r}t} \tag{9.14}$$

It is to be noted that T_2 cannot be triggered unless T_1 is turned off, otherwise T_1 and T_2 will conduct simultaneously which cause short-circuit to the d.c. supply. Therefore, the available off-time (dead zone) must be greater than the turn-off time of the thyristor, t_q .

$$\frac{\pi}{2\pi f_o} - \frac{\pi}{2\pi f_r} = \; t_{off} \; > t_q \tag{9.15}$$

where f_o is the frequency of the output voltage in rad /s. From Eq.(9.15), one can estimate the value of the maximum possible output frequency of the series resonant inverter as

$$f_{omax} = \frac{f_r}{(2f_r t_q \; + 1)} \tag{9.16}$$

Since the term $2f_r t_q$ is negligibly small, we can say that $f_{omax} \cong f_r$.

The resonant inverter in Fig.9.1 is very simple. It gives the principle of operation and basic concepts of utilizing resonant phenomena in *RLC* circuit to generate voltage or current waveforms at desired frequencies. The advantages of the series inverter is that the commutating components are part of the load and also the output waveform is nearly sinusoidal. However, its main disadvantages are, the load current flows through the commutating components *L* and *C*, so they must have high rating current. Also the maximum output frequency obtained is limited to the resonance frequency of the *RLC* circuit. One more distinct disadvantage of the series inverter is that, energy is taken from the source only in one half-cycle, hence high pulsed current from the d.c. supply is required.

The drawback of high pulsed current from the d.c. supply can be overcome by using a half-bridge and full-bridge configurations shown in Fig.9.3(a) and (b) respectively. In the half-bridge circuit of Fig.9.3(a), with $L_1 = L_2$ and $C_1 = C_2$, the power drawn from the source will be during the two half cycles of the output voltage. One half cycle of the load current will be supplied by one capacitor, either C_1 or C_2 and the other half is supplied by V_{dc}. In the full-bridge circuit of Fig.9.3(b), when Q_1 and Q_2 triggered simultaneously a positive voltage appears across the load resulting in positive pulse of current to flow. On the other hand negative pulse of current results when Q_3 and Q_4 are triggered simultaneously. This lead to continuous current drawn from the supply and higher output power is allowed to transfer to the load.

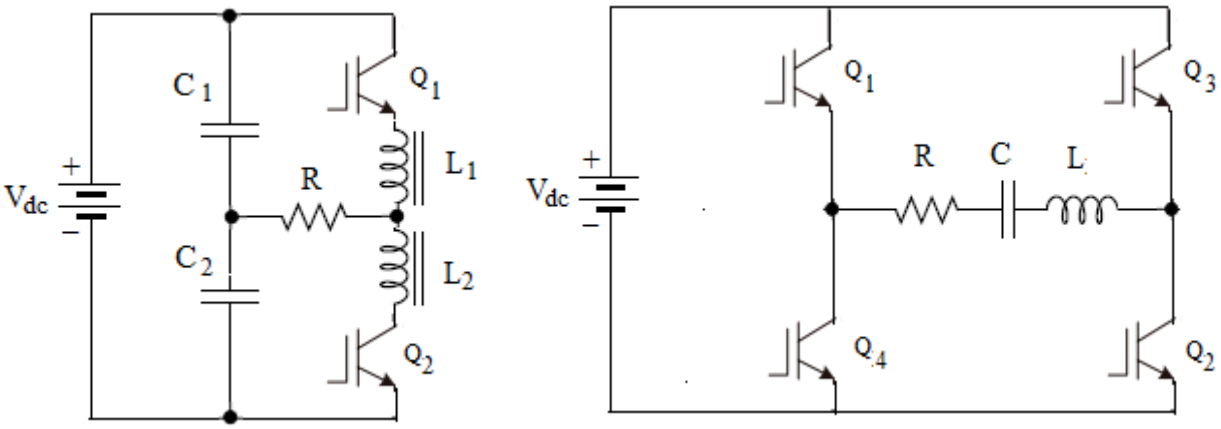

(a) (b)

Fig.9.3 Series resonant inverter : (a) Half-bridge, and (b) Full-bridge.

Analysis of the half-bridge series resonant inverter

The operation of the half-bridge resonant inverter cycle can be divided into two subcycles. To analyse the circuit of Fig.9.4(a), let us assume that, in the first subcycle, transistor Q_1 is closed for a period of t_1 and transistor Q_2 is off for the same period. The equivalent circuit for the first subcycle will be as depicted in Fig.9.4(a). The two capacitors C_1 and C_2 are charged now to V_{c1} and $V_{dc} - V_C$ respectively. The inductance L will store energy due to the flow of load current i_o whereas the capacitors C_1 and C_2 will share equally the load current. Ignoring the capacitor C_1 and by

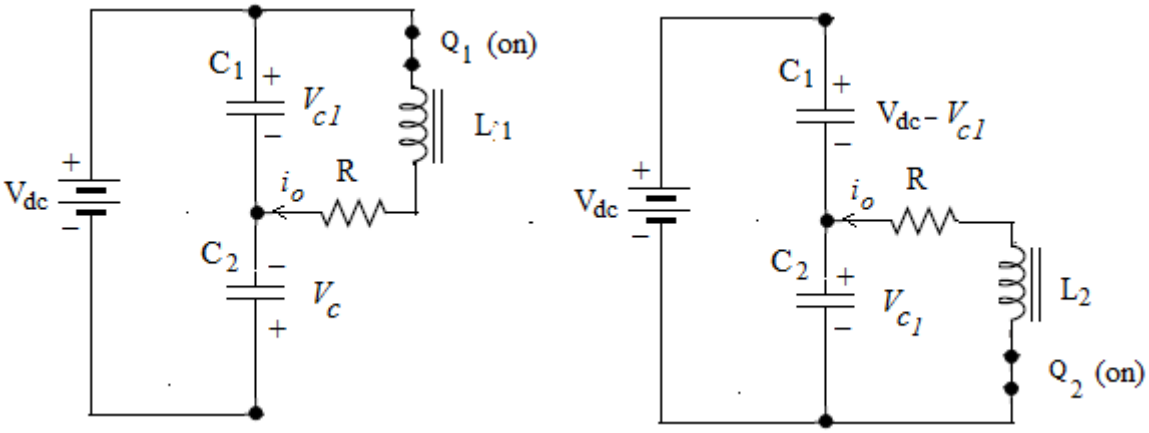

(a) (b)

Fig.9.4 Half-bridge series resonant inverter : (a) Equivalent circuit for the first subcycle, (b) Equivalent circuit for the second subcycle.

considering the outer loop of the equivalent circuit of Fig.9.4(a), the equation that govern this circuit can be written as

$$Ri_o + L\frac{di_o}{dt} + \frac{1}{2C_2}\int i_o dt + v_{c2}(t=0) = 0 \qquad (9.17)$$

If $C_1 = C_2$, for underdamped condition, and at $t = 0$, $i_o = 0$, $v_{c2} = 0$ as initial conditions, thus the load current is given by Eq.(9.18) as

$$i_o = \frac{V_{dc} + V_c}{2\pi f_r L} e^{\frac{-0.5\,R}{L}t} \sin 2\pi f_r\, t \qquad (9.18)$$

and since the effective capacitance is $C_1 + C_2 = 2C$, then the resonance frequency is

$$\omega_r = 2\pi f_r = \sqrt{\frac{1}{2LC} - \frac{R^2}{4L^2}} \qquad (9.19)$$

Example 9.1

The series resonant inverter shown in Fig.9.1(a) has $L_1 = L_2 = 100$ μH, $C = 2$ μF and $R = 1$ Ω. The d.c. input voltage is $V_{dc} = 200$ V and the frequency of output voltage is $f_o = 6.5$ kHz (this is not resonant frequency). The turn-off time of the thyristors is $t_q = 10$ μs. Determine,

(a) The resonant frequency of the circuit.
(b) Available turn-off time.
(c) Maximum permissible frequency.
(d) Time at which the load current is maximum.

Solution

(a) The output frequency is

$$\omega_o = 2\pi f_o = 2\pi \times 6500 = 40829 \text{ rad/s}$$

The resonant frequency is calculated from Eq.(9.4) as

$$f_r = \frac{1}{2\pi}\sqrt{\frac{1}{2 \times 100 \times 10^{-6} \times 2 \times 10^{-6}} - \frac{1^2}{4(100 \times 10^{-6})^2}}$$
$$= 11231 \text{ Hz}$$

$$\omega_r = 2\pi f_r = 2\pi \times 11231 = 70530 \text{ rad/s}$$

$$T_r = \frac{1}{f_r} = \frac{1}{11231} = 89\,\mu s$$

(b) From Eq.(9.15), the available turn-off time is

$$t_{off} = \frac{\pi}{\omega_o} - \frac{\pi}{\omega_r} = \frac{\pi}{40820} - \frac{\pi}{70530} = 32.4\ \mu s$$

(c) From Eq.(9.16) maximum permissible frequency f_{omax} is

$$f_{omax} = \frac{f_r}{(2f_r t_q + 1)} = \frac{11231}{(2 \times 11231 \times 10 \times 10^{-6} + 1)} = 9171 \text{ Hz}$$

(d) The instant of time t_{max} at which the supply current, and hence the load current, be maximum is given by Eq.(9.10) as

$$t_{max} = \frac{1}{2\pi f_r} \tan^{-1} \frac{4\pi f_r L}{R} = \frac{1}{\omega_r} \tan^{-1} \frac{2\omega_r L}{R}$$

$$= \frac{1}{70530} \tan^{-1} \frac{2 \times 70530 \times 100 \times 10^{-6}}{1} = 21.25\ \mu s$$

9.3 SINGLE-PHASE SINGLE-SWITCH RESONANT INVERTER

Another type of d.c. link resonant inverter is shown in Fig.9.5 where the d.c. voltage is used to supply energy to the load. A resonant *LC* circuit is inserted between the supply and load. A power transistor is connected across the capacitor C to control the output voltage.The power transistor is driven on and off at a fixed frequency *fs* and at a low duty cycle as shown in Fig. 9.6. When the transistor Q is turned on for a period 'ton', the current through the inductor *L* rises linearly. During the turn off period ' t_{off} ' of the transistor, a sinusoidal current flows through the capacitor C due to resonance. In the first half period of quasi-sine wave, the capacitor is charged to twice the d.c. input voltage and then it is discharge to zero during the next half period. This process of switching on and off at a fixed frequency with low duty cycle is repeated to obtain quasi-sinusoidal voltage across the capacitor.

Analytical properties of the load current waveform

When a gate pulse applied to transistor Q for a period of t_1 (t_{on}) switch Q closed, current i_s flows through the inductance L which start to store

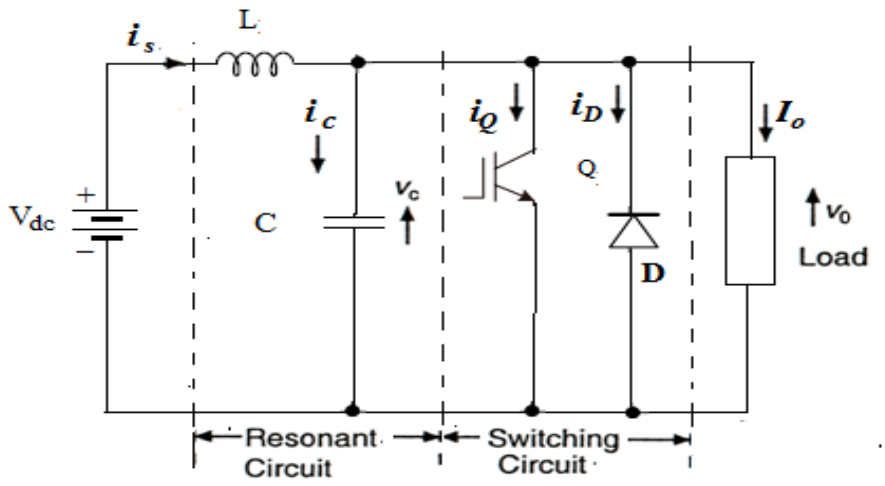

Fig.9.5 Single-phase single-switch resonant d.c. link inverter.

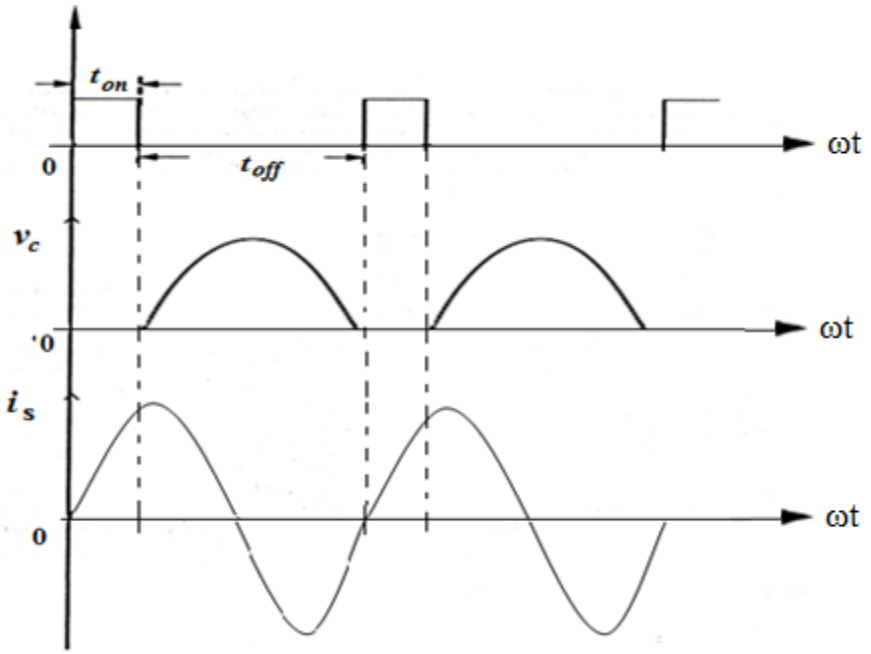

Fig.9.6 Capacitor voltage and inductor current.

energy from the d.c. supply and the circuit is governed by the following equation:

$$V_{dc} = Ri_s + L\frac{di_s}{dt} \qquad for \qquad 0 \le t \le t_{on} \qquad (9.20)$$

where R is the resistance of the non-ideal resonant circuit in ohms.

and $$i_Q = i_s - I_o \qquad (9.21)$$

thus $i_s(t) = \frac{V_{dc}}{R}\left(1 - e^{-t/\tau}\right) + I_1 e^{-t/\tau}$ (9.22)

where $\tau = \frac{L}{R}$

$$i_Q = \frac{V_{dc}}{R}\left(1 - e^{-t/\tau}\right) + I_1 e^{-t/\tau} - I_o \quad (9.23)$$

I_1 is the initial value of the input current i_s (t = 0).

At the end of first subcycle , the input current reach the maximum value I_2, equal to

$$I_2 = i_s(t = t_{on}) = \frac{V_{dc}}{R}\left(1 - e^{\frac{-Rt_{on}}{L}}\right) + I_1 e^{\frac{-Rt_{on}}{L}} \quad (9.24)$$

In the second subcycle, the transistor Q opens and the energy stored in the inductor is discharged through the capacitor. During this subcycle , both the transistor current i_Q and the diode current i_D are zero whereas the capacitor current i_c and the output voltage are given by

$$i_c = i_s - I_o \quad (9.25)$$

$$v_o = \frac{1}{C}\int_0^t i_c dt \quad (9.26)$$

Using KVL, the resonant circuit can be described by the following equation

$$V_{dc} = Ri_s + L\frac{di_s}{dt} + v_o \quad (9.27)$$

Substituting Eq.(9.25) in Eq.(9.26) and Eq.(9.26) in Eq.(9.27) ,yields

$$V_{dc} = Ri_s + L\frac{di_s}{dt} + \frac{1}{C}\int_0^t i_s dt - \frac{I_o}{C}\,t \quad (9.28)$$

If we assume that the resonant circuit is underdamped, the solution of the above equation gives

$$i_c = \left\{\left[\frac{V_{dc} - RI_o}{L\omega_r} + \frac{\alpha}{\omega_r}(I_o - I_2)\right] sin\omega_r t - (I_o - I_2)\cos\omega_r t\right\} e^{-\alpha t} \quad (9.29)$$

$$V_o = V_{dc} - RI_o + \left\{\left[\frac{\alpha}{\omega_r}(V_{dc} - RI_o) - \frac{(I_o - I_2)}{C\omega_r}\right] sin\omega_r t - (V_{dc} - RI_{o)}\cos\omega_r t\right\} e^{-\alpha t} \quad (9.30)$$

where $\alpha = \frac{R}{2L}$ (9.31)

and the damping resonance frequency is,

$$\omega_r = 2\pi f_r = \sqrt{\frac{1}{LC} - \frac{R^2}{4L^2}} \quad (9.32)$$

If the resonant circuit has high quality factor, thus $RI_o \ll V_{dc}$ and $\alpha \ll \omega_r$; then Eqs.(9.29) and (9.30) can mathematically reduced to

$$i_c = I\, sin(\omega_r t + \varphi_1)e^{-\alpha t} \quad (9.33)$$

$$v_o = V_{dc} - Vcos(\omega_r t + \varphi_2)e^{-\alpha t} \quad (9.34)$$

where

$$I = \sqrt{(\frac{V_{dc}}{L\omega_r})^2 + (I_o - I_2)^2} \qquad \varphi_1 = \tan^{-1}\frac{L\omega_r(-I_o + I_2)}{V_{dc}} \quad (9.35)$$

$$V = \sqrt{{V_{dc}}^2 + (\frac{I_o - I_2}{C\omega_r})^2} \qquad \varphi_2 = \tan^{-1}\frac{(-I_o + I_2)}{C\omega_r V_{dc}} \quad (9.36)$$

During the off subcycle (during the period t_{off}) , if we denote the final value of this period by I_3, then

$$I_3 = i_s(t = t_{off}) = I_o + I_c(t = t_{off}) = I_o + I\, sin(\omega_r t + \varphi_1)e^{-\alpha t} \quad (9.37)$$

In the next duration of t_{on2} ,

$$i_D = I_o - i_s \quad (9.38)$$

where i_s can again be found from Eq.(9.22) , that is

$$i_s(t = t_{on2}) = \frac{V_{dc}}{R}\left(1 - e^{\frac{-Rt_{on2}}{L}}\right) + I_3 e^{\frac{-Rt_{on2}}{L}} \quad (9.39)$$

Remember that, $t_{on1} = t_{on2}$ always.

Example 9.2

A series d.c. link resonant inverter in Fig.9.5 has L = 0.25 mH , C = 1 μF and R = 0.0 Ω. The d.c. voltage V_{dc} = 240 V and the frequency of the output voltage is f_o = 8 kHz (this is not resonant frequency).The current drawn from the inverter I_o is constant at 150 A whereas the input current, at the beginning of the operation cycle is 158 A. Determine the average output voltage V_o of the inverter.

Solution

The resonance frequency is calculated from Eq.(9.32) as

$$\omega_r = 2\pi f_r = \sqrt{\frac{1}{LC} - \frac{R^2}{4L^2}} = \sqrt{\frac{1}{LC}} = \sqrt{\frac{1}{0.25 \times 10^{-3} \times 1 \times 10^{-6}}}$$
$$= 63250 \text{ rad/s}$$

From Eq.(9.34) , since $e^{-\alpha t} = 0$

$$v_o = V_{dc} - V\cos(\omega_r t + \varphi_2)$$

where V and φ_2 are given by Eq.(9.36) , hence

$$V = \sqrt{240^2 + (\frac{-150 + 158}{63250 \times 10^{-6}})^2} = 271.3 \text{ V}$$

$$\varphi_2 = \tan^{-1}\frac{(-150 + 158)}{63250 \times 10^{-6} \times 240} = 1.015 \text{ rad} \rightarrow 58.2°$$

The output voltage of the link is

$$v_o = 240 - 271.3\cos(63250t + 1.015)$$

The period t_2 of the resonant subcycle can be calculated as

$$t_2 = \frac{2\pi - \cos^{-1}\frac{240}{271.3} - 1.015}{63250} = 8.38\ \mu s$$

The average value of v_o is calculated as

$$V_o = \frac{1}{T}\int_0^{t_2} v_o\, dt$$

where T = operating period = $1/f$ = 1/8000 =125 μs.

$$V_o = \frac{1}{125x10^{-6}} \int_0^{8.38x10^{-6}} (240 - 271.3\cos(63250t + 1.015))dt$$

9.4 SINGLE-PHASE DISCRETE PULSE MODULATED RESONANT INVERTER (DPMPI)

When the principle of operation of the d.c. link resonant inverter have been understood, single-phase and three-phase resonant voltage source inverter can be constructed in practice. Therefore, to illustrate this techn-ology, consider the single-phase circuit of this type of inverters shown in Fig.9.7. The output voltage v_c of the resonant d.c. link is fed to a single-phase bridge inverter. The resonant circuit consisting of L and C is provided between the d.c. source and the transistor bridge circuit. The operation of the inverter with *R*-load divided into three modes as shown in Fig.9.8.

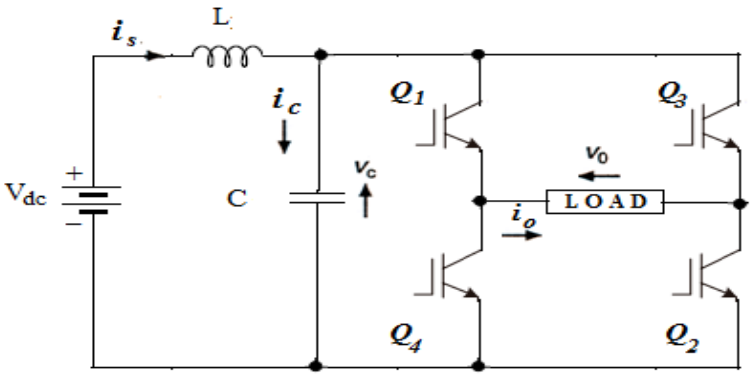

Fig.9.7 Single-phase discrete pulse modulated resonant inverter.

Mode-I (t_0, t_1)

The current through the resonant inductor increases linearly when Q_1 and Q_4 are turned on simultaneously for a period t_{on}. The voltage across the capacitor is zero. This mode ends at the instant t_1, when the base drive pulse for Q_4 is inhibited.

Mode-II (t_1, t_2)

A positive resonant pulse of the output voltage is initiated by driving Q_2 on. The source supplies both the load current and the capacitor charging current. Now the stored energy of the inductor is transferred to the capacitor. This mode ends when the capacitor voltage reaches V_{dc}.

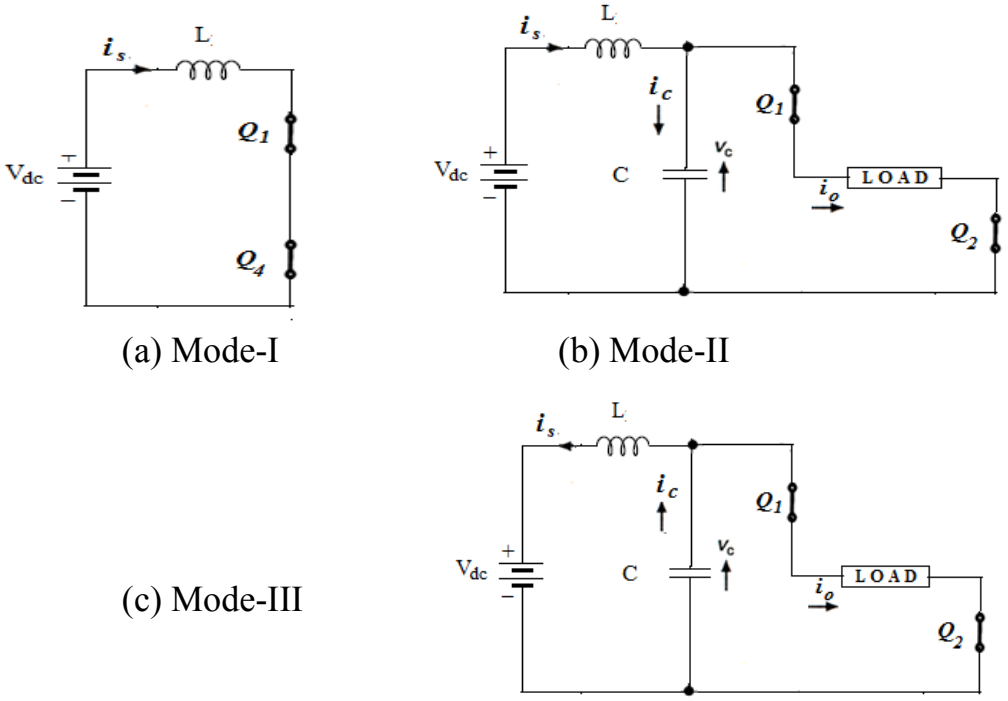

Fig.9.8 Modes of operation of single-phase PMRI with *R*-load.

Mode-III (t_2, t_3)

The base drive pulses to transistors Q_1 and Q_2 are retained. The capacitor discharges through the load and the d.c. source. This mode ends when the capacitor voltage reaches zero.The process of turning on and off is repeated 'm' times every half period of the output voltage. Thus a low frequency a.c. voltage consisting of an integer number of high frequency pulses instead of single pulse is generated. Hence this inverter is called discrete pulse modulation or high frequency integral pulse modulated resonant inverter.

When transistor Q_1 operates in the three modes described above, the inverter generates the positive group of pulses or the positive half-cycle of the output voltage waveform. In the same manner, when Q_3 operates in three modes (Figs.9.9 and 9.10), the inverter generates the negative group of the pulses or the negative half-cycle of the output voltage waveform. The waveforms of the output voltage with four pulses per half-cycle and base drive pulses to various transistors are shown in Fig.9.10. The waveforms of the output voltage with four pulses per half-cycle and base drive pulses to various transistors are shown in Fig.9.11.

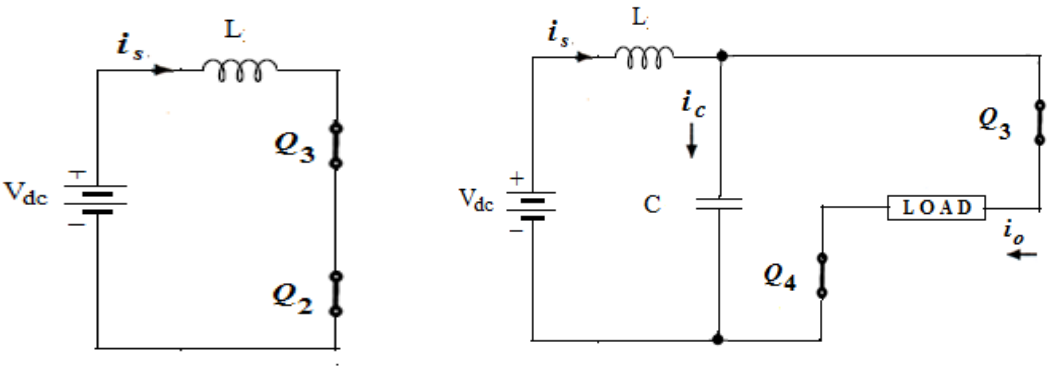

Fig.9.9 Modes of operation of transistor Q_3.

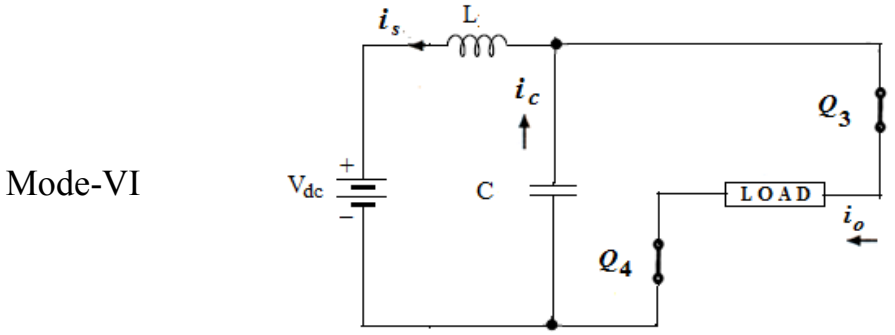

Fig.9.10 Modes of operation of transistor Q_3.

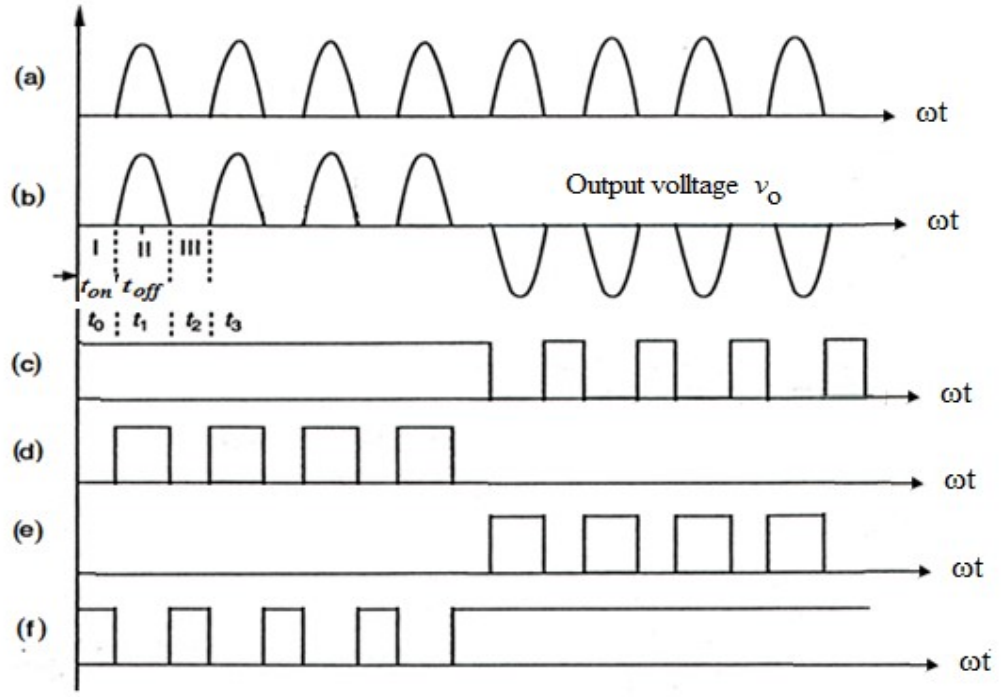

Fig.9.11 Waveforms of DPMPI with *R*-load:Output voltage is shown in (b) and the transistors pulses are shown in (c) to (f).

9.5 MULTILEVEL INVERTERS

In recent years, numerous industrial applications have begun to require higher power apparatus. A multilevel inverter is a power electronic device which is capable of providing high power (MW range) at desired a.c. voltage level and desired frequency by using low level multiple d.c. voltage sources. In high power applications such as motor drives in the range of 1 MW power, for example, would required votages in ranges such as 3.3 kV or 6.6 kV, at 50 Hz supply giving a d.c. link of 5 to 7 kV. The voltage supplied to the motor is also 3.3 kV or 6.6 kV or sometimes up to 12 kV, hence, the power swiching device used must has voltage rating of 8-10 kV which is not available in the market.

In power electronics the problem of handling high currents can be easily be solved by putting power devices in parallel or even connecting several converters in parallel. However, the problem of achieving the desired voltage handling can be solved by two ways : (1) either by using standard converter topologies with devices are connected in series or (2) by using alternative topology converters which a number of low voltage devices and that have some means for distributing the voltage stress amongst those devices. These converters are called multilevel converters. Multilevel converters not only achieve high power ratings, but also enable the use of renewable energy sources and transportation applications.

In order to understand the concept of handling the voltage by series connection of the power devices, consider a two-level inverter shown in Fig.9.12. This leads to creates two different voltages for the load.

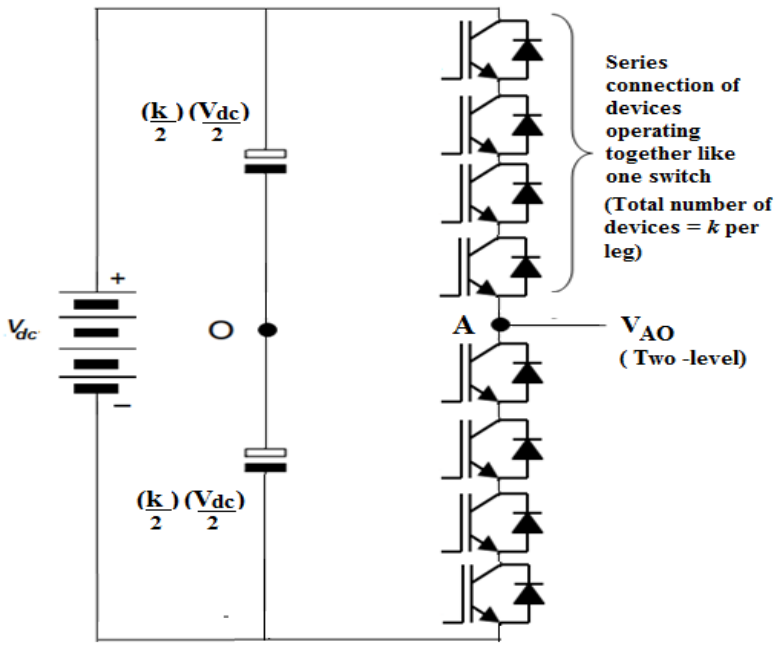

Fig.9.12 One inverter leg of simple 2-level inverter.

Now if a single d.c. source V_{dc} is available as an input to this inverter then it provides two voltages $+V_{dc}/2$ and $-V_{dc}/2$ on output. However, by assuming that the available power swiching devices are each can handles a voltage of V_{dc} , then by using k similar switches in series it can, theoretically, operate with a d.c. voltage of $(k/2)V_{dc}$. When the switches are off, the entire d.c. voltage appears across each switch and and this will be greater than the voltage rating of the individual switching devices.

Types of multilevel converters

There are several topologies of multilevel inverters available in industry. The difference lies in the mechanism of switching and the source of input voltage to the multilevel inverters. Three most commonly used multilevel inverter topologies are:

- Cascaded H-bridge multilevel inverters
- Diode-clamped multilevel inverters
- Flying-capacitor (capacitor-clamped) multilevel inverters

9.5.1 Cascaded H-Bridge Multilevel Inverters

The cascade H-bridge inverter uses several single-phase full-bridge (H-bridge) inverters connected in series to provide a nearly sinusoidal output voltage. Each inverter contains one H-bridge and separate d.c. source V_{dc} and the output voltage generated by this multilevel inverter is actually the sum of all the voltages generated by each individual inverter. This means that, if there are k cells in an H-bridge multilevel inverter then the number of output voltage levels will be $2k+1$. For example, Fig.9.13(a) shows a 5-level cascaded H-bridge inverter. The desired output voltage waveform is synthesized from the separate d.c. sources by generating five quasi-square wave of amplitude V_{dc} , and by proper selections of the triggering angle α ; the cascaded inverter output voltage waveform will be as depicted in Fig.9.13(b). As it can be seen that the output voltage of the multilevel converter is the sum of the individual inverter voltages which is $v_o = v_1 + v_2 + v_3 + v_4 + v_5$. Each inverter level can generate three different voltage outputs $+V_{dc}$, 0 , and $-V_{dc}$.

The H-bridge inverter has advantage over the other two as it requires less number of components as compared to the other two types of inverters and so its overall weight and price is also less. However, the waveform of the output voltage of the multilevel inverter is not a pure sinusoid but it is nearly sinusoidal that has less than 5% total harmonic distortion (THD) which is an acceptable one from the harmonics point of view. For a k cells in an H-bridge multilevel inverter, the output voltage is $v_o = v_1 + v_2 + v_3 + \ldots\ldots + v_k$, each inverter level can generate three different voltage outputs $+V_{dc}$, 0, and $-V_{dc}$.

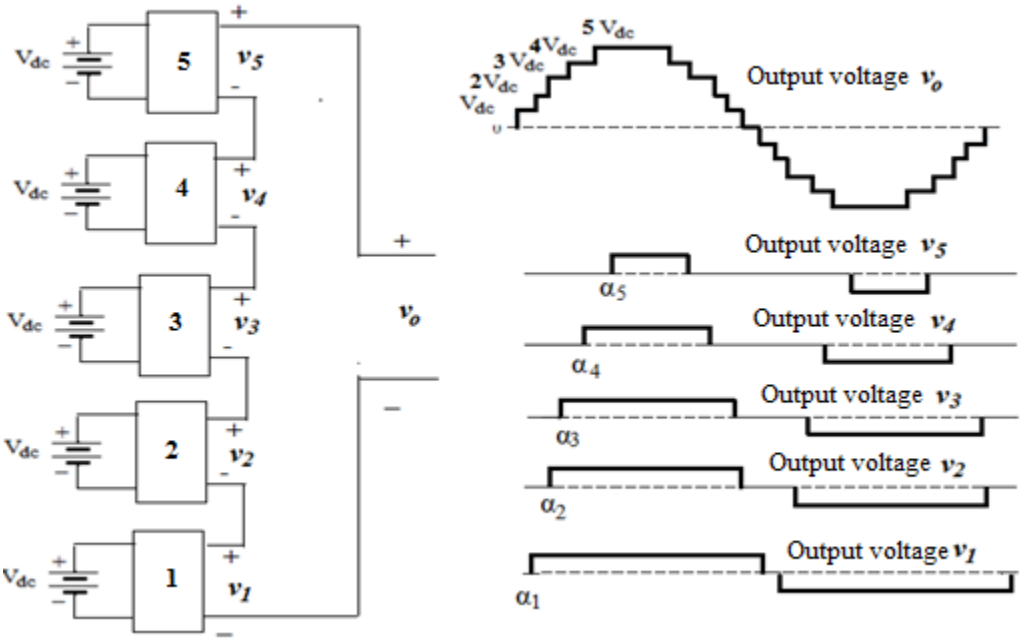

(a) (b)

Fig.9.13 (a) A five-source cascade multilevel converter. (b) Voltages at each output of H-bridge, and the total output voltage v_o.

Harmonic analysis of the multilevel inverter output voltage waveform

To generalize harmonic analysis, the Fourier series for a staircase output voltage waveform for k separate d.c. sources each equal to V_{dc} is given in reference [48] as

$$v_o\,(t) = \frac{4V_{dc}}{\pi} \sum_{n=1,3,5}^{\infty} [\cos(n\alpha_1) + \cos(n\alpha_2) + \cdots \cos(n\alpha_k)] \frac{\sin n\omega_o t}{n} \tag{9.40}$$

and the amplitudes of the nth order harmonic are thus

$$V_n = \frac{4V_{dc}}{n\pi} [\cos(n\alpha_1) + \cos(n\alpha_2) + \cdots \cos(n\alpha_k)] \tag{9.41}$$

for n = 1, 3, 5, 7, . . .

The modulation index Mi is the ratio of the amplitude of the fundamental frequency component of v_o to the amplitude of the fundamental frequency component of a square wave of amplitude kV_{dc}, which is $k\ (4V_{dc}/\pi)$. Hence, the modulation index is given by :

$$M_i = \frac{V_1}{4kV_{dc}/\pi} = \frac{[\cos(n\alpha_1) + \cos(n\alpha_2) + \cdots \cos(n\alpha_k)]}{k} \qquad (9.42)$$

Specific harmonics can be eliminated from the output voltage waveform with the proper selection of the triggering angles α in Eq.(9.40). For the *k*-source converter, harmonic *m* can be eliminated by using triggering angles such that

$$\cos(n\alpha_1) + \cos(n\alpha_2) + \cdots \cos(n\alpha_k) = 0 \qquad (9.43)$$

To eliminate the m^{th} order harmonic and also meet a specified modulation index for the *k*-source inverter requires the simultaneous solution to Eq.(9.43) and the additional equation derived from Eq.(9.42),

$$\cos(n\alpha_1) + \cos(n\alpha_2) + \cdots \cos(n\alpha_k) = kM_i \qquad (9.44)$$

To understand the problem let us take a simple example for a two-source multilevel inverter where k =2 :

Example 9.3

For the 2-source multilevel inverter shown in Fig.9.14 with V_{dc} =150 V:

(a) Determine the Fourier coefficients up to the 9th order harmonic (n = 9) and the modulation index for $\alpha_1 = 20^o$ and $\alpha_2 = 40^o$.

(b) Determine α_1 and α_2 such that the third harmonic (n =3) is eliminated and M_i = 0.795.

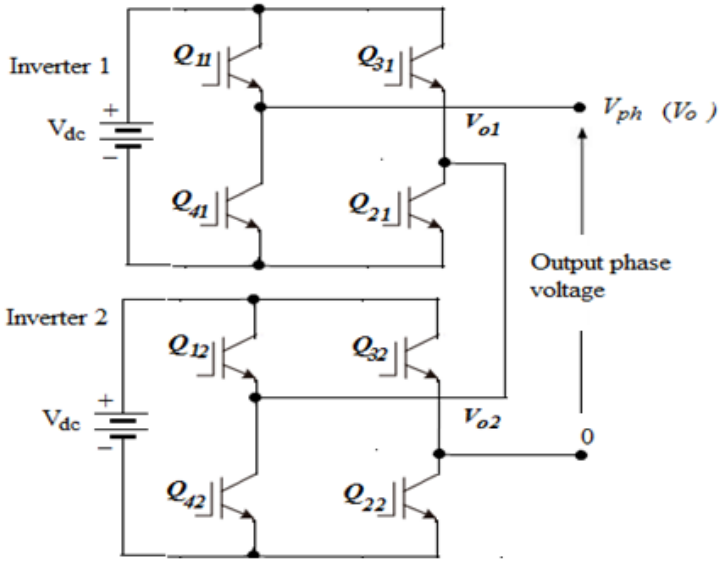

Fig. 9.14 Two-source multilevel inverter .

Solution

(a) Using Eq.(9.41) to evaluate the amplitudes of the harmonics as follows:

$$For\ k = 2: \qquad V_n = \frac{4V_{dc}}{n\pi}[\cos(n\alpha_1) + \cos(n\alpha_2)]$$

$$= \frac{4(150)}{n\pi}[\cos(n20°) + \cos(n40°)]$$

For n =1, 3, 5, 7, 9, this will result in :

$V_1 = 190.2$, $V_3 = 0$, $V_5 = -42.6$, $V_7 = -16.2$, $V_9 = 0$.

The modulation index M_i is calculated from Eq.(9.42) for k =2 ,

$$M_i = \frac{\cos(n\alpha_1) + \cos(n\alpha_2)}{k} = \frac{[\cos(n \times 20°) + \cos(n \times 40°)}{2} = 0.85$$

(b) The third harmonic component can be eliminated for modulation index $M_i = 0.795$ requires the solution of the equations

$$\cos(3\alpha_1) + \cos(3\alpha_2) = 0$$

and

$$\cos(\alpha_1) + \cos(\alpha_2) = 2 \times M_i = 1.59$$

Using numerical solution by iteration technique yields

$\alpha_1 = 7.5°$ and $\alpha_2 = 52°$

Voltage and frequency control in multilevel inverters

It is worth to not that one of the main advantage of the multilevel inverter is the standard PWM techniques can be used to control the output voltage and frequency as shown in Fig.9.15 for 3-level and Fig.9.16 for 5-level inverter respectively. Although this method has advantages in generating alternating voltages but it has disadvatage as it creates harmonic distortions in the output voltage and also has a high *dv/dt* as compared to that of a multilevel inverter. Generally, this method works effectively in many industrial applications. On the other hand, this method, in some applications creates technical problems, particularly, the applications that need low distortion in the output voltage.

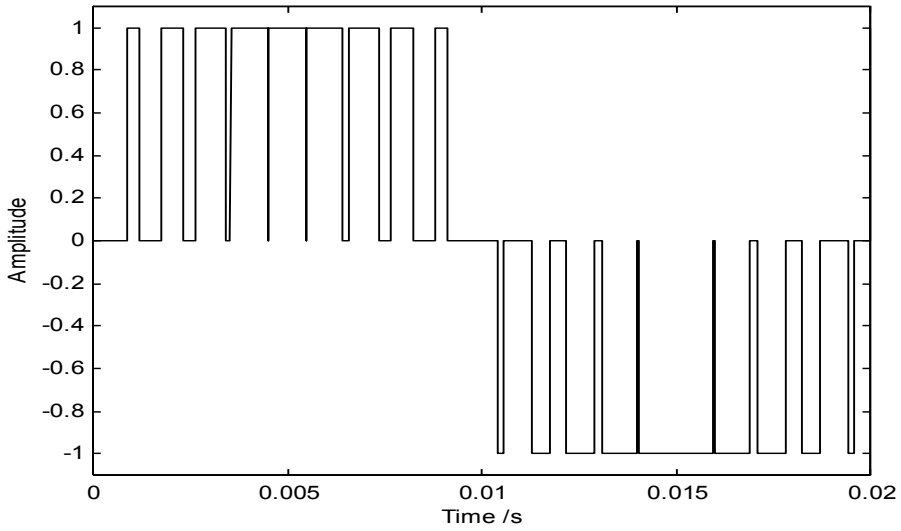

Fig. 9.15 Example of 3-level line-to-line waveform produced by an inverter with standard 2-level inverter legs (H-bridge).

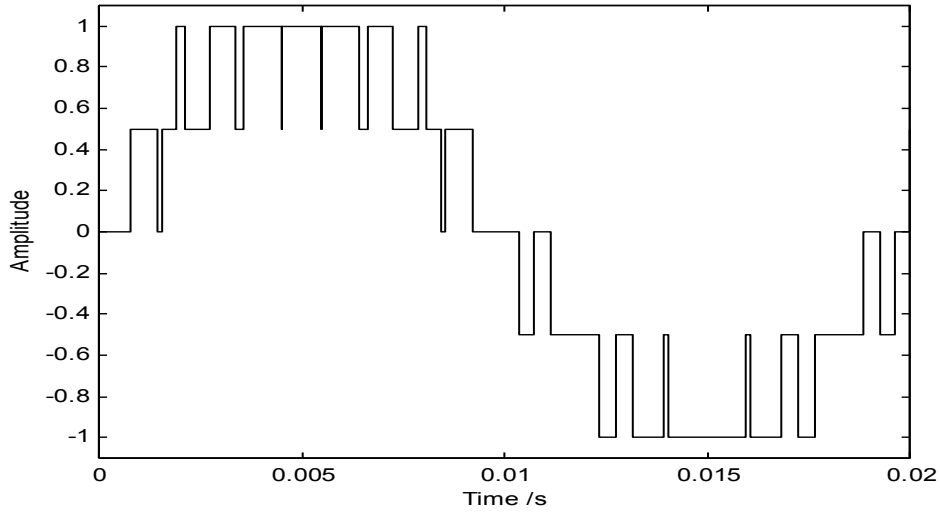

Fig.9.16 Example of 5-level line-to-line waveform produced by an inverter with individual legs that can produce 3-levels.

Applications of Cascaded H-bridge Multilevel Inverters

The main application of the cascaded H-bridge multilevel inverters are mostly used in battery based renewable energy resources as static var applications. Cascaded H-bridge multilevel inverters can be used in a delta or wye form as in photovoltaic cell or fuel cell. This is the example of parallel connectivity of the H-bridge multilevel inverter. H-bridge can

also be used in car batteries to run the electrical components of the car. Also this can be used in electrical braking system of the vehicles.

Scientist and engineers have also proposed the multiplicative factor on Cascade H-Bridge Multilevel. It means that rather than using a d.c. voltage with difference in levels, it uses a multiplying factor between different levels of the multilevel, i.e. every level is a multiplying factor of the previous one.

Advantages of Cascade H-Bridge Multilevel Inverters

1. Output voltage levels are doubled the number of sources.
2. Manufacturing can be done easily and quickly.
3. Packaging and layout is modularized.
4. Easily controllable by using ordinery transformer.
5. Low cost.

Disadvantages of Cascade H-Bridge Multilevel Inverters

1. Every H-bridge needs a separate d.c. source.
2. Large number of d.c. sources needed limits its applications.

9.5.2 Diode-Clamped Multilevel Inverters

The most commonly used multilevel topology is the diode clamped inverter, in which only a single source d.c. volage is used. A diode is used as the clamping device to clamp the d.c. bus voltage so as to achieve steps in the output voltage as shown in Fig.9.17.

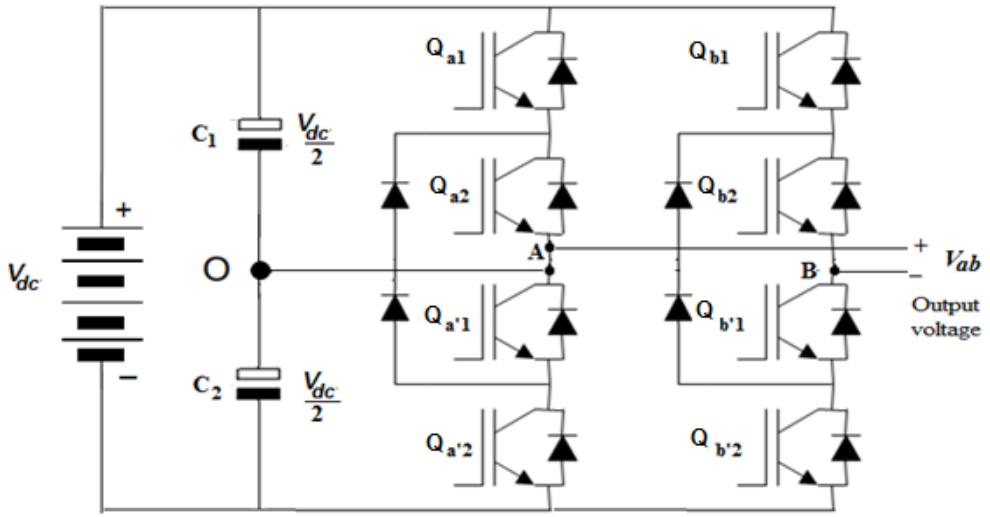

Fig.9.17 Two-phase diode-clamped inverter.

In this circuit, the main concept is to use diodes to limit voltage stress of power devices. It was first proposed in 1981 by Nabae, Takashi and Akagi and it is also known as neutral point converter. In its simple form the diode-clamped inverter consists of two pairs of series switches (upper and lower) connected in parallel with two series capacitors where the anode of the upper diode is connected to the midpoint (neutral) of the capacitors and its cathode to the midpoint of the upper pair of switches; the cathode of the lower diode is connected to the midpoint of the capacitors and divides the main d.c. voltage into smaller voltages, as illustrated in Fig.9.17.

The middle point of the two capacitors is defined as the "neutral point" and the converter uses a single d.c. bus that is subdivided into a number of voltage levels by a series string of capacitors. For a three-level diode clamped-inverter if the point **O** is taken as the ground reference, the output voltage has three values 0 ,+ ½ V_{dc} and -1/2 V_{dc} . In Fig.9.17 which shows a two-phase diode-clamped multilevel inverter, the line to line voltages of two legs with the capacitors are: V_{dc} ,+ ½ V_{dc} , 0 , - ½V_{dc} and - V_{dc} . Three phases are necessary to generate a three-phase voltage.

A k level inverter needs (k-1) voltage sources, 2(k-1) switching devices and (k-1) (k-2) diodes. By increasing the number of voltage levels the quality of the output voltage is improved and the voltage waveform becomes nearly sinusoidal. Figure 9.18 shows a three-level diode-clamped converter in which the d.c. bus consists of two capacitors, C1, and C2. For d.c. bus voltage V_{dc}, the voltage across each capacitor is $V_{dc}/2$ and each device voltage stress will be limited to one capacitor voltage level V_{dc}/2 through clamping diodes.

To explain how the staircase voltage is synthesized, the neutral point n is considered as the output phase voltage reference point. The concept of diode-clamped inverter can better be understood by looking into three-phase three-level diode-clamped inverter shown in Fig.9.18. Here the common d.c. source is supplying all the phases by using two capacitors and three levels. Each capacitor has a voltage of V_{dc}/2 and same is the voltage limit of switching devices. This type of inverter is use mostly for high power applications (500kW – few MW) for motor drives. Fig.9.19 shows the schematic diagram of a 5-level diode-clamped multi-level inverter.

Applications of Diode-Clamped Multilevel Inverters

The most common application of diode-clamped multilevel inverter is when a high voltage d.c. and a.c. transmission lines are interfaced. This can also be used in variable speed control of high power drives. Static variable compensation is also an application of diode-clamped multilevel inverters.

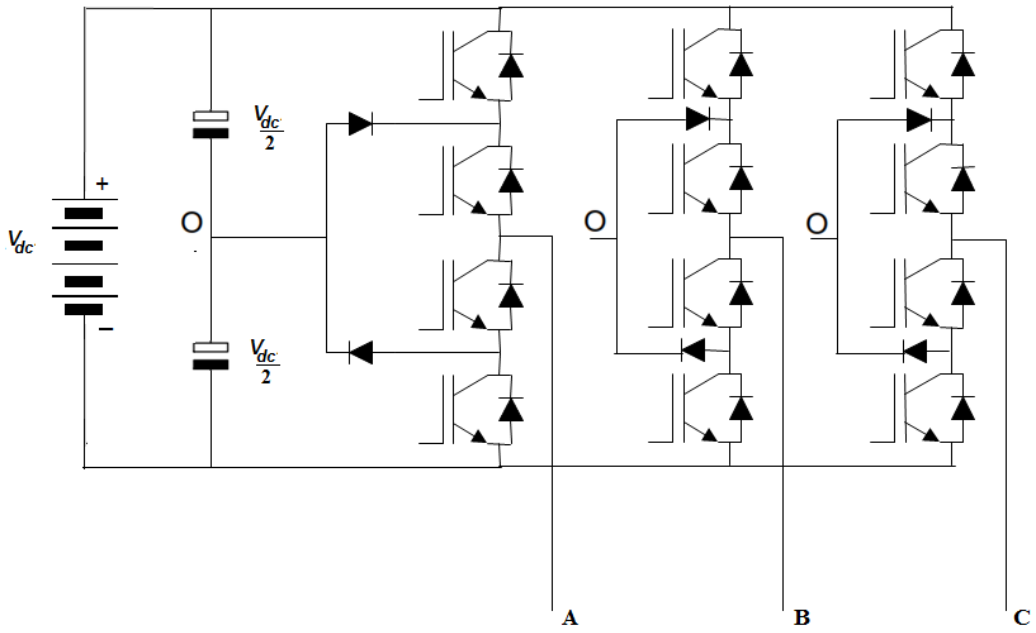

Fig.9.18 Three-level three- phase inverter: V_{AO} etc are 3-level ($+V_{dc}/2$, 0 , $-V_{dc}/2$)V_{AB} etc are 5-level ($+V_{dc}$, $+V_{dc}/2$, 0 , $-V_{dc}/2$, $-V_{dc}$).

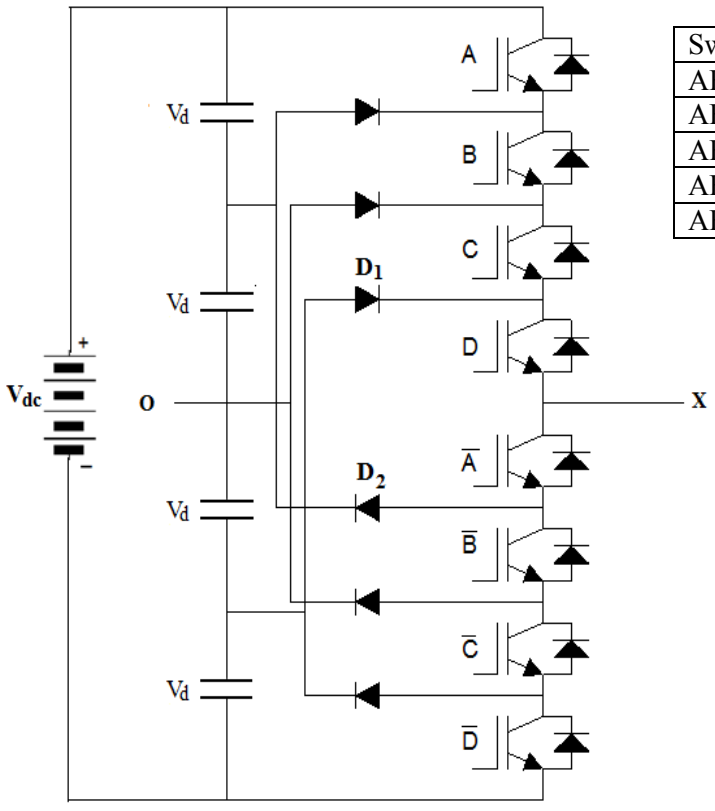

Switches	State	Voltage
ABCD	1111	V_{XO} = +2Vd
ABCD	0111	V_{XO} = +Vd
ABCD	0011	V_{XO} = 0
ABCD	0001	V_{XO} = -Vd
ABCD	0000	V_{XO} = -2Vd

Fig.9.19 Five-level diode-clamp multi-level inverter (only one inverter leg is shown).

Note: D_1 has to block $3V_d$ when ABCD=1111, D_2 has to block $3V_d$ when ABCD=0000.

Advantages of Diode-Clamped Multilevel Inverters:

1. Only one isolated d.c.supply is required.
2. Only one set of split d.c. link caps required
3. With the same number of devices (ignoring clamp diodes) of equal voltage rating, the circuit can produce the same output voltage levels as the isolated H-bridge solution and operate with the same d.c. link voltage as the series switch solution. Outputs of each phase can be understood by the table given next to Fig.9.19. Condition 0 means switch is OFF and vice versa.
4. By operating the circuit such that the output from each leg changes one level at a time, the problem of device voltage sharing during transients (dynamic sharing) is avoided. This however, makes the switching pattern more restricted than the isolated H-bridge solution. Note: static voltage sharing is not guaranteed without parallel resistors.
5. Capacitance of the capacitors used is low.
6. Back to back inverters can be used.
7. Capacitors are pre-charged.
8. At fundamental frequency, efficiency is high.

Disadvantages of Diode-Clamped Multilevel Inverters:

1. As the number of levels increases, some diodes have to block large voltages (e.g. D_1 and D_2 in Fig.9.18) makes the circuits unattractive for more than 5-levels since many diodes in series are required.
2. Difficult to build in redundancy.
3. Clamping diodes are increased with the increase of each level.
4. DC level will discharge when control and monitoring are not precise.

9.5.3 Flying-Capacitor Multilevel Inverters

Fig.9.20 shows one inverter leg of a 3-level flying-capacitor inverter circuit. The structure of this inverter topology is quite similar to diode clamp inverter except the difference that here flying capacitors is used in order to limit the voltage instead of diodes.The flying capacitor involves series connection of capacitor clamped switching cells. This topology has a ladder structure of d.c. side capacitors, where the voltage on each capacitor differs from that of the next capacitor. The voltage increment between two adjacent capacitor legs gives the size of the voltage steps in the output waveform.

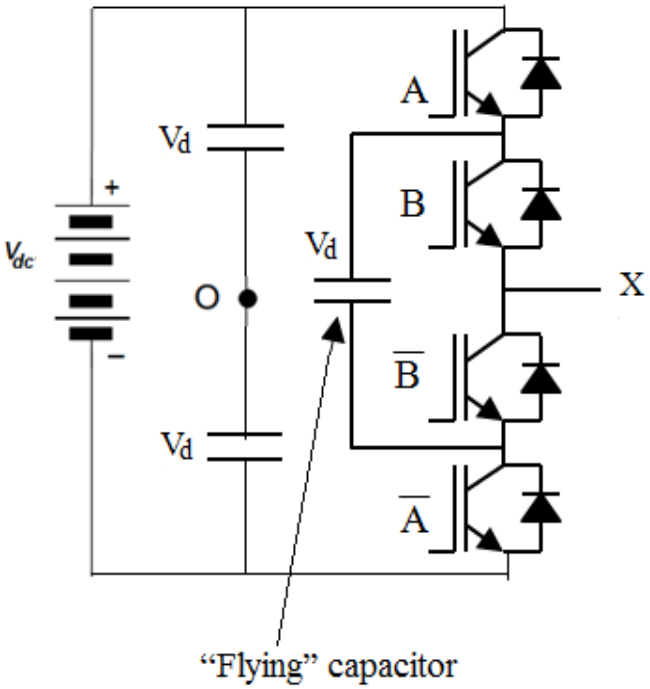

Switches	State	Voltage
AB	11	$V_{XO} = +Vd$
AB	01	$V_{XO} = 0$
AB	10	$V_{XO} = 0$
ABCD	00	$V_{XO} = -Vd$

Fig.9.20 Three-level flying-capacitor inverter circuit.

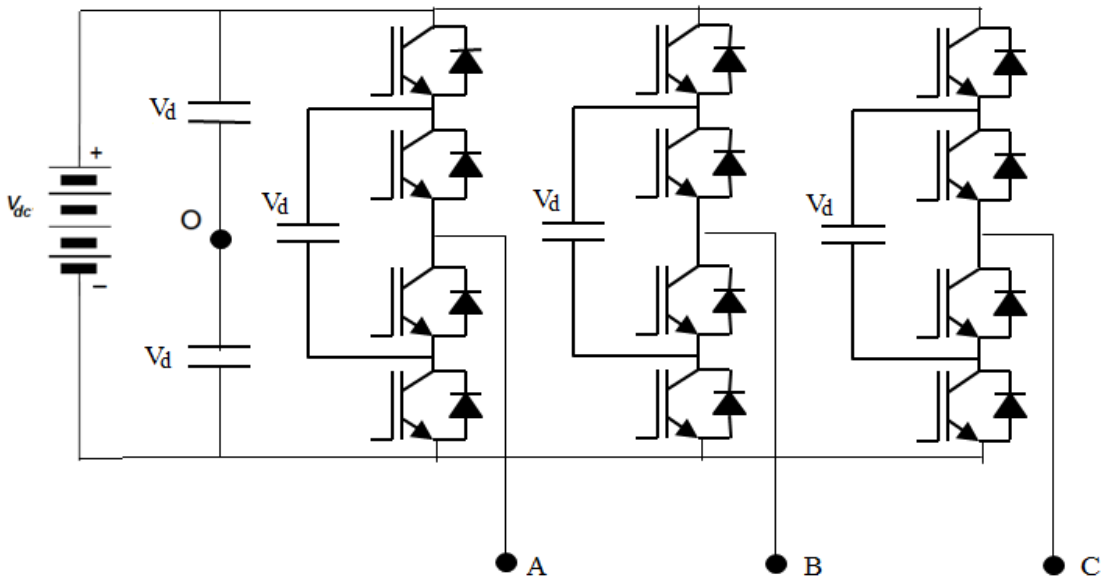

Fig.9.21 Three-phase inverter with 3-level flying-capacitor.

For a 3-level inverter, using flying-capacitor (Fig. 9.20), the voltage of phase-leg "a" output with respect to the neutral point "o" (i.e.Vox), can be synthesized by the switch combinations as given in the table next to the same figure. A complete three-phase inverter with 3-level flying-capacitor legs is depicted in Fig.9.21.

V_{AO} etc are 3-level ($+V_d$, 0 , $-V_d$)

V_{AB} etc are 5-level ($+2V_d$, $+V_d$, 0 , $-V_d$, $-2V_d$)

A k level flying-capacitor inverter with ($2k$ – 2) switches will use (k – 1) number of capacitors in order to operate. Fig.9.22 shows a five level flying-capacitor multilevel inverter. A k level inverter will require a total of (k-1)×(k-2)/2 clamping capacitors per phase leg in addition to (k-1) main d.c. bus capacitors**.** The voltage levels and the arrangements of the flying capacitors in the flying-capacitor multilevel inverter structure assures that the voltage stress across on each main device is same and is equal to V_{dc} /(k-1), for a k-level inverter. The voltage synthesis in a five-level capacitor clamped converter has more flexibility than a diode-clamped converter.

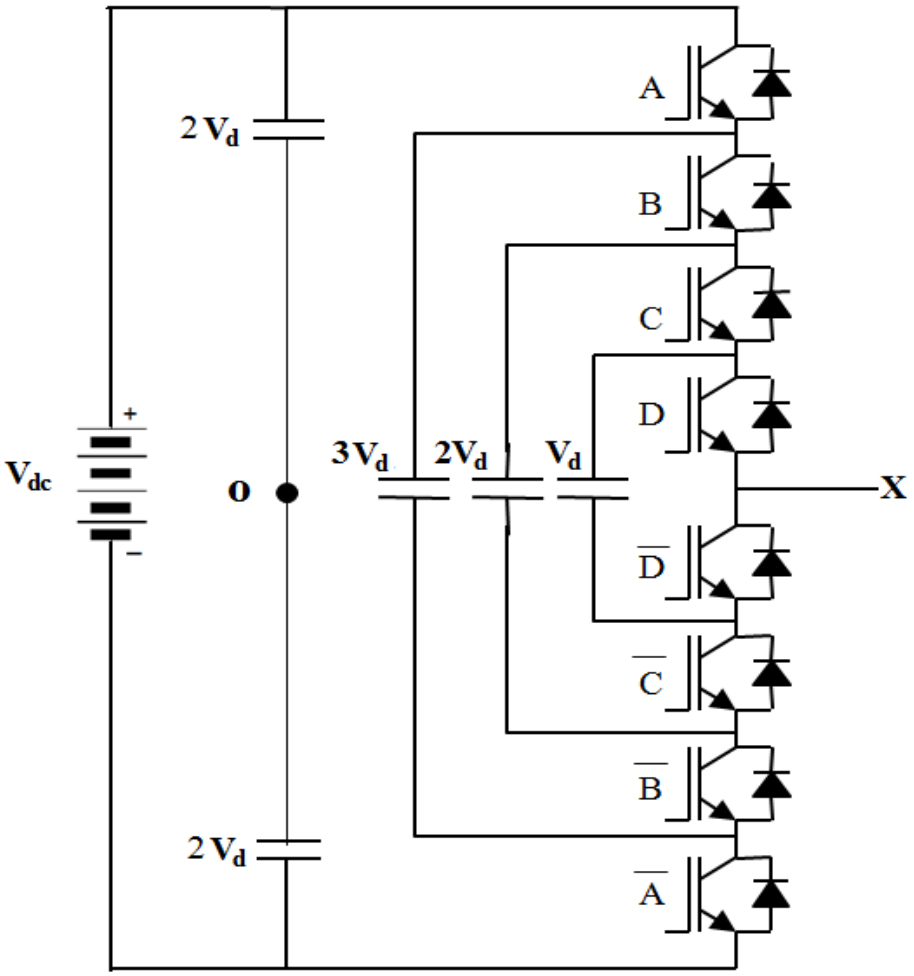

Fig.9.22 Five-level flying-capacitor circuit (One inverter leg shown).

Advantages of Flying-Capacitor Multilevel Inverters:

1. Only one d.c. supply is required.
2. Device voltage sharing is guaranteed (both static and dynamic) if the flying-capacitors are kept charged the correct voltage.
3. No high voltage silicon devices are required (unlike the diodes in the diode-clamped circuit).
4. With the same number of devices of equal voltage rating, the circuit can produce the same output voltage levels as the isolated H-bridge solution and the diode-clamped solution and operate with the same d.c. link voltage as the series switch solution.
5. Capacitor-clamped multilevel inverters are considered to be the best in static var generation .
6. Phase redundancies are available for 'balancing capacitors' voltage levels .
7. Reactive and real power flow can be controlled easily.

Disadvantages of Flying Capacitor Multilevel Inverters:

1. Capacitors are expansive than diodes.
2. "Flying" capacitors need to be pre-charged (Complex startup).
3. Switching strategy must be used to maintain flying-capacitors at the correct voltage. This must be done via some form of feedback mechanism (switching efficiency is poor).
4. As the number of levels increases, the number of capacitors required increases rapidly (note that the flying capacitors supporting more than V_d will generally be made from a number of series connected capacitors).
5. Voltage control is difficult for all the capacitors.

PROBLEMS

9.1 By giving four reasons explain why resonant converters are superior to their hard switched counterparts at higher switching frequencies.

9.2 In a resonant forward converter, the switch is subject to a higher voltage stress than when used in its hard switched counterpart but it produces less EMI (electromagnetic interference). Explain why.

9.3 The basic series resonant inverter shown in Fig.9.1(a) has $L_1 = L_2 = 20$ μH, C = 4 μF and $R = 4$ Ω. The d.c. input voltage is $V_s = 220$ V and the frequency of output voltage is $f_o = 5.5$ kHz. The turn-off time of the thyristors is $t_{off} = 15$ μs. Determine,

(a) The resonant frequency of the circuit.
(b) Available turn-off time.
(c) Maximum permissible frequency.
(d) Time at which the load current is maximum .

[Ans: 7961.78 Hz, 28.1 μs, 6451.6 Hz, 9.26 μs]

9.4 A series d.c. link resonant inverter in Fig.9.5 has $L = 0.24$ mH , $C = 1$μF and $R = 0.0$ Ω. The d.c. voltage $V_{dc} = 200$ V and the frequency of output voltage is $f_o = 10$ kHz (this is not resonant frequency). The current drawn from the inverter I_o is constant at 200 A whereas the input current, at the beginning of the operation cycle is 209 A. Determine the average output voltage V_o of the inverter.

[Ans : 200 V]

9.5 Give at least two distinct reasons why a multilevel power converter may be better than a 2-level topology with series connection of IGBTs for use in medium and high voltage applications.

9.6 Explain why a multilevel power inverter produces a better output voltage waveform compared with that of the 2-level voltage source inverter. Which type is then considered to be more suitable for high power level applications.

9.7 What are the major problems that may be encountered when a high power conventional 2-level PWM inverter with a high d.c. link voltage is constructed. The conventional 2-level topology used series connected devices to achieve the required voltage rating. Explain, with the aid of a sketch showing the circuit arrangement (assume a 3-phase output is

required), how these problems can be overcome using a multi-level circuit employing series connection of isolated H-bridges. Discuss any disadvantages associated with this latter solution.

9.8 Draw a circuit diagram for one leg (including the associated d.c. link capacitors) of a 3-level inverter employing the "flying-capacitor" technique. List the possible gating patterns (clearly indicating which are the gated devices for each) and determine the voltage between the d.c. link center point and the inverter leg output for each state. With the aid of equivalent circuits, show how the two states yielding the same output voltage can be used to control the charge on the output capacitor without affecting the output voltage.

9.9 Figure 9.20 shows one leg of a multilevel capacitor-clamped (flying-capacitor) inverter circuit. Determine the leg output voltage (V_{XO}) for each of the possible switching states and hence determine the number of output voltage levels that the circuit can produce.

9.10 Explain the advantages offered by using multilevel inverter topologies for high power inverters, compared to using conventional inverter topologies employing series connected devices to achieve the required voltage rating. Draw a circuit diagram for one leg (including the associated d.c. link capacitors) of a diode clamped 3-level inverter (5-level line to line). List the possible gating patterns (clearly indicating which are the gated devices for each) and determine the voltage between the d.c. link centre point and the inverter leg output for each state.

9.11 In some indusrial applications it is required to produce a 9-level (line-to-line) load voltage waveform from three-phase multilevel inverters using the "diode-clamped" topology and the "flying-capacitor" topology.

(a) Sketch one of the three inverter legs in detail for each circuit arrangement.

(b) List the advantages and disadvantages of each circuit.

9.12 List the advantages and disadvantages multilevel inverters have over the traditional two-level arrangements.

9.13 A single-phase 5-level inverter using a flying-capacitor multilevel inverter arrangement.

(a) Draw the circuit diagram of this arrangement.

(b) Draw circuit diagram of a diode-clamped inverter having the same number of levels (phase-to-neutral).

(c) By Listing all possible gating patterns, determine the voltage between the d.c.-link centre point and the inverter leg output for each state and prove that the topology is, in fact, produces 5-level output voltage.

(d) By analysing all possible combinations of gating signals for the single-phase diode-clamped arrangement, show that this topology produces a 5-level output voltage.

(e) List the number of components such as power supplies, transistors, capacitors, needed for building the three-phase version of the diode- clamped and the cascaded bridge. Explain which inverter requires less components and you think is the cheaper to build.

9.14 Consider a single-phase, 5-level inverter using a diode clamped multilevel inverter arrangement. The 5-level is referred to phase-to-neutral configuration.

(a) Draw the circuit diagram of this arrangement.

(b) Compare the typical configuration of a 5-level phase-to-neutral voltage with that of a 2-level corresponding inverters operating with the same d.c.-link voltage and state what would be the advantage of the 5-level inverter when working with very low modulation index.

(c) List the number of components such as power supplies, transistors, capacitors, needed for building the three-phase version of the diode-clamped and the cascaded bridge. Explain which inverter requires less components and you think is the cheaper to build.

9.15 An HVDC transmission system is to be used to connect a wind farm to a public transmission line. Assume that the HVDC transmission system has a voltage between the two d.c. poles of 30kV, and the public substation is assumed to be connected to a three-phase a.c. distribution system:

(a) Describe and list the appropriate components needed and suggest which inverter topology would be more convenient if the largest available forced commuted power switch can operate with 7.5kV.

(b) Illustrate this arrangement by drawing the single-line diagram of the circuit.

9.16 In a 5-level inverter of cascade type, it is required to eliminate harmonic components n = 5, 7, 11 and 13 from the output voltage waveform to suit special indusrial application with modulation index $M_i = 0.8$. Determine, approximately, the values of the triggering angles required for each individual inverter to achieve this purpose.

[Ans: $\alpha_1 = 7^o$, $\alpha_2 = 19^o$, $\alpha_3 = 2\ 7^o$, $\alpha_4 = 45^o$, and $\alpha_5 = 62^o$]

PART II : ELECTRICAL DRIVES

CHAPTER TEN

INTRODUCTION TO ELECTRICAL DRIVES

10.1 INTRODUCTION

An **ELECTRIC DRIVE** is defined as an electromechanical device designed to convert electrical energy into mechanical energy to impart motion to different machines and provides electrical control for various kinds of processes by means of "controller".

The aim of the controller is to adjust or stabilize the speed of the motor to suit a given industrial task.

In the past, horse power replaces the hand power drive by using animals. These animals were replaced by mechanical drive powered by wind mills, water wheels and turbines, steam engine, internal combustion engine and electrical machines (Electric Drives).

Development of Electrical Drives

The development of different kinds of electric drives used in industry may be divided into three stages:

(1) Group Electric Drive

This drive consists of a single motor, which drives one or more line shafts supported on bearings. The line shaft may be fitted with either pulleys and belts or gears, by means of which a group of machines or mechanisms may be operated. It is also sometimes called as SHAFT DRIVES.

Advantages

- A single large motor can be used instead of number of small motors.

Disadvantages

- There is no flexibility. If the single motor used develops fault, the whole process will be halted.

(2) Individual Electric Drive

In this drive each individual load is driven by a separate motor. This motor also imparts motion to various parts of the load.

(3) Multi-Motor Electric Drive

In this drive system, there are several individual drives, each of which serves to operate of many working machines or mechanism in some production unit, such as complicated metal cutting machine tools, paper making industries, rolling machines, building cranes, aircrafts, etc.

10.2 GENERAL ELECTRIC DRIVE SYSTEM

Fig.10.1 shows the basic structural diagram of a variable speed electrical drive system which generally has the following components:

- A device that transforms electrical power into mechanical power (An electric motor or electromagnet).
- A device that control the electrically driven assembly to obtain motion of specific form (linear or rotary motion) and response to a master controller.
- A device that converts mechanical energy and impart it to the actuating mechanism (reducers and other intermediate gearing).

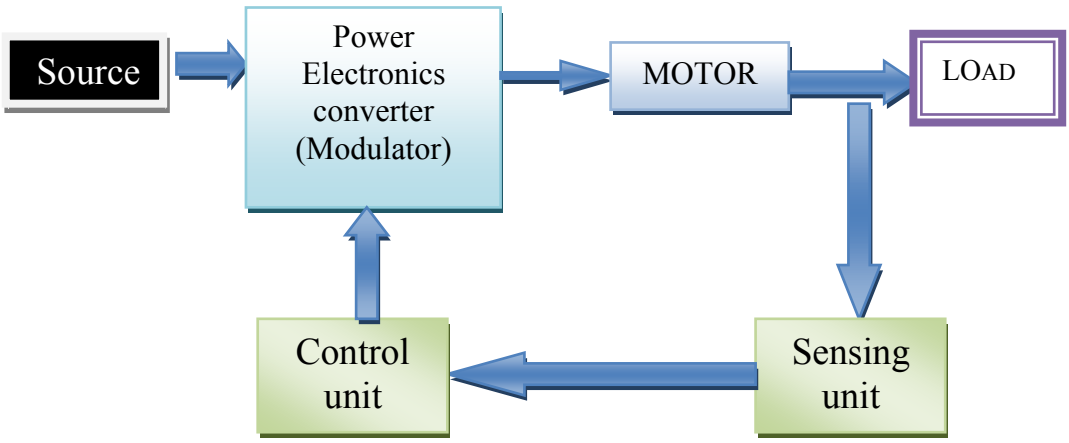

Fig.10.1 Block diagram of drive system.

10.2.1 Drive System Components

1-Electrical Motors

Most commonly used electrical motor for speed control applications are the following:

❖ DC Machines

Separately-excited and permanent magnet, shunt, series, compound motors and switched reluctance machines.

- ❖ AC Machines
  Induction, wound rotor, synchronous, PM synchronous and synchronous reluctance machines.
- ❖ Special Machines
  Brush less d.c. motors, stepper motors, switched reluctance motors are used.

2- Power Modulators

The functions of the power modulator are

- ❖ Modulates flow of power from the source to the motor in such a manner that motor is imparted speed-torque characteristics required by the load.
- ❖ It converts electrical energy of the source in the form suitable to the motor.
- ❖ Selects the mode of operation of the motor, i.e. Motoring or Braking.

Types of Power Modulators

In the electric drive system, the power modulators can be any one of the following:

- Controlled rectifiers (ac-to-dc converters)
- Inverters (dc-to-ac converters)
- AC voltage controllers (ac-to-ac converters)
- DC choppers (dc-to-dc converters)
- Frequency changers (Cycloconverters or PWM Inverters)

3- Electrical Sources (Input Power)

Very low power drives are generally fed from single-phase sources. Rest of the drives is powered from a three-phase source. Low and medium power motors are fed from a 400V supply. For higher ratings, motors may be rated at 3.3 kV, 6.6 kV and 11 kV. Some drives are powered from batteries.

4- Sensing Unit

- Speed Sensing (From Motor)
- Torque Sensing
- Position Sensing
- Current sensing and voltage sensing from lines or from motor terminals or from Load
- Temperature Sensing

5- Controller

Controller for a power modulator matches the motor and power converter to meet the load requirements.

10.2.2 Classification of Electric Drives

Electric drives may be classified as follows:

1. According to Mode of Operation
   - Continuous duty drives
   - Short time duty drives
   - Intermittent duty drives
2. According to Means of Control
   - Manual
   - Semi automatic
   - Automatic
3. According to Number of machines
   - Individual drive
   - Group drive
   - Multi-motor drive
4. Another main classification of electric drive is
   - DC drive
   - AC drive

Table 10.1 gives comparison between DC and AC drives.

Table 10.1 Comparison between DC and AC drives.

DC DRIVES	AC DRIVES
• Well established technology • Requires frequent maintenance • The commutator makes the motor bulky, costly and heavy • Fast response and wide speed range • Speed and design ratings are limited due to commutations • Poor power factor • Environmentally sensitive	• The power circuit and control circuit are complex • Less Maintenance • No commutator problems exist in these motors and they are inexpensive, particularly squirrel-cage induction motors • Good line power factor • Environmentally insensitive

10.2.3 Advantages of the drive system

A modern variable speed electrical drive system are static system using power semiconductor devices such as thyristors (SCRs) and power transistors. These systems have replaced the old pneumatic or hydraulic drives as well as electromechanical and other forms of control to electronic control using SCR's drive which has the following advantages:

1. Basic operation is simple and reliable.
2. Saving in space and capital cost.
3. Higher efficiency.

4. Better speed response.
5. Low maintenance cost and long life.
6. Braking power can be transformed into electrical power and feedback to the main supply.

Applications of Electrical Drives

Electric drives are used in several indusrial applications such as:

- Paper mills
- Cement Mills
- Textile mills
- Sugar Mills
- Steel Mills
- Electric Traction
- Petrochemical Industries
- Electrical Vehicles

10.3 REVIEW OF ROTATIONAL MECHANICS

Rotational mechanics is very important in electric drives studies. The following Table 10.2 gives comparison between rotational and linear mechanics formulae.

Table 10.2 : Rotational mechanics VS linear mechanics.

Rotational Mechanics	Linear Mechanics
θ =Angular displacement (rad)	S = Displacement (m)
ω = Angular velocity (rad/s) $= \frac{d\theta}{dt}$	v = velocity (m/s) $= \frac{dS}{dt}$
α = Angular acceleration (rad/s^2) $= \frac{d\omega}{dt} = \frac{d2\theta}{dt^2}$	a = Acceleration (m / s^2) $= \frac{dv}{dt} = \frac{d2S}{dt^2}$
J = Moment of inertia (kg.m^2)	m = Mass (kg)
T = Torque (Nm) = J α	F = Force (N) = m a
M = Angular momentum (kg.m^2.rad/s) = $J\omega$	M = Momentum (kg.m /s) = m v
Kinetic energy = $\frac{1}{2} J \omega^2$ (Jouls)	Kinetic energy = $\frac{1}{2} m v^2$ (Jouls)
Power = P = T ω (Watts)	Power = F v (Watts)
Work = T θ	Work = F S

10.4 DYNAMICS OF MOTOR- LOAD SYSTEM: FUNDAMENTALS OF TORQUE EQUATIONS

A motor generally drives a load (Machines) through some mechanical transmission systems. The equivalent rotational system of motor and load is shown in the Fig.10.2.

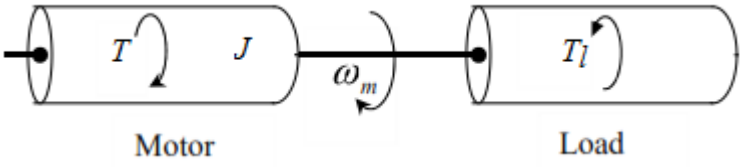

Fig.10.2 Typical motor-load system.

where :

J = Moment of inertia of motor load system referred to the motor shaft kg .m^2.

ω_m = Instantaneous angular velocity of motor shaft, rad /s.

T = Instantaneous value of developed motor torque, Nm.

T_l = Instantaneous value of load torque, referred to the motor shaft, Nm.

Load torque T_l includes *friction* and *windage* torque of motor.

Motor-load system shown in Fig.10.2 can be described by the following fundamental torque equation.

$$T - T_l = \frac{d}{dt}(J\omega_m) = \frac{d\omega_m}{dt} + \omega_m \frac{dJ}{dt} \qquad (10.1)$$

Equation (10.1) is applicable to variable inertia drives such as mine winders, reel drives, Industrial robots.

For drives with constant inertia $\frac{dJ}{dt} = 0$

$$T = T_l + \frac{d\omega_m}{dt} \qquad (10.2)$$

$J\frac{d\omega_m}{dt}$ = Torque component called dynamic torque because it is present only during the transient operations.

At steady state operation $J\frac{d\omega_m}{dt} = 0$.

Note: The energy associated with dynamic torque $J\frac{d\omega_m}{dt}$ is stored in the form of kinetic energy given by

$$KE = \frac{1}{2} J\,\omega^2 \qquad (10.3)$$

10.4.1 Types of Loads

Various load torques can be classified into broad categories, however, the loads are of two types according to the applied torque:

- Active load torques
- Passive load torques

Load torques which has the potential to drive the motor under equilibrium conditions are called ***active*** load torques. Such load torques usually retain their sign when the drive rotation is changed (reversed) , for example :

- ❖ Torque due to gravitational force.
- ❖ Torque due to deformation in elastic bodies and due to tension.
- ❖ Torque due to compression and torsion etc.

Load torques which always oppose the motion and change their sign on the reversal of motion are called ***passive*** load torques, for example :

- ❖ Torque due to friction.
- ❖ Torque due to shear (cutting).
- ❖ Torque due to deformation in inelastic bodies etc.

Components of Load Torque (T_l)

The load torque T_l can be further divided into following components :

(i) Friction Torque (T_F)

Friction will be present at the motor shaft and also in various parts of the load. T_F is the equivalent value of various friction torques referred to the motor shaft. Variation of friction torque with speed is shown in Fig10.3.

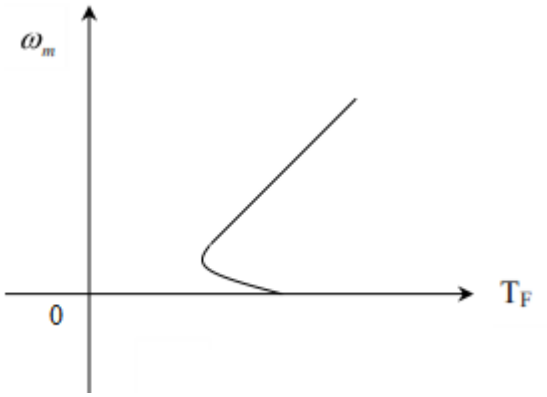

Fig.10.3Variation of friction torque with speed.

Friction torque (T_F) can also be resolved into three components :

(1) VISCOUS friction T_v : Component varies linearly with speed and is given by

$$T_v = B\omega_m \qquad (10.4)$$

where B is viscous friction coefficient.

(2) COULOMB friction T_C : Component which is independent of speed.

(3) STATIC friction T_s : Component T_s accounts for additional torque present at stand still. Since T_s is present only at stand still it is not taken into account in the dynamic analysis. Its value at stand still is much higher than its value slightly above zero speed. Friction at zero speed is called ***stiction*** or static friction. In order to start the drive the motor should at least exceed stiction.

The variation of these three torques are shown in Fig.10.4. Hence, the total friction torque is given by

$$T_F = T_v + T_C + T_S \qquad (10.5)$$

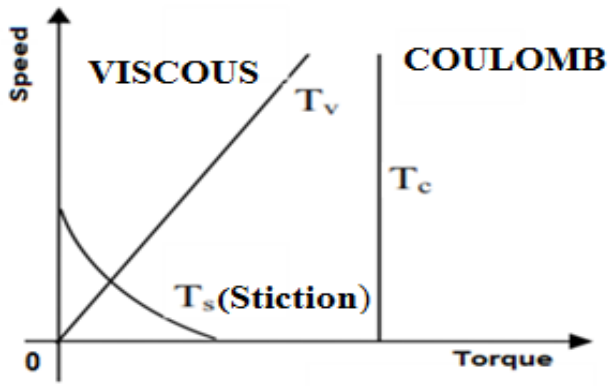

Fig.10.4 Types of friction torques in drive system.

(ii) Windage Torque (T_W)

When motor runs, wind generates a torque opposing the motion. This is known as windage torque. Windage torque, T_w which is proportional to the square of the speed is given by

$$T_W = C\,\omega_m^2 \qquad C \text{ is a constant} \qquad (10.6)$$

(iii) Torque required doing useful mechanical work (T_L).

Nature of this torque depends upon particular application. It may be constant and independent of speed. It may be some function of speed, it may be time invariant or time variant, its nature may also change with the load's mode of operation.

From the above discussions, and for finite speed,the load torque T_l *is*

$$T_l = T_L + B\omega_m + C\,\omega_m^2 + T_C \qquad (10.7)$$

10.4.2 Classifications of Various Types of Loads

Most of the industrial loads can be classified into the following two categories :

(i) Load torques varying with time :

- Constant continuous type loads: Loads oprating continuously for the same loading (same torque) conditions for a long time.
- Continuous variable loads : Loads varying and having duty cycle.
- Pulsating loads : Loads of machines with crank shafts.
- Impact loads : Regular repetitive load peaks such as in rolling mills, forging hammer, etc.
- Short time loads (e.g. hoists).

(ii) Load torques varying with with speed :

- Load torques which are independent of speed (e.g.cranes).
- Load torques proportional to speed (Generator type load) .
- Load torques proportional to square of the speed (Fan type load).
- Torque inversely proportional to speed (Constant power type load).

Load Torque-Speed Charachteristics

Speed-torque characteristics of the load must be known to calculate the acceleration time and to select the proper type of motor to suit the load. The load speed-torque characteristics of industrial loads are generally non-analytical function $T_L = f(\omega)$. However, some of them may be approximated to an analytic form such as :

1- Constant Torque characteristics: $T_L = k$

Most of the working machines that have mechanical nature of work like shaping, cutting, grinding or shearing, require constant torque irrespective of speed, (See Fig.10.5(a)). Similarly cranes during the hoisting and conveyors handling constant weight of material per unit time also exhibit this type of characteristics.

2- Torque Proportional to speed: $T_L = k\omega$

Separately-excited d.c. generators connected to a constant resistance load, eddy current brakes have speed-torque characteristics given by $T_L = k\omega$. (See Fig.10.5(b)).

3- Torque proportional to square of the speed: $T_L = k\omega^2$

Another type of load met in practice is the one in which load torque is proportional to the square of the speed, e.g. : Fans, rotary pumps, compressors and ship propellers. (See Fig.10.6 (a)).

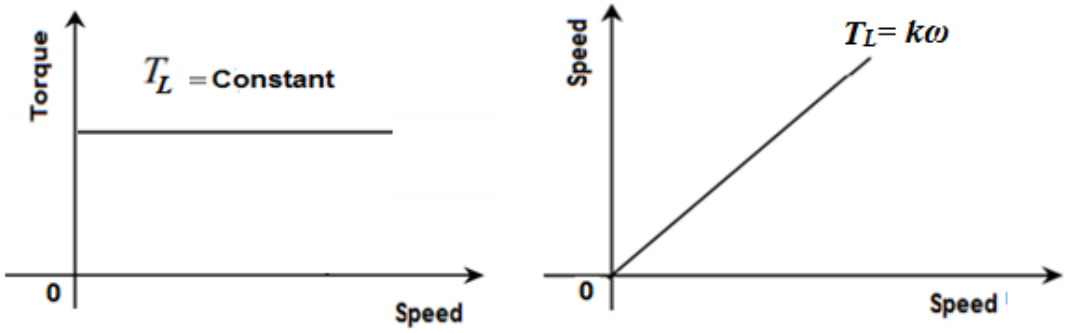

(a) (b)

Fig.10.5 Types of load torque : (a) Constant torque characteristics, (b) Torque proportional to speed.

4. Torque Inversely proportional to speed: $T_L \alpha \frac{1}{\omega}$

Certain types of lathes, boring machines, milling machines, steel mill coiler and electric traction load exhibit hyperbolic speed-torque characteristics as shown in Fig.10.6(b).

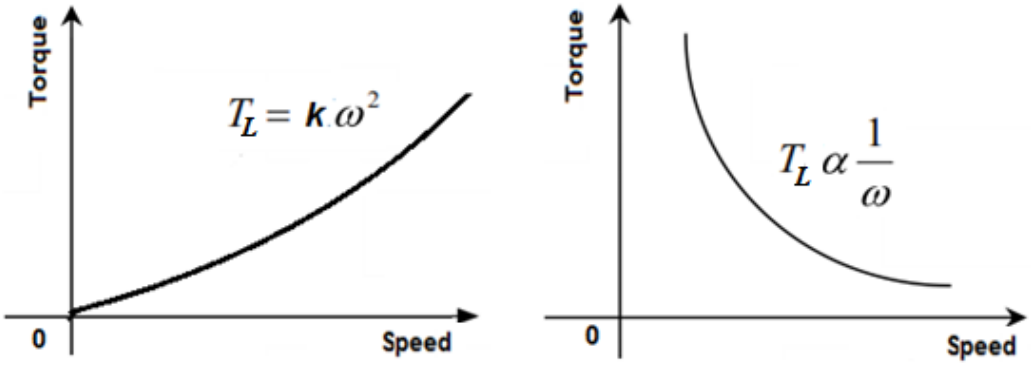

(a) (b)

Fig.10.6 Types of load torque : (a) Torque proportional to square of the speed, (b) Torque inversely proportional to speed .

5. Torque polinomialy related to the speed:

For the particular characteristics of Fig.10.7 each example may be approximated to a polynomial form :

$T_L = k_o + k\omega$ for a hoist or elevator (Fig.10.7(a))

$T_L = k_o + k_1\,\omega + k_2\omega^2 + ...$ for a compressor (Fig.10.7(b))

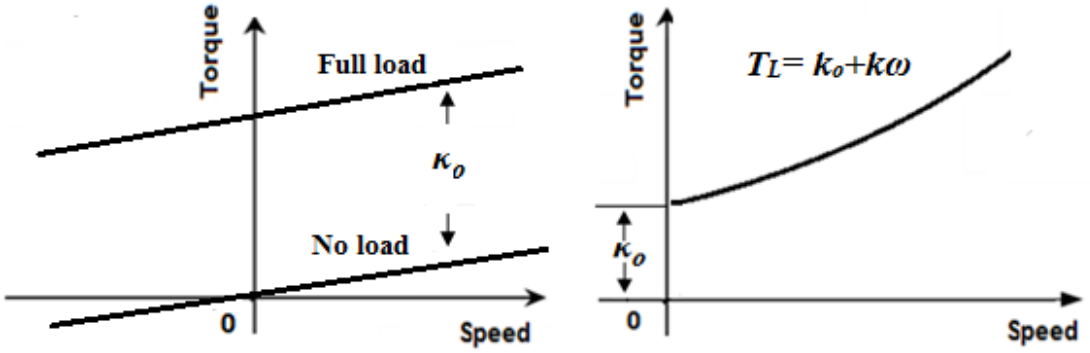

(a) (b)

Fig.10.7 Torque approximated to a polynomial form .

10.4.3 BASIC EQUATION OF MOTION FOR DRIVE SYSTEM

Generally, the basic equation of motion of motor driving a load, Fig.10.8, is given by

$$T_m = T_l + J\frac{d\omega}{dt} = T_L + J\frac{d\omega}{dt} + T_{FW} \qquad (10.8)$$

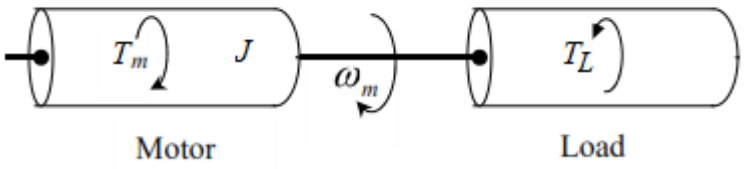

Fig.10.8 Motor-load system.

where

J = Polar moment of inertia of motor-load system referred to the motor shaft, Kg.m^2
ω_m = Instantaneous angular velocity of the motor shaft, rad/sec
T_m = Developed torque of the motor, Nm
T_L = Load (resisting) torque, referred to the motor shaft, Nm
T_{FW} = Friction and windage torque = $T_v + T_c + T_w$

$$= B\omega_m + T_C + C\,\omega_m^2$$

Coulomb friction is generally neglected in drive systems.

If T_{FW} is small then, $T_{FW} = 0$, hence, Eq.(10.7) becomes,

$$T_m = T_L + J\frac{d\omega}{dt} \qquad (10.9)$$

- For motor operation, T_m and ω_m have same directions
- Always T_m and T_L have opposite directions

In the drive systems, depending on the mechanical load, the motor may be subjected to variable operating conditions in its duty cycles. The motor in an electric car can operates in various conditions such as starting, accelerating, steady-state, decelerating and stopping. Fig.10.9 illustrates motor-load torque characteristics, the available starting torque is T_{st}. At this condition, the motor is accelerated and subjected to most severe service. The equation of motion govern the motor in this case is Eq.(10.8).

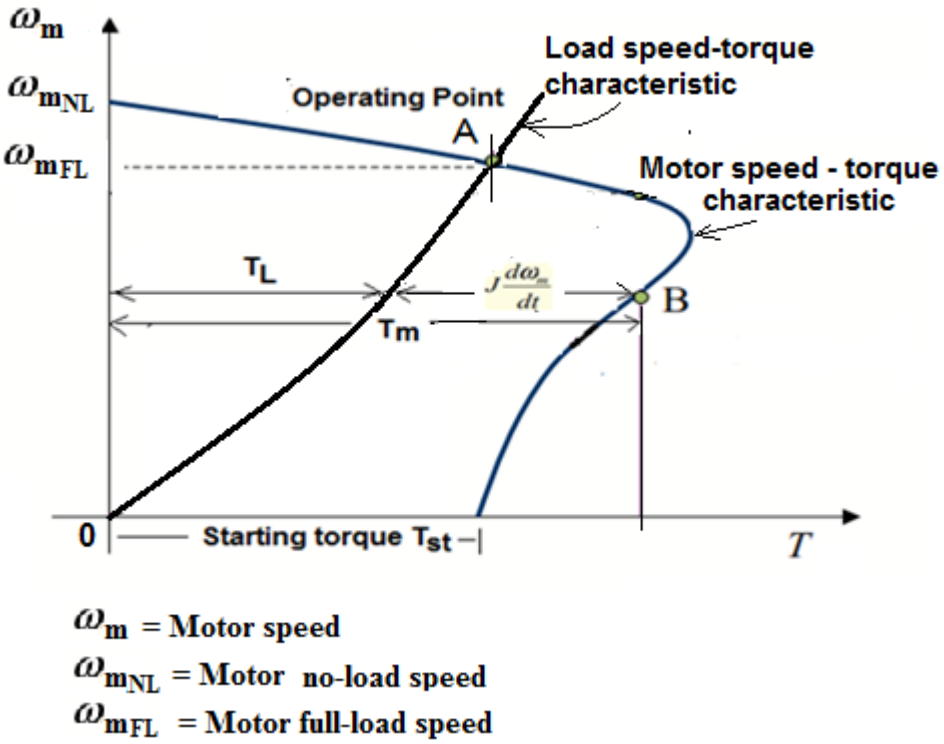

Fig.10.9 Motor and load speed-torque characteristics.

- When the motor operates at steady-state: $\frac{d\omega}{dt} = 0 \Longrightarrow T_m = T_L$
- When $T_m > T_L$, i.e. the dynamic torque $J\frac{d\omega}{dt} > 0$, the drive accelerating.
- When $T_m < T_L$, i.e. the dynamic torque $J\frac{d\omega}{dt} < 0$, the drive decelerating and coming to rest.

- When $T_m = T_L$, i.e. $\frac{d\omega}{dt} = 0$, the drive continues to run at same speed if it was running.

- The steady-state operation of the motor occurs when its speed-torque characteristic intersects with the load speed-torque characteristic at the operating point A as shown in Fig.10.9.

Example 10.1

A variable speed d.c. drive has rated power of 10 kW,rated speed of 1500 rpm drives a load that comprises a constant load of T_L = 30 Nm. The inertia of the drive system is 0.10 kg.m^2. Calculate the time taken to accelerate the load from zero to 800 rpm , assuming the drive develops rated torque during the acceleration phase.

Solution

$$\text{Rated speed} = 1500 \text{ rpm}, \quad \text{in rad/s} = \frac{1500}{60} \times 2\pi = 157 = \omega$$

$$\text{Rated torque} = \frac{P_{\text{rated}}}{\omega} = \frac{10000}{157} = 63.6 \text{ Nm}$$

$$T_a = T_m - T_L = J \frac{d\omega_r}{dt}$$

$$T_a = 63.6 - 30 = 33.6 \text{ Nm}$$

$$T_a = J\frac{\Delta\omega}{\Delta t}$$

$$\Delta t = J\frac{\Delta\omega}{T_a}$$

$$\Delta\omega = (800\ rpm - 0\ rpm) \times \frac{2\pi}{60} = 800 \times \frac{2\pi}{60} = 83.73 \text{ rad/s}$$

$$\Delta t = \frac{0.10 \times 83.73}{33.6} = 250 \text{ ms}$$

Example 10.2

An induction motor directly connected to a 400V, 50Hz supply utility has a rated torque of 30Nm that occurs at a speed of 2940 rpm. The motor drives a fan load that can be approximated by: $T_L = B \cdot \omega_m$

where B = 0.05 Nm/rad/s, and the rated speed of the motor is 3000 rpm. Stating any assumption made, calculate the speed, in equilibrium position at which the torque developed by the motor is equal to the load torque.

Solution

The torque speed characteristic of an induction motor is shown in Fig.10.9, part of which can be approximated as straight line.

Let ω_{mFl} = speed of the motor at full load.
ω_{mNl} = speed of the motor at no load.

At full load $T_m = T_{rated} = 30$ Nm

$$\omega_{mFl} = \frac{2940}{60} \times 2\pi = 307.72 \text{ rad/s}$$

At no-load T_m at $\omega_{mNl} = 0$ Nm

$$\omega_{mNl} = \frac{3000}{60} \times 2\pi = 314.15 \text{ rad/s}$$

For the linear region (only)

$$T_m = K\,(\omega_{mNl} - \omega_m)$$

$$\therefore \quad K = \frac{30}{(314.15 - 307.72)} = 4.66$$

For the load

$$T_L = B\omega_m = 0.05\,\omega_m$$

For the equilibrium position

$$4.66 \times (\omega_{mNl} - \omega_m) = 0.05\,\omega_m$$

$$4.66\,\omega_{mNl} = 4.71\,\omega_m$$

$$\omega_m = \frac{4.66 \times 314.15}{4.71} = 310.8 \text{ rad/s} \quad \rightarrow \quad 2967\text{rpm}$$

Load Torque and Load Power

At steady state $T_m = T_L$.

The output power from a motor running at speed ω_m is

$$P_m = T_m \omega_m$$

The power required by the load is

$$P_L = T_L \omega_L$$

If the motor is connected directly to the load as shown in Fig.10.8, then

$$\omega_m = \omega_L$$

Hence $P_m = P_L$ (10.10)

If η is the efficiency of the motor on full load, then

$$T_m = T_L = \frac{\text{Watts output}}{\eta \omega_m} \quad \text{Nm} \qquad (10.11)$$

In some applications, the motor is connected to the load through a set of gears. The gears have a teeth ratio and can be treated as speed or torque transformers. The motor-gear-load connection is shown in Fig.10.10.

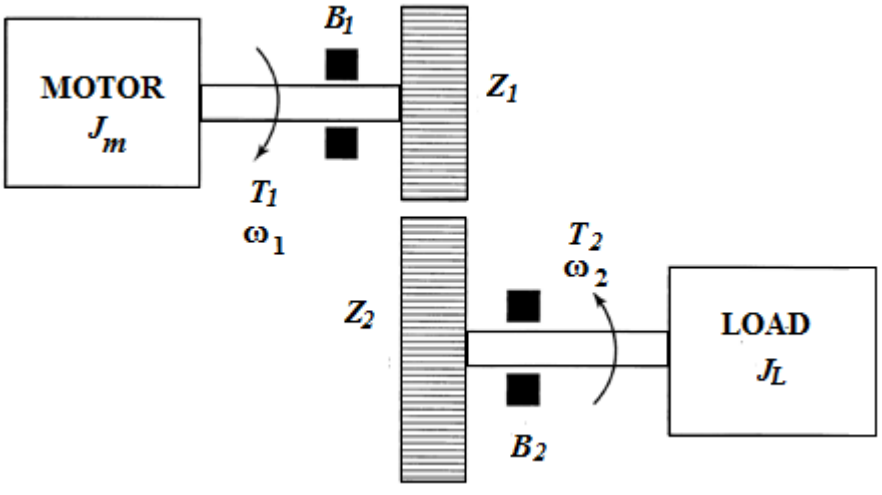

Fig.10.10 Motor connected to the load through a gear.

In Fig.10.10,

Z_1 , Z_2 = Teeth number in the gear

B_1 ,B_2 = Bearings and their coefficients

J_m ,J_L = Moment of inertia of the motor and load

The gears can be modelled from the following facts:

(i) The power handled by the gear is the same on both sides.

(ii) Speed on each side is inversely proportional to its tooth number.

Hence

$$T_1\omega_1 = T_2\omega_2 \tag{10.12}$$

$$T_2 = \frac{\omega_1}{\omega_2}T_1 \tag{10.13}$$

and

$$\frac{\omega_1}{\omega_2} = \frac{Z_2}{Z_1} = g_r \quad = \text{gears ratio} \tag{10.14}$$

Substituting Eq.(10.14) into Eq.(10.13) yields

$$T_2 = \frac{Z_2}{Z_1}T_1 \; = g_r \; T_1 \tag{10.15}$$

At steady-state $T_m = T_L$.

If η is the efficiency of the motor on full load, then

$$T_m = T_L = \frac{\text{Watts input}}{\omega} \times \eta \quad \text{Nm} \tag{10.16}$$

and

$$\text{kW required by the load} = \frac{\text{Watts input}}{1000} \cdot \eta \tag{10.17}$$

Now if the motor is geared to the load, then the torque seen by the load is increased or decreased by the ratio: $\frac{\omega(motor)}{\omega(load)} = \frac{\omega_1}{\omega_2}$.

Determination of Referred Load Torque

In the system of Fig. 10.10, If the speed of the motor shaft ω_1 and that of the motor is ω_2 , T_2 is the load torque , T_2' is the load torque referred to motor shaft , g_r = gear ratio = $\frac{Z_2}{Z_1} = \frac{\omega_1}{\omega_2}$, and η_t = efficiency of transmission, then equating power :

$$T_2\omega_2\frac{1}{\eta_t} = T_2'\,\omega_1$$

$$T_2' = T_2\,\frac{\omega_2}{\omega_1} \times \frac{1}{\eta_t} = \frac{T_2}{g_r\eta_t} \tag{10.18}$$

If the losses in transmission are neglected, then the kinetic energy due to equivalent inertia is

$$\frac{1}{2}J\omega_1^2 = \frac{1}{2}J_2\omega_2^2 = \frac{1}{2}J_2\ \frac{\omega_2^2}{g_r^2}$$

$$\therefore \quad J = J_2 \times \frac{1}{g_r^2} \tag{10.19}$$

When there are number (k) of stages of transmission between the driving motor and the drive load, as shown in Fig.10.11, Eq.(10.18) becomes:

$$T_L^{'} = T_L\ \frac{1}{g_{r1}g_{r2}g_{r3}\ldots\ldots g_{rk}} \times \frac{1}{\eta_{t1}\eta_{t2}\eta_{t3}\ldots\ldots\eta_{tk}} \tag{10.20}$$

where : $g_{r1}g_{r2}g_{r3}\ldots\ldots g_{rk}$, and $\eta_{t1}\eta_{t2}\eta_{t3}\ldots\ldots\eta_{tk}$ are the gear ratios and the efficiencies of the respective transmission.

Similarly the equivalent inertia will be :

$$\frac{1}{2}J^{'}\omega_m^2 = \frac{1}{2}J_m\omega_m^2 + \frac{1}{2}J_1\omega_1^2 + \frac{1}{2}J_2\omega_2^2 + \frac{1}{2}J_3\omega_3^2 + \cdots + \frac{1}{2}J_k\omega_k^2$$

$$J^{'} = J_m + J_1\frac{\omega_1^2}{\omega_m^2} + J_2\frac{\omega_2^2}{\omega_m^2} + J_3\ \frac{\omega_3^2}{\omega_m^2} + \cdots\ldots\ldots\ldots\ldots + J_k\frac{\omega_k^2}{\omega_m^2} \tag{10.21}$$

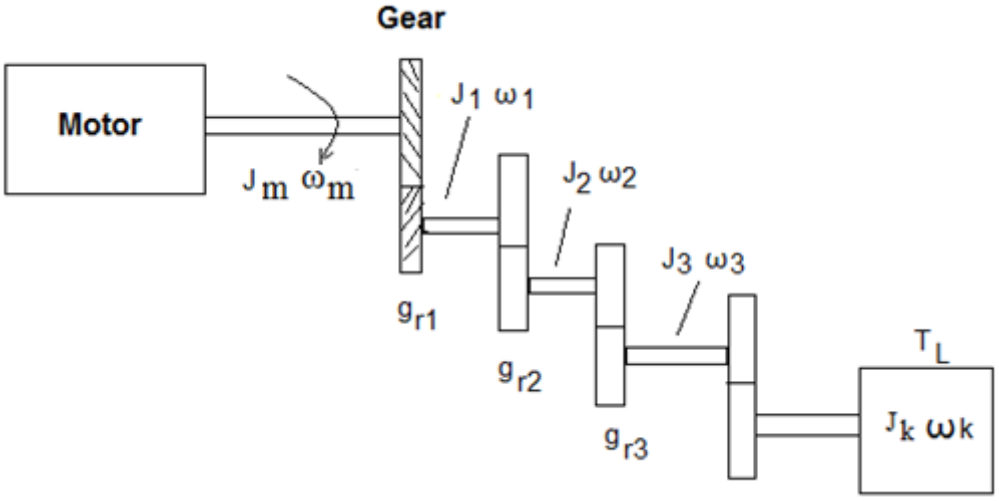

Fig.10.11 Motor-load system with multi gears.

Referring Forces and Masses Having Translation Motion to a Rotating One

In some machines or systems, some moving parts rotate while others undergo translation motion, e.g. cranes, hoists, etc. It is necessary to refer

the translational motion in terms of referred load torque and moment of inertia referred to motor shaft.

Fig.10.12 shows a hoist load lift, wound on drum driven through gears by a motor. If F is the force required due to gravitational pull to lift the moving weight W, η is the efficiency of transmission , v (m/s) is the velocity of the moving mass , and ω_m (rad/s) is the angular velocity of the motor shaft, the referred load torque is obtained by equating the power.

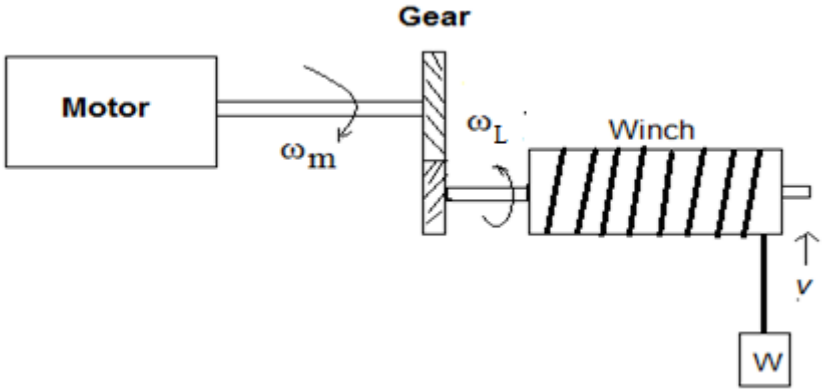

Fig.10.12 Motor-hoist load system.

The referred load torque T_L':

$$T_L^{'} = \frac{F \cdot v}{\eta \cdot \omega_m} \tag{10.22}$$

The moment of inertia referred to the motor shaft is obtained by equating kinetic energy:

$$\frac{1}{2} m\, v^2 = \frac{1}{2} J^{'} \omega_m^2$$

$$\text{or} \quad J^{'} = m \left(\frac{v^2}{\omega_m^2}\right) = \frac{W}{g}\left(\frac{v^2}{\omega_m^2}\right) \tag{10.23}$$

where $m = \frac{W}{g}$ kg weight , g = gravitational accelaration = 9.81 .

Example 10.3

A weight W of (1500 kg) is to be lifted up with a velocity of (1.5 m/s) by means of a motor-hoist system shown in Fig.10.12. The winch has a diameter of (0.35 m) and driven by motor running at (1000 rpm). The inertia of the motor and the winch drum are (1.8 kg.m^2) and (4.2 kg.m^2) respectively. Calculate the total load torque of the system referred to the motor shaft .

Solution

Winch drum diameter = o.5 m
Circumference of the winch drum = 0.5π = 1.57 m
Velocity of the weight = 1.5 m /s
Speed of the winch =1.5/1.57 = 0.955 rev/s
ω of the winch, $\omega_{winch} = 2\pi \times 0.955 = 5.997$ rad / s
speed of the motor = 1000/60 = 16.6 rev / s
ω_m of the motor $= 2\pi \times 16.6 = 104.6$ rad / s
constant load torque = weight × radius of the winch drum
= 1500 × (0.5/2) = 375 kgf . m = 375 Nm at ω_{winch}.
Hence

$$\frac{\omega_L}{\omega_m} = \frac{2\pi \times 0.955}{2\pi \times 16.6} = 0.0575$$

If J' is the moment of inertia of the translation movement of the weight referred to the motor shaft of the motor , then

$$\frac{1}{2}\ mv^2 = \frac{1}{2} J' \omega_m^2$$

$$\therefore \quad J' = \frac{1500}{9.81} \times \frac{1.5^2}{104.6^2} = 0.03144 \text{ kg. m}^2$$

Total torque referred to the motor shaft :

$$T_m = J_m \frac{d\omega}{dt} + W \cdot r \left(\frac{\omega_L}{\omega_m}\right) + J_{winch} \times \left(\frac{\omega_L}{\omega_m}\right)^2 \times \frac{d\omega}{dt} + J' \frac{d\omega}{dt}$$

$$T_m = 1.8 \frac{d\omega}{dt} + 375 \times \left(\frac{\omega_L}{\omega_m}\right) + 4.2 \times (0.0575)^2 \frac{d\omega}{dt} + 0.0144 \frac{d\omega}{dt}$$

If the system operates at steady-state (running continuously without acceleration) ,then

$$\frac{d\omega}{dt} = 0 \quad \text{and} \quad T_m = 375 \times \left(\frac{\omega_L}{\omega_m}\right) = 375 \times 0.0575 = 21.56 \text{ Nm}$$

Example 10.4

A motor has two loads. Load-1 has rotational motion which is coupled to the motor through a reduction gear with gear ratio g_{r1} =10 and efficiency of

90%. Load-1 has a moment of inertia of 10 kg.m^2 and torque of 10 Nm. Load-2 has translation motion and consists of 1000 kg weight to be lifted up at uniform speed of 1.5 m / s. The coupling between load-2 and the motor has an efficiency of 85%.The motor has an inertia of 0.2 kg.m^2 and runs at constant speed of 1420 rpm. Determine the equivalent inertia referred to the motor shaft and the power developed by the motor.

Solution

From equations (10.21) :

$$J' = J_m + J_1 \frac{\omega_1^2}{\omega_m^2} + J_2 \frac{\omega_2^2}{\omega_m^2}$$

$$J' = J_m + J_1 \frac{1}{g_{r1}^2} + m \left(\frac{v^2}{\omega_m^2}\right)$$

J_m= 0.2 kg.m^2 , g_{rl} = 10 , v = 1.5 m /s , and

$$\omega_m = \frac{2\pi n}{60} = 2\pi \times \frac{1420}{60} = 148.7 \text{ rad/s}$$

Hence, substituting these values in the above equation we get;

$$J' = 0.2 + 10 \times \frac{1}{10^2} + 1000 \left(\frac{1.5^2}{148.7^2}\right) = 0.4 \text{ kg. m}^2$$

The referred torques are calculated as follows:

The referred torque for load-1 (T'_{L1}), can be found from Eq.(10.18),

$$T'_{L1} = \frac{T_{L1}}{g_{r1}\eta_{t1}}$$

The referred torque for load-2 (T'_{L2}) can be found from Eq.(10.22),

$$T'_{L2} = \frac{F \cdot v}{\eta_{t1} \cdot \omega_m}$$

The total load torque referred o the motor shaft is,

$$T'_L = T'_{L1} + T'_{L2}$$

or $$T'_L = \frac{T_{L1}}{g_{r1}\eta_{t1}} + \frac{F.v}{\eta_{t1}\omega_m}$$

Here: η_{tl} = 0.9 , g_{rl} = 10 , T_{Ll} = 10 Nm , η_{t2} = 0.85 , F = mg =1000 × 9.81 = 9810 N , v = 1.5 m / s , and ω_m =148.7 rad / s.

Now substitute these values in the above equation yields;

$$T_L^{'} = \frac{10}{10 \times 0.9} + \frac{9810 \times 1.5}{0.85 \times 148.7} = 117.53 \text{ Nm}$$

Example 10.5

A drive used in a hoist to raise and lower weights up to 400 kg at velocities up to ± 2 m/s. The weight hangs from a cable that is wound on a drum of radius of 0.4 m . The drum is driven by the drive motor through a gearbox that has an efficiency of 85% . The maximum speed of the motor is ± 1300 rpm. It is required to:

(a) Sketch the system and find the nearest integer gearbox ratio that will match the maximum speed of the motor to the maximum velocity of the hoist.

(b) Determine the torque and power provided by the motor when lifting the maximum weight at the maximum velocity.

(c) Calculate the torque and power provided by the motor when lowering the maximum weight at the maximum velocity.

Solution

(a) The system is shown in Fig. 10.13.

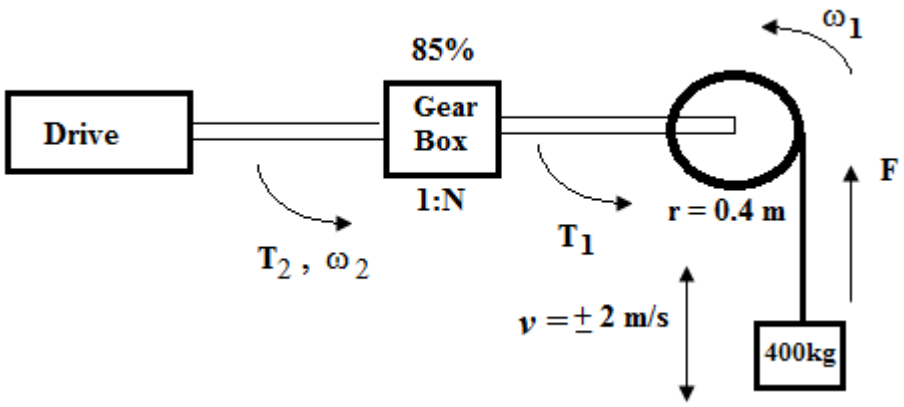

Fig.10.13 System diagram of Example 10.5.

The speed of the weight is given as: $v = 2$ m /s

$$\omega_1 = \frac{v}{r} = \frac{2}{0.4} = 5 \text{ rad/s}$$

The motor speed in rad /s is given by

$$\omega_2 = 1300 \times \frac{2\pi}{60} = 136.06 \text{ rad/s}$$

$$N = \frac{\omega_2}{\omega_1} = \frac{136.06}{5} = 27.21 \quad \rightarrow \quad \text{use } 27$$

$$\frac{\omega_2}{27} = 5$$

$$\therefore \quad \omega_2 = 135 \text{ rad/s} = \frac{135 \times 60}{2\pi} = 1290 \text{ rpm}$$

(b) Now, when lifting and lowering F is upwards, T_1 is in the direction shown (here anticlockwise)

$$T_1 = \text{Force} \times \text{radius} = 400 \times 9.81 \times 0.4 = 1569.6 \text{ Nm}$$

(Since Force = mass × gravity)

When lifting, motor drive supplies the losses in the gearbox :

$$T_2 = \frac{T_1}{N.\eta} = \frac{1569.6}{27 \times 0.85} = 68.4 \text{ Nm}$$

$$T_2 \times \omega_2 \times \eta = T_1 \times \omega_1$$

$$P_{drive} = T_2 \times \omega_2 = 68.4 \times 135 = 9.234 \text{ kW}$$

When lowering , moving mass now supplies gearbox losses, hence

$$T_2 \times \omega_2 = T_1 \times \omega_1 \times \eta$$

$$T_2 = \frac{1569.6 \times 0.85}{27} = 49.41 \text{ Nm}$$

$$P_{drive} = 49.41\ (-135\ ) = -6.67 \text{ kW}$$

The minus sign indicates that the drive is regenerating.

10.5 MECHANICAL TRANSMISSIONS EMPLOYED IN ELECTRICAL DRIVE SYSTEMS

Motion from the electric motor to the actuating or drive system is imparted through a system drives. The electric drive widely employs the mechanical transmission designed to convey and convert the rotational motion of the motor shaft to the desired kind of motion of the actuating mechanism, the speed and torque being changed accordingly.

10.5.1 Reducers

The electric motor generally produces relatively high rpm (speed). Since most of loads in drive systems require low speed operation, therefore it is required to install a reducer, i.e. an encased transmission mechanism, between the motor and the actuating mechanism or load. In order obtain drastic reduction in the speed of motion, the reducers may be fitted with several series-connected mechanical transmissions. The reducers are mainly provided by gears, planetary, worm, and screw-gear transmissions. These types will be discussed briefly hereinafter.

(A) Gear Transmission

(1) Simple reducers with ordinary gear wheels employ external and internal gearing (Fig.10.14) with efficiency of 98% or more in one pair of wheels. Such reducers are simple in construction. One pair of gear wheels is capable of providing small gear ratios ($g_t \approx 6$) which imply the ratio of the input speed ω_1 to the output speed ω_2 , i.e.:

$$g_t = \frac{\omega_1}{\omega_2} = \frac{z_1}{z_2} \tag{10.24}$$

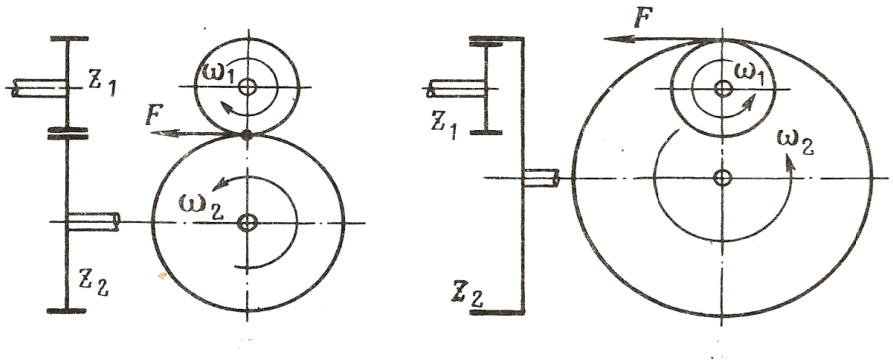

(a) (b)

Fig.1.14 Single- stage gear transmission with : (a) External transmission, and (b) Internal transmission.

where Z_2 and Z_1 are, respectively, the number of teeth on the output and input gear wheels.

(2) Multi-stage gearing: To obtain greater ratios, multi stage transmission as shown in Fig.10.15, is used. This type is mainly used in low-power drive systems.The gear ratio of the multi-stage gearing canbe obtained by the following formula

$$g_t = \frac{Z_2}{Z_1} \times \frac{Z_4}{Z_3} \times \frac{Z_6}{Z_5} \ldots\ldots\ldots \frac{Z_{2n}}{Z_{2n-1}} = g_1 \times g_2 \times g_3 \ldots\ldots\ldots\ldots \times g_n \quad (10.25)$$

where n = number of transmission stages ,

g_n = gear ratio of transmission stage.

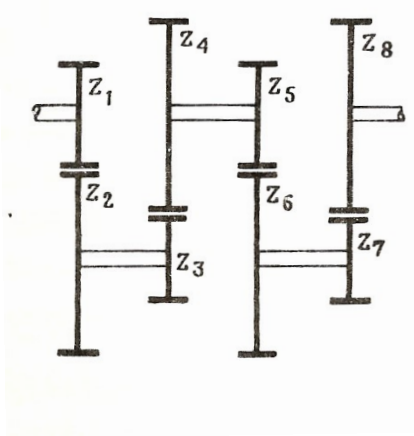

Fig.10.15 Multi-stage gear transmission with pairwise meshing.

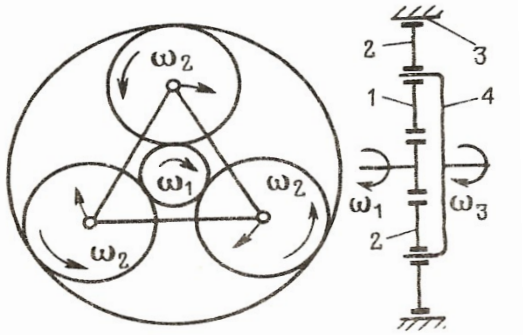

Fig.10.16 Coaxial planetary tray transmission.

(B)The planetary gear transmission

Fig.10.16 shows a simple diagram of a planetary reducer. As compared to simple reducers, the planetary reducers have a relatively small size. The rotary motion is imparted sun gear 1 which is fixed firmly to the driving shaft, to satellite gear 2 (minimum two gears) which ride over a fixed rim gear 3 and rotate carrier 4 linked to the output shaft. The gear ratio of such transmission is determined from

$$g_t = \frac{\omega_1}{\omega_2} = \frac{Z_1 + Z_2}{Z_2} \quad (10.26)$$

It is clear from Eq.(10.26) that the gear ratio in planetary system of transmission does not depends on the number of satellite gears and their teeth number.

(C)The worm gear transmission

These are designed to transmit rotation between two shafts that are located at angle of 90^o to each other and in different planes, Fig.10.17. As the worm rotates, its threads apply pressure to the teeth and drive the gear

wheel. The worm gear transmission consists of worm 1 and worm wheel 2, meshed with each other.

The gear ratio of the worm gear transmission is given may reach comparatively that can be expressed as

$$g_t = \frac{Z}{m} \tag{10.27}$$

where Z = number of teeth on worm wheel.

m= number of threads turns.

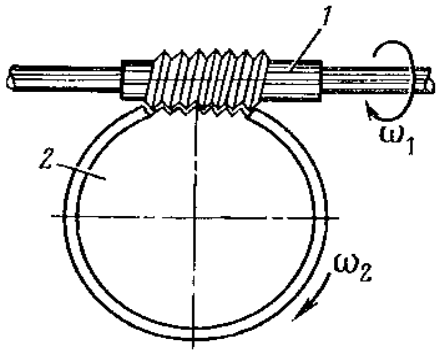

Fig.10.17 Worm transmission.

Disadvantages:

Usually this type of transmission has low transmission efficiency (50% - 85%), rapid wear and relative low power transmission.

(D)The screw transmission

These devices are served to convert rotary, motion to progressive (linear) motion, Fig.10.18 , and usually used in output devices.

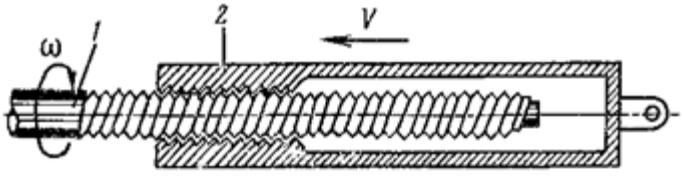

Fig.10.18 Screw transmission.

The gear ratio of such drive is given by:

$$g_t = \frac{\omega}{v} \tag{10.28}$$

where ω = angular speed of the input shaft.

v = linear speed of the output shaft.

The efficiency of such transmission is about 50%. This type of transmission can be made self braking.

10.5.2 Cluches

A clutch is an electromagnetic device designed to join together two shafts of a transmission system, as well as to break either one of them. In general, there are three main types of clutches used in main industrial tasks:

- Friction clutches

- Braking clutches
- Safety clutches

The application of the friction and braking clutches is to preclude malfunction of a controlled mechanism which may occurs due to rundown of the electric motor, after it turned off, and to shorten the transient process when the mechanism responds to a control signal or when it is being reversed. The torque-limiting clutches protect transmission systems from excessive mechanical stress which may developed by overloading. The safety clutches safeguard the electric motors in the event of inadvertent damage ,seizing or any other unexpected failures.

(A) Friction clutches

The electrical mechanisms widely use clutch of mechanical coupling with electromagnetic control; such mechanism is called electromagnetic friction clutch and depicted in Fig.10.19. As winding 2 of the clutch is energized, the electromagnetic force overcomes the tension of the leaf spring 5 and this draws the armature 3 of the clutch toward core 4, and the torque is transmitted from the electric motor to the actuating mechanism.

Fig.10.19 Electromagnetic clutch.

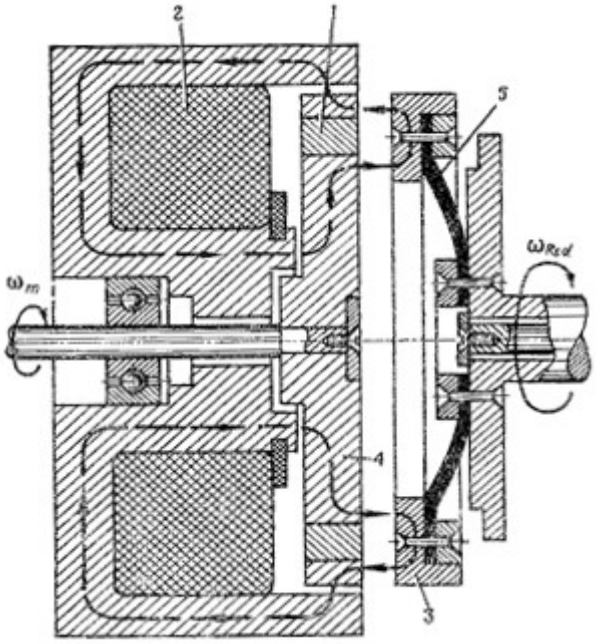

The turning off of the power supply of the motor de-energizes the winding of the clutch. Leaf springs 5 force off armature 3 to the initial position, and the armature of the electric motor disengaged from the actuating mechanism.

(B)The braking clutches

These types of clutches are used in electric drives of low and medium power. A typical breaking clutch is presented in Fig.10.20. The end shield 8

of the electric motor carries electromagnet frame 7. When winding 6 is de-energized, electromagnet armature 4 is pressed by spring 5 to brake ring 3 on disc 2 secured to the motor shaft 1.The frictional forces acting between armature 4 and the brake ring rapidly bring the motor armature to stop. When the electromagnet winding is activated, armature 4 is attracted to core 7 and the electric motor is disengaged.

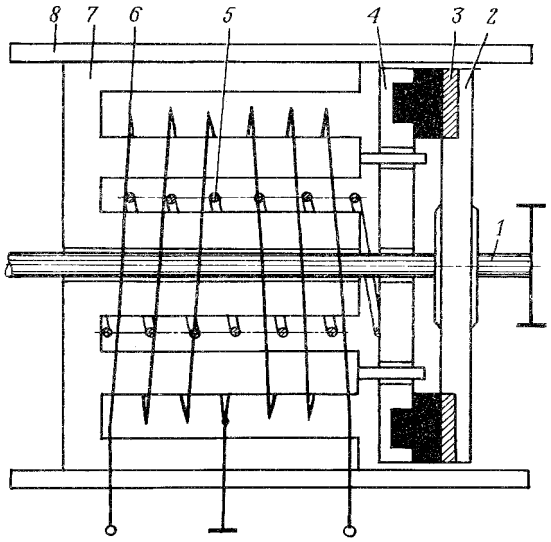

Fig.10.20 Electromagnetic breaking clutch.

(C) The safety clutches

These are installed between the electric motor and the actuating mechanism. In Fig.10.21, the safety friction clutch is presented in the form of two discs 5, 6 and springs 10. The friction torque between the discs depends on the tension of spring 10 and the friction coefficient of the discs. When the resisting (counter) torque on the shaft of the actuating mechanism exceeds the permissible value determined by the slipping torque of the discs, they start slipping with respect to each other, thus limiting the resisting torque transmitted via gear 1 to the shaft of the electric motor.

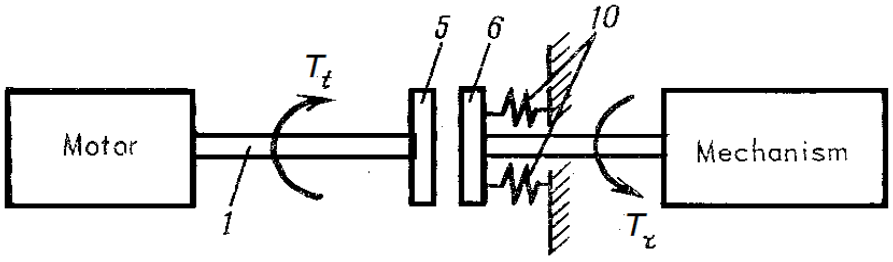

Fig.10.21 Safety clutches.

10.6 RATING OF MOTORS

Rating or size of motor can be selected in accordance to specific industrial applications. Beside the rated voltage and rated frequency, the size of the motor depends also upon:

(1) Temperature rise , which also depend on the duty cycle of the load
- Continuous load
- Intermittent load
- Variable load

(2) Maximum torque required of the motor

Temperature rise :

An electric machine can be considered as a homogeneous body in which heat is internally developed at uniform rate and heat dissipation is not a rate proportional to its temperature rise. The relation between the temperature rise and time is an exponential function which is given by:

$$\theta = \theta_m \left(1 - e^{-\frac{t}{\tau}}\right) \qquad (10.29)$$

where: θ = temperature rise C°
θ_m = Maximum temperature rise C°
τ = heating time constant
t = time in seconds

The temperature rise characteristics is depicted in Fig.10.22.

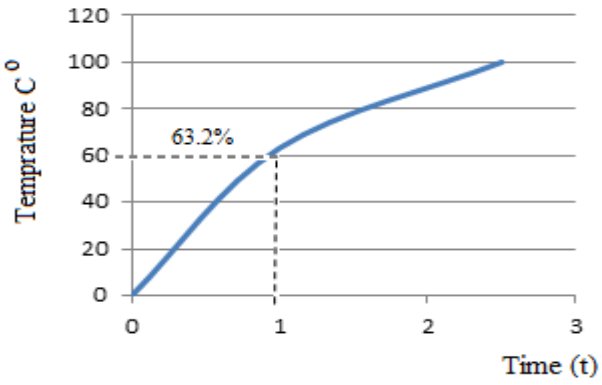

Fig.10.22 Temperature rise in electrical machine.

Cooling:

During cooling period (motor speed reduce or stopped) the temperature equation will be

$$\theta = \theta_m \, e^{-\frac{t}{\tau}} \qquad (10.30)$$

Example10.6

A motor has a thermal heating time constant of 45 min. When the motor runs continuously on full rating; its final temperature rise is 75 C°. (a) What is the temperature rise after two hour if the motor runs continuously on full load? (b) If the temperature on one hour rating is 70 C°, find the maximum steady temperature at this rating.

Solution

(a) Heating time constant τ = 45 min.

$$\Theta = \Theta_\infty \left(1 - e^{-\frac{t}{\tau}}\right) = 80(1 - e^{-\frac{120}{45.0}}) = 69.43\ \text{C°}$$

(b)

$$70 = \Theta_\infty \left(1 - e^{-\frac{120}{45.0}}\right)$$

$$\therefore\ \Theta_\infty = \frac{70}{0.925} = 75.6\ C°$$

10.6.1 Rating of the Motor for Continuous Load

If the motor has load torque T in Nm and it is running at ω rad /sec , the power rating of the motor:

$$p = \frac{T \cdot \omega}{1000} kW \qquad \rightarrow \qquad p = \frac{T \cdot \omega}{746}\ hp \tag{10.31}$$

Such loads are pumps, fan, etc.

10.6.2 Rating of the Motor for Intermittent Loads

Here the motor operating for short time and switch off for long time (motor is loaded for sometime). The motor is switched on before cooling completely to the ambient temperature such loads also referred as fluctuating loads, see Fig.10.23. An approximate and simple method of determined the rating of a motor subjected to fluctuating load is by assuming that the heating is proportional to the square of the current drawn by the motor and hence square of the load. The suitable continuous rating of the motor is the *rms* value of the load curve.

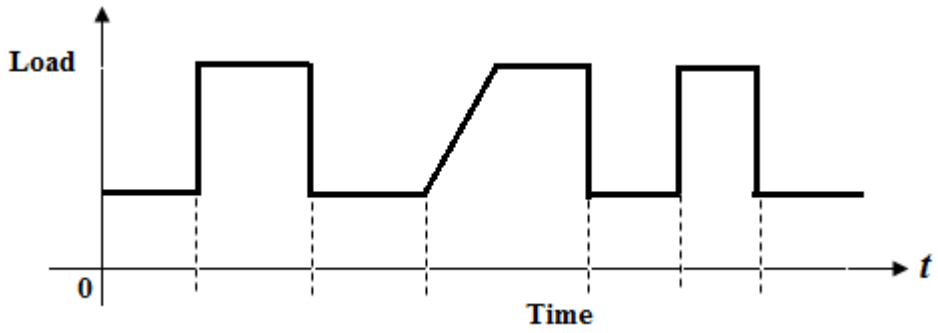

Fig.10.23 Fluctuating loads. e.g. (elevators).

Example10.7

The load cycle of a motor operating an elevator (lift) for 11 minutes is as follows:

Load period at the bottom	5 minutes	2 hp
Load going up	1 minute	25 hp
Load period at the top	4 minutes	2 hp
Load period going down	1 minute	-20 hp

Regenerative braking takes place when the load is disconnected. The cycle is repeated continuously. Estimate suitable *hp* for the motor.

Solution

Load variation is plotted in Fig.10.24.

The total area under the $(\text{hp})^2$ curve:

$$\text{A} = (2)^2 \times 5 + 25^2 \times 1 + 2^2 \times 4 + -20^2 \times 1 = 1061\ (\text{hp})^2.\ \text{min.}$$

$$\therefore \quad \text{hp}^2 = \frac{1061}{11} = 96.45 \qquad \text{or} \qquad \text{hp} = 9.82$$

The nearest standard rating = 10 hp.

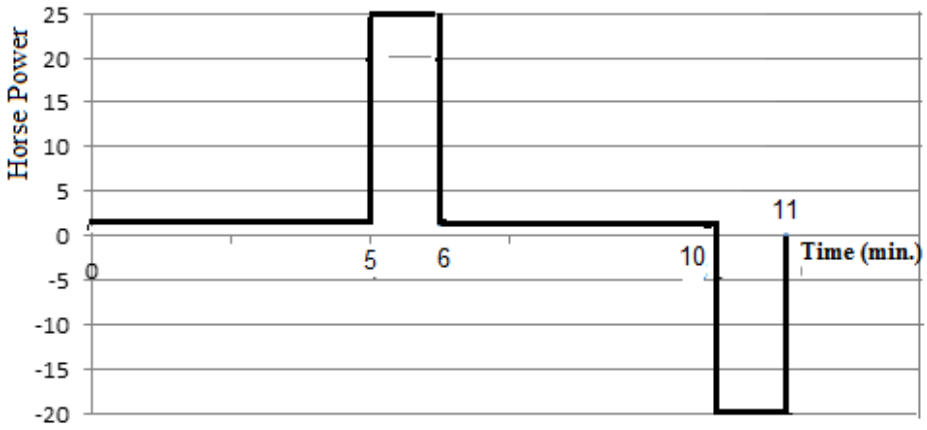

Fig.10.24 Power variation with time.

10.6.3 Rating of the Motor for Variable Load

The rating of the motor under such load conditions can be determined from the load torque vs time carve as depicted in Fig.10.25. This is called the method equivalent torque. In case of machines, whose flux remains constant irrespective of load variation, the equivalent torque rating is given by:

$$T_{eq} = \sqrt{\frac{\sum_{i=0}^{n} T_i^2 \,.\, t_i}{\sum_{i=0}^{n} t_i}} \qquad (10.32)$$

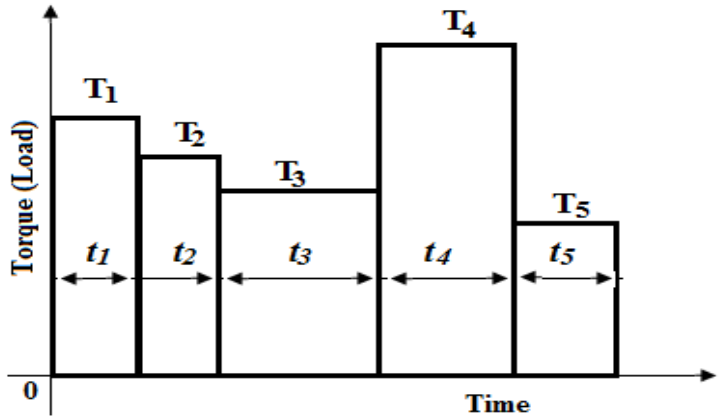

Fig.10.25 Load torque variation with time.

If the speed at which the load operates is approximately constant, the power *P* is proportional to the torque *T* and,

$$P_{eq} = \sqrt{\frac{\sum_{i=0}^{n} P_i^2 \,.\, t_i}{\sum_{i=0}^{n} t_i}} \qquad (10.33)$$

Example 10.8

An electric motor has load variation as:

Torque	250 Nm	for 25 minutes
	150 Nm	for 10 minutes
	320 Nm	for 12 minutes
	180 Nm	for 20 minutes

Find the equivalent torque rating of the motor. If the speed of the motor is 1000 *rpm* find the power rating of the motor?

Solution

$$T_{eq}^2 = \frac{(250)^2 \times 25 + (150)^2 \times 10 + (320)^2 \times 12 + (180)^2 \times 20}{25 + 10 + 12 + 20}$$

$$= 47588.3$$

$$\therefore T_{eq} = \sqrt{47588.3} = 218.14 \text{ Nm}$$

Power rating of the motor

$$P = T_{eq}\,\omega = \frac{218.14 \times 2\pi \times 1000}{60} = 22.8 \text{ kW}$$

Example 10.9

A motor driving an industrial load which follows the following cycles:

Power	50 kW	for 15 minutes
	No load	for 5 minutes
	30 kW	for 10 minutes
	No load	for 8 minutes

The cycle repeated indefinitely. Find the suitable size of the continuously rated motor for the purpose.

Solution

$$P_{eq}^2 = \frac{(50)^2 \times 15 + (30)^2 \times 10}{15 + 5 + 10 + 8} = \frac{46500}{38} = 1223.68$$

$$\therefore \ P_{eq} = 34.98 \text{ kW}$$

The nearest standard motor size is 37 kW or 50 hp.

PROBLEMS

10.1 A motor drive system produces 150 kW at the motor shaft when the motor runs at 1200 rpm.The motor is coupled to a gearbox with a ratio 4:1. The gearbox efficiency is 85%. Calculate the speed, power and torque delivered at the output of the gearbox.

[Ans: 300 rpm, 127.5 kW, 4060.5 Nm]

10.2 An a.c. motor is used to lift a mass of 750 kg through hight of 50 meter as shown in Fig.10.26. It is required that the mass must be lifted in time of 22 s. Calculate the power developed by the motor and the power rating of the motor needed.

[Ans: 16.72 kW ⟶ 18.5 kW]

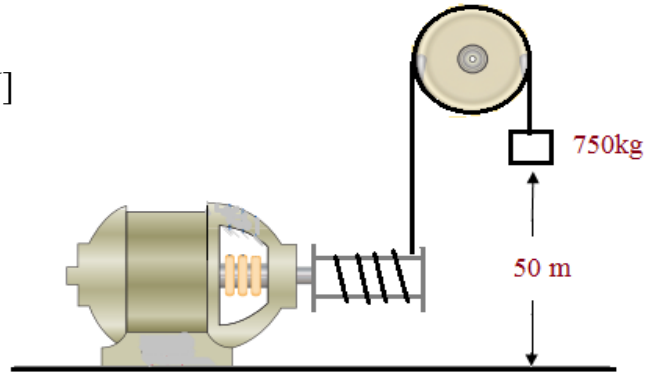

Fig.10.26.

10.3 Figure 10.27 shows a motor lifting a load by means of a winch. The weight lifted is1500 kg at a velocity of 0.5 m/s. The motor runs at a speed of 1250 rpm. The inertia of the winch drum and motor are 1.8 kg.m^2 and 3.6 kg.m^2

respectively. Calculate (i) the total load torque of the system referred to motor shaft, (ii) the inertia referred to the motor shaft.

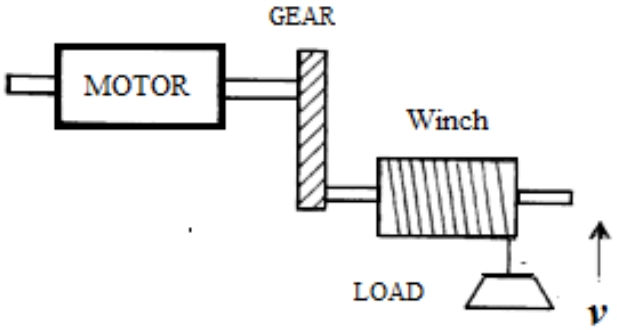

Fig.10.27.

[Ans: (i) 56.23 Nm, (ii) 0.0146 kg.m^2]

10.4 In a textile factory a motor is required to drive the take-up roll on a fabric strip line; the mandrel on which the strip is wound is 0.05 m in diameter and the strip rolls up to a roll 0.25 m in diameter. The strip emerges from the line at a speed of 15 m /s; the strip tension required is 20 kgf. The motor is coupled to the mandrel by a 1:2 reduction gearing. The gears may be considered to be 90% efficient at all speeds. Determine the speed and power rating of the motor needed for this service.

[Ans: 2866 rpm, 16.42 kW – typical ratings would be 3000 rpm, 18.5 kW]

10.5 A crane hoist is required to raise 300 kg weight at a speed of 0.40 m/s. The hook is mounted on a block which carries a single pulley sheave. One end of the hoisting cable is anchored on the crane trolley and the other is wound up on a winch drum 0.30 m in diameter. The drum is driven by a speed reducing gear of 45:1 ratio. The whole mechanism may be considered to be 65% efficient. Determine the power and speed rating of the motor and the braking torque exerted by the motor when it lowers the load at a rate of 0.5 m /s.

[Ans: 1813.3 W, 2296 rpm, – 3.18 Nm]

10.6 A paper manufacturing machine driving a large reel of paper installed at the end of the machine. The reel has a radius of 1 m , length of 4.5 m ,and a moment of inertia of 3750 kg.m^2. The machine employes driving motor a variable-speed driving motor running at 100 rpm. The paper is kept under constant tension of 5500 N.

(a) What is the power of the motor when it runs at 100 rpm.
(b) Calculate the torque and power produced by the motor when the motor speed raised to 150 rpm in 10 s.

[Ans: (a) T = 5500 Nm, P = 57.52 kW, (b) T = 7463.35 Nm, P = 86.38 kW]

10.7 A horizontal conveyer is to be used to move feedstock boxes, with an average of 6 boxes per metre run of conveyer belt. The weight of each box is 2kg. The belt is to move at a speed of 2.5 m /s. Determine the power rating of the motor required, noting that the mechanical power transmission has an efficiency of 60 % , and the motor has an efficiency of 90 % . Length of conveyer = 30 m and the mass of the part of the conveyer belt supporting the load = 1 kg per meter. The system is shown in Fig.10.28.

[Ans: 12.26 kW – typical rating would be 15 kW]

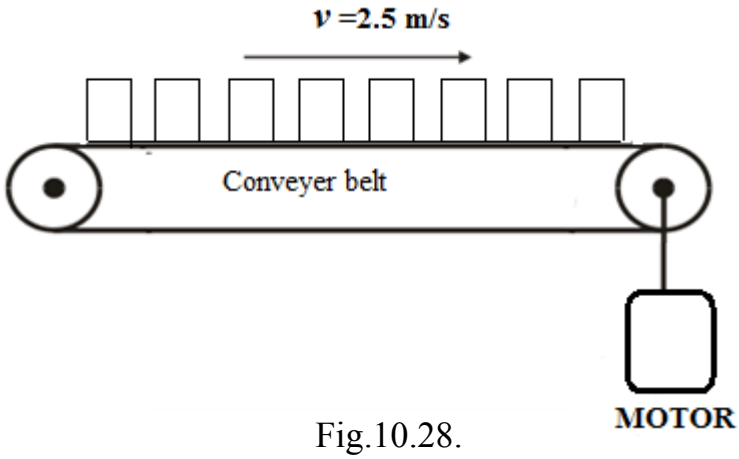

Fig.10.28.

10.8 A motor drive is supplied from a three-phase power converter has conversion efficiency of 90 % when operating at rated load. On the other hand,when the motor operates at rated load, it delivered net output power of 45 kW. The motor electrical and mechanical losses are 1125 W and 1200W respectively. Calculate the efficiency of the system from supply utility to motor shaft.

[Ans : 85.5%]

10.9 A variable speed d.c. drive has a rated power of 15 kW, and a rated speed of 1500 rpm drives a load that comprises a constant load T_L = 45 Nm. The inertia of the drive system is 0.10 kg.m^2. Calculate the time taken to accelerate the load from zero to 1000 rpm assuming the drive develops rated torque during the acceleration phase.

[Ans: 207 ms]

10.10 A drive system is used in the takeup roll in a paper making process. The paper is wound on a drum such that the radius from empty to full varies from 0.3 m to 1.25 m. The drum is driven through a 4:1 lossless reduction

gearbox by the drive motor. The process requires that the tension in the paper is maintained at 75 N and the paper velocity is 15 m /s .

(a) Sketch the torque-speed characteristics of the load as seen by the motor.

(b) Determine the required motor power rating.

[Ans: 4686 W– typical rating would be 5 kW]

10.11 A weight of (1000 kg) is to be lifted up with a velocity of (1 m /s) by means of winch having a diameter of (0.30 m). The winch is driven by motor running at (960 rpm) and inertia of the motor and the winch drum are (1.6 kg.m^2) and (3.2 kg.m^2) respectively. Calculate the total load torque of the system referred to the motor shaft. The system is shown in Fig.10.29.

[Ans :9.9 Nm]

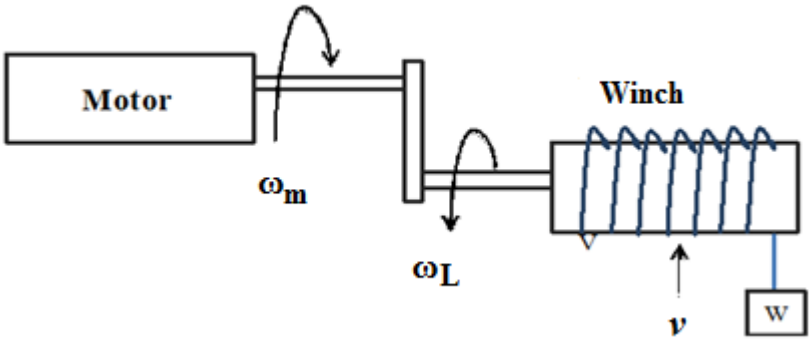

Fig . 10.29.

10.12 A horizontal conveyor belt is moving at a velocity of (1.5 m /s) and moves load at the rate of (60,000 kg/hour). The belt is (90 m) long is driven by a motor with speed of (960 rpm). Determine equivalent rotational inertia at the shaft of the motor. Fig.10.30 shows the system.

[Ans: 0.0227 kg.m^2]

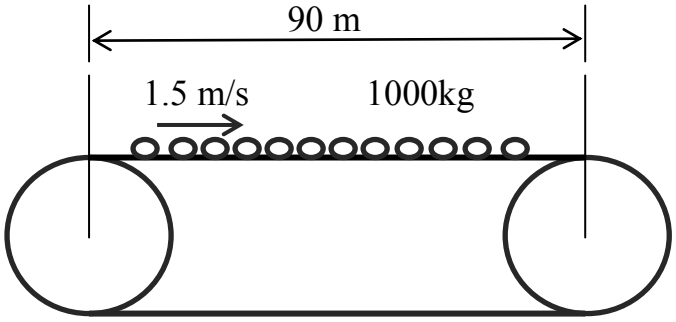

Fig.10.30.

10.13 A load torque of (6000 Nm) is supplied by motor through gears of ratios (1:2:4:8:16). The speed of motor is (960 rpm). Find the load torque referred to the motor shaft if the efficiency of each gear is (85%). Find power

required by the load. Also find the power input to the motor if the motor efficiency is (88 %). The system is shown in Fig.10.31.

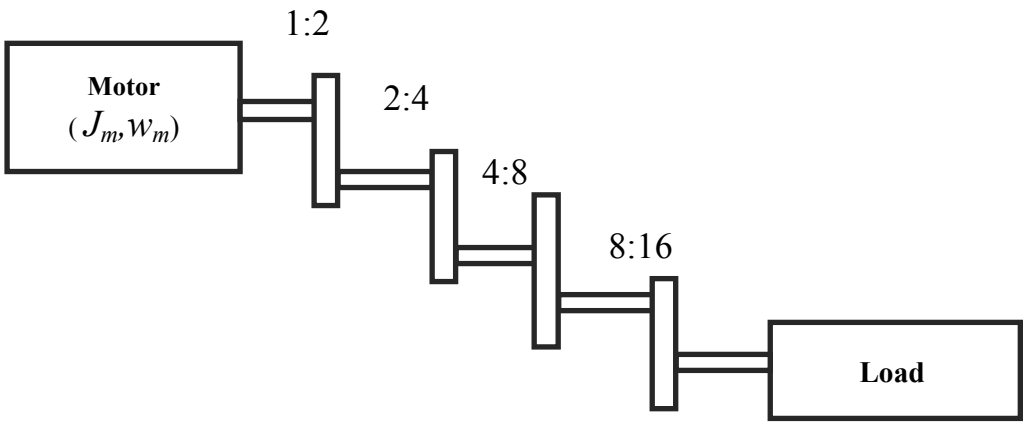

Fig .10.31.

[Ans: 11.22 Nm , 1128 Watts , 1282 Watts]

10.14 In the hoist drive system shown in Fig.10.32 , the mass M is considered being moved upwards with negligible frictional torque. Show that the load torque and the equivalent moment of inertia are given by

$$T_m = J_e \frac{d\omega_m}{dt} + \frac{\omega_2}{\omega_m} M.r$$

$$J_e = J_m + (\frac{\omega_1}{\omega_m})^2 J_1 + (\frac{\omega_2}{\omega_m})^2 [J_2 + M.r^2]$$

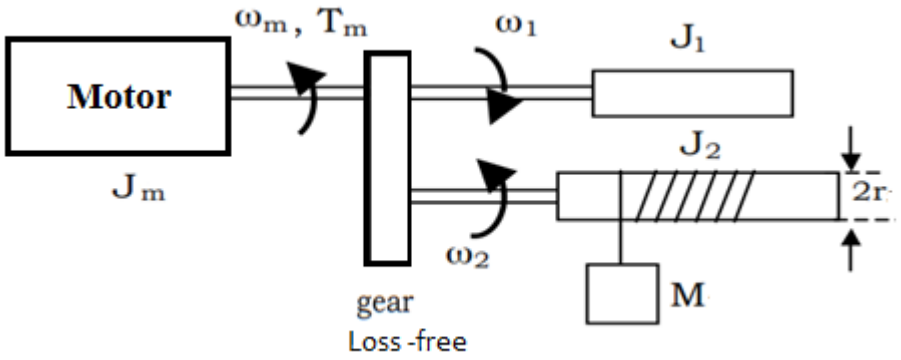

Fig.10.32.

CHAPTER ELEVEN

DC DRIVES : DC MACHINES REVIEW

11. 1 INTRODUCTION

In DC drives d.c. motors are employed in a very large power range, from few watts to several hundreds of kilowatts. Many applications required precise speed control as in textile and spinning and weaving industries, also some applications required very precise position adjustments (as in robotics). Electric trains require smooth speed control as well as the electric cars. In all these industrial applications d.c. motors are used since they provide smooth and precise speed control as compared with a.c. motors. Therefore, optimum performance and efficiency are the main concern in these applications. Variable speed drive (VSD) systems help in optimisation of process so as to reduce operational and maintenance costs. In order to study the DC drives it is important that the d.c. motor and its characteristics must be studied first and reviewed. This will be given in the following sections.

11.2 DC MOTORS

The structure of a direct current (d.c.) motor has two basic components, the field winding and the armature winding. The field winding in a d.c. machine is generally mounted on the frame or stator, while the armature winding invariably mounted on the rotor. Both are supplied from direct current electrical source as shown in Fig.11.1.

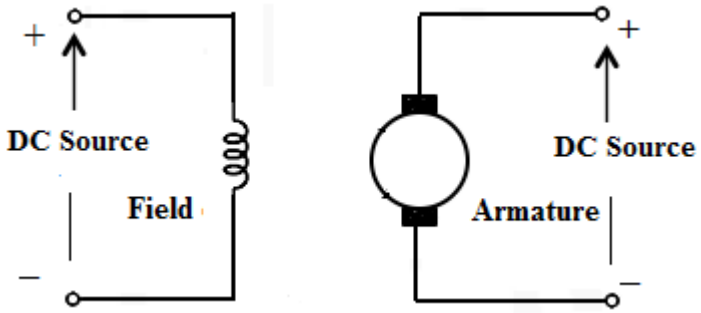

Fig.11.1 Armature and field circuits of a d.c. machine.

11.3 TYPES OF DC MOTORS

The armature circuit and the field circuit may be interconnected in the three basic ways shown in Fig.11.2. Each connection results in particular motor performance and each is suited to particular load applications. These basic types are :

- Separately-excited d.c. motor
- Self-excited d.c. motors
  - (a) Shunt d.c. motor
  - (b) Series d.c. motor
  - (c) Compound d.c. motor

In the separately-excited d.c. motor, (Fig.11.1), the field winding is excited from separate source. In the self-excited d.c. motor, the field winding can be connected in two different ways, the field winding may be connected across the armature (i.e. in shunt), resulting in a shunt motor (Fig.11.2(a)) or the field winding may be connected in series with the armature (Fig.11.2(b)) resulting in a series d.c. motor.

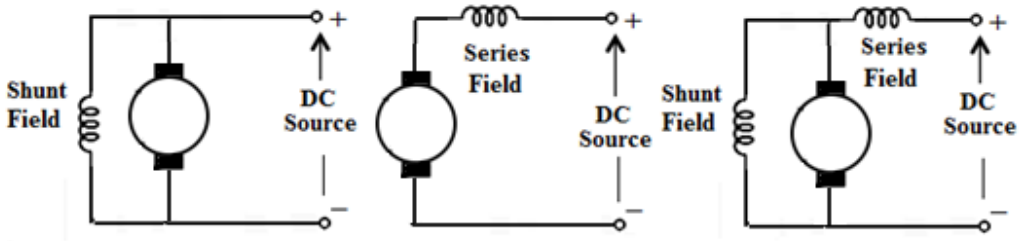

(a) (b) (c)

Fig.11.2 Basic types of self-excited d.c. machines: (a) shunt excited machine, (b) series excited machine, and (c) short-shunt compound machine.

Also these two basic circuits may be connected in such manners to form other types of motors called compound motors that contains both the

shunt and series fields as shown in Fig.11.2(c). If the shunt winding is connected across the armature, it is known as short-shunt motor (Fig.11.2(c)). In an alternative connection, the shunt winding is connected across the series connection of armature and series winding, and the machine is known as long-shunt motor (Fig.11.3). Both shunt field winding and series field winding are practically wound on the same pole as shown in Fig.11.4(a).

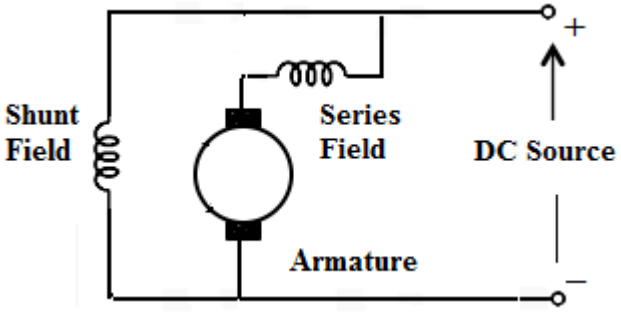

Fig.11.3 Compound d.c. motor: Long-shunt type.

In a compound wound d.c. motor the shunt field is normally stronger than the series field (i.e, has more ampere-turns). Compound motor are also be of two types namely, cumulative compound wound motor and differential compound wound motor. Cumulative compound motor is one in which the field windings are connected in such a way that the shunt winding flux φ_{sh} and the series winding flux φ_s are produced in the same direction so that they add together as shown in Fig.11.4(b).

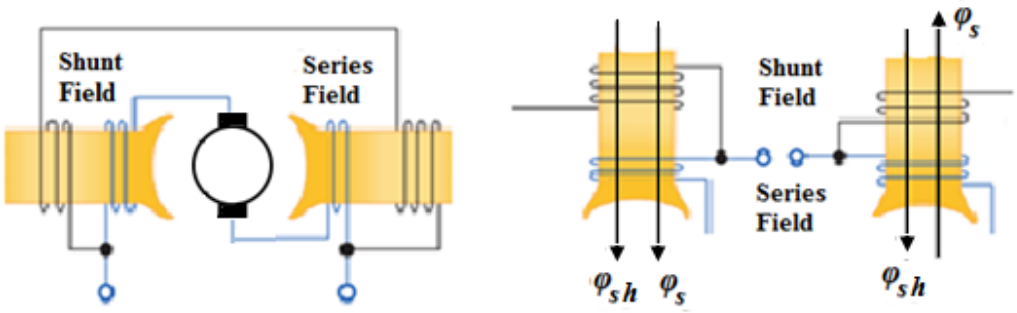

(a) (b) (c)

Fig.11.4 (a) Compound motor field windings, (b) Differential compound, (c) Cumulative compound.

On the other hand, the differential compound wound motor is one in which the field windings are connected in such a way that the series winding flux φ_s opposes the shunt winding flux φ_{sh} and weakens it, as illustrated in Fig.11.4(c).

11.4 PRINCIPLES OF DC MOTORS

11.4 .1 The Equivalent Circuit of a Separately-Excited DC Motor

A separately-excited d.c. motor is a motor whose field circuit is supplied from a separate constant voltage power supply. Fig.11.5 shows the electrical equivalent circuits of a separately-excited d.c. motor. In this figure, the armature circuit is represented by an ideal voltage source E_a and a resistor R_a in series with armature inductance L_a. This representation is really the Thevenin equivalent of the entire rotor structure, including rotor coils, interpoles and compensating windings, if present.

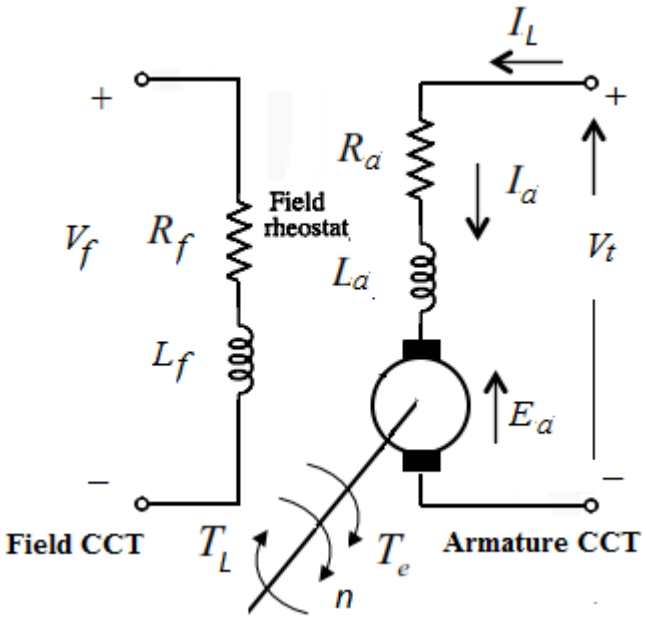

Fig.11.5 Electrical equivalent circuit of a separately-excited d.c. motor.

The field coils, which produce the magnetic flux in the motor, are represented by inductor L_f and resistor R_f. This circuit is approximate because we made some of the few simplifications:

i- The brush drop voltage is often only a very tiny fraction of the generated voltage in the machine. Thus, in cases where it is not too critical, the brush drop voltage may be left out or included in the R_a.

ii- The internal resistance of the field coils is sometimes lumped together with the variable resistor and the total is called R_f.

The principal equations of d.c. machine are:
The internal induced (back) *emf* E_a is given by:

$$E_a = K_e \emptyset \, n \qquad (11.1)$$

and the electromagnetic (developed) torque T_e is

$$T_e = K_T \emptyset \, I_a \tag{11.2}$$

The relation between the terminal voltage V_t and the induced *emf* is

$$V_t = E_a + I_a R_a \tag{11.3}$$

Input electrical power to the armature circuit

$$P_{in} = V_t \, I_a \tag{11.4}$$

Developed power

$$P_d = T_e \, \omega \tag{11.5}$$

Output mechanical power

$$P_{out} = T_L \, \omega \tag{11.6}$$

where

n = speed of the motor in revolution per minute (rpm),
Φ = flux per pole in Weber (Wb),
K_e = machine constant = $p.Z / 60$ a,
P = number of poles, Z = total number of conductors in the armature circuit , a = number of parallel paths (a = p for lap winding, a = 2 for wave winding).
K_T = torque constant = 9.55 K_e ,
I_a = armature current (A).
ω = angular speed = 2πn /60 (rad /s)

11.4.2 Speed and Torque Equations

The output characteristic (speed-torque relationship) of a separately-excited d.c. motor can be derived from the induced voltage equation (11.1) and torque equation (11.2) of the motor plus the motor general equation (11.3) as follows :
From Eq.(11.2) current I_a can be expressed as:

$$I_a = \frac{T_e}{K_T \emptyset} \tag{11.7}$$

Combining the V_t , E_a and I_a equations:

$$V_t = K_e \emptyset \, n + \frac{T_e}{K_T \emptyset} R_a \tag{11.8}$$

Finally, solving for the motor speed:

$$n = \frac{V_t}{K_e \emptyset} - \frac{R_a}{K_e K_T \emptyset^2} T_e \quad (11.9)$$

The later is called the fundamental equation of the speed of d.c. motor. The no load speed n_o is found when $T_e = 0$, hence the no load speed is,

$$n_o = \frac{V_t}{K_e \emptyset} \quad (11.10)$$

Representation of the speed equation of the d.c. motor in terms of the angular velocity ω

Referring to the two basic equations of d.c. motor Eqs.(11.1) and (11.2), in which the constants K_e and K_T are defind previously as the machine constant and the torque constant respectively. The relation between these two constant is, $K_T = 9.55\ K_e$ for all types of d.c. machine. In the SI system of units the constants K_e and K_T are identical ($K_e = K_T = K$) and have the dimensions Newton metres per Weber ampere or Volt seconds per Weber radian. Since the angular velocity $\omega = 2\pi n /60$ rad /s, equations (11.1) and (11.2) can be re-written as,

$$E_a = K_e\ \emptyset\ n = K_e\ \emptyset\ \frac{60}{2\pi}\omega = 9.55\ K_e\ \emptyset\ \omega \quad (11.11)$$

or $$E_a = K_T\ \emptyset\ \omega = K \emptyset\ \omega \quad (11.12)$$

and $$T_e = K\ \emptyset\ I_a \quad (11.13)$$

From which,

$$I_a = \frac{T_e}{K \emptyset} \quad (11.14)$$

Substituting Eq.(11.1) and Eq.(11.2) in Eq.(11.3) yields,

$$V_t = K \emptyset\ \omega + \frac{T_e}{K \emptyset} R_a \quad (11.15)$$

Finally, solving for the motor speed:

$$\omega = \frac{V_T}{K \emptyset} - \frac{R_a}{K^2 \emptyset^2} T_e \quad (11.16)$$

Equation (11.16) represents the general equation of the speed of d.c. motors in terms of the angular velocity ω in rad per second which is used instead of n in rpm in many text books.
The no load speed is when $T_e = 0$, hence the no load speed ω_o :

$$\omega_o = \frac{V_t}{K \emptyset} \tag{11.17}$$

During transient periods where $n \neq$ constrant

$$V_t = E_a + R_a I_a + L_a \frac{di_a}{dt} \tag{11.18}$$

For steady-state , n = constant and $\frac{di_a}{dt} = 0$.

11.5 MECHANICAL CHARACTERISTICS OF DC MOTORS IN DRIVING CONDITIONS

When a d.c. motor is used in driving system, its basic operational characteristics are determined by both the values of the resisting torque T_L created by the load, and the electromechanical properties of the motor itself. In the steady-state operation of the drive, it has been shown in Chapter Ten, Section (10.4) , that the value of the torque T_m developed by the motor should equal to the load torque, i.e. $T_m = T_L$. As it is seen from Eq.(11.2) that the electromagnetic torque $T_e = T_m$ is proportional to the armature current I_a and the effective machine flux per pole Φ. Thus the variation of the load torque T_L should result in variation of the motor torque T_m as well, i.e. variation of armature current I_a and the magnetic flux Φ. The relation between the motor torque and the armature current, $T_m = f(I_a)$, is called the electrical characteristic or internal characteristic of the motor .

In drive systems, the internal characteristic of the motor is not very important, since we are interested in the motor shaft speed and not the current. Therefore, to find out the motor's actual speed corresponding to specific value of the motor torque, one should know the actual relation between the speed and torque n = $f(T_m)$, which is called the external or mechanical characteristic of the motor. In general, the mechanical characteristic of a d.c. motor depends on its type whether it is separately, shunt, series or compound. Each type has its own mechanical characteristic which is different from the others as it will be explained hereinafter.

11.5.1 Mechanical Characteristics of a Separately-Excited d.c. Motor

The output characteristic of a separately excited d.c. motors which is the relation between the torque and speed is given in Eq.(11.9) or

Eq.(11.16). This equation is called the d.c. motor speed equation. Now since V_t , $\emptyset$, Ke, K_T and R_a are all assumed constants, Eq.(11.9) can be expressed analytically as,

$$n = \alpha - \frac{1}{\beta} T_e \ = \alpha - \ m\, T_e \qquad (11.19)$$

which is just a straight line with a negative slope $m = \frac{1}{\beta}$. However, In this equation

$$\alpha = \frac{V_t}{K_e \emptyset} = n_o \qquad (11.20)$$

where n_o = no load speed , i.e. when $T_e = 0$.

$$\beta = \frac{K_T K_e \emptyset^2}{R_a} \qquad (11.21)$$

β is a constant called the coefficient of hardness of the motor.

The resulting mechanical characteristics (speed-torque characteristics) of the separately-excited motor is shown in Fig.11.6 (Curve-1).

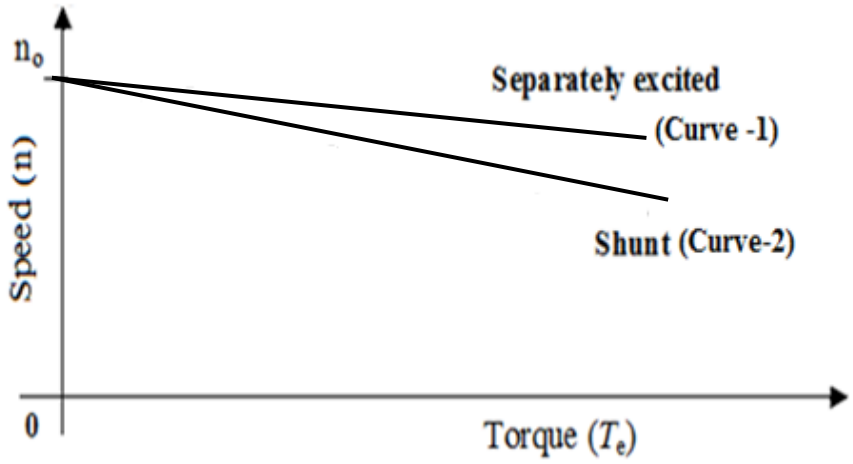

Fig.11.6 Speed-torque characteristic of separately-excited d.c. motor (Curve-1) and shunt (self-excited) d.c. motor (Curve-2).

11.5.2 Mechanical Characteristics of Shunt d.c. Motor

The equivalent circuit of a shunt d.c. motor is shown in Fig.11.7(a). The output characteristic of a shunt and separately-excited d.c. motors are approximately the same. As it has been mentioned that the separately-excited d.c. motor is a motor whose field circuit is supplied from a separate constant-voltage d.c.source, whereas a shunt d.c. motor is a motor whose field circuit gets its power directly across the armature terminals of the motor as shown in Fig.11.7(a). This means that, when the

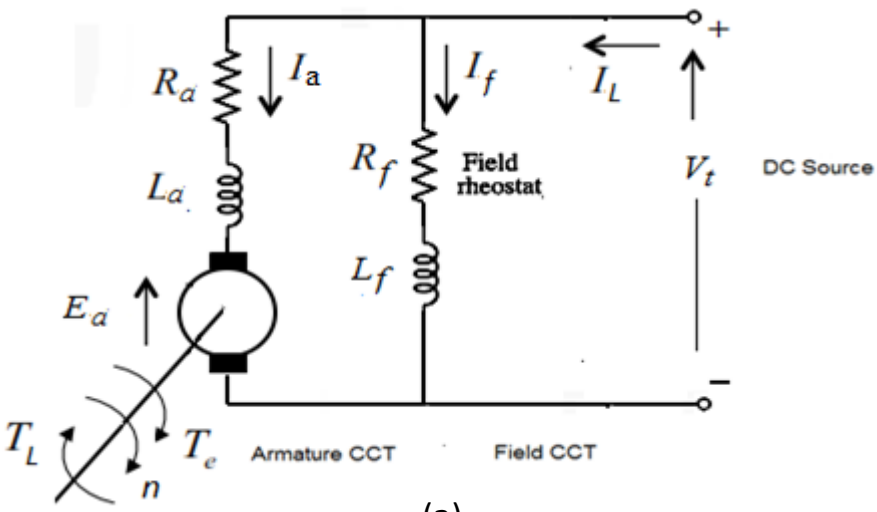

(a)

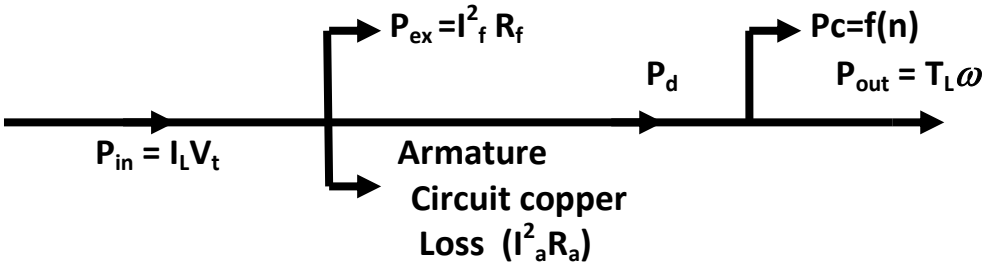

(b)

Fig.11.7 Shunt d.c. motor : (a)The equivalent circuit, (b) Power flow.

supply voltage V_t to a motor is assumed constant, there is no practical difference in behaviour between these two machines. Unless otherwise specified, whenever the behaviour of a shunt motor is described, the separately-excited motor is included too. Hence for shunt motor :
The KVL equation for the armature circuit is

$$V_t = E_a + I_a R_a \qquad (11.22)$$

The currents relations is

$$I_L = I_a + I_f \qquad (11.23)$$

The power flow diagram in shunt motor is shown in Fig.11.7(b).

$$P_d = T_e \omega = I_L V_t - \left(I_f V_t + I_a^2 R_a\right) \qquad (11.24)$$

Note that: Pc = mechanical loss+ iron loss and both are speed dependent.

The speed equation of the shunt motor is the same equation of the separately-excited motor (Eqs.(11.9) and (11.16)). These equations are just a straight line with a negative slope. The resulting torque-speed characteristic of a shunt d.c. motor is also shown in Fig.11.6 (Curve-2).

To explain how does a shunt d.c. motor respond to a load, suppose that the load on the shaft of a shunt motor is increased, then the load torque T_L will exceed the developed torque T_e in the machine, and the motor will start to slow down. When the motor slows down, its internal generated voltage drops ($E_a = Ke\ n\phi\downarrow$), so the armature current in the motor $I_a = (V_t - E_a\downarrow)/R_a$ increases.

As the armature current increases, the developed torque in the motor increases ($T_e = K_T\ I_a\ \phi$) and finally the developed torque will equal the load torque at a lower mechanical speed of rotation.

11.5.3 Mechanical Characteristics of Series d.c. Motor

A series d.c. motor is a d.c. motor whose field windings consist of relatively few turns connected in series with the armature circuit. The equivalent circuitof this type of motor is shown in Fig.11.8. A distinct feature of a series motor is that the field current I_S is equal to the armature current I_a and the current drawn from the supply I_L , i.e.

$$I_S = I_a = I_L \tag{11.25}$$

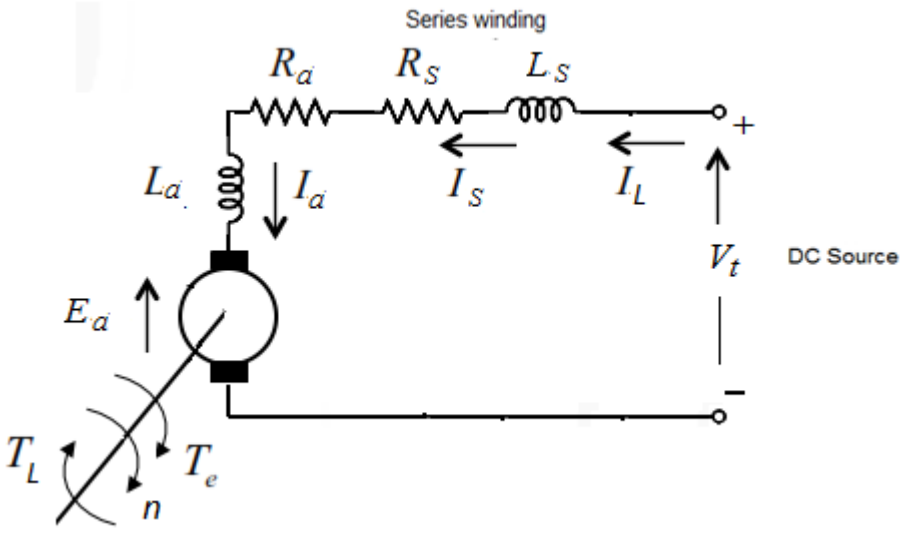

Fig.11.8 Series d.c. motor equivalent circuit.

Induced Torque in a Series d.c. Motor

The basic behaviour of a series d.c. motor is due to the fact that the flux is directly proportional to the armature current, at least until saturation is reached, (Fig.11.9). As the load on the motor increases, its flux increases too. As seen earlier, an increase in flux in the motor causes a decrease in its speed. The result is that a series d.c. motor has a sharply drooping speed-torque characteristic. The developed torque is

$$T_e = K_T \phi I_a \tag{11.26}$$

The flux in this machine is directly proportional to its armature current (at least until iron saturates). Therefore, the flux in the machine can be given by

$$\phi = K_f I_a \tag{11.27}$$

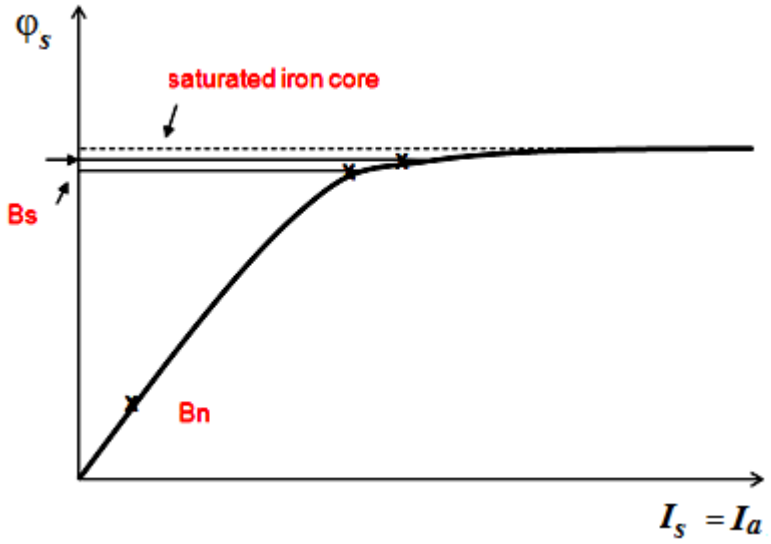

Fig.11.9 Magnetization curve of a series motor.

where K_f is a constant. Thus,

$$T_e = K_T \phi I_A = K_T K_f I_a^2 \tag{11.28}$$

Series d.c. motors are therefore used in applications requiring very high torques. Example: starter motors in cars, elevator motors, tractor motors etc.

The Terminal Characteristic of a Series d.c. Motor

The assumption of a linear magnetization curve implies that the flux in the motor will be given by Eq.(11.27). This equation will be used to derive the speed-torque characteristic curve for the series motor.

Derivation of the speed-torque characteristic:

Referring to Fig.11.8, the KVL for this motor is

$$V_t = E_a + I_a(R_a + R_s) \tag{11.29}$$

The armature current I_a is given by,

$$I_a = \sqrt{\frac{T_e}{K_T\, K_f}} \tag{11.30}$$

Also, $E_a = K_e \emptyset\, n$, thus substituting this and Eq.(11.30) in Eq. (11.29) yields

$$V_t = K_e \emptyset\, n + \sqrt{\frac{T_e}{K_T K_f}}\,(R_a + R_s) \tag{11.31}$$

If the flux can be eliminated from this expression, it will directly relate the torque of a motor to its speed n. Notice that $I_a = \emptyset^2/K_f$ and $T_e = (K_T/K_f)\,\emptyset^2$. Thus ,

$$\emptyset = \sqrt{\frac{K_f}{K_T}}\sqrt{T_e} \tag{11.32}$$

Substituting Eq. (11.32) into Eq. (11.31), and solve for n results in:

$$n = \frac{V_t}{K_e\sqrt{\frac{K_f}{K_T}}} \times \frac{1}{\sqrt{T_e}} - \frac{(R_a + R_s)}{K_e K_f} \tag{11.33}$$

and the torque equation is

$$T_e = T_m = K_T K_f I_a^2 \tag{11.34}$$

The speed-torque curve of series motor will vary, according to Eq.(11.33) as shown in Fig.11.10. It can be easily, from Eq. (11.33), being noted that the speed-torque characteristic of series motor is a hyperbola

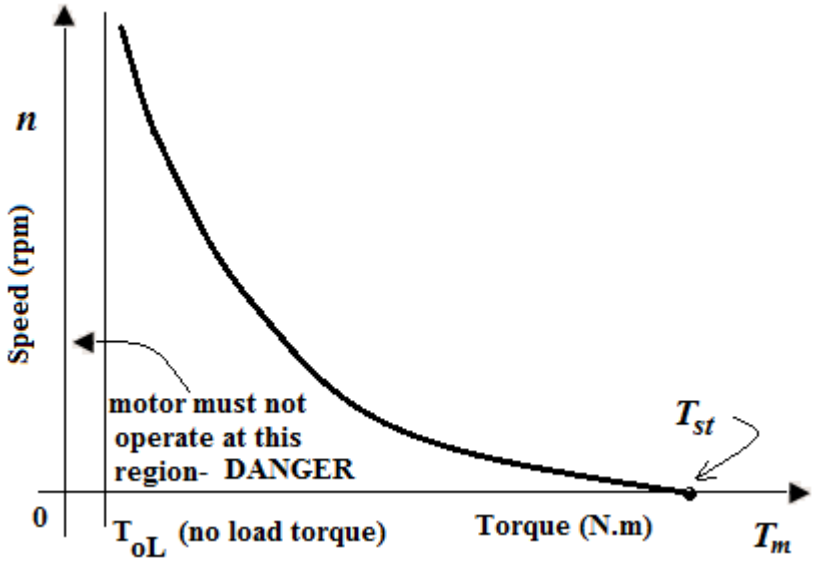

Fig.11.10 The speed-torque characteristic of a series d.c. motor.

with asymptote at the speed axis. To plot this hyperbola, substituting $T_e = 0$ in Eq.(11.33) yields, $n = n_o = \infty$. i.e. , the no load speed at the ideal no load running of the series motor is infinite (excessive speed). Therefore, at very small load torques are likely to cause rapid increase in the motor speed n which is dangerous to the motor mechanical construction (armature winding, bearings, and commutator structure).

Series motors can usually protected against the danger of excessive speeds by a positive connection to their load before starting. However, for small motors, below 200W, the mechanical losses in the motor may be sufficient to prevent excessive no load speed. In high power motors, even a threefold increase, $n = 3n_n$, where n_n is the normal (rated) speed may result in mechanical over stresses dangerous to the armature . Therefore, these machines should not be run at no load condition.

On the other hand, the starting torque T_{st} can be calculated by setting $n = 0$ in Eq. (11.33), thus

$$T_{st} = \frac{V_t^2}{(R_a + R_s)^2} K_T K_f \qquad (11.35)$$

Since the values of R_a and R_s are usually very small, hence the starting torque of the series motor is considerably large compared with that of separately-excited and shunt motors. This feature makes it preferable to be used to start heavy loads such as electric vehicles, electric trains and elevators.

11.5.4 Mechanical Characteristics of Compound d.c. Motor

The connection diagram of a compound motor is shown in Fig.11.11.The mechanical characteristics of the compound motor occupy intermediate position between the characteristics of the shunt and the series motors due to the fact that the compound motors contains both the shunt and the series windings.

Fig.11.12 depicts the speed-torque characteristics of the three types of d.c. motors namely, shunt ,series and compound. As is clear from these characteristics, the compound motor at ideal idle running has an ultimate no load speed n_o . Beside, when compared with shunt motor, the compound machine develop stronger starting electromagnetic torque T_{st} , and when compared with series motor , it exhibits more " rigid " mechanical characteristics.

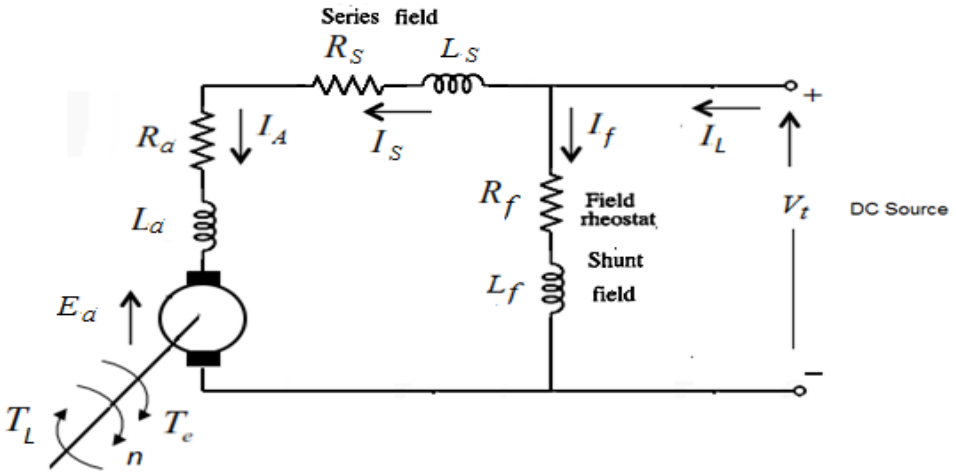

Fig.11.11: Compound motor connection diagram.

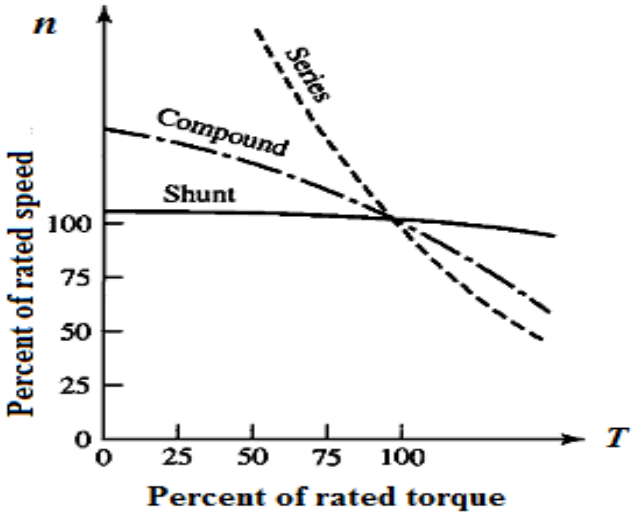

Fig.11.12 Compound motor mechanical characteristics as compared with shunt and series motors.

11.6 DC MOTORS SPEED CONTROL

The speed control of d.c. motors is very important subject in the consideration of the application of these motors. The various methods of speed control follow directly from the fundamental equation of the d.c. motor speed equation (11.9), from which one can predict the ways to control *n* if we write down it in the following simple form,

$$n = \frac{V_t - I_a R_a}{K_e \emptyset} \tag{11.36}$$

This equation shows that the speed is directly proportional to the applied voltage (V_t), inversely proportional to the flux per pole $\emptyset$ and changing the armature resistance R_a by adding an external resistance in series with it. Therefore, it is clear that the motor speed *n* can be varied by the following methods:

(i) Varying the terminal voltage V_t , hence varying the applied voltage to the armature V_a .
(ii) Adjusting the field resistance R_f (and thus varying the field flux $\emptyset$).
(iii) Inserting a resistor in series with the armature circuit ($R_a + R_{add} = \sum R_a$) , (rheostat control).

The first method is the most common method to decrease or increase the spead, while the third one is rarely used now days since it results in excessive losses.

11.6.1 Motor Speed Control of Shunt and Separately Excited d.c. Motors

(A) Changing the Armature Voltage

This method involves changing the voltage applied to the armature of the motor without changing the voltage applied to the field. If the voltage V_a is increased, then I_a rises, since [$I_a = (V_a \uparrow - E_a) / R_a$]. As I_a increases, the developed torque $T_e = K_T \phi I_a$ increases, making $T_e > T_L$, and the speed of the motor increases. Motor accelerated to new speed: (1→2→3) as shown in Fig.11.13. Now, as the speed increases, E_a ($=K_e \phi n \uparrow$) increases, causing the armature current to decrease. This decrease in I_a decreases the developed torque, causing $T_e = T_L$ at a higher rotational speed.

(B) Changing the Field Resistance (Field weakening method

If the field resistance increases, then the field current decreases ($I_f \downarrow = V_t / R_f \uparrow$), and as the field current decreases, the flux decreases as well. A decrease in flux causes an instantaneous decrease in the internal

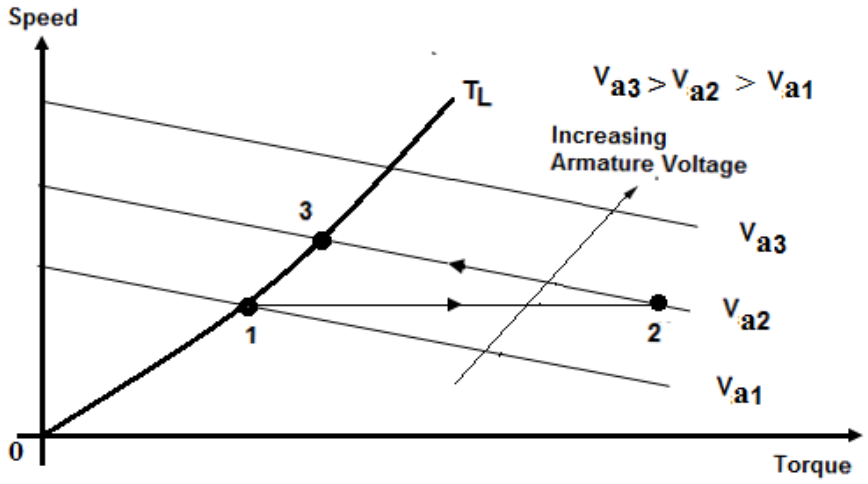

Fig.11.13 The effect of armature voltage variation on speed control of d.c. separately-excited and shunt motor.

generated voltage $E_a\downarrow$ (=$Ke\ \phi \downarrow n$), which causes a large increase in the machine's armature current since, The developed torque in a motor is given by $T_e = K_T \phi\, I_a$. Since the flux in this machine decreases while the current I_a increases, so which way does the developed torque change?

To understand what is happning , the following example will illustrate the sequence of events for the motor shown in Fig.11.14:

$$I_a \uparrow = \frac{V_t - E_a}{R_a}$$

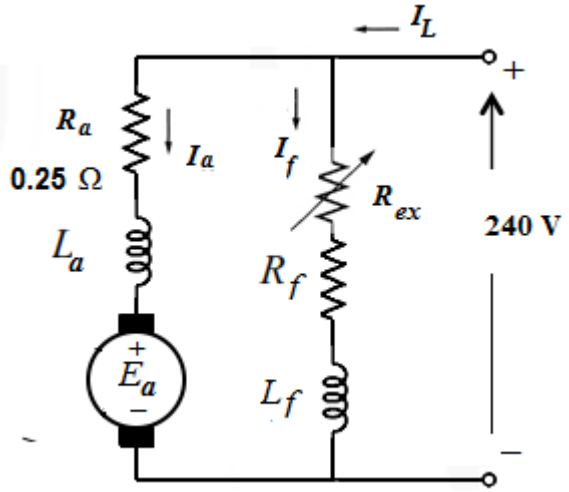

Fig.11.14 Shunt motor with added resistance in the field circuit.

Figure 11.14 shows a shunt d.c. motor with an armature resistance of 0.25 Ω. It is currently operating with a terminal voltage of 240V and an internal generated voltage E_a of 235V. Therefore, the armature current flow is: I_a = (240V-235V) / 0.25Ω = 20A.

Now, what happens in this motor if there is a 1% decrease in flux?

If the flux decrease by 1%, then E_a must decrease by 1% too, because $E_a = Ke\ \phi \downarrow n$. Therefore, E_a will drop to:

$$E_{a2} = 0.99\ E_{a1} = 0.99\ (235) = 232.65\text{V}$$

The armature current must then rise to:

$$I_a = (240\text{-}232.65) / 0.25 = 29.4\ \text{A}$$

Thus, a 1% decrease in flux produced a 47 % increase in armature current.

So, to get back to the original discussion, the increase in current predominates over the decrease in flux, $T_e > T_L$ and the motor speeds up. However, as the motor speeds up, E_a rises, causing I_a to fall. Thus, developed torque T_e drops too, and finally T_e equals T_L at a higher steady-state speed than originally (1 → 2 → 3) , see Fig.11.15.

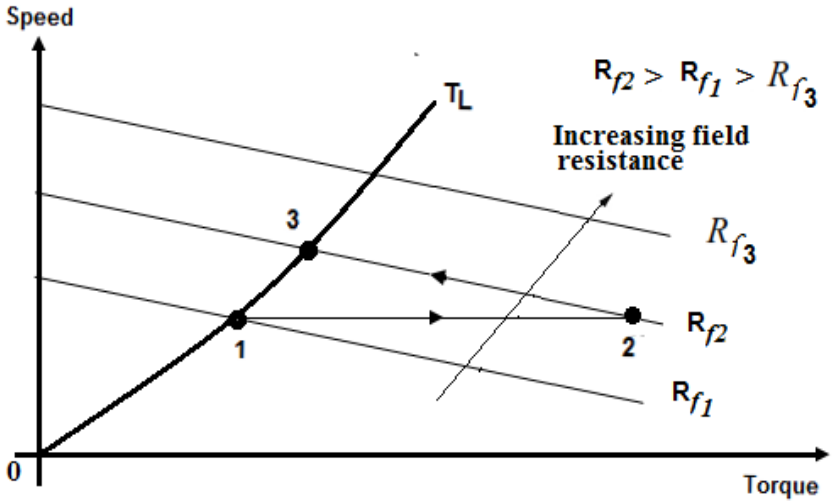

Fig.11.15 The effect of field resistance R_f variation on speed control of a shunt motor's speed-torque characteristics.

The effect of increasing the R_f is depicted in Fig.11.15 . Notice that as the flux in the machine decreases, the no-load speed of the motor increases, while the slope of the speed-torque curve becomes steeper.

(C) Inserting a Resistor in Series with the Armature Circuit

If a resistor is inserted in series with the armature circuit, see Fig.11.16, the effect is to drastically increase the slope of the motor's torque-speed characteristic, making it operates more slowly if loaded. This fact can be seen from the speed equation (11.9) which can be re-written as:

$$n = \frac{V_t}{K_e \emptyset} - \frac{R_a + R_{add}}{K_e K_T \emptyset^2} T_e \qquad (11.37)$$

If $R_{add} \downarrow I_a$ and $T_e \uparrow$, hence motor accelerated (n increased from point 1 to point 3), see Fig.11.17.

If $R_{add} \uparrow I_a$ and $T_e \downarrow$, hence motor decelerated (n reduced from point 4 to point 6).

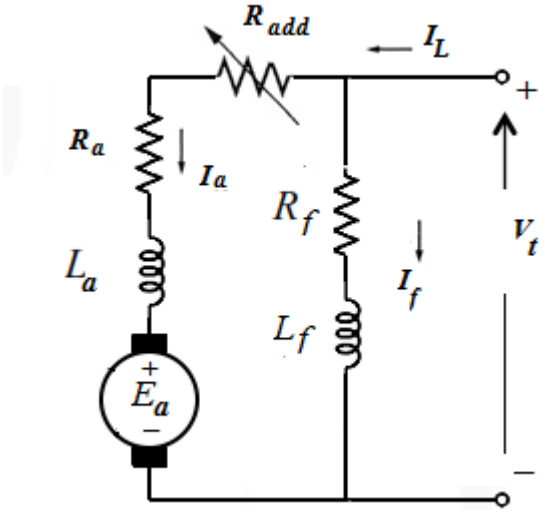

Fig.11.16 Rheostat speed control of shunt motor.

The insertion of a resistor is a very wasteful method of speed control, since the losses in the inserted resistor are very large. For this reason, it is rarely used.

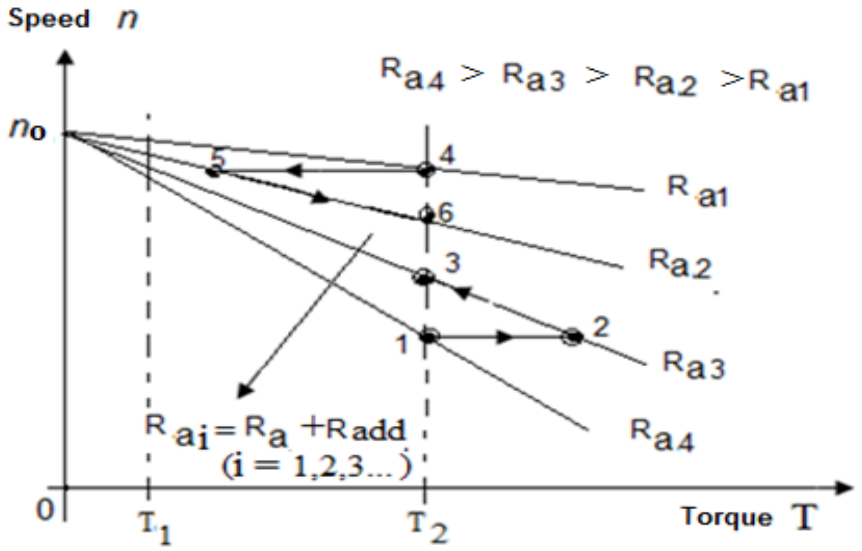

Fig.11.17 Speed variation by insertion additional resistance R_{add} in the armature circuit.

11.6.2 Safe Ranges of Operation for the Two Common Methods

Field Resistance Control

- The lower the field current in a shunt (or separately-excited) d.c. motor, the faster it turns; and the higher the field current, the

slower it turns. Since an increase in field current causes decrease in speed, there is always a minimum achievable speed by field circuit control. This minimum speed occurs when the motor's field circuit has the maximum permissible current flowing through it.

- If a motor is operating at its rated terminal voltage, power and field current, then it will be running at rated speed, also known as base speed. Field resistance control can control the speed of the motor for speeds above base speed but not for speeds below base speed. To achieve a speed slower than base speed by field circuit control would require excessive field current, possibly burning up the field windings.

Armature Voltage Control

- The lower the armature voltage on a separately-excited d.c. motor, the slower it turns, and the higher the armature voltage, the faster it turns. Since an increase in armature voltage causes an increase in speed, there is always a maximum achievable speed by armature voltage control. This maximum speed occurs when the motor's armature voltage reaches its maximum permissible level.

- If a motor is operating at its rated terminal voltage, power and field current, then it will be running at rated speed, also known as base speed. Armature voltage control can control the speed of the motor for speeds below base speed but not for speeds above base speed. To achieve a speed faster than base speed by armature voltage control would require excessive armature voltage, possibly damaging the armature circuit.

These two techniques of speed control are obviously complementary. Armature voltage control works well for speeds below base speed, and field resistance control works well for speeds above base speed.

- There is a significant difference in the torque and power limits on the machine under these two types of speed control. The limiting factor in either case is the heating of the armature conductors, which places an upper limit on the magnitude of the armature current I_a .
  For armature voltage control, the flux in the motor is constant, so the maximum torque in the motor is $\boldsymbol{T}_{max} = K_T \phi I_{a,max}$. This maximum torque is constant regardless of the speed of the rotation of the motor. Since the power out of the motor is given by $P=T\omega$, ($\omega = 2\pi n / 60$) is the angular velocity of the motor shaft), the maximum power is $P_{max} = T_{max}\,\omega$. Thus, the maximum power

out is directly proportional to its operating speed under armature voltage control.

- On the other hand, when field resistance control is used, the flux does change. In this form of control, a speed increase is caused by a decrease in the machine's flux. In order for the armature current limit is not exceeded, the developed torque limit must decrease as the speed of the motor increases. Since the power out of the motor is given by $P=T\omega$ and the torque limit decreases as the speed of the motor increases, the maximum power out of a d.c. motor under field current control is constant, while the maximum torque varies as the reciprocal of the motor's speed, see Fig.11.18.

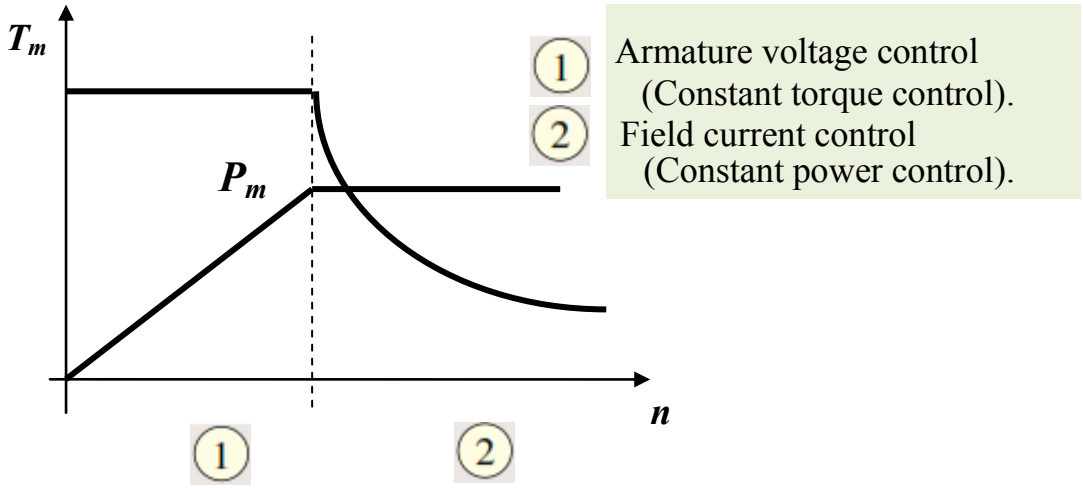

Fig.11.18 Torque and power limits for a d.c. motor.

Example 11.1

A separately-excited d.c. motor used to drive a fan whose torque is proportional to the square of the speed. When the armature circuit of the motor is connected across 200 V, it takes armature current of 16 A and the motor runs at speed of 1000 rpm. If the speed of the motor is to be reduced to 750 rpm, calculate the required terminal voltage and the current drawn by the motor at the new speed. Assume the armature resistance is 0.5 Ω and neglect brush voltage drop.

Solution

Armature current I_{a1} = 16 A

Back *emf* $E_{a1} = V_1 - I_{a1}R_a \; 200 - 16 \times 0.5 = 192$ V

Speed n_1 =1000 rpm

Torque $T_1 \propto n_1^2 \quad \rightarrow \quad T_1 = \mathrm{C}n_1^2$ where C is constant

$$T_1 = K_T \emptyset \, I_{a1}$$

Let the voltage required to lower the speed to 750 rpm be V_2

$$V_2 = E_{a2} - I_{a2}R_a$$

To find V_2 we must find E_{a2} and I_{a2},

To find I_{a2} : since for a separately-excited motor , the flux $\emptyset$ is constant,

$$T_2 = K_T \emptyset \, I_{a2}$$

Also $T_2 = \mathrm{C}n_2^2$

$$\therefore \quad \frac{T_1}{T_2} = \frac{\mathrm{C}n_1^2}{\mathrm{C}n_2^2} = \frac{n_1^2}{n_2^2} = \left(\frac{1000}{750}\right)^2 = 1.778$$

$$T_2 = \frac{T_1}{1.778} = 0.562 \, T_1$$

$$K_T \emptyset \, I_{a2} = 0.562 \, (K_T \emptyset \, I_{a1})$$

$$I_{a2} = 0.562 \times 16 = 9\text{A}$$

To find E_{a2} :

To find E_{a2} : $E_{a1} = K_e \emptyset \, n_1$ and $E_{a2} = K_e \emptyset \, n_2$

$$\therefore \quad \frac{E_{a1}}{E_{a2}} = \frac{K_e \emptyset \, n_1}{K_e \emptyset \, n_2} = \frac{n_1}{n_2} = \frac{1000}{750} = 1.33$$

$$E_{a2} = \frac{E_{a1}}{1.33} = \frac{192}{1.33} = 144.36 \text{ V}$$

Hence $V_2 = 144.36 + 9 \times 0.5 = 148.86 \text{ V} \cong 150 \text{ V}$

Example 11.2

A 240 V d.c. shunt motor has an armature resistance of 0.2 Ω. When the armature current is 40 A, the speed is 1000 rpm. (a) Find additional resistance R_x to be connected in series with armature to reduce the speed to 600 rpm. Assume the armature current remains the same. (b) If the current decreases to 20 A (with resistance R_x connected) find the new speed of the motor.

Solution

(a)

$$E_{a1} = V_1 - I_{a1}R_a$$

$$= 240 - 40 \times 0.2 = 232\ V$$

$$E_{a2} = V_1 - I_{a1}(R_a + R_x)$$

$$= 240 - 40 \times (0.2 + R_x) = 232 - 40R_x$$

But $$\frac{n_2}{n_1} = \frac{E_{a2}}{E_{a1}}$$

$$\frac{600}{1000} = \frac{232 - 40R_x}{232}$$

$$600 \times 232 = 1000 \times (232 - 40R_x)$$

$$R_x = \frac{232 - 0.6 \times 232}{40}$$

From which : $R_x = 2.325\ \Omega$

(b)

$$\frac{n_2}{1000} = \frac{240 - 20(2.325 + 0.2)}{240 - 20 \times 0.2}$$

From which :

$$n_2 = 803\ rpm$$

Example 11.3

A 300 V d.c. shunt motor runs at 1600 rpm when taking an armature current of 40 A. The armature resistance is 0.5 Ω. It is required to :

(a) Calculate the speed when a resistance is inserted in the field circuit as to reduce the flux to 80% of its nominal value (flux weakening),

(b) Calculate the speed when the field resistance is deacrease to a value such that the flux is increasead to 120 % of its nominal value .

Assume that the armature current remains constant in both cases.

Solution

(a) In speed control of d.c. motor using flux variation method, the terminal voltage and armature resistance are kept constant,while the flux $\emptyset$ is varied. Therefore,

$$n_1 = \frac{V_t - R_a I_{a1}}{K_e \emptyset_1} \qquad \text{(a)}$$

$$n_2 = \frac{V_t - R_a I_{a2}}{K_e \emptyset_2} \qquad \text{(b)}$$

By dividing equation (a) by (b) yields,

$$\therefore \quad \frac{n_2}{n_1} = \frac{V_t - R_a I_{a2}}{V_t - R_a I_{a1}} \times \frac{\emptyset_1}{\emptyset_2}$$

Since $I_{a2} = I_{a1}$, hence

$$\frac{n_2}{n_1} = \frac{\emptyset_1}{\emptyset_2}$$

$$n_2 = n_1 \times \frac{\emptyset_1}{\emptyset_2} = 1600 \times \frac{100}{80} = 2000 \text{ rpm}$$

(b) When the flux is increased by 120%

$$n_2 = n_1 \times \frac{\emptyset_1}{\emptyset_2} = 1600 \times \frac{100}{120} = 1333.3 \text{ rpm}$$

Note : Higher speeds can be obtained with field weakening control method.

11.6.3 Speed Control of Series d.c. Motors

Speed control of series d.c. motor may be achieved through either field control, or armature control method:

(A) Field control methods: The speed of a series motor can be controlled by varying the flux in any one of the following ways.

(i) Using field diverting resistor: The field current in a series motor winding can be reduced by connecting a shunt resistance across the field winding so that a small portion of the field current is diverted to the shunt resistance thus reducing the excitation *mmf* and weakening the flux, Fig.11.19 (a).

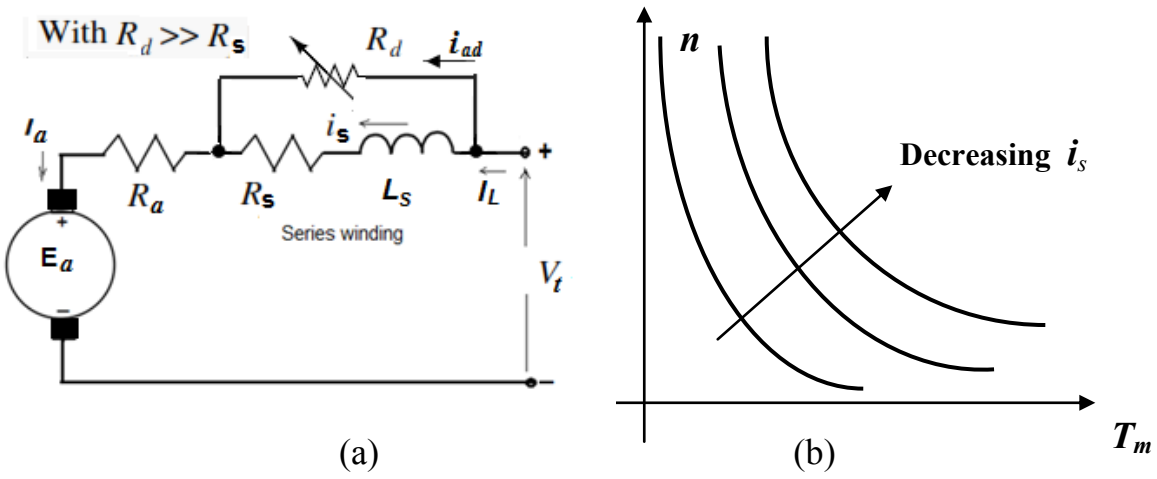

Fig.11.19 Speed control of series motor using diverter resistor R_d (field control): (a) Circuit connection, (b) Characteristics.

As the field current I_s is reduced, ϕ will be reduced accordingly since $\phi = K_s I_s$ and the speed n will increases according to Eq.(11.8) and Eq.(11.9). To find an equation for the speed as a function of the diverting resistance :

By KVL :

$$E_a = V_t - I_L R_a - \frac{R_d R_s}{(R_d + R_s)} I_L$$

$$E_a = K_e \emptyset\, n = K_e K_s I_s n = K_{es} I_s n$$

$$K_{es} I_s n = V_t - I_L R_a - \frac{R_d R_s}{(R_d + R_s)} I_L$$

But

$$I_s = \frac{R_d}{(R_d + R_s)} I_L$$

$$K_{es}\, n \frac{R_d}{(R_d + R_s)}\ I_L = V_T - I_L R_a - \frac{R_d R_s}{(R_d + R_s)}\ I_L$$

that result in :

$$n = \frac{V_t(R_d + R_s)}{K_{es} I_L R_d} - \frac{R_s}{K_{es}} - \frac{(R_d + R_s)R_a}{K_{es} R_d} \qquad (11.38)$$

This method gives speeds above normal because the reduction of the flux. As the field current is decreased, the speed-torque characteristics are shifted upward parallel to each other as shown in Fig.11.19(b). The diverting resistor should be highly inductive so that any change in the load current will not immediately affect the field winding current.

(ii) Using tapped-field winding: To increase the speed of the series motor, the flux is reduced by reducing the number of turns of the field winding. This is achieved by using field winding with a number of tapping brought outside, as shown in Fig.11.20.

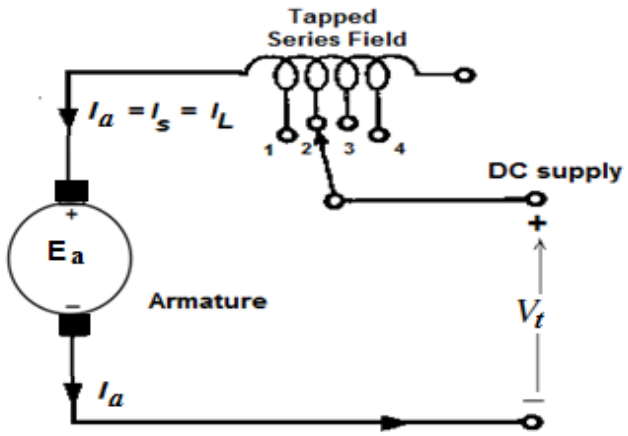

Fig.11.20 Speed control of series motor using tapped-field method.

(B) Armature control methods: speed control of series motor by armature control may be accomplished by one of the following methods,

(i) Armature terminal voltage control: Unlike with the shunt d.c. motor, there is only one efficient way to change the speed of a series d.c. motor. That method is to change the terminal voltage of the motor. If terminal voltage is increased, the speed will increase for any given torque.

From Eq. (11.38), the speed of a series motor can be controlled by variation of the terminal voltage V_t using variable d.c. supplies. Although this method was very expensive to be achieved in the past, it becomes the most common in use now a days due to the advent of the

powerful power semiconductor devices which provide a cheap, small size and reliable variable d.c. supplies such as the d.c. choppers and controlled rectifiers.

(ii) Armature resistance control: This method is obtained by the same way as for d.c. shunt motor with the exception that the control resistance is connected in series with the supply voltage such that the total armature resistance seen by the supply (Thevenin equivalent resistance) is ($\sum R_a = R_a + R_s + R_{add}$), see Fig.11.21(a).

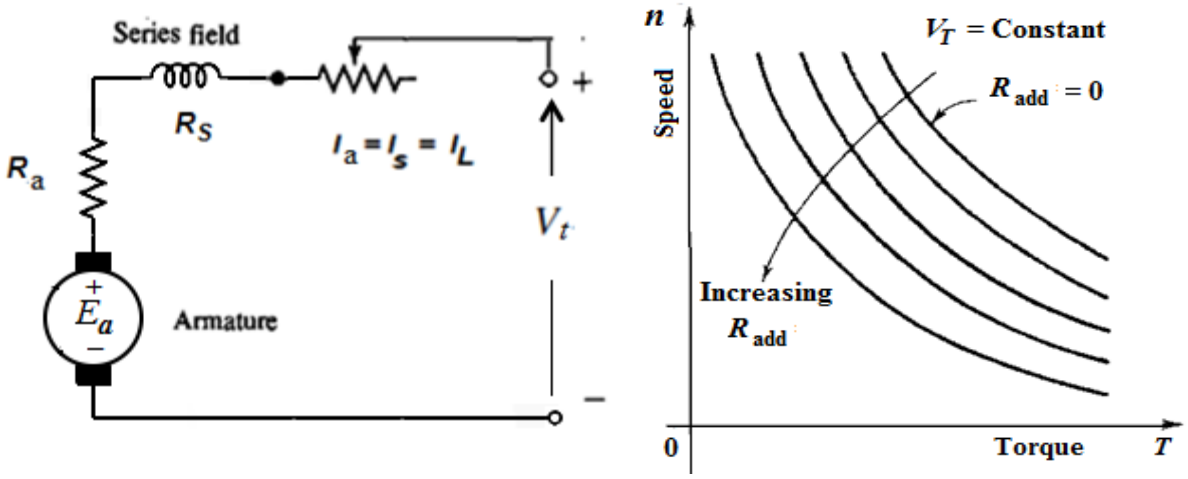

(a) (b)

Fig.11.21 Speed control of series motor using armature resistance control.

The speed-torque characteristics for various values of R_{add} are shown in Fig.11.21(b). For particular value of $R_{add,}$ the speed is almost inversely proportional to the square root of the torque as it can be seen from Eq.(11.39) ,

$$n = \frac{V_t}{\emptyset} \times \frac{1}{\sqrt{T_e}} - \frac{(R_a + R_s + R_{add})}{K_e K_f} \qquad (11.39)$$

A high torque is obtained at low speed and a low torque is obtained at high speed. Series motors are therefore used where large starting torques are required as in hoist, cranes, etc.

Example 11.4

A d.c. series motor draws 22 A from a 240 V line while running at 840 rpm. It has an armature resistance of 0.6 Ω and a series field resistance of 0.5 Ω. A diverter is to be added to the circuit so that the speed increases to

1200 rpm while the line current increases to 28 A. Find the value of the diverter resistance R_d.

Solution

$$I_L R_s = 22 \times 0.5 = 11 \text{ V}$$

$$I_L R_A = 22 \times 0.6 = 13.2 \text{ V}$$

$$n = \frac{V_T - I_L (R_A + R_s)}{K_e \emptyset} = \frac{V_T - I_L (R_A + R_s)}{K_{es} I_L}$$

$$840 = \frac{240 - 11 - 13.2}{K_{es} \times 22}$$

Therefore, $K_{es} = 0.0116$

Now using Eq.(11.38)

$$n = \frac{V_T (R_d + R_s)}{K_{es} I_L R_d} - \frac{R_s}{K_{es}} - \frac{(R_d + R_s) R_A}{K_{es} R_d}$$

$$1200 = \frac{240\ (R_d + 0.5)}{28 \times\ 0.0116 \times R_d} - \frac{0.5}{0.0116} - \frac{(R_d + 0.5) \times 0.6}{0.0116\ R_d}$$

From which

$$556.42 = \frac{343.59}{R_d} \qquad \rightarrow \quad R_d = 0.62\ \Omega$$

11.7 FOUR-QUADRANT OPERATION OF A DRIVE SYSTEM AND MOTOR BRAKING

11.7.1 FOUR-QUADRANT OPERATION OF DC MACHINE

A d.c. machine can operate as a motor, as a generator or as a brake as illustrated in the following diagram (Fig.11.22). It has been assumed in this diagram that the field current is fixed (in magnitude and direction) and the armature reaction is negligible such that $K\varphi$ is constant. In this case the ω –T equation is linear.

$$\omega = \frac{V_T}{K\emptyset} - \frac{R_a}{K^2 \emptyset^2} T_e \qquad (11.40)$$

Assumptions :

- The positive or forward speed is arbitrarily chosen in counterclockwise direction (it can also be chosen as clockwise). The positive torque is in the direction that will produce acceleration in forward speed, as shown in Fig.11.22.

- The plane of Fig.11.22 is divided into four quadrants, thus four modes of operation. The quadrants are marked as: I, II, III and IV.

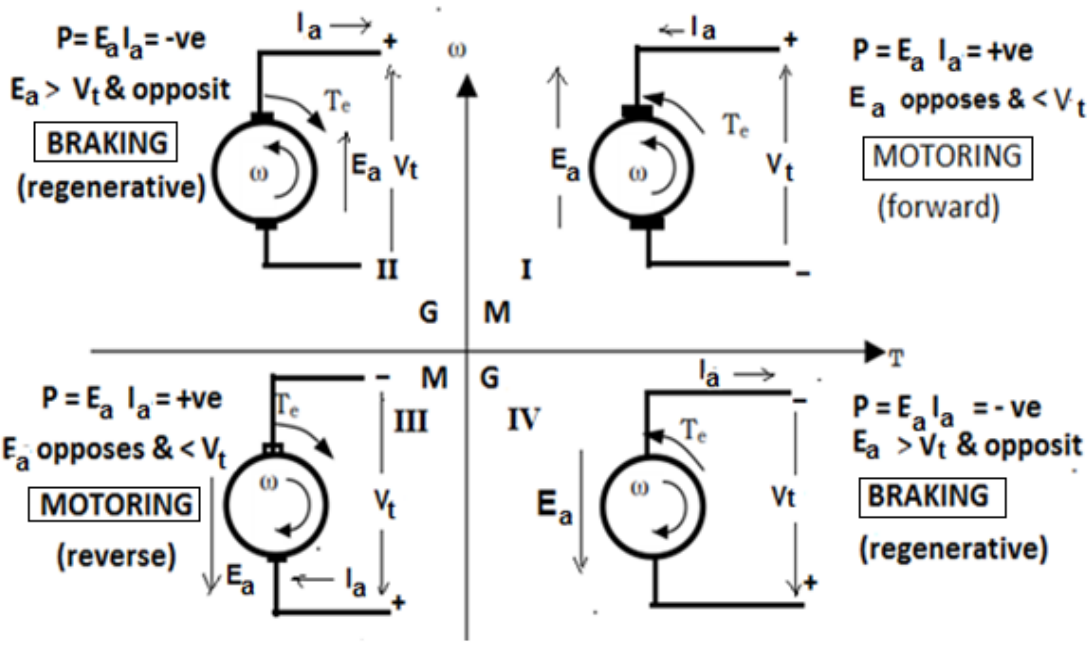

Fig.11.22 Four-quadrant operation of a d.c. motor.

Quadrant I

Both torque and speed are positive – the motor rotates in forward direction, which is in the same direction as the motor torque. The power of the motor is the product of the speed and torque ($P = T_e \omega$), therefore the power of the motor is positive. Energy is converted from electrical form to mechanical form, which is used to rotate the motor. The mode of operation is known as ***forward motoring.***

Quadrant II

The speed is in forward direction but the motor torque is in opposite direction or negative value. The torque produced by the motor is used to **'brake'** the forward rotation of the motor. The mechanical energy during the braking is converted to electrical energy – thus the flow of energy is from the mechanical system to the electrical system. The product of the torque and speed is negative thus the power is negative, implying that the

motor operates in ***braking mode***. The mode of operation is known as ***forward braking***.

Quadrant III

The speed and the torque of the motor are in the same direction but are both negative. The reverse electrical torque is used to rotate the motor in reverse direction. The power, i.e. the product of the torque and speed, is positive implying that the motor operates in **motoring mode.** The energy is converted from electrical form to mechanical form. This mode of operation is known as ***reverse motoring.***

Quadrant IV

The speed is in reverse direction but the torque is positive. The motor torque is used to 'brake' the reverse rotation of the motor. The mechanical energy gained during the braking is converted to electrical form, thus power flow from the mechanical system to the electrical system. The product of the speed and torque is negative implying that the motor operates in **braking mode**. This mode of operation is known as ***reverse braking.***

11.7.2 ELECTRICAL BRAKING OF DC MOTORS

A motor is said to be in braking mode when T_e and ω_m (motor speed) are in opposite direction (Fig.11.23). If $\boldsymbol{E_a}$ becomes $> \boldsymbol{V_T}$ for any reasons, then I_a will become negative (reverse) and T_e will become in the same direction of T_L ; which opposes rotation. Hence the speed will reduced (since negative dynamic torque is acting on the motor shaft) as described in the following equations.

Fig.11.23.

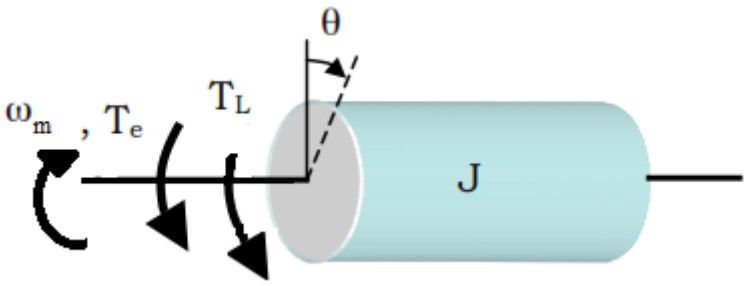

$$T_e = T_L + T_{loss} + T_j \qquad (11.41)$$

$$T_j = J\frac{d\omega_m}{dt} = (T_e - T_L) \qquad (11.42)$$

T_e remain negative until $T_j = 0$.

If the motor supply is disconnected while motor speed is ω_1 then it takes some time, t_{stop} , until it reaches zero speed. In this case the developed motor speed is zero and the accelerated torque T_j is negative (acting to decelerate the motor).

The stop time , t_{stop} , can be determined from

$$t_{stop} = \int_{\omega=\omega_1}^{0} \frac{Jd\omega}{-T_j} = \int_{\omega=\omega_1}^{0} \frac{-Jd\omega}{T_L + T_{loss}}$$
$$= \int_{0}^{\omega_1} \frac{J\, d\omega}{T_L + T_{loss}} \qquad (11.43)$$

During the deceleration period, the stored energy is completely consumed in supplying rotational losses and in supplying the coupled load by the required mechanical energy as input. Finally, the speed of the rotating part (the rotor of the motor and its coupled load) attains zero whereby the stored kinetic energy is zero. Note that T_L and T_{loss} are, in general , rising functions of speed and being very small at low speeds, and therefore t_{stop} is high.

11.7.3 Types of d.c. Motor Electric Braking

There are three types of electrical braking applied to the d.c. motors, namely, regenerative braking, plugging braking and dynamic breaking.

1. Regenerative Braking

- This type of braking happen when the motor speed increases above the no-load speed ω_{mo} (for example, lowering of a load by electrically operated winch and when an electric train goes downhill). The mechanical energy in this type of breaking is converting into electrical energy, part of which is return to the supply and the rest of the energy is lost in the machine.
- Most of the motors pass smoothly from motoring to generating operation if the induced *emf* E_a exceeds the source voltage V_t (due to increase of motor speed from ω_{mp} to ω_{mr}). In this case the current I_a becomes negative and the machine will act as a generator pumping power back into the source. This regeneration created by the negative T_L which accelerates the machine from point **1** to point **2** , picking up the speed in excess of the no load speed ω_{mo} at point **3** as shown in Fig.11.24. Under this condition $E_a = K \phi \omega_{mr}$ ($\omega_{mr} > \omega_{mo}$) becomes greater than the supply voltage V_t.

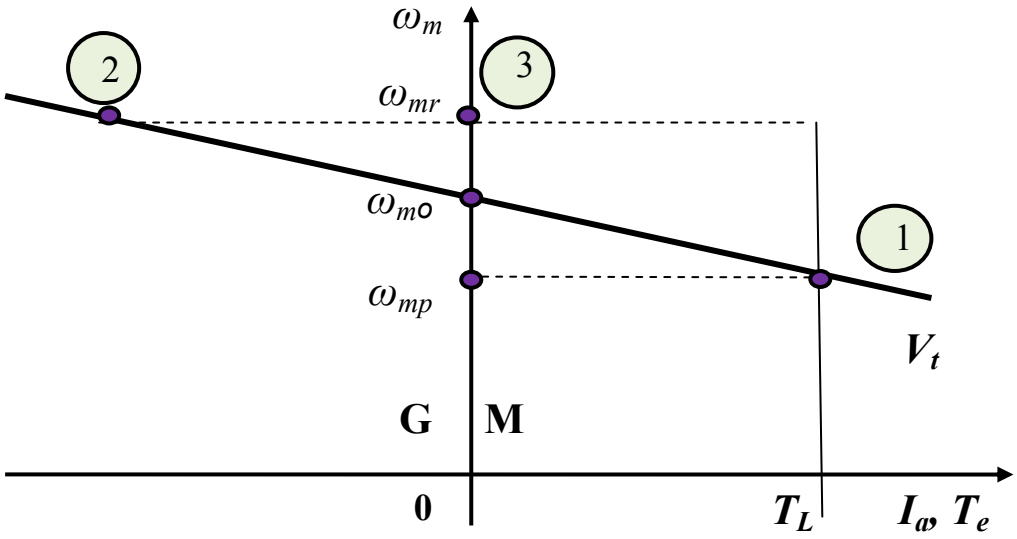

Fig.11.24. Regenerative braking

Consider now a separately-excited d.c. motor in regenerative mode. Fig.11.25(a) shows the motor working at is normal state at point **2**.
Now for the transition from **1** to **2** in general case, for Fig.11.25(b),

$$I_a = \frac{V_t - E_a}{R_a} \qquad (11.44)$$

The equivalent diagram for this transision is depicted in Fig.11.25.
Since in regenerative breaking : $\omega_{mr} > \omega_{mo}$, then at point **2**

$$E_{a2} = K\phi\omega_{mr} > V_t$$

Then $$I_{a2} = \frac{V_t - K\phi\omega_{mr}}{R_a} < 0 \qquad (11.45)$$

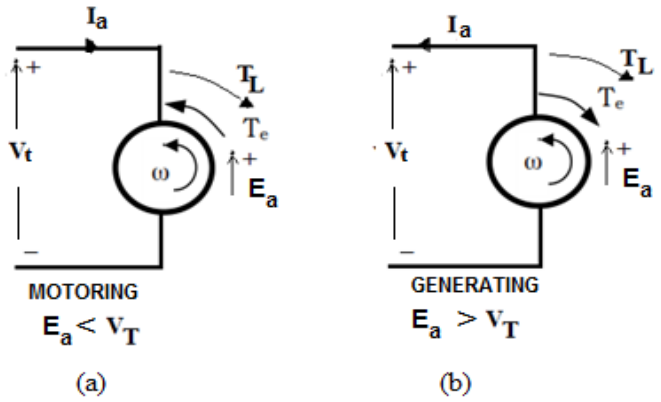

Fig.11.25 Separately-excited d.c. motor in regenerative mode.

To find the value of the electromagnetic torque developed by the motor in the regenerative braking condition, substitute Eq.(11.45) into the following torque equation yields

$$T_{e2} = T_{m2} = K\phi I_{a2} = K\phi \frac{V_t - K\phi\omega_{mr}}{R_a} \quad < 0 \qquad (11.46)$$

Equation (11.46) indicates that, in regenerative breaking condition, the motor torque has negative value.

To find an analytical expression for the mechanical characteristic in regenerative condition, equation (11.46) must be solved with respect to ω_{mr} , that is

$$\omega_{mr} = \omega_{mo} - \frac{R_a}{K^2\phi^2} T_{m2} \qquad (11.47)$$

where $\omega_{mo} = \frac{V_T}{K\emptyset}$ is the no-load ideal speed.

Notes :

- To maintain the current below the maximum permissible value, an external resistance R_x may be needed for this purpose.
- The series motor cannot be used in the regenerative breaking condition, i.e at negative load torque (-T_m).

2. Plugging

This type of breaking is applicable for all types of d.c. motors, namely separately-excited, shunt, compound and series motors. In this method the polarity of the applied terminal voltage of the motor is reversed. As a result the motor torque T_m reverses its direction and acts as a break to the motor shaft by reducing its speed to zero. At this instant, i.e. when $\omega_m = 0$, the supply must be switched off otherwise the motor will run in reverse direction with negative speed. Fig.11.26 shows braking of separately-excited motor by plugging method.

It is important that, during voltage reversal an external resistance R_x should be inserted with the armature circuit to limit the braking current. Referring to Fig.11.27, the sequences of events during plugging for separately excited motor are :

From point **1** to point **2** : Current and torque reversal

$$i_{a2} = \frac{-V_t - E_a}{R_a + R_x} < 0 \qquad (11.48)$$

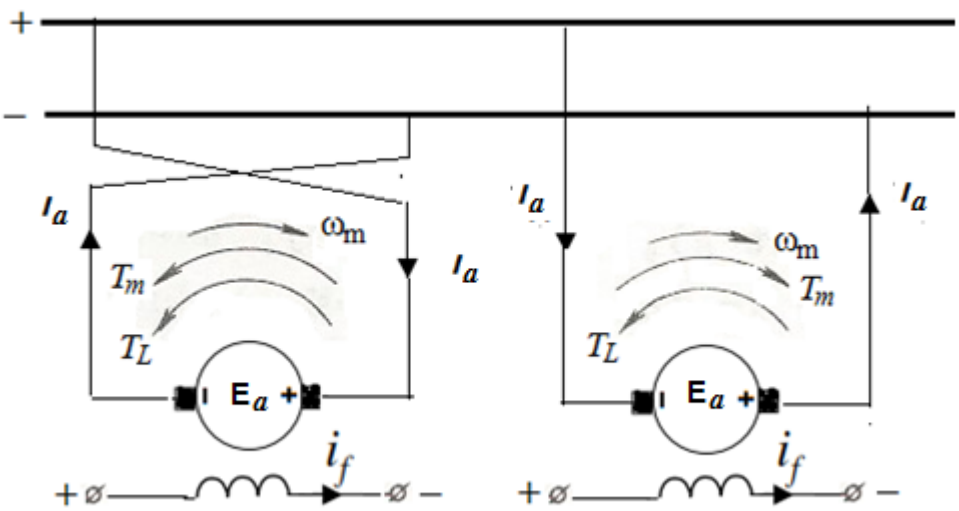

Fig.11.26 Motor braking by plugging.

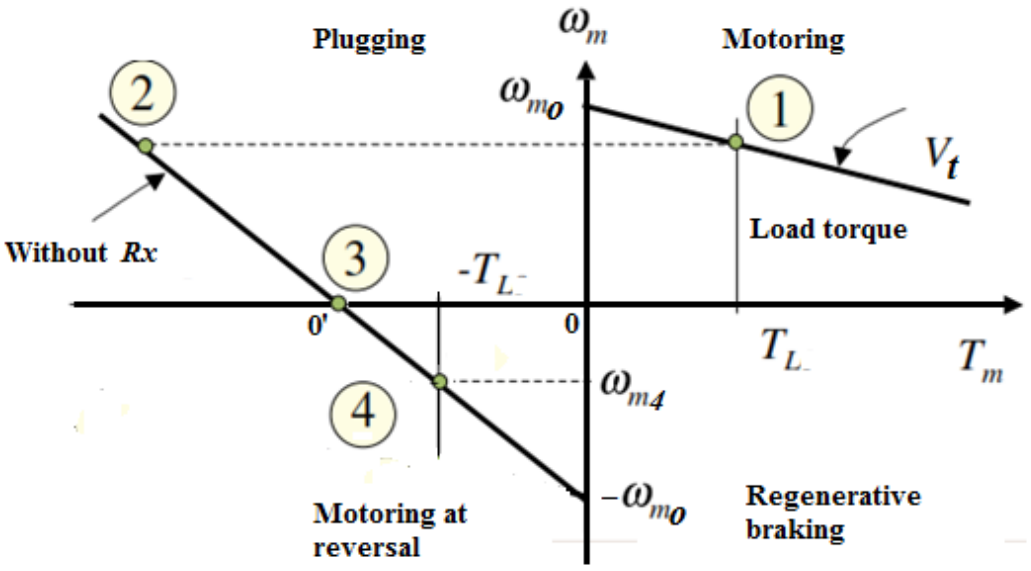

Fig.11.27 Plot of mechanical characteristics of separately-excited motor in plugging mode.

At point 3 :

$\omega_{m3} = 0$ and $T_L =$ negative

The motor start to run in opposite direction toward point **4**.

3. Dynamic Braking

This method of braking the motor is disconnected from the supply and operated as a generator by the kinetic energy of rotor. The kinetic energy is then dissipated in an external resistance connected across the motor. With this technique, the energy required from the supply to brake the motor is eliminated as compared to the previous plugging method. This method of braking can be applied to brake d.c. motors, synchronous a.c. motors as well as a.c. induction motors and generally referred to as *Rheostatic Braking*. See Fig.11.28.

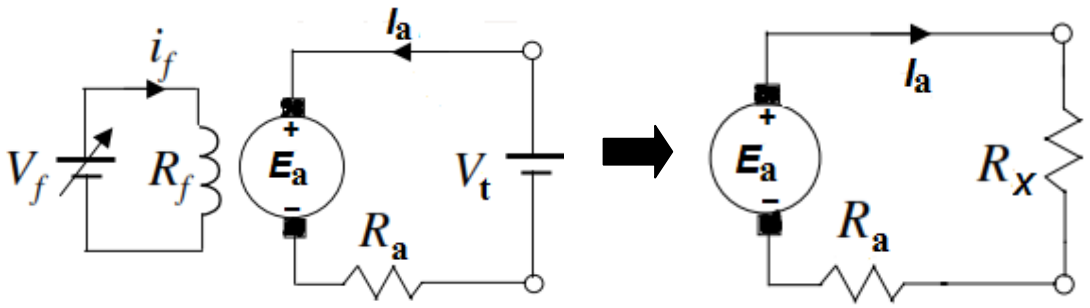

MOTORING BRAKING

Fig.11.28 Dynamic breaking of d.c. separately-excited motor.

The sequences of events during plugging are:

From **1** to **2** : Current reversal

At point **2** : $I_a = \dfrac{E_a}{R_x + R_a}$

At point **3** : $\omega_{m3} = 0$ and $I_a = 0$

Note:

- Short circuiting the motor makes $V_t = 0$.
- R_x is used to limit the current and to dissipate the stored kinetic energy.

Example 11.5

A 30 kW, 415 V d.c. shunt motor is braked by plugging. Calculate the value of the external resistance R_x to be placed in series with the armature circuit to limit braking current to 164 A. The armature resistance of the motor is 0.1 Ω and the full load armature current is 100 A at full load speed of 600 rpm. What is the braking torque obtained from the motor?

Solution

The *emf* induced in the motor

$$E_a = V_t - I_a R_a = 415 - 100 \times 0.1 = 405 \text{ V}$$

Voltage across the armature at the instant of braking

$$= 405 + 415 = 820 \text{ V}$$

The total resistance required to limit the current to 164 A

$$R = \frac{820}{164} = 5\ \Omega = R_{\text{x}} + R_{\text{a}}$$

$$R_{\text{x}} = 5 - 0.1 = 4.9\ \Omega$$

Full load torque :

$$T_{mfl} = \frac{P}{\omega} = \frac{30000}{2\pi n} \times 60 = \frac{30000}{2\pi \times 600} \times 60 = 483.7 \text{ Nm}$$

Since the flux in the shunt motor is constant, hence the torque is proportional to the armature current, hence the initial braking torque is

$$T_b = T_{mfl} \times \frac{I_b}{I_{afl}} = 483.7 \times \frac{164}{100} = 793.26 \text{ Nm}$$

Example 11.6

A 600 V d.c. shunt motor having an efficiency of 80% operates a hoist having an efficiency of 75% . Determine the current taken from the supply when the hoist raise the load of 450 kg at speed of 3 m/s. If rheostat braking is used to brake the motor, what is the value of the external resistance must be put in series with the armature circuit in order to lower the same load at the same speed?

Solution

Work done when raising the load

$$W = F \cdot v = m \cdot g \cdot v = 450 \times 9.81 \times 3$$

$$= 13243.5 \ \text{Nm/s (Watts)}$$

$$\text{power input} = \frac{\text{output}}{\eta_m \times \eta_{hoist}} = \frac{13243.5}{0.8 \times 0.75} = 22072.5 \text{ W}$$

Current drawn from the supply

$$I_m = \frac{\text{power input}}{V} = \frac{22072.5}{600} = 36.78 \text{ A}$$

When the load is lowered, the motor will operate as a generator. The output of the generator will be dissipated in the resistance. Assume the generator has efficiency of 85%, hence,

$$\text{power output of generator} = 600 \times 9.81 \times 3 \times 0.85 \times 0.75$$

$$= 11256.975\text{W}$$

If we neglect the armature resistance, the inserted external resistance is

$$\text{Power dissipated in } (R_x) = \frac{V^2}{R_x}$$

$$\therefore \quad R_x = \frac{600^2}{11256.975} = 31.98 \ \Omega$$

PROBLEMS

11.1 A d.c. drive employs a d.c. series motor to raise and lower a constant weight W which hangs from a cable that wound on a drum of constant radius *r*. The velocity of the weight when rising is 6 m /s . The motor has an armature resistance of 0.4 Ω and series field resistance of 0.08 Ω. The supply voltage to the motor is 460 V. Calculate the value of the external resistance that must be inserted in series with the armature circuit to permit the weight W to be lowered at a speed of 4 m /s.

[Ans: 3.67 Ω]

11.2 A variable d.c. drive system is used to drive a fan which has the load characteristic $T_L \propto n^2$, where T_L is the load torque and n is the mechanical speed in rpm. When the motor runs at 600 rpm the back *emf* generated is 120 V and the current drawn by the armature is 28 A. Calculate the external resistance that must be added to the armature circuit to reduce the speed of the motor to 400 rpm. Neglect all electrical and mechanical losses of the motor including the armature resistance loss.

[Ans: 3.21 Ω]

11.3 A 100 V, 1120 W (1.5 hp), 2900 rpm, permanent magnet d.c. motor has an armature resistance of 0.5 Ω, takes armature current of 14 A at rated load. Calculate the value of the external resistance placed in series with the armature circuit to reduce the speed of the motor to 1800 rpm. Assuming the torque to be constant and neglect brush voltage drop.

[Ans: 2.5 Ω]

11.4 A 240 V, 1000 rpm 100 A, separately-excited d.c. motor has an armature resistance of 0.04 Ω. The motor is braked by plugging from an initial speed of 1100 rpm. Calculate:

(a) The value of the external resistance R_x to be placed in series with the armature circuit to limit braking current to twice the full load value.
(b) The braking torque obtained from the motor.
(c) Torque when the speed has fallen to zero.

[Ans: (a) 2.458 Ω, (b) 450.7 Nm, (c) 216 Nm]

11.5 A 220 V, 20 kW d.c. shunt motor running at its rated speed of 1200 rpm is to be braked by plugging. The armature resistance is 0.1 Ω and the rated efficiency of the motor is 88%. Determine:

(a) The resistance to be connected in series with the armature to limit the initial braking current to twice the rated current.

(b) The initial braking torque.
(c) The torque when the speed of the motor falls to 400 rpm.

[Ans: (a) 1.98 Ω, (b) 318.31 Nm, (c) 214.73 Nm]

11.6 A 40 kW, 500 V d.c. shunt motor having an efficiency of 80% operates a hoist having an efficiency of 70% . Determine the current taken from the supply in order to raise a load of 500 kg at 4 m/s. If the rheostatic braking is employed, what resistance must be put in the armature circuit in order to lower the same load at the same speed?

[Ans: 70 A, 22.75 Ω]

11.7 A 50 hp, 440V d.c. shunt motor is braked by plugging. Calculate the value of the resistance to be connected in series with the armature circuit to limit the initial braking current to 150A . Calculate the braking torque so obtained. Assume armature resistance as 0.1Ω, full-load armature current is 100A and full-load speed is 600 rpm.

[Ans: 5.8 Ω, 878 Nm]

11.8 A 200 V d.c. series motor takes line current of 25 A when runs at 500 rpm. The armature resistance is 0.5 Ω and the series field resistance is 0.3 Ω. If the load torque remains constant, find the value of the additional resistance to be inserted in series with the armature to reduce the speed to 250 rpm.

[Ans: 3.6 Ω]

11.9 A variable-speed drive system uses a d.c. motor which is supplied from a variable voltage source. The torque and power profiles are shown in Fig, 11.7. The drive speed is varied from 0 to 1750 rpm (base-speed) by varying the terminal voltage (from 0 to 600V) with the field current maintained constant,

(a) Determine the motor armature current if the torque is held constant at 250 Nm up to the base-speed.
(b) The speed beyond the base-speed is obtained by field weakening while the armature voltage is held constant at 600 V . Determine the torque available at a speed of 2500 rpm if the armature current is held constant at the value obtained in part (a). Neglect all losses.

[Ans: (a) 76.35 A, (b) 175 Nm]

11.10 A 250 V, 10 hp series motor is mechanically coupled to a fan and draws 30 A and runs at 500 rpm when connected to a 220 V supply with no external resistance connected to the armature circuit (i.e., $R_{add} = 0$). The torque required by the fan is proportional to the square of the speed. $R_a = 0.5\ \Omega$ and $R_s = 0.3\ \Omega$. By neglecting the armature reaction and rotational loss, it is required to:

(a) Determine the power delivered to the fan and the torque developed by the machine,
(b) The speed is to be reduced to 300 rpm by inserting a resistance (R_{add}) in the armature circuit. Determine the value of this resistance and the power delivered to the fan.

[Ans: (a) 129.5 Nm, (b) 10.9 Ω, 1464.5 W]

11.11 A 300 V, d.c. shunt motor runs at a speed of 800 rpm when driving a constant-torque load. The armature resistance is 0.5 Ω and the field resistance is adjusted to give 3A in the field circuit. Under certain load condition the motor draws a line current of 20 A.

(a) Calculate the resistance that must be added to the armature circuit to reduce the speed of the motor to 400 rpm.
(b) What is the value of the additional resistance that must be inserted in the armature circuit to make the motor operates in the stalling condition?

[Ans:(a) 8.57 Ω, (b) 17.14 Ω]

CHAPTER TWELVE

DC CHOPPER DRIVES

12.1 INTRODUCTION

The principle of operation of d.c. chopper with passive loads (*R* and *R-L* loads) is discussed in much details in Chapter Four. Also the operation of the chopper with load consisting back *emf* is discussed in the same chapter briefly. In the present chapter, the operation of the chopper with the d.c. motors shall be discussed in details. The analytical properties of the voltage and current of the motor with d.c. chopper drive are presented.

The d.c. motor is considered a SISO (Single Input and Single Output) system having torque-speed characteristics compatible with most mechanical loads. This makes a d.c. motor controllable over a wide range of speeds by proper adjustment of the terminal voltage.

12.2 ONE-QUADRANT DC CHOPPER DRIVE

A simple chopper-fed d.c. motor drive is shown in Fig.12.1. The basic principle behind d.c. motor speed control is that the output speed of a d.c. motor can be varied by controlling armature voltage for speed below and up to rated value keeping field voltage constant. The armature voltage can be controlled by controlling the duty cycle of the converter (here the converter used is a d.c. chopper).

In Fig. 12.1, the converter output gives the d.c. output voltage V_a required to drive the motor at the desired speed. In this diagram, the d.c. motor is represented by its equivalent circuit consisting of inductor L_a and resistor R_a in series with the ideal source back *emf* (E_a). The thyristor T_1 is triggered by a pulse width modulated (PWM) signal to control the average motor voltage.

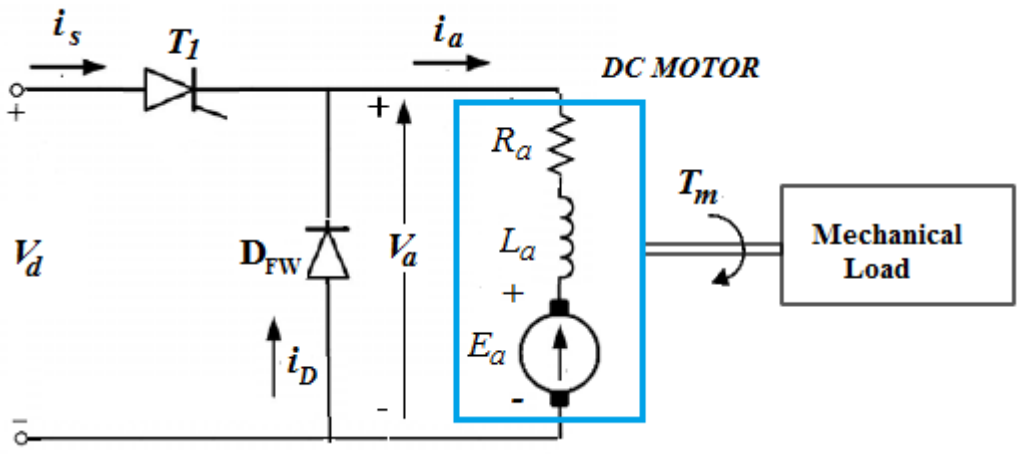

Fig.12.1 Chopper-fed d.c. motor drive.

Theoretical waveforms illustrating the chopper operation are shown in Fig.12.2. In this case the average armature voltage is a direct function of the chopper duty cycle γ, i.e. $V_{av} = \gamma V_d$.

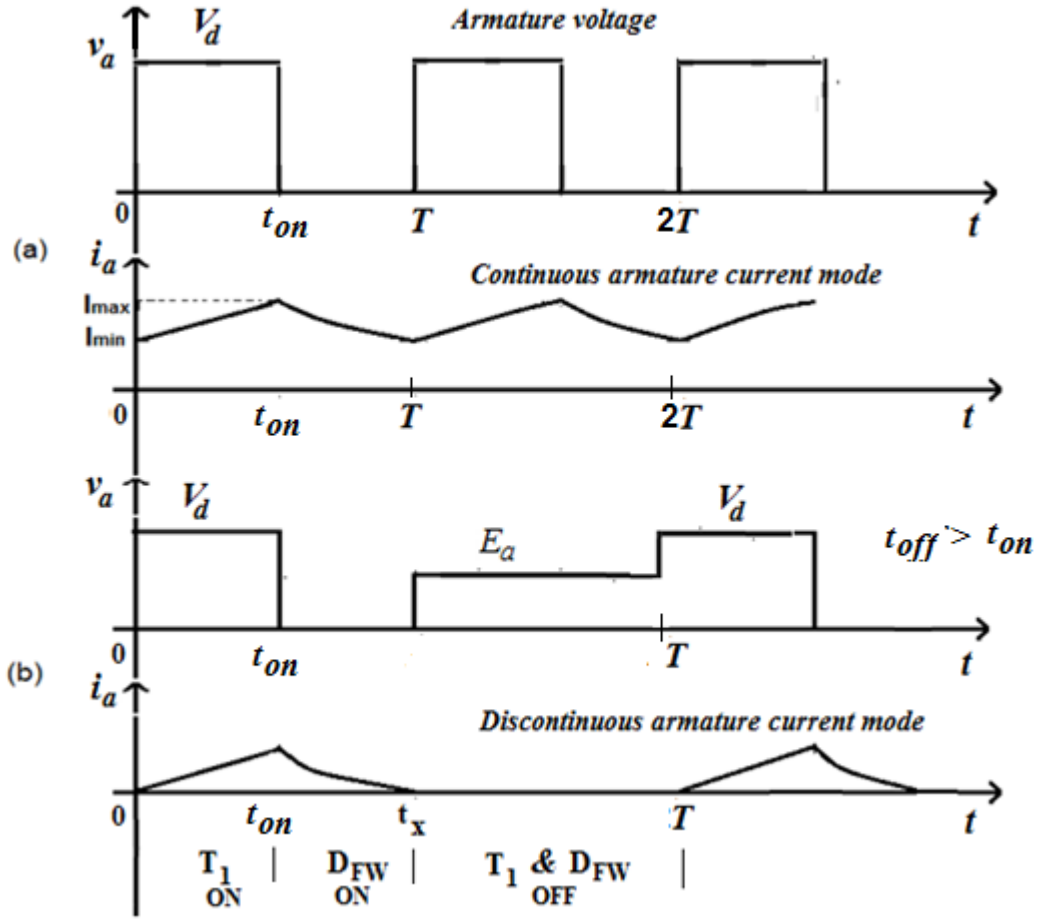

Fig.12.2 Load current and voltage waveforms with motor load: (a) Continuous armature current, (b) Discontinuous armature current.

Like the operation of the d.c. chopper with the passive inductive load discussed in Chapter Four. Two modes of operation may result when the chopper operates with d.c. motor load, namely, continuous armature current operation and discontinuous armature current operation modes as illustrated in Fig.12.2. In both cases, the armature voltage and current waveforms are different in shape and each has its own analytical properties as will be discussed in the following subsections.

12.2.1 Armature Voltage Waveform Analysis for Continuous Armature Current Operation

The armature voltage waveform $v_a(t)$ applied to the d.c. motor for continuous current operating mode shown in Fig.12.2(a) is given by

$$v_a(t) = V_d|_0^{t_{on}} + 0|_{t_{on}}^{T} \qquad (12.1a)$$

In order to analyse all equations in terms of (ωt) rather than the time (t) which gives more convenient and simple way for harmonic analysis, let the repetition periodicity $t_{on} + t_{off}$, Fig.12.2, be designated as 2π radians, hence

$$T \rightarrow t_{on} + t_{off} = 2\pi$$

The ON period of the chopper t_{on} is, $t_{on} = \gamma(t_{on} + t_{off}) = 2\pi\gamma$, therefore, Eq.(12.1) can be re-written as

$$v_a(\omega t) = V_d|_0^{2\pi\gamma} + 0|_{2\pi\gamma}^{2\pi} \qquad (12.1b)$$

Hence, the average value V_a of the armature voltage $v_a(\omega t)$ is

$$V_a = \frac{1}{2\pi}\int_0^{2\pi} v_a(\omega t)\,d\omega t = \frac{1}{2\pi}\int_0^{2\pi\gamma} V_d\,d\omega t = \frac{V_d}{2\pi}[\omega t]_0^{2\pi\gamma}$$

$$\therefore V_a = \gamma V_d \qquad (12.2)$$

The *rms* value of the armature voltage waveform is given by

$$V_{arms} = \sqrt{\frac{1}{2\pi}\int_0^{2\pi} v_a^2(\omega t)\,d\omega t} = \sqrt{\frac{V_d^2}{2\pi}[\omega t]_0^{2\pi\gamma}}$$

$$\therefore V_{a_{rms}} = \sqrt{\gamma}\,V_d \qquad (12.3)$$

The ripple factor, defining the ratio of the a.c. components to the average value, is given by

$$\text{Ripple Factor} = \frac{\sqrt{V_{arms}^2 - V_a^2}}{V_a}$$

$$PF = \frac{V_d\sqrt{\gamma - \gamma^2}}{V_d\,\gamma} = \sqrt{\frac{1-\gamma}{\gamma}} \qquad (12.4)$$

The ripple factor = 0 for full conduction when $\gamma = 1$.
The harmonic analysis of the armature voltage waveform is the same as that given in equations (4.52) – (4.56) in Chapter Four – Part I.

12.2.2 Armature Voltage Waveform Analysis for Discontinuous Armature Current Operation

With some values of the duty cycle γ, the armature current may falls to zero during part of the cycle, as illustrated in Fig.12.2(b), this will occur when switch T_1 and diode D_{FW} are both off. In this case the armature is disconnected from the supply and any *emf* E_a generated in the armature winding will then be appeared across the armature terminals. Therefore, for the interval $t_x \le t \le T$ or $x \le \omega t \le 2\pi$,where t_x is the time at which the current becomes zero and x is the diode extinction angle in Fig.12.2(b), it is seen that there is an armature voltage $v_a(\omega t) = E_a$. If we assume that E_a is constant then

$$\boldsymbol{v_a}(\omega t) = V_d|_0^{2\pi\gamma} + E_a|_x^{2\pi} \qquad (12.5)$$

The average value of this voltage V_a is

$$V_a = \frac{1}{2\pi}\int_0^{2\pi} v_a(\omega t)d\omega t$$

$$= \frac{1}{2\pi}\left(\int_0^{2\pi\gamma} V_d d\omega t + \int_x^{2\pi} E_a\, d\omega t\right) \qquad (12.6)$$

$$\therefore \quad V_a = \gamma V_d + \left(1 - \frac{x}{2\pi}\right)E_a \qquad (12.7)$$

For full conduction $x = 2\pi$ and Eq.(12.7) reduced to Eq.(12.2). The *rms* load voltage is

$$V_{a_{rms}} = \sqrt{\frac{1}{2\pi}\int_0^{2\pi\gamma} V_d^2\, \mathrm{d}\omega t + \int_x^{2\pi\gamma} E_a^2\, \mathrm{d}\omega t}$$

$$= \sqrt{\gamma V_d^2 + E_a^2 \left(1 - \frac{x}{2\pi}\right)} \qquad (12.8)$$

The Fourier components of the armature voltage waveform with discontinuous current are obtained by substituting Eq.(12.1) into Fourier integrals:

$$a_n = \frac{1}{\pi}\int_0^{2\pi} v_a(\omega t)\cos n\omega t\, d\omega t$$

and $$b_n = \frac{1}{\pi}\int_0^{2\pi} v_a(\omega t)\sin n\omega t\, d\omega t$$

to result :

$$a_n = \frac{V_d}{n\pi}\sin 2\pi n\gamma - \frac{E_a}{n\pi}\sin nx \qquad (12.9)$$

$$b_n = \frac{V_d}{n\pi}(1 - \cos 2\pi n\gamma) - \frac{E_a}{n\pi}(1 - \cos nx) \qquad (12.10)$$

From which, the fundament component, (n =1), of the armature voltage, is given by

$$V_{a_1}(\omega t) = \hat{V}_a \sin(\omega t + \varphi_1) \qquad (12.11)$$

where $\hat{V}_a = c_1$

$$= \frac{1}{\pi}\sqrt{(V_d \sin 2\pi\gamma - E_a \sin x)^2 + [V_d(1 - \cos 2\pi\gamma) - E_a(1 - \cos x)]^2} \qquad (12.12)$$

$$\varphi_1 = tan^{-1}\left[\frac{V_d \sin 2\pi\gamma - E_a \sin x}{V_d(1 - \cos 2\pi\gamma) - E_a(1 - \cos x)}\right] \qquad (12.13)$$

12.3 ANALYTICAL PROPERTIES OF THE ARMATURE CURRENT WAVEFORM

When the chopper is loaded with a d.c. motor, having the equivalent circuit representation as in Fig.12.1, the armature current equation is,

$$v_a(\omega t) = R_a i_a + L_a \frac{di_a}{dt} + E_a$$

or $$\frac{di_a}{dt} + \frac{R_a}{L_a} i_a = \frac{v_a - E_a}{L_a} \qquad (12.14)$$

This differential equation represents the armature current behaviour in both the continuous and discontinuous current modes as will be discussed here in after.

(A) Continuous armature current operation

The analytical properties of the armature current of the d.c. motor is very similar to that of the chopper operation with back *emf* given in chapter Four-Part I. Hence, equations (4.29) to (4.34) are also applied to the motor with some modification including designating *T,* the repetition periodicity $t_{on} + t_{off}$ in Fig.12.2 , as 2π radians and t_{on} as $2\pi\gamma$.

- With switch T_1 - ON (and D_{FW} - OFF)

At $\omega t = 0^+$, in Fig.12.2(a) , $v_a = V_d$ and $i_a(\omega t) = I_{min}$, solution of the first order linear differential equation (12.14) gives the result :

For the interval $0 \leq \omega t \leq 2\pi\gamma$,

$$i_a(\omega t) = \frac{V_s - E_a}{R_a}\left(1 - e^{-\omega t/\omega\tau}\right) + \mathrm{I_{min}}\, \mathrm{e}^{-\omega \mathrm{t}/\omega\tau} \qquad (12.15)$$

where $\omega\tau = \omega L_a / R_a$

When $\omega t = 2\pi\gamma$, (t_{on}) in Fig.12.2 (a), $v_a = V_d$, and $i_a(\omega t) = I_{max}$, substituting these values into Eq. (12.15) gives

$$I_{max} = \frac{V_d - E_a}{R_a}\left(1 - e^{-2\pi\gamma/\omega\tau}\right) + I_{min}\, \mathrm{e}^{-2\pi\gamma/\omega\tau} \qquad (12.16)$$

Equation (12.16) is not time dependent and remains true after T_1 switches off.

- With switch T_1 - OFF (and D_{FW} -ON)

At $\omega t = 2\pi\gamma^+$, in Fig.12.2(a) , $v_a = 0$ and $i_a(\omega t) = I_{max}$, hence in the interval $2\pi\gamma \leq \omega t \leq 2\pi$, the load current is given by

$$i_a(\omega t) = \frac{-E_a}{R_a}\left(1 - e^{-(\omega t - 2\pi\gamma)/\omega\tau}\right) + I_{min} e^{-(\omega t - 2\pi\gamma)/\omega\tau} \qquad (12.17)$$

But at $\omega t = 2\pi$, $i_a(\omega t) = I_{min}$, equation (12.17) may then be re-written as

$$I_{min} = \frac{-E_a}{R_a}\left(1 - e^{-2\pi(1-\gamma)/\omega\tau}\right) + \mathrm{I_{max}} \mathrm{e}^{-2\pi(1-\gamma)/\omega\tau} \qquad (12.18)$$

The simultaneous solution of Eq.(12.16) and Eq. (12.18) yields

$$I_{max} = \frac{V_d}{R_a}\left(\frac{1 - e^{-2\pi\gamma/\omega\tau}}{1 - e^{-2\pi/\omega\tau}}\right) - \frac{E_a}{R_a} \tag{12.19}$$

$$I_{min} = \frac{V_d}{R_a}\left(\frac{e^{2\pi\gamma/\omega\tau} - 1}{e^{2\pi/\omega\tau} - 1}\right) - \frac{E_a}{R_a} \tag{12.20}$$

Equations (12.19) and (12.20) are used for the solution of equations (12.15) and (12.17) to determine the value for the armature current $i_a(\omega t)$ at any instant of the cycle during continuous conduction mode.

To find the average armature current, we can use the following basic equation,

$$I_a = \frac{1}{2\pi}\int_0^{2\pi} i_a(\omega t)d\omega t \tag{12.21}$$

For continuous current operation equations (12.15) and (12.18) are substituted into Eq.(12.21) for the intervals $0 \le \omega t \le 2\pi\gamma$ and $2\pi\gamma \le \omega t \le 2\pi$ respectively. Hence, the average armature current in the steady-state is given by

$$I_a = \frac{V_a - E_a}{R_a} = \frac{\gamma V_d - E_a}{R_a} \tag{12.22}$$

where

V_a = average armature voltage = $\gamma\ V_d$
I_a = average armature current
E_a = the internal generated voltage (back *emf*) is given by: $E_a = K_e\ \varphi\ n$

Now solving for the motor's speed using the motor general equation, $V_a = E_a + I_a R_a$,

$$n = \frac{V_a}{K_e \emptyset} - \frac{R_a}{K_T K_e \emptyset^2} T_m$$

or for the chopper drive in the steady-state ,

$$n = \frac{\gamma V_d}{K_e \emptyset} - \frac{R_a}{K_T K_e \emptyset^2} T_m \tag{12.23}$$

where n is the speed in rpm.

and the motor torque is $T_m = K_T\ I_a\ \varphi$

K_T = Torque constant = 9.55 K_e .

At starting, $n = 0$. The starting torque T_{st} may be found as:

$$n = 0 = \frac{\gamma V_d}{K_e \emptyset} - \frac{R_a}{K_T K_e \emptyset^2} T_{st}$$

$$\therefore T_{st} = \frac{9.55\, \gamma V_d}{R_a} K_e \emptyset \qquad (12.24)$$

The speed-torque characteristics of a separately-excited d.c. motor is shown in Fig.12.3 for different values of the duty cycle γ. It is clear that, as the duty cycle is reduced, the no load speed and the starting torque are reduced accordingly and the characteristic lines shift downward in parallel manner.

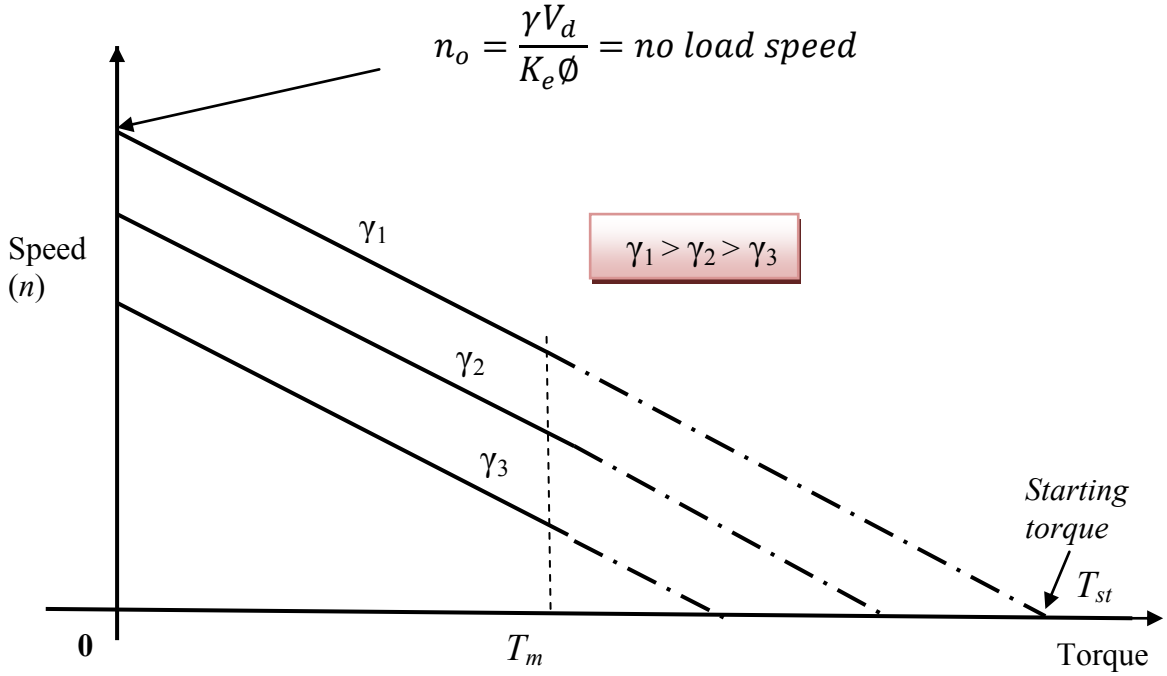

Fig.12.3 Speed-torque characteristics of a d.c. motor with d.c. chopper drive.

(B) Discontinuous armature current operation

Under different loading and duty cycle value conditions, the motor current $i_a(\omega t)$ may fall to zero resulting in the discontinuous current shown in Fig.12.2(b), this waveform can be divided into two parts that may be analysed according to the conduction of switch T_1, whether it is on or off as in **(*A*)** above. In this case the maximum current is different from the value I_{max} obtained with continuous operation and it occurs for a different value of t_{on} . The minimum current for discontinuous operation is, $I_{min} = 0$.

- With switch T_1 - ON, (and diode D_{FW} - OFF)

In Fig.12.2 (b), the current of Eq.(12.14) can be found for the interval $0 \leq \omega t \leq 2\pi\gamma$ by considering that $v_a = V_d$, and $i_a(\omega t) = 0$ at $\omega t = 0+$. This gives

$$i_a(\omega t) = \frac{V_d - E_a}{R_a}\left(1 - e^{-\omega t/\omega\tau}\right) \tag{12.25}$$

Since maximum value of $i_a(\omega t)$ occurs at $\omega t = 2\pi\gamma$ (t_{on} in Fig.12.2(b)) then,

$$I_{max_D} = \frac{V_d - E_a}{R_a}\left(1 - e^{-2\pi\gamma/\omega\tau}\right) \tag{12.26}$$

where I_{maxD} is the maximum value of the motor current for discontinuous operation.

- With switch T_1 - OFF (and diode D_{FW} - ON)

When T_1 in Fig.12.1 is switched off, the motor voltage $v_a(\omega t)$ falls to zero due to the conduction through diode D_{FW}, the circuit differential equation (12.14) is then modified to

$$\frac{di_a}{dt} + \frac{R_a}{L_a} i_a = \frac{-E_a}{L_a} \tag{12.27}$$

This has the solution given in Eq.(12.17) except that the maximum current is now given by Eq.(12.26) to result in,

$$i_a(\omega t) = \frac{-E_a}{R_a}\left(1 - e^{-(\omega t - 2\pi\gamma)/\omega\tau}\right) + \frac{V_d - E_a}{R_a}\left(1 - e^{-2\pi\gamma/\omega\tau}\right) e^{-(\omega t - 2\pi\gamma)/\omega\tau} \tag{12.28}$$

- The current extinction angle x

In Fig.12.2 (b), in order to find the current extinction angle x, let it occurs at $\omega t = x$ at which i_a (ωt) = 0. Now if we substitute these values into Eq.(12.28) and solve for x, the following expression will be obtained:

$$x = \omega\tau \ln\left[e^{(2\pi\gamma)/\omega\tau}\left\{1 + \left(\frac{V_d}{E_a} - 1\right)\left(1 - e^{-2\pi\gamma/\omega\tau}\right)\right\}\right] \tag{12.29}$$

Hence, Eq.(12.27) defines the current in the region $2\pi\gamma \leq \omega t \leq x$, where x is found from Eq. (12.29), and this equation is indeterminate if $E_a = 0$.

- The critical value of the duty cycle γ'

Let switch T_1 in Fig.12.1 have a conduction period of particular value t'_{on} radians that represent the boundary between continuous and discontinuous operation. Then, from Eq.(4.5),

$$\gamma' = \frac{t'_{on}}{2\pi} = \frac{t'_{on}}{t'_{on} + t_{off}} \tag{12.30}$$

At the particular value of conduction γ' the minimum current I_{min} = 0 defined by Eq.(12.20),

$$I_{min} = \frac{V_d}{R_a}\left(\frac{e^{2\pi\gamma'/\omega\tau} - 1}{e^{2\pi/\omega\tau} - 1}\right) - \frac{E_a}{R_a} = 0$$

From this equation we can write,

$$m = \frac{E_a}{V_d} = \frac{\mathrm{e}^{2\pi\gamma'/\omega\tau} - 1}{\mathrm{e}^{2\pi/\omega\tau} - 1} \tag{12.31}$$

The relationship between $m = \frac{E_a}{V_d}$ and γ' is discussed in chapter Four and shown in Fig.4.12 with the factor $\sigma = \mathrm{T}/\tau = 2\pi/\omega\tau$ as parameter. If a circuit operate with a specified value of γ , defined by Eq.(12.30), then the criteria for continuous or discontinuous operation of a d.c. motor are the same as that given in Fig.4.12 in Chapter Four so that ,

$$\left.\begin{array}{l} \gamma > \gamma' \text{ , Continuous current} \\ \gamma < \gamma' \text{ , Discontinuous current} \end{array}\right\} \tag{12.32}$$

where γ' is defined by Eq.(12.30).

It should be noted that the ratio $2\pi/\omega$ is the periodic time of the overall cycle, the parameter $2\pi/\omega\tau$ of the 'state of conduction' curves, Fig.4.12, is

$$\sigma = \frac{2\pi}{\omega\tau} = \frac{\text{period of overall (T = on + off)cycle}}{\text{electrical time constant of the armature circut}} \tag{12.33}$$

The electrical time constant of armature circuit depends on the motor armature inductance L_a which is considered as an important parameter in determining current continuity. For small motors L_a is of the order 10-50 mH and for larger motors the inductance is smaller, being typically 2-10 mH.

12.4 POWER INPUT, SUPPLY CURRENT, AVERAGE ARMATURE CURRENT AND TORQUE CALCULATIONS

The average power in a chopper circuit is transferred from the constant supply V_d to the load by the combination of V_d with average component of the input current $I_{s(av)}$, hence

$$P_{in} = V_d I_{s(av)} \tag{12.34}$$

The instantaneous input current $i_s(\omega t)$ flows only while switch T_1 is conducting in Fig.12.2,

$$i_s = i_a \Big|_{0}^{2\pi\gamma} + 0 \Big|_{2\pi\gamma}^{2\pi} \tag{12.35}$$

The average value of $i_s(\omega t)$ is defined by

$$I_{s(av)} = \frac{1}{2\pi}\int_0^{2\pi\gamma} i_L(\omega t)d\omega t \tag{12.36}$$

For continuous conduction, substituting Eq.(12.15) and Eq.(12.20) into Eq.(12.36) gives

$$I_{s(av)} = \gamma\frac{V_d - E_a}{R_a} - \left(\frac{\omega\tau}{2\pi}\right)\left(\frac{V_d}{R_a}\right)\frac{\left(e^{\frac{2\pi}{\omega\tau}} - e^{\frac{2\pi\gamma}{\omega\tau}}\right)}{\left(e^{\frac{2\pi}{\omega\tau}} - 1\right)}\left(1 - e^{\frac{2\pi\gamma}{\omega\tau}}\right) \tag{12.37}$$

For discontinuous conduction, substituting Eq.(12.25) into Eq. (12.36) gives

$$I_{s(avD)} = \frac{V_d - E_a}{R_a}\left[\gamma - \frac{\omega\tau}{2\pi}\left(1 - e^{\frac{2\pi\gamma}{\omega\tau}}\right)\right] \tag{12.38}$$

Example 12.1

The speed of a separately-excited d.c. motor with R_a = 1.2 Ω and L_a = 30 mH, is to be controlled using class-A thyristor chopper as shown in Fig.12.4. The d.c. supply V_d = 120 V. By ignoring the effect of the armature inductance L_a, it is required to:

(a) Find the no load speed and starting torque of the motor when the duty cycle γ =1.

(b) Draw the speed-torque characteristics for the motor when the duty cycle γ = 1. The motor design constant $Ke\Phi$ has a value of 0.042 V/rpm.

(c) Find the speed of the motor n (rpm) when a torque of 8 Nm is applied on the motor shaft and the duty cycle is set to $\gamma = 0.5$.

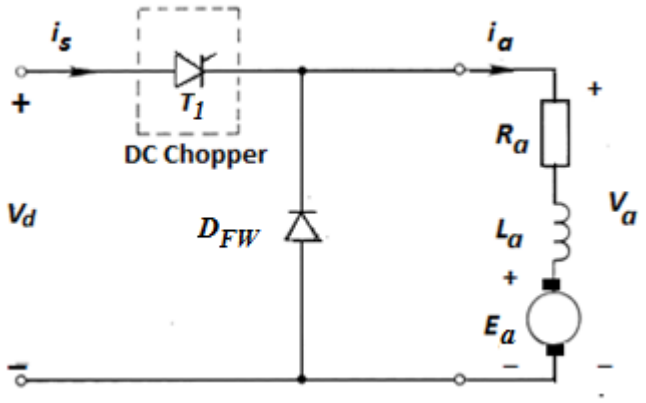

Fig. 12.4 Thyristor chopper drive.

Solution

The average armature voltage for $\gamma = 1$ is

$$V_{av} = \gamma V_d = 1 \times 120 = 120 \text{ V}$$

The motor's speed:

$$n = \frac{V_{av}}{K_e \emptyset} - \frac{R_a}{K_T K_e \emptyset^2} T_d$$

At no load $T_d = 0$, hence

$$\text{or} \quad n_o = \frac{\gamma V_d}{K_e \emptyset} = \frac{120}{0.042} = 2857 \text{ rpm}$$

At starting, $n = 0$. The starting torque T_{st} may be found as:

$$n = 0 = \frac{\gamma V_d}{K_e \emptyset} - \frac{R_a}{K_T K_e \emptyset^2} T_{st}$$

$$T_{st} = \frac{9.55\, \gamma V_d}{R_a} K_e \emptyset$$

$$\therefore \quad T_{st} = \frac{9.55 \times 120}{1.2} \times 0.042 = 40 \text{ Nm}$$

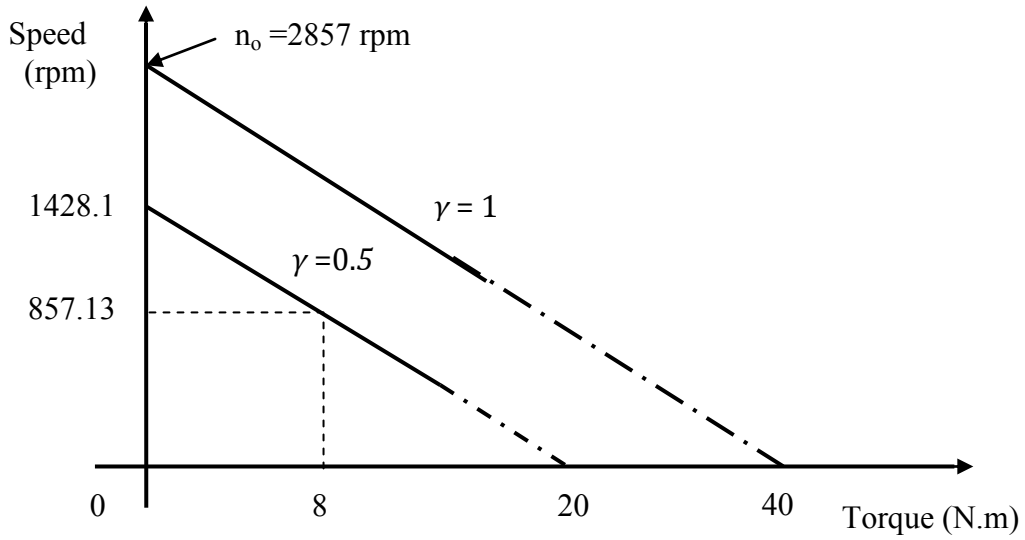

Fig. 12.5 Speed-torque characteristics.

(b) At $\gamma = 0.5$,

$$V_a = \gamma V_d = 0.5 \times 120 = 60 \text{ V}$$

$$n_o = \frac{\gamma V_d}{K_e \emptyset} = \frac{60}{0.042} = 1428.5 \text{ rpm}$$

$$T_{st} = \frac{9.55 \times 60}{1.2} \times 0.042 = 20 \text{ Nm}$$

At $\gamma = 0.5$, $T_L = 8$ Nm

$$n = \frac{60}{0.042} - \frac{1.2}{9.55 \times (0.042)^2} \times 8 = 857.13 \text{ rpm}$$

Note: K_T = Torque constant = 9.55 K_e

Example 12.2

A d.c. motor is driven from a class-A d.c. chopper with source voltage of 220 V and at frequency of 1000 Hz. Determine the range of duty cycle to obtain a speed variation from 0 to 2000 rpm while the motor delivered a constant load of 70 Nm. The motor details as follows:
1kW, 200 V, 2000 rpm, 80% efficiency, R_a = 0.1 Ω, L_a = 0.02 H, and $K\emptyset$ = 0.54 V/rad /s.

Solution

$$\omega = \frac{2\pi n}{60} = \frac{2\pi \times 2000}{60} = 209.3 \text{ rad/s}$$

$$I_{av} = \frac{P_{out}}{\text{Voltage} \times \eta} = \frac{1000}{200 \times 0.80} = 6.25 \text{ A}$$

$$I_{av} = \frac{\gamma V_d - E_a}{R_a} = \frac{\gamma V_d - K\emptyset\, \omega}{R_a}$$

$$T_{av} = K\emptyset\, I_{av}$$

$$T_{av} = K\emptyset \left(\frac{\gamma V_d - K\emptyset\, \omega}{R_a}\right) \text{Nm}$$

For $\omega_m = 0$

$$T_{av} = \frac{\gamma\, K\emptyset\, V_d}{R_a}$$

$$\gamma = \frac{T_{av}\, R_a}{K\emptyset\, V_d} = \frac{70 \times 0.1}{0.54 \times 220} = 0.058$$

$\therefore\ \gamma_{min} = 0.058$

and $\gamma_{max} = \frac{T_{av} R_a}{K\emptyset V_d} + \frac{K\emptyset\omega_m}{V_d} = \frac{70 \times 0.1}{0.54 \times 220} + \frac{0.54 \times 209.3}{220} = 0.571$

Hence the range of γ is $0.058 - 0.571$.

Example 12.3

In the microcomputer-controlled class-A IGBT transistor d.c. chopper shown in Fig.12.6, the input voltage V_d = 260 V, the load is a separately-excited d.c. motor with R_a = 0.28 Ω and L_a = 30 mH. The motor is to be speed controlled over a range 0 – 2500 rpm , provided that the load torque is kept constant and requires an armature current of 30 A .

(a) Calculate the range of the duty cycle γ required if the motor design constant $K_e\Phi$ has a value of 0.10 V/rpm.

(b) Find the speed of the motor n (rpm) when the chopper is switched fully ON such that the duty cycle $\gamma = 1.0$.

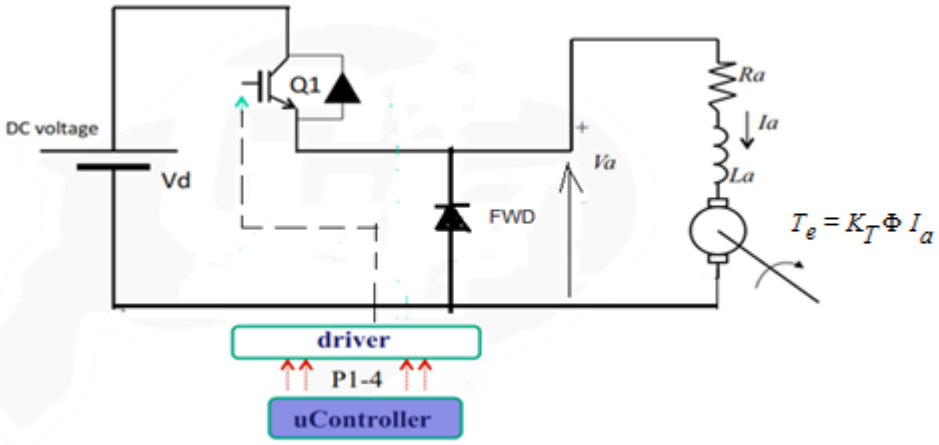

Fig.12.6 IGBT d.c. chopper drive.

Solution

(a) With steady-state operation of the motor, the armature inductance L_a behaves like a short circuit and therefore has no effect at all.

At stand still $n = 0$, and therefore , $E_a = 0$, hence from Eq.(12.22),

$$I_a = \frac{V_a - E_a}{R_a} = \frac{V_{a0} - 0}{0.28} = 30 \text{ A}$$

$$\therefore V_{a0} = 0.28 \times 30 = 8.4 \text{ V}$$

At full speed $n = 2500$ rpm ,

$$E_{a2500} = K_e \phi n = 0.1 \times 2500 = 250 \text{ V}$$

For separately-excited d.c. motor,

$$V_{a2500} = E_a + I_a R_a = 250 + 30 \times 0.28 = 258.4 \text{ V}$$

Therefore the range of the duty cycle γ will be:

$$\gamma_0 = \frac{V_{a0}}{V_d} = \frac{8.4}{260} = 0.0323$$

Similarly

$$\gamma_{2500} = \frac{V_{a2500}}{V_d} = \frac{258.4}{260} = 0.9938$$

(b) When the chopper is switched fully on, i.e. γ =1, then

$$V_a = V_d = 260 \text{ V} .$$

At this condition,

$$V_a|(\gamma = 1) = E_a + I_a R_a = K_e \, \phi \, n + I_a R_a \; = 260\text{V}$$

$$0.1\, n + 30 \; \times \; 0.28 \; = 260 \qquad \rightarrow \quad n = 2516 \text{ rpm}$$

Example 12.4

A separately-excited d.c. motor has the following parameters:

R_a = 0.5 Ω , L_a = 5.0 mH , $K_e \, \Phi$ = 0.078 V/rpm.

The motor speed is controlled by a class-A d.c. chopper fed from an ideal 200 V d.c. source. The motor is driven at a speed of 2180 rpm by switching on the thyristor for a period of 4 ms in each overall period of 6 ms .

(a) State whether the motor will operate in continuous or discontinuous current mode,
(b) Calculate the extinction angle of the current if it exist,
(c) Sketch the armature voltage and current waveforms,
(d) Calculate the maximum and minimum values of the armature current,
(e) Calculate the average armature voltage and current.

Solution

(a) To find whether the motor operates in continuous or discontinuous current modes ,we have to find the values of γ and γ' :

$$\gamma = \frac{t_{on}}{t_{on} - t_{off}} = \frac{t_{on}}{T} = \frac{4ms}{6ms} = 0.667$$

$$T = 6 \, x \, 10^{-3} \text{ s} \qquad \rightarrow \quad \omega = 2\pi \, \frac{1}{T} = 1046.6 \text{ rad/s}$$

The armature circuit tim constant is $\tau = \frac{L_a}{R_a} = \frac{5}{0.5} = 10$ ms

Therefore, $\frac{2\pi}{\omega\tau} = \frac{2 \times 3.14}{1046.7 \times 10 \; \times \; 10^{-3}} = 0.6$

At speed of 2180 rpm , $E_a = \; K_e \, \phi \, n = 0.078 \; \times 2180 = 170$ V

The critical value of γ' will be , (using Eq.(12. 31))

$$\frac{E_a}{V_d} = \frac{e^{2\pi\gamma'/\omega\tau} - 1}{e^{2\pi/\omega\tau} - 1} \; = \frac{170}{200} = \; \frac{e^{0.6\,\gamma'} - 1}{e^{0.6} - 1}$$

From which $\gamma' = 0.0.8829$, therefore , $\gamma' > \gamma$, hence the motor is operating in discontinuous current mode.

(b) The extinction angle x of the current is calculated from Eq.(12.29) as,

$$x = \omega\tau \ln\left[e^{(2\pi\gamma)/\omega\tau}\left\{1 + \left(\frac{V_d}{E_a} - 1\right)\left(1 - e^{-2\pi\gamma/\omega\tau}\right)\right\}\right]$$

$$\omega\tau = 1046.7x10\ x\ 10^{-3} = 10.467 \text{ rad}$$

$$x = 10.467 \ln\left[e^{(2\pi x0.6)/10.467}\left\{1 + \left(\frac{200}{170} - 1\right)\left(1 - e^{-2\pi x0.6/10.467}\right)\right\}\right]$$

From which $x = 4.8$ rad $\rightarrow$ $x = 275.16°$

(c) The armature voltage and current waveforms are shown in Fig.12.7.

(d) The maximum and minimum values of the armature currents are:

$I_{min} = 0$, since it is discontinuous.
I_{maxD} is calculated from Eq.(12.26) as,

$$I_{max_D} = \frac{V_d - E_a}{R_a}\left(1 - e^{-2\pi\gamma/\omega\tau}\right)$$

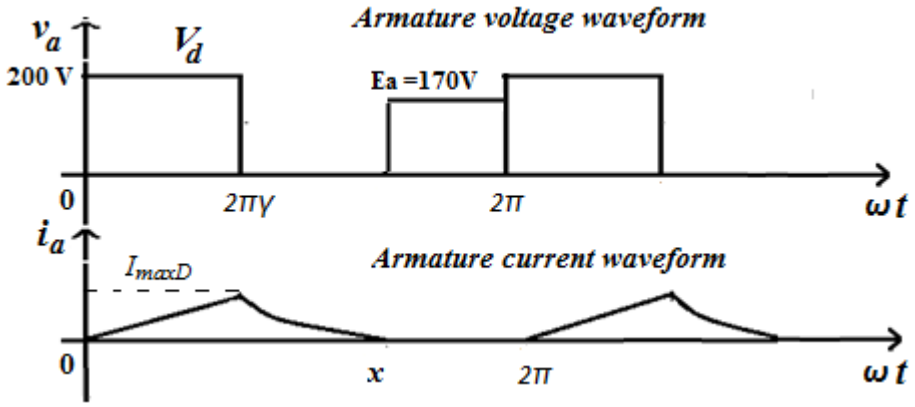

Fig.12.7 Armature voltage and current waveforms.

Example 12.5

A separately-excited d.c. motor with R_a = 0.1 Ω and L_a = 20 mH, is to be controlled using class-A thyristor chopper. The d.c. supply is a battery with V_d = 400 V. The motor voltage constant is 5 V.s/rad. In the steady-state

operation the average armature current I_a = 100 A and it is assumed to be continuous and ripple-free.

(a) For a duty cycle of 0.5, it is required to calculate (i) the input power to the motor, (ii) the speed of the motor, (iii) the developed torque. Mechanical, battery and semiconductor losses may be neglected.

(b) If the duty cycle of the chopper is varied between 20% and 80%, find the difference in speed resulting from this variation.

Solution

(a) Input power to the motor, speed of the motor and the developed torque are calculated as follows:

(i) For continuous current operation the input power is

$$P_{in} = V_a I_a = \gamma V_d I_a = 0.5 \times 400 \times 100 = 20 \text{ kW}$$

(ii) Speed of the motor can be calculated as,
The voltage across the armature circuit

$$V_a = \gamma V_d = 0.5 \times 400 = 200 \text{ V}$$

The induce voltage $E_a = K\emptyset\, \omega$

$$K\emptyset = 5 \text{ V.s/rad.}$$

$$E_a = V_a - I_a R_a = 200 - 100 \times 0.1 = 190 \text{ V}$$

$$\omega = \frac{E_a}{K\emptyset} = \frac{190}{5} = 38 \text{ rad/s}$$

To find the speed *n* in rpm

$$n = \frac{60}{2\pi}\omega = \frac{60}{2\pi} \times 38 = 363 \text{ rpm}$$

(iii) The torque produced by the motor,

$$T_m = \frac{E_a I_a}{\omega} = \frac{190 \times 100}{38} = 500 \text{ Nm}$$

(b) For duty cycle of 20%,

$$E_{a20\%} = \gamma V_d - I_a R_a = 0.2 \times 400 - 100 \times 0.1 = 70\, V$$

$$\omega_{20\%} = \frac{E_{a20\%}}{K\emptyset} = \frac{70}{5} = 14 \ \frac{\text{rad}}{\text{s}} \quad \rightarrow \quad n_{20\%} = 14 \times \frac{60}{2\pi} = 133.7 \text{ rpm}$$

For duty cycle of 80%,

$$E_{a80\%} = \gamma V_d - I_a R_a = 0.8 \times 400 - 100 \times 0.1 = 310 \text{ V}$$

$$\omega_{80\%} = \frac{E_{a80\%}}{K\emptyset} = \frac{310}{5} = 62 \text{ rad/s} \rightarrow n_{80\%} = 62 \times \frac{60}{2\pi} = 592.3 \text{ rpm}$$

Hence the difference in speed is

$$n_{80\%} - n_{20\%} = 592.3 - 133.7 = 458.6 \text{ rpm}$$

Example 12.6

A class-A d.c. chopper operating at a frequency of 500 Hz and feeding a separately-excited d.c. motor from 200 V d.c. source. The load torque is 35 Nm and speed is 1000 rpm. Motor resistance and inductance are 0.15 Ω and 1.0 mH respectively. The *emf* and torque constant of motor are 1.6 V/rad/s and 1.4 Nm /A respectively. Find (a) Maximum and minimum values of motor armature current, and (b) Variation of armature current. Neglect chopper losses.

Solution

(a) Let duty cycle = γ

V_d = 200 V

$V_{av} = \gamma V_d = \gamma \times 200$

Average armature current $I_a = T / K\varphi = 35/1.4 = 25$ A

Back *emf* $E_a = K \varphi \omega = 1.6 \times (950 \times 2\pi/60) = 159.16$ V

$V_{av} = E_a + I_a R_a$

$200 \gamma = 159.16 + 25 \times 0.15 = 162.29$ V

$\gamma = 0.8145$

$T = 1/500 = 2$ ms

$t_{on} = \gamma T = 2 \times 0.8145 = 1.629$ ms

$t_{off} = 2 - 1.629 = 0.371$ ms

From Eq.s (12.19) and (12.20) ,The maximum and minimum currents are calculated as

Let:

$$T = 2\pi \ , \quad t_{on} = 2\pi\gamma = \gamma T \ , \quad \tau = \frac{R_a}{L_a} \ , \text{and} \quad -t_{on}/\tau = \frac{-\gamma T R_a}{L_a}$$

Hence Eq.(12.19) and (12.20) can be re-written as

$$I_{max} = \frac{V_d}{R_a}\left(\frac{1 - e^{-t_{on}/\tau}}{1 - e^{-T/\tau}}\right) - \frac{E_a}{R_a}$$

and

$$I_{min} = \frac{V_d}{R_a}\left(\frac{e^{t_{on}/\tau} - 1}{e^{T/\tau} - 1}\right) - \frac{E_a}{R_a}$$

$$\frac{TR_a}{L_a} = \frac{2 \times 10^{-3} \times 0.15}{1 \times 10^{-3}} = 0.30$$

$$e^{-\frac{\gamma TR_a}{L_a}} = e^{-0.8145 \times 0.3} = e^{-0.24435} = 0.7832$$

$$e^{-\frac{TR_a}{L_a}} = e^{-0.3} = 0.7408$$

$$I_{max} = \frac{200}{0.15}\left(\frac{1 - 0.7832}{1 - 0.7408}\right) - \frac{159.15}{0.15}$$

$$= 1333.34 \times \left(\frac{0.2168}{0.2592}\right) - 1061 = 54{,}2A$$

$$I_{min} = \frac{200}{0.15}\left(\frac{1.2767 - 1}{1.3498 - 1}\right) - \frac{159.15}{0.15}$$

$$= 1333.34 \times \left(\frac{0.2767}{0.3498}\right) - 1061 = 0$$

(b) Variation of armature current = $I_{max} - I_{min} = 54{,}2 - 0 = 54{,}2\text{A}$

PROBLEMS

12.1 A permanent-magnet d.c. motor with R_a = 5 Ω and L_a = 300 mH, is to speed controlled using class-A d.c. chopper. The d.c. power supply is 120 V, armature resistance R_a = 0.5 Ω and L_a = 20 mH. The motor constant $K_e\phi$ = 0.05 V/rpm. The motor is assumed to drive a constant load torque on the motor which required an average armature current of 20 A. Assuming continuous current drawn by the motor, determine:

(a) The ranges of the chopper drive duty cycle.
(b) The range of speed control.

[Ans: (a) $\gamma = (0.083 - 1)$, (b) $n = (0 \ - 2200)$ rpm]

12.2 A separately-excited d.c motor with $R_a = 5\ \Omega$ and $L_a = 300$ mH, is to speed controlled using class-A d.c. chopper. The d.c. supply is 120 V. (a) It is required to draw the speed torque characteristics for the motor for duty cycle, $\gamma = 1$. The motor constant $K_e \phi = 0.7$ (V /rpm). (b) Find the speed of the motor (ω) at a torque of 5 Nm applied on the motor shaft when the duty cycle used is ($\gamma = 0.5$).

[Ans: (b) 34.69 rpm]

12.3 A d.c. motor is driven by a single-quadrant d.c. chopper with source voltage of 240 V.The chopper operates at a frequency of 400 Hz. The motor is loaded such that it draws contiuous and ripple-free current of 80 A and runs at speed of 500 rpm. The armature resistance is $R_a = 0.25\ \Omega$ and the machine constant $K_e\varphi = 0.1$ V/rpm. It is required to:

(a) Draw waveforms of the armature voltage, armature current and the current drawn from the source.
(b) Determine the duty cycle γ and the ON-time t_{on} of the chopper.
(c) Determine the power developed by the motor, power absorbed by the armature resistance and the power drawn from the source.

[Ans (b) $\gamma = 0.291$, $t_{on} = 0.729$ ms, (c) 4000 W, 1600 W, 5600 W]

12.4 A class-A, single-quadrant d.c. chopper is used to feed a d.c. shunt motor motor which has the following parameters:

$R_a = 0.25\ \Omega$, $L_a = 15$ mH, and $K_e \phi = 0.209$ V/rpm.

The chopper is supplied from an ideal battery source of voltage = 500 V. At a certain operating condition, the motor runs at speed of 9000 rpm and the mechanical output power is 9000 W. At the stated condition, the armature current is continuous with peak-to-peak ripple of 8 A. It is required to determine:

(a)The chopper duty cycle.
(b)The approximate switching frequency (neglect the effect of R_a).
(c)The power lost in R_a .

[Ans: (a) 0.4, (b) 1039 Hz, (c) 600 W]

12.5 A small electric train is driven by a 1250 rpm, 400 V d.c. series motor has an armature resistance $R_a = 0.05\ \Omega$ and a series field resistance $R_s = 0.1\ \Omega$. The motor rated full load current is 150 A. The train is to be speed controlled using single-quadrant d.c. chopper fed from 500 V ideal battery. The

chopper frequency varies between 100 Hz and 1800 Hz but the ON time remains constant at 0.5 ms. At stand still, the motor current is limited to 200 A. Calculate:

(a) The chopper switching frequency and the supply current drawn when the motor is at standstill.
(b) The chopper switching frequency and the supply current drawn at rated output.

[Ans: (a) 120 Hz, 12 A, (b) 1600 Hz, 120 A]

12.6 A permanent-magnet d.c. motor is fed by a class-A d.c. chopper. The machine has negligible armature resistance and an armature inductance of 5 mH with machine constant $K_e \phi$ = 0.262 V/rpm. The chopper is fed from a 400 V ideal battery source and operating with a switching frequency of 1000 Hz. It is required to:

(a) Determine the speed of the motor if the duty cycle is 50% and the torque is 100 Nm.
(b) The torque is now reduced to 20 Nm and the duty cycle is maintained at 50%. Show that the armature current is discontinuous and calculate the new motor speed.
(c) For the condition in (b) determine the duty cycle required to bring the motor speed back to the value calculated in (a).

[Ans: (a) 764 rpm, (b) 849 rpm, (c) 44.7 %]

12.7 A d.c. supply with V_d = 250 V supplies power to a separately excited d.c. motor via a class-A thyristor chopper. The motor has an armature circuit resistance of 0.25 Ω and inductance of 10 mH. The chopper is fully ON at the rated motor speed of 1500 rpm when the armature current is 25 A. If the speed is to be reduced to 1000 rpm, with the load torque constant, calculate the necessary duty cycle.

[Ans : γ = 0.675]

12.8 A 100 V battery supplies power to a d.c. separately-excited motor, with R_α = 0.2 Ω and L_α =1 mH, via a class-A d.c. chopper operating at 300 Hz. With a duty cycle of 0.75 the motor back *emf* is 70 V, calculate the average values of the load voltage and current, the average value of input current, the output power and the approximate efficiency of the motor.

[Ans: V_{av}= 75 V, I_{av} = 25 A, I_{sav} = 20.89 A , P_o = 1750 W , η = 84 %]

12.9 A separately-excited d.c. motor with R_a = 0.3 Ω and L_a = 15 mH is to be speed controlled over a range 0 – 1500 rpm using class-A MOSFET d.c. chopper fed from ideal d.c. source with V_d =300 V as shown in Fig.12.8(a). The motor load is a conveyer belt which exerts a constant torque on the motor, as shown in Fig.12.8 (b), and requires an average armature current of 30A. The machine design constant $k_e \varphi$ = 0.17 V/rpm.

(a) Calculate the required range of the duty cycle of the chopper.
(b) Calculate the speed of the motor when the chopper is fully ON.

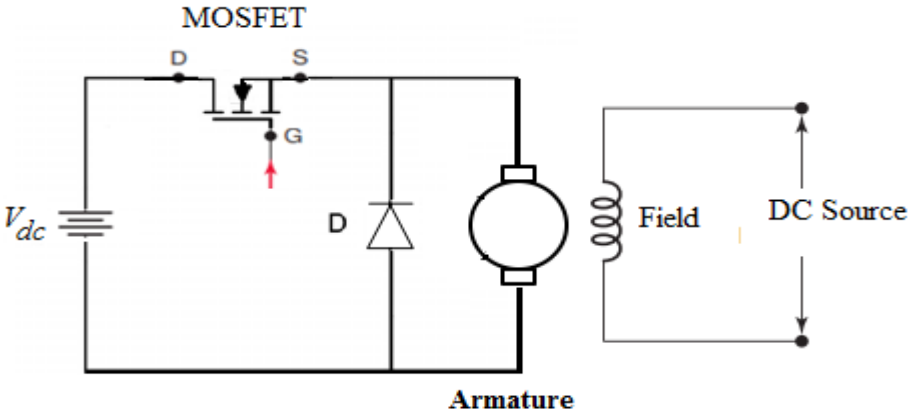

(a)

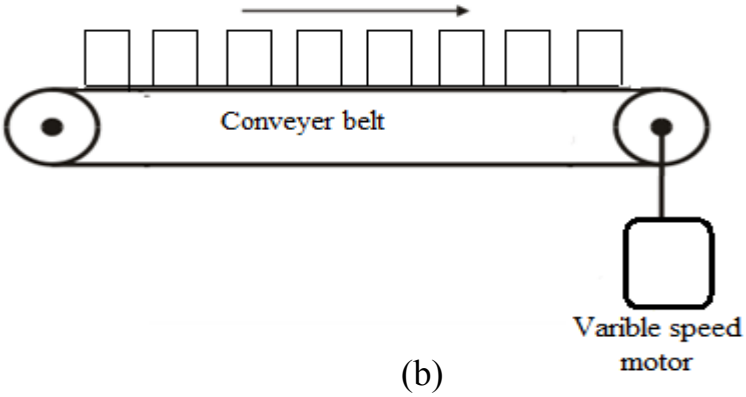

(b)

Fig.12.8.

[Ans : (a) γ Range : 0.03 – 0.91, (b) 1712 rpm]

12.10 A 240 V, 150 kW, 500 rpm separately-excted d.c. motor is controlled by a class-A d.c. chopper. The d.c. supply for the chopper is an ideal battery of 310 V. The chopper is operates with a frequency of 1000 Hz. The motor parameters are as follows:

$$R_a = 0.04\ \Omega\ , \qquad L_a = 1\ \text{mH}\ , \qquad K_T = 4.17\ \text{V/rad/s}$$

If the motor is running at 300 rpm with 0.55 duty cycle, determine the average current taken by the motor and the average load produced by the

motor using steady-state approximation analysis and assume continuous current operation. Neglect any switching losses.

[Ans : 991.8 A , 4138.1 Nm]

12.11 A 20 kHz d.c. chopper is used to drive a separately-excited d.c. motor from 240 V source. Resistance and inductance of armature circuit are 0.6 Ω and 4mH, respectively. At rated conditions, armature current is 10 A and back *emf* is 174 V,

(a) Find the duty cycle of the chopper .

(d) Find the required duty cycle of chopping to reduce motor speed to 80% of rated speed, assuming that the armature current at this speed remains at rated value.

[Ans: (a) 0.75 , (b) 0.605]

12.12 A class-A, single-quadrant d.c. chopper is used for dynamic braking of a separately-excited d.c. motor having armature resstance R_a = 0.2 Ω, and inductance L_a of 30 mH. The braking resistance used is 10 Ω. The voltage constant is 1.3 V/A.rad /s, and the armature current is 100 A. If the field current is 2 A and the duty cycle of chopper is 0.5; find : (a) Average voltage across chopper, (b) Power dissipated in braking resistance, and (c) Motor speed.

[Ans : (a) 500 V ,(b) 15 kW, (c) 1910 rpm]

12.13 A separately-excited d.c. motor is fed from an ideal d.c. source of 500 V through a single-quadrant d.c. chopper. The armature resistance is 0.08 Ω and armature current is 150 A. The voltage and torque constants are 1.3 V/A.rad /s and 1.4 Nm /A^2 respectively. The field current is 1.5 A. The duty cycle of chopper is set to 0.75. Determine: (a) The input power to the motor,(b) The speed of the motor, (c) The output torque.

[Ans : (a) 33.75 kW, (b)782.3 rpm , (c) 390 Nm]

CHAPTER THIRTEEN

DC DRIVES USING CONTROLLED RECTIFIERS

13.1 INTRODUCTION

The speed of d.c. motor can be controlled very easily by means of regulating its supply voltage by the use of phase controlled rectifiers. This control can be applied to either the field or the armature circuit. The motor response with armature control is faster than that with field control since the time constant of the field is very much larger than that of the armature. Generally, field control is used for speeds above rated value and armature control for speeds below rated value.

Controlled rectifiers either single-phase or multi-phase are widely used in d.c. drive applications where a.c. source is available. The single-phase or multi-phase a.c. is converted to d.c. by a controlled rectifier or converter to give a variable d.c. source, by varying the triggering angle of the thyristor or any other power semiconductor device, that could be supplied to a d.c. motor and thus the speed of the motor can be controlled. Controlled rectifiers used in d.c. drives can be classified as follows:

1- Single-phase controlled rectifiers

(i) Single-phase half-wave converter drives.
(ii) Single-phase full-wave half-controlled converter drives.
(iii) Single-phase full-wave fully-controlled converter drives.
(iv) Single-phase dual converter drives.

2. Multi-phase controlled rectifiers

(i) Three-phase half-wave converter drives.
(ii) Three-phase full-wave fully-controlled converter drives.
(iii) Three-phase full-wave half-controlled converter drives.
(iv) Three-phase full-wave dual converter drives.

13.2 SINGLE-PHASE CONVERTER DRIVES

These are used for small and medium power motors up to 75kW (100*hp*) ratings. In the following subsections, the various types of these converters will be discussed.

13.2.1 Single-Phase Half-Wave Converter Drives

Fig.13.1 shows a single-phase half-wave converter drive used to control the speed of separately-excited motor. This d.c. drive is very simple, needs only one power switch and one freewheeling diode connected across the motor terminals for the purpose of dissipation of energy stored in the inductance of the motor and to provide an alternative path for the motor current to allow the power switch to commutate easily.

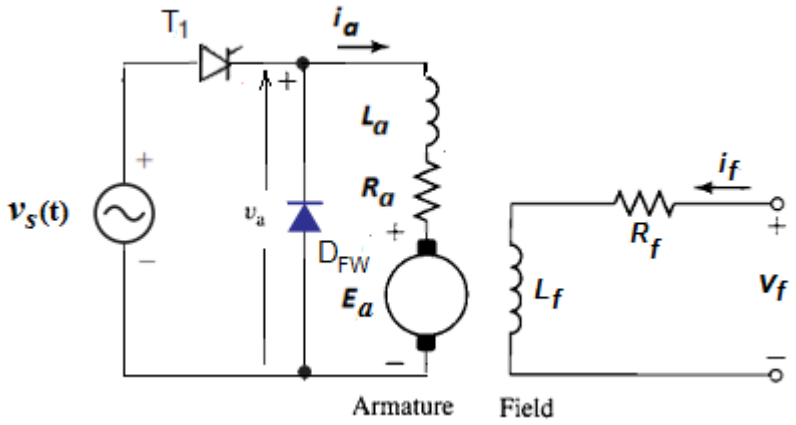

Fig.13.1 Single-phase half-wave converter drive.

Waveforms for steady-state operation of the converter with motor load is shown in Fig.13.2 for the case $\alpha \equiv 80^\circ$. It is clear that during the interval $\beta < \omega t < 2\pi$, the armature current is zero, hence the torque developed by the motor is zero, the speed of the motor will be reduced. Since the mechanical time constant of the motor is larger than its electrical time constant, the inertia of the motor will maintain the speed, but its value will fluctuate resulting in poor motor performance. Therefore, this type of drive is rarely used; it is only used for small d.c. motors below 500 W ratings.

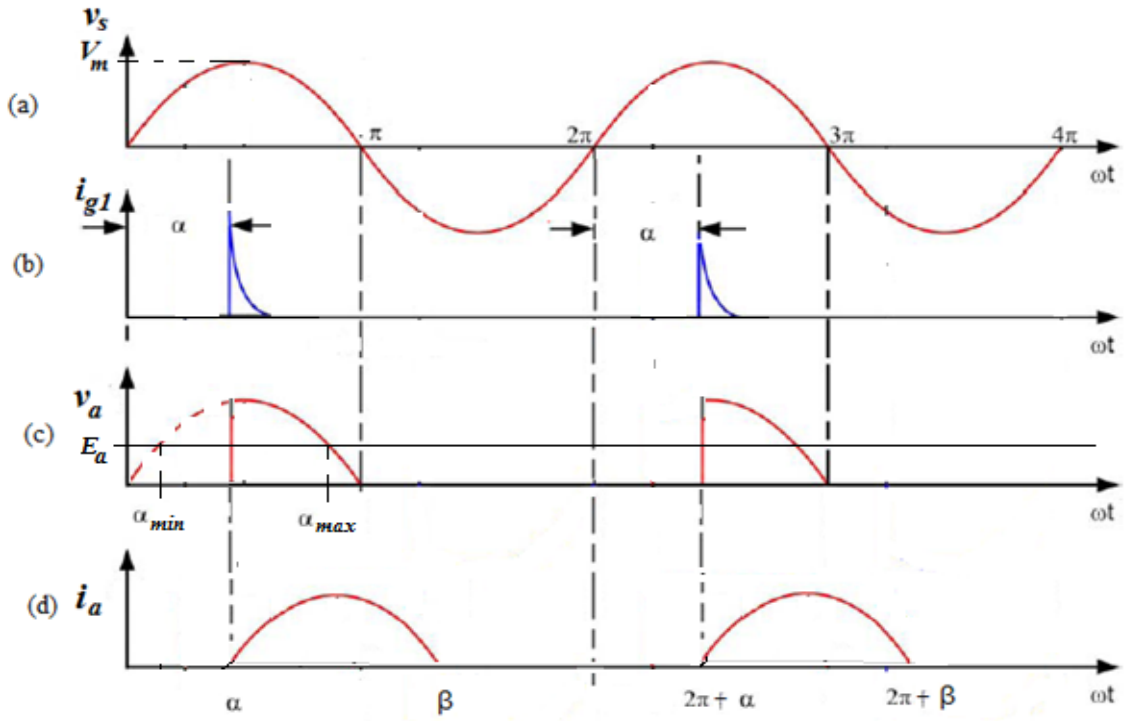

Fig.13.2 Waveforms for steady-state operation of the single-phase half-wave rectifier with motor load.

The average value of the armature voltage can be evaluated as follows:

Assuming the supply voltage $v_s(\omega t) = V_m \sin \omega t$, thus in the positive half-cycle, T_1 will conduct from α to π , where α is the firing angle, and D_{FW} will conduct from π to β, where β is the extinction angle of the current. Hence the average value of the armature current will be,

$$V_{a(av)} = \frac{1}{2\pi}\int_{\alpha}^{\pi} V_s(\omega t)\ d\omega t\ = \frac{1}{2\pi}\int_{\alpha}^{\pi} V_m \sin \omega t\ d\omega t$$
$$= \frac{V_m}{2\pi}\ (1 + \cos \alpha) \qquad (13.1)$$

It is to be noted that the thyristor T_1 is only conducts when supply voltage exceeds back *emf* E_a , therefore, referring to Fig.13.2(c), we define two triggering angles α_{min} and α_{max} as,

α_{min} is the minimum firing angle below which the thyristor cannot be triggered. i.e. when the supply voltage $V_m\ sin\alpha\ >\ E_a$. This angle can be calculated as,

$$V_m\ sin\ \alpha_{min} = E_a \quad \rightarrow \quad \alpha_{min} = sin^{-1}\left(\frac{E_a}{V_m}\right) \qquad (13.2)$$

Similarly α_{max} is the maximum firing angle above which the thyristor cannot be triggered. Its value is given by

$$\alpha_{max} = \pi - \alpha_{min} = \pi - sin^{-1}\left(\frac{E_a}{V_m}\right) \tag{13.3}$$

The speed of the motor can be calculated from the general equation of the speed of d.c. motor as,

$$n = \frac{V_a}{K_e \emptyset} - \frac{R_a}{K_T K_e \emptyset^2} T_L$$

Substituting for $V_{a(av)}$ from Eq.(13.1) into the above equation we get,

$$n = \frac{V_m}{2\pi\, K_e\, \emptyset}(1 + \cos\alpha) - \frac{R_a}{K_T K_e \emptyset^2} T_L \tag{13.4}$$

or in terms of the angular velocity ω using Eq.(11.25),

$$\omega = \frac{V_{a(av)}}{K\emptyset} - \frac{R_a}{K^2 \emptyset^2} T_L$$

Substituting for $V_{a(av)}$ we get,

$$\omega = \frac{V_m}{2\pi K\emptyset}(1 + \cos\alpha) - \frac{R_a}{K^2 \emptyset^2} T_L \tag{13.5}$$

The starting torque can also be calculated from Eq.(13.4) or Eq.(13.5) by setting n or ω equal zero and calculate the torque, (using Eq.(13.5) for example), as

$$0 = \frac{V_m}{2\pi K\emptyset}(1 + \cos\alpha) - \frac{R_a}{K^2 \emptyset^2} T_{st}$$

From which,

$$T_{st} = \frac{K\emptyset V_m}{2\pi R_a}(1 + \cos\alpha) \tag{13.6}$$

And the no load speed is calculated from Eq.(13.5) by setting $T_L = 0$ to give,

$$\omega_o = \frac{V_m}{2\pi K\emptyset}(1 + \cos\alpha) \tag{13.7}$$

By knowing ω_o and T_{st} the mechanical characteristics of the motor can be obtained for various values of the triggering angle α as illustrated in the following example:

Example 13.1

For the d.c. drive circuit of a separately-excited motor shown in Fig.13.1, it is required to calculate and draw the speed-torque characteristics of the motor for firing angles $\alpha = 0°$, $\alpha = 45°$, and $\alpha = 90°$. The supply voltage is 60V (*rms*) , the motor armature resistance R_a = 0.5 Ω and the motor voltage constant $K\emptyset = 1$ V.s / rad.

Solution

Using equations (13.5) , (13.6) and (13.7),

$$T_{st} = \frac{\sqrt{2}K\emptyset V_{rms}}{2\pi R_a}(1 + \cos\alpha)$$

$$\omega_o = \frac{\sqrt{2}V_{rms}}{2\pi K\emptyset}(1 + \cos\alpha)$$

To calculate T_{st} and ω_o , the following values are obtained and drawn in Fig.13.3.

Firing angle α	Starting torque T_{st} (Nm)	No load speed ω_o (rad/s)
0°	54	27
45°	46.1	23
90°	27	13.5

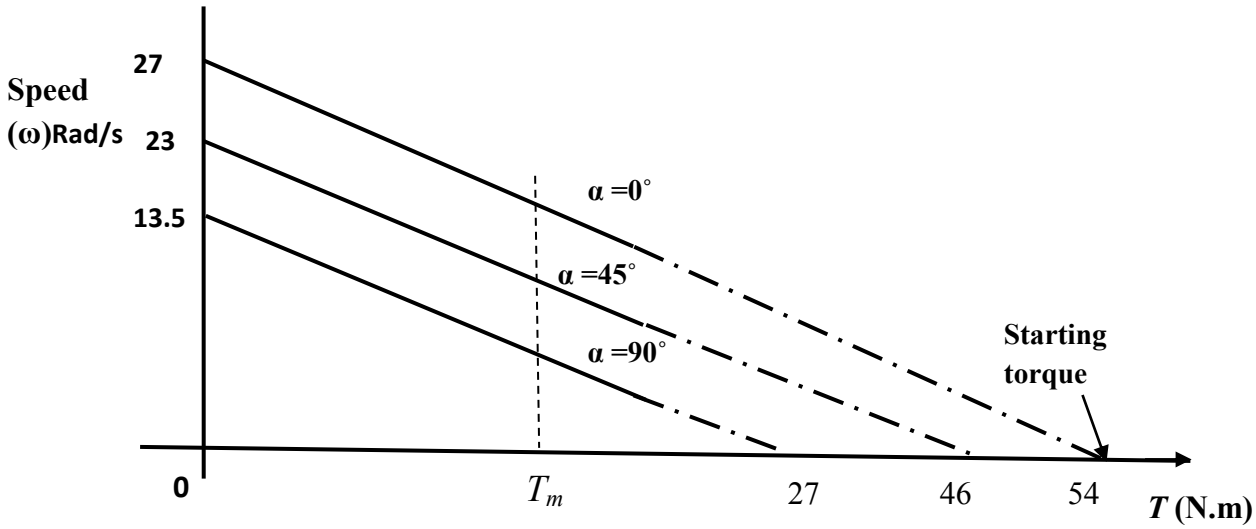

Fig.13.3 Speed-torque characteristics of a separately-excited d.c. motor controlled by single-phase half-wave rectifier drive.

13.2.2 Single-Phase Semiconverter with Separately-Excited d.c. Motor Load

The circuit diagram of a single-phase full-wave half-controlled (semiconverter) drive for controlling a separately-excited d.c. motor is depicted in Fig.13.4. Here a full wave rectifier bridge is supplies the field circuit, and a half-controlled bridge supplies the armature circuit. The vast majority of shunt motors are controlled in this manner.

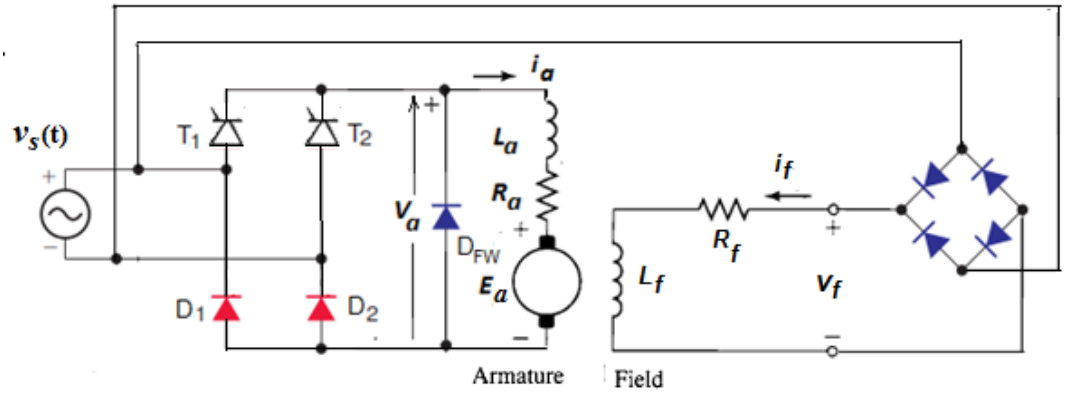

Fig.13.4 Single-phase semiconverter with d.c. motor load.

Assuming the supply voltage $v_s(t) = V_m \sin \omega t$, in the positive half-cycle, T_1 and D_2 will conduct from α to (α + δ), where α is the firing angle and δ is the conduction angle. Generally, for medium and large motors the inductance of the armature is small and hence, for the separately-excited motor, the armature current falls to zero at the instant when the back *emf* E_a is equal to the supply voltage . i.e.

$$\alpha + \delta = \pi - sin^{-1} \frac{E_a}{V_m} \tag{13.8}$$

The waveforms of the voltage v_a across the armature and the current i_a through the armature are shown in Fig.13.5. It is obvious that the armature current is discontinuous.

(A) Discontinuous armature current operation

The differential equations describing the motor system, during the period the thyristors conduct, are

$$v_a = i_a R_a + L_a \frac{di_a}{dt} + e_a = i_a R_a + L_a \frac{di_a}{dt} + K\emptyset\omega_m \tag{13.9}$$

$$T_m = K\emptyset\, I_a = J \frac{d\omega_m}{dt} + B.\omega_m + T_L \tag{13.10}$$

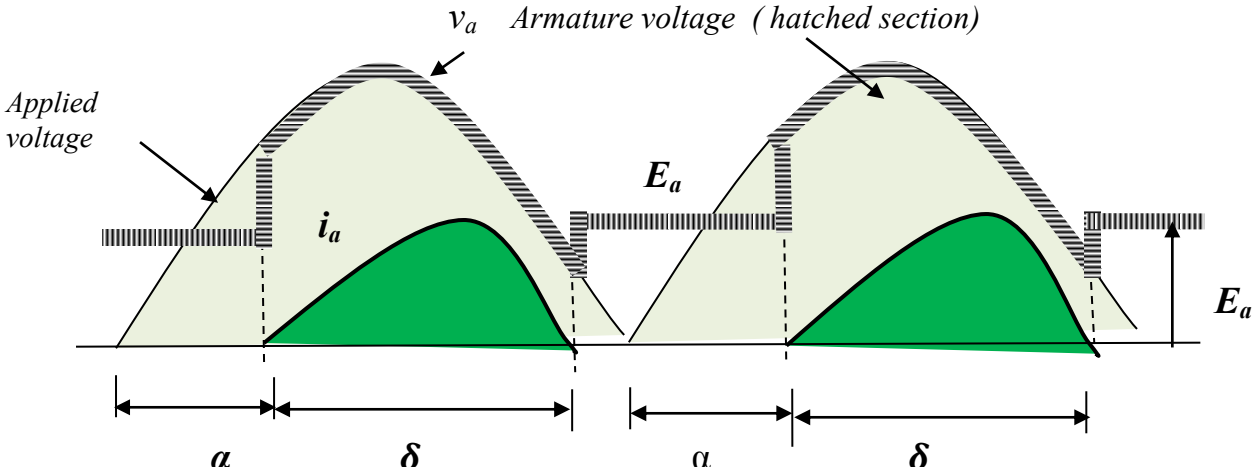

Fig.13.5 Waveforms for single-phase semiconverter operation with discontinuous armature current.

If we assume that the inertia of the rotating system is large then speed fluctuations will be negligible. If each term of v_a is integrated from α to (α + δ) and then divided by π , the instantaneous voltage, current and speed will be converted to their respective average values,

$$V_{a(av)} = \frac{1}{\pi}\int_{\alpha}^{\alpha+\delta} V_m \sin\omega t \; d\omega t$$

$$= \frac{1}{\pi}\int_{\alpha}^{\alpha+\delta} L_a \frac{di_a}{dt} \; d\omega t + \frac{1}{\pi}\int_{\alpha}^{\alpha+\delta} R_a \, i_a \; d\omega t + \frac{1}{\pi}\int_{\alpha}^{\alpha+\delta} K\emptyset \; \omega_m \, d\omega t$$

Thus

$$V_{a(av)} = I_{a(av)}R_a + K\emptyset \; \omega_{m(av)} \qquad (13.11)$$

where

$$V_{a(av)} = \frac{V_m}{\pi}[\cos\alpha - \cos(\alpha+\delta)\,] \qquad (13.12)$$

and the average voltage across L_a is zero.

Similarly,

$$T_{m(av)} = K\emptyset \; I_{a(av)} = B.\omega_{m(av)} + T_L \qquad (13.13)$$

Example 13.2

A d.c. shunt motor , operating from a single-phase half-controlled bridge at speed of 1450 rpm, has an input voltage v_s = 330 sinωt and a back *emf* of 75 V. The thyristors are fired symmetrically at α = π / 4 in every half-cycle, and the armature resistance is 5 Ω. Neglecting the armature inductance, calculate the average armature current and load torque.

Solution

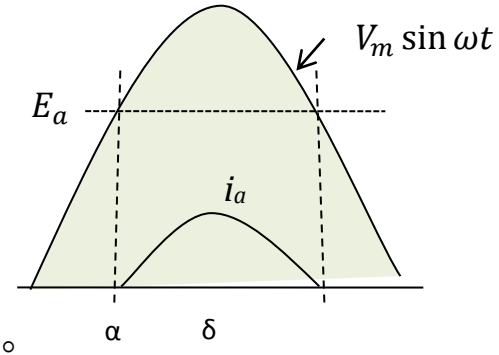

$$\alpha = \pi/4 = 45^\circ$$

$$(\alpha + \delta) = \pi - sin^{-1}\left(\frac{E_a}{V_m}\right)$$

$$= \pi - sin^{-1}\left(\frac{75}{330}\right) = 166.9^\circ$$

$$\omega_{av} = \frac{2\pi n}{60} = \frac{2\pi \times 1450}{60} = 151.8 \text{ rad/s}$$

$$V_{a(av)} = \frac{1}{\pi}\int_{45^\circ}^{166.9^\circ} V_m \sin \omega t \; d\omega t = \frac{V_m}{\pi}[\cos 45^\circ - \cos 166.9^\circ]$$

$$= \frac{330}{\pi} \times 1.68 = 176.6 \text{ V}$$

$$E_a = K \, \emptyset \, \omega_{m(av)}$$

$$75 = 151.8 \, K\emptyset \quad \rightarrow \quad K\emptyset = \frac{75}{151.8} = 0.494 \text{ V. s/rad}$$

Now use the general equation of the shunt motor (13.11),

$$176.6 = 5 \, I_{a(av)} + 75 \quad \therefore \quad I_{a(av)} = 20.32 \text{ A}$$

From Eq.(13.10) , $T_m = K\emptyset \, I_a$

$$\therefore T_{av} = K\emptyset \, I_{a(av)} = 0.494 \times 20.32 = 10.04 \text{ Nm}$$

The torque can also be evaluated as,

$$T_{av} = \frac{P}{\omega_{av}} = \frac{E_a I_{a(av)}}{\omega_{av}} = \frac{75 \times 20.32}{151.8} = 10.04 \text{ Nm}$$

(B) Analysis with Continuous Armature Current Operation

If the armature inductance is large then conduction will continue, even after the supply voltage has reversed, for which typical waveforms are shown in Fig.13.6. Hence assume continuous current operation, the average value of the armature voltage is:

$$V_{a(av)} = \frac{1}{\pi}\int_{0}^{2\pi} V_a(\omega t)d\omega t = \frac{1}{\pi}\int_{\alpha}^{\pi} V_m \sin(\omega t)\, d\omega t$$

$$V_{a(av)} = \frac{V_m}{\pi}(1 + cos\alpha) \qquad (13.14)$$

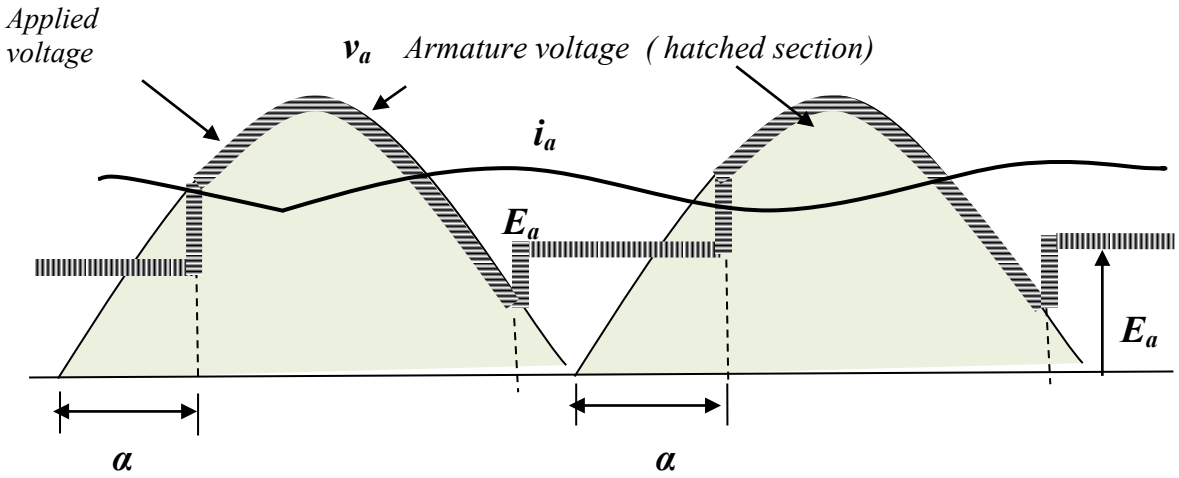

Fig.13.6 Waveforms for single-phase semiconverter operation with continuous armature current.

The average load current is:

$$I_{a(av)} = \frac{V_{a(av)} - E_a}{R_a}$$

$$I_{a(av)} = \frac{V_m}{\pi R_a}(1 + cos\alpha) - \frac{E_a}{R_a} \qquad (13.15)$$

The drive circuit shown in Fig.13.4 can also be used for the variable speed operation of a d.c. series motor. Here the motor field winding is in

series with the armature and hence the armature current becomes continuous, using D_1 or D_2 as freewheeling diodes whenever the supply voltage reverses. Two modes of operation are possible. In one mode current flows through T_1 and D_2 (or T_2 and D_1) and the supply voltage appears across the motor. In the second mode T_1 and D_1 (or T_2 and D_2) conduct and the motor voltage is zero. The motor equations are:

$$v_a = V_m \sin(\omega t) \ = i_a R_T + L_T \frac{di_a}{dt} + e_a \quad \text{for } \alpha \leq \omega t \leq \pi \quad (13.16)$$

and

$$v_a = 0 \ = i_a R_T + L_T \frac{di_a}{dt} + e_a \qquad \text{for } \ \pi \leq \omega t \leq (\pi + \alpha) \ (13.17)$$

where R_T and L_T are the total resistance and inductance in the series circuit respectively.

$$T_m = \ K\emptyset \ I_a = J \frac{d\omega_m}{dt} + B.\omega_m + \ T_L \quad (13.18)$$

Integrating as before gives

$$V_{a(av)} \ = \frac{V_m}{\pi}(1 + cos\alpha) = R_T \ I_{a(av)} + K\emptyset\omega_{m(av)} \quad (13.19)$$

$$T_{av} = \ K\emptyset {I_{a(av)}}^2 = B.\omega_{m(av)} + \ T_L \quad (13.20)$$

For series motor, it is known that, $\emptyset = k_f \ I_{a(av)}$, hence , $K\emptyset = Kk_f I_{a(av)}$.

Now, let $Kk_f = K_{af}$ $\rightarrow$ new constant (henry), thus the above Eq. (13.19) and Eq. (13.20) can be re-written as,

$$V_{a(av)} \ = \frac{V_m}{\pi}(1 + cos\alpha) = R_T \ I_{a(av)} + K_{af} I_{a(av)} \ \omega_{m(av)} \quad (13.21)$$

$$T_{av} = \ K_{af} {I_{a(av)}}^2 = B.\omega_{m(av)} + \ T_L \quad (13.22)$$

Example 13.3

A series d.c. motor is to be controlled by a single-phase, half-controlled, full-wave rectifier bridge as shown in Fig.13.7. The a.c. input voltage has an *rms* value of 240V at 50Hz.The combined armature and field resistance is 2.5Ω and K_{af} = 300 mH. If the load torque is 30 Nm and damping is neglected, calculate the average current and the speed for α = 60˚.

Solution

Using Eq. (13.21),

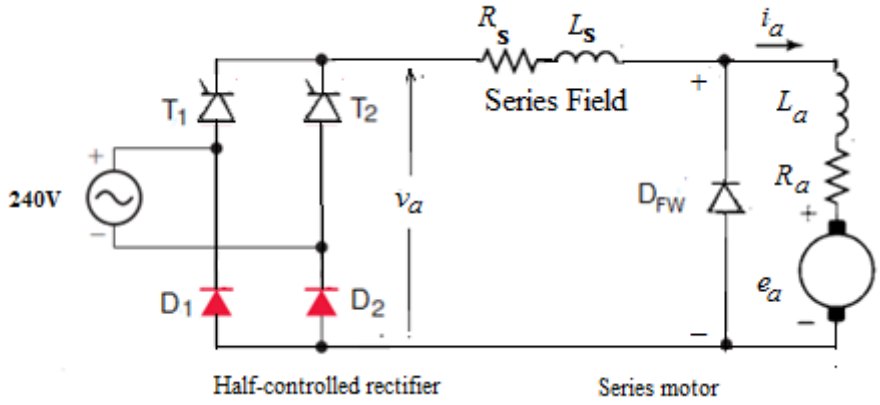

Fig.13.7 Series motor drive.

$$V_{a(av)} = \frac{V_m}{\pi}(1 + cos\alpha) = \frac{\sqrt{2}}{\pi} \times 240\ (1 + \cos 0°) = 162.11\ \text{V}$$

From Eq. (13.22) $\quad T_{av} = K_{af} I_{a(av)}{}^2 = 30 = 300 \times 10^{-3} I_{a(av)}{}^2$

$$\therefore I_{a(av)} = 10\ \text{A}$$

$$V_{a(av)} = R_T\ I_{a(av)} + K_{af} I_{a(av)}\ \omega_{m(av)}$$

$$162.11 = 2.5 \times 10 + 0.3 \times 10\ \omega_{m(av)}$$

$$\therefore \omega_{m(av)} = 45.7\ \text{rad/s} \longrightarrow \text{n} = 436.6\ \text{rpm}$$

13.2.3 Single-Phase Full-Wave Fully-Controlled Rectifier Drives

The circuit diagram of a single-phase full-wave fully-controlled converter drive for controlling a separately-excited d.c. motor is depicted in Fig.13.8.

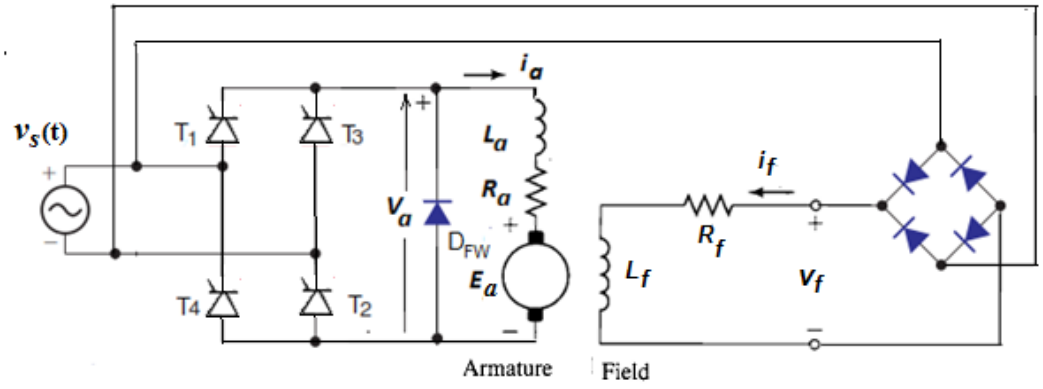

Fig. 13.8 Single-phase full-converter with d.c. motor load.

Here a full-wave rectifier bridge is supplies the field circuit, while the full-converter supplies the armature circuit. The converter has four thyristors that need alternate switching of the pairs of these thyristors T_1 , T_2 or T_3 , T_4 . The converter provides + V_a or – V_a depending on the value of the triggering angle α of the thyristors, thus two quadrant operation is possible. Armature current remains unidirectional due to the converter configuration. The vast majority of shunt motors are also controlled in this manner.

(A) Single-phase full-converter operation with continuous motor current

The waveforms of voltage v_a across the armature and the current i_a through the armature are shown in Fig. 13.9 for continuous current mode of operation.

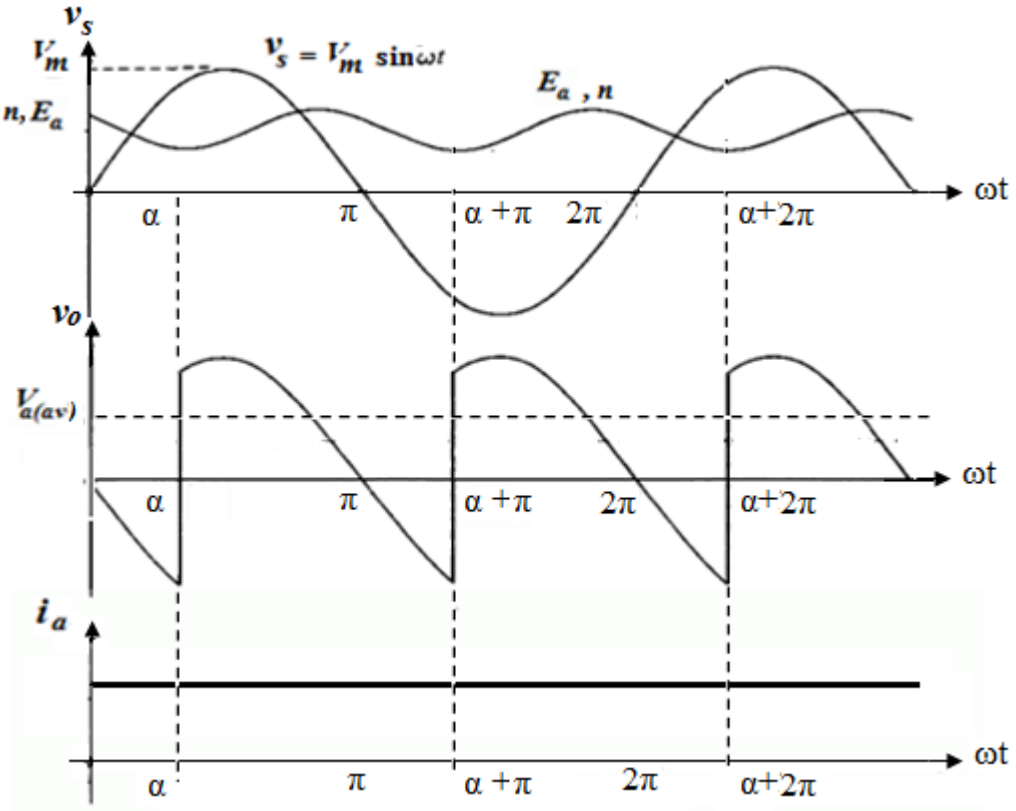

Fig.13.9 Waveforms of the armature voltage and the current for continuous current operating mode.

In any case it is obvious that the thyristor only conducts when supply voltage exceeds the back *emf* , i.e. ($V_m sin\alpha > E_a$).

When thyristors T_1 and T_2 triggered at ωt = α , T_3 and T_4 must be turned off. When thyristors T_3 and T_4 are triggered at ωt = α + π negative voltage is applied across T_1 and T_2 causes them to commutate naturally. The average value of the armature voltage, as can be deduced from Fig.13.9 is

$$V_{a(av)} = \frac{1}{2\pi}\int_0^{2\pi} v_a(\omega t)d\omega t = \frac{2}{2\pi}\int_\alpha^{\pi+\alpha} V_m \sin(\omega t)\, d\omega t$$

$$V_{a(av)} = \frac{2V_m}{\pi}\cos\alpha \tag{13.23}$$

The average current

$$I_{a(va)} = \frac{V_{a(av)} - E_a}{R_a}$$

$$= \frac{2V_m}{\pi R_a}(cos\alpha) - \frac{E_a}{R_a} \tag{13.24}$$

(B) Power and power factor

The power taken by the motor can be calculated as

$$P_{in} = P_a = I_a^2 R_a + E_a I_a \tag{13.25}$$

$E_a I_a$ represents the output power plus the motor friction and windage losses. If the mechanical losses in the motor and electrical losses in the rectifier switches are neglected, the output power and the operating efficiency are

$$P_{out} = E_a I_a = T\omega_m \tag{13.26}$$

$$\eta = \frac{P_{out}}{P_{in}} = \frac{E_a I_a}{P_a} \tag{13.27}$$

Since the input current has *rms* value equal to that of the motor current, thus the operating power factor is

$$\text{Power factor} = \frac{P_a}{\frac{E_m}{\sqrt{2}}.I_L} \tag{13.28}$$

Example 13.4

A separately-excited d.c. motor has the following parameters:

$R_a = 0.25\ \Omega$, $K_e = 0.62$ V/ rpm.Wb , Φ (flux per pole) = 175 mWb.

The motor speed is controlled by a single-phase, full-wave bridge rectifier. The firing angle α is set at 45°, and the average speed is 1300 rpm. The applied a.c. voltage to the bridge is 230 V at 50Hz. Assuming the motor current is continuous; calculate the armature current drawn by the motor and the steady-state torque for the cases of:

(a) Fully-controlled bridge shown in Fig.13.10 (a).
(b) Half-controlled (semiconverter) bridge shown in Fig.13.10 (b).

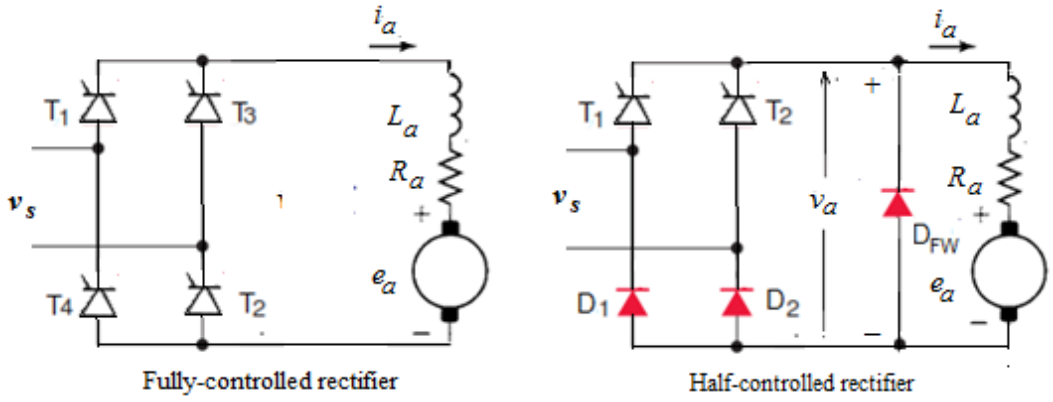

(a) (b)

Fig.13.10.

Solution

(a) For fully-controlled bridge with continuous current operating mode:

$$V_{a(av)} = \frac{2V_m}{\pi}\cos\alpha$$

$V_m = \sqrt{2} \times 230 = 325.2$V

$$V_{a(av)} = \frac{2 \times 325.2}{\pi}\cos 45° = 146.44\ \text{V}$$

$E_a = K_e\, \varphi\, n = 0.62 \times 175 \times 10^{-3} \times 1300 = 141.05$ V

$V_t = V_a = E_a + I_a R_a$

$$\therefore I_a = \frac{V_a - E_a}{R_a} = \frac{146.44 - 141.05}{0.25} = 21.56\ \text{A}$$

Since $T_d = K_T I_a \varphi$

K_T = Torque constant = 9.55 K_e = 9.55 × 0.62 = 6.2

$T_d = 6.2 \times 21.56 \times 175 \times 10^{-3} = 23.4$ Nm

(b) For half-controlled (semiconverter) bridge.

$$V_{a(av)} = \frac{V_m}{\pi}(1 + cos\alpha)$$

$$V_{a(av)} = \frac{325.2}{\pi}(1 + cos45°)$$

$$V_{a(av)} = 176.78\ \text{V}$$

$E_a = K_e \varphi n = 0.62 \times 175 \times 10^{-3} \times 1300 = 141.05$V

$V_t = V_{a(av)} = E_a + I_a R_a$

$$I_a = \frac{V_{a(av)} - E_a}{R_a} = \frac{176.78 - 141.05}{0.25} = 142.95\ \text{A}$$

$T_d = 6.2 \times 142.95 \times 175 \times 10^{-3} = 155.1$ Nm

Example 13.5

A single-phase full converter of Fig.13.8 is used to control the speed of small separately-excited d.c. motor rated at 7.5 kW, 230 V, 1500 rpm. The converter is connected to a single-phase 230 V, 50 Hz supply. The armature resistance is R_a = 0.50 Ω and the armature circuit inductance is L_a = 10 mH. The motor voltage constant is $K_e \Phi$ = 0.07 V/rpm. With the converter operates as a rectifier, the d.c. motor runs at 1200 rpm and carries an armature current of 35 A. Assume that the motor current is continuous, determine:

(a) The firing angle α.
(b) The power delivered to the motor.
(c) The power factor of the supply.

Solution

(a) The back *emf* of the motor at 1200 rpm

$E_a = k_e \varnothing n = 0.07 \times 1200 = 84$ V

The average armature voltage is

$V_{a(av)} = E_a + I_a R_a$

$= 84 + 35 \times 0.5 = 101.5$ V.

For the full-wave full-converter:

$$V_{a(av)} = \frac{2V_m}{\pi}\cos\alpha = \frac{2 \times \sqrt{2} \times 230}{\pi}\cos\alpha = 101.5 \text{ V}$$

.

$$\cos\alpha = \frac{101.5\,\pi}{2\sqrt{2} \times 230} = 0.489 \qquad \text{or} \qquad \alpha = 60.65°$$

(b) The average power: $P = V_{a(av)}\, I_{a(av)} = 101.5 \times 35 = 3552.5$ W.

(c) The supply current has a square wave with amplitude $I_{a(av)} = 35$A as shown in the figure below.

$$I_s = \sqrt{\frac{1}{\pi}\int_0^{\pi} (i_a)^2 d\omega t} = I_a = 35 \text{ A}$$

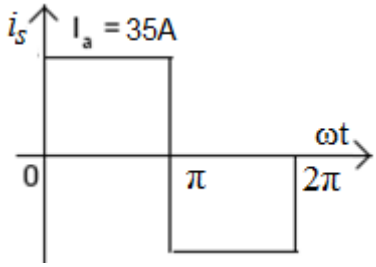

The supply VA = $I_s V_s$ =230 × 35 = 8050

$$\text{power factor} = \frac{\text{Active power (W)}}{\text{apparent power (VA)}} = \frac{3552.5}{8050} = 0.441$$

Example 13.6

A single-phase semiconverter, shown in Fig.13.4, is used to control the speed of small separately-excited d.c. motor rated at 4.5 kW, 220 V, 1500 rpm. The converter is connected to a single-phase 220 V, 50 Hz supply. The armature resistance is R_a = 0.50 Ω and the armature circuit inductance is L_a = 10 mH. The motor voltage constant is $Ke\,\Phi$ = 0.1 V/ rpm. With the converter operates as a rectifier, the d.c. motor runs at 1200 rpm and carries an armature current of 16 A. Assume that the motor current is continuous and ripple-free, determine:

(a) The firing angle α.
(b) The power delivered to the motor.
(c) The supply power factor.

Solution

(a) The back *emf* of the motor at 1200 rpm

$E_a = k_e \Ø\, n$

= 0.1 × 1200 = 120 V.

$V_{a(av)} = E_a + I_{a(av)}\ R_a$

$= 120 + 16\ \times 0.5 = 120 + 8 = 128\text{V}.$

For half-controlled (semiconverter) rectifier:

$$V_{a(av)} = \frac{V_m}{\pi}(1 + \cos\alpha) = \frac{220\ \times\sqrt{2}}{\pi}(1 + \cos\alpha) = 128V$$

$\cos\ \alpha = 1.292 - 1.0 = 0.292.$

$\alpha = 73.0^{\circ}$

(b) $P = V_a\, I_a = 128 \times 16 = 2048$ W.

(c) The supply current is shown in the figure below

$$I_{s(rms)} = \sqrt{\frac{1}{\pi}\int_{\alpha}^{\pi}(I_{a(av)})^2 d\omega t}$$

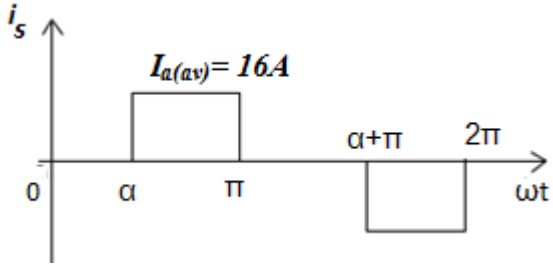

$$= \sqrt{\frac{(I_{a(av)})^2}{\pi}\ [\omega t]_{\alpha}^{\pi}}$$

$$= I_a\sqrt{\frac{\pi - \alpha}{\pi}} = 16 \times \sqrt{\frac{\pi - [73 \times \frac{\pi}{180}]}{\pi}} = 12.33\text{A}$$

The supply VA = 220 × 12.33 = 2712.91

$$\therefore\ PF = \frac{\text{W}}{\text{VA}} = \frac{2048}{2712.91} = 0.7549$$

Example 13.7

The speed of 10 hp, 230 V, 1200 rpm separately-excited d.c. motor is controlled by single-phase fully-controlled full-wave rectifier bridge. The rated armature current is 38 A, R_a = 0.3 Ω, the a.c. supply voltage is 260V. The motor voltage constant is $Ke\Phi$ = 0.182V/rpm. Assume sufficient inductance is present in the armature circuit to make I_a continuous and ripple-free:

(a) For α = 30° and rated motor current calculate,
(i) Motor torque (ii) Motor speed (iii) Supply power factor
(b) The polarity of the armature *emf* is reversed say by reversing the field excitation, calculate:
(i) the firing angle to keep the motor current at its rated value.
(ii) the power fed back to the supply.

Solution

(a) For α = 30° ,

(i) Motor torque is $T = k_e \varnothing I_a$

$K_e \varnothing = 0.182$ V/ rpm

$$= \frac{0.182}{2\pi} \times 60 = 1.74\,\text{V.s/rad} \quad (K_T \emptyset = 9.55 K_e \emptyset)$$

Hence $T = 1.74 \times 38 = 66.12$ Nm.

$$V_{a(av)} = \frac{2\sqrt{2}}{\pi} \times V_m \cos\alpha = \frac{2\sqrt{2} \times 260}{\pi} \cos 30° = 202.82\ \text{V}$$

(ii) $E_a = V_{av} - I_a R_a = 202.82 - 38 \times 0.3 = 191.42$ V.

$$\text{Since } E_a = K_e \emptyset n \quad \rightarrow n = \frac{E_a}{\text{Ke } \emptyset} = \frac{191.42}{0.182} = 1051.8\ \text{rpm}$$

(iii) $$PF = \frac{V_{a(av)} I_a}{V_s I_a} = \frac{V_{a(av)}}{V_s} = \frac{202.82}{260} = 0.78$$

(b) (i) $E_a = -191.42$

$V_{av} = -191.42 + 38 \times 0.3 = -180.02$ V.

$$-180.02 = \frac{2\sqrt{2} \times 260}{\pi} \cos\alpha \quad \rightarrow \quad \alpha = 140.24°\,.$$

(ii) Power fed back to the supply = 180.02 × 38 = 6840.76 W.

Example 13.8

A d.c. series motor has the following parameters:

$$R_a = 3\Omega\ , \qquad R_s = 3\Omega\ , \qquad K_{af} = 0.15\ \text{H}.$$

The motor speed is controlled by a single-phase, full-wave bridge rectifier. The firing angle is set to 45˚ and the average speed is 1450 rpm. The supply a.c. voltage to the bridge is v_s = 330 sinωt volts. Assuming continuous motor current, calculate the steady-state average motor current and torque for,

(a) Fully-controlled bridge,
(b) Half-controlled bridge.

Solution

(a) For fully-controlled bridge:

For continuous current operating mode, using Eq. (13.23)

$$V_{a(av)} = \frac{2V_m}{\pi} cos\alpha = \frac{2 \times 330}{\pi} \cos 45° = 148.53\ \text{V}$$

For series motor,

$$V_{a(av)} = R_T\ I_{a(av)} + K_{af} I_{a(av)}\ \omega_{m(av)}$$

$$148.53 = (3+3) \times I_{a(av)} + 0.15 \times\ I_{a(av)} \times \frac{2\pi \times 1450}{60}$$

$$\therefore\ I_{a(av)} = 5.16\ \text{A}$$

From Eq. (13.22) $\qquad T_{av} = K_{af} {I_{a(av)}}^2 = 0.15 \times (5.16)^2 = 4\ \text{Nm}$

(b) For half-controlled bridge,

$$V_{a(av)} = \frac{V_m}{\pi}(1 + cos\alpha) = \frac{330}{\pi}(1 + \cos 45°) = 179.3\ \text{V}$$

$$179.3 = (3+3) \times I_{a(av)} + 0.15 \times\ I_{a(av)} \times \frac{2\pi \times 1450}{60}$$

$$\therefore\ I_{a(av)} = 6.23\ \text{A}$$

From Eq. (13.22) $\qquad T_{av} = K_{af} {I_{a(av)}}^2 = 0.15 \times (6.23)^2 = 5.82\ \text{Nm}$

13.2.4 Single-Phase Dual Converter Drives

In some industrial applications, d.c. motor may require to be operated in four quadrants without a switching changeover. In this case, duplication of power electronics converters is used. Fig.13.11 shows a simple dual converter drive circuit diagram which consists of two single-phase full bridge converters connected in inverse-parallel supplying a d.c motor. One bridge for one direction of motor current and the other bridge for the opposite direction of current. The controls are interlock to prevent their simultaneous operation to avoid short circuits on one another. Bridge-I provides operation in the first and fourth quadrants while bridge-II provides operation in second and third quadrants. Therefore, the dual converter is a four quadrant drive which allows four quadrant of machine operation without a switching changeover.

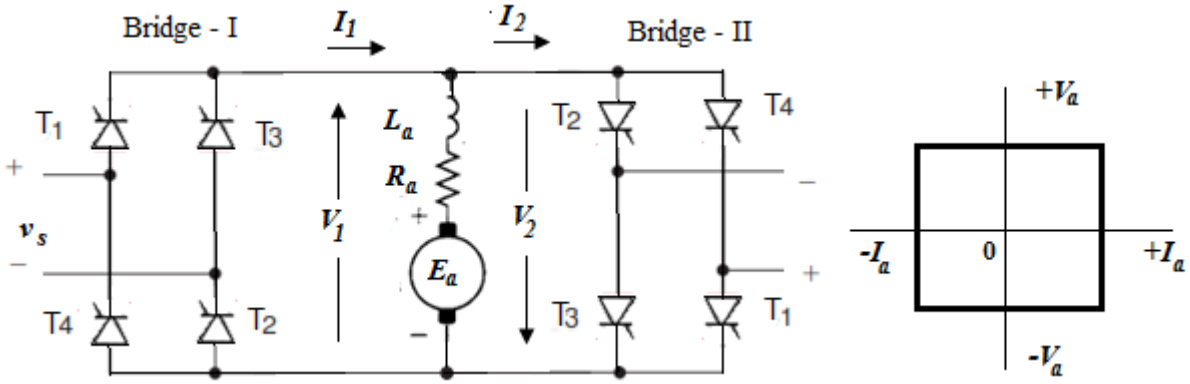

(a) (b)

Fig.13.11 Dual converter drive: (a) Circuit diagram, and (b) Quadrants of operation.

To illustrate how a speed reversal takes place, bridge-I has its firing signals removed; i_1 falls to zero and after few milliseconds delay, bridge-II is fired. This drive is employed for motors of rating up to 15 kW. On the circuit of Fig.13.13, positive voltages are shown by the arrowheads, though in the equations, these voltages may have negative values. These equations are:

Bridge – I operating:

$$V_1 = V_{a(av)\,1} = \frac{2V_m}{\pi}\cos\alpha_1 \; = V_{do}\;\cos\alpha_1 \; = E_a + I_1\;R_a \qquad (13.29)$$

Bridge – II operating:

$$V_2 = V_{a(av)\,2} = -\left(\frac{2V_m}{\pi}\cos\alpha_2\right) = \; V_{do}\;\cos\alpha_2 = E_a - I_1\;R_a \qquad (13.30)$$

where

$$V_{do} = \frac{2V_m}{\pi}$$

Which is the output voltage of the converter when α = 0˚.

Equations (13.29) and (13. 30) are shown as straight lines on Fig.13.12, the intersection of the machine and bridge characteristics giving the operating points.

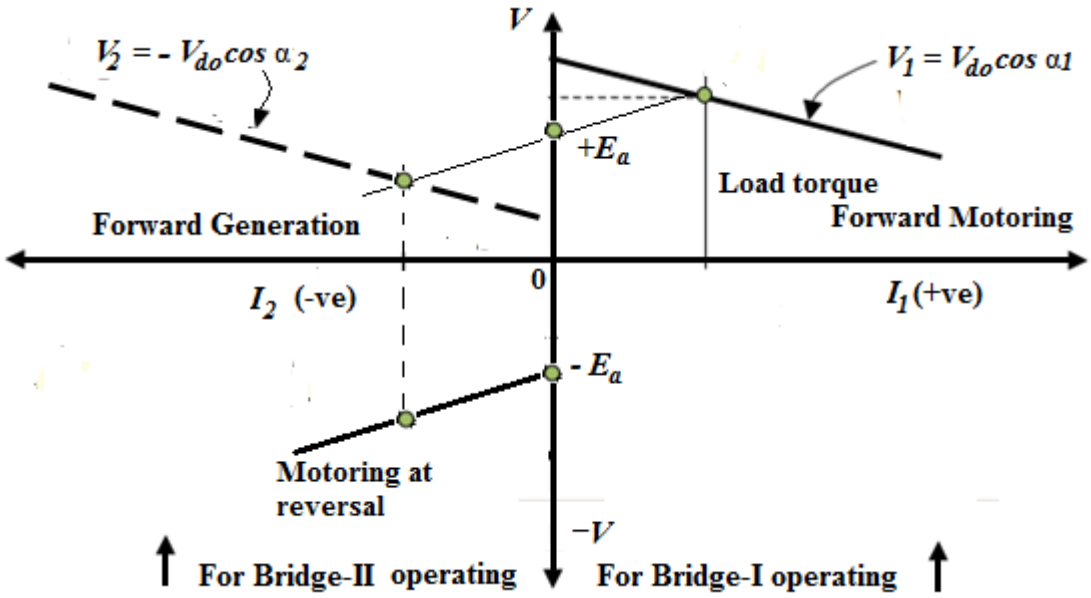

Fig.13.12 Dual converter.

Example 13.9

A d.c. separately-excited motor rated at 10 kW, 200 V is to be controlled by dual converter. The armature circuit resistance is 0.2 Ω and the machine constant $K_e\emptyset$ is 0.35 V/ rpm. For the following conditions, determine the firing angles of the converter, the back *emf* and the machine speed given that for the converter system V_{do} = 250 V. Neglect any losses in the converter circuit.

(a) Machine operates in a forward motoring mode at rated current and with terminal voltage of 200 V.

(b) Machine operates at forward generation mode at rated current and with terminal voltage of 200 V.

Solution

(a) For the motoring case,

$$V = V_{do} \cos\alpha \;\rightarrow\; 200 = 250\cos\alpha \;\rightarrow\; \cos\alpha = \frac{200}{250} = 0.8$$

$$\therefore\ \alpha = cos^{-1}(0.8) = 36.8°$$

The rated current of the machine I_a = 10000 / 200 = 50 A.

$$V = E_a + I_a R_a \;\rightarrow\; 200 = E_a + 50 \times 0.2$$

$$\therefore\quad E_a = 200 - 10 = 190\ \text{V}$$

The speed of the motor can be calculated as,

$$E_a = K_e \emptyset\, n \;\rightarrow\; n = \frac{E_a}{K_e \emptyset} = \frac{190}{0.35} = 542.85\ \text{rpm}$$

(b) For generating mode,

$$-V = V_{do} \cos\alpha \;\rightarrow\; -200 = 250\cos\alpha$$

$$\therefore\ \alpha = cos^{-1}(-0.8) = 143.13°$$

$$E_a = V + I_a R_a \;\rightarrow\; E_a = 200 + 50 \times 0.2 = 210\ \text{V}$$

$$E_a = K_e \emptyset\, n \;\rightarrow\; n = \frac{E_a}{K_e \emptyset} = \frac{210}{0.35} = 600\ \text{rpm}$$

13.3 THREE-PHASE DC DRIVES

Three-phase converters are commonly used in adjustable speed drives from about 15 kW up to several thousand kilowatts ratings. The output voltage of a three-phase converter has less ripple contents than the single-phase converter, and therefore, the armature current will be smoother and mostly continuous.

The theory and operation of all types of the three-phase converters was fully discussed in chapter Three-Part I, for the case of passive impedance load. However, three-phase converters could be half-wave, full-wave fully-controlled, full-wave half-controlled (semiconverter) and dual converter when reversible armature current is needed. The three-phase half-wave circuit is only of theoretical importance and is generally not used in industrial applications because of the d.c. components inherent in its line currents. For medium size motors, in the range 15 – 120 kW, either the full-converters or semiconverter are used.

13.3.1 Three-Phase Half-Wave (or p = *3*) Converter

In the three-phase half-wave converter, the motor load is connected between the converter positive terminal (cathodes of all thyristors) and the supply neutral as shown in Fig.13.13 .The firing angle α is also defined to be zero from the zero crossings of the input voltages. This converter is used for motor ratings from 10 to 50 hp and it is rarely used in practice because of the d.c. component in the line current. Waveforms of the armature (load) voltage and current are shown in Fig.13.14.

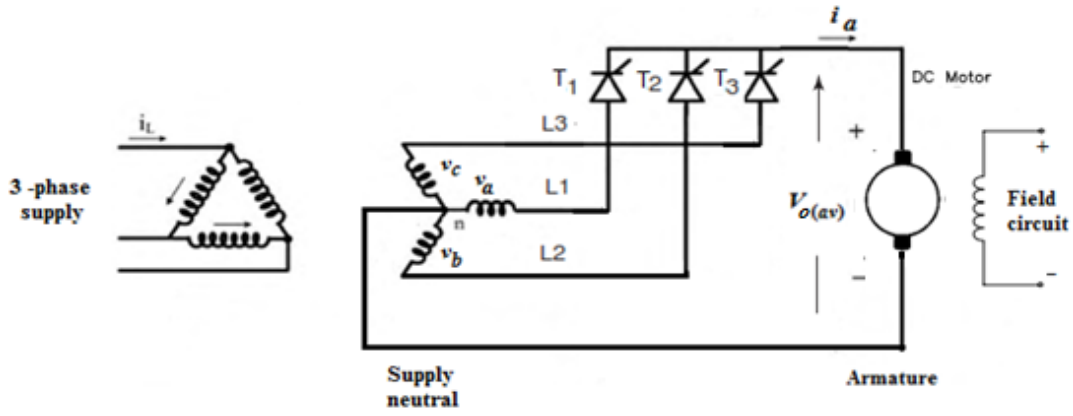

Fig.13.13 Three-phase, half-wave controlled converter with motor load.

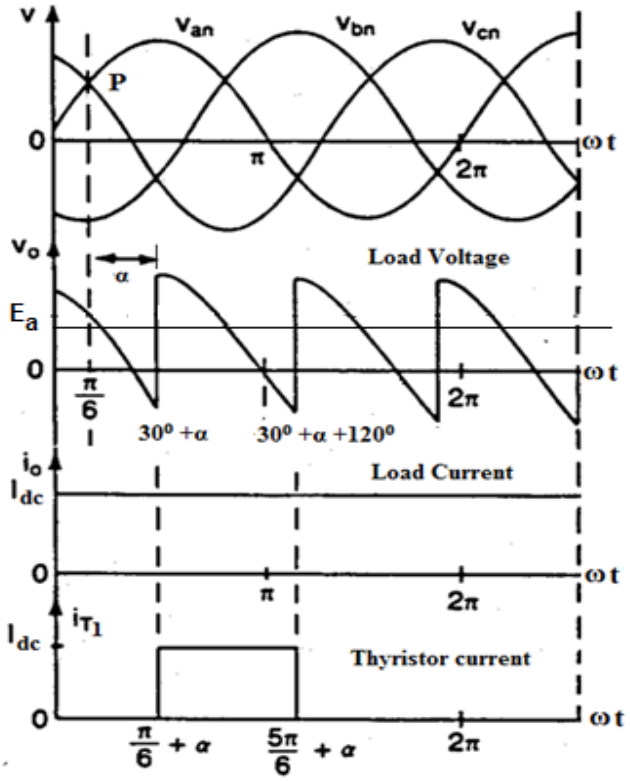

Fig.13.14.Wave forms for the three-phase half-wave converter d.c. drive.

To find the average value of the output d.c. voltage of the converter, let the transformer secondary phase to neutral voltages be,

$$v_{an} = V_m \, sin\omega t$$
$$v_{ab} = V_m \sin(\omega t - 120°)$$
$$v_{ab} = V_m \sin(\omega t - 240°)$$

Assuming continuous current conduction, the average output voltage is,

$$V_{o(av)} = \frac{1}{\frac{2\pi}{3}} \int_{30°+\alpha}^{30°+\alpha+120°} V_m \, sin\omega t \, d\omega t = \frac{3V_m}{2\pi} \, [-cos\omega t] \, \begin{matrix} 150° + \alpha \\ 30° + \alpha \end{matrix}$$

$$V_{o(av)} = \frac{3V_m}{2\pi} [-(\cos(150° + \alpha) - \cos(30° + \alpha))]$$

$$V_{o(av)} = \frac{3\sqrt{3}V_m}{2\pi} cos\alpha \qquad (13.31)$$

where V_m is the peak of the supply line-neutral voltage.

A firing angle of zero degree produces the maximum output d.c. voltage for all ac-to-dc converter circuits. For continuous current conduction, each thyristor carries current for 120˚, followed by 240˚ of non-conduction. The firing angle α can be varied in the range of ±180°. For α > 90°, the output d.c. voltage becomes negative, whilst the motor current is positive and continuous. This implies operation of the converter in the fourth quadrant of the *V-I* plane as shown in Fig.13.15 where the converter operates in the inversion mode. In this mode of operation the motor supplies power to the a.c. source through the converter steadily. This mode of operation is called regenerative conversion. For example, an overhauling motor can supply its energy to the a.c. mains in this way. However, in the case of the overhauling motor, controlled braking is thus possible.

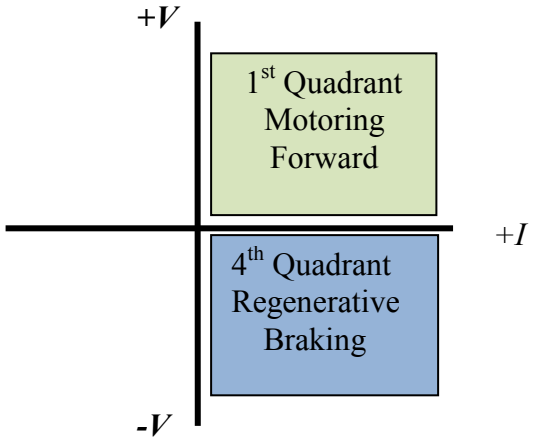

Fig.13.15 Two-quadrant operation of three-phase half-wave converter drive.

Example 13.10

A 100 hp, 1750 rpm, d.c. shunt motor has an armature inductance of 1.15 mH, a resistance of 0.0155 Ω and an armature voltage constant of 1.3V.s/rad. The motor is operated from a three-phase half-wave controlled-rectifier at rated armature current of 35 A. Find the firing angle α, assuming that the supply voltage is 400 V and the motor speed is 1750 rpm. Consider the thyristors to have a forward voltage drop of 1.5 Volt and assume continuous conduction.

Solution

Speed of the motor in rpm: $n = 1750$

Change the speed from rpm to rad/s:

$$\omega = \frac{2\,\pi n}{60} = \frac{2\,\pi}{60} \times 1750 = 183.25 \text{ rad/s}$$

Armature voltage constant $K\emptyset = 1.3$

$$\therefore \mathrm{E_a} = K\emptyset\omega = 1.3 \times 183.25 \text{ V}$$

$$V_m = \sqrt{2} \times \frac{400}{\sqrt{3}} = 326.2 \text{ V}$$

$$V_{o(av)} = \frac{3\sqrt{3}V_m}{2\pi}cos\alpha = \frac{3\sqrt{3} \times 326.2}{2\pi}cos\alpha = 270.08 \cos \alpha$$

$$V_{o(av)} = E_a + I_a\ R_a + V_T \leftarrow \text{Thyristor drop}$$

$$270.08 \cos \alpha = 238.22 + 15.5 \times 10^{-3} \times 35 + 1.5 = 240.26$$

$$\therefore \alpha = \cos^{-1}\frac{240.26}{270.08} = \cos^{-1} 0.8895 = 27.2°$$

13.3.2 Three-Phase Semiconverter Drive

The three-phase semiconverter is a one-quadrant drive. Its circuit includes a freewheeling diode D_{FW} to maintaining continuous load current. It uses three thyristors and three diodes; hence a cost advantage is obtained compared with the full-converter. The circuit diagram for a separately-excited d.c. motor supplied from a three-phase a.c. supply through a three-phase semiconverter is shown in Fig.13.16. This converter

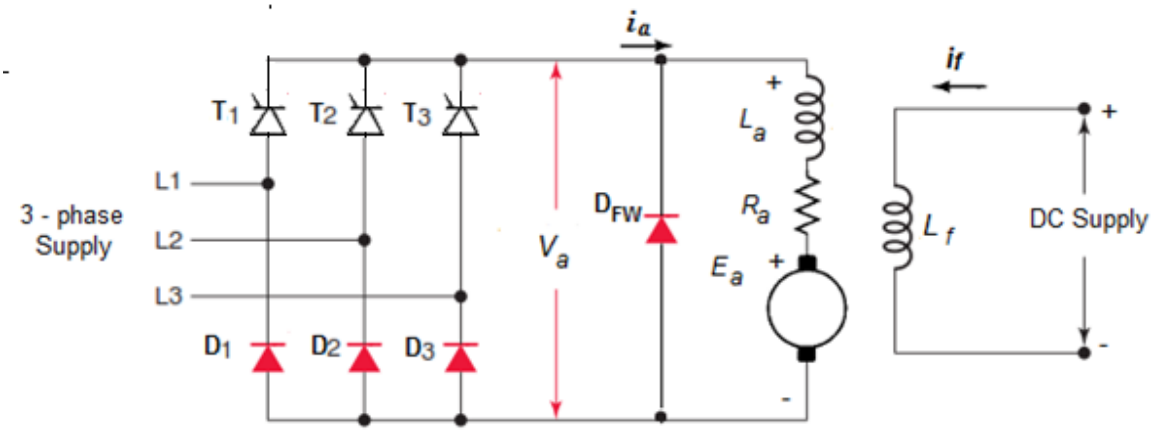

Fig.13.16 Three-phase semiconverter drive.

is used for motor ratings from 15 to 150 hp. The field converter may be single-phase or three-phase semiconverter with firing angle of α_f.

Assuming continuous current operation, the average value of the armature voltage at the motor terminals is a contribution from the upper half-bridge plus a contribution from the uncontrolled lower bridge. Hence for all firing angles we can write:

$$V_{o(av)} = \frac{3\sqrt{3}}{2\pi} V_m \cos\alpha + \frac{3\sqrt{3}}{2\pi} V_m$$

$$= \frac{3\sqrt{3}}{2\pi} V_m(1 + \cos\alpha) \qquad (13.32)$$

The average armature current is:

$$I_{a(va)} = \frac{V_{a(av)} - E_a}{R_a} \qquad (13.33)$$

$$= \frac{3\sqrt{3}V_m}{2\pi R_a}(1 + cos\alpha) - \frac{E_a}{R_a} \qquad (13.34)$$

For discontinuous current operation, the above equations are not valid.

Features:

- Since only three thyristors are used, the circuit is not expensive and a simple control circuitry is required.
- Dynamic braking can be performed by switching armature connection to an external resistance.
- Operation is in the first quadrant only (Fig.13.17). However, bi-directional rotation can be obtained by reversing field current or armature terminals when the motor has been stopped.

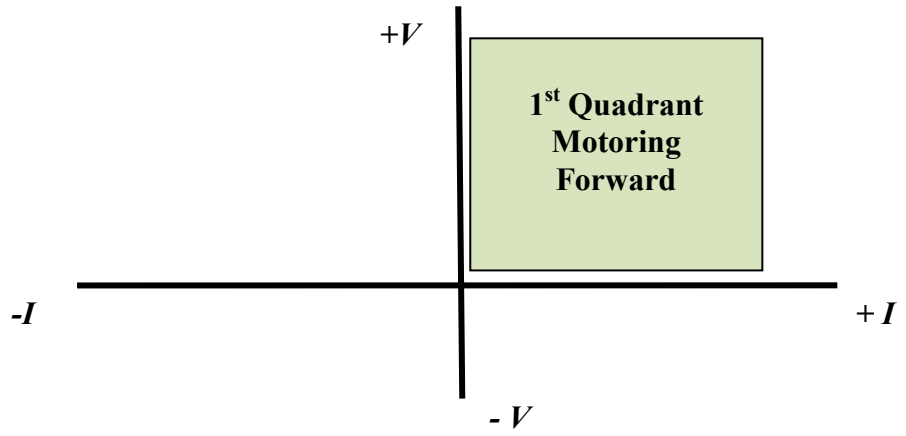

Fig.13.17 One-quadrant operation of the three-phase semiconverter drive.

Example-13.11

A Three-phase half-controlled thyristor bridge with 400 V, three-phase, 50 Hz supply is feeding a separately-excited d.c. motor. Armature resistance is 0.2 Ω, armature rated current is 100 A and back *emf* constant is 0.25 V/rpm. Determine the no-load speed if the no-load armature current is 5 A and firing angle is 45˚. Also determine the firing angle to obtain a speed of 1500 rpm at rated current.

Solution

Armature voltage at no-load,

$$V_{o(o)} = \frac{3\sqrt{3}}{2\pi} V_m(1+\cos\alpha)$$

$$= \frac{3\sqrt{3}}{2\pi} \times \frac{400\sqrt{2}}{\sqrt{3}}(1+cos45°) = 461 \text{ V}$$

Back *emf* at no-load , $E_{ao} = V_{a(o)} - I_{ao}R_a = 461 - 5 \times 0.2 = 460$ V

Speed at no-load

$$n_o = \frac{E_{ao}}{K_e\emptyset} = \frac{460}{0.25} = 1840 \text{ rpm}$$

Back *emf* developed at speed of 1500 rpm

$$E_{ao} = 1500 \times 0.25 = 375 \text{ V}$$

Armature voltage will be:

$$V_o = E_a + I_a R_a = 375 + 100 \times 0.2 = 395 \text{ V}$$

Also

$$V_o = \frac{3\sqrt{3}}{2\pi} V_m (1 + \cos\alpha)$$

$$395 = \frac{3\sqrt{3}}{2\pi} \times \frac{400\sqrt{2}}{\sqrt{3}} (1 + \cos\alpha)$$

$$\alpha = 62.45°$$

13.3.3 Three-Phase Full-Converter Drive

The circuit diagram for a separately-excited d.c. motor supplied from a three-phase a.c. supply through a three-phase full-converter is shown in Fig.13.18.

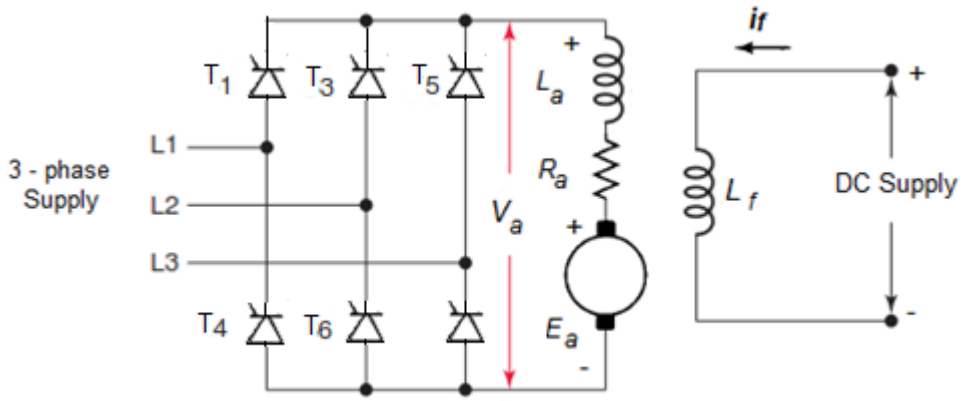

Fig.13.18 Three-phase full-converter with a separately-excited d.c. motor load.

If the motor armature inductance is large and the firing angle is small then the armature current is likely to be continuous. However, with small armature inductance and large firing angles the armature current may become discontinuous particularly when the back *emf* is relatively high.

- For continuous current operation, the armature voltage has an average value which is the same as that given in Eq.(3.40) in Chapter Three - Part I , repeated here,

$$V_{a(av)} = \frac{3\sqrt{3}}{\pi} V_m \cos\alpha \qquad (13.35)$$

Thus, the average armature current is:

$$I_{a(va)} = \frac{V_{a(av)} - E_a}{R_a} \tag{13.36}$$

$$= \frac{3\sqrt{3}V_m}{\pi R_a}\cos\alpha \; - \frac{E_a}{R_a} \tag{13.37}$$

- For discontinuous current operation of the full-converter, the waveforms of the voltage and currents are shown in Fig.13.19.

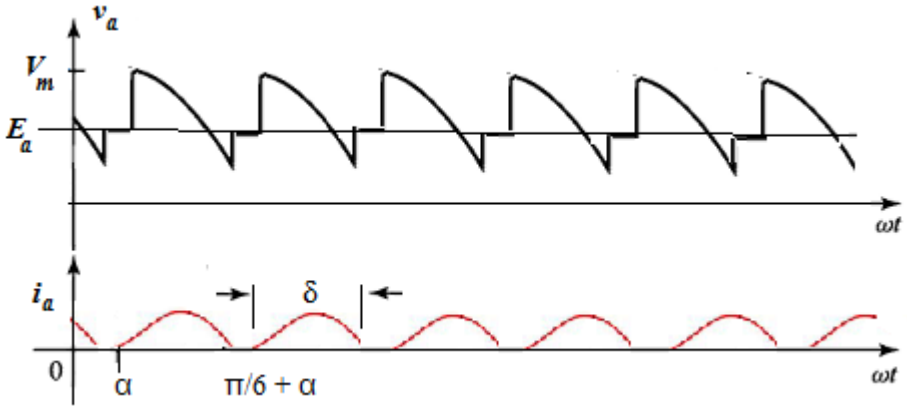

Fig.13.19 Discontinuous current operation waveforms of the full-converter.

The differential equations describing the motor system, during the period the thyristors conduct, are

$$v_a = i_a R_a + L_a \frac{di_a}{dt} + e_a \tag{13.38}$$

$$\sqrt{3}V_m \sin(\omega t + 30°) = i_a R_a + L_a \frac{di_a}{dt} + K\emptyset\omega_m$$

$$T_m = K\emptyset\, I_a = J \frac{d\omega_m}{dt} + B.\omega_m + T_L \tag{13.39}$$

If it is assumed that the inertia of the rotating system is large then speed fluctuations will be negligible. If each term of v_a is integrated from α to (α + π/6) and then divided by π/3, the instantaneous voltage, current and speed will be converted to their respective average values,

$$V_{a(av)} = \frac{3}{\pi}\int_{\alpha}^{\alpha+\pi/6} \sqrt{3}V_m \,(\sin\omega t + 30°)\; d\omega t$$

$$= \frac{1}{\pi}\int_{\alpha}^{\alpha+\pi/6} L_a \frac{di_a}{dt}\, d\omega t + \frac{1}{\pi}\int_{\alpha}^{\alpha+\pi/6} R_a\, i_a\, d\omega t + \frac{1}{\pi}\int_{\alpha}^{\alpha+\pi/6} K\emptyset\, \omega_m\, d\omega t$$

Thus

$$V_{a(av)} = I_{a(av)} R_a + K\emptyset\, \omega_{m(av)} \tag{13.40}$$

where

$$V_{a(av)} = \frac{3\sqrt{3}V_m}{\pi}[\cos(\alpha + 30°) - \cos(\alpha + 90°)] \tag{13.41}$$

and the average voltage across L_a is zero.

Similarly,

$$T_{m(av)} = K\emptyset\, I_{a(av)} = B \cdot \omega_{m(av)} + T_L \tag{13.42}$$

13.3.4 Three-Phase Dual Converter Drive

Four-quadrant operation of a medium and large size d.c. motor drive (200-2000 hp) can be obtained by the three-phase dual converter shown in Fig.13.20. The average motor voltage is required to be equal for both converters, which required that the firing angles of the two sets of the thyristors should sum to 180˚.

The armature voltage supplied by converter-1 (for continuous current operation) is

Bridge – I operating:

$$V_1 = V_{a(av)1} = \frac{3\sqrt{3}V_m}{\pi}\cos\alpha_1$$

$$= V_{do}\cos\alpha_1 = E_a + I_1 R_a \tag{13.43}$$

Bridge – II operating:

$$V_2 = V_{a(av)2} = -\left(\frac{3\sqrt{3}V_m}{\pi}\cos\alpha_2\right)$$

$$= V_{do}\cos\alpha_2 = E_a - I_1 R_a \tag{13.44}$$

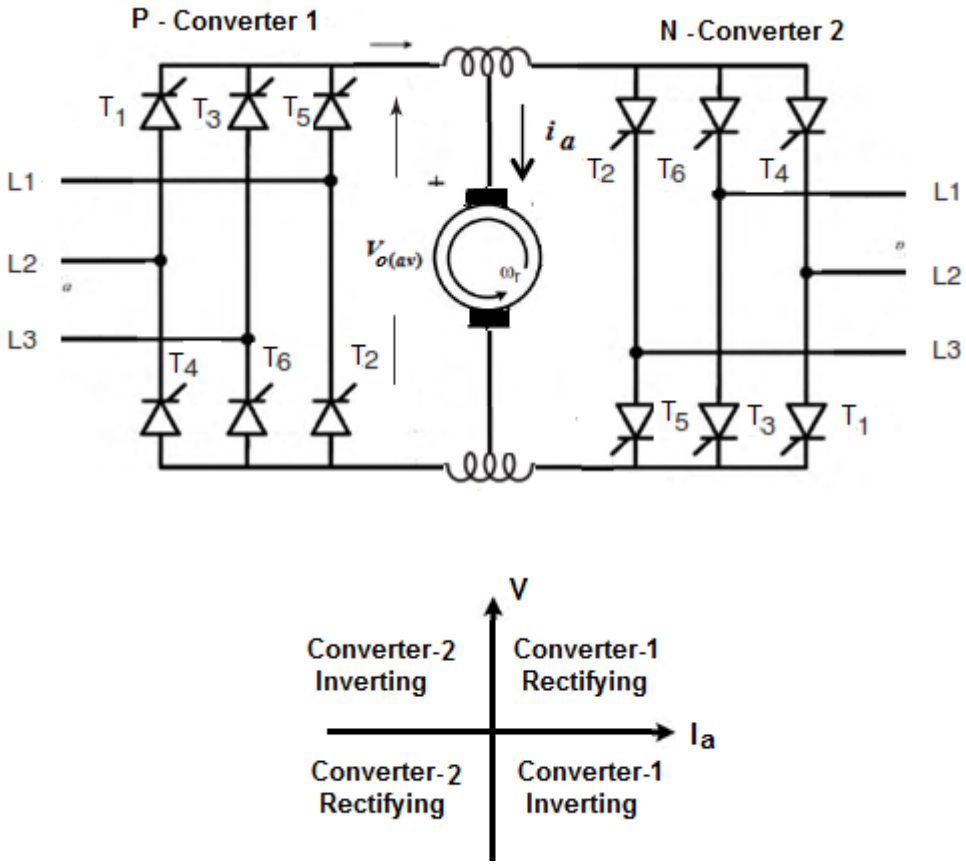

Fig.13.20 Four-quadrant three-phase d.c. drive.

where $V_{do} = \dfrac{3\sqrt{3}V_m}{\pi}$

and $\alpha_2 = \pi - \alpha_1$.

Two modes of operation can be achieved with this circuit:

(a) Circulating current operating mode:

Here, instantaneous values of circulating current are limited by use of reactors and mean level is controlled by current loop. Circulating current may be constant giving linear characteristic or it may be reduced to zero giving higher gain portion of overall characteristic.

Advantage: Continuous bridge current maintain armature current at all times, no discontinuity occurs.

Disadvantage: Presence of circulating current reduces efficiency.

(b) Circulating current-free operation mode:

In this mode only one converter operates at a time. Logic used to prevent the two bridges being turn on at the same time. Reactors or inductors used to maintain continuous current down to acceptable low levels. Discontinuity occurs at zero and also a time delay (*ms*) introduced at the zero current level.

Advantage: Higher efficiency than circulating current schemes, hence used more widely.

Disadvantage: Dead time, discontinuity in zero current regions.

Example 13.12

A three-phase full-converter, shown in Fig.13.21, is used to control the speed of a separately-excited d.c. motor rated at 100 kW, 600 V, 2000 rpm. The converter is connected to a three-phase 400 V, 50 Hz supply.

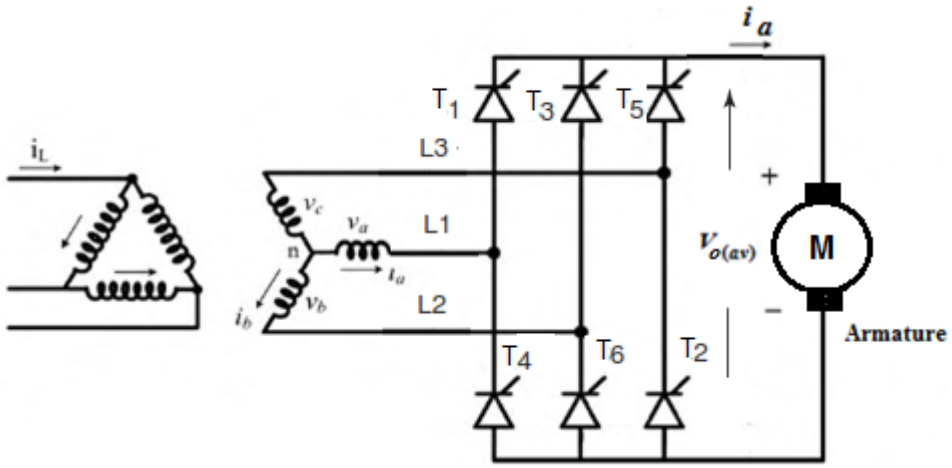

Fig.13.21 Three-phase full-converter d.c. drive.

The armature resistance R_a = 0.051 Ω and the armature circuit inductance is L_a = 10mH. The motor voltage constant is $K_e\Phi$ = 0.25 V/rpm. The rated armature current is 100 A and the no-load current is 10 A.
With the converter operates as a rectifier, and assuming that the motor current is continuous and ripple-free, determine:

(a)The no load speed when the firing angles: $\alpha = 0^0$ and $\alpha = 60^0$.
(b)The firing angle to obtain the rated speed of 2000 rpm at rated motor current.

Solution

(a) At no-load condition

$$V_m = \frac{400}{\sqrt{3}} \times \sqrt{2} = 325.22 \text{ V}$$

Let the converter output voltage = $V_{o(av)}$ = armature terminal voltage V_a :

$$V_{o(av)} = \frac{3\sqrt{3}}{\pi} V_m \cos\alpha$$

$$V_{o(av)} = \frac{3\sqrt{3}}{\pi} \times 325.22 \cos\alpha$$

$V_{o(av)} = 538 \cos\alpha$

For $\alpha = 0^0$, $\longrightarrow$ $V_{o(av)} = 538$ V

$E_a = V_{o(av)} - I_a R_a = 538 - 10 \times 0.051 = 537.5$ V

No-load speed:

since $E_a = K_e \varphi n$

Hence

$$n_o = \frac{E_a}{K_e \emptyset} = \frac{537.5}{0.25} = 2145 \text{ rpm}$$

For $\alpha = 60^0$:

$V_{o(av)} = 538 \cos 60^0 = 269$ V

$E_a = V_{a(av)} - I_a R_a = 269 - 10 \times 0.051 = 268.4$ V

$$n_o = \frac{E_a}{K_e \emptyset} = \frac{268.41}{0.25} = 1073.64 \text{ rpm}$$

(b) At full-load condition

$E_a = K_e \varphi n = 0.25 \times 2000 = 500$ V

$V_t = E_a + I_a R_a = 500 + 100 \times 0.051 = 505$ V

$505 = 538 \cos\alpha$

Hence $\alpha = 20.14^0$

PROBLEMS

13.1 A separately-excited d.c. motor is supplied via a half-control full-wave single-phase rectifier bridge. The supply voltage is 240 V(*rms*), the thyristors are fired at angle of 110 ° and the armature current continues for 50 ° beyond the voltage zero. Determined the motor speed for a torque of 1.8 Nm, given the motor torque characteristics is 1.0 Nm /A and its armature resistance is 6 Ω. Neglect all rectifier losses.

[Ans: 864 rpm.]

13.2 The speed of an 8 kW, 220V, 1250 rpm separately-excited d.c. motor is controlled by a single-phase full converter as shown in Fig.13.22. The rated armature current is 30 A. The armature resistance is R_a = 0.25 Ω and armature inductance is L_a = 15 mH. The a.c. supply voltage is 300 V. The motor voltage constant is $K_e \varphi$ = 0.20 V/rpm. Assume that motor current is continuous and ripple free. For firing angle α = 60° and rated motor current, determine: (a) Speed of the motor, (b) Motor torque, and (c) The input power to the motor.

[Ans : (a) 637.5 rpm , (b) 57.33 Nm , (c) 4050 W]

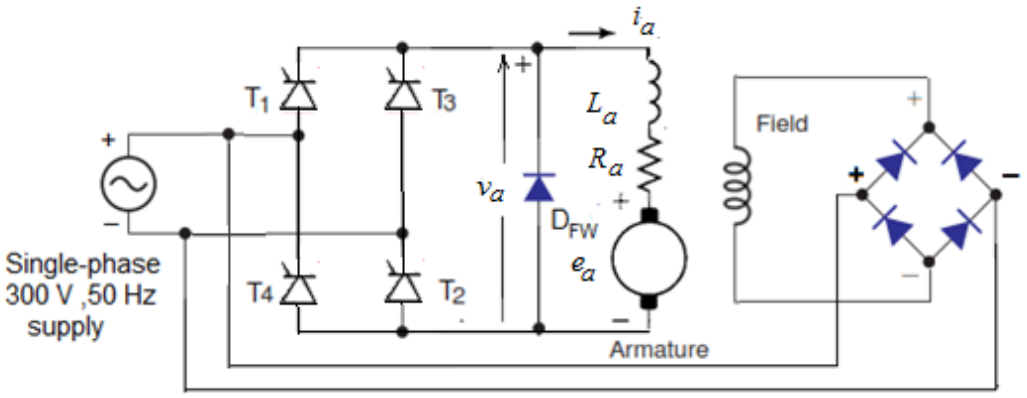

Fig.13.22.

13.3 A single-phase source rated at 230 V, 50 Hz supplies power to a shunt-excited d.c. motor via a full-wave fully-controlled rectifier. The armature resistance R_a = 1.5 Ω and the armature inductance L_a = 25 mH. The motor voltage constant $K_e \phi$ = 0.182 V/rpm. At certain speed of operation the back *emf* is 85.6 V. When the thyristor firing angle is 45°, calculate the average value of the armature current and the power delivered by the motor. Assume that sufficient inductance is present in the armature circuit to make I_a continuous and ripple free.

[Ans: 40.56 A, 3472 W]

13.4 A separately-excited d.c. motor is rated at 8 kW, 230 V, 1200 rpm is supplied with power from a 6-pulse three-phase fully-controlled bridge rectifier. The armature circuit resistance is 0.50 Ω and the machine constant $K\emptyset$ is 1.5 V.s/rad. The motor is assumed to operate in continuous current mode, calculate for firing angles of $\alpha = 0^\circ$ and $\alpha = 30^\circ$, (a) the motor speed in rpm , (b) the power factor , and (c) the efficiency of the system. Neglect any losses in the converter circuit and assume that the load torque remains constant for each case.

[Ans : For $\alpha = 0^\circ$: (a) 1181.14 rpm, (b) PF = 0.80 , (c) η = 89.5%.
For $\alpha = 30^\circ$: (a) 1023.6 rpm, (b) PF = 0.792, (c) η = 88.16%.]

13.5 A d.c. shunt motor operating from a single-phase half control bridge at a speed of 1450 rpm has an input voltage $v_s = 330 \sin\omega t$ and a back *emf* of 75 V. The SCRs are fired symmetrically at ($\alpha = \pi/4$) in every half cycle and the armature resistance is (5 Ω). Neglecting the armature inductance, calculate the average armature current and load torque.

[Ans: I_a = 20.32 V, T = 10.04 Nm]

13.6 A series d.c. motor is supplied from a bridge rectifier, the a.c. input of which has *rms* value of 230 V, 50 Hz. The combined armature and field resistance is 2 Ω and the field constant k'_f of the motor is 0.23 H. If the load torque is 20 Nm and the damping can be neglected, calculate the average current and speed.

[Ans: I_a = 9.33 A, n = 838.5 rpm]

*(Hint: in series motor $E_a = k'_f i\,\omega$, ω = speed (rad/s))

13.7 A 500 V, 1500 rpm d.c. motor is connected to a 400 V, three-phase, 50 Hz line using a three-phase fully-controlled bridge rectifier. The full-load armature current is 1500 A and the armature resistance is 0.05 Ω. Calculate:

(a) The required firing angle α under rated full load conditions.
(b) The firing angle required so that the motor develops its rated torque at 600 rpm.

[Ans: (a) $\alpha = 22.3^o$, $\alpha = 63^o$]

13.8 The speed of a 120 kW, 600 V, 1800 rpm, separately-excited d.c. motor is controlled by a three-phase fully-controlled full-converter (6-pulse converter) as shown in Fig.13.23. The converter is operating from a three-phase 400 V, 50 Hz supply. The rated armature current of the motor is 115 A. The motor parameters are:

R_a = 0.08 Ω , L_a = 7.5 mH , $K_e\Phi$ = 0.278 V/rpm

(a) Find the no-load speeds at firing angles α = 0°, and α = 45°. Assume that, at no-load, the armature current is 10% of the rated current and is continuous.
(b) Find the firing angle to obtain the rated speed of 1800 rpm at rated motor current.

[Ans: (a) For α = 0°, n_o = 1900 rpm. For α = 45°, n_o = 1335 rpm, (b) α = 24°]

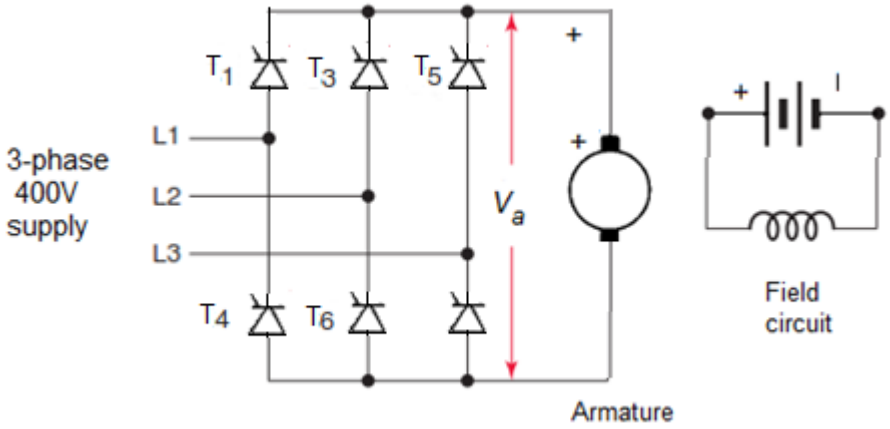

Fig.13.23.

13.9 A 300 V, 1500 rpm d.c. motor is connected to a 400V, three-phase, 50 Hz line using a three-phase fully-controlled bridge rectifier. The full-load armature current is 2000 A and the armature resistance is 0.005 Ω. Calculate:
(a) The required firing angle α under rated full load conditions.
(b) The firing angle required so that the motor develops its rated torque at 500 rpm.

[Ans: 56˚, 76˚]

13.10 A 10 kW , 300 V , 1000 rpm d.c. shunt motor has an armature resistance of 19.4×10^{-3} Ω , armature inductance of 1.1 mH , and a voltage constant of 1.38 V.s/rad. The motor is operated from a fully-controlled, three-phase rectifier. Find the firing angle α in order that the motor is operated at speed of 860 rpm , assuming that the supply voltage is 220V , consider the thyristors to have a forward voltage drop of 1.0 volt and assume continuous current operating mode. Also calculate the efficiency of the drive if the load torque is constant.

[Ans: α = 30°, η = 97 %]

13.11 A separately-excited d.c. motor rated at 10 kW, 400 V, 1000 rpm is supplied with power from a fully-controlled, three-phase bridge rectifier. The supply to the rectifier is assumed ideal and rated at 220 V, 50 Hz. The

motor has an armature resistance of 0.2 Ω and sufficient added inductance to maintain continuous armature current condition. The motor has voltage constant of 1.38 V.s. rad^{-1}, and it delivers rated power at zero firing angle. If the firing angle is retarded to 30˚ calculate the speed, power factor and efficiency of operation if the load torque remains constant.

[Ans: n = 866 rpm, PF = 0.48, η = 97.3 %]

13.12 A 600 V, 50 A d.c. separately-excited motor is fed form a three-phase half-controlled rectifier. The armature resistance of the motor is 0.1 Ω, the armature inductance is 40 mH and the machine constant $K_e \phi$ is 0.3 V/rpm. The rectifier is fed form 400 V, 50 Hz three-phase supply. It is required to calculate:

(a) The no-load speed when the firing angle is 30^o and the no-load current is 5 A.

(b) The firing angle to obtain a speed of 1600 rpm.

[Ans: (a) 1678 rpm, (b) 37.26^o]

13.13 The speed of 75 kW, 600 V, 2000 rpm separately-excited d.c. motor is controlled by a three-phase fully-controlled full-wave rectifier bridge. The rated armature current is 132 A, R_a = 0.15 Ω, and L_a = 15 mH. The converter is operated from a three-phase, 415 V, 50 Hz supply. The motor voltage constant is $K_e\Phi$ = 0.25 V/rpm. Assume sufficient inductance is present in the armature circuit to make I_a continuous and ripple-free:

(a) With the converter operates in rectifying mode, and the machine operates as a motor drawing rated current, determine the value of the firing angle α such that the motor runs at speed of 1400 rpm.

(b) With the converter operates in inverting mode, and the machine operates in regenerative braking mode with speed of 900 rpm and drawing rated current, calculate the firing angle α.

[Ans: (a) 48.72° , (b) 111.47°]

13.14 A separately-excited d.c. motor rated at 55 kW, 500 V, 3000 rpm is supplied with power from a fully-controlled, three-phase bridge rectifier. The bridge is supplied from a three-phase source rated at 400 V, 50 Hz. The motor has an armature resistance of 0.23 Ω. Series inductance is present in the armature circuit to make the current continuous. Speed adjustment is required in the range 2000-3000 rpm while delivering rated torque (at rated current). Calculate the required range of the firing angles.

(Hint: The output power of the motor = $E_a I_a = T\omega$)

[Ans: 0^o < α < 20.3^o]

13.15 A separately-excited d.c. motor rated at 30 kW, 600 V, 2000 rpm with armature resistance R_a= 0.5 Ω and inductance L_a = 30 mH. The motor driving a load whose torque is directly proportional to the speed. The speed of the motor is to be controlled from rated speed to one half speed using a three-phase, fully-controlled bridge rectifier. The rectifier is supplied from a three-phase source of 400 V, 50 Hz. Determine the range of thyristor firing angles required if an additional sufficient inductance is inserted to maintain continuous conduction. The Torque-speed characterristics of the drive is shown in Fig.13.24.

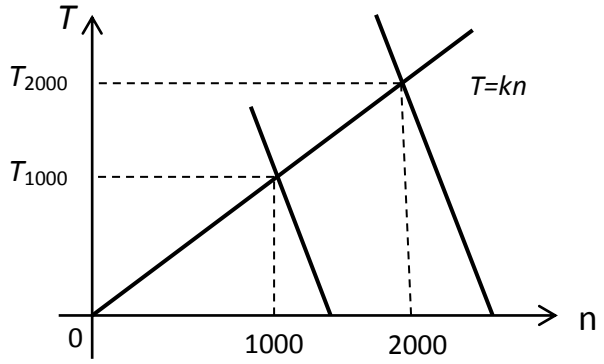

Fig.13.24 Torque-speed characteristics of the drive in problem 13.15.

[Ans : $0^o < \alpha < 69.2^o$]

CHAPTER FOURTEEN

CLOSED-LOOP VARIABLE SPEED DC DRIVES

14.1 INTRODUCTION

In many applications it is necessary to maintain the speed of electric motors constant. In general, speed tends to fall as the motor is loaded; on other hand, for a number of electric motors, it is possible to raise the speed by increasing the applied voltage. Phase controlled rectifiers are widely used in the speed control of d.c. motors, the control circuits are designed in such a way that, as loading increasing, α is made smaller thus raising the applied voltage, and hence attempting to maintain the speed constant.

DC-Drives are widely used in applications requiring adjustable speed and good regulation; Control of the speed of a d.c. motor is extensively used below and above the base (or rated) speed. The methods of control are simple and less expensive than those applicable to a.c. motors. The converters used are controlled rectifiers or choppers. If the supply is a.c. , controlled rectifiers can be used to convert a fixed a.c. voltage into a variable voltage d.c. supply. Several types of controlled rectifier circuits are available: single-phase and three-phase half-wave and full-wave. In general, the type of controlled rectifier adopted depends on the motor power:

- Up to 7.5 kW (10 hp) a single-phase a.c. bridge is customary unless the supply impedance and other users lead to unacceptable supply disturbance, where a three-phase control would be used.
- For more than 7.5 kW, the three-phase bridge converter is universally used with thyristors and diodes where non-regenerative braking is acceptable.

14.2 CLOSED-LOOP VARIABLE SPEED D.C. DRIVE

Regardless of the type of the power circuit (single or three-phase rectifier or chopper) or its mode of operation (i.e. continuous or discount-inuous current mode) the basic requirements for closed-loop variable d.c. drive is essentially the same.

Firing of an SCR switch is accomplished by a train of pulses applied to the gate. These pulses are synchronized with the a.c. supply (in case of rectifier circuits), the amplitude of the pulse is unimportant as long as it drives sufficient gate current (in case of thyristors, GTO or power transistors). The important factor is the firing angle α, since by varying α the applied voltage V_a to the motor and the speed of the driven motor are controlled. Typical closed-loop variable speed drive is shown in Fig.14.1.

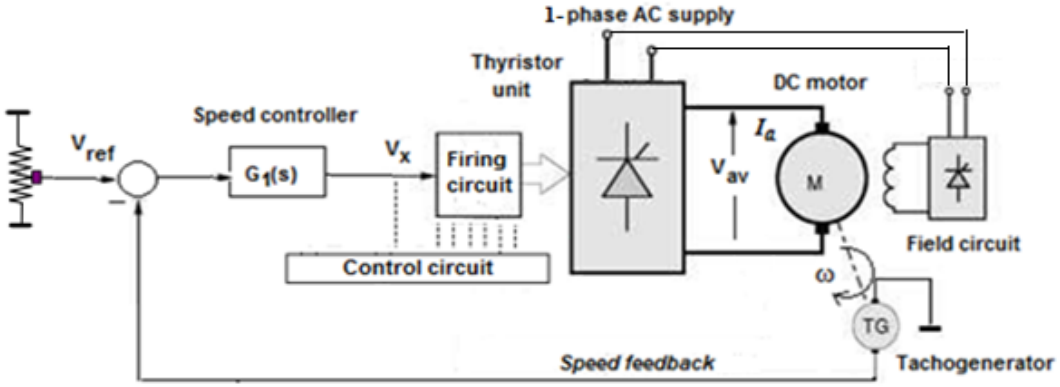

Fig.14.1 Typical closed-loop variable speed d.c. drive.

14.2.1 The Triggering (Firing) Circuit

The train of pulses is generated by triggering circuit. Several type of triggering circuits is used in practice. However, in closed-loop d.c. drive the study will be limited here to their function, which can be defined as in Fig.14.2 : The firing circuit generates a train of pulses whose delay angle α is a function of the input signal Y, which may be a voltage or current input to the firing angle control circuits shown in Fig 14.2.

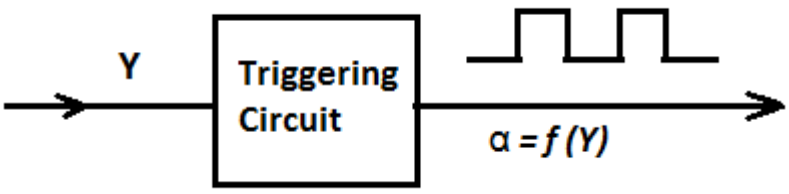

Fig.14.2 Function of the triggering circuit.

14.2.2 Control Signal and Components

The input signals to the triggering circuit, Y, determine the firing angle α and hence the speed of the driven motor. Y itself is determined, essentially by two types of signal:

(1) A reference signal, this is a voltage derived from the a.c. supply or from d.c. supply in case of choppers. It is pre-set (manually, say, by a potentiometer) at some value, and remains constant throughout the entire operation.

(2) Feedback signal (or signals), these are signals proportion to motor speed, voltage or current. Cleary, the feedback signals vary as the motor is loaded.

The signal flow and the function of various control components may be understood by referring to Fig.14.3 which shows a complete drive composes of the following basic parts:

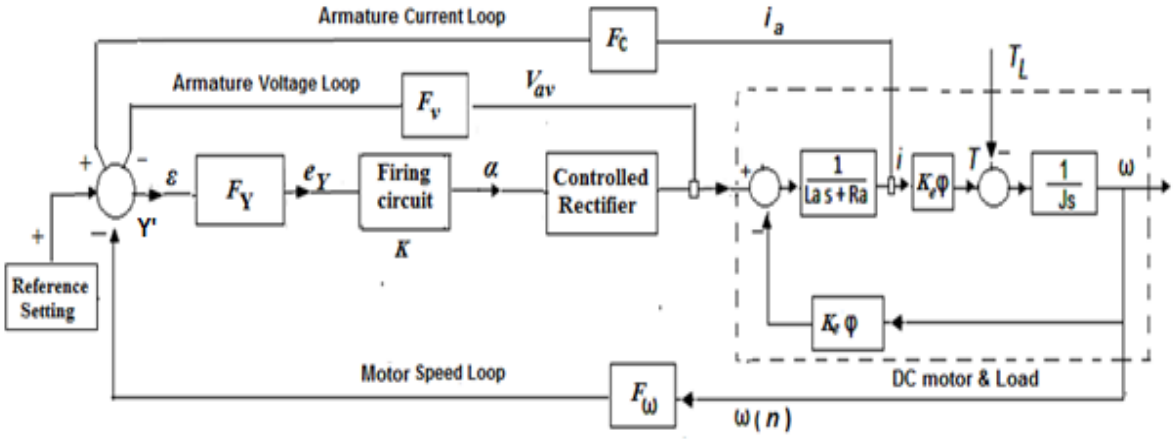

Fig.14.3 SCR control system driving a separately-excited d.c. motor (J and B are, inertia and friction of the motor and load respectively).

(a) Power section: A converter (rectifier or chopper with or without freewheeling diode).

(b) motor and load ; in this case the motor is a separately-excited d.c. motor whose main field flux is constant, the load is assumed to be only inertial (friction is neglected).

(c) Control section: This section comprises the following items,

(i) Triggering (firing) circuit.

(ii) Means for sensing n (ω), voltage V_{av} and current I_a .

(iii) Reference comparison, and signal processing circuits the blocks marked F_y , F_i , F_v ,and F_ω may be an amplifier, attenuator , or other signal processors.

14.3 SPEED CONTROL

DC Motor Speed Control Basic Theory

Before considering the details of speed control, it is required to define the following related terms:

Pre-set speed : The speed to which the drive is pre-set, for example by means of adjusting the reference voltage in the control circuit (n_p in Fig.14.4). Maximum setting of n_p is called the base speed (n_{pmax} in Fig.14.4). Minimum possible setting of n_p is n_{pmin} in the figure.

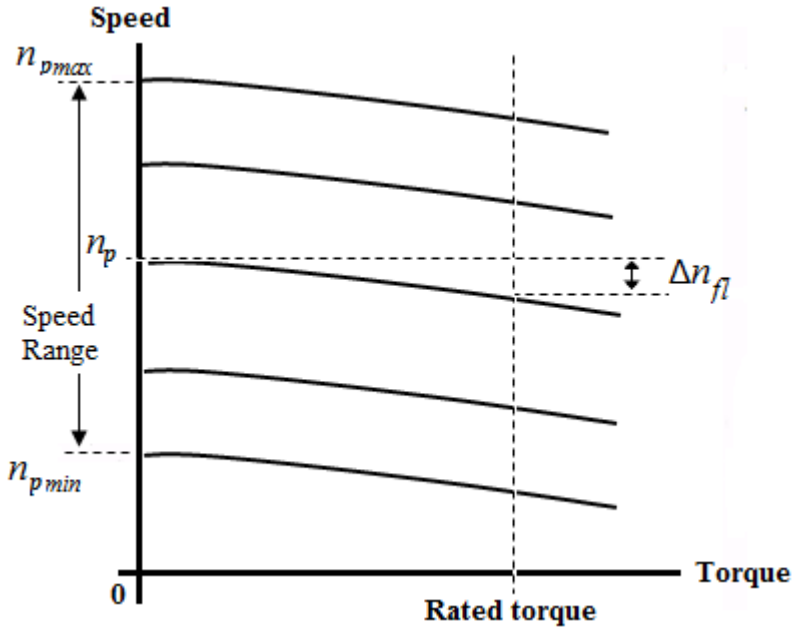

Fig.14.4 Speed-torque characteristics of adjustable-speed drives.

Speed regulation: The change in speed from no-load to full-load in percent of the pre-set speed. Thus at a pre-set speed *n* in Fig.14.4:

$$\text{speed regulation} = \frac{\Delta\, n_{fl}}{n_p} \times 100\% \qquad (14.1)$$

Sometimes the speed regulation is given in percent of the base speed n_{pmax} , i.e.

$$\text{speed regulation} = \frac{\Delta\, n_{fl}}{n_{pmax}} \times 100\% \qquad (14.2)$$

In controlled drives, speed regulation ranges from 1% to 5 % .

Speed range: Is the ratio of the base speed n_{pmax} to the minimum possible speed setting n_{pmin}.

By defining the base speed range, n_{pmin} is defined, and hence the entire range of speeds over which the motor can be controlled. A typical speed range is 6:1. In general, n_{pmin} is determined by limits of temperature rise in the motor.

Having defined the above technical terms, we can state that the objective of speed control is to operate the drive with small speed regulation over a wide speed range.

14.3.1 Open-Loop Operation

If, in Fig.14.3, the speed, voltage and current feedback signals are removed, then Y, and hence the firing angle α are determined solely by the reference signal. For a given pre-set speed, the reference signal is constant; thus the speed drops according to the internal characteristics of the motor, and speed regulation is very large.

14.3.2 Closed-Loop Operation

Speed regulation is greatly improved if a feedback signal proportional to speed is used, the control system compares this feedback signal with the reference signal; the difference, Y' in Fig.14.3, is amplified to control the firing or triggering circuit in such a way as to maintain the speed constant. At no-load, the feedback signal subtracts from the reference voltage to yield a certain Y' (corresponding to the pre-set speed n_p); as the motor is loaded, the speed tends to fall and the feedback signal decreases so that Y' increases; thus α is decreased to increase the motor voltage, tending to restore the speed to its original pre-set value; in fact the speed does not reach the original value, but slightly less. This difference, or error is defined by,

$$\Delta n = n_p - n \tag{14.3}$$

which produces the necessary change in α. Thus the speed regulation ability of the control section depends on two main factors:

1. How well the feedback signal depicts motor speed; this depends on the quality of the speed sensing means and the components present in the feedback path.
2. How much error in speed, Δn is required to produce a given change in the firing angle α. It is desirable that only a small Δn is sufficient to produce large changes in α. Clearly, this factor is related to the amount of amplification available in the control circuit (for example in the block F_Y of Fig.14.3).

Speed sensing

In section 14.2 it was clear that we need a feedback signal which represents the speed in precise manner. The most obvious method of speed sensing is by means of a tachogenerator mounted on the shaft of the motor under control. The tachogenerator generates a voltage proportional to the motor speed with high degree of accuracy (linearity), which is its main advantage; however, the installation of a tachogenerator constitutes a costly item in the drive. A cheaper method of speed sensing is based on motor basic equation which is

$$V_{a(av)} = I_{a(av)} R_a + K_e \emptyset n \qquad (14.4)$$

If the main field flux $\emptyset$ is constant, and the resistive drop $I_{a(av)} R_a$ is negligible, then the average armature voltage $V_{a(av)}$ is proportional to speed n. Thus the armature voltage may be used as the feedback signal represents the speed. This method is cheap because it uses little additional hardware, but it is inaccurate because the feedback signal used is not very good representation of motor speed due to the above assumption. However, this last method may be improved considerably by the use of current feedback. Let us re-write Eq.(14.4) in the form

$$V_{av} - I_{av} R_a = K_e \emptyset n \qquad (14.5)$$

If $\emptyset$ is constant, then the term on the left hand side is in fact, proportional to speed. Thus a feedback signal composed of two components is used: the first component is proportional to armature voltage as before, but the second component is proportional to armature current and is subtracted from the first component (in effect, it is added to the reference signal) to yield an overall feedback signal proportional to the speed as desired. It may be said that current feedback used in this way compensates for the resistive drop of the armature circuit. The current multiplier representing R_a is usually set by test for optimum performance. This method is effective and quite cheap, but it may suffer from stability problems due to positive current feedback.

Amplification

As mentioned in subsection 14.2.2, the amplification, or gain, available in the control loop affects the speed regulation ability of the drive. As the gain increases, a small error in speed ($\Delta n = n_p - n$) is sufficient to produce large changes in the firing angle, these changes being, in turn , sufficient to keep Δn small. Usually, the amplifier stage is located after the comparator stage. With small gains, a relatively large error in speed is needed to advance α sufficiently; in effect speed regulation is large.

Very close speed regulation is achieved by the use of tachogenerator speed sensing together with an operational amplifier; however, the system is expensive, and is used only where the application justifies its high cost. Moreover, high gains may give rise to stability problems, thus limiting the range of operation of the motor.

Transient effects

So far, our analysis has been limited to steady-state conditions where the objectives are to obtain a small value of speed regulation over a wide speed range. Inevitably, transient effects arise whenever the drive experience sharp changes in loading, voltage, or speed. Ideally, after any disturbance, the system should settle quickly to the new steady-state. Any oscillations that arise being damped with a short time constant.

In practice, closed-loop control may give rise to instability over certain ranges of operation, where transient may cause undamped oscillations. It is interesting to note that the devices which improve steady-state performance tend to be the ones that cause transient problem. In particular, transient performance may suffer from high gains in the control loop, and from the use of positive current feedback, especially at high loads. In these cases we shall be interested not only in steady state performance (speed regulation and speed range), but also in the transient effects of such disturbances as starting and run-up, sudden loss of speed, and sudden load shedding. It will also be useful to remember that instability, unless very severe, occurs over only certain ranges of speed and loading.

14.4 DC MOTOR CONTROL CHARACTERISTICS

To study the d.c. motor control characteristics from the control theory point of view, let us consider a separately-excited d.c. motor at loading condition controlled by a power electronics converter as depicted in Fig.14.5. The motor speed is adjusted by setting reference or control voltage , v_r .

Assuming the converter of gain K_c has a linear power characteristics, then, the output voltage of the converter is

$$v_a = K_c\, v_r \tag{14.6}$$

is directly supplied to the armature circuit. Therefore, the closed-loop transfer function of the motor could be evaluated easily by considering first its open-loop transfer function.

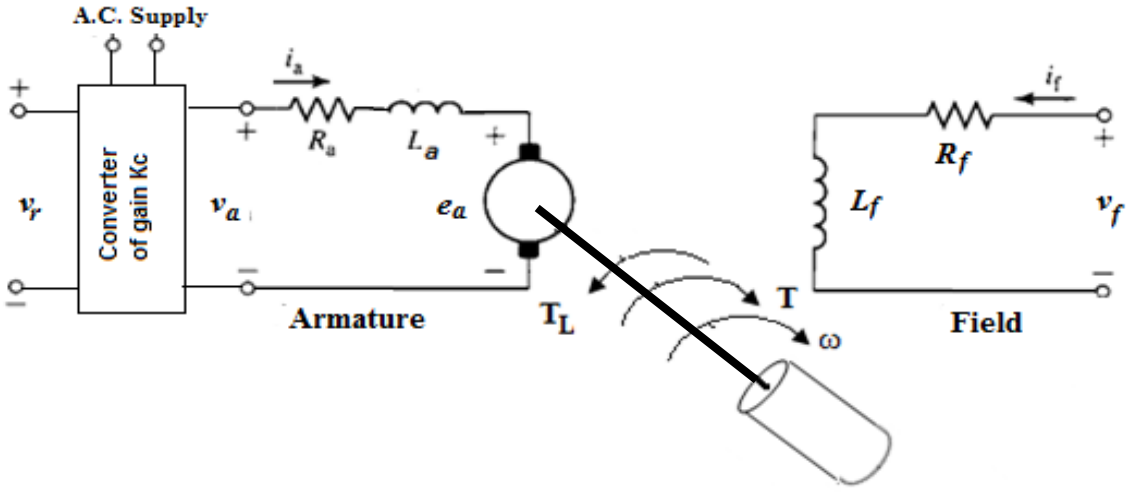

Fig.14.5 Equivalent circuit of a converter fed separately-excited d.c. motor.

14.4.1 Open-Loop Transfer Function of d.c. Motor

To find the open-loop transfer function of a d.c. motor, consider the following basic equations of the d.c. motor :

The general motor electrical equation referred to Fig.14.5 (armature circuit),

$$v_a = R_a i_a + L_a \frac{di_a}{dt} + e_a \tag{14.7}$$

The induced back *emf*

$$e_a = K \phi \omega \tag{14.8}$$

Substituting Eq. (14.8) in Eq. (14.7) yields

$$v_a = R_a i_a + L_a \frac{di_a}{dt} + K \phi \omega \tag{14.9}$$

Also, the mechanical equations of the motor are,

$$T = T_L + J \frac{d\omega}{dt} + B \omega \tag{14.10}$$

and the induced (developed) torque

$$T = K\phi i_a \tag{14.11}$$

The Laplace transform of the above four equations (14.8), (14.9), (14.10) and (14.11), assuming zero initial conditions are,

$$v_a(s) = R_a I_a(s) + L_a s I_a(s) + K\phi\, \omega\,(s) \tag{14.12}$$

$$E_a\,(s) = K\phi\, \omega(s) \tag{14.13}$$

$$T(s) = T_L(s) + Js\omega(s) + B\,\omega(s) \tag{14.14}$$

$$T(s) = K\phi\, I_a(s) \tag{14.15}$$

From equations (14.12), and (14.13) the current is given by

$$I_a(s) = \frac{V_a(s) - E_a\,(s)}{R_a(1 + s\,\tau_a)} = \frac{V_a(s) - K\phi\,\omega\,(s)}{R_a(1 + s\,\tau_a)} \tag{14.16}$$

where $\tau_a = L_a / R_a$ = electrical time constant of the motor.

From equations (14.14), and (14.15)

$$\omega\,(s) = \frac{T(s) - T_L(s)}{B(1 + s\frac{J}{B})} = \frac{K\phi\, I_a(s) - T_L(s)}{B(1 + s\tau_m)} \tag{14.17}$$

where $\tau_m = J / B$ = mechanical time constant of the motor.

The open-loop block diagram of the motor represented by Eqs.(14.13), (14.16) and (14.17) is shown in Fig.14.6. Two possible disturbances may occur to the motor,the terminal voltage V_a (or reference voltage V_r), and the load torque T_L. The steady-state responses can be determined by combining the individual response due to V_a and T_L as follows :

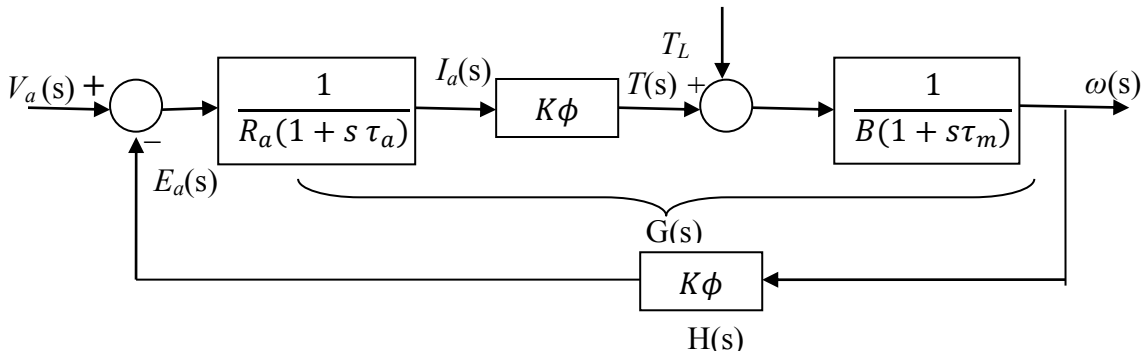

Fig.14.6 Open-loop block diagram representation of a separately-excited d.c. motor.

- The response to change in V_a (or V_r) is obtained by setting $T_L = 0$ (no load condition), hence Fig.14.6 will represent the general negative feedback system with transfer function:

$$TF = \frac{G(s)}{1 + G(s)H(s)} \tag{14.18}$$

$$\frac{\omega(s)}{V_a(s)} = \frac{\dfrac{K\emptyset}{R_a(1 + s\,\tau_a)B(1 + s\tau_m)}}{1 + \dfrac{K\emptyset}{R_a(1 + s\,\tau_a)B(1 + s\tau_m)}.K\emptyset}$$

$$= \frac{K\emptyset}{R_aB(1 + s\,\tau_a)(1 + s\tau_m) + (K\emptyset)^2}$$

$$= \frac{K\emptyset/R_aB}{s^2\tau_a\tau_m + s(\tau_a + \tau_m) + \ 1 + (K\emptyset)^2/R_aB} \tag{14.19}$$

It is clear from Eq.(14.19) that the motor forms a second order system with inherent feedback.

From Fig.14.5, and the relation $v_a = K_c\, v_r$, the response to step change in the control voltage V_r (s) = V_a (s) / K_c can be obtained as,

$$\frac{\omega(s)}{V_r(s)} = \frac{K_c\,K\emptyset/R_aB}{s^2\tau_a\tau_m + s(\tau_a + \tau_m) + \ 1 + (K\emptyset)^2/R_aB} \tag{14.20}$$

- The response to change in the torque T_L is obtained by setting $V_a = 0$ (or $V_r = 0$) , hence the block diagram for step change in load torque will be as depicted in Fig.14.7.

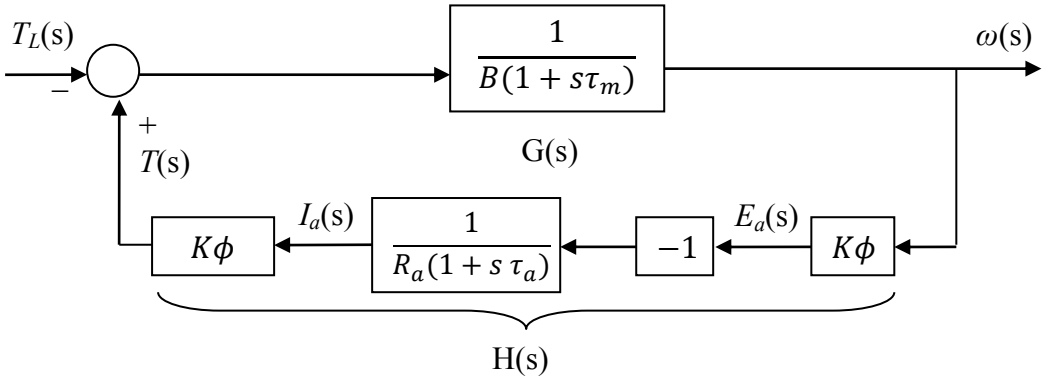

Fig.14.7 Block diagram of a separately-excited d.c. motor with torque disturbance.

For positive feedback, the transfer function of the block diagram of Fig.14.7 is,

$$TF = \frac{G(s)}{1 - G(s)H(s)} \tag{14.21}$$

$$\frac{\omega(s)}{-T_L(s)} = \frac{\frac{1}{B(1+s\tau_m)}}{1 - \frac{1}{B(1+s\tau_m)} x \frac{K\emptyset x(-1) x K\emptyset}{R_a(1+s\,\tau_a)}}$$

$$= \frac{\frac{1}{B}(1+s\,\tau_a)}{(1+s\tau_m)(1+s\,\tau_a) + (K\emptyset)^2/R_aB}$$

$$\frac{\omega(s)}{-T_L(s)} = \frac{\frac{1}{B}(1+s\,\tau_a)}{s^2\tau_a\tau_m + s(\tau_a+\tau_m) + 1 + (K\emptyset)^2/R_aB} \tag{14.22}$$

The steady-state relationship of a change in speed $\Delta\omega$ due to step change in the reference voltage ΔV_r and a step change in load torque ΔT_L, can be found from Eqs.(14.20) and (14.21) respectively by applying the final value theorem in which we substitute s = 0 in both equations to give,

$$\Delta\omega = \frac{K_c K\emptyset}{R_aB + (K\emptyset)^2}\ \Delta V_r \tag{14.23}$$

$$\Delta\omega = \frac{-R_a}{R_aB + (K\emptyset)^2}\ \Delta T_L \tag{14.24}$$

For special case, if the viscous friction B = 0, the above equations become,

$$\Delta\omega = \frac{K_c\Delta V_r}{K\emptyset} = \Delta\omega_o \qquad \text{no-load speed change} \tag{14.25}$$

$$\Delta\omega = \frac{-R_a}{(K\emptyset)^2}\ \Delta T_L \qquad \text{change in } \omega \text{ due to loading} \tag{14.26}$$

or $\omega = \Delta\omega_o + \Delta\omega = \frac{K_c\Delta V_r}{K\emptyset} - \frac{R_a}{(K\emptyset)^2}\ \Delta T_L$

Notes:

(1) The above transfer functions are valid for continuous current operation only.
(2) The motor is always stable in open-loop operation.

14.4.2 Closed-Loop Transfer Function

Open-loop control system for separately-excited d.c. motor of Fig.14.1 may be changed to closed-loop control system by attaching speed sensor to the motor shaft. The output of the sensor (could be a tachogenerator or speed encoder) which is proportional to the speed, is amplified by a factor K_t and compared with a reference voltage v_r to give an error signal v_e. The block diagram for a typical closed-loop control system of a separately-excited d.c. motor is shown in Fig.14.8.

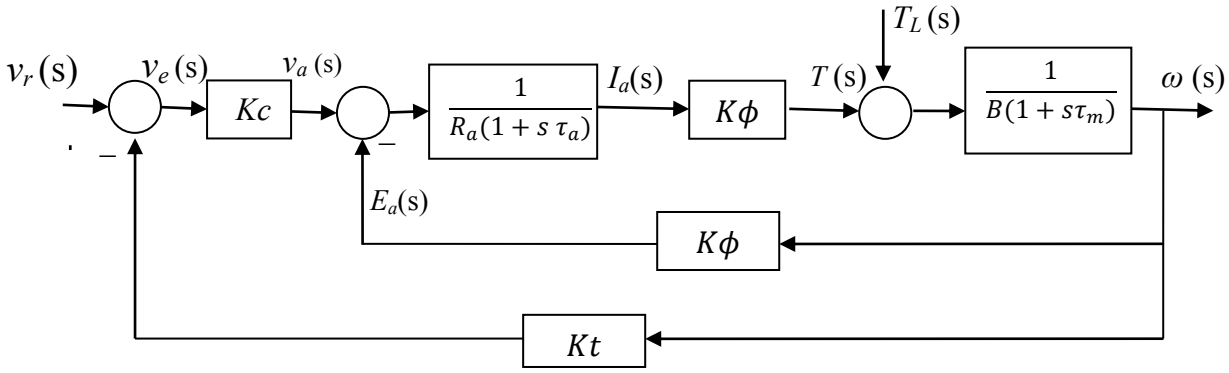

Fig.14.8 Closed-loop control block diagram representation of a separately- excited d.c. motor.

The closed-loop step response due to a change in reference voltage can be obtained from Fig.14.8 with $T_L = 0$.The transfer function is,

$$\frac{\omega(s)}{V_r(s)} = \frac{K_c\, K\emptyset/R_aB}{s^2\tau_a\tau_m + s(\tau_a + \tau_m) + \ 1 + [(K\emptyset)^2 + K_tK_cK\emptyset]\ /R_aB} \qquad (14.27)$$

The closed-loop step response due to a change in load torque T_L can be obtained from Fig.14.8 by setting $V_r = 0$, hence the transfer function is found to be,

$$\frac{\omega(s)}{T_L(s)} = \frac{-\frac{1}{B}(1 + s\,\tau_a)}{s^2\tau_a\tau_m + s(\tau_a + \tau_m) + \ 1 + [(K\emptyset)^2 + K_tK_cK\emptyset]\ /R_aB} \qquad (14.28)$$

The steady-state relationship of a change in speed $\Delta\omega$ due to step change in the reference voltage ΔV_r and a step change in load torque ΔT_L, can be found from equations (14.27) and (14.28) respectively by applying the final value theorem in which we substitute $s = 0$ in both equations to give,

$$\Delta\omega = \frac{K_c K\emptyset}{R_a B + (K\emptyset)^2 + K_t K_c K\emptyset}\ \Delta V_r \qquad (14.29)$$

$$\Delta\omega = \frac{-R_a}{R_a B + (K\emptyset)^2 + K_t K_c K\emptyset}\ \Delta T_L \qquad (14.30)$$

Example 14.1

A 45 kW, 240 V, 2000 rpm, separately-excited d.c. motor is to be speed controlled by a thyristor converter as shown in Fig.14.5. The machine constant $K\emptyset$ =1.0 V.s / rad. The armature resistance R_a = 0.1 Ω and the viscous friction constant B = 0.1 Nm.s/rad. The speed sensor amplification factor K_t = 100 mV.s /rad and the gain of the power control K_c = 100. It is required to determine the following:

(a) The rated torque of the motor.
(b) The reference voltage V_r to drive the motor at rated speed.
(c) The speed at which the motor develops the rated torque if the reference voltage is kept constant.
(d) The motor speed if the load torque is increased by 15% of the rated value.
(e) The motor speed if the reference voltage is reduced by 15%.

Solution

(a) The rated speed ω_R is

$$\omega_R = \frac{2000 \times 2\pi}{60} = 209.44 \text{ rad/s.}$$

Rated torque T_R is

$$T_R = \frac{P}{\omega_R} = \frac{45000}{209.44} = 214.85 \text{ Nm}$$

(b) Since for open-loop $V_a = K_c V_r$, Eq.(14.23) gives

$$\omega = \frac{K_c K\emptyset}{R_a B + (K\emptyset)^2} V_r = \frac{K_c V_r K\emptyset}{R_a B + (K\emptyset)^2} = \frac{V_a K\emptyset}{R_a B + (K\emptyset)^2}$$

$$\therefore V_a = \frac{\omega[R_a B + (K\emptyset)^2]}{K\emptyset} = \frac{209.44[\,(0.1 \times 0.1) + (1.0)^2]}{1.0}$$
$$= 211.53 \text{ V}$$

and the feedback voltage, $E'_a = K_t\,\omega = 100 \times 10^{-3} \times 209.44 = 20.944$ V.

With closed-loop control, the error voltage $V_e = V_r - E'_a$,

$$V_a = V_e K_c = (V_r - E'_a) K_c$$

From which,

$$\therefore V_r = \frac{V_a + K_c E'_a}{K_c} = \frac{211.53 + 20.944 \times 100}{100} = 23.05 \text{ V}$$

(c) For $V_r = 23.05$ V and $T_R = 214.85$ Nm, from Eq.(14.30)

$$\Delta\omega = \frac{-0.1 \times 214.85}{0.1 \times 0.1 + (1.0)^2 + 100 \times 10^{-3} \times 100 \times 1.0} = -1.951 \text{ rad/s}$$

The speed at rated torque = 209.44 – 1.951 =207.49 rad / s.

(d) If the load torque is increased by 15 % of the rated value:

$$\Delta T_L = 1.15 \times 214.85 = 247.07 \text{ Nm}$$

$$\Delta\omega = \frac{-0.1 \times 247.07}{0.1 \times 0.1 + (1.0)^2 + 100 \times 10^{-3} \times 100 \times 1.0} = -2.243 \text{ rad/s}$$

The speed at rated torque = 209.44 – 2.243 = 207.197 rad /s.

(e) Now, $\Delta V_r = -0.15 \times 23.05 = -3.4575\,V$, From Eq.(14.29) ,

$$\omega = \frac{100 \times 1.0}{0.1 \times 0.1 + (1.0)^2 + 100 \times 10^{-3} \times 100\,x1.0} \times (-3.4575)$$
$$= -31.4 \text{ rad/s}$$

The speed at rated torque = 209.44 – 31.4 = 178.04 rad /s.

14.5 PRACTICAL CLOSED-LOOP CONTROL SYSTEM FOR D.C. MOTOR WITH SPEED AND CURRENT CONTROLLERS

In practice d.c. motor closed-loop control schemes do not contains speed feedback only. The scheme must also contain current feedback to meet the load torque which depends on the armature current. When the motor is operating at a particular speed and suddenly load is applied, the

speed will fall and the motor will take time to restore to its original speed. Therefore, a speed feedback with an inner current loop gives faster response to any change in speed, load torque or the supply voltage as depicted in Fig.14.9.

The function of the current loop is to react with the sudden change of the load torque under transient conditions of operation such as starting, breaking, speed reversal, and torque disturbances. The supply current which is the a.c. input current (equivalent to the armature current),sensed

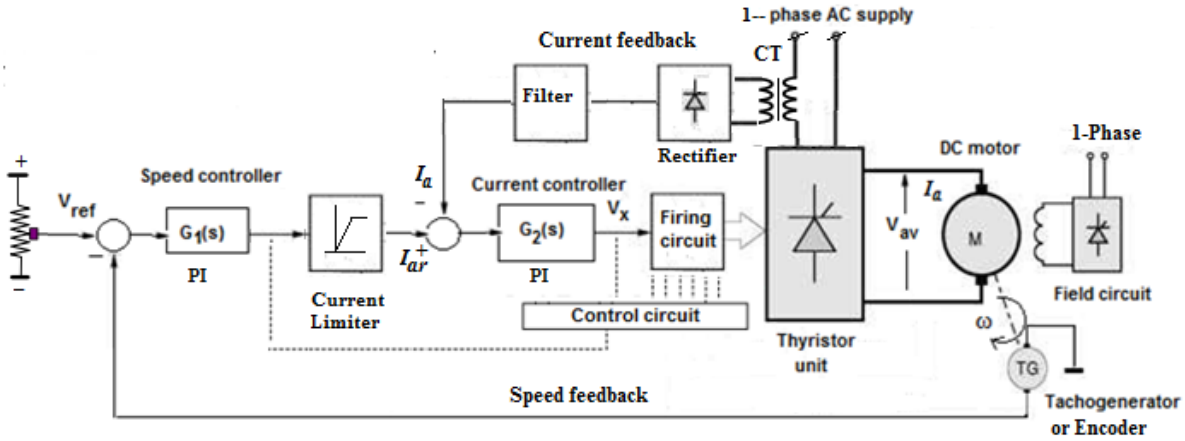

Fig.14.9 Closed-loop control system for d.c. motor with speed and current controllers.

by the current transformer CT, rectified and filtered by an active filter to remove ripples to give the actual d.c. armature current I_a . The output of the speed controller is applied to a current limiter which sets the current reference I_{ar} for the current loop to a safe value, no matter how high the speed error is. The current error (I_a - I_{ar}) is applied to the current controller to adjust the firing angle α of the thyristor unit (or γ for a chopper) to bring the motor speed to the desired value by increasing or decreasing the armature voltage. The reference current is the output of the speed controller.

The function of the current limiter is to saturate and limit the current in case of any large increase in the value of the reference current I_{ar} due to any positive speed error resulting from either increase in the speed command or an increase in the load torque. This variation in I_{ar} is processed by the current controller whose output adjusts the firing angle of the converter to correct the speed error and finally settled to a new $I_{ar,}$ which makes the motor torque equal to the load torque and the speed error closed to zero.

The current control loop is generally faster than the speed control loop, therefore it is preferred that the current loop is designed first by assuming

the motor operates at constant speed. Once the current loop is designed, the speed control loop is then considered to satisfy torque demand.

14.5.1 Speed and Current Controllers Transfer Functions

Types of the Controller-Review:

A controller for a converter-fed variable-speed drive is an electronic device whose input and output values are electrical signal. By suitable electrical design it is possible to obtain the required control action. The four principal types of controllers are:

(1) P-Controller (Proportional-action):

P-controller is mostly used in first order system to stabilize the unstable process. The main usage of the P-controller is to decrease the steady state error of the system. As the proportional gain factor *K* increases, the steady state error of the system decreases. However, despite the reduction, P-control can never manage to eliminate the steady-state error of the system. As we increase the proportional gain, it provides smaller amplitude and phase margin, faster dynamics satisfying wider frequency band and larger sensitivity to the noise. Hence , this type of controller can only be used when the system is tolerable to a constant steady-state error. In addition, it can be easily concluded that applying P-controller decreases the rise time and after a certain value of reduction on the steady state error, increasing *K* only leads to overshoot of the system response. P-control also causes oscillation if sufficiently aggressive in the presence of lags and /or dead time. The more lags (higher order), the more problem it creates.

Operational - Amplifier P- Controller

Fig.14.10 shows a P-controller using operational-amplifier. The transfer function of the circuit is,

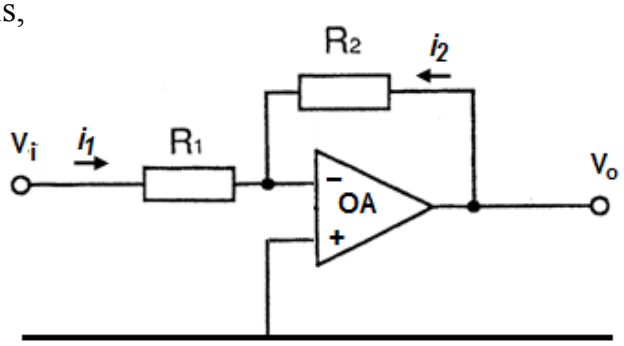

Fig.14.10 Op-amplifier P-controller.

$$\frac{V_i}{R_1} = i_1 \qquad \text{and} \qquad \frac{V_0}{R_2} = -i_2$$

Since $i_1 = i_2$

$$\therefore \frac{V_0}{V_i} = -\frac{R_2}{R_1} = K_C \qquad \text{(Controller gain)} \qquad (14.31)$$

Hence with p-controller the output is directly proportional to the amplitude value of the input, i.e. $V_o = K_c V_i$.

P- Speed controller

In this type of controllers, the transfer function shows that an input change in V_r results in large sudden change in current that decays slowly, this transient overcurrent is undesirable from the stand point of converter rating and protection. This particularly the case for starting or other large change.

P- Current controller

The current drawn by the motor is fed back by the inner loop with current transducer. Relatively there is small overshoot and in practice, there will be a delay due to the armature circuit electrical time constant together with the converter delay. Sometimes a filter is required to reduce the ripple in the current sensor element or in the tachogenerator itself.

(2) PI-Controller (Proportional plus integral action):

PI-controller is mainly used to eliminate the steady state error resulting from P-controller. However, in terms of the speed of the response and overall stability of the system, it has a negative impact. This controller is mostly used in areas where speed of the system is not an issue. Since PI- controller has no ability to predict the future errors of the system it cannot decrease the rise time and eliminate the oscillations. Fig.14.11 shows a PI-controller using Op-amplifier. The transfer function of the circuit is obtained as ,

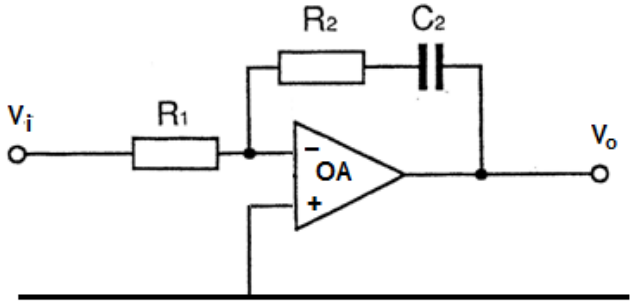

Fig.14.11 Op-amplifier PI-controller.

$$G_c(s) = \frac{v_0}{v_i} = -\frac{R_2}{R_1}\left(1 + \frac{1}{sC_2R_2}\right) = K_c\left(\frac{T_2 s + 1}{T_2 s}\right)$$
$$= K_c \frac{s + a_g}{s} \qquad (14.32)$$

where $T_2 = C_2 R_2$, $a_g = 1/T_2$, and $K_c = -R_2/R_1$.

Hence with PI-controllers the output value is of the aggregate of the amplified input pulse and the integral of the input value. PI-controllers are normally used for speed and current control. The addition of integral

feedback is to eliminate the steady-state error and to reduce the required forward gain.

(3) PD-Controller (proportional plus derivative action):

The aim of using PD-controller is to increase the stability of the system by improving control since it has an ability to predict the future error of the system response. In order to avoid effects of the sudden change in the value of the error signal, the derivative is taken from the output response of the system variable instead of the error signal. Therefore, D mode is designed to be proportional to the change of the output variable to prevent the sudden changes occurring in the control output resulting from sudden changes in the error signal. In addition D directly amplifies process noise therefore D-only control is not used. Fig.14.12 shows a PD-controller using Op-amplifier. The transfer function of the circuit is,

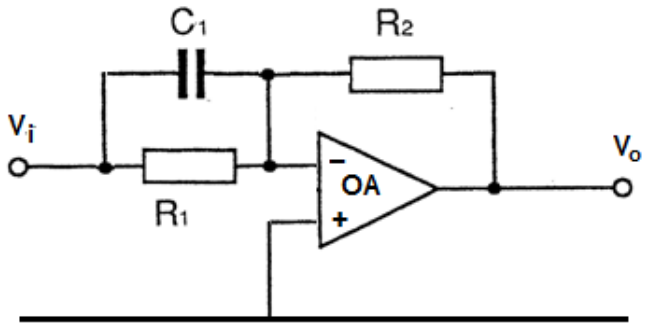

Fig.14.12 Op-amplifier PD-controller.

$$\frac{v_0}{v_i} = -\frac{R_2}{R_1}(1 + sC_1R_1) \qquad (14.33)$$

(4) PID-Controller (Proportional pulse integral plus derivative action):

PID-controller has the optimum control dynamics including zero steady state error, fast response (short rise time), no oscillations and higher stability. The necessity of using a derivative gain component in addition to the PI-controller is to eliminate the overshoot and the oscillations occurring in the output response of the system. One of the main advantages of the PID-controller is that it can be used with higher order systems.PID-controller has the combination of PI and PD characteristics. Fig.14.13 shows a PID-controller using Op-amplifier. The transfer function of the circuit is,

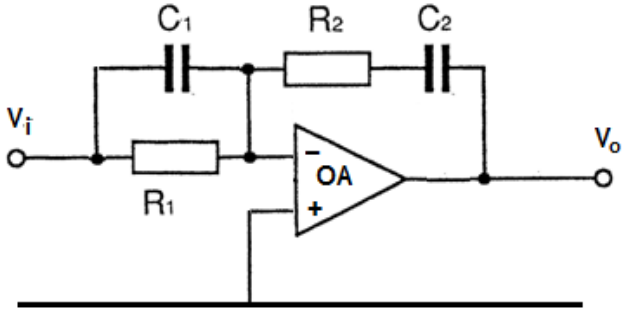

Fig.14.13 Op-amplifier PID-controller.

$$\frac{v_0}{v_i} = K\left(1 + \frac{1}{s\tau_i} + s\,\tau_d\right) \qquad (14.34)$$

where $K = -\left(\frac{R_2}{R_1} + \frac{C_1}{C_2}\right) = -K_o$, $\tau_i = C_1 R_1 K_o$ and $\tau_d = R_2 C_1 / K_o$

The time response for the different types of controller are shown in Fig.14.14. Table 14.1 gives comparison between the characteristics of the four types of controllers.

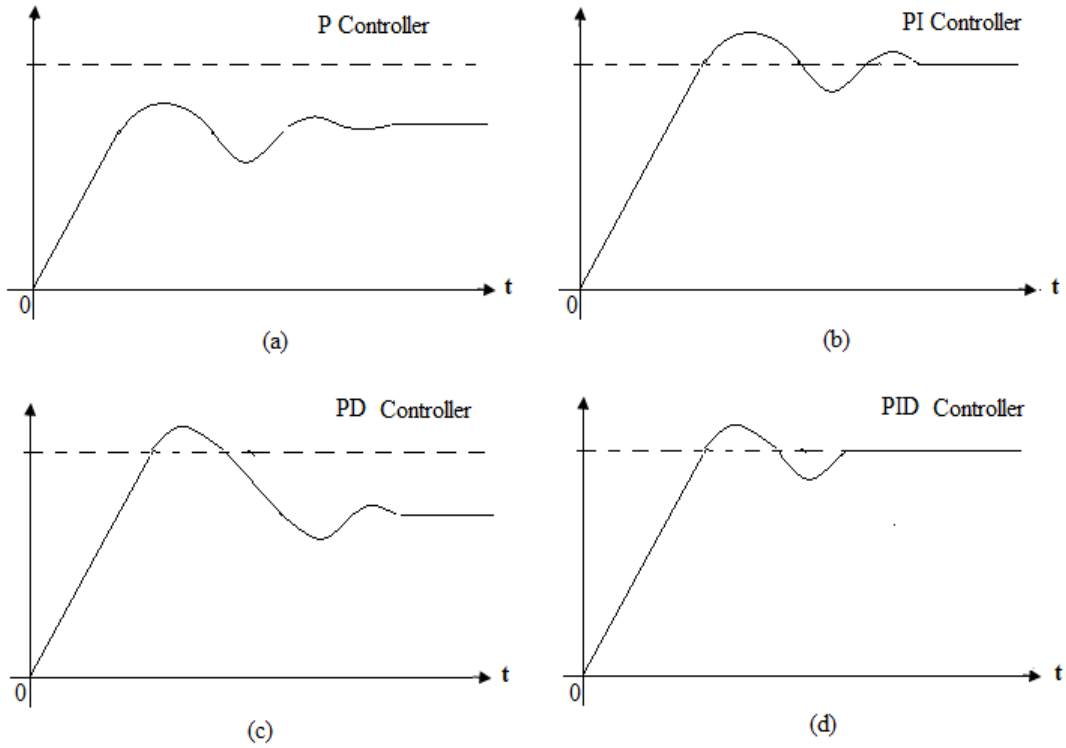

Fig.14.14 Time response and steady-state errors for : (a) P-controller, (b) PI-controller , (c) PD-controller, and (d) PID-controller.

Table 14.1. Comparison between the characteristics of controllers.

Type of controller	**Characteristics**
P-controller	Relatively fast , but low statistical accuracy
PI-controller	Relatively fast , high statistical accuracy
PD-controller	Very fast , but low statistical accuracy
PID-controller	Fast , high statistical accuracy

However, the most common type controller used in d.c. drive is the PI-controller. A complete closed-loop control system with both speed and current control using PI-controllers is shown in Fig.14.15.

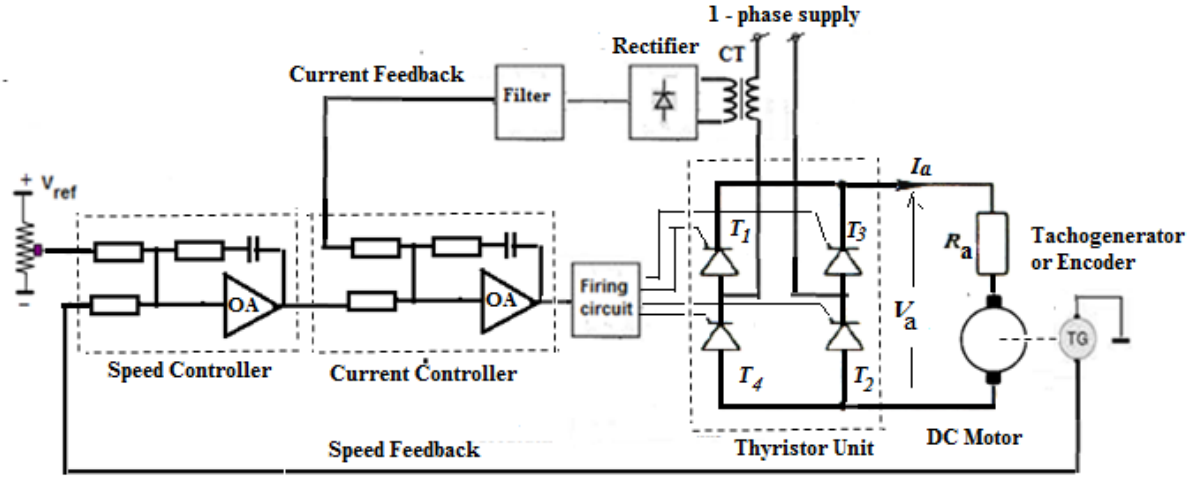

Fig.14.15 Block diagram of thyristor speed control system with speed and current controllers (structure).

14.5.2 Mathematical Modeling of the Power Converter Units

Power converters cannot always be considered purely as simple gain as stated earlier. They usually have a delay associated with them. Therefore, each converter should be studied alone to find its transfer characteristic and its mathematical modeling in order to solve the entire control system. To understand the converter delay and find a control model to represent a specific type of converter, the main two categories of the converters used in d.c. drives namely, controlled rectifiers and d.c. chopper drives will be considered here in after.

1. Thyristor bridge converters

The thyristor bridge converter used in d.c. drives is usually provided with a.c. supply through a single-phase transformer and fast acting a.c. contactors. The d.c. output is fed to the armature of the d.c. motor. For the separately-excited motor, field is separately excited, and the field supply can be kept constant or regulated, depending on the need for the field weakening mode of operation. Here, the feedback control system with the thyristor elements is, in fact, non-linear sample-data system with variable parameters.The block diagram of such system is shown in Fig.14.16. In this case the thyristor unit is considered as sampler with a sampling period T is given by

$$T = \frac{1}{qf} \tag{14.35}$$

where f = supply frequency and the factor (q) depends on the drive type, The values are: q = 1 for half-wave rectifier, q = 2 for full-wave rectifier and q = 6 for three-phase rectifier.

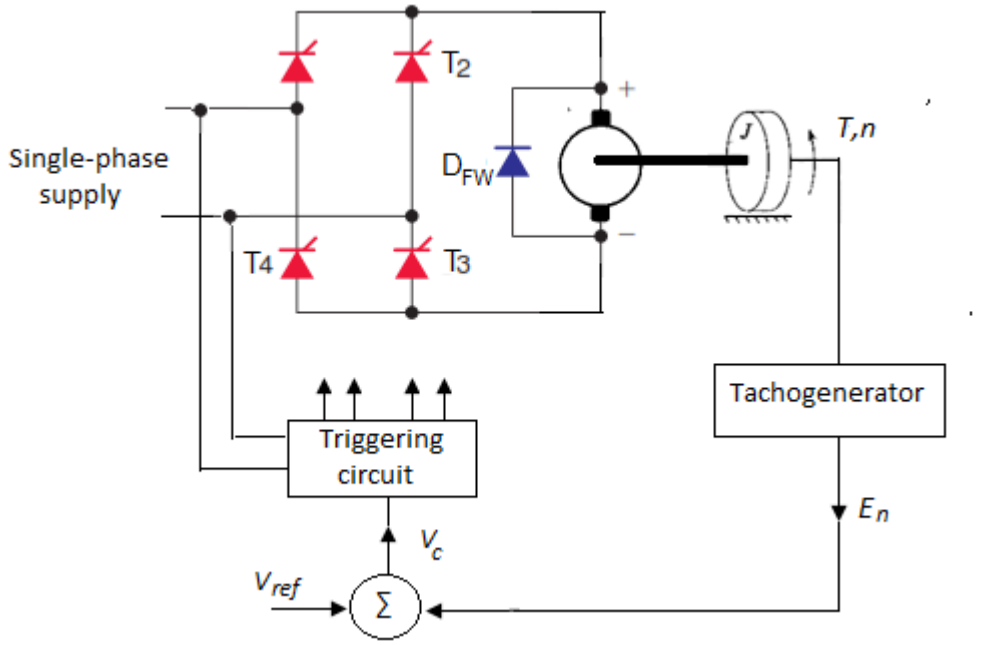

Fig.14.16 Schematic diagram of a thyristor controlled d.c. motor with tachogenerator feedback.

For full-wave rectifier, the static characteristic of the thyristor unit is given by the following equation (Reference 51):

$$V_{av} = \frac{V_m}{\pi}(1 - \cos(\pi \frac{V_c}{V_{cm}})) \tag{14.36}$$

where

V_c = Control voltage of the triggering circuit (usually 0 to 10 V).

V_{cm} = Maximum control (reference) voltage of the triggering circuit (10V).

Equation (14.36) is depicted on Fig.14.17, curve (1). It can be seen that the static characteristic is nonlinear and the gain of thyristor unit is not constant since $\frac{\partial V_{av}}{\partial V_c}$ will be varied according to V_c. The function ($\frac{\partial V_{av}}{\partial V_c} = f\,(V_c/V_{cm})$ is shown in Fig.14.17, Curve (2).

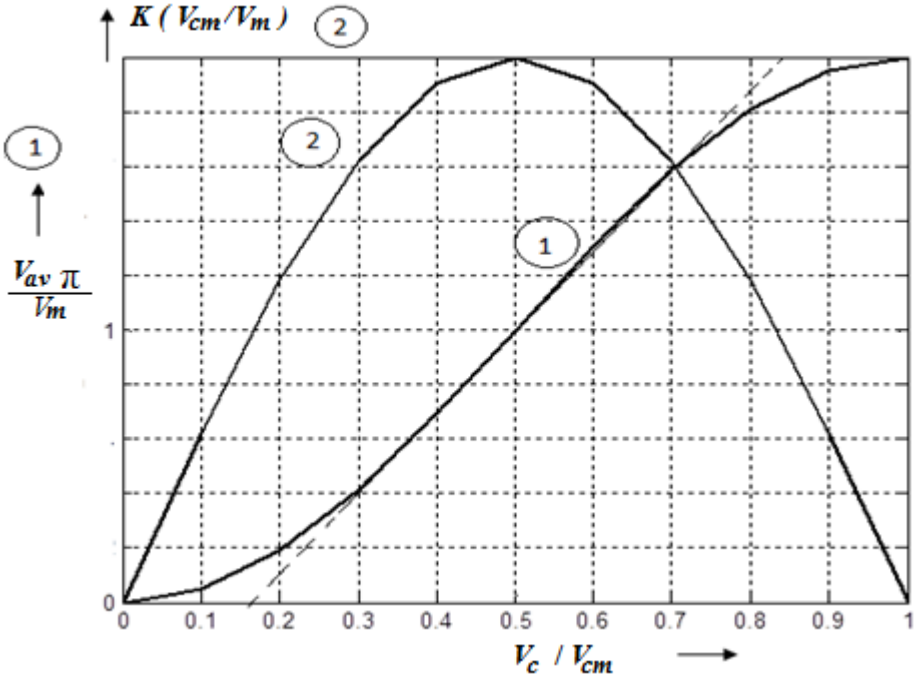

Fig.14.17 Gain of thyristor unit.

The nonlinear characteristic of the power converter shown in Fig.14.17 can be approximated by a linear one. Moreover, the gain of the rectifier unit is assumed to be constant and equal to

$$K_R = \frac{\Delta V_{av}}{\Delta V_c} \tag{14.37}$$

The zero-order hold of the thyristor unit represents a memory holding average voltage until the next coming pulse from the triggering unit. Hence the sampler and hold of the thyristor unit can be replaced by a time delay of T/2 , where *T* is the sampling period as shown in Fig.14.18.

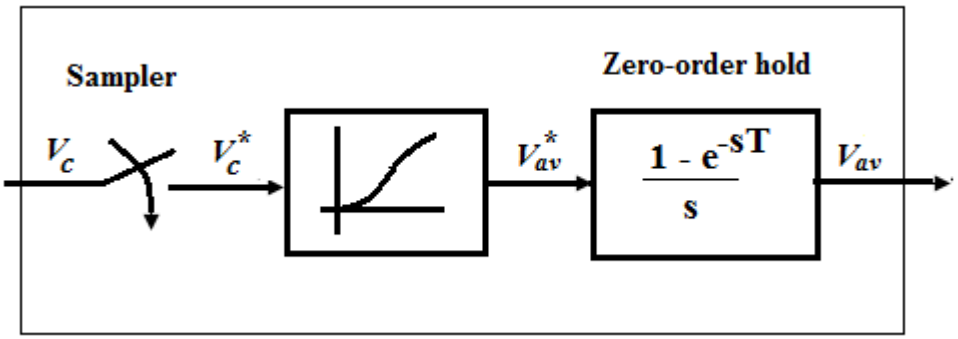

Fig.14.18 Sampled data representation of the thyristor converter unit.

Hence, the dynamic of the ac-to-dc thyristor converter (rectifier) is usually described by a transfer function $G_R(s)$ with a time delay (or transportation lag) and certain gain K_R , i.e.

$$G_R(s) = \frac{V_a(s)}{V_{ar}(s)} = K_R e^{-(T/2)} \tag{14.38}$$

where $T = \frac{1}{qf}$ and K_R = gain of the controller.

The exponential function in the above equation is approximated by rational algebraic function using Pade's approximation so that

$$G_R(s) = \frac{V_a(s)}{V_{ar}(s)} = \frac{K_R}{1 + \frac{T}{2}\, s} \tag{14.39}$$

In this case the thyristor unit is considered as sampler with a sampling period $T=1/q\,f$, where f = supply frequency and the factor (q) depends on the drive type (i.e. the number of pulses), (q = 1 for single-phase half-wave rectifier, q = 2 for single-phase full-wave rectifier and corresp-onding by q = 6 for three-phase rectifier). For full-wave single-phase rectifier with 50 Hz: $= \frac{1}{2\times 50} = 0.01$ s. Therefore, the average delay caused by this type of converter is 5 ms as depicted in Fig.14.19.

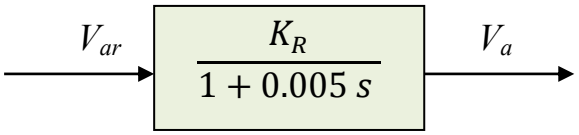

Fig.14.19 Time delay representation of a single-phase full-wave rectifier.

For three-phase rectifier: Maximum delay = 360˚/ 6 = 60˚.In 50 Hz, this is equivalent to 20 ms/6 = 3.3 ms , therefore, the average delay caused by this type of converter is 3.3 ms /2 = 1.67 ms as depicted in Fig.14.20.

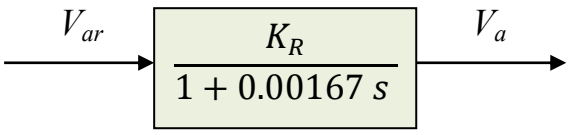

Fig.14.20 Time delay representation of a three-phase full-wave rectifier.

2. DC Chopper drives

Consider a dc-to-dc converter (chopper) with a duty cycle γ ($t_{on} = \gamma T$). According to Eq.(12.2) the average output voltage of the chopper is directly proportional to the duty cycle which is a direct function of the control voltage (usually 0 to 10 V). If V_{cm} is the maximum value of the control voltage (10 V), then the gain K_{cr} of the chopper can be expressed mathematically as

$$K_{cr} = \frac{V_c}{V_{cm}} \tag{14.40}$$

When the chopper operating in the steady-state at a duty cycle γ_1 and the controller demands a new duty cycle γ_2 shortly after triggering of the chopper thyristor then there is a delay of almost T before the chopper can react. Usually, this delay is approximated as a first order lag (1/ (1+sτ)) with a time constant $\tau = T/2$ .Thus the average delay of a chopper with a switching (control) period T is represented as in Fig.14.21.

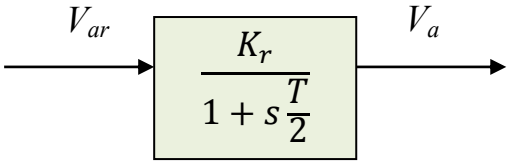

Fig.14.21 Time delay representation of a d.c. chopper.

14.5.3 Closed-Loop Current Control with PI-Controller

As stated before that, in practice, the most type used of current controller is the proportional plus integral (PI). To analyse a drive with both speed (outer loop) and current (inner loop) controllers, it is preferred that the inner loop is analysed first. The simple block diagram of the inner loop is shown in Fig.14.22.

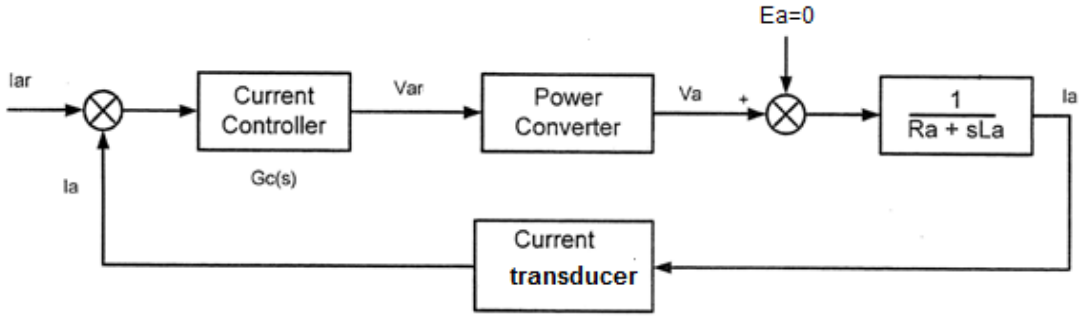

Fig.14.22 Current controller (inner loop).

From Eq.(14.32), the transfer function of the current controller is re-written as

$$G_c(s) = K_c \frac{(s + a_g)}{s} \tag{14.41}$$

To simplify analysis, we initially assume that the power converter is just a simple gain K_R (i.e. ignoring the time lag in the converter) . Therefore the function of the power converter is to convert the input reference voltage V_{ar} , for example 0-12V, to armature voltage V_a , say 0-500V.
If the speed effect is ignored, we set $E_a = 0$ in the block diagram since E_a is directly proportional to the speed.

From the block diagram of Fig.14.19, the forward transfer function G(s) and the closed-loop transfer function T(s) of the system may be obtained as well as the feedback transfer function H(s). The general relation between these transfer functions is

$$T(s) = \frac{G(s)}{1 + G(s)\,H(s)}$$

The characteristic equation of the system can be written as

$$1 + G(s)H(s) = 0$$

which can be rearranged mathematically in the following form

$$s^2 + as + b = 0 \tag{14.42}$$

where a and b are functions of known parameters (R_a , L_a) and unknown parameters (K_c , a_g).

Equation (14.42) is used for the design of the inner loop system and evaluation of its performance. The design specification usually requires a system dominated by a second order pole pair, with natural frequency ω_n , and damping factor ξ . Therefore, the characteristic equation can be written as

$$s^2 + 2\xi\omega_n\, s + \omega_n^2 = 0 \tag{14.43}$$

Now, by equating the coefficients of s_1 and s_0 one can find the desired K_c and a_g for the current controller.

To find how the system is stable, we can use any linear control theory such as root locus method or Bode plot as it will be described in the following examples.

Example 14.2

A block diagram of a d.c. drive control system is shown in Fig.14.23. The drive employs a d.c. separately-excited motor has the following parameters:

$R_a = 0.2\ \Omega,\ L_a = 0.004$ H

Inertia constant $J = 5.5$ kg.m^2

Friction coefficient $B = 0.006$ Nm / (rad /s)

Design a PI - current controller using a current transducer which gives an output of 0.15 V/A. The PI-controller output (V_{ar}) is input to a rectifier that provides the armature circuit of the motor with the voltage V_a , where $V_a / V_{ar} = 40$. The closed-loop band width should be 300 rad /s and the damping factor ξ should be 0.6.

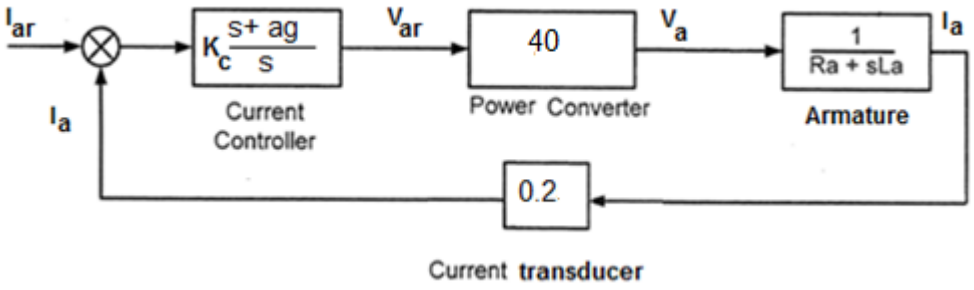

Fig.14.23 Block diagram of d.c. drive system with PI - current controller.

Solution

The forward transfer function is

$$G(s) = K_c \frac{(s + a_g)}{s} \times 40 \times \frac{1}{0.20 + s\,0.004}$$

$$H(s) = 0.15$$

The complete transfer function of the system is

$$T(s) = \frac{G(s)}{1 + G(s)\,H(s)}$$

The characteristic equation is

$$1 + G(s)H(s) = 0$$

$$1 + K_c \frac{(s + a_g)}{s} \times 40 \times \frac{1}{0.20 + s\,0.004} \times 0.15 = 0$$

Simplification of the above equation yield

$$s^2 + (50 + 1500K_c)\, s + 1500\, K_c a_g = 0$$

Compare this equation with the standard second order equation:

$$s^2 + 2\xi\omega_n s + \omega_n^2 = 0$$

$$2\xi\omega_n = 2 \times 0.6 \times 300 = 50 + 100K_c$$

$$K_c = \frac{310}{1500} = 0.206$$

$$1500\ \ K_c a_g = 0.206 \times 1500 a_g = 300^2$$

$$a_g = \frac{90000}{310} = 290$$

The root locus of the system is shown in Fig.14.24 for clarity.

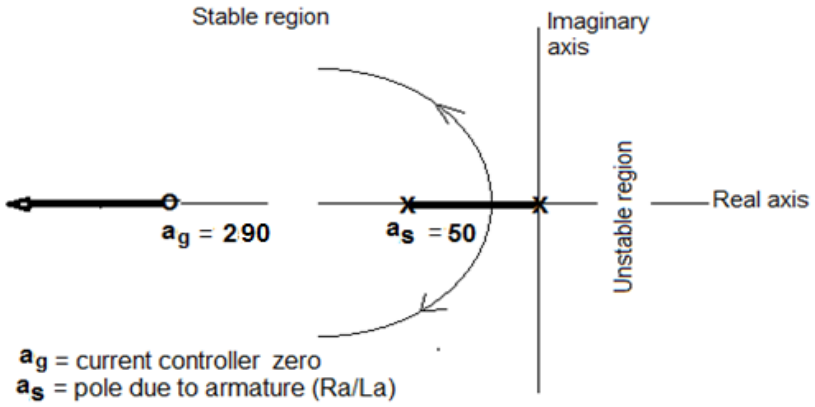

Fig.14.24 Root locus.

14.5.4 Closed-Loop Speed Control with PI-Controller

After analysing the current controller, as shown in the previous subsection, the speed controller is considered in the next step. The speed controller output must be related to torque, the torque must change to change the speed. The speed control (outer) loop is depicted in Fig.14.25. To start design of the controller, we make the speed controller output as the armature current reference I_{ar} . This value of the current must be limited so that the armature current does not exceed the rated value for the power converter. This is usually 150% full load current of the motor.The current loop can be approximated to a second or first order system or even just a simple gain if its bandwidth is very high.

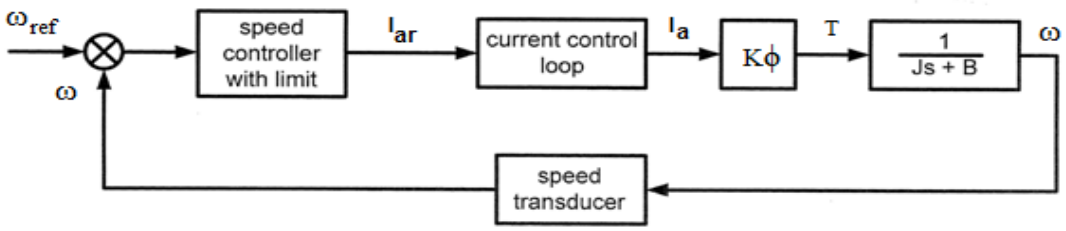

Fig.14.25 Speed controller loop.

From the block diagram of Fig.14.25, the forward transfer function $G(s)$ and the closed loop transfer function $T(s)$ of the system may be obtained as well as the feedback transfer function $H(s)$. The transfer functions function of the system is obtained, as in the case of the current controller, after that the characteristic equation of the system is obtained and written in the standard quadratic equation form (Eq.14.43).

Equation (14.43) is used for the design of the outer loop system and evaluation of its performance. The design specification usually requires a system dominated by a second order pole pair, with natural frequency ω_n , and damping factor ξ. The following example (14.3) illustrates the design procedure for a speed controller.

Example 14.3

A speed controller is to be designed for a 1500 rpm d.c. motor with J = 0.01 Nm / rad / s^2, B = 0.095 Nm /rad /s, using PI-controller. The current controller can be approximated to a first order lag of time constant 20 ms , and torque / back *emf* constant is 9 Nm /A; speed reference is provided by a 0 – 10V supply and speed measurement is from a tachogenerator giving 15 mV/rpm. Assume the armature current is limited to 5 A in control loop,

(a) Sketch the block diagram for the control system.

(b) Find the gain K_c and the factor a_g for the PI-speed controller to provide closed loop control of bandwidth 10 rad/s, damping factor = 0.7. Sketch the root locus.

Solution

(a) The current controller transfer function is

$$G_R(s) = \frac{K_{pc}}{1 + s\tau} = \frac{1}{1 + 20 \times 10^{-3} s} = \frac{50}{s + 50}$$

For the tachogenerator, K_t = 0.015 V/rpm = 0.1432 V /rad /s.

The block diagram for the control system is shown in Fig.14.26.

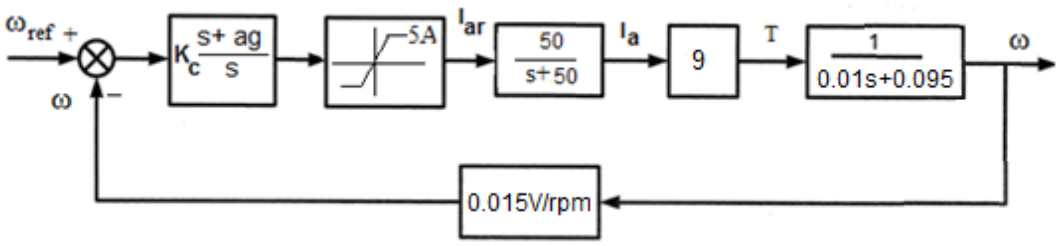

Fig.14.26.

(b) The characteristic equation of the system in Fig.14.26 is

$$1 + K_c \frac{(s + a_g)}{s} \times \frac{50}{s + 50} \times \frac{9}{0.01s + 0.095} \times 0.1432 = 0$$

$$s^3 + 59.5\, s^2 + 475.5\, s + K_c\big(s + a_g\big)\, 6444 = 0 \qquad (A)$$

The reference equation has $\omega_n = 10$, $\xi = 0.7$ and an unknown pole α. Hence,

$$(s + \alpha)(s^2 + 2\xi\omega_n s + \omega_n^2) = 0$$

or $$s^3 + (17 + \alpha)\, s^2 + (100 + 17\alpha)s + 100\,\alpha = 0 \qquad (B)$$

Equating coefficients of Eq.(A) and Eq.(B) :

$$\alpha = 42.5\ , \qquad K_c = 0.0567\ , \qquad a_g = 11.63$$

and the closed loop poles are : -49 , -11.8, -9.5 and 0 . The root locus is shown in Fig.14.27.

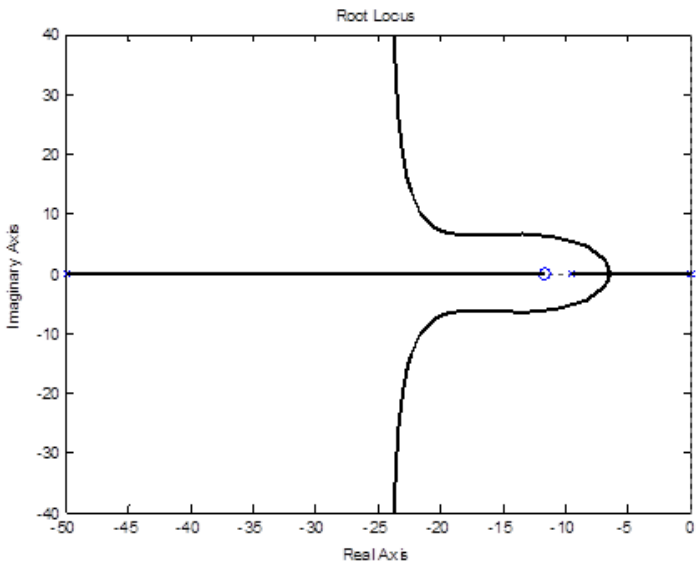

Fig.14.27 System root locus.

14.5.5 Closed-Loop Speed and Current Control with PI Controller Simplified Steady-State Analysis

Fig.14.28 shows a typical block diagram of d.c. drive system with both speed and current control using PI-controllers. The d.c. drive closed-loop system employs ac-to-dc converter using thyristor or any other power semiconductor devices elements is a standard full-wave fully-controlled rectifier bridge.

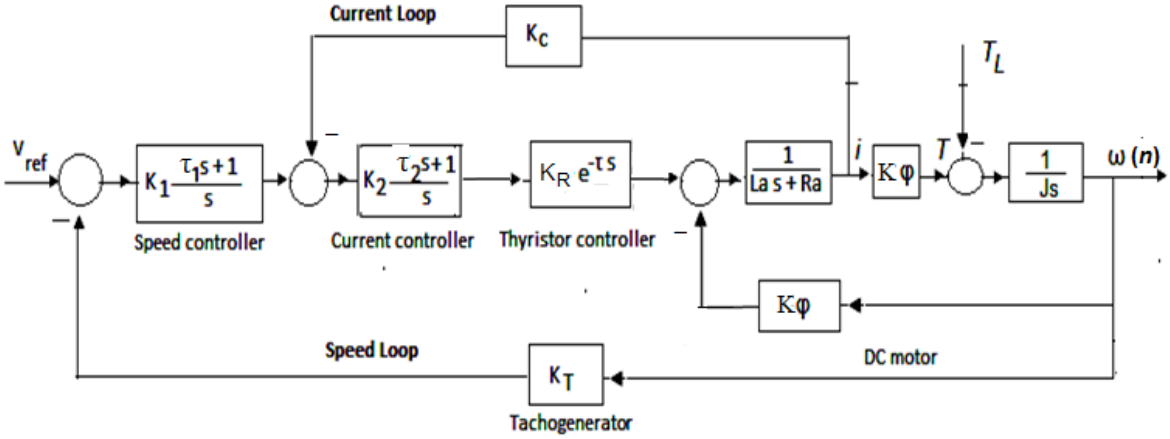

Fig.14.28 Block diagram of thyristor speed control system with speed and current controllers (work diagram).

The thyristor bridge converter is provided with a.c. supply through a single-phase transformer and fast acting ac contactors. The d.c. output is fed to the armature of the d.c. motor. The field is separately excited, and the field supply can be kept constant or regulated, depending on the need for the field weakening mode of operation. Here, the feedback control system with the thyristor elements is, in fact, non-linear sample-data system with variable parameters. In this case the thyristor unit is considered as sampler with a sampling period $T=1/\mathrm{q}\,f$, where f = supply frequency and the factor (q) depends on the drive type, (q=1 for half-wave rectifier, q =2 for full-wave rectifier) as illustrated in subsection 14.5.2. If either speed or current control is used then the above system is reduced to Fig.14.29.

Let G = open loop transfer function.

$$T(s) = \frac{G(s)}{1 + G(s)H(s)}$$

The over all transfer function of the system is

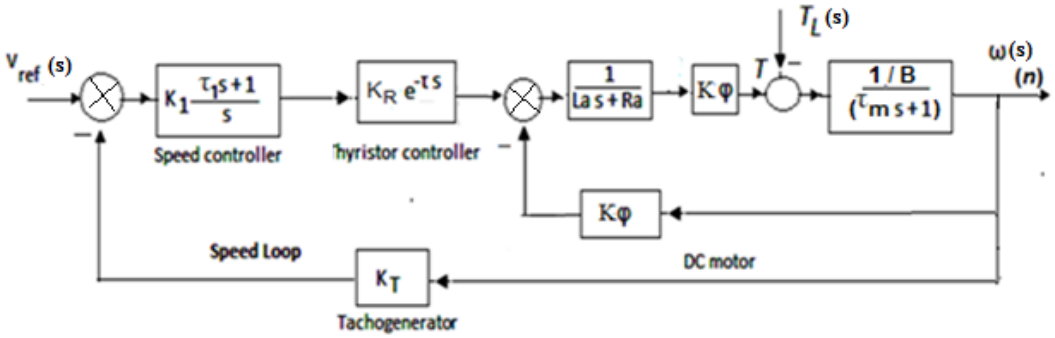

Fig.14.29 Block diagram of thyristor speed control system with PI-speed controller only (work diagram).

$$\frac{N}{V_r} = \frac{K_0}{K_0 + Kt + SsT_m + s^2T_aT_m + 1} \qquad (14.44)$$

where

$$K_o = \frac{K_R K_A}{K_m}$$

Note: this analysis is only valid if the effect of the back *emf* of the motor is neglected.

The steady-state operation of the system can be obtained by applying the final value theorem by setting s = 0, hence the block diagram of the system will reduced to more simple one as depicted in Fig.14.30.

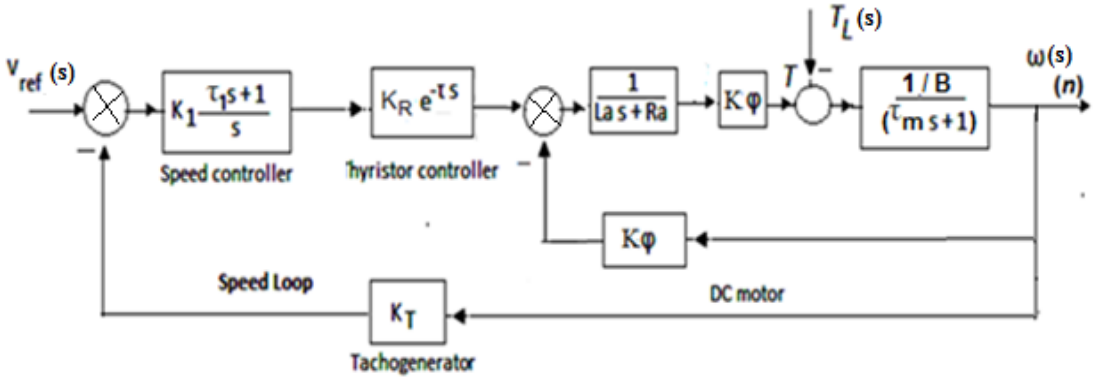

Fig.14.30 Simplified block diagram of the d.c. drive with speed controller only.

Example 14.4

The thyristor speed control of a d.c. separately-excited motor is drawn in Fig.14.31. The d.c. motor has the following data :

Rated armature voltage $V_{a(av)} = 180$ V .
Rated armature current $I_a = 8.7$ A
Rated speed $n = 880$ rpm

Armature resistance $R_a = 3.15\ \Omega$
The thyristor unit has gain $K_R = V_{a(av)} / V_x = 0.2$
The tachogenerator has a gain $K_T = V_T / \omega = 0.2$ Volt / rad/s
Machine constant $K\Phi = 1.655$ V/rad/s

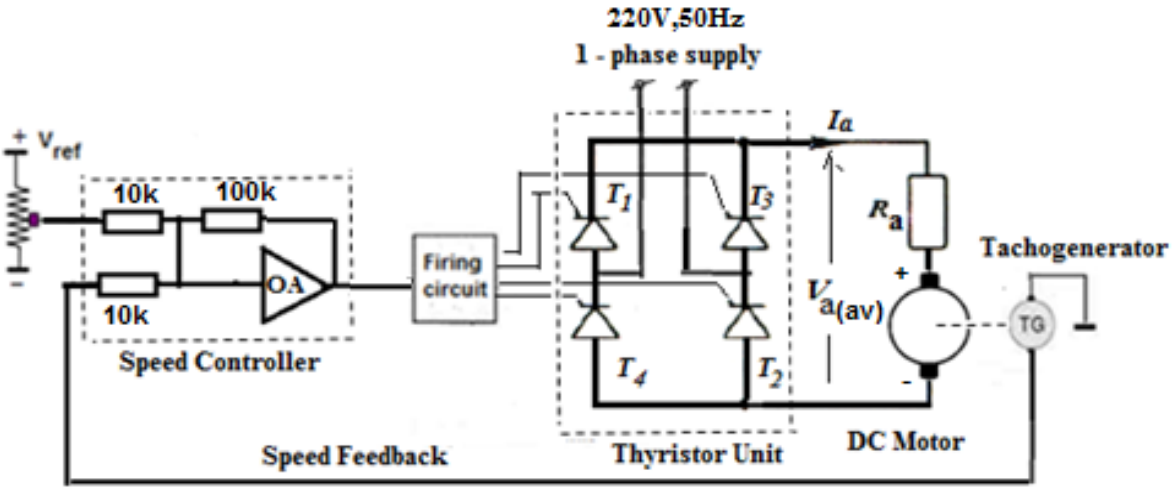

Fig.14.31 Thyristor speed control of a d.c. separately-excited motor.

It is required to solve:

(a) The drop of the speed Δω of the d.c. motor without speed controller (open-loop operation) at rated armature current and at rated voltage.

(b) The drop of the speed Δω for the same armature current in (a) considering the effect of the speed controller and the feedback control if the reference voltage $V_r = 13.55$ V.

Solution

For steady-state operation, the speed of d.c. motor is given by Eq.(11.25) as

$$\omega = \frac{V_{a(av)}}{K\emptyset} - \frac{R_a I_a}{K\emptyset} = \omega_o - \Delta\omega$$

The no load speed is

$$\omega_o = \frac{V_{a(av)}}{K\emptyset}$$

The drop in speed is

$$\Delta\omega = \frac{R_a I_a}{K\emptyset} = \frac{3.15 \times 8.7}{1.655} = 16.5 \text{ rad/s}$$

$$\text{or} \quad \Delta n = \frac{60 \times 16.5}{2\pi} = 157.64 \text{ rpm} \qquad \text{since} \qquad \omega = \frac{2\pi n}{60}$$

(b) Considering the speed controller effect:

The closed-loop block diagram of the d.c. motor with speed controller only is shown in Fig.14.32.

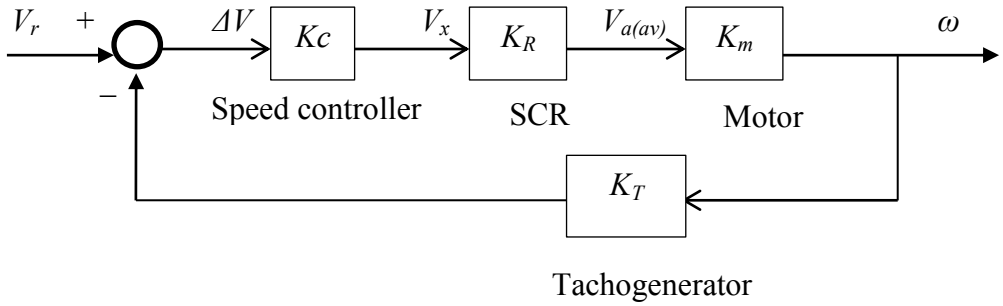

Fig.14.32.

Now $\Delta V = V_r - V_T$

$$V_x = K_C \,.\, \Delta V$$

$$V_{a(av)} = K_R \,.\, V_x = K_C\, K_R\, (V_r - V_T)$$

$$V_T = K_T \,.\, \omega$$

$$T = K \varphi\, I_a = (1/Km) \,.\, I_a$$

since $K_m = 1/K\phi = 1/\ 1.655 = 0.606$ rad /V.s, in this case ,

$$\omega = \frac{V_{a(av)}}{K\emptyset} - \frac{R_a}{K\emptyset} I_a$$

$$\omega = \frac{K_C K_R\ (V_r - K_T \,.\, \omega)}{K\emptyset} - \frac{R_a}{K\emptyset} I_a$$

$$\omega = \frac{K_C K_R\ V_r}{K\emptyset} - \frac{K_C K_R\ K_T \,.\, \omega}{K\emptyset} - \frac{R_a}{K\emptyset} I_a$$

$$\omega \left(1 + \frac{K_C K_R\ K_T}{K\emptyset}\right) = \frac{K_C K_R\ V_r}{K\emptyset} - \frac{R_a}{K\emptyset} I_a$$

$$\omega\ (1 + K_C K_R\ K_T K_m\ ) = K_m K_C K_R\ V_r - K_m R_a I_a$$

Let $K_o = K_C K_R\ K_T K_m$

$\therefore K_o = 10 \times 30 \times 0.2 \times 0.606 = 36.25$

$$\omega = \frac{K_m K_C K_R \ V_r}{(1+K_o)} - \frac{K_m R_a I_a}{(1+K_o)}$$

$$\omega = \omega_o - \Delta\omega'$$

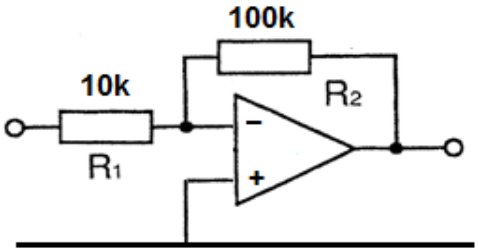

$$K_C = \frac{100k}{10k} = 10$$

The change in speed with closed-loop controllers is

$$\Delta\omega' = \frac{K_m R_a I_a}{(1+K_o)} = \frac{0.606 \times 3.15}{(1+36.25)} \times 8.7 = 0.445 \text{ rad/s}$$

or $$\Delta n' = \frac{0.445 \times 60}{2\pi} = 4.25 \text{ rpm}$$

PROBLEMS

14.1 A separately-excited motor is used in a close-loop speed control system in which the voltage applied to the motor terminals (V_t) is obtained from single-phase full-wave rectifier bridge. The speed controller is a simple proportional type with gain K_c. Draw a block diagram to represent the system, including amongst others, blocks representing the converter, controller and the speed reference voltage V_r, and from the block diagram determine the transfer function (ω/v) for the motor on no load. Show also how the effects of varying load torque are deduced from the block diagram.

14.2 A d.c. motor with constant excitation is used in a control system in which the voltage applied to the armature (v_t) adjust the motor speed (ω). Draw a block diagram to represent the motor, including amongst others, blocks representing the time constant of the armature circuit, the friction torque and the load torque, and from the block diagram determine the transfer function (ω(s) / V_t(s)) for the motor on no load.
Use the transfer function to deduce the shape of a graph showing the transient speeds immediately after suddenly applying a voltage V_t, assuming the inductance of the armature circuit is negligible. Show also how the effect of varying load torques are deduced from the block diagram.

14.3 A d.c. separately-excited motor with voltage control by thyristor switching is used as a drive motor in a close-loop system with tachometric feedback. Sketch such a system in ' block-box ' form. If the system is operating at low speed, what would be the effect the suddenly increasing the reference signal on the motor error signal, the thyristor firing-angle, the motor voltage and the speed? (use Matlab simulation if you could, sketch the type of speed response versus time that you would consider acceptable and reasonable in such a system). What are the advantages and disadvantages of using thyristor chopper and thyristor bridge rectifier for voltage control of a d.c. motor ?

14.4 A separately-excited d.c. motor with machine constant $K\phi$ = 0.54 is controlled by a closed-loop system, as shown in Fig.14.30, including a power converter which has a gain of 100. The armature resistance and inductance of the motor are 0.7 Ω and 0.1 H respectively. The armature inertia J = 0.05 kgm^2 and frictional damping B is negligible. The motor is connected through a 10:1 gearbox to a load which has inertia 5 kg.m^2 and torque which is proportional to (speed)^2 : $T = 0.01\ \omega^2$.
The motor shaft speed is sensed by a tachogenerator, which is a precision permanent magnet d.c. generator producing 9.5 V/1000 rpm. The error signal which is the input to the power converter is derived by subtracting the tachogenerator output from a reference voltage.
By approximating the load torque characteristic about an operating point of 100 rad /s, derive a closed-loop transfer function for the system and calculate its natural frequency and damping ratio. The block diagram of the system is shown in Fig.14.33.

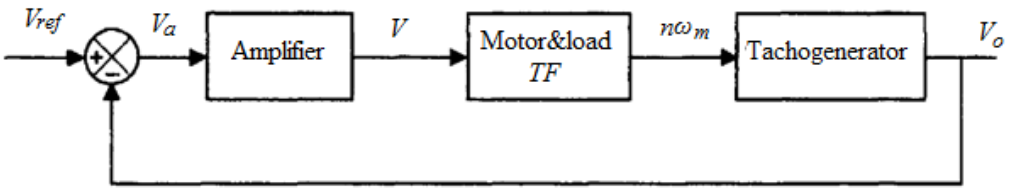

Fig.14.33.

[Ans: $\frac{V_o(s)}{V_{ref}(s)} = \frac{G(s)}{1+G(s)} = \frac{49.14}{s^2+7.2s+50.83}$, $\omega_n = 7.13$ rad/s , $\xi = 0.5$]

14.5 A conveyor is to be speed controlled by a d.c. drive using two d.c. motors coupled on a common shaft. The motor ratings are 300 kW, 600 V, 1250 rpm and 600 kW, 500 V, 1250 rpm. Each motor has its own thyristor converter match its rating, employing conventional current loops. A tachogenerator is fitted on the shaft. Suggest a method or methods of control to provide :

(a) Overall speed control.
(b) Correct load sharing.

14.6 A 30 kW, 240 V, 4000 rpm shunt-excited d.c. motor is by three-phase half-controlled rectifier of gain K_R = 200. The armature resistance of the motor R_a = 0.045 Ω and the armature inductance is 0.72 H. The machine constant $K\phi$ = 0.628 V.s / rad.

(a) Obtain the open-loop transfer functions ω(s) /V_r (s) and ω(s) /T_L(s) for the motor.
(b) If the speed reference voltage V_r is set to 1.0 V and the torque is reduced by 40% of its rated value, calculate the speed of the motor under these conditions.

[Ans: n = 2988 rpm]

14.7 Repeat problem 14.6 if a tachogenerator of amplification factor K_t = 3 mV.s / rad is used to control the speed of the motor in closed-loop mode of operation.

[Ans: n = 1528 rpm]

14.8 Fig.14.34 shows d.c. motor drive system block diagram with PI-current controller. The error signal from I_a loop is fed into the PI-controller. The output of the PI-controller, V_{ar} , is fed to power converter / d.c. motor system. The current control loop is taking into consideration the effect of the mechanical time constant T_m .

(a) Show that the system can be reduced to the block diagram shown in Figs.14.35 and 14.36.
(b) Obtain expressions for the overall gain K , ω_n and ξ in terms of the mechanical and electrical time constants (τ_m and τ_a) of the system,
(c) Given that ω_n = 10 rad /s, ξ = 0.5 and a_g = 18 rad/s , sketch the root locus as K varies from 0 to infinity, given that K_c = 0.095.
(d) Calculate the values of the closed-loop poles when K = 2 and show that the closed-loop transfer function is given by

$$T(s) = \frac{200(s+18)}{(s+20)(s+19)}$$

Note : $$\tau_a = \frac{L_a}{R_a} \ , \tau_m = J\frac{R_a}{K_m{}^2}$$

k_m = Motor constant in SI unit (V.s/rad) , K_i = Current transducer gain.

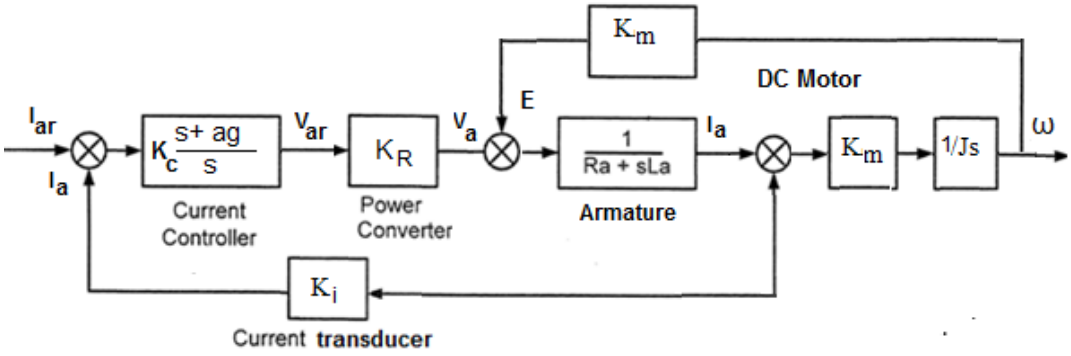

Fig.14.34.

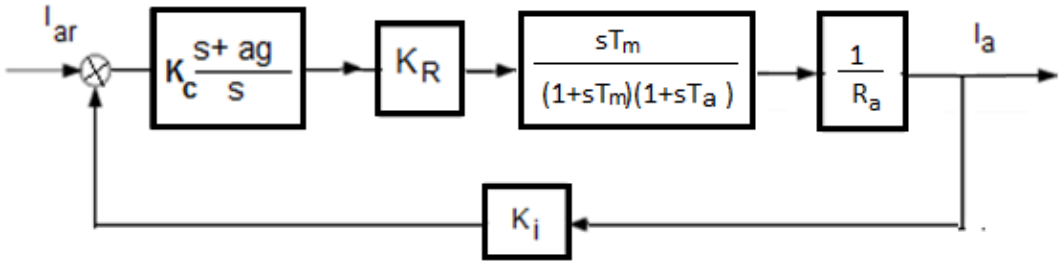

Fig.14.35.

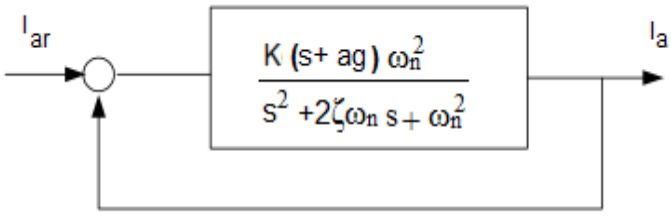

Fig.14.36.

[Ans: (a) $K = \frac{K_R K_c K_i}{R_a}$ τ_m , $\omega_n = \sqrt{\frac{1}{\tau_a \tau_m}}$,

$\xi = \sqrt{\frac{\tau_m}{4\tau_a}}$,$(d) - 20, -190$]

14.9 A separately-excited d.c. motor drives a load with equivalent inertia referred to the motor equal to J . By considering the effect of the armature circuit inductance L_a, show that the response of the current is affected by both the electrical and mechanical time constants defined in problem 14.9.

Hint: Use the fundamental electrical and mechanical equation of the motor to solve for the current respons.

14.10 In a closed-loop speed control of a separately-excited motor, derive the transfer function (ω_m /v) for the motor by considering the load as a pure inertia . Use the superposition theory to show that, by examine the effect of load torque T_m, the speed response will be oscillatory if the electrical time constant of the motor $\tau_a > \tau_m$ /4, hence derive the frequency of oscillation in terms of these time constants. The open loop block diagram of the system is shown in Fig.14.37.

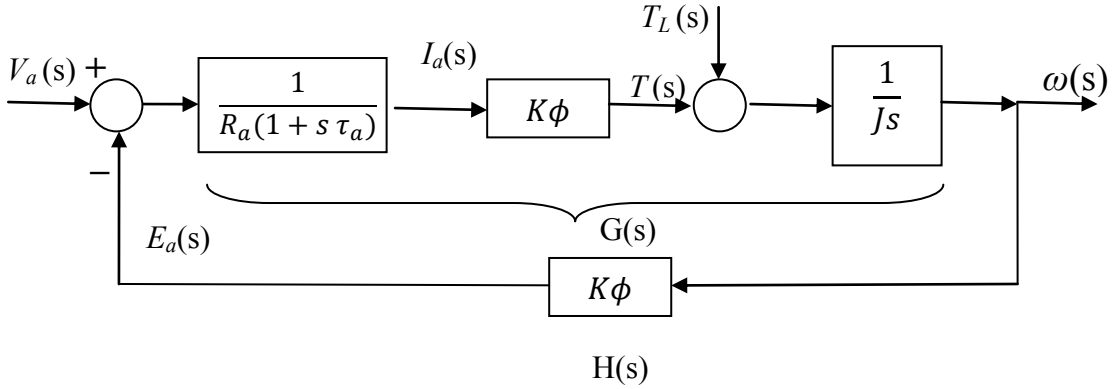

Fig.14.37 Open-loop block diagram of a separately-excited d.c.motor.

[Ans : $TF = \frac{\omega(s)}{V_a(s)} = \frac{1/K\emptyset}{\tau_a\tau_m s^2+\tau_m s+1}$, undamped oscillatory frequency $\omega_n = \sqrt{\frac{1}{\tau_a\tau_m}}$]

14.11 If the motor in problem 14.11 is supplied from an electronic amplifier of linear gain K with a close-loop speed control system, show how will be the effect of adding the amplifier on the speed response. Use the transfer function obtained in problem 14.11.

14.12 Figure 14.38 shows the block diagram of a speed control system of a d.c. motor where V_{in} is the reference input voltage, ω is the output speed and overall feedback loop with constant K_t represents the tachogenerator feedback.

(a) Derive the closed-loop transfer function (ω/V_{in}) in terms of the system constants.

V_{in} is now adjusted to give a steady output speed of 1300 rpm. Due to fault , tachogenerator is reduced to zero and this increases the steady output speed to 1500 rpm. By what factor must K_1 be changed to restore the speed to 1300 rpm.

(b) Discuss the effect of this on the transient behaviour of the system.

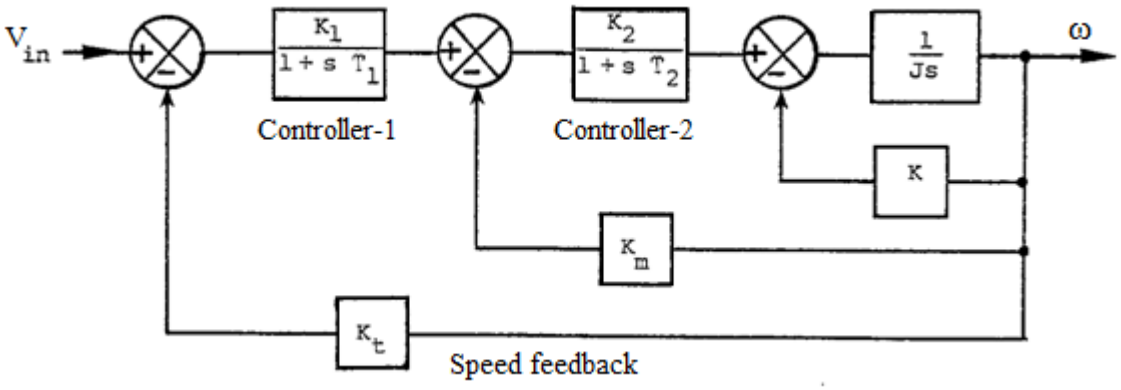

Fig.14.38.

14. 13 A d.c. motor is to be controlled by terminal voltage variation using single-phase fully-controlled rectifier. Sketch a diagram of this arrangement for open-loop control and point out the advantages and disadvantages compared with, say, d.c. chopper control.

The control loop is now closed using a tachogenerator to give negative feedback. Sketch the system in block-diagram form, defining transfer functions or transfer characteristics for each block. Discuss the inherent difficulties of analysing such a system by linear control theory. How would you approach the analysis of such a system ?

The response of motor shaft speed to a step increase of control signal in a typical case is given in Fig.14.39. What do you deduce from this about the nature of the system ?

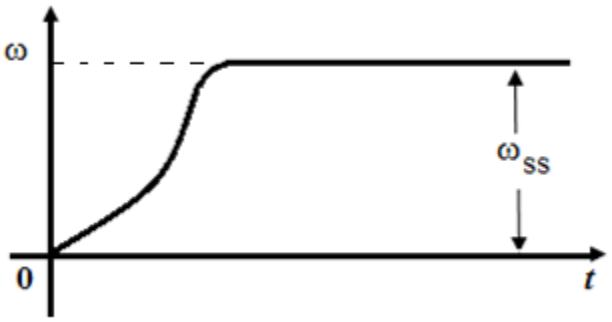

Fig.14.39.

CHAPTER FIFTEEN

AC DRIVES

15.1 INTRODUCTION

AC drives is a term used to refer to equipment designed to control the speed of an a.c. motor. They receive a.c. power and convert it to an adjustable frequency, adjustable voltage output for controlling motor operation. Inverters and other types of frequency changers are typical examples of modern a.c. drives which are also called adjustable frequency drives.

A typical inverter receives 400 V a.c., three-phase, 50 Hz input power and in turn provides the proper voltage and frequency for a given speed to the motor. The three common inverter types are the variable voltage inverter (VVI), current source inverter (CSI), and pulse width modulation (PWM). Another type of a.c. drive is a cycloconverter. These are commonly used for very large motors used in steel industry and mils. The cycloconverters is an arrangement of poly-phase rectifiers in which the firing delay is cyclically varied to synthesise an a.c. output, instead of the set delay for producing a controllable d.c. for the d.c. motor previously mentioned.

A feature of a.c. drives is the ability to increase or decrease the voltage and frequency to a motor gradually. This accelerates the motor smoothly with less stress on the motor and connected load. Smoothing is a feature that can be added to the acceleration/ deceleration operation. This feature smoothes the transition between starting and steady-state operation.

There are several types of a.c. motors used in industrial applications that need real drives to suit a given task. In all types of drives, motors and load have stored energy which can be either regenerated or dissipated as the load speed falls. One third of the world's electricity consumption is used for running induction motors driving pumps, fans, compressors, elevators and machinery of various types. In general, the speed of a.c. motors depends on the frequency of the supply voltage and the number of magnetic poles per phase in the stator. Early speed controllers depended

on switching in different numbers of poles and control was only available manually and in crude steps. Modern electronic drives make continuously variable frequency supplies possible permitting closed-loop speed control. This chapter is intended to provide a basic understanding of a.c. drive terms, types and theory of operations.

Benefits of AC drive

- Large energy savings at lower speed.
- Increased life of rotating components due to lower operating speed.
- Reduced noise and vibration level.
- Reduction of thermal and mechanical stresses.
- Lower kVA.
- High power factor.

15.2 TYPES OF AC MOTORS

The types of a.c. motor available in industry are classified according to the supply as single-phase and poly-phase motors. These two types may also be classified according to the principle of operation into induction type and synchronous type as follows:

1- single-phase motors
  (a) Induction type-squirrel cage
    (i) Split-phase
    (ii) Capacitor start
    (iii) Permanent split capacitor
    (iv) Capacitor start / capacitor run
    (v) Split-phase start / capacitor run
    (vi) Shaded pole
  (b) Induction type-wound rotor
    (i) Repulsion
    (ii) Repulsion start
    (iii) Repulsion induction
  (c) Single-phase synchronous
    (i) Hysteresis
    (ii) Reluctance
    (iii) Permanent magnet
  (d) Single-phase universal motor (AC and DC)

2- Poly-phase motors
  (a) Induction type
    (i) Wound rotor
    (ii) Squirrel – cage
  (b) Synchronous

These motors are summarised in the following diagram (Fig.15.1) ,

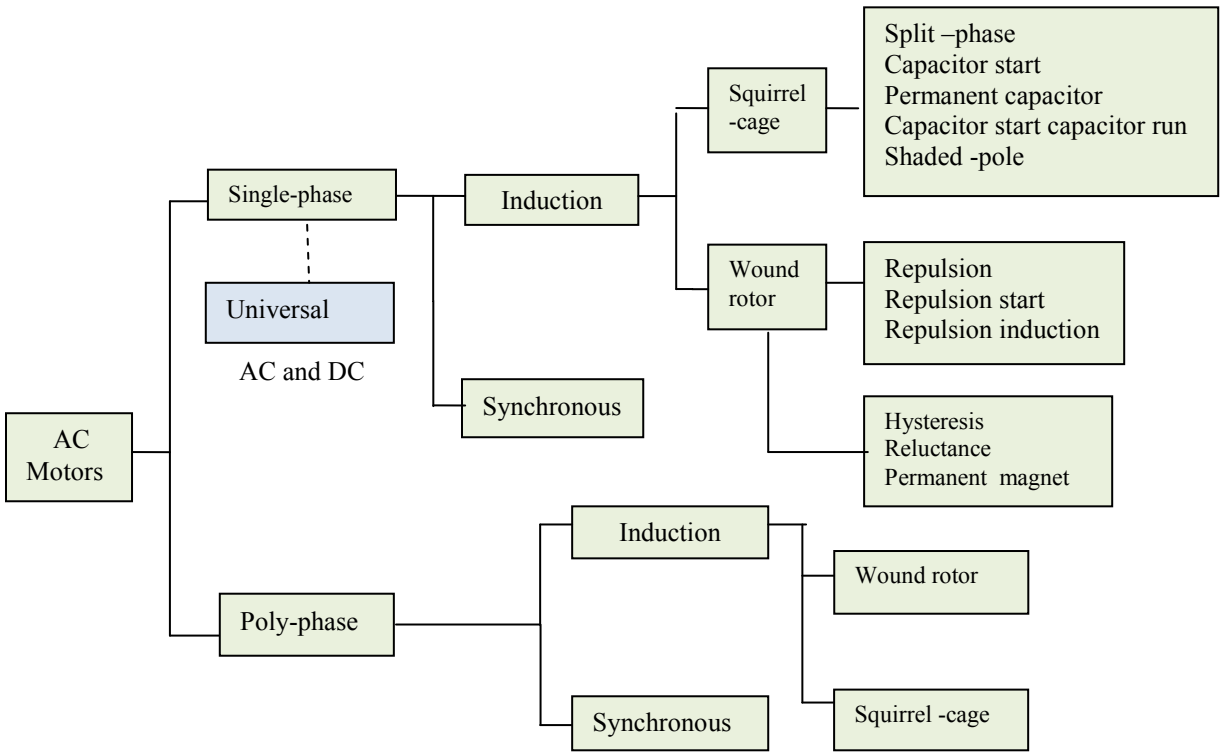

Fig.15.1 Types of a.c. motors.

15.3 THREE-PHASE INDUCTION MOTOR : REVISION OF EQUATIONS

The three-phase induction motors (also called asynchronous motors) are the most widely used electric motors in industry. The popularity of this type of motors in most industrial applications is because of their simple, robust construction because they can build without slip-rings or commutator, rugged, relatively cheap, require little maintenance and have self-starting torque. An induction motor of a medium size may have an efficiency as high as 90 percent and power factor of nearly 0.9. The physical size of such a motor for a given output rating is small as compared with d.c. and a.c. synchronous motors of same rating. There is another distinguishing feature of induction motor is that it is a singly excited machine, i.e. only the stator winding is connected to the a.c. supply, no electrical connection from the supply to the rotor is needed. Finally It can be manufactured with characteristics to suit most industrial requirements.

Beside the above numerous advantages of the induction motor, it has two main inherent disadvantages:

1. Its starting torque is inferior to d.c. shunt motor.
2. It is essentially a constant speed motor and its speed cannot be changed easily.

The speed of an induction motor is determined by the supply frequency and number of poles, with a few percent regulation from no-load to full-load. However, the speed is frequency dependent and consequently these motors are not easily adapted to speed control. A wide range of speed control is only possible by using expensive power electronic circuit with advanced digital control. We usually prefer d.c. motors when large speed variations are required due to its inexpensive methods of control.

15.3.1 Basic Principles of Three-Phase Induction Motor with Sinusoidal Supply Voltages

Like any electric motor, a three-phase induction motor has a stator and a rotor. The stator carries a three-phase winding (called stator winding) while the rotor carries a short-circuited winding (called rotor winding). Only the stator winding is fed from three-phase supply. The rotor winding derives its voltage and power from the externally energized stator winding through electromagnetic induction and hence such a machine is often called the induction machine. The induction motor may be considered to be a transformer with a rotating secondary in the sense that the power is transferred from the stator (primary) to the rotor (secondary) winding only by mutual induction. Hence, it can, therefore, be described as a "transformer type" a.c. machine in which electrical energy is converted into mechanical energy.

When the stator windings are connected to a set of balanced three-phase voltages and the rotor circuit is closed, the resulting three-phase current establish a rotating *mmf* wave that results in a flux wave of constant amplitude rotating at constant speed known as the synchronous speed. The value of the synchronous speed is fixed by two parameters:

(a)The supply frequency, f_1 (Hertz),
(b)The number of poles p for which the primary is wound.

The synchronous speed n_s of the rotating magnetic field is given by

$$n_s = \frac{120\, f_1}{p} \text{ rpm} \qquad (15.1)$$

The number of poles p must be an even integer since for every north pole there is a corresponding south pole. The following Table-15.1 shows motors speeds for motors with different numbers of poles working with different a.c. supply frequencies.

Table 15.1. Synchronous speed of induction motor for different number of poles.

Rotor Speed (rpm)						
Number of poles (p)	2	4	6	8	10	12
Frequency f = 50 Hz	3000	1500	1000	750	600	500
Frequency f = 60 Hz	3600	1800	1200	900	720	600

An induction motor runs at a shaft speed n that is less than the synchronous speed n_s at which the stator rotating field is rotate. The speed difference $n_s - n$ is called the slip speed. The ratio of slip speed to synchronous speed is the most important variable in induction motor operation and is called the per-unit slip s, and is given by:

$$s = \frac{n_s - n}{n_s} \tag{15.2}$$

where s is the slip in per unit, n_s is the synchronous speed in rpm, and n is the rotor speed. Since the rotor current is proportional to the relative motion between the rotating field and the rotor speed, the rotor current and hence the torque are both directly proportional to the slip. For particular cases, the slip of the motor will have the following special values:

- When the motor is running at synchronous speed , i.e. $n = n_s$ and $s = 0$.
- At standstill $n = 0$ and $s = 1$.
- If the motor is rotating at synchronous speed in the reverse direction, then $n = -n$ and $s = 2$.

Squirrel cage motors are built with the slip ranging from about 3 – 20%. Motors with a slip of 5% or higher are used for hard-to-start applications. A motor with a slip of 5% or less is called a *normal slip* motor. A normal slip motor is often referred to as a *constant speed* motor because the speed changes very little with variations in load. At full load the per-unit slip usually 5% for a small motor because $n \approx 0.95 n_s$.

15.3.2 Development of Circuit Model (Equivalent Circuit) Standstill Operation

At standstill, the motor can be considered as a static transformer with primary (stator) winding and secondary (rotor) winding. If the stator is fed from a three-phase supply with voltage V_1 is the phase voltage, the air gap field produced rotates at synchronous speed n_s . This field induces *emfs* E_1 and E_2 in both the stator and rotor winding respectively. The magnitudes of these *emfs* are given by, assuming unity winding factor (k_w =1) ,

$$E_1 = 4.44\, f_1 N_1 \emptyset \qquad (15.3)$$

$$E_2 = 4.44\, f_1 N_2 \emptyset \qquad (15.4)$$

Therefore
$$\frac{E_1}{E_2} = \frac{N_1}{N_2} = a_{eff} \qquad (15.5)$$

where a_{eff} is the effective transformation (turns) ratio between the stator and rotor winding which is usually greater than unity and is typically in the range 1.1 – 1.3. In slip ring wound rotor motor, a_{eff} is easily defined exactly. However, in cage rotor motor because there is no distinct winding on the cage, the rotor quantities can also be referred to the stator side by taking a_{eff} as unity. The induced voltage E_1 (back *emf*) will be differs from V_1 by the voltage drop in the stator leakage impedance $Z_1 = R_1 + jX_1$ as shown in Fig. 15.2.

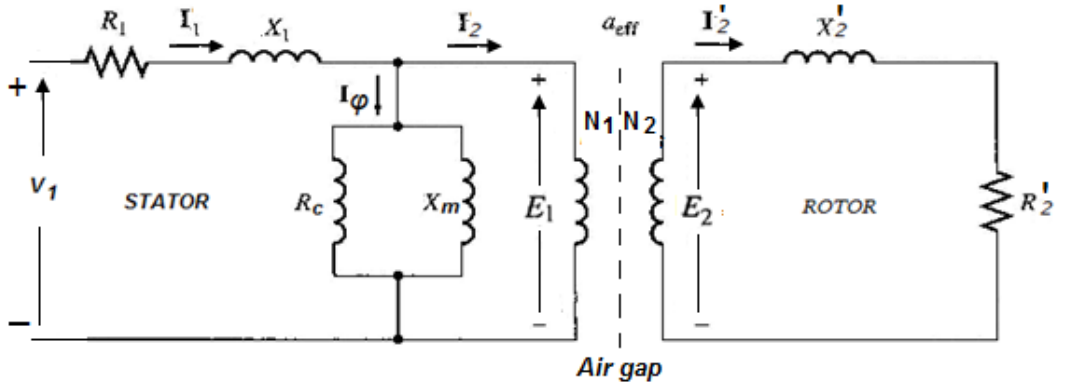

Fig. 15.2 Induction motor per-phase equivalent circuit at standstill.

The stator current I_1 can be resolved into two components: a load component I_2 and an exciting (magnetizing) component I_φ. The load component I_2 produces the rotor *mmf*. The exciting component I_φ is the additional stator current required to create the resultant air-gap flux.
The exciting current I_φ (also called no-load current) is large compared with the transformer because of the air gap (20% - 30% of the full load current for small motors, and 30% - 50% of the full load current for large

motors). I_φ can be resolved into a core-loss component I_c in-phase with E_1 and a magnetizing component I_m lagging E_1 by 90°.
The rotor circuit at standstill consists of E_2 and the rotor leakage impedance $Z'_2 = R'_2 + j\,X'_2$ as shown in Fig.15.2,where in this figure:

V_1 = stator line-to-neutral terminal voltage
E_1 = back *emf* (line-to-neutral) generated by the resultant air-gap flux
stator current I_1
R_1 = stator effective resistance
X_1 = stator leakage reactance at standstill = $2\pi f_1 L_1$
R_c = core loss resistance
X_m = magnetizing branch reactance
X'_2 = rotor leakage reactance at standstill = $2\pi f_1 L_2$
R'_2 = rotor effective resistance at standstill.

Equivalent circuit at running operation

If the rotor conductors rotate at speed n and cut the constant rotating stator flux (which rotates at speed n_s), then at a speed $n_s - n$ the induced *emf* and current in the rotor are of frequency $f_{Rotor} = f_2$, where

$$f_2 = \frac{p}{120}(n_s - n) = \frac{p}{120} s\, n_s = s f_1 \qquad (15.6)$$

Since the flux in the air gap is constant, the secondary *emf* $E_{2(s)}$ at slip s is proportional to the time rate of flux cutting. Hence,

$$E_{2(s)} = 4.44\, f_2 n_s \emptyset = 4.44\, s f_1 n_s \emptyset = s\, E_2 \qquad (15.7)$$

Hence, the exact equivalent circuit at running operation is shown in Fig.15.3.

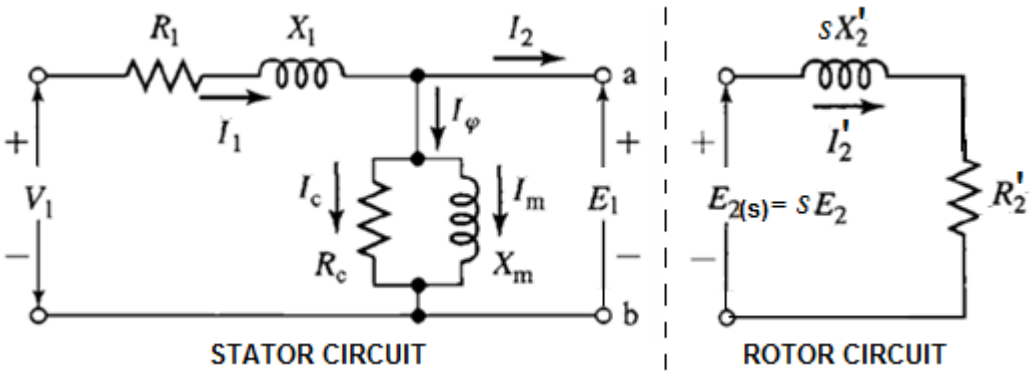

Fig.15.3 The exact equivalent circuit at running operation.

It is clear that, in the equivalent circuit of the rotor of the induction motor shown in Fig.15.3, both the rotor leakage reactance sX'_2 and the back *emf* sE_2, depend on the rotor frequency. But the rotor effective resistance R'_2 doesn't depend on the frequency. Dividing all elements of the equivalent circuit by s, we can obtain the circuit shown in Fig.15.4.

where

R'_2 = rotor effective resistance

X'_2 = rotor leakage reactance

I'_2 = rotor current

E_2 = back *emf* (line-to-neutral) generated by the resultant air-gap flux.

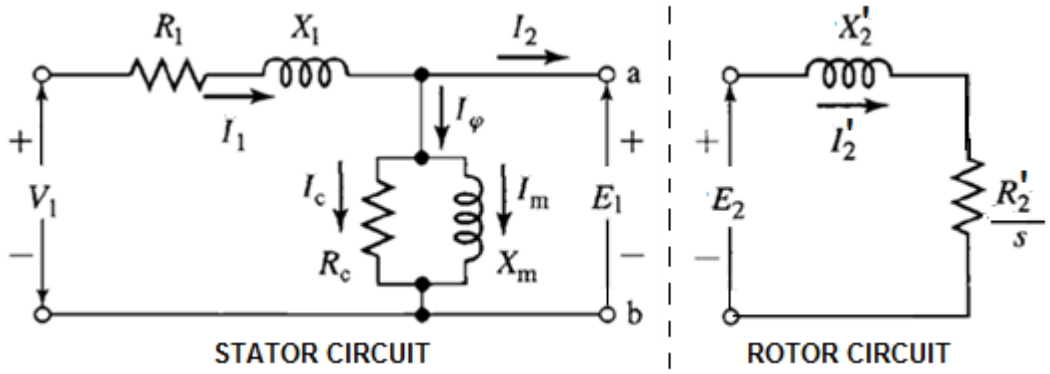

Fig.15.4 Modified exact equivalent circuit at running operation.

To study the performance of induction motor, it is recommended to refer the rotor circuit to the stator circuit similar to that of the transformer, therefore, the overall exact equivalent circuit of the induction motor viewed from the stator is shown in Fig.15.5.

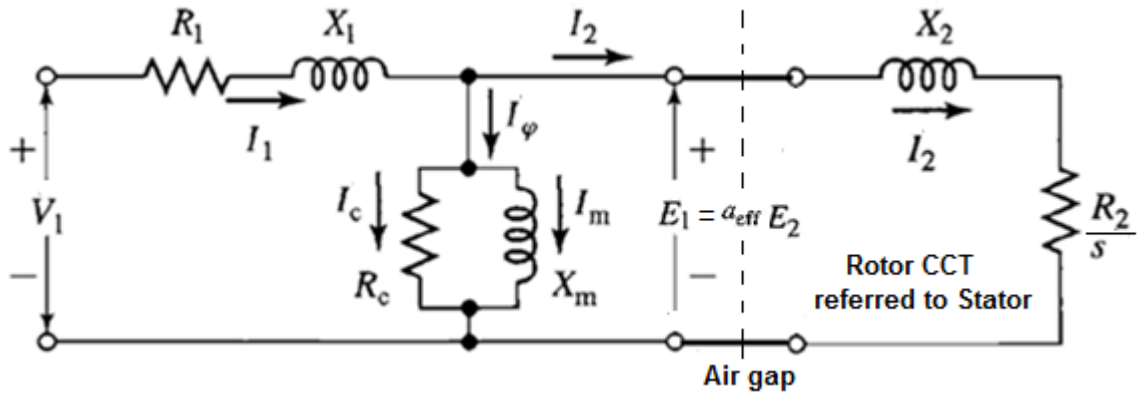

Fig.15.5 Exact equivalent circuit per-phase of a three-phase induction referred to the stator.

15.3.3 The Approximate Equivalent Circuit

In Fig.15.5, the resistance (R_2 / s) can be divided into two resistances R_2 and R_2 (1-s) / s, where R_2 represents the referred rotor resistance and R_2 (1-s) / s represents the mechanical load connected to the motor shaft as shown in Fig.15.6. Now, if the magnetizing branch of R_c and X_m is moved towards the terminal voltage, one can obtain the approximate equivalent circuit as depicted also in Fig.15.6. The equivalent rotor circuit per-phase referred to the stator side is also depicted in Fig.15.7.

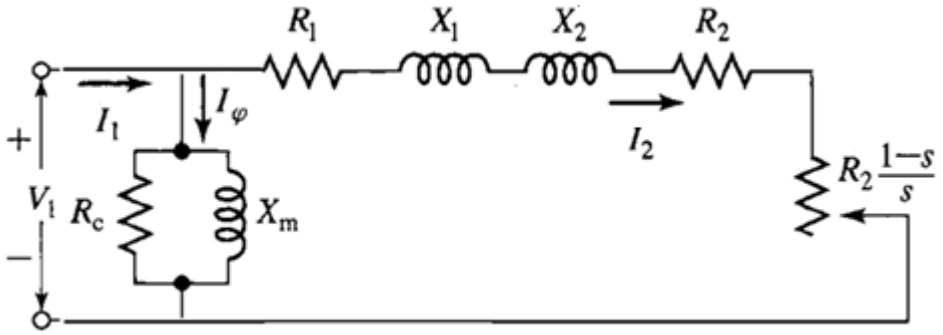

Fig.15.6 Approximate equivalent circuit per-phase of induction motor referred to stator.

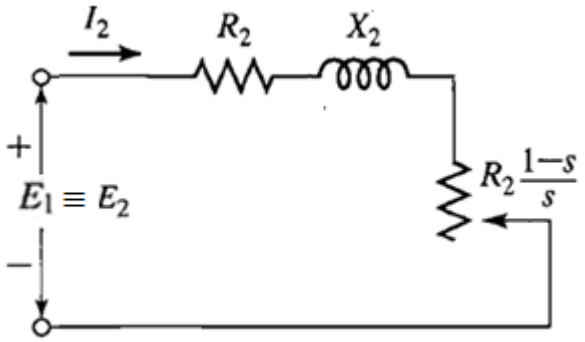

Fig.15.7 The equivalent rotor circuit per-phase referred to the stator.

15.3.4 Power and Torque in Induction Motor

An induction motor can be basically described as a rotating transformer. Its input is a three-phase system of voltages and currents. For an ordinary transformer, the output is electric power from the secondary windings. The secondary windings in an induction motor (the rotor) are shorted out, so no electrical output exists from normal induction motors. Instead, the output is mechanical. The relationship between the input electric power and the output mechanical power of this motor is shown in Fig.15.8.

The input power to an induction motor P_{in} is in the form of three-phase electric voltages and currents. The first losses encountered in the machine are I^2R losses in the stator windings (the stator copper loss P_{SCL}). Then,

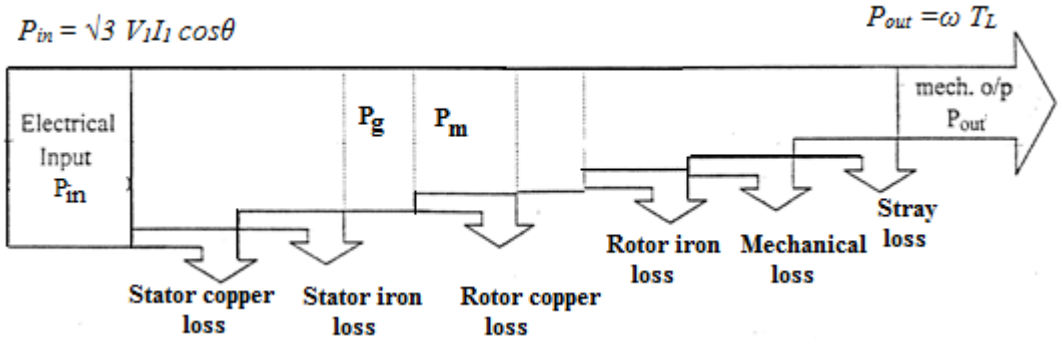

Fig.15.8 Power flow diagram of a three-phase induction motor.

some amount of power is lost as hysteresis and eddy currents in the stator (P_{core}). The power remaining at this point is transferred to the rotor of the machine across the air gap between the stator and rotor. This power is called the air gap power P_{AG} of the machine. After the power is transferred to the rotor, some of it is lost as I^2R losses (the rotor copper loss P_{RCL}), and the rest is converted from electrical to mechanical form ($P_{conv} = P_m$). Finally, friction and windage losses $P_{F\&W}$ and stray losses P_{misc} are subtracted. The remaining power is the output of the motor which is mechanical $P_{out} = \omega T_L$. However, one may simplify the power flow diagram to the form shown in Fig.15.8. This can be validated by considering opposite variations of mechanical loss and rotor iron loss with speed.

By examining the per-phase equivalent circuit, the power and torque equations governing the operation of the motor can be derived. The input current to a phase of the motor is:

$$\mathrm{I}_1 = \frac{\mathrm{V}_1}{\sqrt{(\mathrm{R}_1 + \mathrm{R}_2/s)^2 + (X_1 + X_2)^2}} \qquad (15.8)$$

Thus, the stator copper losses, the core losses, and the rotor copper losses can be found.

The stator copper losses in the three phases are: $P_{SCL} = 3\, I_1^2\, R_1$

The core losses: $P_{core} = 3\, E_1^2 / R_c$

The air-gap power: $P_g = P_{in} - P_{SCL} - P_{core}$

Also, the only element in the equivalent circuit where the air-gap power can be consumed is in the resistor R_2 / s. Thus, the air-gap power:

$$P_g = 3I_2^2 \frac{R_2}{s} \qquad (15.9)$$

The total actual resistive losses in the rotor circuit are given by:

$$P_{RCL} = 3\,(I'_2)^2\,R'_2$$

Since power is unchanged when referred across an ideal transformer, the rotor copper losses can also be expressed as:

$$P_{RCL} = 3\,I_2^2\,R_2 = \mathrm{s}\,P_g$$

where

$$I_2 = \frac{\mathrm{E}_2}{\sqrt{\left(\frac{R_2}{s}\right)^2 + (\mathrm{X}_2)^2}} = \frac{sE_2}{\sqrt{\mathrm{R}_2{}^2 + (\mathrm{sX}_2)^2}} \qquad (15.10)$$

and $$I_2^2 = \frac{s^2E_2^2}{\mathrm{R}_2{}^2 + (\mathrm{sX}_2)^2} \qquad (15.11)$$

After stator copper losses, core losses and rotor copper losses are subtracted from the input power to the motor, the remaining power is converted from electrical to mechanical form. The power converted, which is called developed mechanical power is given as:

$$P_{conv} = P_g - P_{RCL}$$

$$= 3I_2^2\frac{R_2}{s} - 3I_2^2\,R_2$$

$$= 3I_2^2R_2\left(\frac{1}{s} - 1\right)$$

$$\therefore P_{conv} = 3I_2^2R_2\left(\frac{1-s}{s}\right)$$

$$= P_m \text{ (Mechanical developed power)} \qquad (15.12)$$

The rotor copper losses can be given to be equal to the air-gap power times the slip : $P_{RCL} = s\,P_g$. Hence, the lower the slip of the motor, the lower the rotor losses. Also, if the rotor is not turning, the slip is s =1 and the air-gap power is entirely consumed in the rotor. This is logical, since if the rotor is not turning, the output power P_{out} (= $\omega_m\,T_L$) must be zero. Since $P_{conv} = P_g - P_{RCL}$, this also gives another relationship between the air-gap power and the power converted from electrical and mechanical form:

$$P_m = P_g - P_{RCL}$$
$$= P_g - s\,P_g$$
$$P_m = (1- s)\,P_g \qquad (15.13)$$

Note that the proportion of the above quantities is fixed by "s".

Finally, if the friction and windage losses and the stray losses are known, the output power:

$$P_o = P_m - P_{F\&W} - P_{misc} \qquad (15.14)$$

The induced torque in a machine was defined as the torque generated by the internal electric to mechanical power conversion. This torque differs from the torque actually available at the terminals of the motor by an amount equal to the friction and windage torques in the machine. Hence, the developed torque is:

$$T_d = \frac{P_m}{\omega_m} \qquad (15.15)$$

or it can be expressed as

$$T_d = \frac{(1-s)P_g}{(1-s)\omega_s}$$

The output or load torque T_L per-phase can be found from Eq.(15.15) as

$$T_L = \frac{P_o}{\omega} \qquad (15.16)$$

$$T_L = \frac{P_o}{\omega_s(1-s)} = \frac{P_g}{\omega_s} = \frac{I_2^2}{\omega_s}\frac{R_2}{s}$$

Substitute for I_2^2 from Eq.(15.11),

$$T_L = \frac{1}{\omega_s} \times \frac{sE_2{}^2\,R_2}{R_2{}^2 + (sX_2)^2} \qquad (15.17)$$

or $$T_L = \frac{I_2^2}{\omega}\,\frac{R_2}{s}(1-s) \qquad (15.18)$$

From Eq.(15.18), it is revealed that:

(i) At synchronous speed, i.e. when slip *s* is zero, the torque is zero so the torque-speed curve or the external characteristic of the induction motor start from the origin as shown in Fig.15.9.

(ii) At very low slip, i.e. the motor speed near the synchronous speed, the term sX_2 is very small and can be neglected. Therefore, the torque is approximately proportional to the slip and the relation between the torque and speed is approximately straight line.

(iii) When the motor is loaded, the speed will drop and the slip increases and for further increase in the load, torque will reach its maximum value T_m which also called the breakdown torque.

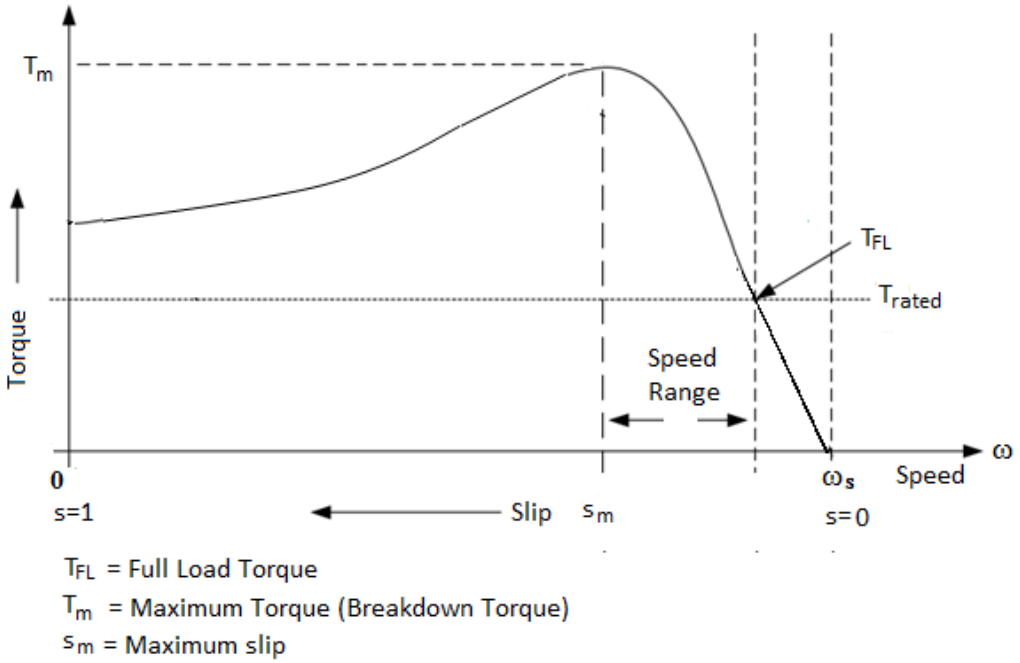

Fig.15.9 Torque-speed curve of an induction motor.

(iv) With further drop in speed due to increase in the load ,slip will increase and if the load increases beyond maximum torque that the motor cold tolerate , the motor start slows down and finally it becomes at stopping position. The value of the torque that results in motor stopping is called the pull-up torque as shown in Fig.15.9.

From the approximate circuit of Fig.15.4, the current I_2 can be expressed in terms of the primary voltage V_1 as

$$I_2 = \frac{V_1}{\sqrt{\left(R_1 + \frac{R_2}{s}\right)^2 + (X_1 + X_2)^2}} \qquad (15.19)$$

Substituting Eq.(15.19) into Eq.(15.18) gives

$$T_{\mathrm{L}}=\frac{\mathrm{V_1}^2}{s\omega_s}\times\frac{R_2}{(R_1+\frac{R_2}{s})^2+(X_1+\mathrm{X_2})^2} \tag{15.20}$$

In Eq.(15.20) slip s is the only variable, hence maximum torque can be found by differentiating this equation with respect to s and equating to zero to give the result the slip s_m at which the peak torque occurs as

$$s_m=\frac{R_2}{\sqrt{\mathrm{R_1}^2+X^2}}\cong\frac{R_2}{X} \tag{15.21}$$

where X = motor total reactance = X_1+X_2 .

Substituting Eq.(15.21) into Eq.(15.20) gives an expression maximum torque T_m (sometimes called the peak torque or breakdown torque)

$$T_{\mathrm{m}}=\frac{\mathrm{V_1}^2}{2\omega_s}\times\frac{R_2}{\sqrt{(R_1)^2+(X_1+\mathrm{X_2})^2}+R_1}\cong\frac{\mathrm{V_1}^2}{2\omega_s X} \tag{15.22}$$

15.4 SPEED CONTROL OF INDUCTION MOTOR

The three-phase induction motor runs at a speed slightly less than synchronous speed and is load dependents. Therefore, it is an inherently a constant speed motor and its output mechanical power depends on the slip s ($P_o=T_L\omega=T_L(1-s)\omega_s$). So it is difficult to control its speed. The speed control of induction motor is done at the cost of decrease in efficiency and low electrical power factor. Before discussing the methods to control the speed of three-phase induction motor one should know the basic formulas of speed and torque of three-phase induction motor as the methods of speed control depends upon these formulae.

The synchronous speed was given by Eq.(15.1) as $n_s\propto\frac{f}{p}$, where f = frequency and p is the number of pole. The speed of induction motor is given by,

$$\mathrm{n}=n_s(1-s) \tag{15.23}$$

Hence, the speed of the induction motor can be changed either from the stator or from the rotor sides. Therefore, from Eq.(15.1), the speed control of three-phase induction motor from stator side are classified as:

1. Changing the number of stator poles (p).
2. Stator voltage control (controlling the supply voltage (V_1)).
3. Supply frequency changing:

(i) Variable-voltage, variable-frequency (V/f) control.
(ii) Variable-current, variable-frequency (I/f) control.

The speed controls of three-phase induction motor from rotor side are further classified as:

1. Adding external resistance on rotor side.
2. Rotor injected voltage / slip energy recovery.
3. Cascade control method.

These methods are sometimes called scalar controls to distinguish them from vector controls. The torque-speed characteristics of the motor differ significantly under different types of control.

15.4.1 Speed Control from Stator Side

(1) Changing the number of stator poles (p)

The stator poles can be changed by three methods

(i) Method of varying the number of consequent poles
(ii) Multiple stator winding method
(iii) Pole amplitude modulation method (PAM)

Method of varying the number of consequent poles: In this method, the number of poles can be changed in the ratio of 2:1 by changing the connection of the coils. Fig.15.10 shows the stator connections for two-speed operation of the thee-phase induction motor. The windings can be connected in series or in parallel.

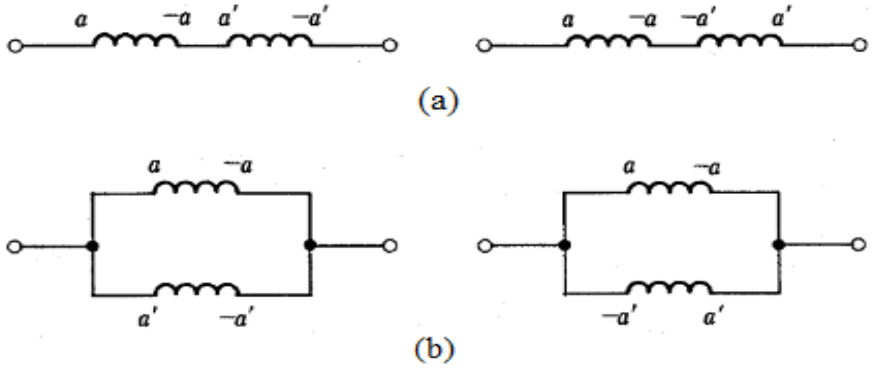

Fig.15.10 Stator windins connections for two-speed operation of induction motor: (a) Series connection, (b) Parallel connection.

Multiple-stator winding method: In this method of speed control of three-phase induction motor, the stator is provided by two separate winding. These two stator windings are electrically isolated from each other and are wound for two different pole numbers. Using switching arrangement, at a time, supply is given to one winding only and hence speed control is possible.

The disadvantage of this method is that, it enable speed changes in terms of 2:1 ratio steps, hence to obtained variations in speed, multiple-stator windings has to be applied. Multiple-stator windings have extra sets of windings that may be switched in or out to obtain the required number of poles. Unfortunately this would an expensive alternative.

Pole amplitude modulation method (PAM): In this method, the original sinusoidal *mmf* wave is modulated by another sinusoidal *mmf* wave having different number of poles. To explain the method, let :

$f_1(\theta)$ be the original *mmf* wave of induction motor whose speed is to be controlled.

$f_2(\theta)$ be the modulation *mmf* wave.

P_1 be the number of poles of induction motor whose speed is to be controlled.

P_2 be the number of poles of modulation wave so that,

$$f_1(\theta) = \mathrm{F}_1 \sin\left(\frac{\mathrm{P}_1\theta}{2}\right) \quad \text{and} \quad f_2(\theta) = \mathrm{F}_2 \sin\left(\frac{\mathrm{P}_2\theta}{2}\right)$$

After modulation, i.e. multiplying $f_1(\theta)$ by $f_1(\theta)$, the resultant *mmf* wave is

$$F_r(\theta) = F_1 F_2 \sin\left(\frac{P1\theta}{2}\right) \sin\left(\frac{P2\theta}{2}\right)$$

Apply formula for: $2\sin A \sin B = \cos\frac{A-B}{2} - \cos\frac{A+B}{2}$

So we get, resultant *mmf* wave

$$F_r(\theta) = F_1 F_2 \frac{\cos\frac{(P_1 - P_2)\theta}{2} - \cos\frac{(P_1 + P_2)\theta}{2}}{2} \qquad (15.24)$$

Therefore, the resultant *mmf* wave will have two different numbers of poles,i.e.

$$P_{11} = P_1 - P_2 \quad \text{and} \quad P_{22} = P_1 + P_2$$

Hence, by changing the number of poles we can easily change the speed of three-phase induction motor.

(2) Controlling supply voltage (Variation of stator voltage)

It is seen from Eq.(15.17) that at any fixed speed, if we neglect the mechanical losses, the developed torque T_L (=T_d) is proportional to the square of the applied stator voltage V_1^2. As the stator voltage is reduced the rotor speed decreases and the maximum torque available from the motor also decreases, Eq.(15.19). If the stator voltage is varied to control the speed then the speed range of this method is limited with a constant-torque load. This can be proved as follows:

The torque produced by running three-phase induction motor was given by Eq.(15.17) as

$$T_L \propto \frac{s\,E_2^2\,R_2}{R_2^2+(sX_2)^2}$$

In low slip region $(sX_2)^2$ is very small as compared to $(R_2)^2$, hence it can be neglected. Therefore the torque becomes,

$$T_L \propto \frac{s\,E_2^2}{R_2} \qquad (15.25)$$

Since rotor resistance, R_2 is constant so the equation of torque further reduces to

$$T_L \propto s\,E_2^2$$

We know that rotor induced *emf* $E_2 \propto V_1$, the supply voltage. So,

$$T_L \propto s\,V_1^2 \qquad (15.26)$$

From the equation above, it is clear that if the supply voltage is decreased voltage by one half the torque reduces to one quarter.Therefore, the low speed performance of the motor with this method is poor because motor current at a given slip is also proportional to the applied voltage whereas the torque varies as the square of the voltage.This means that the torque per ampere becomes lower at reduced speed as large currents are required to develop a sufficient torque. However, in fan or pump drives, the load torque varies approximately as the square of the speed. Hence the torque required for low speed operation and starting is small and may obtained without excessive overheating from a voltage controlled induc-tion motor.

Methods of reducing stator voltage V_1

1- Rheostatic control : The stator voltage can be reduced by conecting external variable resistance or impedance between stator terminals and the a.c. supply as shown in Fig.15.11. Saturable reactors have been used in the past to perform this function.

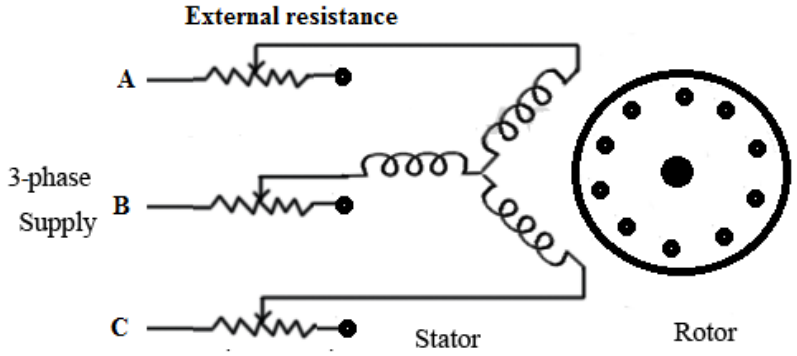

Fig.15.11 Speed control of three-phase induction motor by adding rheostat in the stator circuit.

A high resistance modifies the torque-speed characteristics and a wide range of speed control is obtained. The ohmic losses of this method of speed control are excessive and particularly at low speeds. Since the torque produced in an induction motor is proportional to the square of the supply voltage ($T \propto s\ V_1^2$), then if we decrease V_1, the supply voltage, torque will also decrease. However, this method is not efficient from energy saving point of view and it is rarely used nowadays because small change in speed requires large reduction in voltage, and hence the current drawn by motor increases, which cause overheating of induction motor.

.

2- Electronic control: Nowadays, reduction of stator voltage is performed by using thyristors (or triacs) that offers several advantages. With thyristors different techniques can be used to control the *rms* voltage applied to the motor. Thyristor can be used as:

- AC regulators
- Transformer adjustable tap changers
- Controllers for multi-winding transformer secondary

Reduction of stator voltage of induction motor using three-phase thyristor a.c. regulator is shown schematically in Fig.15.12. When the motor is supplied by balance three-phase voltages of constant frequency, the torque speed characteristics of the motor have the shape shown in Fig.15.13. Now if the supply voltage is reduced by one half, the maximum torque reduces to one quarter of its original value since the maximum torque is also proportional to $|V_1^2|$ as described previously.

The operating point of an induction motor can be located on the torque speed characteristics diagram and it is defined by the point of intersection between the motor characteristics and the load characteristic as shown in Fig.15.13. For small reduction in supply voltage the speed variation will be very small, so that, for example, point 2 in Fig.15.13 is not shown.

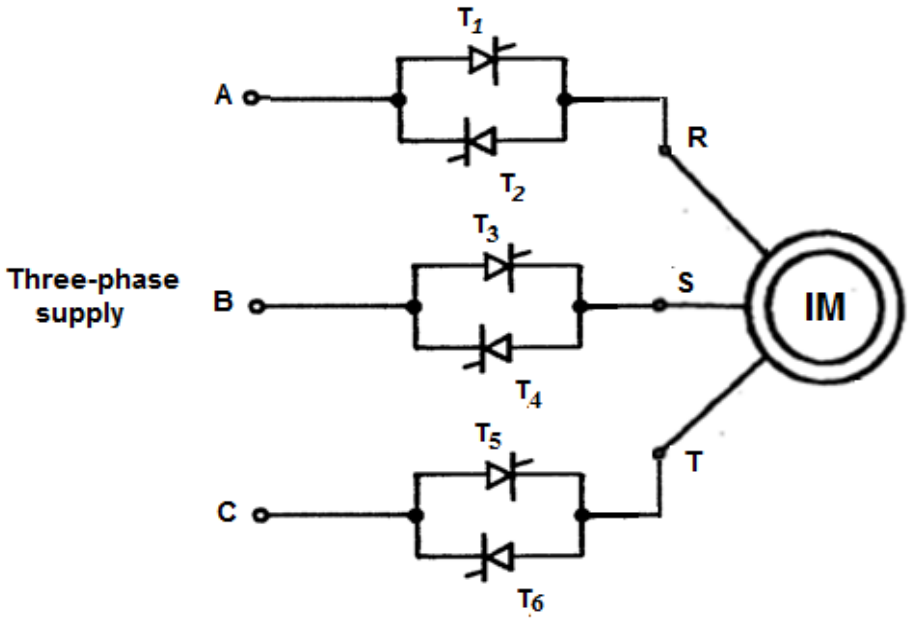

Fig.15.12 Reduction of stator voltage of induction motor using three-phase thyristor a.c. regulator.

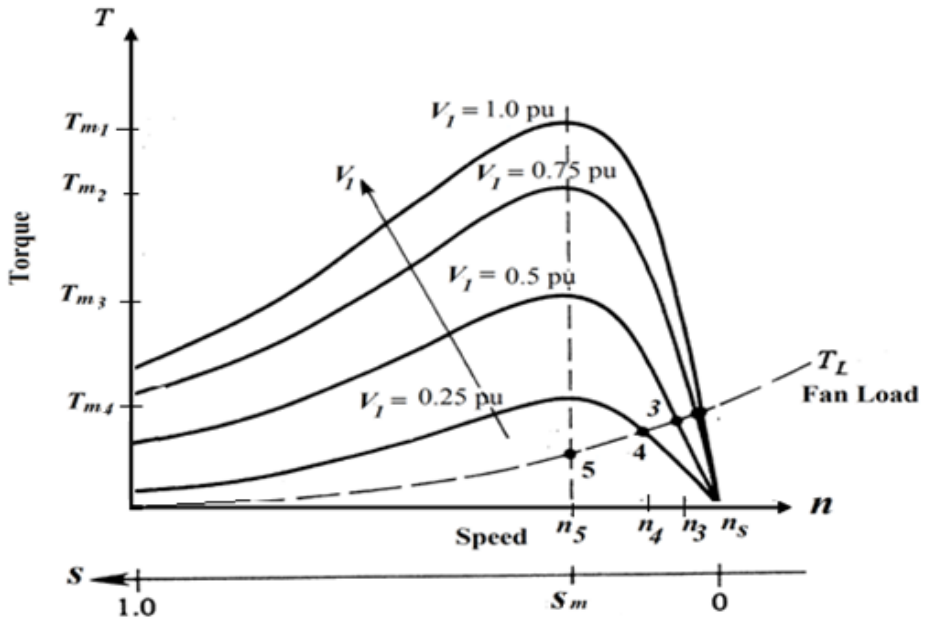

Fig .15.13 Torque-speed characteristic of three-phase induction motor for voltage control with fan load.

The waveform of the motor currents for the connection of Fig.15.12 are very similar to corresponding waveforms for passive series *R-L* load discussed in Chapter Five .The performance analysis of the motor with its thyristor controller would be very complex due to the interaction between the motor and its controller. The accurate analysis would require solution

of several nonlinear differential equations for the voltage, speed and electromagnetic torque. The general solution is only possible using computer simulation techniques such as Matlab and other computer programmes. However, for steady-state solution using the approximate equivalent circuit of Fig.15.6 one can find the performance of the three-phase induction motor when speed controlled by voltage variation technique as illustrated in the following example.

Example 15.1

A 7.5 kW, three-phase, 400 V, 50 Hz, 4-pole, 1400 rpm, star-connected induction motor has the following parameters referred to the stator side:

$R_1 = 2\ \Omega$, $R_2 = 6\ \Omega$, $X_1 = 5.75\ \Omega$, $X_2 = 4.25\ \Omega$, X_m = Very high

The speed of the motor is controlled by voltage variation method using pair of inverse parallel connected thyristors in each line with symmetrical phase angle triggering mode. The delay angles of the thyristors are set to give a line to line voltage of 250 V across the motor windings. Calculate the motor speed, current and torque when driving a fan load its characteristic is given by:

$$T_L = 60\ (1\text{-}s)^2$$

Solusion

Using Eq.(15.20), the torque of the three-phase induction motor for the three phases is

$$\mathrm{T}= \frac{3\mathrm{V}_1{}^2}{s\omega_s} \times \frac{R_2}{(R_1 + \frac{R_2}{s})^2 + (X_1 + \mathrm{X}_2)^2}$$

n_s = Synchronous speed in rpm = $120\,f$ / p = 120×50 /4 =1500.

$$\omega_s = \frac{2\pi n_s}{60} = \frac{2\pi \times 1500}{60} = 50\pi \text{ rad/s}$$

$$\mathrm{T} = \frac{3}{50\pi s} \times \frac{250^2 \times 6}{(2 + \frac{6}{s})^2 + (5.75 + 4.25)^2} = \frac{7165.6\,s}{(104s^2 + 24s + 36)}$$

At steady-state, $T = T_L$, hence

$$\frac{7165.6\,s}{(104s^2+24s+36)} = 60\,(1-s)^2$$

From which ;

$$\therefore \quad 104s^4 - 184s^3 + 92s^2 - 191.42s + 36 = 0$$

Which gives ; s = 0.2005

The torque produced by the motor is

$$T = 60\,(1-0.2005)^2 = 38.35 \text{ Nm}$$

The speed of the motor at 250V is

$$n = n_s\,(1-s)^2 = 1500(1-0.2005)^2 = 958 \text{ rpm}$$

The line current is calculated from Eq.(15.8) ,since X_m is very high , thus $I_1 = I_2$,

$$I_1 = I_2 = \frac{\mathrm{V}_1}{\sqrt{\left(R_1 + \frac{R_2}{s}\right)^2 + (X_1 + \mathrm{X}_2)^2}}$$

$$\therefore \qquad I_1 = \frac{250}{\sqrt{\left(2 + \frac{6}{0.2005}\right)^2 + (10)^2}} = 7.4 \angle 17.35° \text{ A}$$

Approximate method of solution

It is seen from the above example that the equation of the slip *s* obtain is of high order that is mathematically difficult to solve. However, an approximate method of solution for steady-state operation can be used over a range of average speeds to determine the corresponding range of thyristor firing angles. This approximate method uses the motor fundamental equivalent circuit together with the curves giving the relation between the per unit current and the firing angles for both particular speed and load angles. These curves are shown in Fig.15.14(a) and can be approximated by straight line as depicted in Fig. 15.14(b).

For star-connected motors with large phase angle ϕ, the approximated straight line relationship between the current and firing angle α can be represented mathematically as

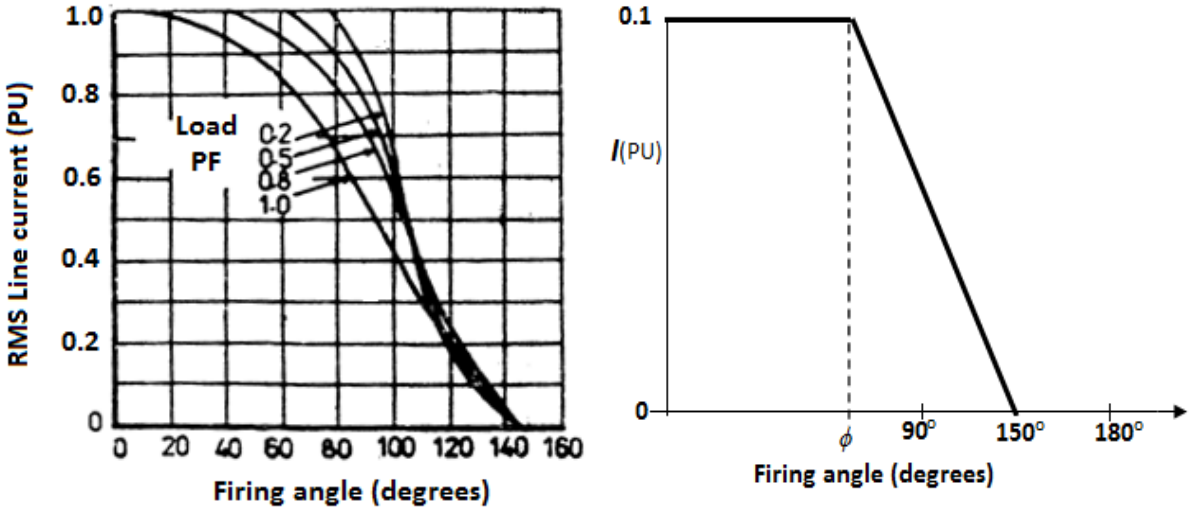

(a) (b)

Fig. 15.14 Current and the firing angles relationship for three-phase star connected *R-L* load : (a) *Rms* line current versus α, (b) Straight line approximation of current (p.u.) for three-wire star-connected induction motor.

$$I(pu) = \frac{150 - \alpha}{150 - \emptyset} \qquad (15.27)$$

For branch-delta connected motor, the approximate relation is found to be roughly as

$$I(pu) = \frac{180 - \alpha}{180 - \emptyset} \qquad (15.28)$$

Example 15.2

A variable speed drive is used to drive a water pump which has a torque-speed curves described by the equation $T_L = 0.005\,\omega^2$ SI units, where ω is the speed of the pump motor. The drive employs a three-phase, 240V, six-pole, 50 Hz, star-connected induction motor controlled by pairs of inverse-parallel connected thyristors in each supply line. The per-phase equivalent circuit parameters of the motor, referred to primary turns are $R_1 = 0.3\ \Omega,\ R_2 = 0.2\ \Omega, X_1 = X_2 = 0.6\ \Omega,\ X_m =$ infinity. The required speed range is 975 - 600 rpm. Use performance curves of current versus firing-angle to calculate, approximately, the necessary ranges of thyristor firing-angles.

Solution

The synchronous speed of the motor n_s

$$n_s = \frac{120\, f_1}{p} = \frac{120 \times 50}{6} = 1000\, rpm$$

The slip is given by Eq.(15.2) as

$$s = \frac{n_s - n}{n_s}$$

Hence

$$s_1 = \frac{1000 - 975}{1000} = 0.025$$

$$s_2 = \frac{1000 - 600}{1000} = 0.4$$

From Eq.(15.13) , the output power for the three phases of the motor is

$$P_o = \omega T_L = 3I_2^2 R_2 \left(\frac{1-s}{s}\right)$$

$$\frac{R_2}{s_1} = \frac{0.2}{0.025} = 8\ \Omega$$

$$\frac{R_2}{s_2} = \frac{0.2}{0.4} = 0.5\ \Omega$$

From the equivalent circuit of Fig.15.6, neglecting the magnetising branch,

$$Z_{in1} = (0.3 + 8) + j1.2 = 8.4\ \angle 8.25^\circ\ \Omega$$

$$Z_{in2} = (0.3 + 0.5) + j1.2 = 1.44\ \angle 56.12^\circ\ \Omega$$

$$T_{L975} = \omega^2/200 = \frac{(975 \times \frac{2\pi}{60})^2}{200} = 52.124\ \text{Nm}$$

$$I = I_2 = \sqrt{\frac{\omega T_{L975} s}{3R_2(1-s_1)}} = \sqrt{\frac{975 \times \frac{2\pi}{60} \times 52.124 \times 0.025}{3 \times 0.2 \times (1 - 0.025)}} = 15.1\ \text{A}$$

$$I_{base} = \frac{240}{\sqrt{3}} \times \frac{1}{8.4} = 16.5 \text{ A}$$

$$I_{pu} = \frac{15.1}{16.5} = 0.989$$

From Fig,15.14 (a) ,

$$PF_1 = \cos 8.25° = 0.989 \qquad \rightarrow \qquad \alpha_1 = 50°.$$

$$T_{L600} = \omega^2/200 = \frac{(600 \times \frac{2\pi}{60})^2}{200} = 19.74 \text{ Nm}$$

$$I = \sqrt{\frac{\omega T_{L600}\, s}{3R_2(1-s_2)}} = \sqrt{\frac{600 \times \frac{2\pi}{60} \times 19.74 \times 0.4}{3 \times 0.2 \times (1-0.4)}} = 37.12 \text{ A}$$

$$I_{base} = \frac{240}{\sqrt{3}} \times \frac{1}{1.44} = 96.23 \text{ A}$$

$$I_{pu} = \frac{37.122}{96.23} = 0.386$$

From Fig,15.14 (a),

$$PF_2 = \cos 56.12° = 0.557 \qquad \rightarrow \qquad \alpha_2 = 110°.$$

Therefore, the range of the delay angles is: $50° \leq \alpha \leq 110°$.

It is obvious that, with this method of speed control, the variation of speed is not great (if the voltage reduced to ½) . It generates harmonics and electromagnetic interferences. However, the method for obtaining speed change is simple and energy saving is possible.

Example 15.3

A fuel pump has load characteristics represented in the speed range by a line given by

$$T_L = \frac{\omega^2}{500} - \frac{\omega^3}{10^6}$$

where ω = motor speed.

A three-phase, 240 V, four-pole, 50 Hz, star-connected, squirrel-cage induction motor is to be used for the speed control of the fuel pump. Per-phase equivalent circuit parameters of the motor, referred to primary turns, are $R_1 = 0.3\,\Omega$, $R_2 = 0.2\,\Omega$, $X_1 = X_2 = 0.72\,\Omega$, $X_m =$ very large. The motor terminal voltages are to be controlled by pairs of inverse-parallel connected thyristors in the supply lines. If steady-state speed control is required in the range 750 - 1450 rpm, calculate the necessary range of thyristor firing-angles.

Solution

The synchronous speed of the motor n_s

$$n_s = \frac{120\,f_1}{p} = \frac{120 \times 50}{4} = 1500 \text{ rpm}$$

The slip is given by Eq.(15.2) as

$$s = \frac{n_s - n}{n_s}$$

Hence

$$s_1 = \frac{1500 - 750}{1500} = 0.5$$

$$s_2 = \frac{1500 - 1450}{1500} = 0.033$$

From Eq.(15.10), the output power for the three phases of the motor is

$$P_o = \omega T_L = 3I_2^2 R_2 \left(\frac{1-s}{s}\right)$$

$$\frac{R_2}{s_1} = \frac{0.2}{0.5} = 0{,}4\,\Omega$$

$$\frac{R_2}{s_2} = \frac{0.2}{0.033} = 6\,\Omega$$

From the equivalent circuit of Fig.15.6, neglecting the magnetising branch,

$$Z_{in1} = (0.3 + 0.4) + j1.44 = 1.6\,\angle 64^\circ\,\Omega$$

$$Z_{in2} = (0.3 + 6) + j1.44 = 6.5 \angle 12.9° \, \Omega$$

$$T_{L750} = \omega^2/200 = \frac{(750 \times \frac{2\pi}{60})^2}{500} - \frac{(750 \times \frac{2\pi}{60})^2}{10^6} = 11.9 \text{ Nm}$$

$$I = I_2 = \sqrt{\frac{\omega T_{L975} s}{3R_2(1 - s_1)}} = \sqrt{\frac{750 \times \frac{2\pi}{60} \times 11.9 \times 0.5}{3 \times 0.2(1 - 0.5)}} = 39.4 \text{ A}$$

$$I_{base} = \frac{240}{\sqrt{3}} \times \frac{1}{Z_{in1}} = \frac{240}{\sqrt{3}} \times \frac{1}{1.6} = 86.6 \text{ A}$$

$$I_{pu} = \frac{39.4}{86.6} = 0.455$$

From Fig,15.14 (a),

$$PF_1 = \cos 64° = 0.438 \qquad \rightarrow \qquad \alpha_1 = 105°.$$

$$T_{L1450} = \omega^2/200 = \frac{(1450 \times \frac{2\pi}{60})^2}{500} - \frac{(1450 \times \frac{2\pi}{60})^2}{10^6} = 42.6 \text{ Nm}$$

$$I = \sqrt{\frac{\omega T_{L1450} s}{3R_2(1 - s_2)}} = \sqrt{\frac{1450 \times \frac{2\pi}{60} \times 42.6 \times 0.033}{3 \times 0.2(1 - 0.033)}} = 19.27 \text{ A}$$

$$I_{base} = \frac{240}{\sqrt{3}} \times \frac{1}{6.5} = 21.32 \text{ A}$$

$$I_{pu} = \frac{19.27}{21.32} = 0.386$$

From Fig.15.14 (a),

$$PF_2 = \cos 12.9° = 0.974 \qquad \rightarrow \qquad \alpha_1 = 50°.$$

3- Supply frequency changing: This method of speed control of induction motor is considered as the most efficient one. The motor is supplied from variable voltage variable frequency source. This is because, in the three-phase induction motor , *emf* is induced by induction similar to that of transformer which is given by

$$E \text{ or } \cong V = 4.44\,\emptyset\, KNf \qquad \text{or} \qquad \emptyset = \frac{V}{4.44\,K\,N\,f}$$

Where K is the winding constant, N is the number of turns per phase and f is frequency. Now since (4.44 K N) is a constant value for any induction motor, therefore the above equation can be written as,

$$\emptyset \propto V/f \qquad \text{or} \qquad \emptyset \propto E/f \qquad (15.29)$$

It is clear from the above equation that, if we change the frequency. the synchronous speed will change (n_s= 120 f / p). So if the frequency is decreased the flux will increase and this change in flux causes saturation of rotor and stator cores that causes increase in no load current of the motor. Hence, it is important to maintain flux, φ constant and this is only possible if the value of the voltage V is changed to keep the ratio of (V / f) as constant. Hence, this technique is known as constant (V / f) method. For controlling the speed of three-phase induction motor by (V/f) method it is necessary to supply variable voltage and frequency which is easily obtained by using converter using solid-state devices / power electronics which has the ability of providing such requirement.

So far, we have calculated torque-speed relationships at single supply frequencies, now we need to find how the torque changes with changing frequency. Consider the circuit diagram shown in Fig.15.15, which shows the induction machine equivalent circuit in terms of inductances, rather than reactances at any effective frequency f_e :

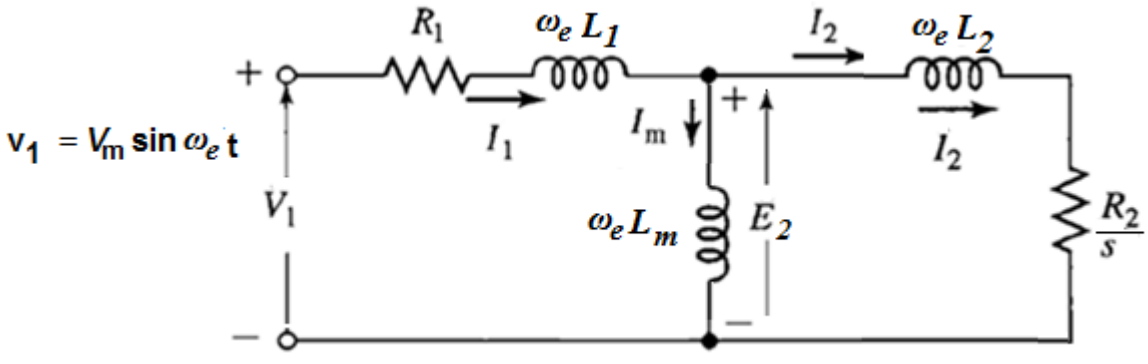

Fig.15.15 Equivalent circuit per-phase for the induction motor in terms of inductace.

Now, from analysis with a constant frequency supply we know that the torque is given by:

$$T_L = \frac{P_o}{\omega} = \frac{I_2^2}{\omega_s}\frac{R_2}{s}$$

$$\text{or} \qquad T_L = \frac{1}{\omega_s} \times \frac{sE_2{}^2 R_2}{R_2{}^2 + (sX_2)^2} = \frac{1}{\omega_s} \times \frac{E_2{}^2 R_2}{\frac{R_2{}^2}{s} + (\omega_e L_2)^2}$$

$$\omega_s = \frac{f_e}{P} \quad \text{rev/s} \qquad (15.30(a))$$

$$\rightarrow \quad \omega_s = \frac{f_e}{P} \times 2\pi = \frac{\omega_e}{P} = \frac{2}{p}\ \omega_e \ \text{rad/s} \qquad (15.30(b))$$

$$\rightarrow \quad n_s = \frac{60 f_e}{P} = \frac{120 f_e}{p} \ \text{rpm} \qquad (15.31)$$

where

$\omega_e = 2\pi f_e$ angular frequency of the supply
p = number of poles
P = number of pole pairs = 2 p.

At small values of slip it is reasonable to say that

$$\frac{R_2}{s} \gg \omega L_2 \qquad \rightarrow \qquad T_L \cong \frac{sE_2{}^2}{\omega_s R_2}$$

and, from Eq.(15.31(b)) $\omega_s = \frac{2}{p}\ \omega_e$, we can re-write this in terms of electrical supply frequency:

$$T_L \cong \frac{p\ sE_2{}^2}{2\ \omega_e R_2} \qquad (15.32)$$

At this point, it is useful to introduce the concepts of *slip frequency* and *slip speed*.

Slip Speed and Slip Frequency

Define simply, slip speed and slip frequency are:

- Slip speed = slip multiplied by synchronous speed
- Slip frequency = slip multiplied by supply frequency

Slip speed may be defined in either rpm (sn_s) or mechanical radians per second ($s\omega_s$).

Slip frequency is usually given in electrical radians per second as

$$\text{Slip frequency } = \omega_{sl} = s\omega_e = \frac{p}{2}\, s\omega_s = \frac{p}{2}\,\frac{2\pi}{60} n_s \qquad (15.33)$$

Note that slip frequency has its own symbol, while slip speed is actually written as the product of slip and synchronous speed.

Now multiplying top and bottom of the torque Eq. (15.32) by ω_e yields

$$T_{\mathrm{L}} \cong \frac{p\ \mathrm{s}\ \omega_e}{2\ R_2}\left(\frac{\mathrm{E_2}^2}{\omega_e^2}\right) \qquad (15.34)$$

Torque as a function of slip speed

From the above, we can now re-write the torque as:

$$T_{\mathrm{L}} \cong \frac{p}{2\ R_2}\left(\frac{\mathrm{E_2}^2}{\omega_e^2}\right) \omega_{sl}$$

It can be seen that, if the ratio E_2 /ω_e is constant the torque will be proportional to slip frequency. Considering another approach to define E_2 from the equivalent circuit:

$$E_2 = j\omega_e L_m\, I_m$$

$$\left|\frac{E_2}{\omega_e}\right| = L_m\, I_m = \lambda \text{ (flux linkage)} \qquad (15.35)$$

where λ is the magnetizing flux in the machine. Substituting we get:

$$T_{\mathrm{L}} \cong \frac{p}{2\ R_2}\lambda^2 \omega_{sl} \qquad (15.36)$$

This is an important result: *At small slips* torque is proportional to flux squared times slip speed

$$T_{\mathrm{L}} \propto \lambda^2\ s\ n_s \qquad (15.37)$$

It is clear from Eq.(15.37) that the maximum torque is independent on frequency at a given flux λ. The torque-speed characteristics of induction motor operates with variable voltage variable frequency source is depicted in Fig.15.16. One great advantage of this method is that the value of the maximum torque for any frequency $f_1, f_2, \ldots\ldots, f_{\mathrm{n}}$ remains constant. This feature is very desirable in many industrial application for speed control.

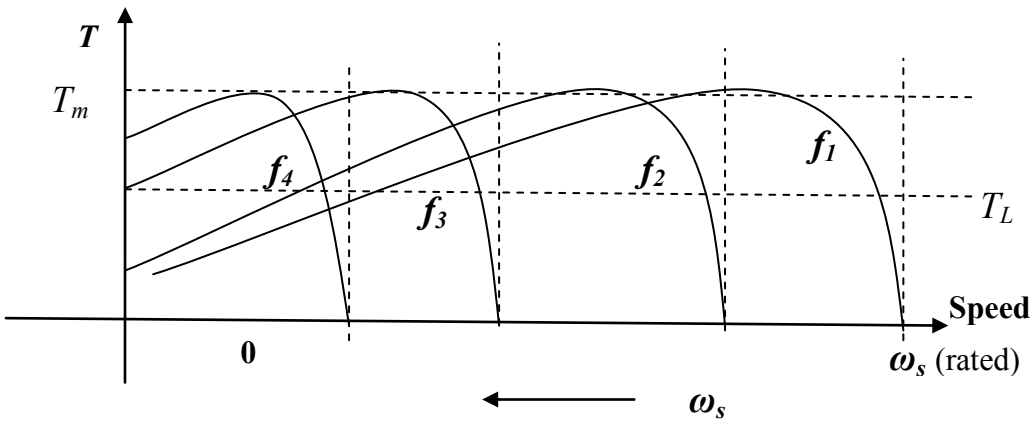

Fig.15.16 Torque-frequency relationship.

Example 15.1

A 400 V, 50 Hz, 4-pole motor has rated speed of 1450 rpm and rated torque of 10 Nm. If a torque of 10 Nm is needed at a mechanical speed of 1250 rpm, find the synchronous speed, supply frequency and line-to-line supply voltage.

Solution

At rated torque, the slip speed will be the rated value. For a 4-pole 50 Hz machine, synchronous speed is 1500 rpm, therefore, rated slip speed = 1500-1450 = 50 rpm. When operating at 1250 rpm, 10 Nm, slip speed will still be 50 rpm and the synchronous speed is given by

$$n_s = n_m + sn_s$$

$$n_s = 1250 + 50 = 1300 \text{ rpm}$$

With the synchronous speed, the supply frequency can be found

$$n_s = 120 f_e / p$$

$$f_e = n_s p/120 = 1300 \times 4/120 = 43.33 \text{ Hz}$$

Finally, if *V/f* is constant, the supply voltage must be

$$V_{L-Lnew} = 400 \times \frac{43.33}{50} = 346.64 \text{ V}$$

Methods of obtaining supply frequency changing

Thyristor circuits can be used to produce variable frequency to control the speed of induction motors.In general the currently available methods of obtaining a variable frequency power output from the constant public supply can be divided into two main techniques:-

1. Indirect frequency conversion using d.c. link (Inverters).
2. Direct frequency conversion (Cycloconverters).

These two frequency changing techniques when applied to speed control of a.c motors are called: variable frequency drives (VFD).These types of drive perform two main functions:

- Controls the speed of an a.c. motor by varying the frequency supplied to the motor.
- Regulates the output voltage in proportion to the output frequency to provide constant ratio of voltage to frequency (V/Hz), required by the characteristics of the a.c. motor to produce adequate torque as discussed before.

(A) Induction motor control using d.c link inverter drive:

Inverter drives are of two types:

- Voltage source inverter drives (VSI)
- Current source inverter drives (CSI)

The voltage source inverter has two stages of power conversion, a *rectifier* and an *inverter*. A block diagram of voltage source inverter drives is shown in Fig.15.17. The rectifier converts the fixed a.c. voltage a to either fixed or adjustable d.c. voltage. The inverter produces a contr-ollable a.c. output voltage at the desired frequency. The term "Inverter" is also used to refer to the entire drive.

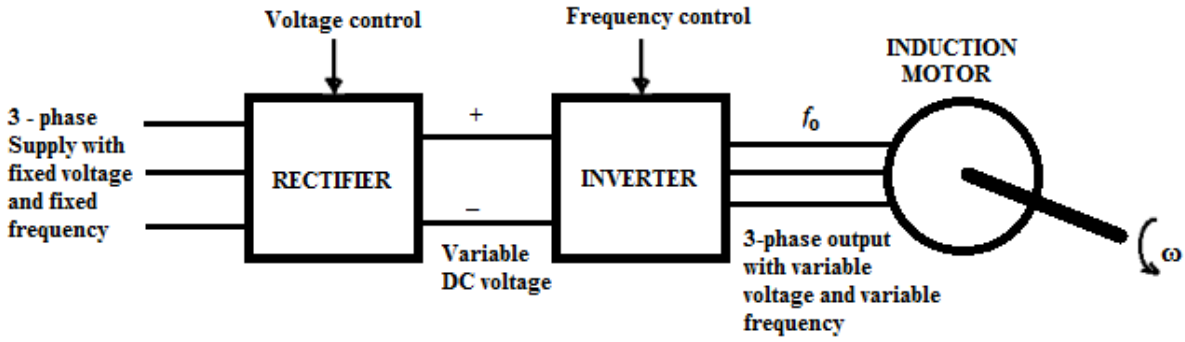

Fig.15.17 Block diagram of voltage source inverter drives.

There are three basic types of inverters commonly employed in adjustable a.c. drives:

(1) The variable voltage inverter (VVI), or square-wave six-step voltage source inverter (VSI), receives d.c. power from a fixed or adjustable voltage source and adjusts the frequency and voltage. A controlled rectifier transforms supply a.c. to variable voltage d.c. as shown in Fig.15.18. The converter can be an SCR (silicon-controlled rectifier) bridge or a diode bridge rectifier with a d.c. chopper to adjusts d.c. bus voltage to motor requirements. The typical output voltage and current waveforms of VVI inverter are shown in Fig.15.19.

The output frequency in the VV I inverter is controlled by switching transistors or thyristors in six steps as shown in Fig.15.20(a), whereas the VVI inverters control voltage in a separate section from the frequency generation output.

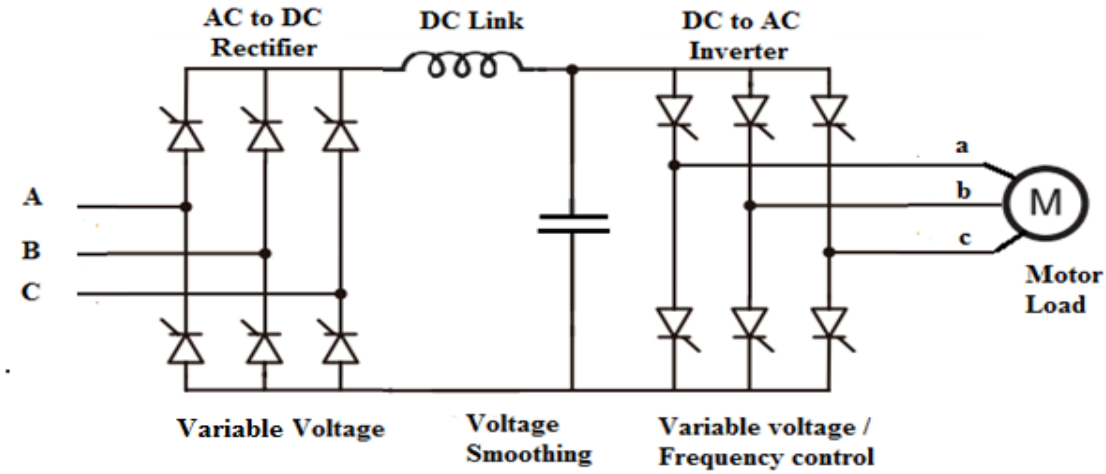

Fig.15.18 VVI – Variable Voltage Inverter.

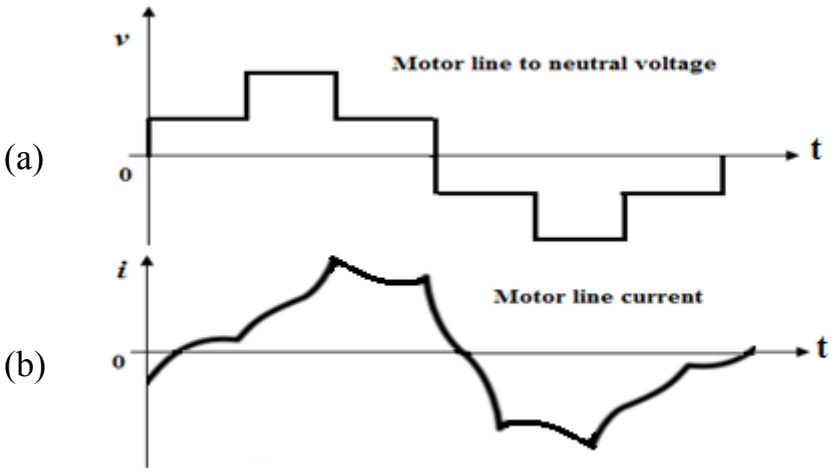

Fig. 15.19 VVI-Variable Voltage Inverter : (a) Phase voltage waveform, (b) Motor line current waveform.

The VVI inverter produces nearly sine current waveform as depicted in Fig.15.19(b). It is considered as the simplest adjustable frequency drive and most economical; however, it has the poorest output voltage waveform. It requires the most filtering to the inverter. The ranges available are typically up to 370 kW or 500 hp.

(2) The current source inverter (CSI) receives d.c. power from an adjustable current source and adjusts the frequency and current. AC current transformers are used to adjust the controlled rectifier. Input converter is similar to the VVI drive. A current regulator presets d.c. bus current. The inverter delivers six step current frequency pulses, which the voltage waveform follows. Switches in the inverter can be transistors, SCR thyristors or gate turnoff thyristors (GTOs). The schematic diagram of typical current source inverter drive is shown in Fig.15.20. The output voltage and current waveforms of the CSI inverter are shown in Fig.15.21.

Features of CSI inverter drives

Because it is difficult to control the motor by current only, the CSI requires a large filter inductor and complex regulator. The capacitor in the inverter must match to motor size, and the voltage exhibits commutation spikes when the thyristors fire. The CSI drives are short circuit proof because of a constant circuit with the motor. Also they are not suitable for parallel motor operation, however, power is returned to the supply easily during braking.

The CSI drive's main advantage is in its ability to control current and, therefore, control torque. This applies in variable torque applications. CSI-type drives have a higher kW range than VVI and PWM (typically up to 3750 kW).

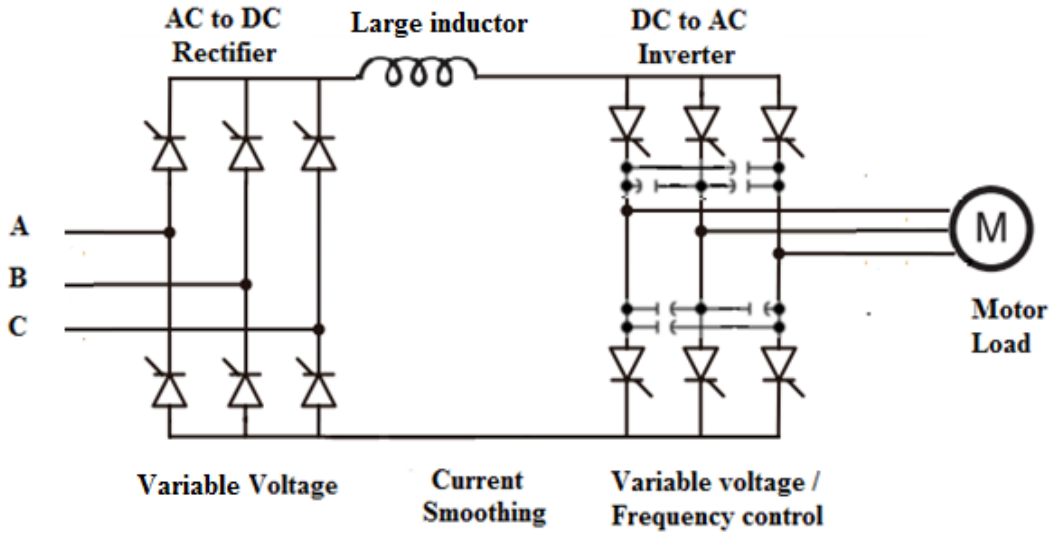

Fig.15.20 Schematic diagram of typical current source inverter drive.

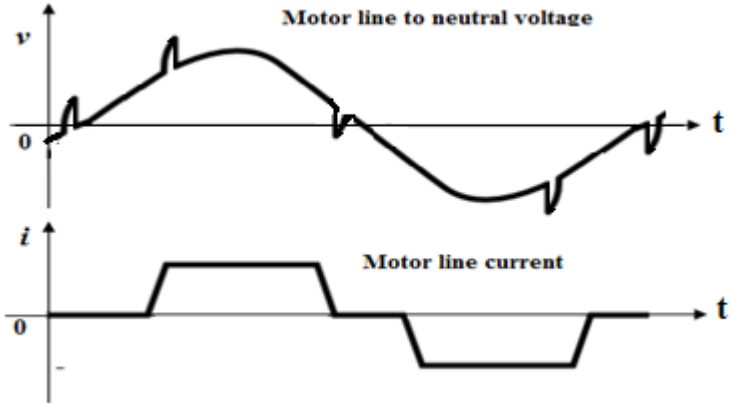

Fig.15.21 CSI drive – motor voltage and current waveforms.

(3) The pulse width modulated (PWM) inverter, this is the most commonly used type of inverters in practice. It receives d.c. power from a fixed voltage source and adjusts the frequency and voltage within the switches of the inverter itself. Block diagram for a typical PWM drive is shown in Fig.15.22.

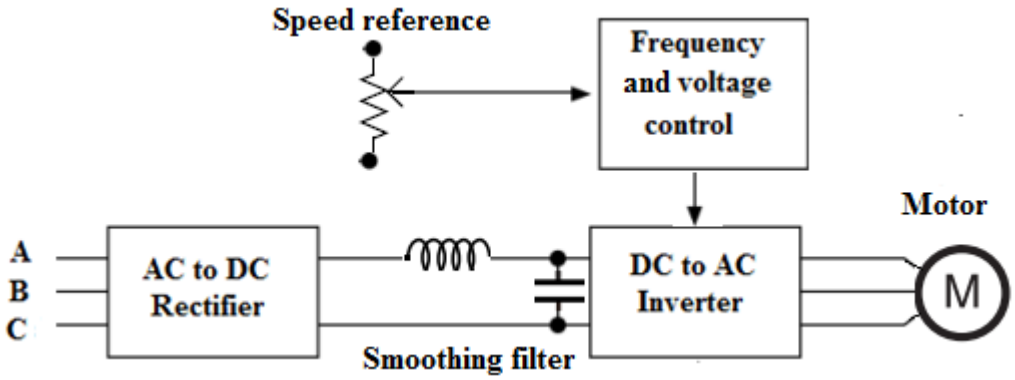

Fig.15.22 Block diagram for a typical PWM drive.

Features of PWM inverter drives:

With PWM inverter drive, motors run smoothly at high and low speed (no cogging); however, they are current limited. PWM drives can run multiple parallel motors with acceleration rate matched to total motor load. At low speeds, PWM drives may require a voltage boost to generate required torque. However, PWM is the most costly of the three main a.c. VSD (Variable Speed Drives) types.

The PWM drive's main advantage is it requires less filtering to produce nearly sinusoidal waveforms for both the voltage and current (PWM types cause the least harmonic noise). The range of PWM inverters is typically up to 2250 kW. The output voltage and current

waveforms of the PWM inverter are shown in Fig.15.23. Of the three most common inverter systems, the pulse width modulated inverter produces output current waveforms that have the least amount of distortion.

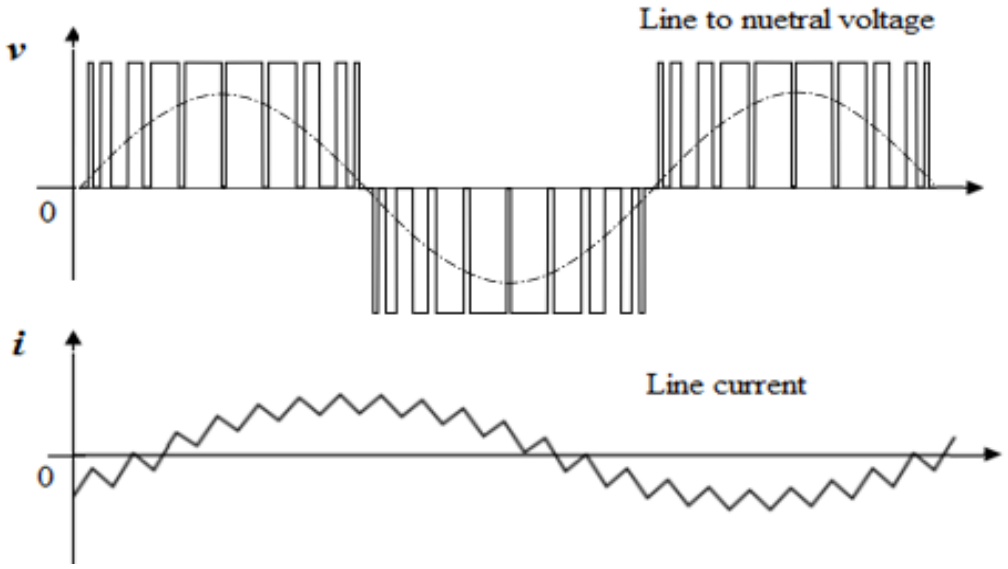

Fig.15.23 PWM inverter : Voltage and current waveforms with motor load.

(B) Induction motor control using direct AC to AC converter

AC to AC direct frequency changers used in AC drive systems are of two types :

(i) Cycloconverter drives

(ii) Load-commutated inverters (LCIs) drives

These are used only for large motor speed control applications (nearly 1000kW and above). Both can be used with induction or synchronous motors. The cycloconverters provide variable frequency variable voltage supply using large number of power switching devices. They are mainly used in low frequency applications such as steel rolling mill end tables, cement mill furnaces, mine hoists and ship propulsion drives. These drives are also called gearless drives since low speed operation is obtained without a reduction gear thus reducing the cost compared to the conventional drives.

Cycloconverters are capable of producing output voltage and current waveforms at frequencies below the mains frequency. This fact make it possible to manufacture large induction or synchronous motors with high-number of poles (e.g. 18) hence, a very low-speed direct (gearless) drive becomes practicable. An 18-pole motor, for example, will have a synchronous speed of only 33.3 rev/min at 5 Hz, making it suitable for mine winders, kilns, crushers, etc. These drives are called gearless drives since low speed operation is obtained without a reduction gear.

The main advantage of the cycloconverter is that naturally commutated devices such as thyristors can be used instead of self-commutating devices, which means that the cost of each device is lower and higher powers can be achieved. The cycloconverters can have different combination of input and output phase numbers, but in practice the three-phase to three-phase version is used for drive of rating 1 MW and above.

A full-wave cycloconverter drive configuration with two three-phase thyristor bridges per motor phase is shown in Fig.15.24. The output of a poly-phase controlled rectifier is approximately $V_d = V_{do} \cos \alpha$, where V_{do} is the output of the rectifier with zero firing angle, and α is the delay angle. When $\alpha > 90^\circ$ the mean output is negative but the output current cannot reverse so that the converter is then returning power from the load back to the supply. A reverse connected converter, bridge – B is used for the reverse half cycle of load current. On an induction motor the power factor presented to the frequency changer is variable so that the change-over of converter circuits cannot be predicted, a current transformer is used to sense the current zero and inhibit the unwanted firing pulses. The waveforms are generated in a converter which produces frequency proportional to control voltage and also imparts the required amplitude / frequency characteristic on the outputs.

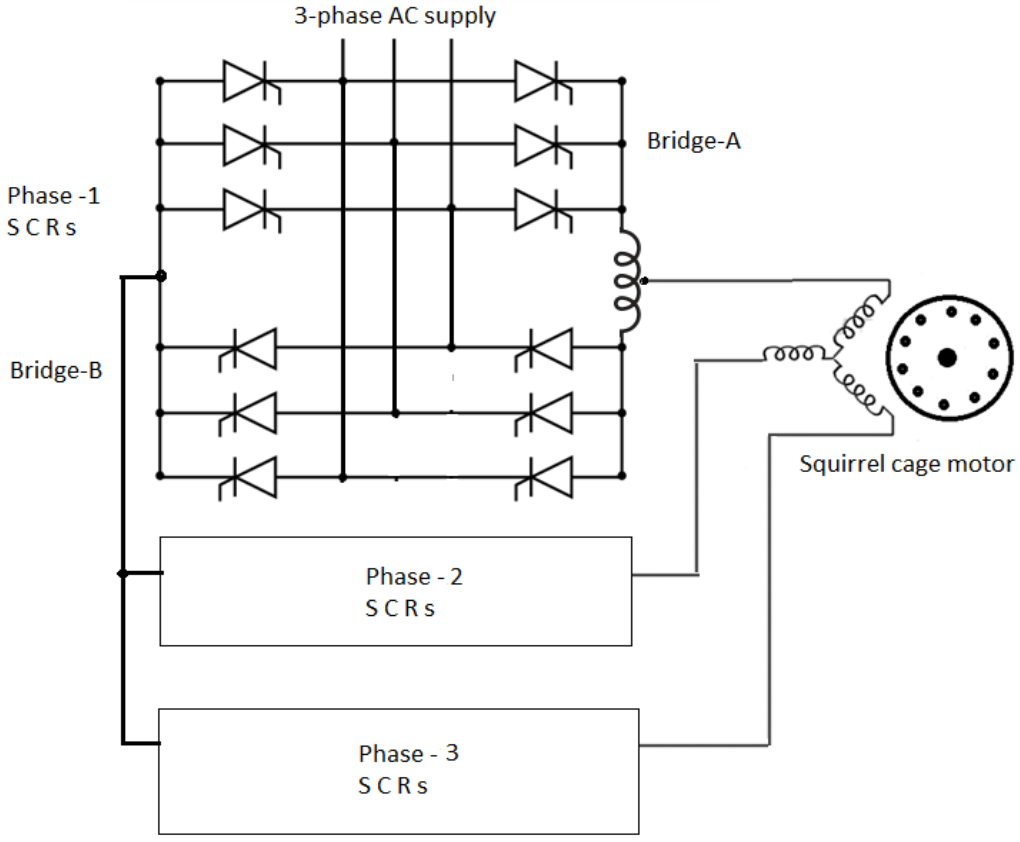

Fig.15. 24 Cycloconvertor drive circuit for a three-phase induction motor.

The voltage and current waveforms produced by direct ac-to-ac conversion systems approximate to pure sine wave due to the large number of thyristors used to synthesis the output voltage and current waveforms. Voltage and current waveforms for squirrel cage medium power motor driven by cycloconverter drive are shown in Fig.15.25. This type of drive has limitation that waveforms become distorted above 40% of input frequency (i.e., 20 Hz from 50 Hz supply). However, it has an advantage that high power factor is obtained when used with synchronous motors.

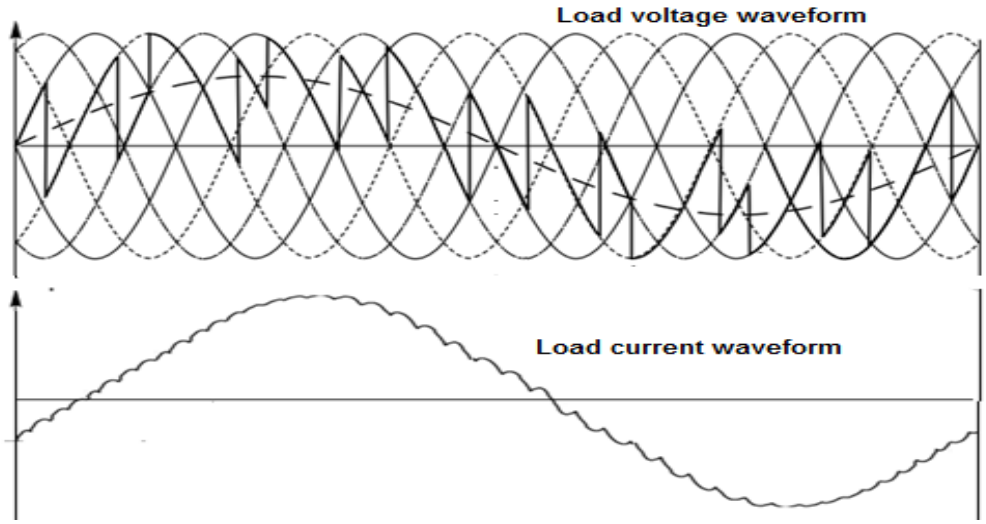

Fig.15.25 Output voltage and current waveforms of a typical cycloconverter.

15.4.2 Speed Control from Rotor Side

(1) Speed control by changing rotor-circuit resistance

It has been shown previously that the slip of an induction motor equals the ratio of rotor copper loss to rotor input. Therefore, changing total resistance of the rotor circuit can change the slip. This may achieved by inserting a rheostat in the rotor circuit as shown in Fig.15.26(a). This method is only possible for wound rotor applications, and not be possible for squirrel-cage rotor, but with a cost of reduced motor efficiency. The changing total resistance of the rotor circuit can change the speed can also be proved as follows:

The equation of torque for three-phase induction motor is given previously in Eq.(15.17) as

$$T\alpha \frac{sE_2^2 \quad R_2}{R_2^2 + (sX_2)^2}$$

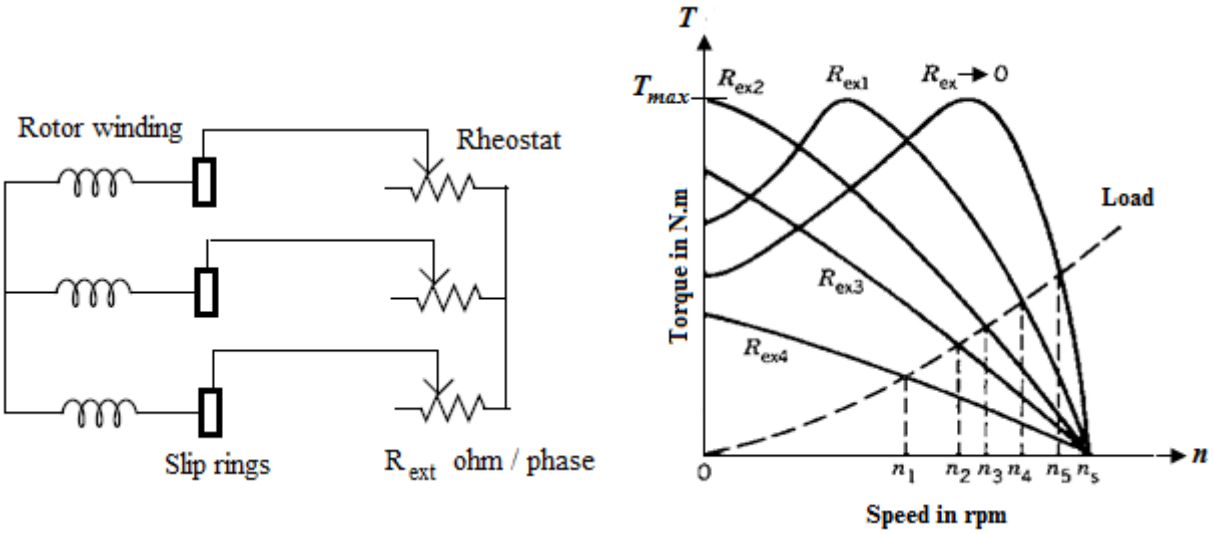

(a) (b)

Fig.15.26 Three-phase induction motor speed control by changing rotor-circuit resistance method.

In general, the three-phase induction motor operates in low slip region, hence the term $(sX_2)^2$ becomes very small as compared to R_2^2, so it can be neglected. Also if we consider that E_2 is constant, then the equation of torque may be written as,

$$T\alpha\frac{s}{R_2}$$

.

It is clear that from the above equation, the torque is inversely proportional to the rotor resistance. Hence, if the rotor resistance R_2 increases, torque decreases, but to supply the same load, torque must remain constant. So, if the slip is increased this will cause further reduction in rotor speed. Thus by adding additional resistance in rotor circuit the speed of three-phase induction motor can be decreased. The main advantage of this method is that with addition of external resistance starting torque increases. However, this method of speed control of three-phase induction motor suffers from some disadvantages:

(a) This method can only reduce the speed below the maximum value correspond to zero external resistance, hence, the speed above the normal value is not possible. Obviously the method is characterised by low efficiency due to high waste of energy. For example, to reduce the speed to 50% of its normal value, one has to dissipate 50% of the power absorbed from the source in the added resistor. The rheostat, which can dissipate this high energy with normal temperature rise, is costly.

(b) Another objection against this method is the departure of the torque-speed characteristic from its original shape of small slop to a new characteristic of considerable slop and the speed regulation is degraded. The slop is dependent on the value of the added resistance as shown in Fig.15.26(b).

Rotor-circuit resistance variation using choppers

The three-phase resistor shown in Fig.15.26 (a) may be replaced by a single resistor and d.c. chopper. The slip power from the rotor is converted to d.c current by rectification. The average resistance across the rotor slip rings will vary from 0 to R depending on the rate of switching of the rapidly pulsed thyristor. There is need only for one main thyristor and an auxiliary thyristor for turn-off. The fact that there is only one resistance is another advantage and this also provides perfect circuit balancing between the three phases. Schematic diagram of the method is shown in Fig.15.27.

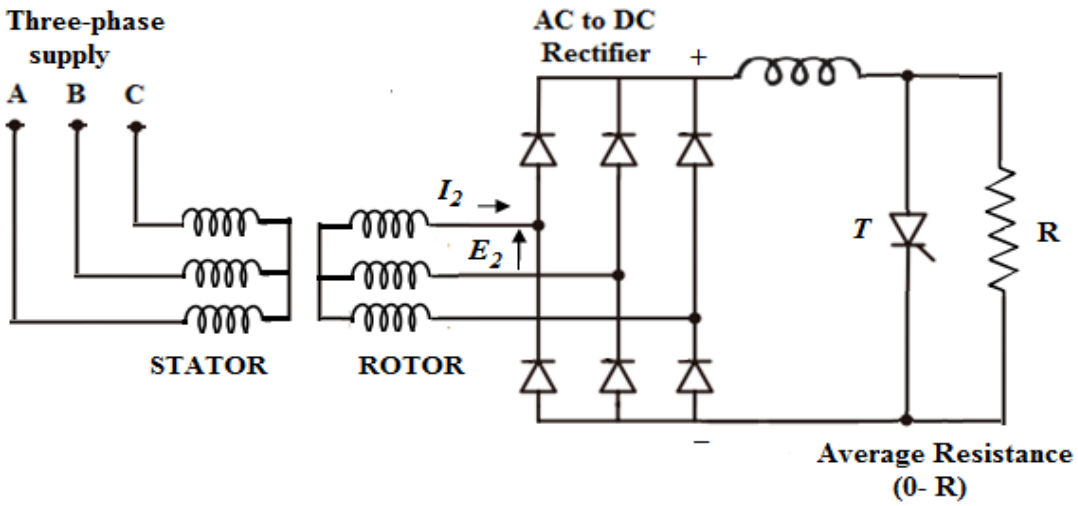

Fig.15.27 Speed control by varying rotor resistance using d.c. chopper.

The external resistances $R_{ex} = 0$ during chopper conduction ($\gamma = 0$) , where γ is the chopper duty cycle and $R_{ex} = R$ during chopper extinction with variation. Therfore,

$$R_{ex} = \frac{t_{off}}{t_{on} + t_{off}} R \ = (1 - \gamma)R \qquad (15.38)$$

Disadvantages: high losses in the commutating circuit at high chopping frequency. At high motor speeds E_2 is low and may be insufficient to provide commutating voltage. So small range of speed can be achieved.

Example 15.4

A 75 kW, 4-pole, 440 V, 50 Hz, star-connected, three-phase induction motor has the following parameters per-phase referred to the stator side:

$R_1 = 0.1\ \Omega,\ R_2 = 0.083\ \Omega,\ X_1 + X_2 = 1.83\ \Omega,\ a_{eff} = N_p / N_s = 2.5$

If the rotor is star connected, determine the external resistance inserted in series with the rotor winding per phase such that the motor develops an output shaft torque of 150 Nm at a speed of 1250 rpm.

Solution

The synchronous speed of the motor is

$$n_s = \frac{120f}{p} = \frac{120 \times 50}{4} = 1500 \text{ rpm}$$

From Eq.(15.2) , the slip is

$$s = \frac{n_s - n}{n_s} = \frac{1500 - 1250}{1500} = 0.167$$

The approximate equivalent circuit of the motor referred to the stator side is shown in Fig.15.28.

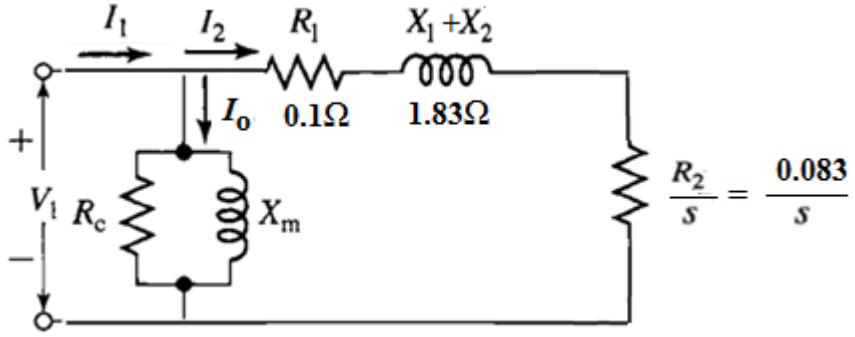

Fig. 15.28 Approximate equivalent circuit of the motor.

Let R_{ext} be the additional resistance inserted in each rotor phase at $s = 0.167$ such that the new rotor resistance becomes R_x , hence from the torque equation Eq.(15.17),

$$T = \frac{3V_1^{\,2}}{s\omega_s} \times \frac{R_2}{(R_1 + \frac{R_2}{s})^2 + (X_1 + X_2)^2}$$

$$T = 150 = \frac{1}{2\pi(\frac{1500}{60})} \times \frac{3(\frac{440}{\sqrt{3}})^2 R_x}{\left[(0.1 + \frac{R_x}{0.167})^2 + (1.83)^2\right]} \times \frac{1}{0.167}$$

This leads to the following quadratic equation

$$35.86\, R_x^2 - 48R_x + 3.359 = 0$$

From which we get,

$$R_x = \frac{48 \pm \sqrt{(48)^2 - 4 \times 35.86 \times 3.359}}{2 \times 35.86}$$

$\therefore \quad R_x = 1.264\ \Omega$ and 0.074Ω

Neglecting the smaller value, hence $R_x = 1.264\ \Omega$.

$R_{ext} = 1.264 - 0.083 = 1.1816\ \Omega$, referred to the stator

This resistance referred to the rotor side as

$$R_{ext} = \frac{1.1816}{a_{eff}^2} = \frac{1.1816}{2.5^2} = 0.19\ \Omega$$

Example 15.5

A 4-pole, 3 hp, 415 V, 50 Hz, star-connected, three-phase induction motor has the following parameters per-phase referred to the stator side:

$R_1 = R_2 = 0.80\ \Omega$, $X_1 = X_2 = 3.5\ \Omega$, $a_{eff} = N_p / N_s = 2.5$
Friction and windage loss = 170 W

(a) Calculate the slip at full load.
(b) If the rotor is star connected, determine the external resistance inserted in series with the rotor winding per-phase such that the slip would increase to four time the value obtained in (a) above with the full load torque remains constant.

Solution

(a) From Eq.(15.9) , the mechanical power is

$$\text{Mechanichal power} = 3P_g(1-s) - \text{ Mechanical loss}$$

$$3 \times 746 = \frac{3(V_1)^2(\frac{R_2}{s})}{\left[\left(R_1 + \frac{R_2}{s}\right)^2 + (X_1 + X_2)^2\right]} \times (1-s) - 170$$

$$2408 = \frac{3(\frac{415}{\sqrt{3}})^2(\frac{0.8}{s})}{\left[\left(0.8 + \frac{0.8}{s}\right)^2 + (7)^2\right]} \times (1-s)$$

Simplifying the above equation yields

$$\frac{1}{s^2} - \frac{87.5}{s} + 167.3 = 0$$

Solving thequadratic equation above ;

$$\frac{1}{s} = \frac{87.5 \pm \sqrt{(87.5)^2 - 4 \times 167.3}}{2}$$

The lower value of s can be obtain as : $\frac{1}{s} = 85.5 \rightarrow s = 0.0011$

(b) From the torque equation (15.14), for the torque to have a fixed value, all other parameters of the equation must be constant. However, if the slip becomes four times, the quantity $\frac{R_2}{s}$ must unchanged .i.e.

$$\frac{R_2}{s} = \frac{R_{2n}}{4s}$$

where $R_{2n} = R_2 + R_x$, hence $R_{2n} = 4R_2 = 4 \times 0.8 = 3.2\ \Omega$, therefore, the extra resistance required is

$$R_x = R_{2n} - 0.8 = 2.4\ \Omega$$

(2) Injecting slip frequency *emf* into rotor side

Induction motor drives with full-power control on the stator side are widely used in industrial applications. Although either a cage-type or wound-rotor machine can be used in the drive, the former is always preferred because a wound-rotor machine is heavier, more expensive, has higher rotor inertia, a higher speed limitation, and maintenance and reliability problems due to brushes and slip rings. When the speed control of three-phase induction motor is done by adding resistance in rotor circuit, some part of power called, the slip power is lost as I^2R

losses. Therefore, the efficiency of the motor is reduced by this method of speed control. This slip power loss can be recovered and supplied back in order to improve the overall efficiency of motor and this scheme of recovering the power is called slip power recovery scheme. This is done by replacing the d.c. chopper and resistor *R* in Fig.15.27 by a three-phase bridge converter as shown in Fig.15.29.

The converter operates in inversion mode with firing angles $90° \leq \alpha \leq 180°$ thereby returning energy to the source. The variation of the triggering angle α results in variation of speed, hence speed control is achieved by this technique. Therefore, one feature of wound rotor machine is that the slip power becomes easily available from the slip rings, which can be electronically controlled to control speed of the motor.

The two well known types of converter use the slip energy recovery technique are:

1. Static Kramer drive: only allows operation at sub-synchronous speed.
2. Static Scherbius Drive: allows operation above and below synchronous speed.

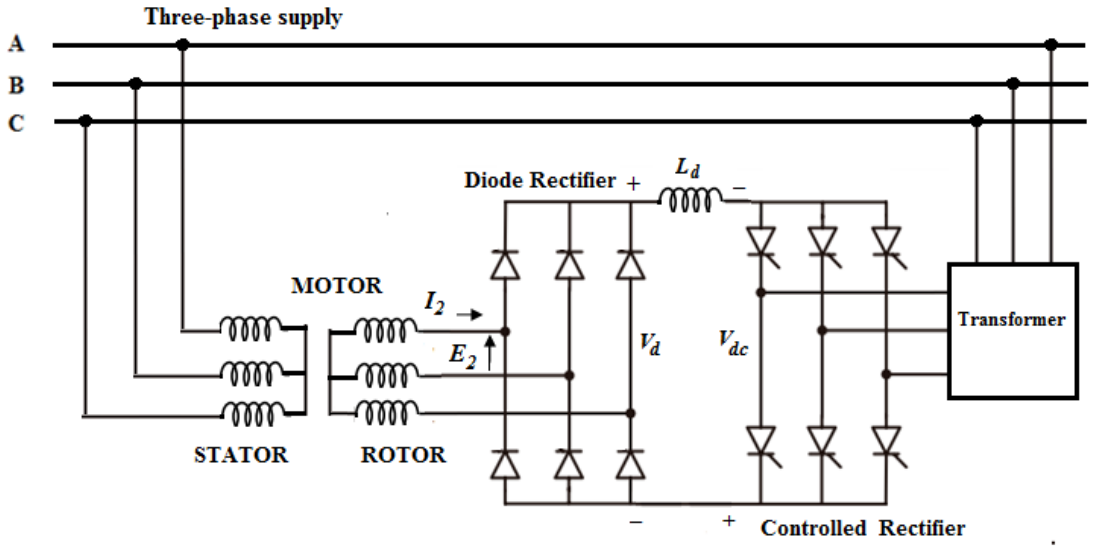

Fig.15.29 Slip power recovery (Static Kramer drive).

Static Kramer drive

A static Kramer drive is a method to obtain an injected voltage that is in phase with the rotor current. The voltage at the slip rings is forced to be in phase with the rotor currents by the diode rectifier. The magnitude of the slip ring voltage is set by the d.c. link voltage, which is in turn set by the inverter connected back to the a.c. supply. The schematic diagram of the converter is depicted in Fig.15.29. The static

Kramer drive is, therefore, a slip power-controlled drive that permits only a sub-synchronous range of speed control through a converter cascade using static power semiconductor devices. It is different from the old original Kramer drive, where rotating machines were used for slip energy recovery.

The static Kramer drive has been very popular in large power pump and fan-type drives, where the range of speed control is limited near, but below the synchronous speed. The drive system is very efficient and the converter power rating is low because it has to handle only the slip power. The additional advantages are that the drive system has d.c. machine-like characteristics and the control is very simple. These advantages largely offset the disadvantages of the wound-rotor induction machine.

Static Scherbius drive

Another technique that employs the principle of slip power returns to the supply is kown as static Scherbius drive shown in Fig.15.30. In this system the bridge rectifier in Fig.15.26 is replaced by cycloconverter (or by three-phase duel converter).

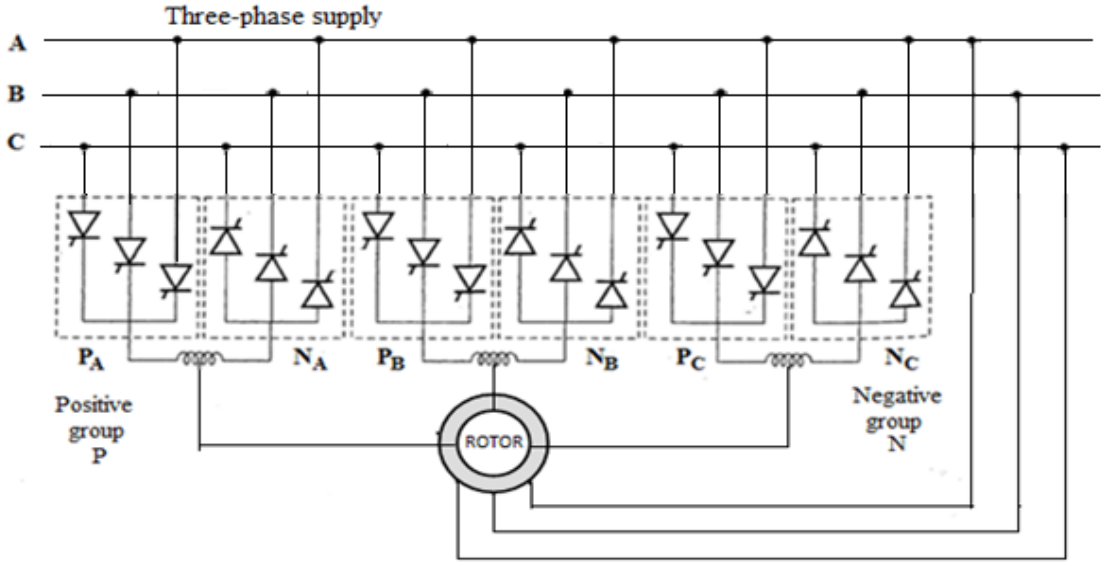

Fig.15.30 Static Scherbius drive.

For limited-range speed control applications, where the slip power is only a fraction of the total power rating of the machine, Kramer and Schrebius drives (slip-power recovery drives) have been used in the following applications:

- Large-capacity pumps and fan drives
- Variable-speed wind energy systems
- Shipboard VSCF (variable-speed/constant-frequency) systems

- Variable-speed hydro pumps/generators
- Utility system flywheel energy storage systems

Simplified analysis of three-phase induction motor with injected secondary voltage

In slip energy recovery, a voltage is applied to the slip ring terminals of a wound rotor induction motor, in phase with the rotor current. Such an external injected voltage must operate at slip frequency for all motor speeds. Using the equivalent circuit of induction motor, the injected voltage V_{iR} to the rotor is shown in Fig.15.31. The magnitude of the secondary current is given by

$$I_2^{'}=\frac{\mathrm{E}_2^{'}-\mathrm{V}_{\mathrm{iR}}}{\sqrt{(R_2^{'})^2+(sX_2^{'})^2}} \tag{15.39}$$

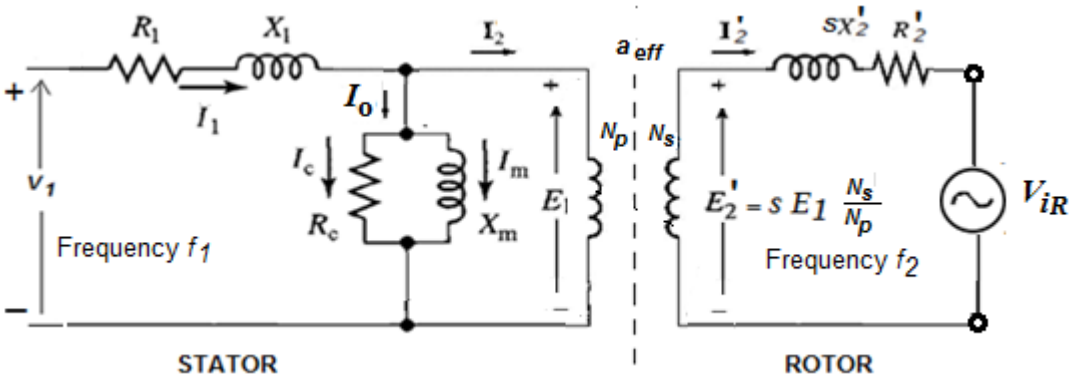

Fig.15.31 Per-phase equivalent circuit of a three-phase induction motor with injected secondary voltage.

The injected voltage can be referred to the stator is

$$V_i = \frac{V_{iR}}{a_{eff}} \tag{15.40}$$

In order to simplify the analysis, assume that the magnetising reactance can be moved to the terminals of the equivalent circuit resulting in the approximate circuit referred to the stator side as shown in Fig.15.32. If the injected voltage is in phase with the rotor current, then the voltages in the equivalent circuit may be written as

$$V_1 = I_2(R_1 + \frac{R_2}{s}) + \frac{V_i}{s} + jI_2(X_1 + X_2) \tag{15.41}$$

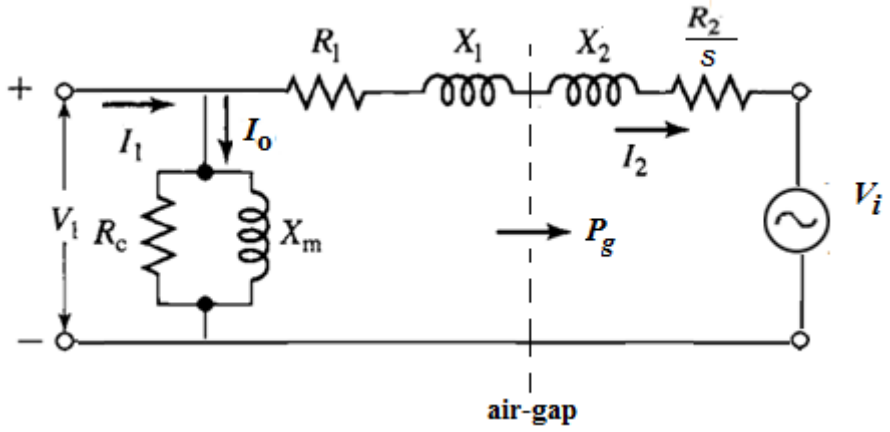

Fig.15.32 Approximated equivalent circuit of induction motor with injected voltage referred to stator side.

By re-arranging Eq.(15.41), the slip may be found as

$$s = \frac{V_i + \mathrm{I}_2\mathrm{R}_2}{(V_1^2 - I_2^2(X_1 + X_2)^2)^{1/2} - \mathrm{I}_2 X_1} \tag{15.42}$$

Power and Torque

The air gap power of the machine may be written as

$$P_g = 3I_2 \frac{(I_2R_2 + V_i)}{s} \tag{15.43}$$

Breaking this equation into parts, it can be seen that the air gap power is the sum of resistive losses, power recovered through the slip rings and the mechanical power.

$$P_g = 3\mathrm{I}_2^2 R_2 + 3I_2V_i + 3I_2(I_2R_2 + V_i)\frac{1-s}{s} \tag{15.44}$$

Using the expression for air gap power, the torque may be written as

$$T = 3I_2 \frac{(I_2R_2 + V_i)}{s\omega_s} \tag{15.45}$$

Now, substituting the slip expression into the torque expression gives the result that torque is only a function of rotor current, not slip or injected voltage:

$$T = \frac{3I_2}{\omega_s}\left[(V_1^2 - I_2^2(X_1 + X_2)^2)^{1/2} - I_2R_1\right] \quad (15.46)$$

The expression above means that for a given torque, the rotor current will always be the same, independent of speed.

No-Load Condition

Consider again the expression for slip given in Eq.(15.42), if the torque is zero, then the rotor current will also be zero and at zero torque, therefore the slip is given by

$$s_o = \frac{V_i}{V_1} \quad (15.47)$$

Efficiency

Since some of the power supplied to the motor is recovered from the rotor circuit, the efficiency cannot be calculated as simply output power over input power. Instead, in slip energy recovery drive the efficiency is

$$\eta = \frac{P_o}{P_{in} - P_{recovered}} \quad (15.48)$$

(3) Cascade control method

In this method of speed control of three-phase induction motor, two motors are required one of them should be a wound rotor type. These two motors are connected on common shaft and hence called cascaded motor as shown in Fig.15.33.

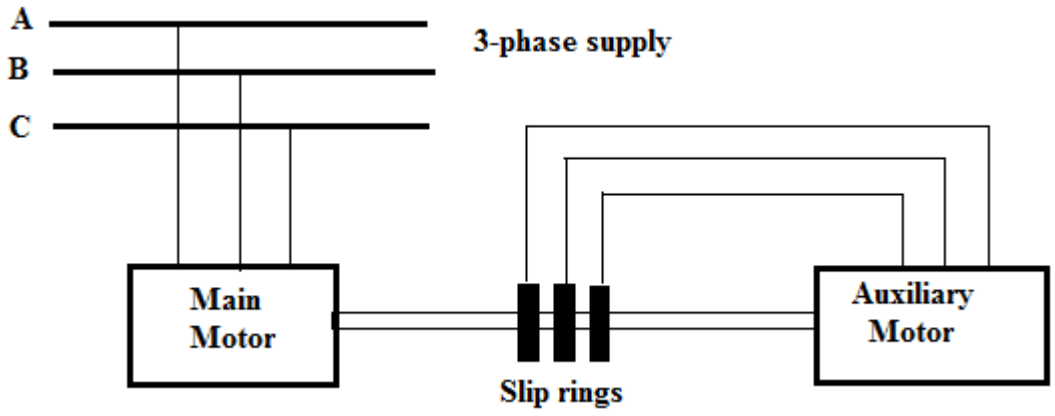

Fig.15.33 Cascade connections of induction motors for speed control.

One motor is the called the main motor and another motor is called the auxiliary motor. The three-phase supply is given to the stator of the main motor while the auxiliary motor is derived at a slip frequency from the slip ring of main motor.

Example 15.6

Two three-phase induction motors are to be speed control by cumulative cascade arrangement as shown in Fig.15.32. The main motor has four poles whereas the auxiliary motor has six poles. The supply voltage is 400 V, 50 Hz for the main motor while the frequency in the rotor of the auxiliary motor is 1.0 Hz. Calculate the slip of each motor and the combined speed of the whole set.

Solution

Let f_{Rm} = Rotor frequency of the main motor
f_{Ra} = Rotor frequency of the auxiliary motor
P_m = Number of poles of the main motor
P_a = Number of poles of the auxiliary motor

The synchronous speed of the set is

$$n_{ss} = \frac{120f}{P_m + P_a} = \frac{120 \times 50}{4 + 6} = 600 \text{ rpm}$$

$$f_{Ra} = sf$$

The slip of the set is

$$s = \frac{600 - n}{600}$$

Where n = speed of the set , which can be evaluated as

$$1 = \frac{600 - n}{600} \times 50$$

$$12 = 600 - n \qquad \rightarrow \qquad n = 588 \text{ rpm}$$

The synchronous speed of main motor is

$$n_{sm} = \frac{120f}{P_m} = \frac{120 \times 50}{4} = 1500 \text{ rpm}$$

The slip of the main motor is

$$s_m = \frac{1500 - 588}{1500} = 0.608$$

The synchronous speed of auxiliary motor is

$$n_{sa} = \frac{120 f_{Rm}}{P_a}$$

But

$$f_{Rm} = s_m f = 0.608 \times 50 = 30.4 \text{ Hz}$$

$$n_{sa} = \frac{120 \times 30.4}{6} = 608\, rpm$$

The slip of the auxiliary motor is

$$s_m = \frac{n_{sa} - n}{n_{sa}} = \frac{608 - 588}{608} = 0.033$$

15.5 SYNCHRONOUS MOTOR DRIVES

A synchronous motor is a constant speed machine, which always rotates at a synchronous speed that is dependent on frequency and the number of poles. The synchronous motors consist of two parts namely; a rotor, which is the rotating part, and a stator, which is a stationary part. The motor has the following characteristics:

1. It runs at synchronous speed only, that is, while running it maintains a constant speed. The only way to change its speed is to vary the supply frequency f or the number of its poles p since the speed of the motor is given by equation (15.49).

$$n_s = 120f/p \qquad (15.49)$$

2. The synchronous motor is not self-starting. It has to run up to synchronous speed by some means before synchronization to the supply.

3. It is capable of being operated under a wide range of power factors both lagging and leading.The synchronous motors have a poly- phase winding on its stator, which is also known as the armature, and a field winding carrying a d.c. current on the rotor.

Therefore, two types of magneto-motive forces are established in the machine air gap, one due to field current and the other due armature current. The armature current is identical to the stator of induction motors but there is no induction in the rotor.

Types of AC Synchronous Motors

Synchronous motors come in different variants:

1. Wound field motor
   (i) Cylindrical rotor wound field
   (ii) Salient pole rotor wound field
2. Permanent magnet (PM) motors
   (i) Surface-mounted permanent-magnet synchronous motor (SPM)
   (ii) Interior or buried permanent-magnet synchronous motor (IPM)
3. Synchronous reluctance motor (SyRM)
4. Permanent-magnet-assisted SyRM (PM-SyRM)
5. Hysteresis motor
6. brushless d.c. and a.c. motors

In the wound rotor type, the rotor steel structure can be either cylindrical or salient like. In either case, the rotor winding carries d.c. , delivered through slip rings, or through a rectified voltage of an inside-out synchronous generator mounted on the same shaft.
In the permanent magnet rotor type**,** instead of supplying d.c. to the rotor, the rotor contains permanent magnets. The effects of permanent magnet rotors include:

(a) The rotor flux can no longer be controlled externally. It is defined by the magnets and the geometry.
(b)The machine becomes simpler to construct, at least for small sizes.

15.5.1 Variable Speed Synchronous Motor Drives (VSD)

In particular applications where synchronous motors are suitable, variable speed drives are required for the following reasons:

(a) Match the speed of a drive to the given application task
(b) Match the torque of a drive to the given application task
(c) Saving energy and improving the efficiency

Today, there are several speed control techniques for a.c. drives, namely:

(a) Scalar control: *V/f* (Volts per Hertz) control
(b) Vector control:
  (i) Field oriented control
  (ii) Sensor less Vector Control
  (iii) Direct torque control
  (iv) Flux Vector Control
  (v) Space vector modulation control

V/Hz control using static frequency changers is a basic control method, providing a variable frequency drive for applications like fan and pump. It provides fair speed and torque control, at a reasonable cost.

Sensor less vector control provides better speed regulation, and the ability to produce high starting torque. Flux vector control provides more precise speed and torque control, with dynamic response. Field Oriented Control drives provide the best speed and torque control available for a.c. motors. It provides d.c. performance for a.c. motors, and is well suited for typical d.c. applications.

As it was shown in Eq.(15.49) that the speed of a synchronous motor can be varied by changing the stator supply frequency, hence the best way is to use the static frequency changers such as inverters and cycloconverters. V/Hz control using inverter is shown schematically in Fig.15.34(a), and depicted as a block diagram in Fig.15.34(b).

Open-loop and closed-loop frequency control

In open-loop frequency control, a separate control mode where the controlling of the inverter frequency is from an independent oscillator which determines the speed of the motor and the stator voltage that are directly controlled.

In closed loop or self-synchronous control, the stator voltage can be controlled directly by varying the stator frequency. For example by a signal obtained from a rotor shaft sensor (these signals are used as firing signals for thyristor gates). The inverter output supplies the three-phase a.c. motor as depicted in Fig.15.35. In this case, by monitoring the rotor position, the magnetic axis of the field winding is determined and since these signals are used for firing the gates of the SCRs of the inverter, as a d.c. machine, a fixed space angle can be maintained between the field winding and the stator magnetomotive force. It is also possible to use terminal voltages of motor for synchronization of the firing signals of the inverter.

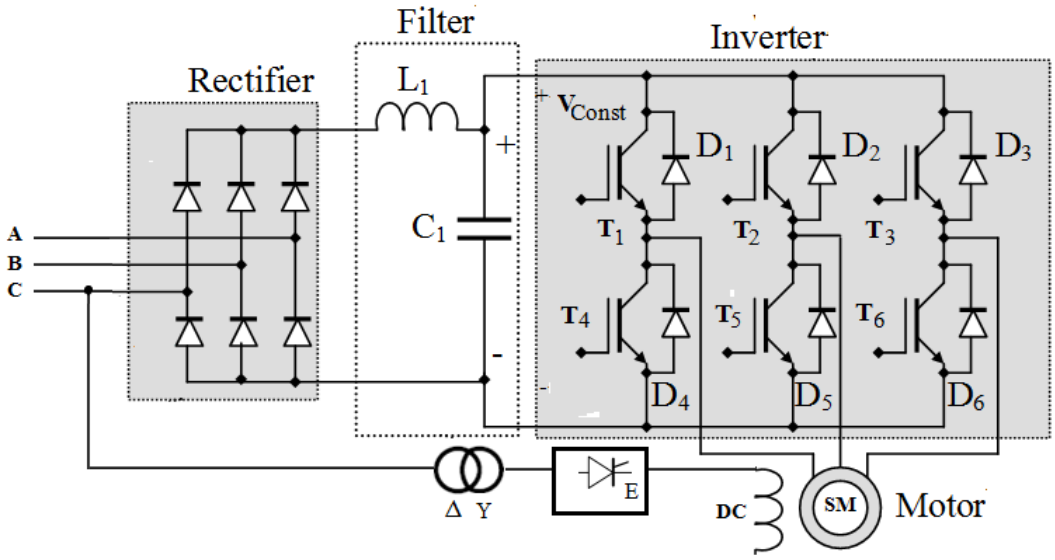

(a)

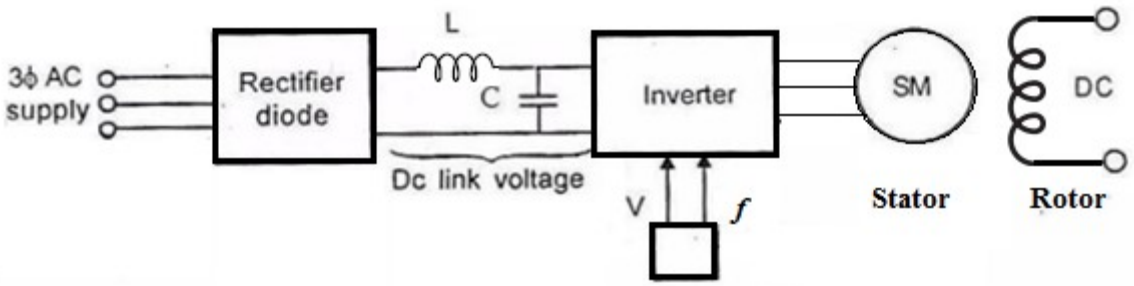

(b)

Fig.15.34 Inverter drive for synchronous motor using *V/f* control.

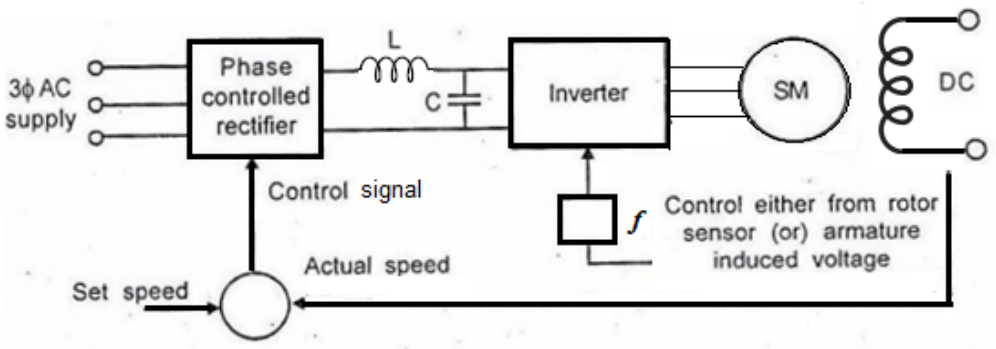

Fig.15.35 Inverter drive for synchronous motor using feedback control.

In self-controlled mode, the frequency and phase of the output wave are controlled by an absolute position sensor mounted on machine shaft, giving it self-control characteristics. The supply frequency is changed so that the synchronous speed is same as that of the rotor speed. Hence, rotor cannot pull-out of slip and hunting oscillations are eliminated. The stator

winding of the machines is fed by an inverter that generates a variable frequency variable voltage sinusoidal supply. Here the pulse train from position sensor may be delayed by the eternal command as shown in Fig.15.35.

15.5.2 Types of Inverters Used in Synchronous Motor Drives

The types of inverters used in synchronous motor drives are:

1. Voltage fed inverter (VFI) where the input voltage remains constant.
2. Current fed inverter (CFI) where the input current remains constant.
3. Variable d.c. link inverter where the input voltage is controlled.

There are two types of voltage fed inverter (VFI);

(i) Square wave inverters in which a controlled rectifier is used. However, the controlled rectifiers suffer from the disadvantages that they have low power factor at low voltage and they suffer from lagging power factor on a.c. supply.

(ii) Pulse Width modulated inverters (PWM*)* where an uncontrolled rectifier is used. Pulse width modulation (PWM) drives provide a more sinusoidal current output to control frequency and voltage supplied to an d.c. motor. PWM drives are more efficient and typically provide higher levels of performance.

The current source inverter (CSI) uses an SCR input to produce a variable voltage d.c. link. The inverter section also uses SCRs for switching the output to the motor. The current source inverter controls the current in the motor. The motor must be carefully matched to the drive current spikes, caused by switching.

Advantages

1. The circuit for CSI is simple since it uses only converter grade thyristor, which should have reverse blocking capability, and also should able to withstand high voltage spikes during commutation.
2. The simultaneous conduction in an inverter arm or an output short circuit is controlled by the ‘controlled current source’ used here, i.e., a current limited voltage source in series with a large inductance.

3. The converter-inverter combined configuration has inherent four-quadrant operation capability without any extra power component.

Disadvantages

1. The commutation capability is dependant upon load current, hence minimum load at the output is required, This limits the operating frequency, and also puts a limitation on its use for UPS systems.
2. At light loads, and high frequency, these inverters have stability problems.

In variable d.c. link inverter, switching devices include thyristors, bipolar transistors, MOSFETS, and IGBTs are used. The control logic uses a microprocessor or logic circuits to switch the transistors on and off providing a variable voltage and frequency to the motor.

Performance of The Synchronous Motor with Inverter Drives

The motor prefers a smooth sine wave; a six-step output is satisfactorily used. The main disadvantage is torque pulsation, which occurs each time a switching device, such as a bipolar, is switched ON. The pulsations can be noticeable at low speeds as speed variations in the motor. These speed variations are referred to as cogging. The nonsinusoidal current waveform causes extra heating in the motor requiring a motor derating. Generally a VSI fed synchronous motor drive has :

(a) Reasonable efficiency.
(b) Converter cost is high.
(c) Multi motor operation is possible.
(d) Open loop (separate) control may pose stability problem at low speeds.
(e) Closed loop mode is very stable.
(f) PWM drive has better dynamic response than square wave drive.

15.5.3 Cycloconverter Drives of Synchronous motors

The inverter drives discussed in the previous sections do not actually convert power directly from a.c power of one frequency to a.c. power of another frequency. Instead, these converters first convert electrical power to d.c. using a rectifier, and then convert power back into a.c. using an inverter . This topology has advantages in that both rectifier and inverter topologies have been studied thoroughly and the techniques used in their implementation are very well known. Control strategies have also been

well developed for increasing the accuracy of producing an output waveform, including Pulse Width Modulation (PWM) of the signal so that output voltage harmonics can be directly controlled. Also, there are no limitations imposed on the input or output frequencies providing semiconductor switching device limits are not reached. However, there are also downsides to this topology.

On the other side ,cycloconverters are a single-stage solution that they change the a.c. iput at a given voltage and frequency to another voltage and frequency at the output without d.c. link as shown in Fig.15.36. They are usually phase-controlled and they traditionally use thyristors due to their ease of phase commutation. Cycloconverters not only eliminate the problem of having multiple systems to perform a single function, they also limit the flow of power to a single switch at any one period in time.

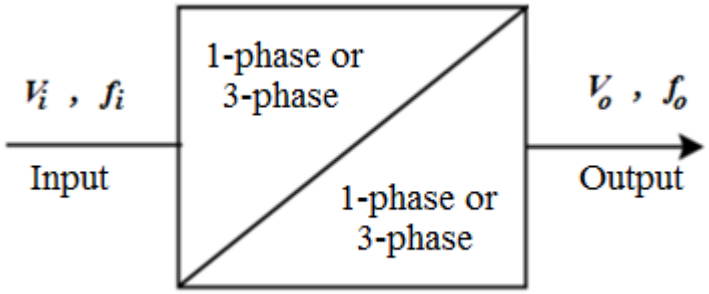

Fig.15.36 Block diagram of a cycloconverter.

The cycloconverters however, have a rash of other problems. Because cycloconverters directly manipulate input signals at alternating intervals, they do not produce output harmonics in the way that an inverter circuit does. The frequencies of the harmonics produced in the inverter are usually multiples of, and are entirely dependent on the inverter switching speed. Instead, cycloconverters produce interharmonics, which are side lobe frequencies based on both the input and output of the system. The presence of these interharmonic frequencies can be especially problematic because they are not necessarily at higher order or greater than than the output frequency.

Harmonics below the output frequency which is called subharmonics can badly affect the load performance. Because these frequencies occur close to the desired output, they are difficult to filter without drastically altering the fundamental, the sinusoidal waveform at the desired output frequency. The subharmonics, which are undesired frequencies constitute one of the most important reasons why cycloconverters are impractical in many applications. Table 15.1 shows frequency components of output waveform of typical cycloconverter.

Table 15.1. Frequency components of output waveform of typical cycloconverter.

harmonic	$f = hf_s$	where h is an integer >0
DC	$f = 0$	$f = hf_s$ where $h = 0$
interharmonic	$f \neq hf_s$	where h is an integer >0
subharmonic	$f > 0$ and $f < f_s$	

where f_s = fundamental or wanted frequency component.

Inverters often produce harmonics, where cycloconverters produce interharmonics, and at times, subharmonics. The occurrence of these harmonics is most noticeable at high output-to-input frequency ratios. Therefore, the easiest solution to limiting these unwanted frequencies is to limit the output-to-input frequency ratio of the cycloconverter. This limit changes with the topology of the cycloconverter, although ratio limits of 0.5 or less are not uncommon on the simplest cycloconverter topologies. As the complexity of the cycloconverter increases, however, this bound on usable output frequencies approaches one.

The use of cycloconverters also creates adverse affects on the input of the cycloconverter system. Harmonics are produced in the input current, and the input power factor can be low depending on the load. These affects are consistent with rectifiers, though harmonics occur at different intervals in cycloconverters than occur in rectifiers.

Inverters, generally cause waste of power through multiple switching stages and include dangerous high voltage d.c. lines. Cycloconverters avoid these problems and consequently are often used in high power industrial applications. Gearless cement mills, steel rolling mills, ore grinding mills, pumps and compressors, and mine winders are all current applications of the cycloconverter because of its benefits with high power, low speed devices.

Additionally, cycloconverters can independently control both output frequency and voltage and have the ability for four quadrant operation, which allows reverse and regeneration. Reverse operation being the situation where currents are run the opposite direction to convention, which can be accomplished in three-phase systems by switching two of the inputs or in cycloconverters by simply changing the controls. This causes the motor to spin in the reverse direction as well. Regeneration is the condition where stored currents in the load are allowed to flow back into the source .

15.5.4 Types of Cycloconverters Used in Synchronous Motor Drives

The most common types of cycloconverters used for synchronous motor drives are :

1. Six-pule three-phase to three-phase cycloconverter :The circuit configuration of the six-pulse cycloconverter drive is shown in Fig.15.37. This type of drives has the following benefits,

   (a)The most cost effective solution
   (b) Saved volume
   (c) Minimum weight

The motor may be star-connected or equipped with galvanically separated windings. The configuration where the motor winding are separated are widly used in ship propulsion.

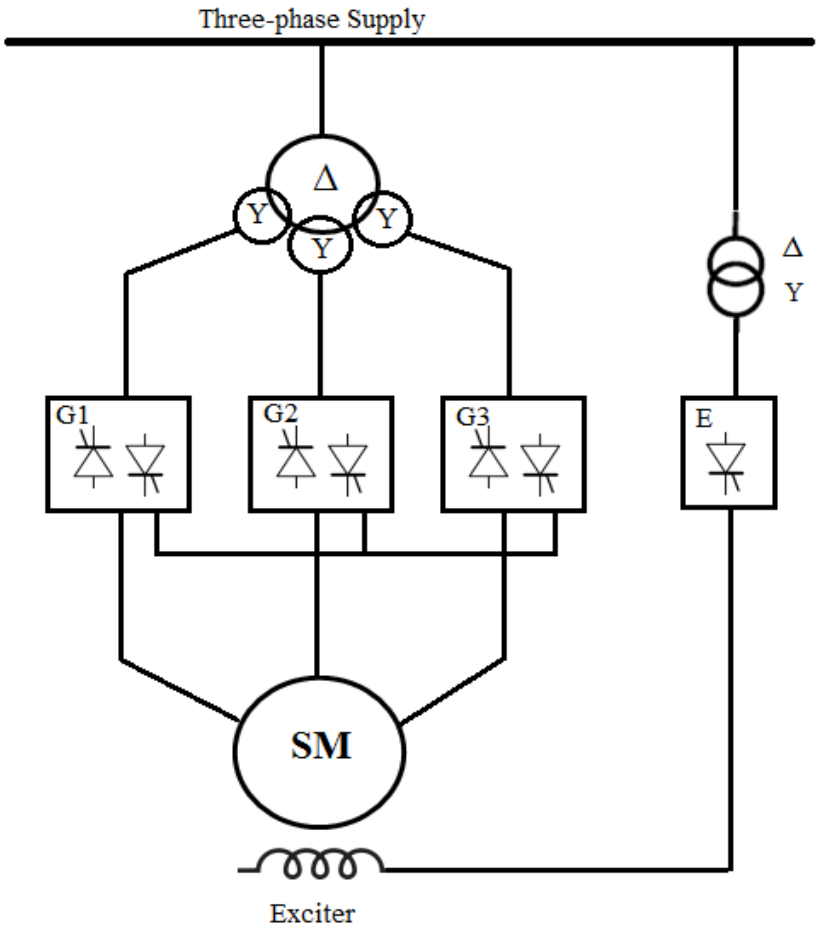

Fig.15.37 Six-pulse three-phase to three-phase cycloconverter synch-ronous motor drive.

2. Twelve-pulse three-phase cycloconverter: The circuit configuration of the six-pulse cycloconverter drive is shown in Fig.15.38. This type of drives has the following benefits,

(a) Fastest response times in current and torque control.
(b) Lowest network harmonic distortion.
(c) Lowest losses.
(d) Lowest shaft torque ripple.
(e) Minimum output frequency.

The torque rise time which can be reached with a motor supplied by twelve-pulse converter is better than the respective value of a six-pulse converter. Furthermore , with this arrangement , the motor voltage can be

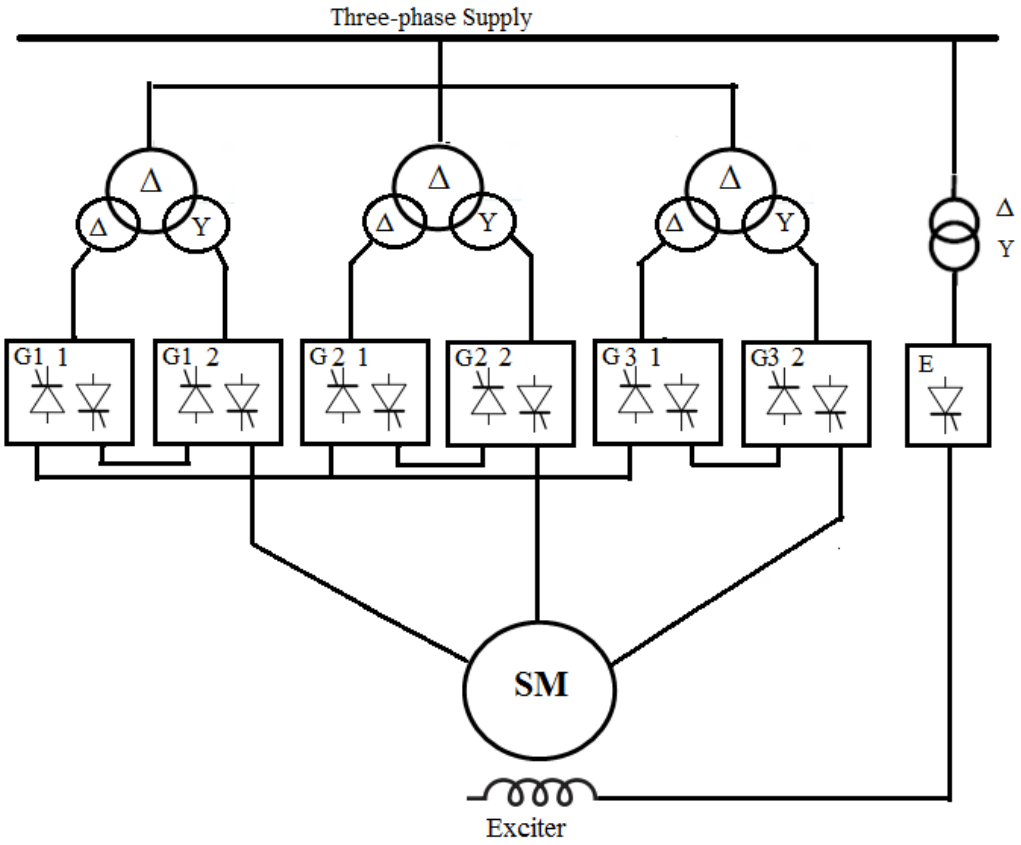

Fig.15.38 Twelve-pule three-phase to three-phase cycloconverter synchronous motor drive.

increased to 3 kV, reducing cable cost and energy losses. The main output current ripple frequency is 600 Hz (760 Hz for 60 Hz supply) compared to the 300 Hz (360 Hz) of a 6-pulse converter. This means that the magnitude of torque ripple caused by current ripple is extremely low, and the torsional vibrations are negligible.

PROBLEMS

15.1 A three-phase, four-pole, star-connected wound-rotor induction motor is to be controlled by terminal voltage variation using one triac in each supply line. Sketch a diagram of this arrangement and list the advantages and disadvantages of triac control compared with sinusoidal voltage variation using auto transformer.

15.2 A Triac control of a three-phase, 30 kW, 400 V, 50 Hz, six-pole, star-connected squirrel-cage induction motor such that it operates at a full load efficiency of 0.85 p.u. and power factor 0.8 lagging. Calculate the average and *rms* current rating and maximum voltage rating required of the triacs.

[Ans : 32 A, 45 A, 326 V]

15.3 The motor in Problem 15.2 drives a load characterised by the relation $T_L = k\,\omega$ where T_L is the shaft torque and ω is the motor speed. Operation is required to give rated torque at rated speed of 960 rpm and also to supply the appropriate load at speed of 640 rpm at which the power factor is dropped to 0.6. If the motor operates at full voltage at its upper speed, estimate roughly, the change of thyristor firing-angle necessary to achieve satisfactory operation of the motor at the lower speed. Assuming that the motor impedance is unchanged between the two speeds.

[Ans: $37^\circ \leq \alpha \leq 90^\circ$]

15.4 It is proposed to use a 240 V, 50 Hz, four-pole, star-connected induction motor with the equivalent circuit parameters (referred to stator turns):

$$R_1 = 0.25\ \Omega,\ X_1 = 0.36\ \Omega,\ R_2 = 0.65\ \Omega,\ X_2 = 0.36\ \Omega,\ X_m = 17.3\ \Omega.$$

to drive a pump has a torque-speed curve given by $T_L = 0.014\ \omega^2$ Nm. The pump speed ω is to vary from full speed 1250 rpm to 750 rpm by voltage control using pairs of back to back connected thyristors in the lines. Calculate the range of firing-angles required.

[Ans : $95^\circ \leq \alpha \leq 118^\circ$]

15.5 A mechanical load represented by the relation

$$T_L = 2 \times 10^{-3}\omega^2 + 1 \times 10^{-6}\omega^2$$

is driven by a three-phase, 140 V, four-pole, 50 Hz, delta-connected squirrel-cage induction motor which provides speed control for a load by

terminal voltage variation method in which terminal voltages are varied by the symmetrical triggering of pairs of inverse-parallel thyristors connected in series with each primary phase winding. The per-phase equivalent circuit parameters of the motor referred to stator side are:

$R_1 = 0.32\ \Omega$, $R_2 = 0.18\ \Omega$, $X_1 = X_2 = 1.65\ \Omega$, X_m : very large.

If speed control is required in the range 1200-1450 rpm, estimate roughly the required range of thyristor firing-angles.

[Ans : $36^\circ \leq \alpha \leq 75.5^\circ$]

15.6 A three-phase induction motor operating from a power supply of constant frequency can be used to supply a range of speed by variation of

(a) The magnitudes of the terminal voltages, or

(b) The magnitudes of the secondary circuit resistances.

Sketch motor torque-speed characteristics to demonstrate each of these control methods, showing intersections with load line representing a constant torque requirement of about rated torque. Point out the relative features of the two schemes for speed control purposes in this case.

Show, by diagrams, how pairs of thyristors connected in the inverse-parallel arrangement may be used to obtain speed control by each of the two methods. Explain the scheme of thyristor triggering that you would recommend. What particular difficulties would you anticipate in correctly triggering the thyristors to obtain secondary resistance control?

15.7 A three-phase, six-pole, squirrel-cage induction motor is to be controlled by terminal voltage variation using pairs of inverse-parallel thyristors in the supply lines with symmetrical phase-angle triggering. The motor is rated at 50 kW, 240 V, 50 Hz. If it operates at a full-load efficiency of 0.9 p.u. and power factor 0.85. Calculate the *rms* current rating and maximum voltage rating required of the thyristors. The motor drives a fan load characterised by the relation $T_L = k\omega^2$, where T_L the shaft torque is and ω is the motor speed. Operation is required to give full load at full speed; which corresponds to 5 % slip, and at three quarters of the full speed. What approximate reduction of motor power is required (compared with full-load, full-speed operation) in order to realise operation at 750 rpm?

If the motor operates at full voltage at upper speed, calculate, approx-imately, the voltage required at the lower speed. Explain and estimate the change of thyristor firing-angle necessary to obtain the required change of voltage.

[Ans: 6.5]

APPENDIX A

Fourier Analysis

A nonsinusoidal periodic function $f(\omega t)$ can be expressed as a summation of harmonic terms:

$$f(\omega t) = \frac{a_o}{2} + \sum_{n=1}^{\infty} a_n \cos n\omega t + \sum_{n=1}^{\infty} b_n \sin n\omega t$$

$$= \frac{a_o}{2} + \sum_{n=1}^{\infty} C_n \sin(n\omega t + \psi_n) \quad V \qquad (A-1)$$

From Eq. (A.1) , it follows that

$$c_n = \sqrt{a_n^2 + b_n^2} \qquad (A-2)$$

and

$$\psi_n = \tan^{-1}\left(\frac{a_n}{b_n}\right) \qquad (A-3)$$

where

a_n = cosine term Fourier coefficient
b_n = sine term Fourier coefficient
c_n = the amplitude of the nth order harmonics
ψ_n = phase angle of the nth harmonic component
n = the nth order harmonics (n=1,2,3,…….)

The Fourier coefficients in Eq. (A-1) are defined by the expressions

$$\frac{a_o}{2} = \frac{1}{2\pi}\int_0^{2\pi} f(\omega t)\, d\omega t \qquad (A-4)$$

$$a_n = \frac{1}{\pi}\int_0^{2\pi} f(\omega t)\cos n\omega t\, d\omega t \qquad (A-5)$$

$$b_n = \frac{1}{\pi}\int_0^{2\pi} f(\omega t)\sin n\omega t\, d\omega t \qquad (A-6)$$

For the fundamental component (n=1):

$$a_1 = \frac{1}{\pi}\int_0^{2\pi} f(\omega t)\cos\omega t\, d\omega t \qquad (\mathrm{A}-7)$$

$$b_1 = \frac{1}{\pi}\int_0^{2\pi} f(\omega t)\sin\omega t\, d\omega t \qquad (\mathrm{A}-8)$$

The amplitude of the fundamental component is

$$c_1 = \sqrt{a_1^2 + b_1^2} \qquad (\mathrm{A}-9)$$

The phase angle of the fundamental component is given as,

$$\psi_1 = \tan^{-1}\frac{a_1}{b_1} \qquad (\mathrm{A}-10)$$

APPENDIX B

Thyristor Forced Commutation Methods

As we have studied in Chapter One, a thyristor can be turned on by triggering gate terminal with low voltage short duration pulse. However, when the supply is d.c., natural commutation is not possible. This is because the polarity of the supply remains unchanged. Therefore, special techniques must be adopted to reduce the current through the SCR below the holding value or to apply a negative voltage across it. This technique is called "FORCED COMMUTATION" and is applied in all circuits where the supply voltage is d.c. The forced commutation techniques of thyristors use basic electronics and electrical components such as inductance and capacitance as commutating elements for commutation purpose. These techniques are classified into different methods as follows:

- Class A: Self commutation by resonating load
- Class B: Self commutated by an LC circuit
- Class C: C or L-C switched by another load carrying SCR
- Class D: C or L-C switched by an auxiliary SCR
- Class E: An external pulse source for commutation

1. Self-Commutated SCR by a Resonating Load (Class A)

Fig.B-1 shows the circuit diagram of a simple self-commutation. When the SCR T_1 is triggered, current start flowing through the load and charges up the capacitor C with the plate *a* as positive. The inductor L, capacitor C and resistor R form a second order under-damped circuit. Because of the inductance the current through the SCR builds up slowly and remains in the same direction through a complete half cycle. The inductor current will then attempt to flow through the SCR in the reverse direction and the SCR will be turned off.

Fig.B-1 Self-commutation circuit (Class A-Commutation).

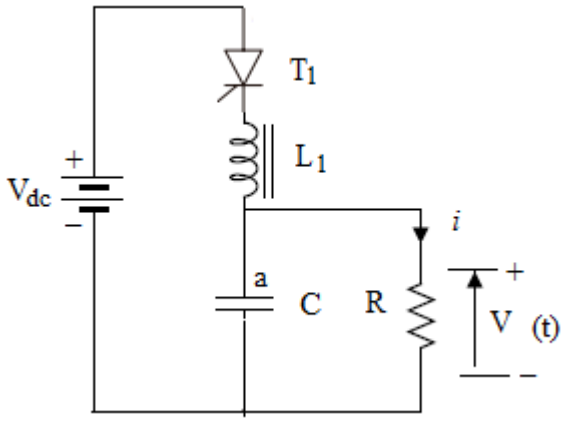

After the thyristor commutation or turning off the thyristor, the capacitor will start discharging from its peak value through the resistor is an exponential manner. The thyristor will be in reverse bias condition until the capacitor voltage returns to the supply voltage level.

2. Self Commutated by a parallel L-C Circuit (Class B)

Fig.B-2 shows another method of self-commutation using series LC elements. The main difference between class-A and class-B SCR commutation techniques is that the LC is connected in series with thyristor in class-A, whereas in parallel with thyristor in class-B. Before triggering on the SCR, the capacitor is charged up (letter (*a*) on the capacitor indicates positive plate).

Fig.B-2 Self Commutated by an L-C Circuit (Class B-Commutation).

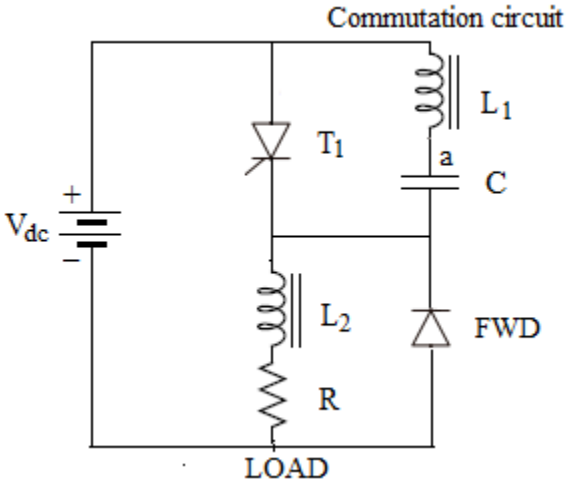

If the SCR is triggered the resulting current has two components. The constant load current flowing through the *R-L* load is ensured by the large reactance L2 connected in series with the load which is clamped with freewheeling diode. If sinusoidal current flows through the resonant L-C circuit, then the capacitor C is charged up with plate (*a*) as negative at the end of the half cycle.

The total current flowing through the SCR becomes zero with the reverse current flowing through the SCR opposing the load current for a small fraction of the negative swing. If the resonant circuit current or reverse current becomes just greater than the load current, then the SCR will be turned OFF.

3. Class C: C or L-C Switched by Another Load Carrying SCR

In this technique of thyristor commutation two SCRs are usually used as shown in Fig.B-3. One SCR is considered as main thyristor and the other as auxiliary thyristor and both the SCRs may act as main SCR carrying the load current. Also, the commutation circuit can be designed with four SCRs to charge and discharge the capacitor as illustrated in chapter Four, Section 4. To commutate the main thyristor.

Fig.B-3 Class C-Commutation.

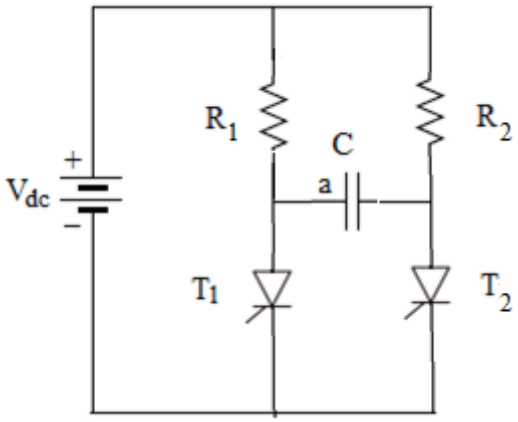

In two thyristors technique shown in Fig.B-3, if the thyristor T_2 is triggered, then the capacitor will be charged up. When the thyristor T_1 is triggered, then the capacitor will discharge and this discharge current of C will oppose the flow of load current in T_2 as the capacitor is switched across T_2 via T_1.

4. Class D: L-C or C Switched by an Auxiliary SCR

In class D thyristor commutation technique the SCR commutation can be illustrated as : only the main thyristor T_m will carry the load current whereas the other auxiliary thyristor T_a acts as commutating one. Large resistor must be connected in series with the anode of the auxiliary thyristor to ensure main thyristor commutation.

When the thyristor T_a is triggered the capacitor C is charged up to source voltage causing T_a to turn OFF. If an extra voltage appears due to effective inductance in the source it will be discharged through the diode D-inductor L and the load circuit.

In Fig.B-4, If the main thyristor T_m is triggered, current will flow in two paths: commutating current will flow through the C-T_m-L-D path and load current will flow through the load. If the charge on the capacitor is

reversed and held at that level using the diode and if T_a is re-triggered, then the voltage across the capacitor will appear across the T_m via T_a. Thus, the main thyristor T_m will be turned off.

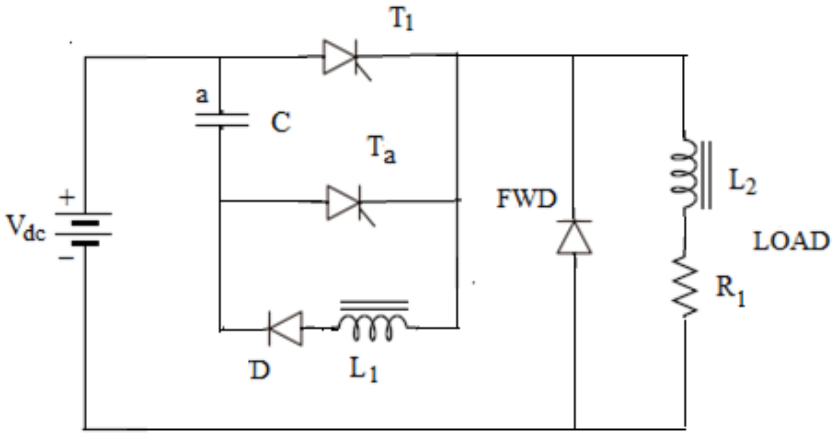

Fig.B-4 Class D-Commutation.

5. Class E: External Pulse Source for Commutation

In this technique, an external pulse generator is used to generate a positive pulse which is supplied to the cathode of the thyristor through pulse transformer as depicted in Fig.B-5. The capacitor C is charged to around 1.0V and it is considered to have zero impedance for the turn off pulse duration. The voltage across the thyristor is reversed by the pulse from the electrical transformer which supplies the reverse recovery current, and for the required turn off time it holds the negative voltage. The pulse transformer is so deign that it cannot saturate easily by using sufficient iron core with large air gap as well as it must capable of carrying the load current with small voltage drop compared with the supply voltage.

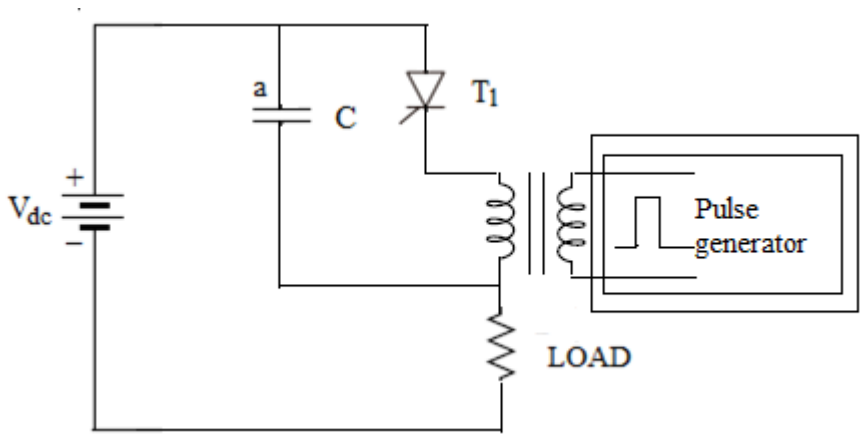

Fig.B-5 Class E-Commutation.

APPENDIX C

Matlab Spectra and Phase Relation Plots

MATLAB (MATrix LABoratory) is a tool for numerical computation and visualization. The basic data element is a matrix, so if we need a program that manipulates array-data it is generally fast to write and run in MATLAB. The following example is how to calculate and plot spectra and phase relationship of a Multi-Conduction and Control Periods Integral Cycle Triggering waveforms.

```
clear;clc
h=1;
N1=1;
N2=1;
N3=1;
N4=1;
T1=2;
T2=3;
m1=0;
m2=0;
t=T1+T2
n=20;
x=0;
d=0;
while h<4
B(1)=0 ;
B(2)=2*pi/3;
B(3)=4*pi/3;
for i=1:n
d=d+1;
u(i)=i*50/t;
if i==t
a(i)=1/(4*pi*t)*(cos(B(h))-2*(2*pi*N1+x)*sin(B(h))-cos(2*x+B(h))-
cos(B(h))+2*(2*pi*N2+x)*sin(B(h))+cos(2*x+B(h))+cos(B(h))-
2*(2*pi*N3+x)*sin(B(h))-cos(2*x+B(h))-
cos(B(h))+2*(2*pi*N4+x)*sin(B(h))+cos(2*x+B(h)));
```

```
b(i)=1/(4*pi*t)*(sin(B(h))+2*(2*pi*N1+x)*cos(B(h))-sin(2*x+B(h))-
sin(B(h))-
2*(2*pi*N2+x)*cos(B(h))+sin(2*x+B(h))+sin(B(h))+2*(2*pi*N3+x)*cos
(B(h))- sin(2*x+B(h))-sin(B(h))-
2*(2*pi*N4+x)*cos(B(h))+sin(2*x+B(h)));
c(i)=sqrt(a(i)^2+b(i)^2);
else
a(i)=t/(pi*(t^2-i^2))*(cos(i/t*B(h))-cos(x)*cos(i/t*(2*pi*N1+x+B(h)))-
i/t*sin(x)*sin(i/t*(2*pi*N1+x+B(h)))-
cos(i/t*(B(h)+2*pi*N1))+cos(x)*cos(i/t*(2*pi*N1+x+B(h)+2*pi*N2))+i/
t*sin(x)*sin(i/t*(2*pi*N1+x+B(h)+2*pi*N2))+cos(i/t*(B(h)+2*pi*T1))-
cos(x)*cos(i/t*(2*pi*N3+x+B(h)+2*pi*T1))-
i/t*sin(x)*sin(i/t*(2*pi*N3+x+B(h)+2*pi*T1))-
cos(i/t*(B(h)+2*pi*T1+2*pi*N3))+cos(x)*cos(i/t*(2*pi*N3+x+B(h)+2*p
i*T1+2*pi*N4))+i/t*sin(x)*sin(i/t*(2*pi*(N4+N3)+x+B(h)+2*pi*T1)));
b(i)=t/(pi*(t^2-i^2))*(sin(i/t*B(h))-
cos(x)*sin(i/t*(2*pi*N1+x+B(h)))+i/t*sin(x)*cos(i/t*(2*pi*N1+x+B(h)))
-sin(i/t*(B(h)+2*pi*N1))+cos(x)*sin(i/t*(2*pi*N1+x+B(h)+2*pi*N2))-
i/t*sin(x)*cos(i/t*(2*pi*N1+x+B(h)+2*pi*N2))+sin(i/t*(B(h)+2*pi*T1))-
cos(x)*sin(i/t*(2*pi*N3+x+B(h)+2*pi*T1))+i/t*sin(x)*cos(i/t*(2*pi*N3
+x+B(h)+2*pi*T1))-
sin(i/t*(B(h)+2*pi*T1+2*pi*N3))+cos(x)*sin(i/t*(2*pi*N3+x+B(h)+2*pi
*T1+2*pi*N4))-i/t*sin(x)*cos(i/t*(2*pi*(N4+N3)+x+B(h)+2*pi*T1)));
c(i)=sqrt(a(i)^2+b(i)^2)
end
pp(d)=a(i);
qq(d)=b(i);
end
stem(u,c);grid
axis([0,160,0,max(c)+.1])
xlabel('Frequency(Hz)')
ylabel('Amplitude(perunit)')
h=h+1;
end
for f=1:n
figure
VV=[pp(f) pp(n+f) pp(2*n+f)];
ee=[qq(f) qq(n+f) qq(2*n+f)];
compass(ee,VV)
text(qq(f),pp(f), 'Va')
text(qq(n+f),pp(n+f), 'Vb')
text(qq(2*n+f),pp(2*n+f),'Vc')
title(['Harmonic Number ',num2str(f)])
end
```

References

1. Bin Wu, Mehdi Narimani, High-Power Converters and AC Drives, Second Edition, Wiley, 2016 - Science.
2. Paul Scherz , Simon Monk , Practical Electronics for Inventors, Fourth Edition 4th Edition, Mc graw Hill Education, 2016.
3. Andrzej M. Trzynadlowski , Introduction to Modern Power Electronics, Third Edition, Wiley, 2015 - Science.
4. M. H. Rashid, Power Electronics: Circuits, Devices, and Applications, Fourth Edition, Pearson, England 2014.
5. M. H. Rashid, Power Electronics Handbook : Circuits, Devices, and Applications, Third Edition , Butterworth-Heinemann – Elsevier, USA 2011.
6. W.Shepherd and D.W. Shepherd, Energy Studies, Imperial college press, 2014.
7. Ned Mohan, Tore M. Undeland, William P.Robbins, Power electronics: converters, applications, and design, Wiley India, 2007.
8. Robert W.Erickson, Dragan Maksimovic, Fundamentals of Power Electronics, Second Edition, Springer Science & Business Media, 2001.
9. Valery Vodovozov, Introduction to power electronics, Ventus publishing APS , 2010.
10. Fang Lin Luo, Hong Ye, Muhammad Rashid, Digital Power Electronics and Applications, Elsevier, USA, 2005.
11. D. M. Divan, remarks in Introduction to Power Electronics, Madison, Wisconsin, USA, 1994.
12. P. Krein, Elements of Power Electronics, Oxford University Press, London, 1997.
13. B.K. Bose, ed., Power Electronics and Variable Frequency Drives: Technology and Applications, New York : IEEE (1996).
14. D.Hart, Introduction to Power Electronics, Prentice-Hall, New York,1996.
15. J. Ross, The Essence of Power Electronics, Prentice-Hall, New York , 1996.
16. P. C. Sen, Principles of Electric Machines and Power Electronics, Second Edition, Wiley, New York , 1996.
17. W. Shepherd, L. N. Hulley and D. T. Liang, Power Electronics and Motor Control, Cambridge University Press, London ,1996.
18. Subramanyam, A Course on Power Electronics, Halsted, New York, 1995.

19. J.Vithayathil, Power Electronics: Principles and Applications, McGraw-Hill, New York, 1995.
20. D. A. Bradley, Power Electronics, Chapman and Hall, London, 1994.
21. C. W. Lander, Power Electronics, McGraw-Hill, New York, 1994.
22. R. Ramshaw, Power Electronics Semiconductor Switches, Chapman and Hall, London ,1993.
23. B. J. Baliga, Modern Power Devices, Kreiger, New York ,1992.
24. R. G. Hoft, Semiconductor Power Electronics, Kreiger, New York, 1991.
25. J. O. Kassakkian, M. F. Schlecht and G. C. Verghese, Principles of Power Electronics, Addison-Wesley, Boston, 1991.
26. R. Erickson, Power Electronics, Chapman and Hall, London ,1997.
27. D. A. Bradley, Power Electronics, Chapman and Hall, London, 1987.
28. J. M. D. Murphy and F. G. Turnbull, Power Electronic Control of AC Motors, Pergamon Press, New York, 1988.
29. S. K. Ghandi, Semiconductor Power Devices-Physics of Operation and Fabrication Technology, John Wiley and Sons, New York, 1977.
30. S. M. Sze, Physics of Semiconductor Devices, 2nd ed., John Wiley and Sons, New York, 1984.
31. F.C. Lee, High-Frequency Resonant, Quasi-Resonant and Multi-Resonant Converters, Virginia Power Electronics Center, 1991.
32. F.C. Lee, High-Frequency Resonant and Soft-Switching Converters, Virginia Power Electronics Center, 1991.
33. M.K. Kazimierczuk and D. Czarkowski, Resonant Power Converters, New York: Wiley Interscience, 1995.
34. R.E. Tarter, Solid-State Power Conversion Handbook, New York: Wiley- Interscience 1993.
35. C. Rombaut, G. Seguier, and R. Bausiere, Power Electronic Converters AC-AC Conversion, McGraw-Hill, New York, 1987.
36. W. Shepherd, Thyristor Control of AC Circuits, Granada Publishing, Great Britain, 1975.
37. B. R. Pelly, Thyristor Phase-Controlled Converters and Cycloconverters, John Wiley, New York, 1971.
38. L. Gyugi and B. R. Pelly, Static Power Frequency Changers: Theory, Design and Applications, Wiley-Interscience, New York, 1976.
39. W. McMurray, The Theory and Design of Cycloconverters, MIT Press. Cambridge, 1972.
40. Leonhard, Control of Electrical Drives, Second Edition, Springer-Verlag, Berlin, 1996.
41. W. Novotny and T. A. Lipo, Vector Control and Dynamics of AC Drives, Oxford University Press, London , 1996.
42. Rajashekara, A. Kawamura and K. Matsuse, Sensorless Control of AC Motor Drives: Speed and Position Sensors, IEEE Press, New York, 1996.

43. Subrahmanyam, Electric Drives: Concepts and Applications, McGraw-Hill, New York , 1996.
44. Wildi, Electrical Machines, Drives and Power Systems, Third Edition Prentice-Hall, New York , 1996.
45. M. P. Kazmierkowski and H. Tunia, Automatic Control of Converter-Fed Drives, Elsevier, Paris , 1994.
46. P.Vas, Electrical Machines and Drives: A Space Vector Theory Approach, Oxford University Press, London, 1993.
47. S. A. Nasar, Vector Control of AC Drives. CRC Press, Boca Raton, Florida, USA, 1992).
48. Daniel . W . Hart, Power Electronics, McGraw-Hill Companies, Inc., New York, 2011.
49. G. R. Slemon, Electric Machines and Drives, Addison-Wesley, Boston ,1992.
50. T. J. E. Miller, Brushless Permanent Magnet and Reluctance Motor Drives, Oxford University Press, London, 1989.
51. M. E. Brumbach, Electronic Variable Speed Drives, Delmar, New York, 1996.
52. P. Idberq, A. Nerman " Motor Drive with Thyristor Converters", Esselet Studium, Royal Swidish Institute of Technology, Sweeden, 1978.

I N D E X

A

Ac drives, 649
Ac-Dc conversion, 38
Accelerating torque, 483
Air-gap power, 658
Amplifier, 625
Anode, 6, 9, 13
Angle
  commutation or overlap, 147
  displacement , 317
  extinction , 46, 193
  phase , 329
  of maximum current, 48
Armature inductance, 512
Armature resistance, 512
Avalanche breakdown, 11
Average power, *see* power, average

B

Back *emf* , 512
Basic equation of motion, 482
Bi-phase converter, 326
Bipolar junction transistors (BJTs), 20
  Safe operation area of, 21
  current gain of, 21
  silicon carbide, 31
    V-I characteristics of, 21
    switching characteristics of, 21
Braking, 538
    Dynamic, 542
    Plugging, 540
    Regenerative, 538
Branch-delta connection, 281
Breakdown voltage, 7
Bridge rectifier, *see* single-phase bridge rectifier *and* three-phase bridge rectifier
Burst firing, 290

C

Cathode, 6, 9, 13
Chopper drives, 548
Choppers, 179
    boost,180, 207
    buck, 180, 218
    buck-boost, 226
    class-A, 184
    class-B, 214
    class-C, 215
    class-D, 215
    class E, 216
    classifications of, 214
    dc-dc, 179, 217
    first quadrant, 179
    first and second quadrant, 215
    four quadrant, 216
    step-down, 181
    step-up, 207
    types of, 180
Chopping frequency, 183
Circulating current, 350, 361
Closed-loop operation, 614
Commutation, 14
    angle, 147
    circuit,15
    natural or line, 14
Controlled rectifier, *see* single-phase bridge rectifier *and* three-phase bridge rectifier.
Copper losses, 517
Current,
    average, 40, 45, 58
    current loop, 633
    circulating mode, 350 , 361
    extinction angle, 46, 194
    rms value, 41, 58, 237, 270
Current source inverter (CSI), 384, 433

Controllers, 474
ac voltage, 234
speed controller, 639
Converters
ac-ac, 234, 27
ac-dc, 38
bi-phase, 114, 148
dc-ac, 384
dc-dc,179
dual, 591, 601
flyback, 180, 222
forward, 218
full-bridge, 151
half-bridge,*see* inverters.
matrix, 379
one-quadrant, 184
semi-, 53, 113, 137, 596
single-phase uncontrolled , 39, 53
single-phase dual, 591
single-phase full-wave , 53
single-phase series, 442
three-phase dual, 601
three-phase full-wave, 68, 127, 134, 135, 151
Cycloconverters, 346, 702
drive, 683, 702
envelope, 365
multi-phase , 354
single-phase, 347
three-phase, 354, 359

D
Dc Chopper, 179
Dc drives, 509
chopper control, 181
closed-loop control of, 611
single-phase converter drives, 573
single-phase dual-converter , 591
single-phase full-converter , 582
three-phase dual-converter , 601
three-phase full-converter, 599
three-phase semiconverter, 596
Dc motors, 509
characteristics of, 515, 516, 518, 522
closed-loop control of, 620, 623
closed-loop transfer function of, 620
compound, 522
separately-excited, 510, 512, 515
shunt, 516
open-loop transfer function, 617
series, 518
speed control of, 523
Diodes, 6
break-down voltage of, 7
characteristics of, 6
fast recovery, 8
forward-biased, 6
freewheeling, 83, 96
leakage current, 6
line frequency, 8
power, 6
reversed-biased, 6
Schottky, 8
silicon carbide, 30
tum-on voltage of, 8
types of, 8
Displacement factor, 42
Distortion
factor, 244, 391
total harmonic, 392
Drives
ac, 649
dc, 509
static Kramer, 691
static Schcrbius, 692
Duty cycle, 183
Dynamic braking, 542
Dynamic torque, 483

F
Factor
damping, 634
displacement, 42
distortion, 244, 391
lowest order harmonics, 392
form, 42
harmonic, 43
input power, 43, 238, 243
power, 43, 238, 243
ripple, 42
transformer utilization, 42
Filters, 182

Firing angle, *see* triggering angle.
Field oriented control, 699
Field weakening, 523
Forced commutation, 14
Forward breakdown voltage, 7, 11
Fourier analysis, 59, 63, 160, 196, 239, 266, 291, 323
Fourier coefficients, 62, 196
Four quadrant operation, 535
Frequency
  chopping ,183
  fundamental , 161, 240, 266, 390
  resonant, 443, 447
  undamped natural, 634
Friction and windage, 482

G
GCT, 30
GTOs, 17, 26
  characteristics of, 17
  snubber circuit of, 19

H
Half-wave uncontrolled , 51, 268
Harmonics, 58,147, 160, 162, 195, 239
  lowest-order, 392
  phase-angle, 240
  reduction, 378, 428
  zero-value, 293
Holding current, 10, 12

I
IGBTs, 25
Induction motors, 650
  equivalent circuit of, 654
  frequency control of, 675
  rotor resistance control of, 685
  speed control of, 662
  stator voltage control of , 665
  voltage and frequency control of, 675
Integral cycle control, 290
  single-phase, 290
  three-phase , 307
Inverters, 384
  current-source, 433
  dc-link, 456
  half-bridge, 384, 397
  load commutated, 683
  multilevel, 456
  parallel , 385
  performance parameters of, 391
  pulse-width-modulated, 418
  single-phase series resonant, 442
  single-phase bridge, 384, 395
  three-phase bridge, 409
  types of, 384
  voltage control, 417, 428
  voltage-source, 384

L
Latching current, 10, 12
Linear mechanics, 476
Load classifications, 480
Load torque, 480, 486
Load commutated inverter, 683

M
Matrix converter, 379
Maximum slip, 662
MCT s, 28
Mechanical transmission, 494
Modulation
  index, 419
  modified sinusoidal pulse-width, 426
  multiple-pulse·width, 421
  single pulse, 419
  sinusoidal pulse-width, 423
  sixty-degree pulse-width, 427
  third-harmonic pulse-width, 427
Modules,
  intelligent, 5
  power, 5
  smart, 5
Moment of inertia, 477
MOSFETs, 24
  steady-state characteristics of, 24
  switching characteristics of, 25
  ratings of, 25

Motors
ac, 650
dc, 509
ratings, 499
synchronous, 651, 698
Multilevel inverters, 456
cascaded, 457
diode-clamped, 462
flying-capacitors, 465
types of, 457

N
Natural commutation, 14
Neutral current, 310, 322

O
Open-loop operation, 614
Overlap, 147
Overmodulation, 425

P
Poly-phase rectification, 64, 127, 165
Performance parameters, 41, 392, 366, 391
phase-angle, 316
Phase displacement, 317
Power semiconductor devices, 4
ideal characteristics, 6, 10
switching characteristics, 6, 10, 17,18
symbols, 6, 9, 16, 18, 26
Types of, 5
Power diodes, 6
Power electronics, 1
applications of, 3
Power factor, 43, 76, 238, 243
Power semiconductors, 4
Power supplies, 217
switched mode ac, 217
switched mode dc, 217
Pulse-width modulation (PWM), 182, 418, 682,701

R
Rectifiers.
Bridge, 38
controlled, 38
efficiency, 42
single-phase full-wave, uncontrolled, 53
with highly inductive load, 57, 109
with *R-L* load, 44, 94, 107, 129
single-phase half-wave, uncontrolled, 39
three-phase, 68,127, 133 , 135, 151
three-phase bridge, 68
uncontrolled, 38
Reducers, 494
Regulators
boost, 222
buck, 218
buck-boost, 226
switching mode, 217
Resonant frequency, 443, 447
Resonant inverters, 441
dc link, 449
series, 442
Reverse recovery time, 7, 8
Ripple factor, 42
Root-mean-square (*rms*) value, 295, 388
Rotational mechanics, 476

S
Schottky diodes, 8
Silicon carbide (SiC), 8
Slip, 653
Slip power, 657, 691
Sinusoidal pulse-width modulation (SPWM), 423
SIT, 29, 30
SITH, 29, 30
Snubbers, 19
Space vector, 699
Speed
control, 523
sensing, 615
SPIC, 5
synchronous, 652
static friction, 479
Static Kramer drive, 691
Static Scherbius drive, 692
Stinction, 479

Subharmonics, 292
Synchronous motor, 651
cylindrical rotor, 698
drives, 697
permanent magnet, 698
reluctance, 698
salient-pole, 698

T
Thyristors, 8
asymmetrical, 235
characteristics of, 10
di/dt capability , 5
dv/dt capability, 5, 14
gate controlled, 30
gate-turn off, 17
insulated gate commutated, 30
light activated, 14
MOS-controlled, 28
phase-control, 8, 235
static induction, 29
parameters , 12
static induction, 29
triggering methods, 13
turn-off of, 12
turn-on of, 12
two-transistor model of, 9
types of, 15
Time
forward recovery, 7
reverse recovery, 7
turn-off, 182
turn-on, 182
THD, 393
Time constant, 46, 187, 263
Torque
accelerating, 483
constant, 513
equation, 477
developed, 477
due to friction, 478
instantaneous , 477
Maximum(breakdown) , 661
Transistors
bipolar, 20
characteristics, 21
Cool MOS, 25, 29
IGBTs, 25
MOSFETs, 24
power, 23
safe operation area, 21
saturation, 20
SIT, 5
types of, 5
Transmission,
mechanical, 494
gear, 494
planetary, 495
screw, 496
worm, 496
TRIAC, 16

V
Variable load, 502
Vector control, 699
Sensor less, 699
Flux, 699
Variable speed drives (VSDs), 698
Viscous friction, 478
Voltage controller, see single-phase voltage controller *and* three-phase voltage controller
Voltage source inverter, 384

W
Wide Gap Semiconductors, 30

Z
Zero current switching, 290, 441
Zero voltage switching, 441